

REVISTA

BRASILEIRA

DE CIÊNCIAS

MECÂNICAS

Journal of the Brazilian
Society of Mechanical Sciences

SPECIAL ISSUE

Proceedings of the International
Symposium on Spacecraft Ground Control
and Flight Dynamics

SCD1



07-11 February 1994
São José dos Campos, Brazil

PUBLICAÇÃO DA ABCM - ASSOCIAÇÃO BRASILEIRA DE CIÊNCIAS MECÂNICAS

Vol. XVI • Special Issue • 1994

ISSN 0100-7386

REVISTA BRASILEIRA DE CIÊNCIAS MECÂNICAS
JOURNAL OF THE BRAZILIAN SOCIETY OF MECHANICAL SCIENCES

SPECIAL ISSUE: PROCEEDINGS OF THE INTERNATIONAL
SYMPOSIUM ON SPACECRAFT GROUND CONTROL
AND FLIGHT DYNAMICS
SCD1

REVISTA BRASILEIRA DE
CIÊNCIAS MECÂNICAS
JOURNAL OF THE BRAZILIAN
SOCIETY OF MECHANICAL
SCIENCES
Vol. 1, N° 1 (1979)
Rio de Janeiro: Associação Brasileira de
Ciências Mecânicas

Trimestral

Inclui referências bibliográficas.

1. Mecânica

ISSN-0100-7386

A REVISTA BRASILEIRA DE
CIÊNCIAS MECÂNICAS
publica trabalhos que cobrem os vários
aspectos da ciência e tecnologia
em Engenharia Mecânica,
incluindo interfaces com as Engenharias
Civil, Elétrica, Química, Naval, Nuclear,
Aeroespacial, Alimentos,
Agrícola, Petróleo, Materiais, etc.,
bem como aplicações
da Física e da Matemática à Mecânica.

Publicação da/Published by
ASSOCIAÇÃO BRASILEIRA DE
CIÊNCIAS MECÂNICAS
THE BRAZILIAN SOCIETY OF
MECHANICAL SCIENCES

Secretária da ABCM: Ana Lúcia
Frões de Souza
Av. Rio Branco, 124-18º andar -
Rio de Janeiro - Brasil
Tel. /Fax (021)222-7128

Presidente: Arthur Palmeira Ripper
Vice-Presidente: Sidney Stuckenbruk
Secret. Geral: Agamenon R. E. Oliveira
Secretário: Carlos Alberto de Almeida
Diretor de Patrimônio: Luiz Fernando
Salgado Candiota

EDITORS FOR THIS SPECIAL ISSUE:

Pawel Rozenfeld
INPE - CRC - C. P. 515
12201-970 São José dos Campos - SP - Brazil
Tel. : (0123)41-8977 R-622 Fax: (0123)41-1873

Hélio Koiti Kuga
INPE - DMC - C. P. 515
12201-970 São José dos Campos - SP - Brazil
Tel. : (0123)41-8977 R-414 Fax: (0123)21-8743

Valcir Orlando
INPE - CRC - C. P. 515
12201-970 São José dos Campos - SP - Brazil
Tel. : (0123)41-8977 R-622 Fax: (0123)41-1873

PROGRAMME COMMITTEE:

Pawel Rozenfeld - "Chairman" - (INPE - Brazil)
Jean P. Carrou (CNES - France)
Giorgio E. O. Giacaglia (USP - Brazil)
Jean F. Kaufeler (ESOC - ESA)
Hélio K. Kuga (INPE - Brazil)
Jean Latour (CNES - France)
Rolf E. Münch (ESOC - ESA)
Valcir Orlando (INPE - Brazil)
José A. G. Pereira (INPE - Brazil)
Peter Piotrowski (DLR - Germany)
Konrad Reinel (DLR - Germany)
Malcolm D. Shuster (APL - USA)

The symposium was realized under the auspices of INPE and ABCM, and sponsored by:



ABCM

BANCO REAL

digital



finep

PROMON

VARIG

FOREWORD

The International Symposium on Spacecraft Ground Control and Flight Dynamics, SCD1 Symposium for short, was the first one of that kind to be held in Brazil. The event was particularly meaningful for Brazil as the symposium was held during the week of the first anniversary of in-orbit operation of the first Brazilian Satellite SCD1. A total of 86 papers and 8 computer demonstrations have been presented during 5 days of the symposium. In terms of participants, 95 from 14 countries and one international organization (ESA) attended the symposium. In particular, INPE had the pleasure of featuring 15 papers covering the operation, control, performance and perspective of the SCD1 mission.

The papers presented constitute a blend of past experiences, challenges of the future comet rendez-vous mission operations, novel solutions for the system architecture, use of the artificial intelligence in the satellite operations, problem of orbit determination for satellites with ion propulsion and much more. Therefore, the symposium constituted a ground for cross-fertilization of ideas valuable for all participants.

All these facts made the SCD1 Symposium Organizing Committee to feel gratified and encouraged to think about the realization of a new symposium in not a too distant future, hopefully, with always growing number of participants from ever growing number of countries, presenting always high level papers.

Pawel Rozenfeld

SCD1 Symposium Chairman

INVITED PAPER

Dias Jr., O.P. (INPE-Brazil):
"An Overview of the MECB Program"

003

RESUMEN

An overview of the MECB program will be presented, including the main milestones reached by this program. The presentation will address the development of the infrastructure, the development activities, the other projects under execution and the future program currently carried out by INPE as planned for the next future.

INTRODUCTION

This text is dedicated to the first anniversary of the MECB launch. The various milestones achieved during the Brazilian space program were acknowledged by the Brazilian society and, in particular, by the Brazilian Government, giving us the necessary confidence to go ahead with the program.

I will take this opportunity to talk about this MECB program as well as about another current program, the CBERS program, and also to say just few words about our future plans regarding satellite programs.

MECB PROGRAM

The SCDF was launched by a BRASUL launcher in February the ninth, 1993, since it was

launched, MECB is performing very well as you will see in the presentation that will follow.

The MECB is the first of a series of satellites to be part of the MECB program. MECB is an artificial Earth satellite launched from the Guiana Space Center by the Brazilian Government in 1993. This program comprises 3 segments:



the satellite development, the launcher development and the launching site construction. The first segment comprises the development of 2 data collecting satellites and 2 remote sensing satellites and is under INPE's responsibility. In the Ministry of Science and Technology.

The second segment is under the responsibility of the Ministry of Aeronautics and will provide the launchers to put the satellites into orbit. The third segment will be at the construction of the

AN OVERVIEW OF THE MECB PROGRAM

Oscar Pereira Dias Jr., Director

Engineering and Technology Directorate

INPE, Brazil

ABSTRACT

An overview of the MECB program will be presented focusing on the major achievements reached by that program. The presentation will address the investments made, the infra-structure installed and the current development activities. It will also address other satellite programs currently carried out by INPE or planned for the near future.

INTRODUCTION

This week we celebrate the first anniversary of the SCD1 launch. That was an important achievement for the Brazilian space program which was acknowledged by the Brazilian society and, in particular, by the Brazilian Government, giving us the necessary confidence to go ahead with the program.

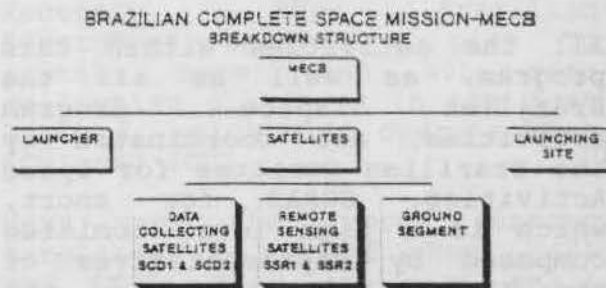
I will take this opportunity to talk about this MECB program as well as about another current program, the CBERS program, and also to say just few words about our near future plans regarding satellite programs.

MECB PROGRAM

The SCD1 was launched by a PEGASUS launcher in February the ninth, 1993. Since it was

launched, SCD1 is performing very well, as you will see in the presentations that will follow me.

The SCD1 is the first of a series of four satellites as part of the MECB program. MECB is an acronym for Brazilian Complete Space Mission, a program approved by the Brazilian Government in 1979. This program comprises 3 segments



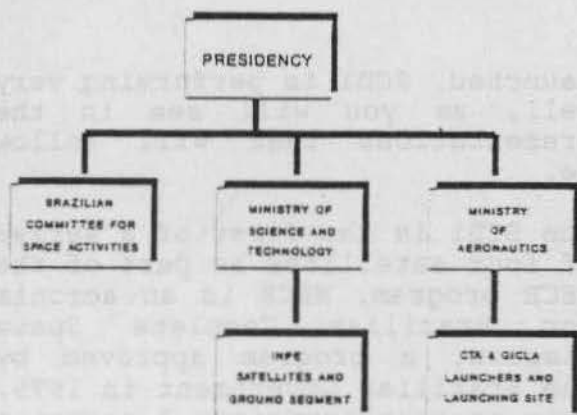
the satellites development, the launcher development and the launching site construction. The first segment comprises the development of 2 data collecting satellites and 2 remote sensing satellites and is under INPE's responsibility, in the Ministry of Science and Technology.

The second segment is under the responsibility of the Ministry of Aeronautics and will provide the launchers to put the satellites into orbit. The third segment aims at the construction of the

launching facilities in Alcântara, state of Maranhão, at 2 degrees latitude South of Equator. This segment is also under the responsibility of the Ministry of Aeronautics.

technical reasons than to administrative and financial constraints and international regulations.

BRAZILIAN SPACE PROGRAM ORGANIZATION



All the activities within this program, as well as all the Brazilian space program activities, are coordinated by the Brazilian Committee for Space Activities, COBAE for short, which is a high level committee composed by representatives of the Ministries involved in the space program. That Committee reports directly to the President of Brazil.

The estimated total cost for the MECB program is around 1 billion dollars for an original 13 years execution plan. According to that plan, the first launch should be done in 1989 and in fact it happened only in 1993, that is, 4 years later. Furthermore the launch was carried out by an American instead of Brazilian launcher. The delays in the satellite and launcher development are due less to

Budget constraints have been very frequent during the execution of the program. So far only 50 to 60% of the total estimated budget was allocated to the program. That had an important impact on the schedule since we had to delay the procurement of parts and materials, to review the design of some facilities to make them simpler and to take other decisions toward the postponement of program targets.

On the other hand, the international market has also played an important role in this subject. The MTCR treaty put some constraints on the exportation of some space components by the international suppliers. This has affected the development of our program leading to the revision of the development plan of the satellites and launcher. The latter was the most affected by these constraints on the exportation of components and technology transfer because of the sensitive nature of the technology involved. As a result the launcher was not ready in time to launch the first Brazilian satellite.

Nevertheless, the program has accomplished several important goals besides the launch of the satellite. During the development phase we have installed the facilities for satellite integration and tests, satellite tracking and control, have trained our team in space technology and involved an important segment of our industry in the program.

The Integration and Tests

Laboratory - LIT tor short - was installed in 1987 and is fully operational. It is a set of laboratories which provides several kinds of services at subsystem and system levels, according to international standards. Besides the Brazilian satellites, this laboratory is involved with other international satellite programs. The Argentine satellite SAC-B, the communication satellite BRASILSAT, made by HUGHES, and the China-Brazil Earth Resources Satellite - CBERS - are using or will use this laboratory for the integration or tests of their models. The Laboratory also provides different kinds of services to the local and national industries in related and non-related space activities.

The facilities for the satellite tracking and control have also been implemented within the scope of the MECB program. As you will see during this Symposium, we have implemented two ground stations, one in Alcântara, state of Maranhão, and the other in Cuiabá, state of Mato Grosso. The first one was very important during the orbit acquisition phase for the SCD1 launch, and the second has an important role in the operational phase of that satellite. Both ground stations are linked to the Satellite Control Center, installed in São José dos Campos, and also built as part of the MECB program.

The facilities in the launching site are not available for satellite launching yet. However, they are operational for sounding rockets launchings. The launching pad for small satellite launchers will be ready in less than two years. Because of its strategic location - very close to the Equator - those facilities can be

used in the future to provide services to other satellite programs in a cooperation basis. They can be used both to launch and to track satellites.

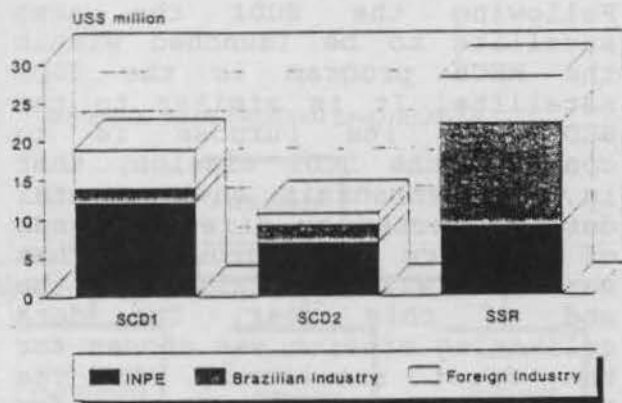
Following the SCD1 the next satellite to be launched within the MECB program is the SCD2 satellite. It is similar to the SCD1 and its purpose is to continue the SCD1 mission, that is, to retransmit environmental data collected by different kinds of sensors on ground. That satellite will be finished by the end of this year. The data collecting mission was chosen for the first satellites for its technological simplicity and for the relevance of that kind of service to a large country like Brazil. Data collecting platforms can provide environmental data from remote areas in the Amazon forest as well as along the hidrographic basins and coast. Recently, the Brazilian Government aproved a plan to install more than 400 data collecting platforms in the next 2 years, which will operate with SCD1 and SCD2.

Next come the remote sensing satellites - two of them, SSR1 and SSR2. They are also small satellites and will carry onboard a CCD camera which will operate in 2 spectral bands producing images of 200 m space resolution with a repetition period of only 4 days. Those satellites will fit our needs to monitor large regions, like the Amazon forest, with a short period of time between observations. These satellites are scheduled for launch in 1996.

An important goal of the MECB program is the involvement of the Brazilian industry in the program. This objective has been

gradually achieved in the development plan.

MECB PROGRAM COST BREAKDOWN



During the SCD1 development the national industry supplied small parts and materials and INPE was responsible for most of the design and manufacturing activities. Exceptions were the structure of the satellite and some products for the ground segment like the communications network and software services for the satellite tracking and control. Those products were supplied by national industries with close supervision of INPE. The SCD1 total cost, including the development and flight models, was around 20 million dollars and more than 70% of these expenses were spent in Brazil, but only 10% due to the national industry activities. The remaining were in-house activities.

For the SCD2 we have involved the industry in a more effective way. It has been dealing with some equipment manufacturing and through this process it was possible to transfer to the industry the management and product assurance procedures

required by space software and hardware. Solar pannels, structures, electronic equipments are examples of hardware produced by the Brazilian industry for the SCD2. The participation of the Brazilian industry in the SCD2 has increased to 30% of the total satellite cost.

The plans for the SSR satellites are to increase that participation to around 50% of the total satellite cost. There will be also a qualitative change. For that satellite, entire subsystems will be designed and built by the industry. For most of the subsystems INPE will only be responsible for the conception and specification and, maybe, the integration and tests. As an example, the payload for that satellite, a CCD camera, was entirely ordered to a Brazilian company as well as the design and manufacturing of the satellite structure.

By this time we have around 10 important companies which have been involved with our satellite program in different levels of involvement. We hope that at the program completion the Brazilian industry will be able to carry out a whole satellite project in compliance with the space quality and reliability requirements .

FUTURE PROGRAMS

All the knowledge and expertise acquired through the MECB program entitled INPE to look for other satellite programs and partnership in the international market.

CURRENT AND FUTURE PROGRAMS

.BRAZILIAN COMPLETE SPACE MISSION
- MECB (current)

.CHINA-BRAZIL EARTH RESOURCES
SATELLITE - CBERS (current)

.COMMUNICATION SATELLITES IN LOW
ORBIT - ECO-8

.ENVIRONMENTAL SATELLITES

.SCIENTIFIC SATELLITES

The main consequence of that initiative was the establishment of a cooperative program with China. Following the signature of a government to government agreement, INPE signed, in 1988, a cooperation agreement with the Chinese Academy of Space Technology - CAST for short - to develop a joint satellite program.

Remote sensing satellites play a very important role for the Brazilian environment monitoring. Brazil is a very large country and most of the population is settled down along the coast. Most of the country area is of difficult access by conventional means and the monitoring of the environment and natural resources is largely facilitated by using remote sensing satellites.

However the development of a remote sensing satellite, with the same operational capabilities as, for example, LANDSAT and SPOT, is very expensive and we cannot afford the cost of its development by ourselves. On the other hand, we do not have the technology to develop some equipments which are fundamental to the satellite configuration and which are not available in the international market. China

was found to be an strategic partner because both countries complement each other.

The CBERS program was, then, started in cooperation with the Chinese. That program aims at the manufacturing of 2 satellites for remote sensing and data collecting purposes. Those satellites will operate within basically the same performance requirements of LANDSAT and SPOT and will also provide the continuity of the MECB mission because they have data collecting capabilities. The total estimated cost for this program is 150 million dollars, including launching costs, and this figure will be shared by the two countries being 30% to Brazil and 70% to China. The launch of the first satellite is scheduled for 1996 and will be carried out by the Chinese launcher Long-March.

And what about the plans for the near future? The SCD1 successful experience encouraged us to go ahead with small satellite programs. Furthermore we can see with gladness the international tendency to go back to small satellites. So we have to take advantage of these positive aspects to speed up our space program. Taking also advantage of the geographic position of Brazil, crossed by the Equator, we have conceived a low orbit satellite communication program. This program, called ECO-8, comprises a set of 8 small satellites in a equatorial orbit of 2,000 km high to provide continuous real time communication between remote regions.

This program seems to better fit our needs for remote and mobile communication than other international proposed programs

using constelations of satellites in different orbit planes. It is a low cost alternative that uses at the same time the country's capabilities both in small satellite technology and for the operation of satellite-based communication networks, by the state company TELEBRAS. This system will provide a coverage range of 30° latitude north to 30° latitude south including areas of the Brazilian territory which are very poorly attended by communication facilities. The total estimated investment for the program is about 200 million dollars. We hope to have the program approved by the Government in a short period of time so that the system can be implemented by 1997. The strategy to carry out this kind of program may foresee the participation of other equatorial countries in the program in a consortium base or any other kind of joint participation. The possibilities are still open.

Small satellites in low equatorial orbit can play a very important role for the environment monitoring. So this is another possible application to our capabilities in dealing with small satellites. The same technology of the MECB satellites can be used to build a network of small earth observation satellites to monitor our remote equatorial regions providing information with a very high frequency. This kind of idea is still in a study phase.

On the other hand small satellites can be used for low cost scientific missions. In this direction we intend to emphasize scientific missions using small satellites. These satellites can use the same buses developed for the MECB satellites which will

make the missions very affordable for the participants. INPE has many research groups which can benefit from this initiative and the universities can benefit too. We know that this kind of program has already proved to be an effective way to involve universities in high technology development. A proposal for a scientific satellite program was already prepared and we hope to have the first scientific satellite launched in 1996.

CONCLUSION

So, many were the initiatives taken after the SCD1 launch and if they are now likely this is certainly due to the success of that first project. Therefore we are thankful to everybody who participated in the SCD1 and made all these plans a reality.

ATTITUDE DETERMINATION

1. Lopes, R.V.F.; Orlando, V.; Kuga, H.K.; Guedes, U.T.V. and Rao, K.R. (INPE-Brazil):
"Attitude Determination of the Brazilian Satellite SCD1" 011
2. Shuster, M.D. (APL-USA):
"Attitude Estimation from the Measurement of a Direction and an Angle" 019
3. Brum, A.G.V. and Ricci, M.C. (INPE-Brazil):
"Horizon Sensors Attitude Errors Simulation for the Brazilian Remote Sensing Satellite" 024
4. Eismont, N. (IKI-Russia); Klas, J. and Shimonek, J. (Academy of Sciences-Czech Rep):
"Onboard Algorithm for Attitude Determination of Spin Stabilized Spacecraft of Interball Project Based on Optical Sensors and Magnetometer Measurements" 032

ATTITUDE DETERMINATION OF THE BRAZILIAN SATELLITE SCD1

Roberto Vieira da Fonseca Lopes[†]

Valcir Orlando

Helio Koiti Kuga

Ulisses Thadeu Vieira Guedes

Kondapalli Rama Rao

Instituto Nacional de Pesquisas Espaciais - INPE

CP 515 - Sao Jose dos Campos

CEP 12201-970 - Brazil

E-Mail: [†]RVFL@DEM.INPE.BR

Abstract

This paper describes the main aspects of the attitude determination related to the first Brazilian satellite: the Data Collection Satellite (SCD1). The satellite was developed by the National Institute for Space Research (INPE) as the first of the four scheduled by the program called Complete Brazilian Space Mission (MECB). It is spin-stabilized and was injected in a near-circular orbit, at an altitude of approximately 760 km. The attitude determination is achieved in two phases. In the first one, a preliminary attitude is computed from sensors' telemetry data corresponding to passes over the tracking station. In the second one, data encompassing all the preliminary attitudes are processed to fit a dynamic model whose parameters are estimated. This paper aims at describing these procedures, their mathematical development and their evolution along time since the conception of the project. We also describe our first experience of a real satellite attitude determination, main difficulties, problems faced, as well as the solutions sketched at the very last minute. The results obtained are presented and discussed based on the expected performance of the software developed by the INPE's flight dynamics team.

Key words: Attitude Determination, Data Pre-processing, SCD1 Mission

INTRODUCTION

The main purpose of this paper is to describe the first experience of INPE's flight dynamics team in determining the attitude of a real satellite, the SCD1. This spin-stabilized data collection satellite turned out to be the first satellite fully conceived, designed and manufactured in Brazil. The launching was a very special oc-

casional and, as far as most of the team members are concerned, it was a significant milestone in their career till that date. Since the early 80's we have been extensively studying state estimation theory (including Kalman filtering, smoothing, adaptive estimation and all that paraphernalia) and its application to attitude determination of artificial satellites¹⁻¹⁰. The attitude determination software, specially for the SCD1 mission, was ready long time ago and its performance predicted from numerical simulations was pretty good¹¹⁻¹². However, unlike the orbit determination software, which could be checked previously against real data from other satellites, the attitude determination software for the SCD1, due to its strong mission dependency, could not show its actual performance until the launch time. It was not a quite straightforward test, definitely! In fact the LEOP (Launch and Early Orbit Phase) unfolded as a sequence of unpredicted problems, each of them being a new, exciting and scary challenge. Indeed, more than just presenting the algorithms (already well depicted in other papers¹¹⁻¹²) and their final numerical results (which fortunately brought nothing else than the expected performance, except for the fact that they came from real data!), we emphasize our experience on achieving them. We hope that this description on how we were driven from the nice theory field (to which we were so well familiarized), into our new real world problem, could not only provide a valuable information source for the development of the attitude determination software for the next Brazilian satellites, but also give some insight to the data pre-processing techniques as well as highlight the helpfulness of some extra support tools especially for beginning missions.

ATTITUDE DETERMINATION SYSTEM

The first Brazilian environmental data collecting satellite (SCD1), developed by the National Institute

of Space Research (INPE), was launched on February 09, 1993 by a North-American launcher named Pegasus. It is a spin-stabilized satellite launched in a near circular orbit of about 760 km altitude. The attitude hardware consists of a fluid-filled nutation damper, a magnetic torque coil, a three-axis fluxgate type magnetometer whose z-axis is aligned with the satellite spin-axis, and two redundant 180° field-of-view digital sun sensors. The attitude sensors are sampled at a rate of 2 Hz. The satellite attitude determination is performed off-line at pre-specified time spans, in several distinct steps. In other words, the attitude determination process is divided into three main sub-processes: attitude data pre-processing; preliminary attitude determination; fine attitude determination and propagation. It is aimed to determine a one-degree accuracy spin-axis attitude, which is useful for monitoring the sun aspect angle outside its prohibited region; for attitude maneuver planning; and for silent zones prediction. The attitude follow-up software, which will be explained in another section, provides an easy way of monitoring the spin-axis attitude.

ATTITUDE DATA PRE-PROCESSING

The data pre-processing reduces the large amount of crude attitude sensors' data stored in the telemetry (TM) data file. The TM corresponding to a satellite single pass over the ground station is pre-processed to yield a record containing the spin-rate, the sun aspect angle, and n magnetic aspect angles, where n is the integer number of 15.5 second-intervals within the pass.

In short, the global output of the SCD1 attitude sensors' pre-processor consists, for a single satellite pass over the ground station, of:

- n estimates of the magnetic aspect angle, n being the number of sets of 32 successive measurements each (corresponding to 15.5 seconds) contained in the pass;
- an estimate of the solar aspect angle and spin-rate, and
- the corresponding standard deviations of the error in the estimates.

The pre-processor is nowadays executed every day, processing all TM accumulated on the previous day and recording the results in the pre-processed attitude data file, which contains also formerly recorded data. This daily routine has become necessary in order not to overload the disk storage capacity of the computer. The compression rate can be as high as 100:1, i.e. 100Kb of TM is compressed as 1Kb of attitude data. The pre-processor output is then used as attitude observations by the Preliminary Attitude Determination Process, which is briefly described in another section.

Magnetometer data pre-processing

Basically the magnetometer measures the intensity of the local geomagnetic field in its three orthogonal axes. The magnetometer z-axis is aligned with the satellite z-axis. So, due to the satellite spin motion, the x-y magnetometer outputs are sinusoidal, synchronized with the satellite spinning frequency, whose amplitude is given by the orthogonal component of the geomagnetic field vector, and the offset given by the x-y magnetic bias due to residual magnetic fields in the satellite as well as magnetic interference near the magnetometer. The magnetometer z-output is given by the component of the geomagnetic vector along the spin-axis shifted by the z-axis magnetic bias of the satellite. The amplitudes and offsets of the x-y magnetometer outputs at each 15.5 seconds are obtained by curve-fitting. Subsequently they are combined in some optimum sense with the biased z-axis magnetometer mean output for the corresponding period, furnishing a set of magnetic aspect angles.

The magnetometer data are preprocessed in consecutive measurement sets. Each set is composed of 32 measurements for each of the three magnetometer axes. Each of these sets will, after the preprocessing, be transformed in only one compressed data which will, in turn, be used as input to the Preliminary Attitude Determination process. The data compression process is valid under the assumption that the geomagnetic field variation along the arc of orbit travelled by the satellite in 15.5 seconds (time span to make 32 measurements) can be neglected. The magnetometer data preprocessing will be described in somewhat more detailed way purposefully, because its preprocessing turned out to be the most problematic component.

From the application of a least-squares sinusoidal curve-fitting procedure to a given set of 32 successive measurements of the magnetometer x-axis, initially obtained are:

- an estimate of the orthogonal projection on the xy plane of the geomagnetic field vector, and
- an estimate of the bias error on the magnetometer x-axis measurement of the geomagnetic field.

In the same fashion, also obtained are a redundant estimate of the geomagnetic field orthogonal projection on the xy plane and an estimate of the bias error on the y-axis measurements. To the measurements corresponding to the z-axis the initial step of the preprocessing consists of the computation of the mean value of the set of 32 measurements. With the help of a mathematical model of the geomagnetic field, the magnitude of the bias in the z-axis measurements is evaluated. This coarse estimate of the bias is considered as an increment of the uncertainty in the computed estimate of the mean value of z-axis measurements. In both the above processes, a procedure for automatic deletion of

data points which have values out of a tolerance range around the fitted sinusoidal curve (in the case of the x and y-axis) or around the evaluated mean value (in the case of the z-axis) is considered. In the next step, the two redundant estimates just obtained for the xy-plane orthogonal projection of the geomagnetic field and the mean value of the z-axis measurements are used as observations for a linearized filter with no a-priori information. By this filter is obtained an estimate of the angle between the geomagnetic field and the satellite spin-axis (magnetic aspect angle) in the time interval corresponding to the current data set. In this process, besides the uncertainties in the observations, also the uncertainties in the reference model used for the evaluation of the geomagnetic field are considered. It is to be mentioned that the application of the filter leads to a transcendental algebraic equation from whose solution the magnetic aspect angle is computed. The solution of this equation is found with the application of the Newton-Raphson method.

Sun sensors' data pre-processing

The digital sun sensors give direct measurements of the angle between the direction of the sun light incidence and the satellite spin-axis, with 1° resolution at the Least Significant Bit. Besides the usual word to measure the sun aspect angle, the sun sensor contains an extra bit which changes its state every 16th crossing of the Sun within the sensor's field-of-view. Given the sampling time, this extra bit provides a measurement of the satellite spin-rate.

The pre-processing of the sun sensors' measurements consists simply of the computation of the mean value of all measurements sampled during a satellite pass over the ground station. This computation, as in the case of the magnetometer data, is combined with a procedure for automatic deletion of invalid data points. It is supposed that the solar aspect angle can be considered constant across the passes (12 minutes average). In brief, the task here consists of a data compression procedure in which all the sun sensors' data collected in a single pass are reduced to only one compressed data.

PRELIMINARY ATTITUDE DETERMINATION

The preliminary attitude determination process obtains a least squares estimate of the spin-axis attitude from the sun aspect angle value and the set of magnetic aspect angle values generated by the pre-processor. This process is purely static and do not take into account the long period attitude dynamics.

Basically, it consists of the application, to the preprocessor output data, of a least squares attitude determination procedure. By this procedure is generated an estimate of the satellite angular velocity vector related to each satellite single pass over the ground station. The

estimation corresponding to a given pass only considers the observations related to this specific pass. The procedure used in the Preliminary Attitude Determination can operate even in the absence of sun sensors' data, by using only the magnetometer data. Situations of co-planarity between the Sun vector, the geomagnetic field vector and the spin-axis are automatically treated. The results of the Preliminary Attitude Determination will be used as an input for the last step of the SCD1 attitude determination: the Fine Attitude Determination Process, discussed in the next section.

FINE ATTITUDE DETERMINATION

The fine Attitude Determination Process has two main objectives:

- to improve the results of the Preliminary Attitude Determination process,
- to estimate two parameters of the attitude dynamical model to be used in the attitude propagation process: the satellite residual magnetic moment (which is the main cause of the satellite spin-axis drift) and the eddy current parameter (which is the main cause of the decrease of the satellite spin-rate)

The input data for the Fine Attitude Determination process consist of the results of the Preliminary Attitude Determination covering a time interval of about one week. From these data the attitude corresponding to a selected epoch is estimated, employing a Least Squares Estimation Method developed with the help of the Householder orthogonal transformation. A Fine Attitude Determination procedure developed with the use of the Extended Kalman Filter combined to an adaptive state noise estimation procedure⁹ was alternatively developed.

The fine attitude estimates allow the realization of long period attitude predictions. The attitude predictions are used to foresee when silent zones of communications between the satellite and the ground station will occur during satellite's passes over the station. They are also used to foresee the need of and to prepare spin-axis maneuvers.

Besides the standard processes described above, another auxiliary process, namely, the attitude follow-up process, was found to play an important role as an efficient tool especially in those troubled few weeks after launch.

ATTITUDE FOLLOW-UP

The attitude follow-up software is aimed at supplying mission analysts with a fast and integrated visualization of the preliminary attitude determination uncertainty and its related aspects. For each orbit during a

specified period, the software prepares and draws on a colour screen (and optionally on a graphic plotter or on a laser printer) a map on an inertial celestial sphere, containing: the geomagnetic field vector trajectory; the sun position; the Earth shadow; the satellite trajectory during its pass over the ground station; and the attitude of the satellite spin-axis enveloped by its predicted uncertainty ellipse. As an additional information, it is indicated on the top of the screen, if the sun sensor is illuminated or not during the pass. Knowledge of uncertainty beforehand is usually helpful to schedule on-board computer tests and magnetic coil polarity commutation times. Since these activities usually invalidate the attitude data, it is preferable to perform them in those passes which would give the worst attitude determination performance. With the help of this map, mission analysts can rationally select an optimum subset of passes in order to retain the best accuracy in the attitude determination process. In fact, however, this software offered several other fruitful applications, some of which had never been thought of before the satellite was launched, as described in the following sections of this paper.

LEOP CONTINGENCIES

In this section we describe several difficulties which the flight mechanics team had to face during the first forty days after launch, while trying to accomplish the attitude determination within the specified accuracy level. Since the orbit became well determined, right from the beginning, we had to face one problem after the other, while hearing all kinds of guesses about what could be happening. Of course the problems did not happen in a quite ordered sequence as they are described here. Actually there were multiple interactions and overlaps which we have omitted now for the sake of clarity.

PROBLEM 1

All data were rejected when accessing and reading the telemetry data file.

Adopted Solution: The parity check was turned off within the TM reader software. This parity check was somewhat unstable and not reliable because ground station engineers were still trying to adjust some signal levels.

PROBLEM 2

All magnetometer data were rejected by the automatic pre-processing software.

Suspected Cause: Noisy data.

Adopted Solution: Pre-processing manually the magnetometer read-out. Soon it became obvious how cumbersome and time-consuming was the manual pre-processing mode for an extended work, despite the

better control and understanding it offers. In order to solve these problems of preprocessing of magnetometer data which became apparent early during the mission, efforts were made to model and evaluate the magnetometer bias fluctuation observed from one pass to the next one. During this phase, the attitude follow-up software was useful in two ways. Firstly, it showed that the unmodelled fluctuations are closely related with the satellite path through the magnetosphere, in terms of the time of the day, among many other factors. And then it permitted to easily select a pair of crossing satellite passes. This was necessary for testing an ingenious method to determine the magnetometer z-axis bias. Eventually, that method did not give consistent results and magnetometer z-axis measurement had to be abandoned. Thus, though not worked at the end, the attitude follow-up software was very useful here to select few passes a day which could have determined the attitude.

PROBLEM 3

Spin-rate measured by sun sensor presented strange oscillations.

The spin-rate is given by:

$$w[\text{rpm}] = 16 \times (N - 1) / (t_N - t_1) \quad (1)$$

where t_i [min], $i = 1, \dots, N$ are the times when the extra bit of the sun sensor changes its value during a pass of the satellite over the ground station. So, at a nominal spin-rate of 120rpm and a sampling rate of 2Hz, the error due to discretization should be less than 0.4rpm for a typical pass longer than five minutes. However the spin-rate presented oscillations of around 5rpm from one pass to the next one. This clearly could not be explained by discretization error.

Suspected Cause: Spurious changes in sun sensor extra bit state, probably due to data transmission noise and momentaneous loss (fluctuations) of the satellite signal. This could only explain unexpected high spin-rates. However the opposite eventually happened as well. Therefore we concluded that other causes should exist.

Other Suspected Cause: Discontinuity in the measurements sequence.

Adopted Solution: Inclusion of data deletion procedure and re-initialization of the computation of the spin-rate every time that $t_i - t_{i-1} > \text{limit} - \text{value}$.

That is, add a validity test for each candidate t_i : $dt_{\min} \leq t_i - t_{i-1} \leq dt_{\max}$; so, premature t_i 's are rejected as spurious; late t_i 's are considered as a new starting time:

$$w = 16 \times \sum_{j=1}^{N_d} (N_j - 1) / \sum_{j=1}^{N_d} (t_{N_j} - t_{1_j}) \quad (2)$$

where N_d is the number of discontinuities in measurement sequence. The values of dt_{\min} and dt_{\max} would

need adjustments along the satellite lifetime due to spin-rate decay.

PROBLEM 4

Purely noisy pattern in some magnetometer data files.

Suspected Cause: Hardware problems on the ground station telemetry unit.

Adopted Solution: Substitute hardware unit.

However, the problem occasionally persisted.

Suspected Cause: High Power Amplifier (HPA) was set with too much power for uplink transmission, causing interference noise in the downlink path.

Adopted Solution: Reduce the power of the ground station transmitter. Along the time, the HPA power was gradually reduced by the ground station staff to adequate levels.

PROBLEM 5

Persistence of PROBLEM 2 after solution of PROBLEM 4.

Suspected Cause: Some isolated spurious data shifted all the others away from the 3-sigma rejection boundary.

Adopted Solution: Add a detector of spurious data by comparison with neighboring data.

Parameters which detect spurious data in some inequality tests should be reviewed along the mission, according to the current spin-rate. This was clearly very troublesome because it implied periodic updating of the software code.

Problem eventually persisted when spurious data was the first or the last of the set.

Adopted Solution: Software was improved with special tests for first or last spurious data detection.

This kind of test becomes less effective as spin-rate decreases, due to increasing phase angle between consecutive magnetometer measurements. Furthermore, this test did not deal with the unlikely case (but not impossible) of consecutive spurious data.

Adopted Solution: Data rejection process was modified to eliminate only one invalid data per iteration (that one with the worst residual).

PROBLEM 6

Preliminary attitude determination process gave meaningless results with enormous residuals.

Suspected Cause: Inaccurate magnetic aspect angle.

Adopted Solution: Activate the geometric attitude determination software.

The solution given by this method spanned randomly over a rough $2^\circ \times 2^\circ$ square, too wrong to start a fine attitude determination process. However, it was found

to be very useful to obtain evidences for the cause of PROBLEM 6.

Due to the erratic movement of the spin-axis attitude determined by the geometric method, we wondered if there was something like a large residual nutation. Fortunately, during some manual data pre-processing, we could see the exact instant when the sun sensor output changed its value of one degree (sensor resolution). So, if there were nutation, due to nutation rate non-synchronism with spin-rate, the transition should not happen at once, as in fact it was. It should oscillate for some period, which could be used to measure the nutation half-cone angle. This fact eliminated the possibility of any detectable nutation on the satellite.

Another remarkable thing was that eventually, the best passes of a day, from the attitude determination point of view, were during the night, when sun sensor measurements are not made. However, since the sun aspect angle changes very slowly and the sun sensor keeps the last measurement done, we tried to consider the last retrieved sun aspect angle measurement as if it had been made during the pass. As the results did not show evidence of inferior performance, such "evening measurement" of the sun aspect angle was considered a normal procedure.

PROBLEM 7

Appearance of third-degree polynomial-like residual patterns in magnetometer data curve-fitting, causing successive rejection of the first and last data point.

Suspected Cause: Non-synchronism between the modeled and measured magnetometer data.

Adopted Solution: Add the model frequency as a new parameter to the curve-fitting process.

Due to the geomagnetic field vector change along the orbit, at first a new complete curve-fitting (now including the frequency) was performed every 15.5 seconds. Later experience showed however that we should fit a single (constant) frequency for each pass.

PROBLEM 8

Curve-fitting including model frequency did not converge.

Suspected Cause: Initial guess of frequency was not accurate enough.

The curve-fitting process is non-linear in frequency. Added to this the fact is that the spin-rate estimate provided by the sun sensor is not accurate enough to be used as initial guess, i.e. the initial guess accuracy should be one order of magnitude more accurate than that provided by the sun sensor extra bit.

Adopted Solution: create a magnetometer based "gyro", i.e. compute the spin-rate from the magnetometer x and y-axis measurements.

Like the extra bit of the sun sensor, the magnetome-

ter based "gyro" measures the spin-rate as a ratio of the number of sign changes over the elapsed time. It was thought here that, unlike in the sun sensor case, the transition times of sign changes can be better determined from the interpolation of the instants corresponding to a pair of consecutive measurements with opposite signs. This results in a more precise spin-rate estimate than that estimated via the sun sensor.

PROBLEM 9

The transition time of x and y magnetometer measurements could not be determined and so the spin could not be computed from magnetometer data.

Suspected Cause: the nominal spin-rate of 120rpm was resonant with the sampling rate of 2Hz; the satellite rotates 2π rad between two consecutive sensor measurements.

The existence of this singularity in the curve-fitting was known a long time ago, during the simulation tests. At that time, however, this fact was of no concern because the specified nominal spin-rate for the SCD1 at launch lied in the range 160rpm - 180rpm, very far from the singularity. After launch, during the routine operations, once the spin is determined, propagated values would be provided during the period spanning the singularity range, and the problem could be overcome. Nevertheless, along the years, the initial spin-rate was successively changed to 140 rpm, to 130 rpm, and at last, exactly to 120rpm! Fortunately the satellite spin-rate in orbit 2 was 119.2rpm, which gave an apparent shift of -0.8rpm. Even this resulted in an apparent rotation of less than $\pi/2$ rad each 15.5 seconds, which was not quite enough for taking a measurement of the magnetometer based "gyro".

Adopted Solution: Wait for a while until spin-rate decays a little bit.

PROBLEM 10

Strange oscillations in the spin-rate computed from magnetometer measurements.

Suspected Cause: Telemetry transmission noise and loss of the satellite signal (the same of PROBLEM 3).

Adopted Solution: The same of PROBLEM 3.

PROBLEM 11

The preliminary attitude determination process presented large residuals and precision around 1° , within mission specification, but not as good as the simulation results. Furthermore, fine attitude determination methods did not converge to consistent results and rejected a lot of data.

Suspected Cause: Persistent inaccuracy in magnetic aspect angle computation.

From a long sequence of maps generated by the attitude follow-up software, one could recognize some pat-

terns which determine the accuracy level in the preliminary attitude determination process. For example, it became clear from those maps that the descending passes over Cuiabá experiences a bigger variation in geomagnetic field direction than the ascending ones, and consequently offers a better attitude observability. As another example, in southern hemisphere winter, small angles between Sun direction and geomagnetic field vector are found to occur very often. This causes a seasonal degradation in attitude observability. At that time we noted that the adjusted x-y magnetometer bias presented an arc of ellipse pattern. The source of inaccuracy was the z-axis magnetometer bias. An attempt was made to estimate this bias.

At first, we thought that it was due to non-symmetric effects related with the sampling rate and the spin-rate. According to this theory, each time the 32 sampled measurements encloses a regular polygon, the bias would be determined exactly, except for a small error due to measurement noise. As the spin-rate decays from one such symmetric value to the next, the error would increase until a maximum value and then reduces. In this case, the best estimate of the bias should be the baricenter of the ellipse. Nevertheless, this was far from being the dominant effect. In fact, when the satellite spin-rate crossed a symmetry value, the bias was the farthest from the ellipse center. So this theory was abandoned.

Luckily, with the help of the attitude follow-up software, it became clear that the estimated bias and the satellite path with respect to the earth were closely related. This meant that the bias has an actual variation from path to path, and there is no sense in taking some mean value of the differently determined bias.

So, the only source of inaccuracy was the z-axis magnetometer bias. An attempt was made to estimate its value from subsequent crossing passes over an earth fixed point, based on the following equality:

$$(M_{z_1} - b)^2 + M_{zy_1}^2 = (M_{z_2} - b)^2 + M_{zy_2}^2 \quad (3)$$

where M_{zy} is the bias free magnetic field normal to spin-axis; M_z is the biased magnetic field along the spin-axis; and b is the z-axis bias. This would give:

$$b = \frac{(M_{z_2}^2 + M_{zy_2}^2) - (M_{z_1}^2 + M_{zy_1}^2)}{2(M_{z_2} - M_{z_1})} \quad (4)$$

Again the attitude follow up software was useful to select the proper passes. Unfortunately the results were not encouraging at all. So the following more drastic solution had to be adopted.

Adopted Solution: The z-axis magnetometer measurements were removed from the algorithm for magnetic aspect angle evaluation, except for solving sign ambiguity.

In addition to all these hindrances, there was the software ageing. For example, the geomagnetic model coefficients had to be updated. The software for evaluating

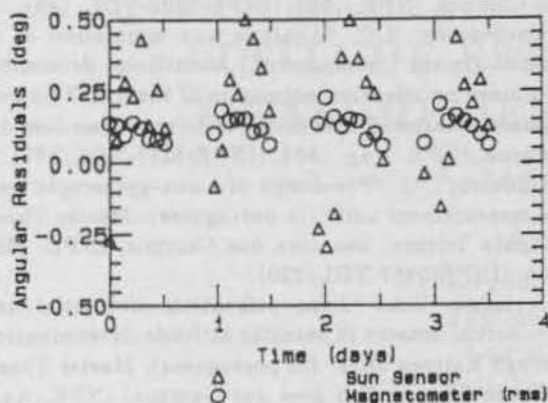


Figure 1: Preliminary Attitude Determination Residuals

the geomagnetic field vector model was ready since a long time ago, and its original version used the IGRF-80 (International Geomagnetic Reference Field) spherical harmonic coefficients. Meanwhile, we updated those coefficients, at first with the IGRF-85, and more recently with the IGRF-90. Nevertheless, at the last updating time, the version existing in the Satellite Control Center computer, had not been updated yet.

After all this, the performance was very good, similar to the simulation results, as we show in the next section. The dynamic parameters were well estimated, presenting also a reasonable agreement between the two fine attitude determination softwares.

TYPICAL RESULTS

The performance of the attitude sensors' data pre-processing procedure may be verified by comparison with the results obtained in the preliminary and fine attitude determination processes. The standard deviations of the estimates of the sun and magnetic aspect angles, which are the outputs of this phase, are of the order of 0.3° . The estimates of the bias due to magnetic interferences in the x and y magnetometer axes are typically of the order of -16 mGauss and 55 mGauss respectively. During the execution of the spin-axis maneuvers, when the magnetic torque coil is activated, the values estimated for the bias in the x and y axes are, respectively, of the order of -5 mGauss and 65 mGauss. Both estimates show a standard deviation of about 0.5 mGauss.

Fig. 1 shows the plot of the residuals for the sun and magnetic aspect angles obtained by the application of the preliminary attitude determination process. These data encompass the period from January 6 to 9, 1994.

Figs. 2 to 4 show the plots of the deviations between the attitude estimates generated in the preliminary attitude determination and the attitude predicted from the most up-to-date fine attitude determination. The

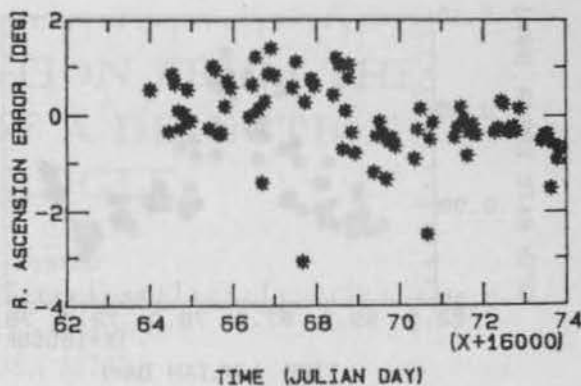


Figure 2: Right Ascension Errors

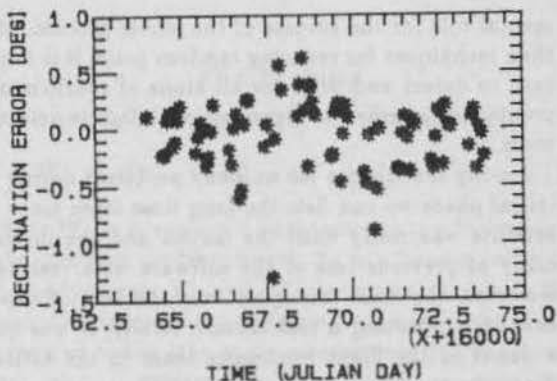


Figure 3: Declination Errors

deviations are given in terms of right ascension, declination and spin-rate, respectively and cover the period from December 25, 1993 to January 4, 1994. Within this period, from 27 to 30 December, 1993 a spin-axis maneuver was performed. As can be seen in the figures, the execution of the maneuver did not affect significantly the attitude determination results.

CONCLUSION

As a first conclusion, we point out that the attitude determination software clearly achieved its goals. After several listed (and solved) problems, the software works properly for almost one year and during this period it provided attitude information for many well succeeded attitude maneuvers, well within the mission requirements.

Nowadays initial guess to the spin-rate estimation process is given from the attitude predicted file which is accurate to better than 0.1rpm. The pre-processor and the preliminary attitude determination software run daily. The fine attitude determination is executed on a weekly basis and extended attitude predictions of up to 02 months are regularly made.

Another conclusion that we clearly draw from our experience is that data pre-processing plays a funda-

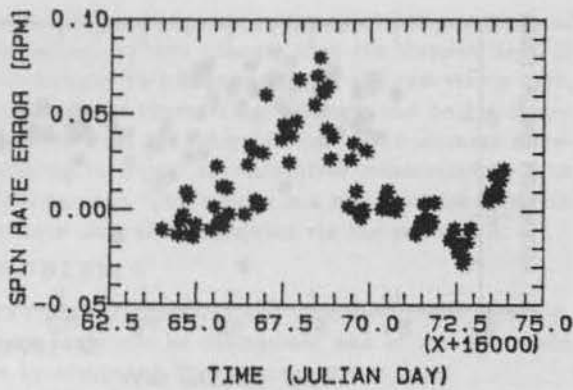


Figure 4: Spin-Rate Errors

mental role for the success of the whole process. More than techniques for reducing random noise, it is important to detect and solve for all kinds of spurious data points, and supply the algorithm with failure detection tools.

Among the reasons for so many problems during the initial phase we can list: the long time lapse since the satellite was ready until the launch and the impossibility of previous test of the software with real data. However, the most important was the lack of experience in supporting a real launch. Really, it was quite a debut of the flight mechanics team in the attitude determination field of a flying satellite.

ACKNOWLEDGEMENTS

We would like to express our sincere gratitude to Dr. Luc Fraiture from ESOC-ESA for the whole review of and invaluable suggestions to the preliminary design of the project. Dr. Malcolm D. Shuster from APL-USA should also be mentioned for his always supportive "attitude" to the team. Last but not least, we should thank all the colleagues whose efforts along the years directly or indirectly contributed significantly to the success of the team. We want them to know that their efforts have not been in vain.

REFERENCES

- ¹ Kuga, H.K. "Adaptive estimation of orbits applied to satellites at low altitude" (in portuguese). Master Thesis in Space Science. Sao Jose dos Campos, INPE, Feb. 1982. (INPE-2316-TDL/079).
- ² Lopes, R.V.F. "Attitude determination of artificial satellites through state estimators" (in portuguese). Master Thesis in Space Science. Sao Jose dos Campos, INPE, Dec. 1982. (INPE-2608-TDL/105).
- ³ Orlando, V. "Stochastic technics applied to smoothing, bias treatment, and compression of tracking or telemetry data from artificial satellites" (in portuguese). PhD. Dissertation in Space Science. Sao Jose

- dos Campos, INPE, 1983. (INPE-2909-TDL/148).
- ⁴ Cardenutto, N.C. "Analysis and simulation of an inertial system ("strapdown") of attitude determination aided by adaptive estimation of the drift" (in portuguese). Master Thesis in Space Science. Sao Jose dos Campos, INPE, Aug. 1984. (INPE-3257-TDL/177).
- ⁵ Trabasso, L.G. "Pre-design of a non-gyroscopic inertial measurement unit" (in portuguese). Master Thesis in Space Science. Sao Jose dos Campos, INPE, May 1986. (INPE-3887-TDL/220).
- ⁶ Ferraresi, V.A. "Joint utilization of inertial and non-inertial sensors in satellite attitude determination through Kalman filter" (in portuguese). Master Thesis in Space Science. Sao Jose dos Campos, INPE, Aug. 1987. (INPE-4313-TDL/280).
- ⁷ Varotto, S.E.C. "Attitude determination of artificial satellites through joint application of static and dynamic optimal estimation technics" (in portuguese). Master Thesis in Space Science. Sao Jose dos Campos, INPE, Oct. 1987. (INPE-4415-TDL/306).
- ⁸ Lopes, R.V.F. "Adaptive state estimation and analysis of sampling rate for linear time-invariant dynamical systems" (in portuguese). PhD. Dissertation in Space Science. Sao Jose dos Campos, INPE, Nov. 1989. (INPE-4960-TDL/389).
- ⁹ Guedes, U.T.V. "Procedure for attitude estimation of a spin-stabilized satellite" (in portuguese). Master Thesis in Space Science. Sao Jose dos Campos, INPE, Aug. 1989 (INPE-4866-TDL/377).
- ¹⁰ Kuga, H.K. "Orbit determination of earth artificial satellites through state estimation technics combined with smoothing technics" (in portuguese). PhD. Dissertation in Space Science. Sao Jose dos Campos, INPE, Nov. 1989. (INPE-4959-TDL/388).
- ¹¹ Kuga, H.K.; Lopes, R.V.F.; Varotto, S.E.C.; Guedes, U.T.V. "Performance analysis of the procedures for attitude determination of the first MECB satellite" (in portuguese). *5th Brazilian Colloquium on Orbital Dynamics*, Curitiba, 26-30 Nov., 1990.
- ¹² Lopes, R.V.F.; Orlando, V.; Kuga, H.K.; Guedes, U.T.V. "Attitude determination system for the Brazilian data collecting satellite" (in portuguese). *Proceedings of the 3rd. Pan-American Congress of Applied Mechanics, PACAM III*, Sao Paulo, Brazil, 4-8 Jan., 1993, p.519-522.

ATTITUDE ESTIMATION FROM THE MEASUREMENT OF A DIRECTION AND AN ANGLE

Malcolm D. Shuster
The Johns Hopkins University
Applied Physics Laboratory
Laurel, MD, USA 20723
Malcolm.Shuster@jhuapl.edu

Abstract

The general problem of determining the attitude from measurements of an angle and a direction is considered. It is shown that there is no continuous ambiguity for this problem, because effectively three data are given. However, the attitude still has generally a two-fold ambiguity which can be removed only by the addition of further data.

Introduction

While numerous algorithms exist for the estimation of the attitude from the measurement of two or more directions, the best known being the TRIAD and QUEST algorithms,¹ no simple algorithm has ever been published for the estimation of the attitude from the measurement of a single vector and a single angle. This particular case is of interest, because there being only three independent equivalent scalar data, it might seem at first glance that a unique solution should exist in this case. For the case of the measurement of two directions on the other hand, a solution is, in general, not defined without additional criteria, because three parameters must be determined from four data.

In the present work a simple construction is given for determining the solution to this problem. It turns out that the solution is not unique but has a two-fold degeneracy. It is also noted that since a deterministic estimate exists, this must also be the maximum-likelihood estimate. This fact is exploited to develop a covariance analysis of the algorithm using the QUEST model² for the measurement errors. The algorithms for solving this attitude problem and the covariance analysis were developed in order to provide rapid analysis of attitude data from the a spacecraft equipped with a three-axis magnetometer and a Sun angle sensor.

The Problem

We seek an attitude matrix A which satisfies

$$\hat{W}_1 = A \hat{V}_1, \quad \hat{S}_2 \cdot A \hat{V}_2 = d, \quad (1)$$

where \hat{W}_1 is a measured unit vector in the body frame (the direction measurement); \hat{S}_2 is a known vector in the body frame; \hat{V}_1 and \hat{V}_2 are known vectors in the primary reference (typically inertial) frame; and d is a measured cosine (the angle measurement). We assume that $|d| \leq 1$; otherwise, a solution will not exist. For a typical spacecraft, \hat{W}_1 might be the measured magnetic field vector and d might be the cosine of the Sun angle as obtained from a spinning digital solar aspect detector.

General Structure of the Solution

We begin by seeking all attitude matrices A which satisfy $\hat{W}_1 = A \hat{V}_1$. These are given by

$$A = R(\hat{W}_1, \theta) A_0, \quad (2)$$

where A_0 is any attitude matrix satisfying $\hat{W}_1 = A_0 \hat{V}_1$; $R(\hat{W}_1, \theta)$ is a the rotation matrix for a rotation about the axis \hat{W}_1 through and angle θ ; and θ is any angle satisfying $0 \leq \theta < 2\pi$. $R(\hat{W}_1, \theta)$ is given by Euler's formula

$$R(\hat{n}, \theta) = \cos \theta I_{3 \times 3} + (1 - \cos \theta) \hat{n} \hat{n}^T + \sin \theta [[\hat{n}]], \quad (3)$$

with

$$[[\hat{v}]] \equiv \begin{bmatrix} 0 & v_3 & -v_2 \\ -v_3 & 0 & v_1 \\ v_2 & -v_1 & 0 \end{bmatrix} \quad (4)$$

To prove the assertion of Equation (2), assume that there exist two distinct attitude matrices, A and A_n ,

satisfying $\hat{W}_1 = A \hat{V}_1$ and $\hat{W}_1 = A_o \hat{V}_1$, respectively. Then

$$\hat{W}_1 = A(A_o^{-1} A_o) \hat{V}_1 \quad (5)$$

$$= (AA_o^{-1}) A_o \hat{V}_1 \quad (6)$$

$$= (AA_o^{-1}) \hat{W}_1. \quad (7)$$

Thus, \hat{W}_1 must be the axis of rotation of the rotation matrix AA_o^{-1} . Since AA_o^{-1} must be different from the identity matrix, the axis of rotation is well-defined and unique. Hence,

$$AA_o^{-1} = R(\hat{W}_1, \theta) \quad (8)$$

for some angle θ . Equation (2) now follows from Equations (6) and (8). Every attitude matrix given by Equation (2) satisfies $\hat{W}_1 = A \hat{V}_1$. Therefore, there is a continuum of solutions, satisfying this equation.

Equation (2) is equivalent to

$$A = A_o R(\hat{V}_1, \theta), \quad (9)$$

with identical A_o and θ . This follows from³

$$A_o R(\hat{V}_1, \theta) A_o^T = R(A_o \hat{V}_1, \theta). \quad (10)$$

A Single Solution for A_o

We must now find a single A_o which satisfies $\hat{W}_1 = A_o \hat{V}_1$. Let us look for an A_o of the form

$$A_o = R(\hat{n}_o, \theta_o), \quad (11)$$

where

$$\hat{n}_o \equiv \frac{\hat{W}_1 \times \hat{V}_1}{|\hat{W}_1 \times \hat{V}_1|}, \quad (12)$$

which is defined provided that $\hat{W}_1 \neq \pm \hat{V}_1$. Then trivially

$$\hat{n}_o \cdot \hat{V}_1 = 0, \quad (13)$$

and

$$\begin{aligned} [[\hat{n}_o]] \hat{V}_1 &= -\hat{n}_o \times \hat{V}_1 \\ &= \frac{\hat{W}_1 - (\hat{W}_1 \cdot \hat{V}_1) \hat{V}_1}{|\hat{W}_1 \times \hat{V}_1|}. \end{aligned} \quad (14)$$

Thus,

$$\begin{aligned} R(\hat{n}_o, \theta_o) \hat{V}_1 &= \cos \theta_o \hat{V}_1 \\ &\quad + \frac{\sin \theta_o}{|\hat{W}_1 \times \hat{V}_1|} (\hat{W}_1 - (\hat{W}_1 \cdot \hat{V}_1) \hat{V}_1) \\ &= \left[\cos \theta_o - \frac{(\hat{W}_1 \cdot \hat{V}_1)}{|\hat{W}_1 \times \hat{V}_1|} \sin \theta_o \right] \hat{V}_1 \\ &\quad + \frac{\sin \theta_o}{|\hat{W}_1 \times \hat{V}_1|} \hat{W}_1. \end{aligned} \quad (15)$$

Since \hat{W}_1 and \hat{V}_1 are linearly independent, a unique solution exists for θ_o , namely,

$$\sin \theta_o = |\hat{W}_1 \times \hat{V}_1|, \quad \cos \theta_o = (\hat{W}_1 \cdot \hat{V}_1), \quad (16)$$

which yields

$$\theta_o = \text{ATAN2}(|\hat{W}_1 \times \hat{V}_1|, (\hat{W}_1 \cdot \hat{V}_1)), \quad (17)$$

where ATAN2 is the familiar FORTRAN function, which for the purpose of calculating θ_o we will adjust so that the values always lie in the interval $-\pi < \theta_o \leq \pi$.

Note that once \hat{n}_o is fixed there can be only one solution for θ_o . We could equally well have chosen

$$\hat{n}'_o \equiv -\frac{\hat{W}_1 \times \hat{V}_1}{|\hat{W}_1 \times \hat{V}_1|}, \quad (18)$$

in which case we would have been led to

$$\theta'_o = \text{ATAN2}(-|\hat{W}_1 \times \hat{V}_1|, (\hat{W}_1 \cdot \hat{V}_1)). \quad (19)$$

The two solutions are equivalent.

The quaternion corresponding to A_o has a very simple form. To calculate the quaternion we note first that

$$\cos(\theta_o/2) = \sqrt{\frac{1 + \cos \theta_o}{2}} = \sqrt{\frac{1 + \hat{W}_1 \cdot \hat{V}_1}{2}}, \quad (20)$$

and

$$\cos(\theta_o/2) \geq 0 \quad \text{for} \quad |\theta_o| \leq \pi. \quad (21)$$

Likewise,

$$\sin(\theta_o) = 2 \sin(\theta_o/2) \cos(\theta_o/2), \quad (22)$$

so that

$$\begin{aligned} \sin(\theta_o/2) &= \frac{\sin(\theta_o)}{2 \cos(\theta_o/2)} \\ &= \frac{|\hat{W}_1 \times \hat{V}_1|}{\sqrt{2(1 + \hat{W}_1 \cdot \hat{V}_1)}}. \end{aligned} \quad (23)$$

Hence,

$$\sin(\theta_o/2) \hat{n}_o = \frac{\hat{W}_1 \times \hat{V}_1}{\sqrt{2(1 + \hat{W}_1 \cdot \hat{V}_1)}}, \quad (24)$$

and the corresponding quaternion is given by

$$\begin{aligned} \hat{q}_o &= \sqrt{\frac{1 + \hat{W}_1 \cdot \hat{V}_1}{2}} \\ &\quad \times \left[\begin{array}{c} \left(\frac{\hat{W}_1 \times \hat{V}_1}{1 + \hat{W}_1 \cdot \hat{V}_1} \right) \\ 1 \end{array} \right], \end{aligned} \quad (25)$$

which can now be computed without the need to compute θ_o . The Rodrigues vector ρ_o (also called the Gibbs vector) is given obviously by³

$$\rho_o = \frac{\hat{W}_1 \times \hat{V}_1}{1 + \hat{W}_1 \cdot \hat{V}_1} \quad (26)$$

and the matrix A_0 is given equivalently by

$$A_0 = (\hat{W}_1 \cdot \hat{V}_1) I_{3 \times 3} + \frac{(\hat{W}_1 \times \hat{V}_1)(\hat{W}_1 \times \hat{V}_1)^T}{1 + \hat{W}_1 \cdot \hat{V}_1} + [(\hat{W}_1 \times \hat{V}_1)] \quad (27)$$

Complete Solution for A

Given θ_0 we must now compute θ . Define

$$\hat{W}_3 \equiv A_0 \hat{V}_2 \quad (28)$$

Then θ is a solution of

$$\hat{S}_2 \cdot R(\hat{W}_1, \theta) \hat{W}_3 = d \quad (29)$$

Substituting Euler's formula leads to

$$\begin{aligned} \hat{S}_2 \cdot [\hat{W}_3 - \sin \theta (\hat{W}_1 \times \hat{W}_3) \\ + (1 - \cos \theta) (\hat{W}_1 \times (\hat{W}_1 \times \hat{W}_3))] \\ = d \end{aligned} \quad (30)$$

which can be rearranged to yield

$$\begin{aligned} [\hat{S}_2 \cdot (\hat{W}_1 \times (\hat{W}_1 \times \hat{W}_3))] \cos \theta \\ + [\hat{S}_2 \cdot (\hat{W}_1 \times \hat{W}_3)] \sin \theta \\ = (\hat{S}_2 \cdot \hat{W}_1)(\hat{W}_1 \cdot \hat{W}_3) - d \end{aligned} \quad (31)$$

There are clearly two solutions for θ , in general. To see this define

$$B \equiv |\hat{S}_2 \times \hat{W}_1| |\hat{W}_1 \times \hat{W}_3| \quad (32)$$

$$\beta \equiv \text{ATAN2} \left([\hat{S}_2 \cdot (\hat{W}_1 \times \hat{W}_3)], [\hat{S}_2 \cdot (\hat{W}_1 \times (\hat{W}_1 \times \hat{W}_3))] \right) \quad (33)$$

Then Equation (31) can be rewritten as

$$B \cos(\theta - \beta) = (\hat{S}_2 \cdot \hat{W}_1)(\hat{W}_1 \cdot \hat{W}_3) - d \quad (34)$$

From Equation (34) we see that a necessary condition that a solution exist is that

$$\begin{aligned} |(\hat{S}_2 \cdot \hat{W}_1)(\hat{W}_1 \cdot \hat{W}_3) - d| \\ \leq |\hat{S}_2 \times \hat{W}_1| |\hat{W}_1 \times \hat{W}_3| \end{aligned} \quad (35)$$

If this condition is satisfied, then θ has the solutions

$$\theta = \beta + \cos^{-1} \left[\frac{(\hat{S}_2 \cdot \hat{W}_1)(\hat{W}_1 \cdot \hat{W}_3) - d}{|\hat{S}_2 \times \hat{W}_1| |\hat{W}_1 \times \hat{W}_3|} \right] \quad (36)$$

and the inverse cosine is indeed two-valued. Given A_0 and θ we can now construct the attitude matrix solutions according to Equations (2) and (27).

Covariance Analysis

The attitude matrices constructed by the above algorithm solve Equations (1) exactly. Therefore, if attitude solutions exist, they each certainly minimize the cost function

$$J(A) = \frac{1}{\sigma_1^2} |\hat{W}_1 - A \hat{V}_1|^2 + \frac{1}{\sigma_d^2} |\hat{S}_2 \cdot A \hat{V}_2 - d|^2 \quad (37)$$

where σ_1 and σ_d are standard deviations characterizing the weights. If a deterministic attitude solution constructed according to the above methodology does not exist (say, because Equation (35) is not satisfied due to the effect of measurement noise) then one can at least find an attitude solution (generally two) which minimizes the cost function of Equation (37). The discussion of this section will still be valid in the latter case.

We recognize the first term as the negative-log-likelihood corresponding to the error model²

$$\hat{W}_1 = A^{\text{true}} \hat{V}_1 + \Delta \hat{W}_1 \quad (38)$$

where $\Delta \hat{W}_1$ is the equivalent measurement noise, which is assumed to be Gaussian and to satisfy

$$E\{\Delta \hat{W}_1\} = 0 \quad (39)$$

and

$$\begin{aligned} E\{\Delta \hat{W}_1 \Delta \hat{W}_1^T\} \\ = \sigma_1^2 (I_{3 \times 3} - \hat{W}_1^{\text{true}} \hat{W}_1^{\text{true}T}) \end{aligned} \quad (40)$$

where $E\{\cdot\}$ denotes the expectation. Likewise, the second term of Equation (37) is the negative-log-likelihood corresponding to the error model

$$d = \hat{S}_2 \cdot A \hat{V}_2 + \Delta d \quad (41)$$

where Δd is a zero-mean Gaussian random noise with variance σ_d^2 . Thus, the attitude matrices computed by the above algorithm are also (non-unique) maximum-likelihood estimates of the attitude. We may, therefore, compute the attitude covariance matrix as the inverse of the Fisher information matrix by interpreting Equation (37) as a negative-log-likelihood function.^{2,4} The calculation of the Fisher information is tedious but straightforward. The result for the attitude covariance matrix, which we define as the covariance matrix of the infinitesimal rotation vector, ξ , connecting the true attitude to the estimated attitude, is

$$\begin{aligned} P_{\xi\xi} = & \left[\frac{1}{\sigma_1^2} (I_{3 \times 3} - \hat{W}_1 \hat{W}_1^T) \right. \\ & \left. + \frac{1}{\sigma_d^2} (\hat{W}_2 \times \hat{S}_2)(\hat{W}_2 \times \hat{S}_2)^T \right]^{-1} \end{aligned} \quad (42)$$

where \hat{W}_2 is defined as

$$\hat{W}_2 \equiv A \hat{V}_2 \quad (43)$$

Note that generally

$$\dot{W}_2 \neq \dot{S}_2, \quad (44)$$

even in the absence of measurement noise. For this reason we have used the notation \dot{S}_2 rather than \dot{W}_2 . Note also that $P_{\xi\xi}$ will not exist unless

$$\dot{W}_1 \cdot (\dot{W}_2 \times \dot{S}_2) \neq 0, \quad (45)$$

or, equivalently, unless

$$\dot{S}_2 \cdot (\dot{W}_1 \times (A \dot{V}_2)) = (A \dot{V}_2) \cdot (\dot{S}_2 \times \dot{W}_1) \neq 0. \quad (46)$$

Even though the attitude matrix may be defined in this case the geometry represents an extremum situation in which the sensitivity of the attitude to the measurements vanishes along one direction in parameter space.

Remarks

Note that the fact that we have equivalently three independent measurements (two for the direction and one for the cosine) does not guarantee a unique solution, only that the solutions be elements of a discrete set. Uniqueness would be obtained only if the equations for the three independent attitude parameters were linear, which is almost never the case.

We are not restricted to choosing

$$\hat{n}_o \equiv \pm \frac{\dot{W}_1 \times \dot{V}_1}{|\dot{W}_1 \times \dot{V}_1|}. \quad (47)$$

In fact, any vector \hat{n}_o satisfying

$$\hat{n}_o \cdot \dot{W}_1 = \hat{n}_o \cdot \dot{V}_1, \quad (48)$$

will do. We have selected one of the simpler cases. An alternate choice is examined below.

In fact, the construction of \hat{n}_o fails if $\dot{W}_1 = \pm \dot{V}_1$. If $\dot{W}_1 = \dot{V}_1$, we may choose $A_o = I_{3 \times 3}$. If, on the other hand, $\dot{W}_1 = -\dot{V}_1$, then we may choose \hat{n}_o to be any vector perpendicular to \dot{W}_1 and $\theta_o = \pi$.

Note that we have avoided using the relation,

$$\sin(\theta_o/2) = \sqrt{\frac{1 - \cos \theta_o}{2}}, \quad (49)$$

in developing an analytic expression for the quaternion. This would have led to an unnecessary sign ambiguity which would have been complicated to resolve.

In developing the expression for the attitude covariance matrix we assumed a particular model for the measurement errors of the direction. We could, in fact have used an arbitrary measurement model for \dot{W}_1 , namely,

$$E\{\Delta \dot{W}_1\} = 0, \quad (50)$$

$$E\{\Delta \dot{W}_1 \Delta \dot{W}_1^T\} = P_{\dot{W}_1}, \quad (51)$$

where $P_{\dot{W}_1}$ is an arbitrary covariance matrix for \dot{W}_1 , which must, because of the unit-norm constraint, satisfy

$$P_{\dot{W}_1} \dot{W}_1 = 0, \quad (52)$$

so that $P_{\dot{W}_1}$ is singular (rank deficient). Equation (37) then generalizes to

$$J(A) = (\dot{W}_1 - A \dot{V}_1)^T P_{\dot{W}_1}^\# (\dot{W}_1 - A \dot{V}_1) + \frac{1}{\sigma_d^2} |\dot{S}_2 \cdot A \dot{V}_2 - d|^2, \quad (53)$$

where $\#$ denotes the pseudo-inverse. The attitude covariance matrix generalizes to

$$P_{\xi\xi} = \left[\left[(\dot{W}_1) \right]^T P_{\dot{W}_1}^\# \left[(\dot{W}_1) \right] + \frac{1}{\sigma_d^2} (\dot{W}_2 \times \dot{S}_2) (\dot{W}_2 \times \dot{S}_2)^T \right]^{-1}. \quad (54)$$

If the measured direction is that of the geomagnetic field, then in general the entire three-vector is known and need not have unit norm. In that case the we replace \dot{W}_1 and \dot{V}_1 by the unnormalized W_1 and V_1 and the covariance matrix is now full rank (Equation (52) no longer applies). Equations (53) and (54) remain unaltered except for the replacement

$$P_{\dot{W}_1}^\# \rightarrow P_{W_1}^{-1}. \quad (55)$$

In many practical circumstances, however, the simple model of Equation (37) has proven to be adequate.

Note that the covariance matrix characterizes the probability of the estimate compared to other solutions within its immediate neighborhood. The algorithm, however, has two solutions, the correct one of which cannot be identified except by bringing additional information to bear on the attitude problem. Thus, even though the attitude variances may be small the estimated solution, if it happens to be the false solution, may be very far from the truth.

An Alternate Choice for the Initial Rotation

Instead of Equation (12) we could have chosen

$$\hat{n}'_o = \frac{\dot{W}_1 + \dot{V}_1}{|\dot{W}_1 + \dot{V}_1|}. \quad (56)$$

Then it is easy to show that

$$A'_o = R(\hat{n}'_o, \pi) \quad (57)$$

$$= -I_{3 \times 3} + \frac{(\dot{W}_1 + \dot{V}_1)(\dot{W}_1 + \dot{V}_1)^T}{1 + \dot{W}_1 \cdot \dot{V}_1}. \quad (58)$$

The quaternion in this case is simply

$$q'_o = \begin{bmatrix} \hat{n}'_o \\ 0 \end{bmatrix}. \quad (59)$$

The special case $\hat{W}_1 = \hat{V}_1$ no longer requires special attention for this choice of A'_0 . The treatment of the special case $\hat{W}_1 = -\hat{V}_1$ is as previously. The computation of β' (corresponding to the earlier β) and θ' (corresponding to the earlier θ) proceeds as before.

A More Direct Solution for the Attitude Matrix

Instead of first calculating the attitude matrix from the data and then determining a vector \hat{W}_2 which satisfies

$$\hat{W}_2 = A \hat{V}_2. \quad (60)$$

in order to carry out the covariance analysis, we might try instead to calculate this \hat{W}_2 directly and, once this vector has been determined, calculate A using the triad algorithm.¹

To compute \hat{W}_2 we write

$$\hat{W}_2 = a \hat{W}_1 + b \hat{S}_2 + c \frac{\hat{W}_1 \times \hat{S}_2}{|\hat{W}_1 \times \hat{S}_2|}, \quad (61)$$

which is possible provided that $\hat{W}_1 \neq \pm \hat{S}_2$. It then follows that

$$\hat{W}_1 \cdot \hat{W}_2 = a + b(\hat{W}_1 \cdot \hat{S}_2) = \hat{V}_1 \cdot \hat{V}_2, \quad (62)$$

$$\hat{S}_2 \cdot \hat{W}_2 = a(\hat{W}_1 \cdot \hat{S}_2) + b = d, \quad (63)$$

$$\begin{aligned} \hat{W}_2 \cdot \hat{W}_2 &= a^2 + 2ab(\hat{W}_1 \cdot \hat{S}_2) \\ &+ b^2 + c^2 = 1. \end{aligned} \quad (64)$$

The solution for a and b is immediate and is given by

$$a = \frac{(\hat{V}_1 \cdot \hat{V}_2) - (\hat{W}_1 \cdot \hat{S}_2) d}{|\hat{W}_1 \times \hat{S}_2|^2}, \quad (65)$$

$$b = \frac{d - (\hat{W}_1 \cdot \hat{S}_2)(\hat{V}_1 \cdot \hat{V}_2)}{|\hat{W}_1 \times \hat{S}_2|^2}. \quad (66)$$

The solution for c is now given by

$$c = \pm \sqrt{1 - (a^2 + 2ab(\hat{W}_1 \cdot \hat{S}_2) + b^2)}. \quad (67)$$

This last calculation can be simplified by noting that

$$\begin{aligned} &a^2 + 2ab(\hat{W}_1 \cdot \hat{S}_2) + b^2 \\ &= \frac{1}{|\hat{W}_1 \times \hat{S}_2|^2} \left[d^2 - 2d(\hat{V}_1 \cdot \hat{V}_2)(\hat{W}_1 \cdot \hat{S}_2) \right. \\ &\quad \left. + (\hat{V}_1 \cdot \hat{V}_2)^2 \right]. \end{aligned} \quad (68)$$

The lack of a unique solution is now obvious from Equation (67). Although the triad algorithm¹ can now be used to calculate the attitude from the four vectors \hat{V}_1 , \hat{V}_2 , \hat{W}_1 , and \hat{W}_2 , the measured unit vectors are no longer uncorrelated, and the attitude covariance matrix is still that computed earlier (Equations (42) or (54)).

While the present algorithm is clearly more efficient than that developed in the main text, it also suffers

from some numerical problems. Because of round-off error it is not guaranteed that \hat{W}_2 is a unit vector. Worse still, large measurement errors may cause the argument of the square root in Equation (67) to be negative.

Discussion

We note with some dismay that for three data there is no single unambiguous solution to the attitude determination problem. On the other hand, for two vectors, which are equivalent to four data, the solution is generally overdetermined, so that no solution will exist. If we are given three angles, two of which are to the same body-fixed vector, then there will clearly be four possible attitude solutions, in general. We conjecture that for three angles, each one to a different body-fixed vector, there will be eight possible attitude solutions. It would appear, therefore, that the non-optimal attitude determination problem is always ambiguous or nonexistent, and only least-square solutions of the overdetermined problem yield unique results.

Acknowledgment

The author is grateful to J. Courtney Ray for suggesting this problem and to F. Landis Markley for a critical reading of the manuscript.

References

- ¹Shuster, M. D., and Oh, S. D., "Three-Axis Attitude Determination from Vector Observations," *Journal of Guidance and Control*, Vol. 4, No. 1, 1981, pp. 70-77.
- ²Shuster, M. D., "Maximum Likelihood Estimation of Spacecraft Attitude," *Journal of the Astronautical Sciences*, Vol. 37, No. 1, 1989, pp. 79-88.
- ³Shuster, M. D., "A Survey of Attitude Representations," *Journal of the Astronautical Sciences*, Vol. 41, No. 4, 1993, pp. 438-517.
- ⁴Sorenson, H., *Parameter Estimation*, Marcel Dekker, New York, 1980.

HORIZON SENSORS ATTITUDE ERRORS SIMULATION FOR THE BRAZILIAN REMOTE SENSING SATELLITE

Antonio Gil Vicente de Brum and Mario Cesar Ricci
Space Mechanics and Control Division
Brazilian National Institute of Space Research - INPE
C.P. 515-cep 12201-970 S.J. Campos/SP- E-Mail: BRUM@DEM.INPE.BR

ABSTRACT

Remote sensing, meteorological and other types of satellites require an increasingly better earth related positioning. From the past experience it is well known that the thermal horizon in the 15μ band provides conditions of determining the local vertical at any time. This detection is done by horizon sensors which are accurate instruments for earth referred attitude sensing and control whose performance is limited by systematic and random errors amounting about 0.5° . Using the computer programs OBLATE, SEASON, ELETRO and MISALIGN, developed at Inpe to simulate four distinct facets of conical scanning horizon sensors, attitude errors are obtained for the brazilian remote sensing satellite (The first one, SSR-1, is scheduled to fly in 1996). These errors are due to the oblate shape of the earth, seasonal and latitudinal variations of the 15μ infrared radiation, electronic processing time delay and misalignment of sensor axis. The sensor related attitude errors are thus properly quantified in this work and will, together with other systematic errors (for instance, ambient temperature variation) take part in the pre-launch analysis of the brazilian remote sensing satellite, with respect to the horizon sensor performance.

Key words: Horizon sensor, attitude errors, errors simulation.

INTRODUCTION

By detecting the thermal horizon of the Earth, a horizon sensor system pro-

vides the spacecraft with conditions to determine the local vertical at any time. This local vertical becomes a reference for spacecraft stabilization and attitude measurements. With this goal, horizon sensors were developed with high sensitivity in the $14-16\mu$ band associated with CO_2 absorption in the atmosphere. This band effectively shields a sensor from clouds and other low-altitude effects, however, makes it sensitive to relatively slowly varying temperature changes in the atmosphere above 20 Km, thereby introducing variations caused by seasonal and geographic effects¹.

A scanning horizon sensor consists of an infrared optics, spectral band-pass filter for $14-16\mu$, thermistor bolometer and processing electronics. The field of view (FOV) of the sensor is tilted by using a germanium prism. The rotation of the prism results in a conical scan of the space by the FOV (Fig. 1). During the scan, the FOV cone intersects the Earth's horizon which is detected by the sensor. The period between space-to-Earth and Earth-to-space crossings produces an electronic pulse, whose width corresponds to the chord of the Earth, as scanned by the sensor. The chord length when compared with a standard chord length determines the roll angle. The scan mechanism also generates a reference pulse signal, corresponding to the time when the FOV is oriented towards the local vertical, at pitch zero condition. When there is a pitch angle it results in an asymmetry of the reference pulse with respect to the chord length. The asymmetry is a measure of the pitch angle (Fig. 2).

Remote sensing, weather and other satellites demand an increasingly better accuracy in their earth referred

positioning. This accuracy is limited by systematic and random errors which amount about 0.5° . Some of these errors arise from Earth oblateness, seasonal and latitudinal variations of Earth infrared radiation, electronic processing time delay, misalignment of sensor axis and were properly quantified in earlier works. With the same authorship of this paper, the programs OBLATE, SEASON, ELETRO and MISALIGN were developed to simulate the errors mentioned above² and are used here to simulate errors expected to be found in the forthcoming Brazilian SSR missions. The SSR horizon sensor analysis follows a brief introduction of the programs, which is done by simulating some aspects of past missions and then comparing the results obtained with the published ones.

Program OBLATE

For the purpose of testing results obtained from it, OBLATE program has been first utilized in the attempt to reproduce the results of Alex and Shrivastava³ in their simulation for a typical conical scanning Earth sensor (CSES) used in a sun-synchronous orbit (904 Km altitude and 97° inclination). The oblateness errors obtained by them were compared with the errors obtained via OBLATE (the details of such comparison are better explained in Ref. 2). From that comparison one can see how well, quantitatively and qualitatively, the expected results were achieved with the use of the program OBLATE.

For the SEASAT mission⁴ we only knew the magnitude of the expected oblateness errors taken from a summary of pitch and roll standard deviations, where one can see that the errors magnitude is approximately:

	Pitch	Roll
sensor 1:	0.25°	0.05°
sensor 2:	0.14°	0.23°

Which are practically the same as those found using the OBLATE program (see Fig. 3).

Program SEASON

As a first test to the program we tried to reproduce the prediction of Ward⁵ about the on-orbit performance of the conical scan horizon sensor system model 13-166-9. The orbital radiance errors were computed for a sun-synchronous polar orbit (inclination 98°) for an altitude of 100 NM in the northern hemisphere only. With the use of program SEASON, radiance errors were simulated². The similarity between obtained and expected errors is remarkable.

As a second test we compared simulated roll and pitch errors for the LANDSAT 4 mission⁴ with the residual errors obtained in-flight. Figures 4 and 5 show respectively the in-flight data and the simulated (via SEASON) ones. All biases have been removed for the comparison. From them one can see a good similarity in shape and magnitude.

As a third program test the agreement between the prediction of Weiss⁶ for a conical scan horizon sensor, in Earth orbits up to 6000 NM for a range of inclinations and the simulation of this sensor undertaken via SEASON (Ref. 2 presents the simulated errors). Again the comparison showed a remarkable agreement between expected and obtained errors.

Program ELETRO

This program² is used to simulate the electronic processing of a conical scan horizon sensor and is useful to identify the triggering levels (usually 50% of the positive/negative peaks of the processed input intensity) and/or, for fixed triggering heights, to help finding out the time delay introduced by the electronic processing. Even though all time constants of the SSR electronic components are not well known yet, a previous simulation seemed worth doing. The results are presented in the next sections.

Program MISALIGN

The misalignment between spin axis and optical axis is one of the error sources that has been observed to affect the accuracy of earth sensors

but has not been studied in sufficient detail. The program MISALIGN was only recently developed and represents a new effort in the comprehension of the errors due to misalignment of sensor axes. As input data, the parameters σ and ϕ_B , which stand for, respectively, offset angle between spin axis and optical axis, and phase of the FOV. Once fixed these two parameters one can simulate roll and pitch errors introduced by such misalignment. Some results for one optical head are presented (Fig. 6). They show that sign and magnitude of the sensor errors vary with orbital parameters and sensor position. The errors increase with the eccentricity for the same semi major axis and sensor position. Figure 6 shows, for 45° half cone angle, and for several eccentricities, roll and pitch errors due to 0.05° of misalignment (σ), 180° of FOV phase (ϕ_B), in a 7,282.14 Km semi major axis orbit and with spin axis positioned according to the angles α (canting angle = 20°) and β (rotation angle from pitch-yaw plane up to spin axis = 30°). As one can see the errors are small if compared with other sources as oblate shape or radiance effects. For circular orbits the error is constant. In the case mentioned the magnitude of the roll and pitch errors for null eccentricity is 10^{-6}° but can be majored to 10^{-4}° if changed the spin axis for pitch or roll axes.

SSR Errors Simulation

SSR Parameters

The simulated sensors (Fig. 1) have their optical heads disposed in diametrically opposite directions ("back to back"). The first one has his optical axis bent α_1 degrees down with respect to the positive pitch axis while the second has his optical axis bent α_2 degrees down with respect to the negative pitch axis. The orbit is circular sun-synchronous with 639.73 Km altitude and 97.7° inclination. Some of the defined parameters are as follows:

α_1, α_2 : canting angles ($0^\circ, 0^\circ$)

γ_1, γ_2 : half cone angles (between 45° and 60°)

FOV dimension: $1.5^\circ \times 2.6^\circ$

The parameters for the simulation of the electronic processing are presented below. Some of them were not well defined yet and, for previous simulation purposes, they were taken from similar projects (see Ref. 3).

Bolometer time constant: 2.25 ms

Bolometer responsivity: 155 V/W

Coupling circuit time constant: .16 s

High-pass filter time constant: 1.6ms

Low-pass filter time constant: 0.01 s

The simulation undertaken resulted in the following graphics where one can see the errors and their respective sources (Fig. 7, 8 and 9)

Results and Conclusions

Figure 7 shows the simulated SSR oblateness errors. When the average of both sensors outputs is used, the roll error reduces considerably (maximum 0.05°) while the pitch oblateness error is not affected significantly (max. 0.15°).

Figure 8 shows the simulated errors due to seasonal and latitudinal variation of the 15μ infrared radiation. Again the average, if used, reduces the roll error (max. 0.07°), but the pitch error remains not significantly affected (max. 0.3°). It should be mentioned here that the use of some kind of normalization technique could reduce these errors to 0.04° roll and 0.08° pitch (see reference 5).

The electronic processing simulation is undertaken. Results are shown in Fig. 9. From it one is able to identify bias errors introduced by electronic processing delays and/or better estimates for triggering heights (usually taken as 50% of positive/negative peaks, V_p and V_N). Figure 9 identifies the time when the

FOV crosses from space-to-Earth, ϕ_{in} , and from Earth-to-space, ϕ_{out} . Note that these crossing times are shifted in a quantity introduced by the electronic processing delay. The simulation is useful to identify this quantity and/or to identify triggering heights that are able to nullify such delay.

As we have mentioned, some electronic parameters were not defined yet. The simulations that have been undertaken here represent a previous analysis effort on the expected errors and will take part as starting points in the forthcoming SSR pre-launch analysis in the branch concerned with horizon sensors.

References

¹DODGEN, J. A.; CURFMAN JR., H. J. *Accuracy of IR horizon sensors as affected by atmospheric considerations.* s.n.t.

²BRUM, A. G. V. de; *Horizon sensor mathematical modeling in digital computers for low earth orbits.* M.s.C. thesis (in portuguese). Brazilian National Institute of Space Research, INPE, São José dos Campos, São Paulo, 1993.

³ALEX, T. K.; SHRIVASTAVA, S. K. *On-Board Correction of Systematic Errors of Earth Sensors.* IEE Transactions on Aerospace and Electronic Systems, 25(3):373-379, May 1989.

⁴PHENNEGER, M. C.; SINGHAL, S. P.; LEE, T. H.; STENGLE, T. H. *Infrared horizon sensor modeling for attitude determination and control: Analysis and mission experience.* s.l., March, 1985. (NASA TM-86181).

⁵WARD, K. A. *Modeling of the atmosphere for analysis of horizon sensor performance.* SPIE Sensor Design Using Computer Tools. Los Angeles, CA, 1982, v. 327.

⁶WEISS, R. *Sensing accuracy of a conical scan CO₂ horizon sensor.* Journal of Spacecraft and Rockets. s.l., 1972, v. 9, p. 606-612.

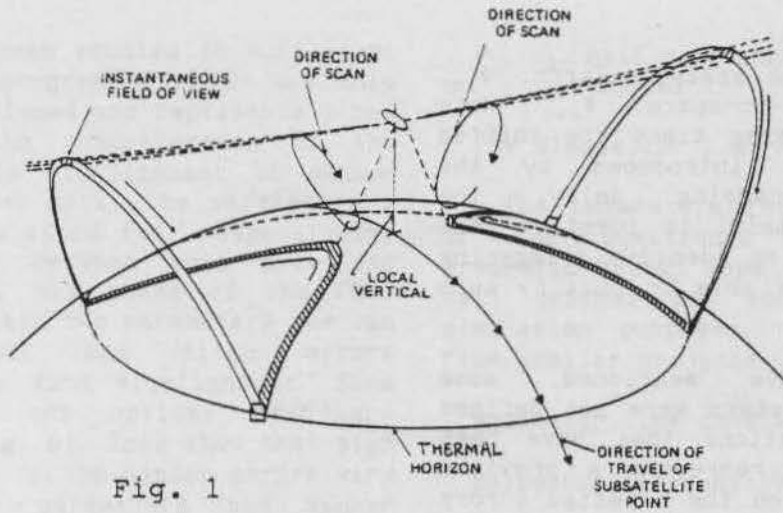


Fig. 1

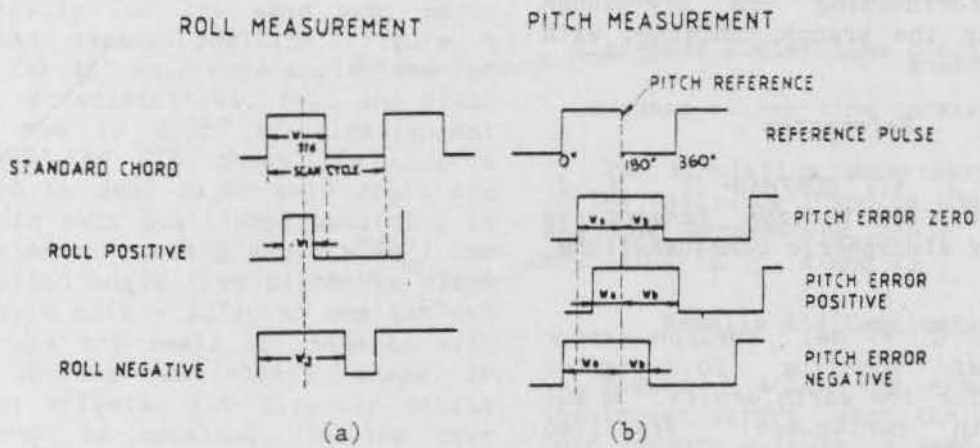


Fig. 2

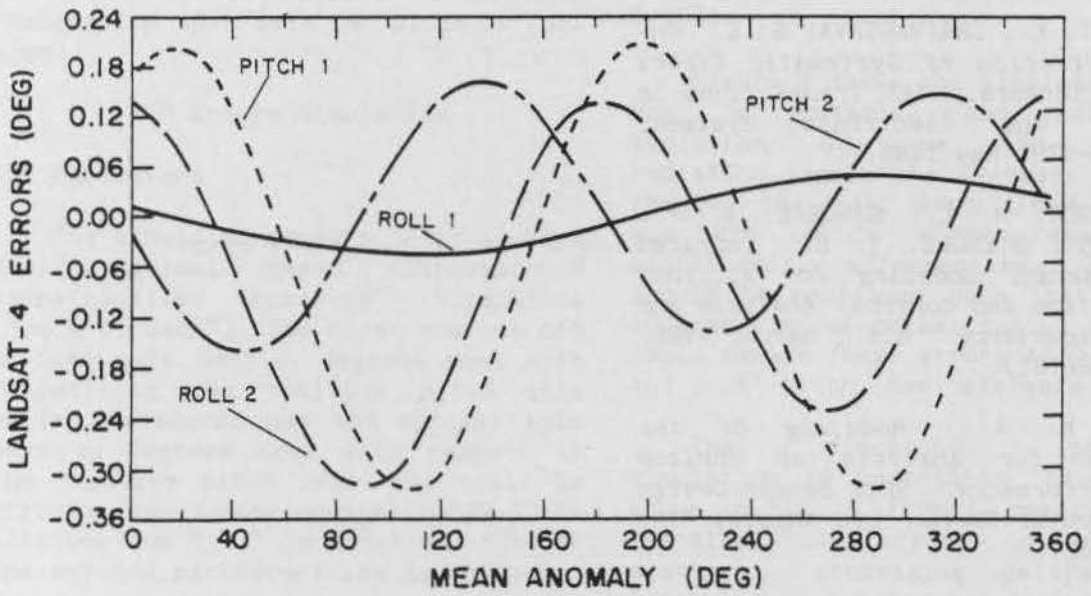


Fig. 3 - LANDSAT-4 Oblateness errors.

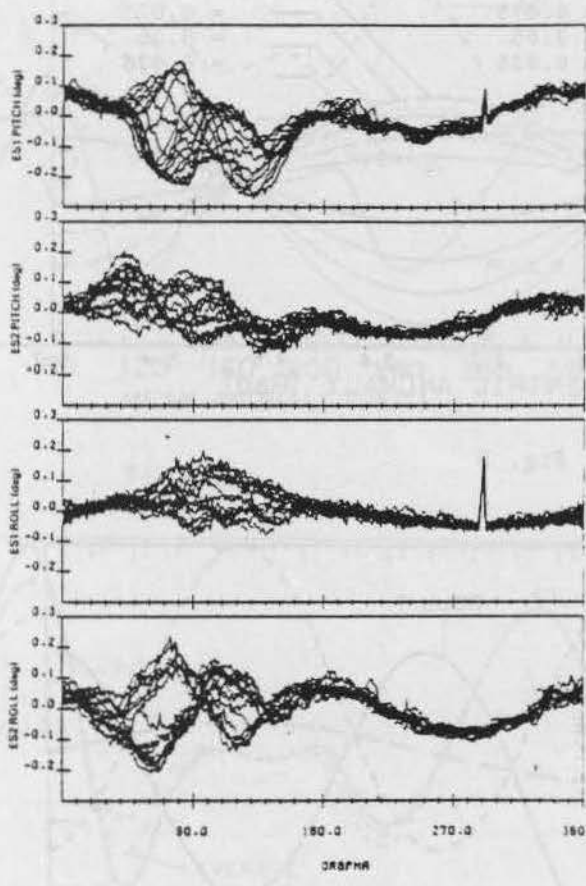


Fig. 4

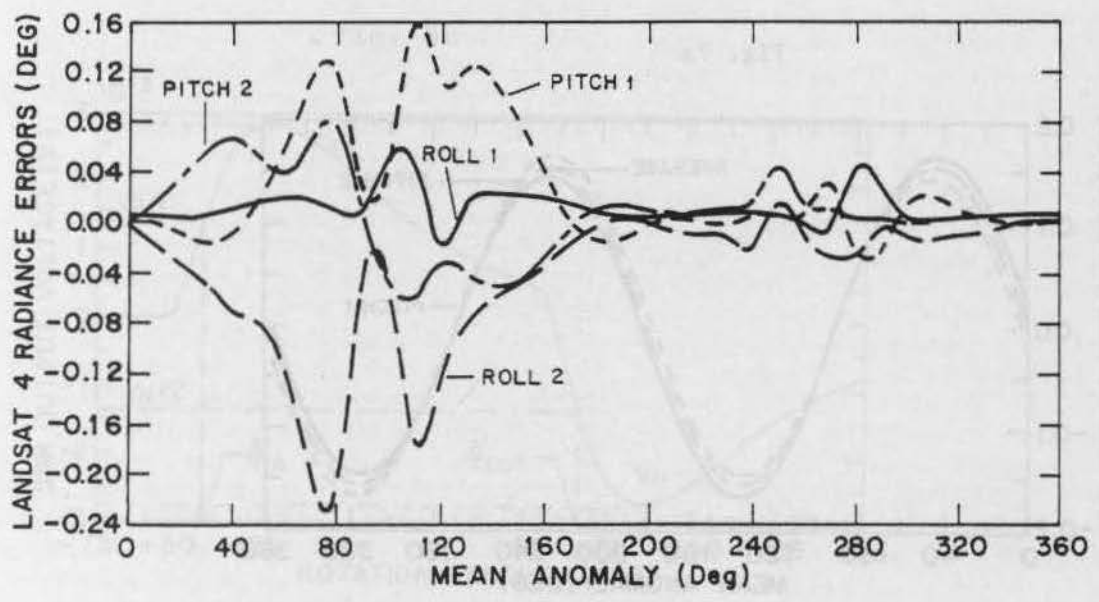


Fig. 5

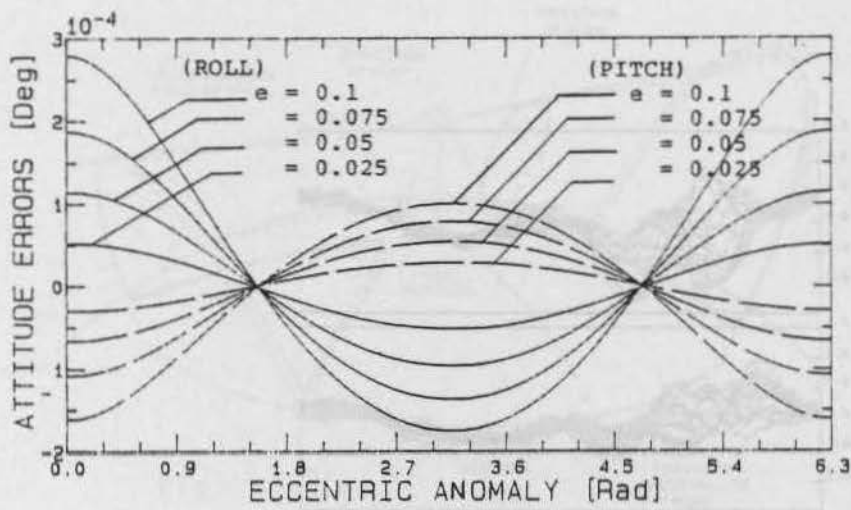


Fig. 6

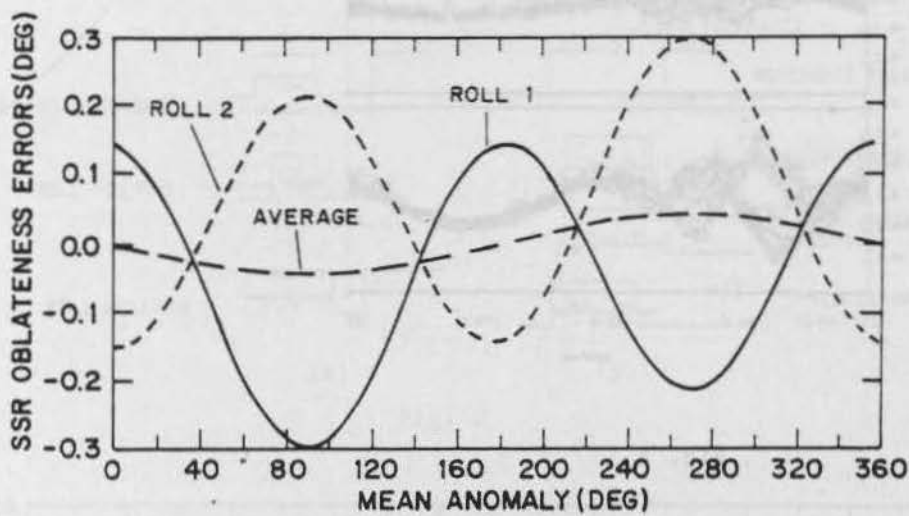


Fig. 7a

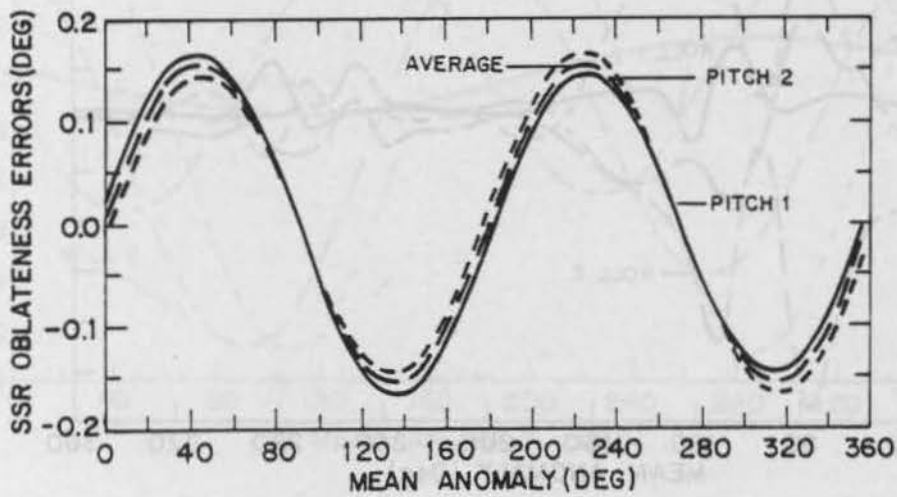


Fig. 7b

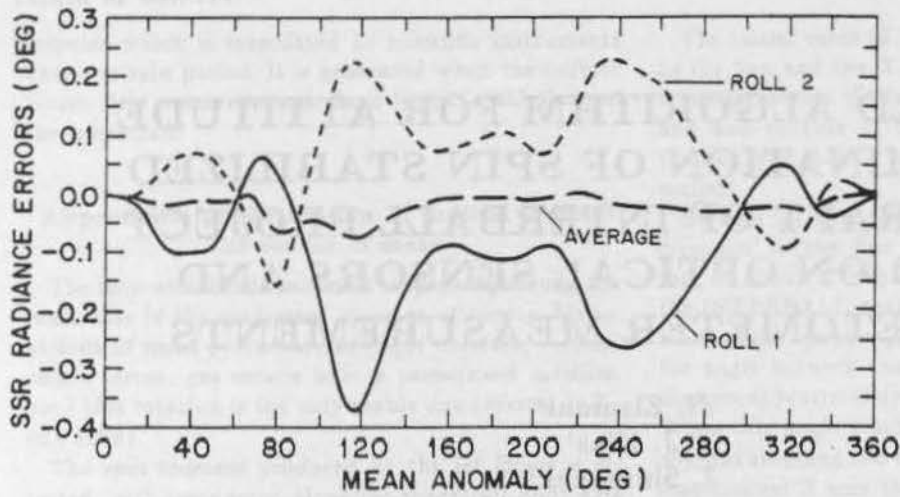


Fig. 8a

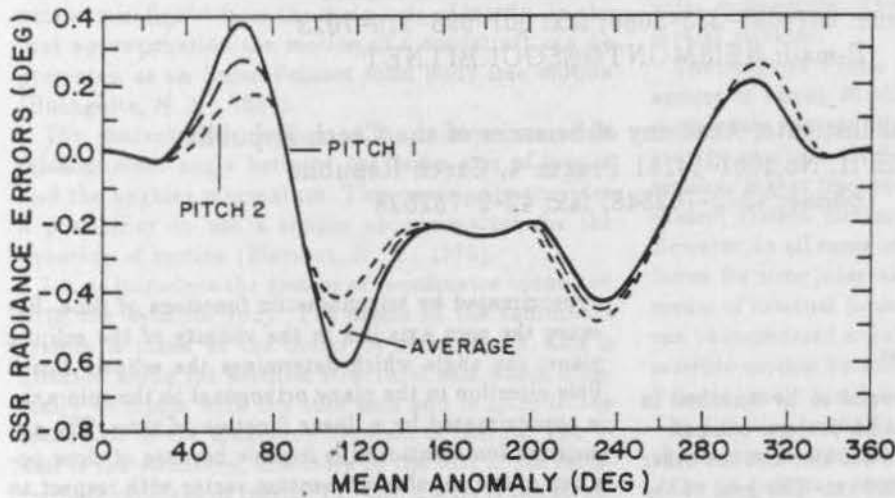


Fig. 8b

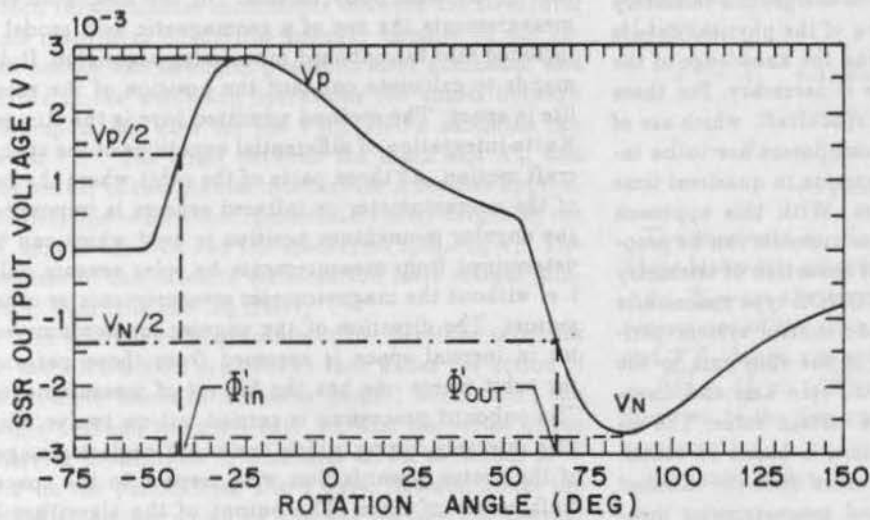


Fig. 9

ONBOARD ALGORITHM FOR ATTITUDE DETERMINATION OF SPIN STABILIZED SPACECRAFT OF INTERBALL PROJECT BASED ON OPTICAL SENSORS AND MAGNETOMETER MEASUREMENTS

N. Eismont*

J. Klas†

J. Shimonek†

*Space Research Institute of Russian Academy of Sciences
Profsoyuznaya 84/32, 117810 Moscow, Russia
phone: 007-095-333-5089; fax: 007-095-310-7023
E-mail: NEISMONT@ESOC1.BITNET

†Geophysical Institute, Academy of Sciences of the Czech Republic
Bocni II, No.1401-14131 Prague 4, Czech Republic
phone: 42-2-762548; fax: 42-2-762528

Abstract

Four Earth satellites are planned to be launched in the framework of the INTERBALL project: one pair—into orbit with apogee height 20 000 km, and the other pair—with apogee height 200 000 km. The goal of the project is to explore phenomena in the Earth magnetosphere and in the solar wind. To reduce the information flow to be transmitted to the ground telemetry stations, the onboard processing of the physical data is planned. To fulfill this processing the knowledge of the spacecraft attitude parameters is necessary. For these reasons onboard the two main spacecraft, which are of the PROGNOZ type, special computers are to be installed which will allow to determine in quasireal time the actual attitude parameters. With this approach measurements of the onboard instruments can be properly organised, and a significant reduction of telemetry data flow is achieved. The PROGNOZ type spacecrafts are spin stabilized. The attitude control system periodically restores the direction of the spin axis to the Sun, when the angle between the spin axis and direction towards the Sun exceeds a certain value. The algorithm of attitude determination is based on statistical processing of the solar sensors data (or infrared Earth horizon sensors data) and magnetometer measurements. For this purpose the angles which characterize the Sun direction in the spacecraft frame are

approximated by trigonometric functions of time. Because the spin axis lies in the vicinity of the ecliptic plane, the angle which determines the ecliptic North Pole direction in the plane orthogonal to the spin axis, is approximated by a linear function of time. The approximation mentioned is feasible because of close position of the angular momentum vector with respect to the principal inertia axis of the spacecraft which attitude motion is very precisely modelled by the Euler case of the solid body motion. For the magnetometer measurements the use of a geomagnetic field model is included into the onboard processing algorithm. It demands to calculate onboard the position of the satellite in space. The method admitted here is the Runge-Kutta integration of differential equations of the spacecraft motion. At those parts of the orbit where the use of the magnetometer or infrared sensors is impossible the angular momentum position is used which can be determined from measurements by solar sensors only, i. e. without the magnetometer measurements or other sensors. The direction of the angular momentum vector in inertial space is assumed from those parts of the orbit where one has the full set of measurements. The onboard processing is carried out on twelve minutes intervals during which one could neglect changes of the vector towards Sun with respect to the spacecraft center of mass. The output of the algorithm is a set of constants in the approximated law of spacecraft motion including the so called "top of spin"—an

impulse which is transmitted to scientific instruments once per spin period. It is generated when the ecliptic North Pole passes through fixed longitudinal plane of the spacecraft.

Approximation for the law of motion around the center of mass

The spin-stabilized spacecraft is spinning around the main axis of the maximum moment of inertia. Under actions of small perturbations (light pressure, aerodynamic forces, gas escape from a pressurized satellite, etc.) this rotation is the only stable one (Wertz, J. R., ed., 1978).

The spin moment produced by the jet forces is directed, with some error, along the spacecraft body axis which does not exactly coincide with the main central axis of inertia due to errors of the spacecraft balancing. Therefore, after a spinning up, the spacecraft spin axis is misaligned from the main axis of inertia. In the first approximation the motion of a spacecraft can be presented as an Euler-Poinsot solid body free motion (Buchgoltz, N. N., 1967).

The characteristic feature of the motion is a small misalignment angle between the main axis of inertia and the angular momentum. This peculiarity provides a possibility to use a simple approximation for the equation of motion (Eismont, N. A., 1975).

Let us introduce the system of coordinates connected with the satellite body. The origin of the coordinate system is taken at the center of mass, the X axis is directed along the satellite structural axis which nominally coincides with the spin axis and is close to the main axis of the maximum moment of inertia. The Y axis is the structural axis close to the axis of the intermediate moment of inertia Y_m ; the Z axis is the structural axis close to the axis of the minimum moment of inertia Z_m . Balancing of the satellite is performed to reach the maximum coincidence between the structural and main axes of inertia, however because of not exact booms and antennas positions after extension, and errors in the balancing operations the angles between corresponding axes for the PROGNOZ satellites can reach 1.5° . The angle between the main axis X_m and the vector of the angular momentum \vec{L} reaches approximately the same value immediately after targeting the X axis to the Sun and the spacecraft spinning up. The process of the satellite stabilization lasts several minutes, then it is moving freely.

The analysis of the motion of the previous satellites of the PROGNOZ type shows that under the action of dissipative forces in the solar panels, booms etc., the angle between the main axis X_m and the vector of the angular momentum \vec{L} decreases down to values of $\sim 0.2^\circ$ in the period from 1 to 4 days. Besides, under the effect of forces caused by the gas leakage the angular velocity of the satellite motion is changing linearly by the value of up to 1.5% for 10 days.

The initial value of the angle between the direction to the Sun and the X axis of the satellite, because of a misalignment of the main axis X_m from the X axis, and also because of the errors of the orientation to the Sun was about $1 \div 1.5^\circ$ for the satellites launched earlier.

Because of the orbital motion of the Earth the direction to the Sun changes its position with the rate of about $1^\circ/\text{day}$. For the Tail Probe satellite of the INTERBALL project the direction of the angular momentum remains practically unchanged. Therefore the angle between the longitudinal axis and the Sun changes approximately with the same rate, i. e. $1^\circ/\text{day}$. When this angle reaches the value 10° it is planned, without stopping the rotation, to redirect the satellite longitudinal X -axis to the Sun. In this case the attitude control system should suppress the nutation motion of the spacecraft down to the value corresponding to the angle of 1° between the main axis and the angular momentum. The reorientation process can last several minutes.

The Auroral Probe satellite has an orbit with the apogee of about 20 000 km. The vector of its angular momentum can change its position under the effect of gravity gradient with the mean rate up to $5^\circ/\text{day}$. It requires higher frequencies of switchings of the attitude control system for targeting the X axis to the Sun. However, in all cases of the motion without controlling forces for time intervals up to 10 min the level of moments of external forces and internal dissipative forces can be considered as sufficiently low to approximate the satellite motion by solid body free motion (the Euler-Poinsot case), i. e. to neglect the disturbing moments. The direction to the Sun within such a time interval (in the inertial frame) can also be considered invariable.

Let us designate as α and β the angles formed by the projections of the direction to the Sun from the spacecraft to the planes XY and YZ with the X -axis. These angles can be approximated by the following functions of time t :

$$\alpha = A_1 + A_2 \sin \omega_1 t + A_3 \cos \omega_1 t + A_4 \sin \omega_2 t + A_5 \cos \omega_2 t, \quad (1)$$

$$\beta = B_1 + B_2 \sin \omega_1 t + B_3 \cos \omega_1 t + B_4 \sin \omega_2 t + B_5 \cos \omega_2 t. \quad (2)$$

The constants A_i , B_i , ω_1 , ω_2 are not all independent. Their kinematic meaning is as follows:

A_1 , B_1 —are the angles between the X axis and the projections of the main axis of inertia X_m to the XY and XZ planes, respectively;

$\sqrt{A_2^2 + A_3^2} = \sqrt{B_2^2 + B_3^2}$ is the angle between the direction to the Sun and the vector of the angular momentum;

$\omega_2 = c\omega_1$, where

$$c = \sqrt{\frac{(J_x - J_y) \cdot (J_x - J_z)}{J_y \cdot J_z}}; \quad (3)$$

$J_x > J_y > J_z$ are the spacecraft main central moments of inertia;

ω_1 is the angular velocity of the satellite rotation around the main axis X_m ;

ω_2 is the angular velocity of the rotation of the angular momentum relative to the satellite;

$$\sqrt{B_4^2 + B_5^2} = d\sqrt{A_4^2 + A_5^2}, \quad (4)$$

where

$$d = \sqrt{\frac{J_z(J_x - J_y)}{J_y(J_x - J_z)}} \quad (5)$$

Besides, the constants satisfy the relations:

$$\arcsin\left(\frac{A_3}{\sqrt{A_2^2 + A_3^2}}\right) - \frac{\pi}{2} = \arcsin\left(\frac{B_3}{\sqrt{B_2^2 + B_3^2}}\right),$$

$$\arcsin\left(\frac{A_5}{\sqrt{A_4^2 + A_5^2}}\right) - \frac{\pi}{2} = \arcsin\left(\frac{B_5}{\sqrt{B_4^2 + B_5^2}}\right)$$

Thus the angular momentum relative to the satellite is moving along the surface close to the elliptic cone. While giving its position by angles α and β similar to the position of the Sun in the phase plane α, β the motion of the angular momentum vector is characterized by the ellipse with semi-axes a and b

$$a = \sqrt{A_4^2 + A_5^2} \text{—along axis } \alpha \text{ (i. e. along } Y);$$

$$b = \sqrt{B_4^2 + B_5^2} = da \text{—along axis } \beta \text{ (i. e. along } Z).$$

The center of this ellipse has the coordinates A_1, B_1 .

Attitude sensors

As the instantaneous axis of the satellite rotation lies sufficiently close to the ecliptic plane and misaligned from its mean position by no more than by $\sim 1.5^\circ$, for the Tail Probe and $\sim 10^\circ$ for the Auroral Probe the projection of direction, orthogonal to the ecliptic plane, to the YZ plane of the satellite is rotating practically with the constant velocity. It gives the position of this projection by angle γ , counted from axis Y :

$$\gamma = c_1 + c_2 t,$$

where c_1 is the initial phase, $c_2 = -\omega_1$.

It is planned to use the solar sensor and the magnetometer for the determination of the spacecraft attitude.

The solar sensor measures the quantities providing to calculate angles α and β for the time instants of measurements. The minimum interval between measurements is ~ 0.2 sec. However the interface between the attitude onboard processor and the solar sensor should provide a possibility to select the sensor measurements with an arbitrary data step exceeding 0.2 sec.

The magnetometer measures three components of the magnetic field vector over the whole possible range of the flight altitudes. But these measurements can be used only at altitudes for which there is a reliable model of the magnetic field.

For the Auroral and the Tail Probes the initial perigee altitude is about 500 km, apogee altitudes are 20 000 km and 200 000 km respectively. Under actions of the Moon and the Sun perturbations, the perigee altitude of the Tail Probe is increasing up to 12 000 km in a year after the launch and reaching its maximum of 18 000 km in a year and a half.

Algorithm for the "top of spin" calculation

The algorithm objective is to calculate the time instants when the direction to the North pole of the ecliptic passes through the XY plane of the satellite from the data of the onboard magnetometer and the solar sensor.

For the altitudes when it is possible to apply the model of the magnetic field, the algorithm is reduced to the following sequence of operations.

1. Using initial conditions the numerical integration determines the cartesian coordinates and projections of the velocity vector of the satellite into equatorial non-rotating system of coordinates ("absolute" frame).

2. For the calculated satellite coordinates the simulative model vector of the magnetic field \vec{H}_0 and the vector of direction to the Sun \vec{S}_0 are calculated in the same system of coordinates.

3. For every mentioned point the matrix is plotted from the data of the solar sensor \vec{S}_m and magnetometer \vec{H}_m measurements:

$$W_m = \left\| \vec{S}_m \left| \frac{\vec{S}_m \times \vec{H}_m}{|\vec{S}_m \times \vec{H}_m|} \right| \frac{\vec{S}_m \times \vec{H}_m}{|\vec{S}_m \times \vec{H}_m|} \times \vec{S}_m \right\| \quad (6)$$

The matrix is calculated from \vec{H}_0 and \vec{S}_0 :

$$W_0 = \left\| \vec{S}_0 \left| \frac{\vec{S}_0 \times \vec{H}_0}{|\vec{S}_0 \times \vec{H}_0|} \right| \frac{\vec{S}_0 \times \vec{H}_0}{|\vec{S}_0 \times \vec{H}_0|} \times \vec{S}_0 \right\| \quad (7)$$

and then the transition matrix—from the system of the satellite coordinates to "absolute" system is calculated

$$M = W_0 * W_m^T. \quad (8)$$

If the vector of the direction to the North pole of the ecliptic in the "absolute" frame is denoted as $\vec{N} = (N_x, N_y, N_z)$, the angle γ between the Y axis of the satellite and the \vec{N} projection onto the YZ plane is determined by projections N_{cy}, N_{cz} of \vec{N} vector to the plane YZ :

$$\begin{pmatrix} N_{cy} \\ N_{cz} \end{pmatrix} = M * \vec{N}$$

Using the symbols of functions from the library of Fortran standard functions

$$\gamma = \text{ATAN2}(N_{cx}, N_{cy}) \quad (9)$$

4. These operations are made with the step of 30 sec, their results are values γ_i within the time interval of about 10 min.

The array of γ_i is built so that $\gamma_1 = \gamma(t_1)$, where t_1 is the moment of the first measurement. Then, till $(\gamma_i - \gamma_{i+1} - \epsilon) < 0$, where, for example, $\epsilon = \pi/4$ and $i = 1, 2, \dots$ the value γ_{i+1} can be taken as $\gamma_{i+1} - 2\pi$.

5. The values γ_i thus obtained are approximated by the function

$$\gamma = c_1 + c_2 t \quad (10)$$

where c_1 and c_2 are defined by the method of least squares while processing the measurements in the form of γ_i .

Further the moments t_k for the "top of spin" are calculated using the following equations:

$$\gamma_k = c_1 + c_2 t_k = -2\pi k \quad (k = 0, 1, 2). \quad (11)$$

For altitudes where there is no reliable model of the magnetic field, the "top of spin" moments t_k are calculated by using the vector of the direction to the Sun (\vec{S}_0 —in the absolute frame; \vec{S}_m —in the satellite frame) and the vector of the angular momentum (\vec{L}_0 —in the absolute frame, \vec{L}_m —in the satellite frame).

The vector of the angular momentum \vec{L}_m in the satellite frame is defined by the processing of measurements of the solar sensor. The processing consists in the minimization of the sum of squares of residuals J of measured values $\tilde{\alpha}_i, \tilde{\beta}_j$ of angles α and β and their calculated values α_i, β_j . The index i corresponds to the times of measurements t_i ; j —to the times t_j now,

$$J = \sum [(\alpha_i - \tilde{\alpha}_i)^2 + (\beta_j - \tilde{\beta}_j)^2] \quad (12)$$

The minimization of J is carried out for the chosen phase frequency ω_i and coefficients A_k, B_k in ratios (1), (2). In this case the algorithm is formed in such a way that for each ω_1 the values of A_k, B_k are calculated, which result in a minimum of J magnitude.

$$E(\omega_1) = \min_{A_k, B_k} J(A_k, B_k, \omega_1) \quad (13)$$

This problem comes to the solution of two systems of linear equations

$$\sum_i \begin{pmatrix} 1 \\ \sin \omega_1 t_i \\ \cos \omega_1 t_i \\ \sin \omega_2 t_i \\ \cos \omega_2 t_i \end{pmatrix} * \begin{pmatrix} 1 \\ \sin \omega_1 t_i \\ \cos \omega_2 t_i \\ \sin \omega_1 t_i \\ \cos \omega_2 t_i \end{pmatrix}^T * \begin{pmatrix} A_1 \\ A_2 \\ A_3 \\ A_4 \\ A_5 \end{pmatrix} = \sum_i \tilde{\alpha}_i \begin{pmatrix} 1 \\ \sin \omega_1 t_i \\ \cos \omega_1 t_i \\ \sin \omega_2 t_i \\ \cos \omega_2 t_i \end{pmatrix} \quad (14)$$

$$\sum_j \begin{pmatrix} 1 \\ \sin \omega_1 t_j \\ \cos \omega_1 t_j \\ \sin \omega_2 t_j \\ \cos \omega_2 t_j \end{pmatrix} * \begin{pmatrix} 1 \\ \sin \omega_1 t_j \\ \cos \omega_1 t_j \\ \sin \omega_2 t_j \\ \cos \omega_2 t_j \end{pmatrix}^T * \begin{pmatrix} B_1 \\ B_2 \\ B_3 \\ B_4 \\ B_5 \end{pmatrix} = \sum_j \tilde{\beta}_j \begin{pmatrix} 1 \\ \sin \omega_1 t_j \\ \cos \omega_1 t_j \\ \sin \omega_2 t_j \\ \cos \omega_2 t_j \end{pmatrix} \quad (15)$$

If measurements are taken with a constant step, i. e. $t_i = (i - 1)\Delta t$; ($i = 1, 2, 3, \dots$) then while calculating the trigonometric functions, the recursive method can be used.

$$\begin{aligned} \sin(n+1)\Delta\phi &= \sin n\Delta\phi \cos \Delta\phi + \cos n\Delta\phi \sin \Delta\phi, \\ \cos(n+1)\Delta\phi &= \cos n\Delta\phi \cos \Delta\phi - \sin n\Delta\phi \sin \Delta\phi. \end{aligned} \quad (16)$$

It should be mentioned that the coefficients with unknown A_k, B_k in the systems of equations (14), (15) do not depend on measurements if measurements in each point t_i, t_j are involved in the data processing. In this case it is sufficient to calculate the matrices $M_A(\omega)$ and $M_B(\omega)$. (It is evident that with $t_i = t_j$ $M_A(\omega_1) = M_B(\omega_1)$).

The minimization of $E(\omega_1)$ for ω_1 can be made by the method of parabolic approximation. In this case three values of matrix $M_A(\omega_{11}), M_A(\omega_{12}), M_A(\omega_{13})$ are calculated.

The value ω_{13} can be taken from the data of processing at altitudes, where the magnetic field model can be used.

$$\omega_{13} = -c_1$$

Then for each subsequent interval the value of ω_{13} is taken from the solution of the task during the preceding step of processing.

The vector of the angular momentum of the satellite \vec{L}_m is defined in the satellite frame by angles α_L, β_L

$$\alpha_L = A_1 + A_4 \sin \omega_2 t + A_5 \cos \omega_2 t$$

$$\beta_L = B_1 + B_4 \sin \omega_2 t + B_5 \cos \omega_2 t$$

The vector of the angular momentum in the absolute space is calculated for altitudes where the models of the magnetic field can be used

$$\vec{L}_0 = M^T * \vec{L}_m$$

For the Tail Probe which orbit goes out of the limits of the altitudes of the reliable magnetic field model it is taken

$$\vec{L}_0 = \text{const}$$

(A version is possible when the time change of \bar{L}_0 is taken into account. In this case for the Tail Probe the differential equations are integrated with the step of several hours).

Then the "top of spin" (TS) is calculated with the use of equations (6)-(11), where in (6) and (7), \bar{L}_m and \bar{L}_0 are used instead of \bar{H}_m and \bar{H}_0 .

Admissible levels of the calculation discreteness. Required arrays of processed information.

The calculation of the "top of spin" is made by various algorithms; by the Algorithm I at altitudes where the model of the magnetic field is used, and by Algorithm II at altitudes where the previously acquired knowledge of the angular momentum position in space is used instead of the model vector of the magnetic field.

In the first case it is sufficient to calculate, in the satellite frame the magnetic field vector and the direction to the Sun once per 30 s, i. e. to solve the same problem that is performed by the ADO instrument in the project AKTIVNYI (J. Klas et al., 1987) with the step of 10 s.

The additional operations are the calculations of the angle between the Y-axis of the satellite and the projection to the satellite plane YZ of direction to the ecliptic North pole.

From values γ the array is formed corresponding to 10-20 min of the flight. Then the system of linear equations is solved, in this case the coefficients c_1 and c_2 are calculated in the equation for γ and from them the "top of spin" is determined for the subsequent interval of 10-20 min.

Auroral Probe is moving along the orbit with the apogee of 20 000 km, i. e. in the region of distances of the Earth where the use of the magnetic field model is possible. Therefore for the Auroral Probe the use of only Algorithm I is sufficient.

The simplest method of the orientation calculation when the spacecraft enters the Earth shadow is the extension of the extrapolation interval of 10-20 min up to 1 hour (duration of the satellite shadowing).

A more complex Algorithm II uses the knowledge of the position of the angular momentum. For the Tail Probe the determination of the position of the angular momentum in space by measurements near the perigee area of the orbit is the necessary part of the attitude restitution algorithm.

In this case the solar sensor data are sent to the computer each 5 sec.

Calculating the matrices of equations (14) and (13) for $\omega = -c_2$ is possible simultaneously with the formation of the array $\bar{\alpha}_i, \bar{\beta}_j$.

At the end of the 10 minutes interval the equations (14), (15) are solved and the position of the angular

momentum vector in space \bar{L}_0 is calculated. These calculations are made for altitudes beginning with those of > 7 000 km where vector of the angular momentum in space remains stable with the accuracy up to the measurements of the direction to the Sun.

Beginning with altitudes of 20000 km within each 10 minutes interval the system of equations (14) and (15) is solved for three values of the ω_1 : $\omega_{11}, \omega_{12}, \omega_{13}$, and the values $J(\omega_{11}), J(\omega_{12}), J(\omega_{13})$ are calculated. Then the ω_{1m} giving the minimum $J(\omega_1)$ is calculated by quadratic approximation:

$$J(\omega_{1m}) = \min_{\omega_1} J(\omega_1)$$

When systems (14) and (15) are solved and $J(\omega_1)$ is minimized, the input of new data on $\bar{\alpha}_i, \bar{\beta}_j$ can be blocked. An organization of calculations is possible with which the interval of time of the formation of the measurement array is equal to the time interval of processing of these arrays for determining the "top of spin". In any case it is evident that the interval of the extrapolation is equal to the sum of the intervals of the formation of the array of measurements and their processing.

Description of some programs used for the ground-based processing

During the ground-based processing of measurements of the solar and Earth's sensors of the PROGNOZ satellites launched before the satellite coordinates were determined by the integration of differential equations of the satellite motion, the Sun and the Moon in non-rotating geocentric equatorial system of coordinates. The effects of the Sun and the Moon and the field of the Earth's gravitation forces were taken into account with the accuracy up to the second zonal harmonics.

Runge-Kutta method (RK) of the fourth order was used for integration with the variable step. In the program RK realising this method the right-hand parts of differential equations of the motion were calculated by DIF subroutine.

Subroutines RK and DIF have a common block COMMON/T/ T, R(18), F(18), RA(6), RL(6), T1, TK. Besides the Subroutine DIF has a common block /G/ GE, GS, GL, SPL, RE.

Before calling the RK the following values should be given to:

- gravitation parameter of the Earth GE = 398.6004;
- gravitation parameter of the Sun GS = 132712517;
- gravitation parameter of the Moon GL = 4.90265;
- parameter of the Earth flattening SPL = 0.0678913965;
- average radius of the Earth RE = 6.371.

In array R(18) there should be put down (for the moment T1) the initial coordinates and the projections of the satellite velocities (projections of the satellite radius-vector on axes X, Y, Z and then the projections of the satellite velocity vector to the same axes), Sun and Moon.

The dimension of variables: thousands of km; (thousands of km)/(thousands of sec). Besides there should be given the initial time T1 and the final time TK in thousands of seconds calculated from the arbitrary defined moment of time.

As a result of the subroutine RK operation, after leaving RK, we obtain in the array R(18) the parameters of the satellite motion, of the Sun and the Moon for the final moment of time TK.

The initial parameters of the Sun and the Moon motion are taken from the Addition to the Astronomical Almanach or from the DE-118 model.

Algorithms for cases of non-standard operation of the attitude determination system

The main objective of the device is to form the TS for scientific instruments. In this case it is essential to send this signal with the period equal to the period of the satellite rotation. The moment of "the first" TS is not critical for the operation of the most instruments, i. e. just the relative position of reference marks is important. Thus, in a non-standard case their absolute reference direction can be obtained by the ground-based processing.

For the Auroral Probe the algorithm is possible which uses only the information on the magnetic field. It can be assumed in this case that the X -axis of the satellite is directed to the point coinciding with the Sun position during the orientation.

The algorithm can be more accurate if it is based on the assumption about the coincidence of the angular momentum vector direction with the direction to the Sun at the final moment of spacecraft axis targeting towards Sun. Then the angular momentum vector is defined by the integration of equations averaged during the satellite rotation. The X axis of the satellite is assumed to coincide with the angular momentum vector.

Such an approach is possible if there are no magnetometer data and if the measurements are sent only from the solar sensor. It is also assumed here that the angular momentum during the initial moment (orientation moment) is directed to the Sun. Then the TS is calculated on the basis of the knowledge of the direction vector to the Sun and the angular momentum vector relative to the satellite as it was described above. The realization of algorithms which use the knowledge of the position of the angular momentum in space should assume the possibility of sending the information about the angular momentum vector position from the Earth via the command radiolink.

To calculate it on the Earth there can be used the telemetry data of the device recording the Earth passing through the field of view (such as DOK, UVAI).

List of parameters sent by the device to the telemetry system

To control the device operation and for the subsequent ground-based processing of the scientific instrument data the following parameters are sent to the telemetry system:

1. The start of the processing interval, coefficients $A_1, A_2, A_3, A_4, A_5, B_1, B_2, B_3, B_4, B_5$ and phase frequencies $\omega_1 = -\omega_2, \omega_2$. These data are transmitted once per ten minutes.
2. Cosines of the angular momentum.
3. TS—the moments of the passing through Y axis, of the satellite YZ plane projection of the direction to the North pole of the ecliptic.

The enumerated parameters are sent from the computer to the buffer device with the memory volume 1024 bytes.

Control of the computer operation

The possibility of sending the following parameters through the command radiolink should be envisaged for the computer operation:

1. The initial conditions of the motion of the satellite mass center (time and six Cartesian coordinates).
2. The initial position of the angular momentum vector in space.
3. The relationship between phase angular velocities of the satellite and the angular momentum relative to the satellite.
4. The initial phase and the angular velocity of the satellite rotation.
5. The initial moment of the passing of the ecliptic North pole of direction projection to the YZ plane through Y axis and the period of the satellite rotation.

Besides the following commands should be envisaged:

- a) transfer to the calculation program using the given vector of the angular momentum and the solar sensor data;
- b) transfer to the calculation program using the given vector of the angular moment and the magnetic field measurements.

Input of measured parameters

Angles α and β are calculated as functions of K_1, K_2 values basing on the fact that the unit vector \bar{S}_m in the satellite frame

$$\bar{S}_m = \begin{pmatrix} S_x \\ S_y \\ S_z \end{pmatrix}$$

is determined by equaltions

$$S_x = \cos \delta_1 \cdot \cos \delta_2$$

$$S_y = \frac{\sqrt{2}}{2} \cdot (-\sin \delta_2 + \sin \delta_1 \cdot \cos \delta_2)$$

$$S_z = \frac{\sqrt{2}}{2} \cdot (-\sin \delta_2 - \sin \delta_1 \cdot \cos \delta_2)$$

In this case δ_1 and δ_2 (in minutes) are found from

$$\delta_1 = 0,5(K_1 + 0,5K_2) + \theta,$$

$$\delta_2 = 0,5K_2 + \psi,$$

where θ and ψ are constants.

References

- [1] Buchgoltz, N. N., Basic course of theoretical mechanics, Part II, (in Russian) "NAUKA" Publ. House, Moscow, 1967.
- [2] Eismont, N. A., Attitude restitution of spacecraft stabilized by rotation, from onboard optical measurements, in: "Spacecraft motion determination", (in Russian) "NAUKA" Publ. House, Moscow, 1975.
- [3] Klas, J., M. L. Pivovarov, V. M. Sinitzyn, N. A. Eismont, Onboard computer for navigation calculations on the AKTIVNYI project, Prepr. IKI Pr.-1221, 1987.
- [4] Wertz, J. R. (ed.), Spacecraft attitude determination and control, D. Reidel Publ. Comp., Dordrecht, Holland, 1978.

ATTITUDE AND ORBIT CONTROL I

ORBIT CONTROL OF SPOT SATELLITES

1. Darrigan, C.; Dulot, J.L.; Forcioli, D. and Micheau, P. (CNES-France):
 "Orbit Control of Spot Satellites" 041
2. Thomas, G.R. (Science Systems-UK):
 "Computer Based Training for Flight Dynamics and Meteosat Spacecraft" 049
3. Leibold, A. (DLR-Germany):
 "Insertion from Supersynchronous and Subsynchronous Transfer Orbit and Navigation Around Active Geostationary Satellites Encountered During Station Acquisition Drift Phase" 055
4. Nagarajan, N. and Rayan, H.R. (ISRO-India):
 "Frozen Orbit Realization Using LQR Analogy" 064
5. Nazirov, R.R. and Timokhova, T.A. (IKI-Russia):
 "Optimal and Quasioptimal Transfer Between Neighboring Elliptical Orbits" 068

ORBIT CONTROL OF SPOT SATELLITES

Christian DARRIGAN, Jean-Louis DULOT,
 Dominique FORCIOLI, Pascal MICHEAU

CNES, Toulouse, France

Abstract

The SPOT system is operational since the February 22nd 1986, SPOT 1 launch date; SPOT 2, the second satellite, was put in orbit on the February 21st 1990, and the station acquisition of SPOT 3, the last first generation satellite, was successfully performed after the September 26th 1993 through an Ariane launch.

Now, three satellites are in orbit, and their relative positions depend on the respect to the station keeping requirements specified for each one. Only SPOT 2 and SPOT 3 products are presently commercialized, SPOT 1 being kept in standby. The topic of this document is to give the main information about the flight dynamics aspects of the system. In that, it synthesizes the specifications related to this field, and recalls specific remarks resulting from the mission analysis. Among following parts, one is described more in detail: the station acquisition, referring to the operational results of SPOT 3 launch: launch phase, description of the operations, station acquisition, maneuvers strategy, definition of the parameters monitored for station keeping, automatic management of maneuvers, relative deviation of the 3 satellites.

Key words: SPOT, station keeping, station acquisition, maneuver, launch.

Context of SPOT attitude and orbit control

Main characteristics of the system

The main mission, already introduced through several publications is now well known. Many passengers are asking for use the infrastructure of SPOT platform to proceed to various experiments: DORIS (SPOT 2/3/4) performs highly accurate altimetric measures which enable to locate the satellite better than 10 cm in radial and 20 cm along track; POAM (SPOT 3) performs measures of the ozone layer; PASTEL terminal (SPOT 4) will realize an optical link with a geostationary satellite (SILEX system).

The platform used for those payloads is hence more and more in demand and has been improved on an on-board concept now well tested.

The AOCS (Attitude and Orbit Control System) management is ensured by a sophisticated and reliable flight software which keeps the three axis stabilization at less than 0.15 degree in the most precise mode. This mode uses inertial wheels for correcting the attitude, thus limiting perturbations which could affect the images quality. Other modes provide a control by thrust (3.5 newtons): they are modes used for operating the propulsion system (long thrusts > 20 s and short thrusts), and specific modes used when the flight software or some equipments are faulty (rough acquisition, sun pointing in survival mode).

The selected orbit has to satisfy most of the observation demands, preferring the scenes located between ± 60 degrees of latitude and reducing the elapsed time to satisfy those demands. Therefore, the orbit is phased on a 26-day cycle for 369 orbits. The 369 ground tracks are characterized by their longitude at the equator; the reference of the track 1 is 330.24 degrees. The distance between successive ground tracks at the equator is 108.6 km, and the two successive ground tracks (i, i+1) are 2823.7 km apart.

On days J and J+5, the ground tracks are one inter-track apart, thus providing accessibility to a five-day sub-cycle as indicated on the following figure.



Figure 1 : Passing days to inter-tracks located between two successive ground tracks

The selection of phasing and repetitivity defines the orbital period, hence the semi-major axis. To maintain an altitude and a constant lighting above a given point is necessary for comparative study of the images. Stability of the altitude is ensured by the constraints on the eccentricity vector (frozen perigee). A constant lighting will be obtained through sun-synchronous (the precession of the orbit plane is linked to the sun rotation speed). This choice imposes this inclination value in relation with the semi-major axis:

$$\frac{d\Omega}{dt} = -\frac{3}{2} \cdot J_2 \cdot a_e^2 \cdot \sqrt{\mu} \cdot \frac{\cos i}{a^{7/2}} = .98561 \text{ degree / day}$$

Therefore, the orbit will be a quasi-polar one, and the lighting level above covered areas depends on the selection of the pass local time at the descending node (at 10:30).

Such an orbit leads to the notion of pass set as shown on the following figure.

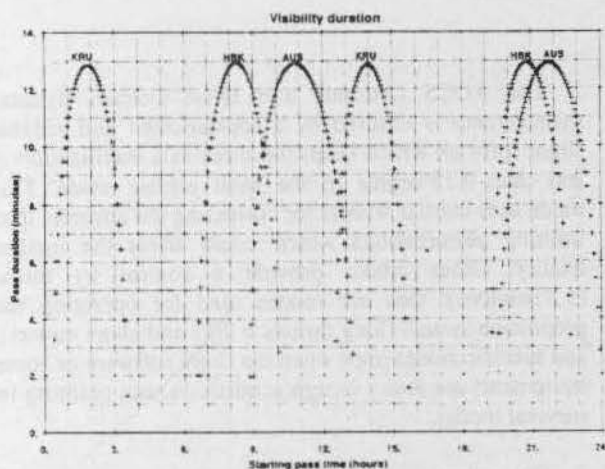


Figure 2 : Set of SPOT passes above AUS (Toulouse), KRU (Kourou), HBK (Pretoria)

The passes above Toulouse [9h - 13h] and [19h - 24h] mark the rhythm of the exploitation; the satellites tracking data enable to refresh the information about the orbit, the maneuvers previsions, the parameters of the correspondance between the on-board clock and the Universal Time, and to elaborate the data required for programming the next day mission. This programming will be done during the afternoon and the corresponding commands are sent during the evening passes.

A daily planning (7 days / 7) is established where all utility tasks are inserted; it is the operational routine during which the orbit corrections needed for station keeping are performed (from 15 days to 6 weeks for the ground tracks keeping at 0 degree, every 14 months for the ground tracks keeping at 60 degrees).

Some perturbations can affect the routine, as anomaly in the payload or in the flight software, and lead to an altered mission capacity; but those cases are rare. Some specific gathering of perturbations can be very critical and lead to the survival of the satellite: in this situation a very simplified attitude control mode is used, which does not need the flight software, and ensures a coarse sun pointing for a sufficient charge of batteries; it happened once for SPOT 1, on the December 16th 1992, and was quickly fixed; it served as a valuable experience to the operational teams.

Main requirements

Concerning the flight dynamics functions and data, there are 2 classes of needs: for the follow-up of the platform (utility) and the payload (programming and pre-processing of images). They are assumed by a specific entity of the ground segment. The first class of needs mainly consists in refreshing the flight software parameters which affect the attitude control; in particular, a deviation less than 2 degrees must be maintained, between the on-board estimated position and real position determined on ground. Sensors masking is also controlled.

The other needs are exploitation aids, and all these data are elaborated from the standard orbit determination. The second class of needs concerns accuracy requirements for the orbit mission determination and the dating precision of image pixels:

Table 1 : Orbit accuracy requirements (max. values)

	Determination	Prediction at 36h
radial	300 m	350 m
across the orbit	300 m	300 m
along the orbit	500 m	1000 m

As the orbit parameters used for pre-processing of the images are transmitted using the payload telemetry, the accuracy should be assessed over the next 36h in prediction for SPOT 4, and it was specified in determination for SPOT 1, 2, 3.

Requirements for the station keeping are the bounds windows:

1. ± 3 km for the reference longitudes at the equator,
2. ± 5 km for the reference longitudes at $\pm 60^\circ$ latitude,
3. ± 10 mn for local time.

The 2nd and 3rd constraints induce an inclination correction, but the third is ensured by the respect of the second one.

The cost of station keeping is conditioned by the inclination drift (.038°/year) and by the semi-major axis drift (from 4 m/day to 26 m/day according to the solar activity). As the mission stretches over 5 years, the dimensioning value considered for SPOT 4 are 0.15 degree for the inclination, and 9 km for the semi-major axis: 33 kg propellant consumption is also dimensioning the station keeping coast.

The requirements set of the system led to use 3 types of orbit modelling. The first one is useful for mission analysis and system reference.

Table 2 : Simplified SPOT orbit model

a	=	7200547	+	8946	.	cos (2 . α_M)
ex	=	0	+	0,000725	.	cos (3 . α_M)
			-	0,000282	.	cos (α_M)
ey	=	0,001144	+	0,000725	.	sin (3 . α_M)
			-	0,000904	.	sin (α_M)
i	=	98,721646	-	0,005466	.	cos (2 . α_M)
Ω	=	Ω_M	-	0,005522	.	sin (2 . α_M)
α	=	α_M	+	0,052587	.	sin (2 . α_M)

(a in meter, and i, Ω , α in degrees)

Ω_M : mean value of ascending node right ascension in inertial reference

$$= \theta(t) + \left(\frac{h_1 - h}{24} \right) \cdot 360 + 180$$

$\theta(t)$: sidereal time at t

α_M : mean value of α
 $= 179.8689 + \dot{\alpha}(t-t_1)$

$$\dot{\alpha} = \frac{369 \times 360}{26} \text{ degrees / day}$$

(t,h) (time, hour) of parameters

(t_1, h_1) (time, hour) of node 1 passage

$$h_1 = 10:30$$

$$t_1 = j_1 + \left(\frac{h_1}{24} - \frac{\varphi_1}{360} \right)$$

j_1 = day of node 1 passage

φ_1 = node 1 longitude = 330.24 degrees

It enables to represent the theoretical tracks of the phased orbit, without considering the perturbations which require phasing keeping at various latitudes: the atmospheric drag and the moon-solar potential. On the day J of the cycle, the pass on the required tracks is conditioned by the α_M value.

The second one is at the operational level: a more sophisticated analytic development is used for the maneuvers computation needs which are based on a mean parameters notion, and to ensure the standard orbit determination.

The corresponding software package is integrated into the image processing centers (SPOT 4), the initial orbit parameters being provided by the ground interfaces or transmitted through the image telemetry.

In the first generation SPOT system, the orbit determination is based on a numerical integration of the main perturbation functions, thus providing the respect of required accuracies ; this is the third model used.

Station acquisition

Launch

- The characteristics of the orbit targeted by the launcher are specified according to the description of Table 2. With this approach, Arianespace can readjust the numerical values of the parameters to be reached: from the preliminary study to the final mission review, 3rd stage orientation phase included, the latitude of the separation point varies, bringing subsequent changes in the injection point coordinates. This technique enables a maximum coherence between the trajectories of both launcher and SPOT.

Furthermore, the values of constant terms differ from nominal values for 3 parameters: the semi-major axis is reduced by the accuracy at 3 σ planned by Arianespace (3.6 km), thus avoiding later any chance of collision on the nominal orbit; the decreased value depends also on the drift rate relative to SPOT satellites already in orbit, and on the lapse time needed for reaching the assigned positions. The inclination and the right ascension of the ascending node are in the same way corrected by a value which corresponds to their drifts observed during the nominal lapse time between two successive corrections (ref. station keeping).

- Afterwards, characteristics of the launcher trajectory are defined according to the mass to be satellized and the available performance; for SPOT 3 launch, the payload included 8 satellites (SPOT 3 / STELLA / 6 micro-sats) weighting up to 2300 kg, for a capacity of 2800 kg; this margin permits a 20 mn launch window, and the possibility to keep a sufficient performance reserve which could ensure the required parameters to be obtained before the propellants exhausting.

This margin was beneficial for SPOT 3 because launch occurred at the end of the window due to bad weather condition: the same reasons forbid the first try, the September 25th. The launch time is defined by the flight duration until the moment the separation occurs and by separation time; those two parameters are depending upon the characteristics of SPOT orbital plane and particularly the local time (22:30) at the ascending node. An other important sequence of the launch lays in the orientation phase of the 3rd stage, which occurs after the 3rd stage propeller extinction: it is intended to ensure the correct attitude of SPOT at the separation, as well for the 7 other satellites, through various orientation maneuvers and speed increments.

Those characteristics are completed by a last element: the dispersion matrix concerning the orbital parameters reached; it considers dispersions connected to the guidance, the propulsion, the flight duration, the attitude error during the orientation phase. The main contribution is provided by an inertial platform; the last flights used an efficiency gyro-laser platform. The Table hereafter shows the typical accuracy:

Table 3 : Theoretical injection accuracy at 1 σ launcher

a (meters)	1.2
e	.00017
ω (degrees)	6.23
i (-)	.027
Ω (-)	.0031
α (-)	.22

The total duration of Ariane mission for SPOT 3 was 29 minutes, and the separation of SPOT 3 occurred after 17 minutes.

The launch diagnosis is performed following the first orbit determinations and is confirmed before switching to the fine pointing attitude mode. Though indicative only, a first diagnosis is quickly known after the separation, using the Ariane telemetry and Wallops radar tracking data. All SPOT launch were successfully performed by Arianespace (AR 1 / SPOT 1, AR 40 / SPOT 2 and 3) as indicated in Table 4.

Table 4 : Observed accuracy for SPOT launch (in σ launcher)

	SPOT 1	SPOT 2	SPOT 3
a	+ 0.1	- 2.4	- 0.7
e	+ 0.2	+ 0.4	- 0.35
ω	- 0.2	+ 2.9	+ 1.2
i	- 0.15	- 0.6	- 2.3
Ω	+ 0.15	+ 0.9	- 2.1
α	+ 1.0	+ 1.8	- 0.2

Description of the operations

The station acquisition of SPOT satellites includes the attitude acquisition, the orbit acquisition and the payload starting, and particularly the acquisition of the first image obtained within the 48 hours following the launch. SPOT 3 operations represents so far the maximum density workload as the whole set of positioning phase operations were completed in less than a week.

The succession of the different phases is shown in Table 5 (H0 is the launch time):

Table 5 : Main steps of the positioning phase

Step	Start	End	Duration
Launch pad	H0 - 10h30	H0	
Launch	H0	separation	17 min
Pyrotechnic sequence	separation	solar panel deployment	30 min
Attitude stabilization	solar panel deployment	switching to MPF	10 hours
$\Delta V1$	switching to MPF	switching to MCO1	36 hours
$\Delta V2$	switching to MPF after MCO1	switching to MCO2	48 hours
$\Delta V3$	switching to MPF after MCO2	switching to MCO3	48 hours

MPF : Fine pointing attitude mode.

MCO : Maneuver mode (thrust duration > 20s).

MCC : Maneuver mode (thrust duration < 20s).

The first MPF is switched by the ground control, but the others, after maneuvers, are automatically switched by on-board software.

Timing of the activities depends on the passes above Toulouse. For the launch, the tracking stations network is reinforced by Wallops (WPS), Prince Albert (PAS), Katsura (KTS) and Santiago (AGO) stations which are a great contribution to an optimum observation of the attitude acquisition sequence. Kourou (KRU), Kiruna (KRN) and Pretoria (HBK) stations complete the network. Immediately after MPF switch, which occurs at the second pass above Toulouse, the ground segment is operating in routine mode. This mode corresponds to the starting of all interface data transfers enabling the image scheduling system. This mode stays open to any manual intervention which could be necessary during first steps, such as maneuvers computing and orbit determination.

The flight dynamics entity is a part of the SPOT ground segment; its task is to compute the orbits and maneuvers required for a good running of SPOT mission. Moreover, some AOCS parameters used by the flight software are updated, and sent to satellite through the associated teleloading: the position in orbit used in on-board software, the sensors masking, the coefficients of guidance. It ensures the elaboration and optimisation of the maneuvers programming, and after the maneuver, the assessment of the performances using telemetry data.

Finally, it also defines parameters for the board and ground reference time synchronization.

An important human potential is necessary for performing these operations. For the orbit control, three mixed teams (flight dynamics and operational specialists) are used for the station acquisition phase. During the first orbits, key meetings are held between project managers after each main phase; everyday, specialized boards (satellite, orbit, maneuver, payload) assess past and future operations, and are represented to the main board which after an overall synthesis takes decisions about the future operations.

Attitude acquisition

The flight software starts at the identification of the separation, and control the pyrotechnic sequence, which unlatches and puts on the latched equipments during the launch phase; it runs automatically until deployment and spinning of the solar panel. If a defect occurs, the ground segment must immediately send the necessary commands, this requires the best tracking capacity during this phase.

List of the main events are given in Table 6, along with the timing since the separation time.

Table 6 : Attitude acquisition

Separation SPOT 3 / AR 40	t0	WPS (=11 mn)
Mirrors payload releasing and positioning		
Arm spreading of solar panels		
Angular speeds reduction	+ 3 mn	PAL (=10 mn)
Roll and pitch acquisition		
Yaw acquisition		
Fine attitude acquisition	+ 11 mn	
Solar panels deployment	+ 28 mn	KTS (=12 mn)
Starting of the solar panels spin (at $\alpha = +177$ degrees)		
End of pyrotechnic sequence	+ 30 mn	
Starting of mission attitude control	+ 10 h 30 mn	
($\theta_{xyz} < 0.15$ degree ; $\dot{\theta}_{xyz} < 0.05$ degree/sec)		

This sequence includes the attitude acquisition, managed automatically by on-board software which change on various modes as: speed reduction, coarse acquisition, and fine acquisition.

Then, the attitude control is done by control thrusts. This state is maintained and monitored during

4/5 revolutions to ensure a stable guidance. After that, the ground commands switch on the "mission" attitude control mode (MPF), which is controlled by inertial actuators; this mode is kept during the complete mission, except for maneuvers programming during which, the attitude control by thrust is temporarily used, and for contingency situations (survival mode, equipment failure). The total propellant consumption during SPOT 3 attitude acquisition phase was 1.3 kg.

Orbit acquisition

Quality and reliability of the AR 40 launcher entails no particular arrangement for the first orbit determinations. They are ensured using the 2 GHz network tracking data.

The quick set up of the transponder enables the first orbit determination using range and range rate measurements.

Table 7 : First orbit determinations at separation time

	a (meters)	e	ω (degrees)	i (degrees)	Ω (degrees)	α (degrees)
Orbite visée	7182689	0.00135	112.603	98.7438	341.6291	38.071
OD1 AGO1-WPS2	7181930	0.00127	118.384	98.6803	341.6068	38.272
OD2 AGO2-GDS1	7181899	0.00127	118.299	98.6807	341.6071	38.270
OD3 GDS2-KRN1 -HBK1	7181891	0.00127	118.167	98.6809	341.6085	38.270
OD4 KRN2-AUS1 -HBK2	7181821	0.00128	118.367	98.6815	341.6062	38.268
OD5 KRN3-AUS2	7181800	0.00128	119.106	98.6822	341.6064	38.266

The orbit determination strategy is very simple:

- OD1: adjustment of the position on orbit using AGO1 and WPS2 measures,
- OD2: adjustments of the 6 parameters,
- OD3, OD4: idem,
- OD5: adjustment of drag coefficient.

Manoeuvres

• The station acquisition has a dual aim: to obtain matching of the ground tracks with the longitudes specified when passing at the equator, and to place the satellite on orbit at a given angular distance from the other two satellites.

The phase lag between ground tracks and the relative distance between satellites are conditioned by the orbital period, hence the semi-major axis value.

The successive adjustments necessary to achieve these requirements will be done on this parameter.

The launcher trajectory has been designed to achieve a maximum performance in the acquisition of the local time. On the contrary, the inclination can be degraded by a deviation equivalent to a two-year natural drift, this leads a correction included in the station acquisition. Finally, the eccentricity vector will be adjusted to match the stability and altitude criteria above a given point. Those corrections will be performed jointly with the semi-major axis ones.

- The maneuvers strategy consists to inject the satellite on a drift orbit, this ensures a significant relative motion with the other satellites orbiting. The semi-major axis selected is 20 km below the nominal value (i.e. the value ensuring the ground tracks phasing with the required longitudes); so, in the worst case the maximal delay for the station acquisition is 17 days. Moreover, it avoids to get SPOT orbit jammed by the other items orbiting (3rd stage and other passengers).

Two parameters are conditioning a drift readjustment: the launcher dispersion on the semi-major axis (± 3.6 km at 3σ) can increase or decrease the drift, and the launch time within the window modifies the angular distance between satellites. The geometrical configuration depends also on the launch day. The mission analysis covers these possibilities and enables identification of all the situations, particularly the S-band jamming which occurs when a satellite passes "under" another.

- Concerning the station acquisition, the selected option consists in performing the three following maneuvers:

- ΔV_1 is a readjustment of the drift speed, this according to the hazards encountered, the geometrical configuration of the satellites on the launch day, and the time needed to compute following maneuvers; it happens rather quickly (36h after SPOT 3 launch) and enables to proceed a first thrust calibration.

This is done by two speed increments performed at 180 degrees offset position on orbit (this is necessary to include a preliminary correction of the eccentricity vector).

- ΔV_2 is an inclination maneuver which needs a 90° tilting of the satellite around its yaw axis, this results from the thrusts position on the platform. As the attitude control cannot ensure the thrust will be strictly

perpendicular to the orbit plane, this entails a dispersion in the orbit plane.

Programming a bias yaw angle is possible to offset this effect; nevertheless, this is a delicate action to estimate.

- ΔV_3 targets the semi-major axis nominal value, when the relative distance between the SPOT satellites is reached. Priority is given in the ground tracks freezing in their keeping windows around the reference longitudes; the accepted deviation about the mutual angular position between satellites is ± 3 degrees.

- This last maneuver completed, the orbit complies with the requirements of the mission. However, keeping the phasing window can require quickly a semi-major axis readjustment. For all maneuvers performed during the positioning phase, the MCC mode (long thrusts) is used; this is not so fine accurate than short thrust mode (MCC) which enables a better management of control thrusts during the station keeping maneuvers.

The programming of a maneuver is made in two steps: the elaboration of orbital characteristics (date, position, speed increment), the elaboration of thrust control, and updating of AOCS parameters used by the attitude control.

The first step is conventional: two speed increments nearly diametrically opposite in the orbit plane to correct [a, ex, ey], and one speed increment across the orbit plane at the ascending or descending node pass to correct the inclination correction.

Two kinds of requirement are considered: AOCS requirements (sensor masking, limitation of the thrust duration according to the season, etc...), and operations requirements (real time, post maneuver tracking data quickly available for analysis).

The second step takes into account the characteristics of SPOT platform propulsion system and the attitude control performed during the maneuvers.

The main optimization factors are the consideration of a pressure drop during the thrust, the estimation of tank pressure, the efficiency evaluation, the possibility to program a yaw bias angle for maneuvers outside the plane.

The station acquisition of SPOT 3 has been realized according to the pattern previously described in record time (5 days) and with excellent results of maneuvers, particularly the last one.

The post-maneuver orbit determination adjusts speed increments: the transparency of routine maneuvers in the ground segment operation is a main requirement for the future SPOT 4 system.

Table 8 : Main results of the SPOT 3 station acquisition

	$\Delta V1$	$\Delta V2$	$\Delta V3$
Parameters deviation	$\Delta a = 12.94 \text{ km}$ $\Delta e = 1.10^{-4}$ $\Delta \omega = -3 \text{ deg}$	$\Delta i = 6.3 \times 10^{-2} \text{ deg}$	$\Delta a = 8.13 \text{ km}$ $\Delta \omega = -3 \text{ deg}$
ΔV	6.71 m/s	8.19 m/s	4.21 m/s
Thrust duration	232 s + 246 s	620 s	158 s + 181 s
Consumption	5.4 kg	7.4 kg	3.3 kg
Accuracy	$\Delta a = -297 \text{ m}$	$\Delta i = 1.6 \times 10^{-3} \text{ deg}$	$\Delta a = 8 \text{ m}$
Efficiency	.977	.975	.998

Station keeping

The monitored parameters (P1, P2, P3, P4) enable the specifications required checking.

- Holding of the phasing at a 0 degree latitude (P1) is shown by the deviation at the equator between the ground track longitude of the descending node orbit and the corresponding reference longitude; orbits are numbered from 1 to 369, the orbit 1 passes at reference longitude 330.24 degrees (cf. Table 2).

The evolution of this deviation depends on the semi-major axis drift, hence on the solar activity effect upon the atmospheric density along the orbit.

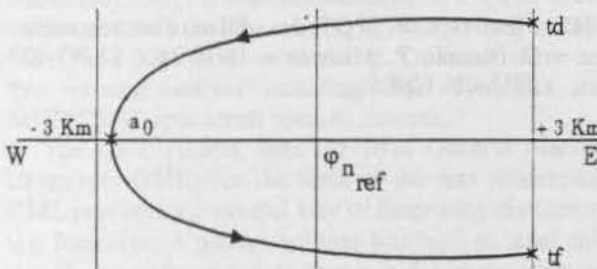


Figure 3 : P1: evolution of the phasing at a 0 degree latitude

ϕ_{n_ref} : reference longitude for the orbit n
td, tf : initial and final time of the keeping in bounds window

If during the period [td, tf] the semi-major axis drift is constant, the P1 parameter describes a parabola, the which top is reached when the semi-major axis passes through its nominal value $a_{(0)}$.

This is the value which would ensure stability of the phasing if the semi-major axis drift value could remain at

zero. This nominal value depends on the inclination by the sun-synchronous relation ($\dot{\Omega} = \text{constant}$). Between two inclination corrections, the nominal value of semi-major axis decreases of 100 meters.

At tf, the window outgoing needs the phasing holding maneuver which consists in the semi-major axis correction to optimize the course within the window (beginning at +3 km and pass on top at -3 km). Range of the corrections vary from 20 to 300 meters (thrust duration < 20 s).

- Holding of the phasing at a ± 60 degrees latitude (P2) is controlled with the same considerations, but margins are increased at $\pm 5 \text{ km}$ to consider the inclination drift.

Holding of the phasing at a 0 degree latitude ensures the holding at 60 degrees, until the inclination causes an outgoing from the window; an inclination correction ($\approx 0.04 \text{ degree}$) is also needed.

- The difference (P3) between the local time at the descending node and the theoretical local time (10:30) describes a parabola in accordance with the inclination.

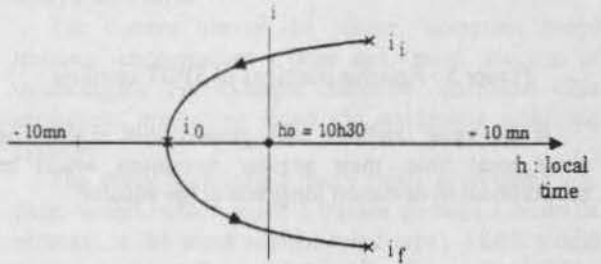


Figure 4 : Evolution of the local time

The principle of the window course is similar to the phasing holding one: the top of the parabola corresponds to the pass at the nominal value of the inclination; it is the value which would ensure the stability of the local time, if the inclination drift could be zero. i_0 and $a_0(i_0)$ values appear as constant terms in the reference model of SPOT orbit (Table 2). As the evolution of the inclination is conditioned by an external criteria (phasing holding at ± 60 degrees), the local time clearance is limited to ± 40 seconds for the 10 minutes specified.

- Stability of the altitude (P4) depends on holding of the eccentricity vector characteristics: the radius of the circle described by the end of the eccentricity vector must be very small against the eccentricity value.

In fact, these corrections are integrated in the phasing holding maneuver and ensure the parameters e and ω to stay in specified values.

• Furthermore, as the system is made up of 3 satellites, SPOT IMAGE has expressed requirements about their relative position as to obtain stereoscopic images. SPOT 1 is kept in standby to induce a minimum perturbation to the two remaining satellites.

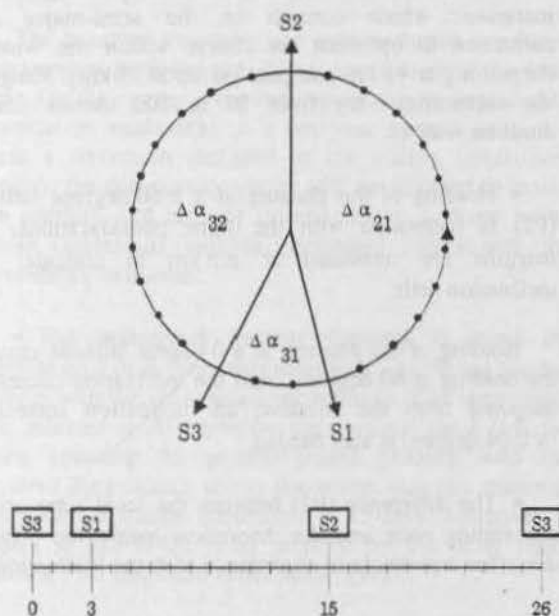


Figure 5 : Relative positions of SPOT satellites

If the three satellites were phased with exactly the same local time, their angular deviations would be proportional to deviation longitude at the equator:

$$\Delta\alpha_{31} = \frac{3}{26} \times 360 = 41.5 \text{ degrees}$$

$$\Delta\alpha_{32} = \frac{11}{26} \times 360 = 152 \text{ degrees}$$

More precisions of station keeping are available in ref. 1.

All these maneuvers are automatically provided during the daily processes performed by the ground segment; they ensure follow-up of parameters previously described, identification of windows outgoings hence the dates of maneuvers, and generation of the on-board programming.

Conclusion

With a favourable injection configuration with regard to the position of SPOT 1 and SPOT 2, the SPOT 3 station acquisition has been quickly achieved: three maneuvers in less than 6 days have been performed taking into account programming constraints of the first image acquisition. This delay is the minimum possible for such operations and the reliability of satellite and ground system team has been again demonstrated.

Now, a new ground system has been developed with more efficiency and ergonomics for the future SPOT 4 and next satellites; new possibilities are offered such as autonomous navigation and station keeping using DORIS measurements. That will be a subject for further publication.

References

- [1] Survey on SPOT system orbit-keeping exploitation (1986-1990) - P. Micheau - 3rd International Symposium on Spacecraft Flight Dynamics, Darmstadt, Germany, 30 Sep.-04 Oct. 1991, p.171-176 - ESA SP.326.
- [2] Analyse de mission pour la mise à poste SPOT 3 - D. Forcioli, P. Micheau - 10/09/93 - S3-NT-633-2560-CN, CNES.
- [3] Définition de l'orbite visée pour SPOT 3 / SPOT 4 après séparation du lanceur - J.L. Dulot, P. Micheau - 22/05/91 - S3-NT-0-1411-CN, CNES.
- [4] Mise à poste SPOT 3 - Bilan d'orbitographie - D. Forcioli, P. Micheau - 15/10/93 - S3-NT-633-2913-CN, CNES.

COMPUTER BASED TRAINING FOR FLIGHT DYNAMICS AND METEOSAT SPACECRAFT

Graham Roland Thomas
Science Systems (Space) Ltd
c/o ESOC
Robert Bosch Strasse 5
64293 Darmstadt, Germany
gthomas@esoc.bitnet

Abstract

With its friendly language and completely integrated graphics and communications capabilities the Flight Dynamics Computer Based Training (CBT) Facility is everything the developer requires to turn their knowledge into sophisticated, technical training courses. It incorporates high quality graphics and has an open communications interface to allow current and future connections to external applications. For the author it provides a simple and effective suite of commands to develop training material. For the trainee, logical layout and access to help and graphical data via hypertext, provides a quick and pleasant learning system.

Key words: Authoring Language, Hypertext.

Introduction

The CBT facility at the European Space Operations Centre (ESOC) was developed between March 1991 and September 1992. It was implemented on a Sun workstation and was the first training system written specifically for a high level of learning. Currently there are five training courses including flight dynamics and METEOSAT spacecraft specific courses.

The CBT system uses the IBM General Markup Language (GML) for the basis of the text processing. GML provides a powerful way of describing mathematical formulae. A picture scanner was used to input colour photographs and data sheets and a graph viewing tool gives access to these pictures. The creation of the CBT facility pulled together a mass of technical data onto a workstation. The training facility is now also being used to store reference documents and manuals.

The paper covers the full story of the development and implementation of the training facility. The background provides information on the CBT technologies and the requirements that were created. The training facility is broken down into its key areas, each of which is described in detail. The areas covered are: authoring language, applications, communications and course structure. A list of available courses is given at the end.

Background

Recurrent or long-duration projects, like METEOSAT Operations (MOP) and Ulysses, have produced a requirement for staff re-training and training of new staff. A dedicated computerised training facility was implemented in order to provide this and to achieve a consistent and guaranteed quality of training.

Two studies were made before the systems final implementation and these are summarized below.

CBT Technology and Product Survey¹

The aim of the survey was to establish the current technologies and system features of third party computer based training products and to summarize these in a comparable form.

The current use of the phrase "computer based training" encompasses a large and varied selection of technologies. For example computer controlled slide projectors, interactive video and mainframe authoring systems.

The study highlighted many types of systems e.g. page turners, which guide a trainee through a series of screens, to the more sophisticated types which would guide a trainee through a series of exercises. Often these exercises are enhanced with graphical, sound and video information. Such systems would take trainee input via a keyboard, mouse or lightpen. They also provide analysis tools in order to monitor the performance of a trainee.

The survey noted that, "A system which requires user interaction can obtain longer and higher levels of attention and therefore result in an improved performance from a training system".

In summary the current most advanced CBT systems have the following features:

- ✓ Control of the learning route.
- ✓ Checking and marking trainee work.
- ✓ Lesson presentation management.
- ✓ Record keeping.
- ✓ Statistical analysis of results.

COMPUTER BASED TRAINING FOR FLIGHT DYNAMICS AND METEOSAT SPACECRAFT

Graham Roland Thomas
Science Systems (Space) Ltd
c/o ESOC
Robert Bosch Strasse 5
64293 Darmstadt, Germany
gthomas@esoc.bitnet

Abstract

With its friendly language and completely integrated graphics and communications capabilities the Flight Dynamics Computer Based Training (CBT) Facility is everything the developer requires to turn their knowledge into sophisticated, technical training courses. It incorporates high quality graphics and has an open communications interface to allow current and future connections to external applications. For the author it provides a simple and effective suite of commands to develop training material. For the trainee, logical layout and access to help and graphical data via hypertext, provides a quick and pleasant learning system.

Key words: Authoring Language, Hypertext.

Introduction

The CBT facility at the European Space Operations Centre (ESOC) was developed between March 1991 and September 1992. It was implemented on a Sun workstation and was the first training system written specifically for a high level of learning. Currently there are five training courses including flight dynamics and METEOSAT spacecraft specific courses.

The CBT system uses the IBM General Markup Language (GML) for the basis of the text processing. GML provides a powerful way of describing mathematical formulae. A picture scanner was used to input colour photographs and data sheets and a graph viewing tool gives access to these pictures. The creation of the CBT facility pulled together a mass of technical data onto a workstation. The training facility is now also being used to store reference documents and manuals.

The paper covers the full story of the development and implementation of the training facility. The background provides information on the CBT technologies and the requirements that were created. The training facility is broken down into its key areas, each of which is described in detail. The areas covered are: authoring language, applications, communications and course structure. A list of available courses is given at the end.

Background

Recurrent or long-duration projects, like METEOSAT Operations (MOP) and Ulysses, have produced a requirement for staff re-training and training of new staff. A dedicated computerised training facility was implemented in order to provide this and to achieve a consistent and guaranteed quality of training.

Two studies were made before the systems final implementation and these are summarized below.

CBT Technology and Product Survey¹

The aim of the survey was to establish the current technologies and system features of third party computer based training products and to summarize these in a comparable form.

The current use of the phrase "computer based training" encompasses a large and varied selection of technologies. For example computer controlled slide projectors, interactive video and mainframe authoring systems.

The study highlighted many types of systems e.g. page turners, which guide a trainee through a series of screens, to the more sophisticated types which would guide a trainee through a series of exercises. Often these exercises are enhanced with graphical, sound and video information. Such systems would take trainee input via a keyboard, mouse or lightpen. They also provide analysis tools in order to monitor the performance of a trainee.

The survey noted that, "A system which requires user interaction can obtain longer and higher levels of attention and therefore result in an improved performance from a training system".

In summary the current most advanced CBT systems have the following features:

- ✓ Control of the learning route.
- ✓ Checking and marking trainee work.
- ✓ Lesson presentation management.
- ✓ Record keeping.
- ✓ Statistical analysis of results.

Training Facility General System Requirements

The second study highlighted the expected requirements of a training system for the Orbit and Attitude Division at ESOC. These requirements were obtained from discussions with end users and from the product survey. The following is an overview of the top level requirements:

- A training system author will be able to define multiple paths through any training sessions to cater for varying trainee abilities. It also allows the training session to be tailored to achieve different course goals.
- The production of training material should be quick and easy with the use of preferred editors. The choice of the authoring language should not itself require extensive training. It should be effective and simple.
- The authoring method should include the automatic checking of the integrity of the course material so that debugging is achieved before releasing into the training facility.
- The presentation of graphical data is essential in the flight dynamics discipline. Graphical output will be produced by external programs and therefore the training system must be able to display this data.
- Similarly the training system must be capable of displaying mathematical symbols and equations. The equations will form part of the reference material to the course work.
- The presentation style of the course work must be consistent throughout all courses.
- The use of various fonts and text highlighting will assist in the presentation of course material.
- One main advantage of a computer training system is that a trainee is able to take course work at an individual pace. Therefore the trainee must be able to logout from a training session and return at a later date to the same position, this function is similar to a bookmark.

Man-Machine Interface

The interaction between trainee and the training system will be in the form of questions and answers. Each answer will be marked to give immediate feedback. The trainee will be required to provide the answers in one of the following forms:

- Selection of true or false.
- Multiple choice - Selection of one answer from a number of options
- Numerical - Input of numerical solutions, this can be either a single number or a related set of numbers.

If the trainee fails to answer the question correctly the system should give immediate feedback so that the trainee may do the following:

- Repeat the question up to a defined or default number of tries.
- Access general help, which is made available at all times.
- Access a hint, which is a list of keywords to give access to specific help.

Finally the access to the pages of the training material will be done with the selection of the previous, next, first, last or a required page by number, by mouse or by keyboard command.

Environment

The training course will operate on UNIX based Sun Sparc machines. The training courses will be made available at all times and from a number of terminals.

Orbit and Attitude Division Computer Training Facility

The third party products that were available could not comply with the user requirements. Many of these products were only available for PC's and none of them could display the level of equation complexity needed.

Authoring Language

An authoring language must contain all that is necessary to describe the layout of text and also allow the description of the training aspects of the text. The language for the current version of CBT is the IBM's General Markup Language (GML). The GML syntax is a set of keywords which are used to describe document and page layouts. The GML syntax was used for the following reasons:

- The mathematical description language incorporated into GML, called the Mathematical Formula Formatter (MFF), is a complete, powerful and simple method to describe mathematical equations. The description of an equation is achieved with the use of English language terms which can be understood without the need for any special graphical output.
- Most of the technical documentation written within the Orbit and Attitude Division, prior to the start of the project, was produced on an IBM GML system.

The use of the GML syntax also allowed the development of the software to coexist with the production of training material. The first training exercises were tested and debugged on paper.

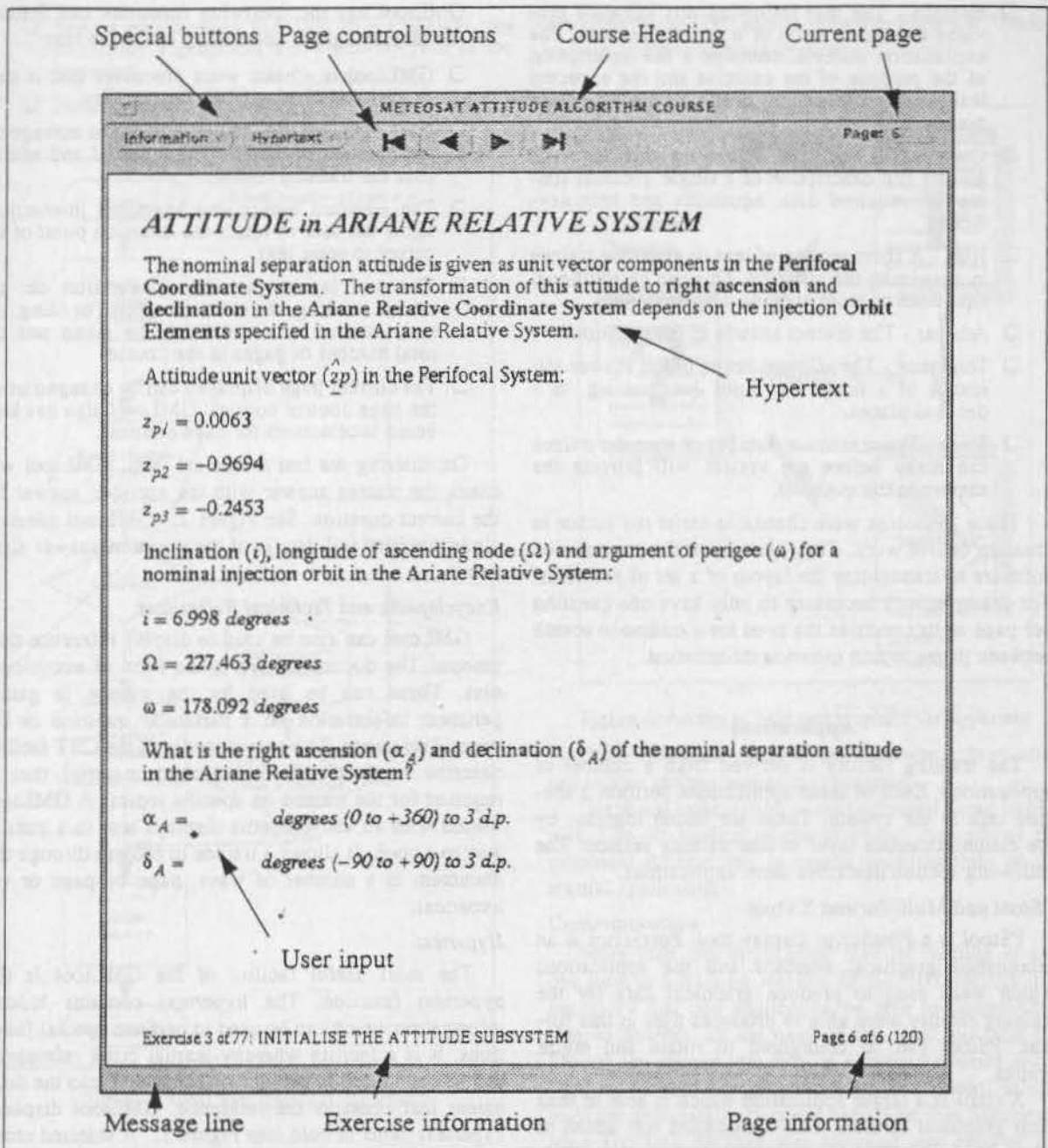


Figure 1: GMLtool main window

A sub-set of the GML syntax for the presentation of text was taken. This ensured that current and future course material would conform to the same format and presentation style. The subset allowed the creation of the standard types of page objects. These are:

- Headings (six levels).
- Paragraphs.
- Line and page breaks.

- Bulleted, ordered and unordered lists.
- Text highlighting using font changes and bold or italicized lettering.

GML Extensions

The GML language was extended with the use of additional keywords to allow the creation of course material. The following is a list of some of the keywords that are available:

- Explain - The text following this keyword provides the introduction of a set of questions. The explanation material contains a full description of the purpose of the exercise and the expected level of comprehension of the problem on completion.
- Question - The text following this keyword gives a full description of a single question stating the required data, equations and help keywords.
- Hint - A short section of text to assist the trainee in answering the question. This can be additional equations or more specific help keywords.
- Answer - The correct answer to the question.
- Tolerance - The allowed limits of the answer tolerance of a numerical input question e.g. to 5 decimal places.
- Tries - The maximum number of tries the trainee can make before the system will provide the answer to the question.

These keywords were chosen to assist the author in creating course work. They also allow the presentation software to standardize the layout of a set of exercises. For example, it is necessary to only have one question per page as this reduces the need for a trainee to search between pages to find question information.

Applications

The training facility is derived from a number of applications. Each of these applications perform a specific task in the system. These are bound together by the communications layer in one training session. The following section describes these applications.

PSstool and Multi-format XVtool

PSstool is a PostScript display tool. PostScript is an established graphical standard and the applications which were used to produce graphical data for the training facility were able to produce files in this format. PSstool can be configured to rotate and resize graphs.

XVtool is a larger application which is able to read most graphical formats. This application was added to allow colour pictures to be presented on the screen. A high resolution colour scanner was installed into the training facility and this was used to import colour pictures and spacecraft data sheets.

GMLtool

The main window of GMLtool is shown in Figure 1: "GMLtool main window". It shows a typical input window which requires a numerical answer. Note the simple layout which provides easy comprehension of the question text.

GMLtool has the following functions and features for the displaying and controlling of course text:

- GMLtool is a basic word processor that is used to load and display GML format files.
- GMLtool uses the CBT extensions to manage the presentation of the training material and administer the training course.
- The standard mouse and keyboard interactions allow the user to select the insertion point of the cursor to enter text.
- The tool layout includes information on: the course heading, the current exercise heading, the total number of exercises to be taken and the total number of pages in the course.
- The current page displayed can be changed using the page control buttons. GMLtool also has keyboard accelerators for page controls.

On entering the last numerical item, GMLtool will check the trainee answer with the encoded answer for the current question. See Figure 2: "GMLtool question algorithm" for full details of the question/answer algorithm.

Encyclopedia and Technical References

GMLtool can also be used to display reference documents. The documents are in the form of encyclopedias. These can be used by the trainee to gather pertinent information on a particular question or for general reference. The encyclopedia in the CBT facility describe in detail the background material that is required for the trainee on specific topics. A GMLtool loaded with an encyclopedia displays text in a similar way to a book. It allows a trainee to browse through the document in a number of ways, page by page or via hypertext.

Hypertext

The most useful facility of the GMLtool is the hypertext function. The hypertext contains hidden information which can be used to perform special functions. It is a facility whereby textual cross references can be configured to provide direct access into the document that contains the reference. GMLtool displays hypertext items in bold (see Figure 3: "A selected cross reference").

By placing the cursor over a hypertext item and performing a double click, with the select mouse key, one of 3 actions is invoked. These are:

- A request for a cross referenced document to be displayed. The system will automatically open the document at the position of the cross reference which is given in the keyword.

- Send a message via ToolTalk to a graphical tool to display a graphical file which is given in the keyword.
- Send a generic message.

afforded by the GMLtool is shown in Figure 4: "Access to help and graphics via hypertext".

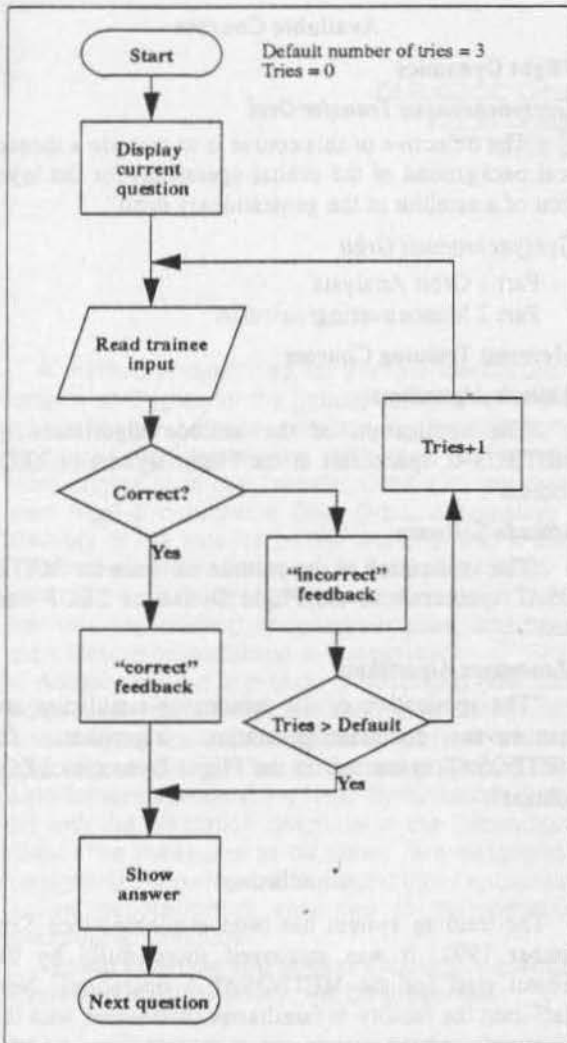


Figure 2: GMLtool question algorithm

system. The transformation of this attitude to the **Ariane Relative Coordinate System** depicted in the Ariane Relative System.

Figure 3: A selected cross reference

Hypertext items include text cross references, figures displayed on a graphics viewer and tables. Selection of these items may require a CBT application to start. This is handled automatically by the communication package. The access to information which is

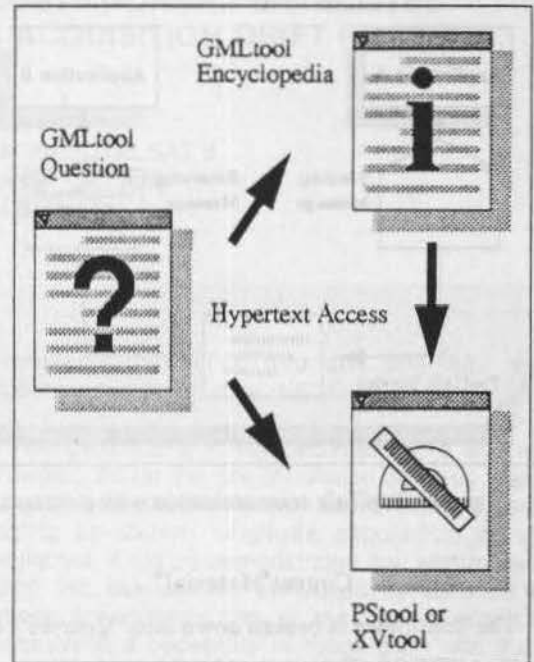


Figure 4: Access to help and graphics via hypertext

Other reference material provided are abbreviation definitions and mathematical constants.

Graphical information is also accessed using hypertext. The off loading of the graphical data allows the graphical applications to evolve independently of the textual applications.

Communication

More than one application may be running at any one time in a training session. In the CBT facility it is necessary that one application be able to communicate to another. In the case of the GMLtool and the PStool, the trainee selection of a figure keyword in the GMLtool would be communicated to a PStool to display the associated graphical data. The Sun Microsystems ToolTalk package was installed into each of the applications (see Figure 5: "ToolTalk communication with messages"). It is an intelligent messaging system which can be configured with application parameters. The parameters include information on how to start applications. It therefore allows each application to be automatically started when required by the training session.

In addition to the specific hypertext objects the author is able to place into the training material special tags which can be converted into ToolTalk messages. The ToolTalk product is standard across the Sun Open-

windows system applications and therefore the training system is capable of linking to other applications.

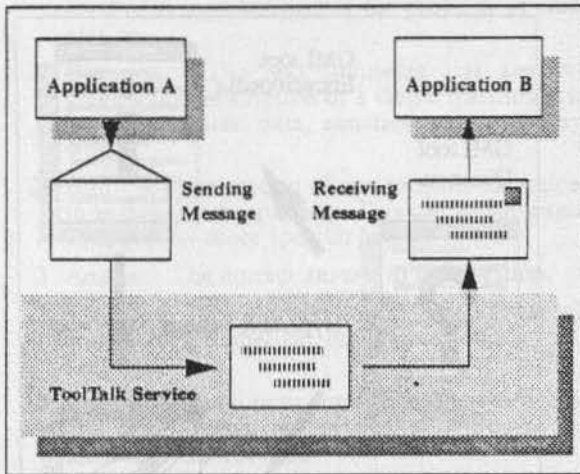


Figure 5: ToolTalk communication with messages

Course Material⁴

The Teachware is broken down into "Courses", e.g.:

- METEOSAT Attitude Algorithms.
- ARTEMIS Command Generation Software.
- Motion in Synchronous Orbit.
- Injection into Synchronous Orbit.

A given Course is broken down into "Tasks" which are actions performed during operations or overall goals, e.g.:

- Monitor Spacecraft Nutation.
- Generate Spin-up Manoeuvre Command.
- Calculate Perturbations on Geosynchronous Orbit.

A given Task is further broken down into question-units or "Exercises" in such a way that an Exercise may be presented on the monitor in a user-friendly and efficient manner, e.g.:

- Addresses of accelerometer datations in the TM.
- Conversion of accelerometer datations to engineering units.
- Determine Sun Position.
- Evaluate Sun Pressure Acceleration.

To support the trainee in the solving of the exercises, he is given hypertext access (managed by the CBT) to other teachware files containing background Information. These files are currently split into 3 generic groups or levels;

- Encyclopedias.
- Dictionaries.
- Miscellaneous Information (Abbreviations, Constants etc.).

Available Courses

Flight Dynamics

Geosynchronous Transfer Orbi

"The objective of this course is to provide a theoretical background of the orbital operations for the injection of a satellite in the geostationary orbit".

Geosynchronous Orbit

- Part 1 Orbit Analysis
- Part 2 Manoeuvring

Meteosat Training Courses

Attitude Algorithms

"The application of the attitude algorithms for METEOSAT spacecraft in the Flight Dynamics LEOP context".

Attitude Software

"The application of the attitude software for METEOSAT spacecraft in the Flight Dynamics LEOP context".

Manoeuvre Algorithms

"The application of the manoeuvre-simulation and manoeuvre command-generation algorithms for METEOSAT spacecraft in the Flight Dynamics LEOP context".

Conclusion

The training system has been available since September 1992. It was employed successfully by the project staff for the METEOSAT 6 operations. New staff used the facility to familiarise themselves with the spacecraft and the system encyclopedias were used for references during the launch operations.

References

- ¹I. Graham, CBT Technology and Product Survey 5th November 1990.
- ²I. Graham, Training Facilities General System Requirements Document, 28th November 1990.
- ³P. Cornes, The Computer BULLETIN, The British Computer Society, May 1991, Volume 3, Part 4, p. 8-10
- ⁴F.M. Martinez-Fadrique, J.B. Palmer, G.R. Thomas Flight Dynamics Computer Based Training Teachware Authors Guide, November 1992.

INSERTION FROM SUPERSYNCHRONOUS AND SUBSYNCHRONOUS TRANSFER ORBIT AND NAVIGATION AROUND ACTIVE GEOSTATIONARY SATELLITES ENCOUNTERED DURING STATION ACQUISITION DRIFT PHASE

Alois F. Leibold
DLR/GSOC Orbit Engineer for EUTELSAT II
82230 Oberpfaffenhofen - Germany
RM38@DLRVM.BITNET

Abstract

A method is described for the fast identification of optimal strategies for the ground stations-commanded geostationary satellite insertion by several apogee and/or perigee maneuvers performed with a restartable engine from the Transfer Orbit into any prescribed Near-Synchronous Drift Orbit, anticipating the delivery of the satellite by the launcher into a Supersynchronous, Geostationary or Subsynchronous Transfer Orbit. Sufficient simultaneous dual-site maneuver visibility, backup apogees/perigees, and optimal orbit inclination reduction is guaranteed.

Additionally, an approach is described how station acquisition maneuvers, including orbit determination and thruster calibration aspects, as well as cross-coupling effects, can be scheduled and sized for the satellite rendezvous in the Near-Synchronous Drift Orbit with the on-station longitude in the Geostationary Orbit. The measures to be taken are described for navigating the own satellite around other encountered active geostationary satellites to its operational geographic longitude.

Typical insertion and station acquisition examples, exercised at DLR-GSOC, will be presented.

Keywords: Geostationary Satellite Transfer Orbits, Geostationary Satellite Positioning.

Introduction

The optimal transfer orbit for a geostationary satellite is usually the so-called Standard Geostationary Transfer Orbit (GTO). However, depending on the geographic latitude of the launch site, the satellite weight and the launcher performance, injection into an Extreme Supersynchronous (ESPTO) or Supersynchronous (SPTO) or Subsynchronous Transfer Orbit (SBTO) can provide better alternatives under the aspect of increasing the satellite propellant available after positioning at begin of satellite in-orbit lifetime. In the sequel it is shown how to generate in a simple way strategies for insertion from these types of

Transfer Orbits (TO) into any specified Near-Synchronous Drift Orbits (NSDO).

The geostationary ring becomes more and more crowded. So far the risk of collision between the own satellite and another known active satellite passed during on-station longitude acquisition is often neglected. It will be demonstrated that with moderate effort this risk can be eliminated by accurate and proper scheduling/sizing of the station acquisition maneuvers, if necessary in cooperation with the respective owner(s) of the encountered satellite(s).

Transfer Orbit Apogee Altitude

For a launcher with launch capability for transfer orbit injection (far) beyond GTO, a SPTO¹ or even ESPTO is very attractive to correct more efficiently the orbit inclination reducing by this the satellite velocity correction requirements - for the case that the transfer orbit has a high inclination as a result of the launch site latitude considerably different from zero. It has, however, to be anticipated that the satellite subsystems (e.g. attitude determination and control subsystem) allows such an orbit. The maneuver sequence and sizes for an ESPTO with 90 000 km

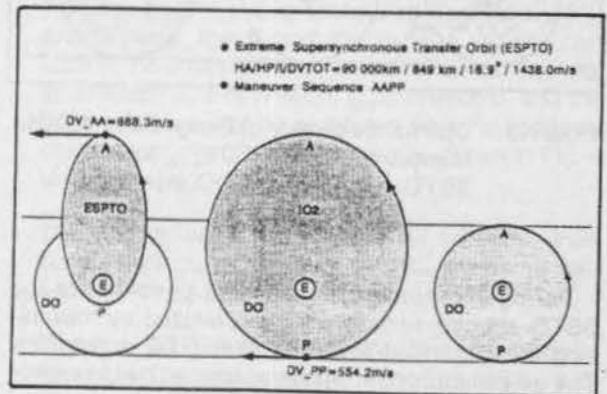


Figure 1: Optimal Sequence of Apogee and Perigee Maneuvers $DV_{A(A)}$ and $DV_{P(P)}$ for ESPTO → NSDO Insertion

apogee altitude is illustrated in Fig. 1.

The satellite velocity correction requirements / in-orbit lifetime may decrease / increase considerably even for a moderate SPTO as demonstrated in Fig. 2 for a SPTO with 750 km perigee altitude and for an apogee altitude range between 36 000 and 50 000 km and inclination range from 0° to 26°.

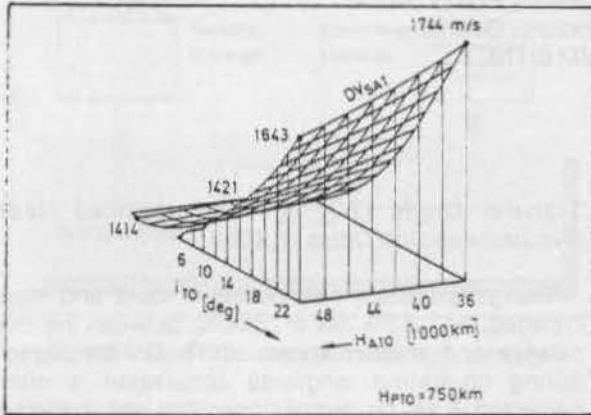


Figure 2: Decreasing DV_{Sat} for Different Inclinations in SPTO with $H_{ASPTO} > 36\ 000$ km

For a satellite which exceeds the launcher GTO launch capability and which has a propellant tank large with respect to its dry mass the injection into a SBTO by the launcher, followed by a perigee maneuver executed by the satellite to reach the GTO can be an interesting solution towards maximizing the satellite propellant at satellite lifetime begin. This is suggested in Fig. 3.



Figure 3: Optimal Sequence of Perigee and Apogee Maneuvers DV_P and $DV_{A(AA)}$ for SBTO \rightarrow GTO \rightarrow NSDO Insertion

Taking into account the launcher performance the SBTO apogee altitude will be optimized by maximizing the propellant available after GTO is reached. The propellant for the satellite-provided perigee velocity augmentation burn DV_P and for the apogee burns $DV_{A(AA)}$ to reduce the inclination and to insert the satellite into its target drift orbit are entering this propellant budget. See Table 1 for a typical example.

Table 1: DV_P and $DV_{A(AA)}$ as Function of the Apogee Altitude for SBTO with 200 km Perigee Altitude and 7° Inclination.

Apo Alt (km)	DV_{AAA} (m/s)	DV_P (m/s)
27 688		160.2
28 000		152.8
29 000		129.8
30 000		108.0
31 000	1499.7	87.2
32 000		67.3
33 000		48.4
34 000		30.3
35 000		12.9
35 786		0.0

As an example the achievable gain of in-orbit lifetime is shown in Table 2 for an ATLAS-launched satellite².

Table 2: Mission Benefits of Subsynchronous Transfer

	GTO	SBTO
S/C mass (kg):	3654	3654
S/C ofload to meet GTO launch capab. (kg):	-160	0
Transfer orbit parameters:		
Perigee altitude (km):	167	167
Apogee altitude (km):	35 786	30 000
Orbit inclination (deg):	27.0	27.0
Argument of perigee (deg):	180	180
Final orbit:	GSO	GSO
S/C ΔV required for GSO insertion (m/s):	1806	1913
S/C mass at beginning of life (kg):	1916	1933
Estimated mission lifetime (years):	12.1	12.6

S/C gains propellant for an additional 1/2 year in-orbit lifetime

Insertion Strategy Finding

Operational and Mission Requirements

The following minimal requirements must be fulfilled for a TO \rightarrow NSDO Insertion Strategy Candidate :

- i) Sufficient geometric ground station visibility (dual site visibility if requested) during all apogee/perigee maneuver preparations and executions must be guaranteed.
- ii) The satellite has to reach a prescribed NSDO in terms of apogee and perigee altitude biases with respect to the geostationary altitude, and specified values for the NSDO inclination and geographic longitude after the last insertion maneuver.
- iii) The sum of the satellite velocity correction increments for insertion and station acquisition

must be minimized.

Additional requested features for the selected *Final Insertion Strategy* are:

- i) For each scheduled apogee/perigee maneuver a reasonably early backup apogee/perigee providing again dual site maneuver visibility should be available.
- ii) The final insertion strategy should be robust with respect to maneuver execution errors, i.e. the chosen maneuver apogee/perigee/ground station - combination should not change in case of occurrence of maneuver execution errors within the $\pm 3\sigma$ range.

Problem Formulation

How the Optimal Insertion Strategy Maneuver Parameters can be determined from the set of prescribed Target Parameters reflecting the operational and mission requirements described before will be shown using the ESPTO as an example.

Reasonable *Target Parameters* assuming the suggested maneuver sequence of 2 apogee maneuvers followed by 2 perigee maneuvers are:

L_{DV2}	= geogr longitude for apogee impulse DV_2 ,
L_{DV4}	= geogr longitude for perigee impulse DV_4 ,
DH_{PDO}	= perigee height deviation of DO from GEO,
DH_{ADO}	= apogee height deviation of DO from GEO,
i_{DO}	= inclination of DO,
i_{IO2}	= optimal inclination of IO2.

By specifying the geographic longitudes for the apogee and perigee maneuvers, DV_2 and DV_4 , to be accomplished by proper sizing of apogee and perigee - maneuvers, DV_1 and DV_3 , the ground station visibility during the insertion maneuvers are to be controlled. The next three parameters describe the target NSDO, whereas the last parameter, the optimal inclination of the intermediate orbit IO2 reached after DV_2 , guarantees minimal total DV_{sat} - requirement for the insertion and station acquisition.

Owing to the restarting capability of the insertion motor anticipated earlier the apogee and perigee maneuvers were suggested to be split each into two maneuvers delivered at different times with the advantages that long burn losses are reduced and that thruster calibrations between the maneuvers are possible. This leads to the following

Maneuver Parameters

DV_1	= size of first apogee impulse,
DV_2	= size of second apogee impulse,
DV_3	= size of first perigee impulse,
DV_4	= size of second perigee impulse,
δ_{AA}	= declination for apogee impulses,
δ_{PP}	= declination for perigee impulses.

The Target Parameters are now expressed as functions of the Maneuver Parameters leading to the following set of equations

$$\begin{aligned}
 L_{DV2} &= f_1 (DV_1, \delta_{AA}, n_0, n_1) \\
 L_{DV4} &= f_2 (DV_1, DV_2, \delta_{AA}, DV_3, \delta_{PP}, L_{DV2}, n_2, n_3) \\
 DH_{PDO} &= f_3 (DV_1, DV_2, \delta_{AA}) \\
 DH_{ADO} &= f_4 (DV_1, DV_2, \delta_{AA}, DV_3, DV_4, \delta_{PP}) \quad (1) \\
 i_{DO} &= f_5 (DV_1, DV_2, \delta_{AA}, DV_3, DV_4, \delta_{PP}) \\
 i_{IO2} &= f_6 (DV_1, DV_2, \delta_{AA})
 \end{aligned}$$

Problem Solution

Insertion Strategy Candidates

The unknown maneuver parameters could now be found for example by a 6-dimensional Newton-Raphson Method. This is not suggested here. As the insertion problem has to be solved maybe hundreds of times for different combinations of maneuver longitudes and maneuver apogee(s)/perigee(s) (the latter expressed by the number of revolutions in TO and Intermediate Orbits IO, n) until the ideal insertion strategy is found, certain insertion strategies might be missed due to possible numerical problems which may be encountered without notice by the user when solving for the maneuver parameters of certain insertion strategies during the search process.

The following Mixed Approach is suggested which has the advantage to be simpler, faster and which does not involve the risk of numerical problems. Its components are:

- For the given ESPTO and the specified target NSDO the sum of the apogee velocity correction increments, DV_{AA} , and associated declination, δ_{AA} , and likewise, the sum of the perigee velocity correction increments, DV_{PP} , and declination, δ_{PP} , for an arbitrary IO2-inclination, i_{IO2} (between 0° and the TO inclination), can be computed from the apogee/-perigee velocity correction triangles shown in Fig. 4 using Equ. (2).
- The optimal value for i_{IO2} will now be determined such as the sum $DV = DV_{AA} + DV_{PP}$ will be minimized.
- The first apogee impulsive DV_1 and first perigee impulsive DV_3 are computed from Equ. (3) by a 2-dimensional Newton-Raphson Method for a given set of maneuver longitudes, L_{DV2} and L_{DV4} , and a given set of numbers of revolutions, n_i ($i=1, \dots, 3$), in TO and the Intermediate Orbits IO, i.e. for a given

set of preselected maneuver apogees/perigees.

Note: The maneuver longitude, L_{DV1} , in TO is given by the apogee selected for DV_1 , and the maneuver longitude, L_{DV3} , in IO₂ is defined by L_{DV2} , DV_2 and n_2 .

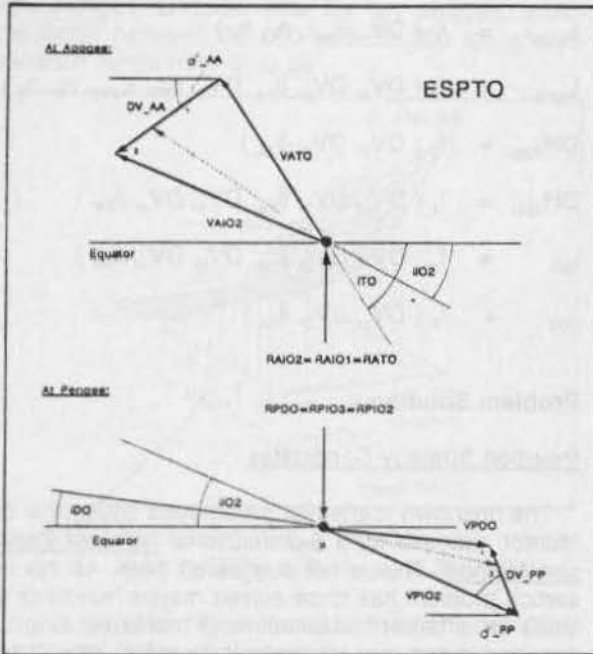


Figure 4: DV_{AA} ($=DV_1 + DV_2$) and DV_{PP} ($=DV_3 + DV_4$) and Optimization of i_{IO2} for Given ESPTO and Prescribed NSDO

- Knowing $DV_{AA} = DV_1 + DV_2$ and $DV_{PP} = DV_3 + DV_4$, the second apogee impulsive DV_2 and second perigee impulse DV_4 can be calculated. Insertion strategies for which DV_1 , DV_2 , DV_3 or DV_4 exceed their lower or upper allowed limits will be discarded.
- By an exhaustive search with respect to all reasonable orbit revolutions, n_1 (i.e. allowed maneuver apogees/perigees) and maneuver longitudes L_{DV2} , L_{DV4} (related to particular ground stations envisaged for certain apogee/perigee maneuvers), a large number of insertion strategies is generated, and simultaneously, the station visibilities for a prescribed time before and after the theoretical passage of the maneuver apogees/perigees, corresponding to the prescribed/computed maneuver longitudes L_{DVI} , are computed. The same visibility checks are done for a series of backup apogees/perigees in TO and in the following IO_i ($i=1, \dots, 3$).

Insertion Strategy Candidates are now those strategies which guarantee sufficient geometric visibility by at least 2 stations before and after each maneuver performed at the selected / prescribed / computed maneuver longitudes L_{DVI} ($i=1, \dots, 4$).

$$DV_{AA} = \sqrt{V_{ATO}^2 + V_{AI02}^2 - 2 \cos(i_{TO} - i_{IO2}) V_{ATO} V_{AI02}}$$

$$\delta_{AA} = -\arcsin \left[\frac{V_{ATO} \sin(i_{TO} - i_{IO2})}{DV_{AA}} \right] < 0$$

$$DV_{PP} = \sqrt{DV_{PPX}^2 + DV_{PPY}^2}$$

$$\delta_{PP} = \arctan \frac{DV_{PPY}}{DV_{PPX}} > 0$$

$$DV_{TOT} = DV_{AA} + DV_{PP}$$

where

$$V_{AI02} = \sqrt{\frac{2\mu}{R_{ATO} + R_{PDO}} \frac{R_{PDO}}{R_{ATO}}}$$

$$R_{PDO} = R_{SO} + DH_{PDO}$$

$$R_{SO} = \text{geostationary radius}$$

$$DV_{PPX} = -V_{PDO} \cos i_{DO} + V_{PI02} \cos i_{IO2} \quad (2)$$

$$DV_{PPY} = -V_{PDO} \sin i_{DO} + V_{PI02} \sin i_{IO2}$$

$$V_{PDO} = \sqrt{\frac{2\mu}{R_{ADO} + R_{PDO}} \frac{R_{ADO}}{R_{PDO}}}$$

$$R_{ADO} = R_{SO} + DH_{ADO}$$

$$V_{PI02} = \sqrt{\frac{2\mu}{R_{ATO} + R_{PDO}} \frac{R_{ATO}}{R_{PDO}}}$$

i_{IO2} is found by minimizing DV_{TOT}

$$L_{DV2} = L_0 + \pi(n_0 + n_1) - \pi \omega_E \left(\frac{n_0}{n_{TO}} + \frac{n_1}{n_{IO1}} \right)$$

$$n_{TO} = \text{mean motion of TO}$$

$$n_{IO1} = \sqrt{\mu \left(\frac{2}{R_{ATO}} - \frac{V_{AI01}^2}{\mu} \right)}$$

$$V_{AI01}^2 = (V_{ATO} \cos i_{TO} + DV_1 \cos \delta_{AA})^2 + (V_{ATO} \sin i_{TO} + DV_1 \sin \delta_{AA})^2$$

n_0, n_1 = number of half revolutions in Transfer Orbit and Intermediate Orbit

$$L_{DV4} = L_{DV2} + \pi (n_2 + n_3) - \pi \omega_E \left(\frac{n_2}{\Omega_{IO2}} + \frac{n_3}{\Omega_{IO3}} \right)$$

$$n_{IO2} = \sqrt{\frac{8 \mu}{(R_{ATO} + R_{PTO})^3}}$$

$$n_{IO3} = \sqrt{\mu \left(\frac{2}{R_{PTO}} - \frac{V_{PTO}^2}{\mu} \right)}$$

$$V_{PTO}^2 = (V_{PTO} \cos i_{IO2} - DV_3 \cos \delta_{PP})^2 + (V_{PTO} \sin i_{IO2} - DV_3 \sin \delta_{PP})^2$$

DV_1, DV_2 - computation by Newton-Raphson

$$DV_2 = DV_{AA} - DV_1, DV_4 = DV_{PP} - DV_3$$

Final Insertion Strategy

From the list of insertion strategy candidates the final insertion strategy will be selected fulfilling the following criteria:

- Proper Backup Apogee/Perigee longitudes with sufficient dual site ground station visibility for each nominal maneuver are available, preferably 2 revolutions after the respective nominal maneuvers, only 1 revolution between the last maneuver and its backup.
- Sufficient station visibility during DV_1 maneuver preparation and execution in case of $\pm 3\sigma$ execution errors of $DV_{1,1}$.
- Longitudes of last maneuver and of its backup are close to the on-station longitude.

A numerical example for the Insertion from an Extreme Supersynchronous Transfer Orbit into an Near-Synchronous Drift Orbit is given in Table 3. The suggested strategy has not yet been used for a real satellite positioning.

Table 3: Four Impulse Insertion Maneuver Strategy for ESPTO \rightarrow NSDO Insertion

	TO/DV1	IO1/DV2	IO2/DV3	IO3/DV4	NSDO
NO. OF A.A.P.P	3	5	5	5	5
IMPULSE (M/SEC)	851.2	32.5	464.1	30.1	5
DECL (DG)	+13.0	-13.3	7.1	7.3	7.3
DRIFT R (DG/REV)	-130.2	-177.5	-196.7	-14.2	-0.45

LONGITUDES (GROUND STATION VISIBILITIES):

MAIN STRAT	24(02300)	-11(12000)	114(00140)	12(12300)	
NEXT APSIDE	-106(00005)	-29(12000)	77(02300)	-22(12000)	
NEXT APSIDE	124(00040)	-48(12000)	41(12300)	-56(12005)	
NEXT APSIDE	-7(12000)	-64(10000)	4(12300)	+9(00005)	

ORBITAL ELEMENTS:

APD R (KM)	96378.155	96378.16	96378.16	47561.95	42264.18
PER R (KM)	7222.483	29652.60	41994.18	41994.18	41994.18
INCL (DG)	27.80	27.88	2.18	0.29	0.28
NODE (DG)	154.97	154.97	154.97	154.97	154.97
PERI (DG)	180.00	180.00	180.00	180.00	180.00
NA (DG)	180.00	180.00	3.00	3.00	3.00
IMP DATE	91-09-23	91-09-27	91-09-30	91-10-03	
IMP TIME	08:16:27	10:40:00	14:08:42	20:43:42	
TOTAL IMPULSE OF THE ABOVE STRATEGY (N/S)				1438.0	
IMPULSE ESTIMATE FOR ACQUISITION (N/S)				4.9	
TOTAL IMPULSE (N/S)				1443.0	

FINITE BURN PARAMETERS ESTIMATES

IGN DATE	91-09-23	91-09-27	91-09-30	91-10-03	
IGN TIME	08:07:52	11:16:11	14:32:06	20:41:41	
DUR (MIN)	57.3	1.4	25.0	4.0	
FUEL (KG)	466.4	12.4	203.0	32.5	
MASS (KG)	1880.0	1413.6	1402.3	1195.0	1366.4

Legend

TO	Transfer Orbit,
IO1	Intermediate Orbit 1 obtained after DV1 execution,
IO2	Intermediate Orbit 2 obtained after DV2 execution,
IO3	Intermediate Orbit 3 obtained after DV3 execution,
NSDO	Near-Synchronous Drift Orbit obtained after DV4 execution.

Longitudes (Ground Station Visibilities)

Main	Maneuver longitudes for DV1, DV2, DV3, DV4,
Next...	Longitudes of apogees/perigees following nominal apogee/perigee maneuver longitudes = possible longitude candidates for backup maneuvers.
(m,W,B,c,g)	indication that stations Weilheim and Bangalore would have geometric visibility of the satellite each one for at least 4 hours before and 1 hour after the theoretical apogee/perigee passage, where as madrid, canberra and goldstone have no or at least not sufficient visibility.

Possible Program Messages:

- "Geographic longitude for last impulse is beyond stationkeeping longitude in error case of impulse before last one".
This message indicates that perigee maneuver 2 (=DV₃) would be performed east of on-station longitude 16° in case -3σ error during perigee maneuver 1 (=DV₁).
- "Not sufficient station visibility before impulse 2 by station 1 in case of -3σ error of impulse 1".
This message would indicate that station 1 (Madrid) would not have sufficient visibility for maneuver preparation and execution of apogee maneuver DV₂ in case of underperformance of the apogee motor during apogee maneuver DV1.

Station Acquisition

In the following the station acquisition strategies for two EUTELSAT II satellites are summarized. Their maneuvers were scheduled and sized such as to guarantee safe navigation around the active geostationary satellites encountered during station acquisition.

The first one outlines the strategy as envisaged during LEOP mission preparation simulations for EUTELSAT II - F5. Unfortunately, due the failure of the ARIANE Flight 63 the satellite did not reach its GTO and the foreseen station acquisition strategy could not be applied.

The second one describes the steps of generating the station acquisition strategy for EUTELSAT II - F4

which was actually also operationally applied.

Using these two examples the process of obtaining fast and safe station acquisition strategies as developed and applied at DLA-GSOC is described in the sequel. The different steps of this process are:

1) Generation of a longitude/radial plot (see Fig. 5) for the satellite motion in NSDO starting after last insertion maneuver and ending when satellite reaches its on-station longitude before applying any correction maneuver. The idea is

- to get a first estimate on the expected duration of the station acquisition phase,
- to study the structure of the satellite motion in latitude and longitude over time,
- to visualize the location of the apogees and perigees above and below the geostationary altitude, and finally,
- to picture the control boxes of the satellites which must be passed during station acquisition (see Table 4).

2) Production of a major number of attainable station acquisition strategies (in general consisting of 3 maneuvers, described by their velocity increments and maneuver times) and Preliminary Strategy Selection (see Table 5). Requirements for this "Strategy Cross-Planning" are:

- at least 1/2 revolution must be foreseen between maneuvers which use different thrusters, and for maneuvers which correct only the drift rate and not in parallel the eccentricity vector with the same thruster.
- at least 1 revolution must be foreseen between maneuvers which use the same thruster and which require thruster calibration, maneuver replanning and maneuver tuning (for thruster calibration only 1/2 day tracking after the maneuver would be sufficient).
- in general: the 3rd maneuver will be preferably scheduled soon after the 2nd maneuver in case its size becomes large (5 m/s or so). By this a major longitude offset at time of the drift rate stop maneuver will be avoided.
- in particular: for the different maneuver sequences (E = East maneuver, decreasing mean satellite velocity, W = West maneuver, increasing mean satellite velocity) the following aspects are taken into account:

-- E_E_W: the 2nd East maneuver can be calibrated leading to an accurate longitude for the West maneuver execution; however, the drift rate after this West maneuver will not

be accurate, requesting for an 4th (additional) small drift rate correction maneuver.

-- W_E_W: the 2nd West maneuver can be calibrated and accurately sized such that the satellite enters its control box with optimal drift rate; no 4th trim maneuver will be necessary.

-- E_W_W, 2nd and 3rd maneuver separated by 1 revolution, should be reasonably small and be preferably of the same size; by this, a small longitude error at time of the 3rd maneuver and an accurate drift rate after the calibrated 3rd maneuver can be guaranteed; no 4th trim maneuver is then expected to be necessary.

-- W_E_E:

3) Maneuver Fine Planning^{3,4} for the selected maneuver strategy taking into account

- thruster cross couplings,
- station keeping target elements, and
- difference between mean and osculating elements.

4) Generation of longitude/radial plot as in 1), however, including the maneuvers and checking whether any encountered control boxes of geostationary satellites are violated (see Fig. 6 and Fig. 7). In case of problems or doubts:

- i) either another strategy indicating no box violation is selected,
- ii) or the respective satellite owner is contacted to get orbital elements for assessing the collision risk by computation of relative distances of the own and passed satellite by a proximity check (see Fig. 8) and if necessary, selecting of another strategy (see Fig. 9),
- iii) or possibly disregarding the risk resulting from entering the respective control box.

There is no fixed rule what approach will be used. Anyway, the strategy chosen now will be strictly applied in the sequel, only minor modifications will be made if it will be necessary.

5) Realization and execution of (1st, 2nd or 3rd) maneuver.

6) Orbit determination including estimation of the executed maneuver and computation of the maneuver magnitude and thruster cross couplings. The nominal cross couplings are known. If significant deviations are found, the thruster efficiency and the cross coupling values are properly

adjusted for the replanning of the next maneuver to be performed by the same thruster.

- 7) If necessary, adjusting of the sizes and times of the remaining maneuvers by hand via trial and error to correct as far as possible the effect of maneuver execution errors on the achieved station keeping target elements.
- 8) Repetition of steps 4 (without 4a), 5), 6) and 7) for 2nd and 3rd (4th) maneuver observing the principles as applied for the 1st maneuver.

Strategy for EUTELSAT II - F5

The last insertion maneuver is often performed close to the satellite's on-station longitude. By this a short station acquisition time can be achieved and the chance to encounter a other satellite is smaller.

The DV₃-maneuver longitude of F5 is ca. 20° west of its operational on-station longitude. This large longitude offset was the result of a series of requirements which the insertion strategies for the EUTELSAT II satellites have to fulfil. The most important ones are:

- no apogee insertion maneuver should be larger in size than 900 m/s,
- dual-site ground station visibility including Weilheim during each nominal and - whenever possible - backup maneuver preferably 2 revolutions later, should be guaranteed, and in particular,
- the satellite should be not more than ca. 10° east of its on-station longitude for the case that DV₃ (the last insertion maneuver) has to be performed in the backup apogee.

Table 4: Longitudes and Control Boxes of Satellites Encountered by EUTELSAT II - F5

15.8° E	Eutelsat II - F5	DV ₃ nominal
16.0° E ± 0.08°	E/W	Eutelsat II - F3
19.2° E ± 0.10°	E/W	Astra 1A, 1B, 1C
20.0° E ± 0.10°	E/W	Arabsat 1D
21.5° E ± 0.10°	E/W	ECS1 - F5
22.5° E ± 0.30°	E/W	Marecs A
23.5° E ± 0.07°	E/W	DFS-3
25.5° E ± 0.10°	E/W	ECS1 - F4
28.5° E ± 0.07°	E/W	DFS-2
31.0° E ± 0.10°	E/W	Arabsat 1C
33.5° E ± 0.07°	E/W	DFS-1
36.0° E ± 0.08°	E/W	Eutelsat II - F5

As a consequence of the 20° longitude offset F5 was scheduled to pass the satellites listed in Table 4, with the respective control boxes as pictured in Fig. 5.

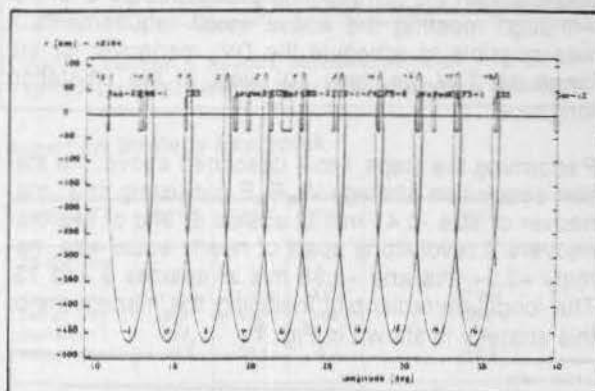


Figure 5: Simulated Drift Orbit After Apogee Manuever DV₃ for EUTELSAT II - F5

The final station acquisition strategy selected during the F5 mission preparation simulations corresponds roughly with the second strategy listed in Table 5. It has, however, been refined as described above in step 3, such as to guarantee that the satellite will be safely navigated around the control boxes of the encountered satellites (see Fig. 6). The observed box violation of EUTELSAT II - F3 at 16°E was regarded to be a manageable internal problem between DLR-GSOC and EUTELSAT, the owner of both, of the F5 and of the F3 satellite.

Table 5: Station Acquisition Strategy Candidates for EUTELSAT II - F5

	1	2	3	TOTAL DV	N1	N2	N3
					K1	K2	K3
DV (m/s)	-1.333	1.348	1.388	10.367	10	13	17
LANDBA2	1887.38	2427.38	2147.38				
TIME (DAYS)	4.48344	5.24456	7.35183				
DV (m/s)	-1.333	1.334	1.438	10.378	10	15	17
LANDBA2	1887.38	2187.38	2147.38				
TIME (DAYS)	4.48344	4.25597	7.35183				
DV (m/s)	1.868	-1.534	1.688	10.388	11	12	17
LANDBA2	2087.38	2247.38	2147.38				
TIME (DAYS)	4.87869	5.47484	7.35183				
DV (m/s)	1.750	-1.334	1.204	10.388	11	16	17
LANDBA2	2087.38	2607.38	2147.38				
TIME (DAYS)	4.97869	4.46633	7.35183				

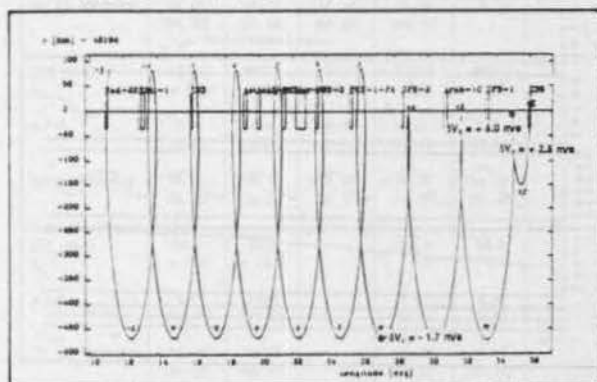


Figure 6: Simulated Station Acquisition Strategy for EUTELSAT II - F5

Strategy for EUTELSAT II - F4

The on-station longitude for F4 was 8°E. This longitude is more favorable for Weilheim under positioning aspects than the corresponding longitude 36°E for F5. Although meeting the above listed requirements it was possible to schedule the DV₃ maneuver for the longitude 2°W, i.e. only 10° west of the on-station longitude.

Performing the steps 1 to 4 described above, the station acquisition strategy W_E_E consisting of a maneuver of size -0.41 m/s at apside 6, and of two maneuvers 2 revolutions apart of nearly equal size, namely +3.04 m/s and +2.98 m/s at apsides 9 and 13. The longitude/radial plot including the maneuvers of this strategy is shown in Fig. 7.

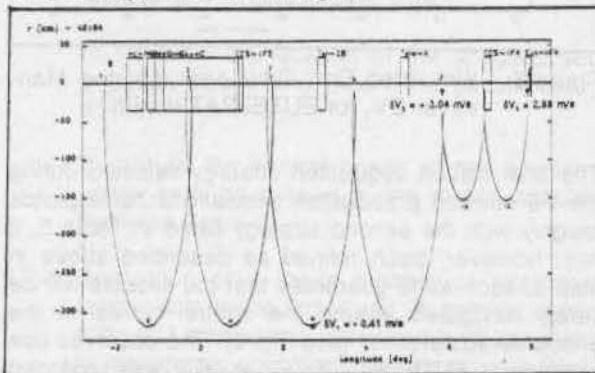


Figure 7: Initially Envisaged Station Acquisition Strategy for EUTELSAT II - F4

Violations of two control boxes are observed. The first one is the $\pm 1^\circ$ control box of Meteosat 4 positioned at longitude 0°, the second one the $\pm 0.1^\circ$ control box of ECS1 - F4 stationed at 7°E. To clarify the situation the two station keeping control centers in charge of these satellites were contacted. It turned out that there is no collision risk at the time when F4 enters the Meteosat control box, it was, however, found by a proximity check that the closest distance between EUTELSAT II - F4 and ECS1 - F4 will be 11.8 km (see Fig. 8).

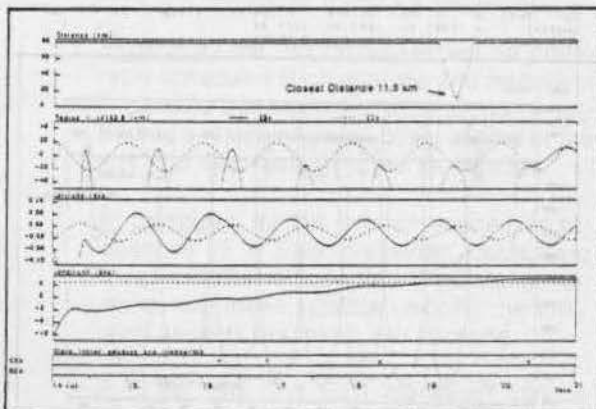


Figure 8: Proximity Check for EUTELSAT II - F4 and ECS1 - F4

To eliminate any collision risk - even if it is still small - GSOC decided to abandon the nice strategy with small and balanced East maneuvers in favor of two fairly unbalanced maneuvers of sizes +5.26 m/s and +0.76 m/s in the 11 and 13 as pictured in Fig. 9 and Fig. 10⁵.

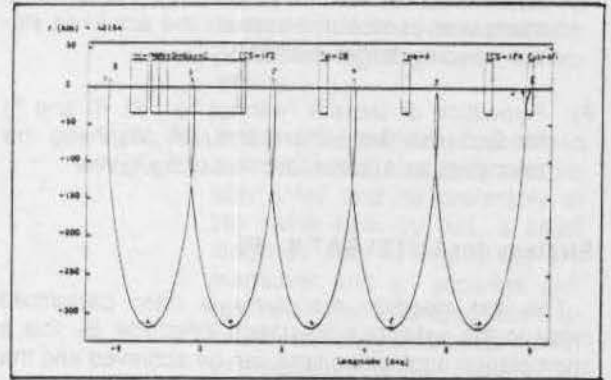


Figure 9: Final Station Acquisition Strategy for EUTELSAT II - F4

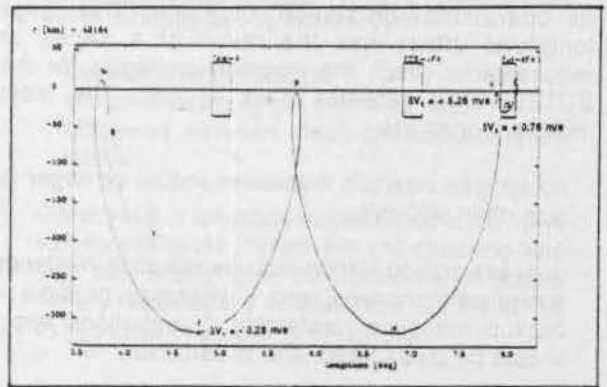


Figure 10: Blow-up of Longitude/Radial Motion Near ECS1 - F4

References

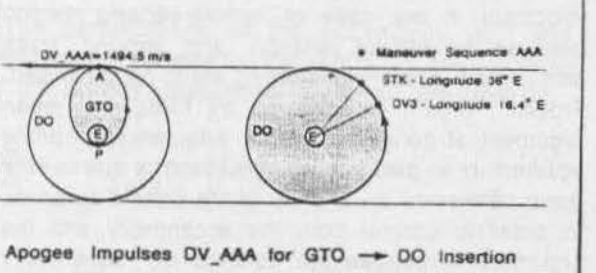
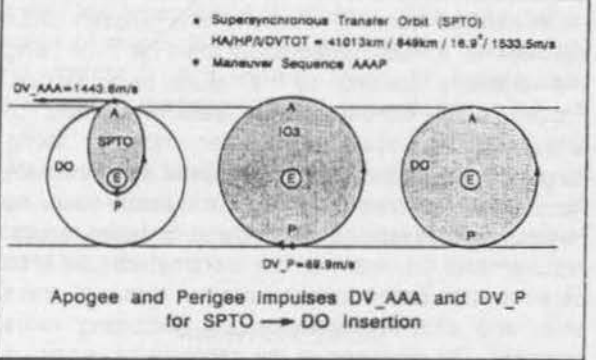
- Leibold, A. F. "Positioning of EUTELSAT II Satellite from Supersynchronous Transfer Orbit to Reduce Satellite Velocity Correction Requirements", AAS/AIAA Astrodynamics Specialist Conference, AAS 91-408, Durango, Colorado, August 19-22, 1991
- Mission Planner's Guide for Atlas Launch Vehicle Family, Revision 4, July 1993, General Dynamics Launch Services, Inc.
- Pietraß, A., Eckstein, M. C., Montenbruck, O. "Software for Station Keeping of Co-located Geostationary Satellites", 11th European Space Conference (EAC 91), Paris, France, 12 - 16 May 1991, EAS SP-342 (October 1991)
- Montenbruck, O., Eckstein, M. C., Gonner J., "The Geo-Control System for Station Keeping and Colocation of Geostationary Satellites", Second Symposium, Ground Data Systems for Space Mission

5 Eutelsat II LEOP Services, Post Mission Flight Report, Launch and Early Orbit Phase (LEOP), Doc. No.: LEO-RPT-DLR-52077, Issue: 1.0, August 21, 1992

Appendix

Target and Maneuver Parameters for (E)SPTO and GTO

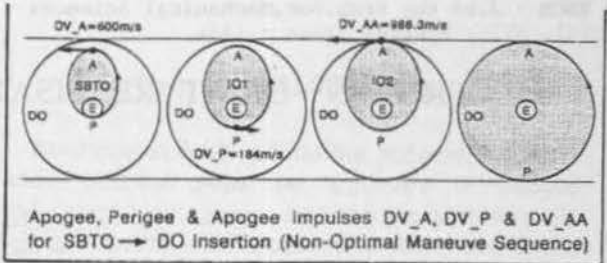
TO/ Man. Sequ.	Target Parameters	Maneuver Parameters	Comment
ESPTO/ AAPP	$L_{over}, DH_{100}, l_{02}$ $L_{over}, DH_{100}, l_{00}$ l_{02} pre-optimized	DV_1, DV_P, δ_{AA} DV_2, DV_P, δ_{AP}	For TO with high inclination and with no restriction on Apogee Altitude by Satellite
SPTO/ AAAP	$L_{over}, L_{01}, DH_{100}, l_{02}$ DH_{100}, l_{02} l_{02} pre-optimized	$DV_1, DV_P, DV_2, \delta_{AA}$ DV_2, δ_P	For TO with high inclination and with restriction on Apogee Altitude by Satellite
AAA	$L_{over}, L_{01}, DH_{100}, l_{02}$	$DV_1, DV_P, DV_2, \delta_{AA}$	Maneuver Sequence for GTO added for completeness



Target and Maneuver Parameters for SBTO

Man. Sequ.	Target Parameters	Maneuver Parameters	Comment
FAAA	DH_{100}, l_{02} $L_{01}, L_{02}, DH_{100}, l_{00}$	$DV_1, \delta_P = -l_{02}$ $DV_P, DV_2, DV_3, \delta_{AA}$	Optimal Maneuver Sequence (without Ground Station Visibility during Perigee Assist Maneuver)
APAA	$L_{01}, L_{02}, DH_{100}, l_{02}$ L_{01}, DH_{100}, l_{00} l_{01}, l_{02} as function of DV_1 pre-optimized	$DV_1, \delta_2, DV_P, \delta_P$ DV_2, DV_3, δ_{AA}	Possible DV-saving when only SBTO (with an 180°) rather than GTO was achieved due to minor launch injection errors or launcher issues
AAAP	$L_{01}, L_{02}, DH_{100}, l_{02}$ DH_{100}, l_{00} l_{01} pre-optimized	$DV_1, DV_P, DV_2, \delta_{AA}$ DV_2, δ_P	Maneuver Sequence included for comparison of DV_{tot} with DV_{tot} of Sequence FAAA, APAA

• Subynchronous Transfer Orbit (SBTO)
 $HA/HP/DVTOT = 27988km / 200km / 7.7^\circ / 1767.6m/s$
 • Maneuver Sequence APAA



Insertion Strategy Examples

TO Type	ESPTO	SPTO	GTO	SBTO		
TO Elements						
App alt. [km]	90 000	41 013	35776	27 688		
Peri alt. [km]	849	849	206	200		
Inclination [°]	18.9	18.9	7.0	7.0		
1st per. long. [°]	-10.3	-10.3	-9.3	-10.3		
Man. Sequ.	AAPP	AAAP	AAA	PAAA	APAA	AAAP

Target Parameters during Insertion

Incl_IO1 [°]				7	3.7
Long_DV2 [°]	-11.0	+33.0	+44.3		+63.9
Incl_IO2 [°]	1.2				
Long_DV3 [°]		+62.0	+16.4	-20	-40.6
Incl_IO3 [°]					
Long_DV4 [°]	+12			+21	+14.4

Target Parameters in Drift Orbit

Inclination [°]	0.08	0.08	0.08	0.08	0.08
App Alt [km]	+100	+100		-10	-10
Peri Alt [km]	-170	-170	-335	-100	-100
Drift ["/day]			+2.2		
STK Long. [°]	+16	+16	+36	+26	+26

Maneuver Parameters

DV_1 [m/s]	851.2	771.1	527.5	160.1	600.0
δ_1 [°]	-13.0	-16.5	-7.3	-7	-7.3
A / P	3 A (6 A)	3 A (5 A)	4 A (6 A)	2 P	4 A (7 A)
Gr. St. Visibility	W, B (M, W)	B, C/W (B, C/W)	M, W (M, W)	no visib. (no visib)	B, C (B, C)
DV_2 [m/s]	36.6	519.8	878.0	601.6	184.0
δ_2 [°]	-13.0	-16.5	-7.3	-7.3	-3.7
A / P	5 A (6 A)	6 A (9 A)	6 A (8 A)	4 A (6 A)	5 P
Gr. St. Visibility	M, W (M, W)	M, W (M, W)	M, W (M, G)	M, W (M, W)	B *)
DV_3 [m/s]	464.1	152.7	88.9	837.9	900.0
δ_3 [°]	+7.3	-16.5	-7.3	-7.3	-7.5
A / P	6 P (7 P)	8 A (10 A)	8 A (9 A)	5 A (8 A)	6 A (8 A)
Gr. St. Visibility	B, C (B, C)	W, B (B, C)	M, W (M, W)	M, W (M, W)	M, W (M, G)
DV_4 [m/s]	90.1	89.9		60.4	86.3
δ_4 [°]	+7.3	+15.6		-7.3	-7.5
A / P	9 P (10 P)	10 P (11 P)		8 A (9 A)	8 A (9 A)
Gr. St. Visibility	M, W (M, W)	M, W (M, W)		M, W (M, W)	M, W (M, W)
DV_{tot} [m/s]	1438.0	1533.5	1494.5	1660.0	1767.6
				1846.0	

FROZEN ORBIT REALISATION USING LQR ANALOGY

N. Nagarajan

H. Reno Rayan

Indian Space Research Organisation

Flight Dynamics Division

ISRO Satellite Centre

Bangalore - 560 017, INDIA

Abstract

In case of remote sensing orbits, the Frozen Orbit concept minimises the altitude variations over a given region using passive means. This is achieved by establishing the mean eccentricity vector at the orbital poles i.e., by fixing the mean argument of perigee at 90 deg with an appropriate eccentricity to balance the perturbations due to zonal harmonics J_2 and J_3 of the Earth's potential. Eccentricity vector is a vector whose magnitude is the eccentricity and direction is the argument of perigee. The launcher dispersions result in an eccentricity vector which is away from the frozen orbit values. The objective is then to formulate an orbit maneuver strategy to optimise the fuel required to achieve the frozen orbit in the presence of visibility and impulse constraints. It is shown that the motion of the eccentricity vector around the frozen perigee can be approximated as a circle.

Combining the circular motion of the eccentricity vector around the frozen point and the maneuver equation, the following discrete equation is obtained,

$X(k+1) = AX(k) + Bu(k)$, where X is the state (i.e. eccentricity vector components), A the state transition matrix, u the scalar control force (i.e. dV in this case) and B the control matrix which transforms dV into eccentricity vector change.

Based on this, it is shown that the problem of optimising the fuel, can be treated as an Linear Quadratic Regulator (LQR) problem in which the state is driven to the origin by a feedback control law in an optimal manner. The constraints on visibility during the maneuver is handled by appropriately defining the matrix B and the constraints on magnitude of the impulse is handled by a proper choice of the weighting matrix R . By solving the algebraic Riccati Equation, the set of impulses and their firing positions are computed. Through various case studies it is shown, how a problem of orbit

maneuver can be solved by using the control system design tools like MATLAB by deriving an analogy to LQR design.

Introduction

In remote sensing missions, the Frozen Orbit concept is a much talked about topic for minimising the variations caused by the natural perturbations. Frozen orbit concept is a passive method of arresting the eccentricity vector motion taking advantage of the perturbations caused by J_2 and J_3 for near circular orbits. As the remote sensing missions are advancing for better and better results, requirements on many of the parameters like orbit determination/prediction accuracies, ground track shift, and altitude variations are becoming more stringent. The arresting of the eccentricity vector is important in the case of remote sensing mission because the altitude variation and ground track shift which affect the imaging are to be minimised. Frozen orbit is achieved by fixing the mean argument of perigee at 90° with an appropriate eccentricity to balance the perturbations due to the zonal harmonics J_2 and J_3 of the Earth's potential. In order to control both the eccentricity and the argument of perigee the concept of eccentricity vector is found to be very useful in formulating the Frozen Orbit acquisition problem. Eccentricity vector is a vector whose magnitude is the eccentricity and direction is the argument of perigee.

Due to the launch dispersions the frozen orbit is not directly achieved. One strategy could be to achieve frozen orbit by combining it with the orbit acquisition maneuvers. On the other hand, if the realised orbit after injection is close to the nominal one in terms of semi-major axis (a), then the frozen orbit acquisition can be decoupled from the trim maneuvers for ' a '. The objective of this paper is to formulate an orbit maneuver strategy to optimise the fuel requirement to achieve frozen orbit in the presence of visibility and impulse constraints assuming that the nominal values of ' a ' and ' i ' are acquired.

While analysing the IRS-1A and IRS-1B (Indian Remote Sensing Satellites) data it is found that the motion of the eccentricity vector around the frozen perigee can be approximated by a circle and the rate of motion is also a constant. This forms the dynamics of the state, and the velocity impulse (dV) necessary to change the eccentricity vector forms the control part of the problem². Combining both the state dynamics and control parts, the following discrete equation is obtained $X(k+1) = AX(k) + Bu(k)$, where X is the state (ie eccentricity vector components), A the state transition matrix, u the scalar control force (= dv) and B the control matrix which transforms dv into eccentricity vector change.

Thus the fuel optimising problem can be treated as a Linear Quadratic Regulator (LQR) problem in which the state is driven to the origin by a feedback control law in an optimal manner. The appropriate choice of matrix B handles the visibility constraint and matrix Q and R are tuned to handle the constraint on the magnitude of the impulse.

Various case studies on the optimal fuel budget has been brought out with different visibility and impulse constraints using the control system design tool MATLAB.

Motion of e vector

The perturbations of the eccentricity (e) and argument of perigee (ω) caused by J_2 and J_3 terms of the Earth's gravitational potential² are given by,

$$\frac{de}{dt} = -\frac{3\eta J_3 R^3 \sin i}{2p^2 a} \left(1 - \frac{5}{4} \sin^2 i\right) \cos \omega \quad (1)$$

$$\frac{d\omega}{dt} = \frac{3\eta J_2 R^2}{p^2} \left(1 - \frac{5}{4} \sin^2 i\right) \left[1 + \frac{J_3 R}{2J_2 p} \left(\frac{\sin^2 i - e \cos^2 i}{\sin i}\right) \frac{\sin \omega}{e}\right] \quad (2)$$

where η is the mean motion,

J_2 and J_3 are second and third zonal harmonics

R the equatorial radius of the earth

a the semi major axis

i the inclination and $p = a(1-e^2)$.

The analytical solution for the variation of e and ω have been compared with the actual data using the orbital history of IRS-1A and IRS-1B³ and it is shown that the cyclic behaviour of the eccentricity vector has a periodicity of about 131 days. Fig.1 gives the eccentricity vector motion for IRS-1B studied over a span of one year.

Derivation of LQR analogy

As shown in fig.2 let \bar{e} be the eccentricity vector whose direction gives the argument of perigee and magnitude gives the eccentricity of the orbit. Let \bar{e}_0 be the initial eccentricity vector and \bar{e}_r the frozen eccentricity vector with respect to the line of node. Then $\Delta \bar{e}$ is given by,

$$\Delta \bar{e} = \bar{e}_0 - \bar{e}_r \quad (3)$$

Based on one year of data, fig.3 shows the magnitude and directional variation of $\Delta \bar{e}$ per day alongwith their computed averages⁴. This analysis justifies the assumption that $\Delta \bar{e}$ motion can be approximated to a circle around the frozen perigee point, with a constant angular rate.

Thus the problem of the $\Delta \bar{e}$ motion could be expressed in a recursive form as given below.

$$i.e. X_{k+1} = AX_k \quad (4)$$

where the X is $\Delta \bar{e}$ at any instant of time. In the full form the above equation is written as,

$$\begin{pmatrix} \Delta e_x \\ \Delta e_y \end{pmatrix}_{k+1} = \begin{pmatrix} \cos \Delta \theta & -\sin \Delta \theta \\ \sin \Delta \theta & \cos \Delta \theta \end{pmatrix} \begin{pmatrix} \Delta e_x \\ \Delta e_y \end{pmatrix}_k \quad (5)$$

where $\Delta \theta$ is the motion of $\Delta \bar{e}$ between the times k and k+1. This forms the dynamics of the discrete state equation and describes the motion of $\Delta \bar{e}$ without any control force acting on it.

The maneuver equation is given by

$$\Delta \bar{e} = \frac{2Vdv}{\mu} \hat{r} \quad (6)$$

where, $|\Delta \bar{e}| = \frac{2Vdv}{\mu} r$ and direction

$$\hat{\Delta e} = \hat{r} = \begin{pmatrix} \cos \theta \\ \sin \theta \end{pmatrix}, \theta \text{ being the argument of}$$

latitude of the maneuver point.

Thus $\Delta \bar{e}$ in terms of dV is given by

$$\Delta e = \begin{pmatrix} D \cos \theta \\ D \sin \theta \end{pmatrix} dV, \text{ where } D = \frac{2Vr}{\mu} \quad (7)$$

Thus, the motion of $\Delta \bar{e}$ alongwith the effect of control force on the state is given by,

$$X_{k+1} = AX_k + Bu_k \quad (8)$$

with A given by (5), B by (7) and $u = dV$.

Analogous to the control problem, here the correction eccentricity vector components with respect to the frozen point has to be reduced to zero with minimum fuel (ie minimum total dV) using the feedback control law,

$$ie \ u = -FX \quad (9)$$

In the design of control systems, the above problem can be treated as an Linear Quadratic Regulator (LQR) where the cost function,

$$J = X^T QX + u^T Ru \quad (10)$$

is minimised. By solving the Algebraic Riccati Equation,

$$P = A^T PA - A^T PB(B^T PB + R)^{-1} B^T PA + Q$$

the feedback gain is calculated. i.e.,

$$F = (B^T PB + R)^{-1} B^T PA \quad (11)$$

$$\text{The minimum cost, } J_{\min} = X_0^T P_0 X_0 \quad (12)$$

We find F such that, with all constraints like visibility, maximum impulse and time gap between maneuvers, the cost function is minimum. While using LQR analogy for Frozen perigee acquisition, the different constraints are handled in the following manner. The constraint on magnitude of velocity impulse is handled by a proper choice of R. A higher value of R reduces the amplitude of the velocity impulses. The point of maneuver is given by the argument of latitude which appears in the control matrix B. Thus by manipulating the contents of B the visibility constraint can be taken care of. For instance, if the maneuver is to be done always at equator, then $B = (D, 0)^T$. Simulation studies were made using the control system design tools MATLAB.

Simulation Study

For the case study, the considered orbit is a sun synchronous type of orbit at 904 km altitude. For frozen orbit, an eccentricity of .001 and an argument of perigee of 90 deg are to be realised. Initial position of eccentricity vector is assumed to be .001 units away from the frozen perigee point. The maneuver point is assumed to be at the equator as it provides the visibility for the Indian network stations. The interval between maneuvers is taken to be one day with three burn maneuver strategy to avoid ground trace disturbances⁴. Fig.4 shows the trajectory of the eccentricity vector as the frozen point is achieved for various initial locations of

the eccentricity vector. Fig.5 gives the typical velocity impulse history. It is found from fig.6 that the total dV required to achieve frozen perigee depends on the initial location of the eccentricity vector with respect to the allowed region for the maneuvers. The minimised cost function given by (12) is a function of the initial location of eccentricity vector. This is depicted in fig. 6. Table-1 shows the effect of Q and R on the maximum impulse needed and the acquisition time.

TABLE-1 : Effect of Q and R

Q	R	Maximum impulse (m/sec)	Acquisition Time (days)
	10	0.288	84
	30	0.191	139
	50	0.156	159

Conclusion

This method of orbit correction to achieve frozen orbit is well suited for on-board implementation of the strategy. Once the gains are calculated on the ground and uplinked alongwith the initial eccentricity vector, only the equations (8) and (9) need to be executed onboard to calculate the control force. Thus this onboard logic could do the necessary correction automatically. Occasionally the orbit determination on ground could verify the correction and in case of inconsistency, the strategy can be modified by uplinking the parameters A,B,X and F.

References

- [1] Nagarajan, N., and Reno Rayan, H., "Effect of Apisides Rotation on Altitude and Ground Trace Pattern for IRS-1C" DOC.No.IRS-1C-42-90-02-05-03
- [2] Rosengren, M., "Improved Technique for Passive eccentricity Control", Advances in Astronautical Sciences, Vol..69, 1989, paper No.AAS-89-155
- [3] Jayashree, M.S., and Nagarajan, N., "On the motion of the eccentricity vector for IRS-1A ,IRS-1B", Journal of Spacecraft Technology, Vol.2, No.2, July 1992, pp:44-51
- [4] Reno Rayan, H., and Nagarajan, N., "Realisation of Frozen Orbit Parameter for IRS-1B with visibility and impulse constraints" DOC.No.ISRO-IRS-1A/ 1B-93-02-10-27

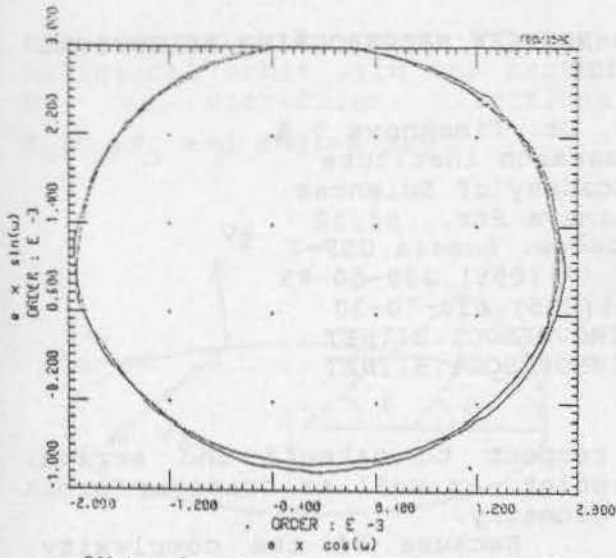


FIG. 1 - Eccentricity vector motion for IRS-18

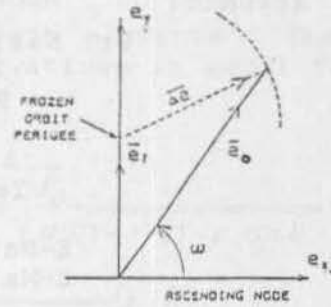


FIG. 2. GEOMETRY OF ECCENTRICITY VECTOR

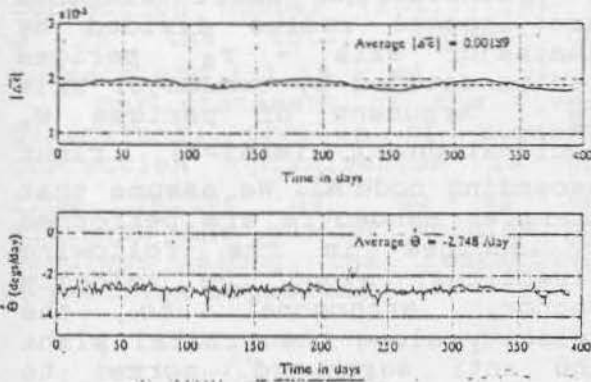


FIG. 3 - Magnitude and directional variation of $\dot{\theta}$ / day

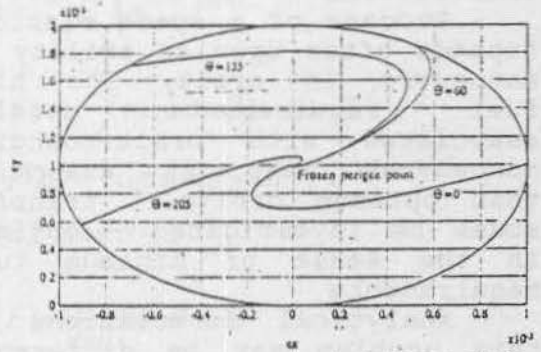


FIG. 4 - Frozen perigee acquisition for different initial locations

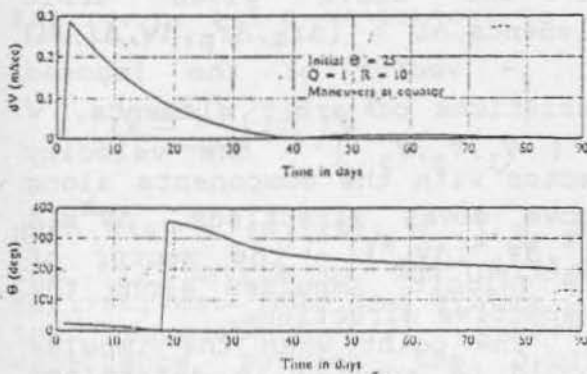


FIG. 5 - Typical velocity impulse and θ history for $\theta_0 = 25^\circ$

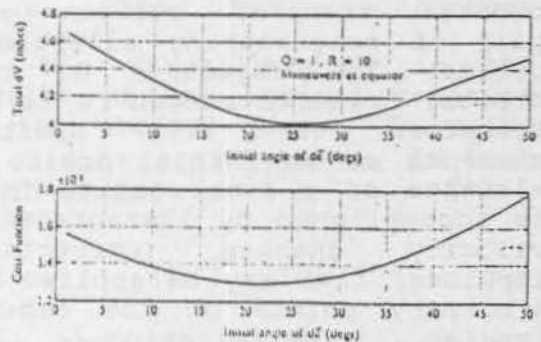


FIG. 6 - Total Δv & Cost function as function of initial θ

OPTIMAL AND QUAZIOPTIMAL TRANSFER BETWEEN NEIGHBOURING ELLIPTICAL ORBITS

Dr. Nazirov R.R., Dr. Timokhova T.A.
Space Research Institute
Russian Academy of Sciences
Profsoyuznaya Str., 84/32
117810, Moscow, Russia, GSP-7
Telephone: (7)(095) 333-50-89
Fax: (7)(095) 310-70-23
E-Mail: RNAZIROV@ESOC1.BITNET
E-Mail: TTIMOKHO@ESOC1.BITNET

Abstract

This paper gives analytical solution of the problem how to optimize the impulse transfer between neighbouring elliptical orbits when a transfer manoeuvre is performed by engines along the velocity vector, orthogonal to the velocity vector or normal to the orbital plane.

Introduction

Success of a space missions depends often upon an ability to manoeuvre in orbit. The high fuel requirements usually associated with orbit-changing manoeuvres make it essential that optimum orbital transfer modes be investigated - optimum in the sense of minimum fuel requirements.

Analytical formulations of this problem may be different. It is possible to consider the motion in oblate or central gravity field, discrete or continued control, prescribed or free final time.

This paper concerns optimum orbital transfer between any pair of neighbouring elliptical orbits. The objective of the orbital transfer manoeuvre is to transform the five orbital elements of an initial orbit to elements of a final orbit. This is accomplished by instantaneous velocity changes (correction impulses) that may be applied at arbitrary points on the orbit. Impulse optimization is accomplished for free end point: i.e., impulse is minimized with

respect to takeoff and arrival point, as well as transfer orbit geometry.

Because of its complexity, this problem of optimal transfer can only be analytically solved in some special cases. In our case minimized functional differ from usual one and problem is solving in linear formulation.

Considering orbit elements are: apogee radius divided by semimajor axis - r_a , perigee radius divided by semimajor axis r_p , argument of perigee w , inclination i ($\sin i \neq 0$), right ascending node Ω . We assume that transfer manoeuvre are performed by engines in the following directions: along the velocity vector, orthogonal to the velocity along the orbital plane and anti earthward, normal to the orbital plane.

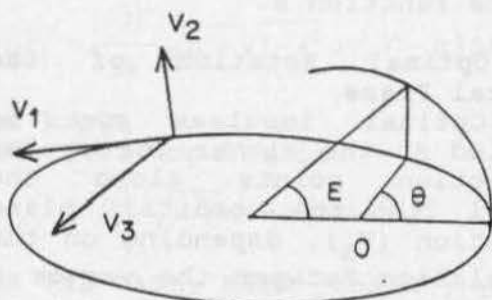
1 Analytical Formulation

Note:

$L = \{r_a, r_p, w, i, \Omega\}$ - vector of the above given orbit elements, $\Delta L = \{\Delta r_a, \Delta r_p, \Delta w, \Delta i, \Delta \Omega\}$ - vector of the imposed variations of orbit elements, $V = \{v_1, v_2, v_3\}$ - the velocity vector with the components along above given directions, $\Delta v^k = \{\Delta v_1^k, \Delta v_2^k, \Delta v_3^k\}$ - the vector of the velocity impulses along the respective directions.

The point when the impulse should be applied is determined by the correction points either the eccentricity anomaly E or

true anomaly ϑ . Fig. 1 shows elliptical orbit with the center O. the correction directions v_1, v_2, v_3 and angles E, ϑ .



At the correction point E^k (or ϑ^k) impulses $\Delta v_1^k, \Delta v_2^k, \Delta v_3^k$ are applied along the respective directions where K is the correction number ($K=1, \dots, n$), n is the total number of corrections ($1 \leq n < \infty$).

Our statement of the five-dimensional problem of element correction optimization is to find vector Δv^k so as to minimize the sum of modules of impulses along the respective directions separately

$$S = \sum_{k=1}^n (|\Delta v_1^k| + |\Delta v_2^k| + |\Delta v_3^k|) \quad (1)$$

over the set of all possible values $\Delta v_1^k, \Delta v_2^k, \Delta v_3^k$ at any correction points $E^k \geq 0$, for $K=1, \dots, n, 1 \leq n < \infty$ subject to

$$\Delta L = \sum_{k=1}^n Q(E^k) W^k \quad (2)$$

Here $G(E) = \{G_{ij}(E)\} = \partial L / \partial v$ is the 5×3 matrix of the partial derivatives. Thus the system of the equalities (2) express dependence between the orbit element variation and correction impulses in a linear

approximation. The partial derivatives are derived using well-known formulas for spacecraft elements. The matrix of derivatives is equal to

$$G(E) = \sqrt{\frac{P}{\mu}} \frac{1}{\sqrt{1-e^2} \sqrt{1-e^2 \cos E^2}} G^1(E) + \sqrt{\frac{P}{\mu}} \frac{1}{\sqrt{1-e} \cos \vartheta} G^2(E)$$

where non-zero elements are equal

$$G_{11}^1(E) = 2(1+e)(1+\cos E)$$

$$G_{21}^1(E) = 2(1-e)(1-\cos E)$$

$$G_{12}^1(E) = -G_{22}^1(E) = \sqrt{1-e^2} \sin E (1-e \cos E)$$

$$G_{13}^1(E) = \left(\frac{2}{e}\right) \left(\sqrt{\frac{1}{e^2}}\right) \sin E$$

$$G_{33}^1(E) = -\frac{1}{e} (\cos E + e) (1-e \cos E)$$

$$G_{33}^2(E) = -\text{ctg} \vartheta \sin(\vartheta + \omega)$$

$$G_{43}^2(E) = \cos(\vartheta + \omega)$$

$$G_{53}^2(E) = \frac{1}{\sin i} \sin(\vartheta + \omega)$$

where e is the eccentricity of elliptical orbit ($0 < e < 1$), p is the orbit element, μ is the gravitational constant.

This optimization problem falls into two independent problems.

The first problem is the problem of the optimal rotation of the orbital plane. To solve it we must find impulses Δv_3^k so as to minimize

$$Q = \sum_{k=1}^n |\Delta v_3^k|$$

over the set of all possible values Δv_3^k at any correction

points $\vartheta^k \geq 0$, for $k=1, \dots, n$, $1 \leq n < \infty$ subject to

$$\Delta P = \sum_{k=1}^n C(\vartheta^k) \Delta V_3^k \quad (3)$$

where

$$\Delta P = \{\Delta i, \sin i \Delta \Omega\},$$

$$C(\vartheta) = \{G_{43}(\vartheta), \sin i G_{53}(\vartheta)\}$$

The second problem is the problem of the optimal modification in the orbital plan. To solve it we must find impulses $\Delta v_1^k, \Delta v_2^k$ so as to minimize

$$R = \sum_{k=1}^n (|\Delta V_1^k| + |\Delta V_2^k|)$$

over the set of all possible values $\Delta v_1^k, \Delta v_2^k$ at any correction points $E^k \geq 0$, for $k=1, \dots, n$, $1 \leq n < \infty$, subject to

$$\Delta M = \sum_{k=1}^n (A(E^k) \Delta V_1^k + B(E^k) \Delta V_2^k), \quad (4)$$

where

$$\Delta M = \{\Delta r_s, \Delta r_{s1}, \Delta \varpi\},$$

$$A(E) = \{G_{11}(E), G_{21}(E), G_{31}(E)\},$$

$$B(E) = \{G_{12}(E), G_{22}(E), G_{32}(E)\},$$

$$\Delta \varpi = \Delta \omega + \cos i \Delta \Omega$$

Let us show that the solutions of the two separate problems are equivalent to the solution of the initial problem. Consider the 5×5 matrix H which non-zero elements are equal

$$h_{11} = h_{22} = h_{33} = h_{44} = 1,$$

$$h_{35} = \cos i,$$

$$h_{55} = \sin i$$

It is a non-degenerate one. Consequently, equalities (3) and

(4), obtained by multiplying equalities (2) by matrix H , are equivalent to (2). Moreover, it is possible to write the function (1) in the form $S = Q + R$. Since $Q \geq 0$, $R \geq 0$ we can minimize the functions Q and R separately to obtain the minimum of the function S .

2. Optimal Rotation of the Orbital Plane

Optimal impulses may be applied at the either one or two correction points along the normal to the orbital plane direction (V_3), depending on the correlation between the vector ΔP components and value ω . Note: α - the angle from the vector $(\cos \omega, \sin \omega)$ to the vector ΔP . Then

$$\cos \alpha = \frac{(\Delta i \cos \omega + \sin i \sin \omega \Delta \Omega)}{|\Delta P|},$$

$$\sin \alpha = \frac{(\Delta i \sin \omega - \sin i \cos \omega \Delta \Omega)}{|\Delta P|},$$

$$|\Delta P| = \sqrt{\Delta i^2 + \sin^2 \Delta \Omega^2}$$

2.1 THE - CASE, WHEN $|\cos \alpha| < e$

In this case optimal transfer is two-impulse one. The impulses are applied at the correction points ϑ^1, ϑ^2 , which satisfy the equalities:

$$\cos \vartheta^1 = \cos \vartheta^2 = e,$$

$$\sin \vartheta^1 = \sqrt{1-e^2}, \sin \vartheta^2 = \sqrt{1-e^2}$$

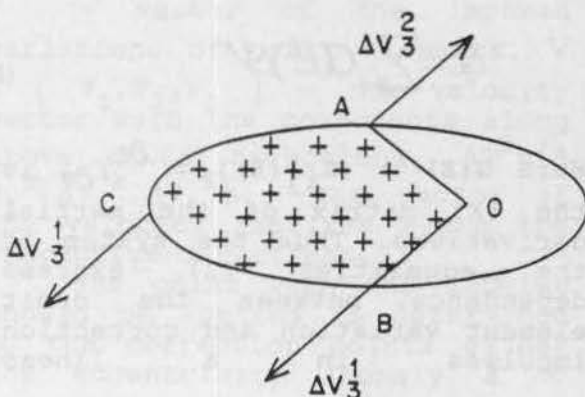


Fig. 2 shows SC orbit with the center O and points A, B corresponding to angles ϑ^1, ϑ^2 , the value of impulses are

$$\Delta V_3^k = \frac{(-1)^k}{2e} \sqrt{\mu/p} \sqrt{1-e^2} \sin(\vartheta^k - \alpha) |\Delta P|,$$

for $k=1, 2$

The total impulse is

$$Q = \sqrt{\mu/p} \sqrt{1-e^2} |\sin \alpha| |\Delta P|$$

2.2 THE CASE, WHEN $|\cos \alpha| \geq e$

In this case optimal transfer is one-impulse one. The impulse is applied at the correction point, ϑ^1 , which satisfy the equalities:

$$\cos \vartheta^1 = -|\cos \alpha|, \sin \vartheta^1 = -\text{sign}(\cos \alpha) \sin \alpha$$

Fig. 2 shows hatching part of CS orbit where the angle ϑ^1 may be and point C corresponding to the probable angle ϑ^1 . The value of the optimal impulse is

$$\Delta V_3^1 = -\text{sign}(\cos \vartheta^1) N$$

where N is equal to the total impulse

$$Q = N = \sqrt{\mu/p} (1+e \cos \vartheta^1) |\Delta P|$$

3. Optimal Modifications in the Orbital Plane.

If there are some restrictions to the value of e, optimal impulses may be applied at the either one or two correction points along the velocity vector direction (\mathbf{v}_1), depending on the correlation between the vector $\Delta \mathbf{M}$ components.

3.1 THE CASE, WHEN $\Delta \varpi = 0$

In this case optimal transfer is two-impulse one. The impulses are applied at the

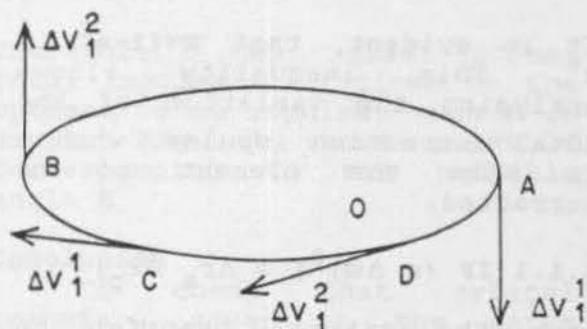
correction points E^1, E^2 , which satisfy the equalities: $E^1 = 2\pi q$, $E^2 = \pi(2L+1)$, where q, L are natural numbers. The values of impulses are

$$\begin{aligned} \Delta V_1^1 &= W_1 = \frac{1}{4} \sqrt{\frac{\mu}{p}} (1-e) \Delta r_a, \\ \Delta V_1^2 &= W_2 = \frac{1}{4} \sqrt{\frac{\mu}{p}} (1+e) \Delta r_p \end{aligned} \quad (5)$$

The total impulse is

$$R = R^0 = \frac{1}{4} \sqrt{\frac{\mu}{p}} [(1-e) \Delta r_a + (1+e) \Delta r_p] \quad (6)$$

Note that this theorem agrees well with known results². Fig. 3 shows SC orbit with the center O and points A, B corresponding to the angles E^1, E^2 .



3.1 THE CASE, WHEN

$$\Delta \varpi \neq 0, (e \Delta \varpi^2) \leq \Delta r_a \Delta r_p$$

In this case if either $e \leq 2 \leq \sqrt{5}$ or it is possible to use impulses only along the velocity vector direction (\mathbf{v}_1), then optimal transfer is following one. The impulses are applied at the correction points

$$E^1 = E^*, E^2 = \pi - E^*$$

such that

$$\sin E^* = \frac{2\Delta\omega e\sqrt{1-e^2}}{(1-e)\Delta r_a + (1+e)\Delta r_p}$$

Fig. 3 shows the points C, D corresponding to the probable angles E^1, E^2 . The total impulse is

$$R = \left(\frac{1}{\cos \theta^*} \right) R^0$$

where the values R^0 was determined in (6), θ^* is the angle between velocity vector and the orthogonal to the orbit radius direction. It satisfy the equation

$$\cos \theta^* = \frac{\sqrt{1-e^2}}{\sqrt{1-e^2 \cos^2 E^*}} \quad (7)$$

It is evident, that $R\sqrt{1-e^2} \leq R^0$. This inequality allows analysing the variation of the total correction impulse, when ω is also the element to be corrected.

3.1.1 IF $(e \Delta\omega)^2 = \Delta r_a \Delta r_p$,

then the optimal transfer is one-impulse one. The impulse is applied at the point $E^1 = E^*$ and is equal

$$\Delta V_1^1 = \text{sign}(\Delta r_a) R^0$$

where the value R^0 was determined in (6).

3.1.2 IF $(e \Delta\omega)^2 < \Delta r_a \Delta r_p$,

then the optimal transfer is two-impulse one. The impulses are applied at the correction

points $E^1 = E^*, E^2 = \pi - E^*$ and are equal

$$\Delta V_1^k = F(E^*),$$

where

$$F(E^*) = \left(\frac{1}{\cos \theta^*} \right) \left[1 - \frac{(-1)^k}{\cos(E^*)} \right] W_1 + \frac{1}{\cos \theta^*} \left[1 + \frac{(-1)^k}{\cos(E^*)} \right] W_2$$

where W_1, W_2 were determined in (5), $k = 1, 2$.

3.2 THE CASES WHEN

$$\Delta\omega \neq 0, (e\Delta\omega)^2 > \Delta r_a \Delta r_p$$

In this case if either $e \leq \sqrt{3}/2$ or it is possible to use impulses only along the velocity vector direction (V_1), then optimal transfer is the following one. The impulses are applied at the correction points $E^1 = E', E^2 = \pi - E'$ such that

$$\text{ctg } E' = \frac{(1-e)\Delta r_a - (1+e)\Delta r_p}{2\Delta\omega e\sqrt{1-e^2}}$$

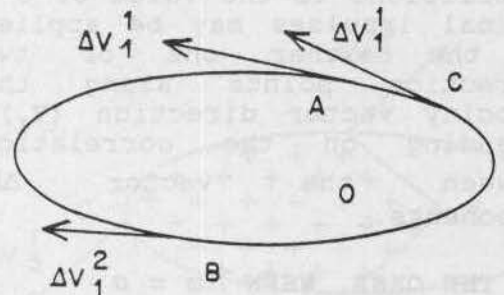


Fig. 4 shows the SC orbit with the center O and points A, B corresponding to the probable angles E^1, E^2

3.2.1 IF $(1-e)\Delta r_a \neq (1+e)\Delta r_p$ then the values of the impulses are

$$\Delta V_1^k = F(E^k)$$

where function F was determined in (8), $k = 1, 2$. The total impulses is

$$R = \frac{1}{\cos \theta} \left| \frac{1}{\cos E} (W_1 - W_2) \right|$$

where W_1, W_2 were determined in (5) the angle θ satisfies (7).

3.2.2 IF $(1-e)\Delta r_a = (1+e)\Delta r_p$ then the values of the impulses are

$$\Delta V_1^k = \frac{(-1)^k}{4} \sqrt{\frac{\mu}{p}} \Delta \varpi$$

where $k=1, 2$.

The total impulses is

$$R = \frac{1}{2} \sqrt{\frac{\mu}{p}} |\Delta \varpi|$$

4. Quasi-optimal Modifications in the Orbital Plane

Assume that the optimal transfer is not suitable or only a one-impulse manoeuvre is allowed and variation of the element ω is not important (it is usually true for small e). Here we demonstrate the case, when the so-called quasi-optimal one-impulse correction of elements r_a, r_p along the velocity vector direction (V_1) exists. And the quasi-optimal total impulse is close to the

optimal one if the eccentricity is small.

If $\Delta r_a \Delta r_p > 0$ it is possible to become a sub-optimal solution of the transfer problem by one-impulse manoeuvre at the point $E^1 = E^2$ such that

$$\cos E^* = \frac{(1-e)\Delta r_a - (1+e)\Delta r_p}{(1-e)\Delta r_a + (1+e)\Delta r_p}$$

The value of this impulse is

$$\Delta V_1^1 = \text{sign}(\Delta r_a) \frac{1}{\cos \theta^*} R^0$$

where the value R^0 was determined in (6), θ satisfies (7). The quasi-optimal correction value is

$$R = \frac{R^0}{\cos \theta^*}$$

From this follows that $R\sqrt{1-e^2} \leq R^0$,

Therefore, the quasi-optimal total impulse R is close to the optimal total impulse, when e is small. Fig. 4 shows point C corresponding to the probable angle E^*

Conclusion

To check that orbital transfers given in the parts 2, 3, 4 are suitable, one must simply put them to the equations (3), (4).

To prove that the above chosen solutions of the transfer problem are optimal, we will use the so-called Kuhn-Tucker theorem which gives the criteria of optimum (see Appendix).

For our statement of the optimal transfer problem we have obtained a full analytical solution of the problem of optimal rotation of the orbital plane. Solution of the problem

of optimal modifications in the orbital plane is not so full because of in a general case the are orbital parameters (e, p) and the required variations of orbital parameters when above given solution is not optimal. But it is not so important for applications because of the restrictions to the value of excentrecety are not essential and are close to unit.

Appendix : Criteria of Optimum

According to the theory, the following nonlinear problem: to find $x = \{x_1, \dots, x_n\}$ so as to minimize

(A1)

$$\sum_{k=1}^n |x_k| \quad (\text{for } k=1, \dots, n, 1 \leq n < \infty)$$

subject to

$$C = Ux \quad (\text{A2})$$

where C is an m -dimensional vector, U is an $m \times n$ matrix, is equivalent to the following linear programming problem, to find $y = \{y_1, \dots, y_{k2n}\}$ so as to minimize

$$\sum_{i=1}^{2n} y_i \quad (\text{for } i=1, \dots, 2n, 1 \leq n < \infty)$$

subject to

$c = Zy, y_i \geq 0, \text{ for } i=1, \dots, 2n,$
 where $Z = \{U, -U\}, X_k = y_k - y_{n+k}$
 Hence, the linear programming form of the Kuhn - Tucker theorem can be used for the problem (A1), (A2). That is:

feasible solution x^* is the optimal solution of the problem (A1), (A2) if and only if an m -dimensional vector d exists such that all of the following conditions are satisfied

$$U_k d^T = \text{sign}(x_k^*), \text{ at } x_k^* \neq 0,$$

$$|U_k d^T| \leq 1 \quad \text{at } x_k^* = 0,$$

for $k=1, \dots, N, 1 \leq N < \infty,$
 where U_k is the column of matrix U, T is the transposition sign.

To prove the above results one must use this theorem with corresponding x^*, U_k .

References:

- 1 Eliasberg, P.E.:1965. Introduction into the Fight Theory of the articial Earth Satellite, Nauka, Moscow.
- 2 Ivashkin, W.W.:1975. Optimization of the space manouevres., Nauka, Moscow.

ATTITUDE AND ORBIT CONTROL II

ATTITUDE MEASUREMENT AND CONTROL SUBSYSTEM

1. Bollner, M.; Feucht, U.; Frank, H. and Rupp, T.
(DLR-Germany):
**"Flight Experience with the ROSAT Attitude
Measurement and Control Subsystem"** 077
2. Carrara, V. and Guedes, U.T.V. (INPE-Brazil):
"Attitude Control Aspects for SCD1 and SCD2" 083
3. Anigstein, P.A. (U.B.A.-Argentina); Pe/a, R.S.S.;
Yasielski, R.; Jáuregui, M. and Alonso, R. (CONAE-
Argentina):
"Mission Mode Attitude Control for SAC-B" 088
4. Kono, J. and Santana, C.E. (INPE-Brazil):
"SCD1: One Year in Orbit" 096

FLIGHT EXPERIENCE WITH THE ROSAT ATTITUDE MEASUREMENT AND CONTROL SUBSYSTEM

M. Bollner, U. Feucht, H. Frank, T. Rupp
DLR / German Space Operations Center
D-82234 Wessling / Germany

Abstract

Experience gained during the flight operations of the Attitude Control System of the ROSAT spacecraft is described. The ROSAT spacecraft comprises a three-axes stabilized satellite supporting the largest X-ray telescope flown up to now. The control system consists of high precision star trackers and gyros for attitude reference and reaction wheels for maneuvers. The satellite has successfully performed the first all-sky survey with an imaging X-ray telescope. During the following pointing observations of selected sources, severe degradation of the gyros forced modifications of the onboard software to use the available magnetometer and coarse sun sensor measurements. The attitude control accuracy could thereby be improved again to allow an autonomous star acquisition by the star trackers for high precision pointing. This allowed the resumption of the nominal mission under conditions specified prior to launch. Further software changes as results of other device failures are also described.

Key words: Flight experience, high accuracy pointing, attitude subsystem, CCD star trackers, ground segment, device failures.

Introduction

With the launch of ROSAT (ROentgen SATellite) a new area of X-ray astronomy has begun. With this mission the first all-sky survey with an imaging X-ray telescope was performed. Additionally the spacecraft has observed many thousands of celestial sources with unprecedented accuracy and sensitivity. ROSAT is a cooperative project between Germany, the United States and the United Kingdom. Main contractor for ROSAT is Dornier, responsibility for the Attitude Measurement and Control Subsystem (AMCS) is with MBB, both part of Deutsche Aerospace. The spacecraft comprises a three-axes stabilized satellite supporting the largest X-ray telescope flown up to now (83 cm aperture). It is of Woiter type, with a focal plane assembly carrying two imaging proportional counters (PSPC), and one high

resolution imaging channel plate detector (HRI). The main telescope is supplemented by a XUV wide field camera, for observations in the extreme ultraviolet spectral area. Germany developed ROSAT and conducts the operations, the US provided the launcher and one of the detectors, and the UK has built the XUV camera.

The spacecraft of 2500 kg weight has been launched on June 1, 1990 with a Delta II launch vehicle, into the nominal circular orbit of 580 km altitude inclined at 53 degrees.

GSOC (German Space Operations Center) is responsible for mission operations. It provides all tracking, telemetry, command and data processing capabilities to support the mission, with additional facilities to provide interfaces with NASA ground stations in the event of contingency operations. The use of the single Weilheim Ground Station for the low Earth satellite leads to a daily visibility pattern of 5-6 short consecutive contacts of approx. 10 min duration each, separated by 1.5 h, followed by an invisibility period of approx. 16 h. The collected data are stored onboard on tape recorders.

As of December 1993, ROSAT has completed three and a half years of operation. After the survey and three months into the pointing phase, the mission was severely hampered, mainly by gyro degradation. The paper will concentrate on the measures taken to rescue the mission.

The Attitude Measurement and Control Subsystem (AMCS)

The AMCS is a digital control system based on a microprocessor. It uses a strapdown system (which is updated by star tracker measurements every second) and quaternion notation. A RAM area of 6k words is available for onboard software modifications.

The main operating modes are:

- Safe Mode:

to provide survival capability to avoid loss of spacecraft in an AMCS Emergency and/or spacecraft

malfunction situation. It shall maintain two-axes solar oriented attitude.

- Normal Mode:

covers the normal operations scan and pointing including scan at rates between 3 and 5 arcmin/s around the spacecraft x-axis, inertially fixed pointing to selected targets, slewing from one target to the next.

The satellite has a solar array fixed to the spacecraft structure (see Fig. 1). The array must be oriented to within ± 15 deg of the perpendicular to the sun direction. Therefore the observable part of the sky is coupled with the apparent motion of the sun.

A mission planning facility establishes the ROSAT Mission Timeline according to observation requests and applied constraints. This timeline is the base for the AMCS operations. It is used by a complex ground software system to perform an automatic command generation for all attitude related telecommands. This approach is necessary due to the stringent requirement to uplink up to 2500 attitude related telecommands per day nominally during two of the short contacts. Peak uplink is 8000 commands during three contacts. The main part of the attitude commands comprises the star catalogues required by the onboard system.

The spacecraft is equipped with the following attitude devices:

- two imaging star trackers (STC) with CCD devices
- four rate-integrating gyros
- four reaction wheels
- three magnetic coils for wheel unloading
- a three-axes fluxgate magnetometer, originally only for coil steering for the unloading
- a set of three two-axes sun sensors, originally only as safety devices

The following accuracies were specified for the system during pointing:

- deviation of telescope axis from commanded attitude: < 3 arcmin
- rate limits: < 5 arcsec/s
- STC bias: < 2 arcsec
- STC noise: < 1 arcsec

The original design of the attitude control system used three of four gyros for slews between X-ray targets. The accuracy of the gyros with respect to scale factor errors and fixed/random drifts was such, that errors accumulated during slews or Earth occultations were less than 15 arcmin. This allowed an unambiguous star identification and consecutive control with the star trackers. The typical number of autonomously observed targets was 25 per day.

Flight Experience

Launch and early operations

The performance in the early phases of the mission was perfect. Especially the commissioning phase went extremely smooth. All devices were found to fulfill their specifications. Gyro drifts were in the order of 0.006 arcsec/s. The slew times were found to be in accordance with the pre-launch simulations. Momentum management provided appropriate unloading of the wheels without disturbance of the system. A minor problem was the magnitude calibration of the star trackers, which showed some offsets compared to laboratory results.

First anomalies

Four month after launch one of the two star trackers failed, apparently due to a problem in the RAM area of the electronics. This reduced the number of available reference stars from six to three, causing restrictions for the selection of targets when not at least two stars were available for attitude control.

Gyro degradation and loss

Six month after launch severe signs of degradation were observed on three gyros: Scale factor errors ten times larger than specified, drift values up to ± 7 arcsec/sec for the x-gyro, which additionally were dependant from the sign of the rotation performed. The x-gyro was therefore replaced by the redundant 4th skewed gyro. This allowed to finish the survey and to start the pointing phase. However, after three months pointing, in May 1991 the y-gyro failed totally. So the x-gyro had to be used again, despite its bad performance. The usage of these degraded devices caused now slew errors considerably larger than 0.5 degrees, a value which was the maximum for the original star identification to perform well. Also loss of a second gyro would have terminated the mission immediately. Therefore an attitude control concept was designed and implemented, which even has the capability to work with only one gyro. Up to now six versions of onboard software have been developed by the MBB subsidiary of Deutsche Aerospace, requiring each time a code uplink of more than 8000 commands. These onboard changes had also considerable consequences for the already very complex ground segment. It was necessary to implement a realtime star identification software, to change several times the star catalogue generation software, and to operate a hardware-in-the-loop spacecraft simulator to test the new onboard software. Fortunately, from the mission preparation phase this simulator was still available at GSOC. It

combines the AMCS microcomputer with a software simulation of the spacecraft dynamics, the sensor and actuators, and the environment (magnetic field, stars, etc.). This allowed to load the new code to the computer and to verify the performance.

Software modifications

The different software versions cover the following features:

- an angular momentum bias around the nominal sun direction for safety reasons. The momentum is stored in the wheels.
- update of the onboard attitude quaternion after star identification on ground. This was an intermediate solution during development of the modified control concept.
- Survival mode using only one gyro
- Normal mode gyro usage selectable from ground. Mode possible with three, two or one gyro.
- onboard implementation of an 8th order Earth magnetic field model.
- update of the attitude quaternion with sun sensor and/or magnetometer measurements according to availability. Thereby usage of one of the available two-axes sun sensors and the three-axes magnetometer for the attitude measurement.
- automatic selection of angular rate information according to availability from gyros, star trackers, sun sensors, magnetometer, or integration of the Euler equations. This feature is only enabled when less than three gyros are available.
- implementation of advanced star identification algorithms which tolerate large attitude errors.
- onboard gyro drift estimation and compensation.
- extended command capability for gyro scale factors. The original possible range was too small for the degraded devices.
- usage of a star tracker of the XUV camera payload to replace the original attitude subsystem star trackers. This feature has been developed in advance and is not used up to now.

Further mission events

Reduced Mission

During the first phase of the software development a restricted mission had to be defined, during which only one target was observed per day. This was possible by support from a new realtime attitude determination on ground, derived from star tracker measurements, gained after the slew. The attitude solution was then uplinked to the spacecraft, to update the onboard attitude.

Uplink of new mode

After five month in this mission mode, the new control mode with magnetometer and sun sensor for attitude updates and various sources for velocity information could be uplinked. The sun sensor is aligned with the s/c -x-axis (see Fig. 2), and performs updates around the y- and z-axis. Its accuracy is ca. 0.5 degrees. The magnetometer is used for updates around the x-axis. Both devices serve to update the attitude quaternion, when deviations caused by the gyros (which still are input to the strapdown algorithm as long as three are available) exceed certain limits. This means that with three gyros the velocity information during slews is still derived from the gyros, but the necessary accuracy can be very poor.

The new software has three main functions:

- survival mode
- attitude surveillance in Normal mode
- star acquisition support in Normal mode

Survival mode is used to reorient the solar array (s/c -x-axis) to the sun from an arbitrary orientation with the usage of the sun sensors alone. The rate information for the wheel unloading is taken from the x- or s-gyro. So a survival with one gyro only is possible. In eclipse no attitude control and unloading is performed. The wheels are controlled to constant speed, and the sun orientation is roughly kept by the stored angular momentum.

Attitude surveillance in Normal mode ensures a correct orientation of the solar array with respect to the sun. It is only enabled, when no identified reference stars are available.

- in sun driven by the sun sensors
- in eclipse driven by the magnetometer

Star acquisition support ensures an attitude, which is consistent with the tolerances allowed by the star identification algorithm which requires an accuracy of ca. 2 degrees. This can normally be achieved only by a combined update of magnetometer and sun sensor, thus outside eclipse periods (which last up to 35 minutes during the 96 minutes orbit).

In both cases, for the magnetic field computation an up to date 8th order field model is used. It is based on recent updates to the IGRF model. The model has

an accuracy of ca. one degree, which together with a high measurement accuracy of the magnetometer, gives a control accuracy, which satisfies the needs of the star identification algorithm.

The software proved to work very successful, and so in October 1991 the nominal mission could be resumed. Up to November 1993 there was a smooth continuation of the mission. Only some minor problems had to be corrected. During this time also the remaining star tracker showed some anomalies which led to the above mentioned decision to develop a mode using a further payload star tracker.

Two-gyro operations

In November 1993 the z-gyro failed. This left the spacecraft with only two gyros. Thanks to the already uplinked software, a resumption of the scientific mission after 10 days of tests was possible. The consequences of the two-gyro operations are as follows:

- as the rate information around z must be derived in eclipse from the magnetometer, slews during eclipse are no longer possible. Reason is that magnetometer readings can be used only every two minutes due to disturbance by the unloading coils. With this update rate the high velocities during slew maneuvers cannot be controlled to the necessary extent. This had the consequence that the timeline generation software had to be modified to schedule the slews appropriately.

- to use the magnetometer for three-axes attitude control in Normal mode, the inertial reference must be established immediately after leaving the Survival mode in the same short ground contact. Otherwise a fallback to Survival mode in the next eclipse would occur. This requires a realtime attitude determination from one sample of magnetometer measurements at the begin of the contact and consecutive uplink to the spacecraft.

- eclipse conditions during steady state pointing but without reference stars also lead to deviations from the nominal attitude. This behavior is currently under investigation to reduce the offsets which are somewhat larger than expected.

- rate inputs from the star trackers for motion around the z-axis are affected by the noise of the CCD and/or unfavorable star constellations. This leads to jumps in the calculated rate values, which then cause generation of larger wheel torques than necessary. As this situation changes each second, the torque level of the wheels is higher than in the past.

But in general the two-gyro control system works very promising and allows to continue the scientific mission with only minor restrictions.

- Latest developments show that the 2-gyro-S/W causes control problems under special conditions: During shadow there is a rate unobservability around an axis perpendicular to the x- and s-gyro axis, if the earth magnetic field vector coincides with it.

If only external torques would exist, there still would be no problem. However, magnetic unloading of reaction wheels causes considerable internal torques. Thus, during inobservability periods large excursions are possible (up to 45 degr. within 4 min.).

A corrective action is underway, which will disable wheel unloading during shadow periods. The wheels are always kept far away from saturation. Therefore, unloading can wait until the next sun phase.

Respective S/W development is in progress, extensive tests with the simulator are planned. The new code will be uplinked and used around mid-february 1994, providing the basis again for the conduct of a nominal mission.

Conclusions

Despite all problems the ROSAT mission is an outstanding success. ROSAT provides unprecedented scientific results, which will significantly contribute to the understanding of the structure and evolution of the universe. It could be demonstrated that due to the capability to modify onboard software it was possible to overcome hardware deficiencies. The success can mainly be devoted to the high accuracy of both the magnetic field model and the magnetometer measurements, as well as the sensor placement which allowed three-axes measurements. As the orbital lifetime of ROSAT goes beyond the year 2000, it is hoped that the mission can be successfully continued for some more years.

Acknowledgement

The described achievements are the result of a joint effort of teams from MBB, Ottobrunn, Max-Planck-Institute for Extraterrestrial Physics, Garching and GSOC, Oberpfaffenhofen.

References

1. M. Bollner, A concept for operations of the ROSAT attitude measurement and control subsystem. Paper 86-2043, *AIAA Guidance, Navigation & Control Conference*, Williamsburg, Va. (1986)
2. M. Bollner and G. Schneiders, Attitude determination and control for the X-ray satellite ROSAT. *Proceedings of the 2nd International*

Symposium Spacecraft Flight Dynamics, Darmstadt (1986)

3. W. Schrempp et al., Design and test of the ROSAT AMCS. *Proceedings of the 10th IFAC World Congress on Automatic Control, Munich (1987)*

4. M. Bollner and U. Feucht, Ground operations to support the attitude control system of the ROSAT spacecraft. Paper 89/113, *Proceedings of the International Symposium on Space Dynamics, Toulouse (1989)*

5. G. Schneiders and T. Rupp, Flight results of the high accuracy attitude determination concept for the X-ray satellite ROSAT. Paper 90-3494, *AIAA Guidance, Navigation and Control Conference, Portland, Ore. (1990)*

6. M. Bollner, On-orbit control system performance of the ROSAT spacecraft. *Acta Astronautica Vol. 25, No. 8/9, pp. 487-495, (1991)*

7. D. Purl, N. Gradmann, M. Bollner, The ROSAT star tracker - flight experience. Paper, *1st International Conference on Spacecraft Guidance, Navigation and Control Systems, Noordwijk (1991)*

8. T. Rupp and M. Bollner, In-flight sensor performance of the ROSAT spacecraft and consequences for the attitude reconstruction on ground. Paper 91-353, *42nd Congress of the International Astronautical Federation, Montreal (1991)*

9. W. Schrempp, E. Bruederle, L. Kaffer, In-flight performance of the ROSAT attitude measurement and control system, Paper, *1st International Conference on Spacecraft Guidance, Navigation and Control Systems, Noordwijk (1991)*

10. W. Schrempp et al., Evaluation of flight results of the ROSAT AMCS. Paper, *14th AAS Guidance and Control Conference, Keystone, Col. (1991)*

11. M. Bollner, T. Rupp, U. Feucht, Usage of a sun sensor/magnetometer combination to replace gyros within a high accuracy attitude control system. Paper IAF-92-0045, *43rd Congress of the International Astronautical Federation, Washington DC (1992)*

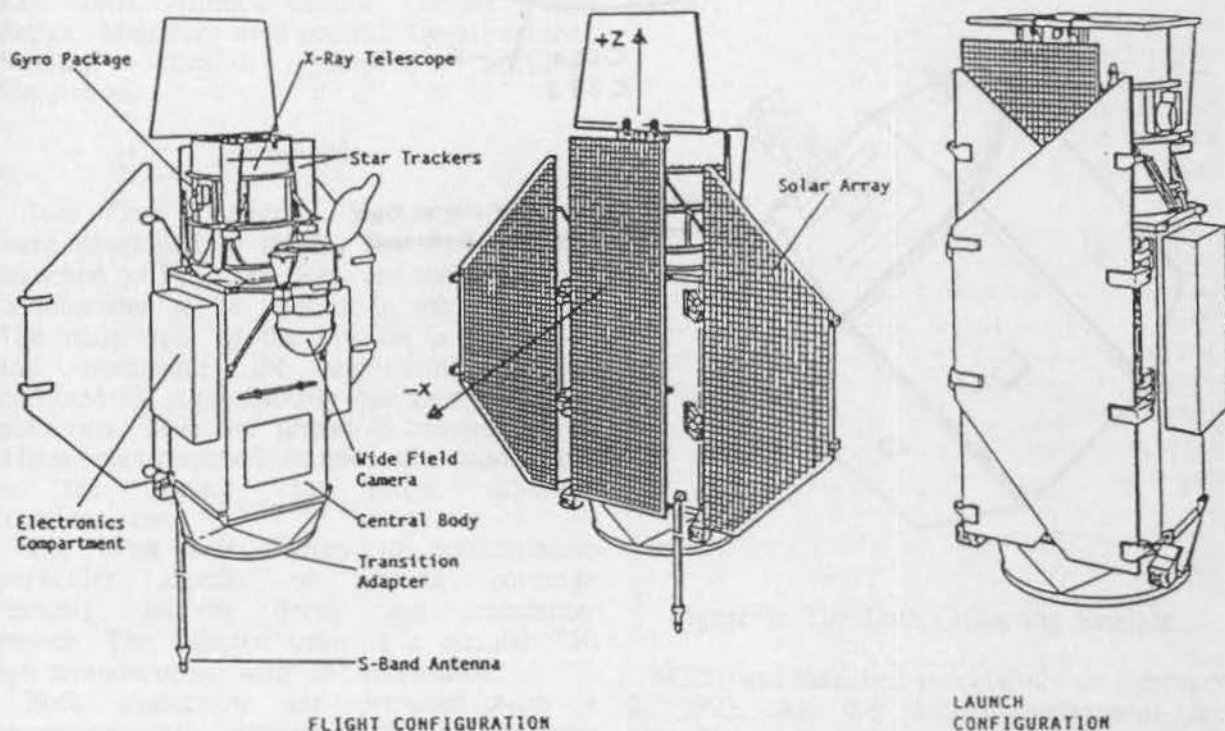


Figure 1.
ROSAT configuration

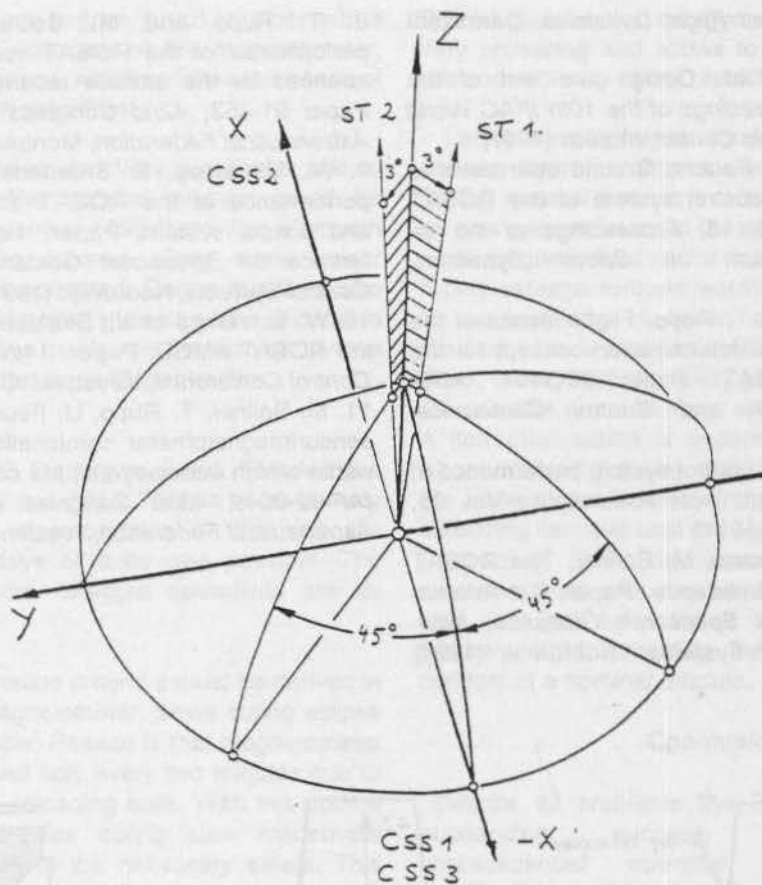


Fig.:2: Geometry of Sensor Line of Sight with respect to Spacecraft Coordinates

ATTITUDE CONTROL ASPECTS FOR SCD1 AND SCD2

Valdemir Carrara

Ulisses Thadeu Vieira Guedes

INPE - Instituto Nacional de Pesquisas Espaciais

POBox 515, 12201-970 - S.J. Campos, SP, Brazil

e-mail: val@dem.inpe.br

Abstract

The Data Collecting Satellites (SCD) were developed and integrated at INPE, Brazil, with an aim of retransmitting meteorological data collected by automatic platforms spread over the country. The specified orbit for SCD1 and SCD2 are circular at 750 km altitude and 25° inclination. SCD1 was launched in February 1993 by the Pegasus launcher (OSC). Both are spin stabilized, with magnetic attitude control coils. The angular velocity of the SCD2 spacecraft will be controlled by a spin plane magnetic coil, commanded by an on-board magnetometer.

Key words: Attitude control, Control system design, Minimum time control, On-off control, Satellite control, Satellite artificial, Simulation.

Introduction

Two Data Collecting Satellites (Fig. 1) were developed at INPE. The first one was launched on February 1993, and the second one is scheduled to be injected in orbit in 1995. The main goal of the mission is to receive and retransmit the environmental data collected by autonomously operated on-ground platforms. They are spread in remote regions where man-operated stations are inadequate, as the tropical rain forest, off-shore locations, etc.

The orbit was chosen to accommodate particular aspects of ground coverage (Brazil), altitude decay and transmitter power. The selected orbit is a circular 750 km altitude orbit, with 25° inclination.

Both spacecrafts are provided with a transponder as a payload. Internal subsystems are: Power Supply, Structure and Thermal Control, Telemetry and Telecommand Subsystem (TMTC), an experimental On-Board Computer and Attitude Control Subsystem. An experimental reaction wheel (only the shaft, bearings and electronics, without the wheel mass) will also be integrated in SCD2.

SCD1 satellite

The Attitude Control Subsystem (ACS) is responsible to stabilize and control the spacecraft orientation with respect to the Sun. To perform these tasks, the ACS is provided with two digital one-axis Sun Sensors, one analogue Magnetometer, one spin axis air core Magnetic Coil and a passive Nutation Damper. The stabilization is achieved by a rotation around its major principal axis imparted to the spacecraft by the launcher's last stage. Attitude determination and control are both performed on-ground, by using the telemetered sensor signals and commanding the appropriate coil polarity.

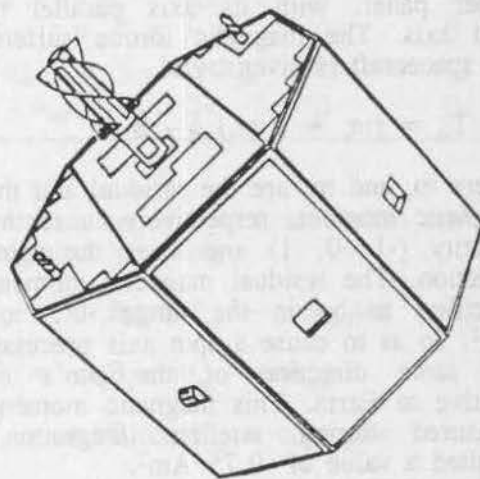


Figure 1: The Data Collecting Satellite.

SCD1 was launched successfully on February 9, 1993. All the internal subsystems are operating according to specifications. Orbit and attitude determinations are being performed properly.

Due to the launcher restrictions (Pegasus), the injection angular velocity was limited to 120 rpm, rather than the specified 140 rpm. Eddy current torques caused by the Earth's magnetic field decrease exponentially the

angular velocity of the satellite. Pre-flight calculations predicted a spin decay from 120 rpm, at the beginning of life, to 20 rpm, approximately, after 1 year (expected spacecraft life). This torque is approximately described by¹:

$$\bar{T}_e = p (\bar{\omega} \times \bar{B}) \times \bar{B} \quad (1)$$

where p is a constant coefficient, function of the spacecraft's geometry and its surface electrical properties. $\bar{\omega}$ is the satellite angular velocity and \bar{B} the Earth's magnetic flux density. Theoretical approaches gave to p a value close to 1920 m²/Ohm.

In addition, magnetic torques due to unbalanced electrical currents in the spacecraft equipments precess the satellite spin axis, around the Earth's magnetic dipole. After some period, the change in the satellite attitude relative to the Sun would illuminate the thermal bottom panel, so an attitude maneuver would be necessary to reorient the spin axis. In this case, the magnetic air core coil shall be activated, in such a way as to drive the spin axis in a safe attitude with respect to Sun. The 6 Am² torque coil is located in the spacecraft upper panel, with its axis parallel to the spin axis. The magnetic torque suffered by the spacecraft is given by:

$$\bar{T}_m = (m_r + u m_c) \bar{\omega} \times \bar{B} \quad (2)$$

where m_r and m_c are the residual and the coil magnetic moment, respectively. u is the coil polarity (-1, 0, 1) and $\bar{\omega}$ is the spin axis direction. The residual magnetic moment was specified to be in the range -0.5 to -1.5 Am², so as to cause a spin axis precession in the same direction of the sun's motion relative to Earth. This magnetic moment was measured during satellite integration and resulted a value of -0.75 Am².

The SCD1 has no attitude pointing requirements. The only restriction is that the bottom radiator panel should be kept out from the Sun direct incidence. Periodic attitude maneuvers take place whenever necessary as to achieve the correct orientation with respect to the Sun. The coil polarity is selected by an attitude simulation program, in such a way as to reduce the Sun aspect angle (angle between the Sun and the spin axis). A telecommand is then transmitted to switch the coil to the specified polarity. The maneuver can be spread for several days.

SCD2 satellite

As SCD1, SCD2 will also be spin stabilized. Nevertheless, its angular velocity will be controlled close to 30 rpm, by means of a magnetic air core coil (4 Am² magnetic moment) located in the lateral panel. The angular velocity control will be autonomously activated whenever the rotation falls below 28 rpm and will be deactivated when the rotation reaches 32 rpm. Also, the SCD2 spin axis orientation will be controlled in such a way as to point the rotation axis to the ecliptic north pole. Residual magnetic torques shall slowly precess this axis, so after a few weeks the required pointing is no longer assured. To correct the attitude, periodical spin axis maneuvers are predicted, whenever the angle between the spin and the ecliptic normal is greater than 10°.

Spin Axis Maneuvers

The coil polarity as a function of time can be derived from the attitude error²⁻³:

$$\bar{E} = \hat{s}_r - \hat{H} \quad (3)$$

where \hat{s}_r is the desired spin axis direction, after the maneuver, and \hat{H} is the angular momentum direction. In order to reduce the attitude error, E^2 is derived with respect to time, resulting

$$d(E^2)/dt = (-2/H) \bar{E} \cdot \bar{T}_m \quad (4)$$

It is assumed that the magnetic torque causes only precession (the magnitude of the angular momentum remains unchanged) and the perturbing torques are neglected. Substituting Equation 1 in the above equation results

$$d(E^2)/dt = -2/H (m_r + u m_c) s_w \quad (5)$$

The switching function s_w , given by

$$s_w = \bar{E} \cdot \bar{\omega} \times \bar{B} \quad (6)$$

determines the appropriate coil polarity in order to decrease the attitude error, since $m_c \gg m_r$ (the specified values are 12 Am² and ±0.1 Am², respectively). Therefore,

$$u = 1 \text{ for } s_w > 0 \quad (7a)$$

$$u = -1 \text{ for } s_w < 0 \quad (7b)$$

$$u = 0 \text{ if } s_w = 0. \quad (7c)$$

Time-tagged maneuvers will be calculated on-ground, telemetered to the spacecraft and stored in the on-board computer. Each time-tagged command informs the computer the spin axis coil (located at the spacecraft's upper panel) polarity, activation and deactivation times. It is expected to point the spin axis to the ecliptic pole with accuracy better than 1° . To calculate the maneuver, the coil polarity is obtained at defined time intervals (5 minutes, in the simulations) using the above equations. The resulting maneuver provides a significant saving of the maneuvering time with respect to a QOMAC (quarter orbit magnetic attitude control) type maneuver. Both spin axis and angular velocity maneuvers shall last a few hours (6 to 18) with time interval between maneuvers around 25 days.

Simulations were carried out to check the control algorithms and to adjust an optimal coil magnetic moment. The strategy consists in driving the spin axis inside the 1° cone around the ecliptic north pole. Environmental torques will slowly precess the spin axis, and after some days it reaches the 10° cone around the ecliptic pole. A new maneuver is then calculated on-ground, transmitted and stored in the on-board computer. The maneuvers consist in a set of switching times and the corresponding coil polarities.

Spin Plane Maneuvers

To control the angular velocity of the spacecraft around 30 rpm, two (a main and a backup unit) spin plane magnetic coils will be employed. They are individually activated, by on-ground telecommand. Also, the on-board computer will monitor the angular velocity using the sun sensor outputs and autonomously will activate the coil electronics when the velocity falls below 28 rpm. To accelerate the spacecraft from 28 to 32 rpm, the maneuver time is estimated in 8 hours, approximately. The coil switching is performed automatically by a dedicated electronics that process the 3-axis fluxgate magnetometer signals. Each coil is commanded by the magnetometer sensor orthogonal to both the coil axis and the the spin direction. To avoid the interference in the magnetometer output caused by the magnetic field of the coil, a threshold activation and deactivation level was implemented in the commutation electronics. These levels differ each other to prevent feedback: the activation value is $B_{on} = 120$ and $B_{off} = 60$ mGauss.

Considering a spin plane coil rotating in a XY plane, such that the geomagnetic component in this plane lies along the X direction, the instantaneous torque experienced by the satellite is given by:

$$\vec{T} = \nu m_s (\cos\theta \hat{i} + \sin\theta \hat{j}) \times \vec{B} \quad (8)$$

where ν is the coil polarity, m_s is the spin plane magnetic moment ($m_s = 4 \text{ Am}^2$) and $\theta = \omega t$. If B_x and B_z are the components of the geomagnetic flux intensity in the X and Z directions, the commutation limits are then:

$$\theta_{on} = \arcsin B_{on}/B_x \quad (9a)$$

$$\theta_{off} = \arcsin B_{off}/B_x \quad (9b)$$

For a spin-up and a spin-down maneuvers, the coil polarity as a function of the position angle is given in Table 1

Table 1: Spin coil polarities

θ limits	Spin up	Spin down
$0 \leq \theta < \theta_{on}$	0	0
$\theta_{on} \leq \theta < \pi - \theta_{off}$	-1	+1
$\pi - \theta_{off} \leq \theta < \pi + \theta_{on}$	0	0
$\pi + \theta_{on} \leq \theta < 2\pi - \theta_{off}$	+1	-1
$2\pi - \theta_{off} \leq \theta < 2\pi$	0	0

The mean torque over a revolution can now be integrated, resulting⁺:

$$T_x = -m_s B_z (\cos\theta_{on} + \cos\theta_{off})/\pi \quad (10)$$

$$T_y = -m_s B_z (\sin\theta_{on} - \sin\theta_{off})/\pi \quad (11)$$

$$T_z = m_s B_x (\cos\theta_{on} + \cos\theta_{off})/\pi \quad (12)$$

Note that the torque along the Y direction can be neglected, as θ_{on} and θ_{off} are normally small.

Results

Attitude determination of the SCD's spacecrafts is performed on-ground, using the sensor signals, telemetered to the Earth during the ground station contact. The satellite shall count with two sensors: one-axis digital sun sensor with meridian sun crossing indicator and a 3-axis fluxgate

magnetometer. The sensors are sampled at a 2 Hz frequency, by the on-board TMTC subsystem. The digital sun sensor measures the sun's aspect angle, between the spin axis and the direction of the sun. The magnetometer gives the Earth's magnetic field vector, allowing the determination of the attitude by solving the ambiguous orientation. The meridian sun crossing indicator is also sampled and gives information about the spacecraft angular velocity. Both SCD1 and SCD2 are provided with nutation dampers to reduce perturbations in the angular velocity of the satellite during separation from the launcher. They are toroidal shape rings, partially filled with oil and located in an off-center position at the upper panel.

The first year results are presented in Figures 2 to 6. Figure 2 presents the attitude maneuvers times, through the coil polarities history. Since the satellite launch, the requirement for pointing the spin axis is not only to avoid the sun incidence in the bottom panel, but also to maximize the electrical energy and to adjust the equipment temperatures by placing the spacecraft in a specific orientation with respect to the sun. These requirements are achieved for sun aspect angles between 70 and 90°. Several spin axis maneuvers were performed in order to conform to this requirement, with negative coil polarity (against the angular velocity vector). The sun aspect angle history is shown in Figure 3. Except during the initial 40 days, the sun angle remained constricted to the specified range.

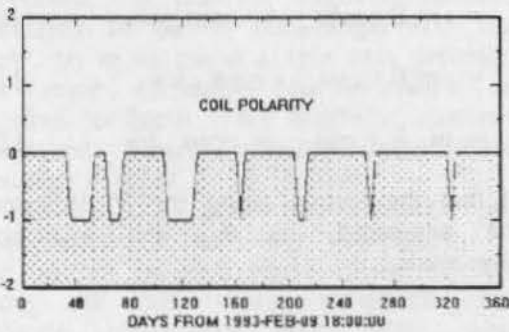


Figure 2: Coil polarity history.

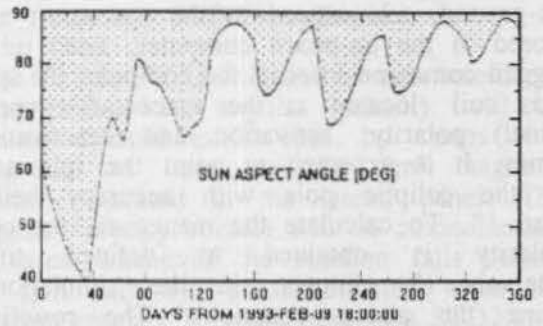


Figure 3: Sun aspect angle history.

Figure 4 presents the path of the spin direction in celestial coordinates (right ascension and declination). Note that the attitude maneuvers caused the spacecraft spin axis to align to the Earth's magnetic pole.

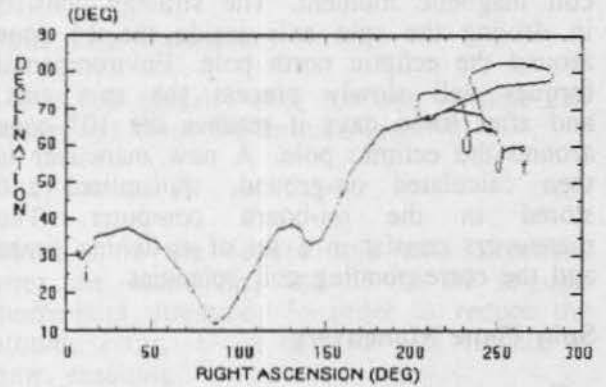


Figure 4: Spin axis motion.

Spin decay history is presented in Figure 5, where the exponential decay behavior due to the induced electrical currents in the spacecraft structure by the Earth's magnetic field is clearly seen. It should be noted the high discrepancy between the predicted and the in-flight values of the decay rate. In fact, as shown in Figure 6, the estimate of the Foucault parameter p through filtering technics resulted $500 \text{ m}^+/\Omega$ mean, smaller than the calculated $1920 \text{ m}^+/\Omega$ from theory.

References

¹Wertz, J. R. (1978) *Spacecraft Attitude Determination and Control*. London, Reidel.

²Ferreira, L. D. D., Cruz, J. J. (1989) *Attitude and Spin Rate Control of a Spinning Satellite Using Geomagnetic Field*. INPE, S. J. Campos. INPE-4818-NTE/289.

³Shigehara, M. (1972) Geomagnetic Attitude Control of an Axisymmetric Spinning Satellite. *Journal of Spacecraft and Rockets*, Vol. 9, June, pp. 391-398.

⁴Carrara, V.; Padilha, O. S.; Varotto, S. E. C.; Ricci, M. C. (1992) *An experiment to test the spin plane coil of SCD2*. INPE, S. J. Campos (in Portuguese). INPE-5404-RPQ/658.

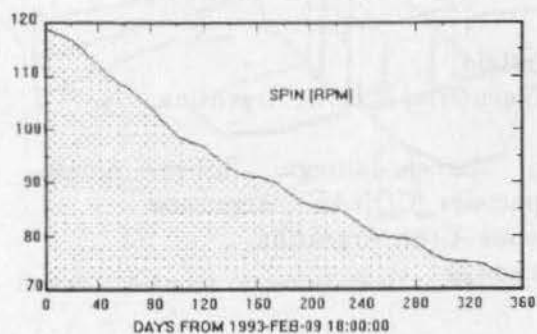


Figure 5: Spin rate history.

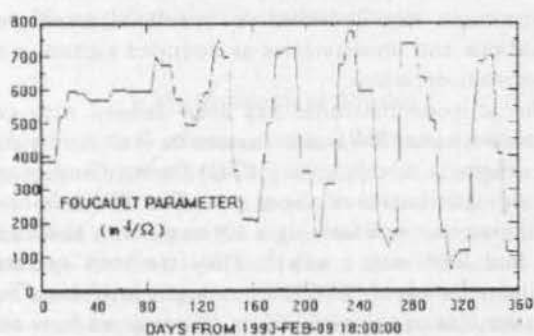


Figure 6: Foucault parameter.

The spacecraft residual magnetic moment is also estimated by the attitude determination procedures. In the Figure 7, the estimated magnetic moment of the satellite reflects the coil activation when a maneuver is performed. The mean value of the residual magnetic moment (when no maneuver is on way) is around -0.65 Am^2 , close to the -0.75 Am^2 measured on-ground before launch.

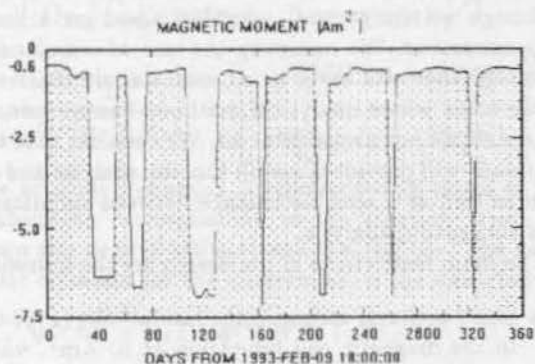


Figure 7: Magnetic moment estimation.

Mission Mode Attitude Control for SAC-B

Pablo A. Anigstein

*Depto. de Electrónica, Facultad de Ingeniería, U.B.A., Argentina.

Ricardo S. Sánchez Peña* Roberto Yasielski Marcela Jáuregui Roberto Alonso
Comisión Nacional de Actividades Espaciales (CONAE), Argentina.
Av. Dorrego 4010, (1425) Buenos Aires, Argentina
marcela@conae.gov.ar

Abstract

We describe the Mission mode attitude control of the scientific argentine satellite SAC-B. Based on the mathematical model of the system, an LQR controller with integral action has been designed. Robustness against parametric and dynamic uncertainty is evaluated. Performance is defined in terms of pointing accuracy under sets of perturbations and measurement noise, and evaluated by means of the singular value plots. Several pointing maneuvers and failure conditions are simulated and plotted.

Key words: Attitude control, optimal linear regulator, robustness, flexible modes.

Introduction

SAC-B is the first scientific argentine satellite, designed by CONAE and INVAP in a joint program with NASA. The PDR and CDR meetings have been held in december 1991 and april 1993 respectively. At this time, the satellite is being constructed and tested. The launch is scheduled in april 1995. Several scientific instruments will be carried, the circular orbit will have an altitude of approximately 550 Km. and an inclination of 38°. This orbit has a 90 min. period with an average eclipse of between 20 and 30 minutes.

The objective of the Mission Mode is to maintain the x axis of the satellite in a 3° circle, as required by the Cosmic Unresolved X-ray Background Instrument using CCD's (CUBIC). Due to the specifications of the Hard X-Ray Spectrometer (HXRS) and SoXS, and for minimum available power, the $-z$ axis (normal to solar panels) should point to the Sun within a 10° angle. Although these requirements are not extremely precise, the main objective in terms of analysis is to rely as much as possible in analytical tools to support the controller design. These analytical tools take into account all perturbations on the system, measurement and estimation errors in the attitude determination, modelling

uncertainty and actuator errors. The errors, perturbations and uncertainties are considered in a *worst case* deterministic way. Therefore we consider all errors, perturbations and uncertainties as bounded signals, a realistic consideration.

The attitude controller has been defined with two reaction wheels (RW) as actuators in the (x, z) plane, and magnetic torque coils (MTC) for momentum unloading and control in the y axis. The RW have a V configuration, both forming a 10° angle with the z axis (80° and 100° with x axis)⁵. They are both operated at a nominal speed of 2500 rpm, which provides a momentum bias to the satellite. In this way we have reasonable torques in both the x and z axes which will basically rotate the satellite around the y and z axes respectively, due to the gyroscopic stiffness effect. This is necessary because the CUBIC experiment is located in the x axis, therefore all maneuvers consist in rotating the y and z axes in a reasonable amount of time.

The sensors are triaxial magnetometers (TAM) and a digital Sun sensor (DSS), providing two vectors from which attitude can be determined.

We take into account the physical limitations on the actuators (saturation, small angle between sun and magnetic field), the measurement noises and errors as well as the complete nonlinear behavior of the system, although we design the controller based on a linear approximation. We minimize the use of simulations, although they will serve as an essential alternative in those cases where analytical methods become conservative or are not available at all. We consider that this approach will provide a useful tool for analysis and design as well as a sensible balance between simulations and conceptual analysis.

The main restrictions in the design are the following:

- Small actuator torque in the lateral axes (x, y) due to the magnetic coil limitation of 10 Am², which provides a maximum of $0.35 \cdot 10^{-3}$ Nm for the best orientation of B , against $15 \cdot 10^{-3}$ Nm from each reaction wheel.
- High error in the z axis quaternion due to the error

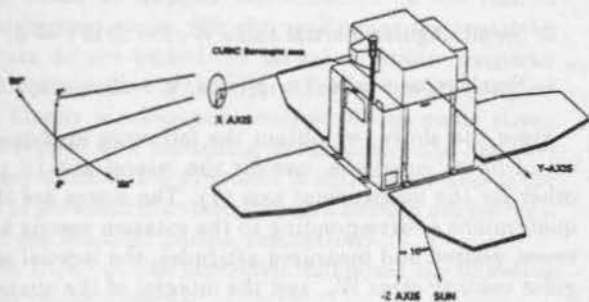


Figure 1: Attitude control elements of SAC-B.

in the magnetometer and magnetic field determination.

- No angular velocity measurements.

Mathematical Model

A conceptual scheme of the satellite can be seen in figure 1. The mathematical model of the satellite has been derived from the basic Newton-Euler dynamic equations considering a rigid satellite body with two reaction wheels tilted from the z axis by α_1 and $-\alpha_2$. The inertial angular velocity of the satellite in body axis is defined as $W_{is}^s = W$. The dynamic equation is the following:

$$\dot{W} = I_{ws}^{-1} [L(\Omega)W + J(W) + T_p + T_w + T_c] \quad (1)$$

where $J(W) = W \times I_T W$ represents the nonlinear terms, I_T the total inertia of the satellite and the wheels, I_{ws} the satellite and transversal wheel inertia, I_s the satellite inertia, and $L(\Omega)$ is a matrix which is linear in Ω (wheel velocities). The perturbation, wheels and magnetic control torques are defined as T_p , T_w and T_c respectively.

The equation for the angular velocities of both reaction wheels is:

$$\begin{bmatrix} \dot{\Omega}_1 \\ \dot{\Omega}_2 \end{bmatrix} = \begin{bmatrix} -\sin(\alpha_1) & 0 & -\cos(\alpha_1) \\ \sin(\alpha_2) & 0 & -\cos(\alpha_2) \end{bmatrix} \dot{W} \quad (2)$$

$$+ \frac{1}{\sin(\alpha_1 + \alpha_2)} \begin{bmatrix} -\frac{\cos(\alpha_2)}{I_{s1}} & 0 & -\frac{\sin(\alpha_2)}{I_{s1}} \\ \frac{\cos(\alpha_1)}{I_{s2}} & 0 & -\frac{\sin(\alpha_1)}{I_{s2}} \end{bmatrix} T_w$$

The attitude dynamics is represented in terms of the quaternions corresponding to the rotation error between the *desired* attitude and the *real* one. The kinematic equation for the quaternions is the following:

$$\dot{q} = \frac{1}{2} (q_0 I + q^{*k}) W = \Gamma_q W \quad (3)$$

$$\Gamma_q = \frac{1}{2} \begin{bmatrix} q_0 & -q_3 & q_2 \\ q_3 & q_0 & -q_1 \\ -q_2 & q_1 & q_0 \end{bmatrix} \quad (4)$$

$$q_0^2 + q_1^2 + q_2^2 + q_3^2 = 1 \quad (5)$$

All the nonlinear dynamics have been taken into account. The magnetic, gravitational and aerodynamic perturbations have been concentrated in vector T_p . The attitude and velocity outputs are the Euler quaternions (q) and the satellite angular velocity with respect to an inertial frame, measured in body axes ($W_{is}^s \triangleq W$). The q vector is computed from the solar and magnetic sensors as measured in body axes, therefore we have considered a computation error which is related to the sensor measurement errors (see section). We have also estimated the angular velocity W through a nonlinear observer and therefore we also consider an estimation error (see section).

Both actuators, the wheels (T_w) and the magnetic coils (T_c) will also have errors. For simplicity these have been also considered in T_p .

Attitude Estimation

The quaternion vector is obtained from the attitude matrix which is computed via the TRIAD algorithm³. This matrix is obtained from the *measurement* of the Sun (S) and magnetic field (B) vectors projected over the satellite reference frame and the *computed* theoretical Sun and magnetic field vectors in inertial frame. We also consider the desired reference frame C_d^i as follows:

$$C_d^s = [c_{ij}] = C_m^s \cdot C_i^m \cdot C_d^i \quad (6)$$

$$C_m^s = \begin{bmatrix} \frac{(S \times S \times B)^s}{\|S \times S \times B\|^s} & \frac{(S \times B)^s}{\|S \times B\|^s} & S^s \end{bmatrix} \quad (7)$$

$$C_i^m = \begin{bmatrix} \frac{(S \times S \times B)^i}{\|S \times S \times B\|^i} & \frac{(S \times B)^i}{\|S \times B\|^i} & S^i \end{bmatrix} \quad (8)$$

From simple calculations we obtain:

$$q_0 = \frac{1}{2} \sqrt{1 + c_{11} + c_{22} + c_{33}} \quad (9)$$

$$q_1 = \frac{c_{23} - c_{32}}{4q_0} \quad (10)$$

$$q_2 = \frac{c_{31} - c_{13}}{4q_0} \quad (11)$$

$$q_3 = \frac{c_{12} - c_{21}}{4q_0} \quad (12)$$

We have considered q as the quaternion of the error matrix, i.e. the rotation between the desired attitude (d) and the "measured" one (s). This not only allows the possibility of including both stabilization and attitude maneuvers in the same algorithm, but also solves the usual uncertainty in the sign of q_0 at a 180° rotation. We define the sign of q_0 as positive, which will be valid unless we have a 180° attitude error.

A nonlinear reduced order observer has been designed, which uses the "measurements" of the quaternions (as computed from TRIAD) to derive a "measured" \dot{W} and estimates the value of W from the dynamics. To this end, we consider the dynamic equations which represent the quaternions of the attitude error matrix and angular velocity error $W_e = W - W_d$, being W_d the desired velocity trajectory.

$$\dot{W} = I_{ws}^{-1} [L(\Omega)W + J(W) + T_p + T_w + T_c] \quad (13)$$

$$\begin{bmatrix} \dot{q}_0 \\ \dot{q}_1 \\ \dot{q}_2 \\ \dot{q}_3 \end{bmatrix} = \frac{1}{2} \begin{bmatrix} q_1 & q_2 & q_3 \\ q_0 & -q_3 & q_2 \\ q_3 & q_0 & -q_1 \\ -q_2 & q_1 & q_0 \end{bmatrix} W_e$$

$$\hat{=} \Gamma_1(q_0, q) W_e \quad (14)$$

From this last equation, and with $\Gamma_1^T \Gamma_1 = \frac{1}{4} I_{3 \times 3}$, we obtain

$$W_e = 4\Gamma_1^T \begin{bmatrix} \dot{q}_0 \\ \dot{q} \end{bmatrix} \quad (15)$$

which we will use in order to compute \dot{W} from "measured" quaternions (\hat{q}_0, \hat{q})

$$\dot{W} = W_d + 4\Gamma_1^T(\hat{q}_0, \hat{q}) \frac{1}{\Delta t} \begin{bmatrix} q_0(t_k) - q_0(t_{k-1}) \\ q(t_k) - q(t_{k-1}) \end{bmatrix} \quad (16)$$

We propose the following observer:

$$\dot{\hat{W}} = (I_{ws}^{-1})_o [L_o(\hat{\Omega})\hat{W} + J_o(\hat{W}) + T_w + T_c] + K(\hat{W} - W) \quad (17)$$

$$\dot{W}_e = \dot{\hat{W}} - \dot{W}_d \quad (18)$$

where $[(I_{ws}^{-1})_o, L_o, J_o]$ are the nominal values of these functions and $\hat{\Omega}$ the measured value of the wheel velocities. The observer gain K will be determined according to the stability and estimation error analysis. The error dynamics ($e = W - \hat{W}$) is the following:

$$\begin{aligned} \dot{e} &= [(I_{ws}^{-1})_o L_o(\hat{\Omega}) - K] e \\ &+ [I_{ws}^{-1} L(\Omega) - (I_{ws}^{-1})_o L_o(\hat{\Omega})] W \\ &+ (I_{ws}^{-1} - (I_{ws}^{-1})_o) T_c \\ &+ [I_{ws}^{-1} J(W) - (I_{ws}^{-1})_o J_o(\hat{W})] \\ &+ I_{ws}^{-1} T_p - K n_W \end{aligned} \quad (19)$$

being n_W the noise in the W measurement (i.e. $n_W = \hat{W} - W$) which is due to measurement errors in \hat{q} and to the calculation of the difference instead of the derivative of q in (16).

For simplicity, when the maneuvers slow down or the steady state has been reached, the term $J_o(\hat{W})$ may be eliminated from the observer equations.

Control

A first approach is to reduce the nonlinear equations in (1-3) according to the following assumptions:

1. Identical reaction wheels in terms of inertia, speeds and cant angles, i.e. $I_{i1} = I_{i2} = I_i$ ($i = \ell, a$ which holds for lateral and axial), $\Omega_1 = \Omega_2 = \Omega$ and $\alpha_1 = \alpha_2 = \alpha$ respectively.

2. Principal axis of both, satellite and wheels.
3. Small angular inertial rates W , i.e. $J(W) \rightarrow 0$.
4. Small error angles, i.e. $q_0 \rightarrow 1, q_i \rightarrow 0, i = 1, 2, 3$.

From the above, we obtain the following uncoupled set of linear equations, one for the lateral axis (x, y), other for the longitudinal axis (z). The states are the quaternions q corresponding to the rotation matrix between desired and measured attitudes, the inertial angular velocity error W_e , and the integral of the quaternion q_I , i.e. $x = [W_e^T \quad q^T \quad q_I^T]^T$.

$$\dot{x} = \begin{bmatrix} 0 & -\frac{k}{I_{xx}} & 0 & 0_{3 \times 3} & 0_{3 \times 3} \\ \frac{k}{I_{yy}} & 0 & 0 & 0_{3 \times 3} & 0_{3 \times 3} \\ 0 & 0 & 0 & 0_{3 \times 3} & 0_{3 \times 3} \\ \frac{1}{2} I_{3 \times 3} & 0_{3 \times 3} & 0_{3 \times 3} & 0_{3 \times 3} & 0_{3 \times 3} \\ 0_{3 \times 3} & 0_{3 \times 3} & 0_{3 \times 3} & I_{3 \times 3} & 0_{3 \times 3} \end{bmatrix} x$$

$$+ \begin{bmatrix} I_{xx}^{-1} & 0 & 0 \\ 0 & I_{yy}^{-1} & 0 \\ 0 & 0 & I_{zz}^{-1} \\ 0_{3 \times 3} & 0_{3 \times 3} & 0_{3 \times 3} \end{bmatrix} \begin{bmatrix} T_x \\ T_y \\ T_z \end{bmatrix} \quad (20)$$

$$q = [0_{3 \times 3} \quad I_{3 \times 3} \quad 0_{3 \times 3}] x \quad (21)$$

where we have defined:

$$k = 2I_z \Omega \cos \alpha \quad (22)$$

$$I_{xx} = I_{s11} + 2I_\ell \cos^2 \alpha \quad (23)$$

$$I_{yy} = I_{s22} + 2I_\ell \quad (24)$$

$$I_{zz} = I_{s33} + 2I_a \sin^2 \alpha \quad (25)$$

Model uncertainty

For the linear model approximation, the uncertainties can be separated in two different classes:

1. **Parametric.** These uncertainties will appear when the first two assumptions are eliminated. Therefore by considering different wheels, angles and cross inertia terms, new elements will appear in the linear model and there is no decoupling between lateral and longitudinal axes.
2. **Dynamic.** This uncertainty comes from the fact that only the rigid body model has been considered. If we take into account the flexible modes which come from the solar panels, this is no longer true.

Both have been analyzed in greater detail in the CDR report⁶.

Design

We have designed a very simple optimal linear state feedback controller F for the nominal (uncoupled) system described in (20)-(21), which includes integral action. Although we assume perfect measurements in

both cases, we analyze the controller in the case of measurement errors. We also verify that the controller torques do not exceed the actuators limits (magnetic coils and reaction wheels) and follow the tracking error. Finally a robustness analysis of the whole closed loop system with modelling uncertainties and high frequency unmodelled dynamics is performed. This is the case of parametric uncertainty and flexible modes coming from the solar panels, respectively.

The LQR optimal controller minimizes the following performance integral:

$$\int_0^{\infty} [W^T(t)Q_W W(t) + q^T(t)Q_q q(t) + q_I^T(t)Q_I q_I(t) + u^T(t)Ru(t)] dt \quad (26)$$

The state and input weights are chosen according to the particular relevance of the axis in consideration. The CUBIC axis is the most important one in terms of tracking error, therefore rotations around the y and z axes should be significantly smaller, i.e. the state weight should be higher for (y, z) than for x axis. In terms of control, the y axis is the one with the most restrictive actuator bound (magnetic coils), therefore the control weight should be higher for this axis. Although the reaction torques of both wheels actuate over x and z , the first component is projected through an angle of 10° , therefore there is a significant difference between these axes as well.

With this controller, the closed loop equations are the following:

$$\dot{x}(t) = Ax(t) + Bu(t) \quad (27)$$

$$q(t) = Cx(t) \quad (28)$$

$$u(t) = -F[x(t) + n(t)] + T_p(t) \quad (29)$$

where n is the estimation error in W and the "measurement" error in the quaternions, and matrices (A, B, C) are obtained from (20)-(21).

For stability robustness we evaluate the complementary sensitivity function $T(s)$. If the open loop transfer function is $L(s) = F(sI - A)^{-1}B$, then $T(s) = L(s)[I + L(s)]^{-1}$, which has the following state space representation:

$$T(s) \equiv \left[\begin{array}{c|c} A - BF & B \\ \hline F & 0 \end{array} \right] \quad (30)$$

For performance, the transfer functions to be analyzed are the ones which relate the output angular error q and the control torque u with perturbation torques and measurement errors, this is:

$$q(s) \equiv \left[\begin{array}{c|c} A - BF & B \\ \hline C & 0 \end{array} \right] T_p(s) + \left[\begin{array}{c|c} A - BF & -BF \\ \hline C & 0 \end{array} \right] n(s) \quad (31)$$

$$u(s) \equiv \left[\begin{array}{c|c} A - BF & B \\ \hline -F & I \end{array} \right] T_p(s) + \left[\begin{array}{c|c} A - BF & -BF \\ \hline -F & -F \end{array} \right] n(s) \quad (32)$$

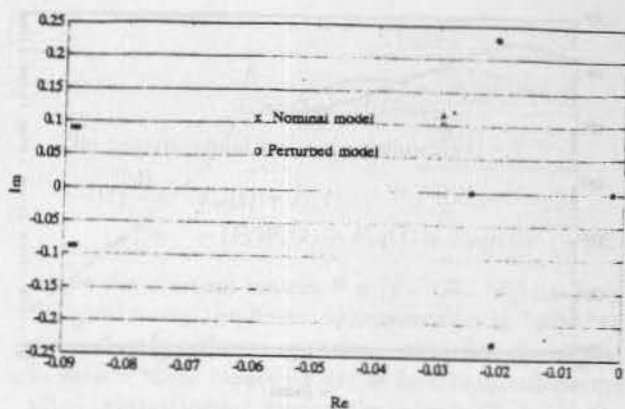


Figure 2: Closed loop poles of uncertain system.

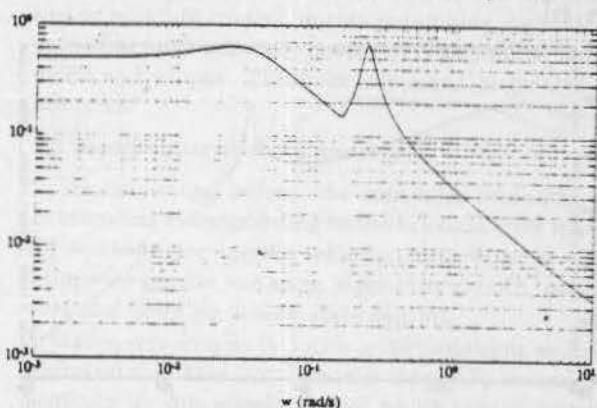


Figure 3: Robustness against dynamic uncertainty.

Analysis

Stability robustness

First we have evaluated the influence of *structured* uncertainty in the parameters of the A and B matrices of the model in (20), which result in a perturbed coupled model (assumptions 1. and 2. of the linear approximation are no longer valid). The transformation of this parametric uncertainty into *unstructured* dynamic uncertainty is excessively conservative. Therefore we have plotted the closed loop poles of the uncertain system (see figure 2). These values have been obtained by studying the functional dependency of the characteristic polynomial with the unknown parameters and computing the roots of this polynomial over a grid of values of the uncertain parameters. We have concluded that the stability of the system is robust against this type of uncertainty⁶.

In terms of stability robustness against dynamic uncertainty due to the higher order flexible modes, we have used the singular values $\bar{\sigma}[T(j\omega)W_\Delta(j\omega)]$. The weight $W_\Delta(s)$ has been defined as the uncertainty "distribution" of the solar panels as a function of frequency. According to the robust stability equivalent condition⁸ $\|T(s)W_\Delta(s)\|_\infty < 1$, the plot in figure 3 verifies that closed loop stability is robust against uncertain higher order flexible modes, which come from the solar panels.

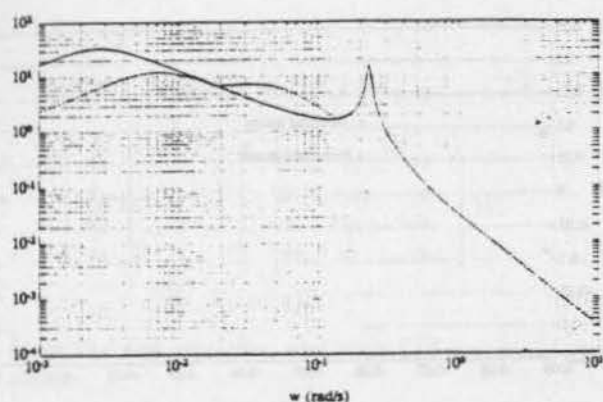


Figure 4: Maximum singular value of T_p to q_1 and $[q_2, q_3]$.

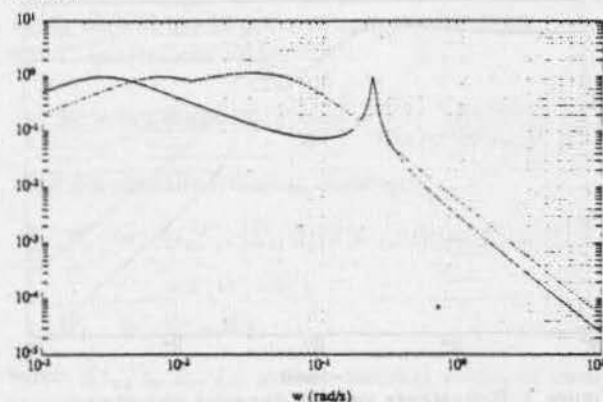


Figure 5: Maximum singular value of n_θ to q_1 and $[q_2, q_3]$.

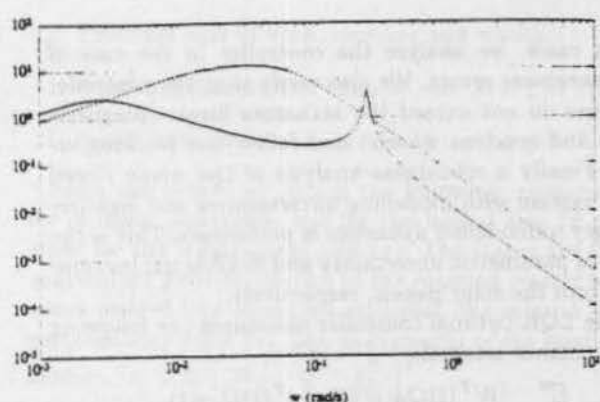


Figure 6: Maximum singular value of n_W to q_1 and $[q_2, q_3]$.

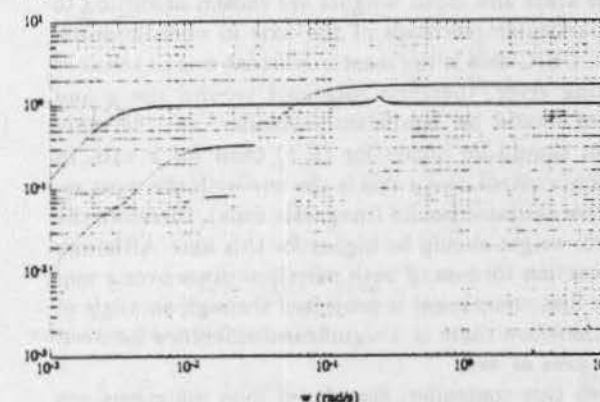


Figure 7: Maximum singular value of $[T_p, n_\theta, n_W]$ to u .

the perturbations and measurement/estimation errors.

Performance

We have defined performance in a worst case sense, as rejection of sets of disturbances and perturbations. To this end, we have plotted the maximum singular value frequency responses of the transfer functions in (31)-(32) (see figures 4 to 7). These represent the worst case gains, considering all possible input vector directions and all possible input signal waveform, under the restriction of bounded energy. Because rotations around y and z axes are more critical than the ones around the x axis due to the CUBIC experiment, we have separated the influence of T_p and n over these two groups. A worst case performance error can be obtained, by considering torque perturbations and measurement errors. Considering small angle errors, the rotation error around each axis can be approximated as $\delta\theta_x = 2q_1$, $\delta\theta_y = 2q_2$ and $\delta\theta_z = 2q_3$. The total rotation error in each axis which result from the singular value plots are the following:

$$\delta\theta_x = 60 \cdot \|T_p\| + \|n_\theta\| + 6 \cdot \|n_W\| \quad (33)$$

$$\delta\theta_i = 22 \cdot \|T_p\| + \|n_\theta\| + 21 \cdot \|n_W\|, \quad (34)$$

$(i = y, z)$

These equations give a good idea of how critical are

1. The most critical is the angular measurement errors n_θ , due to the fact that they have a 1 to 1 relation with the final error and are of the order of the desired attitude error⁶.
2. If we assume the velocity estimation errors $n_W \leq 0.01$ °/s, their contribution in the attitude error is in the order of 0.21° in (y, z) , well below the requirements.
3. Assuming maximum values of perturbations $T_p \leq 10^{-5}$ Nm due to gravitational, magnetic and aerodynamic torques, the contribution in the attitude error is in the order of 0.01° in (y, z) and 0.03° in x , well below the requirements. As we have mentioned before, the errors when applying the control torques with both momentum wheels and magnetic coils are also included in T_p . This means that these errors become relevant, because they are multiplied by a factor of 22 in both critical axes y and z .

Magnetic coils have a maximum possible torque of 0.35 mNm for the best orientation of B . For the momentum wheels, the misalignment error ($\approx \pm 0.35^\circ$ around the nominal values $\alpha_1 = \alpha_2 =$

10°) produces a torque error in the order of 10^{-5} Nm. Instead, there is a great uncertainty component due to the drag. The only available data¹ is the maximum drag torque, which is in the order of 10 mNm. Even if the error in the value of the actual drag could be determined with a 10% precision¹, we would still have a perturbing torque of 10^{-3} Nm, two orders of magnitude above the other perturbations. Therefore its influence in the total error is in the order of 1°.

For this reason, an integrator has been included which eliminates the static errors of the actuators, in particular the wheels drag. Although the $\|\cdot\|_\infty$ obtained from the singular value plot is still 22, the low frequency singular value goes to zero, due to the integral action.

A second alternative, which has also been explored, is to eliminate the uncertainty in the reaction torques due to the drag. To this end, a (software) velocity feedback has been implemented in both wheels, which counteracts the effect of this uncertainty. This speed control is also used in starting up the wheels to nominal speed, maintaining them at constant speed when angle $(B, S) \in [0, 30^\circ]$, or taking one wheel to 4500 rpm while the other runs down at wheel failure mode. The speed control is simply a constant plus integral feedback⁶.

The conclusion of this analysis is the following. The worst case perturbations torques and estimation errors, all combined in the worst possible way (because we have considered the transfer functions measured by the peak value of their maximum singular value, i.e. $\|\cdot\|_\infty$), with the worst possible situation, this is $\theta_{SB} = 30^\circ$ gives a very conservative measure of performance. This combination gives a target error rectangle of $(0.54^\circ, 3.66^\circ)$ due to rotations around y and z axes respectively. If instead we consider a stochastic value for the errors and add them quadratically, still considering their worst possible combination and worst angle θ_{SB} , we achieve a much smaller error rectangle of $(0.4^\circ, 1.46^\circ)$. Still the actual error will be significantly smaller, because very seldom we will have perturbations, estimation errors and θ_{SB} combined in the worst possible way. Therefore, simulations should give a smaller error, as will be verified in the next plots.

Although in this analysis we have made certain assumptions which produce a linear model of the system, certain nonlinear robustness analysis can also be made. This analysis can be performed in certain cases, by means of Lyapunov theory and also through a generalization of the small gain theorem⁹. In cases as the one considered, where the control torques depend on the Earth magnetic field, the complete analysis of robust stability cannot be performed, and as a consequence, the final test is made through simulations.

Control Modes

The control equation is the following:

$$\begin{aligned} u(t) &= T_w(t) + T_c(t) \\ &= -[F_1 W_e(t) + F_2 q(t) + F_3 q_I(t)] \end{aligned} \quad (35)$$

where the constant matrix $F = [F_1 \ F_2 \ F_3]$ has been designed using the linear approximation in (20)-(21). According to different situations, we define the modes. In each of these modes we decide how to distribute the total control torque among the wheels (T_w) and the magnetic coils (T_c). We should also decide the priorities on pointing control, nutation damping, momentum unloading and pointing maneuvers, as well as failure mode and eclipse. These are explained in greater detail next.

Pointing control & Maneuvers

As mentioned before, the controller feedbacks the quaternions corresponding to the attitude error matrix C_e^* and the error angular velocity vector $W_e = W - W_d$. Therefore we use the same algorithm in both, maneuvers and pointing steady state control.

Maneuvers consist in z axis $\pm 180^\circ$ rotations and $\pm 5^\circ$ precession. In this last case, the torque T_x is made essentially by the wheels, one of which should decrease velocity while the other should increase it above the nominal (2500 rpm). For a 5° maneuver this amount to 3800 rpm for one wheel and 1200 for the other.

The procedure in these cases is to stabilize both velocities at these values (and not at the nominal) during the whole observation period, while their speeds do not fall out of the interval [1000, 4000] rpm. In this way, the return from the target to the nominal steady state situation (z axis pointing to Sun) is performed basically with the wheel reaction torques and will return both to approximately their nominal speed. Furthermore we save energy coming from the magnetic coils and minimize possible torque perturbations during the observation period, as will be explained next.

If instead we proceeded by forcing the wheels to their nominal speeds after the maneuver, the coil actuators would have to counteract the speed dispersion in both wheels to return them to 2500 rpm. Furthermore, after the observation period to return the z axis towards the Sun, the same desaturation procedure should be performed again with the magnetic coils. In these situations the coils apply, during a long time, maximum power to counteract this extra momentum, which also may introduce extra torque perturbations into the system.

Nutation damping

In the linear approximation design, we have considered a state feedback control which performs nutation damping, stabilization and maneuvers all together. Furthermore, we have also considered uncertainty in

the parameters, which eliminates the assumption of maneuver dynamics and lateral nutation decoupled, for which the same controller performed efficiently. Therefore there is no separation between nutation damping, stabilization and tracking maneuvers.

Momentum unloading

Two procedures have been tested for momentum unloading and from both we have obtained satisfactory results. The one which has been used is standard in attitude control⁴, and performs a continuous unloading.

Eclipse mode

During eclipse, we can decide to keep the last observed Sun vector S^s to form the TRIAD matrix or the last momentum vector $H^s = I_{ws}W + H_{wheels}$.

In the first case any control torque from coils or wheels, as well as perturbations torques T_p will produce an attitude error due to the misleading S^s . Assuming a worst case sinusoidal $T_p(t)$ of 10^{-5} Nm amplitude applied in x during a 30 minute eclipse, we obtain an attitude error in the correct x direction, due to a rotation around y , of approximately 0.16° . If we do not apply wheel control torques during the eclipse, the x direction error is greater than 50° , due to a rotation around the z axis.

The second option instead is sensitive only to external torques, i.e. T_p and coils. This is so because the wheel torques do not change the momentum vector H^s . Therefore we only consider the error of 0.16° due to T_p and do not apply any magnetic coil torques during this mode. This does not affect the attitude, because the coil torque along y gives rotations around x . This is the option we have selected.

Low θ_{SB} angle mode

As we have mentioned in section 2.1, the errors increase significantly when the angle between vectors S and B are in the region $[-30^\circ, 30^\circ]$ and $[150^\circ, 210^\circ]$. In fact the attitude error duplicates when $\theta_{SB} = 30^\circ$. Therefore in these situations we do not apply any control which uses the TRIAD computation. The wheels are stabilized at a constant speed, by using the speed control mentioned in last section⁵.

We have analyzed a worst case group of orbits in the sense of the angle θ_{SB} . This case is when we obtain the Earth magnetic vector, the radius vector of the orbit, with respect to the center of the Earth, and the Solar vector as close as possible. This happens in the North hemisphere during summer, approximately at June 21st. We have simulated ± 14 hours around this condition and obtained several situations in which $\theta_{SB} \in [150^\circ, 180^\circ]$. The worst of these situations has a 10 minute period. Therefore, we compute the influence of a worst case sinusoidal magnetic perturbation T_p of 10^{-5} Nm amplitude and a 45 minute period. If this torque is applied to the z axis (without control) during the 10 minute period, it produces a 5° shift in the CUBIC boresight axis (x). During these situations,

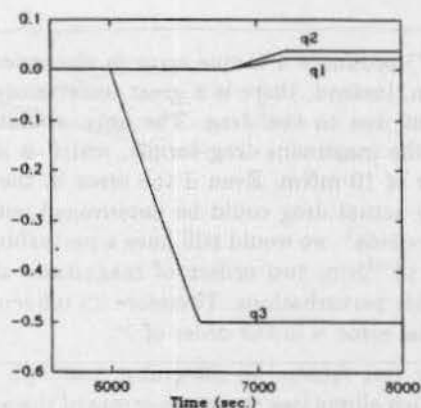


Figure 8: Desired quaternions.

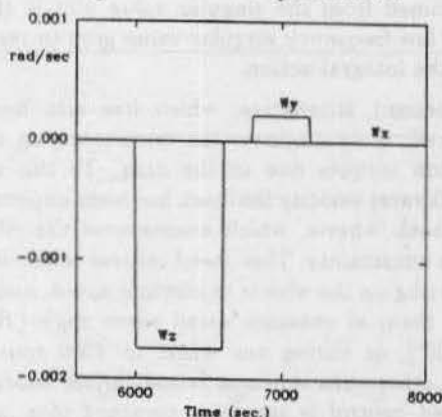


Figure 9: Desired angular velocities during the maneuver.

the experiment should be cancelled, because there is no way of measuring the attitude deviation without a significant error.

Nevertheless, by simulations we can observe that we can still control efficiently up to smaller angle intervals ($[165^\circ, 195^\circ]$ and $[-15^\circ, 15^\circ]$), therefore this means that the critical situation in which the control should be turned off is reduced, which also reduces the attitude error in those cases.

Simulations

A spacecraft simulator for design and analysis has been programmed in MatLab-386 which includes all the satellite and wheels dynamics. Simplified perturbations, measurement, estimation errors and model uncertainty have also been included, as well as flexible solar panel modes, and observer dynamics and control strategies. A Simulator⁷, programmed in Fortran, which includes also the orbital and magnetic models, has been used to simulate different maneuvers and events, as well as failure modes. These simulations for a typical maneuver can be seen in figures 8 to 13.

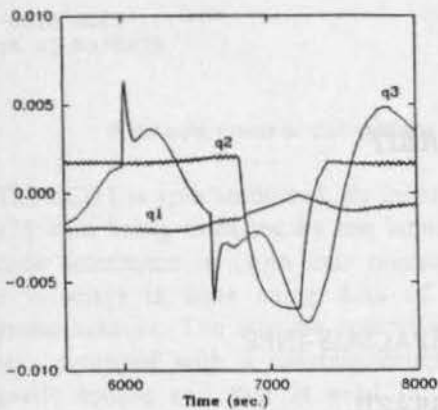


Figure 10: Quaternion errors.

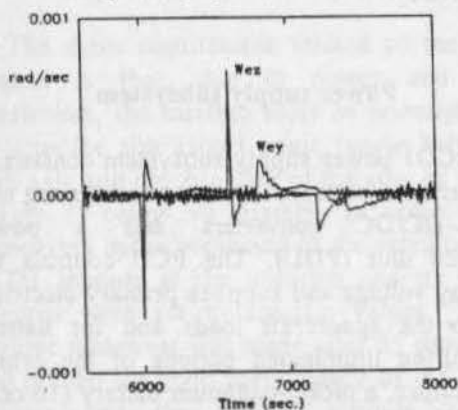


Figure 11: Angular velocity errors.

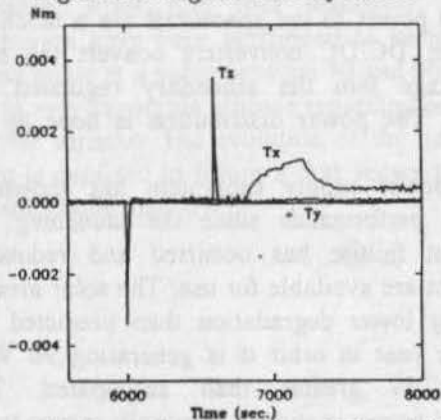


Figure 12: Control torques from RW and MTC.

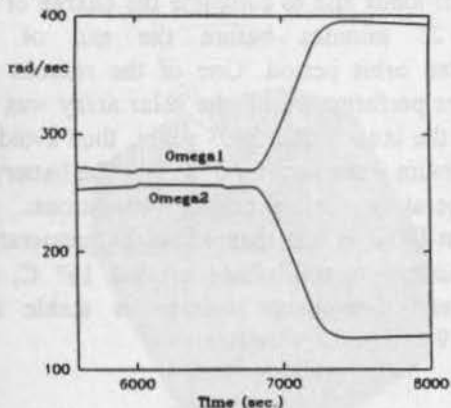


Figure 13: RW angular velocities.

Acknowledgments

The authors are indebted to Henry Hoffman, Chief Engineer of the Guidance & Control Branch at GSFC, for his enlightening suggestions.

References

¹ ITHACO, "T-Reaction Wheel Interface Control Document", Report 94190; "Proposal for SAC-B", Proposal 98123; "Response to SAC-B questions", KLE/92/0795, 1992.

² Sánchez Peña R., P. Anigstein, "Control Robusto No lineal: Aplicación al Satélite SAC-B", (in spanish) Proceedings of the XIII Simposio Nacional de Control Automático, Buenos Aires, 1992.

³ Schuster M.D., Oh S.D., "Three-Axis Attitude Determination from Vector Observations", *AIAA Journal of Guidance, Control & Dynamics*, Vol. 4, No. 1, 1981.

⁴ Stickler A.C., Alfriend K.T., "Elementary Magnetic Attitude Control System", *AIAA Journal of Spacecraft*, pp. 282-7, 1976.

⁵ Suggested by H. Hoffman's, Head of the Guidance & Control Branch at the NASA/CONAE Preliminary Design Review, Buenos Aires, November 1991.

⁶ CONAE ACS Team, "Mission Mode Design, Analysis & Simulation", presented at the NASA/CONAE Critical Design Review, Bariloche, April 1993.

⁷ Jáuregui M., Anigstein P., "Low-Fi Simulator", Document presented at the NASA/CONAE Critical Design Review, Bariloche, April 1993.

⁸ Doyle J.C., Francis B., Tannembaum A., *Feedback Control Theory*, Maxwell McMillan, 1992.

⁹ Anigstein P.A., *Análisis Robusto de Sistemas no lineales: Aplicación al Control de Actitud*, (in spanish) Electronic Engineer degree Thesis, Fac. de Ing., Universidad de Buenos Aires, 1993.

SCD1: ONE YEAR IN ORBIT

Janio Kono
Carlos E. Santana

INSTITUTO NACIONAL DE PESQUISAS ESPACIAIS-INPE
Av. dos Astronautas, 1758
12227-010 São José dos Campos-SP BRAZIL
MECB%CCS@BRFAPESP.BITNET

Abstract

The first Brazilian satellite, the Data Collecting Satellite (SCD1) is a Low Earth Orbit spin stabilized satellite for real time reception and retransmission of data on the environment. The SCD1, was launched in its 25 degree inclination orbit at 750 km altitude in February 9th, 1993, by a Pegasus launch vehicle.

This paper presents an evaluation of the in-orbit performance of the SCD1 satellite based on the analysis of its telemetry which has been recorded since the first orbit. An analysis of the SCD1 performance in its first year of operation shows that the satellite design lifetime of one year can be extended by at least one year.

Introduction

The SCD1 satellite is dedicated to the collection and distribution of environmental data emitted by Data Collecting Platforms (DCP's) distributed over Brazilian territory. The DCP's are small automatic, unattended earth stations which collect weather and other local environmental data for transmission in short intermittent bursts, with an average repetition period of two minutes. During a satellite pass in which it is visible both from a certain DCP and from the Cuiabá Tracking Station, the data emitted by that DCP are relayed by the satellite and received in Cuiabá. Up to 500 DCP's can be set in operation, at arbitrary locations, over the Brazilian territory. The system is designed so that any DCP has probability greater than 70% of being acquired at least once a day.

Power supply subsystem

The SCD1 power supply subsystem consists of a solar array, a battery, a power conditioning unit (PCU), DC/DC converters and a power distribution unit (PDU). The PCU controls the solar array voltage and supplies primary electrical power to the spacecraft loads and for battery charge during illuminated periods of the orbits. During eclipse, a nickel-cadmium battery (16 cells of 8-Ah nominal capacity) supplies secondary electrical power to the spacecraft via a discharge controller. DC/DC converters convert the main bus voltage into the secondary regulated bus voltages. The power distribution is done by the PDU.

The power supply subsystem has shown an excellent performance since the launching. No equipment failure has occurred and redundant equipment are available for use. The solar array is exhibiting lower degradation than predicted and after one year in orbit it is generating 90 W, a power 10% greater than anticipated. This generated power is enough to supply energy to the spacecraft loads and to complete the charge of the battery 25 minutes before the end of the illuminated orbit period. One of the reasons for this better performance of the solar array was the delay of the launch date by 3 years, thus avoiding the maximum solar activity of 1990. The battery is also operating in excellent conditions: the maximum DOD is less than 15%; the temperature of the battery is stable and around 16° C; the battery end-of-discharge voltage is stable and around 19.5 V (1.22 V/cell).

Attitude control subsystem

The SCD1 is spin stabilized, its initial rotation of 120 rpm being imparted by the launcher. The attitude determination (spin axis orientation and spin velocity) is done using data of sun and magnetic sensors. The attitude control subsystem is also equipped with a nutation damper and a magnetic torque coil that is used in spin axis reorientation maneuvers.

The main requirement related to the attitude control is that, due to power and thermal constraints, the satellite must be oriented such as to keep the sun aspect angle (angle between the spin axis and the direction of the sun, as shown in Figure 1) below 90 degrees. In order to avoid maneuvers in the beginning of the satellite life, the SCD1 attitude at the injection and its magnetic moment were set to specific values. The first attitude maneuver was made after 35 days in orbit and proved the good performance of the magnetic torquer and the ground attitude estimation software. After this first maneuver, frequent maneuvers have been performed to keep the sun aspect angle at a value between 70 and 90 degrees, that is very favorable attitude regarding power and thermal aspects. The evolution of the sun aspect angle is depicted in figure 2 that shows the effect of the attitude maneuvers.

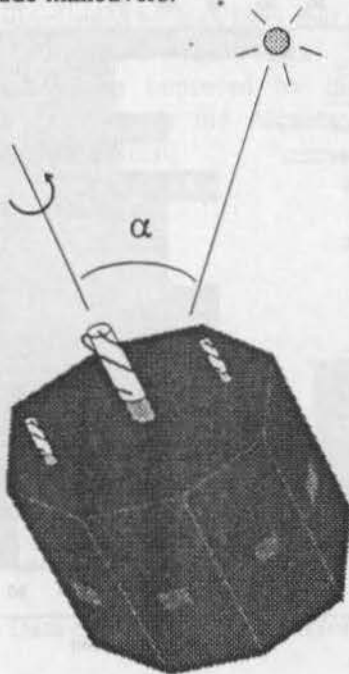


Fig. 1 - Sun aspect angle

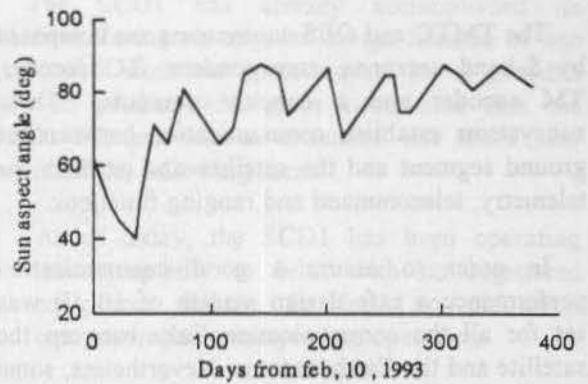


Fig. 2 - Sun aspect angle evolution

The SCD1 has no means to control its spin velocity, so the spin velocity will decrease gradually up to a value (< 10 rpm) for which the satellite stabilization will be lost. Figure 3 shows the evolution of spin rate since the launching. The approximately exponential decay of the spin rate is occurring at a rate significantly smaller than estimated before the launching. It will take more than one year for the spin rate to reach half of its initial value. The original calculation estimated a half-life of approximately 110 days.

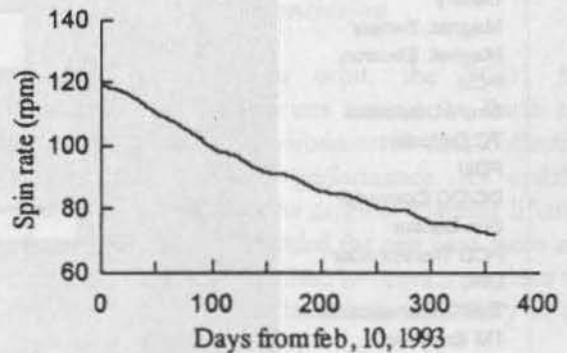


Fig. 3 - Spin rate evolution

Service telecommunications (TMTC) and onboard supervision (OBS) subsystems

The TMTC and OBS subsystems are composed by S-band antennas, transponders, TC decoder, TM encoder and an onboard computer. These subsystems establish communication between the ground segment and the satellite and perform the telemetry, telecommand and ranging functions.

In order to assure a good communication performance a safe design margin of 10 dB was set for all the communication links between the satellite and the Earth stations. Nevertheless, some loss of communication was expected when the stations are in the satellite "blind zone" (a region within ± 10 degrees from satellite the equator) caused by to interference between two antennas using the same polarization. In practice the loss of communication has been less severe than expected. No tracking loss or TC carrier loss were reported in the "blind zones". Telemetry data losses have been reported only for angles within ± 3 degrees from the satellite equator.

The experimental computer composed of a Communication and Processing Unit (UPC) and of a Distributed Processing and Communication Unit

(UPD/C) acquires telemetry data when the spacecraft is not in visibility of the stations and distributes time-tagged commands. An error in the onboard software was causing the UPC to reset few days after being loaded. The problem was identified, the software repaired and both units are operating faultless since then.

Thermal control subsystem

The thermal control of the spacecraft is achieved using passive means: selective painting and coating of the interior surfaces and electronic boxes and control of the heat conduction paths. The disposal of the excess heat is done through the bottom panel which is the only one that is not covered with solar cells.

Telemetry data has shown a very good correlation between the temperatures predicted in the SCD1 thermal model and the actual in orbit temperatures and show good temperature margins for all equipment of the satellite. Figures 4 shows the predicted values, the actual values and the margins of equipment temperatures.

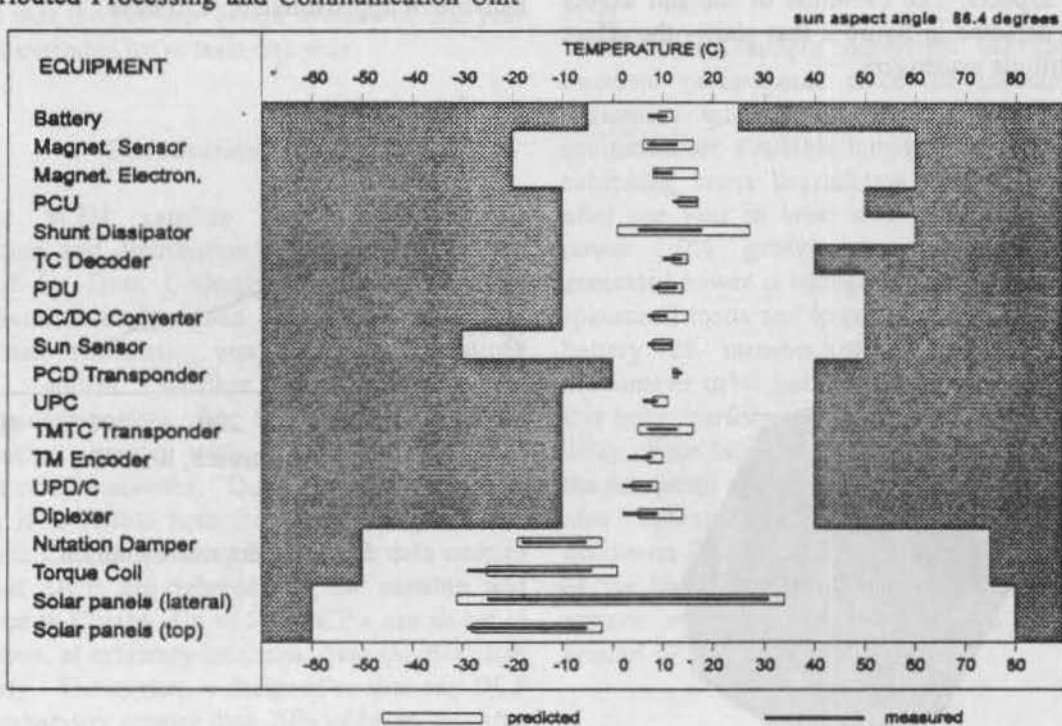


Fig. 4 - SCD1 temperatures

Solar cell experiment

The solar cell experiment comprises a small solar array, made by cells manufactured in Brazil, attached to one of the spacecraft lateral panels. Its purpose is to assess the performance of the Brazilian solar cells in the space environment. The cells are working well and after one year in orbit they have not shown any observable degradation.

Data Collecting Payload

The data collecting payload receives Data Collecting Platforms (DCPs) signals in the UHF band and transmits these signals to the ground, phase-modulated in a S-Band carrier. The Cuiabá station receives and demodulates the DCP signals and send then to the Mission Center (Cachoeira Paulista), which disseminates the data to the users.

The SCD1 is relaying DCP signals regularly since march 93 and complies with the requirement of at least one data reception each day for DCPs in Brazilian territory. Figure 5 shows the performance of the system for several locations. It is interesting to notice that the number of receptions in Manaus is less than in Atol das Rocas although Manaus is closer to Cuiabá than Atol das Rocas. This happens because the DCP in Manaus is surrounded by high trees that impair the signal transmission. The data collecting performance can be improved by installing a second PCD receiver in the Alcantara station, located in northeast Brazil.

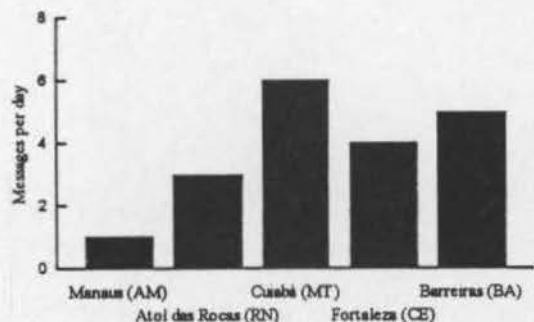


Fig. 5 - Data collecting system performance

Lifetime prediction

The SCD1 has already accomplished its mission, during its original design lifetime of one year, with excellent performance. Its is possible now to predict with great confidence that the SCD1 lifetime will be extended one more year based on the following facts:

- As of today, the SCD1 has been operating uninterruptedly in orbit with no registered equipment failure. In fact, no redundant equipment has come yet into operation.
- Equipment that are subject to wear-out such as the battery and the solar arrays are in excellent conditions and have not shown any significant degradation.
- Attitude maneuvers keep the sun aspect angle near 90 degrees. This attitude will provide a very comfortable temperature range for all the equipment, thus extending the components lifetime.
- An estimation of the spin rate decay shows that the attitude stabilization is well guaranteed for at least one more year.

Conclusion

After one year in orbit, the SCD1 has completed over 5000 orbits around the Earth and its carrying out its environmental data collecting mission with excellent performance. An updated prediction shows that the original planned lifetime of one year can be extended for one year more and that the SCD1 will continue to operate to close the gap until the SCD2 is launched, nominally in the beginning of 1995

ATTITUDE AND ORBIT CONTROL III

1. Martins Neto, A.F. (INPE-Brazil):
"Design of Controllers for Satellites Subjected to Gravitational and Drag Torques Using Liapunov Function Techniques" 103
2. Líbero, C. and Mauceri, G. (TELESPAZIO-Italy):
"On-Ground AOCs Support Software for the SAX Satellite" 108
3. Souza, L.C.G. (INPE-Brazil):
"Robust Controller Design for a Flexible Space System With Mixed Uncertainty Model" 116
4. Lin, H. (CAST-China) and Feng, X. (Beiging Institute of Control Engineering-China):
"The Orbit-Maintenance for a New China's Recoverable Satellite" 124
5. Ovchinnikov, M. and Dyachenko, A.I. (Keldysh Inst. Appl. Math-Russia):
"Universal Small Space Platform: Orientation Aspects" 129
6. Pivovarov, M. (IKI-Russia); Triska, P. and Voita, J. (Geophysical Inst. Czech Rep.):
"Magnetically Stabilized Satellite with Viscous Annular Damper Attitude Motion" 134

DESIGN OF CONTROLLERS FOR SATELLITES SUBJECTED TO GRAVITATIONAL AND DRAG TORQUES USING LIAPUNOV FUNCTION TECHNIQUES

Antonio Felix Martins Neto
Instituto Nacional de Pesquisas Espaciais
Avenida dos Astronautas, 1758, C.P. 515
12201-970 São José dos Campos, SP
e-mail: mneto@dem.inpe.br

Abstract

Nonlinear design procedures are presented for obtaining attitude and angular momentum control laws for a rigid satellite. Besides the gravitational torque, a drag torque is supposed to be applied to the satellite. By making use of physical and mathematical considerations, a Liapunov function is proposed that leads to a asymptotically stable attitude control law. The problem of identifying some parameters related to the drag torque is also dealt by adding new terms to the proposed Liapunov function. A mechanism for adjusting the parameters on line is obtained by forcing a condition in the time derivative of the modified Liapunov function that will imply stability for the whole system. Both types of controllers will be valid for large angular displacements and can be easily implemented, competing successfully with the usual algorithms based on linear control techniques.

Key words: Satellite Control, Liapunov Function, Adaptive Systems.

Introduction

Usually the design of a satellite attitude control system is based on a linearized model valid only for the region around the desired equilibrium point. In order to avoid this limitation some procedures have been proposed taking into account the nonlinear nature of the problem. Vadali and Oh¹ have used Liapunov functions for obtaining attitude and momentum control laws for the space station.

The purpose of this paper is to extend some results of their work for the case when the satellite is also subjected to a drag torque besides the gravity gradient torque. An adaptive procedure is also developed in order to adjust the parameters of the controller that

depend on the satellite configuration and on the environment through which the satellite is travelling.

Description of the satellite and its environment

The satellite to be modelled will be considered as a rigid body. Its attitude will be controlled by the use of three wheels, one for each principal axis. The principal axes of inertia will be called respectively roll, pitch and yaw axes and the moments of inertia with respect to these axes will be denoted by I_1, I_2, I_3 , respectively. The moments of inertia of the three wheels about their symmetry axes will be called J_1, J_2, J_3 for the roll, pitch and yaw wheels. Using the approach proposed by Hughes², the satellite dynamics can be modelled by the equations:

$$\dot{h} = -\omega^x(I\omega + J\Omega) + \mathcal{G} \quad (1)$$

$$\dot{h}_w = u \quad (2)$$

$$\dot{C} = -(\omega - \omega_f)^x C \quad (3)$$

where h is the satellite absolute angular momentum with respect to the center of mass, $I = \text{diag}\{I_1, I_2, I_3\}$, ω is the angular velocity of the satellite with respect to the reference frame solidary to the satellite body whose origin is the satellite center of mass and has the axes aligned with the principal axes of inertia, $J = \text{diag}\{J_1, J_2, J_3\}$, $\Omega = (\Omega_1, \Omega_2, \Omega_3)^T$, where Ω_i , $i=1, 2, 3$, is the angular velocity of the i wheel with respect to the satellite body, h_w is the vector whose components are the values of the wheel angular momenta along their motor spin axes, \mathcal{G} is the external torque being applied to the satellite, u is the vector of the axial torques being applied to each wheel rotor, C is the direction cosine matrix between the orbital frame and the reference frame solidary to the satellite body, $\omega_f = -n\mathbf{c}_2$, where n is the satellite orbital rate and

c_2 is the second column of C , and ω^x is the angular velocity cross product operator defined as

$$\omega^x = \begin{pmatrix} 0 & -\omega_3 & \omega_2 \\ \omega_3 & 0 & -\omega_1 \\ -\omega_2 & \omega_1 & 0 \end{pmatrix} \quad (4)$$

Since

$$h = I\omega + J\Omega \quad (5)$$

$$h_w = J(\omega + \Omega) \quad (6)$$

one obtains:

$$(I - J)\dot{\omega} = -\omega^x[(I - J)\omega + h_w] + \mathcal{G} - u \quad (7)$$

Defining $I - J \doteq I^*$, the above equations can be rewritten as:

$$I^*\dot{\omega} = -\omega^x[I^*\omega + h_w] + \mathcal{G} - u \quad (8)$$

$$\dot{h}_w = u \quad (9)$$

$$\dot{C} = -(\omega - \omega_f)^x C \quad (10)$$

The external torques to be considered will be the gravitational torque T and an aerodynamic torque T_a . So:

$$\mathcal{G} = T + T_a \quad (11)$$

$$T = 3n^2 c_3^x I c_3 \quad (12)$$

$$T_a = \rho_a V_R^2 A_p c_p^x \hat{V}_R \quad (13)$$

where n is the satellite circular orbital rate, c_3 is the third column of C , the direction cosine matrix between the orbital frame and the reference frame solidary to the satellite body, ρ_a is the atmospheric density, V_R is the modulus of the velocity of the local atmosphere with respect to the surface of the satellite, A_p is the total projected area, c_p is the coordinate of the centre of pressure with respect to the solidary frame and \hat{V}_R is the direction cosine vector of the velocity of the local atmosphere with respect to the solidary reference frame.

For simplicity, $\alpha \doteq \rho_a V_R^2 A_p$, $\hat{V}_R \doteq C v_R$, where v_R is the direction cosines of the velocity of the local atmosphere with respect to the orbital frame. So it can be written:

$$T_a = \alpha c_p^x C v_R \quad (14)$$

The kinetic energy of the whole system is given by:

$$T = \frac{1}{2} \omega^T I \omega + \frac{1}{2} \Omega^T J \Omega + \Omega^T J \omega \quad (15)$$

and its derivative by:

$$\dot{T} = \mathcal{G}^T \omega + u^T \Omega \quad (16)$$

Torque equilibria

The purpose of the attitude control system should be to achieve LVLH (local vertical, local horizontal) orientation so the unitary vector in the roll direction should point along the local horizontal (velocity vector), the unitary vector in the pitch direction should point along the orbit normal, and the unitary vector in yaw direction should point along the local vertical. Defining:

$$\omega_f \doteq C \omega_0 = -n c_2 \quad (17)$$

$$\omega_0 = \begin{pmatrix} 0 \\ -n \\ 0 \end{pmatrix} \quad (18)$$

where ω_0 is the velocity of the orbital reference frame in its own coordinates, c_2 is the second column of C , the following conditions should be met for $\dot{\omega} \equiv 0$:

$$\omega_f^x I \omega_f + \omega_f^x J \Omega - 3n^2 c_3^x I c_3 - \alpha c_p^x C v_R + u = 0 \quad (19)$$

Imposing the condition:

$$u = \alpha c_p^x C v_R - \omega_f^x J \Omega \quad (20)$$

one obtains from equation (19) the condition:

$$3n^2 c_3^x I c_3 - \omega_f^x I \omega_f = 0 \quad (21)$$

The above condition implies that the solidary reference frame will be aligned with the LVLH orientation³. The matrix C will be an identity matrix and ω_f will be equal to ω_0 . Under this condition equation (20) reduces to:

$$u = \alpha c_p^x v_R - \omega_0^x J \Omega \quad (22)$$

or

$$J \Omega = \alpha c_p^x v_R - \omega_0^x J \Omega \quad (23)$$

So in order to align the satellite with the LVLH orientation, the control torque that should be applied to each wheel rotor will correspond to the coordinates of the vector u given in equation (22).

Attitude control law design

The aim of an attitude controller for a satellite should be to keep the satellite aligned with the LVLH orientation and, at the same time, to restrain the wheel momenta to become unbounded. Since a nonlinear controller is being search to comply to these conditions and one way of obtaining them is through the use of the Liapunov second method, a natural candidate for a Liapunov function should be the Hamiltonian for the

system composed of the satellite body plus wheels. This function is given by:

$$H = \Phi + \frac{1}{2}(\omega - \omega_f)^T I^* (\omega - \omega_f) + \frac{1}{2}(\omega + \Omega - \omega_f)^T J (\omega + \Omega - \omega_f) \quad (24)$$

where the attitude dependent dynamic potential Φ is given by:

$$\Phi = \frac{3}{2}n^2 c_3^T I c_3 - \frac{1}{2}n^2 c_2^T I c_2 - \frac{1}{2}n^2 (3I_3 - I_2) \quad (25)$$

The above function is locally positive definite (around the equilibrium point $\omega = \omega_0$, C equals to the identity matrix) only if the moments of inertia satisfy the gravity gradient stability conditions, $\Phi \geq 0$. In terms of the principal moments of inertia, this condition implies $I_2 > I_1 > I_3$. For dealing with the design of controllers, a modified Hamiltonian should be constructed:

$$L = \Phi + \frac{1}{2}(\omega - \omega_f)^T I^* (\omega - \omega_f) + \frac{k_1}{2}(\omega - \omega_f + \Omega - J^{-1}y)^T J (\omega - \omega_f + \Omega - J^{-1}y) \quad (26)$$

where the scalar k_1 should be greater than zero and the auxiliary variable y is defined by the equation:

$$\dot{y} = \alpha c_p^x C v_R - \omega^x J \Omega \quad (27)$$

Taking the derivative of L with respect to time and rearranging terms, it is obtained:

$$\dot{L} = [(k_1 - 1)(\omega - \omega_f) + k_1(\Omega - J^{-1}y)]^T (u - T_a + \omega^x J \Omega - J \dot{\omega}_f) \quad (28)$$

where it was used the facts that:

$$\dot{\Phi} = (\omega - \omega_f)^T (-T + \omega_f^x I \omega_f) \quad (29)$$

and

$$(\omega - \omega_f)^T (-\omega^x I \omega - I \dot{\omega}_f) = (\omega - \omega_f)^T (-\omega_f^x I \omega_f) \quad (30)$$

Choosing the control law specified by:

$$u = T_a - \omega^x J \Omega + J \dot{\omega}_f - D(\omega - \omega_f) - K(\Omega - J^{-1}y) \quad (31)$$

with $D = (k_1 - 1)Q$ and $K = k_1 Q$, where Q is a positive definite matrix and substituting it in equation (28) gives the following expression:

$$\dot{L} = -[(k_1 - 1)(\omega - \omega_f) + k_1(\Omega - J^{-1}y)]^T Q [(k_1 - 1)(\omega - \omega_f) + k_1(\Omega - J^{-1}y)] \quad (32)$$

So \dot{L} is non positive definite and the system is Liapunov stable. To prove asymptotic stability, the condition:

$$(k_1 - 1)(\omega - \omega_f) + k_1(\Omega - J^{-1}y) \equiv 0 \quad (33)$$

should be examined. With this in mind, one can use condition (31), together with equations (6), (9) and (27) to get the equalities below for the trajectories satisfying (33):

$$\dot{\omega} = \dot{\omega}_f \quad (34)$$

$$\dot{\Omega} = J^{-1} \dot{y} \quad (35)$$

Since

$$\dot{\omega}_f = -\omega^x \omega_f \quad (36)$$

$$\frac{d}{dt} \left(\frac{1}{2} \omega^T \omega \right) = \omega^T \dot{\omega} \quad (37)$$

condition (34) implies ω is constant and $\dot{\omega} \equiv 0$. So equation (8) gives the identity below for points in the trajectories:

$$0 = -\omega^x I \omega + T \quad (38)$$

This equality can be only satisfied at the equilibrium point. Therefore $\dot{L} = 0$ occurs only for $\omega = \omega_0$ and C equals to the identity matrix. So the following conditions are going to be valid:

$$\lim_{t \rightarrow \infty} \omega = \omega_0 \quad (39)$$

$$\lim_{t \rightarrow \infty} y = J \Omega \quad (40)$$

The vector of torques that should be applied to the wheels at steady state should satisfy the equation:

$$u = \alpha c_p^x v_R - \omega_0^x J \Omega \quad (41)$$

Adaptive redesign of the attitude control law

The control law just proposed suffers from the drawback that the parameters related to the aerodynamic torque are not well known. To deal with this problem a redesign of the controller just obtained is needed. To simplify the problem the local atmosphere will be supposed to be moving in the roll direction, what is the usual case. With this hypothesis, $v_R = (1, 0, 0)^T$ and the torque T_a can be rewritten as:

$$\alpha c_p^x C v_R = -\alpha c_1^x c_p = -c_1^x d_p \quad (42)$$

where c_1 is the first column of the matrix C and $d_p \doteq \alpha c_p$.

If \hat{d}_p is an estimate of the vector d_p , one can propose the modified Liapunov function L_m in order to try to identify this parameter on line:

$$L_m = \Phi + \frac{1}{2}(\omega - \omega_f)^T I^* (\omega - \omega_f) + \frac{k_1}{2}(\omega - \omega_f + \Omega - J^{-1}y_m)^T J (\omega - \omega_f + \Omega - J^{-1}y_m) + \frac{1}{2} \gamma (\Delta d_p)^T (\Delta d_p) \quad (43)$$

where $\Delta d_p = \hat{d}_p - d_p$, and:

$$\dot{y}_m = -c_1^x \hat{d}_p - \omega^x J \Omega \quad (44)$$

Taking the derivative with respect to time, one finds after some rearrangements and cancellations the following expression:

$$\begin{aligned} \dot{L}_m = & (\omega - \omega_f)^T c_1^x \Delta d_p + \gamma (\Delta d_p)^T \left(\frac{d}{dt} \Delta d_p \right) \\ & [(k_1 - 1)(\omega - \omega_f) + k_1(\Omega - J^{-1} y_m)]^T \\ & (u + c_1^x \hat{d}_p + \omega^x J \Omega - J \dot{\omega}_f) \end{aligned} \quad (45)$$

Using the control law:

$$u = -c_1^x \hat{d}_p - \omega^x J \Omega + J \dot{\omega}_f - D(\omega - \omega_f) - K(\Omega - J^{-1} y_m) \quad (46)$$

and imposing:

$$\frac{d}{dt} \Delta d_p = -\frac{1}{\gamma} (\omega - \omega_f)^x c_1 \quad (47)$$

The expression for \dot{L}_m reduces to:

$$\begin{aligned} \dot{L}_m = & -[(k_1 - 1)(\omega - \omega_f) + k_1(\Omega - J^{-1} y_m)]^T \\ & Q[(k_1 - 1)(\omega - \omega_f) + \\ & k_1(\Omega - J^{-1} y_m)] \end{aligned} \quad (48)$$

Since d_p is constant ,

$$\frac{d}{dt} \Delta d_p = \frac{d}{dt} \hat{d}_p$$

and, using equation (47), the estimate for d_p can be obtained by:

$$\frac{d}{dt} \hat{d}_p = -\frac{1}{\gamma} (\omega - \omega_f)^x c_1 \quad (49)$$

The expression (48) shows that $\dot{L}_m \leq 0$, consequently one should look the case

$$(k_1 - 1)(\omega - \omega_f) + k_1(\Omega - J^{-1} y) \equiv 0.$$

Using the same procedure as before, it is possible to show that $\dot{\omega} = \dot{\omega}_f$, $\dot{\Omega} = J^{-1} \dot{y}$, $\dot{\omega} \equiv 0$. The difference now is that equation (8) gives the following condition for the trajectories:

$$0 = -\omega^x I \omega + T + c_1^x \Delta d_p \quad (50)$$

The equation above can be satisfied outside the equilibrium point. It will mean that the satellite can align itself with a direction that it is fixed with the orbital reference frame, but different from the desired one.

Using the fact that:

$$\dot{c}_1 = -(\omega - \omega_f)^x c_1 \quad (51)$$

equation(49) can be rewritten:

$$\frac{d}{dt} \hat{d}_p = \frac{1}{\gamma} \dot{c}_1 \quad (52)$$

so

$$\dot{\hat{d}}_p = \delta + c_1$$

where δ is a constant vector corresponding to the difference between the parameter initial guess and the initial position of c_1 . Using this result in equation (8), one obtains:

$$0 = -\omega^x I \omega + T + c_1^x (\delta - d_p) \quad (53)$$

So the error of the alignment will be function of the precision the coordinate of the center of pressure is known at the beginning of the process of controlling the satellite and there is no improvement during the attitude control process. In order to change this, a new Liapunov function should be constructed and a new controller should be designed. Consider a modified function L_n :

$$\begin{aligned} L_n = & (k + 1)\Phi + \frac{1}{2}(\omega - \omega_f)^T I^* (\omega - \omega_f) \\ & + \frac{1}{2}(\omega + \Omega - \omega_f - J^{-1} y_m)^T g [(k + 1)J^2 \\ & - gkI^* J] (\omega + \Omega - \omega_f - J^{-1} y_m) \\ & + (\omega + \Omega - \omega_f - J^{-1} y_m)^T gkJI^* \\ & (\omega - \omega_f) + \frac{1}{2}(\Delta d_p)^T \Gamma (\Delta d_p) \end{aligned} \quad (54)$$

where k and g are positive constants and the condition, $gk < \frac{1}{I^*}$, ensures local positive definiteness of L_n . The derivative of this function is:

$$\begin{aligned} \dot{L}_n = & [(I + gkJ)(\omega - \omega_f) + gk(J\Omega - y_m)]^T \\ & c_1^x \Delta d_p + (\Delta d_p)^T \Gamma \left(\frac{d}{dt} \Delta d_p \right) \\ & + [(I - gJ)(\omega - \omega_f) - g(J\Omega - y_m)]^T \\ & [-k(T - \omega^x I \omega - I \dot{\omega}_f) + (gkI^* - I) \\ & (u - J \dot{\omega}_f + \omega^x J \Omega + c_1^x \hat{d}_p)] \end{aligned} \quad (55)$$

where I corresponds to the identity matrix. Imposing:

$$\begin{aligned} u = & J \dot{\omega}_f - \omega^x J \Omega - c_1^x \hat{d}_p + (gkI^* - I)^{-1} \\ & [k(T - \omega^x I \omega - I \dot{\omega}_f) - D(I - gJ) \\ & (\omega - \omega_f) - gD(J\Omega - y_m)] \end{aligned} \quad (56)$$

$$\begin{aligned} \frac{d}{dt} \hat{d}_p = & -\Gamma^{-1} [(I + gkJ)(\omega - \omega_f) \\ & + gk(J\Omega - y_m)]^x c_1 \end{aligned} \quad (57)$$

the value of \dot{L}_n becomes:

$$\begin{aligned} \dot{L}_n = & -[(I - gJ)(\omega - \omega_f) - g(J\Omega - y_m)]^T \\ & D[(I - gJ)(\omega - \omega_f) - g(J\Omega - y_m)] \end{aligned} \quad (58)$$

To ensure the proper momentum management for the system the control law just designed must be modified. With this purpose a new variable should be defined:

$$\begin{aligned} z = & -kI^* (\omega - \omega_f) + [-(k + 1)I + gkI^*] \\ & [J(\omega + \Omega) - J\omega_f - y_m] \\ & + \int D[(I - gJ)(\omega - \omega_f) \\ & - g(J\Omega - y_m)] dt \end{aligned} \quad (59)$$

The momentum manager is obtained by using a controller satisfying the following equation:

$$\dot{x} = -K_2 x \quad (60)$$

where $K_2 > 0$. With this constraint the final control law is given by:

$$u = J\dot{\omega}_f - \omega^x J\Omega - c_1^x \dot{d}_p + (gkI^* - I)^{-1} [k(T - \omega^x I\omega - I\dot{\omega}_f) - D(I - gJ)(\omega - \omega_f) - gD(J\Omega - y_m) - K_2 x] \quad (61)$$

The estimation variable d_p should satisfy:

$$\frac{d}{dt} \hat{d}_p = -\Gamma^{-1}(\omega - \omega_f)^x c_1 \quad (62)$$

So, as in the previous design, $\dot{L}_n \leq 0$, the system is stable, and, for assuring asymptotical stability, one should examine the trajectories for which:

$$(I - gJ)(\omega - \omega_f) - g(J\Omega - y_m) \equiv 0 \quad (63)$$

$$x \equiv 0 \quad (64)$$

It can be shown the above conditions imply:

$$\dot{\omega} = \dot{\omega}_f$$

$$\dot{\omega} = 0$$

$$\omega = \text{constant}$$

$$\omega = \omega_f$$

$$\dot{d}_p = \text{constant}$$

So for the trajectories satisfying (62) and (63) it is possible that the satellite attitude will not follow the orbital reference frame. It may occur an alignment error given by the following equation:

$$0 = [I - k(gkI^* - I)^{-1}](T - \omega^x I\omega) + c_1^x \Gamma^{-1} c_1 + c_1^x \delta \quad (65)$$

where δ is a vector depending on the initial value given to the estimate and the initial value of c_1 .

Conclusions

Some methods of obtaining attitude and angular momentum control laws using Liapunov functions were presented. It was shown that when the aerodynamic disturbance is exactly known it is possible to find a controller that keeps the satellite aligned with the orbital reference frame. In the case one is uncertain about the disturbance, an adaptive procedure can be tried, but the stronger results obtained earlier are not met. The reason for this behaviour lies in the fact long known that in order to identify the control objective should be relaxed and one should let the system be driven by signals that are able to excite its complete dynamics. So,

since the main interest consists in controlling the attitude and momentum of the satellite, one has to be satisfied with procedures that do not estimate the involved parameters completely and keep the satellite attitude close to the desired one, in some kind of compromise between the two objectives. Simulations for comparing various algorithms should be performed, but unhappily it was not possible to present in this paper.

Acknowledgments

The support given by Conselho Nacional de Desenvolvimento Científico e Tecnológico (CNPq) through a postdoctoral scholarship is acknowledged. The author would also like to thank Dr. S.R. Vadali for the helpful discussions during his stay at the Department of Aerospace Engineering, Texas A&M University.

References

- ¹Vadali, S.R.; Oh, H.-S. Space station attitude control and momentum management: a nonlinear look. *Journal of Guidance, Control, and Dynamics*, Vol. 15, No. 3, 1992, pp. 577-586.
- ²Hughes, P.C. *Spacecraft Attitude Dynamics*, Wiley, New York, 1986.
- ³Sperling, H.J. The general equilibria of a spinning satellite in a circular orbit. *Celestial Mechanics*, Vol. 6, 1972, pp. 278-293.

ON-GROUND AOCS SUPPORT SOFTWARE FOR THE SAX SATELLITE

Carlo De Libero
Gianni Mauceri

Telespazio S.p.A. per le Comunicazioni Spaziali
Via Tiburtina, 965 I-00156 ROME ITALY

Abstract

The SAX (X-ray Astronomy Satellite) mission, sponsored by the Italian Space Agency (ASI), aims to carry out systematic and comprehensive observations of celestial X-ray sources, using both Narrow Field Instruments (NFI) and Wide Field Cameras (WFC). The spacecraft is three-axis stabilized, using Reaction Wheels System (RWS) as actuators and Gyros (GYRs) and Star Trackers (STRs) as main sensors.

The paper describes the Attitude and Orbit Control Ground Support System (AOCSS) which is being developed to support the on ground operations of the SAX AOCS and which will be integrated in the SAX Operations Control Centre (OCC). The main tasks of this software include computation of attitude manoeuvres, attitude reconstruction and sensor calibration. A high precision attitude determination software shall also be described; this module, based on the Kalman filtering technique, uses the measurements coming from STRs and GYRs. The latter replace the state dynamics model in the filter, and will be run off-line as a post facto activity. The internal and external interfaces with the other software systems installed at OCC are highlighted, together with all operational constraints which rule the proper working of the software. Testing activities for software validation are described briefly with reference to the availability and use of the SAX Simulator (SAXSIM), developed in the framework of the same project.

Key words: SAX, AOCS Ground Support, Attitude Determination, Kalman Filter, Star Tracker, Sensors Calibrations, SAXSIM.

Introduction

The SAX spacecraft is a three-axis stabilized satellite whose objectives are to perform systematic and comprehensive observation of celestial X-ray sources over the 0.1 to 300 keV energy range. The following payload instruments are mounted on-board:

- Low Energy Concentrator Spectrometer (LECS) covering the 0.1 - 10 keV range with a field of view (FOV) of 40 arcmin;
- Medium Energy Concentrator Spectrometer (MECS) covering the 1.3 - 10 keV range having a FOV of 30 arcmin;

- High Pressure Concentrator Proportional Counter (HP-GSPC) covering the 3.5 - 120 keV range having a FOV of 1.1 degrees;
- Phoswich Detector System (PDS) covering the 15 - 300 keV range having a FOV of 1.5 degrees;
- Two Wide Field Cameras (WFC) covering the 2 - 30 keV range having a FOV of 20x20 degrees.

The NFI have the boresight directed as the satellite Z axis whereas the WFCs are mounted along the +Y and -Y satellite axes (see Fig.1).

SAX is a joint program of the Italian Space Agency and the Dutch Government. The satellite main contractor is the Italian company ALENIA SPAZIO (Turin). The Netherlands provides a number of Government Furnished Equipment (GFE), specifically LECS and WFC, and the AOCS, developed by FOKKER Space and Systems as an ALENIA subcontractor. TELESPIAZIO is responsible for the development of the Ground Support System (GSS). In particular, the following subsystems are being implemented: TT&C Ground Station, STation Computer (STC), Data Relay System (DRS), Operations Control Centre (OCC) Scientific Data Centre (SDC), SAX SIMulator (SAXSIM). SAX will be launched by the end of 1995 with an Atlas Centaur vehicle into a near circular orbit at 600 Km altitude with an inclination of less than 5 degrees. It will have a lifetime of at least two years. Should the satellite altitude fall below 450km due to the atmospheric drag, it will be possible to perform Delta-V manoeuvres using the Reaction Control Subsystem (RCS). This consists of twelve 10N thrusters (two branches of 6 thrusters). The total SAX mass at launch will be about 1400 Kg, propellant included. The RCS will also be used in case of contingency of the launcher third stage to reach an altitude close to the nominal one.

The SAX Ground Station will be placed in Singapore and connected via Intelsat Business Service (IBS) to OCC and SDC located in Rome. Ground/SAX contact will last a minimum of 10 minutes at 600 Km in a 97 minute orbit. Data collected during the non visibility period are stored on the on-board tape recorder and sent to the ground station during each passage at a HBR (High Bit Rate) of 1.2 Mbit/s together with real time telemetry.

SAX Attitude and Orbit Control Subsystem (AOCS)¹

The AOCS is a modular subsystem consisting of a number of units which communicate with the Attitude Control Computer (ACC) via a redundant digital serial MACS-bus. The SAX attitude is always constrained to remain within one of the two Pointing Domains: the Default Pointing Domain, defined by the constraint of keeping the +X satellite axis within 30° from the sun-vector ($0 \leq \text{SAA} \leq 30^\circ$), and the Extended Pointing Domain in which the angle can be relaxed to 45° and the sun is constrained in the XY plane ($0 \leq \text{SAA} \leq 45^\circ$, $\text{SIA} = 90^\circ$ see Fig.2). The pointing domain is selected depending on whether NFI or WFC operations are performed; both are necessary in order to guarantee the required power generation from the Solar Array Subsystem (SAS) to avoid sun impingement of the NFIs FOV. The AOCS is designed to autonomously obtain and keep a safe attitude and to support scientific observations by using safeguards which ensure the detection of errors and a proper unit reconfiguration. It will be capable of pointing the Z-axis within an Absolute Pointing Error (APE) of 1.5 arcmin and the Y-axis within an APE of 16.5 arcmin with a rate limit of 40 arcsec/sec. The accuracy required for the post facto attitude solution, obtained on ground using data coming from GYRs and STRs, is defined by an Absolute Measurements Accuracy (AMA) of 0.5 arcmin; this means that for each axis the error between the actual and the measured directions shall be less than 0.5 arcmin.

AOCS Units

The AOCS consists of the following units, through which full redundancy shall be provided for all essential functions:

- ACC, composed of two identical computers each connected to a dedicated MACS-bus;
- Power Distribution Unit (PDU) (internal redundancy);
- Two Sun Acquisition Sensors (SAS) composed of 8 Sun Presence Indicators (SPIs) redunded along both the +X and -X axis direction; one Quadrant Sun Sensor (QSS) only present on +X side. These sensors are used both during the first sun acquisition and to keep the sun in the active pointing domain during attitude slews;
- Monitoring and Reconfiguration Unit (MRU) containing the subsystem watchdog and two set of electronics to process the signals coming from the two SASs;
- Four Rate Integrating Gyroscopes (GYR) in an all-skewed configuration for three out of four hot redundancy; they can operate in two internal modes, coarse and fine, measuring angular change during the AOCS cycle (0.5 sec) respectively in the ranges $\pm 1.25^\circ/\text{sec}$ and $\pm 0.36^\circ/\text{sec}$.
- Three STRs (-X, +Y, +Z); two out of three STRs provide accurate pointing capability. Availability of the STRs depends on their health and on the attitude relative to the Earth, Moon and some Bright Objects;
- Four Reaction Wheels (RWL) in an all-skewed configuration for three out of four cold redundancy. Each RWL stores up to

20Nms of angular momentum and provides a torque up to 0.2 Nm;

- Three Magnetic Torquers (MTR) along the X, Y and Z axes. They will be used for momentum unloading and provide a magnetic moment of $100 \pm 10 \text{ Am}^2$.
- Two Magnetometers (MGM) used either in attitude acquisition after SAX-launcher separation or during the RWL unloading; they provide the measurement of the Earth Magnetic Field (EMF) vector along the spacecraft axes in the range of $\pm 50 \mu\text{T}$ with a resolution of $0.5 \mu\text{T}$.

The two ACC computers consist of an 80C86 microprocessor supplemented with the 8087 co-processor to achieve the required performance. Each one contains both Basic Software (BSW) and Application Software (ASW). The first one provides the real time executive, performs ASW tasks scheduling and execution, their synchronisation and timing, and controls of the ACC interface with the external device (e.g. MACS-bus and OBDH). The ASW consists of the attitude control tasks which are responsible for the sensors data processing, control laws execution and actuators commanding. In order to separate the aspects of autonomous actions and ground commanded operations, the ASW is divided in two blocks, BAC-ASW and EAC-ASW. BAC ASW aims for robustness and safety and deals with automatic initialization after power up, autonomous attitude acquisition using direct measurement of local sun vector and the EMF, safe-keeping, housekeeping telemetry (HKTLM) generation, telecommands processing and redundancy management for all units essential for safe-keeping attitude control. The EAC-ASW is responsible for the inertial attitude control with full pointing performance during science operations, support to the attitude and orbital manoeuvres, comprehensive telemetry production and full AOP handling.

The STRs are the main attitude sensors, two of which are used during scientific observations in order to reach the required pointing accuracy. The detector of the STR sensor is a CCD with 384×288 pixels, each of them having 39.5 arcsec of dimension, thus providing a total FOV of $4^\circ \times 3^\circ$. The STR is able to detect each star having visual magnitude, m_V , in the range [2,8] and to track five stars simultaneously. The Elementary Search Window (ESW), the maximum window that the STR can use for star search, has 62×46 pixels dimension. STR accuracies are 5.7 arcsec in position and from 0.2 to 0.62 m_V in magnitude depending on the star class. The STR electronics are microprocessor-based and contain the software for sensor data processing and drives the STR operating modes executing the relevant tasks. The AOCS EAC-ASW uses the STR to track one star at a time; moreover it uses the following STR modes: stand-by, search/track, mapping.

AOCS Operating Modes

According to SAX mission requirements, the AOCS operates in the following modes:

- BAC modes:
 - Initialization Mode (IM)
 - Acquisition Mode BAC (AM-BAC)

• EAC modes:

- Acquisition Mode EAC (AM-EAC)
- Default Pointing Mode (DPM)
- Science Pointing Mode (SPM)
- Delta-V Mode (DVM)
- Slow Scan Mode (SSM)

Mode transitions are implemented as shown in Fig.3.

IM performs hardware and software initialization in order to prepare the AOCS units for BAC, to start communication with the OBDH and to perform autonomous transition to AM-BAC.

AM-BAC brings the satellite to a safe attitude from a wide range of possible initial conditions. Its target is to point the X satellite axis to the Sun and put the EMF vector in the XZ plane, Z pointing North. It is able to absorb a worst case angular velocity (0.84°/sec) caused by the SAX-launcher separation. When this mode enters for the first time, the satellite attitude w.r.t. the inertial frame used during the operations is not known on-board.

AM-EAC performs the same functions of AM-BAC and the EAC initializations including, through two dedicated ground commands, the upload of the attitude quaternion and Sun vector in the inertial frame.

DPM points the Z satellite axis to a default guide star (Polaris), whose coordinates and brightness are read from the on-board database, and keeps the sun vector in the XZ plane. This attitude is accurately and autonomously determined using the on-board maintained sun vector and the default guide star data; the Science Pointing can be started from this mode.

SPM performs scientific observations of up to 10^5 sec., by pointing the instrument fundamental axis towards any target in the active pointing domain, using the data contained in the SP AOP (target attitude quaternion and STRs data). This mode is also used to achieve the proper attitude before SSM and DVM.

SSM is used for calibration of scientific instruments by performing a rotation, at constant rate, of the satellite about a predefined axis by using data contained in the SS AOP (initial target attitude quaternion and rotation quaternion).

DVM is used for orbital manoeuvres using the RCS and starting from an attitude characterised by Z axis tangent to the orbit, Y axis normal to the orbit plane and X axis within 30° to the Sun. This mode is similar to SSM because in this case a slow scan is also performed, about the Y axis, in order to keep the thrust axis Z always directed along the satellite velocity vector.

AOCSSS - Attitude and Orbit Control Ground Support System Environment²⁻³

Although the AOCS is designed to operate largely autonomously, situations may arise in which ground intervention is required. When a scientific observation has to be performed, for example, a SP AOP is sent to the AOCS, in order to drive the satellite to the target attitude required to carry out the observation and to define the sensors configurations used for attitude keeping. Since the AOCS commands have well defined structures and contain many parameters, and are in general rather complex, an On-Ground

AOCS Support Software, responsible for parameter computation and AOCS commands preparation has been foreseen. These functions are performed by the AOCSSS, part of the OCC. The OCC is the core of the satellite management and its scope is to carry out all routine and contingency activities to be performed during the mission. It is composed of four systems:

- 1) Spacecraft Control System (SCS), whose tasks are the management of the spacecraft, system and workstations databases; handling of telemetry data; telecommand generation and transmission;
- 2) AOCSSS, which implements AOCS operations support functions for preparation of the AOCS complex commands (e.g. AOPs), attitude determination, sensors calibrations, auxiliary computations;
- 3) Orbit Determination and Dynamics System (ODDS), where preprocessing of tracking data, orbit determination and prediction, auxiliary data generation functions are performed;
- 4) Scientific Operation Centre (SOC), where long and short term scheduling of scientific payload activities and data archiving are done.

AOCSSS forms a unique working environment with the OCC systems, for handling all operational mission activities. Communication is achieved by means of external interfaces based on special input/output files used for transfer of data (Fig.4). A nominal operational sequence involving all OCC systems can be summarized as follows:

- the Nominal Pointing File (NPF) is produced by the short term scheduler in the Observation Scheduling Subsystem (OSS) of SOC, on a weekly basis and five days before the start of each application week; this contains a set of requested science pointings and the slow scans to be performed;
- the satellite state vector predictions for the application week are taken from the ARCHIVE file in ODDS; this is a cyclic file, refreshed daily after orbit determination; this contains the satellite state vector data over three months, twelve days into the future and the remaining in the past;
- the AOCSSS tasks AOPSPM and AOPSSM, read the science pointing and slow scan requests from the NPF and the satellite state vector predictions from the ARCHIVE file for the time span covered by each observation. Using these data, together with the reference Mission Star Catalogue and the Sun, Moon and Planets ephemerides, AOPSPM and AOPSSM produce the relevant SP and SS AOP commands, storing them in two dedicated files AOPSPM.OUT and AOPSSM.OUT; the Mission Star Catalogue will be involved in the SP AOPs preparation only, because in SSM attitude keeping is not performed using STRs;
- the SCS task for the preparation of telecommands takes each AOP command structure contained in the files AOPSPM.OUT and AOPSSM.OUT and inserts it into a telecommand structure used for the successive AOP uplinking;
- the ODDS computes the predicted ground visibility start and stop times for the next twelve days' orbits and stores them in the file Sequence Orbit Events (SOE);

- the AOCSS task ANTSWI reads these data from the file SOE, the target attitude quaternions relevant to the SP AOPs active during each visibility periods from the file AOPSPM.OUT, and the satellite state vector predictions, for the same time slot, from the ARCHIVE file. Next, it produces the file ANTSWI.OUT containing, for the following week's passages, a prediction of the antenna used for the link with the Ground Station and antenna switching information. This file has to be transferred to the STC in order to automatize the Link Acquisition (LAP) and the Antenna Switching (ASP) procedures.

As off-line activities and for scientific purposes only, the following steps have to be taken:

- for each SP AOP, the satellite attitude has to be accurately reconstructed for the entire duration in order to give a precise attitude reference for the scientific data acquired during the observations; this is performed by the AOCSS task POSATT, which uses the Attitude Reconstruction Data (ARD) file handled by SCS, the satellite state vector from the ARCHIVE file, the star coordinates from the Mission Star Catalogue. The computed attitude solutions in a selected time interval are stored into the POSATT.OUT file;
- once POSATT.OUT has been created, a message is sent to the Archive Subsystem of SOC which takes this file and transfers it to SDC.

From the aforementioned AOCSS functions it is evident that, in addition to the support in commands preparation activities, processing of telemetry data is also performed. The latter is required, in fact, both for attitude determination and sensors calibration. Therefore the AOCSS is a data management and processing system which prepares the AOCS complex commands, determines the post facto attitude solution, performs the sensors calibrations and determines the antenna in visibility at the start of each ground contact and possible switching occurrence. In the remainder of the paper, the AOCSS software components are presented, with a description of their functionalities.

AOCSS - The SAX On-Ground AOCS Support Software²⁻³

AOCSS software tasks have been organised in the following four functional components:

- Manoeuvre Support Software;
- Attitude Determination Software;
- Sensor Processing Software;
- Auxiliary Software.

This top level software decomposition is illustrated in Fig.5, which also shows the main tasks included in each block.

Manoeuvre Support Software

The software tasks included in this block are responsible for the computation of the parameters and the preparation of the

structures of the AOCS ground commands to be sent to the satellite to support AM, DPM, SPM, DVM and SSM.

Acquisition Mode Attitude Calibration (ATTCAL)¹⁻²⁻³ is the software for to the preparation of the AOCS Attitude Calibration and Memory Patch commands which have to be sent before commanding the first transition to DPM. The former command replaces the on-board attitude quaternion with the required AM target attitude w.r.t. the inertial frame, while the latter is used to define a suitable default guide star for DPM. The outputs of this task are the two files ATTCAL.OUT and DEFGST.OUT containing the structures of the two commands. For the production of the second command the DPM guide star inertial vector, visual magnitude and related memory addresses are needed; the star data are read from the mission star catalogue, and used to compute the inertial default guide star vector.

Sun Vector Maintenance (SUNVEC)¹⁻²⁻³ is the software for the preparation of the AOCS Sun Vector and Memory Patch commands. These commands are required to initialise/calibrate the on-board maintained inertial sun vector and to calibrate the time step quaternion; the latter is used by the ASW to update the sun vector taking into account the rotation of the Earth around the Sun. The inertial sun vector initialization has to be performed because it is used together with the default guide star vector to fully specify the DPM attitude. As the quaternion calculation used on-board to maintain the sun vector introduces round-off errors, this vector has to be updated periodically during the mission because error on this vector directly influences the accuracy of the next science pointings. Moreover the time step quaternion, used to propagate the sun vector, depends on the time rate of change of the sun ecliptic longitude ($d\lambda/dt$). As the latter is constant on-board, that is the Earth orbit around the Sun is considered circular, this quaternion has to be updated periodically in order to take into account the actual variation of $d\lambda/dt$. This task performs the computation of both inertial sun vector and the time step quaternion, preparing the relevant commands and inserting them inside two dedicated files: SUNVEC.OUT and SUNVEL.OUT. The inertial sun vector is computed using the JPL library routines.

AOP Parameters for SPM (AOPSPM)¹⁻²⁻³ is the software devoted either to the preparation of the AOCS SP AOP commands relevant to the science pointing requests coming from OSS/SOC or to perform a slew to any desired attitude. With this type of command the target attitude is defined together with the STRs which the on-board control loop has to use for attitude keeping, including the data needed for STRs handling purposes. A STR is defined as available for attitude keeping if at least a star ($2 \leq m_V \leq 8$) falls into the FOV, only Earth obstructions occur and a time span exists, along each orbit, during which the STR is not obscured. Moreover, to fulfil the requirements on the pointing accuracy, two STRs shall be available during each science observation.

The functions provided by this task for each observation request are the following: 1) compute the target attitude quaternion corresponding to the X-ray sources to be pointed; 2) determine the STRs availability configuration taking into account the mission star catalogue, the target attitude, celestial

objects and satellite ephemerides; 3) for each available STR compute the guide star coordinates in the STR functional frame using the mission star catalogue, determine if the STR is obscured by the Earth and the start and stop times in which the first obstruction occurs, determine the search window length and width. These data, together with the magnitude threshold used by STR to search the guide star, are used to prepare the SP AOP command for a generic observation request. The magnitude threshold shall be a value slightly below the brightness of the guide star as measured by the STR but above that of the stars close to it. At the end of this process the file AOPSPM.OUT contains an SP AOP command for each science pointing required and the time at which it has to be enabled.

AOP Parameter for DVM (AOPDVM)¹⁻²⁻³ is the software for the preparation of the AOCS Delta-V command required to perform Delta-V manoeuvres. With this command the initial target attitude at the manoeuvre start time (AOP enable time) is defined together with the rotation quaternion required to keep the thrust axis tangent to the orbit and defining the angular rotation to be performed at each AOCS cycle, the RCS branch to be used and the manoeuvre maximum duration. It should be noted that before and after the DV AOP execution, an SP AOP must be enabled in order to calibrate the satellite attitude. The initial target attitude specified in the DV AOP is constrained to be within 2° of the actual attitude when the manoeuvre starts. Therefore from the above considerations the functions provided by this task are the following: 1) compute the initial target quaternion having the Z axis tangent to the orbit, Y axis normal to the orbit plane and whose direction is defined by the sun position in order to keep X axis inside the pointing domain; 2) compute the total rotation angle using the angular separation between the satellite velocity vectors at manoeuvre start and stop times; 3) compute the rotation quaternion, using the Y axis as rotation axis, the step angle for AOCS cycle from the total rotation angle and the manoeuvre duration provided by ODDS. The DV AOP command prepared using the parameters computed previously is stored in the file AOPDVM.OUT.

AOP Parameter for SSM (AOPSSM)¹⁻²⁻³ is the software for the preparation of the SS AOP command required to carry out slow scan manoeuvres around a predefined axis to perform scientific instruments calibrations. The SS AOP structure is the same as the DV AOP except for the definition of the RCS branch which is not foreseen, since during the SSM the RWLs are used as actuators. This task computes the same parameters indicated for DV AOP except that the input data come from SOC via NPF instead of ODDS. For SS, in fact, NPF specifies the axis around which the scan has to be performed, the rotation amplitude and the angular velocity (less than 5°/min) used to carry out the scan. In this case, before and after a SS AOP is commanded, a SP AOP shall be foreseen. The SS AOP commands prepared by this module are stored in the file AOPSSM.OUT.

A Mission Star Catalogue, containing the stars having visual magnitude in the range [2,8] and their position in mean system of 2000.0 coordinates, is used as reference. It will be provided by ASI and tailored for the SAX mission taking into account STR performances and mission constraints. To this end, a

software with a number of routines for mission star catalogue handling is also being developed. These are used extensively for SP AOPs preparation and attitude determination. The main functions of this software are: 1) extract from the mission star catalogue, for a well defined attitude, the coordinates and brightness of the guide stars which fall in the STR FOV; 2) perform star pattern recognition using data coming from the STR when it performs a map of its FOV.

Attitude Determination Software

Although for SAX the attitude is autonomously computed on-board by using attitude sensor information and special pointings, the success of the mission largely depends on the accuracy of the final on-ground attitude solution, the so called post-facto attitude. In fact, the scientific nature of the mission requires that observation data collected have to be correlated with the particular attitude achieved during the different science pointings. Moreover, during the mission, a module which computes the attitude from sensors outputs is required both for verification and calibration purposes. The two modules contained in this functional component provide different accuracy levels for the solutions, one simply based on a deterministic approach and the other implementing a Kalman filtering technique.

Quick Attitude Determination (QUIATT)¹⁻²⁻³ is the software which computes the satellite attitude at a given time using a simple deterministic approach. This task uses the outputs of the sensors being used, their sensor to body transformation matrices and all orbital and celestial ephemerides of interest. For example, this task is used when the satellite does not find the default guide star in a transition to DPM and locks onto an unknown star as a result of an insufficiently accurate initial attitude; in this case both the STRs not used for control can be commanded to perform a map of their FOV. Using the star pattern recognition, the new attitude is computed and uplinked on-board using the Attitude Calibration command. The output file ATTCAL.OUT contains the structure of the above command.

Post Facto Attitude Determination (POSATT)⁴⁻⁵⁻⁶ is the software module which computes the attitude for a time interval in which a scientific observation was performed (AOCS in SPM) making use, for requirements on accuracy, of a Kalman filtering technique. The attitude solution calculated by this task will be used in order to correctly place the observed sources in a well defined inertial reference. As for the Kalman filter, it generally consists of a state dynamic model described by a set of non-linear differential equations and a set of non-linear measurement equations. Since for SAX the gyro measurements are available and provide information about the angular velocity present on-board the satellite, a model replacement approach is used; the measurements include alignment errors, drift biases and noise. The kinematic equations are represented in quaternion notation and the on-board computed attitude quaternion is used to initialise the algorithm. So the starting point of the generic algorithm is the integration of the kinematic equations which computes the

predicted attitude quaternion $q(k+1/k)$. As for the propagation of the state errors foreseen inside the Kalman filter, the quaternion error is expressed not as the difference between the true and the estimated quaternions, but as the quaternion composed by means of quaternion algebra with the estimated one in order to obtain the true one. From that an approximate representation of the state vector and covariance matrix is used. Being this incremental quaternion a small rotation, the fourth component is close to unity and the attitude information is contained in the three vector components. Therefore the state vector defined as a six component vector given by the three components of the error quaternion and the gyros drift biases provide a non redundant representation of the state error. Moreover the STR measurements are modelled to perform the correction of the predicted estimate. The attitude solution in the selected time interval is stored into the file POSATT.OUT.

Sensor Processing Software

The software described in this paragraph determines all sensor parameters which impact the sensors and the on-board control loop. It is strictly linked to both manoeuvre support and attitude determination software, whose activation always requires a preliminary check of the sensor parameters involved and if necessary a run of the related sensor processing software. It contains software tasks used either to perform the computation of the sensor misalignments (QSS, STR and GYR), due to the changes of thermal environment and launch shocks, or to estimate internal parameters which characterise the sensor performances (GYR drift and scale factor). Except for STR misalignments which need only be taken into account in the AOCSS when required in a computation, the others must be updated on-board by means of dedicated memory patch commands.

QSSs Misalignments Calibration (QSSMIS)¹⁻²⁻³ is the software which computes the QSSs misalignments. It is required because the QSS influences the AOCS performance as it is used by the safeguard function. The dedicated memory patch command data has to be uplinked if the computed misalignment quaternion is larger than 0.01° per axis. In order to compute the misalignment quaternion a dedicated procedure (suggested by Fokker) has to be implemented; it foresees memory dumps and the execution of three SP AOPs based on the use of two STRs. The former are commanded for the Sun vector in satellite axes determined from QSS measurement and the commanded attitude quaternion. The algorithm implemented in this module compares the sun vector in the satellite axes, computed using the on-ground determined inertial sun vector, and the attitude quaternion corresponding to the commanded pointing, with the Sun vector determined by the QSS for each of the three pointings. The latter is computed taking into account the nominal misalignment quaternion and the sun vector in ACA frame obtained from memory dump. The memory patch command prepared is stored in QSSMIS.OUT file.

Gyros Drift Determination (GYRDRI)¹⁻²⁻³ computes the Gyros Drifts. Again, a dedicated procedure (suggested by Fokker) has

to be implemented. It foresees the execution of a SP AOP based on the use of two STRs. As drifts are input for the computation of scale factors and misalignments, this calibration has to be performed before the one for scale factors. The algorithm implemented in this module uses the gyro counter variation during a 30 minute time interval in which the aforementioned AOP is active. As attitude keeping is performed using two STRs, the limit cycle attitude variation and gyro noise average out, therefore the measured gyro counter variation is only due to gyro drift.

The memory patch prepared containing the computed gyro drifts are stored in the file GYRDRI.OUT.

Gyros Scale Factor and Misalignments (GYRSFM)¹⁻²⁻³ computes the gyros scale factor and misalignment. A ground procedure has to be implemented in order to perform these calibrations, and foresees the execution of three slews about the satellite axes; each of them starts and ends with pointings in which two STRs are used. The algorithm used to compute the scale factors and the four alignment matrices for each possible gyro combination compares the angles of the commanded slews with the corresponding gyros current counters variation. The latter are computed for each slew by processing the counts of each gyro stored in the ARD and corrected for the gyro drift computed with the previous task. The memory patch commands relevant to the scale factors and the four alignment matrices are stored respectively inside the files GYRSCF.OUT and GYRMIS.OUT.

The importance of the last two calibrations depends on the effects that drift and scale factor have on the gyro performance. Typical situations are those in which a gyro is used to replace a STR temporarily obscured by the Earth or when a large slew is commanded. In the first case, the gyro has to guarantee that at the end of the obstruction period the guide star used for the pointing shall be within the same window used before. For large slews, the attitude reached at the end needs to be such that the guide star falls inside the ESW.

STRs Misalignments Estimation (STRMIS) computes the alignment quaternions defining the orientation of each STR w.r.t. the satellite axes. These quaternions include misalignments of the STRs measured during a dedicated calibration procedure. Both the procedure and the algorithm required to perform the misalignment estimation are being investigated. As there are contributions to the STR misalignments from systematic, periodic, short-term quasi systematic and random error sources, a Kalman filtering technique could be used to perform an estimation of the interested misalignments. The fundamental requirement to take into account in performing the calibration is that two STRs must have at least two stars simultaneously within their FOV during the calibration phase; this fact provides both direction and rotational information. The computed alignment quaternions shall not be uplinked on-board, but taken into account in the above software modules each time the coordinates of a guide star w.r.t. STR axes need to be computed.

STRs Calibration (STRCAL) computes the instrumental magnitude of each guide star as measured from the STR. In general it is a little different from the visual magnitude

reported in the mission star catalogue and computed taking into account the star spectral class and the CCD response. The m_V computed value shall be inserted into the SP AOP to define the magnitude threshold used by the STR during the guide star search; the procedure to perform this type of calibration is currently under investigation.

Auxiliary Software

This block contains a number of more general modules which are either used as check tools during operation or as low level modules for the tasks specified above. Examples of these routines are: the Earth Magnetic Field Model, the JPL module to compute the Planet, Sun and Moon Ephemerides, conversion routines from calendar date to MJD2000 and vice versa. However, the most important software included in this block is the Antenna Switching task.

Antenna Switching (ANTSWI)^{1-2,3} predicts the on-board antenna which comes into visibility of the ground station at each passage and the time at which a possible antenna switching may occur. Both these predictions depend on the satellite orbit and attitude during the ODDS provided ground station visibility period. In fact, for the reasons presented so far and due to the position of the two SAX antenna (see Fig.6) directions, the angles between the directions of the satellite-ground station and each antenna could be such that the same antenna may not come and remain in visibility. The prediction performed by this software will be used at STC to prepare two telecommands needed respectively to uplink the data used by the on-board sequence responsible for initializing the TT&C link acquisition and to perform antenna switching. The data computed by this software for each on ground station passage, taking into account the expected attitude, are: 1) antenna which initiates the link with the ground station in case of nominal, DPM and AM attitude; 2) a flag indicating if the antenna switching occurs; 3) the time, for each attitude, at which the antenna switching occurs. These computations are repeated for each SP contained in the AOPSPM.OUT file and results are stored into the SOEMOD.OUT file, which is sent to STC five days before the application week.

AOCGSS Testing and Validation

Unit, subsystem and system tests are planned for the AOCGSS software in order to verify its ability to support AOCSS operations. SAXSIM shall be used for these activities: this is a real-time, software simulator of all the subsystems and operating modes of the SAX satellite, together with a model of the SAX mission orbit and environment. Use of the AOCSS on-board software would enhance exploitation of the simulator at the OCC, accuracy of AOCSS simulated data and the reliability of operations. It can be used either in local or in remote mode. In local mode (i.e. SAXSIM not connected to the OCC) some software details can be refined and major flight dynamics concepts tested and verified by using a local OCC which foresees telecommand structures and telemetry displays similar

to those available at the real OCC. The testing procedure in this mode is an open-loop, as no direct links exist between the AOCGSS tasks and the (simulated) satellite. In remote mode (i.e. SAXSIM connected to the OCC through the same X.25 link used for the real environment) the AOCGSS tasks will interface with the simulator as if it were the real satellite. All data coming from AOCGSS shall in fact be stored at the OCC in SAXSIM dedicated files, used to send telecommands and AOPs to the simulator as shall be done for the satellite. Similarly, operations performed by the software during the mission on satellite data coming from the ground station shall be carried out, during the planned simulations, on SAXSIM generated data. Therefore execution of all commands and attitude plans can be accurately verified, all satellite modes and modes transitions appropriately forced, studied and tested. Finally, all telemetry of interest can be used to check and validate filtering and calibration algorithms.

Conclusion

This paper has presented the functional description of the software under development for the AOCGSS for the SAX mission, and its planned operational use. AOCGSS is currently in the ADD phase and finally integration with the OCC is planned for mid 1995.

References

- ¹SAX AOCSS Users' Manual for Flight Operations; Document: SX-MA-AI-019 Vol.3 (Feb. 1993).
- ²SAX AOCSS Support Software Requirements; Document: TPZ/GO.AST-100/SRD-SAX (Nov. 1992)
- ³SAX AOCSS Support Software Architectural Design; Document: TPZ/GO.AST-100/ADD-SAX (Feb.1993).
- ⁴E.J. Lafferts, F.L. Markley, M.D. Shuster; Kalman Filtering for Spacecraft Attitude Estimation. *Journal of Guidance, Navigation and Control*, Vol.5, NO 5, Sept.-Oct. 82, pp.417-429.
- ⁵M. Bollner & G. Schneiders; Attitude Determination & Control for the X-Ray Satellite Rosat. *39th Congress of the International Astronautical Federation*, Bangalore, India, 08-15 Oct.88.
- ⁶T. Rupp, G. Schneiders; High Precision Post Facto Attitude Determination of the X-Ray Satellite Rosat. *2nd International Symposium on Spacecraft Flight Dynamics*, Germany, 20-23 Oct.86.

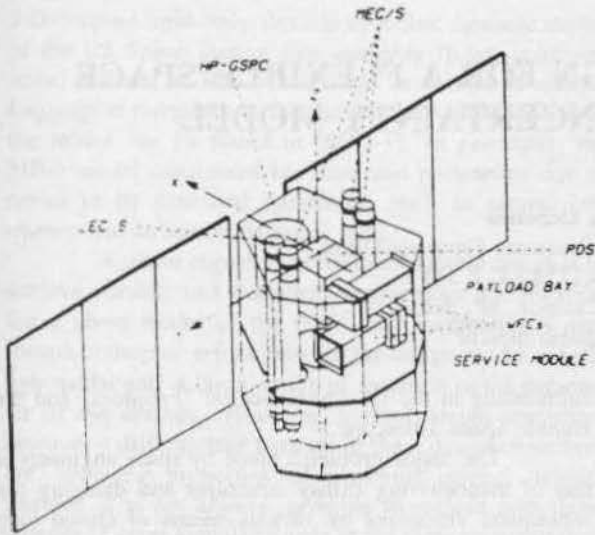


Figure 1: Satellite Configuration and Instruments locations

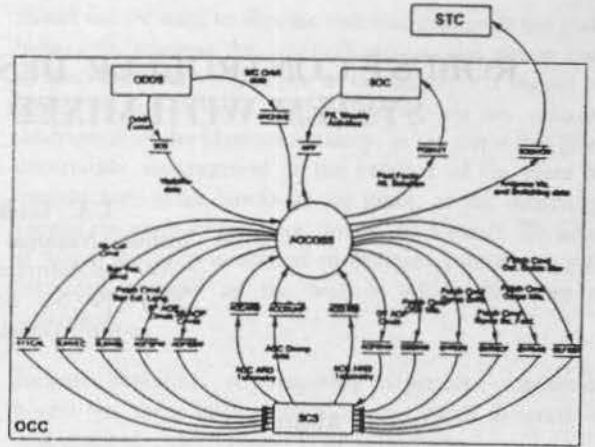


Figure 3: AOCSS Environment and External Interfaces

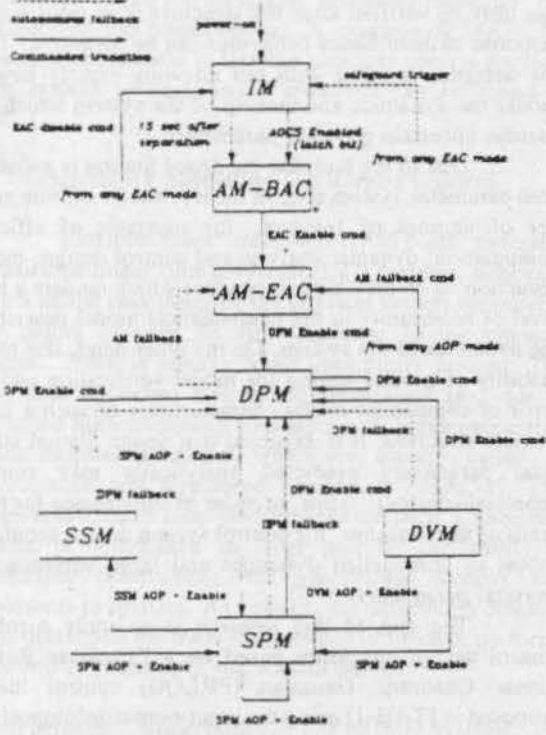


Figure 2: AOCS Modes Transitions

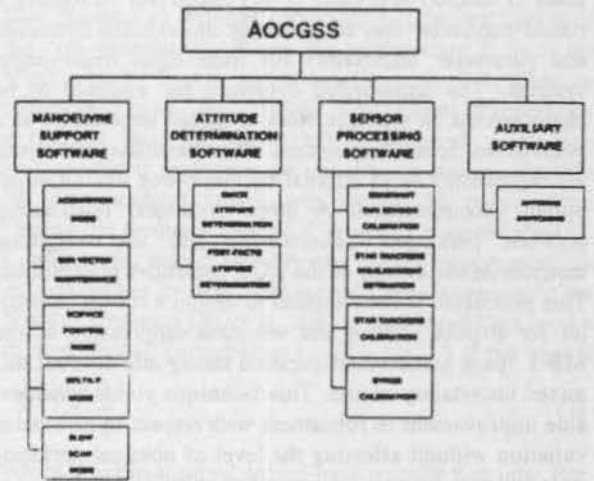


Figure 4: AOCSS Top Level Software decomposition

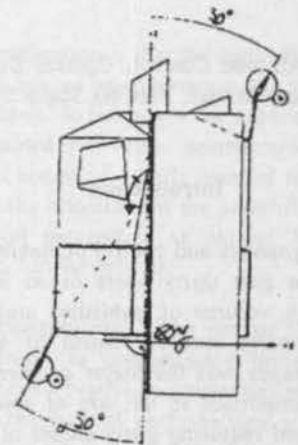


Figure 5: SAX On board Antennas location

ROBUST CONTROLLER DESIGN FOR A FLEXIBLE SPACE SYSTEM WITH MIXED UNCERTAINTY MODEL

L.C. Gadelha DeSouza

INPE - Instituto Nacional de Pesquisas Espaciais/DEM
Av. dos Astronautas, 1758 - C.P. 515
12201-970 - S.J. dos Campos, SP, Brazil
e-mail: Gadelha@dem.inpe.br

Abstract

In this paper an asymptotic Linear Quadratic Gaussian (LQG) design procedure based on a modified version of the Parameter Robust Linear Quadratic Gaussian (PRLQG) approach is developed for designing a robust controller that accounts for unmodelled dynamics and parameter uncertainty for multi-input multi-output systems. The unmodelled dynamics are assumed to be characterized as a single block dynamic uncertainty at a point in the closed-loop system. Plant parameter variations are represented as an internal feedback loop via the input-output decomposition. A direct structural relationship between parameter uncertainties and the weighting matrices in the design of the LQG controller is exploited. This procedure is then applied to design a robust controller for attitude control and vibration suppression of the MB-1 Space Station configuration taking into account this mixed uncertainty model. This technique yields considerable improvement in robustness with respect to parameter variation without affecting the level of nominal performance and robustness with respect to unmodelled dynamics achieved during the design. Simulations have shown that when the system is submitted to unit impulse the controller was able to impose quick convergence properties to the system.

Key words : Attitude Control, Control Design, Robustness, Uncertainty Model, Flexible Space System.

Introduction

The dynamics and control of flexible space structures over the past thirty years or so has led to an incredibly large volume of published and unpublished research. Originally attitude control of satellites with flexible appendages was the major problem area which became more important as the size of solar panels and antenna increased requiring many modes of vibration for accurate representation of the dynamic behaviour. In more recent years the advent of large flexible structure has compounded the problem of stability and attitude control

culminating in the US Space Station "Freedom" and the Hubble Space Telescope.

The major problems faced by space engineers is that of manoeuvring flimsy structures and damping out subsequent vibrations by various means of closed loop active damping, ensuring stability, maintaining static shape as in the case of dish antenna and ensuring in the case of "Freedom" that microgravity experiments are not affected by structural vibrations. The reference [MEI-1] provide an extensive bibliography to survey the developments of particular importance to control and dynamics modelling of large space structure.

A study of the physical characteristics of many space structure components indicates that dynamic modelling is an approximation to the actual system and can only be verified after the structure is in orbit and its response to disturbance behaviour can be measured. Thus the designer is faced with not knowing exactly how to model the dynamics and control of the system which has various uncertain physical parameters.

Due to the fact that the Space Station is a distributed parameter system and, in theory, has an infinite number of degrees of freedom, for purposes of efficient computation, dynamic analysis and control design, model reduction is an inevitable procedure which renders a high level of uncertainty in the mathematical model describing the dynamics of the system. On the other hand, due to the inability of ground testing for model verification and the error of component modal characteristics of such a large flexible structure, it is expected that Space Station structural parameters predicted analytically may contain appreciable errors. Thus, in order to compensate for both kinds of uncertainties, the control system design should be robust to unmodelled dynamics and large variations in physical parameters.

The aim of this research is to study a robust control design procedure based on a Parameter Robust Linear Quadratic Gaussian (PRLQG) control theory proposed in [TAH-1] using the input-output decomposition concept in [MOR-1] to incorporate parameter variations into a modal state-space representation of the system. Therefore, a mixed uncertainty model consisting of unmodelled dynamics and parameter variation is constructed. In order to perform this robust control design a

3-D coupled rigid body/flexible structural dynamic model of the US Space Station first assembly flight configuration, referred as MB-1 [MOD-1], is developed using a Lagrangian formulation. Details about the development of the model can be found in [SOU-1]. In particular, the MB-1 model considered has uncertain parameters due to errors in its structural parameters such as natural frequency and structural damping ratio.

A major objective of feedback system design is to achieve stability and a nominal performance specification for a given model of the plant, and maintain this performance despite errors between the design model and the true model and a large range of variation in the parameter of the system. However, control design procedure becomes a difficult task because of these design objectives are opposing properties of a robust control design. Besides, it is not always possible to include both these sources of error simultaneously in the same robust control design procedure, since the first one is usually characterized by the frequency domain error model, while the second one is more suitably represented as a state space model. In [HEI-1] a robust control design is applied for controlling a flexible truss structure with respect parameter uncertainty and high frequency unmodelled dynamics optimizing both the LQG performance index and the H_{∞} norm. However, since the H_{∞} control theory [FRA-2] basically deals with unmodelled dynamics plant variations, design for parameter variations based on H_{∞} can become too conservative. A example of LQG/LTR approach application to flexible structure control problem with respect to unmodelled dynamics can be found in [JOS-1].

Uncertainty Modelling for Robust Control.

Flexible space structures (FSS) are generally modeled as linear time invariant (LTI) systems, although, such a model may describe the physical system accurately, any model is only an approximation to the physical system. There is always some uncertainty present. The two most important sources of uncertainty are due to neglected high frequency dynamics and parameter errors in the modeled dynamics, which are, usually, called as unstructured and structured uncertainty [MAC-1]. The achievable closed loop performance of such a uncertain system is determined in large part by the ability to synthesize controllers with guaranteed stability and robustness properties. As a result, the uncertainty descriptions determine the trade-off between achievable performance and robustness of the control design.

Unstructured Uncertainty. For MIMO systems the unstructured description of the uncertainty occurring in different parts of the system is usually lumped into one single perturbation L which is a full matrix with the same dimension of the plant. The three description more commonly used to represent L are, additive, multiplicative output and multiplicative input. The additive uncertainty

model can be used to express absolute change in the plant behaviour, whereas the multiplicative model can be used to describe relative changes in the model. It should be noted that any of these unstructured models are external description of the plant uncertainty, in the sense that plant uncertainty are modeled at the exterior of the plant by introducing extra blocks at the input, at the output, or around the plant as feedback loops. As a result, the point at which the loop is opened to examine robustness will, therefore, depend on the way in which the error is described.

Robust Stability: A frequency dependent magnitude bound on these uncertainties can be stated in terms of maximum singular values ($\bar{\sigma}$) of L given by

$$L(s) = l(s)\Delta(s), \quad \bar{\sigma}(\Delta(j\omega)) \leq 1 \quad \forall \omega \quad (1)$$

The bound $l(\omega)$ can also be interpreted as a scalar weight on a normalized perturbation $\Delta(s)$. Generally the magnitude bound $l(\omega)$ will not constitute a tight description of the real uncertainty. When the perturbation L is of the form given by Eq.(1) and Δ satisfies $\bar{\sigma}(\Delta) \leq 1$, it can be represented in an "M- Δ model". The symbol M represents a transfer function matrix of the nominal closed-loop system, and Δ represents an uncertainty matrix acting on M . The nominal closed-loop system M results from closing the feedback control K around a nominal plant G . Condition for robust stability of a closed-loop system can be determined by the multivariable generalization of the Nyquist Criterion [ROS-3], that is, the closed loop system is stable for all perturbation L ($\bar{\sigma}(L) \leq 1$) if and only if

$$\bar{\sigma}(T) < \frac{1}{l} \quad (2)$$

where T is the nominal closed-loop transfer function. For high frequencies the loop transfer function KG is small and therefore Eq.(2) becomes

$$\bar{\sigma}(KG) < \frac{1}{l} \quad (3)$$

The design implication is that the controller gain for high frequencies is limited by uncertainty, the loop gain $\bar{\sigma}(KG)$ has to be "shaped" to fall below the uncertainty bound $1/l$. It should be noted that when unstructured uncertainty is used to model errors of lightly damped flexible structure it does not take into account the possibility that inaccurate in physical parameters as natural frequencies and damping ratio can be present.

Structured Uncertainty: The use of the unstructured uncertainty leads to compensator designs which are unnecessarily conservative, because they perform satisfactory even in the face of perturbations which can never occur. On the other hand, particular parameters in a state-space model may be known to vary over known ranges which is certainly highly structured information. For lightly damped, flexible structures with uncertain frequency and damping ratio, this is certainly the case.

A linear, time-invariant MIMO system can be written in state-space form as

$$\begin{aligned} \dot{x}(t) &= Ax(t) + B_1 w(t) + B_2 u(t) \\ z(t) &= C_1 x(t) + D_{11} w(t) + D_{12} u(t) \\ y(t) &= C_2 x(t) + D_{21} w(t) + D_{22} u(t) \end{aligned} \quad (4)$$

where $x(t)$ is an n -dimensional state vector, $w(t)$ an r_1 -dimensional disturbance vector, $u(t)$ an r_2 -dimensional control vector, $z(t)$ an r_3 -dimensional controlled output vector, and $y(t)$ an m -dimensional measured vector.

An Internal Feedback Loop Model of the state-space representation of a uncertainty dynamical system can be described by

$$\begin{bmatrix} \dot{x} \\ z \\ y \end{bmatrix} = \left\{ \begin{bmatrix} A & B_1 & B_2 \\ C_1 & D_{11} & D_{12} \\ C_2 & D_{21} & D_{22} \end{bmatrix} + \Delta_p \right\} \begin{bmatrix} x \\ w \\ u \end{bmatrix} \quad (5)$$

where the first matrix in the right-hand side is the nominal system matrix and Δ_p is the perturbation matrix. Assuming that C_1 , D_{11} and D_{12} are not subject to parameter variations Δ_p and that there are m independent parameters p_1, \dots, p_m and that they are bounded as $|\Delta_p| \leq 1$. The perturbation matrix Δ_p is can be decomposed with respect to each parameter variation [MOR-1] and written in matrix form as

$$\Delta_p = - \begin{bmatrix} M_x \\ 0 \\ M_y \end{bmatrix} \Delta [N_x \ N_w \ N_u] = -M \Delta N \quad (6)$$

By introducing the following new variables for the internal feedback loop

$$z_p \triangleq [N_x \ 0 \ N_w \ N_u] \begin{bmatrix} x \\ w_p \\ w \\ u \end{bmatrix}, \quad w_p = -\Delta z_p \quad (7)$$

the perturbed system in Eq.(5), and the input-output decomposition in Eq.(6), can be combined as

$$\begin{bmatrix} \dot{x} \\ z_p \\ z \\ y \end{bmatrix} = \begin{bmatrix} A & M_x & B_1 & B_2 \\ N_x & 0 & N_w & N_u \\ C_1 & 0 & D_{11} & D_{12} \\ C_2 & M_y & D_{21} & D_{22} \end{bmatrix} \begin{bmatrix} x \\ w_p \\ w \\ u \end{bmatrix}, \quad w_p = -\Delta z_p \quad (8)$$

where w_p and z_p are considered as the fictitious input and output, respectively, due to the plant perturbation; and Δ is considered as a fictitious, internal feedback loop gain matrix.

The perturbed system model can be obtained from the transfer function (\hat{G}) representation with a stabilizing controller which for the closed-loop transfer function

matrix from w to z with plant perturbations becomes

$$T_{zw} = \hat{G}_{22} - \hat{G}_{21} \Delta (I + \hat{G}_{11} \Delta)^{-1} \hat{G}_{12} \quad (9)$$

The stability condition for T_{zw} is equivalent to establish condition for \hat{G}_{11} [MAC-1]. The transfer function given by \hat{G}_{11} is conventional denoted $F_1(G_{11}, K)$, and is referred to as robustness function [TAH-1].

Robust Control Design

The unstructured uncertainty model is an external description of the errors in the plant, in the sense that plant uncertainties are modeled at its exterior, this modelling method is not convenient at all in handling parameter uncertainty. Many difficulties arise from the fact that parameter uncertainty are usually given in state-space forms while in current design techniques, plant uncertainties are characterized by frequency domain errors models and evaluated by singular values techniques. By using the concept of internal feedback loop and the input-output decomposition the structured parameter variation can be represented in a state space form. In [TAH-1], stability robustness analysis has been made in detail for structured parameter variation, and the LQG/LTR technique has been extended to PRLQG design technique by employing an asymptotic robustness recovery procedure. However, as the inclusion of a asymptotic recovery procedure implies a high gain characteristic, usually achieved by placing the compensator poles sufficiently far to the left from the imaginary axis, a very high bandwidth controller that becomes sensitive to noises and unmodelled high-frequency dynamics can be expected. In order to avoid this undesirable sensitivity, we exploit here a robust control design procedure based on the structured uncertainty modelling concept which takes into account the unstructured uncertainty model, resulting in a robust control design technique which is the combination of LQG/LTR and PRLQG, denoted LTR/PRLQG.

LQG/LTR Design Methodology: The LQG/LTR design procedure, introduced by Doyle and Stein [DOY-1], enables a controller design by combining frequency domain and state-space techniques for a minimal-phase system. The fundamental idea in the LTR-design is to recover a target feedback loop (TFL) with a suitable asymptotic design. The loop transfer function matrix associated with the TFL is given by $K_r \phi B$ if the recovery to be achieved is at the input of the plant or $C \phi K_r$ if the recovery is at the output of the plant, where $\phi = (sI - A)^{-1}$ is the state transition matrix of the plant, K_r and K_f are the gain matrices associated with the Linear Quadratic Regulator (LQR) and Kalman Filter (KF) problem, respectively. These gains depend on the selection of the weighting matrices Q and R or V and W associated, respectively, with the LQR and KF problem which in turn are chosen such that the TFL satisfies the imposed stability, robustness, and performance specifications. The loop transfer

function matrix of the LTR design is given by KG , where G is the open-loop transfer function matrix of the plant and K is the dynamic compensator matrix to be designed.

PRLQG Design Methodology: The PRLQG design procedure, developed by Tahk and Speyer [TAH-1], is in fact a generalization of the LQG/LTR technique, and serves to improve the stability robustness and reduce the sensitivity to structured plant perturbation. The fundamental idea in PRLQG methodology is to formulate the structured parameter variation as an internal feedback loop via the input-output decomposition. In doing that, the perturbation is seen essentially as additional noise in the plant model. The robust controller design turns into a disturbance attenuation problem [TAH-1]. From this incorporation it is possible to establish a direct structural relationship between the class of parameter uncertainty and the choice of weighting matrices in the LQR and KF designs.

Input-Output Decomposition

We are interested in applying the LTR/PRLQG design taking into account parameter variation in the state matrix A . Particularly, when this matrix is written in modal form, which means that parameter variation can be analyzed in terms of errors in frequency and damping ratio.

The modal state-space form for a simple system with one flexible mode considering one input and one output, with one collocated sensor/actuator pair, is given by

$$\dot{X} = \begin{bmatrix} 0 & 1 \\ -\omega^2 & -2\zeta\omega \end{bmatrix} X + \begin{bmatrix} 0 \\ 1 \end{bmatrix} U, \quad Y = [0 \ 1]X \quad (10)$$

and, ω and ζ are modal natural frequency and damping ratio, respectively.

The matrices N_x and M_x depend on how the input-output decomposition of A and Δ_p is established and what parameter is being considered to vary. Therefore, let us, consider that the perturbation (uncertainty) occurs in frequency and damping in the terms ω^2 and $2\zeta\omega$. Then, separating the uncertainties from the nominal matrix A , the perturbed system matrix can be written as

$$A = \begin{bmatrix} 0 & 1 \\ -\omega^2(1+\Delta_1) & -2\zeta\omega(1+\Delta_2) \end{bmatrix} \quad (11)$$

$$= \begin{bmatrix} 0 & 1 \\ -\omega^2 & 2\zeta\omega \end{bmatrix} + \begin{bmatrix} 0 & 0 \\ -\omega^2\Delta_1 & -2\zeta\omega\Delta_2 \end{bmatrix}$$

where Δ_i ($|\Delta_i| \leq 1$, $i=1,2$) is the perturbation in the terms ω^2 and $2\zeta\omega$, respectively. The perturbation matrix Δ_p is represented by the second term on the right-hand side of Eq.(11) which can be decomposed with respect to each parameter variation as

$$\Delta_p = \begin{bmatrix} 0 & 0 \\ \omega & \omega \end{bmatrix} \begin{bmatrix} \Delta_2 & 0 \\ 0 & \Delta_1 \end{bmatrix} \begin{bmatrix} 0 & -2\zeta \\ -\omega & 0 \end{bmatrix} = M_x \Delta N_x \quad (12)$$

It should be noticed that this input-output decomposition is not unique [TAH-1], and that the matrix Δ , which represents the uncertainty acting on nominal matrix A , is diagonal with real elements, characterizing real parameter variations. Usually, in using the LQG/LTR approach one sets $R=I$ and the parameter Q is manipulated to achieve performance specification and improve robustness, respectively, this is the view-point adopted in [BLE-1]. In [JOS-1] the uncertainty is only due to unmodelled dynamics and basically the tuning parameter Q are used to obtain appropriate gains at 0db cross-over frequency which is an indicator of performance, while the design is done subject to an unstructured barrier profile. Yet, in the LTR/PRLQG approach Q is set as $N_x^T N_x$ to improve robustness with respect to parameters variation and R is used as tuning parameter.

Robustness Based on Mixed Uncertainty Model.

When using the LTR/PRLQG approach to design a robust control system with respect to unstructured and structured uncertainty, these uncertainties are modeled in two distinctly different ways. The unstructured uncertainty modeled at the exterior of the plant to represent unmodelled dynamics, and the structured uncertainty modeled as internal feedback loop to represent parameter variation. Such a mixed uncertainty model appears appropriate when the system is represented in modal state-space form. First, because the neglected dynamics can be relatively easily separated from the design model using a model reduction approach available in the literature [CRA-1]. Second, because of the structural characteristics like modal frequencies, damping ratios, and mode shape appear explicit in modal state-space form as physically meaningful parameters, which is suitable to deal with parameter variation. Thus the overall uncertainty model allows the incorporation of both sources of uncertainty into the robust controller design. This procedure is based on the fact that sensitivity to plant parameter variation is an internal property of the closed loop system [SHA-1], while loop gain is an input/output property. As a result, it can be possible to improve robustness with respect to parameter variations while maintaining essentially the same performance specification on the loop gain without increasing its sensitivity to noises and unmodelled high-frequency dynamics. Accommodating unstructured and structured uncertainties into the LTR/PRLQG design procedure, the designer has a systematic way of trading off the nominal performance and robust stability.

Design Objectives: The LTR/PRLQG design approach imply designing a controller trading-off nominal performance and robust stability with respect to unmodelled dynamic and parameter variations. Therefore, the design

function matrix of the LTR design is given by KG , where G is the open-loop transfer function matrix of the plant and K is the dynamic compensator matrix to be designed.

PRLQG Design Methodology: The PRLQG design procedure, developed by Tahk and Speyer [TAH-1], is in fact a generalization of the LQG/LTR technique, and serves to improve the stability robustness and reduce the sensitivity to structured plant perturbation. The fundamental idea in PRLQG methodology is to formulate the structured parameter variation as an internal feedback loop via the input-output decomposition. In doing that, the perturbation is seen essentially as additional noise in the plant model. The robust controller design turns into a disturbance attenuation problem [TAH-1]. From this incorporation it is possible to establish a direct structural relationship between the class of parameter uncertainty and the choice of weighting matrices in the LQR and KF designs.

Input-Output Decomposition

We are interested in applying the LTR/PRLQG design taking into account parameter variation in the state matrix A . Particularly, when this matrix is written in modal form, which means that parameter variation can be analyzed in terms of errors in frequency and damping ratio.

The modal state-space form for a simple system with one flexible mode considering one input and one output, with one collocated sensor/actuator pair, is given by

$$\dot{X} = \begin{bmatrix} 0 & 1 \\ -\omega^2 & -2\zeta\omega \end{bmatrix} X + \begin{bmatrix} 0 \\ 1 \end{bmatrix} U, \quad Y = [0 \ 1]X \quad (10)$$

and, ω and ζ are modal natural frequency and damping ratio, respectively.

The matrices N_x and M_x depend on how the input-output decomposition of A and Δ_p is established and what parameter is being considered to vary. Therefore, let us, consider that the perturbation (uncertainty) occurs in frequency and damping in the terms ω^2 and $2\zeta\omega$. Then, separating the uncertainties from the nominal matrix A , the perturbed system matrix can be written as

$$A = \begin{bmatrix} 0 & 1 \\ -\omega^2(1+\Delta_1) & -2\zeta\omega(1+\Delta_2) \end{bmatrix} \quad (11)$$

$$= \begin{bmatrix} 0 & 1 \\ -\omega^2 & 2\zeta\omega \end{bmatrix} + \begin{bmatrix} 0 & 0 \\ -\omega^2\Delta_1 & -2\zeta\omega\Delta_2 \end{bmatrix}$$

where Δ_i ($|\Delta_i| \leq 1$, $i=1,2$) is the perturbation in the terms ω^2 and $2\zeta\omega$, respectively. The perturbation matrix Δ_p is represented by the second term on the right-hand side of Eq.(11) which can be decomposed with respect to each parameter variation as

$$\Delta_p = \begin{bmatrix} 0 & 0 \\ \omega & \omega \end{bmatrix} \begin{bmatrix} \Delta_2 & 0 \\ 0 & \Delta_1 \end{bmatrix} \begin{bmatrix} 0 & -2\zeta \\ -\omega & 0 \end{bmatrix} = M_x \Delta N_x \quad (12)$$

It should be noticed that this input-output decomposition is not unique [TAH-1], and that the matrix Δ , which represents the uncertainty acting on nominal matrix A , is diagonal with real elements, characterizing real parameter variations. Usually, in using the LQG/LTR approach one sets $R=I$ and the parameter Q is manipulated to achieve performance specification and improve robustness, respectively, this is the view-point adopted in [BLE-1]. In [JOS-1] the uncertainty is only due to unmodelled dynamics and basically the tuning parameter Q are used to obtain appropriate gains at 0db cross-over frequency which is an indicator of performance, while the design is done subject to an unstructured barrier profile. Yet, in the LTR/PRLQG approach Q is set as $N_x^T N_x$ to improve robustness with respect to parameters variation and R is used as tuning parameter.

Robustness Based on Mixed Uncertainty Model.

When using the LTR/PRLQG approach to design a robust control system with respect to unstructured and structured uncertainty, these uncertainties are modeled in two distinctly different ways. The unstructured uncertainty modeled at the exterior of the plant to represent unmodelled dynamics, and the structured uncertainty modeled as internal feedback loop to represent parameter variation. Such a mixed uncertainty model appears appropriate when the system is represented in modal state-space form. First, because the neglected dynamics can be relatively easily separated from the design model using a model reduction approach available in the literature [CRA-1]. Second, because of the structural characteristics like modal frequencies, damping ratios, and mode shape appear explicit in modal state-space form as physically meaningful parameters, which is suitable to deal with parameter variation. Thus the overall uncertainty model allows the incorporation of both sources of uncertainty into the robust controller design. This procedure is based on the fact that sensitivity to plant parameter variation is an internal property of the closed loop system [SHA-1], while loop gain is an input/output property. As a result, it can be possible to improve robustness with respect to parameter variations while maintaining essentially the same performance specification on the loop gain without increasing its sensitivity to noises and unmodelled high-frequency dynamics. Accommodating unstructured and structured uncertainties into the LTR/PRLQG design procedure, the designer has a systematic way of trading off the nominal performance and robust stability.

Design Objectives: The LTR/PRLQG design approach imply designing a controller trading-off nominal performance and robust stability with respect to unmodelled dynamic and parameter variations. Therefore, the design

sequence is divided in two phases as follows: one starts the first phase designing a controller which achieves nominal performance based on high open-loop gains. However, in order to avoid a high bandwidth controller which can become sensitive to unmodelled high-frequency dynamics the design is performed taking into account an unmodelled high dynamics barrier. Once the initial control objectives (nominal performance and robustness with respect to unmodelled dynamics) have been achieved we carry on the second phase of the design trying to improve the controller robustness with respect to parameter variation. In both phase of the design the locus of the closed loop poles is used as an indicator of stability and the relative control effort applied to the various modes.

The selection of a upper limit on the bandwidth is not specified "a priori" but it is desired that it should be as high as possible, as long as the robustness barrier associated with unmodelled dynamics is not violated. In doing that we are establishing a compromise between performance and robustness with respect to unmodelled dynamics. The multivariable bandwidth is defined as the frequency in which the minimum singular value of loop transfer function KG is equal to unity, i.e., $\underline{\sigma}(KG) = 1$.

Robustness Barrier. Based on the approximate balanced singular values approach the order of MB-1 model with 12 DOF was reduced to a design model with 6 DOF consisting of the three rotational rigid-body modes plus the first three flexible modes. Consequently, the unmodelled dynamics barrier is built taking into account the six flexible modes remained, so that the transfer function $G_r(s)$ of the full order model can be written as $G_r(s) = G(s) + \Delta G(s)$; where $G(s)$ and $\Delta G(s)$ represent the transfer function of the design model and the remaining unmodelled model. Therefore, an upper bound for multiplicative unstructured uncertainty acting at the plant input (the robustness barrier $L_r(\omega)$) in terms of additive uncertainty is given by

$$\bar{\sigma}[L_r(\omega)] = \frac{\bar{\sigma}[\Delta G(s)]}{\sigma[G(s)]} \quad (14)$$

where $\Delta G = G_r - G$. It should be noted that all this manipulation is extremely facilitated due to the fact that we are dealing with the system represented in modal form.

Dynamics Model of MB-1

Though the main purpose of the mathematical model for MB-1 Space Station "Freedom" configuration developed is its use in a linearized robust control design, it is not to the author's knowledge that such model have been done in the literature using a Lagrangian formulation. The details of the coupled rigid body/flexible structural dynamic modelling of the MB-1 derivation can be found in [SOU-1]. The dynamic equations derived in physical coordinates are transformed into a set of

decoupled equations in modal state space. This procedure leads to computational advantages and facilitates to address issues such as model order reduction, truncation, and robustness with respect parameter variation and unmodelled dynamics in the context of the robust control design methodology proposed here. With the availability of the MB-1's model, its frequency characterization can be determined solving the eigenvalues problem for the undamped open-loop case, which yields the eigenvalues (natural frequency) and the modes shapes. We have considered a model with 9 degree of freedom consisting of: 3 rigid body motions (rotation) and 6 flexible modes, that is, the first bending mode plus torsion for the central truss; the first two bending mode for the radiator; and the first two bending mode for the two solar panels.

Design with respect to unmodelled dynamics

It should be noted that in the first phase of the design we are not worrying about parameter uncertainty, that is, we are dealing with the nominal system, there is no uncertainty in the structural parameter. To simplify the procedure in the LQR problem the weighting matrix Q is set as $Q=I$, and weighting matrix R is selected in the following form

$$R = r^2 [I_3] \quad (14)$$

where r is a scalar (design parameter) which will be manipulated to obtain suitable performance specification of the LQR target feedback loop (TFL).

Design #1: Let us start off designing a controller with a "desired" high bandwidth, e.g., a bandwidth of approximately half of the first flexible mode (0.635 rad/sec) (see SOU-1), which will characterize the TFL of LQR. After a number of trials we get the TFL with $r^2 = 1.0E-02$. The plots of $\underline{\sigma}(G_{LQR})$ and $\bar{\sigma}(G_{LQR})$ is shown in Fig.(1) which indicates that the bandwidth obtained is approximately 0.27 rad/sec, which in terms of performance is quite good compared to the frequency of the first flexible mode.

Having obtained satisfactory singular values behaviour of LQR, the next step is design a KF so that its TFL asymptotically approaches "recovers" that of LQR (LTF). The recovery is accomplished by setting the matrix $W=I$ and selecting the matrix V as follows

$$V = v^2 [I_3] \quad (15)$$

where v is a scalar (design parameter) which will be manipulated so that recovery is achieved. We manage to recover the LQR (LTF) with $v^2 = 1.0E-03$. The resulting loop transfer function $\underline{\sigma}(K(s)G(s))$, $\bar{\sigma}(K(s)G(s))$ plots and the robustness barrier are shown in Fig.(2). The plots indicate that the performance objective has been achieved for a frequency close to 0.27 rad/sec. However, the plot of $\bar{\sigma}(K(s)G(s))$ indicates that the robustness barrier has been violated. Therefore, one observes that high perform-

ance requirement (high bandwidth) has led to less stability robustness with respect unmodelled dynamics. As result, the set of performance-robustness conditions needs to be re-evaluated. Fig.(3) shown the locations of the poles, where their right-shift suggest that the compensator was designed to concentrate on stabilizing the rigid body modes, affecting very little the stability of the elastic modes of the design model, which is also indicates that much more control effort were applied to the rigid body modes than to the flexible modes.

Design #2: In the second design the performance objective is established as the higher as possible bandwidth without violating the robustness barrier. Following the same procedure of the Design #1, we have obtained the LQR (TFL) with $r^2=1.0E-01$. Fig.(4) shows the plots of the $\sigma(G_{LQR})$ and $\bar{\sigma}(G_{LQR})$ which indicate that the bandwidth obtained is approximately 0.14 rad/sec, which is still quite good compared with the frequency of the first flexible mode (0.635 rad/sec). In designing the KF we recover the LQR (LTF) with $v^2=1.0E-02$. Performance-robustness design conditions can be evaluated through the plots of the $\sigma(K(s)G(s))$, $\bar{\sigma}(K(s)G(s))$ which are shown in Fig.(5). The plot of $\sigma(K(s)G(s))$ indicate that the performance objective has been meet once the overall loop bandwidth has been achieved for 0.14 rad/sec. The plot of $\bar{\sigma}(K(s)G(s))$ indicate that the robustness barrier has not been violated. Therefore, the controller of Design #2 has met suitable the performance-robustness design conditions, which means that besides its good performance behaviour it is robust with respect to unmodelled dynamics. As a result, the procedure of reducing the target bandwidth of LQR resulted in designing a compensator with appropriated compromise between performance and robustness stability. The locations of the poles, not shown, indicate that in the Design #2 the compensator was also designed to concentrate on stabilizing the rigid body modes. To make a comparison between the control effort applied to the rigid modes and flexible modes in the Design #1 and #2 in Fig.(6) the closed-loop eigenvalues of both Designs are presented, which clearly shows that the closed-loop poles of Design #2 are less left shifted than those of Design #1.

Design with respect to parameter variation

Design #3 : In applying the design methodology using the input-output decomposition concept to incorporate parameter variations into the modal state-space form we have to use the matrices N_x and M_x in the solution of LQR and KF problems, respectively. Hence, the weighting matrix Q and W have the form suggested by the input-output decomposition given by Eq.(12), which for the design model with three rotational rigid body modes and three flexible modes can be written as

$$Q = N_x^T N_x = \text{diag} [I_3 \omega_i^2 I_3 \zeta_i^2] , \quad i=3 \quad (16)$$

$$W = M_x M_x^T = \text{diag} [I_3 0_3 I_3 \omega_i^2] , \quad i=3 \quad (17)$$

The new terms that appear in the weighting matrices Q and W can be seem as weighting on robustness with respect parameter variation. We keep the weighting $R=r^2=1.0E-01$ and $V=v^2=1.0E-02$ since these were the weighting matrices with which we achieve satisfactory performance-robustness in terms of the design objective of the Design #2. Therefore, the introduction of the terms ω_i^2 , ζ_i^2 and ω_i^2 in the weighting matrices Q and W have the function of improving robustness of the compensator $K(s)$ with respect parameter variation. Fig.(7) shows the closed-loop eigenvalues of Design #2 and #3 considering a variation in frequency and damping of -30%. It illustrates that the real part of poles associated with the flexible modes were left shifted while the location of poles associated with the rigid modes were not practically altered. Therefore, in the Design #3 the controller $K(s)$ is placing no further control effort on the rigid body modes, while applying a lot of effort to the flexible modes, which shows that robustness of controller $K(s)$ with respect parameter variation has been improved. Fig.(8) presents the plots of $\sigma(K(s)G(s))$, $\bar{\sigma}(K(s)G(s))$ and the robustness barrier for the Design #3 which shows that the loop gain and the bandwidth obtained in the Design #2 have not been changed.

Performance of the controller $K(s)$: The performance of the resulting controller can be evaluated considering the attitude (roll,pitch and yaw) time history of the MB-1 when responding under closed-loop control to a unit impulse as presented in Fig.(9), which shows that for an impulse level of 1500N-sec, the maximum roll, pitch and yaw excursion are no more than 1.2, 0.8 and 2.0 (deg), respectively. The impulsive perturbation is damped out in all three axes in less than 160 s.

Conclusions.

A modified version of the parameter robust linear quadratic Gaussian (PRLQG) approach has been applied for designing a robust controller to control attitude of the MB-1 Space Station configuration. Applications of this approach take into account uncertainty due to unmodelled dynamics and parameter variation where the first one appears in the design process as a frequency-dependent constraint called robustness barrier while the second one is included in the design process introducing into the weighting matrices the input-output decomposition associated with the parameter variation. Characterization of both sources of uncertainties is facilitated by representing the system in modal state space form which also is appropriate

form to obtain the reduced design model using the approximate balanced singular values approach.

The suitable controller is obtained through two design process, which are called Design #2 and Design #3. In the Design #2 a controller with bandwidth of 0.023 (Hz), approximately a decade below the first flexible mode (0.101 Hz), has been achieved with a high level of stability robustness with respect to unmodelled dynamics. In order to improve parameter insensitivity of the controller the Design #3 is performed considering errors of up to 30 percent in the structural parameter of the system (frequencies and damping ratios). At the end of the Design #3 the robustness of the controller with respect to unmodelled dynamics has been checked which has shown that despite the large parameter variations its stability robustness characteristics was maintained.

The performance of the control system was checked through the response of the MB-1 space station subject to disturbance of unit impulse. In the simulation the rotational rigid body mode in roll and pitch dominate the system response while in yaw a strong coupling between the rotational rigid body mode and the asymmetric bending mode of the two solar arrays and the first bending mode of the radiator has been observed which suggests that as far controlling attitude of the MB-1 concern this axis will be the crucial one.

References.

[BLE-1] Blelloch, P. A., "Robust Linear Quadratic Gaussian Control for Flexible Structure," *Journal of Guidance, Control and Dynamics*, Vol. 13, No. 1, Jan-Feb., pp. 66-72, 1990.

[CRA-1] Craig, R. R & Su, T. J., "A Review of Model Reduction Methods for Structural Control Design," in *Dynamics of Flexible Structure in Space*, Ed. C.L. Kirk & J.L. Junkins, Computational Mechanics Publications, Springer Verlag, pp. 121-134, 1990.

[DOY-1] Doyle, J.C. & Stein, G., "Multivariable Feedback Design: Concepts for a Classical/Modern Synthesis," *IEEE Trans. Auto. Contr.*, Vol. AC-26, No. 1, pp. 4-16, 1981.

[FRA-1] Francis, B.A.; Helton, J.W. & Zames, G., "H-infinity Optimal Feedback Controllers for Multivariable Systems," *IEEE Trans. Auto. Contr.*, Vol. AC-29, No. 10, Oct., pp. 888-899, 1984.

[HEI-1] Heise, S.; Banda, S. & Yeh, H., "Robust Control of a Flexible Structure in the Presence of Parameter Variations and Unmodelled Dynamics." 28th Aerospace Sciences Meeting, Nevada, Jan., pp.1-9, AIAA 90-0752 paper, 1990.

[JOS-1] Joshi, S.M., "Control of Large Flexible Space Structure," Vol. 131 of the *Lecture Notes in Control and Information Sciences*, Ed. M. Thoma and Wyner, Springer-Verlag, 1989.

[MAC-1] Macielojowski, J.M., "Multivariable Feedback Design," Addison Wesley, U.K., 1989. ISBN 0-201-

18243-2.

[MEI-1] Meirovitch, L. & Kwak, M.K., "On the Maneuvering and Control of Space Structures," in *Dynamics of Flexible Structures in Space*, Ed. C.L. Kirk and J.L. Junkins, Computational Mechanics Publications, Springer-Verlag, pp. 3-17, 1990.

[MOD-1] Modi, V.J.; Suleman, A. & Ng, A.C., "Modal Analysis and Dynamics Response of the Evolving Space Station," in *Modal Representation of Flexible Structure by Continuum Methods*, ESTEC Work shop Proc., pp. 299-337, Jun., 1989.

[MOR-1] Morton, B.G.; McAffos, R.M., "A Mu-Test for Robustness Analysis of a Real Parameter Variation Problem." *Proc. Amer. Contr. Conf.*, pp. 135-138. 1985.

[SHA-1] Shaked, U. & Soroka, E., "On the Stability Robustness of Continuous Time LQG Optimal Control," *IEEE Trans. Auto. Contr.*, Vol. AC-30, No.10, pp.1039-1043, 1985.

[SOU-1] Souza, L.C.G., "Robust Control Design for a Flexible Space System," Ph.D Dissertation, Cranfield Institute of Technology, Cranfield, England, 1992.

[TAH-1] Tahk, M. & Speyer, J.L., "Modelling of Parameter Variations and Asymptotic LQG Synthesis," *IEEE Trans. Auto. Contr.*, Vol. AC-32, No. 9, Sept., pp. 793-801, 1987.

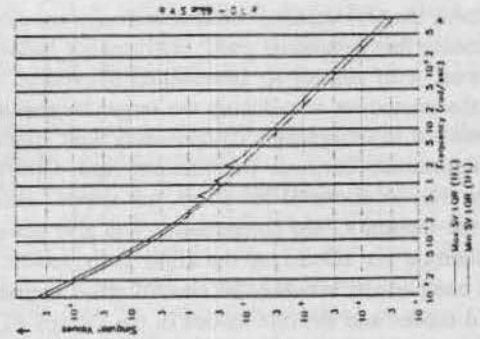


Figure 11 LQR target feedback loop (1971) Design #1.

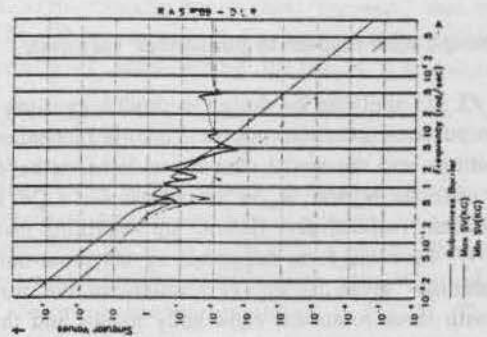


Figure 12 Performance stability Substantive Test Design #1.

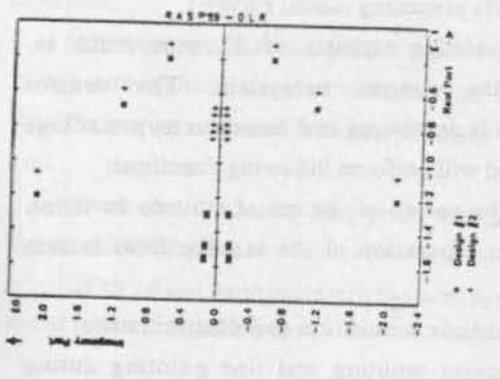


Figure (6) Closed-Loop Signal-to-Noise Ratio vs. Rad Point.

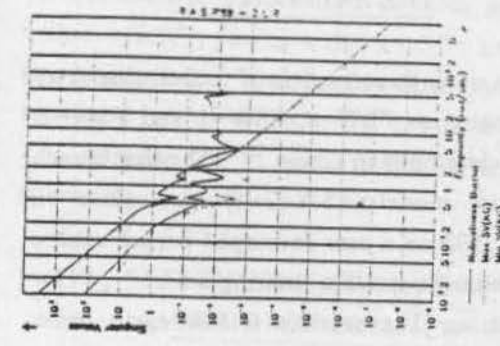


Figure (5) Performance Stability Substrate Design #2.

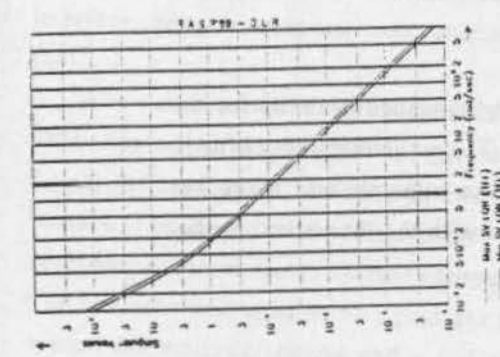


Figure (4) LQR Target Feedback Loop (TFL) Design #3.

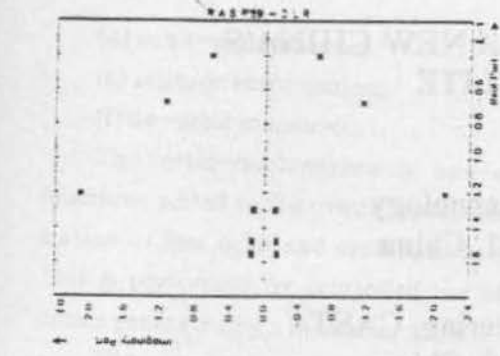


Figure (1) Closed-Loop Signal-to-Noise Ratio vs. Rad Point.

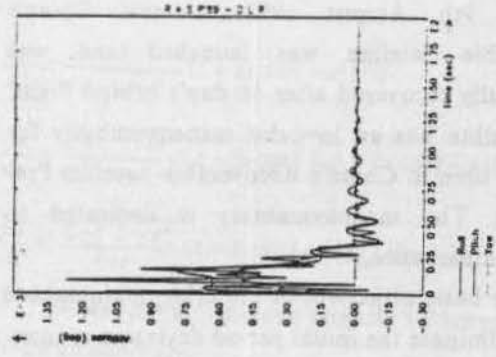


Figure (8) Roll, Pitch, Yaw responding to an orbit impulse.

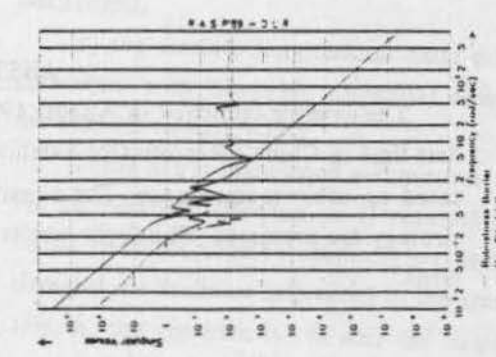


Figure (3) Performance Substrate Design #3.

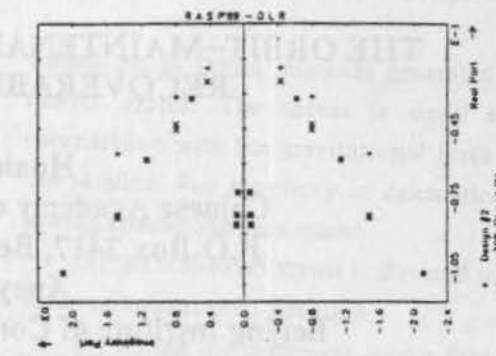


Figure (7) Closed-Loop Signal-to-Noise Ratio vs. Rad Point.

- (d) orbit-maintenance;
- (e) attitude reacquisition;
- (f) de-orbit maneuver.

The orbit-maintenance is one of the new functions added to the control subsystem in consideration of low orbit and prolonged orbit duration. This is performed by controlled use of thrust impulses generated by a maneuver motor.

The control subsystem consists of a measurement unit, an information processing and interface unit, a computer unit and an actuator unit.

The measurement unit consists of three fluid-floated rated integrating gyroscopes, two digital infrared earth sensors and two digital sun sensors. The computer unit is a triple-redundant two-out-of-three fault-tolerant computer system. The actuator unit consists of a cold gas propulsion system for attitude control and a hot gas propulsion system for orbit-maintenance. The attitude control accuracy is specified as pitch and roll to within $\pm 0.5^\circ$, yaw to within $\pm 0.7^\circ$, angular rate to within $\pm 0.02^\circ / \text{sec}$ for fine earth pointing; and pitch and roll to within $\pm 1.5^\circ$, yaw to within $\pm 2^\circ$, angular rate to within $\pm 0.2^\circ / \text{sec}$ for maneuver transfer mode.

BASIC OBJECTIVES OF ORBIT MAINTENANCE

(a) to eliminate the initial period deviation at injection;

(b) to compensate the orbital period decay due to the atmospheric drag perturbation so to ensure that the perigee altitude will not be lower than 170 km;

(c) to ensure the landing point will be within the preselected area;

(d) to adjust appropriately the arrangement of the satellite ground track.

ANALYTICAL TREATMENT

The orbit-maintenance is performed by con-

trolled use of thrust impulses generated by a maneuver motor. The thrust is small enough in comparison with the gravitational force acting on the satellite. For simplicity in calculation, the following assumptions are made:

(a) the maneuver thrust is directed in the satellite longitudinal axial direction;

(b) during the maneuver motor firing, the satellite mass including the maneuver motor remains unchanged;

(c) the satellite longitudinal axial direction is coincident with the orbit tangential direction, i.e. the satellite velocity vector.

Under above mentioned assumptions the satellite acceleration, denoted as U resulted from the thrust remains constant. Among six basic orbital elements we are most interested in the semi-major axis, a , the eccentricity, e , and the argument of perigee, ω . Starting with the Lagrange perturbation motion equations we can get the differential equations for maneuver transfer ^{(4) (5)}.

$$\left. \begin{aligned} \frac{da}{dt} &= \frac{2}{n\sqrt{1-e^2}} (1+2e\cos f+e^2)^{\frac{1}{2}} U \\ \frac{de}{dt} &= \frac{2\sqrt{1-e^2}}{na} (1+2e\cos f+e^2)^{-\frac{1}{2}} (\cos f+e) U \\ \frac{d\omega}{dt} &= \frac{2\sqrt{1-e^2}}{nae} (1+2e\cos f+e^2)^{-\frac{1}{2}} \sin f \cdot U \end{aligned} \right\} (1)$$

Where $n = a^{-1.5}$ is mean angular velocity and f is the true anomaly.

Expanding the right parts of above equations into power series of e and neglecting the terms $O(e^3U)$, yields .

$$\left. \begin{aligned} \frac{da}{dt} &= \frac{2}{n} \left[(1+e^2) + e\cos f - \frac{e^2}{2} \cos^2 f \right] U \\ \frac{de}{dt} &= \frac{2}{na} \left[e + \cos f - e\cos^2 f + e^2 \left(\frac{3}{2} \cos^3 f - 2 \cos f \right) \right] U \\ \frac{d\omega}{dt} &= \frac{2}{nae} \left[1 - e\cos f + e^2 \left(\frac{3}{2} \cos^2 f - 1 \right) \right] \sin f \cdot U \end{aligned} \right\} (2)$$

Using transformation expression

THE ORBIT-MAINTENANCE FOR A NEW CHINA'S RECOVERABLE SATELLITE

Huabao Lin

Chinese Academy of Space Technology
P.O.Box 2417, Beijing 100081, China

Xueyi Feng

Beijing Institute of Control Engineering, CAST
P.O.Box 2729, Beijing 100080, China

ABSTRACT

The satellite launched in August 1992 has an in-orbit maneuverability for the first time in China's Recoverable Satellite Programme. The maneuverability is dedicated to orbit-maintenance. The constitution, operation principle and maneuver strategy are presented. The flight results are well agreed with the theoretical predictions.

INTRODUCTION

On 9th August 1992, a new China's recoverable satellite was launched and was successfully recovered after 16 day's orbital flight. The satellite has an in-orbit maneuverability for the first time in China's Recoverable Satellite Programme. The maneuverability is dedicated to orbit-maintenance.

The basic objectives of the orbit-maintenance are to eliminate the initial period deviation at injection, to compensate the orbital period decay due to the atmospheric drag perturbation and to ensure the landing point will be within the preselected area. This is done by controlled use of thrust generated by a maneuver motor which in turn is a hydrazine monopropellant propulsion system.

In order to economize the consumption of propellant it is intended to eliminate the injection error and atmospheric drag perturbation in the earlier stage of the flight. It is planned to use a 4-impulse maneuvers and each impulse for every three days.

The flight results are well agreed with the theoretical predictions.

BRIEF DESCRIPTION OF THE SATELLITE

Up to now, three models of recoverable satellite, designated as FSW-0, FSW-1 and FSW-2, have been developed in China⁽¹⁾. The first launch of the third model (FSW-2-1) took place on August 9, 1992 on a new developed launch vehicle LM-2D with the satellite entering a 63.1° , 175×355 km orbit. The satellite is low earth orbit, three-axis stabilized, earth oriented and weights 2600 kg. The orbit lifetime is 16 days, twice as long as that of its preceding model FSW-1.

The satellite consists of 12 subsystems including the control subsystem. The control subsystem is developed and based on its precedings^{(2) (3)}, and will perform following functions:

(a) elimination of the initial attitude deviation resulted at separation of the satellite from launch vehicle;

(b) attitude acquisition and determination;

(c) coarse pointing and fine pointing during the orbital phase and attitude keeping during the maneuver;

$$dt = \frac{(1-e^2)^2}{n} \left(1 + \frac{e^2}{2} - 2e \cos f + 3e^2 \cos^2 f \right) df \quad (3)$$

equations (2) become

$$\left. \begin{aligned} da &= \frac{(1-e^2)^2}{n^2} U (2(1+2e^2) - 2e \cos f + e^2 \cos 2f) df \\ de &= \frac{2(1-e^2)^2}{n^2 a} U \left[-e + \left(2 + \frac{11}{4} e^2 \right) \cos f \right. \\ &\quad \left. - 3e \cos 2f + \frac{13}{4} e^2 \cos 3f \right] df \\ d\omega &= \frac{(1-e^2)^2}{n^2 a e} U \left[\left(2 + \frac{9}{4} e^2 \right) \sin f \right. \\ &\quad \left. - 3e \sin 2f + \frac{13}{4} e^2 \sin 3f \right] df \end{aligned} \right\} (4)$$

It is important to keep the perigee altitude and two alternatives are open to do this.

(a) Thrust impulse is applied just ^{as} apogee is reached. This is a conventional method to raise the perigee altitude. Since the apogee is located in the Southern Hemisphere, the satellite is out of the visibility of our ground tracking stations.

(b) Thrust impulse is applied at the point near the perigee, i.e. at certain true anomaly for instance $f = \pm 30^\circ$ bilaterally symmetrical relative to the perigee. With this alternative both perigee and apogee will be raised and without any loss of efficiency as indicated by calculation.

MANEUVER MOTOR

The maneuver motor is a conventional hydrazine mon-propellant propulsion system with nominal thrust 20N. The thrust versus time curve is imitated by a polynomial as a function of time t .

NOMINAL ORBIT

The nominal orbit is a design reference orbit in which only the non-sphere earth perturbation, i.e. harmonic coefficients of earth's gravitational potential J_2, J_3, J_4, A_{22} and B_{22} , has been considered, and the atmospheric drag perturbation has not been taken into account. The nominal orbit is the basic reference for orbit maintenance. The actual

flight orbit will be adjusted or corrected by multiple thrust impulses to bring the satellite close to the nominal orbit. The basic orbital elements of the nominal orbit for each flight mission are given beforehand with the mission definition.

MANEUVER STRATEGY

(a) In selecting the maneuver orbit account must be taken of the fact that following the maneuver orbit there will be 2~3 observable and trackable orbits passing through our territory.

(b) The maneuver will be executed compatibly with the attitude control. If the attitude deviation of the satellite or the thrust deviation of the maneuver motor will go beyond the design bounds, must temporarily cut-off the motor or turn the motor to work on pulse-modulation mode.

(c) In order to economize the consumption of propellant it is intended to eliminate the injection error and atmospheric drag perturbation in the earlier stage of flight, i.e. to execute the maneuver earlier on, especially in case of serious injection error. Thus, it is planned to use a four-impulse transfer and to apply a forward tangential impulse every three days. The first one or two maneuvers are intended to eliminate the errors in orbit injection and to compensate the aerodynamic perturbation. The second and third are intended to raise appropriately the orbit altitude and the last one is only a final trimming.

IN-ORBIT CALIBRATION

The calibration of real thrust curve resulted in maneuver transfer is conducted after each maneuver using ground tracking data and telemetry data before and after firing. With this calibration data the next predetermined value of period compensation will be corrected.

FLIGHT PRACTICE

Computers in Xi'an Satellite Control Centre

(XSCC) process the data obtained from ground tracking stations located around our country, predict the future orbital parameters and combine them with the desired one, calculate the details of the maneuvers, such as required period compensation value, velocity increment, thrusting time and propellant consumption etc for each maneuver, and form as control programmes which are then transmitted to the satellite onboard computers via telecommand. The onboard computers in turn process the data from ground stations and dispatch as a command to the maneuver motor to produce a desired velocity increment (Figure 1). After each maneuver the calibration of the thrust curve of the maneuver motor and calculation of propellant consumption are made in XSCC using ground tracking data and telemetry data.

The flight was made on 9th August, 1992. The first maneuver was performed on 12th August on 45th orbit with thrusting time $\Delta t = 687$ sec and period compensation value $\Delta T = 15.4$ sec. The postmaneuver calibration of thrust curve indicated that the deviation from the theoretical imitated thrust curve is 98%. The second and third maneuvers took place on 15th August and 18th August respectively. The deviations of thrust curve for both maneuvers were 95%. After calculation it is showed that no more maneuver is needed to conduct.

The results of the first orbit flight are well agreed with the theoretical predictions.

ACKNOWLEDGEMENTS

The authors are very grateful to prof. Yiqing CHEN, prof. Zugui CHEN, Mr. Gongtian YAN and Xudong WANG of Beijing Institute of Control Engineering. They are responsible for the development of the orbit maintenance unit for control subsystem of the satellite.

REFERENCES

1. Huabao LIN, Guirong MIN. "Aspect of the China's Recoverable Satellite-Platform", IAF-93-552, 1993
2. Jiachi YANG, Guifu ZHANG, Chengqi SUN, Xueyi FENG, et al. "Three Axis Stabilization Attitude Control System for Chinese Near Earth Orbit Satellite", VIII IFAC Symposium on Automatic Control in Space. Oxford, UK. 2-6. July 1979
3. Yiqing CHEN, Zugui CHEN, Chengqi SUN, Xueyi FENG, et al. "Digital Attitude Determination and Control System of Chinese Recoverable Satellite for Scientific Exploration and Technical Experiments" AAS 89-653, 1989
4. Lin LIU, "Orbit Mechanics of Artificial Earth Satellites" (in Chinese), Higher Education Press, Beijing, 1992, pp. 541-542
5. Rongbao ZHANG, "The Method for Artificial Satellite Orbit Maintenance" (in Chinese), Chinese Space Science and Techuology, No.1, February, 1988, pp.48-55

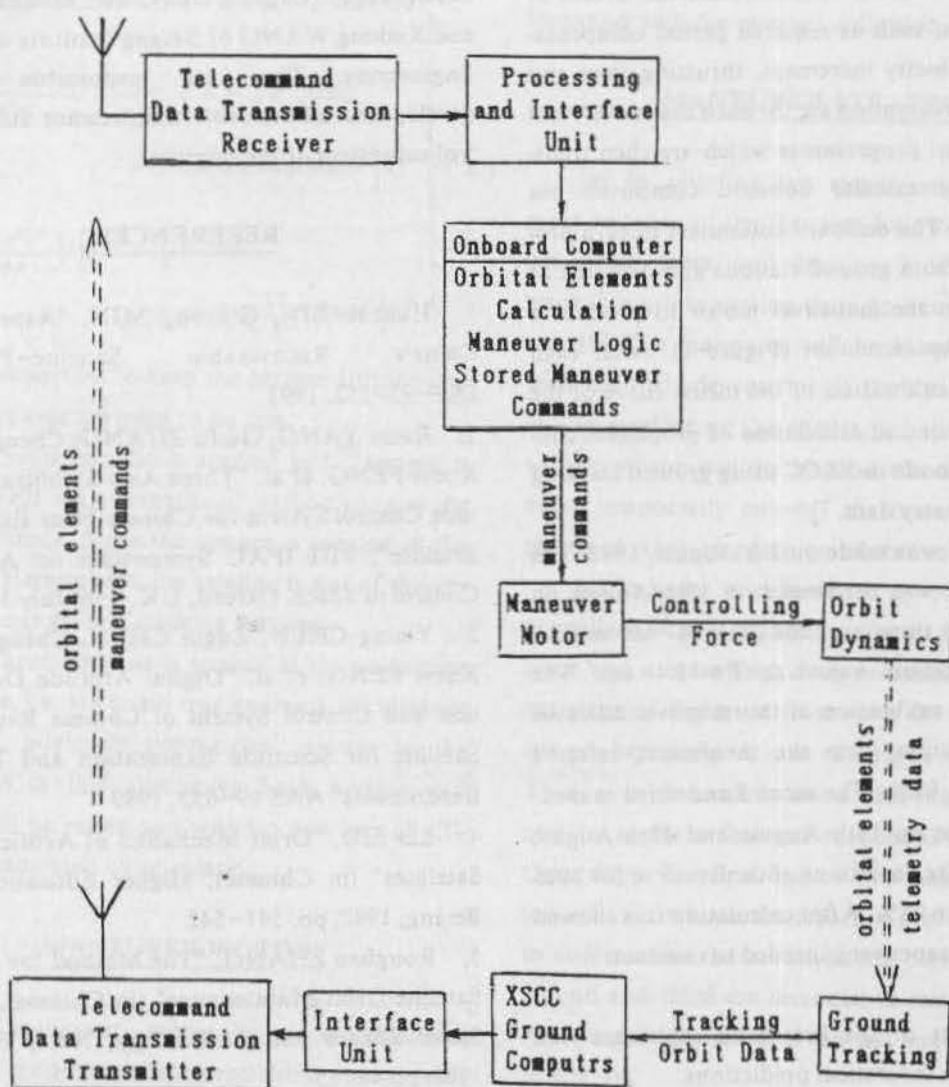


Figure 1. Orbit-Maintenance Block Diagram

UNIVERSAL SMALL SPACE PLATFORM: ORIENTATION ASPECTS

Michael Yu. Ovchinnikov

Alexander I. Dyachenko

Keldysh Institute of Applied Mathematics,

Russian Academy of Science

4, Miusskaya Sq., Moscow, 125047, Russia

Phone: 7-(095)-250-56-15, Fax: 7-(095)-972-07-37

Telex: 411700 Box 6540 For ARGONSPACE

E-mail: ovchin@applmat.msk.su

Abstract

This paper considers the Russian small satellite projects developed during the last years. The most appropriate opportunities to launch these satellites into orbits are discussed. An essential subject is their attitude control systems (ACS). The results of mathematical modeling, computer simulation of dynamics, and design of ACS for Universal Small Space Platform (USSP) are presented. USSP is designed as a small-sized multiple-purpose universal stabilized satellite for commercial use by any customers. USSP is provided by a Gravity Gradient ACS (GGACS) and a Preliminary Magnetic ACS (PMACS) with total weight of about 6 kg. These two ACS direct the satellite's longitudinal axis toward Earth uniquely with pointing accuracy 5-7°. In the mathematical modeling stage the steady-state periodic solutions of the approximate equations are used as a nominal motion of USSP. It is an appropriate way to work out the detailed analysis of the most important characteristics of periodic solutions when the values of parameters are widely varied. The authenticity of results obtained is confirmed by numerical simulation with complete dynamic models and laboratory testing.

Key words: Small Satellite, Attitude Control System, Universal Platform

Introduction

During the recent years an increasing interest has been observed on the part of designers and users of spacecraft toward small satellites—relatively cheap spacecraft characterized by a mass of several to several hundred kilograms, a size under one meter and a relatively simple set of scientific, telemetry, instrumentation and auxiliary equipment. They can be orbited as piggyback with a main satellite, or by a specialized low-power launcher, or by a "shuttle" spacecraft.

The analysis of the problems that may be solved by such satellites and the composition of their payload and auxiliary equipment allow to draw the following conclusion. Apparently, the interest toward small satellites is due to the possibility of simpler solutions that they offer to the financial and ecological problems that arise whenever an orbital system is being designed. This interest has been objectively predetermined by the currently achieved stage of space technology development with its theoretical and element bases. The extension of the scope of organizations and countries participating in development, design, manufacture and application of satellites has also played a significant role. Among such organizations are some universities and small companies from the leading space countries.

Other countries possessing means for purchasing space system components and financing satellite launches, but not planning or claiming able to develop their own space programs and corresponding infrastructures in the near future, are at present a considerable addition to the space technology market as well. The structural economic reforms under way in Russia, the processes of conversion and simultaneous reduction in science and space industry funding require new solutions to the problems faced by researchers and other space technology users. Small satellites are expected to offer a good opportunity in this field, too.

Brief overview of small satellite projects in Russia

The overwhelming majority of the small satellite projects recently developed in Russia are aimed at construction of regional and cross-regional satellite communication systems. The current deficit of communication means is frustratingly large, and it remains practically unmet despite the apparent liquidity of this market segment. The absence of stable long-term investment in space technologies is forcing the communication system designers to look for cheaper and faster ap-

proaches to creating such systems. Small satellites offer the most optimal cost, length of design, and orbiting characteristics. Because of the low capacity of power sources, limited weight and bulk of on-board equipment, such satellites are usually used in low-orbital communication systems. All required territories can be covered by launching satellites into near-polar orbits. Low-orbital systems allow not only to satisfy the limits to on-board equipment but also to use relatively simple portable on-ground receivers and transmitters. The link between two correspondents not within the visibility zone of a single satellite is established either by transmitting the message from on-board computer memory toward the visibility zone of the addressee using the electronic mail principle, or by organizing inter-satellite networks. The latter allows any two or more locations on the globe to communicate in real time. Low near-polar orbits are in many cases superior to geostationary orbits, which are known to be far from perfect. Here follows a list of the most commonly known Russian projects of small communication satellites.

In 1990 NPO Prikladnoy Mekhaniky and NPO Tochnykh Priborov proposed to set up a commercial communication system "Gonets" [1] based on low-orbit military satellites. Two satellites "Gonets-D" of this system were successfully orbited at altitude 1500 km and inclination 74° in July 1992 by "Tsyklon" launcher. The satellite's body is cylindrical, with weight about 250 kg. Solar batteries are mounted on the side surface of the body. The satellite is provided with a GGACS and has two conal weak-directional aerials that allow to establish two- or three-channel connection on frequencies 200–400 MHz. The on-board memory storage is 8 Mb.

In 1991 Ural-Cosmos Corp. announced that work was begun on the Personal Satellite Communication System (PSCS). The general contractor was Makeyev Design Bureau of Machinostroyeniya (Miass city). The satellites (SPC-Satellites) were to be orbited by a modified production-type submarine missile "Shtil" at altitude 560–700 km and inclination 76° . The satellite being developed weighs about 280 kg, has a GGACS and a PMACS, jointly designed by All-Russia Scientific Research Institute of Electromechanics (VNIIEM) and Keldysh Institute of Applied Mathematics (KIAM). These two ACS provide the satellite with a unique orientation to the Earth's surface. During the first stage of design of PSCS it is planned to establish electronic-mail communication mode. The work on the project is currently suspended.

Satellite "Start-1", which is a part of the space rocket complex with the same name, is being developed by a consortium headed by the Moscow Institute Teplotekhniki, which designs and manufactures mobile ballistic surface-based missiles SS-25. These missiles are subject to destruction according to the Strategic Arms Reduction Agreement. With a slight modification this rocket is able to orbit, if inclination is 83° , a load of 350–

400 kg at altitude 700 km. In early 1993 a demonstration variant of the satellite with mass of about 250 kg was orbited. It was provided with a GGACS with variable boom length. By manipulating the boom length the satellite can be overturned if necessary to ensure a unique orientation. The turn-over is made around the normal axis to the orbit plane. At the first stage of development electronic-mail and real-time communication modes are planned (the latter for two correspondents within visibility zone of one satellite only).

In 1992 NPO Polyot (Omsk) orbited an experimental communication satellite "Informator-2", which was based on the satellite used in COSPAS-SARSAT system. It weighed about 900 kg and was provided with a GGACS with controlled boom position relative to the satellite body, which allowed to decrease the amplitude of forced oscillations of the satellite in the steady-state mode.

The joint global communication project announced by NPO Polyot and NPO ELAS is based on a small satellite "Courier-2" with mass about 870 kg, altitude 1000 km, inclination 83° . The ACS includes four controlled electric flywheels.

The space communication system Radiokniga is being designed by Space Research Institute and SLV Company. Presumably, production-type UHF/FM radio stations and currently working on-ground systems (MVD's, Russian Central Bank's, Vostok Bank's) will be used. The commercial re-transmitter is a non-oriented satellite with mass about 10 kg and an octo-rod aerial. It is planned to be orbited from the equator by a geodetic rocket or an airplane-based rocket.

The second most intensive field of small satellite applications is the scientific and technological experiments. The Moscow Aviation Institute continues to develop a series of SAC (Small Autonomous Canister) satellites. These weigh about 15–40 kg and are non-oriented, with the exception of SAC-A satellite (aerodynamical), which has a passive aerodynamical ACS with magnetic hysteresis rods [2]. Several such satellites were orbited through the docking openings of Saljut-7 and Mir orbital stations.

NTC Photon of Samara Aviation Institute jointly with Central Specialised Design Bureau (Samara) during the period 1989–1993 designed and orbited five non-oriented satellites PION for conducting control of current atmosphere state along the satellite trajectory using external trajectory measurements. These satellites are spherical, with diameter 0.33 m and mass about 50 kg. They were orbited as piggyback with the Resurs-F research satellite.

The satellites Magion-1 (15 kg), Magion-2 and Magion-3 (50 kg each) were designed by Space Research Institute jointly with Czechoslovak Academy of Science. They were orbited in 1978, 1989 and 1991 together with Intercosmos-18, 24 and 25 satellites respectively. Magion-1 had a passive magnetic ACS with magnetic hysteresis rods, and the other two had a liquid nuta-

tional damper. They were used for an investigation of the geomagnetic field and the processes in the Earth's magnetosphere.

More small satellite projects are described in [4].

Universal Small Space Platform (USSP)

On the basis of wide use of the practical experience gained during the design, manufacture and operation of multi-purpose spacecraft Meteor, Resurs-O, Planeta, for the purpose of meeting the demand for cheap spacecraft both in Russia and abroad, a series of small satellites are currently being developed. These satellites are designed as universal space platforms which can carry payload equipment for various scientific and commercial purposes.

USSP is designed as a compact universal stabilized platform for commercial, applied, scientific and research purposes. The main characteristics of USSP are as follows. Firstly, the platform is non-hermetic. This reduces the mass and cost and allows to easily rearrange the payload equipment. It also increases reliability of the satellite because one of the most probable causes of failures of its elements over a long period of time is decompression. The accumulated experience of non-hermetic structures design, including provision of a certain thermal mode for on-board devices in orbit makes it possible to successfully solve all arising technical problems.

Here are the basic technical characteristics of USSP.

- Total weight 60 kg including payload weight upto 25 kg.
- Circular orbit with altitude 900 km and inclination 82° (if orbited as piggyback with Meteor satellite) or sun-synchronous orbit with altitude 650 km and inclination 98° (if orbited with Resurs-O).
- Attitude pointing precision toward Earth $5-7^\circ$.
- Tightless body and bearing structure are based on formed and sheet carbon-composite materials.
- GGACS with Eddy-Current Damper (ECD), deployable boom and a PMACS with total weight about 6 kg provide the satellite by unique pointing attitude orientation toward Earth. If necessary, a pitch flywheel is installed to provide three-axis orientation.
- Electrical power supply system consists of an orientable solar battery and an accumulator. It supplies a power of 20 or 40 W. On-board voltage is 27 V.
- Passive thermocontrol system consists of heat protectable materials, heat pipes, special coatings and radiators.

- Service radiomeasuring system consists of command, hardwired telemetry and trajectory measuring sub-systems with weight 6 kg.
- Aerial-feeder equipment is proposed for transmitting telemetry and payload's information.
- On-board systems control is done by a computer.
- The first experimental satellite is going to be launched in 1995 as piggy-back on the Resurs-O satellite board.

The satellite is being designed and manufactured by VNIEM in cooperation with other industry organizations and KIAM and NPP ARGON. KIAM and NPP ARGON build software and carry out mathematical modeling of the satellite dynamics, as well as processing of flight testing data.

Let us now proceed to the questions of mathematical modeling of satellite attitude dynamics and ACS parameter choice.

When a satellite project is designed, a strong attention is given to mathematical modeling of the satellite's dynamics. If a passive ACS is used with characteristics that are not measurable or variable during the flight, motion modeling becomes extremely important for both ACS parameter choice and orientation sensor data processing.

ACS Composition and Operating Scheme

ASC composition for USSP is defined by two basic requirements for attitude motion mode: a small amplitude of oscillations of the longitudinal axis around the local vertical (orientation accuracy) and a unique orientation of the boom with the damper with respect to the Earth (orientation uniqueness). The ACS described includes a deployable boom with an ECD at the tip, a "magnetic spring", cages and other auxiliary devices. The boom with the damper, when deployed along the axis oriented, creates a restoring torque in pitch and roll. The ECD consists of two concentric spheres. The inner magnetized sphere (the "float") tracks the local geomagnetic field direction, the outer non-magnetic conducting sphere is fixed to the boom. When the float rotates with respect to the outer sphere eddy currents are created in the latter and the rotational kinetic energy of the satellite is dissipated, the satellite thus being drawn into one of the asymptotic equilibriums.

The problem of uniqueness of attitude mode is solved by using a PMACS. After separation from the launcher the satellite is brought into a preliminary orientation mode. This mode is so chosen that it provides initial conditions of motion after boom deployment, needed for unique orientation. In contrast from current coils traditionally used for creating a dipole magnetic moment, here a so called magnetic spring is applied—a device that provides an elastic link between the float

and the body of the satellite [3, 4]. An analogous system was proposed for the SPC-Satellite [3]. It allows to decrease the ACS mass and energy consumption.

Let us consider a brief ACS operation scheme. After separation of the satellite from the launcher float is uncaged and magnetic spring is turned on. The float (a strong permanent magnet) is quickly drawn into rotation by vector H of the local geomagnetic field intensity, the dipole moment axis of the former nearly tracking the direction of the latter. Relative rotation of the damper spheres creates a viscous friction torque (damping torque). The satellite, whose motion is basically determined by this torque (gravity torque may be considered a perturbing one), is carried along with the float. Simultaneously, initial angular velocity perturbations arising from separation are damped. After a certain period of time the angular velocities of the float and the satellite become nearly equal; the satellite enters an asymptotically stable rotation together with the geomagnetic field vector. Up to this moment the influence of the spring is not substantial. The spring allows to orient the longitudinal axis of the satellite along H uniquely. This effect is due to the fact that the float has only one asymptotical equilibrium with respect to the satellite body, when there is a magnetic spring. The satellite is in the magnetic orientation mode.

When the satellite passes a near-geomagnetic-pole area, where H is almost vertical, the spring is turned off and the gravity boom is deployed. After the transient motion period the longitudinal axis tracks the local vertical and the satellite is in a uni-axis gravity gradient orientation mode. This mode is similar to forced periodic oscillations, whose parameters are essentially determined by the gravity restoring torque and disturbance damping and aerodynamical torques. The characteristics of such motions can be calculated and, provided the right choice of torque approximation, used for ACS parameter determination.

ACS Parameter Choice

ACS parameter choice is made in two steps. First, taken the magnitudes of disturbance torques, possible deviation of the longitudinal axis from the local vertical in the nominal mode, and constructive requirements, the main parameters of the GGACS are chosen—boom length, ECD mass and its damping coefficient. Further, given these characteristics as well as tensor of inertia of the satellite with undeployed boom, we choose magnetic moment of the float and magnetic spring parameters. The main PMACS characteristics are fast response and reliability of providing the needed initial conditions at the stage of boom deployment. GGACS and PMACS parameter choice is made using simplified motion models which only take account of the basic factors of motion. This permits to lessen the dimensionality of GGACS, PMACS and satellite parameter space. The parameter choice can then be seen as a pro-

cess of optimization of required characteristics in this parameter space.

The satellite is in a near-polar orbit with inclination close to 90° and a negligibly small eccentricity. Therefore, on this stage of dynamics analysis the nominal motion could be taken to be the motion in a polar circular orbit. This motion exists under some traditional assumptions made in the research of this kind. These assumptions deal with the models of geomagnetic and gravity fields, the atmosphere, the interaction between the latter and the satellite body, the interaction between float and geomagnetic field and between float and magnetic spring. The basic advantage of the model built on these assumptions is that the dynamics equations have periodical solutions, which can be analyzed by the well developed mathematical procedure. Periodic motions are a good approximation of the real motions, and thus can be used as nominal attitude motions. These periodic motions are found by using the Newton method, and their behavior for various sets of satellite and ACS parameters (amplitude, stability, etc) is analyzed by method of prolongation by a parameter [5].

It should be mentioned that the USSP GGACS parameter choice scheme is analogous to that of SPC-Satellite.

Let's now consider the process of GGACS parameter choice. The relationship between the damping coefficient k_d and the equatorial and axial moments of inertia of the satellite, A and B , are chosen with regard to the characteristics of nominal motions in gravitational orientation mode (boom deployed, satellite is considered axi-symmetrical). While choosing the values of k_d , A , and B two contradictory requirements have to be held in consideration: reduction of oscillation amplitude and transient period length. As a main criterion we will use the orientation accuracy, i.e. the maximal deviation α_{max} (during one revolution) of the longitudinal axis and the local vertical. To calculate the aerodynamical perturbations, reliable information must be obtained about the state of the atmosphere for the needed period. Moreover, there is in principle a possibility to vary the aerodynamical perturbations, for instance, by shifting somewhat the center of pressure of the satellite. Therefore, when choosing the damping coefficient k_d , given α_{max} , only damping torque, but not aerodynamical, is reckoned. The contribution of the aerodynamical torque is estimated afterwards. Besides that, the satellite will be orbited at altitude of 800 km, where aerodynamical torque is not large.

When choosing the equatorial moment of inertia of the satellite A , active perturbative torques must be considered. The main perturbation in this construction is, apparently, due to residual magnetization. Given its characteristic values, as well as known empirical relationships between ECD mass and its damping coefficient and magnetic momentum of the float, we took a value of $50 \text{ kg}\cdot\text{m}^2$ for equatorial moment of iner-

tia. This value may be changed later. If the satellite with undeployed boom has equatorial moment of inertia $1.91 \text{ kg}\cdot\text{m}^2$ and axial moment of inertia $1.56 \text{ kg}\cdot\text{m}^2$, an equatorial moment of inertia with deployed boom requires approximately a boom length 6 m and ECD mass 1 kg. Then, with $\alpha_{\max}=3^\circ$, we have k_d about $0.0026 \text{ N}\cdot\text{m}\cdot\text{s}$.

The first stage of motion is the transient period and preliminary magnetic orientation. The ECD float's magnetic momentum m_d should be defined in advance. From the results of the research of periodic motions of the satellite with a permanent magnet, it follows that m_d can be chosen so that the amplitude of oscillations of such a satellite is small enough and the oscillations are separated from the resonance areas. These conditions are satisfied by m_d value of $2.7 \text{ A}\cdot\text{m}^2$. This value lies in the optimal area of possible values of m_d with respect to the criteria of minimal amplitude and minimal value of m_d itself.

The value of magnetic field intensity H_c in the center of magnetic spring is found from the condition of minimization of the transient motion period and the angle of deviation of the longitudinal axis from the local vertical above a geographical pole in the magnetic orientation mode. In order to accomplish this, periodic oscillations of the satellite around vector H were analyzed. The shortest transient period corresponds to H_c about 9 A/m .

At the second stage complete dynamics models are used. These modes include accurate representations of the Earth's magnetic and gravitational fields. The orbit is defined as a predetermined trajectory in the inertial space. Non-stationary orbit may be used, by setting revolution-averaged oscillating elements.

The Earth's magnetic and gravitational fields are approximated using the known theory of expansion of the Earth's magnetic and gravitational potentials in series of spherical functions. Two representations are created for the magnetic field. One, the faster, uses the four first multi-poles. The other is the standard expansion into a series of Legendre polynomials upto 10th order, with complex coefficients. The aerodynamical torque is defined by the location of the center of pressure in the satellite body, the section area and the drag coefficient.

Numerical modeling of the satellite dynamics in the magnetic and gravitational orientation modes that were made using a software complex for exact numerical modeling has given satisfactory results.

Acknowledgements

The authors wish to thank Finep - Financiadora de Estudos e Projetos (Brazil) and the Organizing Committee of the "International Symposium on Spacecraft Ground Control and Flight Dynamics—SCD1" for sponsorship and useful help that made possible the authors' participation in the Symposium with this paper.

References

- [1] M.V.Tarasenko. Military aspects of the Soviet Cosmonautics. M., Russian Press Agency, Nikol Ltd., 1992, 164p. (in Russian)
- [2] M.Yu.Ovchinnikov, V.I.Pen'kov. Aerodynamic stabilization system of small scientific satellite. Proceedings of the 3rd International Symposium on Spacecraft Flight Dynamics, Darmstadt, Germany, 30 Sept.- 4 Oct. 1991, ESA SP-326, pp.347-353
- [3] M.Yu.Ovchinnikov. Gravity gradient attitude control system for small communication satellite. Papers AAS/GSFC International Symposium on Space Flight Dynamics, GSFC, Greenbelt, Maryland, USA, 28-30 Apr.1993, v.1, N 93-282, 15p.
- [4] V.A.Sarychev, M.Yu.Ovchinnikov. Magnetic Orientation Systems of Artificial Earth Satellites. Survey of Science and Technology. Series: Exploration of Space. Moscow, 1985, 104pp. (in Russian)
- [5] V.A.Sarychev, V.V.Sazonov, and N.V.Mel'nik, Spatial Periodic Oscillations of a Satellite Relative to Its Center of Mass, Cosmic research, Oct., 1980

MAGNETICALLY STABILIZED SATELLITE WITH VISCOUS ANNULAR DAMPER ATTITUDE MOTION

Michael Pivovarov¹

Pavel Triska²

Jaroslav Voita²

¹Space Research Institute - IKI, Moscow
Profsoyuznaja St. 84/32, Moscow, Russia

E-mail: mpivovar@esocl.bitnet

²Geophysical Institute, Prague

Bochni 11, No. 1401-14131 Praha 4, Czech Republic

E-mail: triska@seis.ig.cas.cz

Abstract

In course of the international missions "Activniy" and "Apex" Czecho-Slovakian Magion-2 & Magion-3 subsatellite with a magnetic stabilization have been separated from Russian gravity-gradient stabilized Intercosmos-24 & Intercosmos-25 satellite respectively. Perhaps Magion-2 is the first magnetically stabilized spacecraft with viscous annular damper.

This paper describes oscillation damping for a spacecraft, containing a constant magnet and a toroidal cavity, filled up with viscous incompressible fluid. The averaging method was used to get closed form solution for the spacecraft oscillation amplitude with respect to the magnetic field line. The optimal damper parameters are found. The results of a laboratory experiment in which oscillations about vertical of a rigid body, suspended by elastic string and carrying toroidal viscous damper are presented. The observed damping and predicted one are compared. The results of the Magion-2 & Magion-3 spacecraft attitude determination are presented.

Key words: Magnetic stabilization, Viscous fluid damper.

1 Introduction

Traditionally the spacecraft stabilized along the magnetic field line is equipped by oscillation damping system using magnetic hysteresis. On the other hand toroidal fluid damper is widely used for spin stabilized spacecraft nutation damping. To avoid unpredictable distortions of the magnetic situation on Magion-2 & Magion-3 subsatellite it was decided to abandon a traditional damping system and to use viscous fluid damper. The paper presents some results in this new problem.

The content of the paper is as the following. Section

2 presents a new approach used to get closed form solutions in the field of magnetically stabilized spacecraft attitude motion. In section 3 we study the oscillations of a rigid body with toroidal fluid damper. Section 4 presents laboratory experiment results in comparison with analytical one. In section 5, combining the technique of section 3 and the approach of section 2 we get approximately closed form solution to the problem of a spacecraft with viscous fluid damper attitude motion. In section 6 we discuss the main results of subsatellites actual attitude determination.

2 Oscillations of a spacecraft with a large magnetic moment

We will consider the spacecraft oscillations in the plane of magnetopolar, Keplerian, elliptical orbit on the assumption that the spacecraft possesses a large magnetic moment. The two-dimensional problem is much simpler than three-dimensional and can serve as a model. However, this problem includes fundamental perturbations of stabilization with the magnetic field due to motion of a spacecraft along nearly polar orbits, which makes it very important.

We will introduce the coordinate system $OXYZ$, the plane of which coincides with the plane of the polar orbit, while axis X is directed toward the ascending node and axis Y is directed toward the pole of the earth. We will assume that the axis of the magnetic dipole coincides with axis Y . Oscillations of the spacecraft in the plane of a magnetopolar elliptical orbit is determined by the equations

$$A\ddot{\varphi} = -I_S H \sin(\varphi - \gamma), \quad (1)$$
$$H = \frac{\mu_0}{R_S} \sqrt{1 + 3 \sin^2(\omega + \vartheta)}$$

In Eq. (1), φ is the angle between the axis of the satellite magnet and axis X ; A is the spacecraft principal moment of inertia relative to the axis orthogonal to the

plane of the orbit; I_S is the magnetic moment of the spacecraft; H is the magnetic field at a current point along the orbit; γ is the angle between the direction of the magnetic field line at a current point along the orbit and axis X ; μ_E is the magnitude of the magnetic moment of the earth's dipole; R_S is the magnitude of the radius vector; ω is the longitude of perigee; and ϑ is true anomaly at time t . One should note that other torques acting on the spacecraft are not taken into account in (1). It is assumed that they are much less than magnetic moment.

Eq. (1) can be reduced to its dimensionless form by substitution

$$\tau - \tau_\pi = \omega_O(t - t_\pi),$$

where ω_O is the mean motion, $\tau - \tau_\pi$ is the mean anomaly. The index " π " corresponds to the moment when the satellite passes the perigee. In dimensionless form

$$\frac{d^2\varphi}{d\tau^2} = -\alpha c(\vartheta) \sin(\varphi - \gamma), \quad \alpha = I_S \mu_E / A \mu \quad (2)$$

$$c(\vartheta) = \left(\frac{1 + \epsilon \cos \vartheta}{1 - \epsilon^2} \right)^2 \sqrt{1 + 3 \sin^2(\omega + \vartheta)}$$

Let $\alpha \gg 1$ so that

$$\epsilon = 1/\sqrt{\alpha} = \omega_O/\omega_H \ll 1,$$

where ω_H is the rate of the spacecraft small oscillations in the magnetic field corresponding to the orbital perigee. Now we consider the fast time z

$$\epsilon z = \tau - \tau_0$$

Then, taking into account that variables ϑ and γ are some functions of slow time τ , we obtain

$$d^2\varphi/dz^2 + Q(\tau, \varphi) = 0, \quad (3)$$

$$Q(\tau, \varphi) = c(\vartheta) \sin(\varphi - \gamma)$$

To analyse Eq. (3) we will use the averaging method^{1,2}. The unperturbed problem ($\epsilon = 0$, $\tau = \tau_0$, $\vartheta = \vartheta_0$, $\gamma = \gamma_0$) describes the motion of simple pendulum with the equilibrium position γ_0 . Introduce the pendulum energy

$$\mathcal{H} = (d\varphi/dz)^2/2 + V(\tau, \varphi) \quad (4)$$

$$V(\tau, \varphi) = \int Q(\tau, \varphi) d\varphi = c(\vartheta)[1 - \cos(\varphi - \gamma)]$$

If in the initial moment $\mathcal{H} < 2c$, then the system is in the domain of oscillations, if the inverse inequality is satisfied then it is in domain of rotations. The amplitude of oscillations F is an essential parameter of the motion in oscillation domain, the energy \mathcal{H} - in rotation domain. We will now study the evolution of F variable in the oscillation domain. The results for rotation domain are presented in³.

Equation (3) describes a Hamiltonian system with a single degree of freedom with a Hamiltonian that is a function of the slow time. The action integral I in this problem is an adiabatic invariant. In the unperturbed

system, the oscillations are symmetric relative to the equilibrium position with an amplitude F that is constant along each solution. We will define in terms of $F_1(\tau)$ the maximum, and in terms of $F_2(\tau)$ the minimum value of coordinate F for perturbed motion. As it is known², for the domain of oscillations

$$I = \int_{F_2}^{F_1} \sqrt{2 \int_{\varphi}^{F_1} Q(\tau, \varphi) d\varphi} dq = const, \quad (5)$$

$$\int_{F_2}^{F_1} Q(\tau, \varphi) d\varphi = 0 \quad (6)$$

From (6), taking into account (3), we find that

$$\frac{1}{2}(F_1 + F_2) = \gamma,$$

and then

$$F_1 = \gamma + F, \quad F_2 = \gamma - F, \quad (7)$$

i.e., perturbed oscillations are symmetric relative to slowly changing values of γ with the amplitude F . Substituting (7) into (5), we obtain an equation for determining F . Omitting complex calculations, we find that

$$\sqrt{c(\vartheta)} \int_0^F \sqrt{\cos x - \cos F} dx = const$$

It can be shown that

$$\int_0^F \sqrt{\cos x - \cos F} dx = 2\sqrt{2} W(F), \quad (8)$$

$$W(F) = E(k) - k'^2 K(k),$$

$$k = \sin(F/2), \quad k'^2 = 1 - k^2,$$

where K and E are complete elliptical integrals of the first and second kind with a modulus of k . Using the second Eq. (2), we finally have

$$W(F) = W(F_0)G(\vartheta), \quad (9)$$

$$G(\vartheta) = \left[\frac{1+3\sin^2(\omega+\vartheta_0)}{1+3\sin^2(\omega+\vartheta)} \right]^{1/4} \left[\frac{1+\epsilon\cos\vartheta_0}{1+\epsilon\cos\vartheta} \right]^{3/2},$$

where F_0 is the initial value of the amplitude.

Numerically solving Eq. (9) does present any difficulties. On the other hand, using an expansion of complete elliptical integral in a series with the modulus k and taking into account two of the first terms, we obtain an approximate closed form solution in the form

$$F = F_0 \sqrt{G(\vartheta)} \quad (10)$$

3 Oscillations of a rigid body with a toroidal cavity filled with a viscous liquid

We consider the planar oscillations of a rigid body, in which there is a toroidal cavity entirely filled with a viscous incompressible liquid of density ρ_* , about an axis parallel to the axis of the torus. To simplify matters we will assume that the centre of the torus is at

the centre of mass of the system or at a fixed (stationary) point, if the latter exists. We shall assume that $\epsilon = a/R \ll 1$, where R is the radius of the torus and a the radius of the tube forming the torus.

We introduce a cylindrical system of coordinates with its origin at the centre of the torus, the z axis directed along the axis of the torus and the coordinate lines r and ϕ in a plane perpendicular to the z axis. For small ϵ the component of the absolute velocity vector V satisfies the conditions $V_r \ll V_\phi$, $V_z \ll V_\phi$. We will therefore drop the terms containing V_r , V_z in the Navier-Stokes equations for V_ϕ . The equations of the motion for the body with liquid become

$$\begin{aligned} A \frac{d^2 \varphi}{dt^2} + M \sin \varphi &= N(V_\phi) & (11) \\ \frac{\partial V_\phi}{\partial t} &= \nu \left(\frac{\partial^2 V_\phi}{\partial r^2} + \frac{1}{r} \frac{\partial V_\phi}{\partial r} + \frac{\partial^2 V_\phi}{\partial z^2} - \frac{V_\phi}{r^2} \right), \\ V_\phi|_S &= \frac{d\varphi}{dt} r|_S \end{aligned}$$

where A is principal central moment of inertia of the rigid body about the z axis, φ is the angle of rotation of the body about the z axis, $M \sin \varphi$ is restoring torque, N is the moment of the forces exerted by the liquid on the body, ν is the kinematic viscosity of the liquid, and S is surface of the torus.

System (11) will subsequently be reduced to an integrodifferential equation describing the oscillations of the rigid body. We will transform the coordinates by putting $r = z + R$ in the last two equations of the (11) and reduce the system to non-dimensional form by means of the substitution

$$\tau = \omega t, \quad u = V_\phi / (\omega R), \quad \xi = z/a, \quad \zeta = z/a, \quad \omega^2 = M/A$$

where ω is the frequency of small oscillations of the rigid body. We obtain

$$\begin{aligned} \ddot{\varphi} + \sin \varphi &= N/(A\omega^2) & (12) \\ \dot{u} &= \frac{\nu}{\omega a^2} \left[\frac{\partial^2 u}{\partial \xi^2} + \left(\frac{\epsilon}{1 + \epsilon \xi} \right) \frac{\partial u}{\partial \xi} + \right. \\ &\quad \left. \frac{\partial^2 u}{\partial \zeta^2} - \left(\frac{\epsilon}{1 + \epsilon \xi} \right)^2 u \right], \\ u|_{\xi^2 + \zeta^2 = 1} &= \dot{\varphi}(1 + \epsilon \xi) & (13) \end{aligned}$$

where as before $\epsilon = a/R$; the dot denotes differential with respect to τ .

If the solution of the boundary-value problem (13) is sought as a series in powers of ϵ , the expression for the principal terms is

$$\dot{u} = \frac{\nu}{\omega a^2} \left(\frac{\partial^2 u}{\partial \xi^2} + \frac{\partial^2 u}{\partial \zeta^2} \right), \quad u|_{\xi^2 + \zeta^2 = 1} = \dot{\varphi} \quad (14)$$

We shall seek a solution of problem (14) satisfying the initial condition $u|_{t=0} = 0$. In the ξ, ζ plane we introduce coordinate ρ, θ by putting $\xi = \rho \cos \theta$, $\zeta = \rho \sin \theta$. Thanks to the symmetry of problem (14), for zero initial data u depends only on ρ and τ , and Eq.

(14) becomes:

$$\begin{aligned} \dot{u} &= \nu_0 \left(\frac{\partial^2 u}{\partial \rho^2} + \frac{1}{\rho} \frac{\partial u}{\partial \rho} \right), & (15) \\ u|_{\rho=1} &= u|_S; \quad \nu_0 = \nu / (\omega a^2), \quad u|_S = \dot{\varphi} \end{aligned}$$

Following Joukowski's we will find the solution of problem (15) such that $u|_S = 1$ and then use the Duhamel integral.

We now take a Laplace transformation of (15). The solution of Eq. (15) in transforms, which is bounded at $\rho = 0$ and satisfies the boundary condition, has the form

$$u_*(\rho, p) = I_0(\rho \sqrt{p/\nu_0}) / I_0(\sqrt{p/\nu_0})$$

where I_0 is the Bessel function of an imaginary argument of order zero and p is transformation parameter.

By the inversion formula, we have

$$u(\rho, \tau) = \frac{1}{2\pi i} \int_{\sigma-i\infty}^{\sigma+i\infty} \frac{1}{p} \exp(p\tau) u_*(\rho, p) dp \quad (16)$$

The singular points of the integrand are pole at zero and poles at a denumerable sequence of points p_k - the roots of the equation $I_0(\sqrt{p_k/\nu_0}) = 0$. We will use the following notation: c_0 is the residue of the integrand at $p = 0$ and c_k is the residue at p_k . Noting that $I_0(x) \rightarrow 1$ as $x \rightarrow 0$ and changing to Bessel functions of real argument of zero and first orders, we obtain

$$\begin{aligned} c_0 &= 1, & (17) \\ c_k &= -2 \exp(-\lambda_k^2 \nu_0 \tau) J_0(\rho \lambda_k) / [\lambda_k J_1(\lambda_k)] \end{aligned}$$

where λ_k are the zeros of J_0 . Eqs. (16) and (18) yield the solution of the boundary-value problem 15 when $u_S = 1$. When $u_S = \dot{\varphi}$ we use the Duhamel integral to obtain

$$\begin{aligned} u(\rho, \tau) &= \int_0^\tau \frac{d^2 \varphi(\eta)}{d\eta^2} \left\{ 1 - 2 \sum_{k=1}^{\infty} \exp \right. \\ &\quad \left. [-\lambda_k^2 \nu_0 (\tau - \eta)] \frac{J_0(\rho \lambda_k)}{\lambda_k J_1(\lambda_k)} \right\} d\eta & (18) \end{aligned}$$

In this approximation the viscous force exerted by the liquid on the torus wall per unit area is $\rho_* \nu [\partial V_\phi / \partial (a\rho)]|_{\rho=1}$ (we recall that ρ_* is the density of the liquid) and the torque of the forces exerted by the liquid on the rigid body is $N = -4\pi^2 R^3 \omega \rho_* \nu (\partial u / \partial \rho)|_{\rho=1}$. Using the fact that $J'_0 = -J_1$ we deduce from (18), (12) that

$$\begin{aligned} \ddot{\varphi} + \sin \varphi &= -\alpha \int_0^\tau \frac{d^2 \varphi(\eta)}{d\eta^2} \Sigma(\tau - \eta) d\eta, & (19) \\ \Sigma(\tau - \eta) &= \sum_{k=1}^{\infty} \exp[-\lambda_k^2 \nu_0 (\tau - \eta)], \\ \alpha &= 8\pi^2 R^3 \rho_* \nu / (A\omega), \quad \nu_0 = \nu / (\omega a^2) \end{aligned}$$

To obtain a bound for the value g of the right-hand side of Eq. (19) we proceed as follows:

$$\begin{aligned}
 |g| &\leq \alpha K \int_0^{\tau} \Sigma(\tau - \eta) d\eta \\
 &= \alpha K \sum_{k=1}^{\infty} \frac{1}{\lambda_k^2 \nu_0} [1 - \exp(-\lambda_k^2 \nu_0 \tau)] \\
 &\leq \frac{\alpha K}{\nu_0} \sum_{k=1}^{\infty} \frac{1}{\lambda_k^2} = \mu K; \quad K = \max |\dot{\varphi}|, \quad \mu = \frac{B}{A}
 \end{aligned}$$

Here we have taken into account that

$$\begin{aligned}
 \lambda_1^{-2} + \lambda_2^{-2} + \dots &= 1/4, \\
 \alpha/(4\nu_0) &= B/A, \quad B = 2\pi^2 R^3 a^2 \rho.
 \end{aligned} \quad (20)$$

where B is the moment of inertia of the liquid about the axis of the torus.

On the other hand, it follows from (19) that $K \leq 1 + |g| \leq 1 + \mu K$, which yields $K \leq (1 - \mu)^{-1}$.

Let us assume that the moment of inertia of the liquid is significantly less than that of the body; then $\mu \ll 1$ and $g = O(\mu)$. We consider small oscillations. To analyse (19) we use the method of averaging.

In the unperturbed problem ($\mu = 0$, $|\varphi| \ll 1$) we have

$$\begin{aligned}
 \varphi &= a_* \sin \tau + b_* \cos \tau \\
 \dot{\varphi} &= a_* \cos \tau - b_* \sin \tau
 \end{aligned}$$

Choose a_* , b_* as the new variables in problem (19). After some standard algebra, omitting terms of second order in μ on the right, we obtain

$$\begin{aligned}
 \frac{\dot{a}_*}{\alpha \cos \tau} &= -\frac{\dot{b}_*}{\alpha \sin \tau} = \\
 \int_0^{\tau} [a_*(\eta) \sin \eta + b_*(\eta) \cos \eta] \Sigma(\tau - \eta) d\eta & \quad (21)
 \end{aligned}$$

Carrying out the integration and dropping terms of the second order in μ , we get

$$\begin{aligned}
 \dot{a}_* &= \alpha \cos \tau \sum_{k=1}^{\infty} G_k(\tau), \\
 \dot{b}_* &= -\alpha \sin \tau \sum_{k=1}^{\infty} G_k(\tau), \\
 G_k &= \{b_*(\tau) \sin \tau - a_*(\tau) \cos \tau + \\
 &\quad \lambda_k^2 \nu_0 [a_*(\tau) \sin \tau + b_*(\tau) \cos \tau] + \\
 &\quad [a_*(0) - \lambda_k^2 \nu_0 b_*(0)] \exp(-\lambda_k^2 \nu_0 \tau)\} / (1 + \lambda_k^4 \nu_0^2)^{-1}
 \end{aligned} \quad (22)$$

Averaging the right-hand sides of Eq. (22) with respect to τ from 0 to ∞ , we find that

$$\begin{aligned}
 \dot{a}_* &= \alpha(-a_* \Sigma_1 + b_* \Sigma_2)/2, \\
 \dot{b}_* &= \alpha(-a_* \Sigma_2 - b_* \Sigma_1)/2, \\
 \Sigma_1 &= \sum_{k=1}^{\infty} \frac{1}{1 + \lambda_k^4 \nu_0^2}, \\
 \Sigma_2 &= \sum_{k=1}^{\infty} \frac{\lambda_k^2 \nu_0}{1 + \lambda_k^4 \nu_0^2},
 \end{aligned}$$

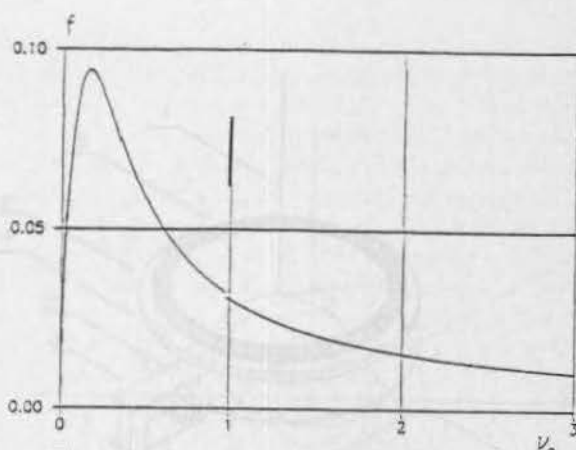


Figure 1: The optimal damper parameter

Integrating these equations with due allowance for the value of α as in (19), we obtain the following expression for the amplitude $F = \sqrt{a^2 + b^2}$ of the oscillations:

$$\begin{aligned}
 F &= F_0 \exp(-2 \frac{B}{A} f \omega t), \\
 f &= \sum_{k=1}^{\infty} \frac{\nu_0}{1 + \lambda_k^4 \nu_0^2}, \quad \nu_0 = \frac{\nu}{\omega a^2}
 \end{aligned}$$

The damper will be optimal if f is a maximum. The figure 1 represents the function $f(\nu_0)$. The optimum value of the nondimensional viscosity ν_0 is 0.158.

4 The laboratory experiment

The analytical results presented above are approximate and have been obtained under some assumptions. To estimate these closed form solutions accuracy the laboratory experiment has been carried out.

The figure 2 presents the sketchy description of the experiment. We study the plane oscillations about vertical of the steel disc⁽³⁾ suspended by the steel string⁽¹⁾ and carrying damper in the form of toroidal tube⁽²⁾ entirely filled with a viscous fluid. The plate⁽⁴⁾ with the number of holes (dots on the plate) is attached to the disc. At some time the light of the bulb⁽⁵⁾ falls down on light-dependent resistor⁽⁶⁾ passing through the corresponding hole. The signal from light-resistor is displayed on the plotter⁽⁷⁾ against time.

The disc oscillations will be determined by the Eq. (11) if we add in the first of them the term describing the energy dissipation in the air and in the string. We assume that this term is linearly proportional to the disc angular rate.

Three experiment have been pursued: with damper filled with water, mercury and without damper. The last experiment have been performed to obtain and exclude the energy dissipation in air and in the string.

The figure 3 shows the decrease of the oscillations amplitude F against time. The curves marked by "W" and "M" present closed form solution in the experiment with water and mercury respectively. The dots mean measurements. Taking into account that the measurement accuracy in the experiment is about 1 degree one

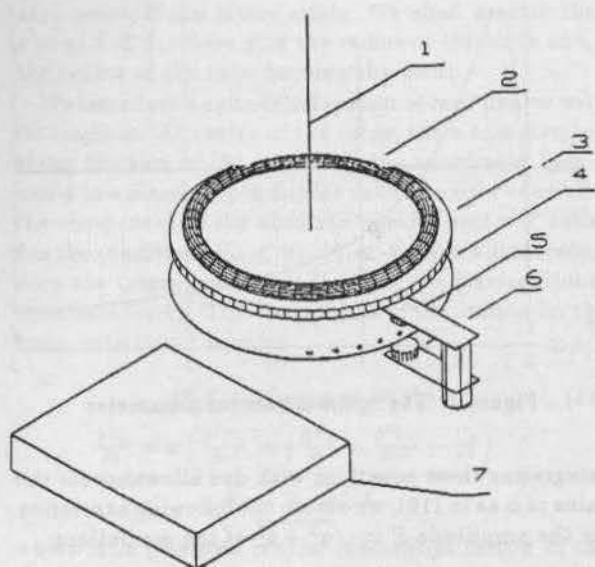


Figure 2: The description of the experiment

can conclude that analytical and experimental results are in good agreement

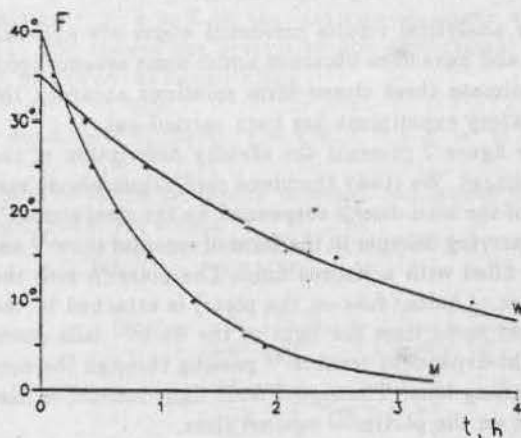


Figure 3: The results of the experiment

5 The damping of a spacecraft oscillations using annular fluid damper

We will consider oscillation damping for a magnetically stabilized spacecraft with toroidal fluid damper. We study the spacecraft oscillations in the plane of magnetopolar elliptical orbit. We assume that torus is located in this plane. The spacecraft equations of motion will take the following form (see Eqs. (1), (11))

$$A \frac{d^2 \varphi}{dt^2} + IH \sin(\varphi - \gamma) = N(V_\phi)$$

$$\frac{\partial V_\phi}{\partial t} = \nu \left(\frac{\partial^2 V_\phi}{\partial r^2} + \frac{1}{r} \frac{\partial V_\phi}{\partial r} + \frac{\partial^2 V_\phi}{\partial \vartheta^2} - \frac{V_\phi}{r^2} \right),$$

$$V_\phi|_S = \frac{d\varphi}{dt} r|_S$$

Using the approach of section 2 and technique of section 3 one can obtain the closed form solution to the amplitude F of spacecraft oscillations with respect to magnetic field line⁴. We give here a final result:

$$F = F_0 \left[\frac{c(\vartheta_0)}{c(\vartheta)} \right]^{1/4} \exp \left[\frac{-2B\Lambda(\vartheta)}{\epsilon A} \right], \quad (23)$$

$$\Lambda = (1 - e^2)^{3/2} \int_{\vartheta_0}^{\vartheta} c(\vartheta) f(1 + e \cos \vartheta)^{-2} d\vartheta,$$

$$f = \nu_0 \sum_{k=1}^{\infty} [c(\vartheta) + \lambda_k^2 \nu_0^2]^{-1}$$

As it follows from (23) the damper influence is determined by one dimensionless parameter ν_0 . Since the integrand in (23) is a 2π -periodic function with respect to ϑ , it is possible to seek for an optimal value of ν_0 such that $\Lambda(2\pi) \rightarrow \max$.

It turns out that for diameter of torus about 20 cm, diameter of tube about 1 cm and period of spacecraft oscillation with respect to magnetic field line about 4 min optimal value ν_0^{opt} is very close to dimensionless viscosity of mercury.

6 Magion-2 & Magion-3 subsatellite attitude determination results

Each of the subsatellite has onboard two toroidal fluid dampers filled up with mercury. The damper parameters are close to ones mentioned above.

To present actual attitude motion we consider the unit vector along a magnetic field line and project the end of this vector onto the plane orthogonal to the magnet axis (see Figure 4-6). If a point belongs to the smallest circle the angle between the magnet axis and magnetic field line is equal to 5 deg. If it belongs to the next circle this angle is equal to 10 deg and so on. A number on a curve means time (min). Figure 4, shows the typical Magion-2 spacecraft attitude determination results. One can see that maximum amplitude of oscillations with respect to magnetic field line is about 25 deg.

The Magion-3 attitude motion differs from one described above. The subsatellite is equipped by gas jets to provide orbital maneuvers. Unfortunately we've got a large eccentricity between $\delta \vec{V}$ direction and the center of mass position. This causes a large disturbing torque and can lead to loss of stabilization.

Figures 5, 6 show the orbital maneuver influence on spacecraft stabilization. The moments of maneuver are marked by M_1, \dots, M_4 . The time separation between the motion presented on these two figures is about 1 day. It should be pointed out that the amplitude of oscillations is rather small before the first maneuver M_1 and before the maneuver M_3 , in other words in this case the damper restores the spacecraft stabilization in a time about 1 day.

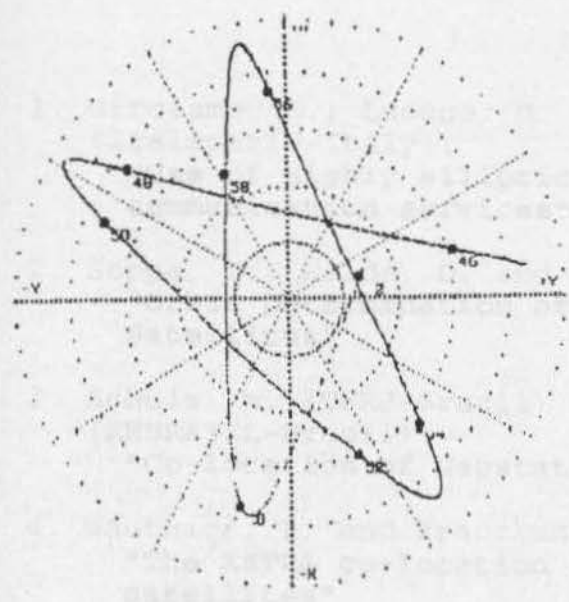


Figure 4: Magion-2 spacecraft attitude determination. Revolution 2402.

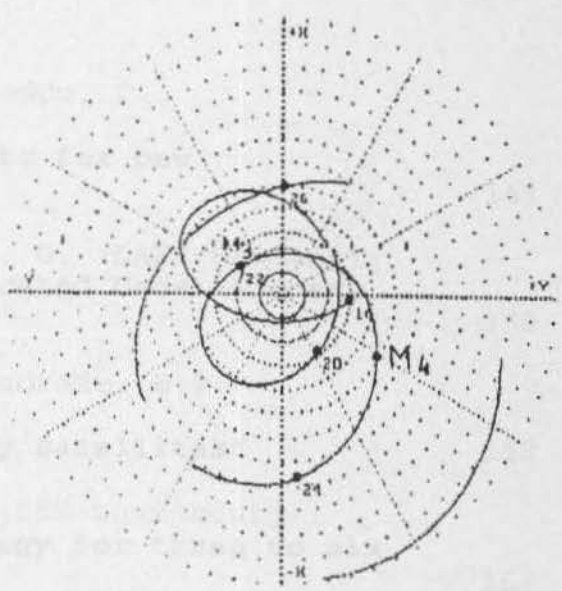


Figure 6: Magion-3 spacecraft attitude determination. Revolution 325.

Acknowledgement

This paper is presented thanks to financial support of Symposium Organizing Committee. The authors are indebted for this support.

References

- ¹Arnold, V.I. (Ed.) 1988, Encyclopaedia of Mathematical Sciences, V. 3, Dynamical Systems III, Springer-Verlag, Berlin, 291 p.
- ²Volosov, V.M., Morgunov, B.I. 1971, The averaging method in the theory of nonlinear oscillatory systems, Izdatel'stvo MGU, Moscow, 507 p. (Russian)
- ³Pivovarov, M.L. 1986, Rotation of a satellite with a large magnetic moment, *Kosm. Issled. (Cosmic Research)*, 24, 6, 816-820. (Russian)
- ⁴Pivovarov, M.L. Magnetically stabilized satellite attitude motion and differential equations with slowly changing coefficients. *3rd International Symposium on Spacecraft Flight Dynamics*, Darmstadt, Germany, 30 Sep.-04 Oct. 1991, p. 317-322. ESA SP-326.

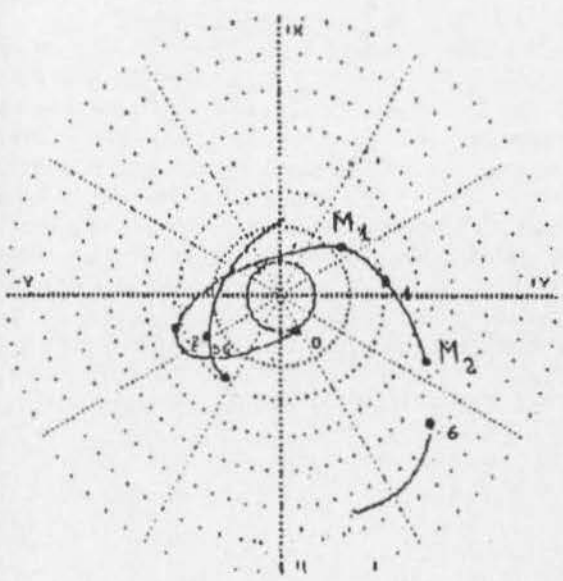


Figure 5: Magion-3 spacecraft attitude determination. Revolution 313.

CONSTELLATION & CO-LOCATION I

1. Girolamo, S.; Luongo, M. and Soddu, C. (Italspazio-Italy): "Use of highly elliptic orbits for new communication services"	143
2. Soppa, U.; Wilde, D. and Baetz, O. (DASA-Germany): "Orbit Determination of Colocated Geostationary Satellites"	150
3. Schulz, W. (UFRJ-Brazil) and Andrade, E.P. (EMBRATEL-Brazil): "Co-location of Geostationary Satellites"	158
4. Wauthier, P. and Francken, P. (SES-Luxembourg): "The ASTRA co-location strategy for three to six satellites"	163

Use of highly elliptic orbits for new communication services

S. Di Girolamo, M. Luongo, C. Soddu

ITALSPAZIO, Via Saccomuro 24 - ROMA - 00131-
Ph. 396 41512293, Fax 396 41512102

Abstract

The use of highly elliptic orbits for communication services can be analyzed according to several parameters, but the final parameter which will determine the adoption of a system instead of another one is the cost of the space infrastructure, when deployed into the selected orbit. Thus, the selection of mission parameters has to be made by comparing their impact on overall system costs. The major parameters concern with:

- coverage;
- number of satellites;
- orbit altitude, inclination, ellipticity.

In general, above parameters have to be selected according to the service requirements, but from their choice will derive the system complexity and the cost, including also the launch cost. Thus, the definition of a convenient space infrastructure for new services has to be assessed through extended trade-offs of above elements, at least. The purpose of this paper is to identify major rules capable to help and simplify the system definition process.

Several architectures are analyzed and compared with many orbit periods. The following topics are considered:

- coverage requirements and mask angle selection;
- radiation environment typical of the selected orbit;
- orbit acquisition and orbit control strategies.

Orbit acquisition is of paramount importance, since, in general, launch cost is a large share of overall system deployment costs. So, the orbit acquisition has to be considered also with reference to the performances of the available launchers, in order to correctly use the launcher capability. A comparison among three launch strategies is presented.

The orbit control is also an important parameter, since it determines the mass of spacecraft, the relevant cost and the launch cost. So, a control strategy having reduced requirement of propellant mass has to be adopted, as the in-plane maneuvers.

Orbit selection has also to be considered with respect to spacecraft attitude, as dictated by the

specific service requirements. In general, the major technical and cost problems concern with the antenna system, which may assume very different configurations according to the orbit choice. For instance, the compensation of zooming, the steering of antenna beams, the rotation of the antenna pattern around the spacecraft nadir axis are typical elements impacting the spacecraft complexity and cost. All above elements are dependent on the selected orbit.

The paper addresses above matter and try to identify the problem solution and the rules applicable to similar cases.

Introduction

The adoption of elliptic orbits for mobile services allows a valuable reduction of multipath interferences at high latitude zones. The multipath reduction is obtained through the combined effect of: a) increasing the grazing angle at the user site; b) adopting directive antennas, still low gain and large beam, but with no gain at low altitude angles. In any other system, the user's terminal makes use of an omni-directional antenna, which makes the terminal sensibly affected by signal reflections, especially at low grazing angles. This is the typical case of mobile services provided with geostationary satellites at high latitude zones.

A wide variety of elliptical orbits may potentially solve the problem of increasing the grazing angle at the user site. Orbits having inclined of about 64° , can be preferred because of:

- their stability,
- the advantage they present with respect to polar orbits in terms of launch performances.

The orbit altitude is a parameter which has to be considered in terms of:

- number of satellites necessary to a continuous service,
- total mass in orbit,
- launch requirements,
- impact on space environment.

Above aspects have to be considered case by case.

Review of Candidate Orbits

A review is presented of some typical orbits and constellations, with different orbit period, ranging from 6 to 24 h. The reference mission is a communication service in the northern Earth hemisphere.

ORBITS	Orbit Period (h)	COVERAGES
TUNDRA	24	40° user's min. elevation over Northern America;
MIO /16h	16	45° user's min. elevation over Europe;
MOLNYIA	12	45° user's min. elevation over Far East.
MIO/8h	8	
MIO/6h	6	

All above constellations can provide continuous coverage over the northern Earth hemisphere. Of course, the spacecraft design and the launcher requirements will be different according to the mission.

The following cases have been analyzed, in order to evidence the geographical zones of potential service:

1. use of 2 satellites in Tundra 24h orbit;
2. use of 6 satellites in MIO/16 orbit;
3. use of 3 satellites in Molnyia 12h orbit;
- 4&5. use of 5 and 6 satellites in MIO8h orbit;
6. use of 8 satellites in MIO/6h orbit.

In the case of Tundra orbit (see Fig. 1), a limited area is covered with two satellites. The advantage of Tundra orbit is the possibility to introduce a service in a selected area with limited investment. The deployments for worldwide service may be made in steps, in correspondance of the areas of interest, as the market requirements arise. Satellites in Tundra orbit may be of interest for radio broadcasting.

Molnyia orbits (see Fig. 2) also may be used. It has to be noted that in Molnyia orbits the delta losses, due to change of satellite-to-earth range distance, have greater impact on the overall system performances, due to the higher dynamic variation of the orbit altitude with respect to Tundra orbit type. Delta losses arise when the spacecraft goes from the hand-off initial point to the apogee point and viceversa to the final hand-off point. Also the zooming of the antenna coverage is more enhanced in Molnyia orbit, making more complex (and costly) the spacecraft antenna design, when referred to Tundra orbit, for instance.

In the case of MIO/16h (see Fig. 3) a system of 4 satellites would present coverage limitations, while a constellation of 5 satellites might be a good solution, with five different orbit planes. Another solution, which could be convenient in terms of coverage and launch deployment, is a constellation of 6 satellites in 3 orbit planes. This configuration provides 50° of mask angle for Europe and Far East.

For MIO 8h orbits we present two cases:

- a) 5 satellites (see Fig. 4);
- b) 6 satellites (see Fig. 5).

A solution with MIO 6h orbit case and 8 satellites (see Fig. 6) may also be adopted. The potential advantage of this configuration is the low altitude of the orbits. The increased number of satellites does not directly imply higher mission costs since the production cost of several spacecraft is driven by the production organization and the cost per Kg may become very low in a mass production.

Another point which may suggest the adoption of a numerous constellation is the possibility to have coverage overlappings which provide additional resources to selected zones. Of course, the interference problem has to be solved. In general, the adoption of spread spectrum techniques makes possible this type of approach.

Orbit Control Strategy

Orbit control is of paramount importance when dealing with inclined and eccentric orbits.

The spacecraft orbit control strategy must be considered in the frame of the selected constellations. The spacecraft must be maintained properly phased in order to avoid any discontinuity in the service coverage. That is: in order to satisfy the mission requirements and to continuously provide the selected services it is needed to maintain the constellation geometry.

Due to the perturbation effects the nominal constellation geometry and phasing will degrade. Hence, an orbit control strategy has to be implemented in order to maintain the constellation architecture.

A low-cost orbit control strategy can be adopted which is addressed only to control the orbit subtrack and the relative shift of satellites in same orbit planes.

This control strategy is based on in-plane maneuvers only. It consists in determining a semiaxis variation which cancels the total subtrack shift or puts the subtrack on the other side with respect to the nominal position.

Above strategy has been specifically studied for HEO orbits and may be applied to any altitude (see [1]). The principally advantage of this kind of strategy is due to the reduced propellant consumption with respect to classical strategies that imply out-of-plane maneuvers.

Antenna Zooming

The antenna zooming should be compensated in order to balance the higher slant range losses when the spacecraft is in proximity of the apogee.

The following delta gain are required, when moving from satellite hand-off points to apogee:

ORBITS	APOGEE (Km)	HAND-OFF (Km)	DELTA LOSSES (dB)
Tundra - 2 sat.s	47256	38700	1.7
MIO/16h - 6 sat.s	50716	40405	2.0
Molnyia - 3 sat.s	39464	23571	4.4
MIO/8 h - 5 sat.s	26859	17690	3.6
MIO/8 h - 6 sat.s	26859	20606	2.3
MIO/6 h - 8 sat.s	19771	14912	2.4

From data shown in the above table it appears that Molnyia constellations present the worst conditions, while the best solution from the delta losses point of view is the adoption of a constellation made up of Tundra orbits.

Radiation Environment

The satellites in Tundra orbit are outside of the intense zone of Van Allen belts, but also MIO orbits present satisfactory characteristics for what concern the radiation integrated during the life.

The Fig. 7 shows the results of the computations which indicate the viability of the system in MIO orbits, since the radiation doses result comparable with GEO satellites; this means that all equipment already qualified for geostationary satellites could be adopted for satellites in MIO orbits, without additional qualification process.

Hand-Over Telecommunication Problems

When a MIO satellite crosses over the first hand-over point, the Earth Surface Footprint has a specific orientation. Then the satellite continues its trajectory, while reaching the apogee point it rotates around the Yaw axis. So, the antenna footprint rotates, as shown in Fig. 8, if the antenna is rigidly connected to spacecraft body.

However a pointing mechanism of the on board antenna can be foreseen according to the mission requirements, especially in the case of a cell coverage over the service area. The adoption of a

counter-rotation mechanism or an electronic beam steering introduces additional complexity on the spacecraft antenna. This fact may represent a limitation on the use of elliptic orbits. Of course, with a broad beam and a single coverage, the antenna rotation has no impact on mission performances. This may be the case of a broadcasting service to a large area, without any frequency reuse.

In Fig. 9 is shown the spacecraft rotation law around Yaw axis for the MIO 8h orbit.

Launch Strategies

The in orbit mass is the most important requirement, when dealing with a multitude of spacecraft. So, the strategies for orbit acquisition have importance, since a new system should be studied in

order to fit as much as possible with the expected launcher performances. In this way it will be possible to optimize the launch costs. Otherwise, a residual mass will be available which will only be reflected into launch extra-costs per Kg of the usefull mass.

The considered constellations present one satellite per orbit plane.

In order to assess the problem areas we have prepared a comparison among three cases:

- 1- injection of satellites in groups into low earth circular orbit and transfer to the final orbit, satellite by satellite, with correct phasing;
- 2- injection of satellites in groups into an orbit higher than the final orbit and transfer to the final orbit, satellite by satellite, with correct phasing.
- 3- direct injection, taken as reference;

An auxiliary propulsion system is necessary for the orbit transfer in the cases 1 and 2.

Fig. 10 indicates the maximum mass availability in the final orbit (BOL mass) and the propellant mass necessary for orbit acquisition. The first table of Fig. 10 illustrates a possible solution for the in orbit injection of more satellites into different orbital planes when a multiple launch configuration is foreseen. Nodal regression provides the necessary drift to reach the wanted orbital plane.

The following two tables of Fig. 10 consider the above mentioned launch strategies making use of two launchers: ARIANE 44 L and PROTON.

The BOL mass has to be optimized to better match the launcher capability. Different sets of requirements derive from the selection of the orbit and the launcher. It has to be remarked anyhow that:

- strategy of injection into low orbit may be convenient for MIO/6h orbit;
- use of 6h orbit with double coverage is equivalent to half the satellite mass.

Conclusion

Six different kinds of satellite constellations for communications services have been considered. The topics which have been analyzed provide a preliminary assessment and to suggest a possible guideline for constellation selection. Of course, a more detailed definition is required with reference to any selected mission, to assess the cost benefits, technology and reliability aspects.

Acknowledgement

The authors wish to acknowledge the contribution and the support of Dr A. Teofilatto President of ITALSPAZIO.

References

- [1] G. Rondinelli, F. Graziani: Orbit Acquisition and Control Strategy for Small Satellites in Inclined Eccentric Orbits, CNES Int. Symp. on Space Dynamics, 6-10 Nov. 1989.
- [2] L. Broglio: Una politica spaziale per il nostro Paese; Il sistema quadriglio; S. Marco project, Roma 1981.
- [3] Comparative analysis of highly inclined orbits for mobile communications and navigation system, ITS-TR-073.A/87, ESA-CONTRACT N.7301/87/F/RD(SC), May 1987.
- [4] Archimedes - Land mobile communication from non-geostationary orbits, An analysis on alternative orbit-keeping methodologies, ITS-TR-127-/88, ESA- CONTRACT N.7301 /87/ F/ RD(SC) RIDER N.1 PART B, Dec. 1988.

ORBIT	ORBIT PERIOD (h)	AVAILAB. (h)	NUMBER OF SAT.s	PERIGEE/APOGEE (Kms)	TRUE ANOMALIES (deg.)	R.A.A.N. (deg.)
TUNDRA	24	12	2	24470/47256	240/120	85/265
MIO/16h*	16	8	5	1000/25716	50/0/180/180/180	50/170/290/50/170/290
MOLNYA	12	8	3	1000/23464	140/215/180	235/115/355
MIO/8 h*	8	4.8	5	1000/25859	141/218/165/0/190	211/139/67/355/283
MIO/8 h*	8	4	6	1000/25859	150/209/150/209/150/209	205/145/85/25/325/265
MIO/6 h*	6	3	8	1000/19771	144.7/215.2/144.7/215.2 144.7/215.2/144.7/215.2	197.5/152.5/107.5/62.5 17.5/332.5/287.5/242.5

* Mio = Multistationary Inclined Orbit
 ** = Availability over the service zone

--- = For one service zone
 --- = A constellation with 5 sat.s is possible, but 6 sat.s concern with only 3 orbit planes.

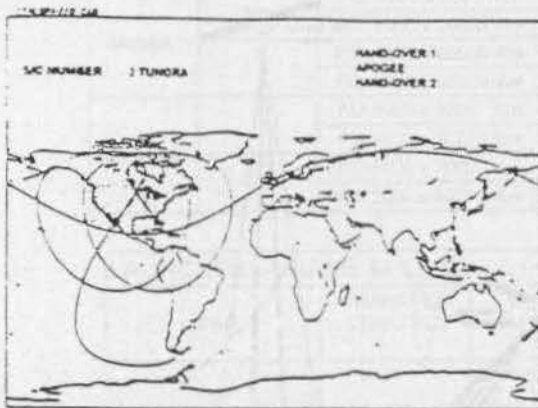


Fig. 1 - 2 S/C in TUNDRA Orbit;
 A service area with 40° of mask angle.

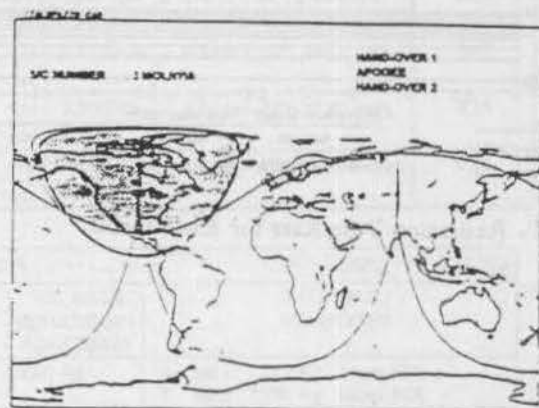


Fig. 2 - 3 S/C in MOLNYA Orbit;
 A service area with 40° of mask angle.

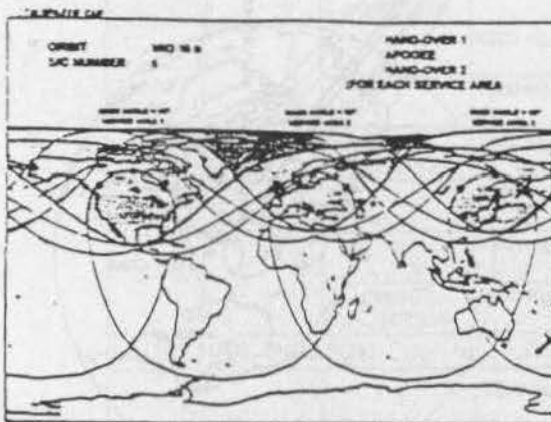


Fig. 3 - 5 S/C in MIO 16h Orbit;
 3 different areas with different mask angles.

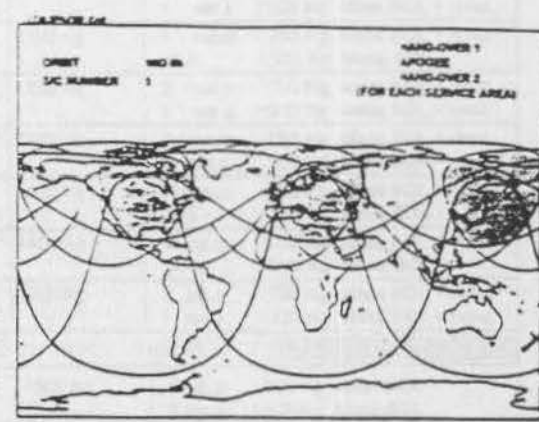


Fig. 4 - 5 S/C in MIO 8h Orbit;
 3 service areas with 40° of mask angle.

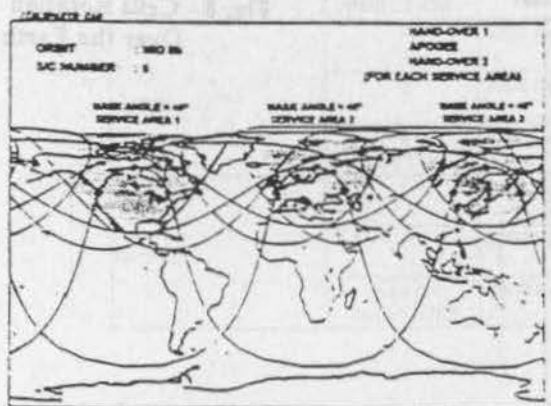


Fig. 5 - 5 S/C in MIO 8h Orbit;
 3 service areas with different mask angles.

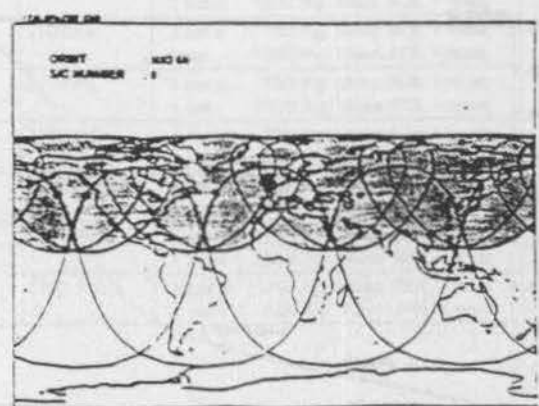


Fig. 6 - 8 S/C in MIO 6h Orbit;
 Earth coverage with 40° of mask angle.

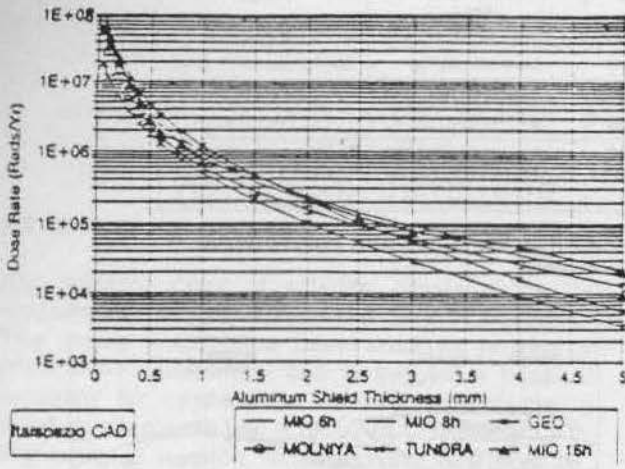


Fig. 7 - Radiation Dose Rate for Each Orbit

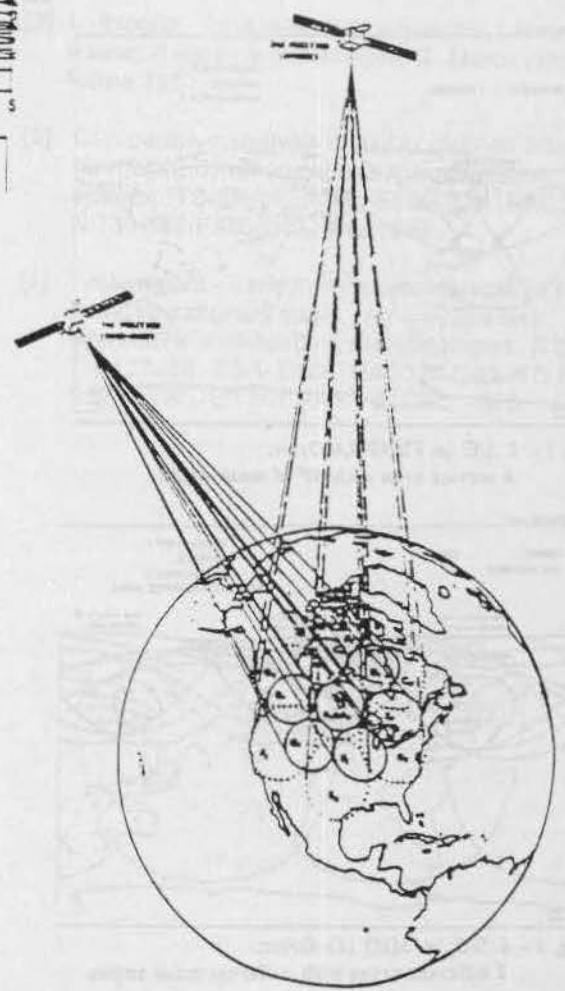
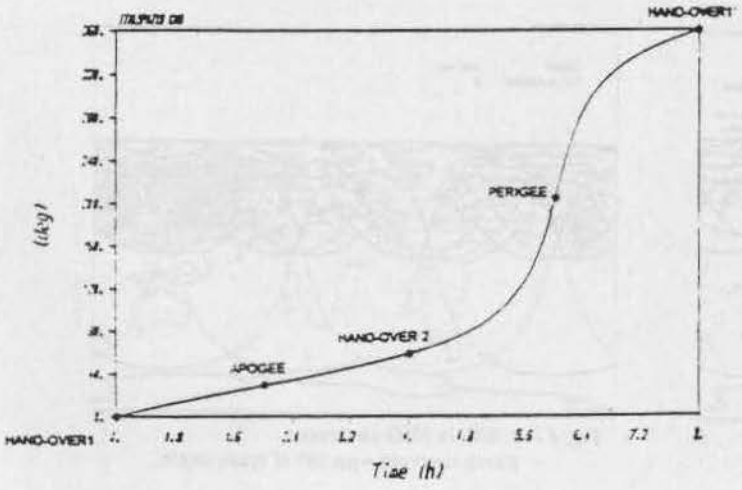


Fig. 8 - Cells Rotation Over the Earth

Fig. 9 - Rotation Law around Yaw axis for MIO 8h Orbit



TRANSFER STRATEGIES						
ORBIT	TRANSFER STRATEGY	PARKING ORBIT (PO)	NODAL REGRESSION			MASS BOL / LAUNCH
		FINAL ORBIT (FO)	DRIFT PER DAYS	Δ DRIFT PER DAY	DAYS FOR Δ RAAN	
MIO/6h	1	PO: 1000 x 1000 Km	-0.27"/day	-2.38"/day	Δ RAAN = 30"; 12.6 days	0.51
		FO: 1000 x 19771 Km	-0.321"/day			
	2	PO: 1000 x 50000 Km	-0.096"/day	-0.225"/day	Δ RAAN = 30"; 133.3 days	0.81
		FO: 1000 x 19771 Km	-0.321"/day			
MIO/8h	1	PO: 1000 x 1000 Km	-2.7"/day	-2.48"/day	Δ RAAN = 60"; 24.2 days	0.24
		FO: 1000 x 26859 Km	-0.22"/day			
	2	PO: 1000 x 50000 Km	-0.096"/day	-0.124"/day	Δ RAAN = 60"; 483.9 days	0.87
		FO: 1000 x 26859 Km	-0.22"/day			
MIO/16h	1	PO: 1000 x 1000 Km	-2.7"/day	-2.606"/day	Δ RAAN = 72"; 27.63 days	0.18
		FO: 1000 x 50716 Km	-0.094"/day			
	2	PO: 1000 x 70000 Km	-0.06"/day	-0.034/day	Δ RAAN = 72"; 2117.6 days	0.95
		FO: 1000 x 50716 Km	-0.094"/day			

LAUNCHER: ARIANE 44 L

ORBIT	TRANSFER STRATEGY	LAUNCH CAPABILITY	BOL MASS (EXCLUDING ADAPTORS)	POSSIBLE SOLUTIONS
MIO/6h	1	6200 Kg	3000 Kg	4 sat.s: 750 Kg Mass BOL 2 sat.s: 1500 Kg Mass BOL
	2	2000 Kg	1500 Kg	2 sat.s: 750 Kg Mass BOL 1 sat.s: 1500 Kg Mass BOL
	DIRECT INJECTION	2900 Kg	2700 Kg	3 sat.s: 750 Kg Mass BOL + resid. 1 sat.s: 1500 Kg Mass BOL + resid.
MIO/8h	1	6200 Kg	1400 Kg	1 sat.s: 750 Kg Mass BOL + resid. N.A. : 1500 Kg Mass BOL
	2	2000 Kg	1650 Kg	2 sat.s: 750 Kg Mass BOL + resid. 1 sat.s: 1500 Kg Mass BOL + resid.
	DIRECT INJECTION	2300 Kg	2100 Kg	2 sat.s: 750 Kg Mass BOL + resid. 1 sat.s: 1500 Kg Mass BOL + resid.
MIO/16h	1	6200 Kg	1000 Kg	1 sat.s: 750 Kg Mass BOL + resid. N.A. : 1500 Kg Mass BOL
	2	1600 Kg	1400 Kg	1 sat.s: 750 Kg Mass BOL + resid. N.A. : 1500 Kg Mass BOL
	DIRECT INJECTION	1900 Kg	1700 Kg	2 sat.s: 750 Kg Mass BOL + resid. 1 sat.s: 1500 Kg Mass BOL + resid.

LAUNCHER: PROTON

ORBIT	TRANSFER STRATEGY	LAUNCH CAPABILITY	BOL MASS (EXCLUDING ADAPTORS)	POSSIBLE SOLUTIONS
MIO/6h	1	9200 Kg	4500 Kg	6 sat.s: 750 Kg Mass BOL 3 sat.s: 1500 Kg Mass BOL
	2	3300 Kg	2500 Kg	3 sat.s: 750 Kg Mass BOL + resid. 1 sat.s: 1500 Kg Mass BOL + resid.
	DIRECT INJECTION	4200 Kg	4000 Kg	5 sat.s: 750 Kg Mass BOL + resid. 2 sat.s: 1500 Kg Mass BOL + resid.
MIO/8h	1	9200 Kg	2100 Kg	2 sat.s: 750 Kg Mass BOL + resid. 1 sat.s: 1500 Kg Mass BOL + resid.
	2	3300 Kg	2750 Kg	3 sat.s: 750 Kg Mass BOL + resid. 1 sat.s: 1500 Kg Mass BOL + resid.
	DIRECT INJECTION	3400 Kg	3200 Kg	4 sat.s: 750 Kg Mass BOL + resid. 2 sat.s: 1500 Kg Mass BOL + resid.
MIO/16h	1	9200 Kg	1500 Kg	2 sat.s: 750 Kg Mass BOL 1 sat.s: 1500 Kg Mass BOL
	2	3300 Kg	2200 Kg	2 sat.s: 750 Kg Mass BOL + resid. 1 sat.s: 1500 Kg Mass BOL + resid.
	DIRECT INJECTION	2800 Kg	2500 Kg	3 sat.s: 750 Kg Mass BOL + resid. 1 sat.s: 1500 Kg Mass BOL + resid.

Fig. 10 - Launch Strategies Comparison.

ORBIT DETERMINATION OF COLOCATED GEOSTATIONARY SATELLITES

U. Soppa, DASA/ERNO, PO Box 105909, D-28259 Bremen, Germany, uwe.soppa@erno.de
D. Wilde, DASA/ERNO, PO Box 105909, D-28259 Bremen, Germany, detlef.wilde@emo.de
O. Baetz, DASA/RS, PO Box 801169, D-81603 Munich, Germany

Abstract

The paper presents the results of two studies on the design, the performance, and a potential application of a tracking system applicable for geostationary satellites which are collocated in the same station keeping window. The first study comprises the analysis of a feasible design for the necessary onboard hardware supporting intersatellite measurements and a performance analysis, carried out as a covariance analysis based on the method of weighted least squares. The results indicate that such a system can provide a significant improvement of the orbit determination enabling even advanced cluster control strategies based on relative navigation. The second study was intended to analyze strategies and techniques for a close collocation of two satellites within only 0.01 deg (≈ 7.3 km) of geocentric arc allowing simultaneous access by a single ground station antenna. The investigations included the development of appropriate control strategies and detailed simulations for their verification. The Monte-Carlo analysis using an Extended Kalman Filter indicate that this so called 'dual-illumination' collocation may be performed with an advanced orbit control strategy combining single ground station range data with intersatellite tracking data.

Key words: Collocation, Intersatellite Tracking, Relative Motion, Station Keeping

Introduction

The steady growth of the geostationary satellite population today already requires to group satellites within clusters sharing the same station keeping window. The satellite density is assessed to increase even more in the next decades especially at those longitudes already frequented above the average today. Therefore, strategies and tools have to be developed in order to operate larger clusters safely within station keeping windows which may be even smaller than 0.1° used today.

So far, collocated geostationary satellites are controlled rather independently, following a coordinated, but not a common control scheme. The safety of the operations is ensured by separation techniques which yield a short term safety by an appropriate separation of the trajectories and allow the orbital parameters to deviate from their nominal values due to perturbations within certain margins.

An advanced control strategy would replace this passive safety concept by a relative navigation which then requires a more frequent determination of the relative orbit. In turn, strategies such as the eccentricity separation or a pure longitude separation, which are difficult to realize due to the poor performance of the traditional tracking system in the along track direction, would become feasible.

In order to support this control concept, the tracking system with intersatellite tracking (ISTRA) needs to be more accurate especially in the direction where the ground based tracking is poor. Also, a fast orbit determination is needed in order to ensure safety after station keeping maneuvers of which the performance errors are the largest perturbation source in the geostationary orbit.

Intersatellite measurements are an attractive candidate for additional tracking data because they can enhance the poor measurement performance of ground stations perpendicular to the ground-to-satellite line of sight.

In particular when dealing with a tight separation like 'dual-illumination' collocation within 0.01 deg of geocentric arc the station keeping performance will benefit from intersatellite tracking data. They provide the base for collocation control maneuvers required in addition to the nominal North/South and East/West maneuvers to maintain within the separation limits.

Onboard Hardware Design

The intersatellite measurements are envisaged to be a complementary tracking device added to the traditional ground station measurements. The general constraints pointed out before can be translated into the following subsystem requirements:

- the measurement shall be obtained by an exchange of an RF signal between the cluster members which needs to support an intersatellite range of about 1 to 100 km, i.e. a dynamical signal range of 40 dB,
- a minimum number of antennas shall be used providing spherical antenna coverage, without using moving parts or other antenna pointing devices.
- interference with other services or other satellites shall be excluded.
- the new system shall be of low weight, low cost, and make a maximum reuse of existing hardware.

Different measurement principles, pure intersatellite ranging and Doppler as well as ranging from ground across the intersatellite link have been considered a priori as applicable measurements subject to a detailed analysis.

The design study has identified four problem areas which will affect the trade off of conceivable designs.

Interference Protection

The problem of interference between the intersatellite tracking devices and other services has a major impact onto other problem areas such as the selection of a suitable frequency

band and the satellite discrimination methods to be applied. Principally, one can distinguish:

- interference of the intersatellite tracking link with any ground - satellite signal and vice versa (e.g. TM/TC)
- interference of the intersatellite transmit signal with the TC signal received by another satellite
- interference of different intersatellite tracking signals within the same satellite cluster

In order to protect the system against any of the a.m. interference cases, a protection margin of at least 20dB has been assessed and the necessary protection methods have been analyzed. For the analysis, typical values have been presumed for the link budgets, such as

- ground station antenna diameter 10m
- ground station signal EIRP is 80dBW
- the received power of the ground station TC uplink signal and of the ISTRA signal is approximately equal
- the ISTRA and the TC receiver onboard the satellite have about the same sensitivity.
- the ISTRA antennas provide a gain range of +3 ... -14dBi within a toroidal area

Taking into account these design parameters, the suppression of the unwanted signal which is required to omit either the interference of the ISTRA transmit signal onto the TM downlink or the TC uplink onto the tracking receiver can be assessed to be 64 and 79 dB, respectively. The only way to realize the suppression requirements is by means of a frequency separation. Filters of any kind are certainly undesirable for the ground stations and would have to be placed onboard resulting in a higher complexity of the onboard system.

The protection of the ISTRA receiver w.r.t. the TM transmit signal from another cluster member requires a signal protection ratio of about 77dB composed of the protection margin (20 dB) plus the gain range of the ISTRA antenna (17 dB) assuming equal EIRP for all cluster members and the envisaged dynamical range of the ISTRA signals (40dB). For this, dedicated discrimination techniques will be discussed below.

It has to be noted however that the strongest interferer will be located onboard the same satellite since every satellite will host receiver and transmitter in order to be able to track any other member of the cluster. Depending on the frequency applied, a protection ratio of 170 dB (VHF-band) up to 190 dB (S-band) will be required. For this, a transmit / receive diplexer shall be used and the transmit / receive frequencies shall be separated by at least 10 %.

Satellite Discrimination

If the geostationary satellite cluster becomes larger than 2 satellites, the discrimination problem has to be solved, be-

cause for almost any satellite separation technique more than one satellite will be inside the antenna field of view at the same time (toroidal coverage assumed).

The following discrimination techniques have been studied:

- time separation (TDMA)
- code separation (CDMA)
- frequency separation (FDMA)

regarding the following trade off criteria:

- number of required RF channels
- number of transmitters / receivers
- cluster growth capability
- length of duty cycle

Here, the time discrimination technique has been selected because it has shown the best characteristics for the first three criteria, which have a considerable impact on the amount of resources (in terms of bandwidth) and hardware (in terms of equipment) to be provided.

The duty cycle, i.e. the fraction of a given reference period which is assigned to a particular intersatellite link, must be seen in relation to the orbital period of 1 day. Tracking data should be equally spaced along this time in order to be able to track the librations of the satellites caused by the residual eccentricity or inclination. Considering that an intersatellite link between two arbitrary satellites yields the same tracking information as the reverse link, the duty cycle for each link within a cluster of 8 satellites is still about 3.5%, i.e. ≈ 50 minutes per day which is available for tracking.

Frequency Allocation

Radio frequencies have been assigned to groups of services established by the ITU. The service of an intersatellite tracking link for satellite collocation has primarily to be allocated to the 'Space Operation Service' (SOS).

Within the study, the available frequency bands within the range from 100 MHz to 100 GHz have been reviewed for a potential use for an intersatellite tracking system. The trade off was made by means of the following criteria:

- potential interference with other services and complexity of protection methods
- RF power demand, which is determined by the receiver threshold and radio frequency dependent free space loss
- the available bandwidth in order to establish a two way measurement system
- availability of H/W components which are ideally space qualified or can be reused from other onboard (sub)systems.

The required transmit power of an ISTRA signal to be used will be determined by the antenna gain characteristics, the dynamical range to be covered, the receiver acquisition threshold and the losses in cables (respectively waveguides) and signal processing equipment.

The values given in fig.1. were calculated applying the design parameters assessed before (minimum antenna gain

-14dB_i, margin for receiver acquisition threshold 0dB). Space qualified hardware is existing for 5W at S-band and about 20W at C-band. Considering the system requirement for a low cost design and acceptable DC power consumption, the solutions above S-band have been disregarded further.

RF band	Transmit Power [W]
VHF	0.008
UHF	0.03
L	1.5
S	5.0
C	80
Ku	300
Ka	2512

Fig. 1.: Transmit Power required to meet the Receiver Acquisition Threshold

As candidates for an implementation of an intersatellite tracking system, the following preferences have been recommended:

- VHF-band (SOS, 137 - 150 MHz)
- L-band (SOS, 1.427 - 1.535 GHz)
- UHF-band (SOS, 272 - 273 MHz)

Measurement Performance

In the simplest case, the measurement error parameters to be used for an analysis of the tracking system performance can be split into stochastic errors and systematic errors, respectively. Preliminary analyses made in the beginning of the study have lead to design objectives for the overall error budget which should be met in order to achieve the performance goals which can be derived from the global requirements of the study drivers.

For example, in order to be able to detect a maneuver burn execution error of about 1.5% for an inclination maneuver (about 2.5 m/s), the desired measurement accuracy has been assessed to be 1 ... 3 % of this error, i.e. ≈ 1 mm/s.

Applying basic relative motion dynamics, one can also set a maximum admissible error for relative position measurements from the desire to determine a maneuver execution error only by means of relative position measurements. Within 3 hours, an in plane maneuver error of the a.m. size yields a position error of about 600 m such that an admissible 3 σ -range error dispersion of 10 m has been assessed as design objective.

Random Errors

The intersatellite range information is obtained on the basis of a sinewave rangetone of 80 kHz, which is used for phase-modulation of the selected RF carrier. After demodulation, the noise impact shall be reduced by a narrow band phase lock loop and an adequate integration time. This yields, for the range tone frequency assumed above, a random error of 10 m (1σ). This error can be achieved with an integration time of

- < 1 sec for 2-way at VHF (100 mW transmit power)
- 10 sec at 2-way S- / L-band

Further reduction is possible by averaging over a number of samples, i.e. an extended integration time.

The error characteristics of the r.m.s. ranging error follows almost a quadratic relationship to the intersatellite distance. Fig. 2. shows the analysis result for the S-band, however, the results are representative also for other bands if the transmit power requirements given in fig. 1. are met. Using a 100 mW transmitter and the VHF band, one even gets a margin of at least 10 dB.

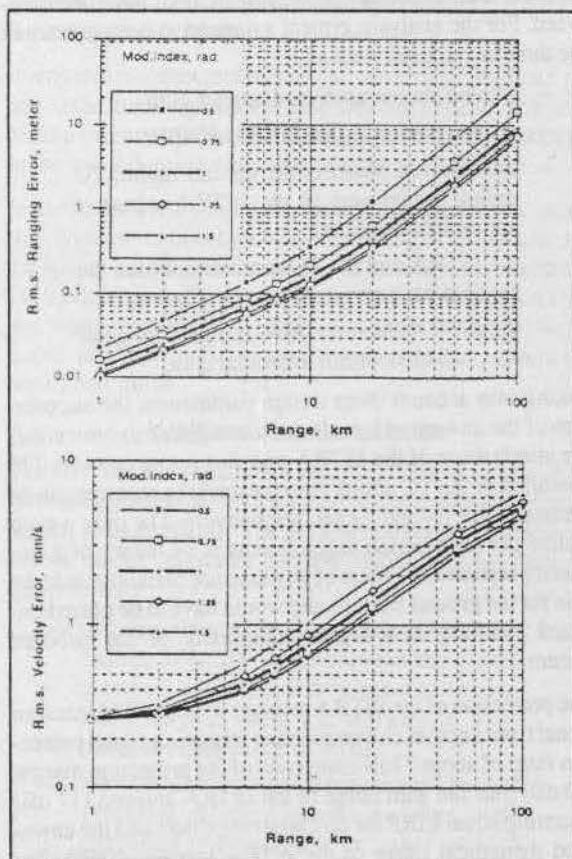


Fig 2.: R.m.s. ranging and Doppler error vs range (2-way system)

Similar characteristics are obtained for other range measurement principles. The three- and four way ranging measurements show a minimum threshold for the r.m.s. ranging error which cannot be passed below due to the fact that the up- and downlink legs from/to earth contribute to the error budget independently from the intersatellite range. This threshold is about 2...5 m for the S-band example, depending on the modulation index.

The error characteristics for range rate measurements is determined by the signal to noise ratio on the RF-link for ranges down to 5 km. The dispersion values shown in fig.2. were obtained for an S-band link and an integration time of 1 second. The slope of the curve is less than 2dB/dB which is due to the counteracting effects of decreasing RF power

and decreasing PLL noise bandwidth, if no AGC (Automatic Gain Control) is implemented. The stochastic error for a given distance can be further reduced by increasing the integration period such that the desired value of a 3σ -dispersion of 1 mm/s can be obtained after ≈ 15 sec.

Systematic Errors

Systematic errors are characterized by relatively slow variations with spectral components below 0.1 ... 1 Hz. Within the scope of the study, systematic errors have been taken into account as constants vs time, accounting for variations within the tracking period by an uncertainty boundary which encloses probable long term variations.

Systematic errors for the application envisaged for ISTRA break down into

- uncertainty of the transponder delay
- errors from the ranging equipment
- errors from the velocity meter
- time tagging error for measurement downlink (for range and velocity measurements)

Systematical ranging errors can be significantly reduced if the equipment is calibrated. Following ESA standard requirements, the resulting systematic errors originating from transponder and ranging equipment will be 4.5 m without calibration and 0.75 m with calibration (S-band, 2-way measurement). Systematic errors originating from the digital measurement of the signal phase delay are in the range of 2.5 ... 5.1 m.

Systematic velocity measurement errors can be limited to 0.75 mm/s for a 2-way system, applying ultra stable oscillators with a frequency stability of $5e-9$.

Time tagging errors are assessed to be not more than 500 ms which is the average TM frame period.

Design Specification

The design studies presented above have resulted in the specification of a feasible hardware design satisfying the design constraints of the study and which is supposed to meet the performance objectives.

In order to ensure continuous coverage, an antenna configuration composed of two quarter-wavelength monopoles arranged on opposite sides of the S/C. This provides approximately a half-wave dipole characteristic and a visibility of 360° inside the orbital plane, and $\pm 55^\circ$ out of plane, respectively.

The overall weight for a non redundant onboard device has been evaluated to be about 4.2 kg, and the DC power consumption will be less than 15 W.

Tracking System Performance Analysis

In order to investigate whether a tracking system as described in the previous chapter can enable an orbit determination which is sufficient for advanced cluster control operations, a numerical analysis of the residual estimation errors using intersatellite measurements has been performed.

Typical ground station performance has been assessed and for all variations except those explicitly focussing onto the sensitivity of the estimation to intersatellite tracking system errors, the performance data derived from the onboard H/W design has been used.

Since the application of intersatellite measurements is supposed to be an add-on to the traditional orbit determination operations, the analysis has been built on the method of weighted least squares used for most orbit determination applications today. The covariance analysis was chosen because the need for a considerable amount of parameter variations disqualified the execution of intensive Monte Carlo studies.

The applied analysis method provides an estimate of the uncertainty of an orbit determination run which is due to the uncertainty of the measurements, system parameter uncertainties and the a priori uncertainty of the solve for parameter vector.

The analysis presumes that the orbit determination has converged and the result is sufficiently close to the reference trajectory such that the error of the estimated covariance matrix is negligible. Under this circumstances, the observation matrices can be calculated on the basis of the reference trajectory data.

The system parameters subject to the error analysis were split into (maximum number of parameters given in parentheses)

- solve for or consider parameters
 - satellite Cartesian state vector w.r.t. the nominal station keeping point (2 x 6)
 - maneuver burn components (2 x 3)
 - area-to-mass ratio (2 x 1)
 - ground station biases (2 x 3)
 - measurement biases (constant or state vector dependant, e.g. the time tagging error)
- 'non formal' parameters
 - reference trajectory shape
 - maneuvers
 - tracking schedule
 - measurement noise characteristics

The analysis of the tracking system was carried out as a variation of the a.m. system parameters and a comparison of the residual estimation uncertainty. For interpretation purposes, the estimation errors of the relative state variables have been used, focussing on the goal to use intersatellite tracking as a means to introduce relative navigation within the geostationary cluster rather than maneuvering the satellites relative to their nominal station keeping point.

Free Flight Orbit Determination

In a first step, the achievable orbit determination accuracy for a two satellite cluster without station keeping maneuvers

was investigated. In opposition to pure ground station tracking, the separation strategy considerably affects the measurement geometry and therefore the accuracy of the estimation.

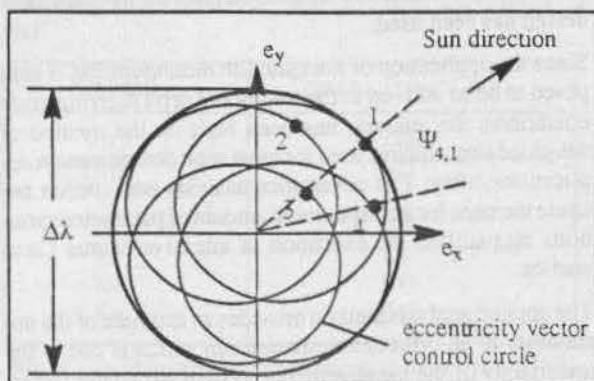


Fig. 3.: Eccentricity separation strategy for a cluster of 4 satellites

Within a larger cluster, the eccentricity and inclination vectors are usually arranged according to a certain pattern such as the one shown in fig. 3. The separation of two satellites is consequently described by the station keeping window size $\Delta\lambda$ and the separation angle Ψ . The closer the eccentricity (or inclination) vectors are set, the closer the satellite separation comes to a pure longitude separation.

The analysis was at first carried out without any dynamics system biases, i.e. assuming an error free state prediction. By this, the calculated estimation uncertainty was only due to the geometrical measurement conditions and due to measurement errors. Although differences in the estimation uncertainty were found for different separation strategies, the errors due to measurement imperfection were rather insensitive to the separation strategy and small w.r.t. the errors induced by orbit prediction uncertainties. Overall, the worst performance still yielded residual estimation uncertainties of $< 5\text{m}$ and 0.5mm/s in plane and 20m (1mm/s) out of plane.

A closer collocation enhanced this orbit determination performance due to the improvement of the measurement performance.

Secondly, the effect of dynamics system biases due to

- an uncertain area-to-mass ratio (causing differential solar radiation pressure effects)
- autonomous S/C maneuvers, in particular wheel momentum offloading, which may cause a ΔV of several mm/s/day

have been taken into account as consider parameters. The results revealed that these effects are dominating the error budget of the orbit determination, overruling the smaller effects of the intersatellite measurement types and the separation strategy.

One can observe that the secular growth of the prediction error of in plane state components cannot be removed completely by the estimation. In opposition, the error of the out

of plane component, only little affected by the perturbation decreases due to the larger tracking data sample size.

However, already after a short tracking period of 1 day, the residual relative position error is in the order of $5\text{...}30\text{m}$ for all three spatial directions, and still below 100m even in the presence of uncertain maneuvers of 5mm/s/day which have been assumed as a worst case assumption on the effect of wheel offloading compensation.

In opposition, the ground station tracking without intersatellite measurements required much longer tracking period before the minimum position error was achieved and the magnitude of this residual error was much larger, i.e. about 150m radial, 400m along track and 1400m out of plane.

Maneuver Error Estimation

The second major point for the numerical tracking system analysis was to investigate the benefit of intersatellite measurements to the estimation of station keeping maneuvers respectively their performance errors. In particular, the size of the (unwanted) in plane components of the maneuver needs to be estimated in order to counteract a potential relative drift of the cluster members.

The analysis considered three different scenarios

- inclination maneuvers with chemical propulsion
- inclination maneuver with ion propulsion
- longitude maneuver with chemical propulsion

As a representative case, the inclination maneuver imposing the largest execution errors shall be discussed hereafter.

It has been presumed that the two satellites execute their maneuvers simultaneously. One can take advantage of the possibility to solve for the relative effect of the maneuver which may even vanish if the satellites are in a pure longitude separation. Only the deviation from the nominal relative effect needs to be compensated quickly whereas an offset of the absolute maneuver vector from its nominal value may be tolerable if no station keeping window violation occurs.

Different tracking schedules and separation strategies have been tried within the analysis and the best results have been obtained for a scenario splitting the tracking period at the maneuver epoch and solving for the satellite state vector only. The obtained result is then used as an a priori estimator for the maneuver burn estimation following after a period of intense (every $10\text{...}15\text{min}$) tracking for several hours.

This method reduces the amount of solve for variables for every part of the estimation and consequently reduces the amount of tracking data to be acquired.

The results can be summarized as follows:

- the in plane maneuver error components can be estimated within a tolerance of 1mm/s in about $3\text{...}6$ hours following the maneuver
- intersatellite velocity measurements by means of Doppler or integrated Doppler yield

the best results for the time immediately after a maneuver

- if the available tracking period after the maneuver is longer than 6 hours, intersatellite range measurements yielded better results

The application of ion thrust propulsion for inclination station keeping requires a thruster firing once or twice per day. This reduces the time available for tracking because it has proven to be impractical to solve for two consecutive maneuvers at once. The typical performance of ion thrusters available today requires to fire the engine for a few hours.

Analysis runs have been performed for this type of scenario and the estimated residual error for the maneuver was found to be $< 1\%$ for the magnitude and $\approx 1.0^\circ$ (radial) respectively 0.1° (tangential) for the vector misalignment. Though 1° is of the same order of magnitude as performance specifications for ion thrusters, the good observability of the along track component would be sufficient for safe relative navigation.

Perturbations due to Autonomous S/C Maneuvers

As mentioned earlier, the side effects of autonomous spacecraft operations may induce significant perturbations into the relative motion. Reaction wheels carried onboard of geostationary satellites are an example for this. As well, the orientation of the solar arrays may be done autonomously which alters the area-to-mass ratio of the satellite.

Unfortunately, these actions are mostly unpredictable and can therefore not be taken into account properly in the orbit determination process. Considering future collocation scenarios which may require intersatellite distances of only a few kilometers, a drift of about 800 m/day introduced by a velocity increment of only 5 mm/s along track is not acceptable.

In opposition to the solar radiation pressure, the error in position and velocity building up due to a maneuver unknown in magnitude, direction and epoch is not reflected by the linearized equations of motion used for the differential correction of the a priori estimate.

If the maneuver epoch is made available to the orbit determination process, it can be solved for by the orbit determination program. The minimum residual estimation uncertainty however is limited if the perturbation occurs once a day or even more often. Assuming a daily offloading maneuver, the analysis has shown that the induced ΔV can be estimated to an accuracy of about 10 % of the expected effect.

Operational Concepts

Although the baseline for the tracking system performance analysis has been a two satellite cluster, the conclusions can be transferred to larger clusters. For clusters of more than two satellites, a cooperation of different satellite control centers is rather likely. Within the intersatellite tracking study, the organization of such a cooperation has been investigated in order to ensure operational flexibility and inde-

pendence on one side while maintaining safety and station keeping accuracy on the other side.

The results obtained by the numerical performance analysis allow the conclusions that

- the proposed system allows collocation within less than 10 km intersatellite distance
- one ground station in combination with intersatellite tracking is sufficient to ensure the required relative orbit determination accuracy
- decentralized orbit determination is feasible such as outlined in fig. 4, where a full visibility of the relative states is supplied without control center communication.

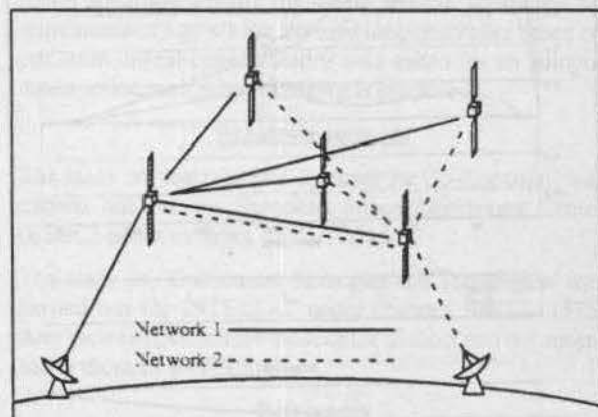


Fig. 4.: Tracking Configuration for a cluster operated by two control centers

Collocation Control Strategies

For the control aspect of cluster operations, the conventional station keeping activities and the relative motion control maneuvers have to be distinguished. With intersatellite tracking, it appears to be possible

- to perform conventional station keeping maneuvers simultaneously which requires to centralize the maneuver planning activities
- to execute relative motion control maneuvers whenever they are necessary to avoid window or proximity violations.

In case of heterogeneous clusters it would be suitable to perform a decentralized planning of relative maneuvers. Although the results from the tracking system performance analysis indicate sufficient control margins to do so, the feasibility of this concept still needs some further analyses. For the purpose of dual-illumination collocation under responsibility of a single control center, two control strategies have been developed and verified.

The first concept is a digital controller based on optimum control theory. It uses the discrete inplane state equations of the solution of the Clohessy-Wiltshire equations describing the relative motion of two closely separated satellites. Applying a quadratic cost function the steady state inplane con-

control law was derived by solving the discrete Riccati equation [2.]. The control law is then

$$\begin{bmatrix} \Delta v_{rad} \\ \Delta v_{tang} \end{bmatrix} = -\underline{G} [\underline{x} - \underline{x}_{nom}]$$

where \underline{x} and \underline{x}_{nom} are the actual and nominal inplane position and velocity vector. Figure 5. illustrates the elements of the 2x4 gain matrix G as function of the step size. Note that in GEO 15 deg are equivalent to 1 hour.

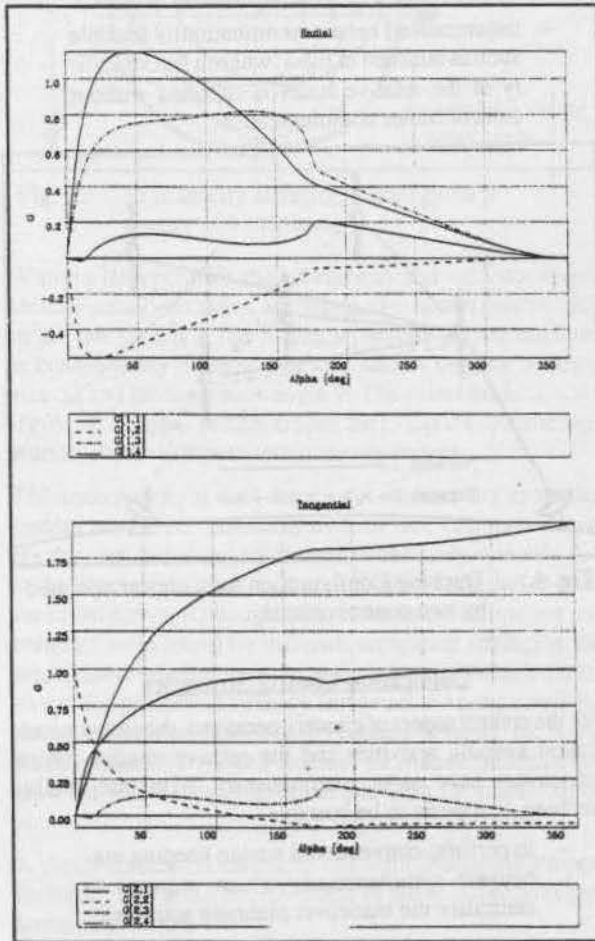


Fig. 5.: Closed loop controller gains

The simulations performed indicated that with such a closed loop control concept very high collocation control performances can be achieved, i.e. for dual-illumination collocation within 0.01 deg large margins w.r.t. to the limits are obtained. Optimum controller cycles of about 8 hours and an extra Δv of about 1-10 % to maintain collocation were found. It can be concluded that such a control concept should be applied for a potential future autonomous station keeping within very close limits of e.g. < 1 km. However for the purpose of collocation within 0.01 deg (7.3 km) it does not make best use the time and tolerance margins. Therefore a second so called adaptive open loop control concept was developed and tested trying to make use of those margins in or-

der to minimize as far possible additional thruster control activities.

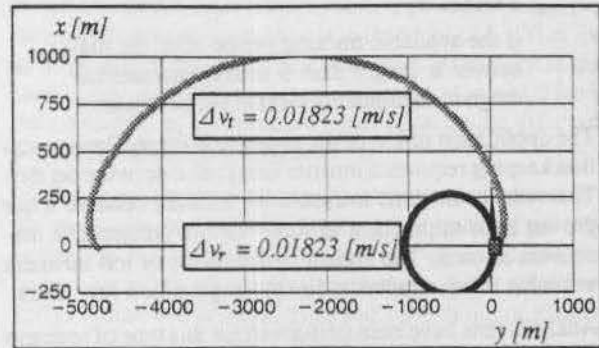


Fig. 6.: N/S maneuver cross couplings

With the adaptive open loop control concept an extra collocation control maneuver (relative motion station keeping) is performed only in case of a predicted violation. For this only the standard East/West thrusters are applied, i.e. only tangential control maneuvers can be executed. The strategy makes use of the statistic behavior of the most critical collocation violation source, i.e. the cross couplings of a North/South maneuver. Depending on the size and the direction of the cross couplings different control demands are given. Figure 6. shows that in particular the drift effects of tangential velocity error increments are critical, whereas radial errors are of less importance.

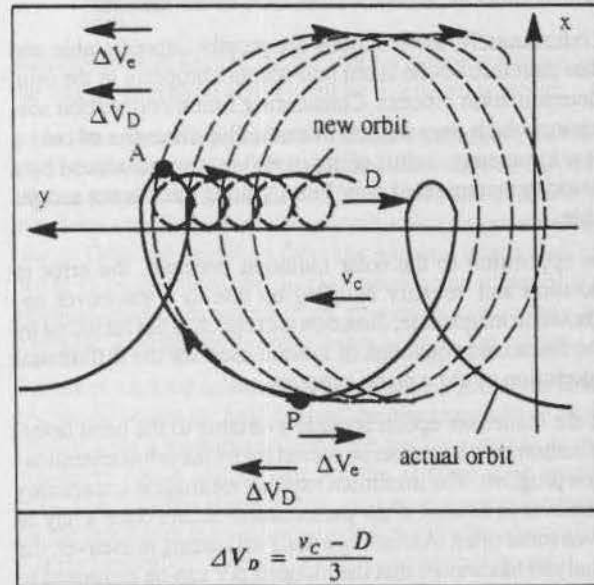


Fig. 7.: Optimum drift maneuver

In case of small statistical errors collocation can be maintained up to the next nominal East/West maneuver without any additional control activity. In case of larger errors the relative drift needs to be controlled, where typically sufficient time is available to wait to the next optimum maneuver point allowing a simultaneous improvement of the relative eccentricity (see figure 7.). Only in extreme situations the drift correction must be performed very soon. By this the effects of tangential cross couplings can be compensated

however radial error effects cannot be covered. Fortunately they are rather small and can be covered by providing sufficient margin w.r.t. the collocation limits at the North/South maneuver.

The tasks of the adaptive open loop control strategy thus is twofold :

- monitoring of the collocation geometry up to the next nominal station keeping maneuver
- determination and execution of a dedicated relative drift maneuver in case of a predicted collocation violation

The simulations confirmed that with such strategy a dual-illumination collocation within 0.01 deg of geocentric arc can be performed with an effort of about 1 - 1.5 collocation control maneuvers per 14 day station keeping cycle (chemical thrusters) and an extra Δv of less than 0.5 % as long as the differential area to mass ratio is negligible. Relevant area to mass ratios lead to station keeping cycle limitations of e.g. 7 days for 0.01 m²/kg difference, collocation however is still feasible. The combination of single station range with the ISL RF link gives better results than a two station ranging, although it should be noted that both are feasible tracking schemes. Wheel unloading must have a statistical character while the maneuver epoch should be known. A longitude/inclination separation is advantageous w.r.t. an eccentricity/inclination separation. For the application of ion North/South thrusters with daily inclination station keeping maneuvers similar performances were achieved.

Conclusions & Recommendations

The study of an intersatellite tracking system applicable for the orbit determination of geostationary satellite clusters has shown that a system based on RF signals providing either intersatellite range or range rate would be sufficient to achieve the goal to navigate the satellites within a proximity of a few kilometers. Within the cluster, the satellites will then be controlled relative to each other rather than w.r.t. the nominal geostationary station keeping point.

This has been analyzed by means of a covariance analysis indicating that the required position and velocity estimation accuracy can be realized and that the performance errors of station keeping maneuvers can be detected within a few hours after the maneuver has been executed which is sufficient to compensate an unwanted relative drift.

The dominating contribution to the estimation error budget originates from the uncertainty of system parameters such as the satellite area-to-mass ratio or autonomous S/C maneuvers. However, intersatellite tracking can help to keep the position and velocity uncertainty small even in the presence of this perturbations. This especially holds for the tangential direction which is the most crucial component w.r.t. safety considerations.

The type of satellite separation strategy applied was found to be of minor relevance for the system performance and it can be concluded that intersatellite tracking allows to operate the cluster even with separation strategies which are not feasible today.

As a combined trade off of the results obtained from the design analysis and the performance analysis a recommendation for an onboard system is made which is composed of a two-way measurement system operating in the VHF band and providing range and (integrated) Doppler simultaneously. Hemispherical coverage is required and satellite discrimination shall preferably be performed by time multiplexing.

Depending on the separation limits different collocation control strategies are proposed. For larger limits of e.g. 0.1 deg no specific collocation control maneuvers are required if the satellites involved follow a coordinated nominal station keeping strategy [6],[7]. For medium separation requirements like dual-illumination collocation within 0.01 deg an adaptive control strategy performing relative drift control maneuvers only in case of a predicted violation was found adequate. Finally for strong relative separation requirements of e.g. < 1 km a closed loop controller based on optimum digital control theory well suited for an autonomous collocation station keeping is proposed.

Acknowledgement

The study on 'Intersatellite Tracking for Co-Location' was carried out for the European Space Operations Center (ESOC) under contract 10035/92/D/CS.

The study on 'Collocation Strategies and Techniques' was carried out for INTELSAT under contract INTEL-1335. Any views expressed are those of the authors and not necessarily those of INTELSAT.

References

- [1.] E.M.Soop; Introduction to geostationary orbits; ESA-SP-1053
- [2.] R.H.Vassar, R.B.Sherwood; Formation Keeping for a Pair of Satellites in a Circular Orbit; Journal Guidance, No.2, March / April 1985
- [3.] Station Keeping Strategies for Colocated Satellites; Final Report; ESA study contract 9297/91/NL/PM
- [4.] Mathematical Theory of the Goddard Trajectory Determination System; NASA-TM-X-71006, April 1976
- [5.] U. Soppa & O. Baetz ; Orbit Determination of Colocated Geostationary Satellites using Intersatellite Tracking Data; IAF-93-A.5.37, Graz, Austria, 1993
- [6.] T. Görlach & U. Brüge; A Solution for the Collocation Problem at 19 deg W and for Future Design; FAC-Symposium, Ottobrunn, Germany, 1992
- [7.] T. Görlach & U. Brüge; Solutions for the Geostationary Collocation Problem; AIAA GNC Conference, Monterey, CA, USA, 1993

CO-LOCATION OF GEOSTATIONARY SATELLITES

Walkiria Schulz
Evandro Paiva de Andrade

Universidade Federal do Rio de Janeiro
DTS-33 - Applied Celestial Mechanics Section - Space Segment Division - EMBRATEL
Av. Pres. Vargas, 1012 / 610 - Centro - Rio de Janeiro - RJ - Brasil
walkiria@dts-3.ebt.anrj.br

Abstract

Over the past years, several studies have established a solid basis for the development of close-by and dual illumination co-location control strategies. The scope of this paper is to evaluate them in order to plan the transition of services from BRASILSAT A2 to BRASILSAT B1 using one of these technics. A number of separation strategies for the co-located satellites were considered, in particular the strategy of inclination and/or eccentricity vector separation. The inclination and eccentricity vector separation were found promising for dual illumination co-location of the BRASILSATs with minimal collision and occultation risks.

Key words: Co-location, Strategies, BRASILSATs.

1. Introduction

Co-location is the maintenance of more than one satellite in the same tolerance window.

If a single satellite is to be kept within a given angular region around its nominal position, in spite of the continuously acting perturbations, orbit correction maneuvers have to be performed from time to time. This is done by means of an on-board propulsion system which is, in general, able to produce thrusts in north/south or in east/west directions. It is operationally convenient to perform the correction maneuvers periodically, as a sequence of repeating correction cycles on such a way that the maneuvers acquire typical characteristics which form a first criterion to verify them. EMBRATEL accomplishes its orbital corrections maneuvers with periods equal to an integer number of weeks so as to plan the maneuvers always on the same weekday.

The maneuver epochs and the velocity increments are computed on the basis of the latest orbit determination and a set of orbital elements, which have to be reached at prescribed times, are computed at the end of each cycle. The target orbital elements are time-dependent and defined for each correction cycle by the stationkeeping strategy in terms of:

Mean drift rate;

Mean longitude offset from the window center;

Eccentricity vector components:

$$e_x = e \cos(\Omega + \omega)$$

$$e_y = e \sin(\Omega + \omega);$$

Inclination vector components:

$$i_x = i \cos(\Omega)$$

$$i_y = i \sin(\Omega).$$

with the aim to minimize the fuel required and to extended satellite lifetime. In these definitions the symbols e , i , ω , Ω denote the classical orbital elements with the usual meaning.

At a specific orbital location, a pair of satellites can be operated in two ways: "close-by" configuration where the two satellites would remain within the $\pm 0.1^\circ$ window but have completely separate ground network for communication links. This configuration is relatively straight forward, where two satellites would be maintained in adjacent and exclusive $\pm 0.05^\circ$ longitude bands, requiring minimum of stationkeeping coordination.

The second configuration is designed "dual illumination", where the spacecraft separation is maintained within 0.05° or less. This would allow simultaneous access of both satellites from a single antenna.

2. Orbital Control

To further improve the performance for smaller communication antennas and particularly to allow the use of larger antennas used for control, without excessive link losses, the maximum separation between two satellites should preferably be reduced to 0.05° according to previous analysis done by EMBRATEL.

The lower limit for co-location is set by the need to avoid sensor interference between two closely located satellites, to allow for the inaccuracy in orbit determination and the need to reduce, as much as possible, the probability of any physical contact between the two satellites. Based on recommended Hughes

procedure, it is confirmed that smaller than 0.01° (7 Km) separation between two satellites would result in excessive risk.

A numbers of factors control the upper angular separation limit between two co-located satellites. If, after the co-location, only the natural forces were allowed to act on both the satellites (i.e. no stationkeeping or attitude control maneuver were performed) then the two satellites would remain stationary in respect to each other, assuming their area/mass ratios are equal.

However, solar radiation and the gravitational forces would not allow the satellites to stay within their respective east/west and north/south stationkeeping boxes; therefore, each satellite needs to be controlled to keep it in the assigned orbital location and also to maintain its proper attitude.

The total time required for collecting sufficient range data, planning and executing the maneuver is approximately twenty-four hours. The disturbing forces resulting from the north/south maneuver in east/west direction could be up to 0.005° per day for a single satellite. For co-located satellites, in the worst case, where both satellites would have opposite errors, the effective change in the separation angle could be up to 0.01° in one day. To ensure the lower limit of 0.01° , the maneuvers would have to be done at 0.02° separation angle and therefore, the upper limit would be 0.03° ($0.02^\circ + 0.01^\circ$).

For some co-location strategies the stationkeeping maneuvers need to be simultaneous and, in this case, for both north/south and east/west maneuvers a delay of up to thirty minutes could be tolerated without exceeding the co-location limits of either or both satellites. If the maneuvers are delayed for both satellites, the impact is smaller and could be tolerated for much longer time (up to next maneuver cycle), since both are synchronously affected. If a maneuver is delayed for one satellite for more than thirty minutes but not for the other, the relative motion would be affected and an additional corrective maneuver would probably be required within twenty-four hours. Considering the operational restrictions that such strategies impose, EMBRATEL is not planning to accomplish simultaneous maneuvers.

When two satellites are co-located, it's more important to perform all the maneuvers in proper sequence at scheduled time compared to the singly located satellite.

North/South Stationkeeping

The gravitational attraction of the sun and moon causes the orbit plane to precess relative to the equatorial plane at about 0.85 deg/year.

To meet the co-location requirements, the orbit planes would be nearly coincident to allow the separation margin to be used for the more difficult east/west stationkeeping. A small separation of 0.005° would be maintained between the orbital planes. This assures some latitude separation except twice per day when the satellites are at the intersection of the orbital planes. A benefit of this is to

increase the magnitude of physical separation in the event that co-location is interrupted, and one satellite passes the other in longitude.

East/West Stationkeeping

The east/west motion is the superposition of two effects: acceleration in longitude caused by the Earth's triaxiality and a 24 hour oscillation in longitude from the orbit eccentricity caused by solar radiation force. The first effect is the same for both satellites because their longitudinal separation is so small. The second effect is a property of the satellite, specifically its area/mass ratio.

The east/west maneuvers are nominally performed at 18:00 Hs satellite local time for BRASILSATs, so, the eccentricity and longitude acceleration effects can both be controlled simultaneously, without the needed of fuel consumption for the eccentricity control.

3. Co-location Strategies

Latitude / Radius Separation

In this strategy the orbital parameters inclination and eccentricity are controlled in such a way as to guarantee that when the two satellites' latitudes are equal, their radii are significantly different and vice versa.

One advantage of this method is that longitude separation is never required. However, the two longitude/drift cycles should be exactly out of phase with each other on such a way that the maneuvers on the two satellites should be one half cycle apart, and that when one satellite's mean longitude is on the western end of its path, the other satellite's mean longitude is on the eastern end. The reasons for this are related to the fact that each inclination maneuver should be followed (by about two days) by drift and eccentricity maneuvers.

The first reason comes from the fact that, in each half cycle, the stationkeeping operations can be concentrated on just one satellite. The only maneuvers required for the other satellite will be the attitude control. This is the least complicated way of stationkeeping two satellites simultaneously.

The second reason is to maintain a systematic difference between the two satellites' inclination vectors. If both satellites' inclination maneuvers were to be scheduled on the same day, then since the targeting strategies used for both are the same, the two satellites' inclination vectors would be kept approximately equal, and then their latitudes would be near equal all the time. The latitude/radius separation strategy rather relies upon the fact that the two satellites latitudes will agree at two predictable times each day and the rest of the time they will be significantly different.

A derivation of the times at which the two satellites' latitudes will agree depends on an understanding of the perturbations affecting inclination and of the strategy

followed to control inclination under the influence of those perturbations. Among the perturbations on the inclination vector, the main long period terms are the secular and the $2\omega_s$ term, where ω_s is the sun frequency (0.9856 deg/day). The secular term is the largest one and varies over an 18.6 year cycle, with:

$$\dot{k}2_{\text{sec}} = -0.132 \sin(\Lambda_M) \quad (1)$$

$$\dot{h}2_{\text{sec}} = 0.0852 + 0.098 \cos(\Lambda_M) \quad (2)$$

where Λ_M is the right ascension of the ascending node of the moon orbit. Thus the magnitude of the secular term varies between approximately 0.75 and 0.95 deg/year.

The $2\omega_s$ term, if it were acting by itself, would pull the inclination vector around a cycle of radius 0.023° every 6 months.

Over each half cycle, the two inclination vectors will experience the same perturbations effects and will maintain a constant relative difference.

The two times of the day at which the two satellites' latitudes are equal will be when the right ascension of the two satellites equals the right ascension of the ascending or descending node of the relative inclination vector between the two satellites^[1].

For $N = 1, 2$:

i_N = inclination of satellite N

Ω_N = ascending node of satellite N

S = right ascension of both satellites

$L_N = i_N \sin(S - \Omega_N)$ = latitude of satellite N

$k2_N = i_N \cos(\Omega_N)$

$h2_N = i_N \sin(\Omega_N)$

then:

$$\Delta k2 = k2_2 - k2_1 = i_2 \cos(\Omega_2) - i_1 \cos(\Omega_1) \quad (3)$$

$$\Delta h2 = h2_2 - h2_1 = i_2 \sin(\Omega_2) - i_1 \sin(\Omega_1) \quad (4)$$

$$\tan(\Omega_{\text{rel}}) = \frac{\Delta h2}{\Delta k2} = \frac{i_2 \sin(\Omega_2) - i_1 \sin(\Omega_1)}{i_2 \cos(\Omega_2) - i_1 \cos(\Omega_1)} \quad (5)$$

$$L_N = i_N \sin(S) \cos(\Omega_N) - i_N \cos(S) \sin(\Omega_N) \quad (6)$$

$L_1 = L_2$ implies:

$$\sin(S) [i_2 \cos(\Omega_2) - i_1 \cos(\Omega_1)] = \cos(S) [i_2 \sin(\Omega_2) - i_1 \sin(\Omega_1)] \quad (7)$$

then:

$$\tan(S) = \frac{\sin(S)}{\cos(S)} = \frac{i_2 \sin(\Omega_2) - i_1 \sin(\Omega_1)}{i_2 \cos(\Omega_2) - i_1 \cos(\Omega_1)} \quad (8)$$

$$(5) = (8) \rightarrow \tan(\Omega_{\text{rel}}) = \tan(S) \quad (9)$$

which implies $S = \Omega_{\text{rel}}$ or $\Omega_{\text{rel}} + 180^\circ$. But the relative node is always along the secular direction, so the two satellites' latitudes will be equal only at the two times of the day that the satellites right ascension equals the right ascension of the secular direction or 180° away.

It is possible to prove that at the two times of the day when the satellites' latitudes are equal, the satellites' radii will be significantly different. This radius separation can be accomplished via the method that the two satellites' eccentricity vectors are controlled.

For $N = 1, 2$:

a_N = semimajor axis of satellite N

e_N = eccentricity of satellite N

ω_N = argument of perigee of satellite N

$\Omega_N = \omega_N + \Omega_N$

E_N = eccentric anomaly of satellite N

$k1_N = e_N \cos(\omega_N + \Omega_N)$

$h1_N = e_N \sin(\omega_N + \Omega_N)$

then:

$$r_N = a_N [1 - e_N \cos(E_N)] = \text{radius of satellite N}$$

and:

$$r_2 - r_1 = (a_2 - a_1) - [a_2 e_2 \cos(E_2) - a_1 e_1 \cos(E_1)] \quad (10)$$

The difference between the two semimajor axis is small compared to each one of them, which will always be near synchronous radius. Therefore in the equation (10) the second appearance of a_2 can be approximated by a_1 . Also, since the two orbits will be nearly circular, eccentric anomaly can be approximated by satellite right ascension of perigee.

$$\begin{aligned} r_2 - r_1 &= (a_2 - a_1) - a_1 [e_2 \cos(S - \omega_2) - e_1 \cos(S - \omega_1)] \\ &= (a_2 - a_1) - a_1 [e_2 [\cos(S) \cos(\omega_2) + \sin(S) \sin(\omega_2)] - e_1 [\cos(S) \cos(\omega_1) + \sin(S) \sin(\omega_1)]] \\ &= (a_2 - a_1) - a_1 [\cos(S) [k1_2 - k1_1] + \sin(S) [h1_2 - h1_1]] \end{aligned} \quad (11)$$

The expression in brackets happens to be the component of the relative eccentricity vector, it means, the difference between the two eccentricity vectors, along the right ascension S direction. The first term $(a_2 - a_1)$ has a nearly constant magnitude. So the magnitude of $(r_2 - r_1)$ can be forced to be large when the two satellites' latitudes are equal by making the second term dominate the first one at those times, which can be accomplished by maintaining a relative eccentricity vector magnitude large enough along the secular direction.

Since both satellites are at the same longitude, they experience the same triaxial acceleration. Assuming that

their solar radiation force and mass are about the same, and that they are being controlled by the same strategy, their target eccentricity vectors should be nearly equal.

the other. The same occurring to the eccentricity vectors. Each satellite relative motion around the reference position is an ellipse with the minor axis along the radial

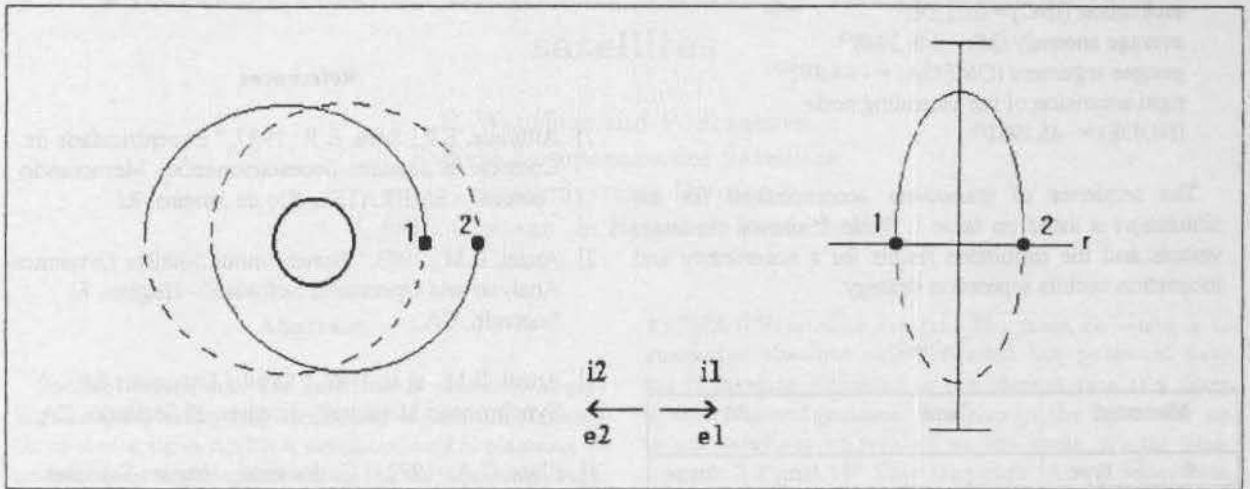


Figure 1

The satellites will not be maneuvered on the same date, so there will be some difference in their eccentricity vectors at any time, but this difference will be relatively small. Thus assuming that the eccentricity vectors are approximately the same, adding large enough offsets

direction and the major axis perpendicular to it, due to the satellites vectors eccentricity and inclination magnitudes. This example indicates the possibility of eclipses, a solution to this could be a displacement between each satellite's eccentricity and inclination vectors, in such a

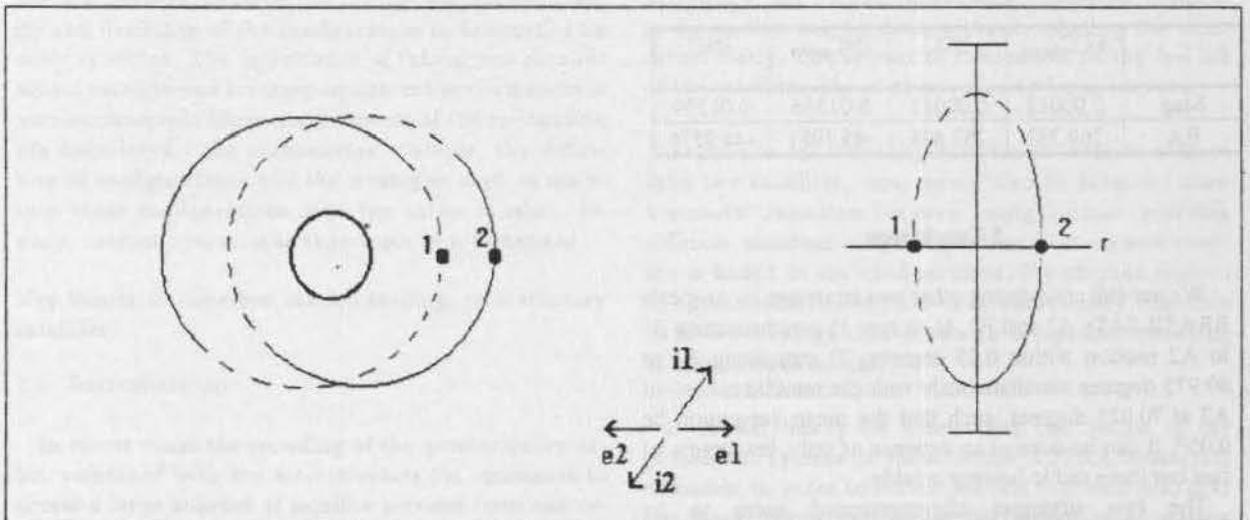


Figure 2

along the opposite secular direction will establish a constant substantial separation along this direction. This will guarantee that collision will be clearly impossible at all times.

way that it changes the relative ellipse plane normal orientation (figure 2).

Eccentricity and Inclination Vector Separation

An example for the two co-located satellites' vector variations is showed on figure 1, where the inclination vector of one satellite is parallel to the inclination vector of

4. The Results

We simulated a BRASILSAT A2, B1 co-location, after moving B1 from 61 degrees, where it was kept initially for in orbit acceptance test, to A2 longitude at 70 degrees, targeting at the orbit:

semi-major axis (SMA) = 42163.59 Km
 eccentricity (ECC) = 0.00012 rad
 inclination (INC) = 0.01556°
 average anomaly (M) = 348.3948°
 perigee argument (OMEGA) = - 44.802°
 right ascension of the ascending node
 (NODE) = -45.1981°

The sequence of maneuvers accomplished for the simulation is listed on table 1. Table 2 shows the target vectors and the simulation results for a eccentricity and inclination vectors separation strategy.

Table 1

Maneuver		Time	ΔV	
#	type		tang	norm
1	D/E	93,6,24,10,50,20	0.946	-0.130
2	INC	93,7,17,15,32,50	-0.056	-13.92
3	D/E	93,7,20,21,39,04	0.008	-0.001
4	D/E	93,7,22,09,35,15	-0.824	-0.114
5	D/E	93,7,22,21,33,24	-0.185	-0.026

Table 2: Simulation results

	ECC _{target}	ECC	INC _{target}	INC
Mag	0.00012	0.00012	0.01556	0.01539
RA	269.333	263.498	-45.1981	-44.9276

5. Conclusion

We are still considering other two strategies to co-locate BRASILSATs A2 and B1, as to say: 1) synchronizing B1 to A2 motion within 0.05 degrees; 2) initializing B1 at 69.975 degrees simultaneously with the reinitialization of A2 at 70.025 degrees, such that the mean separation be 0.05°. It can be done at an expense of only few grams of fuel but turns out to be very reliable.

The two strategies aforementioned seem to be operationally simpler to accomplish although the other two cases approached in this paper are more interesting for a permanent co-location. The final conclusion to which strategy is the best for the transition of services between BRASILSAT generations is still an open issue, expecting further analysis and simulations that proceed until the launch of BRASILSAT B1.

Acknowledgements

Authors wish to thank EMBRATEL for supporting this research and to extend their acknowledgements to the

former Minister Mr. Renato Archer for his important act as the person that actually started the training program at the Co.

References

- 1] Andrade, E.P., Silva, R.P.; 1987, "Excentricidade de Controle de Satélites Geoestacionarios - Memorando Técnico" - EMBRATEL, Rio de Janeiro, RJ.
- 2] Anzel, B.M.; 1983, "Synchronous Satellite Dynamics Analysis and Operations Software" - Hughes, El Segundo, CA.
- 3] Anzel, B.M., et al; 1982, "Orbital Dynamics for Synchronous Missions" - Hughes, El Segundo, CA.
- 4] Elliot, C.A.; 1992, "Co-location: Hugues Satellites Owner/Operators Conference" - Hugues, El Segundo, CA.
- 5] Smart, W.M.; 1953, "Celestial Mechanics"

The ASTRA co-location strategy for three to six satellites

P. Wauthier and P. Francken
Société Européenne des Satellites
Space Systems Division
L-6815 Château de Betzdorf, Luxembourg

Abstract

Société Européenne des Satellites is currently applying the eccentricity and inclination separation strategy to co-locate three ASTRA satellites, and is planning to co-locate up to six spacecraft in the forthcoming years. We describe how, starting from the general formalism of the strategy, adaptations of control methods, extensive simulations and ground systems enhancements have allowed to realize the co-location while guaranteeing absolute safety against the potential risk of collision. Special attention is paid to the role of specific mission constraints: minimization of the fuel consumption, avoidance of radio frequency shadowing and sensor interferences, reduction of the operational complexity and flexibility of the configuration to accommodate more satellites. The importance of taking into account actual satellite and tracking equipment performances is also emphasized. Three main aspects of the co-location are considered: the manoeuvres schedule, the definition of configurations and the strategies used to maintain these configurations over the entire mission. Finally, current operational experience is summarized.

Key Words: Co-location, station keeping, geostationary satellites.

1 Introduction

In recent years the crowding of the geostationary orbit, combined with the attractiveness for customers to access a large amount of satellite services from one orbital position, have stimulated an increasing interest in the concept of satellites co-location. In particular a number of studies¹⁻³ were devoted to an analysis of the respective merits of different co-location strategies. These strategies were essentially designed to prevent, or at least reduce the potential danger of satellite collisions. However, additional requirements need to be taken into account when considering the actual implementation of co-location strategies.

In this paper, we describe how the problem of satellite co-location has been addressed by Société Européenne des Satellites (SES) in order to co-locate the

ASTRA TV-satellite system. The main objective is to guarantee absolute safety against the potential danger of satellite collisions in the present case of a three spacecraft configuration, but also in the future for up to six satellites co-located at the same orbital position of $19.2^\circ \pm 0.10^\circ$ East longitude. A safe separation between the various spacecraft must be ensured not only in normal circumstances, but also in the case of possible manoeuvre errors. The strategy must also be robust against the effects of orbit estimation errors; we will show below that this is indeed the case, and that safe co-location can even be guaranteed using standard tracking equipment. In addition any degradation of the service that may occur through mutual Radio Frequency (RF) signal shadowing should be avoided, as far as this can be done without reducing the separation safety. The impact of co-location on the fuel life of the satellites has of course also to be minimized.

As soon as one is dealing with the co-location of more than two satellites, care should also be taken to allow a smooth transition between configurations involving different numbers of spacecraft, each time a new satellite is added to the configuration. For obvious reasons of operational convenience it is additionally desirable to have a strategy that allows an acceptable spreading of manoeuvres in time.

It should finally be noted that the design of the propulsion system of some of the ASTRA spacecraft demands, in order to reduce the fuel consumption, that no North/South manoeuvre be performed at certain periods of the year. This requires a non-standard inclination control scheme, which has to be integrated in the co-location strategy.

We describe below how the eccentricity and inclination separation strategy^{1,2} was selected and adapted by SES in order to fulfil the above requirements. We show how co-location configuration parameters were chosen and subsequently fine-tuned by means of realistic computer simulations. We finally present the operational implementation of the co-location as it was realized so far in the case of three satellites.

2 The ASTRA co-location strategy

All ASTRA spacecraft are geostationary, three axis stabilized, direct broadcasting TV satellites. The current configuration (February 1994) consists of three satellites, but is planned to be extended to six satellites in the coming years. Major station-keeping characteristics of these satellites are summarized in Table 1.

Table 1: Station keeping characteristics of the ASTRA 1A, 1B and 1C satellites. ASTRA 1D, 1E and 1F will be Hughes HS-601 satellites, like ASTRA 1C.

Satellite	Astra 1A	Astra 1B	Astra 1C
Built by	GE	GE	Hughes
Series	4000	5000	HS-601
mass* (kg)	1015	1580	1684
area/mass* (m ² /kg)	0.023	0.030	0.028
<u>manoeuvre errors</u>			
E/W (1-σ)	2 %	4 %	2 %
N/S (1-σ)	4 %	4 %	2 %
<u>N/S coupling</u>			
tangential	< 2 %	< 1 %	< 1.5 %
radial	< 3 %	< 2 %	< 4 %

* At beginning of life

2.1 The normalized $3 \times 3\sigma$ separation

Current tracking equipment consists of a unique, accurate antenna successively pointing on all satellites of the configuration and of TV-ranging equipment⁶. The system allows raw measurement accuracies better than 0.01° in azimuth and elevation and of the order of one metre in range. The corresponding orbit determination uncertainties were estimated by means of Monte Carlo simulations of the errors, using a dedicated software program. Estimated values of the positional errors along the radial, tangential and out-of-plane directions are summarized in Table 2.

Based on these uncertainties about the respective positions of the spacecraft a *safe threshold*, which represents the minimum separation that can be tolerated between any two satellites of the configuration so as to guarantee a null collision risk, is now defined.

Table 2: 3σ position errors resulting from Orbit Determinations, assuming 2 days of tracking data collected from a unique tracking antenna and TV-ranging and a 7-days orbit propagation

Typical position errors (3σ)	
radial direction	400 m
tangential direction	4000 m
normal direction	1800 m

The position uncertainty of each satellite can be represented by an error ellipsoid, with the largest axis in the longitudinal direction⁷. The semi-major axes of the ellipsoid, that means the radial, tangential and out of plane positional uncertainties, can be defined as the 3σ orbit determination uncertainties after a seven-days propagation (see Table 2). In order to ensure a *significant* separation between two satellites, it is not sufficient that their respective error ellipsoids do not intersect: they must somehow be separated. As a convention we will therefore require that the separation along any direction in space remains always greater than *three times* the positional uncertainty along that direction. This leads to the concept of *normalized $3 \times 3\sigma$ separation*:

$$\Delta(3 \times 3\sigma) = \sqrt{\left(\frac{\Delta_\ell}{\epsilon_\ell}\right)^2 + \left(\frac{\Delta_r}{\epsilon_r}\right)^2 + \left(\frac{\Delta_z}{\epsilon_z}\right)^2} \quad (1)$$

where Δ_ℓ , Δ_r and Δ_z are the longitude, radial and out-of-plane separations and ϵ_ℓ , ϵ_r and ϵ_z are equal to three times the corresponding 3σ uncertainties. The total separation is then considered to be safe if $\Delta(3 \times 3\sigma) \geq 1$. By contrast close approaches are identified as situations for which $\Delta(3 \times 3\sigma) < 1$.

2.2 The e&i co-location strategy

The eccentricity and inclination (e&i) separation strategy consists in ensuring a separation of the satellites by a proper selection of their eccentricity vectors, $\vec{e} = [e \cos(\Omega + \omega), e \sin(\Omega + \omega)]^T$ and inclination node vectors, $\vec{i} = [i \cos \Omega, i \sin \Omega]^T$. In these expressions e , i , Ω and ω stand for the orbit's eccentricity, inclination, right ascension of the ascending node and argument of perigee, respectively.

In the case of two co-located satellites, numerical simulations performed by GSOC² and CNES³ have clearly demonstrated the advantages of the e&i strategy in terms of separation safety compared to other strategies, like the longitude and eccentricity separation strategies. This has further been confirmed, for a constellation of up to six satellites, by realistic simulations⁴ taking into account the actual performances of current tracking equipment and of the ASTRA satellites, as well as station-keeping and co-location algorithms identical to those used in operations. Besides, simulations have demonstrated that by allowing a larger eccentricity control circle than the longitude and eccentricity separation methods and by avoiding corrective manoeuvres, the e&i strategy allows to minimize the fuel consumption.

For these reasons the e&i strategy was selected by SES for the co-location of three and more spacecraft. It has been successfully applied to the co-location of ASTRA 1A and 1B since October 1992, and of ASTRA 1A, 1B and 1C since July 1993. Experience has

proved that by requiring neither corrective manoeuvres nor manoeuvres to be performed simultaneously on all satellites at once, the $e&i$ strategy is particularly convenient from an operational viewpoint.

In spite of the important advantages discussed above, the $e&i$ strategy involves some problems of its own. One of these problems results from the required phasing between radial and out-of-plane oscillations of the various satellite motions. An important parameter for the control of this phasing is the angle between the inter-satellite eccentricity and inclination node vectors, which we call ν . When this angle ν is equal to 0° or 180° the out-of-plane separation comes to a maximum when the radial separation vanishes, and vice-versa. This therefore guarantees a maximum separation between the satellites. However it makes the latitude and longitude separations likely to vanish simultaneously. Such situations should be avoided, for they result in the occultation of one spacecraft by another as seen from an observer on Earth and may cause one spacecraft to enter the field of view of the infrared sensors of another spacecraft, thereby causing attitude disturbances. On the other hand, when the angle ν increases from 0 to 90° the risk of occultation decreases, whereas the risk of close approach increases. This indicates that some kind of trade-off has to be found between the risks of close approach and occultation.

In the case of ASTRA, another difficulty associated to the $e&i$ strategy arises from its requirements in terms of inclination control. Indeed some ASTRA satellites use, in order to improve the efficiency of North/South manoeuvres, electrically heated thrusters. These thrusters require an amount of electrical power that cannot be provided by the satellite's power subsystem during eclipse periods thereby preventing (except at the expense of a higher fuel consumption) North/South manoeuvres from being performed at these times of the year. Note that this constraint requires the ASTRA satellites to be operated within a relatively large inclination window of 0.1° .

In the next Sections we describe in more detail how the $e&i$ separation strategy has been adapted to the station keeping of the ASTRA satellites. The generic case of N satellites ($N = 2, \dots, 6$) will be considered. The leading criteria are the minimization of the probability of close approaches (even in the case of manoeuvre errors), the reduction of the fuel consumption and the minimization of the operational complexity. The strategy described below has not been specifically developed to minimize the occurrence of RF signal shadowing and sensor interferences. However numerical simulations have demonstrated *a posteriori* that the corresponding risk stays within quite acceptable limits. In consequence a discussion of this question is postponed to Section 3.

2.3 The eccentricity and inclination configurations

Let us first consider how the configuration is defined in the *inclination node vector plane* (which will be referred hereafter, for simplicity, as the *inclination plane*). The reference *inclination configuration* can be visualized as a regular polygon in this plane, each apex of which is occupied by a satellite of the configuration. The size and orientation of this polygon can be defined by the vector joining the centre of the configuration to one reference apex. The orientation of this vector can be defined by an angle α , measured relative to a reference direction. This reference is chosen as the direction of the secular inclination drift, which forms an angle θ with the x -axis of the inclination plane (see Fig. 1.a). The norm of the vector, which we will denote Δi_c , determines the size of inclination separations. In particular the inclination separation between any two adjacent spacecraft is given by $\Delta i = 2\Delta i_c \sin(\pi/N)$.

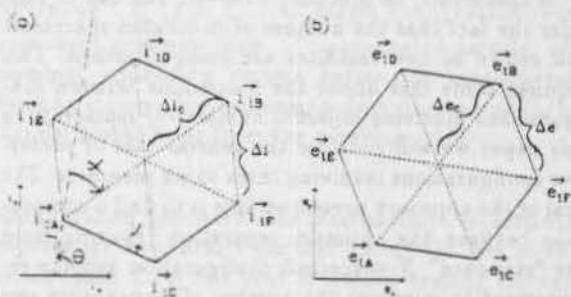


Figure 1: (a) Reference inclination configuration for six satellites. (b) Corresponding eccentricity configuration. Short dashed lines: satellite inclination (resp. eccentricity) vectors relative to the configuration centre. Long dashed line: secular inclination drift direction. Dotted line: direction of the relative eccentricity vector between two satellites of a same group (group 1: 1A/1C; group 2: 1E/1F; group 3: 1D/1B).

The *eccentricity configuration* is obtained by a rotation of the reference inclination configuration by the angle ν (see Fig. 1.b). In this way the configuration in the eccentricity vector plane turns out to be also a regular polygon, which must be scaled in order to determine the eccentricity separations. By analogy to the inclination configuration, a vector of norm Δe_c can be defined such that the eccentricity separation between two adjacent spacecraft is given by $\Delta e = 2\Delta e_c \sin(\pi/N)$. We will address below the question of specifying the eccentricity configuration centre, *i.e.* the point of the eccentricity plane on which the polygon will be centred.

As appears from the above discussion the configuration is entirely determined, for a given number N of satellites, by the four parameters α , ν , Δi_c , Δe_c . We

will now analyze how these parameters can be defined in order to fulfil the mission requirements.

Firstly, the eccentricity and inclination separations must ensure safety in the case of normal manoeuvre performance and orbit determination errors, as well as in the exceptional case of manoeuvre aborts. In addition, as large an eccentricity control circle as possible should be chosen in order to minimize the fuel consumption. However the size of these separations is limited by the requirement that each satellite remains within the assigned longitude and latitude windows during a whole station keeping cycle of fourteen days. In the case of the inclination configuration, tolerable separations are even further limited by the restriction affecting North/South manoeuvres during eclipse periods. These considerations essentially determine the values of the configuration parameters Δe_c and Δi_c .

Before discussing the choice of the parameters α and ν , one should remark that the above considerations apply to the reference configuration for a fixed number N of spacecraft. In practice, however, one has to consider the fact that the number of co-located spacecraft will evolve as new satellites are being launched. This requires some care about the *transitions between configurations involving different numbers of spacecraft*: in this paper we will consider the general case of successive configurations involving three to six members. The goal of the approach presented here is to find a compromise between the optimum separation resulting from the "standard" N -spacecraft configuration and the requirement to minimize the number of manoeuvres and the fuel consumption associated to each modification of the configuration. In fact, depending on the time elapsed between the launches of consecutive satellites one may then decide, either to always work with a reference N -spacecraft configuration (in case each configuration has to be maintained long enough), or to realize immediately a configuration valid for a larger number of satellites than those being currently operated, say $N+1$ or $N+2$. In the latter case of course, a transition will be avoided at the expense of smaller separations and of a higher fuel consumption, because of a tighter station keeping control. To be noted is also the fact that transitions will in general not be realized by simultaneous burns on all satellites, but will result from a longer sequence of smaller corrections distributed over many station keeping cycles, in order to avoid close approaches and minimize fuel requirements.

The requirement to ensure smooth transitions between successive configurations determines the optimal value of the angle α , for any number N of satellites, once the corresponding value is known for the $N-1$ or $N-2$ configuration. As an example Fig. 2 shows how, starting from a given four-spacecraft configuration, a six-spacecraft configuration can be achieved with minimum fuel expenditure (and avoiding close approaches),

and how this transition affects the angle α . In this way the problem is reduced to the determination of the initial value of the angle α for the smallest configuration, $N=2$. Realistic simulations have been performed for the successive configurations $N=2, \dots, 6$ in order to determine the optimal value of this initial angle, which avoids close approaches and minimizes the occurrences of RF signal blockage.

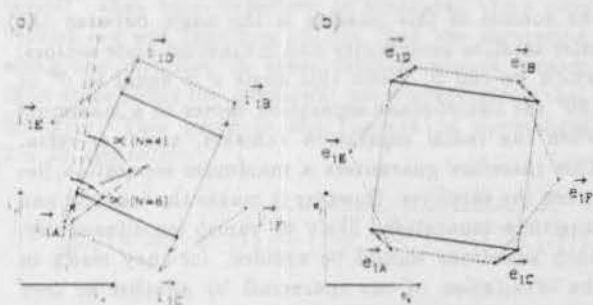


Figure 2: Optimum transition between four spacecraft (solid lines) and six spacecraft (dashed lines) configurations. (a) Inclination plane. (b) Eccentricity plane. Arrows: required orbit corrections. Long dashed line: secular inclination drift direction.

The angle ν is finally determined so as to avoid that the inter-satellite eccentricity and inclination vectors become perpendicular in case of manoeuvre errors. As will be described in more detail in paragraph 2.4 the constellation of satellites is subdivided, from the point of view of the manoeuvres schedule, into *groups of spacecraft* on which North/South manoeuvres are performed simultaneously. Small variations of the angle ν in case of North/South manoeuvre errors can then be ensured by choosing the relative eccentricity vector between two satellites of a same group perpendicular to the secular inclination drift direction (*i.e.* the direction along which North/South manoeuvres are performed). This is shown in Fig. 3.

Theoretical studies based on the manoeuvre performances of the ASTRA satellites and orbit determination accuracies have been performed to adjust the parameters of the $e&i$ configuration. Values of these parameters have further been refined by extensive numerical simulations⁴. Table 3 summarizes the nominal parameters of the ASTRA configuration.

2.4 Manoeuvre planning

As mentioned in the introduction, the operation of a large number of satellites calls for a manoeuvre planning that allows the workload to be distributed in time. This led us to subdivide the spacecraft into groups of two, such that North/South (resp. East/West) manoeuvres are performed on different days on spacecraft belonging to different groups. Considering a station

configuration will never be exactly identical to the reference or alternate one. In order to minimize the fuel consumption, it is generally not desirable to completely correct these errors during the next cycle, except in cases where this may lead to a risk of close approach. In consequence one has to define how far from the nominal configuration the target configuration can be such as to still keep a null close approach risk, and use this tolerance to keep the North/South manoeuvres direction as close as possible to the optimum direction defined above. This led us to introduce the concept of an "inclination configuration variation set", which can be represented by tolerance circles centred around each spacecraft inclination vector.

The inclination control strategy allows to compute target inclination vectors for a given cycle (referenced hereafter as "computed cycle") and for a given group of satellites. This comprises three steps:

1. First inclination vectors of all satellites are propagated from the end of the previous cycle to a reference epoch. It should be noted that the reference epochs are different from one group of satellites to another, due to the dephasing of the manoeuvres. Since only relative positions actually matter from the point of view of the co-location, however, any global shift of the configuration caused by manoeuvre errors of the previous cycle should be tolerated, and not compensated for. We therefore offset the propagated inclination configuration by a vector that accounts for this global error (see Fig. 5). The resulting configuration is then called the "nominal inclination configuration".

2. From the "nominal inclination configuration" a "nominal target inclination configuration" can be obtained by adding the computed inclination corrections.

3. Finally the actual inclination vectors of the various satellites are propagated to their respective reference epochs, and the same inclination corrections as defined in step 2 are applied to the resulting "actual configuration". This directly defines the "actual target inclination configuration", but this target configuration is corrected if any individual satellite leaves a given tolerance circle centred around the corresponding apex of the "nominal target inclination configuration" computed in step 2 (see Fig. 6).

2.6 Eccentricity control strategy

In paragraph 2.3, we presented the eccentricity configuration as resulting from a rotation of the reference inclination configuration by an angle ν . Since this angle ν plays an important role in the minimization of the close approach risk, the eccentricity control strategy must keep it within specified margins. This can be realized by applying to each satellite the "Sun pointing perigee" strategy² relative to a specific control circle centre (one per satellite). These centres define the

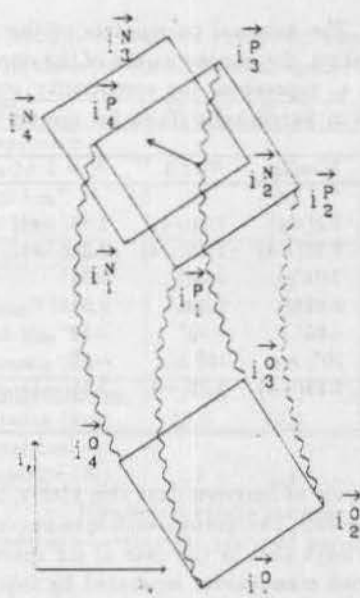


Figure 5: Construction of the "nominal inclination configuration". \vec{i}_j^j ($j = 1, \dots, 4$): target configuration vectors from previous cycle. \vec{i}_j^P : propagated targets. \vec{i}_j^N : nominal inclination vectors before the manoeuvres. Waving curves: free inclination drift during one cycle. Arrow: global error from the previous cycle.

configuration geometry. The inter-satellite eccentricity vectors are kept nearly parallel during the free eccentricity drift. Over one year of station keeping the various satellites keep the same relative positions within the eccentricity configuration, whereas the centre of the configuration describes a circle in the eccentricity vector plane. Combined with the fact that the inclination configuration also maintains a nearly constant orientation, this guarantees that the angle ν will not undergo significant variations.

3 Validation of the strategy

In order to validate the co-location strategy described in Section 2 and fine-tune the corresponding co-location parameters (Table 3), extensive realistic simulations have been performed⁴ over periods which are representative of spacecraft lifetimes. The main results are summarized in Table 4. We will successively consider below how the various criteria defined in the introduction are fulfilled according to these simulations.

3.1 Risk of close approach

Simulations have confirmed that the selected large eccentricity and inclination separations and small value of the angle ν (Table 3) ensure a safe separation. In other words no close approach does occur, the normalized $3 \times 3\sigma$ separation defined in Section 2 always remaining greater than one. This implies that no cor-

Table 3: The nominal parameters of the ASTRA e&i configuration, for various values of the number of satellites, N . e_r represents the eccentricity control radius. Numbers in parenthesis stand for powers of 10.

	$N = 3$	$N = 4$	$N = 5$	$N = 6$
Δe	3.2(-4)	3.2(-4)	2.55(-4)	2.25(-4)
Δe_s	2.25(-4)	2.25(-4)	2.25(-4)	2.25(-4)
Δi	0.03°	0.03°	0.03°	0.025°
Δi_s	0.021°	0.021°	0.025°	0.025°
α	-60°	-60°	-32°	-40°
ν	10°	10°	-4°	8°
e_r	2.25(-4)	2.25(-4)	2.25(-4)	2.25(-4)

keeping cycle of fourteen days this yields, in the case of four spacecraft, two groups with manoeuvres separated by seven days and, in the case of six spacecraft, three groups with manoeuvres separated by four or five days (see Fig. 3). In addition to the workload distribution already mentioned, this planning offers the advantage of a greater flexibility in the sense that a problem with the execution of one manoeuvre will not impact the planning of manoeuvres for a different group of satellites. Moreover it allows the manoeuvres of one group of satellites to be optimized based on the performances of the manoeuvres of the other groups.

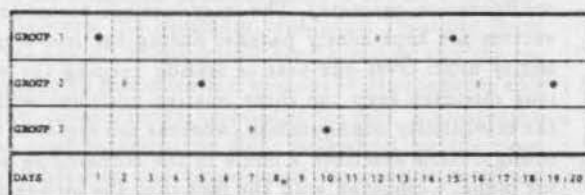


Figure 3: Typical manoeuvres schedule for six satellites. Dots (•) represent East/West manoeuvres; diamonds (◊) represent North/South manoeuvres.

Due to the dephasing of station keeping cycles, the reference inclination configuration will only be maintained during a portion of the cycle. During the rest of the time, the reference inclination configuration is replaced by so-called *alternate inclination configurations*; this causes a decrease of the minimum inter-satellite $3 \times 3\sigma$ separation compared to the case of simultaneous manoeuvres on all satellites. However, extensive realistic simulations have demonstrated that the impact on the risk of close approach remains negligible. Note that, although the eccentricity configuration also undergoes similar deformations, these are small and have a negligible impact.

Another small complication comes, in the case of the ASTRA satellites, from the fact that the spacecraft have to enter the eclipse period in the reference configuration. This is because the reference configuration

is smaller than the alternate ones, making it easier to stay within the prescribed inclination window during the eclipse period (restriction on North/South manoeuvres). This imposes that the manoeuvre planning be modified upon entry and exit of the eclipse period, as shown in Fig. 4. For operational convenience, a yearly manoeuvre planning is defined that takes these constraints into account.

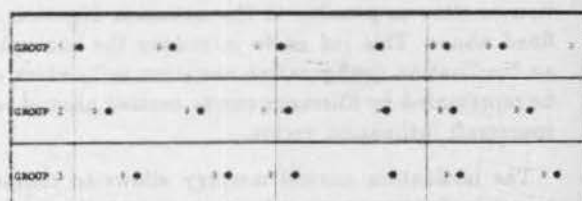


Figure 4: Modification of the manoeuvres schedule on entry and exit of the eclipse period. Dots (•) represent East/West manoeuvres; diamonds (◊) represent North/South manoeuvres. The shaded area corresponds to the eclipse period.

2.5 Inclination control strategy

The inclination control strategy involves two main aspects: the computation of the optimum inclination corrections on one hand, and inclination control in itself, on the other hand. The problem of determining the optimum direction of inclination corrections results from the requirement to maintain not a single satellite⁵ but a whole inclination configuration, as well as from the limitation affecting North/South manoeuvres during the eclipse season. Therefore, instead of exactly following the secular inclination drift direction, one computes the optimum North/South manoeuvres inclination correction as follows:

1. the current inclination configuration is propagated, with simulation of North/South manoeuvres performed at specified dates over the year (according to the planning discussed in Section 2.4) and along a fixed direction until one of the satellites leaves the box.
2. Both the direction and size of the inclination correction are then iteratively adjusted in order to maximize the time that the configuration stays inside the inclination tolerance window.

Once the optimum inclination correction has been determined, a strategy needs to be developed in order to maintain the inclination configuration defined in Section 2.3, under the two following constraints:

1. In the case of non-simultaneous North/South manoeuvres, the usual notion of inclination configuration has to be revised as a consequence of the transitions between the reference and alternate configurations.
2. Due to manoeuvre errors, the actual inclination

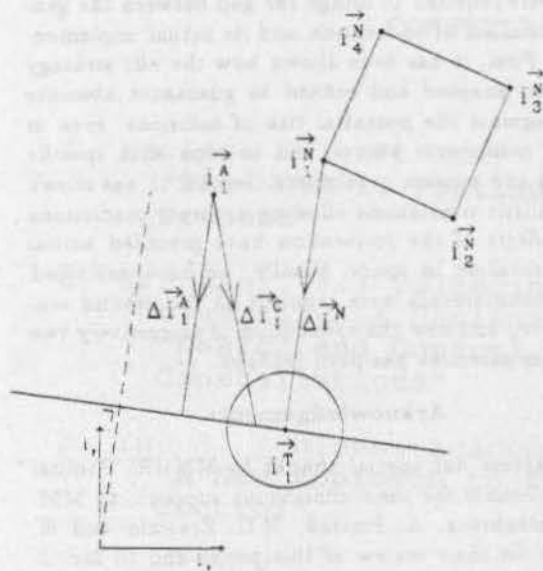


Figure 6: Construction of the "corrected target inclination configuration". \vec{i}_j^N : nominal inclination vectors before the manoeuvres ($j = 1, \dots, 4$). \vec{i}_j^A : nominal targets. \vec{i}_j^A : actual inclination vectors before manoeuvres. $\Delta \vec{i}_1^N$: optimum inclination correction applied to the nominal configuration. $\Delta \vec{i}_1^A$: optimum correction applied to the first spacecraft of the actual configuration. $\Delta \vec{i}_1^C$: correction applied to the first spacecraft of the actual configuration to bring the resulting inclination vector within the tolerance circle. Long dashed line: optimum inclination correction direction.

rective manoeuvre is required in order to guarantee a null risk of close approach. Even in the case of manoeuvre aborts, no close approach below the safe threshold occurs within the two days following the event. This time interval is long enough to perform efficient and safe corrective manoeuvres.

3.2 Fuel consumption

The additional fraction of fuel required for the co-location of three to six spacecraft compared to the single satellite case is seen to vary from 1% to 5%. This relatively small amount reflects the good efficiency of the developed strategy.

3.3 RF shadowing and sensor interferences

With the selected configuration parameters (Table 3), RF signal shadowing events are predicted to occur, depending on the number N of co-located satellites, from one per month ($N = 2$) to one per week ($N = 6$), per satellite and on the average. Earth sensor interference events are even more frequent, for the sensors field of view is generally significantly wider than the aperture

Table 4: Results of realistic computer simulations for a baseline of three to six co-located spacecraft

EVENTS	$N = 3$	$N = 4$	$N = 5$	$N = 6$
Close approaches				
Min $3 \times 3\sigma$	3.5	3.0	2.2	1.5
Below 10 km*	5	20	406	2400
Below 5 km*	0	0	0	0
RF signal blockage				
Mean**	28	35	50	55
Maximum**	39	45	60	65
Below 10 km**	1	1	6	10
Min distance (km)	9.7	9.0	6.5	6.0
Sensor interferences				
Min distance (km)	10.0	10.0	6.9	6.0
Additional fuel vs single satellite (%)	1.2	1.5	4.4	4.9

* Number of events per year

** Number of events per year and per spacecraft

of the RF antenna beam. However, because the selected e&zi strategy has been developed mainly to minimize the risk of close approach, signal shadowing and Earth sensor interference events occur at large inter-satellite distances (typically above 6000 metres for $N = 6$). At these large inter-satellite distances the gain loss due to RF antenna beam blockage is expected to be small. Moreover the duration of one shadowing event above a given point of the antenna footprint lasts no longer than one minute. Similarly, the impact of Earth sensor interferences on the attitude is expected to be negligible when the inter-satellite distance is large.

4 Operational implementation

Implementation of the e&zi strategy required several enhancements of existing tracking equipment, data collection, station-keeping and monitoring software applications. All tracking data used for the station-keeping of the ASTRA satellites are obtained from a unique station located in Betzdorf (Luxembourg). The main improvement of our tracking equipment consisted, on one hand, in the installation of a unique accurate antenna driven by a dedicated computer, commanding the sequential tracking of all satellites. This solution minimizes the relative biases and systematic errors arising when different antennae are used to measure the relative positions of the satellites. On the other hand, accurate TV ranging equipment⁶ was installed and provides a continuous stream of data at all times.

In addition to more accurate tracking systems, co-location imposes specific requirements on orbital software like a higher demand in terms of modelling accuracy than for single satellites, and a multi-satellite operations concept. For these reasons, SES elected to buy the *GeoControl* system developed by the German Space Operations Center⁷. In order to implement the special concept of co-location planning and targeting

described in Section 2, an additional module has been added to GeoControl by SES. This module generates target elements for all co-located spacecraft in a form that can directly be processed by the standard manoeuvre planning module of GeoControl. It thereby allows a centralized control of the configuration.

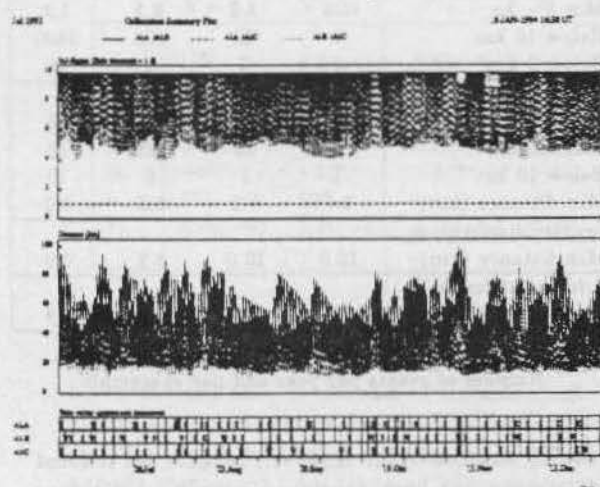


Figure 7: e&I strategy for ASTRA 1A, 1B and 1C from July to December 1993. The plot shows the normalized $3 \times 3\sigma$ separation and intersatellite distance as a function of time, and the occurrence of manoeuvres. Solid lines : 1A/1B separation. Dashed lines : 1A/1C separation. Dotted lines : 1B/1C separation.

Besides, particular attention was paid to the development of systems allowing a continuous monitoring of the co-location. A first system automates orbit determination activities. It allows to continuously monitor tracking data quality, orbital parameters and manoeuvre performances and gives alarms when abnormal situations are detected. Based on the latest orbital information provided by this system for the various satellites, a second system continuously evaluates configuration parameters and the risk of close approach.

The developed e&I strategy was applied to ASTRA 1A and 1B from October 1992 to July 1993. Operational experience has confirmed the results of numerical simulations and the efficiency of the e&I strategy. This further increased our confidence in the capability of this strategy to be applied to three and more satellites. Since July 1993 ASTRA 1A, 1B and 1C have also been safely co-located using this strategy (see Fig. 7). Since the next satellite, ASTRA 1D, is to be launched in 1994, the three spacecraft are currently operated using a configuration which is already valid for four spacecraft. As discussed in paragraph 2.4 this will simplify the insertion of ASTRA 1D in the constellation.

5 Conclusions

We have described the method of proceeding used by SES to achieve the goal of efficiently co-locating up

to six spacecraft. We have shown, in particular, which steps were required to bridge the gap between the general formalism of co-location and its actual implementation. First, it has been shown how the e&I strategy has been adapted and refined to guarantee absolute safety against the potential risk of collisions, even in case of manoeuvre aborts, and to cope with specific satellite and mission constraints. Second, it was shown how realistic simulations allowing accurate predictions of all effects of the co-location have preceded actual implementation in space. Finally, we have described what enhancements were required at the ground segment level, and how the co-location of successively two and three satellites has been realized.

Acknowledgements

We express our special thanks to MM. R. Pontual and J. Gonner for their continuous support, to MM. O. Montenbruck, A. Pietraß, M.C. Eckstein and H. Laroche for their review of this paper and to Mr. J. Wouters for a careful preparation of the figures.

References

- ¹Hubert S. and Swale J., *Stationkeeping of a Constellation of Geostationary Communication Satellites*, AIAA Paper 84-2042, Seattle (USA), 1984.
- ²Eckstein M.C., Rajasingh C.K. and Blumer P., *Co-location Strategy and Collision Avoidance for the Geostationary Satellites at 19 degrees West*, in *Space Dynamics*, pp 85-97, ed. Cepadues, Toulouse (France), 1991, and references therein.
- ³Maisonobe L. and Dejoie C., *Analysis of Separation Strategies for Co-located Satellites*, Proceedings 3d International Symposium on Spacecraft Flight Dynamics, ESA SP-326, pp. 5-9, Darmstadt (Germany), 1991.
- ⁴Francken P. and Wauthier P., *Numerical Simulations of the ASTRA Co-location*, to be published.
- ⁵Soop E.M., *Geostationary Orbit Inclination Strategy*, ESA Journal 9, pp. 65-74, 1985.
- ⁶De Agostini A., Palutan F., Detomo E. and Leschiutta S., *Telecommunications Satellite Orbit Determination via Television-Signal Range Measurements*, ESA Journal 7, pp. 247-256, 1983.
- ⁷Pietraß A., Eckstein M.C., Montenbruck O., *Software for Station Keeping of Co-located Geostationary Satellites*, Proceedings IVth European Aerospace Conference (EAC 91), ESA SP-342, pp. 329-335, 1991.

CONSTELLATION & CO-LOCATION II

1. Heyler, G. (APL-USA):
"The NOVA-II Postlaunch Orbit Adjustment Process" 173
2. Graziani, F.; Palmerini, G.B. and Teofillato, P.
(University La Sapienza-Italy):
"Design and Control Strategies for Global Coverage Constellations" 181
3. Yu, S. (Chinese Academy of Sciences-China):
"A New Approach to Spacecraft Relative Motion Control" 188

THE NOVA-II POSTLAUNCH ORBIT ADJUSTMENT PROCESS

Mr. Gene A. Heyler
Johns Hopkins University Applied Physics Lab
Johns Hopkins Road
Laurel, MD 20723
Internet: glh@aplcomm.jhuapl.edu

Abstract

The NOVA-II satellite was the last of three "drag free" spacecraft to be placed into the Transit Navigation System's constellation of satellites. After its launch from Vandenberg Air Force Base into an initial 510 x 170 nmi near polar orbit, an intensive two-week operations schedule was implemented to: raise the orbit approximately 450 nmi to within .015 sec of desired period, trim eccentricity to within .003, trim inclination to within .006 degrees of requirement, freeze the phase of the spacecraft in orbit relative to the other two "drag free" satellites, dump extra fuel by deliberately designing fuel wasting burns, and transition the spacecraft from a slow spin mode to gravity gradient.

This paper will briefly discuss the concept of a "drag free" satellite, the selection of the orbit plane in the constellation, and the derivation of the required final orbit parameters.

The paper will also discuss peripheral support needed to assist the OATS (Orbit Adjust and Transfer System) ground software, including attitude determination and maneuvers, orbit determination, and orbit prediction through the burns. However, the specific focus of this paper is on the design and execution of the nine OATS burns that accomplished the orbital maneuvers.

Introduction

The Navy Navigation Satellite System, also known as the Transit system, has been in operation since 1964 and available to the public since 1967. At the time of NOVA-II launch, the constellation consisted of 11 satellites in eight near polar orbit planes as shown in Figure 1¹. Satellites included three first generation Oscar spacecraft in individual orbits, six second generation Oscar spacecraft called SOOS (Stacked Oscar On Scout) in three orbit planes (each containing two Oscars launched on the same Scout rocket), and finally, two third generation spacecraft called NOVA which not only contained on-board

fuel (hydrazine) for initial orbit adjustment, but also utilized a DISturbance COmensation System (DISCOS) to neutralize drag and other external effects to maintain an exact orbital period.

The "Drag-Free" Satellite

A user of the Transit system depends on a satellite to broadcast its current position to the ground. This position is predicted on-board from a recently uplinked set of orbit elements. Any error in the predicted position of the satellite will cause an equivalent error in the user's derived position. Even at altitudes of over 600 nmi (nearly 1100 km), drag and especially radiation pressure will affect a typical satellite's predicted orbit sufficiently such that daily uplinks of new orbit parameters are necessary. To alleviate this problem, three "drag free" satellites were inserted into the constellation.

The "drag-free" satellite utilizes a DISCOS composed of a free floating proof mass contained in an internal cavity, and a set of thrusters that react to proof mass position. While the three-axis DISCOS was pioneered first at Stanford University², the single-axis DISCOS was designed and developed at The Johns Hopkins University Applied Physics Laboratory for use on the NOVAs. The DISCOS consists of a cylindrical proof mass floating about a suspension wire in a cavity that is shielded from external surface forces (drag and radiation pressure). These forces perturb the spacecraft body only, causing the proof mass to move off center. When this happens, optical sensors detect the change in proof mass position and fire teflon plasma thrusters that cause the spacecraft to move and re-center the proof mass. Consequently, the spacecraft is slaved to follow the drag-free orbit of the proof mass.

Orbit Requirements

Five of the six Kepler elements for the final orbit were specified prior to launch. Argument of perigee

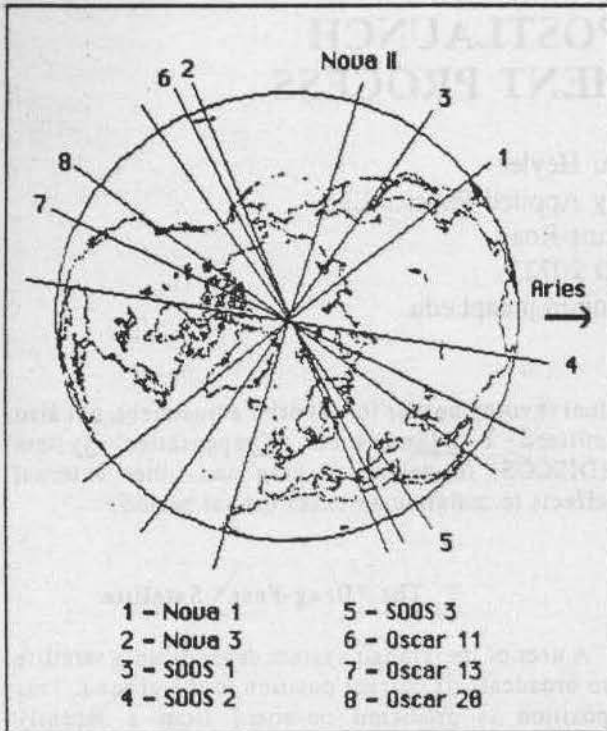


Figure 1 Transit constellation after NOVA-II insertion. Labels depict ascending node.

was ignored since eccentricity would be small.

Ascending node and mean anomaly (phasing)

Ascending node and phasing requirements were specified by considering the NOVA's as a separate constellation from the other spacecraft in the Transit system. This was possible because the "drag-free" NOVA's presented a greatly enhanced 24-hr ephemeris prediction over the Oscars³. Because they provided the highest valued navigation fix to the user, it was advantageous to provide the widest possible coverage by maximizing the separation distance in inertial space between any two NOVA's over an orbit.

Figure 1 shows the Transit constellation including the final chosen NOVA-II orbit plane. Labels are placed next to the ascending nodes. Ascending nodes for NOVA-I and NOVA-III were 24 degrees and 112 degrees respectively. The term "phasing" refers to the relative angle between two satellites measured from the equator. NOVA-I and NOVA-III were phased exactly 180 degrees apart, meaning they would be over opposite poles or at ascending and descending nodes respectively at some given time.

A computer simulation showed that the minimum distance between any two NOVA satellites over one

orbit was maximized if NOVA-II's ascending node was 68 degrees, exactly half way between NOVA-I and NOVA-III, and if phase angle was +90 degrees relative to NOVA-I. When NOVA's I and III would be over the south and north pole respectively, NOVA-II would be at its ascending node.

Semi-major axis

A semi-major axis of 4079.715 nmi was required that would match the 6539.850 second nodal periods of the other NOVA's, with a tolerance of 0.015 seconds. Period error within this tolerance would be trimmed by using the DISCOS as a low energy orbit adjust device by biasing the proof mass position off-center and causing persistent teflon thruster firing.

Eccentricity

The eccentricity requirement was only that the orbit be "near circular", which was arbitrarily defined as any value 0.005 or less.

Inclination

The choice of inclination was critical for the long-term precession of the ascending node. A NOVA constellation requirement was to maintain the initial orbit plane separations between the NOVA's to a tolerance of four degrees over six years.

A software system called the Orbit Determination Program (ODP) is used to support Transit operations. One portion of ODP, called the Analytic Integrator (AI), is used for long-term (several years) orbit predictions of the mean Kepler elements. The AI is a high fidelity integrator, including a 35x35 gravitational model, drag, radiation pressure, sun, moon, and tidal effects. These perturbations are computed analytically for each Kepler element over an exact nodal orbit (equator to equator). By treating each orbit as a single integration step, reliable predictions are obtained over long periods of time. As a test case, the AI was proven to predict the orbit elements of NOVA-I (launched in 1981) to within .004 degrees in inclination and 0.18 degrees in node over a period of six years.

The orbits for NOVA-I and NOVA-III were predicted for six years to obtain node information. The six year node value for NOVA-II was predicted using a starting inclination value of 90 degrees, then iterated until the node value was midway between that of NOVA-I and NOVA-III. Because inclination changes daily due to lunar effects, the precise final inclination value could not be chosen until the day of the last burn of the orbit adjust phase. A preliminary value of 90.008 degrees, with a

tolerance of .006 degrees, was agreed upon based on the estimated last maneuver date.

Supporting Operations

Operations center

Post-launch operations were conducted from the Test and Evaluation Center located at Point Mugu Naval Air Station near Oxnard, California. All commanding and telemetry processing was performed on site. Telemetry was also received from remote stations in Hawaii, Maine, and Minnesota.

Tracking

During the post-launch phase, orbit elements from radar tracking were received at least twice daily from NORAD (now USSPACECOM) located in Colorado. It was also required that predicted orbit elements (as a result of the orbit maneuver burns) be sent to NORAD to aid acquisition by their tracking sites, since these burns would alter predicted rise and set times by several minutes.

Attitude control and determination

A vital part of the orbit adjust phase was the ability to control spin rate and attitude of the spacecraft, and to determine the current attitude in a timely and accurate fashion. Attitude control devices consisted of a magnetic z-coil (electromagnet aligned with the z-axis) for changing z-axis attitude, electromagnetic torquer rods for changing the spacecraft (s/c) spin rate, and nutation dampers at the end of the solar panels. The torquer rods were controlled by the on-board computer that, by reading the magnetometers, would switch the polarity of the rods once per revolution to utilize Earth's magnetic field to create an overall torque around the s/c spin axis.

Similarly, the z-coil was commanded to a given polarity and used to slue the s/c spin axis and momentum vector to desired locations. Typically, a sequence of several slues (defined by polarities and on-off times) were required to move the s/c to the desired attitude over a period of hours or, in some cases, days. Ground software was written to compute the optimal sequence of slues. The original attitude maneuver plan consisted of despinning the s/c so the z-coil would be more effective, perform the attitude slues, then spinup the s/c to provide better stability during the OATS burns. Unfortunately, it was soon apparent that the process of spinning up the s/c perturbed the attitude enough to cause the OATS burns to be less than optimal. Thus, the plan to

despin the s/c for the attitude maneuvers was abandoned midway through the post-launch phase.

Attitude determination was performed via ground processing of magnetometer and spinning DSAD (Digital Solar Attitude Detector) data. Three magnetometers provided data to form field line vectors in body coordinates. The DSAD provided solar elevation in body coordinates and a time of solar passage of the slit opening. By knowing the azimuth mounting of the DSAD on the spinning s/c, az-el coordinates of the sun were derived in body coordinates. Ground processing used a batch least squares technique with the attitude data and truth model data to determine inertial orientation of the s/c z-axis.

Attitude was described with inertial right ascension (RA) and declination (DEC) angles for the s/c z-axis, nominally the spin axis. RA is measured as the positive angle from the Line of Aries towards the celestial Y-axis, while DEC is measured positive from the equatorial plane towards the north.

OATS software

The OATS software programs were written in Iverson's A Programming Language (APL) and operated on a simple IBM compatible PC. Although mission operations employed the use of PL1 programs on a large mainframe computer for attitude and telemetry purposes, the OATS software was deliberately kept separate to utilize APL's powerful graphics display capabilities.

Blowdown curves

One function of the OATS software was to produce so-called 'blowdown' curves, which were a set of polynomial coefficients describing the performance of the OATS engine over time. The combination of diminishing thrust and s/c weight during fuel depletion had to be modelled in the burn algorithms.

Inputs to the blowdown algorithm were: dry spacecraft weight (304 lbs), fuel load (61 lbs), and initial tank pressure (350 psi). Outputs from the algorithm were: total burn time (3399 sec), available delta-v (1314 fps), sets of fourth-order polynomial coefficients for acceleration and fuel weight, and plots of fuel weight and acceleration as a function of total burn time. The acceleration polynomial was utilized by the OATS burn design program to integrate orbit elements throughout the burns.

Orbit perturbation equations

OATS burn design was based on the following set of equations which relate changes to the six mean Kepler elements given an acceleration in HLC (Height, aLong-track, Cross-track) coordinates.⁵ These are sometimes also called the radial, in-track, and cross-track elements of a local vertical, local horizontal coordinate system.

Declare:

a = semi-major axis,
e = eccentricity,
i = inclination,
 Ω = ascending node,
 ω = argument of perigee,
M = mean anomaly,
f = true anomaly,
E = eccentric anomaly,
n = mean motion,
H = radial acceleration component,
L = in-track acceleration component,
C = cross-track acceleration component, and
 β = argument of latitude.

if

$$\gamma = 1 - e(\cos E) \quad \text{and}$$

$$\rho = (1 - e^2)^{-5/2}, \quad \text{then}$$

$$\dot{a} = (2/\rho n) [e(\sin f)H + (1 + e(\cos f))L] \quad (1)$$

$$\dot{e} = (\rho/na) [(\sin f)H + ((\cos E) + (\cos f))L] \quad (2)$$

$$\dot{i} = (\gamma/\rho na)(\cos \beta)C \quad (3)$$

$$\dot{\Omega} = (\gamma/\rho na)C(\sin \beta)/(\sin i) \quad (4)$$

$$\dot{\omega} = (\rho/nae) [-H(\cos f) + (1 + \gamma/(1 - e^2))(\sin f)L - (\cos i)\dot{\Omega}] \quad (5)$$

$$\dot{M} = (2\gamma/\rho na)H - \rho(\dot{\omega} + (\cos i)\dot{\Omega}) + n \quad (6)$$

Burn computations

Inputs to the burn computation program were current orbit elements from NORAD, target orbit elements (a, e, i), total accumulated burn time, orbit number to burn on, and burn duration. Outputs were desired s/c attitude, time of center of the burn, post-burn mean Kepler elements, fuel remaining, and total delta-v used.

Each burn was designed to adjust semi-major axis, eccentricity, and inclination optimally and simultaneously towards the target elements. As such, ascending node, argument of perigee, and mean

anomaly were allowed to freely vary, although phasing of the s/c (sum of perigee and mean anomaly) was accomplished by controlling the overall timeline of the burns. The software could design each burn as an optimal individual burn only, or was capable of automatically generating optimal pairs of burns such as Hohmann transfers. Burn design was based on solving simultaneously for the forces in equations (1) through (3).⁶

Post-Launch Scenario

Spacecraft Configuration

Launch of NOVA-II was southward from Vandenberg AFB, California in June of 1988. Burnout of the booster occurred near the equator, providing an initial 510 x 170 nmi orbit with perigee at the descending node, an inclination of 90.13 degrees, and ascending node at 67.75 degrees.

After separation from the launch vehicle, the spacecraft was despun from its imparted high rotational rate by releasing despun (yo-yo) cables and their attached weights. The deployment of the four solar panels further reduced the rate to about two rpm, and the orbit adjust phase commenced.

Figure 2 shows the spin stabilized s/c configuration during this phase. The momentum wheel and DISCOS were disabled. The despun rods were used to increase or decrease the spin rate to accomplish attitude maneuvers to support the burns. The OATS tank formed the top of the s/c and was held in place by a clamp strap; it was eventually deployed on a 40-foot boom when the s/c went into gravity gradient capture.

Burn constraints

Figure 3 shows the initial and target orbit as viewed from the negative orbit normal. Spacecraft motion is clockwise. The configuration is set up for a classic textbook Hohmann transfer solution, with the first burn occurring at initial orbit apogee to raise perigee, and a second burn at this point to circularize the orbit. However, there were two operational constraints that would prohibit a classical solution to this scenario.

First, there was insufficient delta-v available during any one burn to accomplish the desired maneuver using an inertially pointed thrust vector. Thus, a series of several burns was needed to raise the orbit.

Second, the attitude maneuver rate was quite slow,

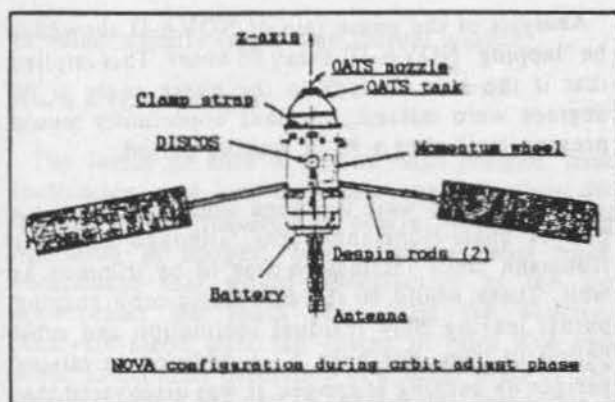


Figure 2

given the limited power of the z-coil, and at times would consume up to 30 hours for the larger slues. Because contacts with the s/c were arranged in twelve hour clusters, attitude maneuvers were sometimes cut short by a few hours in the interest of saving twelve. This, coupled with fuel slosh perturbations, meant that very rarely did the achieved attitude state actually match the desired. Thus burns were hastily redesigned with the achieved attitude and were somewhat sub-optimal in performance.

Burn 1 (L + 1 day)

Orbit elements were obtained from NORAD approximately six hours after launch, and used to design the first burn. This was a calibration burn required to be observed in real time over the operations center, located at 34 degrees latitude. Referring to Figure 3, the burn would occur 34 degrees north of apogee on an ascending pass. The initial attitude after the solar panel deployment had a declination of -29 degrees, which was favorable for an in-track force component over the station. Because it would only take one hour, it was decided to maneuver to (RA=68, DEC=-45) putting the force vector close to the orbit plane (for small inclination adjustments) and optimal energy for burns over the mid-latitudes.

Unfortunately, an erroneous orbit was used to generate the slue commands. The resulting attitude became (RA=114, DEC=-37), and although the cross-track component would actually increase inclination slightly, it was decided to perform a 60 second duration test burn commencing in view of the station, approximately 36 hours after launch. By the time of burn execution, the attitude had drifted to (RA=108, DEC=-39), so the predicted burn results were quickly recomputed and forwarded to NORAD. The spacecraft spin rate had been lowered to two rpm during the attitude maneuver, and because the

burn would be short, was left at that value instead of increased for stability purposes.

Within three hours, a tracked orbit was received and compared with the predicted results. Predicted orbit changes were ($\Delta a=9.92$, $\Delta e=-.00183$, $\Delta i=.037$), and compared excellently with the tracked changes of ($\Delta a=9.91$, $\Delta e=-.0019$, $\Delta i=.041$). With confidence that the onboard OATS system was operating nominally, the remaining burns were designed for greater performance.

Burn 2 (L + 3 days)

Burn 2 was designed to increase perigee as quickly as possible, since its very low altitude was keeping contact times on that half of the orbit to under ten minutes. This was severely limiting mission operation's ability to uplink commands and obtain telemetry. Like burn 1, it was decided to choose an attitude with thrust vector in the orbit plane (to reduce cross-track thrust) and a declination so that burns over the ascending north mid-latitudes would have a large in-track component. Attitude was targeted for (RA=66, DEC=-50) which would give a slight negative cross-track component for reducing inclination. This attitude was matched perfectly by the maneuver; however, when the spin rate was increased from two to three rpm, attitude drifted to (RA=69, DEC=-45) causing a cross-track component unfavorable for inclination adjustment.

This incident prompted the decision to increase the s/c spin rate to four rpm and keep it there for the duration of the post-launch exercise, at the expense of increased slue times for the attitude maneuvers. Commands were uplinked for the spinup and slue over to (RA=60, DEC=-53) (a less time consuming slue than originally planned); however, sub-optimal performance resulted in only 3.8 rpm at (RA=55, DEC=-50). Rather than spend at least an extra half day trimming the attitude, it was decided to perform the burn as scheduled despite an unnecessarily large cross-track component. To avoid overshooting inclination, the burn duration was decreased from 480 seconds to 300.

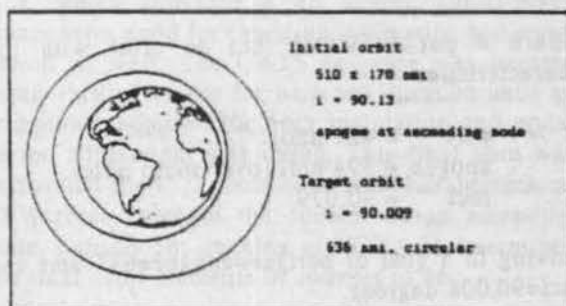


Figure 3

Post-burn orbit tracking once again verified the nominal performance of the onboard OATS system and the ability of the ground software prediction capabilities. Tracked orbit values were within 0.01 nmi semi-major axis and .001 degrees inclination of the predicted values.

After burn two, the phase angle and phase rate of NOVA-II relative to NOVA-III was calculated, primarily as a dry-run exercise, by a computer program utilizing input orbit elements for the two spacecraft. At this early time, NOVA-II was "lapping" NOVA-I every 20 hours.

Burns 3/4 (L + 4 days)

Burns 3 and 4 were designed simultaneously as a consecutive orbit pair, and were very similar to the highly successful burn 2. The goal of these two burns was to continue to raise perigee and trim inclination. Because the first two burns had some radial component and had not been centered exactly at apogee, apogee altitude itself was slowly increasing along with perigee. By deliberately designing these types of slightly inefficient burns (there was at least a 15 percent fuel margin), it would be possible to chip away at apogee and hopefully avoid a potential 180 degree slue for a burn later in the sequence.

A residual effect of the first two burns was that apogee had been driven 30 degrees south of the equator. It was desired to move burns 3 and 4 farther south as well, at least to the equator, and to do so meant a large negative declination was required. An attitude maneuver was put into effect, resulting in a final attitude of (RA=60, DEC=-71). This was favorable for inclination adjustment, and two 480 second burns, centered over the equator and 30 degrees south latitude respectively, were performed on consecutive orbits. Note that burn 4 was performed 'in the blind', meaning the attitude and orbit results of burn 3 were unknown at the time. The confidence gained in burns 1 and 2 permitted this risk to be taken.

Burn 5 (L + 5 days)

Burn 4 put NOVA-II into an orbit with the characteristics

peri = 421 nmi,
apogee = 594 nmi (over south pole),
incl = 90.079,

moving to a goal of perigee=apogee=635 nmi and incl=90.008 degrees.

Analysis of the phase rate of NOVA-II showed it be "lapping" NOVA-III every 36 hours. This implied that if the burn to lock-in the phase angle at 90 degrees were missed, the next opportunity would present itself after a 36-hr waiting period.

Burns 5 and 6 were designed simultaneously as a pair of quasi-Hohmann burns, although not truly Hohmann since inclination was to be trimmed as well. These would be the last major orbit shaping burns, leaving only residual inclination and orbit period to trim. For burn 5, in addition to raising perigee by burning at apogee, it was discovered that by designing a particular inefficient burn near apogee, apogee itself could be raised to the 635 nmi goal. Then a truly efficient burn 6 would be performed exactly at apogee to circularize the orbit. Timing of burn 6 would be critical since it was the burn that would nearly freeze the phase angle to about 90 degrees, so would have to occur on an orbit where the phase angle passes through 90 degrees.

Choices for (RA, DEC) for burn 5 were selected empirically. It was desired to have at least some cross-track component to continue to trim inclination, and that necessitated moving the burn somewhat north of apogee (currently over the south pole) on an ascending node. The computer model also showed that by applying a small nadir component to the force vector, apogee could be raised to 625 nmi where it would remain.

A major attitude slue of nearly 180 degrees was implemented to support this burn. Final values of (RA=266, DEC=-35) meant that a burn performed 70 degrees south of the equator on an ascending node would impart force generally in-track, but with about 17 and 15 degrees negative cross-track and nadir components respectively. A 570 second burn was performed with these parameters.

Burn 5 performed exactly as expected, putting NOVA-II into an orbit with the characteristics

incl = 90.042 degrees
peri = 516 nmi,
apogee = 625 nmi (36 deg south of descending node),

moving to a goal of perigee=apogee=635 nmi and incl=90.008 degrees. Although apogee was 10 nmi lower than needed for a truly circular orbit, it would allow eccentricity to fall below the 0.005 requirement given that perigee would be raised to guarantee the desired nodal period. Thus, the current apogee was considered adequate, and attention turned to burn six which would be centered exactly at apogee to raise opposing perigee to its final value

(a value actually larger than current apogee).

Burn 6 (L + 7 days)

The intent of burn 6 was to raise perigee, trim inclination, and lock the phase angle to about 90 degrees. This required a nearly in-track force operating at apogee, with a minor cross track component that would be effective as the s/c approached the south pole from the equator. Analysis made after the design of burn five had made an accurate prediction of a phase angle of 250 degrees with a rate of 115 degrees/day immediately after the burn. This implied burn 6 should occur 42 hours after burn 5, else wait an additional three days for the next opportunity.

An attitude slue was performed, lasting the better part of a day, that brought the force vector nearly into the orbit plane, leaving an eight degree cross-track component, and changed declination from -35 degrees to 45 degrees. Final values were (RA=240, DEC=45). After an additional wait of 16 hours until phase angle drifted to 90, a 587 second burn was performed with these parameters centered about a point 45 degrees south of the equator.

Burn 6 performance was nearly nominal, and produced an orbit with the characteristics

- $T_N = 2.85$ seconds higher than desired,
- $i = 90.006$ deg, within tolerance but 0.002 deg less than desired,
- $e = 0.0035$, within tolerance.

Phase angle was 92.3 degrees with a rate of -0.03 degrees per day, and decreed acceptable.

Burns 7/8 (L + 8 days)

With the above favorable results, the final activity in the burn schedule was to trim nodal period, trim eccentricity, and waste fuel at the same time. This would be implemented as a sequence of two burns, one each at the south pole and north pole. The attitude slue was to nearly the orbit normal with a slight offset in RA, such that there would be small in-track components at the poles. By moving one of the burns a few degrees off the poles to avoid self-cancellation, minor changes in inclination were achieved. The absolute burn durations were set to waste about ten pounds of remaining fuel. Offsetting the burn durations would provide some of the desired change in T_N , although this was not targeted exactly because there would be one small final burn specifically designed to trim T_N without disturbing inclination.

The attitude slue was to (RA=342, DEC=0.4) leaving the force vector with a residual six degree in-track component, with a small .4 degree radial component. The latter would be a negligible effect because of near self-cancellation and small eccentricity (see eq.(1)).

The duration for burn 7 was set at 330 seconds and was centered exactly over the south pole. Because the blowdown characteristics imparted a slightly greater acceleration early in the burn, a net small gain in inclination, from 90.006 to 90.007, was observed. Nodal period was changed from 2.85 seconds too high to -.75 seconds too low.

Burn 8 was centered 1.3 degrees beyond the north pole on the same orbit, about 50 minutes later, with duration 162 seconds. The slight offsetting of position gave a slightly increase inclination performance to an expected final value of 90.01. Nodal period was increased to an expected 6540.78 which was nearly one second too high, but would be taken out on the next and final burn, as burns 7 and 8 were primarily fuel dumping burns.

Burn 9 (L + 11 days)

After burn 8, an effort was performed to obtain a high fidelity orbit track. After three days of doppler track, orbit parameters of interest were determined to be $T_N = 6540.85$, exactly one second too high, and $incl = 90.014$, about .005 too high.

The final burn was designed to trim both these parameters to their desired values. An attitude maneuver was performed to move the thrust vector farther away from the orbit normal so that the in-track component of thrust was more controllable. It had been noticed that the sub-optimal performance of burns 7 and 8 were due to the unknown drifting of attitude from six degrees in-track component to about four. Thus the in-track force component was only about two-thirds of that required, resulting in an erroneous nodal period.

The final attitude for burn 9 was (RA=23, DEC=-5.5), which provided a 45 degree out-of-plane component, good for changing inclination and nodal period as well. The OATS software was iterated using various values for beta and duration until an acceptable solution for both inclination and nodal period adjustment was found. This final burn was performed for 11.2 seconds at beta=323 degrees, or 37 degrees south of the equator on an ascending node. Subsequent tracking of NOVA-II determined the final orbit elements of interest to be

$$T_N = 6539.692,$$

$e = 0.0029,$
 $i = 90.0094.$

These values were in the acceptable tolerance range, except T_N , off by 0.15 seconds, outside its given tolerance of 0.015 by a factor of ten. The desire to wrap up events quickly prompted a second look at the ability of the DISCOS system to alter orbital period, and it was determined the DISCOS could indeed remove 0.15 seconds of period over time. The original nodal period tolerance level was determined to be much too conservative, so burn 9 was declared to be the last burn in the sequence.

Gravity gradient stabilization

Once the target orbit had been achieved, any remaining fuel was vented through pressure valves and the spacecraft was ready for transition from inertial spin stabilization to gravity gradient capture through a method called the "dual spin turn".⁴ Although this process could be the subject of a complete paper by itself, the main points will be summarized here.

The s/c was slued so that its z-axis (the spin axis) was aligned with the orbit normal and spin angular momentum aligned with orbital angular momentum. The spacecraft was given a spin rate such that its current angular momentum value matched the predicted final angular momentum value of the subsequent gravity gradient mode. While in this mode, the momentum wheel, with spin axis about the s/c body y-axis, was turned on and accelerated to a pre-specified value. This action transferred momentum from the s/c body to the wheel causing the spacecraft y-axis to be nominally aligned with the orbit normal. The momentum wheel speed was selected to give the s/c an approximate 2 rpo tumble around the orbit, similar to the changing magnetic field lines. After many hours of nutation damping, the 40-foot boom was extended at a precise moment causing the s/c rate to drop to one rpo and attitude capture by the gravity gradient.

Figure 4 shows the s/c in this configuration. The empty OATS tank serves as the boom end mass to enhance the gravity gradient effect. Two solar panels are rotatable while two are not. Pitch control is maintained by the gravity gradient force only, while roll and yaw stability are maintained by the momentum wheel whose spin axis points cross-track. Passive nutation dampers located at the ends of the solar panels absorb rotational energy and help minimize attitude disturbances.

Despite the immediate post-launch efforts described herein, several weeks of attitude damping

and testing of sub-system components prevailed before the spacecraft could be declared operational.

References

¹Robert Danchik and Lee Pryor, "The Navy Navigation Satellite System (Transit)", Johns Hopkins APL Technical Digest, Vol 11, No.1&2, 1990.

²Staff of the Space Department, The Johns Hopkins University Applied Physics Laboratory, and Staff of the Guidance and Control Laboratory, Stanford University, "A Satellite Freed of All But Gravitational Forces: TRIAD-I", J. Spacecraft and Rockets, Vol 11, No.9, Sept. 1974, pp. 637-644.

³A. Eisner and S. M. Yionoulis, "NOVA-I - The Drag-Free Navigation Satellite", The Johns Hopkins University Applied Physics Laboratory.

⁴Terry Tracy, "Alternate Gravity Gradient Mode Capture Sequence for NOVA", RCA internal memo # 81N-ADC-0097, May 7, 1981.

⁵W. M. Smart, Celestial Mechanics, p. 221.

⁶R. E. Jenkins, The Johns Hopkins University Applied Physics Laboratory, personal notes.

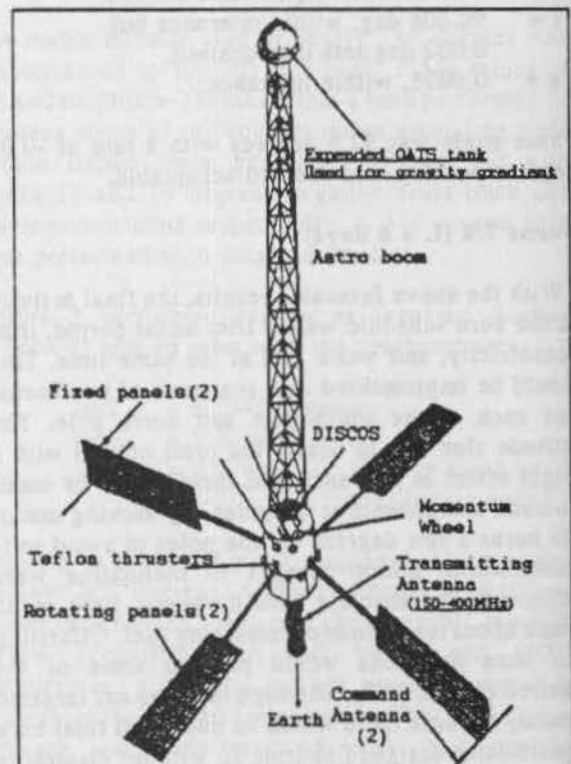


Figure 4 NOVA-II in gravity-gradient stabilization

DESIGN AND CONTROL STRATEGIES FOR GLOBAL COVERAGE CONSTELLATIONS

Filippo Graziani
Giovanni B. Palmerini
Paolo Teofilatto

Scuola di Ingegneria Aerospaziale
Università degli Studi di Roma 'La Sapienza'
Via Eudossiana, 18 - 00184 Roma (Italy)

Abstract

Absolute control of each satellite belonging to a large constellation means a huge work to be performed by ground in order to keep each satellite in its own place, no regarding other satellite motion.

Two possible ways to reduce this heavy ground-segment, and the related amount of consumption penalty, are discussed in this paper.

The first one deals with a good positioning of the constellations planes: some simulation shows that, depending on altitude, parameter's bias, due to the third body perturbation, between designed and actual constellation, could be reduced in a significant way. Above all, this reduction basically affects the out of plane parameters, that are of course the most expensive. So an optimal choice with respect to this perturbing force, constrained on the other side to the inter-plane coverage request, means a reduction on both the maneuver's number and strength.

The second way could be identified with an optimal strategy in constellation orbital control.

In the lack of literature about this subject, we propose, as a first approach, a simple model based on the Lagrange multipliers rule. This kind of solution, differently suitable for the variety of geometrical models studied till today, allows a relative control strategy, i.e. to control each satellite with respect to the others and not with respect to the Earth, in a cheapest way than the traditional one.

Key Words: Satellite Constellations, Orbital Control.

Introduction

Satellite constellation is today an increasing popular option in space mission design, with regard to different purposes (i.e. communication or navigation systems). Since early 60's, a strong effort was made to imagine a network of satellite to cover the entire globe.

The amount of this work was directed to define the best geometric configuration, with papers devoted to theoretical or numerical considerations.

A first approach, by Gobetz¹, started to consider the family of regular polyhedra enclosing the globe and placed the satellites onto the planes perpendicular to these polyhedra's faces. This geometrical approach was followed by Drain^{2,3} who found, on the basis of a couple of theorems, the minimal constellation, designed on 4 satellites placed on orbital planes parallel to the 4 faces of a tetrahedron. Orbits are elliptic and, as the time goes on, the tetrahedron shifts around the globe, making sure the four satellites cover everytime the entire Earth; major disadvantage of this design is the period ($T > 26.49$ h) too long and the related high altitude of the satellites (trade-off with their minimum number).

A second approach was chosen by Walker⁴, who looked for a uniform disposition of a total number of t satellites, placing the same number of platforms, equally spaced, on p orbital planes equally inclined (inclination is called δ), with equally spaced ascendent nodes.

These are the delta pattern models, defined by triple code $t/p/f$ (where f denotes the difference in phase between a reference satellite and the satellite on the immediately easterly contiguous plane). Walker solution is the optimal one till today for low-orbit constellation, but no analytical criterium is available to define exactly the coverage properties assured by this configuration. Inclination δ , if no constrained, could be chosen in a way to optimize coverage.

Really different approach was followed by Lüders⁵, Beste⁶, Adams and Rider⁷. Their work deals with the polar constellations, starting with the problem of the coverage above a certain latitude, then obtaining global coverage as a special case; properties of constellations, also in analytical meaning, were found on the basis of *street-of-coverage* technique. From the amount of these paper, particular features of polar constellations, as the possibility to have interphased or not interphased configurations (depending if constraints between satellites on different planes have to be satisfied or not), with the difference between co- and counterrotating orbits for the latter case, grows up. Polar constellations requires a slight greater number of satellites than Walker models, involving also some stronger constraint in the platforms spacing (two

points are touched by all the satellites, where Walker model allows less intersections: it means that the debris problem has to be considered in a different way); on the other side, this model is not sensitive do J_2 perturbation effect on inclination. Adams and Rider model was chosen for the most advanced, today developing, design.

With the first, effective design of constellation devoted to telecommunication services, to be deployed in next few years, the attention slightly turned from the geometry to the control of the configuration.

Techniques became usual for single, large geostationary platforms, i.e. to keep the satellites in a state $\underline{X} \pm \Delta \underline{X}$, where \underline{X} is the vector of Lagrangian parameters, are not easily suitable when the number of satellites grows up, more than be an expensive solution.

Lamy and Pascal⁸ firstly proposed in an organic manner a control strategy based not on the satellites position with respect to the Earth, but on mutual positions of the orbiting platforms. The goal of their approach is to keep a *mean constellation*, defined as the constellation nearest to the actual perturbed positions of all the satellites, and designed in such a way to satisfy coverage requirements. Mean constellation was calculated by a least square approach, possibly with the interposition of weighting functions. They exploited this way for Walker constellation model, remarking the advantage of this strategy, above all in terms of maneuvers frequency.

In this paper, we propose another way, actually trivial and simple, to pass from the actual positions of the satellites to a mean constellation that preserves the distances between them.

Before to do that, we consider in the next section a constraint condition not enough remembered in litterature, that, related to the desired lifetime, could take some relevant place in mission and launch analysis of a constellation.

Choice of Ascending Nodes

Relative position of the Moon respect to the orbits could have a significant effect on the satellites motion; of course, this effect is stronger as the orbit altitude increases. It means that, depending on the orbit choice, we shall have to counteract a quite different level of perturbation, and so on to perform different amount of orbital control. This effect was previously observed for space mission as Archimedes.

Because we are dealing with a global coverage, the position of the orbital planes with respect to the Earth is not constrained. So, we can go to see what happens if we change the initial RAAN (right ascension of ascending node): in Figs. 1-2 parameter's variation vs. initial RAAN values are plotted, referred to a Draim configuration, where the effect is easily evaluable (data of simulation, starting 1-1-94, are $T=36$ h, $a=55352$ km, $i=31.3^\circ$, $e=0.263$).

It is possible to check the right identification of the

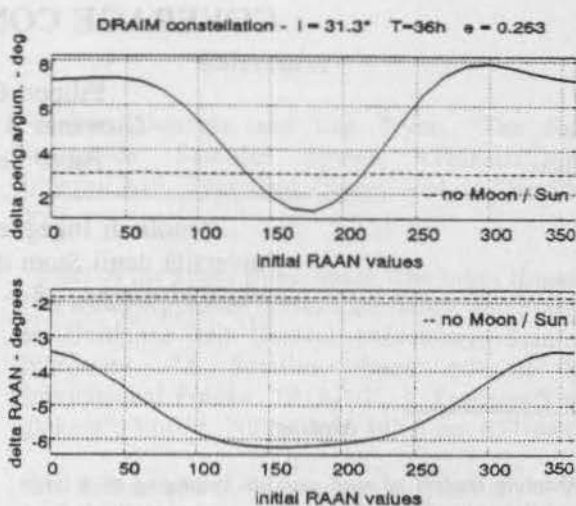


Figure 1: 1 year max parameter variation vs. initial RAAN values (argument of perigee, ascension of ascending node).

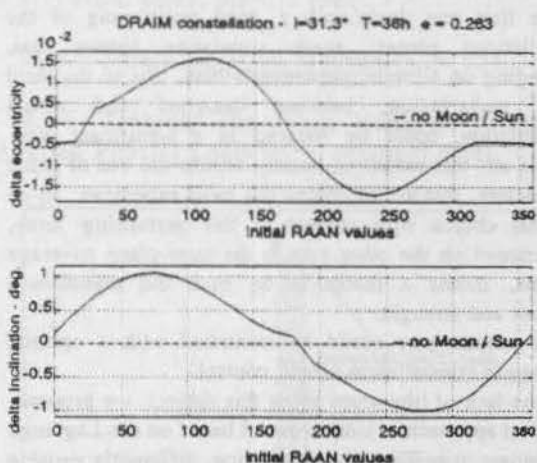


Figure 2: 1 year max parameter's variation vs. initial RAAN (inclination, eccentricity)

perturbing source comparing to the reported results where no 3rd body (Sun+Moon) effect was included.

It arises obviously some question about the periodicity of this phenomena. A series of simulations, with an initial value of 180° for RAAN, each one during 1 year, conducted for 30 years starting 1-1-90, shows clearly a period near 18 years for the maximum of parameter's variation (see Figs.3-4). This value matches quite good the Moon's nutation period, so explaining the problem. Fig.5 shows that things are similar also starting from a different position (initial RAAN equal to 270°).

It could be emphasized that this period is maybe longer than designed lifetime for a constellation, so arising the problem to find an optimal configuration (as exemple of expected lifetime, we could remember the value of 7.5

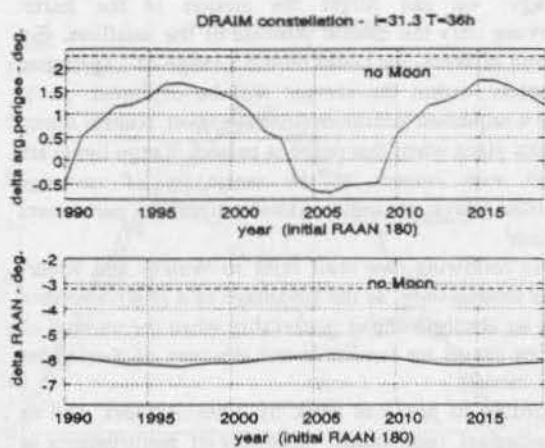


Figure 3: Long term behaviour (argument of perigee, RAAN); maximum displacement per year vs year.

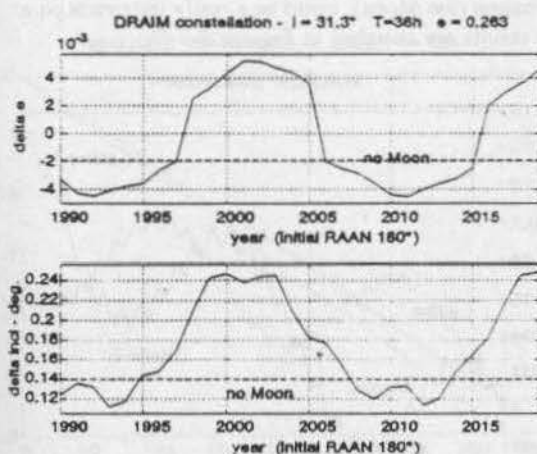


Figure 4: Long term behaviour (argument of perigee, RAAN); maximum displacement per year vs year.

years for one of design now developing).

Basic concern, not enough remarked in literature, is that, dealing with constellations, we don't have to think just about one orbital plane, but to place in a good way numerous planes.

To solve optimally this kind of problem, a useful suggestion could arise following this procedure:

- 1) check the maximum of displacement from desired values for each parameter for a time history, i.e. a propagation of the orbits for the desired lifetime, prepared for one satellite only, starting from a certain set of initial conditions in RAAN (for example, 12 equally spaced planes at $\Omega^* = 0^\circ, 30^\circ, 60^\circ, \dots$);
- 2) figure out with the parameters most expensive (usually out-of-plane corrections)
- 3) working on the most expensive parameter plot, look for

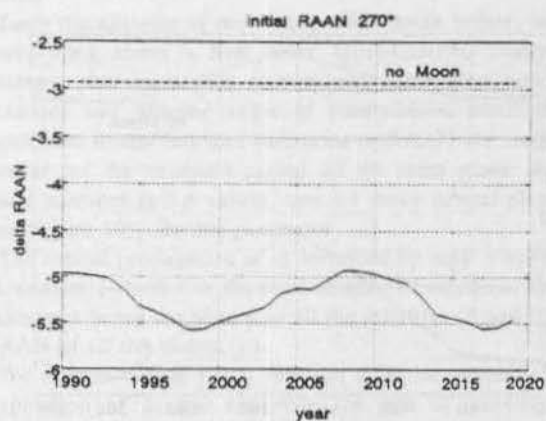


Figure 5: Long term behaviour - Maximum RAAN displacement per year vs years.

the cheaper set of planes.

Meaning of this recipe could be matched from Figs. 6-7, where maximum parameter's variations during a (short) 5 years lifetime are considered.

Mathematically, say $\delta_n(\Omega^*)$ the function that gives the displacement of n th parameter from desired values, and e_n the error range accepted for the parameter, it is possible, for example, to do work on the functions best fitting datas from graphics as Figs. 6-7. Problem is transposed, about n th parameter, in the way to find:

$$\min \varphi_n(\Omega^*) = |\delta_n(\Omega^*) - e_n| + \sum_{i=1}^{p-1} \left| \delta_n(\Omega^* + i \frac{360}{p}) - e_n \right| \quad (1)$$

with Ω^* equal to initial RAAN of the first plane, where we wrote the condition for p planes equally spaced (as in the case of Walker model); the condition is easy to rewrite for other cases.

This procedure is right if we decide to act over one parameter only (i.e. the most expensive, that is usually out-of-plane). Generally, we shall prefer to account for more than one parameter. Relation (1) becomes:

$$\min \phi(\Omega^*) = \sum_{n=1}^p \alpha_n \varphi_n(\Omega^*) \quad (2)$$

where α_n are the weights we have to choose for different parameter errors terms.

About these weights, a good choice must take into account relative penalty of different parameter corrections, and could be established once the way to correct this penalty is chosen.

It is really important to remark that the described solution is not optimal, due to the fact it is based only on

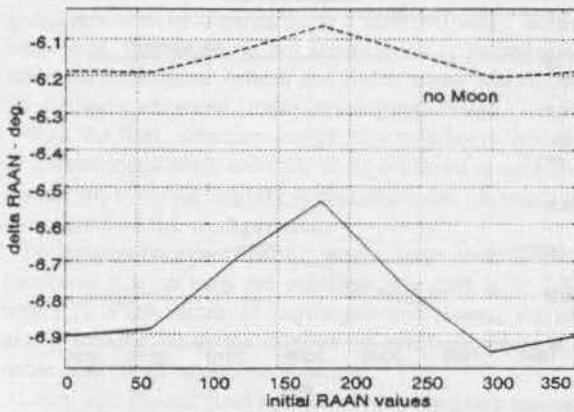


Figure 6: Maximum RAAN's variation for different initial RAANs - 1.5 years analysis.

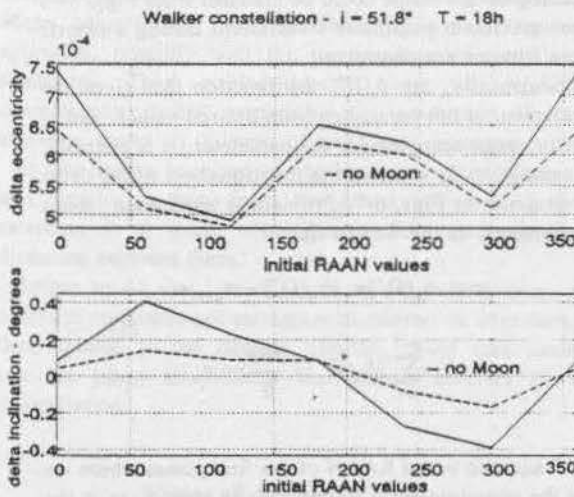


Figure 7: Maximum eccentricity and inclination variation for different initial RAANs - 1.5 years analysis.

the maximum of variation (for example, it could be cheaper to correct just once a strong variation, than to counteract a perturbing effect higher on average).

Nevertheless, there is no doubt that going away from strong perturbing effect shown in the graphics could be a good strategy, in order to obtain a first design solution: this approach become of course optimal in the (lucky) case where we are able to find p points, correctly spaced, where $\delta_n > \epsilon_n$, for all the n of interest, so no corrections are needed.

Relative Control Strategy

Due to the fact that we are dealing with a global

coverage, we can forget the motion of the Earth, preserving only the mutual position of the satellites. For each one of these, we could define a range of Lagrangian parameters within the service will be exploited; so to ensure a requested minimum coverage level, control action will take place when this range is passed. Range limits are defined with respect to the sensitivity of coverage properties (elevation angle, visibility time) vs. parameters variation⁹.

In the following, we shall refer to Walker and Rider-Adams models only, as the advantage of a relative control versus an absolute one is remarkable when the number of satellites grows up (and it is not the case of 4-satellites Draim model).

According to previous work by other Authors, and to our numerical simulations, the effect of perturbations at the altitudes of interest is strongly dependent on the orbits actually chosen; nevertheless, this effect could be summarized in this way: eccentricity and inclination variations are not remarkable, true anomaly shift (phasing) is an important concern, and ascending node (RAAN) shift, especially in the presence of strong third body perturbation (the Moon), could be a really important point (these results are sketched in Figures 8-9-10).

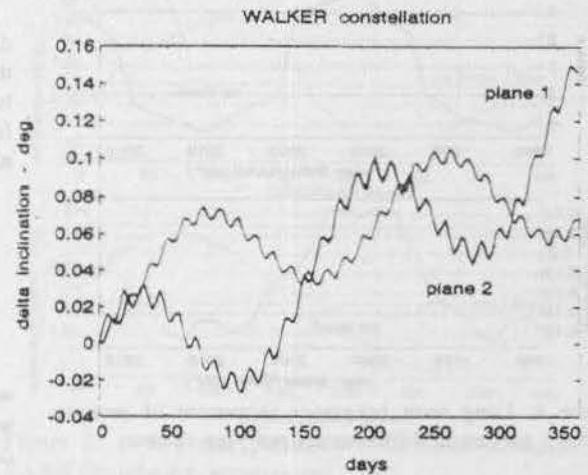


Figure 8: 4 satellites of Walker constellation (9/3/2 T=18h i=60°).

Perturbations of argument of perigee are of course not negligible, but they actually occur only on elliptic orbit constellation, as Draim model, we are not dealing with.

These considerations should be revisited in designing the actual constellation, because particular values of some parameter could enhance or reduce the sensitivity of the coverage properties with respect to the parameter's shift.

About the nature of perturbation, it is no difficult to observe that phasing is particularly affected by the air-drag; the generalized shift in the ascension of ascending node is caused by higher order terms in Earth potential, where the differences between planes are due to lunisolar effect; radiation pressure also with the related eclipse

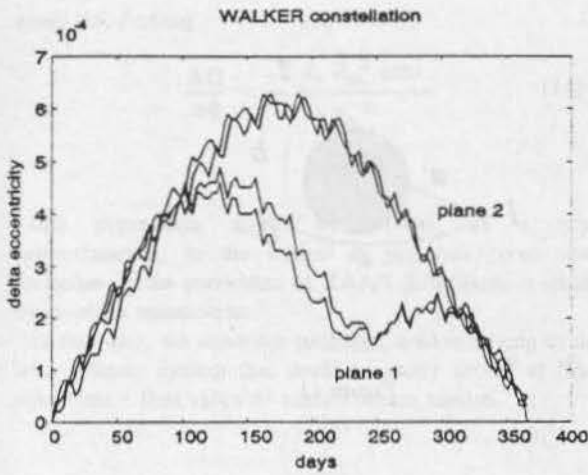


Figure 9: 4 satellites of Walker constellation (9/3/2 T=18h $i=60^\circ$).

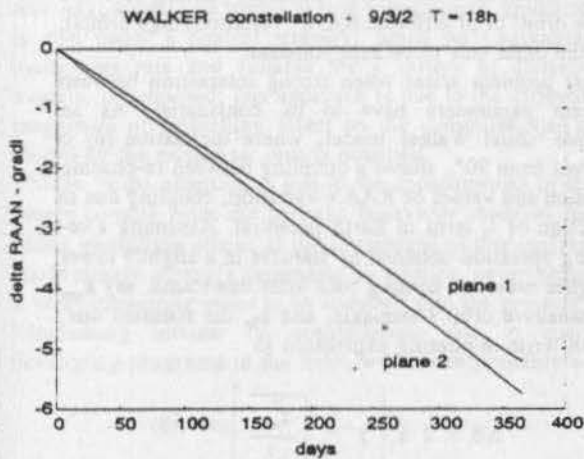


Figure 10: 4 satellites of Walker constellation (9/3/2 T=18h $i=60^\circ$).

periods do not seem to have strong impact, as we can expect using a cannon ball configuration for the satellite. The results presented, together with this note, are confirmed by the literature (see ⁵ as an example).

As we remembered in the previous introduction, Lamy and Pascal recently suggested a way to control satellites configuration based on the mean constellation, in order to reduce frequency and strenght of the manoeuvres. The problem arising is the way to define the mean constellation: Lamy and Pascal proposed⁸ a least square calculation for a Walker model. In the following, we propose a different approach, based on a simple application of Lagrangian multipliers rule: it gives an approximated but really simple method, useful for every

model.

Since the analysis of perturbing effect made before, we could think about a first order approximation control strategy, that takes into account only ascending nodes positions and phasing angle of constellation satellites; more, due to the fact that variations in RAAN are really similar for the satellites placed on the same plane, we could consider just p values, one for every orbital plane (see Figure 10), for this parameter.

The orbital propagation is so described by only $N=t+p$ parameters (where t is the total number of satellites, the unknowns being the phases of all the satellites (t) and the RAAN of all the planes (p)).

We start to define a cost function ψ , to be minimized. Expression of ψ , that conceives the cost of manoeuvre considered as the angle difference to be corrected, is:

$$\psi = \sum_{i=1}^t (\theta_i - \theta^0)^2 - \sum_{j=1}^p \alpha_j (\Omega_j - \Omega^0)^2 \quad (3)$$

with θ_i the optimal phase to be achieved (i.e. the mean constellation parameter) for the satellite i , Ω_j the optimal value of RAAN for the satellites on the j -plane, and θ^0 and Ω^0 the uncontrolled, perturbed values, chosen at the moment in which control action starts; α_j are the weights defining the cost of a RAAN correction with respect to a phase correction, in the sense we told before.

Constraints to be added are dependent on the model chosen. For example, let's start with a simple Rider-Adams model without interphasing, i.e. with arbitrary spacing in the phases of satellites placed on different planes (this model allows obviously a certain penalty with respect to the interphased one in the total number t of satellites needed to assure the coverage). In this case, we could consider the spacing between the satellites placed in the same plane as a first set of constraints:

$$g(\theta_{i+1}, \theta_i) = \theta_{i+1} - \theta_i = \frac{360^\circ}{t} p \quad (4)$$

$$(i = 1, \dots, \frac{t}{p} - 1)$$

to be evaluated for p planes, and the spacing between planes as a second set:

$$h(\Omega_{j+1}, \Omega_j) = \Omega_{j+1} - \Omega_j = \frac{360^\circ}{p} \quad (5)$$

$$(j = 1, \dots, p - 1)$$

so having $p(t/p-1)+p-1=T-1$ constraints to be satisfied (for the $t+np$ unknowns).

It should be remarked that using Lagrangian multipliers method when constraints are linear is not usually a nice and good way to follow, since the problem is easier to solve by substituting constraints expressions in cost formula and minimizing it as a one-variable function.

Nevertheless, due to the dimensions of a constellation simulation, the possibility to work with arrays should be gained.

So we could write the augmented function

$$\Psi = \psi + \sum_{k=1}^{r-p} \lambda_k g_k + \sum_{l=1}^{p-1} \eta_l h_l \quad (6)$$

and solve the problem with the linear system:

$$\begin{pmatrix} \frac{\partial \Psi}{\partial \theta_1} \\ \dots \\ \frac{\partial \Psi}{\partial \theta_r} \\ \frac{\partial \Psi}{\partial \lambda_1} \\ \dots \\ \frac{\partial \Psi}{\partial \lambda_{r-p}} \\ \frac{\partial \Psi}{\partial \eta_1} \\ \dots \\ \frac{\partial \Psi}{\partial \eta_{p-1}} \end{pmatrix} = (Q) \quad (7)$$

Indeed, the solution of controlled propagation for a non-interphased Rider-Adams model could be summarized in such a manner: (i) starting from desired conditions, propagation goes on, until some parameter's variation exceeds suitable limits (for the requested coverage service); (ii) at that time, linear system (7) is solved, obtaining optimal corrections to come back to desired conditions. Due to operator's choice, it is possible to act over all the satellites, or just over that one that exceeded limits, and to correct all parameters or not.

In the other cases, i.e. for different models, as interphased Rider-Adams or Walker, the constraints to be satisfied are different, and usually not so simple.

First of all, we have an increase in the constraints number, because we have to think about relations between phases of satellites in contiguous planes. In this case, we can observe in Fig. 11 that the link to be preserved is responding to the side a of the spherical triangle limited by the points 1 (1st satellite), 2 (2nd satellite) and 0 (ascending node of 2nd satellite). Side b variations depends on phasing error of both the satellites, side c depends on differential regression of nodes. But, due to the different sources of these two perturbations (mainly drag for phasing, and 3rd body effect for differences in RAAN rate) we can divide the field of interest in two parts. One side includes low orbit, where drag is strong, and the deformation of the spherical triangle (and so the widening or shortening of the a side) is mainly due to the

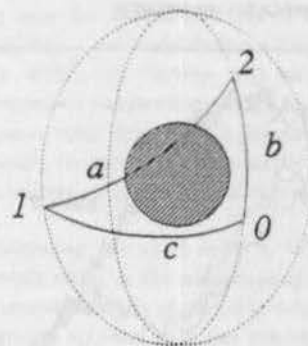


Figure 11

modification of b side. Other side is for higher orbits, where c side is mainly responsible for modifying the triangle. As a first choice we could always consider as a constraint that the length of a side of the triangle has to be equal to a fixed value, with a certain tolerance; this length being written as a function of different phasing of 1 and 2 (low orbit) or of different RAAN variation (high orbits), with the other side to be kept constant.

Other problem arises when strong interaction between different parameters have to be considered. As an example, usual Walker model, where inclination (δ) is different from 90° , allows a coupling between re-phasing operation and values of RAAN variation, coupling due to the action of J_2 term in Earth potential. Assuming a re-phasing operation obtained by transfer in a slightly lower or higher orbit and coming back after one round, say a_{man} the manoeuvre orbit's semiaxis, and a_{fn} the standard one, we can write re-phasing expression as

$$\Delta \theta = 2 \pi \left[1 - \sqrt{\frac{a_{man}^3}{a_{fn}^3}} \right] \quad (8)$$

solving for a_{man} and substituting into the expression of RAAN perturbation due to J_2 term for the two orbits, for small eccentricities

$$\Delta \Omega = -3 \pi J_2 R_{\oplus}^2 \cos i \left[a_{man}^{-2} - a_{fn}^{-2} \right] \quad (9)$$

we can obtain an expression of $\Delta \Omega$ (with respect to 1 orbit) as a function of a_{fn} and of $\Delta \theta$ to be imposed

$$\Delta \Omega = \frac{-3 \pi J_2 R_{\oplus}^2 \cos i}{a_{fn}^2} \left[\frac{1}{(1 - \Delta \theta)^{\frac{4}{3}}} - 1 \right] \quad (10)$$

and, at the end, for a first order theory, we linearize for

small $\Delta\theta$, finding

$$\frac{\Delta\Omega}{\Delta\theta} = \frac{-2 J_2 R_{\oplus}^2 \cos i}{a_{\text{fm}}^2} \quad (11)$$

this expression might be related, as a first approximation, to the weight in previous given cost formulae, if the correction of RAAN differences is made by in-plane maneuvers.

In this way, we solve the problem, always having to do with a linear system that could be easily solved to find everytime a first value of control action needed.

Conclusions

Quoting Lamy and Bonneau⁹, *the study of constellations is not quite easy*, due to the large amount of time needed by numerical simulation and to the intrinsic complexity of the problem, with a quite high number of variables. On this way, it could be useful to find some simple approach: in this paper a control strategy, based on Lagrangian multipliers rule and suitable for a variety of classical models, is proposed; this approach is due to the different magnitude of perturbing effect on the constellations, as shown by the numerical results obtained.

More, some attention is due to the consequences in the design coming from the periodic behaviour observed for Moon perturbing effect; as the advantages of this analysis could change strongly depending on altitude, nevertheless it is an interesting point to be focussed into the projects.

Increasing interest on constellation, due to many developing programs in the field, will create probably a

lot of work to be done on this subject, and above all on orbit deployment and keeping, forgotten fields in the past. Hopefully, this job will be as a first step for more general, less approximated modelling theories.

References

- ¹ Gobetz, F.W. Satellite Networks for Global Coverage. *Advances in the Astronautical Sciences*, Vol.9, 1963, pp.134-156.
- ² Draim, J.E. Three- and Four-Satellite Continuous-Coverage Constellation. *J. Guidance*, Vol.8, No.6, Nov-Dec 1985, pp. 725-730.
- ³ Draim, J.E. A Common-Period Four-Satellite Continuous Global Coverage Constellation. *J. Guidance*, Vol.10, No.5, Sept-Oct 1987, pp. 492-499.
- ⁴ Walker, J.G. Continuous Whole Earth Coverage by Circular-Orbit Satellite Patterns. Royal Aircraft Establishment, Tech.Rept.77044, March 1977.
- ⁵ Lüders, R.D. Satellite Networks for Continuous Zonal Coverage. *ARS Journal*, February 1961, pp.179-184.
- ⁶ Beste, D.C. Design of Satellite Constellations for Optimal Continuous Coverage. *IEEE Transactions on Aerospace and Electronics Systems*, AES 14, No.3, March 1978, pp.466-473.
- ⁷ Adams, W.S.; Rider, L. Circular Polar Constellations Providing Continuous Single or Multiple Coverage Above a Specified Latitude. *The Journal of Astronautical Sciences*, Vol.35, No.2, Apr-June 1987, pp. 155-192.
- ⁸ Lamy, A.; Pascal, S. Station Keeping Strategies for Constellations of Satellites. AAS-93-306.
- ⁹ Lamy, A.; Bonneau, F. Design of Constellations of Satellites. IAF-93-A.2.17. *44th IAF Congress*, Oct. 16/22, 1993, Graz, Austria.

A NEW APPROACH TO SPACECRAFT RELATIVE MOTION CONTROL

Shaohua YU

The Center for Space Science and Applied
 Research, Chinese Academy of Sciences
 P.O. Box 8701, Beijing 100080, PR China

Abstract

The dynamics of a relative motion between two nearby spacecraft is investigated in a local orbital coordinate system. A phase plane analysis shows that a stable equilibrium state may exist in the motion; Based on this analysis, a control method called a Range-Rate Control Algorithm (RRCA) has been established. Furthermore, an omni-directional version of RRCA (ODRRCA) has also been introduced. The controlled trajectory is stable and straight-line, whose orientation is a choice. The choice is completely free for ODRRCA and partially free for RRCA. The numerical computation, correlated measurement and propulsion implementation for the algorithm is very simple. As a illustration example, the tethered satellite system as well as in-orbit spacecraft rendezvous are simulated by the algorithm.

Key words: Equilibrium State, Stability, Range-Rate Control Algorithm

Equations of Motion

Under some assumptions, the terminal phase of a space transportation vehicle's rendezvous with an orbital station as well as the tethered satellite system may be considered as two typical examples of spacecraft relative motion at LEO, in which the mutual position and velocity between two involved spacecraft is of considerable importance. In such cases, one of the spacecraft is regarded as a reference spacecraft; its orbital coordinate system—as a reference coordinate system (Oxyz in Fig.1). In the system, the position of the second spacecraft, called a manoeuver spacecraft, is represented by a vector radius \vec{p} . Then the relative motion between the two spacecraft is described by a variation of the vector \vec{p} .

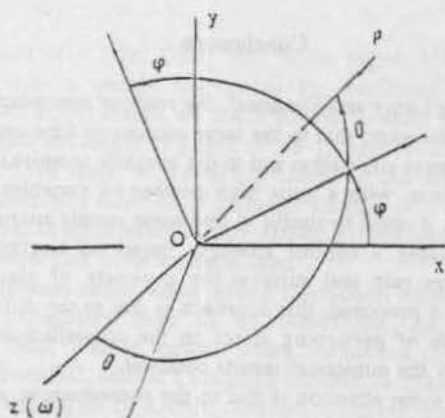


Fig. 1 Coordinate System

Assume the reference spacecraft is on a circle orbit; the orbital angular velocity is ω . Then for relatively small distances between two spacecraft (for example, less than 100 km), the relative motion is described by the C-W Equations¹. Their equivalent but in spherical coordinates is given by

$$\dot{\rho} - \rho\dot{\theta}^2 - \rho(\omega + \dot{\phi})^2 \cos^2 \theta - \rho\omega^2 (3\sin^2 \phi \cos^2 \theta - 1) = a_r \quad (1)$$

$$\rho\dot{\phi} + 2\dot{\rho}(\omega + \dot{\phi}) - 2\rho(\omega + \dot{\phi})\dot{\theta}\tan\theta - 1.5\rho\omega^2 \sin 2\phi = a_\phi / \cos\theta \quad (2)$$

$$\rho\dot{\theta} + 2\dot{\rho}\dot{\theta} + \rho(\omega + \dot{\phi})^2 \sin\theta\cos\theta + 1.5\rho\omega^2 \sin 2\theta \sin^2 \phi = a_\theta \quad (3)$$

$$x = \rho\cos\theta\cos\phi, \quad y = \rho\cos\theta\sin\phi, \quad z = -\rho\sin\theta$$

Equation (1) describes a variation of the magnitude of \vec{p} , while Eqns.(2) and (3) describe a variation of the direction of \vec{p} . Vector \vec{p} has two direction angles: φ and θ (see Fig.1). θ is the angle between \vec{p} and the orbital plane Oxy (out-of-plane or yaw angle). φ is the angle between the projection of \vec{p} on the plane Oxy and the axis Ox (in-plane phase or pitch angle). a_x, a_y, a_z are the differenced components of the accelerations of two spacecraft, resulted by all applied (except for gravitational) forces such as the propulsion, tether tension and other disturbance forces. Equations (1), (2) and (3) are called the distance motion (DM), phase angle motion (PAM) and out-of-plane angle motion (OPM) respectively. In practice, the OPM must be made small so that we can assume $\theta=0$ as to simplify some theoretical arguments displayed in this paper.

To divide the relative motion into two coupled motions, i.e. the DM and PAM motions of \vec{p} , is more convenient for a dynamics analysis of the motion. The dynamics analysis consists of determination of an equilibrium state of the motion, a stability analysis of the equilibrium state and a synthesis of control strategy of the motion. The importance of dynamics analysis is obvious. For example, owing to the gravitational stabilization theory of satellite attitude motion in a circle orbit, there exists a stable equilibrium state, in which one of the satellite body axes aligns with the orbit radius, hence a simple three-axis attitude control can be easily implemented for a earth pointed satellite. To this point, a good question may be asked for: is there any stable equilibrium state in the relative motion between two spacecraft as well? If there is one, then what is about the control strategy in this case?

Equilibrium State, Stability and Control

We start the analysis by DM. Assume that DM is determined according to the following program

$$\dot{\rho} = k\omega\rho \quad (4)$$

It implies such a variation of the propulsion a_x that the measured rate $\dot{\rho}$ must be equal to the programed rate $\dot{\rho}_{pr}$ by (4). We can assume a simple algorithm for the variation as

$$a_x = c(\dot{\rho} - \dot{\rho}_{pr}), \quad c > 0$$

The propulsion a_x is aligned with the line of sight between the two spacecraft and called an in-line propulsion. The parameter k in (4) is choosable. With $k > 0, k = 0$ or $k < 0$, the DM is of a departing

($\dot{\rho} > 0$), station-keeping ($\dot{\rho} = 0$) or closing ($\dot{\rho} < 0$) mode of the relative motion between two spacecraft, respectively; and hence k may be regarded as mode parameter. Once k is chosen, the DM is completely determined. To analyse the PAM, we substitute Eqn.(4) into Eqn.(2) to obtain a new form of the PAM as follows (assume $a_y = 0, a_z = 0, \theta = 0$ for the moment)

$$\dot{\varphi}' + 2k\omega\dot{\varphi} - 1.5\omega^2 \sin 2\varphi = -2k\omega^2 \quad (5)$$

A stationary solution of (5) is defined as an equilibrium state φ_e which is determined through

$$E(\varphi) = \sin 2\varphi_e - \frac{4}{3}k = 0 \quad (6)$$

The condition by which the equilibrium state exists is $k \in (-0.75, 0.75)$. The -0.75 and 0.75 are called as critical values of k , beyond which no equilibrium states can exist. For each selected k , there are four equilibrium states: $\varphi_{e1}, \varphi_{e2}, \varphi_{e3}, \varphi_{e4}$ (Fig.2). φ_{e1} and φ_{e3} correspond with the negative slope of $E(\varphi)$, they are 180° apart; φ_{e2} and φ_{e4} correspond with the positive slope of $E(\varphi)$, they are 180° apart, too.

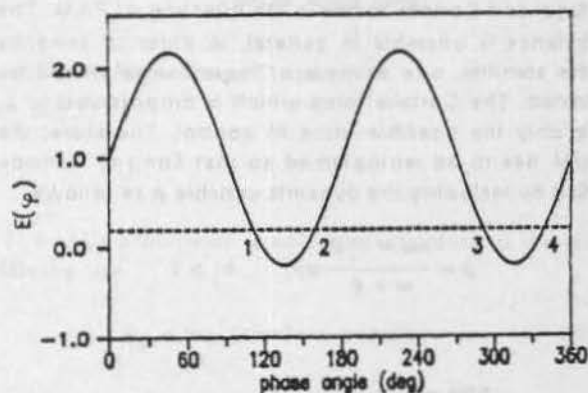


Figure 2. Location of Equilibrium states

In the equilibrium state, the manoeuvre craft is moving toward or away from the reference craft along a straight line in the coordinate plane Oxy, whose orientation is given by φ_e . While the distance and distance rate are determined by Eqn.(4): $\rho = \rho_0 e^{k\omega t}, \dot{\rho} = \dot{\rho}_0 e^{k\omega t}$; $\rho_0, \dot{\rho}_0$ are the initial values in the equilibrium state.

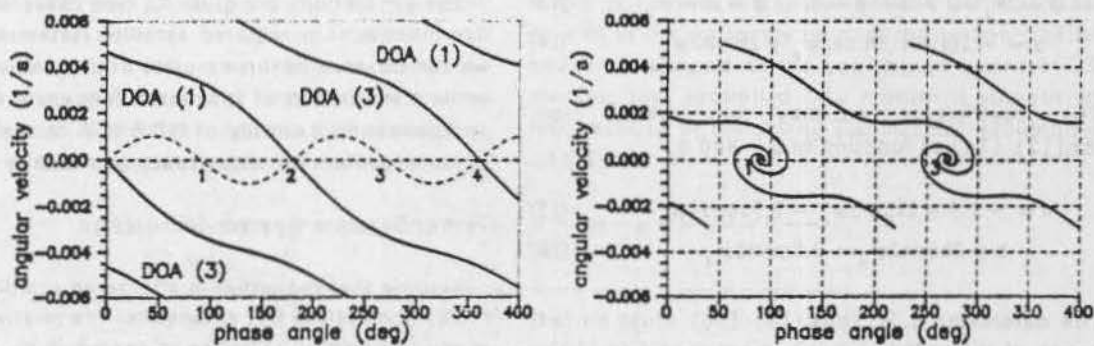


Figure 4. Domains of Attraction (DOA) / Phase Plane Trajectories
($k = 0.0, k_1 = 0.5$)

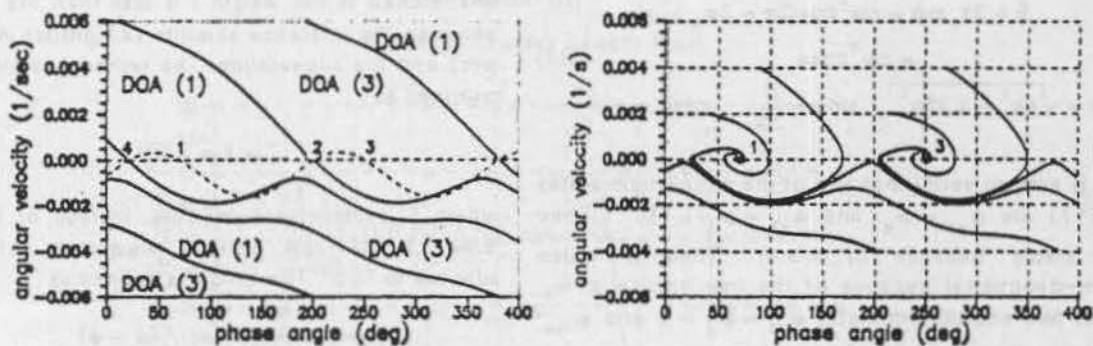


Figure 5. Domains of Attraction (DOA) / Phase Plane Trajectories
($k = 0.5, k_1 = 0.5$)

Omni-Directional RRCA

Because the parameter k of RRCA is limited to $(-0.75, 0.75)$, a small interval, the stable and straight-line trajectories of the equilibrium-states can exist only in some specific sectors in the orbital plane Oxy (see Fig.2); Besides, the range rate ρ in (8) can not be large, a fact which makes the controlled process relatively slow. To overcome these problems, we shall use the PAM's propulsion a_p in addition to a . The newly added propulsion force a_p may dramatically affect the above mentioned dynamic balance (equilibria) of PAM. In fact, the stable and straight-line trajectories now can be located anywhere at will in the whole orbital plane (omni-directionality), and the parameter k could be chosen as large as needed. This is the so called Omni-Directional Range-Rate Control Algorithm (ODRRCA)^{6,7}. ODRRCA consists of two parts:

1. in-line propulsion control based on RRCA of (8)

2. PAM's propulsion is adjusted according to the following law

$$a_p = \rho \omega^2 (a \sin 2\varphi + b \cos 2\varphi) \quad (10)$$

The coefficients a, b of Eqn.(10) are determined such that the equilibrium states of ODRRCA must meet both requirements of stability and omni-directionality. Substitute Eqns.(8) (10) into Eqn.(2) to obtain the PAM as

$$\ddot{\varphi} + 2k_1 \omega \dot{\varphi} - (a + 1.5)\omega^2 \sin 2\varphi - b\omega^2 \cos 2\varphi = -2k\omega^2 \quad (11)$$

An equilibrium state φ_d of Eqn.(11) satisfies the following relation

$$(a + 1.5)\sin 2\varphi_d + b \cos 2\varphi_d = 2k \quad (12)$$

This kind of control is simple on the one hand. It requires only to measure the distance and distance rate, and to adjust only in-line propulsion a_p . On the other hand, the resulted trajectory should be a straight line of known direction, a fact of great advantage for making up a mission profile. However, whether the control is implementable or not in practice depends on the stability of the equilibrium state. Only a stable equilibrium state has a practical interest.

To investigate the stability of an equilibrium state, the well known technique of linearized motion of small deviation is adopted. Thus the PAM is expanded about the equilibrium state to obtain a linearized motion as follows

$$\ddot{\tilde{\varphi}} + 2k\omega\dot{\tilde{\varphi}} - 3\omega^2 \cos 2\varphi_e \tilde{\varphi} = 0, \quad \tilde{\varphi} = \varphi - \varphi_e \quad (7)$$

The eigenvalues of Eqn.(7) are

$$\lambda_{1,2} = -k\omega \pm \omega \sqrt{k^2 + 3\cos 2\varphi_e}$$

An equilibrium state is stable, if all of its eigenvalues have negative real parts. Therefore, only φ_{e1} and φ_{e3} ($\cos 2\varphi_e < 0$ for them) are stable if only $k > 0$; for $k = 0$ or $k < 0$, no stable equilibrium states at all.

From the mechanics point of view, the equilibria is a dynamic balance between the gravitational, centrifugal and Coriolis forces in the direction of PAM. The balance is unstable in general. In order to enhance the stability, one or more of these forces should be varied. The Coriolis force which is proportional to ρ , is only the possible force to control. Therefore, the DM has to be reprogramed so that Eqn.(4) is modified by including the dynamic variable $\dot{\varphi}$ as follows.

$$\dot{\rho} = \frac{k\omega + k_1 \dot{\varphi}}{\omega + \dot{\varphi}} \omega \rho, \quad k_1 > 0 \quad (8)$$

Equation (8) has been defined as the Range-Rate Control Algorithm (RRCA)²⁻⁴. According to RRCA, the PAM has the following form

$$\ddot{\varphi} + 2k_1 \omega \dot{\varphi} - 1.5\omega^2 \sin 2\varphi = -2k\omega^2 \quad (9)$$

The RRCA has the same equilibrium states shown in Fig.2: But their stability property now is quite different. The linearized motion of (9) has the following eigenvalues

$$\lambda_{1,2} = -k_1 \omega \pm \omega \sqrt{k_1^2 + 3\cos 2\varphi_e}$$

Because $k_1 > 0$, the φ_{e1} and φ_{e3} are always stable. In the phase plane ($\varphi, \dot{\varphi}$), φ_{e1} and φ_{e3} might be stable nodes or stable focuses depending on whether $k_1^2 + 3\cos 2\varphi_{e2} > 0$ or < 0 ; The φ_{e2} and φ_{e4} are always unstable equilibrium states. This should not be surprised, because inbetween two stable equilibrium states ($\varphi_{e1}, \varphi_{e3}$) there must be a separation point, and the separation point is no one else but the unstable equilibrium states φ_{e2} and φ_{e4} .

So far, we have done the so called local stability analysis of the equilibrium states, that is the stability of PAM near by an equilibrium states. However, what is about the PAM, if it is far away from the equilibrium states? This is the subject of a global stability analysis. One method of the global stability analysis is to build a domain of attraction (DOA) of the stable equilibrium states in the phase plane ($\varphi, \dot{\varphi}$)^{4,5}. If the initial state of a PAM is inner the DOA of one of the equilibrium states, then the PAM will eventually converge with the stable equilibrium state after some transient process. Figures 3-5 give some variants of the DOA and the associated phase plane trajectories. The form and size of a DOA depends on the values of k , k_1 and ω .

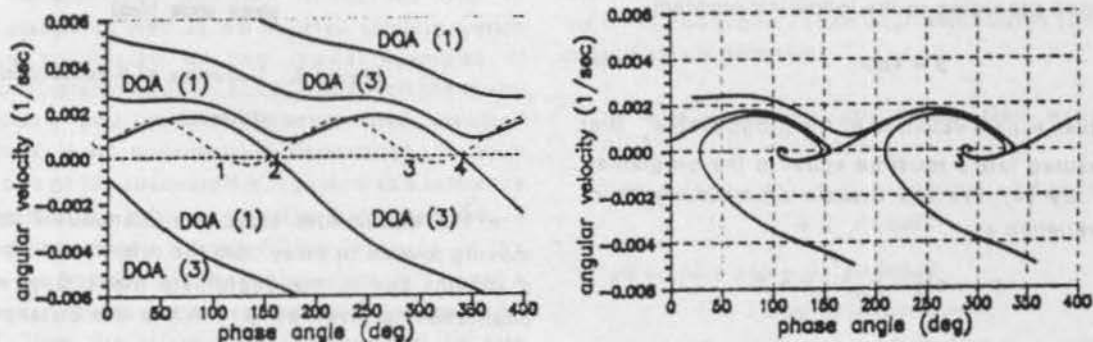


Figure 3. Domains of Attraction (DOA) / Phase Plane Trajectories

($k = -0.5, k_1 = 2.0$)

The linearized motion of Eqn.(11) is given by

$$\ddot{\bar{\phi}} + 2k_1 \omega \dot{\bar{\phi}} + q\omega^2 \bar{\phi} = 0, \quad \bar{\phi} = \phi - \phi_d \quad (13)$$

$$q = -2(a + 1.5)\cos 2\phi_d + 2b\sin 2\phi_d \quad (14)$$

The coefficients a,b may be solved from Eqns.(12) (14) as function of ϕ_d and q:

$$a = -1.5 + 2k\sin 2\phi_d - 0.5q\cos 2\phi_d \quad (15)$$

$$b = 2k\cos 2\phi_d + 0.5q\sin 2\phi_d \quad (16)$$

The parameter q in Eqns.(15) (16) must be > 0 because of the stability requirement (see Eqn.(13)); ϕ_d can be fixed at any value from $[0^\circ, 360^\circ]$ as to meet the omni-directionality requirement.

Substitute Eqns.(15) (16) into Eqn.(11) to obtain new form of PAM

$$\ddot{\bar{\phi}} + 2k_1 \omega \dot{\bar{\phi}} + c\omega^2 \cos(2\phi - 2\phi_d - \alpha) = c\omega^2 \cos \alpha \quad (17)$$

$$c = \sqrt{4k^2 + 0.25q^2}, \quad \sin \alpha = \frac{q}{2c}, \quad \cos \alpha = -\frac{2k}{c}$$

It is easy to verify that two of the equilibrium states of (17) are $\phi_{e1} = \phi_d$ and $\phi_{e3} = \phi_d + 180^\circ$; They are stable because of $q > 0$. They are also omni-directional because of the free choice of ϕ_d . Other two equilibrium states $\phi_{e2} = \phi_d + \alpha$ and $\phi_{e4} = \phi_d + \alpha + 180^\circ$ are unstable; they must separate ϕ_{e1} and ϕ_{e3} in the phase plane.

In principle, k may not be confined in ODRRCA. However, a reasonable value of k should be selected for speed up the control process and at the same time to ensure a suitable DOA for the stable equilibrium states of the motion. The parameters of ODRRCA such as k, k_1, ϕ_d, q may also be considered as control variables during the process so that some optimal controls may be solved⁶.

Computer Simulations

The simulations are given to two cases of the relative motion. In a tethered satellite system simulation we can observe all three modes of the relative motion, while a simulation of spacecraft rendezvous provides an application example of ODRRCA to the most important problem for today space technology.

Tether Satellite System Simulation

Assume that the tether in a tethered satellite system (TSS) is massless but extensible. The relative motion of the tethered subsatellite is described by the same Eqns.(1)-(3). However, an in-line tether tension force and aerodynamic force are included instead of the propulsions (which are not assumed in the subsatellite). For a normal operation of the system, the tether must keep a tension all time. Therefore, the unstretched tether length l is less than the distance between the reference satellite (an orbiter in the system) and the subsatellite. The tether tension T is determined as

$$T = E(\rho - l) / l$$

where E is the elastic module. Instead of RRCA, a tether length rate control algorithm (LRCA) is adapted to TSS⁸. The LRCA is defined as

$$\dot{l} = (k\omega + k_1 \dot{\phi})\omega l / (\omega + \dot{\phi}) \quad (14)$$

The mode parameter $k > 0$ is for the deployment phase, $k = 0$ is for the station-keeping phase and $k < 0$ is for the retrieval phase of the system. The station-keeping phase, especially the retrieval phase is basically unstable, and the control of the system is a challenging problem. However, the LRCA is very effective to control this system. A computer simulation of the US-Italy joint TSS-1 mission⁸ demonstrates the excellent performance of LRCA.

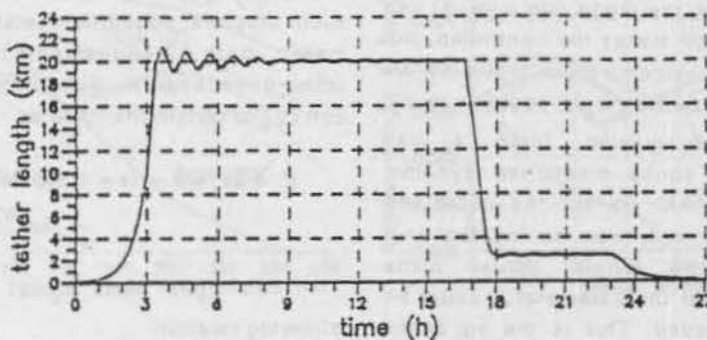


Figure 6. Tether Length's Variation

In the simulation, the orbiter circles the Earth at 250 km altitude, subsatellite weighs 500 kg and the E is equal to 34285 n. A round motion of the tethered subsatellite consists of upward deployment, station-keeping at 20 km, retrieval, second station-keeping at 2.4 km and final retrieval of the subsatellite into the orbiter. Figures 6-9 show the variations of tether length, length rate, tether tension

and the closed in-plane and out-of-plane motion paths of the subsatellite. The straight-line segments in the trajectories of deployment and retrieval phases as well as the stationary point of the station-keeping phase correspond to the equilibrium states of TSS motion. The controlled TSS motion is smooth and fast because of the strong stabilization capability of LRCA.

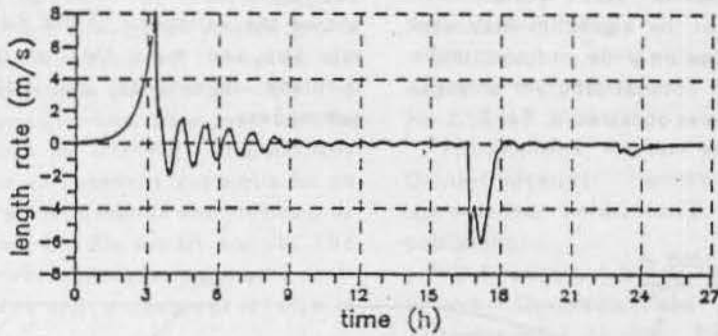


Figure 7. Tether Length Rate

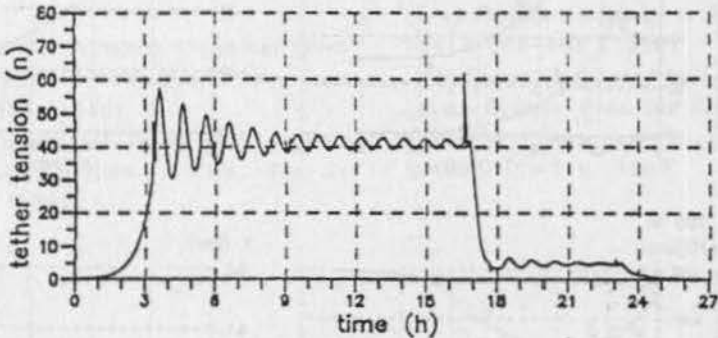


Figure 8. Tether Tension

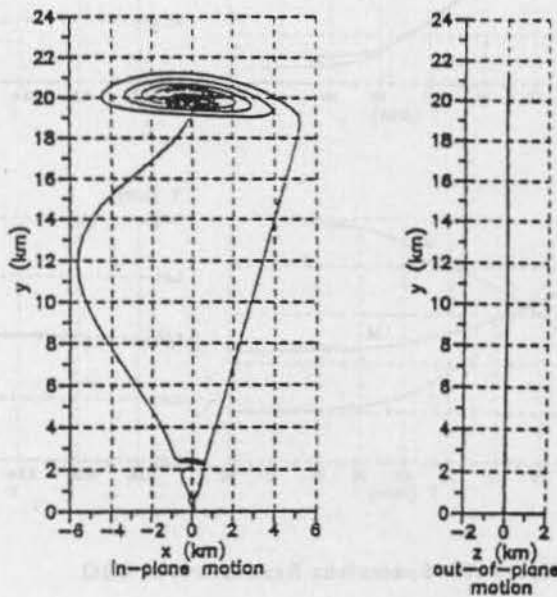


Figure 9. Three Dimensional Tethered Subsattelite Motion Path

Spacecraft Rendezvous Simulation

For a rendezvous control, the mode parameter k must be negative so that by the end of the process the distance as well as the distance rate are gradually decaying to zero, which is favourable for a consequent docking with the space station. In any cases, the universal ODRRCA is very useful. The parameters k , k_1 , φ_d , q of the algorithm may vary during the process provided only the end conditions are met. For example, an optimal program of variation of the parameter φ_d was obtained in Ref.7.

A computer simulation has been done for a rendezvous of the european HERMES spaceplane with the space station. The total rendezvous is divided into three sequential subprocesses in distance²: 100 km-1 km, 1 km-100 m and 100 m-20 m. By the end of each subprocess the spaceplane should be at the hold points located on the horizontal at 1 km, 100 m and 20 m behind the space station. Figure 10 shows the variations of the distance (D), distance rate (V) and mass (M) of the spaceplane; the in-plane trajectories are also given for each subprocess.

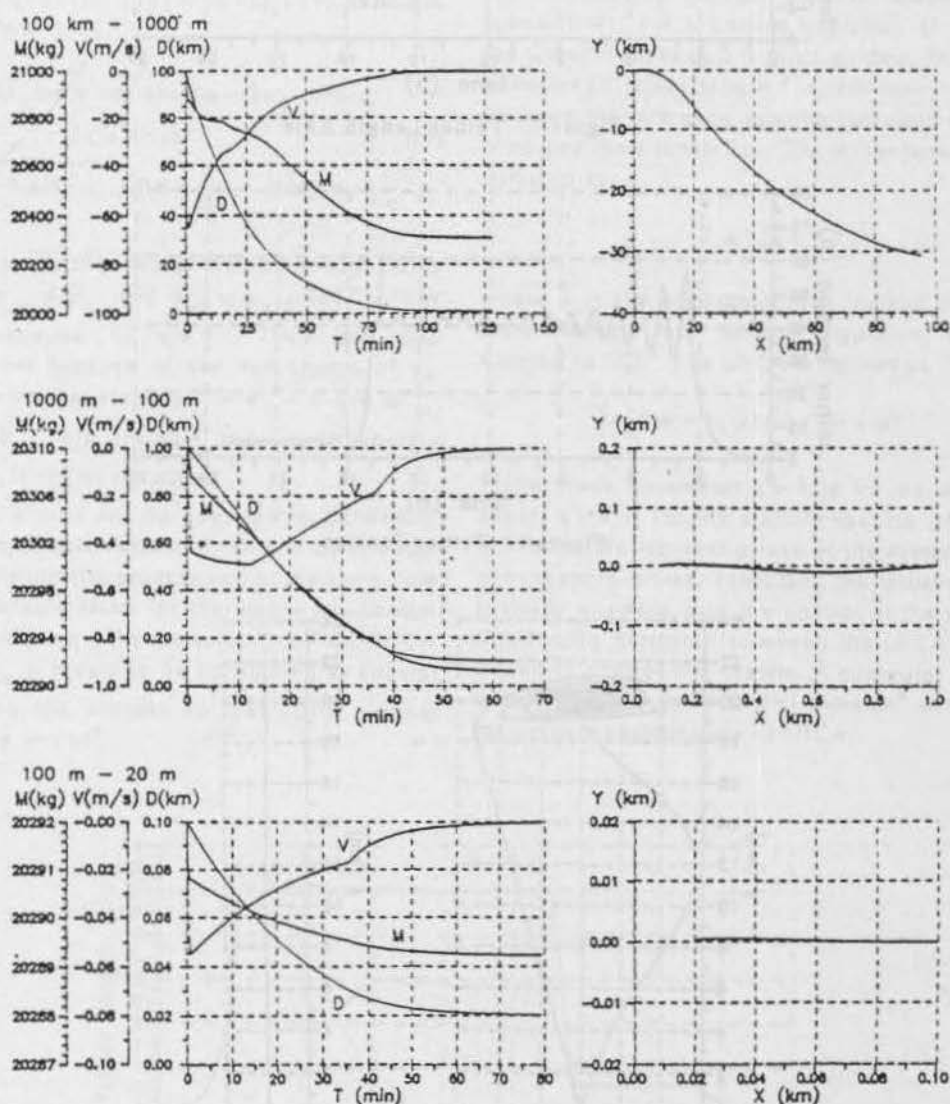


Figure 10. Spaceplane Rendezvous at LEO.

Conclusions

More and more space missions involve the relative motion between two spacecraft. The Range-Rate Control Algorithm (RRCA) and its modification ODRRCA have been worked out to control all modes of the relative motion (departing, station-keeping and closing). The most important point is that the algorithm ensures the existence of a stable equilibrium state in the motion. The controlled trajectory is stationary, stable and straight-line. The orientation of the straight-line trajectory can be chosen completely free for ODRRCA and partially free for RRCA. This is an excellent technique for an autonomous spacecraft rendezvous and docking as well as for the tethered satellite system control. The realization of the control technique, that is the computation, measurement and propulsion scheme is very simple.

REFERENCES

- ¹W.H.Clohesy and R.S.Wiltshire, Terminal Guidance System for Satellite Rendezvous, *J. Aerospace Science*, Vol.27, 653-658 (1960)
- ²YU Shaohua, On Straight-Line Mode of Autonomous Space Rendezvous Motion *J. Chin. Soc. Astronaut.* No.1, 22-27 (1992)
- ³YU Shaohua and R. Akiba, A Range-Rate Algorithm to Control the Relative Motion of Two Spacecraft, *Proc. Eighteenth International Symposium on Space Technology and Science*, Kagoshima, Japan, 579-584 (1992)
- ⁴YU Shaohua, Spacecraft Rendezvous Trajectory Control, *J. Chin. Soc. Astronaut.*, 1993(1), 44-51
- ⁵Andronov, et al., *Theory of Oscillators*, Pergamon Press, Oxford, 1966
- ⁶YU Shaohua, Omni-Directional Autonomous Rendezvous Control, *J. Chin. Soc. Astronaut.*, No.3, 10-17 (1993)
- ⁷YU Shaohua, R.Akiba and H.Matsuo, Control of Omni-Directional Rendezvous Trajectories, *Acta Astronautica*, Vol.00, No.00, pp.000-000 (1993) (in publishing)
- ⁸YU Shaohua, A Study on Space Tethered Satellite System Dynamics and Control, *J. Chin. Soc. Astronaut.*, No.2, 87-94 (1992)
- ⁹B.Musetti et al., Tethered Satellite System Dynamics and Control, *Proc. First Intern. Conf. on The Dynamics of Flexible Structures in Space*, Cranfield, UK, May 15-18, 563-585 (1990)
- ¹⁰M.Frezet et al., HERMES Rendez-Vous and Navigation System, *Proc. 2nd European In-Orbit Operation Technology Symposium*, Toulouse, France, 12-14 September, 207-218 (1989)

GROUND SYSTEM HARDWARE & SOFTWARE I

The Data Handling System for the Second German

1. Drexler, M. (DLR-Germany):
"The Data Handling System for the Second German
Spacelab Mission D-2" 199
2. Yamaguti, W.; Ribeiro, E.A.; Becceneri, J.C. and
Itami, S.N. (INPE-Brazil):
"Collection and Treatment of the Environmental
Data with Brazilian Satellite SCD1" 205
3. Beltan, T.; Jalbaud, M.; Fronton, J.F. (CNES-France):
"Automatic Generation of Reports at the Telecom
S.C.C." 212
4. Becceneri, J.C. (INPE-Brazil):
"Operational Facilities of Remote Control Software
of Ranging Measurement Equipment" 217
5. Garton, D. (CAM-Germany) and Frank, H. (DLR-Germany):
"The ROSAT Observation Timeline Scheduling
Algorithm and its Applicability to Future
Scientific Mission" 220
6. Pujo, O.; Head, N.C. and Jones, M. (ESOC-ESA):
"Object Oriented Design, the Software Life Cycle
and the Software Engineering Standards" 227

Support System which is installed at Cologne.

ESOC served as the Payload Operations Control Center (POCC) while NASA handled the System Element of the Spacelab and defining the NASA/GSFC interface used as a communication gateway between ESOC and GSOC. In addition to Payload Manufacturing Data Management, GSOC provided services for Data Recovery, Data Distribution, and Data Query Scheduling and Archiving.

1. NASA-GSOC Communication

The Goddard Space Flight Center (GSFC) served as GSOC's main site for NASA communications. Various NASA/GSFC operations communications links between GSFC and ESOC were established.

Initially the payload operations links were developed as the PPOC for uplink to the Spacelab Data Base and the Ground Data Base (GDB).

Four different intermediate types were to be communicated: High Rate Data (HRM) via CCSDS Transfer Frame (TFM), Low Rate Data (via NASCOM protocol and JSCD), Audio Data (ADPDM) signals, and Attenuated Low Rate Data (via TDM transmission facility, and Spacelab payload query, video, telemetry, and a separate communications link).

2. GSOC Data Handling

The GSOC Data Handling System consisted the following subsystems: a communications interface (CI), a HRM subsystem providing CCSDS data, a ground data processing subsystem (DPS), a NASCOM subsystem to address a Voice Linkdown

The Data Handling System for the Second German Spacelab Mission D-2

Manfred Drexler

Space Operations Department (GSOC)
German Aerospace Research Establishment (DLR)
Münchner Str. 20, D-82234 Oberpfaffenhofen, Germany

1. Overview

This paper describes the Data Handling System for the Second German Spacelab Mission D-2. In this manned mission, 88 scientific experiments were performed in 10 days (launch: 26/04/93, landing: 06/05/93). Research areas encompassed Life Sciences (biology, human physiology, radiation biology), Material Sciences (fluid physics, solidification), Technology (telescience, robotics), and Earth Observation and Astronomy. Experimenters were located at GSOC, except the MUSC (Microgravity User Support Center) which is established in Cologne.

GSOC served as the Payload Operations Control Center (POCC), while NASA handled the System Control of the Spacelab and orbiting Shuttle. NASA's GSFC facility acted as a communications gateway between JSC and GSOC. In addition to Payload Housekeeping Data Management, GSOC provided services for Data Archiving, Data Distribution, and Data Quality Monitoring and Accounting.

2. NASA-GSOC Communications

The Goddard Space Flight Center (GSFC) served as GSOC's entry into the NASA communications framework. Various transatlantic communications links between GSFC and GSOC were established:

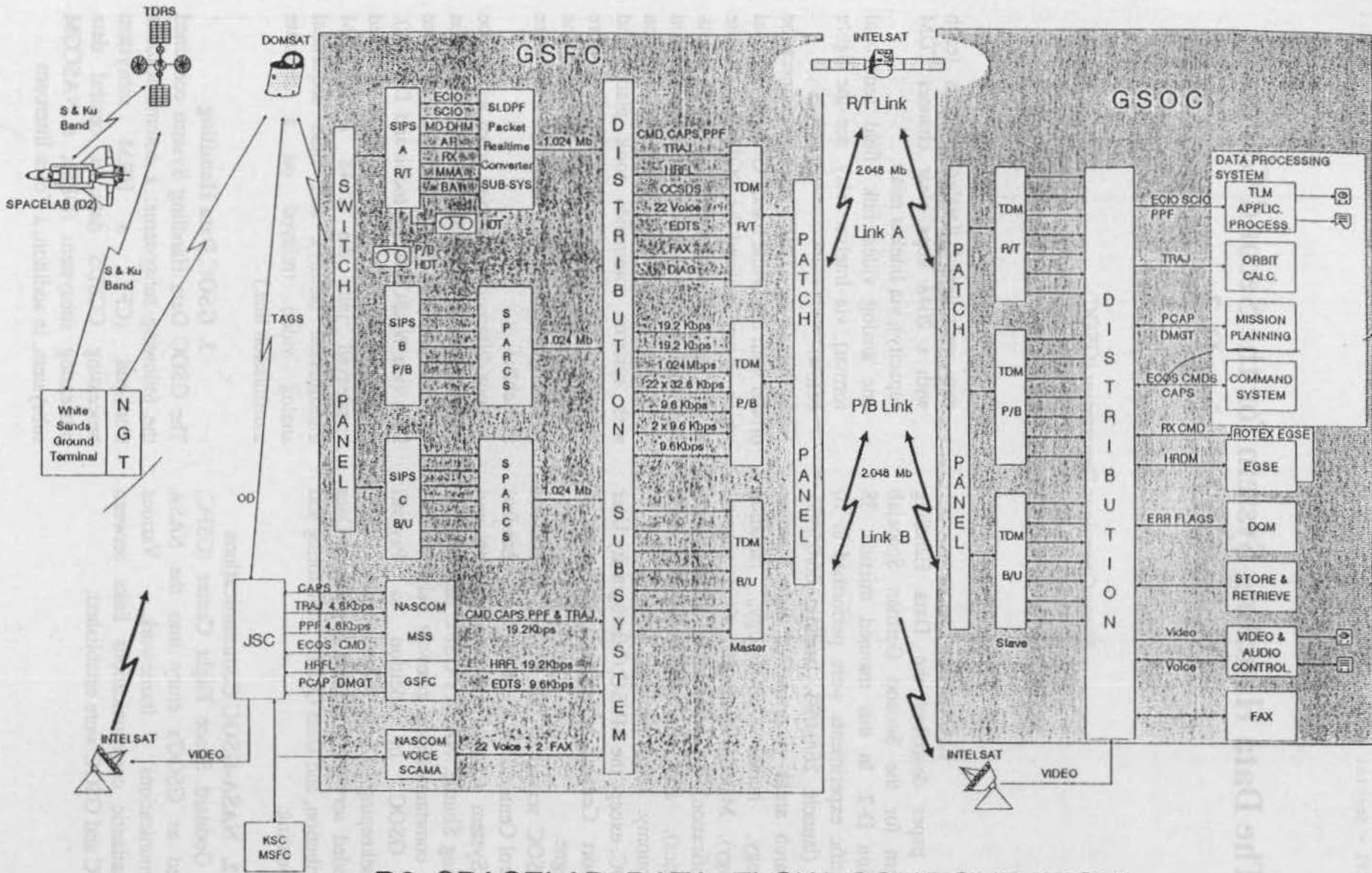
- two multiplexed data/voice links (each with a 2048 kbps clear channel TDM capacity), via Intelsat relay
- one analog video link (field sequential format), via Intelsat relay, see the figure below.

NASA employed TDRSS relay to connect the orbiter with the White Sands Ground Terminal which, in turn, utilized the DOMSAT satellite to link to JSC and GSFC. Payload uplink commands were issued at GSOC, passed on to GSFC, relayed to JSC where integration with systems commands took place, and eventually the merged command strings were transferred to the WSGT for uplink to the Shuttle (Ku Band and S Band RF links were available.)

Four different information types were to be communicated: High Rate Data HRM (via CCSDS Transfer Frame format), Low Rate Data (via NASCOM protocol and DECnet), Audio Data (ADPCM digitized and interleaved into the 2048 kbps TDM transmission facility), and field sequential analog video (relayed on a separate transmission line.)

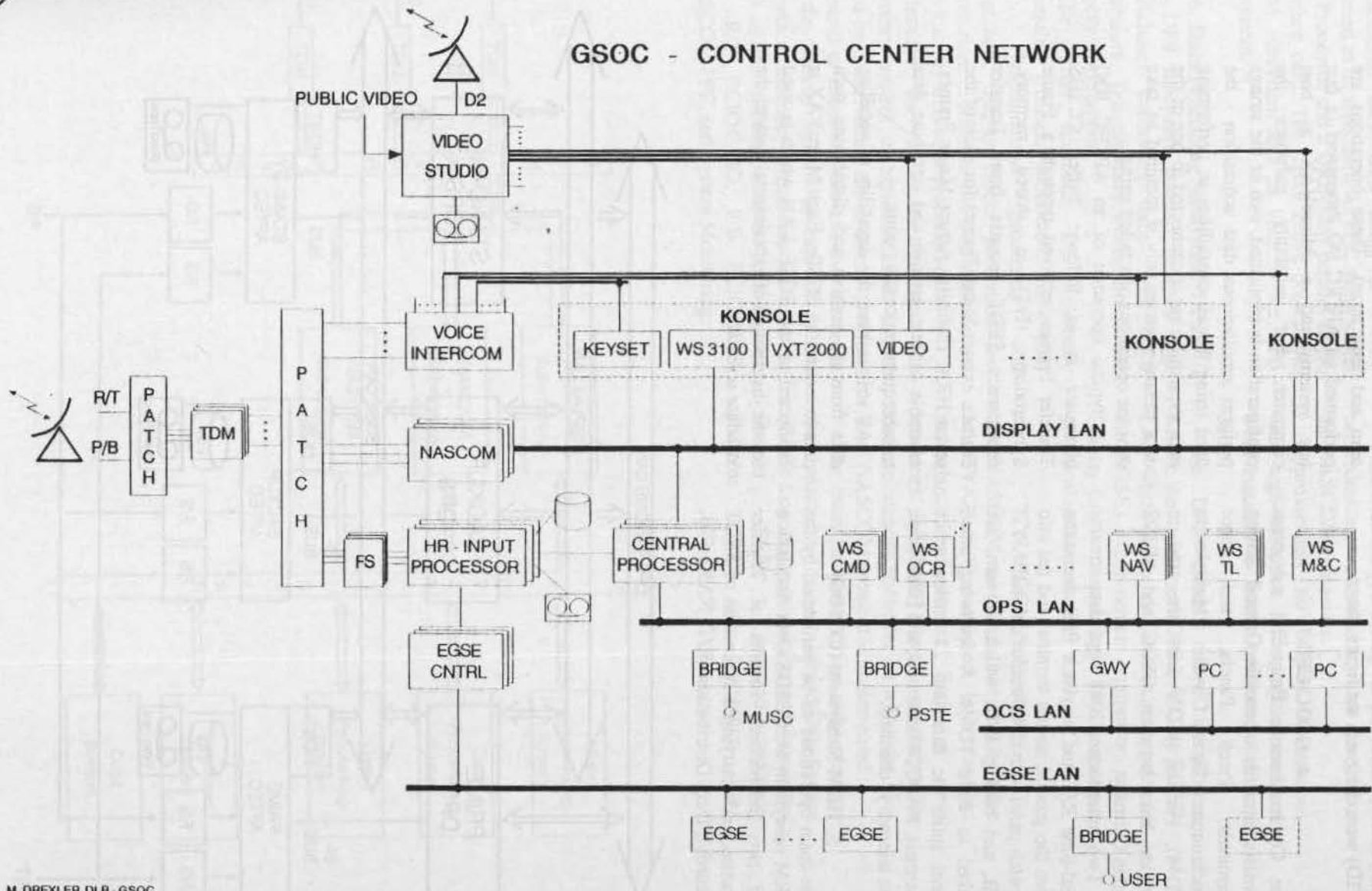
3. GSOC Data Handling

The GSOC Data Handling System contained the following subsystems: a communications front-end (CFE), a HRM subsystem processing CCSDS data, a central data processing subsystem (DPS), a NASCOM subsystem. In addition, a Voice Intercom



D2 SPACELAB DATA FLOW CONFIGURATION

GSOC - CONTROL CENTER NETWORK



201

Subsystem (VIS), and a Video Subsystem (VID) were designed, see figure above.

4. GSOC CFE

The Communications Front-End subsystem consists primarily of mobile Ground Station Terminals, Patch Panels, and three synchronous Time Division Multiplexers (TDM). Further, ISDN lines are used to provide links between GSOC and MUSC within Germany.

Two independent 2048 kbps data streams (real-time R/T and playback P/B) are taken from the ground station terminal and fed into a patch panel with three output channels: R/T, P/B, and backup B/U, which, in turn, are linked to three TDMs. A following patch panel splits the data into 21 analog voice channels, NASCOM channels, and HRM (high rate telemetry) channels.

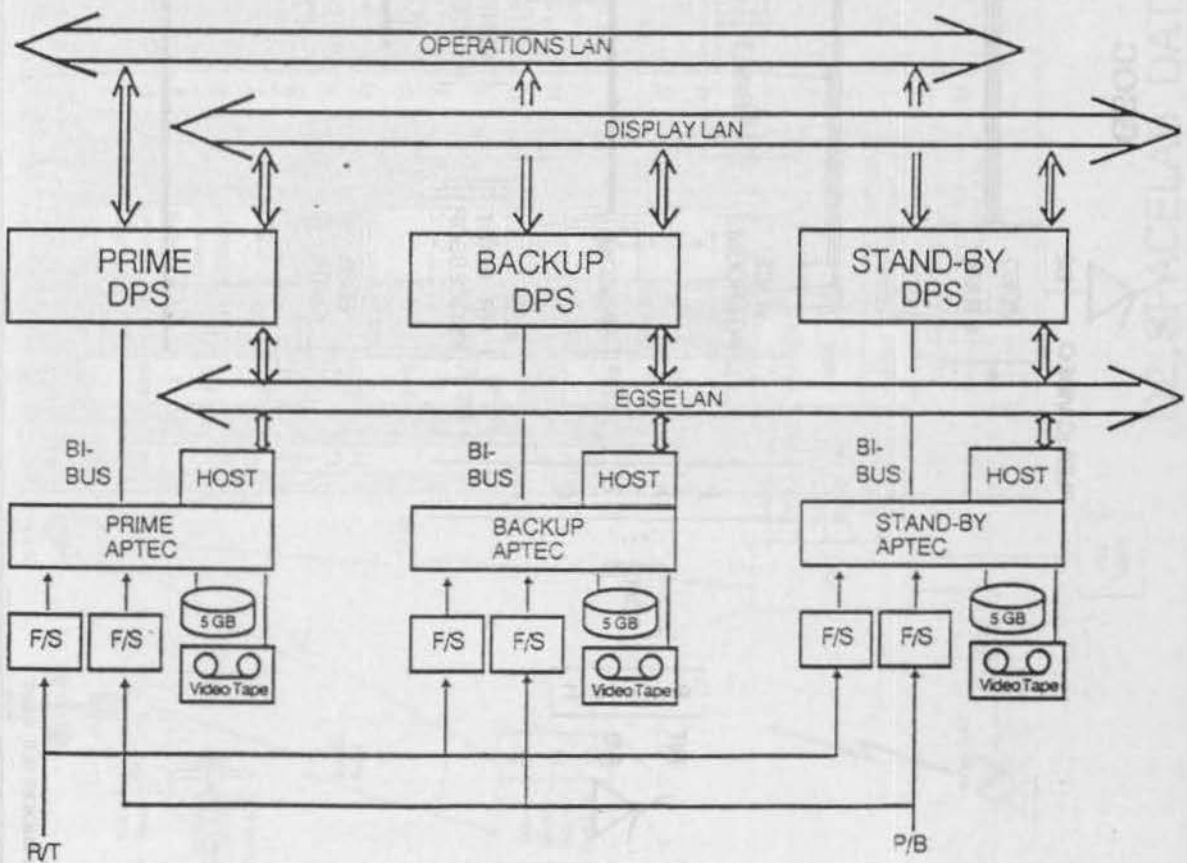
5. HRM Subsystem (CCSDS)

The main operations to be performed by the HRM subsystem are CCSDS Data Acquisition (of two independent streams of Transfer Frames, each carrying a succession of SEDT records), Data Distribution (R/T, NASA P/B,

and GSOC Recall), and Data Archiving (short term and long term). These operations are performed on APTEC I/O Processors (a fast bus system) and a MicroVAX as host computer. For reliability purposes the configuration is triplicated, two of the strings perform simultaneous data acquisition - the third string has all capabilities to performing data acquisition but is connected to one of the data stream sources only if required to take over the operations of a failed string.

A typical operation of an APTEC IOC computer is as follows: buffer CCSDS Transfer Frames received through a Frame Synchronizer (F/S) in shared memory, reconstruct SEDT records from Transfer Frames, extract Minor Frames for each of the seven HRM channels, extract Major Frames, assemble subsets, archive and distribute data to subsequent processing units.

All strings have the capability of recalling data from the archive and distributing such data to requesting EGSEs. Each MicroVAX is connected to the EGSE LAN which is used for the distribution of experimental data to the in-house scientists.



In addition, each DPS string is directly attached to its associated APTEC string via an I/O Processor and a DRB-32M parallel DMA interface card. The figure above depicts the HRM subsystem and its links to the DPS subsystem.

6. Data Processing Subsystem (DPS)

The DPS subsystem consists basically of a VAXcluster containing three VAX 6320 processors, Telecommand workstations, and Display workstations.

The main functions are Telemetry processing (receipt, calibration, quick-look, etc.), Telecommand processing and integration, Display blocks generation and distribution. In addition, the DPS maintains its own internal archive of processed data.

Because the DPS is triplicated the telemetry system is triplicated too. In the stand-by cluster string the telemetry system is prepared to adopt the role of either the prime or the backup system in case of failure. Individual telemetry processors are used for each of the different received data sources, i.e., R/T ECIO/SCIO, P/B ECIO/SCIO, NASCOM PPF, and System Monitoring.

Telecommand processing is performed on two redundant workstations which interface to the NASCOM computers.

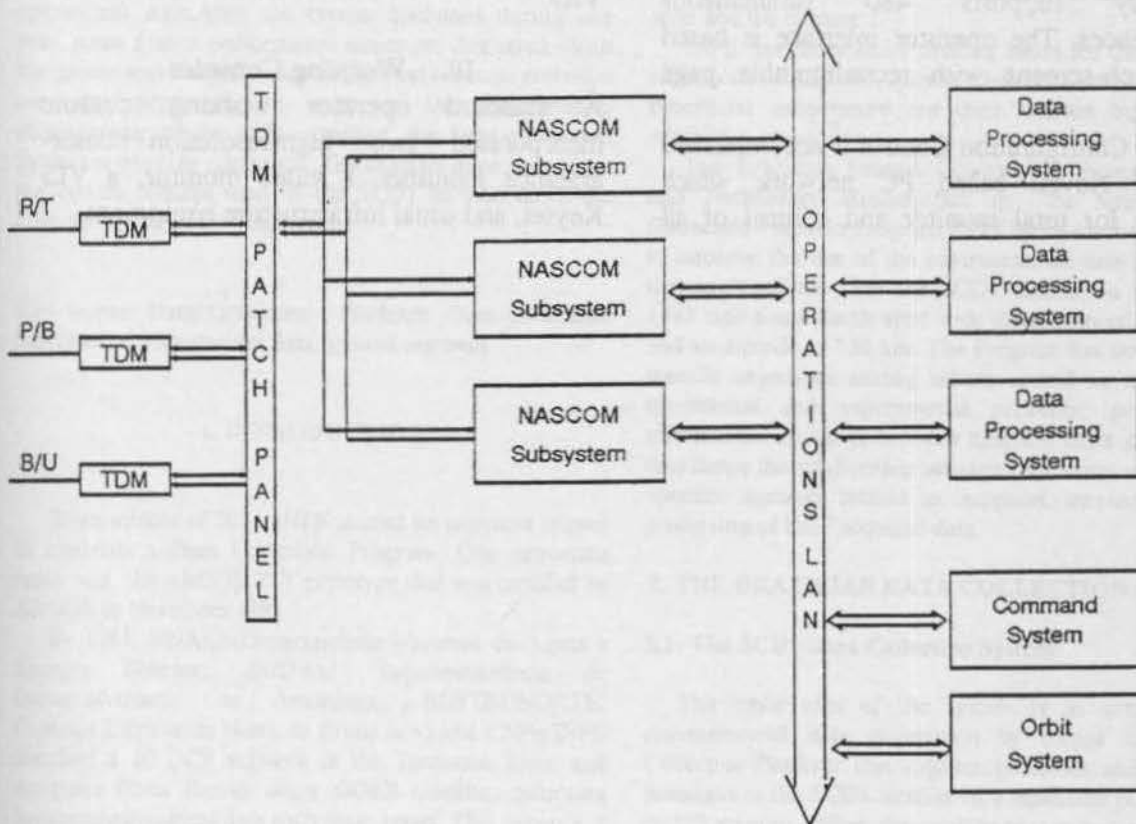
Approximately 60 Display workstations with high-resolution color-graphics monitors were installed to render processed telemetry data.

The DPS contains three independent LANs: the operational OPS-LAN, the EGSE-LAN which serves as a demarcation point to the EGSEs experimenters equipment, and a Display-LAN supporting the operator graphical user interface.

7. NASCOM Subsystem

The NASCOM subsystem incorporates three MicroVAX 3300 computers in a threefold redundant configuration. Each of these machines embeds two programmable communications controller on which the low-level NASCOM protocol is implemented.

The main functions of this subsystem are the provision of a Ground-Data-System (GDS) Log (for received Payload-Parameter-Frames (PPF), Command-Acceptance-Patterns (CAP), and Navigation data);



transferring standard telecommands to TDMs for uplink; handling a special low-latency High-Rate-Forward-Link (HRFL) command channel to the Spacelab robotics experiment ROTEX.

Via OPS-LAN the NASCOM subsystem is linked to the Telecommand workstations which, in turn, house the telecommand planning and execution software, see diagram above.

Shuttle trajectory data is routed through the NASCOM subsystem to a dedicated computer which processes orbit data.

Payload Timelining software is installed on a separate workstation and utilizes file transfer to communicate the D-2 timeline to NASA.

8. Audio Subsystem

The Voice Intercom Subsystem (VIS) features a total non-blocking distributed digital architecture utilizing dedicated microprocessor controlled 2 wire/4 wire and ISDN interfaces. The GSOC configuration currently supports 480 simultaneous conferences. The operator interface is based on touch-screens with reconfigurable page layouts.

VIS Configuration Control is accomplished via an Novell based PC network which enables for total monitor and control of all

VIS resources, even a partitioning of the subsystem, e.g. to provide support for separate parallel missions, is possible. 'Remote' Keysets are hooked up to the central switch via ISDN and digital leased lines to provide complete voice functionality to MUSC/Cologne.

Via a patch panel, the VIS subsystem is connected to the TDMs (approximately 600 kbps are used for 21 voice channels to NASA.)

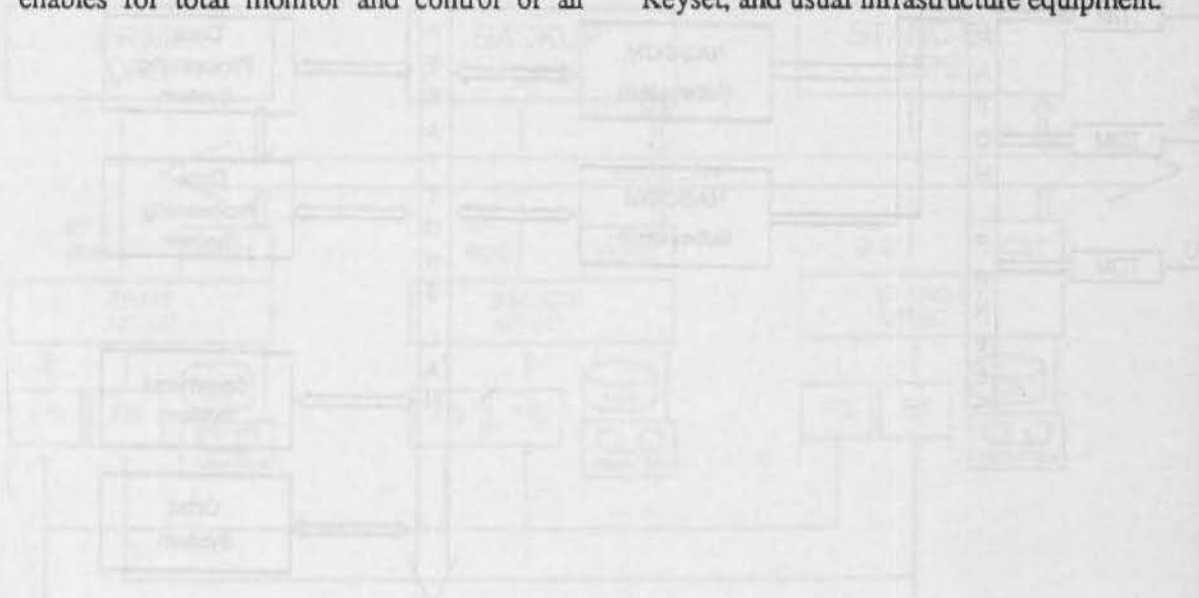
9. Video Subsystem

The heart of the Video Subsystem (VID) is a 20x120 Video Switch Matrix which connects to more than 60 video monitors (each equipped with a channel select panel.)

In addition, a converter is installed to transform NASA field sequential video into NTSC and PAL formats. Storage of the Shuttle video and other sources was done on Betacam SP recorders. A separate audio cross matrix was available to complement the VID.

10. Working Consoles

A standard operator working console incorporated two high-resolution color-graphics monitors, a video monitor, a VIS Keyset, and usual infrastructure equipment.



COLLECTION AND TREATMENT OF THE ENVIRONMENTAL DATA WITH THE BRAZILIAN SATELLITE SCD1

Wilson Yamaguti
Edson Alves Ribeiro
José Carlos Becceneri
Sergio Norio Itami

INSTITUTO NACIONAL DE PESQUISAS ESPACIAIS-INPE
Av. dos Astronautas, 1758
12227-010 São José dos Campos-SP BRAZIL
MECB%CCS@BRFAPESP.BITNET

ABSTRACT

This paper describes the Brazilian Data Collection System set up into operational state after the SCD1 launch on 9 February 1993 into a low Earth orbit with inclination of 25 degrees and an altitude of 750 km. The system is composed by: Data Collection Platform (DCP) Networks where each DCP acquires the environmental data and transmits it to the SCD1 satellite in a predefined repetition rate; the SCD1 satellite with a message relay function; and the Ground Segment Infrastructure that acquires the payload data retransmitted by the satellite to the ground, processes and disseminates to the users, and that has the tracking and control functions to maintain the SCD1 in a operational state. After the system operation during one year, some system performance issues are discussed. With the gained experience, future steps toward system evolution are also presented. In spite of the experimental characteristic of the SCD1 satellite, the Data Collection System is working quite well. The analysis done shows that the system concept used in the SCD1 as well as in the Ground Segment was reasonable.

Key words: Data Collection Platform, Data Collection Satellites, environmental data, ground segment

1. INTRODUCTION

Since middle of 70's, INPE started its activities related to establish a Data Collection Program. One important result was the ARGOS PTT prototype that was certified by ARGOS in November 1983.¹

By 1981, DNAEE (Departamento Nacional de Águas e Energia Elétrica), SUDAM (Superintendência do Desenvolvimento da Amazônia), ELETRONORTE (Centrais Elétricas do Norte do Brasil S/A) and CNPq/INPE installed a 10 DCP network in the Tocantins River and Araguaia River Basins using GOES satellite, collecting hydrometeorological data each three hours. This network is

operated by ELETRONORTE using INPE facilities at Cachoeira Paulista and it is an auxiliary system to the operation of Tucuruí Hydroelectric Power Station¹.

Another national experience was the efforts made by DNAEE and ORSTOM (Office de la Recherche Scientifique et Technique Outre-Mer) in the operation and in the installation of a network composed by 23 ARGOS compatible DCPs to monitor the Amazon Basin. The DCPs messages are obtained directly from the TIROS/NOAA satellites using a mini station¹.

FUNCEME (Fundação Cearense de Meteorologia e Recursos Hídricos) installed a DCP network in the Ceara state measuring the temperature, the wind direction and speed, the precipitation and humidity to monitor the water level and the climate.

INPE has been using drifting buoys for the studies of superficial maritime current dynamics through water superficial temperature and their location by means of ARGOS system²⁻³.

The Brazilian Federal Government through Science and Technology Ministry set up the National Data Collection Platform Program (PNPCD)¹ with the main goal to improve the use of the environmental data acquisition through satellites after the SCD1 launch on 9 February 1993 into a low Earth orbit with inclination of 25 degrees and an altitude of 750 km. The Program has the following specific objectives among others: install in the country operational and experimental networks; promote the information exchange between different users groups; and coordinate the relationship between DCP users and satellite operator agencies related to reception, transmission and processing of DCP acquired data.

2. THE BRAZILIAN DATA COLLECTION SYSTEM

2.1- The SCD1 Data Collection System

The basic idea of the system is to automate the environmental data acquisition by means of a Data Collection Platform that acquires, processes, and transmits messages to the SCD1 satellite in a repetition period of 90 to 220 seconds. When the satellite passes over the mutual

visibility of the DCP and the Cuiabá Ground Station, a communication link is established between the DCP and the Data Collection Processor (PROCOD) at the Cuiabá Station as shown in the Fig. 1. Once a day, all the received message are sent to the Data Collection Mission Center (CMCD) at Cachoeira Paulista for further processing, data base management and data dissemination to the users.

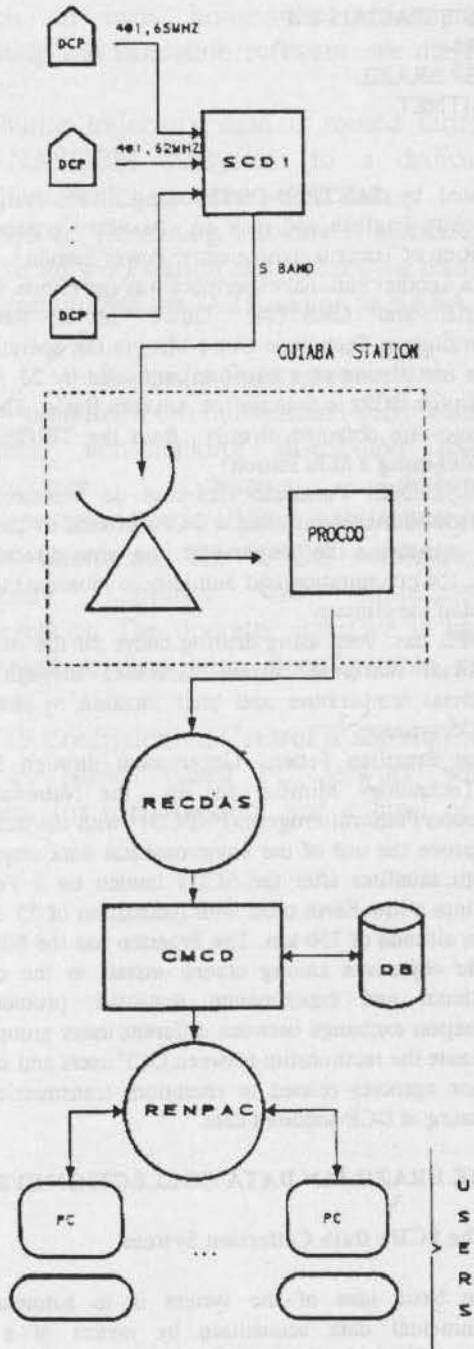


Figure 1 - Data Collection System Block Diagram

Due to existing DCP network and the experimental characteristics of the SCD1 Mission, the SCD1 satellite was equipped with a DCP Transponder that retransmits all the received message in 401.65 MHz (same as ARGOS System) or in 401.62 MHz to the S Band (2.267 GHz) for Cuiaba Station. Thus, the SCD1 System receives all DCPs in operation with ARGOS compatibility in the visibility of Cuiaba Station. As the SCD1 satellite has an orbit period of 100 min., it passes over the Cuiaba Station 8 passes per day.

In the SCD1 satellite there is no any type of on board processing or even a message storage capability for latter retransmission. All processing is done at the Ground Station by the PROCOD. The DCP Transponder just converts the messages in UHF Band to the S Band. This simplifies the on board equipment, as well as it is suitable for experimental purposes. The DCP message format is not fixed and depends only of PROCOD subsystem. In case of use another DCP message format it is sufficient to change the PROCOD configuration.

2.2- Experimental network installed for the SCD1 Mission

The environmental data acquisition by means of a platform and a satellite has several advantages⁴. The platform can be installed in any place such as remote region of Amazon forest and where the access is very difficult.

The INPE data collection experimental networks installed for the SCD1 mission are composed by:

- a) Amazon Program network⁵⁻⁶ for environmental sciences, with initial 10 DCPs as shown in Fig.2, related to Ozone Layer studies, greenhouse effects studies, biomass burning studies. The sensors available are atmospheric pressure, wind direction and speed, ultra violet radiation, CO2 concentration, CO2 temperature, Ozone concentration, air temperature. The DCPs have repetition rate between 205 and 215 seconds.
- b) Amazon Program network for studies of tropical forest regeneration with 3 DCPs installed near to Manaus. The sensors acquire the following data: ground temperature, heat flow, air temperature, humidity, incident and reflected radiation, and wind speed, with a repetition rate of 180 seconds.
- c) Tide-gauge network⁷ enables for the first time a systematic data collection of South Atlantic (coast and oceanic area) with 4 DCPs installed acquiring sea level in an hourly basis through the submarine pressure and water temperature. Soon the sensors for atmospheric pressure and water salinity will be installed. This data will enable the fishing forecast for the northeast region based on better understating the mean sea level and temperature of the ocean and their current.

All these networks are being coordinated by the National Data Collection Platform Program (PNPCD-Programa Nacional de Plataformas de Coleta de Dados), as mentioned before.



Figure 2 - Amazon Program Network DCP locations.
Source: Kirchhoff⁶

3. GROUND SEGMENT INFRASTRUCTURE

The Ground Segment has the responsibilities of monitoring and controlling the SCD1 Satellite, and receiving, processing and distributing the payload data. To realize these objectives the Ground Segment comprises: the DCP Networks; the Satellite Control Center (CCS); the Ground Segment Data Communications Network (RECDAS); the Data Collection Mission Center (CMCD) located in Cachoeira Paulista-SP; and by the Cuiabá and Alcântara Stations.

3.1- Data Collection Mission Center

The CMCD main role⁸ is to receive the DCP data sent through the RECDAS by the Cuiabá Ground Station, storing and processing these data to engineering units and keeping them available for remote user through the public Packet Switch Network (RENPA). The CMCD monitors the mission payload performance to the MECB Program management.

The current configuration is based on system among the existing national alternatives (the Digirede DGR 8000) that employs a Motorola 68010 microprocessor, a UNIX-like multi-user operating system and a relational database package with a C language interface. To perform all process of data acquisition and treatment, the CMCD⁸ is implemented as a set of functions interacting with external entities and operating over the data base.

The main functions are : Acquire payload data; Check Acquired Data; Process Sensor Data; Send User Requested

Data; Update Directories; Generate Reports. The data sets over which the functions above will act are: Raw Data; Pass Events; DCP Sensor Data; Processed Data; DCP directory; Sensor Directory; and User Directory. The function "Acquire Payload Data" receives payload data from the Cuiabá Ground Station through the RECDAS , performs message header checkout and stores the data into the Raw Data file for further processing.

The function "Check Acquired Data" reads the Raw Data file, checks the DCP directory for platform registration, identifies incomplete or erroneous messages, eliminates redundancies from the valid message and stores them into "DCP Sensor Data" for further processing. The Event Data (time-tagged, occurrence of "good" and "bad" messages, source and other relevant information like associated Doppler Shift) are stored in a cumulative data set "Pass Events" for use of other functions.

The function "Process Sensor Data" reads the packed sensor data (DCP Sensor Data) received from each DCP and converts them to engineering units according to the corresponding DCP directory and Sensor directory records. The converted data are stored in a cumulative data set (Processed Data) for consultation.

The function "Send user-requested data" handles the user interface (connection, password, protocol, dialog and disconnection), retrieves the requested Processed Data and sends the obtained information down the communication line or to a printer report to be mailed to the user.

Today for each users group, an account was defined in the CYBER computer just for file transfer all the received and processed data via RENPA.

3.2- Satellite Control Center

The CCS, located in São José dos Campos-SP, is responsible for the coordination of all activities of satellite control. It allows the execution of following tasks : monitor and control the satellite equipments ; determine and propagate orbits and attitudes; prepare and execute maneuvers; make mission analysis ; maintain the mission historical files ; monitor and configure the ground station equipments ; record operational information ; and generate activity schedule to CCS and ground stations.

The CCS computational is based on two VAX-8350 and one VAX-11/780. The application software is composed by Satellite Control System Software (SICS)⁹⁻¹⁰⁻¹¹⁻¹² responsible for all real-time functions of the CCS and Station Computers, Flight Dynamics Software, SCD1 Simulator , and other software packages for analysis, operation and maintenance support facilities.

3.3- Data Communication Network

RECDAS allows the data communication between CCS , the ground stations and CMCD. It is a private packet switching network that utilizes the X.25 protocol and the X.28 protocol, and is composed by three nodes and one Network Control Center (NCC). The NCC is

installed in the CCS building and utilizes a Cobra 580 computer. The network has a star configuration, being São José dos Campos the central node and today only the Cuiabá Station has its own RECDAS node installed physically.

3.4- Ground Stations

The MECB ground segment includes two ground stations: the first, in Cuiabá, is able to perform telemetry reception, tracking and command of satellites, as well as to receive payload telemetry data; the second, located in Alcântara, is configured just as a telemetry, tracking and command (TT&C) station. The main functions of a MECB station¹³ are: to receive satellite attitude and status data; to command attitude and orbit changes and/or corrections as well as satellite status modifications; to perform range and range-rate measurements for orbit determination; to receive payload data (Cuiabá station only).

It also performs the following ancillary functions: automatic supervision of station equipment; time code and frequency reference generation and distribution; station operation log files maintenance; weather data collection for ranging corrections.

The station is functionally divided into: front-end; housekeeping telemetry equipment; telecommand encoder; ranging equipment; station computer; time and frequency reference equipment; PROCOD, the payload telemetry equipment.

As mentioned before, the DCP messages received at Cuiabá Station is processed by PROCOD. This equipment¹⁴ receives down converted DCP messages in 68-92 KHz band for 401.62 MHz, or in 98-122 KHz band for 401.65MHz. For each band, the PROCOD has the capability to process up to 2 simultaneous messages. Due to random characteristics in time and in frequency of DCP transmitted signals, a search and a detection process should be executed. Once the signal is detected, a message processing channel is associated to recover the DCP message. A standard payload message is stored in a floppy disk unit with this recovered message and auxiliary data such as carrier frequency, channel status, message length, and a time stamp. According to the established operational procedures, the files with DCP messages are transmitted once a day to the Mission Center.

4. SYSTEM PERFORMANCE EVALUATION

4.1 - System Performance goals related to DCP Reception

The SCD1 mission is capable of operating simultaneously¹⁵ with up to 500 DCPs with message format compatible with ARGOS System. Half these platforms can operate in the same transmission frequency as ARGOS System (401.65 MHz).

The capability of the System to receive a message from a DCP depends on primary the location in the coverage region of receiving Ground Station, the DCP power transmitted (1 to 2 Watts), and its repetition rate (90 to 220 seconds).

Up to 4 simultaneously DCP message can be processed by the PROCOD subsystem.

Today, as mentioned before, only Cuiabá Station is equipped with PROCOD subsystem. This implies that the DCP should installed inside the coverage region shown in the Fig. 3. This coverage region⁴ corresponds to a circle of 3000 km radius centered in Cuiabá, south limited by parallel 38.



Figure 3 - DCP covered location from Cuiabá

The data of all DCPs located less than 1200 km from Cuiabá are received at least seven times a day. The message of DCPs located between 1200 km and 3000 km are received less frequently, up to the minimum limit of once a day for DCPs located in the borders of the coverage region.

4.2- DCP Message Received analysis

To verify if the Data Collection System meets its performance requirements related to the reception of DCP messages, all received messages are accounted and the following charts summarizes some conclusions.

The Fig.4 shows that the system is receiving about 550 messages per day. From this quantity, 420 of them are valid one.

These valid messages means that the DCP identification is OK and the message length is compatible in the format. The system is receiving about 80 different DCP per day and half of them are not registered in the Mission Center files.

The Fig.5 and Fig.6 show the DCP reception capabilities related to the DCP location. It is interesting to see that in spite of the distance of the DCP installed in

ATOL DAS ROCAS (3.86° S; 33.80° W) the system is receiving better than NATAL (5.22° S; 35.34° W) due to the visibility circle angle elevation restricted by obstacles.

The Figures 7, 8 and 9 show the distribution of received messages per day for DCPs located in Cuiabá, Atol das Rocas and Barreiras during March/1993 to January/1994. Apparently the system is receiving less than expected, but analysing in detail, some satellite passes are lost and for DCP located near to the Cuiabá Station (aprox. less than 1200 km), the system received at least one message per SCD1 pass, and for DCPs located in the borders of visibility circle, the system received at least one DCP message per day as expected.

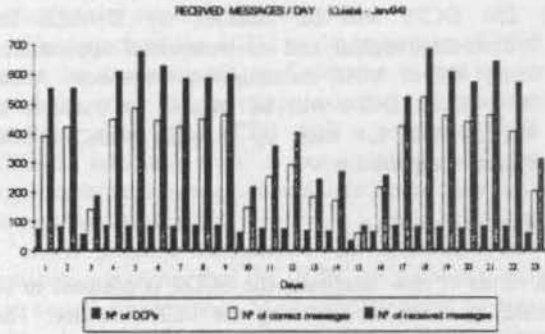


Figure 4 - Received message per day during Jan/94

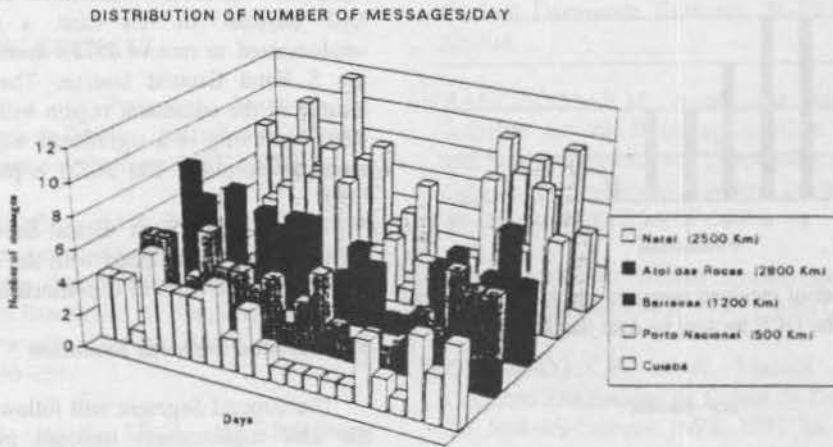


Figure 5 - DCP message reception according to location from Cuiabá during Jan/94

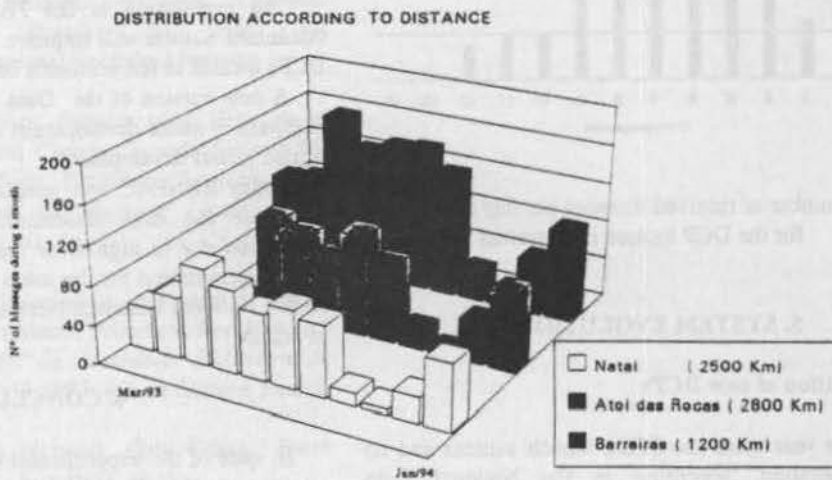


Figure 6 - Number of DCP message per month during Mar/93 to Jan/94. The left most column corresponds to Mar/93

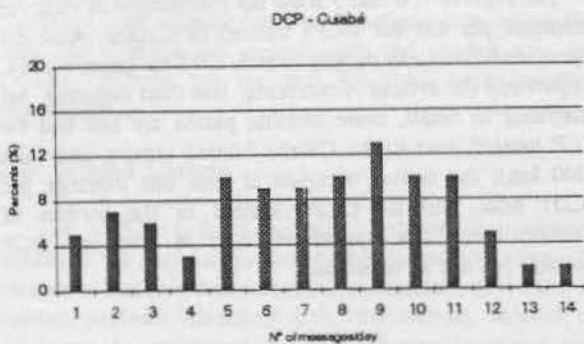


Figure 7 - Number of received message per day distribution for DCP located in Cuiabá

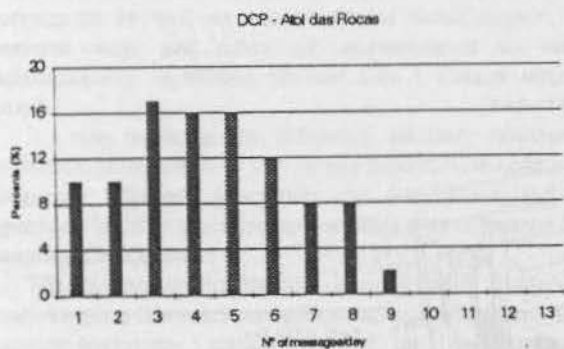


Figure 8 - Number of received message per day distribution for the DCP located in Atol das Rocas

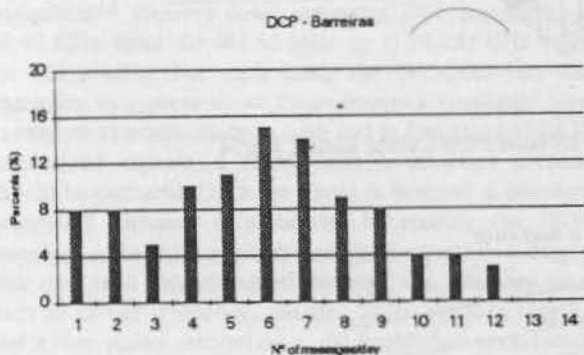


Figure 9 - Number of received message per day distribution for the DCP located in Barreiras

5. SYSTEM EVOLUTION

5.1 - Installation of new DCPs

After one year since the SCD1 launch success and its nominal operation, according to the National Data Collection Platform Program the number of DCPs will raise soon:

- 10 DCPs are being furnished by SUTRON for installation in the Itajaí Basin (Santa Catarina State) ; Minas Gerais State; Ceará State; INPE Magnetometer Network (Cachoeira Paulista).
- 250 DCPs will be installed by DNAEE for hydrometeorological and environmental applications using 401.62 MHz transmission frequency. About 30% of the DCPs will be capable to transmit in 401.65 MHz for back up purpose with ARGOS System compatibility.

5.2 - Future Satellites

In terms of new satellites, the SCD2 is planned to be launched by 1995 for assuring the SCD1 service. The SCD2 is similar to SCD1 with the payload down link using the S band and 25 degrees of orbit inclination.

The SCD3 will have a equatorial orbit and it will be equipped with another transmitter in the UHF band for the DCP payload. In this case, a mini station will be implemented to receive DCPs message independently of the S Band Ground Station. The message from DCP located in the equatorial region will be received each 100 min. improving in a significant way the number of DCP message reception. The SCD3 is planned to be launch in 1996.

The CBERS (China -Brazil Earth Resources Satellite) satellites will be equipped with the DCP transponder in a polar orbit. The CBERS is planned to be launch in 1996.

5.3 - Ground Segment Evolution

The Ground Segment will follow the evolution to meet the new requirements imposed by the next satellites. Related to the Data Collection System , a evolution of PROCOD is being planned by the use of Digital Signal Processor technologies and a version of PROCOD for mini station is under specification for the SCD3 and CBERS satellites.

The installation of the PROCOD equipment in the Alcântara Station will improve the reception of data from DCPs located in the northeast coastline.

A new version of the Data Collection Mission Center Software is under development and DCP location software is also under development.

Today RENPAC and telephone line access are being used for the data dissemination , but this imposes restriction due to high error rate of telephones lines. The data dissemination for the users will be improved by using RNP (National Research Network), bitnet and other forms of access.

6. CONCLUSION

In spite of the experimental characteristic of the SCD1 satellite, the Data Collection System is working quite well. The analysis done shows that the system concept used in

the SCD1 as well as in the Ground Segment was reasonable.

Future steps were presented based on the experience gained mainly in the operational and maintenance aspects, added by new available technologies.

The launch of the SCD2 in the beginning of 1995 will assure the continuity of Data Collection System service and could also cover the gap of approximately 10 hours without satellite passes. The SCD3 with a equatorial orbit and CBERS satellites with a polar orbits will increase significantly the number of satellites passes over Brazil for data collection purpose.

Some problem detected in the DCP operation and maintenance shows that the DCPs are submitted to severe and hostile environment. Maintenance should be organized with adequate financial support to recover the system and to reduce down time periods so that a better service can be provided to the users than today.

REFERENCES

- ¹MOTTA, A.G. et al. O Programa Nacional de Plataformas de Coleta de Dados - Informações Técnicas aos Usuários. São José dos Campos, INPE, 1984.
- ²SOUZA, R.B.; STEVENSON, M.R. Descrição de frentes oceânicas a partir de uma bóia de deriva rastreada por satélite e de dados hidrográficos durante a VII Expedição Antártica Brasileira. *VII Simposio Brasileiro de Sensoriamento Remoto*, Curitiba, Brazil, may 10-14, 1993, Vol(IV) pg 290-299.
- ³STEVENSON, M.R. et al. SIMA- An Integrated Environmental Monitoring System. *VII Simposio Brasileiro de Sensoriamento Remoto*, Curitiba, Brazil, May 10-14, 1993. Vol (IV) pg 300-310.
- ⁴AGUIRRE, J.L.B. Uma introdução ao Sistema de Coleta de Dados através dos Satélites Brasileiros da Missão Espacial Completa Brasileira. São José dos Campos, INPE, 1993 (Internal Technical Report).
- ⁵KIRCHHOFF, V.W.J.H. First Results of a Network of Tropospheric Ozone and Carbon Dioxide Sensors for Operation with the First Brazilian Satellite. *EOS Transaction. American Geophysical Union*, 1993 Spring Meeting, vol 74(16), Apr 20.
- ⁶KIRCHHOFF, V.W.J.H. Plataformas de Coleta de Dados do primeiro Satélite Brasileiro: Primeiros Resultados. *3 Congresso Internacional da Sociedade Brasileira de Geofísica*. November 7-11, 1993. Rio de Janeiro, Brazil.
- ⁷VIANNA, M. Brazilian Network Gets Going. *Earth Challenge*. CLS Argos, July 1993, N(3).
- ⁸MELLO, F.G.A. et al. Data Collection Mission Center. Technical Description. São José dos Campos, INPE, 1987(A-REV-0029).
- ⁹CARDOSO, L.S. et al. Telemetry Processing and Displaying Software for the Brazilian Complete Space Mission. *International Symposium on Ground Data Systems for Spacecraft Control*, Darmstadt, Germany, 26-29 June 1990. ESA SP-308.
- ¹⁰YAMAGUTI, W. et al. Satellite Control System Nucleus for the Brazilian Complete Space Mission. *International Symposium on Ground Data Systems for Spacecraft Control*, Darmstadt, Germany, 26-29 June 1990. ESA SP-308.
- ¹¹YAMAGUTI, W. et al. Telecommand Software for the Brazilian Complete Space Mission. *International Symposium on Ground Data Systems for Spacecraft Control*, Darmstadt, Germany, 26-29 June 1990. ESA SP-308.
- ¹²FRANCISCO, M.F.M. et al. The Antenna Manager Software for the Brazilian Satellite: Implementation and Study. *International Symposium on Ground Data Systems for Spacecraft Control*, Darmstadt, Germany, 26-29 June 1990. ESA SP-308.
- ¹³BARROS, P.M.M. Ground Station Specifications. São José dos Campos, INPE, 1989. (A-ETC-0019).
- ¹⁴SOBRINHO, L.C.P. et al. Manual de Sistema do Conjunto Processador de Coleta de Dados (PROCOD). São José dos Campos, INPE, 1991. (A-MIN-0036).
- ¹⁵TUDE, E.A.P. et al. Análise do Sistema de Coleta de Dados da MECB/SS. São José dos Campos, INPE, 1984 (Internal Technical Report).

AUTOMATIC GENERATION OF REPORTS AT THE TELECOM S.C.C.

Author: Thierry BELTAN, CNES - FRANCE.

Co-authors: Myriam JALBAUD, Jean François FRONTON, CNES - FRANCE.

Address: CNES - ET/EO/ER/TC
18, Avenue Edouard BELIN
31055 TOULOUSE CEDEX
FRANCE

Abstract

In-orbit satellite follow-up produces a certain amount of reports on a regular basis (daily, weekly, quarterly, annually). Most of these documents use the information of former issues with the increments of the last period of time. They are made up of text, tables, graphs or pictures.

The name of the system presented here is SGM (Système de Gestion de la Mémoire Technique), which means Technical Memory Management System.

It provides the system operators with tools to generate the greatest part of these reports, as automatically as possible.

It gives an easy access to the reports and the large amount of available memory enables the user to consult data on the complete lifetime of a satellite family.

Key words: Satellite follow-up reports, automatic generation

Introduction

The TELECOM S.C.C. is in charge of the control and the follow-up of the French TELECOM satellites. Three satellites are today in orbit. TELECOM 1-C is the last satellite from the TELECOM 1 family. TELECOM 2-A and TELECOM 2-B are the firsts flight models of the TELECOM 2 family.

One of the recurrent task of the S.C.C. is to publish operation reports and health reports for the different satellite sub-systems.

The spacecraft analysts are in charge of these reports. The main information source is the satellite telemetry, provided by the real-time control system or by a technical data base. The reports also use manually collected information.

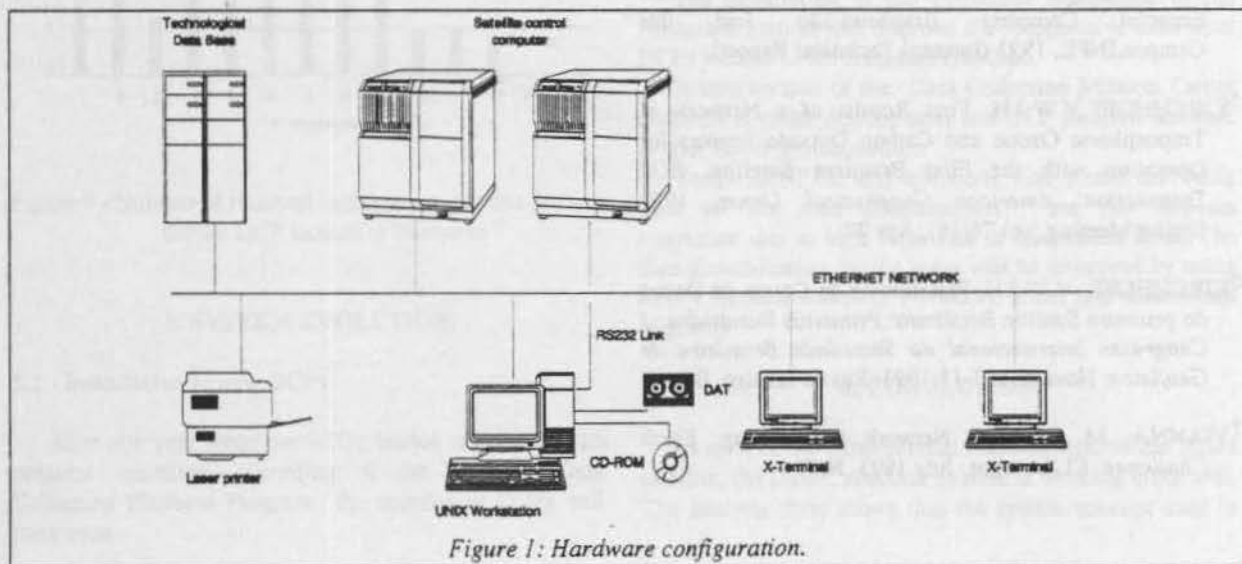


Figure 1: Hardware configuration.

For the build-up of the reports, the analysts were using personal computers connected to the information sources. They used spreadsheet programs to generate charts and tables, and text editors for the written part of the report. This method needed floppy disks and documents manipulations, manual cut/paste operations.

For a given type of document, the successive issues are often similar. The differences are the actual telemetry values, the comments and, if available, the increment of the historical part.

The evolution in the computer field and the need in terms of efficiency, ergonomics and quality led to the definition and the realisation of a system able to cover the full range of the report generation, and to be adapted to different telemetry or data sources.

General description

Hardware environment

The SGMT is supported by a UNIX platform under an OSF/MOTIF X-Window environment. We use a SUN 4/370 server with a 1.6 Gb disk, 64 Mb of RAM memory, a 2 Gb DAT unit and a 6 CD-ROM juke box. The capacity of a CD-ROM is 640 Mb.

The DAT unit is used to make periodical back-ups of the complete system environment (including the database but not all the reports).

The CD-ROM Juke box contains the generated reports. These reports are first saved on a temporary space on the disk. When the size of a CD-ROM is reached, the content of this temporary space is transferred to the definitive support, using the UFS format (standard UNIX format).

The CD-ROM has been chosen for its very good access time performance, its easy operating and its excellent data integrity.

To provide multiple user access, X terminals are connected to the SGMT via an ETHERNET network.

The SGMT may be connected to several data sources. For example, a technological data base or a satellite control computer. For the latter, we use the ETHERNET network or a serial RS-232 link.

The documents are printed on a Postscript laser printer.

Software choice

To take advantage of the continuous improvements in software science, we have chosen to use "On The Shelf" products as much as possible.

The choice criteria were:

- Standard aspect and portability.
- Easy communication between the different programs.

- Ergonomics, performance and evolution capability.

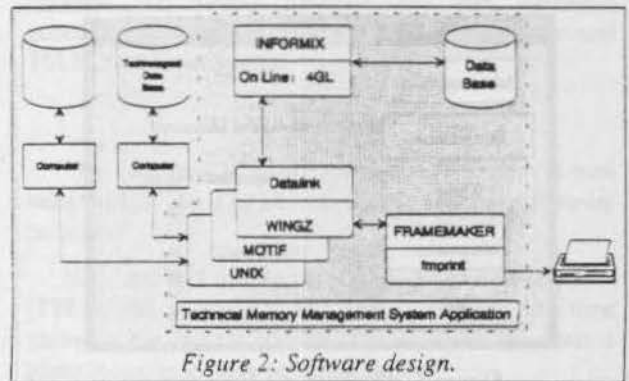


Figure 2: Software design.

The system is based on a Relational Data Base Management System (RDBMS). It uses a spreadsheet program to make calculation and charts, and a publishing tool to set up the lay-out of the final report.

The spreadsheet program is WINGZ. This product can compute and present results through graphics or tables. It also provides a script language, named Hyperscript, for the easy development of user programs.

The application supervisor has been written in Hyperscript, using the WINGZ-DataLink module, which enables access and update of the data base.

The RDBMS is INFORMIX On-Line. It was chosen for its good ability to communicate with the spreadsheet program and the good matching of its data type with the required ones.

As a publishing tool, we have chosen FRAMEMAKER, which is widely used on UNIX work stations.

Application description

The application has a user-friendly interface with push-buttons and scrolling menus.

The main menu enables the user to start administration or exploitation sessions. It allows to access directly and separately WINGZ and FRAMEMAKER.

The application manages the different users access rights. You don't get the same privileges if you are the system administrator or a simple user (e.g., only the system administrator can access directly the Data Base by using SQL statements...).

The Administration menu (see figure 4 below) gives an outline of these possibilities. In this menu, a simple user is only allowed to consult or add items to the data base. He also may start a work session on a remote calculator, but has no access to the archive functions.

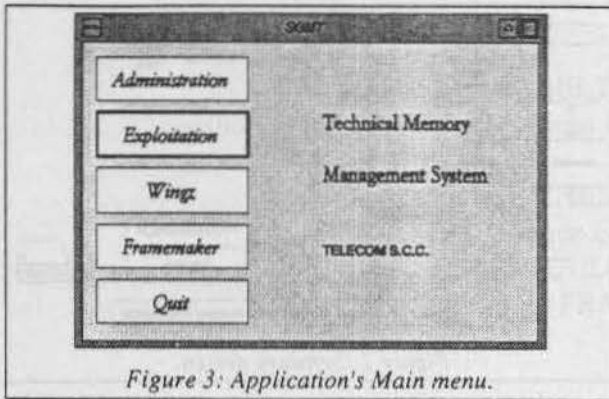


Figure 3: Application's Main menu.

In the following, we'll describe the different steps in making a report.

Document (report) definition

The first action is to create the report type in the data base. The report type is the generic name you will use to generate the actual reports later (e.g., "Annual thermal report"...). A report in the data base is attached to a satellite.

Then you have to create a template for your report. This will be made by using the publishing tool, FRAMEMAKER. In the blank document presented by the application, you can write fixed text, prepare tables, reserve space for the later generated charts or tables and insert pictures (e.g., scanned schemes...).

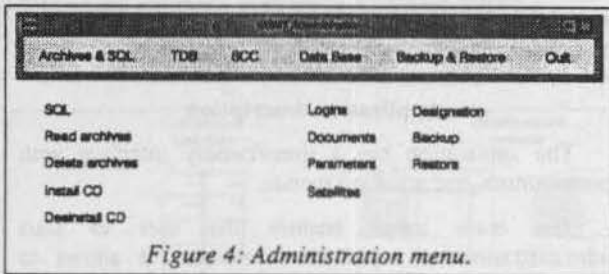


Figure 4: Administration menu.

The same sequence is requested for each script you want to define for the generation of your report. First a creation in the database, and then the actual writing of the script (in Hypertext language) using a standard text editor (choice of each user). You have to write a script for each page of the report containing a chart or a table resulting from calculations.

Document generation

This function is the main feature of the application. The user has to select successively the six options of the generation menu.

At first, you have to create the designation of your report in the database. This is only a logical creation.

The second step is the data collection. The data are provided by the technical data base or by the satellite control computer system. Some additional data may be provided by the user. In this case he must make sure that the data are available at the place he has specified in the script.

The generation itself takes place after the data collection. In this phase, the system runs sequentially all the scripts attached to the type of report.

When the generation is completed, the user can suppress or modify any part of the report. He can add comments, modify fixed text, using the publishing tool. He can modify charts or tables, using the spreadsheet program.

The validation step is the last step of this sequence. When a report is validated, it is impossible to modify any part of it. The report is frozen as if it was printed. It is saved on a temporary space, waiting to be definitely stored on a CD-ROM.

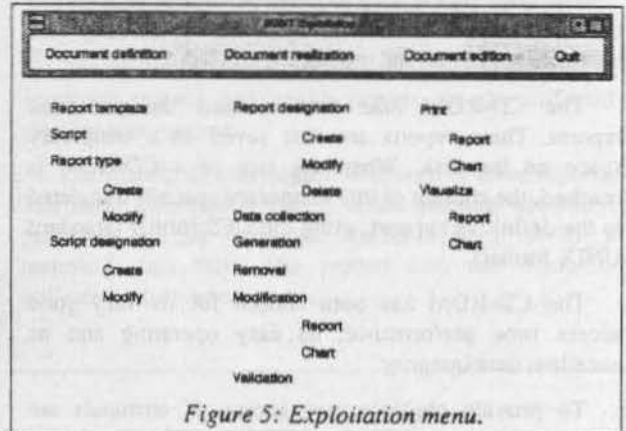


Figure 5: Exploitation menu.

Document consultation

The last feature of the SGM application is the document consultation.

As described above, the generated documents are saved on the disk or on a CD-ROM. These documents and all the related references can be consulted using the RDBMS.

The system manages the available media resources and ask the user to install the needed CD-ROM if not installed.

The user may print all or any part of the reports or visualize these on the screen. The capacity of the CD-ROM juke-box (6 x 640 Mb) allows to store the

complete life of a TELECOM satellite family on-line (3 satellites over 10 years).

Using the system

The system has been used in the TELECOM S.C.C. since the end of 1992.

The staff people training lasted about two weeks, including a UNIX training module.

The next phase was the development of all the TELECOM 1 periodical reports. The content of these reports is now frozen (after more than 8 years in orbit) and the full range of charts and tables is represented.

Document type	"Manual" methods	Automatic generation
Thermal (4/year, about 100 pages)	2 to 3 Weeks	1 Day
Eclipse (2/year, about 30 pages)	1,5 Weeks	2 Days
Maximum/Minimum (1/year, about 35 pages)	3 Days	3 Hours

Figure 6: Time comparisons.

A good example is the quarterly thermal report. This report is published for each characteristic season (equinox, solstice) and is made of:

- 40 thermal telemetry charts (24 hours). Each chart shows one or two telemetry measurement point.
- 75 historical charts. For each telemetry point and for each season, we plot the minimum and maximum value.
- 10 configuration schemes.
- 10 picture showing the geographic location of the measurement points.
- Presentation and explanation text.

Such a report required about three weeks to define completely all the scripts making up the different figures.

This amount of time is approximately the time spent with the former methods, to build the report.

Now, the generation of the thermal report requires about 4 hours to collect the telemetry from the Technical Data Base. Then, 4 more hours are required to build and print the report.

The spacecraft analyst may correct any part of the generated document and add text or comments, before validating it.

The table (Figure 6, above) gives a comparison between the former methods and the automatic generation of reports, using the SGMT, for several TELECOM 1 documents.

Conclusion

The Technical Memory Management System is now integrated in the TELECOM S.C.C. satellite follow-up facilities.

Now, this tool is used for all the TELECOM satellites (TELECOM 1 and TELECOM 2). Through the time gained in the reports construction, it allows the users a better focus on the non recurrent tasks.

The architecture of the system, based on "On The Shelf" products, may be adapted to many other data of the same or other types. In this case, the only need would be to develop new interfaces between the application and the data sources.

Examples

In the following, we show some examples of report pages. These pages are part of the TELECOM 1-C thermal report or of the TELECOM 1-C eclipse report.

These examples are given to give a better idea of the system capabilities, but don't represent all its possibilities.

Table

In this table, the numeric values in column 4 come from the telemetry. The figures in column 5 and 6 are results of spreadsheet calculations, using the values in column 7 (the user provides this information at the beginning of report generation)

	CANAL	TUBE	Reflux (mA)	PUISS. THERMIQUE DISSIPÉE (W)		RECU DE SORTIE (dB)
				EPC	TOP	
412	1	1H01	1.41	13.75	34.62	SATURATION
	2	1H02	1.22	14.51	34.50	SATURATION
	3	1H03	1.56	14.14	35.90	SATURATION
	4	1H04	1.87	13.88	37.43	-0.20
	5	1H05	1.96	12.91	31.30	SATURATION
	6	1H06	0.50	7.64	29.90	-12.00
34	1	2H01				TOP OFF
	2	2H02				TOP OFF
	3	2H03	0.24	3.20	22.40	-15.00
	4	2H04				TOP OFF

Figure 7: Table.

Configuration scheme

All the boxes and connection lines in this scheme are generated by a Wingz script. The numeric values come from the telemetry.

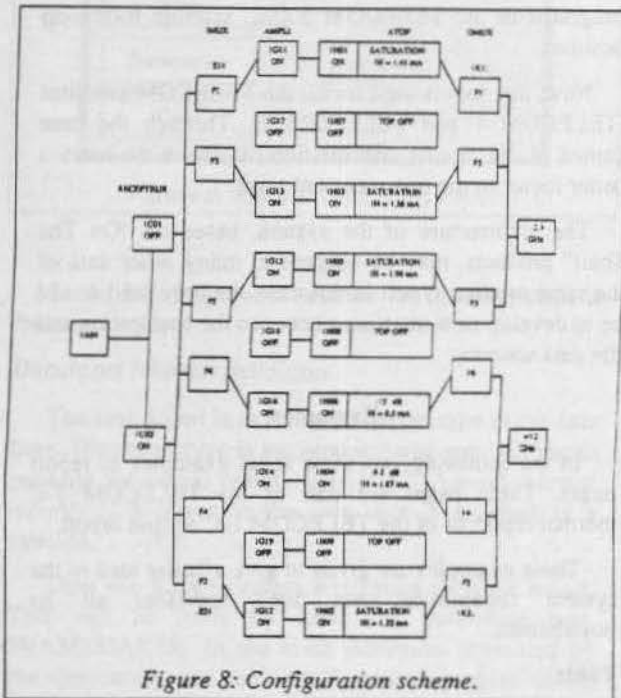


Figure 8: Configuration scheme.

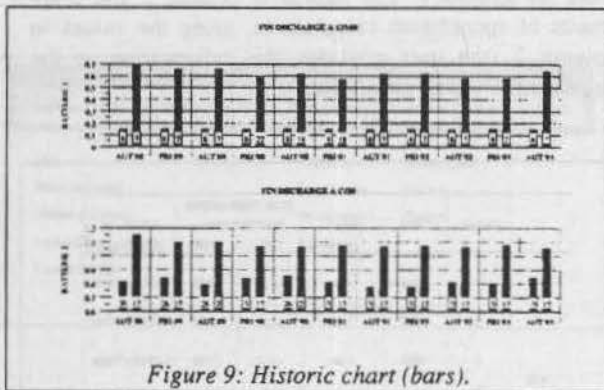


Figure 9: Historic chart (bars).

24 hours chart

The telemetry information under the chart is provided by the Data Base. The scale is computed in the script. The maximum and minimum information is stored in the Data Base and will be used for the historic charts.

Historic chart

The values come from the Data base. The scale is computed in the script.

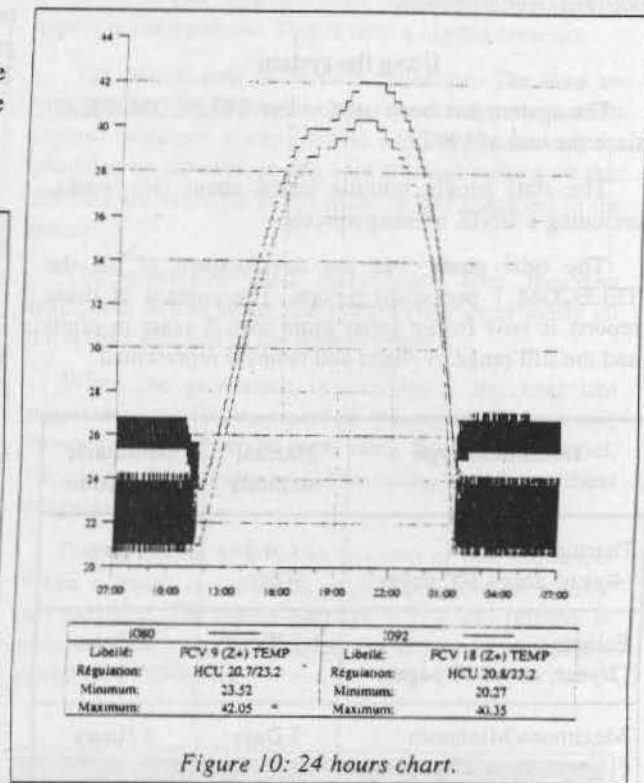


Figure 10: 24 hours chart.

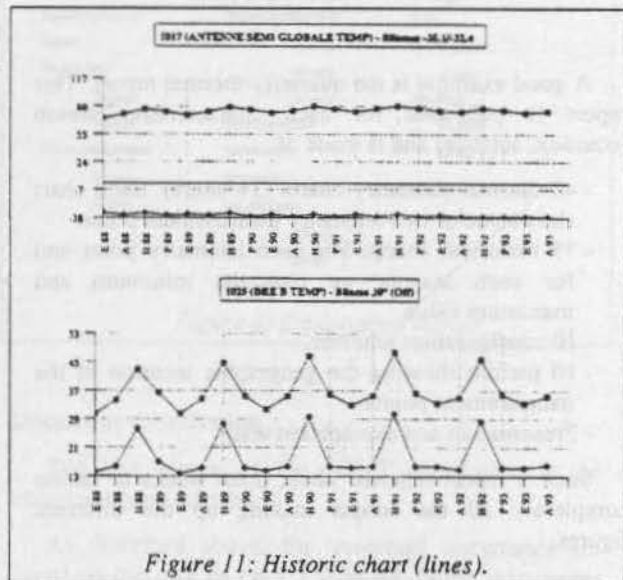


Figure 11: Historic chart (lines).

The charts may use single lines like in the examples above. It also may use bars with or without labels, or combination of lines and bars. The limits are the possibilities of the spreadsheet program.

OPERATIONAL FACILITIES OF REMOTE CONTROL SOFTWARE OF RANGING MEASUREMENT EQUIPMENT

José Carlos Becceneri

INSTITUTO NACIONAL DE PESQUISAS ESPACIAIS
Av. dos Astronautas, 1758
12227-010, São José dos Campos, SP, Brazil
RAN&CCS@BRFAPEP.BITNET

Abstract

The basic purpose of this paper is to document, in this symposium, the work made for the construction of Ranging Measurement Software (RAN) which is one of the functions of Satellite Control System (SICS), software developed by INPE to control the Brazilian satellites of MECB (Brazilian Complete Space Mission). This paper shows the RAN basic architecture as well as a set of functions which facilitates both the operation and the ranging system test.

key words : ranging, software test

1. Introduction

The team for the construction of the SICS was formed in 1986 with approximately 15 persons, which few had had some experience in satellite control software. In 1987 a software-house was contracted to help the development of SICS. The number of people involved in the project oscillated along the project, with approximately 40 persons maximum. This team was divided into three groups: a development one, a technical coordination one and another of support. Today there is a team of 10 persons, all from INPE, to maintain the current system and to define new ones.

In end of 1986, the system basic requirements had already been partially described. From these requirements, Structured Analysis was utilized to the definition of the system logical functions. To help in this phase, the only automatized software tool available was a Data Dictionary. The Data Flow Diagrams (DFD) were generally drawn by hand. This phase lasted, approximately, two years. In the following phase of the project (design phase), the only automatized software

tool available was a Software Catalog, developed by part of the team, which made of the cadastre the elements which would be controlled by the quality control of the system and the relationship among these elements.

In the programming phase, structured programming was utilized and the chosen language was FORTRAN.

Each SICS function had a test plan which was analysed by a inspection team. Each plan took from two weeks to one month to be analysed. Important suggestions were made to improve the quality of each function.

In 1990, almost all the functions had already been tested. For integration purpose of the SICS, functional chains were defined, composed by MECB ground segment subsystems. Chain and system tests were developed. For each chain, such as ranging, telecommand, telemetry, supervision, etc, a team to elaborate the chain tests was constituted.

Regarding the RAN function, the analysis team was composed of three persons. In the other phases, the team was reduced to only one person.

2. RAN Architecture

To describe the RAN facilities it is necessary to delineate shortly the RAN functional architecture. This software has two modules (or programs) [1]. The main module (SOFTRAN) interacts with the ranging measurement equipment (CMD) located at ground stations and coordinates the execution of ranging measurement.

RAN exchanges messages with CMD through RECDAS (Data Communication Network from Ground Segment). The protocol used to this exchange of message is the SDID (Station Data Interchange Document).

The second module of ranging software (VIS) accesses the special file generated by the main module when in test mode and shows all messages included in it with the

interpretation of all SDID message fields, and generating reports by demand.

3. RAN Operation

The screen of the main module is shown in figure 1.

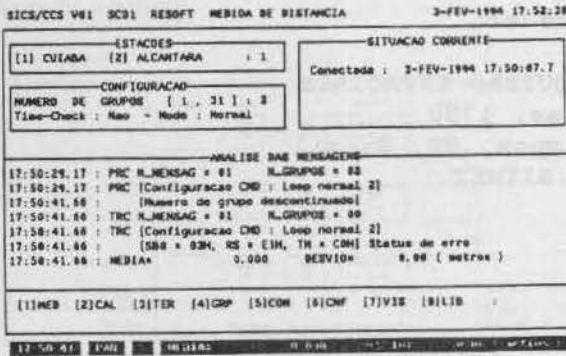


Figure 1: screen of the main module

In a normal situation, the following steps are executed by the satellite operator :

- connection request [option 5] ;
- selection of measurement group number to be executed by CMD [option 4] ;
- transaction desired request. The possible transactions are : range measurement, calibration measurement and premature termination of current measurement [options 1, 2 and 3] .

The right upper corner window indicates if the above requests were successful or not. In case of fail, the line 22 of the screen will show a message indicating the reason . This message is logged in the system event log.

The central window of the screen (ANALISE DAS MENSAGENS) indicates the status of SDID messages sent by CMD.

The complete operation is described in [2].

4. RAN Facilities

The main module can work in three different operational modes. The first mode, the normal mode, does not allow the operator to alter the standart format message (SDID format) which will be sent to CMD and, in the mission history files, only good messages are recorded.

In the second one, the test mode without alteration of SDID message , all message, valid or not, sent or received by the system, are recorded in a special file to be analysed in the future by the second module. This mode can be used to the integration of RAN with the other

parts of the ranging system thus, verifying everything that comes in or goes out through RAN.

The third mode is the mode test which allows alteration of SDID message to be sent to CMD (request message). This mode is similar to the second one but it allows, in real time, the operator to alter the request message. This mode can be used to validate the interface between RAN and CMD, by the alteration of the request message checking thus, the system behaviour facing an established error by the operator.

The first facility is an option from the main menu of SOFTRAN which allows the operator to put the module in one of the three operational modes. This is the option 6 of the main menu. After selecting this option, the screen showed in the figure 2 is presented. The operator can, then, select the desire mode of operation.

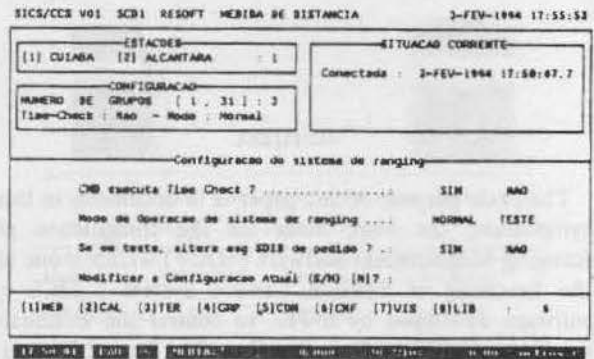


Figure 2: operational mode selection

If the operator selects the test mode with alteration of SDID message, before this message is sent to CMD, it will be showed in the screen (figure 3). The operator can, then, alter any byte of this message. This has proven to be very useful to test the CMD and in the integration phase, when RAN and CMD exchanged messages for the first time. It was possible to know if an error was in the RAN or in CMD.



Figure 3: SDID message to be modified

When a SDID message is received, all heading bytes are analysed and these analyzes are shown in the window 'ANALISE DAS MENSAGENS', which have eight lines. The module has a buffer which holds forty lines of this window. The second facility (option 7 from the menu) allows the operator to scroll this buffer to check the most recent events. The mission history files will be accessed only to a more specific verification of the whole system.

The third facility allows the operator to execute a local reset in the SOFTRAN avoiding, in many cases, the necessity of exiting and reloading the module again. This facility has proven to be useful when there is loss of message in the network and it simplifies the program logic avoiding the use of timers which complicate the depuration of the logic as well as the planning of test cases. Timers should be used only when the lack of perception of a problem by the operator can cause problems to the system.

The fourth facility is the second module of ranging software, which accesses the special file generated by the first module when in test mode and shows all included messages in it with the interpretation of all SDID message fields, and generating reports by demand. This module has proven to be useful in the integration phase and in cases where it is necessary to make tests in the system because it displays the messages that came in and went out of the system with the interpretation of all status bytes and without accessing the history files.

5. Conclusion

The facilities described here showed that :

- there was a small increase of source code (about 20 %). The current SOFTRAN has 2664 lines of code (without comments). Without the facilities, it would have, approximately, 2100 lines. The current VIS has 840 lines of code (without comments).

- the implemented tests facilities do not interfere with the system normal operation ;

- in critical situations happening during the system operation, it is convenient to have facilities that permit to check, in real time, the system functioning. It is not necessary to load any extra program in situations which claim for fast actions ;

- it was avoided to construct extra programs to make tests in the system which would have many similar functions as the RAN. This reduced, thus, documentation, test cases and training time, things that are expensive, mainly when the team is reduced.

6. References

[1] Becceneri, J.C. Projeto do Software de Medidas de Distância. São José dos Campos, INPE (A-DPS-0027).

THE ROSAT OBSERVATION TIMELINE SCHEDULING ALGORITHM AND ITS APPLICABILITY TO FUTURE SCIENTIFIC MISSIONS

D. Garton¹, H. Frank²

¹Computer Anwendung für Management (CAM) GmbH
Rudolf-Diesel-Str. 7a, 82205 Gilching, Germany

²German Space Operations Center, DLR, Oberpfaffenhofen, Germany

Abstract

ROSAT is a scientific spacecraft designed to perform the first all-sky survey with a high-resolution X-ray telescope and to investigate the emission of specific celestial sources. The mission can be broadly divided into three phases: calibration, survey and pointing. The pointing phase presents the most demanding requirements on mission planning. This article presents the mathematical basis of the method successfully used to tackle the optimisation problem, Dynamic Programming. The article concludes with a discussion of how the method can be implemented using the declarative programming language, CLP(R).

Key words: ROSAT, Mission Planning, Scheduling, Dynamic Programming, Optimisation, declarative programming, CLP(R).

Mission Overview

Rosat

ROSAT - ROentgen SATellit - is a project of the German Bundesministerium für Forschung und Technologie in co-operation with NASA and the Science and Engineering Research Council of Great Britain. Scientific management of the project is at the Max Planck Institut für Extraterrestrische Physik (MPE) at Garching near Munich. The responsibility for satellite operations and timeline generation lies with German Space Operations Center (GSOC) which is a department of DLR in Oberpfaffenhofen near Munich.

Scientific Objectives

The two main objectives of the mission are the performance of the first all-sky survey with an imaging X-ray telescope and detailed observation of selected sources with respect to spatial structure, spectrum and time variability.

Payload

The scientific payload of ROSAT (see Fig. 1) consists of a large X-ray telescope (XRT) with an energy range of 0.1 KeV to 2.0 KeV and a wide field camera (WFC) with an energy range of 0.041 KeV to 0.21 KeV.

Two different detectors can be put in the focal plane of the XRT. The Position Sensitive Proportional Counter (PSPC) with a resolution of 30 arc seconds and the High Resolution Imager (HRI) with a resolution of 10 arc seconds.

The WFC is mounted alongside the XRT and points in the same direction. It has a resolution of 1 arc minute and is fitted with several filters which can be inserted into the optical path.

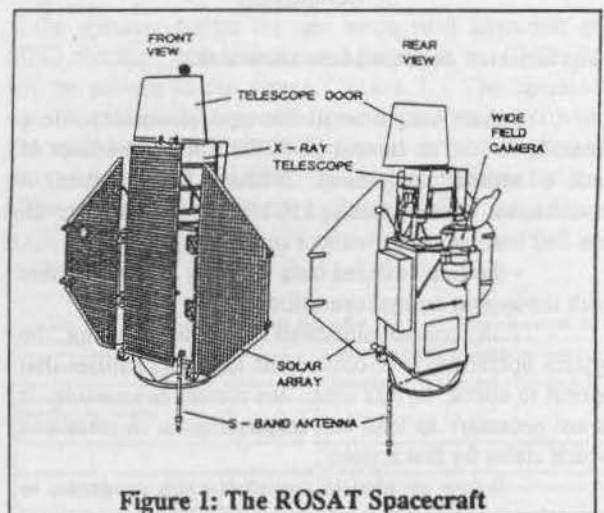


Figure 1: The ROSAT Spacecraft

Launch and Orbit

ROSAT was successfully launched from Cape Canaveral by a Delta II rocket on June 1st 1990 at 21:48 GMT. The orbit is nearly circular with an altitude of 580 km and an inclination of 53°.

Ground Station

The prime ground station is at DLR's Weilheim complex in Oberbayern, south of Munich. Due to the characteristics of the orbit, only 6 to 7 passes of about 8 minutes duration are available each day for receiving telemetry and transmitting commands. Because of the expected high volume of data transfer, both telemetry and commands, these contacts must be carefully planned.

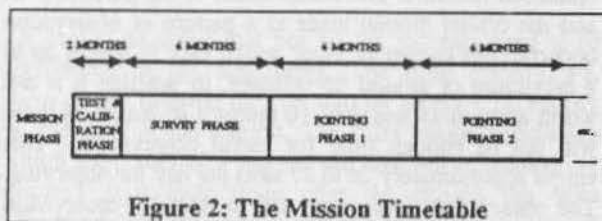


Figure 2: The Mission Timetable

Mission Timetable

The mission is divided up into three phases (see Fig. 2). In the first phase, the spacecraft systems and payload are checked out and the instruments calibrated. The second, or survey phase requires the implementation of a law governing the operation of the scan. The timeline generation procedure is automatic and needs no user intervention and no optimisation. The third phase consists of several pointing sub-phases which present the most demanding requirements on mission planning. Many thousands of requests for observations must be satisfied. These need to be scheduled as efficiently as possible to avoid wasting valuable observing time and produce an optimised timeline. This optimisation must take into account all the constraints placed on the spacecraft and observations and consider other necessary activities such as calibrations and data transmission.

Mission Planning

Requests

Mission planning is a common effort between MPE and GSOC. The primary input to planning is the REQUEST which represents a desired spacecraft activity. All requests originate from MPE. There are two main types: observation requests and calibration requests. Observation requests ask for pointing or survey operations in a standardised format. They are used to schedule the requested activity within the constraints. Calibrations and tests are also requested by MPE in a standardised format. Each request must be scheduled taking the constraints into account.

Constraints

There are several factors which affect the operation of ROSAT and have an important impact on mission planning. These are collectively referred to as 'constraints':

- **Sun constraint.** The plane of the solar arrays must be perpendicular to the Sun direction with a maximum deviation of 15 degrees. This is both to protect the telescopes and ensure proper operation of the solar arrays. This constraint places a window on the observability of a given source called the Sun Constraint Window (SCW). For example, sources near the ecliptic plane will have an SCW of about 30 consecutive days.
- **High energy particle belts.** These include the north and south auroral zones and the South Atlantic Anomaly. The telescopes cannot be operated while passing through these regions. The positions of the belts are shown in Fig. 3.
- **Atomic oxygen.** The telescope must not be pointed in the direction of the velocity vector of the satellite because atomic oxygen, swept up by the telescopes, can oxidise carbon in the detectors or filters and damage them. PSPC and WFC are affected but both have safe filters. HRI is not affected. The avoidance cone has a half angle of 28.1 degrees.
- **Weilheim constraints.** To ensure good communication during the contact periods, the spacecraft antenna aspect angle must not exceed 150 degrees. Manoeuvres from one source to another, called slews (see below), must also be avoided during contacts.
- **Earth blockage.** In the pointing phases, the Earth appearing in the pointing direction can result in a degraded attitude solution and the scientific value of the data will be diminished. Earth blockage will normally be avoided anyway by the scheduling process but if it occurs it must not last longer than 2400 seconds.

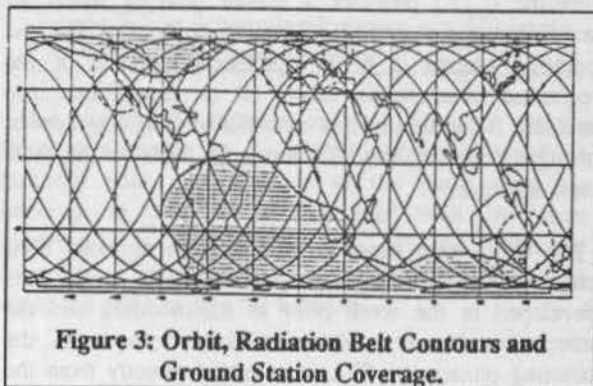


Figure 3: Orbit, Radiation Belt Contours and Ground Station Coverage.

- **Moon blockage.** In the pointing phases a degraded attitude solution may result if the XRT direction is within 14.5 degrees of the Moon (20 degrees for WFC).
- **Detector changes.** Only one of the XRT detectors can be in the focal plane at any one time. Thus a request cannot be scheduled unless the correct detector is in the focal plane. Detector changes must be made regularly (about every 20 days) for mechanical reasons. The WFC is mounted separately and thus can always observe.
- **Strong sources.** The PSPC detector could be damaged by high X-ray fluxes. The telescope must not be directed towards a strong X-ray source if the PSPC is in the focal plane or it must be switched off. MPE has supplied a table of known strong sources which is used in timeline generation. In the pointing phases, requests for observations near to known strong sources will be rejected.
- **AMCD memory capacity.** The onboard attitude control system has a limited memory capacity to store 'time tagged' commands. This restricts the number of slews and thus pointings that can be scheduled in one day to around 35.
- **Request priority.** There are three levels of request priority: mandatory (P1), important (P2) and optional (P3). The percentage of observation time allocated to P1 requests must not exceed 15% and that for P1 and P2 together must not exceed 80% of the total available observation time.
- **Country time allocation.** Each observation request comes from one of the 3 participating countries. The allowed percentage observing times are fixed at USA:50%, Germany:38% and UK:12%. The scheduling process must ensure that these figures are adhered to.

Timeline Generation

The timeline is the master plan of spacecraft activity and is used to operate the satellite. The long term timeline (LTL) provides a master plan of spacecraft activities over a period of around 6 months. For the pointing phases it is an optimised schedule of the requested observations taking all the constraints into account. It can be updated or modified following new or changed requests. The LTL forms the basis for the short term timeline.

The short term timeline uses a more accurate orbit prediction and covers a period of about 1 week. It is developed in the week prior to commanding and the telecommands are produced directly from it. In the pointing phases the STL is extracted directly from the

corresponding part of the LTL by adjusting the observations. No new optimisation is made. The STL also reflects changes to requests made after LTL approval.

The ROSAT Scheduling Problem

The problem in the pointing phases is how to schedule several hundreds or thousands of requests within the constraints as efficiently as possible to produce an optimised timeline. The combination of the particle belts and the orbital motion leads to a pattern of observation opportunities known as 'slots' which vary in length up to a maximum of around 85 minutes. In practice it is not worth using slots less than 10 minutes in length as there will not be enough time for useful observations. This leaves approximately 26 to 27 slots per day for observing. The observation times requested in ROSAT observation requests vary from around 15 minutes to over 2000 minutes (34 hours !) with an average of around 120 minutes. This means that observations cannot generally be completed in one slot and will need to be spread over several and will not be contiguous in time.

The implication of all this is that, for each slot, a decision must be made as to whether to stay with the observation from the previous slot or move ROSAT to point to a different source. The manoeuvre to change the spacecraft attitude from pointing at one source to pointing at another is known as a 'slew'. Attention must be paid to the length of time required to slew. If a slew is so long that it ends in the next slot, then this means that observation time will be lost. Although the slew process is, in practice, not completely deterministic it can be modelled by a mathematical formula which takes as input the angular distance between two sources. The duration varies from 11 minutes for a minimal slew up to 18 minutes for a full length slew of 180°.

The knowledge of the visibility of each source must, of course, also exist. This depends on the constraints and can be calculated beforehand from a long-term orbit prediction. This leads to a visibility pattern, or 'profile' for each source. Fig. 4 shows typical slot and visibility profiles.

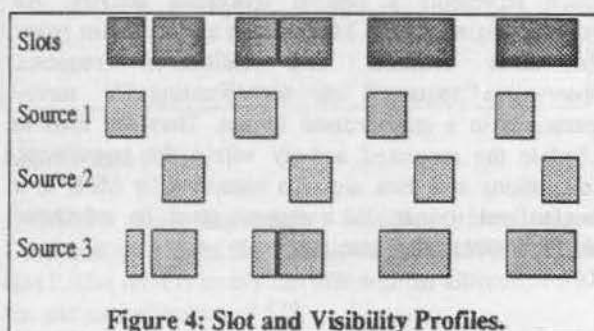


Figure 4: Slot and Visibility Profiles.

Solution of the ROSAT scheduling problem thus reduces to the choice of a strategy for deciding which source to observe in a given slot. This choice must be driven by the requirement to maximise the time for observations by using as much of the available time in the slots as possible. If this is achieved then the timeline can be said to be optimised. The slot pattern forms a natural time-frame on which to base a scheduling method although other time frames also exist. For example, a decision could be made after a given time increment - 10 minutes would be a natural choice.

It should be noted that not all the requests need to be considered in the scheduling. The high priority, P1, requests are inserted directly into an empty LTL exactly as specified in the request. The filter usage percentages which form part of a request are also not scheduled but inserted at a later stage after the request has been scheduled. The calibration and test requests are inserted into the timeline at STL generation time. The scheduling process must thus only consider the P2 and P3 requests. There is overbooking of observation time in any one pointing phase so that the P3 observations in general serve as 'fillers' although the 20% constraint mentioned previously must be adhered to. Other areas which need not be covered are detector changes, guide star optimisation and consumables. Positioning of detector changes is not part of the scheduling process. They are positioned by hand using information on the general source visibilities. It is assumed that there will always be enough guide stars available for the star trackers to establish the attitude at the end of each slew. ROSAT is fortunate in that, although consumables exist, they need not be considered in the scheduling process.

The problem can be seen as a multi-stage process in which a series of interrelated decisions must be made, where each decision depends only on the decision made in the previous stage (slot) and the effectiveness of the whole process is to be maximised (optimum usage of the available observation time).

This is exactly the type of problem that the mathematical optimisation method of Dynamic Programming¹⁻³ is designed to solve. This method provides a systematic procedure for determining the combination of decisions to maximise the overall productivity. The method is not a specific algorithm but rather a general approach to solving problems of this kind. Individual cases must be considered in their own right. The normal mode of solution, analogous to mathematical induction, is to treat the sequence in reverse order by solving the simplest problem first. The problem is then gradually enlarged by finding the current best solution from the one previously found.

This process continues until the complete problem is solved. In certain cases, however, the problem can be

solved by approaching the problem in the forwards direction, for example in the case of minimal chain networks⁴. This is true for the ROSAT scheduling problem. Here, there is no well defined end configuration from which to work back from. Also, as the observations are of a limited duration, the best solution must be found by moving forwards in time.

The problem is cast as a chain network consisting of nodes and links between nodes. This is represented diagrammatically in Fig. 5 which is a chain network corresponding to the slot and source profiles shown in Fig. 4. The nodes represent performing an observation of a particular source in a given slot. The lengths of the individual links correspond to the cost of moving from one node to the other in terms of lost observation time. The values in the nodes of the first column represent the costs of moving to these nodes from some starting point - usually the last observation from the previous schedule. Consider the node (1,2) and find the cheapest way of reaching it from the nodes in column 1. The answer is obviously from node (1,1) with a cost of 39 lost minutes. This fact is recorded by putting a 39 in the node and an arrow on the link leading to the node. In a similar manner the costs of reaching the other nodes in column 2 and the paths are marked on the network. For the nodes in column 3, the routes are computed in the same way by considering all the paths to a given node and working out the costs using the accumulated values from the previous column. The process can be stopped at any time by choosing the cheapest observation in the current column and working backwards to the start using the recorded directions to give the optimum observing sequence. In this way a timeline can be generated.

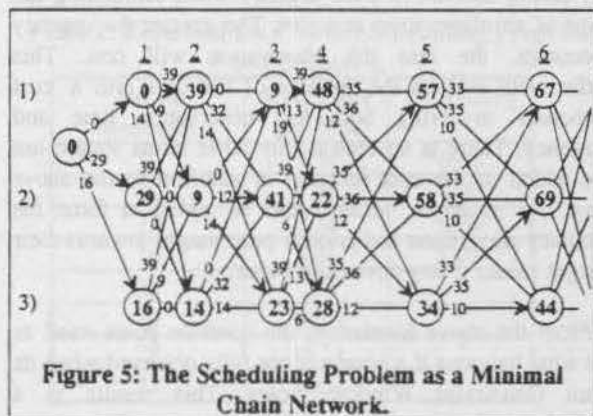


Figure 5: The Scheduling Problem as a Minimal Chain Network.

This procedure is repeated for each slot until either a limit is exceeded or a 'terminal node' is found. A terminal node occurs when all the paths from the previous to the current slot start with the same observation in the previous slot. At this point the sequence of cheapest observations can be traced back along the paths to give the timeline.

Given the assumptions of a slot-based approach and a complete set of requests then the solution provided by the method is the optimum one. Note that only those observations schedulable in the slot are considered i.e. those whose SCW is open.

On every step of the process the cost of moving from N sources to observing each source in the current slot must be computed. The effort thus varies as N^2 and as N increases the problem quickly becomes intractable. This is known as the dimensionality problem associated with Dynamic Programming. Investigations of the visibility of sources has shown that there are around 400 (300 P2 and 100 P3) observable at any given time. It is not practical to consider all of these at once and a subset must be used instead. This implies the choice of the sources to be considered based on some selection procedure. The most obvious method would be based on the observation's priority. Other methods are, however, possible. As discussed above under Constraints, the Sun constraint forces a window on a source's observability. It is advisable that the observation of a source be completed within its SCW (note that the window may be split depending when the phase starts) otherwise the scientific value of the observation may be diminished. One method of choosing a subset would then be to order the sources according to how close the end of their SCW is i.e. how urgent it is that the observation be completed as soon as possible.

Although this guarantees their inclusion in the set of requests to be scheduled, it does not, in itself, ensure that the most urgent ones will be given preference during scheduling. One way to do this is to favour such requests by taking account of their urgency when calculating the cost of an observation in a slot. The greater the urgency becomes, the less the observation will cost. This effectively widens the concept of the cost into a 'cost function' involving both lost observation time and urgency. There is no reason why other terms should not be added to the cost function in addition to the above two. For example, terms could be added to force the country allocations and priority percentages towards their target values if any deviations occur.

From the above discussion, the question poses itself as to what happens if a source is not fully observed when its Sun Constraint Window closes. This results in a scheduling failure and the action to be taken depends on the priority of the request. If the request is important enough that action must be taken then 'backtracking' must be performed. Backtracking is the process whereby the schedule is 'unwound' back to some point in the past and a reschedule attempted. This only makes sense, of course, if some of the scheduling parameters are changed, otherwise the same problem may crop up again. There must also be a guarantee that the process does not go on indefinitely. In the case of ROSAT scheduling the

obvious point to return to would be the start of the window where the offending source first became visible.

The following is a summary of how the constraints are accommodated by the method:

- **Sun constraint.** A source is not considered for scheduling unless its SCW is open. If the window is split then the longest part is chosen.
- **High energy particle belts.** Taken into account by scheduling only in slots and making the constraint part of the source profiles.
- **Atomic oxygen.** Covered by the source's profile.
- **Weilheim constraints.** The antenna aspect angle constraint is taken into account in the profiles. For the slew avoidance, special action must be taken during Weilheim contacts. This would need a special profile to cover these periods.
- **Earth blockage.** Covered by the profile.
- **Moon blockage.**
- **Detector changes.** During scheduling it is necessary to check that the correct detector is in the focal plane before scheduling an observation.
- **Strong sources.** Sources violating this constraint are removed at request processing time.
- **AMCD memory capacity.** This is not normally a problem with the slot based approach since the number of slots used is less than 35.
- **Request priority.** The ratio of P2 to P3 requests is maintained via the cost function.
- **Country time allocation.** The country allocations are maintained via the cost function.

To summarise, the Dynamic Programming method based on the slot approximation is an algorithm which is easily implemented and produces good schedules. The current implementation gives efficiencies around 84%. The method can cope with all the constraints which affect the ROSAT satellite. The problem of dimensionality can be easily surmounted and even advantages gained from the solution enabling further constraints to be automatically taken care of.

Implementation

From the foregoing discussion, the question naturally arises as to what is the best way to implement the algorithm. The current implementation at GSOC is in FORTRAN. This can be seen as a natural choice given

the mathematical nature of many of the calculations involved. On the hand, combinatorial problems of this nature are well handled by declarative languages such as Prolog⁵. With this in mind, a study was made to see how this could best be done with Prolog or a similar language. There are examples in the literature of the application of such languages to Dynamic Programming problems⁶, albeit in the language Datalog.

Declarative versus Procedural

The 'normal' programming languages FORTRAN, Pascal, C, Lisp etc. are procedural in nature. They are concerned with *how* a problem is to be solved. Progress in programming languages means moving away from the procedural and towards the declarative aspects of programming, thus forcing the system to worry about the procedural details. Procedural languages ask *how* the output is to be obtained and *how* the relations are actually programmed. Declarative languages, on the other hand, are concerned with the relations defined by the program and what will be the output of the program. They enable programs to be more easily formulated and understandable. Declarative language systems work out many of the procedural details themselves, leaving the programmer free to consider the declarative meaning of a program. Prolog helps in this respect but only partly: it is possible to write programs which are procedurally wrong. In addition, the declarative approach is not always sufficient and the procedural aspects of programming cannot always be ignored. The procedural aspect is particularly important for efficiency. Prolog and related languages have the advantage that they allow the programmer the freedom to use both approaches. One major problem of declarative languages is that programs declaratively can be correct but either not work or be useless or inefficient in practice. Examples of this are trivial equivalences or left recursion.

Logic- and Constrained Logic- Programming

Prolog, as a logic programming language, is very well suited to solving general problems of a non-numerical nature. However, it was never intended as a general programming language and is certainly not suited to the solution of numerical problems. Recent advances⁷ in logic programming, involving constraint logic programming (CLP) languages are, however, much more interesting from the application programmer's point of view. A particular instance of a CLP programming language, CLP(R), was chosen for this investigation since a readily available public domain compiler could be used^{8,9}. Many examples of the application of CLP(R) to mathematical problems can be found in the literature. In these languages, the process of variable unification is replaced by constraint solving. In the case of CLP(R) this is in the domain of uninterpreted functors over real arithmetic. As opposed to Prolog, variables in CLP

behave like mathematical variables. A CLP(R) program is a collection of rules similar to a Prolog program but differs in that rules can contain constraints (both equality and inequality) and the definition of terms is more general. Among other useful features, this leads to invertibility of clauses. This means that, for example, a clause which implements the calculation of a formula based on an input value can also deliver the input value if the result is given instead.

CLP(R) Applied to the ROSAT Scheduling Problem

The ROSAT problem was programmed in CLP(R) and tested on data from pointing phase 10 (June to December, 1992) of the ROSAT mission. The test program consisted of only 180 lines of CLP(R) code. The data sets used were as follows:

1. on 30.8.92 at 22:09 for 12.4 hours (13 slots)
2. on 31.8.92 at 22:52 for 23.6 hours (27 slots)

The tests were aimed at investigating the effect on run time and efficiency of increasing the number of requests to be scheduled from 4 up to 32 in steps of 4. The results are presented in Tables 1 and 2. The efficiency is measured as the percentage of the time in slots which was used for observation. As can be seen from the table, the process is very efficient from the start and rapidly reaches the point of diminishing returns of ~90 % efficiency with 12 to 16 requests. Assuming the use of a stack size of 16 slots then the approximate run time to generate an LTL for 6 months (~5000 slots) would be around 6.5 hours. On the other hand, good results with an efficiency of ~70% could be obtained with fast run times of less than 1 hour. The increasing run times show that the effort increases as N^2 as predicted by theory.

Table 1: Results of the CLP(R) Scheduling Program and Dataset 1.

No. of Requests	Run Time per Slot	Efficiency
4	0.3s	69%
8	1.3s	74%
12	2.5s	86%
16	4.6s	88%
20	7.2s	"
24	10.4s	"
28	15.3s	"
32	20.5s	"

The CLP(R) system (version 1.02) was installed on a PC 486 (25 MHz, 8Mb memory) running the Linux operating system and the GNU C compiler.

Table 2: Results of the CLP(R) Scheduling Program and Dataset 2 (Run Times as in Table 1).

No. of Requests	Efficiency
4	69%
8	72%
12	91%
16	91%
20	"
24	"
28	"
32	"

Summary and Conclusions

The Dynamic Programming, slot-based, limited stack size solution of the ROSAT scheduling problem is easily implemented and produces very good results.

The price of the high efficiencies is, however, the long run times for producing the solutions. The tests indicate, on the other hand that very good run times (~1 hour for a 6 months optimised timeline) can easily be achieved with an efficiency of around 70%.

CLP(R) allows very compact programs to be written. It is a language worthy of further investigation, especially in the area of mathematical and scientific programming.

Several problems were encountered with the CLP(R) system including file system corruption if virtual memory is exhausted and lack of a garbage collection feature. This indicates that there is still some development work to be done before the system matures.

Acknowledgements

The authors would like to thank Stefan Hücke of DLR/GSOC for his assistance in providing test data for this study and Reinhold Swoboda, Georg Stockinger and Janet Butcher-Weisner of the ROSAT Mission Planning group for their valuable contributions in discussions on the ROSAT scheduling problem.

References

- ¹ R. Bellman, *Dynamic Programming*, Princeton University Press, Princeton, New Jersey, 1957.
- ² O. L. R. Jacobs, *An Introduction to Dynamic Programming*, Chapman and Hall, 1967.
- ³ W. Ledermann (ed.), *Handbook of Applicable Mathematics, Volume IV - Analysis*, Chapter 16, John Wiley and Sons Ltd., 1982.

⁴ D. A. Pierre, *Optimization Theory with Applications*, Chapter 7-5, John Wiley and Sons Inc., 1969.

⁵ I. Bratko, *Prolog Programming for Artificial Intelligence*, Addison-Wesley, 1986.

⁶ S. Greco, D. Saccà and C. Zaniolo, *Dynamic Programming Optimization for Logic Queries with Aggregates*, Proceedings of the 1993 International Symposium on Logic Programming, Vancouver, 1993, pp 575-589.

⁷ J. Cohen, *Constraint Programming Languages*, Communications of the ACM, 33, 7 (July 1990).

⁸ J. Jaffar, S. Michaylov, P.J. Stuckey and R.H.C. Yap, *The CLP(R) Language and System*, Distributed with the CLP(R) System.

⁹ N. Heintze, J. Jaffar, S. Michaylov, P.J. Stuckey and R.H.C. Yap, *The CLP(R) Programmer's Manual*, Distributed with the CLP(R) System.

OBJECT ORIENTED DESIGN, THE SOFTWARE LIFE CYCLE, AND SOFTWARE ENGINEERING STANDARDS

Olivier Pujol
Nigel C. Head, Michael Jones
European Space Operations Center (ESOC)
Robert Bosch Str. 5
D-64293 Darmstadt

Abstract

The ESA software engineering standards ESA PSS-05-0 define a software life cycle comprising a number of phases. Specifically for development, it consists of the user requirements, software requirements, architectural design, detailed design and transfer phases. These standard are influenced by the functional decomposition and predominantly waterfall lifecycle approaches used in most of ESA's software developments up to the publication of Issue 2 of ESA PSS-05-0 in 1991. At ESOC a number of object-oriented developments have recently taken place or are in progress. The ESA software engineering standards are applicable to all ESA software development so the question arises how does the object-oriented method fit with ESA PSS-05-0? We discuss this question in the light of several quite different object-oriented developments: (1) the PASTEL Communications Monitor (2) the PASTEL Mission Planning System and (3) SCOS II, ESA's new infrastructure for spacecraft control. These projects are rather different in size and environment and so we consider that they represent a broad cross-section of the problems encountered in applying existing software engineering standards to object-oriented developments. The impact on the software life cycle, on the management of software projects and on the various management plans is also discussed. Areas of possible modifications to the Standards are outlined.

Key words: Software Engineering, Object-Oriented, Life Cycle

Introduction

The ESA software engineering standards ESA PSS-05-0¹ define a software life cycle comprising a number of phases. Specifically for development, it consists of the user requirements, software requirements, architectural design, detailed design and transfer phases. These standard are influenced by

the functional decomposition and predominantly waterfall lifecycle approaches used in most of ESA's software developments up to the publication of Issue 2 of ESA PSS-05-0 in 1991. The standards detail the products of the phases, including expected documents for each phase. Issue 2 also described other life cycle approaches or process models such as incremental delivery and evolutionary development approaches.

At ESOC a number of object-oriented developments have recently taken place or are in progress. The ESA software engineering standards are applicable to all ESA software development so the question arises how does the object-oriented method fit with ESA PSS-05-0? We discuss this question in the light of several quite different object-oriented developments: (1) the PASTEL Communications Monitor (2) the PASTEL Mission Planning System and (3) SCOS II, ESA's new infrastructure for spacecraft control.

These projects are rather different in size and environment and so we consider that they represent a broad cross-section of the problems encountered in applying existing software engineering standards to object-oriented developments. They are also at different stages of development: (1) has already been delivered, (2) will be delivered mid-94 and (3) will be delivered in stages from early-94 to end 95.

For each of these projects we recall first the development objective, drivers and constraints, then we describe the process model followed, and thirdly we present our results and findings. The paper concludes with a summary of the three experiences and an outline of possible areas of modifications for the ESA PSS-05-0 Standards.

PASTEL and the SILEX experiment

PASTEL is an optical terminal which will be carried as a passenger on-board the SPOT-4 satellite controlled by CNES. A counterpart terminal, OPALE, will be mounted on the ARTEMIS satellite controlled by ESA. PASTEL and OPALE form the

SILEX (Semiconductor Inter-Satellite Link Experiment) mission which will be used to downlink high rate data generated by SPOT's optical camera, using ARTEMIS as a data relay.

The PASTEL terminal will be operated by ESA from the PASTEL Mission Control System (MCS) located in the ESA Redu station. Control and monitoring information will transit through the SPOT-4 Control Centre, the Centre de Mise et maintien à Poste (CMP) at Toulouse, in a cross-support scenario. The planning of the SILEX experiment is under the responsibility of the PASTEL MCS, which will coordinate with the SPOT-4 CMP and the ARTEMIS MCS.

The PASTEL MCS comprises three principal subsystems, (1) a Control and Monitoring System, (2) a Mission Planning System, and (3) a Communications Monitor. The developments of (2) and (3) are performed according to ESA PSS-05-0 Standards and follow an object-oriented approach.

PASTEL Communications Monitor (CM) development

Development objectives, drivers and constraints

The PASTEL CM provides services for file transfer to the external Control Centres (those of SPOT-4 and ARTEMIS). These services include transferring files, which conform to file naming and formatting rules, acknowledging files reception, providing an user interface for monitoring, and handling of link drops and other errors.

In order to provide the flexibility and potential for re-use/upgrade necessary for future use for the PASTEL CM, an object-oriented approach was adopted for the specification phase. This approach was also compatible with the targeted programming language C++ including its object-oriented facilities.

Because the time available for performing acceptance tests with CNES was expected to be short and no preliminary access to CNES facilities was foreseen, it was important to ensure that a highly reliable system was produced in view of acceptance testing.

Life cycle

Although the life cycle followed appeared in terms of document production to be a standard waterfall life cycle because of the sequential phasing (UR, SR, AD, DD), in practice an iterative development

scheme was installed in parallel through a prototyping exercise.

It was acknowledged from the beginning that prototyping was a very useful complementary to the specified PSS-05-0 analysis and design work and that it should aim not only to reduce risks by the validation at an early stage of critical parts but also to support an iterative build up of the system. Therefore some building blocks of the system, such as the user interface and the file transfer using the RPC (i.e. FTP) were worked on at an early stage and expanded during the course of the development.

The software life cycle documents were modified to accommodate the object oriented approach we adopted, which was the development methodology proposed by L.R. Hodge *et al.*². This approach identifies three types of analysis, namely (i) the requirements analysis, which aim is to define the purpose, scope, and functionality of the system, (ii) the information analysis, which aim is to model the entities in the problem domain and their inter-relationships, and (iii) the event analysis, which aim is to model the dynamic behaviour of the system.

The PSS-05-0 links the requirements analysis to the construction of a logical model derived by top-down functional decomposition. The essence of the object-oriented approach, on the other hand, is that the allocation of functions should follow the object model derived during the course of information analysis.

Therefore, the Software Requirements Document (SRD) structure was revised to comprise (a) the System Model, which resulted from (ii) and was presented in the form of an Object Relationship Diagram (see ref.³), (b) the Software Requirements as specified in ESA PSS-05-0, and (c) Description of each object identified in (a), providing a cross-reference to the Software Requirements (b).

The Architectural Design Document (ADD) structure was also revised to accommodate the object-oriented approach. The objects described in part (c) of the SRD were carried forward and detailed as appropriate. Client Server Diagrams (see ref.³) were incorporated to illustrate the interactions between objects in a more dynamic view (showing messages exchanged, cardinalities of relations, etc.) and the allocation of objects to UNIX processes.

The Detailed Design Document (DDD) was replaced by a Design Document, which is an extension of the ADD to cover design issues such as attribute, services or objects needed solely for design purposes, and other information relevant to the DD

phase (e.g. programming standard, naming conventions, etc.).

The approach adopted for unit testing included the integration testing: the unit test performed for any object included real objects of the remainder of the system. The potential drawback being that changes to one object would lead to invalid unit tests of other objects that used it. However the experience proved it not to be a problem.

Results and findings

The PASTEL CM was developed within cost (195 man days) and successfully passed its acceptance testing in January 1993 against the SPOT-4 CMP. The total number of lines of code produced (excluding test code) is 6477 (out of a total 12574 lines including comments and blanks).

On a small/medium scale development, such as the PASTEL CM, it seems that the object-oriented approach can very well mapped on to a waterfall life cycle as described in the ESA PSS-05-0. The waterfall life cycle provides milestones, such as reviews of SRD, ADD... which are most useful, if not mandatory, rendez-vous between users and producers. Moreover it does not preclude prototyping activities to run in parallel, as supporting tasks, to the analysis and design.

The object-oriented approach allows a clear definition of interfaces at a very low level (object level encapsulation) and promotes strong typing. These two elements contribute to ensure that coding errors are identified early at unit testing level. Therefore it was little surprise that we encountered very few problems at system and acceptance testing (most of them actually were due to misformulated software requirements). We have now high expectations concerning the software robustness and reliability.

On the cost side we have met the original estimate, although this estimate was derived from past experience with traditional development methodologies. However we cannot draw a general conclusion on cost from this single experience, because only one engineer was involved.

From our experience with the PASTEL CM we see that ESA PSS-05-0 provides a very good framework in terms both of software development standard and of management tool. However care is needed in mapping the object-oriented process to interpret the standard (specifically in documentation structure) to avoid, e.g. forcing the object model into a functional model.

PASTEL Mission Planning System (MPS) development

Development objectives, drivers and constraints

The PASTEL MPS main functions are:

- (A) to allow the MPS operator to coordinate the production of the Reservation Plan, (which defines the periods in which PASTEL can communicate with ARTEMIS, and the periods where star tracking can be performed by PASTEL),
- (B) to produce an Operations Timeline, containing all the details of the operations to be scheduled from the PASTEL MCS, under MPS operator control.

The object-oriented approach was adopted for this development in view of the potential re-use of it in the frame of the ARTEMIS MCS development to support the scheduling of OPALE and also because it was consistent with the C++ language which was being used for the user interface.

It was also decided to follow a different object-oriented development methodology, the Object Modelling approach from Rumbaugh *et al*³ in order to take advantage of tools supporting this methodology. For the PASTEL CM we had just been using drawing packages but no CASE tools.

Life Cycle

As for the PASTEL CM, a traditional waterfall lifecycle is being followed. Since the PASTEL MPS is primarily an user-driven system, a prototype of the user interface was developed early in the SR phase to support the production of the software requirements. During the SR phase the logical model was constructed using the object model from Rumbaugh. However, because users had had some difficulty in reading the Object Relationship Diagrams and Object Descriptions for the PASTEL CM, it was decided not to integrate the logical model as such in the SRD. Only a very high traditional data flow diagram (as per DeMarco Structured Analysis Method⁴) was provided in the SRD, followed by what looked like a listing of requirements. These were in fact attributes and services of the objects defined in the object model listed in a sequence, which was structured according to the object decomposition. This was very well received by all reviewers.

The ADD expanded, where relevant, the three models defined by Rumbaugh *et al*, i.e. (i) the object model, which provides the static decomposition of the

system in classes (in a very similar way to the system model of L.R. Hodge *et al*), (ii) the dynamic model, which is a collection of small models, each one of which models the dynamic behaviour of some part of the system, and (iii) the functional model, which should only be used to model the processing required, e.g. to calculate the value of an attribute (pseudo-code was actually used for (iii)).

As for the PASTEL CM the DDD will be replaced by a Design Document, and the unit tests will also support the integration tests.

Results and findings

As the DD phase is currently on-going, it is too early to draw conclusions over the full lifecycle. Nevertheless we can observe that so far no significant deviation from the planned schedule and cost. The overall effort for the PASTEL MPS is in the area of 50 man-months, which is roughly 5 times more than for the PASTEL CM.

The waterfall life cycle has not been a major problem to follow but has provided a useful basis, particularly in terms of reviews and management related documents (such as Software Project Management Plan (SPMP), Software Quality Assurance Plan (SQAP), Software Configuration Management Plan (SCMP), etc.).

As for the PASTEL CM, it has been decided to alter the layout of design and test documentation in order to reflect the object-oriented approach. The core of the modifications concerned the adoption of a Design Document, which is an update of the ADD and replaces the DDD, and the issue of an Unit Test Plan, which includes also integration tests, and does not change fundamentally the contents of the documents which are described in ESA PSS-05-0.

SCOSII

Development objectives, drivers and constraints

The SCOSII project is somewhat different in nature to the preceding examples. Instead of producing a complete software system the major objective is to produce a collection of components from which future Mission Control systems can be constructed. It is assumed that, during this construction process, the mission specific teams will need to customise the behaviour of the stock components to match special needs of the mission in question. Of course, in order to provide a basis for the mission teams, SCOSII will also provide a standardised "system" employing stock

components but this should be viewed as a secondary objective.

Given this emphasis on the "flexible component" nature of SCOSII it was decided, almost inevitably, to implement SCOSII as a C++ class library. Customisation of the components will be done by inheritance (specialisation) of an appropriate base class with polymorphic collections being used within the system to ensure that these specialised (for a mission) components can be used at any place the original SCOSII component would be used.

A further important objective of the SCOSII project was to reduce to a minimum the lead time for the production of software systems; this applies both to SCOSII itself and to control systems constructed from the components. In the past the lead time required for implementation of software according to a waterfall lifecycle has led to a demand for mission specific information at a stage of mission preparations at which the information was not available. Alternatively stated - it was almost taking longer to prepare the control system for a mission than it was to prepare the hardware and flight software for the mission itself!

Life Cycle

As mentioned earlier it was essential to allow for a more or less continuous evolution of the User Requirements. There were two major reasons for this:

- the scope and complexity of systems built from the SCOSII components will far exceed that of previous ESA control systems. This means that the underlying Operations Concept will almost certainly require modification in the light of operational experience gained with these systems.
- the continuous process of customisation of the stock components for support of missions will require the feedback of many of the customisations into the standard components.

Additionally, management and schedule considerations required availability of preliminary systems as soon as possible (before user requirements were completed) in order to provide visibility that the project was progressing towards its eventual goal.

The availability of a comprehensive body of experience (in the form of existing control systems) provided a convenient escape from this conflict

between evolution and early visibility. The SCOSII system is being developed in two major versions:

the "Basic System" which contains only facilities equivalent in nature to those provided by existing systems (and therefore with relatively stable User Requirements)

the "Advanced System" which contains any facilities which go beyond those of existing systems.

Each of these systems will of course contain a number of intermediate deliveries, in particular the Advanced System where the early feedback from the initial deliveries will certainly influence the contents of the later ones.

Results and findings

The URD has been written with both the Basic and Advanced systems in mind, as has the SRD. It is intended to add annotation to both of these documents indicating with requirements will be satisfied by which version of the system. This provides an appropriate level of traceability between the various system versions and the user level documentation while ensuring that the final documentation set is consistent between the various versions of the system.

Considerable difficulties were encountered early in the project when it was necessary to define the contents of the various PSS-05 lifecycle documents in terms of the methodology adopted. These difficulties were in part due to the infrastructure nature of the software but largely arose from the use of an object oriented approach. It was eventually decided to maintain the partitioning proposed in Coad, Yourdon⁵ as the basis for the split between the various documents:

Problem Domain Component:
"Software Requirements Document"

Data Management Component: "Architectural Design Document"

Task Management Component: "Architectural Design Document"

Human Interface Component:
"User Requirements Document" & Prototyping Activities

In other words, the logical model was restricted to modelling the problem domain and the physical model was used to address issues related to the

implementation of the system, in particular those related to the distributed nature of the system.

The management of the human resources also proved problematic. It was difficult to clearly define sufficiently clear workpackages in the face of the evolution of requirements and the need to provide early visibility through preliminary deliveries. The concept of an "Statement of Work" was introduced as the definition of a piece of work allocated to an individual and reported on to the project management hierarchy. In a project of the size of SCOSII (400-500 man-months) it is expected that several hundred such Statements of Work will be produced and completed; this level of detail was judged to be inappropriate for the Software Project Management Plan.

The SCOSII project is not yet complete. It is already clear that a number of the issues involved in the planning and execution of an object-oriented project of this magnitude were not ideally covered and require some further modification and extension to the ESA Software Engineering Standards. The SCOSII project team is in the process of updating its internal standards document to reflect the experience gained and intends to submit this to the ESA standards authorities in the next few months so that it may be considered for inclusion in the next issue of the ESA standards.

Discussion

The first two projects, (1) the PASTEL CM and (2) the PASTEL MPS, are of relatively limited size and duration. (3) SCOSII is in comparison larger by a scale factor of 10 to 50. Whilst it was possible to capture the user requirements for (1) and (2) in one pass, and consequently to start the development on a relatively stable baseline, this was not the case for (3) in which incremental provision of user requirements had to be foreseen. We discuss how these aspects, i.e. project size, user requirements availability and object-oriented approach, relate to two major topics of the ESA PSS-05-0: the life cycle and the logical model.

Life cycle

The ESA PSS-05-0 software life cycle model comprises six basis phases, namely the User Requirements (UR) Phase, the Software Requirements (SR) Phase, the Architectural Design (AD) Phase, the Detailed Design (DD) Phase, the Transfer (TR) Phase and the Operations and Maintenance (OM) Phase. Quoting the Standards, "A

'life cycle approach is a combination of the basic phases of the life cycle model'. The Standard mentions three life cycle approaches: (l) the waterfall approach, which is the simplest approach whereby phases are executed sequentially, (m) the incremental delivery approach, which is a variant of the waterfall, where the DD, TR and OM are split into a number of more manageable units after the complete architectural design has been defined, (n) the evolutionary approach, which is characterized by the planned development of multiple releases where each release incorporates the experience of earlier ones.

The life cycle (l) and (m) are based on the assumption that all users requirements are available at the start of the analysis. The life cycle (n) assumes this is not the case, rather that the user requirements will be produced by increments in an iteration cycle where the user refines his requirement from the knowledge he gains from using the delivery corresponding to the output of the previous iteration.

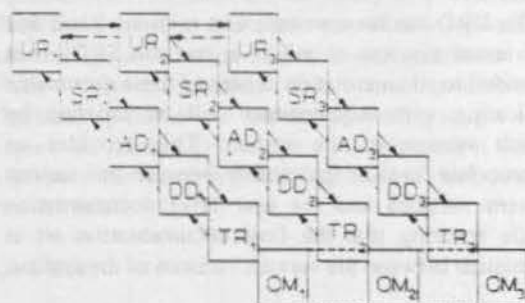
However, there is an alternative to (n), which is not considered in PSS-05-0 and avoids the long loop implied by life cycle (n). This alternative allows the User Requirements Document (URD) to be produced in increments provided that the first increment defines a meaningful subset of the system whilst leaving open the details of the other parts (or even of details of some parts of the subset) to be filled in later increments.

We call this alternative *the incremental requirements approach*. It is characterised by incremental deliveries of user requirements which are matched by as many deliveries of the software. The major difference with the *incremental delivery approach* is that the development of increment [n+1] may have to start before increment [n] is delivered. Although there should be no constraint on the frequency of increments, it would be preferable that the schedule for URD increments and corresponding system deliveries is agreed to with the users before the start of the project.

This *incremental requirements approach* may also be beneficial in the relatively common situation where the requirements for a number of areas cannot be defined at project start depending on some external constraints. This happens quite frequently in development of ground systems for space operations, in which parallel space segment development means that users lack on-board design knowledge needed for the user requirements definition.

The *incremental requirements approach* can result in phase overlapping. Assuming that for each increment the duration of phases are roughly

constant, and that increments follow each other by the average duration of phases, one can quickly encounter a situation where phase DD of increment [n] overlaps with phase AD of increment [n+1] and phase SR of increment [n+2]. And related to this approach is the provision of ESA PSS-05-0 required plan documents. Since 17 such documents are required, the provision of them for each increment would seem to be ruled out. An approach based on one set of the complete suite combined with updates as required would seem to be the practical way. It is however acknowledged that this set is probably insufficient to guarantee a good control of the project both at technical and managerial levels. At technical level it is quite obvious that we need to define how to relate two or more increments of documents such as SRD, ADD, DDD (e.g. to handle traceability) but also that we need to define a Software Validation and Verification (SVV) policy.



< The incremental requirements approach life cycle >

One further question is: how do these increments relate to (the iterations and increments of) the object-oriented approach? The object-oriented approach is often associated with the concepts of prototyping, iterations and incremental development of a system. That is the idea of "design a bit, implement a bit, test a bit". We believe this to be largely due to the exceptional facilities available within the development environment of SMALLTALK, the "father" of object-oriented languages. Its first successors, which were LISP-based (ART, KEE, LOOPS, etc.) contributed to enforce this image of easy evolution from a prototype into an operational system. Whether or not it is appropriate to "institutionalise" this experience into a methodology is still to be elucidated. But first the difference between iteration and increment has to be clarified.

An iteration is the repetition of sequences of development steps (design-code-test is the common example). The *increment* usually means development deliverable, i.e. the software product. On the other hand an *increment* implies additional functions. Again this can apply to one or a sequence of development

steps, e.g. in the *incremental delivery approach* it applies to the DD phase only, whereas it would apply to the UR-SR-AD-DD if user requirements are provided incrementally. This may result from some additional user requirements being considered at analysis level, as in the *incremental requirements approach* described above. Iterations and increments are therefore related but distinct, an increment is usually the result of the last iteration on an analysis or design baseline (i.e. a set of user requirements or a set of functions to be implemented), but there is not necessarily one increment per iteration. And the object-oriented increment is not different from the increment mentioned above.

The object-oriented approach promotes to a large extent the iterative process, which is sometimes referred to as the *object-oriented life cycle* in the object-oriented literature. This is found to be somewhat misleading in the context of ESA PSS-05-0 in which the object-oriented paradigm would be seen as a method and not as a life cycle corresponding to some or several process model. Furthermore, as the object-oriented approach has proved to be successful with various life cycles (see above case studies), there seems to be no good reason for it to be allocated to a new type of life cycle. An explanation for this apparent 'contradiction' might be that the term *object-oriented life cycle* is frequently (and in our view wrongly) as a synonym for *object-oriented design*.

In the context of larger projects (in this case SCOSII) it is difficult to conceive of applying an iterative or incremental lifecycle without the flexibility offered by an object oriented approach. While it is true that an object-oriented approach can be used in a more traditional lifecycle (waterfall for example) we believe that if there is a need for one of the more flexible life cycles, in particular the incremental requirements approach described above, there is little alternative to the adoption of an object oriented view as the clear compartmentalisation of the knowledge and localisation of changes resulting from requirements evolution is unequalled by any other approach.

Logical model

ESA PSS-05-0 distinguishes two analysis phases, the 'problem definition phase' performed by the users during the User Requirements (UR) Phase, and the 'problem analysis phase' performed by the development team during the Software Requirements (SR) Phase, and one design phase, the Architectural Design (AD) Phase. Once the problem is defined, the main analysis activity is to produce the *logical model*. The *logical model* is an implementation-independent

model of what is needed by the user and it is used to produce the software requirements. In the design phase the developer constructs a *physical model* which is derived from the *logical model* and describes the design of the software using implementation terms.

Similarly with the object-oriented approach it is possible to distinguish an object-oriented analysis and an object-oriented design. For example in Rumbaugh *et al*³ a mapping between the analysis models concepts and the *logical model* can easily be made, and the steps of constructing the *physical model* are very clearly described. It is worthwhile noting that actually ref.³ describe object-oriented design as being an iterative process, giving the view that iteration is bounded to Design and does not encompass analysis.

Therefore it seems that the concepts of *logical model* (and *physical model*) can very well accommodate the object-oriented approach. However the Standard would need to reference some of the most widely spread methodologies for analysis and design.

In a project which follows the Coad/Yourdon approach there is a clear correlation between the logical model and the "Problem Domain"; similarly the Data and Task Management Components can be clearly matched to the Architectural Design Document.

Conclusions

A survey of the utilisation of object-oriented approach in the framework of the ESA Software Engineering Standards for a number of ESA spacecraft mission control system projects has been presented.

From the survey and from the discussion which follows, there is evidence that the Standard needs a number of updates and clarifications. However it is to be noted that at this stage no major changes are foreseen. Updates needed are:

- Confirmation of the object-oriented analysis and design as valid methods. This may have some impact in standard documents layout and some clarification on the documents naming in relation to that used in the object-oriented will be needed.
- Addition of another life cycle ("*incremental requirements approach*").
- Development of the notion of iteration.

These points are being worked upon currently within ESOC in the frame of local standards for SCOSII and other projects. These will be inputs to the ESA Board for Software Standardisation and Control (BSSC), who will be preparing Issue 3 of PSS-05-0 in 1994.

Although outside the scope of this paper there is further work required to ensure that the flexibility available to users of an object oriented approach can be safely planned, monitored, controlled and assessed. This will require changes to the management documents and procedures prescribed in the PSS-05 standards.

References

¹ESA Software Engineering Standards", ESA PSS-05-0 Issue 2, February 1991.

²L.R. Hodge *et al.* A proposed object-oriented development methodology. *Software Engineering Journal*, March 1992.

³J. Rumbaugh *et al.* Object-Oriented Modelling and Design. *Prentice-Hall International* (1991).

⁴T. DeMarco. Structured Analysis and System Specification. *Prentice-Hall* (1979).

⁵P. Coad, E. Yourdon. Object-Oriented Analysis. *Yourdon press* (1991)

GROUND SYSTEM HARDWARE AND SOFTWARE II

ESA's Future Flight Dynamics Operations System

1. Twynam, D. and Williams, P. (Science Systems-U.K.):
**"Aspects of ORATOS-ESA's Future Flight Dynamics
Operations System"** 237
2. Baize, L. and Pasquier, H. (CNES-France):
"Tracing in a Control Center Development" 245
3. Ambrosio, A.M. and Kuga, H.K. (INPE-Brazil):
**"GAN - An Automated System for Acquisition and
Tracking of Satellites by Ground Stations"** 248
4. Goettlich, P.; Oku, Y. and Hucke, S. (DLR-Germany):
**"A Neural Network for Solving a Spacecraft
Scheduling Optimization Problem"** 254
5. Pasquier, H. and Baize, L. (CNES-France):
**"Data Exportation in TELECOM 2 Satellite Control
System"** 259

Aspects of ORATOS - ESA's Future Flight Dynamics Operations System

David Twyuan
Peter Williams

Science Systems (Space) Ltd
c/o ESOC
Robert Bosch Strasse 5
64293 Darmstadt

Abstract

ESA is currently in the midst of developing a state-of-the-art system for flight dynamics operations. The Orbit and Attitude Operations System (ORATOS) is due to be fully operational in the mid 1990's. ORATOS brings together over 25 years of flight dynamics expertise with the best of today's distributed computer hardware. ORATOS is split into three layers, one of which is the support layer. The support layer software consists of a suite of applications, libraries and utilities written both in-house and by third parties. A number of the software packages which have been written in-house are detailed here. One of the applications which is detailed is a generic telemetry processor, this gives a good example of how different aspects of the ORATOS support layer are used together.

Introduction

ORATOS is ESOC's future orbit and attitude operations system. It is being developed by, and will be used by the Orbit and Attitude Division (OAD) within the European Space Operations Centre (ESOC).

The concept of providing a dedicated environment for flight dynamics operations has a long history in ESOC, ESA's operations centre, the first of these appearing in the early seventies.

The relatively recent decision to move from mainframes to distributed networks of UNIX workstations has required the development of a new operations system, which can take maximum advantage of this new environment as well as taking account of the existing base of flight dynamics software. The synthesis of these requirements is ORATOS.

ORATOS consists of three layers, the operating system layer, the support layer and the applications layer.

The operating system layer is provided exclusively by third party software. It constitutes Sun's implementation of the UNIX operating system and the necessary software to enable the operation of a distributed hardware system. The applications layer is provided by the flight dynamics

experts within OAD. These applications are generally written in Fortran. The support layer lies between the operating system layer and the applications layer. It provides all interfaces between the operating system layer and the applications layer.

This paper details various aspects of the ORATOS support layer which have been developed by a team of engineers from Science Systems (Space) Ltd. Amongst these are examples of utilities, libraries and applications, which are all described independently.

To give a feel for how this software all works together, one of the higher level support applications, the Generic Telemetry Processor (GTP), will also be described.

Overview of ORATOS Support Layer

The ORATOS support layer consists of a wealth of applications, libraries and utilities to provide full software support for the applications layer. The higher level support layer applications also tend to depend on many of the other support applications, libraries and utilities available. Within ORATOS, utilities are considered to be applications that work in conjunction with a driving application. Libraries and applications are defined in the traditional sense of being linkable code modules and stand-alone executables respectively.

Where possible, support layer software has been either bought off the shelf or obtained from the public domain. When the requirements for software cannot be satisfied by these methods, it has been developed in-house.

Some examples of third party software used is a networked relational database from Oracle Corporation, a three-dimensional animated drawing package from Wavefront Technologies and a graphical user interface C++ class library from ParcPlace Systems.

Descriptions of some of the software and concepts developed in-house now follow.

Data Storage and Retrieval (DSR)

DSR provides the functionality of a simple database

system, including indexed access and sequential access but without the processing overhead of a relational database system. DSR consists of a programmatic interface, callable from C and Fortran, a number of support applications, and on-line manual pages.

DSR is essential for applications which produce data for display in either near real time e.g. for monitoring, or in a "batch" mode e.g. for plotting a graph. This is because DSR is the primary data interface for the data display module (DDM).

The DSR system manages data in tables. The tables can be pictured as a matrix that has a number of rows and columns. At the intersection of each row and column lies a data value.

Rows represent one set of values within a table. Each row has associated with it a unique key value. A DSR table has an optional fixed upper bound on the number of rows that can be stored in it. This value is defined by the programmer when the table is created. If a row is stored in a table that is full, then the row with the lowest key value is overwritten.

A column represents a particular set of values that recur in each row of the table. Columns are referenced by name - a name defined by the programmer when the table is first created. A column may contain data of one type only. Again the type is defined by the programmer when the table is first created. One column in every table must be designated the key of that table. This column is used to reference rows in the table.

KEY DOUBLE TIME	INTEGER SPIN NO	DOUBLE OMEGA _x	DOUBLE OMEGA _y	DOUBLE OMEGA _z
14652.00	21	0.12814	-0.98732	3.19864
14652.10	35	0.12857	-0.98798	3.19828
14652.20	49	0.12857	-0.98757	3.19873
14652.30	63	0.12887	-0.98708	3.19809
14652.40	77	0.12834	-0.98720	3.19853

Figure 1: An Example DSR Table

REACH

REACH (remote extended access to circular history files) is used to access telemetry files that reside on platforms other than SUN workstations. It employs a client-server design, where the server resides on the remote platform, and provides remote access to circular history files from Sun based ORATOS applications. Current implementations of the REACH server have been developed for Vax and Gould computers.

Data Display Module

The ORATOS Data Display Module (DDM) enables the display of data within charts and tables. The user can specify the layout of charts, tables, legends and titles within a graphics window. He can then specify which columns of data need be plotted against which, what type of axes to display and other such details. Having done this data can be displayed either statically from an existing DSR file to analyse results, or dynamically in near real time to monitor data as soon as it becomes available (again, the data is obtained from a DSR file). Having specified a particular layout for a given set of data, this layout can be saved as an ORATOS definition file (the format of which is detailed later in this paper) for reuse at a later date.

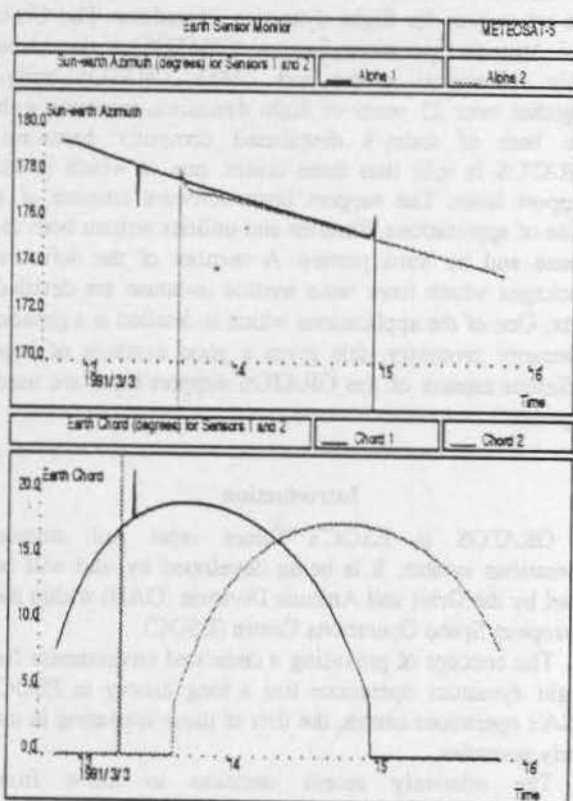


Figure 2: DDM PostScript Output Showing the Results from a GTP Implementation

Communications Package

The ORATOS communications package provides a range of inter-process communications. These communications may be local to a single machine, or across a network. Communications may be synchronous or asynchronous. A communicating process may set up point to point communications with another process, or

alternatively broadcast a message which can be picked up by any number of processes. A series of filters can be applied to a broadcast message so that it is directed to a specific subset of processes. Programmatic interfaces are provided to the communications package both as a C++ class library and a set of oScript operators (oScript is detailed later in this paper).

Definition Files

There are many occasions on which it is necessary to save a relatively small amount of data to file so that it can be retrieved at some time in the future. The data involved is often used to configure or define items such as applications or panels used in the graphical user interface.

The format used within definition files needs to satisfy a number of requirements, it has to be easily readable both by eye and machine, and it has to be flexible, so that the format used for a specific application can be altered without having to make any unnecessary changes to the software used to read and write the files.

The Definition File Format

An ORATOS definition file consists of a number of key-value pairs. Values can take one of five types, *integer*, *real*, *boolean*, *string* or *block*. Key-value pairs are separated by white space (one or more occurrences of tab, newline or space characters).

Comments can be placed in a definition file by adding a “#” character. The comment consists of everything between the “#” and the next newline. Comments are treated as white space.

```
telemetry_processor 0
#####
# #
# TMS Configuration File for METEOSAT-5 #
# #
#####
input_stream
<
    type 'reach'
    maximum_record_length 2000
    remote_host 'GMSCS'
    acam_directory
        GMSCS2:[PNSLIB.TMS]DFIL.DAT'
    acam_file 'TMS5'
>
output_stream
<
    name 'tm_ss'
    dsr
    <
        path
        '/home/oad13/acoss/dsr/meteosat6/tm_ss'
    >
>
record
<
    uid 0
    raw_parameter
    <
        name 'scosTime'
        type 'integer*4'
        number_of_elements 2
        offset -24
        period 4
    >
    derived_parameter
    <
        name 'mjd2000'
        type 'real*8'
        output_stream 'tm_ss'
        output_stream 'tm_irs'
        output_stream 'meas_saa'
        output_stream 'meas_ssr'
    >
>
```

Figure 3: Extracts from a GTP Definition File

The definition file in the figure above gives examples of *string*, *block* and *integer* types. The file is laid out for easy readability by eye, with different levels of indentation being used for each new block level (a block is anything within “<” and “>”).

In general, strings are enclosed within start (‘) and end (’) quotes. However, if a value is not recognised as being any other type, it is taken to be a string.

Integers are composed of an optional sign followed by one or more decimal digits.

A real consists of an optional sign followed by one or

more decimal digits with an embedded period, a trailing exponent, or both.

E.g.

```
12.9  
-14.7e3  
45.0E-4
```

Alternatively, a real may be represented as a hexadecimal code.

E.g.

```
x-4029cccccccccccd # is equivalent to 12.9
```

This format could not be described as human readable, but it is a precise representation of a double precision real. This is the format in which in which reals are output to definition files by ORATOS support layer software (to aid readability, the more legible format is output alongside as a comment).

A boolean is either TRUE or FALSE.

Definition File Identification

The very first item in all ORATOS definition files is an integer key-value pair. The key uniquely identifies the type of definition file which follows, whilst the integer represents the version of the specific definition format being used.

E.g.

```
telemetry_processor 2
```

This identifies the file as a GTP definition file. The GTP application can check for this keyword when loading in GTP files, and abort the load if it does not exist.

Software

The ORATOS definition file format is supported by a library of C++ classes which provide straight-forward save and restore facilities.

Additionally, the ORATOS interpreter, oScript, provides two levels of access to definition file. Firstly, a dumb conversion of definition file key-value pairs to oScript dictionary key-value pairs. Secondly, the C++ classes mentioned above are also available as oScript objects and operators, providing a more manageable interface.

An application using definition files will expect to find specific key-value pairs within a given file. The application will interface with the restore software by asking for the occurrence of a specific keyword within a given block. If it exists, the value of the key can be obtained. It is up to the application to decide if the absence of an expected keyword indicates an error or merely the use of a default value. Similarly, it is possible to give a list of expected keywords, and raise an error if keywords not in this list are encountered.

As an application develops the information required in a definition file tends to change. Generally this means the addition of new key-value pairs, sometimes the removal of key-value pairs and on very rare occasions, changing the

type of a key-value pair. If the application software always uses a default for a key-value pair which was not found in a definition file, definition files created by the old version of the application can be read in by the new version with no additional changes to the application software required when new key-value pairs are added. Removal of key-value pairs presents no problem if the existence of unrequired key-value pairs is not checked for. Changing the type of a key-value pair would mean needing to change the version of the definition file, and reading the key-value pair differently depending on the version number of the definition file being read. So far it has never been necessary to change the type of a key-value pair in the ORATOS support layer.

Inter-process Communications

This section has dealt with the saving and restoring of data to and from file. The same data can also be saved and restored to and from strings. These strings can easily be passed between different applications on different machines using the ORATOS communications package.

oScript - the ORATOS Interpreter

The ORATOS interpreter gives access to ORATOS applications at the command line level. The interpreter is known as oScript and is based upon the PostScript language. PostScript is generally thought of as a page description language, but is equally applicable as a general-purpose programming language.

Text typed in at the command line is translated to operators which are mapped to individual routines within the application. These operators can accept parameters, which are also typed in at the keyboard. Additionally, features are available which enabling looping, conditional control flow and the on-line creation of procedures. The interpreter can accept input from a file as well as the command line.

Using oScript

Any C++ class within ORATOS can be made *interpretable*, allowing the class to be manipulated at the command line. The example below shows a timer being used in the interpreter.

```
/msg { (hello) print flush } def  
/timer /msg 20 createTimer def  
timer|activate;
```

Figure 4: oScript Example 1

The first line of the example is pure oScript - it creates a procedure called msg which prints the string "hello" to standard out. The second line creates an instance of the timer class. The createTimer operator takes two

parameters: the oScript procedure to call every time the timer interval is up, and the timer interval expressed in tenths of a second. The third line starts the timer running. The result of typing these three lines of oScript is to print the message "hello" to standard out once every two seconds.

In this way it is possible to combine many different classes at the command line to build up sequences of any complexity. The next example combines a UNIX and a graphics interface together with the timer.

```
/window (pswind.pdf) restore def
/msg
{
  (date)unixCmd
  window:dateText!setString;
} def
/timer /msg 20 createTimer def
timer!activate;
```

Figure 5: oScript Example 2

The first line of this example creates a graphics window by restoring its definition from a given file. The definition of the msg procedure is still there, but it has been expanded. The first line of msg calls unixCmd, which interfaces to UNIX, with a string specifying a UNIX command to be executed. The second line of msg takes the result of unixCmd and displays it in a text field of the window. As previously, this procedure is called every two seconds, resulting in the date and time being continually updated in a window displayed on the screen, as shown below.

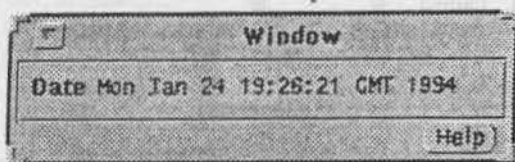


Figure 6: Output from oScript Example 2

Because the ORATOS communications package is also interpretable, it is possible to combine functionality like that shown above not only within one application, but between many. This is the way in which the Panel Server works.

Panel Server

The ORATOS Panel Server provides graphical user interfaces for applications which have none. This is enabled by the non-graphical application communicating with a graphical panel server via oScript by means of a programmatic interface.

The Panel Server Application

The panel server application consists of a basic oScript interpreter supplemented by oScript operators which provide a graphical user interface and inter-process communications.

The panel server processes requests made by client applications. These requests take three basic forms. Firstly, to load specific panels from a given definition file and to display them on the screen (and hide them when necessary). Secondly, to load application specific data into these panel's items. Thirdly, to read data from panel items into the client applications.

Once panels are available on the screen, users can interact with them. These interactions generate events which are received by the panel server. In turn, the panel builder can inform client applications that these events have occurred. In this way, client applications can find out when they should be asking for data from the panel server.

The Programmatic Interface

The programmatic interface is linked in to the client application. It consists of a number of subroutines which allow the client to make the requests described in the previous section as well as notifying the client when events occur on panels.

This interface is available in a number of programming languages: Fortran, C, C++ and oScript.

Panel Builder

The panel builder allows the creation and editing of panels and panel items. Panels may be saved to and restored from definition files. The file format is also readable by the Panel Server.

The graphical user interfaces for all ORATOS applications are created using the panel builder.

The panel builder application consists of a basic oScript interpreter supplemented by oScript operators which provide a graphical user interface.

Generic Telemetry Processor

The Generic Telemetry Processor (GTP) is a program to manipulate streams or packets of raw telemetry into more useful data, known as derived telemetry data. The Telemetry Processor is *generic* in that it can be applied to different telemetry streams without alteration to the program itself, by configuring the GTP at start-up to the particular application.

The GTP is designed to integrate with other ORATOS support layer components including REACH, the panel server, DSR and DDM.

One possible arrangement of ORATOS components can provide a generic monitoring tool. Parameters can be

displayed on panels under the control of the ORATOS Panel Server and can be stored in DSR files, and hence displayed in plots using the DDM (see figure 2).

Another arrangement provides a data archiving system. Parameters are stored on large DSR files which can be archived onto tape, CD WORM etc.

The GTP is configured at run-time to the particular flight application. This configuration can be quite detailed and so an ORATOS definition file is used to hold the information. These definition files are used throughout ORATOS and the general concept underlying them is described elsewhere in the paper. The major configurable areas are the telemetry packet descriptions, declarations of derived parameters, definitions of data mappings and definition of output streams.

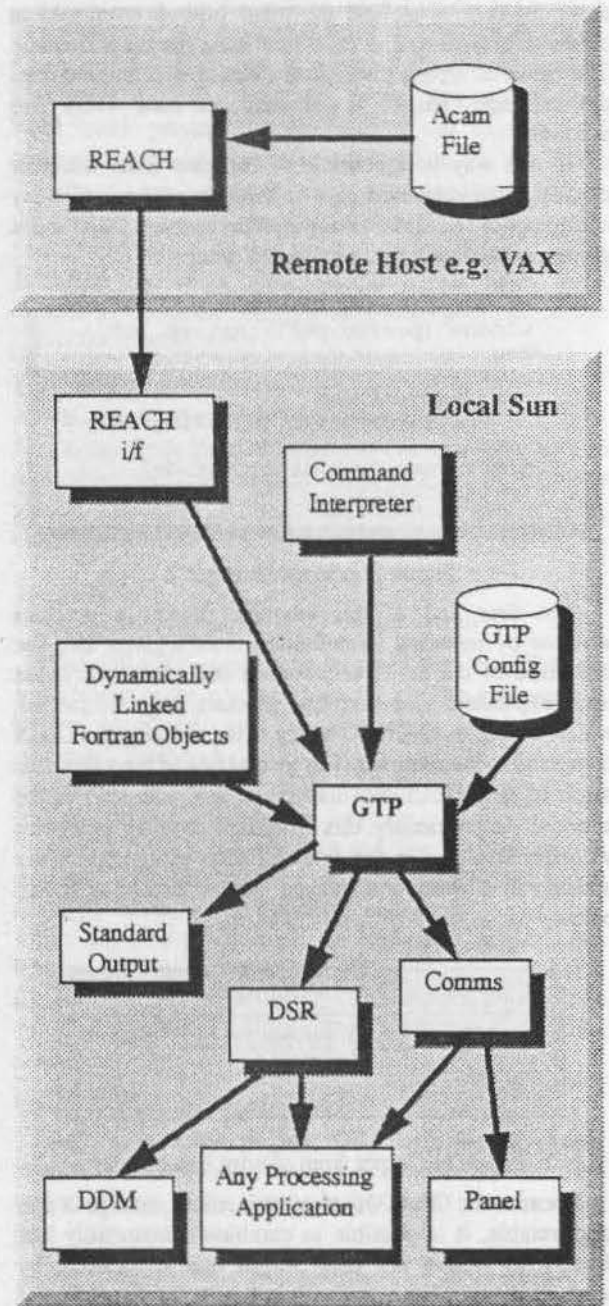


Figure 7: ORATOS Monitoring System Architecture

The Telemetry Packet Description

The GTP can read telemetry packets and the more traditional serialised telemetry streams. In the following description the term telemetry packet is used but telemetry format is equally applicable.

The set of telemetry packets can be thought of as having a tree-like structure, where the contents of a

particular packet correspond to a particular navigation of the tree from root node to leaf node.

The root node contains that part of the telemetry packet that is common to all packets, normally a packet header. The packet header contains a packet identification field, which provides the information necessary to navigate to, at least, the next level of hierarchy in the tree, and at most to completely navigate the tree.

In figure 10 the highlighted navigation of the tree shows the contents of the attitude and orbit control subsystem (AOCS) extended housekeeping telemetry packet, i.e. the primary header, the AOCS secondary header and the AOCS extended housekeeping data. The figure also shows the data handling subsystem (DHS).

Derived Parameters

Parameters that are calculated directly or indirectly from raw parameters are known as *derived*. Derived parameters are declared in the definition file. Each derived parameter must be the output of exactly one data mapping but can be an input to many data mappings.

```

derived_parameter
<
  name 'mjd2000'
  type 'real*8'
  output_stream 'stdout'
  output_stream 'tm_sa'
  output_stream 'met5panel'
>
  
```

Figure 8: GTP derived parameter declaration

Output Streams

Any parameter (raw or derived) can be output once it has been calculated. Currently there are 3 types of output streams implemented:

- Alphanumeric display on the standard output.
- Output to DSR table. The DSR table can be used as input to other applications including the DDM.
- Output direct to a panel under the control of the panel server.

```

output_stream
<
  name 'met5panel'
  panel
  <
    path 'met5sir.pdf'
  >
>
  
```

Figure 9: GTP output stream declaration

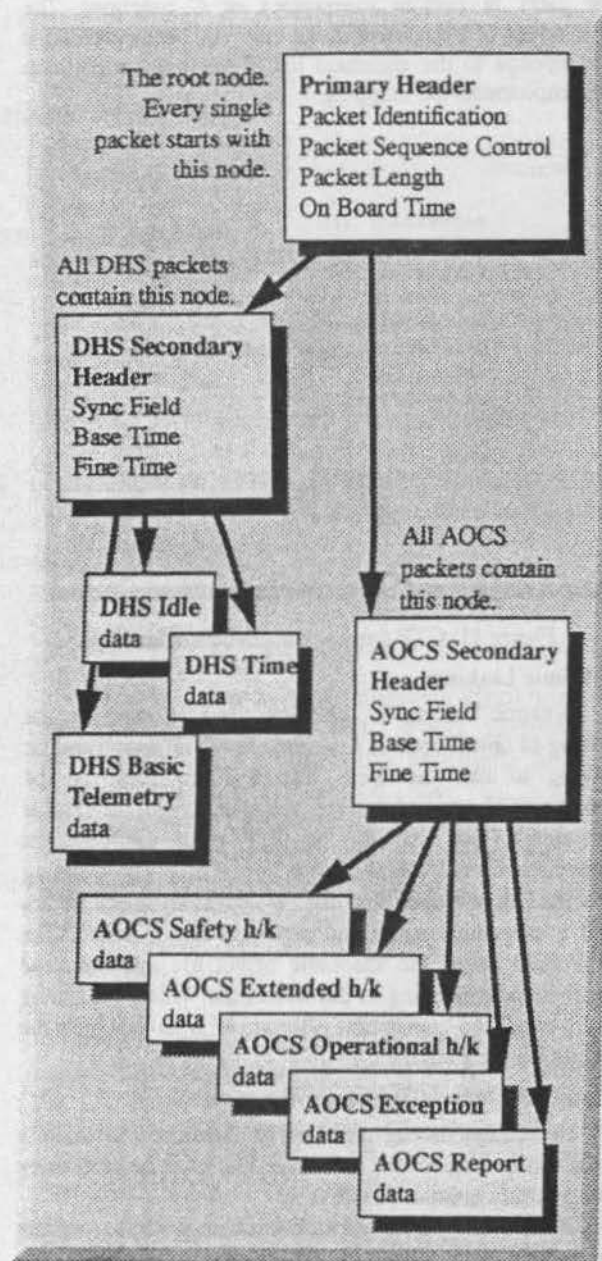


Figure 10: Example Packet Telemetry Tree Hierarchy Data Mappings

A mapping in the context of the GTP is comprised of a set of input parameters, either raw or derived parameters, a set of output parameters i.e. derived parameters and a function that prescribes the relationship between the input and output parameters sets.

The mapping of raw parameters to derived parameters can involve mathematical algorithms that are too varied and complicated to be described in a definition file. However the interface to the function can be described in

the definition file. These algorithms are implemented by the users in Fortran subroutines or C functions. The ordered set of parameters in the mapping declaration must correspond to the argument list in the users subroutine that implements the mapping.

```
mapping
<
  parameter `srp`
  parameter `sep`
  parameter `tsrp`
  parameter `tsep`
  parameter `spinrs`
  parameter `spinrate`
  active TRUE
  user_defined
<
  function p2tims`
  shareable_object
    `libmet5.so.1`
>
>
```

Figure 11: GTP derived parameter declaration

Dynamic Linking

Dynamic linking is the term used to describe the linking of object code at run-time. The GTP uses dynamic linking to link the users fortran subroutines for the processing of raw and derived parameters, with the GTP at run time. Upon start-up the GTP reads the pertinent information from the definition file. For every mapping specified in the definition file, a shareable object library and a subroutine name and signature are specified. The GTP then opens the shareable object file and links the symbol corresponding to the subroutine. When a mapping is invoked, the appropriate subroutine is called, with the appropriate arguments.

Using the Generic Telemetry Processor

To summarise, in order for a developer to build a monitoring system for a particular spacecraft he must carry out a certain amount of work.

A REACH server must be running on the remote machine where the spacecraft telemetry history file is located. (A DSR file can also be used to simulate a short history file).

The user-defined functions used to implement the mapping of raw to derived parameters must be written (e.g. in Fortran), compiled and loaded into shareable object library.

The GTP definition file must be constructed. This requires detailed knowledge of the telemetry packets or formats, descriptions of the required derived parameters, references to user-defined functions and the shareable object libraries, and references to any output streams -

DSR files and panel definition files.

The DSR files referenced in the definition file must be initialised and the panel definition files referenced in the definition file must be built using the panel builder.

Thus the ORATOS components that go together to form the generic monitoring system provide the developer with a powerful and cost-efficient way to build a monitoring system by maximising the re-use of software between monitoring systems.

Tracing in a Control Center Development

Lionel BAIZE - Hélène PASQUIER

C.N.E.S. - CT/TI/PS/SI
18 av. E. Belin
31055 TOULOUSE Cedex - FRANCE

Abstract

From user requirements definition to accepted software system, the software project management wants to be sure that the system will meet the requirements. For the development of a telecommunication satellites Control Centre, C.N.E.S. has used new rules to make the use of tracing matrix easier. From Requirements to Acceptance Tests, each item of a document must have an identifier. A unique matrix traces the system and allows the tracking of the consequences of a change in the requirements. A tool has been developed, to import documents into a relational data base. Each record of the data base corresponds to an item of a document, the access key is the item identifier. Tracing matrix is also processed, providing automatically links between the different documents. It enables the reading on the same screen of traced items. For example one can read simultaneously the User Requirements items, the corresponding Software Requirements items and the Acceptance Tests.

Keywords : Requirements, development, tracing matrix, tool.

1. DOCUMENTATION MANAGEMENT

1.1 Identification of requirements

The problem of identifying precisely the requirements when developing software, is known by any one who has had to manage a subcontracted development on behalf of a final client : the operational team.

One expects the project manager to answer such question as "what about this requirement, are you sure the modification we wanted has been

correctly taken into account.... ?".

Thus to avoid ambiguity and inaccuracy, for the development of a telecommunication satellites control centre, C.N.E.S. decided as early as 1989 to introduce identifiers in the User Requirement Documents.

1.2 Identifiers

In order to have a representative identification (trying to avoid FRED1253), it was decided that an identifier must contain the acronyms of the main functionality concerned (TM, TC,...) and of the requirement, followed by a number, e.g. TMVISU090 for a requirement dealing with telemetry visualization.

1.3 Editing rules

In order to have a tool based on the use of a DataBase Management System, we chose editing rules to allow an automatic feeding of the database. To be followed the rules have to be simple :

- an identifier must be preceded by a carriage return character and followed by a tabulation character,
- when a modification is made to the requirement, the identifier must be preceded by a "£" character in the next version of the document.

2. THE DOCUMENT DATABASE

2.1 Definition of the database

The need at this stage was to gain an automatic access to an identifier, the main key of the

database.

But we also wanted to know :

- which document it comes from,
- which edition/revision of the document,
- which paragraph (number and title) containing it,
- the text of the requirement.

For a requirement subject to a change we also wanted the change request number which it originated from.

2.2 The database

With 4th DIMENSION® which is a user friendly DBMS running on a Macintosh® we have developed a tool named "TBD-pro" for "Traceur de Besoins durant le Développement - version probatoire".

TBD-pro was designed and developed at C.N.E.S. by M. Studnia, P. Pacholczyk, L. Baize.

To avoid to be dependent on the word processor used to edit the document, the automatic feeding of the database is done on ASCII files. For the first "import" of a document, you create as many records as identifiers, for the next ones you only import into the database the requirements whose identifiers are flagged with "E", the previous records of the database with the same identifier are flagged as invalid.

In order to be able to trace the user requirements with other documents, we followed the same syntactic rules for the Software Requirement Document and for the System Acceptance Tests Document which were added to the database.

3. THE TRACING DATABASE

3.1 Definition of the tracing matrix

We wanted to cross check the user requirements with the acceptance tests. The acceptance tests are a subset of the validation tests, which have to be checked against the software requirement. Thus it was decided to have a unique matrix containing the user requirements, the software requirements, the corresponding tests and the phases (validation/acceptance) the test is

performed. Each identifier is followed by a tabulation character and a carriage return character separates each line of the matrix.

UR Ident.->SR Ident.->Test->PhasesCR

FONCTIONS

Reference: REQ-012 Etat: VALID

Synthese: This is an aspect of the requirement

Auto Reference: REQ-012 CM:

Nominaature: Introduction to S.C. 100 Edition: 1 Revision: 1

Paragraph: Introduction to S.C. 100


Description: here is the very precise, unique, second version of the User Requirement which shall facilitate the presentation of TBD-pro at the first international Symposium on Spacecraft Ground Control and Flight Dynamics

3.2 The database

One of the main problems one has, reading a tracing matrix, is that very often the identifiers are not explicit. Thus the only way to study it, is to have on one side the matrix, on the other side the concerned documents.

As we had the document database, we decided to link the records with the matrix to offer a new matrix presenting the contents of the requirements or tests and not only the identifiers.

Thus a new version of TBD-pro was developed, to include this functionality.

 T.B.D pro	
SPECIFICATION de BESOINS	
Reference	<input type="text"/>
Perigramme	<input type="text"/>
Synthese	<input type="text"/>
Description	<p>Here is the very precise details second version of the functional requirements which describe the organization of TBD and its hierarchical organization on Specimen Ground Control and Flight Control.</p>
SPECIFICATION FONCTIONNELLE	
Reference	<input type="text"/>
Perigramme	<input type="text"/>
Description	<p>Here is the very precise details second version of the software architecture which describe the organization of TBD and its hierarchical organization on Specimen Ground Control and Flight Control.</p>
DOSSIER de VALIDATION	
Reference	<input type="text"/>
Perigramme	<input type="text"/>
Description	<p>Here is the validation and which describe the organization of TBD and its hierarchical organization on Specimen Ground Control and Flight Control. ISSUE SOFTWARE_10</p>
Phase	<input type="text"/>
Commentaire	<input type="text"/>
Révisé N°	<input type="text"/>

4. UTILIZATION OF TBD-pro

4.1 Completeness of the matrix

Because the documentation is in the database, TBD-pro offers the automatic check of the completeness of the matrix. You may print and/or store in a file the missing requirements.

4.2 Searches in documents

TBD-pro offers the capability of searching through the documents. For instance, one may :

- search requirements involved in a precise change request,
- rebuild an out of date version of a document,
- combine searches e.g. one may look for requirements containing strings like "telecommand" and "operator" and not "alarm", and then store and/or print the result.

4.3 Other facilities

TBD-pro offers the capabilities of searching through the documents on top of searching through the tracing matrix.

One may perform any search he wants through the documents, and get onto the screen the corresponding selection of requirements and/or tests from other documents.

4.4 Performances

Our User Requirement Document contains 1100 requirements, whole import takes less than one hour.

The full matrix contains about 4000 lines. It takes about two seconds to change from one line of the matrix to the next one.

Checking that no identifier from a document has been omitted takes about one hour and a half.

4.5 Current upgrades

Up to now, the version of TBD-pro was an interpreted one. In order to gain rapidly, it will be updated, to be compatible with the latest version of 4^e DIMENSION® (version 5) and compiled.

To be widely distributed, it will be an industrial product with a real documentation and not only some developers' notes.

5. CONCLUSION

TBD-pro has shown it could be very helpful, because it is exhaustive, simple to use (menus, the result of any search may be stored and/or printed). It is the technical configuration management tool of the project.

Macintosh is a registered trademark of Apple Computer, Inc.

4^e DIMENSION is a registered trademark of ACI.

GAN: AN AUTOMATED SYSTEM FOR ACQUISITION AND TRACKING OF SATELLITES BY GROUND STATIONS

Ana Maria Ambrosio*
Hélio Koiti kuga**

*Divisão de Sistemas de Solo - DSS

**Divisão de Mecânica Espacial e Controle - DMC

Instituto Nacional de Pesquisas Espaciais - INPE
P.O.Box 515
São José dos Campos - 12201-970 - Brasil

e-mail: GAN@CCS.INPE.br

ABSTRACT

This paper presents the architecture and the concepts of the GAN (Antenna Manager Software) designed to execute pre-defined strategies to acquire the Brazilian satellite SCD1 on the horizon as well as to monitor and recover the satellite in any abnormal situation. Its primary objective is to allow ground station operators to track automatically the satellite from the beginning to the end of the satellite pass. Four acquisition strategies are available in order to cover all the situations. In addition GAN is able to command the antenna, to perform uplink sweeps, to release telecommands and to record angular measurements. The flight dynamics aspects, performance, and results from the pre-launch test phase until the routine operation are presented. During the validation and test phase three different satellites (SPOT, ERS-1, and Hipparcos) served as benchmarks and were tracked. The prospect considering the re-usability of GAN for other mission types is presented at the end.

Keywords: acquisition and tracking software, ground station automation, flight dynamics for tracking

1- INTRODUCTION

The Brazilian ground segment for the MECB (Complete Brazilian Space Mission) encloses a set of ground station equipments located in two different sites: one in the central region of South America (Cuiabá at 15° 33'S; 45° 51'W) and another in the north of the country (Alcântara at 02° 20'S; 44° 24'W). Both ground stations have the same characteristics with respect to TT&C capabilities. Antennas are 11 meters in diameter and operate in the S-band frequency range.

As part of the front-end, besides the antenna there is the Antenna Control Unit (ACU) that provides:

- pointing of the antenna.
- acquisition of successive points along the orbit being effectively tracked by the antenna when it is in "autotrack mode".
- monitoring of the antenna status that notifies the controller on the capture and loss of the satellite signal.
- modification of the antenna system configuration parameters.

In order to improve the front-end was developed a control software named GAN - Antenna Manager Software which enables to execute pre-defined strategies to acquire and track the satellite over the ground station. GAN is currently running in a micro-Vax II computer connected to the ACU through the IEEE-488 interface.

2- ACQUISITION STRATEGIES

The GAN was primarily designed to execute pre-defined strategies to acquire the Brazilian satellite SCD1 Ref.[1].

To satisfy the SCD1 satellite tracking needs, four strategies were developed:

1) SCAN Mode - prepared for the first passes right after launch, when the on-board transmitter should be ON. It is assumed that it is not necessary to send telecommands to activate telemetry reception. However, it is necessary to increase the range of acquisition with the antenna scanning the horizon, to minimize the orbit injection errors caused by the launcher.

2) TAA Mode - applied when the satellite orbits are well known, it considers that the on-board transmitter is OFF. Succession of antenna pointing positions covering the probable horizon region where the satellite should rise is computed. Then, for each antenna position, it is necessary to execute the frequency sweeping and to send telecommands to turn ON the on-board transmitter.

3) Programmed Mode - in this strategy the antenna follows pre-computed pointing angles and may be activated prior or during the satellite pass. Indeed a simplified numerical generator, accounting only for the J2 earth flattening coefficient factor, computes the orbit and generates the sequence of antenna pointing angles. It may therefore be selected to cover some special cases, for instance, when malfunction of the antenna autotrack system occurs, or when there is a loss of contact (silent zone) in the horizon. In this mode, the frequency sweeping may be activated or aborted at any time. It also assumes that the orbit knowledge is sufficiently accurate so as to assure satellite tracking during the whole pass.

4) Assisted Tracking - it is activated automatically to recover the satellite after a gap of the downlink signal, by means of a real-time simplified orbit determination and prediction scheme Ref. [2]. The difference is that this process is always active from the beginning of the pass. While the antenna is in auto-track mode it only performs real time orbit determination here called orbit refinement. When the satellite signal is lost, i.e. drop of the auto-track mode is detected, a prediction of antenna pointing positions is generated and the ACU is commanded to these positions at the corresponding times.

All the strategies have the same proposal, that is to acquire the satellite signal. After reaching this goal, the software GAN starts to read angular measurements from ACU. These measurements feed, in real-time, the orbit refinement algorithm (of assisted tracking process) and are also stored in the ground station computer. After the pass, the angular measurements are delivered to the Satellite Control Center, in São José dos Campos.

The strategy selection is made by the station operator through the GAN screen options. The activation or deactivation of the frequency sweeping might be set too. All the important events about the automatic tracking are showed at the screen and, if necessary, the operator might abort the system at any time. To choose one strategy, the operator must to enter the orbit number. This number is used to recover the corresponding record of the pass prediction file, which contains all the necessary information to implement the strategies.

In short, the two first strategies described above (Scan and TAA) cover only the satellite acquisition at the horizon. The programmed mode covers the whole pass and may be selected prior or during the pass. However, independent of the strategy choice, the Assisted Tracking process is always active.

3- THE SOFTWARE ARCHITECTURE

In order to meet the GAN requirements and well understand the problem and the details of each strategy, a finite state automaton was developed, as was shown in the Ref.[1].

The mechanism of the automaton was implemented in a machine process, GAN_P_GERAQS, which centralize the decisions made over the event occurrences. Under the implementation view, three groups of events could be recognized:

1- events from the ACU (Antenna Control Unit), that include acquisition-loss of autotrack, or manual-remote operation mode. Its occurrence is detected by one Asynchronous System Trap (AST), an operational system mechanism of VAX/VMS that allows to run an independent routine. This routine "GAN_Q_LESTATUS" accesses the ACU, reads the convenient memory position and sets the corresponding event. It is activated on each 500 milliseconds.

2- events from the operator screen such as strategy activation (SCAN, TAA or Programmed Mode), activation-deactivation of the frequency sweeping, abortion of the current processing. Considering that all these events come from the same source, it was convenient to conceive an AST routine, GAN_Q_COMANDOS, to both attend and interpret an operator option and translate it to an event.

3- internal events such as time-out and end-of-file that indicate the end of the strategy computations.

The main process, GAN_P_GERAQS, manages the system based on a decision table where each element encompasses two informations: the number of the action to be executed and the next state (that will be the current one after the event occurrence). Two auxiliary variables are most important: one to inform the number of the occurred event and other to save the current state. These variables set, respectively, the line and the column that determine the new element of the matrix which implements the automaton. The occurred event variable is updated by routines that recognize the events. To solve the case of two or more event occurrences at same time, there is actually an array where each element represent one event and the priority treatment is defined previously through the element position.

Thus, each strategy has imbedded the following software elements:

- a machine process to calculate the points (Observe that these calculations are made in the ground station before the satellite pass and after the operator choice);
- an AST to send synchronously the points in the precise time to ACU;
- a routine to initialize the data structures before the calculation;
- a routine to finalize the strategy after the delivery of the last antenna pointing angle without success, i.e., without getting autotrack;
- finally, a routine to finalize the strategy after the autotrack acquisition.

There are other important ASTs, one is GAN_Q_LEMED, responsible for reading the angular measurements every 1.0 second. Another one, GAN_Q_CONFCONTR, is activated when it is necessary to configure the ACU.

To make the software independent of the ACU model, and considering some object-oriented design aspects, a set of interface routines was defined to access the ACU. Therefore the ACU is a real world object so that it can be accessed only through this set of routines.

Finally, there are three processes to execute the different frequency sweeping types, each associated to one strategy.

With this software design it has been very easy to include, modify or exclude one strategy.

The final code is composed by:

- nine machine process;
- ten ASTs (Asynchronous System Traps) working at different rates;

- fifty six routines; and
- two functions.

The code has all been coded in VAX-VMS Fortran language and its size is 15,323 lines, excluding the comment lines; or 35,332 lines, including the comment lines.

4- THE TEST PHASE

The test phase consisted of two subphases: one dealing with the integration and test of parts of GAN; other to integrate and test GAN in the ground station.

4.1 - INTEGRATION AND TEST OF GAN PARTS

The GAN's design was basically divided in three main modules:

- Manager - responsible for implementing the automaton mechanism.
- Frequency Sweeping - which has three independent machine processes (as said in the section 3).
- Assisted Tracking - that implements the part of strategies that depends of the operator decision. It includes the Orbit Propagation and Refinement.

In this way, to test and integrate the GAN, firstly one aimed to validate the automaton implementation into the manager process (GAN_P_GERAQS). After that, it was implemented the routines that represent the automaton actions and the service routines that recognize and set the events to the automaton.

However, although the other modules were implemented as independent machine processes and tested independently, in fact, they are also activated by the automaton.

So the sequence imposed on the integration phase of the GAN was to validate the automaton codification as a framework at first and after to complete it small and consistent software elements (routines, functions, programs).

In this phase all the external (software and hardware) components interacting with GAN were simulated.

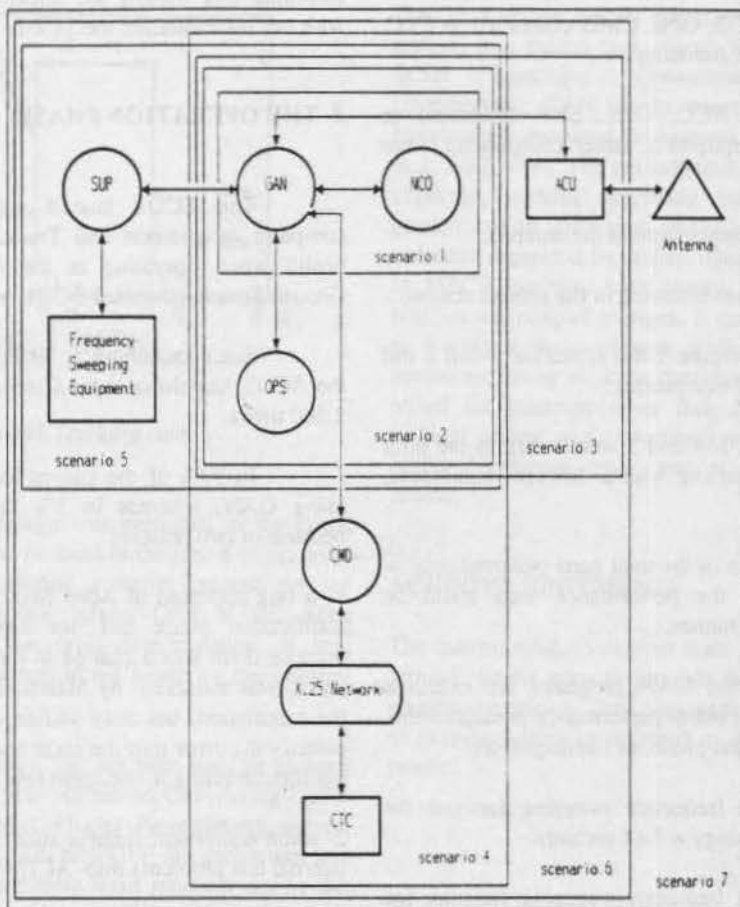


Figure 1 - The scenarios of the Acquisition and Tracking Chain

4.2- THE INTEGRATION AND TEST OF GAN IN THE GROUND STATION

The full system is composed by software and hardware components. Then to integrate all parts, a brick philosophy was adopted. The complete Satellite Control System (SICS) that includes GAN was divided in "CHAINS". For instance, Telecommand Chain, Telemetry Chain and among others, the Acquisition and Tracking Chain.

The chain has the feature of focusing the external interfaces integration and validation. As the GAN has many external interfaces, among software and hardware elements, the Acquisition and Tracking Chain was broken in scenarios. The figure 1 shows the elements that compose the Acquisition and Tracking Chain, where the circles represent the software and the squares represent the hardware elements that include:

NCO - Nucleus of the Satellite Control System Ref.[3],

OPS - Ground Segment Operation that manages the screen functions,

CMD - Telecommand Software Ref.[4],

SUP - Supervision of the ground station,

CTC - Telecommand Equipment Set,

ACU - Antenna Control Unit.

The scenarios validate with safety and increase the completeness, brick on brick, the chain. The several scenarios of the Acquisition and Tracking Chain are mentioned below:

Scenario 1 - GAN, NCO, other components were simulated.

Scenario 2 - GAN, NCO, OPS, other components were simulated.

Scenario 3 - GAN, NCO, OPS, ACU (without the antenna), other components were simulated.

Scenario 4 - GAN, NCO, OPS, CMD connected to CTC, other components were simulated.

Scenario 5 - GAN, NCO, OPS, SUP connected to frequency sweeping equipment, other components were simulated.

Scenario 6 - all components without the antenna.

Scenario 7 - complete environment in the ground station.

As shown in figure 1 the scenarios 1 and 2 did not include the external equipments.

The scenarios 3, 4 and 5 were tested in the pilot station, each one interacting with a different equipment, independently.

The integration of the total parts occurred only in the scenario 6 when the performance tests could be applied and the system tuned.

Considering that GAN programs are executed with real time priority, many performance measurements were taken during the test phase, in tuning effort:

- duration time of the frequency sweeping function for Programmed Mode strategy = 7.44 seconds.

- duration time of the frequency sweeping function for TAA Mode = 2.5 seconds.

- time between two points sent to ACU in the Programmed Mode = 0.1 seconds.
Assisted Tracking = 0.1 seconds.

- time between two angular measurements stored in the history file = 1.4 seconds.

In the scenario 7 the functional and the performance tests were repeated, now considering the antenna motion.

All these preliminary tests could be applied by the orbit simulation software, specially tailored to permit a new valid pass prediction from any initial instant of time.

After the simulated orbit tests the Acquisition and Tracking Chain was submitted to the most important challenge, i.e. to acquire and track a real satellite. In this case three different satellites were used, the SPOT, ERS-1 and also the HIPPARCOS.

Of course, the TC transmitter was always in local position to avoid sending a real TC. So some strategies as TAA, were only partially tested. The test to validate the

complete strategy that includes pointing, sending TC to turn ON the on-board transmitter, executing the frequency sweeping and waiting the tracking, only could be tested with our own satellite, the SCD1.

5- THE OPERATION PHASE

The SCD1 launch was a success and the complete Acquisition and Tracking Chain was in good health when operating at the first orbit over Cuiabá Ground Station (the third SCD1 orbit).

Since launching at 09 Feb. 1993 until nowadays the SCD1 has flown over Cuiabá station approximately 2,800 times.

In 99% of the passes the acquisition was made using GAN, whereas in 1% the GAN was not used because of two reasons:

1- a bug appeared at April first, caused by a fail in the codification phase and not detected during the tests because there was a change in the data conversion where April was mistaken by March. This error did not abort the calculation, but only shifted the pointing angles. To identify the error into the code one spent about one week, but for correcting it one spent few minutes.

2- some equipment failures such as bad connections, and internal bus problems into ACU were recorded.

The most adopted strategy to track the SCD1 has been the Programmed Mode. Since the beginning it was realized the good accuracy of the orbit determination. Then there was no need of any type of search in the horizon region, excluding therefore the use of the Scan and TAA strategies.

In 5% of the passes, that is about 140 of them, the Assisted Tracking was automatically activated due to a signal loss. The figure 2 illustrates the action of the Assisted Tracking in a singular case. In this case, a zenithal pass was the reason for LOS (Loss Of Signal). The figure shows clearly the shift that the antenna had to do in the Azimuth axis when elevation neared 90 degrees. We can see that the Assisted Tracking took about 01 minute to detect LOS, to predict the pointing angles and to command the antenna. After a few fluctuations the signal stabilized, characterizing the AOS. This was one of the hardest cases ever experienced by the Assisted Tracking. Other cases included power shortage, horizon passes (low elevation passes), and silent zones.

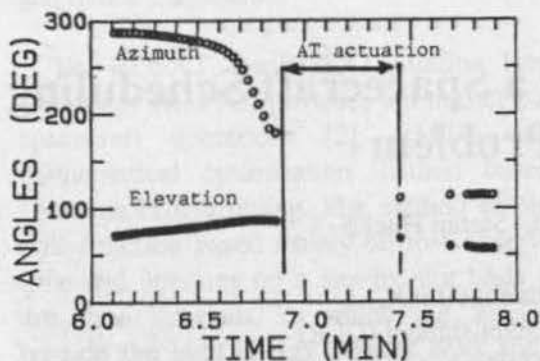


Figure 2 - Assisted Tracking case

The SCAN strategy was predicted in the initial Flight Operations Plan to be used in the first 6 orbits only. However, it was used during a month because the on-board transmitter was not turned OFF at all. After accuracy analysis of the orbit determination, it was decided to adopt the programmed mode as the primary acquisition strategy.

The TAA strategy, has not been used as planned because the transmitter was not turned OFF during LEOP (Launch and Early Orbit Phase) Nevertheless we on purpose used some passes to turn OFF the transmitter and test the strategy. No problems were reported during the tests.

To overcome a premature software decision about the autotrack event occurring in the beginning of the pass and to avoid that the autotrack begins in the secondary lobe, a manual solution was adopted. It consists of increasing the acquire level in the ACU panel until the signal stabilization.

However, even during the test phase, when this problem was detected, the GAN could nonetheless acquire the signal successfully. What happens is that when the signal is detected by ACU, and by GAN, the strategy in execution, chosen by the operator, is finalized, and the Orbit Refinement takes place. But if it is a premature-false alarm, the autotrack loss is detected immediately after, and then the software commands the antenna according to the antenna pointing angles computed by the Assisted Tracking algorithm. This switching occurred many times, about 10 or 20 times in several test cases, but in all of them the satellite signal was re-acquired at the end. This overload of the assisted tracking was considered unnecessary and the signal acquire level was raised up to 10 dB.

6- FINAL COMMENTS

The GAN system is fully operational in the Cuiabá ground station, in a shared-basis micro-Vax computer, since the SCDI launching. Considering the re-usability characteristic, GAN can be migrated to any VAX-VMS environment provided the external interfaces are available (e.g. IEEE-488). The performance has been considered as expected, without degrading other parallelly running ground station softwares, and major improvements have not been requested by station operators. For the satellites of MECB, analyses have shown that GAN can be used without meaningful changes. It can be almost considered as having a multi-mission profile despite the need of parameterization of some configuration tables. This need arised for missions other than MECB (for which the original design was conceived) such as highly elliptical orbits (Hipparcos orbit case) or geo-stationary transfer orbits.

ACKNOWLEDGEMENTS

The authors wish to express their gratitude to the Cuiabá ground station team to provide the statistics data of the routine operations. They also wish to express their thanks to everybody that contributed to the whole sucess of the project.

REFERENCES

- Ref. [1] - Francisco, M. F. M. et al., 1990 "The Antenna Manager Software for the Brazilian satellite: implementation and study" - Proceedings of first International Symposium on Ground Data System for Spacecraft Control, Darmstad, FRG
- Ref. [2] Kuga, H.K.; Carrara, V. "Real time assisted tracking for low earth satellites", São José dos Campos, INPE, Oct. 1990 (INPE-5157- PRE/1636). Presented at First Brazilian Symposium of Aerospace Technology, São José dos Campos, Bazil, 27-31 Aug. 1990.
- Ref. [3] - Yamaguti et al., 1990 "Satellite control system nucleus for the Brazilian Complete Space Mission" - Proceedings of first International Symposium on Data System Spacecraft Control, Darmstad, FRG
- Ref. [4] - Yamaguti, W. et al., 1990 "Telecommand software for the Brazilian Complete Space Mission" - Proceedings of first International Symposium on Ground Data System for Spacecraft Control, Darmstad, FRG

A Neural Network for Solving a Spacecraft Scheduling Optimization Problem ¹

Peter Göttlich, Yukio Oku, Stefan Hucke

Space Operations Department (GSOC)
German Aerospace Research Establishment (DLR)
Münchner Str. 20, D-82234 Oberpfaffenhofen, Germany
rm3c@vm.op.dlr.de

1. Introduction

This paper describes a constraint satisfaction problem (CSP) solver, applied to the complex task of scheduling a scientific satellite's entire system and payload operations. The core problem is to optimally match a given set of resources with a set of resource-utilization requests, subject to a substantial number of constraints. During the assignment process, conflicts, i.e., constraint violations, must be minimized. However, it's a well known fact that the general scheduling task is an NP-hard combinatorial optimization problem (COP).

The traditional constructive approach that incrementally expands a consistent partial assignment doesn't cope effectively with large-scale real-world scheduling problems. The kernel of a very different novel approach consists of an artificial neural network (ANN) developed for scheduling the Hubble Space Telescope (HST), referred to as the Guarded Discrete Stochastic (GDS) network [1], which is a derivative of the Hopfield thermodynamic recurrent network [3]. We present empirical evidence that for the type of scheduling problem mentioned, the GDS network with its heuristically controlled stochastic neuron selection rule is considerably more efficient than the conventional partial assignment method.

The second chapter describes a traditional mathematical optimization approach for the ROSAT satellite mission timeline (T/L) generation. Chapter three addresses the specifics of the GDS artificial neural network architecture. In chapter four, the conventional RMTG technique is compared with the GDS neural network approach, and the performance is evaluated. Some concluding remarks in chapter five close the paper.

2. ROSAT Mission Planning

ROSAT is a scientific spacecraft designed to perform the first all-sky survey with a high-resolution X-ray telescope and to investigate the emission of specific celestial sources.

The pointing phases of the mission, in which detailed observation of selected sources with respect to spatial structure, spectrum, and time variability is performed, present the most demanding requirements on mission planning. Many thousands of observation tasks must be satisfied. These need to be scheduled as efficient as possible to avoid wasting valuable observation time. The optimization must take into account all the constraints placed on the spacecraft and observations, and consider

¹We wish to thank Dr.M.D.Johnston and H.-M.Adorf for their collaboration; Dr.F.Schlude, Dr.K.Reinel, and H.Frank for their project support.

other necessary activities such as calibrations and data transmission.

For ROSAT, the ROSAT Mission Timeline Generator (RMTG) provides the master plan of spacecraft operations [2]. RMTG uses a mathematical optimization method based on Dynamic Programming. The method employs a cost function based mainly on lost observation time and operates on a slot-by-slot basis (slots are time intervals, in which the satellite is outside the high energy particle belts and thus observations can be performed.)

3. The GDS Neural Network Approach

Unlike RMTG, the neural network based scheduler employs a clear separation between the constraint representation level and the strategic scheduling level.

In this scheduler constraint knowledge is captured by so-called 'suitability functions' [4], which resemble the membership functions of fuzzy sets [5]. The time dependent suitability

functions are used to represent and propagate not only different types of constraints but also preferences. In addition, the suitability function framework allows for incorporation of 'multiplier combinations' of constraints, thus enabling introduction of more complex constraint definitions. The numerical value of the suitability function is a measure of the degree of preference for scheduling an activity at any given time.

In this new approach the actual scheduling of activities is done by a modified binary Hopfield neural network. The neurons are arranged as a matrix where each row corresponds to an activity and each column corresponds to a time bin. An active neuron in row n and column m means that activity n is scheduled for time bin m . The suitability functions can be automatically transformed into the biases and the connection weights of the excitatory and inhibitory links of the neural network so that no network training is required. Formally, the input to the neuron labeled ij is given by:

$$x_{ij} = \sum_{mn} W_{ij,mn} y_{mn} + b_{ij},$$

where y_{mn} denotes the output of the neuron labeled mn , and is given by

$$y_{mn} = \begin{cases} 1 & \text{if } x_{mn} \geq 0 \\ 0 & \text{otherwise} \end{cases},$$

b_{ij} is a bias term, and $W_{ij,mn}$ is the connection matrix defined by

$$W_{ij,mn} = \begin{cases} -\omega & \text{if a pair of activity assignments is forbidden by any constraint} \\ -\eta & \text{if } i=m, j \neq n \\ 0 & \text{otherwise} \end{cases}$$

with non-negative constants ω, η .

To overcome a drawback of the Hopfield model, that is, casually settling in local minima of the energy function, an asymmetrically coupled, excitatory 'guard' neuron is added: a

guard neuron with bias b_1^g , input x_1^g , and output y_1^g is connected to each neuron on the row it guards. The input to the guard is

$x_i^g = -\theta \sum y_{ij} + b_i^g$, while the contribution by

the guard to the input of neuron ij is ϕy_i^g . If we

choose the guard bias to be $b_i^g = \gamma > 0$ and

choose $\theta > \gamma$ and $\phi > 0$ sufficiently large, then the guard on row i will fire only when no neurons on row i are firing. When the guard fires, a large positive value ϕ is added to the input of each neuron on the row: if ϕ is chosen to be large enough to overcome the effect of any number of inhibitory links, then any neurons on the row can transition from off to on, thereby reducing the energy of the network. Thus, local minima due to the absence of any firing neurons on a row are eliminated.

This extended network is called *guarded discrete stochastic (GDS) network*. The guard neurons modify the network in such a way that it can escape from local minima and seek a state with lower energy, thereby providing an improved solution for the scheduling problem. Unlike the standard Hopfield model, the GDS network is equipped with a sequential, stochastic neuron update rule, which is motivated by heuristics.

4. ROSAT Timelining with the GDS Network

To investigate the performance of the GDS scheduler for real-world application domains, we examined it on ROSAT-like scheduling problems. Thus, a comparison could be made with the results of the operational RMTG

system. The main task of the ROSAT scheduling is the generation of the master timeline. This is a complex and demanding task, requiring the processing of about 1500 requests and scheduling of approximately 5000 time slots for a period of half a year.

We ran the schedulers in their current configuration: RMTG on a VAXstation/VMS 3100, and the GDS scheduler on a SPARCstation IPX. For the actual ROSAT case with an average of 1500 requests, it typically takes about 40 hours to generate a six-months timeline with RMTG. In contrast, we found that the GDS scheduler is about a factor of 20 faster on solving the same problem. Though the two platforms do not offer precisely the same throughput, the significantly higher performance of GDS mainly reflects the superiority of its approach compared to the Operations Research method of RMTG.

In order to estimate the efficiency of the GDS scheduler and judge its limitations, we ran a different number of requests and analyzed the scheduling process in more detail. While RMTG scheduling is achieved in a single comprehensive step, GDS schedule development is performed in two successive stages. The first stage is the preprocessing phase, in which the construction of the suitability functions and the transformation into the connection weights of the network is done. The second stage is the actual scheduling process, i.e., the network run.

Table 1
GDS scheduler execution time

Number of Requests		Execution time (sec)	
n	rejected	preprocessing	T/L generation
100	52	607.	1.
600	291	3545.	5.
1000	496	5970.	12.
2000	995	12211.	54.
3000	1494	18247.	181.
4000	1993	24562.	624.

Table 1 compares -for different number of requests- the duration of the two stages. The first column shows the number of requests n initially contained in the input. A request is rejected (during preprocessing) if it isn't possible to schedule it at any given time during the mission period due to continuous violation of one or more constraints. This is one advantage of employing suitability functions for constraint representation and propagation. It substantially reduces the chores of the subsequent scheduling process.

We observed that almost all time is spent on preprocessing, less than 2% is needed for the network run. This reveals the extremely high performance of the GDS network for scheduling. In addition, it turned out that the computational effort for the timeline generation increases roughly exponentially with the problem size, i.e., the number of requests. With respect to this, the GDS network does not differ from other algorithms for solving NP-hard COPs. However, within the scope of our task, scheduling must be viewed as an integrated pursuit consisting of constraint processing and network run. But the dominant factor for the total execution time is the preprocessing part, which grows $O(n)$. Thus, for problem domain dimensions n which are relevant to us, the overall execution time increases only linearly with n too. So it is possible for the GDS scheduler to find solutions even beyond the ROSAT dimensionality.

Additionally, an important advantage arises from the high performance of the network in combination with the stochastic neuron update rule. Most of the time is spent on the configuration of the network during preprocessing. Thus, if network configuration is finished, multiple network runs are possible in reasonable time. Because of the stochastic nature of the network update rule, two runs will generate different schedules corresponding to different solutions of the same problem. Through comparison of different schedules, a quality estimation can be performed and the schedule that is best with

respect to certain criteria (e.g., observation time, robustness) can be selected. In contrast, a scheduler that uses a strictly deterministic algorithm, like RMTG, will always generate the same schedule, given the same input data.

5. Conclusions

We have applied the ROSAT astronomical observations scheduling task to the GDS neural network paradigm and have shown the following results:

- ◆ GDS' run-time conduct impressively outperforms RMTG
- ◆ the overwhelming part of absorbed CPU time is spent on preprocessing (i.e., creating suitability functions and translating them into connection weight updates); after preprocessing, only about 2% of GDS' overall CPU consumption is needed to generate the desired timeline
- ◆ the amount of CPU time necessary for preprocessing is approximately proportional to the number of observation tasks. Thus, overall CPU time for timeline formation is about proportional to the number of observation tasks.

Finally, we mention some open problems subject to forthcoming research: a) Is the GDS algorithm readily portable to a massively parallel SIMD/MIMD computing architecture? What could be said about possible performance gains? b) In addition to COP type problems, is the GDS approach applicable to other spacecraft related operations such as adaptive spacecraft telemetry interpretation as well?

References

- [1] Adorf, H.-M. and Johnston, M.D.: 1990, "A Discrete Stochastic Neural Network Algorithm for Constraint Satisfaction Problems", in: Proc. Int. Joint Conf. on Neural Networks (IJCNN '90), 17-21 Jun. 1990, San Diego, CA, Vol III, 917-924
- [2] Frank, H. and Garton, D.: 1990, "ROSAT Mission Planning and its Perspectives for Planning Future Scientific Missions", in:

Proc. Second Int. Symp. on Space Information Systems, 17-19 Sep. 1990, Pasadena, CA, Vol II, 1241-1248

[3] Hopfield, J.J.: 1982, "Neural Networks and physical systems with emergent collective computational abilities", Proc. Nat. Acad. Sci. 79, 2554-2558

[4] Johnston, M.D.: 1989, "Reasoning with Scheduling Constraints and Preferences", SPIKE Tech. Rep. 1989-2, Space Telescope Science Institute, Baltimore, MD, 1-21

[5] Zadeh, L.A.: 1965, "Fuzzy Sets", Information and Control, Vol. 8, 338-353

DATA EXPORTATION IN TELECOM2 SATELLITE CONTROL SYSTEM

Hélène Pasquier, Lionel Baize

Centre National d'Etudes Spatiales
 18 avenue Edouard Belin
 31055 TOULOUSE CEDEX
 FRANCE

ABSTRACT

This paper describes the data exportation function in the satellite control center for the TELECOM2 geostationary satellites family. First, the architecture of the SCC is discussed. Then the paper focuses on the Data Server function explaining the functional and technical protocols used to perform dialogue between the SCC Data Server and its subscribers.

KEYWORDS : Satellite control system architecture, data exportation, network, telemetry processing.

- the TT&C TC2 stations allowing telemetry and telecommanding links with satellites as well as tracking during on station keeping phase.
- the TT&C stations of CNES 2 GHz network allowing telemetry and telecommanding links with satellites as well as localisation during launch and early orbit phases.
- the X25 TC2 specific data transmission network allowing links between some of the above components.

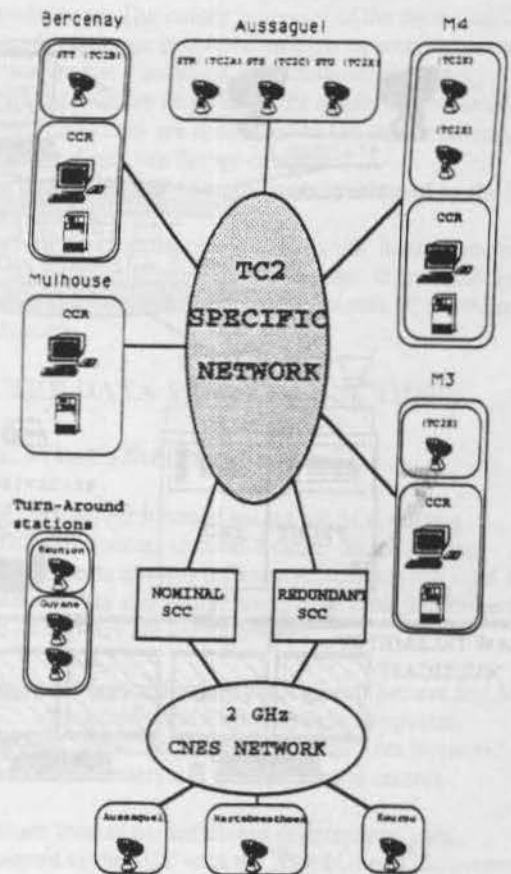
1. INTRODUCTION

The TELECOM2 geostationary satellite family is today composed of 2 satellites TELECOM2A and TELECOM2B whose main missions are business communications service and telephone and television service. The business communications service uses the 14/12 GHz band. The telephone and television service establishes links between the French mainland and its overseas territories, using the 6/4 GHz band. TELECOM2C and TELECOM2D are planned. France Telecom is in charge of development and operation of the French public telecommunications network. On behalf of France Telecom, CNES is responsible for the control of the satellites.

2. GENERAL ARCHITECTURE

The main components of the TELECOM2 satellite ground segment are the followings :

- the satellite control center in charge of telemetry, telecommanding and localisation function 24/24 h.
- the payload control centers in charge of telemetry payload monitoring (CCR).



2.1. The satellite control center architecture

Today, the SCC is designed for the control of 3 satellites and one dynamic simulator. A telemetry frame is composed of 48 bytes received and processed every 1.2 seconds.

Real time telemetry function (TM acquisition, TM processing, TM monitoring, TM storage, link with TC, TM visualisation, TM audible alarm) can not be interrupted more than 5 minutes during critical phases (positioning phase, critical manoeuvres).

The SCC architecture is based on the DIGITAL VAX range of processors running the VMS operating system with DECnet networking between processors.

The system comprises the following prime components :

- Front End Processor (MICROVAX 4000/200 packaged MIRA)
- Back End/Data Server Processor (MICROVAX 4000/200 packaged MIRA)

- Operator Workstations (VAX STATION 4000/60). These entities are interconnected using a thick-wire ethernet Local Area Network.

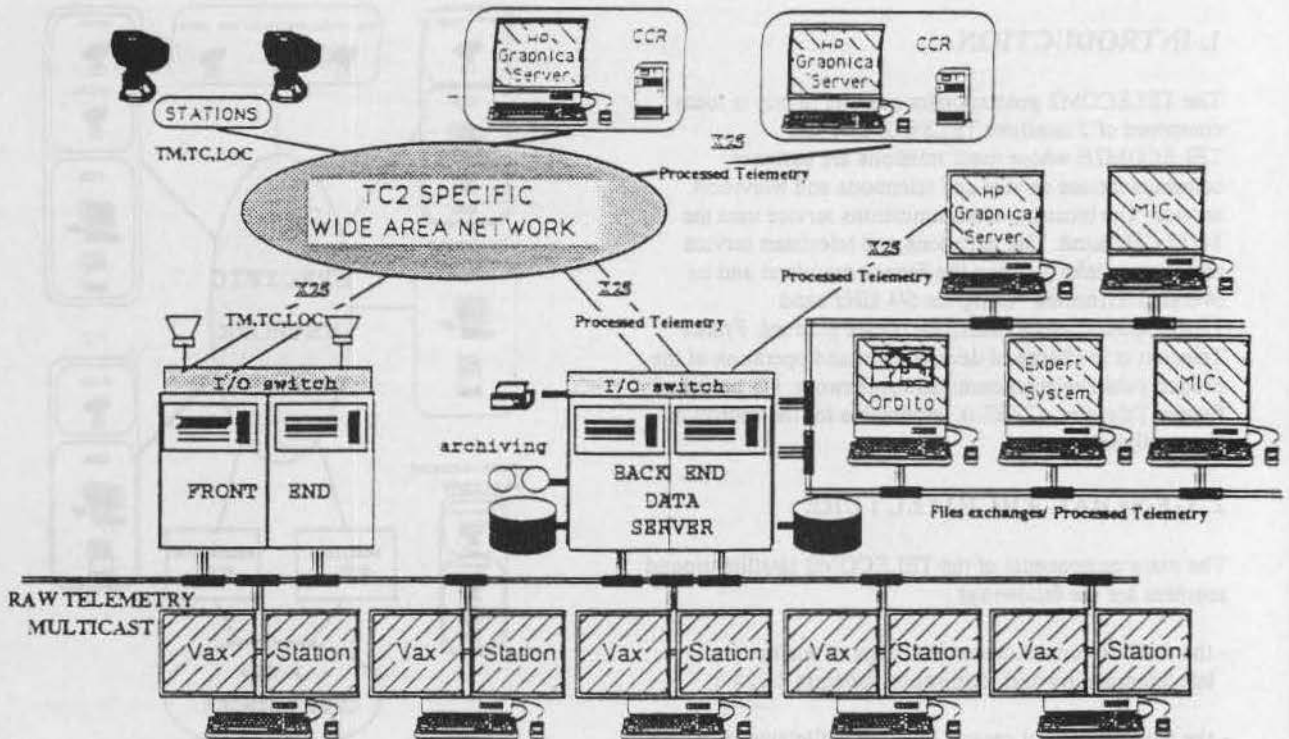
- Graphical Server processors (HP 900/834) They are connected to the Back End/Data Server processor via X25 specialised lines.

- local subscribers as :

- MIC (PC computers) responsible for real time and off line data processing,
- ORBITOGRAPHY processor (SUN station),
- EXPERT SYSTEM (SUN station) for fault analysis.

They are interconnected to the Back End/Data Server processor using a thin wire ethernet Local Area Network.

A simplified diagram of the SCC architecture is given here after.



The Front End processor is responsible for the real-time processing functions including telemetry reception, processing and monitoring and telecommand transmission.

The Back End/Data Server processor is mainly responsible for :

- data filing and archiving, telemetry trending analysis, data base management,
- data exportation towards local and remote subscribers.

The Operator Workstation is responsible for both real time and off line telemetry visualisation and telecommanding. It also offers local data base management.

The Graphical Server processors are responsible for real time telemetry visualisation.

The Front End and Back End/Data Server processors are MICROVAX 4000/200 packaged MIRA. A MIRA processor is composed of 2 redundant VAX 4000/200 processors and of a I/O lines switch. The MIRA system offers the facility of being able to switch I/O lines between two systems to cater for processor failure, and thus provide a packaged master/standby computer system. The switch can also be operated manually to cater for maintenance requirements. For these reasons the MIRA system is used for the functions involved with I/O external devices, such as telemetry/telecommand/localisation I/O, remote systems, printers and plotters. It provides a fast failure detection and reconfiguration and uses proprietary software to perform the system failure detection and I/O lines switching function.

The operator workstations are twin screens workstations allowing advanced man machine interface techniques.

2.2. Functional description

The main features of this architecture are the following ones :

- raw telemetry frame received and processed by the Front End MIRA,
- raw telemetry, derived parameters and monitoring results multicasted over the LAN by the Front-End MIRA after processing,
- multicasted data processed by Back End/Data Server MIRA to be dispatched towards local and remote subscribers,
- multicasted data processed by Operator Workstations for visualisation purpose.

A more detailed functional description of each processor is given here after :

The master processor of the Front End computer receives telemetry from the TTC stations and/or from the dynamic simulator,

The master processor of the Front End computer processes the real time telemetry on a frame by frame basis every 1.2 seconds (i. e. frame acquisition, parameter calibration, parameter monitoring) and multicasts the raw telemetry frame, the derived parameters and the TM monitoring results towards the other components,

the master and standby processors of the Back End/Data Server computer simultaneously archive the received telemetry,

the operator workstations process the TM blocks multicasted on the network by the Front End computer for telemetry visualisation and monitoring alarms visualisation,

the master processor of the Back End/Data Server computer processes the TM blocks multicasted on the network by the Front End computer for telemetry exportation towards subscribers,

telemetry replay is done by reading telemetry archive on Back End/Data Server computer and transmitting to the Front End computer for processing,

trending analysis are defined by the operator from its workstation. The master processor of the Back End/Data Server computer extracts data from its archive, processes it and makes it available for visualisation purpose, tracking data are received by the master processor of the Front End. They are condensed by the master processor of the Back End/Data Server computer,

the transmission of telecommands is achieved by the Front End processor,

the time synchronisation is done by the master processor of the Back End/Data Server computer. It cyclically gets Universal Time and dispatches it towards all the other computers.

3. THE DATA SERVER FUNCTION

3.1. What's the Data Server ?

The Data Server function within the SCC offers a standardised access to control center data. The Data Server exports towards different subscribers real time and processed data and gets requests from those subscribers. The subscribers are the followings :

- local ones depicted before as Graphical Servers and MIC PC, Orbitography and Expert System computers. They are connected to the main Local Area Network.
- remote subscribers i. e. payload control centers.

They are located on distributed geographical sites connected to the SCC with the X25 TC2 specific network.

The design of the Data Server within the SCC has been guided by the following needs :

- dispatching of real time monitored telemetry towards local and remote subscribers with the same user interface,
- dispatching of data files towards local subscribers,
- dynamic data requests by the subscribers,
- centralised management of data distribution,
- data flow control and management,
- easy addition of a new subscriber,
- use of standard market protocols.

3.2. What kind of data ?

The subscribers are separated into two categories : real time ones and off line ones.

The real time subscribers are :

- graphical servers both local and remote
- PC computers both local and remote

The off line subscribers are :

- local PC computers
- orbitography computers
- expert system computer

The data exchanged between Data Server and real time subscribers is telemetry parameters from various sources (satellites, simulator, replay) with telemetry monitoring results.

The data exchanged between Data Server and off line subscribers are data files as operational data base, telemetry off-line analysis results, logbook off-line analysis results, localisation and calibration files, stored and archived telemetry files.

3.3. Why a data server ?

* dispatching of real time monitored telemetry towards local and remote subscribers with the same user interface

The processors and software installed in the remote payload control centers are the same ones as those installed locally in the SCC. So, there was a need to standardise the data distribution for both local and remote subscribers.

* dispatching of data files towards local subscribers

The data server must allow file distribution and transfer. For this purpose the files to transfer are made available to

subscribers in a specific data server area named "export area" with limited access rights.

* dynamic data requests by the subscribers

According to the telemetry it wants to visualise, a subscriber can ask dynamically to the data server for one or more "subset" of telemetry parameters it needs.

* centralised management of data distribution

The subsets are predefined in a SCC data base. This data base is managed by the data server function giving access rights to subsets depending on the subscribers. The authorisation of subset transmission is given by the SCC which is in charge of opening the X25 virtual circuits when needed or allowing TCP/IP session.

* data flow control and management

The specific TC2 network has a data rate of 19.2 kbits/s.

According to the need of information of each remote subscriber and to the volume needed, a maximum number of parameters has been defined for each subscriber and can be parameterised in the satellite characteristics file within the data base.

Today our system is able to broadcast about 3800 parameters towards its subscribers for 3 satellites.

* easy addition of a new subscriber

This can be achieved without modifying the software. Only data base files must be updated.

* use of standard market protocols

ISO8802. 3 is used for ethernet transmission, TCP/IP and sockets are used for ethernet real time transmission, X25 is used for both local and remote real time subscribers, TCP/IP and FTP are used for data file exchanges, Real IEEE coding is used for transmission of parameter physical value.

A more detailed functional description of the Data Server function is given here after.

3.4. real time exchanges functional description

On-line telemetry exportation may be achieved towards the Ethernet, local X25 and remote X25 subscribers.

On-line telemetry exportation is done on data links different of those used for off-line processing.

- For Ethernet subscribers, exportation is achieved within a TCP/IP session. The subscriber opens the session by sending a call to the suited TCP/IP address and port number on the Data Server.

When an Ethernet subscriber wants to establish a connection with the on-line telemetry server, the caller address is controlled. If access is not allowed, a 'denied access message' is sent to the subscriber and the TCP/IP session is cleared.

A TCP/IP session is opened for on-line telemetry exportation concerning one satellite and one mode (live, replay or simulation). To allow exportation to begin, the subscriber must send to the Data Server, a request to associate the session with an entity and a mode. A subscriber may only have one session opened at a time with a given entity and mode. The number of simultaneous treated entities for a subscriber is controlled against the quota specified in the subscribers characteristics file.

- For X25 subscribers, exportation is achieved over a virtual circuit. It is the Data Server which opens virtual circuits by an action of the operator who activates an association between the port associated with the subscriber address on one side, and the subscriber, the satellite and the mode (live, replay or simulation) for which the virtual circuit is opened in the port configuration on the other side. A subscriber may only have one session opened at a time with a given entity and mode.

Nature of exported data

Exported data for an exportation session is either live telemetry from a given entity, or replay telemetry.

For each telemetry frame multicasted on the Ethernet LAN, for one entity and one mode (live/replay) the following data is sent within an exportation session :

- frame date,
- station identifier,
- frame number,
- frame and (date and time) quality,
- for each parameter requested and present in the frame
 - . raw and engineering values
 - . alarm state

Subset requests management

In a given export session, a subscriber receives parameters whose transmission is allowed by the Data Server for this session.

There are two ways to allow the transmission of parameters within an export session :

- automatic transmission at session beginning,
- transmission on request from the subscriber.

Automatic transmissions occur when, in the subscribers characteristics file, a list of subset identifiers to send automatically is specified for the destination subscriber.

There are two kinds of subset requests :

- a total request specifying a subset name, this name identifying a parameter list. This request concerns all the parameters of the subset.
- A partial request specifying a subset name and a list of parameters, the specified list having to be a part of the list associated with the subset name. This request concerns a part of the parameters of the subset.
- The total number of parameters for a given subscriber must be less than the maximum number of parameters specified for the appropriate subscriber in the subscribers characteristics file.
- The subset name must be known by the Data Server.
- The subset must be valid for the concerned entity (satellites or simulator).
- The subset must be allowed for the subscriber.
- In case of partial request, the specified subset name and list of parameters must be compatible (i. e. each parameter of the list must belong to the specified subset).

If the request is accepted, telemetry data is sent to the requester when the next beginning of frame occurs.

When a subscriber no longer wants to receive a subset, it has to send an appropriate request specifying the subset identifier. If there is no corresponding subset active, no action is performed.

When an export session is closed either by the Data Server, (case of X25 subscribers) either by a subscriber (case of Ethernet subscribers) either accidentally, all subsets transmissions for this session are cancelled.

3.5. off line exchanges functional description

The exportation function allows the exportation of the following data to Ethernet subscribers :

- TM/TC database files
- localisation and calibration files
- off-line telemetry analysis result files
- logbook analysis results
- raw telemetry

Exportation is done from export area which are respectively :

- a TM/TC database export area
- a localisation export area
- an off-line analysis results export area
- a logbook analysis results export area
- a telemetry files export area

The exportation function allows exportation by file transfer over Ethernet TCP/IP. The exportation function waits for subscribers connections. A connection is performed as the opening by a subscriber, of a FTP session, this subscriber providing connection information (user ID, password). A connection is accepted, if the given User ID and password have been registered in the data-server VMS Authorise database, if a communication port has been defined for the given network access (FTP user ID, internet address), if this port has been associated with a subscriber in the port configuration, and if this association is active, the connection is accepted else it is refused.

The exportation function then waits for file transfers which are initialised by the connected subscriber.

Ethernet subscriber's access to export areas is limited to 'read' access.

Each file access by a subscriber, successful or not is recorded in the SCC logbook. Each file and directory access is restricted to the rights granted to the subscriber.

Each export area may be managed by a data management operator. Management actions are :

- display of file list
- file deletion
- file transfer from their origin location

4. CONCLUSION

The main advantages of our system are standardisation and extensiveness.

This concept can be easily reused for other projects.

5. REFERENCES

1. Spécification technique de besoin du SICS-D TC2. Centre National d'Etudes Spatiales, Toulouse, France.
2. Spécifications d'interfaces SICS-D/MIC, CCR, Serveur Graphique, SE. Centre National d'Etudes Spatiales, Toulouse, France.
3. Dossier de spécification fonctionnelle du SICS-D TC2. Matra Marconi Space France et Syseca, Toulouse, France.
4. Dossier d'architecture matérielle et logicielle du SICS-D TC2. Matra Marconi Space France et Syseca, Toulouse, France.
5. Dossier des interfaces entre le SICS-D TC2 et les MIC, CCR, Orbito, SE, SGI. Matra Marconi Space France et Syseca, Toulouse, France.

GROUND SYSTEM HARDWARE AND SOFTWARE III

1. Pilgram, M. and Goertz, C. (DLR-Germany):
 "D2 Data Presentation System" 267
2. Pacola, L.C. and Ferrari, C.A. (INPE-Brazil):
 **"A Compact and Low Cost TT&C S-band Ground Station
 for Low Orbit Satellites"** 271
3. Oberto, J.M. (Matra Marconi Space-France):
 **"Ground Segment and Operations Concepts of Small
 Satellite Missions"** 277
4. Huc, C.; Reich, R.; Aubron, R. and Pieplu, J.L.
 (CNES-France):
 **"Consequences Arising from the Long-Term Need to
 Archive and Access Data Relating to Ground System
 Specifications and Architecture"** 286
5. Jones, M.; Head, N. (ESA-Germany); Keyte, K.
 (VITROCISET-Italy) and Symonds, M. (CRI-Denmark):
 **"SCOS II: ESA's New Generation of Mission Control
 System"** 290
6. Jansen, N. (DLR-Germany):
 **"The ROSAT Telecommand System-from Command
 Generation to Command Verification"** 296
7. Uesuji, K.; Nakatani, I.; Mukai, T.; Hashimoto, M.;
 Obara, T. (ISAS-Japan) and Nishigori, N. (Fujitsu-
 Japan):
 **"ISACS of ISAS - An Intelligent Satellite Control
 Software"** 305
8. Kaufeler, J.F.; Kaufeler, P. (ESOC-ESA) and Parkes, A.
 (Nova Space-U.K.):
 "The ESA Packet Utilization Standard - P.U.S." 311

D2 DATA PRESENTATION SYSTEM

Martin Pilgram, Christine Görtz
DLR - GSOC
Münchener Str. 20
D-82234 Wessling
Germany

email: Pilgram@GSOC0007.rm.op.dlr.de

Abstract

Data presentation is one element in a data processing system. In space centers such as the German Space Operations Center (GSOC), located at Oberpfaffenhofen near Munich, data presentation systems are used for the realtime display of telemetry, command user interfaces and for the system monitoring and control consoles. The form of data presentation may vary depending on the employment of the relevant system and the scope has increased considerably during previous years by the development of advanced hardware devices. Consequently alphanumeric terminals have evolved into X-window terminals with all their graphic capabilities included.

This evolution can be seen in the systems used at GSOC and this paper will detail the systems used to support the Spacelab D-2 mission.

Keywords : Display-System, Man-Machine-Interface (MMI), Data Presentation

General

The GSOC has controlled German scientific satellite and manned spaceflight projects throughout the lifetime of their respective missions and also commercial communication satellites during Launch and Early Orbit (LEOP) phases.

One of the tasks of this control center is to display spacecraft 'housekeeping' telemetry for the spacecraft controllers or in the case of the Spacelab D-2 manned mission, provide experiment data to the various mission scientists. Other MMI tasks include the command user interface and the system monitor and control consoles.

These tasks have been performed at GSOC in support of scientific satellite missions such as Helios, Ampté, Rosat (operative) and IRS, manned missions such as Spacelab 1, D1, D2 and also for the TV-SAT1/2, DFS1/2/3 and Eutelsat F2/I-V commercial communication satellites.

A data presentation system, otherwise known as a 'Display System', will vary in accordance with the utility requirements but is generally located at the User end of a data processing system. Data processing systems for the aforementioned missions follow the following schematic :

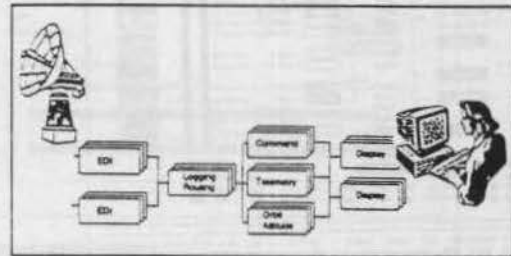


Figure 1: Overview of a GSOC data processing system.

History

The D2 display system was developed from devices dating back to the early 1980's. Due to the cost factor, video-based systems were replaced by terminal based systems and these systems (initially the alphanumeric type) were driven by a display control computer which served approximately 16 terminals. The display control computer was a VAX II class machine which was also used for telemetry processing. With the growing requirement for graphics the VAX II machines were eventually replaced by VAX III class systems. These systems supported telemetry processors using the non-transparent, DEC-

net, task-to-task communication protocol with transfer of only the telemetry updates but also included an additional feature to transfer all parameters to refresh the display screen. These systems are based on an 8 colour graphic terminal, driven by escape (ESC) sequences from the display control computer and include the features:

- alphanumeric
- symbol plots
- line plots
- bar graphs
- project specific interface (ROSAT Star Map)

All these features can be combined into a 'Display Page'. For mission support the page numbers and graphical requirements increase considerably. The Eutelsat system has 170 display pages allocated with 140 alpha and all others graphical. These include 100 line plots with a computer held history.

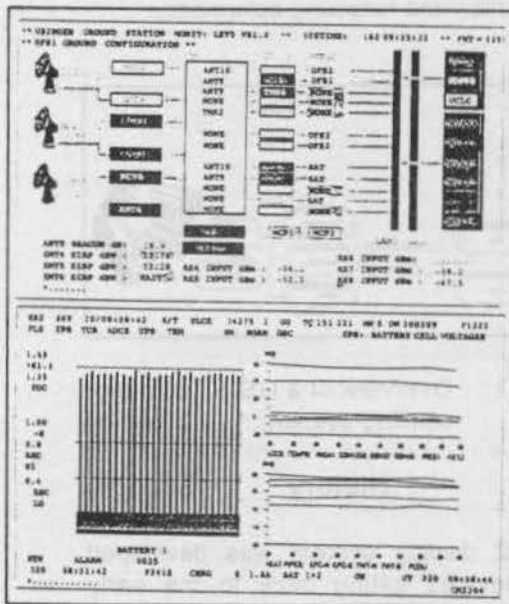


Figure 2: alphanumeric, line-plot, symbol-plot, bar-graph elements of the display systems.

Display page hardcopies are created by pressing the keyboard print button, producing an alphanumeric print to the direct connected line printer. Graphic hardcopies are created by sending a request to the display computer which generates a laser print copy to a specific printer.

TM, TC, M&C

The display system features are primarily used to display telemetry parameters with a minimum capability to accept inputs (H for hardcopy, F for format selection, etc.) and is therefore not considered a useful tool for commanding and monitor/control. To provide an input capability a second system was built based on the concept to drive a single terminal. If more than one terminal was required the process was initiated on each terminal, which is a disadvantage when as many as 100 terminals may need to be activated. The variable requirements of display system usage is listed below :

GSOC	TM	TC	M&C
Formats	200	10	10 - 300
Graphic	-	-	**
input	-	-	-
Consoles	100 1-10	1(3)	1(3)

Table 1: Requirements for TM, TC, M&C.

There are currently two separate systems in operation at the MMI for satellite control. Both systems are based on the use of terminals with added graphical capability.

D2 Display System

GSOC support of manned spaceflight commenced with the first Spacelab mission in 1983. Subsequently a Remote POC was constructed at Oberpfaffenhofen to support D1 and D2. To accommodate telemetry presentation requirements GSOC developed a customized D2 Display System that was evolved from experience gained from previous missions. The requirements included maximum status availability, a mouse based user interface and service to four large control rooms.

One of the new features included the User-group workstation account access that created monitoring capability for a specific experiment. Printers and graphical hardcopy devices were made available in close-

proximity to the VAXstation 3100 workstations.

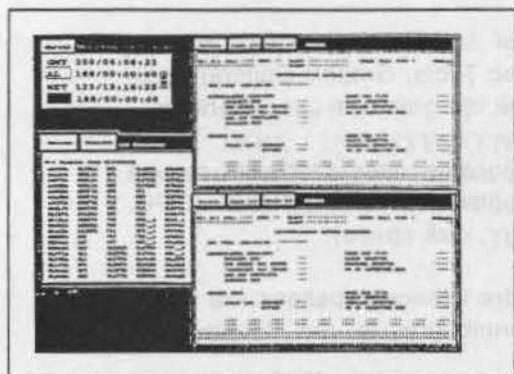


Figure 3: D2 Workstation Layout

Without specific Window standards provided for development GSOC created its own "D2 Standard" with UIS, which is a predecessor of the VAX/VMS X-Windows. The D2 Standard provided a rectangular area on the screen with a title bar, an options menu and two buttons to initiate alphanumeric and graphic hardcopies. Windows can be moved using a mouse and can be resized by a predefined factor (2* enlarge, 6* reduce) according to requirements.

The D2 Display System provides a 'Quick Look' of downlinked ECIO, SCIO and PPF telemetry. A maximum of two formats can be displayed per workstation in a predefined alphanumeric or graphic format, with hardcopy print capability. Furthermore a 'Transfer' terminal option provides an additional format on a remote terminal with an alphanumeric print capability.

	Display Pages		Parameter Processed	
	Alpha numeric	Graphic	according POCC DB	Special Processing
ECIO	1		2	
SCIO	3		62	
PPF	7		123	
ECIO	8		121	2
SCIO	2		29	1
PPF	9	7	161	2
ECIO	10		365	28
SCIO	12		513	22
PPF	11	6	362	172
ECIO	1	13	81	72
SCIO	25	7	838	235
PPF	9	2	216	52
Total	105	38	3187	529

Table 2: D2 Telemetry Statistic Summary

The D2 Display system is divided into two

sections :

1. Telemetry :
Each Usergroup has an account login name and password. The Usergroup determines the selectable formats required.
The D2 Display System has a total of 140 display pages with 105 alphanumeric and 35 graphical.
2. M&C :
M&C can only be accessed via a privileged account. This process monitors the behaviour of each workstation and status of the data lines with the display of data reception and quality. Monitoring is capable as an overview or in more detail (e.g. the status of a single workstation).

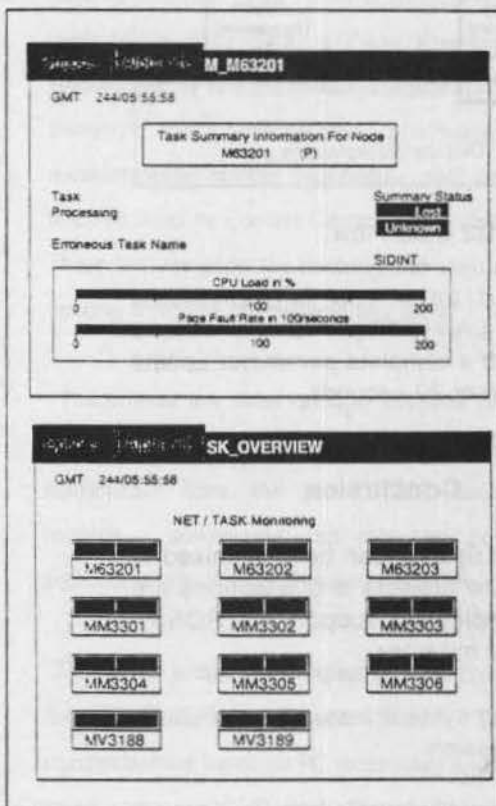


Figure 4: Net/Task Monitoring

D2 Data Flow

RT (realtime), PB (playback) and PPF (payload parameter frame) telemetry parame-

ters are introduced to the Display LAN by the Multicast Write process. Every active workstation will read the multicast parameters and update the selected pages displayed. Graphic updates are performed in the background to maintain status history.

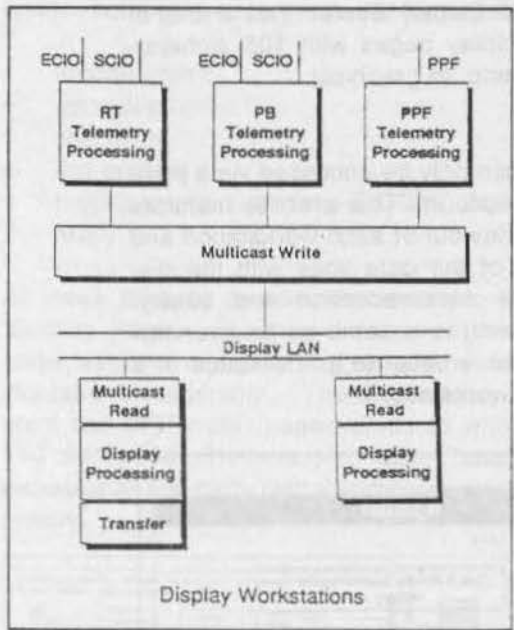


Figure 5: D2 Data Flow

An updated parameter is transmitted across the LAN (3Kbps) at one second intervals with a complete parameter update (24Kbps) every 20 seconds:

Conclusion

The Display System can be customised to support future projects and adaptations are already complete to support the ROSAT and Eutelsat missions.

The following system features were criticized post mission :

- Only two display pages per workstation were possible.
- On-line page definition changes were not possible.

This criticism, coupled with the ongoing development process produced the following conclusion :

- Use Window Standards (X-Windows Motif, ?) which provide a consistent look and feel.
- Use of software tools (GUI builder, Graphic Tools, Graphic Editors) accommodate the graphical user interface.
- Sophisticated user interfaces require more powerful workstations (CPU, memory, disk space).
- Software licence expenses are a major contribution to the development costs.

Emphasis is on future missions, such as the Columbus Project and therefore with more regard to a dynamic system accommodating all possible requirements.

A COMPACT AND LOW COST TT&C S-BAND GROUND STATION FOR LOW ORBIT SATELLITES.

Luiz C. Pacola
Carlos A. Ferrari

INPE - INSTITUTO NACIONAL DE PESQUISAS ESPACIAIS
Av. dos Astronautas, 1758 - Sao Jose dos Campos, S.P., Brazil.
CEP. 12227-010 - Phone :(123) 41.8977 - FAX: (0123) 21.8743

ABSTRACT

INPE's S-Band Ground Station for satellite control and monitoring is revised considering the current software and hardware technology.

A Ground Station conception for low orbit satellites is presented. The front-end uses small antenna and low cost associated equipments without loss of performance. The baseband equipments are highly standardized and developed on a personal computer IBM compatible using extensively Digital Signal Processing (DSP). A link budget for ranging, telecommand and telemetry is also presented.

INTRODUCTION

TT&C Ground Station have traditionally required expensive and lengthy programmes. They have been based on large antennas, costly high power amplifiers and complex baseband equipments in order to perform properly its main functions: to process and uplink telecommands, to receive and process telemetry, to carry

out angle and ranging measurements and to allow remote supervising.

INPE's S-Band Ground Station located at Cuiaba consists basically of an 11 meter antenna with a figure of merit (G/T) of 22 dB/K, a 2 kW Klystron high power amplifier (HPA) and associated equipments for tracking, telemetry and telecommand processing, ranging measurements, remote supervising and communication with the Satellite Control Center via a wide area network. These facilities allow the tracking and control of satellites ranging from low to geostationary orbit.

The present low orbit satellite missions profile and the current available technology for both space and ground equipments drive the new TT&C Ground Stations towards a downsizing and low cost design without significant loss of reliability and flexibility.

This paper presents a compact and low cost architecture for TT&C S-Band Ground Station. The baseband equipments are based on PC technology and implemented using extensively Digital Signal Processing (DSP) techniques. This approach reduces cost and implementation time, resulting in highly standardized equipments. The Front End uses small antennas and low cost solid state power amplifier. All the Ground Station subsystems are connected to a local area network (LAN)

communication with a not co-located control center via a wide area network (WAN) or telephone link.

ARCHITECTURE DESCRIPTION

Figure 1 presents the INPE's Ground Station architecture. All the equipments are remote monitored and/or controlled by the station computer through monitoring and control units (MCUs) using a RS 232C interface. This solution was adopted because the variety of equipments interfaces (IEEE 488, RS 232C, digital signals), the limited number of ports available on the station computer and in order to avoid useless data exchange. Concerning the communication with the Satellite Control Center at Sao Jose dos Campos, all the baseband equipments, but the telecommand, are connected to the wide area network through a serial communication unit (SCU) and a protocol converter. The INPE's Ground Station was conceived in the middle of the 80s using the technology available at that time, resulting in a large number of equipments and interconnections. Besides that, the use of a large antenna, 2 kW HPA and RF associated equipments implied in a costly and complex system in terms of installation, operation, maintenance and upgrade.

The low orbit satellite mission requirements which includes cost and complexity reduction, easy upgrading and maintenance, operation and configuration flexibility lead us to conceive a compact low cost architecture based on the present hardware and software technology. This does not imply in loss of performance or overall flexibility as it will be shown. A typical link budget for a low orbit (800 km) satellite, operating in the S-Band (2033.2 MHz uplink and 2208 MHz downlink), is shown in Table 1. A 3m antenna and tracking for elevation angle greater than 10 degrees are assumed. All

subsystems operate with margin greater than 2 dB and no significant loss of performance is noticed.

The overall compact ground station architecture is shown in Figure 2 and its main subsystems are:

- Ranging and Range Rate
- Acquisition and Tracking Control
- Front End and RF Equipments
- Telemetry and Telecommand
- Time and Frequency
- Supervision and Communication.

All the baseband equipments are developed in a compatible personal computer (PC) platform to which are added dedicated hardware and software. The hardware is as always as possible implemented as dedicated PC board connected to the computer bus. Digital Signal Processing (DSP) tools and support facilities commercially available for IBM PC are extensively used providing standardization, reliability and flexibility. The data exchange between the equipments (ranging and range rate, telemetry, telecommand and supervising) is extremely simplified employing a local area network (LAN) implemented with cheap off the shelf tools. The LAN is connected to a wide area network (WAN) allowing communication with the control center.

The software for acquisition and tracking, telecommand, telemetry, ranging and range rate processing is distributed over the PC network. Once the PCs can do local control and monitoring, supervising functions are simplified. Log, backup and other operational functions can be performed by a single computer connected to the LAN. Therefore the ground station can operate independently from the control center.

Table 1 - Typical Low Orbit Satellite Link Budget.

UP LINK		DOWN LINK	
Earth Station (E/S) EIRP	52.0 dBW	S/C EIRP	10.0 dBm
Free Space Loss	166.1 dB	Free Space Loss	166.8 dB
E/S Pointing Loss	0.5 dB	E/S Antenna Pointing Loss	0.5 dB
Atmospheric Loss	0.5 dB	Atmospheric Loss	0.5 dB
Polarization Loss	1.5 dB	Polarization Loss	1.5 dB
Boltzmann constant	-228.6 dB	Boltzmann constant	-228.6 dB
S/C G/T	-48.0 dB/K	Earth Station G/T	12.0 dB/K
<hr/>		<hr/>	
Up-link S/No	63.9 dBHz	Down Link S/No	51.3 dB
Carrier Modulation Loss (1.31 rad)	3.9 dB	Carrier Modulation Loss (1.26 rad)	6.9 dB
Carrier C/No	60.0 dBHz	Carrier C/No	44.4 dBHz
C/N (PLL Noise BW=800 Hz)	31.0 dB	Carrier Required C/No	40.0 dBHz
Receiver Threshold	10.0 dB	<hr/>	
CARRIER MARGIN	21.0 dB	CARRIER MARGIN	4.4 dB
RANGING (RG)		Major tone mod. loss (.34 rad)	19.2 dB
RG major tone mod. loss (.82 rad)	7.8 dB	Major tone down-link S/No	32.1 dBHz
Up-link major tone S/No	56.1 dBHz	Total Major tone S/No	32.0 dBHz
RG minor tone mod. loss (.42 rad)	14.2 dB	Major tone required S/No	25.0 dBHz
Up-link minor tone S/No	49.7 dBHz	<hr/>	
TELECOMMAND (TC)		MAJOR TONE MARGIN	7.0 dB
TC Modulation Loss (0.93 rad)	6.5 dB	Minor tone mod. loss (.16 rad)	25.7 dB
TC S/No	57.4 dBHz	Minor tone down link S/No	25.6 dBHz
Required TC S/No	49.0 dB	Total minor tone S/No	25.5 dBHz
<hr/>		Minor tone required S/No	16.0 dBHz
TC MARGIN	8.4 dB	MINOR TONE MARGIN	9.5 dB
TM Modulation Loss (1.03 rad)	3.4 dB	TM Modulation Loss (1.03 rad)	3.4 dB
TM S/No	47.9 dBHz	TM S/No	47.9 dBHz
TM Required S/No	45.7 dBHz	TM Required S/No	45.7 dBHz
<hr/>		<hr/>	
TM MARGIN	2.2 dB	TM MARGIN	2.2 dB

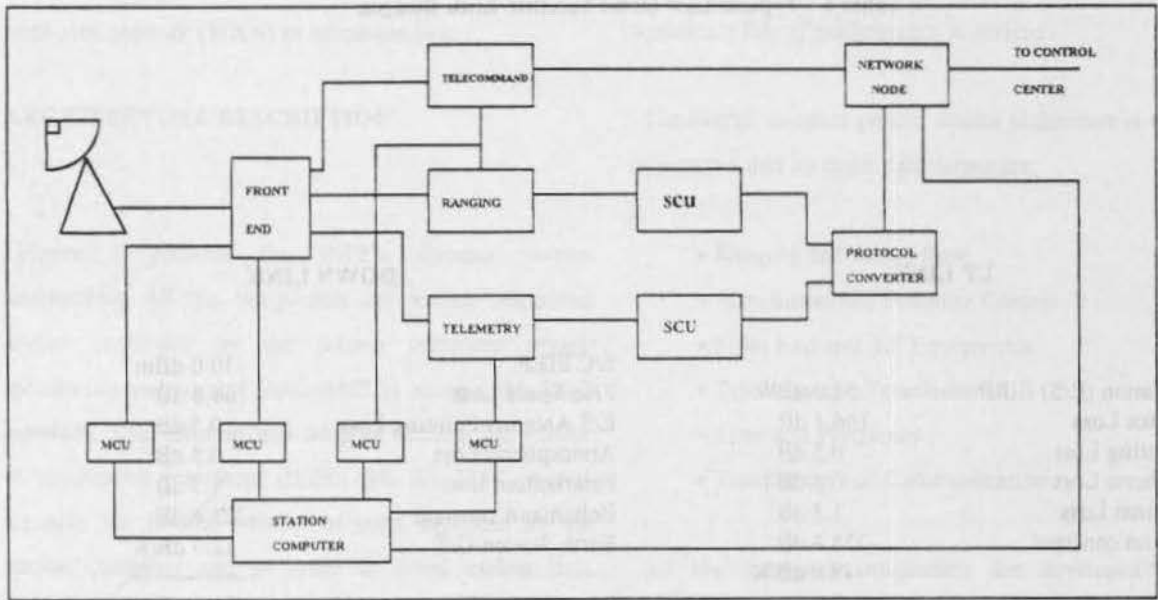


Figure 1 - INPE's S-Band Ground Station Simplified Block Diagram.

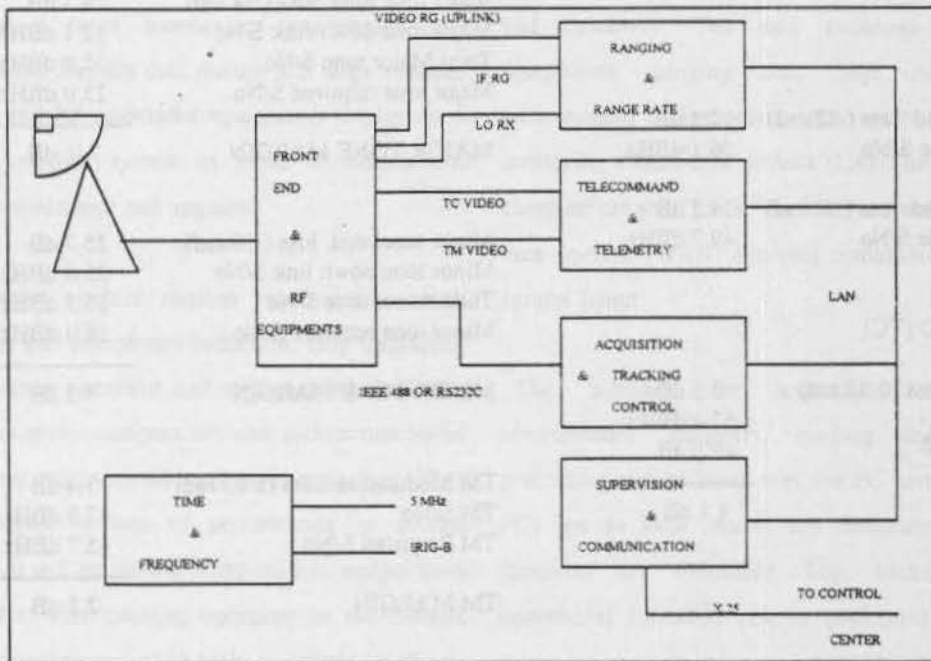


Figure 2 - Overall Architecture of the Compact and Low Cost Ground Station.

FRONT END AND RF EQUIPMENTS

The front end equipments consist basically of a 3 meter antenna and an 1 dB LNA giving a figure of merit of 12 dB/K, an 100 Watts power amplifier, commercial receivers and RF components implying in cost reduction.

ACQUISITION AND TRACKING

The front end equipments control/monitoring and the software needed for acquisition and tracking function runs in a PC connected to the LAN.

TIME AND FREQUENCY

The time and frequency references necessary for synchronization of all subsystems are obtained from a commercial GPS receiver that provides an accurate 5 MHz and an IRIG-B time standard.

TELECOMMAND AND TELEMETRY

The telecommand and telemetry processing is done by a single PC platform to which the necessary hardware and software are developed.

The hardware, including telecommand video modulation, telemetry video demodulation, bit and frame

synchronization, frame integrity checking and self test facilities, is plugged directly in the PC bus. An implementation loss less than 3 dB is obtained for telemetry video signal demodulation and bit synchronization.

The software is implemented under Windows environment having the following main functions:

- to receive telecommand request from the control center;
- to format and transmit telecommands;
- to receive and to store continuously the telemetry data, displaying locally the processed telemetry data in engineering units and doing limit checking on specified telemetries;
- to send the telemetry to the control center;
- to control and monitor the hardware parameters;
- to maintain log of the main events such as telecommand request and transmission, hardware configuration etc.

RANGING AND RANGE RATE

All ranging and range rate functions are implemented on single PC platform. The range rate hardware is put into the computer while the ranging hardware is a separate module connected to the PC via RS 232C or IEEE 488 interface.

SUPERVISING AND COMMUNICATION

The supervising data from all subsystems is sent to the supervising computer which displays locally all necessary data related to ground station hardware and software status. It is also possible to configure all the main ground station parameters from the supervising and communication computer, providing a high degree of automation. This computer is responsible for the communication with the control center which can control remotely the ground station operation.

CONCLUSIONS

The ground station conception presented here provides operation flexibility and reability besides a significant development time and cost reduction by using commercially available software and hardware and developping high standardized dedicated equipments. No redundancy is assumed and when reability must be improved this can be achieved by means of spare parts with only incremental costs.

The installation, operation and maintenance are greatly simplified because the high degree of system integration and standardization. Upgrade can be easily done due to the modular approach adopted in the system design, increasing system lifetime.

This conception allows the ground station to operate both in standalone mode or under control of the satellite control center.

REFERENCES

1. Barros, P. M. M. Ground Station Specifications. INPE technical report, Sao Jose dos Campos, Brazil, 31 January 1989. INPE A-ETC-0019.
2. Thompson, R. S.; Ashton, C. J.; Pidgeon, A. N. A Proposed Ground Segment Design For Small Satellites. International Symposium on Small Satellites Systems and Services, Arcachon, France, 29 June - 3 July 1992.

Ground Segment and Operations concepts of Small Satellite Missions

J.M OBERTO

MATRA MARCONI SPACE

31 rue des Cosmonautes
31077 TOULOUSE CEDEX
FRANCE

ABSTRACT

Small Satellite Missions are raising a growing interest among the user community as their potential benefits in terms of cost and schedule are becoming more and more evident.

On the other hand, for the traditional missions, the ever-increasing science and performance requirements lead to corresponding increases in performance, complexity, novelty and high cost of Ground Segment and Operations.

The goal of this paper is to show the main results of a study led by MATRA.MARCONI.SPAC for ESA/ESOC called "Ground Segment & Operations concepts for Small Satellite Missions".

The objective of this study is to increase the ESOC's understanding on the Ground Segment aspects for Small Satellite Missions in identifying areas of potential optimisation with a view to achieve acceptable ratios between Space segment and Ground segment costs.

The study approach is composed of two main steps; firstly, traditional missions are evaluated in order to highlight the main cost drivers and sizing components costs.

In a second step, from the selected Small Model Missions, Ground Segment and Operations concepts are defined for each kind of mission (Science, Earth Observation, Telecomms).

Finally, for each mission, three options (low cost, low risk, reuse of ESOC) are designed and costed.

During the first part, the following conventional missions have been evaluated in terms of sizing cost: HIPPARCOS, ERS1/SPOT, HISPASAT.

For each mission, a cost breakdown is given showing the repartition of the costs between the components of the Ground Segment (Mission Control Center, Ground Stations, Communication, Operations ...). The main cost drivers and the major cost components are highlighted.

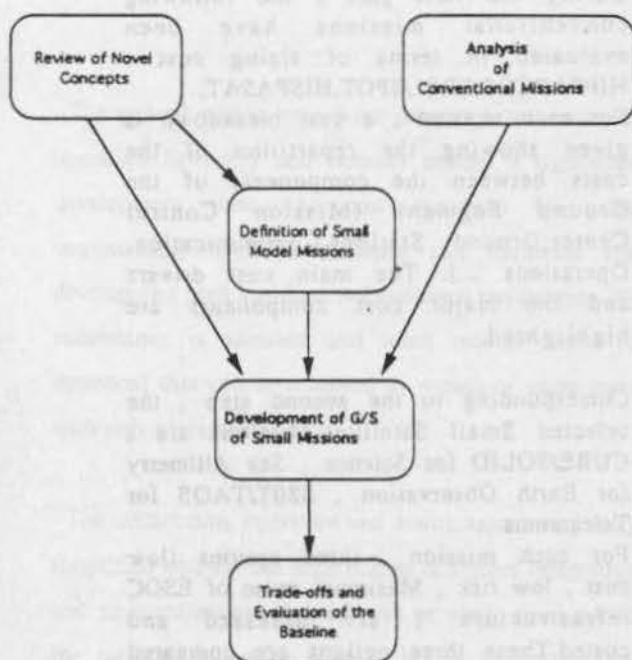
Corresponding to the second step, the selected Small Satellite Missions are: CUBE/SOLID for Science, Sea Altimetry for Earth Observation, S80T/TAOS for Telecomms.

For each mission, three options (low cost, low risk, Maximum reuse of ESOC infrastructure) are assessed and costed. These three options are compared w.r.t costs and risks and a preferred baseline is chosen in terms of "Mission Return / Cost Unit".

In developing Ground Segment and Operations concepts for future Small Satellite Missions, it is natural to start from the basis of the experience gained with past and present ESA missions. A critical analysis of the cost elements and cost drivers for conventional missions can yield important clues as to how the Ground Segment and Operations costs may be reduced for Small Satellite Missions in a similar proportion to those of the Space Segment, such that the overall cost envelope can be achieved.

1 STUDY APPROACH :

In order to reach the objective of the study, a study approach associated with a study logic has been defined (fig 1).



The study approach is divided into three main steps.

The first step is composed of three main tasks performed in parallel. The major one corresponds to the "Analysis of Conventional Missions" like HIPPARCOS, ERS1/SPOT, HISPASAT. Two other tasks are performed in parallel; a Review of Novel concepts for Ground Segment and Operations, and a definition of Small Model Missions (e.g. ESA missions for CUBE/SOLID).

The second step is the heart of the study and corresponds to build Ground Segment and to define the Operations concepts for the selected Small Model Missions.

The third step consists in performing a costing of each component leading to the overall cost (bottom-up approach) of each option. Finally, trade-offs are performed and a preferred baseline is chosen.

2. CONVENTIONAL MISSIONS :

2.1 SELECTION OF MISSIONS :

The conventional missions which have been selected are :

- HIPPARCOS for Science
- ERS1 & SPOT for Earth Observation
- HISPASAT for Telecommunications

The selection of these missions has been performed on the major following criteria :

- Their representativity in each discipline
- Existing programmes
- Availability of data
- European programmes
- Different customers (European versus National)
- Programmes of different natures (commercial versus governmental)
- Expertise of the company
- Common background between ESOC and MATRA MARCONI SPACE.

2.2 EVALUATION OF MISSIONS :

2.2.1 Methodology :

A special emphasis of the study is to identify cost drivers that directly impact segment and operations. This analysis relies on a realistic cost database issued from MATRA.MARCONI.SPACE and ESA experience that entails all components of a programme cost such as the satellite development costs : the interrelations between Ground Segment and Operations definition and the Satellite design are highlighted so that the feasibility of a Ground design option or new operations concepts could be assessed .

A detailed preliminary list of cost drivers is proposed with a clear correspondance with the mission definition , but also with the system design and programme management approach (Fig 2).

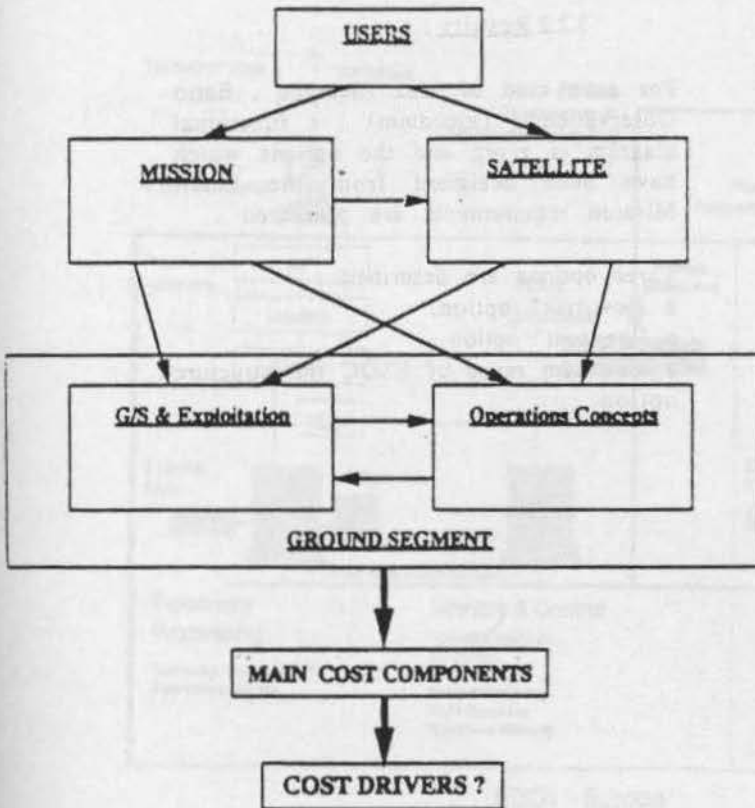


Fig 2 : Methodology

Finally , a reference grid is established with the main cost drivers . A cost breakdown is given for each conventional mission (Fig 3).

COST DRIVERS	GROUND STATIONS	COMMS INFRASTRUCT.	MISSION CONTROL CENTER			
			Flight Dynamics	Mission Planning	TMA/TC Processing	Other MCC Functions
USERS REQUIREMENTS						
MISSION PURPOSE						
PAYLOAD PROGRAMMING MODES						
PERMITTED MISSION OUTAGE						
NON ACCESS TELECOMMAND						
AVAILABILITY OF DATA PAYLOAD						
MISSION REQUIREMENTS						
LAUNCHER						
MISSION LIFE TIME						
LEOP CONSTRAINTS						
PAYLOAD INTERFACES						
ORBIT PARAMETERS						
ORBIT REQUIREMENTS						
POINTING REQUIREMENTS						
LOCALISATION						
DATA DURATION						
R/F PAYLOAD CONSTRAINTS						
SINGLE S/L WITHIN CONSTEL.						
DEORBITING STRATEGY						

Fig 3 : List of cost drivers

2.2.2 Results :

The main results about the evaluation of the conventional missions are given hereafter .

For each kind of mission , two cost breakdowns are shown :

- the first one corresponds to the "Implementation phase" including the development of the Ground Segment and the preparation of the Operations
- the second one corresponds to the "Operational phase" including the running costs for Ground Segment and Operations during the lifetime of the Satellite (or family of satellites).

The main cost drivers and the major cost components are highlighted.

3. SMALL MISSIONS :

3.2 EVALUATION OF MISSIONS :

3.1 SELECTION OF MISSIONS :

The mission which have been selected are :

- CUBE/SOLID for Science Mission :

The CUBE mission will support a Cosmic Background Observation . The SOLID mission will support a Sun Observation Mission (measurement of the Solar diameter and measurement of the Solar irradiance)

The choice of these mission as a Small Model Mission for Science area has been made for two major reasons ;

- the first one is due to the fact that this mission is one of them selected by ESA in the "call for ideas for small missions" as mentioned ,

- the second one is that this mission presents some similarities with HIPPARCOS mission and thus appears fully in line within the frame of the study.

- Altimetry mission for Earth Observation Mission :

The Altimetry mission is composed of three main functions ; measurement of the distance between Satellite and Sea surface , measurement of the wet tropospheric disturbance , subdecimetric orbit determination .

This mission corresponds to an example of descoping of ERS mission which has been evaluated in the previous step .

- S80/TAOS Mission for Telecommunications Mission :

The most promising Small Telecommunications Mission could be based on LEO constellations . As a reference Mission , a data transmission/localisation mission has been chosen specialised in communications with mobiles. It is one of the more simple, the space segment being limited to 5 satellites and it is one of the major reason to justify the choice of this mission.

3.2.1 Methodology :

This section corresponds to the central activity of the study where the different operations concepts and design options of the Ground Segment will be defined in relation with mission definition and satellite design characteristics . A cost driver approach is necessary to select solutions compatible with budgets of a small mission programme , but on the other hand the mission objectives and the feasibility of the overall design (satellite + operations + ground segment) are clearly considered. An iterative approach with successive refinements of the design and cost information is performed , many design options and cost implications are identified hereafter .

Before to establish the design of the Ground Segment & Operations concepts , the main requirements from Mission definition and Satellite design are identified for each kind of mission.

3.2.2 Results :

For each kind of area (Science , Earth Observation , Telecomm) , a functional diagram is given and the options which have been designed from the Small Mission requirements are presented .

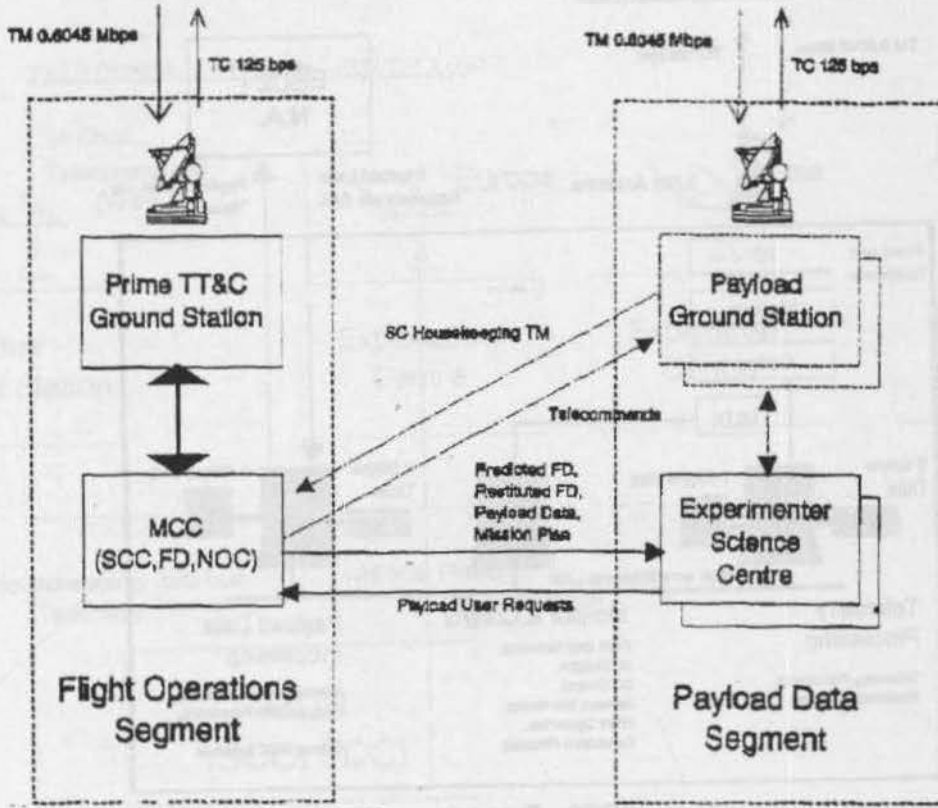
Three options are described ;

a "low-risk" option,

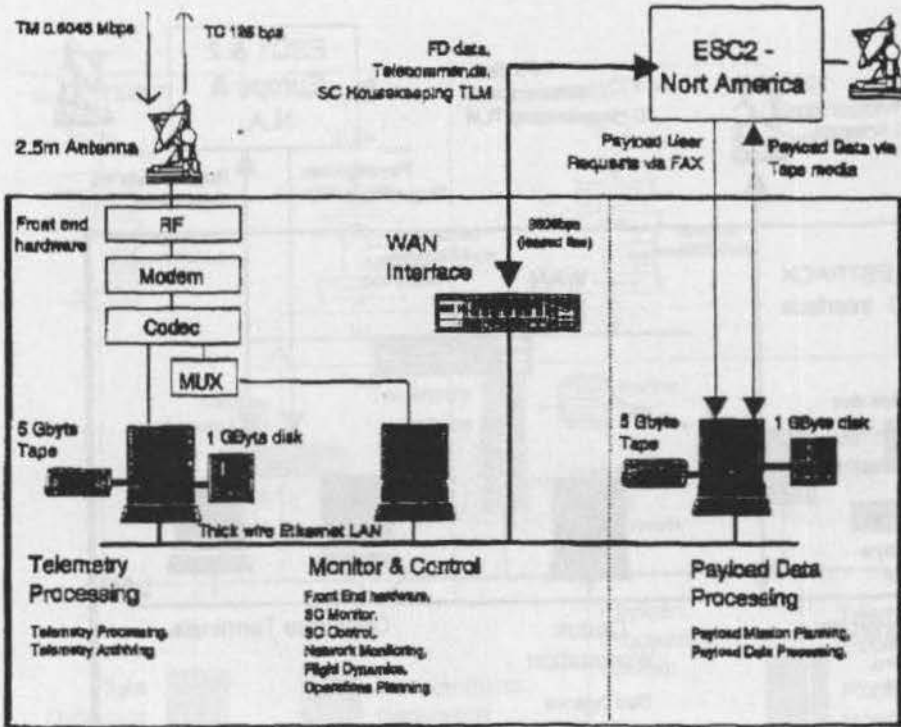
a "low-cost" option ,

a maximum reuse of ESOC infrastructure option

SCIENCE MODEL MISSION (SOLID)

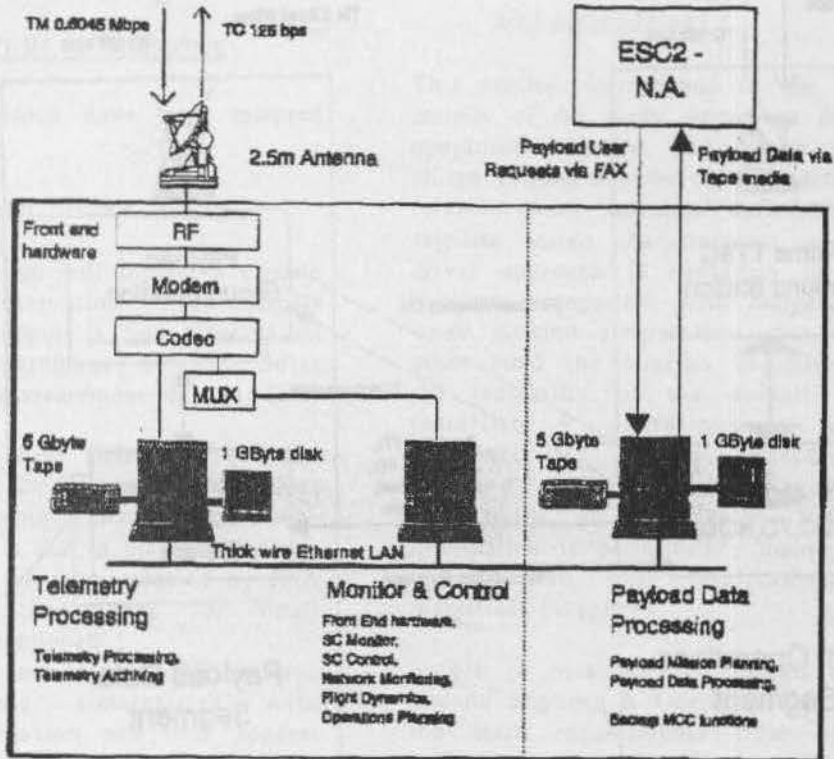


OVERALL SYSTEM DEFINITION

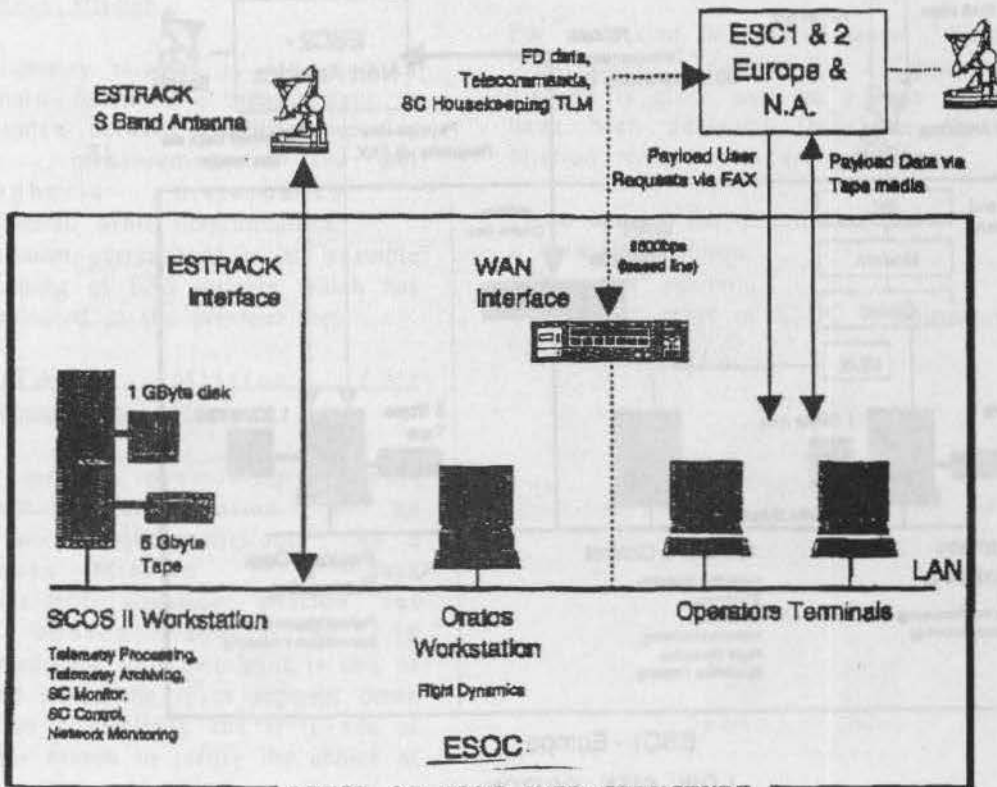


ESC1 - Europe
LOW RISK OPTION

SCIENCE MODEL MISSION (SOLID)

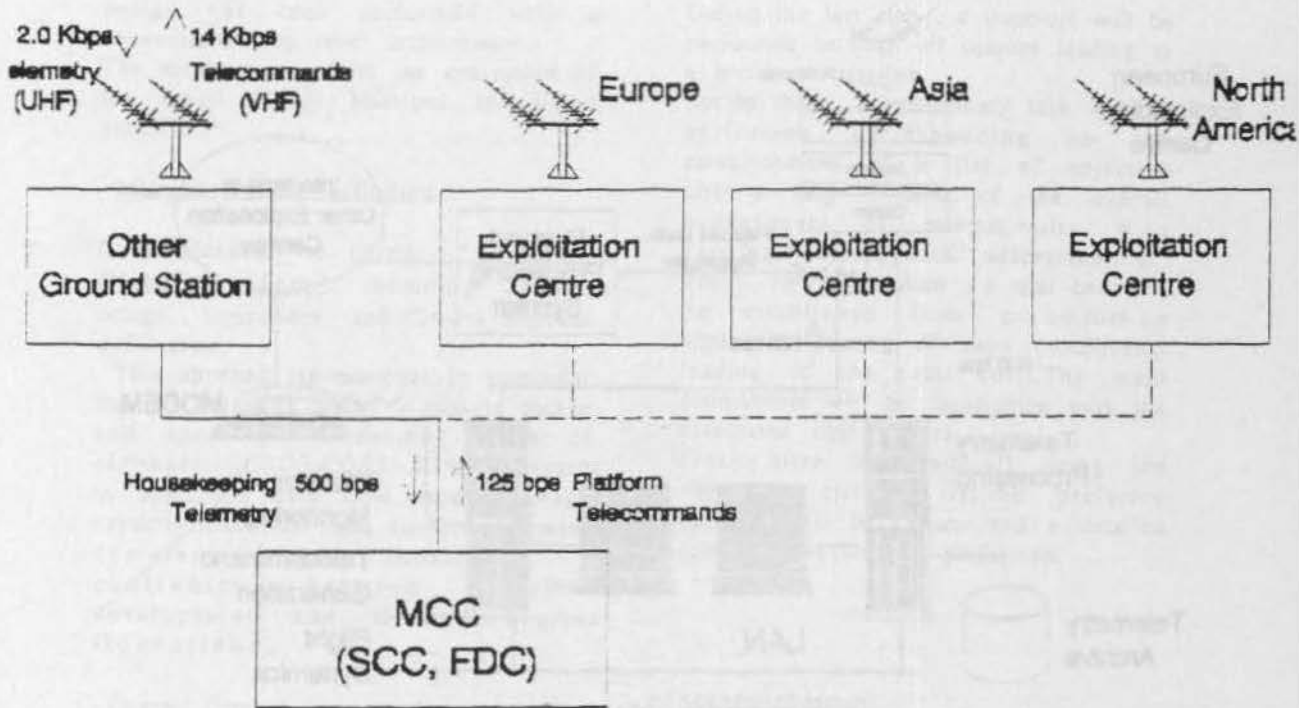


ESC2 - Europe
LOW COST OPTION

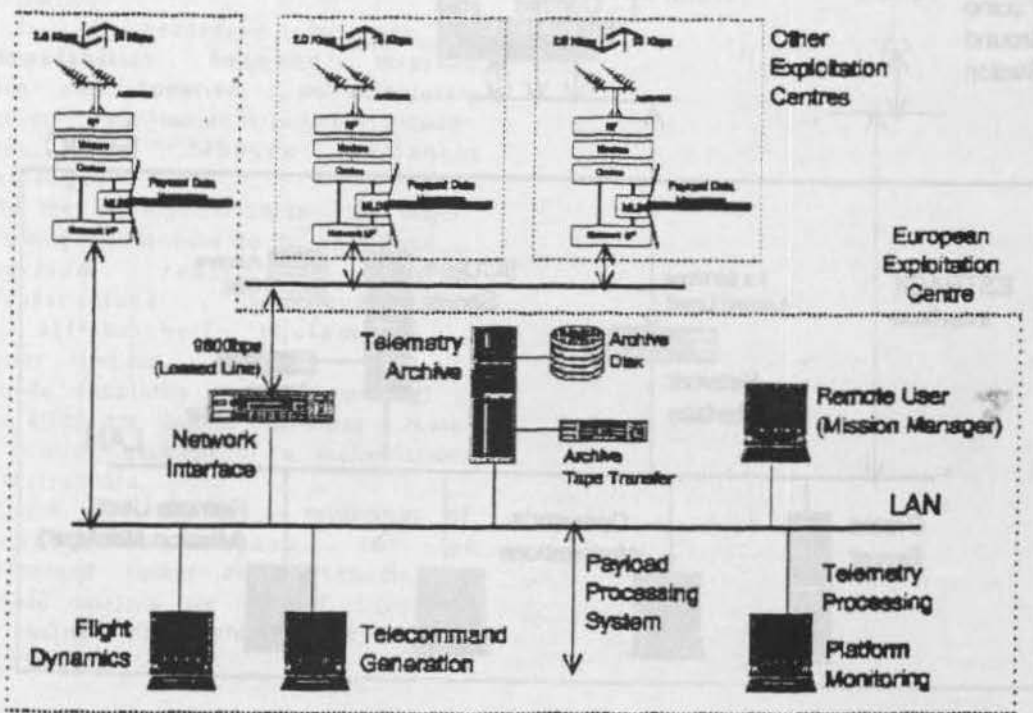


REUSE OF ESOC INFRASTRUCTURE

TELECOMM. MISSION (S80T/TAOS)

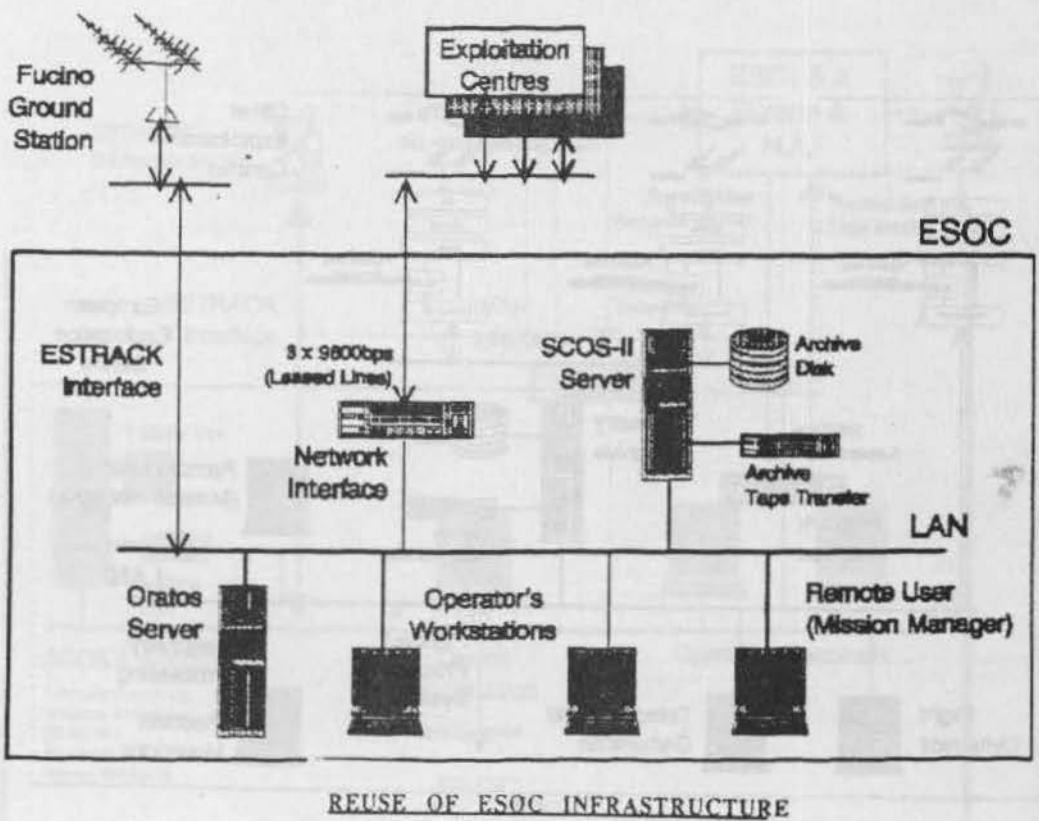
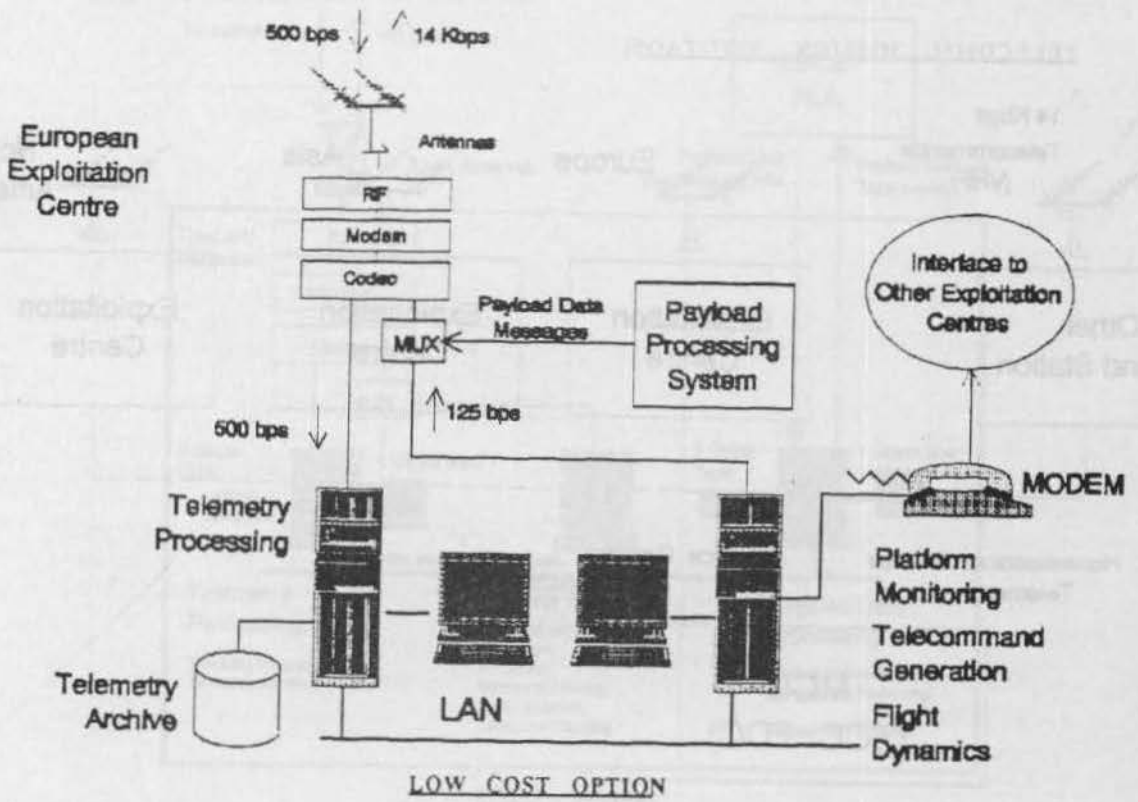


OVERALL SYSTEM DEFINITION



LOW RISK OPTION

TELECOMM MISSION (S80T/TAOS)



- Synthesis on Small Missions

A strong innovation for function and design has been performed with a conventional top level architecture .
The major points from the evaluation of the Small Model Missions are listed hereafter :

- Mission System definition :

It is necessary to think "Integrated Global System" including Satellite design , Operations and Ground Segment definition.

This approach is essential in particular for the following points ; mission outage and spacecraft autonomy , use of standards (CCSDS, COES,...) with regards to costs, size data flow versus storage capacity, spacecraft and Ground Segment complexity, LEOP constraints , continuity between Satellite development and Ground Segment Operations.

- Overall Ground Segment design :

For the design of the Ground Segment and the associated Operations concepts , some of the major issues are described hereafter :

- it is necessary to get a compatibility between mission price and duration ; no compulsory back-up w.r.t major risks on ground (fire...) , no 24hours permanent staffing...
- for the development phase , the major following points have to be considered ; maximum reuse of existing infrastructure , maximum reuse of off-the-shelf equipments , shorter lifetime...
- trade simplicity (e.g commanding) ; man effort for routine operations , reuse of existing package of a multimission infrastructure...
- Users involvement : a minimum of preprocessing have to be performed (users directly handle the payload data), a low level of interaction for using the payload have to be necessary.

4. EVALUATION OF THE BASELINE

During the last step , a trade-off will be performed between all options leading to a preferred baseline .

To do that , a preliminary task will be performed corresponding to the establishment of a list of objective criteria (e.g : 20% of the overall budget, level of compatibility w.r.t existing flexibility, risk assessment...) Then , for each option , a total cost will be established from a bottom-up approach (costing of each components leading to the total cost). The main components will be highlighted with the associated cost drivers.

Finally, after the trade-off using the objective criteria list, the preferred baseline will be chosen and a detailed cost analysis will be performed.

Acknowledgement :

A. PARKES (NOVA)
G. MACE (MMS)
A. SALVATORI (MMS)
C. PAYNE (CRAY)

CONSEQUENCES ARISING FROM THE LONG-TERM NEED TO ARCHIVE AND ACCESS DATA RELATING TO GROUND SYSTEM SPECIFICATIONS AND ARCHITECTURE

Claude HUC

Roger REICH, Rémy AUBRON, Jean-Louis PIEPLU

French Space Agency

CNES, CT/TI/PS/AP

18 Avenue Edouard BELIN

31055 Toulouse Cedex

France

HUC@MELIES.CNES.FR

Abstract

After analysing why it is vital to keep data from spaceborne scientific experiments in the long term, attention is drawn to the insufficient use of existing data. The second part summarizes the technical requirements that must now be taken into account as far as ground systems are concerned in order to preserve future data and make it as independent as possible from operating systems. Finally, the data access needs of the scientific community will be investigated and certain consequences on the architecture of project ground systems identified.

Key words: archival, scientific data, data access

Foreword

This paper does not describe any particular technical accomplishment. It presents a synthetic approach to the long-term archival needs applying to data from spaceborne scientific experiments and the consequences of such needs on ground systems. The term "ground system" is here used in its widest sense, not being limited to the control of in-flight operations. More especially, it includes all archival and data availability functionalities arising from spaceborne experiments.

Long-term scientific data archival needs

An enormous amount of data from scientific space missions has been accumulated since the beginning of the space era. Such data covers all space-related scientific disciplines: astronomy, planetology, geodesy, space physics, solar physics, the Earth's environment sciences, biology, chemistry etc. The data is stored in numerous different agencies, institutes and laboratories and their state of storage and accessibility varies widely from one to another. It would be quite reasonable to wonder whether all this data is of much interest nowadays and whether archiving it serves any useful purpose.

Since 1992, CNES has been working with French research laboratories to assess the current scientific interest in data from space missions that have been being analysed for the past 20 years or more. This evaluation covered quite a wide range both of international missions

flying French experiments and of scientific disciplines. We could quote the following missions in particular: OSO-8 (1975: solar physics), GEOS1 and GEOS2 (1977 and 1978: study of the terrestrial magnetosphere), ISEE1 and ISEE2 (1972: study of boundary regions between the solar wind and the magnetosphere), ISEE3-ICE (1978, continuing to operate even today: study of the solar wind, the magnetosphere's tail, flight through the tail of the Giacobinni-Zinner comet), ARCAD-3 (1981: space physics), VIKING (1986: Swedish satellite studying the auroral magnetosphere), PHOBOS (1988: studies of PHOBOS, MARS and the interplanetary/interstellar environment), HIPPARCOS (1989: astrometry) etc.

The main comment from users was that the lines of investigation arising from such data are far from exhausted and most of it is still of major scientific interest:

- numerous observations are unique as they were made in regions not planned to be revisited by similar missions or because they are related to specific events such as the passing of a comet, gamma-ray bursts etc.,

- in other cases, they play an important role in the preparation of future missions,

- a certain number of theories have been revised and data can now be reinvestigated from a new viewpoint,

- the scientific community is making increasing numbers of correlations between data from various different instruments (multispectral analysis) and is also investigating changes in observed phenomena over several decades, such phenomena not always coming under the heading of environmental sciences,

- certain phenomena are far from clear and various contradictory scientific theories are advanced (such as the origin of cosmic gamma bursts), requiring that observational data be kept,

- some data is currently used for new applications distinct from the initial objectives: Emission of electromagnetic waves from the epicentre of earthquakes and amplified within the ionosphere and magnetosphere has been observed on the GEOS2 data. This could lead to the use of such space data within disciplines such as seismology and geology.

Needless to say, all these considerations do not rule out the sifting through of data so as to eliminate that

considered to be of no use (no doubt a considerable amount!).

These conclusions agree with the views of other international space agencies. The USA has set up institutions to be responsible for or to organize the preservation of the precious heritage that space data represents. The European Space Agency is currently taking steps to provide for the long-term archival and availability of experimental data, and this for each scientific mission.

Technical review of the state of existing data

The assets represented by space data are not used to the full at the moment for three main reasons:

Firstly, because data access is not always simple. Despite the efforts made by the various national space agencies to save data, it has suffered badly from the successive generations of computers and operating systems. In the past, file structures were often dependent upon operating systems that have since become obsolete. Similarly, the binary coding of integers and floating decimals have not proved portable. The inexactitude, incompleteness or even absence of data descriptors have also proved major obstacles to data access. What is certain, because this was a factor we were able to quantify, is that the more accessible the data, the more it is used.

The second reason is linked to the fact that existing archives were rarely designed for use by scientists other than those taking part in the original investigations. This aspect affects not only the nature of archived data, but the completeness and legibility of documentation and, finally, the way data access is organized.

Finally, it must be recognised that until the 1980s, there was no international catalogue listing all space data available. Up till then, a considerable amount of data remained unknown. Data was mainly used by the teams of the principal investigators. The rule stating that data shall be opened up to the whole scientific community once the principal investigators' period of exclusive use is over, is not always put into practice.

In the light of this situation, the various space agencies have begun restoring data open to such a possibility: NASA's Space Science Data Center, for example, has set up the "data restoration program", and CNES has also begun such a programme. However, the cost of these programmes and the difficult conditions in which they are carried out force us to seek surer means for the data from future missions.

New needs

The volume of data produced by space missions and the length of time during which data needs to be kept are both increasing. For some missions, data has to be kept

for several decades. The current situation is characterized by three aspects: firstly, the needs for such data to be placed at the disposal of a large community are becoming increasingly explicit; secondly and concurrently, technological advances in data storage facilities are leading to a significant drop in storage costs; and thirdly, perhaps most importantly, there is a gradual emergence of a certain number of data-related standards. These observations, together with our own experience in the management and restoral of existing data, have led us to a new stage in which data preservation needs are analysed very early in the project - during the feasibility study - and all the consequences on the project's ground system specifications are set out at that point in time. When the time for the ground system specification phase comes, space science projects must be able to reply to the following three questions:

1. Which data from this project will need to be kept in the long term?
2. With which special technical specifications does this data need to comply?
3. What data access facilities will the Principal Investigators and, afterwards, the scientific community, be offered?

The answer to the first question is a scientific one; an accurate answer can only be given on a case-by-case basis. Two general observations should, however, be made. The use currently made of data gathered from the major missions of the 1970s, and particularly the multiplicity of investigations and applications not thought of at the beginning of such missions lead us to believe that it is vital to keep high-resolution data. The long-term conservation of data also implies that scientists who did not participate in the original investigations and who do not have full knowledge of the spaceborne instruments used will also use this data. This is why we consider it preferable to seek to systematically keep data in its physical values, though this does not exclude keeping raw data too.

The answer to the second question, relating to the technical specifications applicable to data, will be developed below, whereas the means used to access the data will be examined in the last part of the paper.

First of all, we have to define what we mean by "long-term archival". Taking an arbitrary figure, we would say that "long-term" implies storage longer than five years. In practical terms, data is always stored on a physical storage medium and read by a computer and software (software packages, languages, user software programs etc.). It can also be transferred over a network and copied onto a physical medium for circulation. After five years, it is highly probable that one or more of the parts just mentioned (physical medium, computer, software, network) will have been upgraded or even changed quite radically. Consequently, the system used to access the data in question also has to change.

New technical requirements applying to data

- Long-term archival must satisfy the following needs:
- to physically preserve the data; i.e. to guarantee its integrity (and thus its "durability") for a defined or undefined period and guarantee physical access to the data
 - associate with the data all items needed for its interpretation, and keep both.
 - minimize the impact of changes in archive and data access systems by making the data as independent as possible from such systems.
 - keep or make the user community aware of the data and its accessibility by that same community.

The technical requirements summarized below were drawn up on the basis of these needs:

Ensuring the physical preservation of data and associated items

The physical durability of data and all the computerized constituents must be ensured throughout the planned archival lifetime. This requirement implies that, taking into account:

- physical storage media used,
- planned storage conditions (temperature, humidity, security etc.),
- checking and media renewal procedures
- measures taken to avoid the accidental destruction of data,
- the physical and human organization required for these tasks,

the physical durability of data, documents, photographs, films etc. will be ensured with an evaluated and accepted risk of loss. The question of durability also concerns the hardware used to read the physical media on which the data is stored.

Data characteristics and structure

Archived files must be sequential and not contain information specific to the operating system on which the data was either created or managed.

Data shall be structured: at least in conformance with CCSDS recommendations as regards SFDUs, or in conformance with recognised science data formats such as FITS or CDF.

Coding modes authorized will in the main be restricted to ASCII for coded data. For binary data, the IEEE representation will be used for floating numbers and the MSB (Most Significant Byte first) representation with two's complement on 8, 16 or 32 bits for integers. Finally, CGM, JPEG and GIF standards will be used for coding graphic data.

The representation of time and dates shall comply with CCSDS recommendation 301.0-B-2: Time Code Formats (blue book).

Metadata

The detailed syntactical and semantic content of data shall be described in a data description document. In the absence of internationally recognised standards in this area, a CNES standard¹ has been defined so as to guarantee the homogeneity and exhaustivity of data description documents.

Catalogues are special files which point, either directly or indirectly, to data files and enable the user to find out their contents. There shall be an ASCII-coded sequential version of these catalogues.

An overall description of each data set shall be drawn up in accordance with the Directory Interchange Format (DIF) standard². Furthermore, when data is considered "public" insofar as it may be used by the scientific community, the Directory Interchange Format shall be introduced into the international database constituted by the Master Directory, which everybody may access through the International Directory Network.

Reference documentation shall be written for each data set, including a data user's manual to specify in particular the precautions to be taken when using the data, in the light of the experiment's actual operation. This documentation shall also include a description of the spaceborne instruments and in-flight operations, a list of scientific publications associated with the data etc.

Data-associated parameters

Auxiliary data, calibration parameters, location data (orbit, trajectory) and attitude data shall all be kept in the same way and respect the same requirements as main data.

Data-associated software

The cost of maintaining software can be extremely high in the long-term. Only perfectly justifiable cases will therefore be accepted for software maintenance. Furthermore, such software will only be accepted if it respects a certain number of strict rules: delivery of the source code, conformance to ISO, FORTRAN, C or Ada standards, availability of a validation environment etc. On the other hand, if no maintenance is required, the source codes for software used to create the data shall be kept frozen when the data is archived.

Application

The technical requirements summarized above will be applied for the future systems used to process and archive data from future scientific missions being prepared by CNES - missions such as MARS 94 or the Mass Processing Centre for data from French spaceborne experiments flown during the European mission CLUSTER. These requirements constitute additional constraints, but that is a small price to pay compared

with both the value of the scientific heritage to be preserved and the international community's outlay for the construction and implementation of scientific missions. Finally, it may be said that while we believe that these requirements constitute a condition necessary for the conservation of data, they are not all-sufficient: an in-depth scientific knowledge of data which could be called scientific expertise must also be kept active and alive at the same time. This is an aspect that will not be developed further in this paper.

The scientific community's access to data

Our thoughts on the long-term preservation of data are sufficiently well formalized to be able to move on to the state of applicable specifications. This is not yet the case for the question of data access systems. This is why this section will limit itself to laying out a certain number of guidelines and new constraints to be taken into account.

The lifetime of ground systems for projects is often limited to the satellite's lifetime or the time needed for data preprocessing. The data itself, however, must be made durable for much longer. Depending on the situation, the data could either be archived directly in a durable structure or, at the end of the mission, transferred to such a structure. The cost of the transfer and the temporary break in data access that might be involved shall be taken into account when defining the system.

Data users will firstly be Principal and Co-Investigators, then the whole scientific community once the data is opened up. A new category of users with incomplete knowledge of the experiment and resulting data will call upon the data access system. This system must therefore be thought out with both categories of user in mind.

Users must have at their disposal means of knowing what data exists in order to be able to select whichever data interests them and then access the data itself. These requirements point to a three-level functional architecture, with:

a) a directory level, b) an inventory level, and c) a basic level.

a) The directory level is the highest and allows the user to find out what data currently exists and in which data centre it is stored. This level is ensured by the International Directory Network.

b) The inventory level is where the user finds the scientific and technical characteristics of each data granule archived. It is by inputting his search criteria at this level that the user can see which data corresponds to his criteria. The search criteria may be very varied (time, measurement location, events, conditions etc.) but must be perfectly intelligible and relevant for users. The inventory level, which also contains data characteristics and the pointers to physical storage units, will most often be organized using a relational or object-oriented data base management system. Data bases constructed in this

way are not static - they must be living objects, offering scientists functionalities with which they can gradually enrich the inventory level by adding key words, events peculiar to their discipline etc.

c) The basic level corresponds to all the data archived.

This three-level model also offers a response to the interoperability question. Without developing this aspect further, we must be aware that the need for different data systems to be interoperable will increase in line with the multiplication of both means of communication and data access.

The technological developments in the area of storage, robotic access to physical media and network capacity have greatly increased the possibilities of immediate, on-line access to data. Consequently, the data archive centre and the main data access point need not be in close geographical proximity. Data archive centres responsible for keeping large volumes of data require specialised technical facilities and technicians. Similarly, scientific expertise on the data is far more useful at the access point than at the archive centre.

Part of the above considerations are being put into practice for the international solar observation mission SOHO (whose launch is planned for 1995). Of the 11 experiments to be flown, three are French and two others have French participants. The long-term archival of data from all five experiments is currently planned in France on the basis of a technical archive centre at CNES Toulouse and a scientific centre 700 km away at the *Institut d'Astrophysique Spatiale* (Institute of Space Astrophysics). The technical centre will be responsible for the inclusion of data in the archives and its maintenance as part of multimission facilities. The scientific centre will be the main data access point. This centre will have activities relating to the programming of instruments during flight and to the processing and analysis of data. The data base should be set up in the scientific centre.

Conclusion

Our main preoccupation has been the technical aspects of data preservation and access. It should be pointed out, however, that these technical aspects must go hand-in-hand with measures that concern human organization, and in particular the durability of structures responsible for archiving data and making it available to scientific users.

References

- 1 Minguillon, D. Standard de document de description de données (Data description document standard). 30 July 1993, CNES CT/TI/PS/MP/N° 93.25
- 2 Directory Interchange Format manual, version 4.1, April 1993. NSSDC 93-20

SCOS II: ESA'S NEW GENERATION OF MISSION CONTROL SYSTEMS

M. Jones, N. Head
Flight Control Systems Department
European Space Operations Centre
Darmstadt, Germany

K. Keyte
VITROCISET S.p.A.
Via Salaria 1027
Roma, Italy

M. Symonds
Computer Resources International AS (CRI)
Bregnerødvej 144
Birkerød, Denmark

ABSTRACT

This article describes the new Mission Control infrastructure software that is being developed at the European Space Operations Centre in Darmstadt. This infrastructure is the second generation of the Spacecraft Control Operations System (SCOSII). The reasons behind the production of the new infrastructure software are given followed by an introduction to the subject of Mission Control. A sketch of the way in which a future SCOS II systems will address some of the issues involved in mission control is provided. By way of contrast brief comparisons with the current infrastructure system (SCOS I) are made. To complete the picture the Project status and plans are summarised.

Why do we need a new infrastructure?

Before embarking on a major development such as SCOSII it is important to have a good view of the reasons or aims for the investment of such large amounts of money and manpower. These can be broadly categorised as follows:

- *financial*
The development and maintenance of Mission Control systems based on the

current generation of infrastructure software (SCOS I) has become costly. This is due, at least in part, to the inflexibility of the SCOS I system structure and the resulting difficulty of customising SCOS I software to a mission and of adding mission specific software to the basic system.

- *functional*

The increasing complexity of missions requires a corresponding increase in the capabilities of the control systems. For the same reason the effort involved in preparing for mission operations is increasing. The SCOSII infrastructure will improve the support provided to the operations staff in both mission operations and mission preparation. Improved support is also expected to help reduce operations costs.

- *strategic*

The cost of computer hardware for previous systems has been an item for concern. This is partly due to the centralised architecture of current systems which, together with the mounting performance requirements and complexity of processing required, has led to the need for large and powerful host computers to support the systems. This has resulted in dependence on the operating system and basic software provided by vendors of the particular host computers chosen, thus effectively

tying the Agency to these vendors. To avoid this the SCOSII infrastructure is required to operate in a hardware and basic software environment which is vendor independent.

What is Mission Control?

In general terms "Mission Control" refers to the tasks of preparing, planning, executing and subsequently reporting on the operations of a spacecraft mission.

• Mission Preparation

A vast amount of information (mainly in the form of documents) is produced during the manufacture of a spacecraft. A portion of this information is essential to the operations of the spacecraft. The corresponding documents must be isolated, collected and then used as a basis for defining operations in terms of procedures, each procedure having a specific operational goal.

SCOSII based control systems will provide facilities for electronic storage and review of documents in many common formats and for the creation of links between documents to allow easier correlation of related information.

• Mission Planning

For reasons of both safety and efficiency it is normal practice to pre-plan and automate operations as far as possible. This pre-planning can be done in the form of manual procedures prepared before launch. However, in general, not all operations can be defined and scheduled before launch. In particular, for operations of payloads, operations schedules will be prepared a day or several days in advance. These schedules must attempt to achieve a set of goals (e.g. satisfy requests for payload utilisation for its end users) subject to any applicable constraints (e.g. onboard power, available ground station contacts, payload instrument conflicts etc.). To date, mission planning has been done on a special-to-project basis.

ESOC is currently studying the possibilities of providing generic support for the planning process. Once identified, such generic support can be included in a future release of the SCOSII infrastructure.

The result of Mission planning is a

detailed schedule of activities or high-level operations. Whatever the nature of the planning process we plan that SCOSII will be able to translate the operations timeline or schedule into a specific set of spacecraft commands.

• Mission Execution

The schedules resulting from the planning will result in operations which will in general affect both the ground facilities ("ground segment") and the spacecraft ("space segment"). The resulting behaviour must be monitored. Discrepancies between the expected behaviour (as contained in the schedule) and the actual behaviour must be identified and corrective action taken.

Systems based on the SCOSII infrastructure will make major improvements in the support for mission execution. We hope to reduce the time spent by operations staff in mechanical or repetitive activities by providing a system which automates many of these functions. We also hope to achieve a better match between the user's view of the mission and the one embedded in the control system. Space segment monitor and control activities are often complicated by the limitations on the access to the spacecraft, e.g. due to limited data rates on telemetry and telecommand links, periods in which the ground station is out of contact with the spacecraft etc. It follows that an area of particular interest is to try to correct for the distortions introduced by the limitations in access to the spacecraft, thus allowing operations engineers to concentrate more on the end object (the spacecraft) and less on the methods used to access it (telemetry parameters, network links, telecommands etc.)

• Mission Reporting

In order to determine whether the mission goals are being achieved the long term behaviour of the spacecraft and the ground segment must be evaluated and reports provided to the mission management. This is also commonly referred to by the general term Spacecraft Performance Evaluation.

Future SCOSII based systems will contain integrated support for analysis and summary work as opposed to the loosely coupled and independently implemented service provided to date. We plan to take advantage of commercial analysis &

visualisation packages (e.g. PV-WAVE*) rather than relying exclusively on purpose-built software.

Despite the apparently sequential nature of the activities described above each usually continues for the duration of the mission. For example feedback from the reporting often affects the planning of subsequent operations, procedures may be updated as a result of execution anomalies and replanning takes place at fairly short intervals to optimise resource usage or to correct deviations from the overall mission goals. Mission preparation may need to be done during a mission if a major anomaly occurs, necessitating adjustment to new mission assumptions or goals.

Each of these activities has its own special challenges for both the users and the providers of Mission Control Systems; the SCOSII infrastructure system will become the foundation of a coordinated set of tools which will meet these challenges providing a Mission Control Infrastructure which, for the first time, covers all of these activities.

How can we approach these issues?

This section covers some of the more interesting facets of SCOSII and shows their application to some of the mission control activities summarised earlier. Most of the material covered here arises from proposed improvements to the execution phase software, the area in which most of the original thought has been invested. The improvements to the support for the other phases will depend on integration of a carefully chosen set of commercial tools (for example, in the area of Mission Preparation, publishing software with hypertext link capabilities and, in the area of reporting, statistical or visual data analysis packages).

Modelling as an aid to monitoring

Previous control systems have approached the monitor and control task in a manner which is closely linked to the way in which they have been forced to access the spacecraft - as a collection of telemetry parameters and telecommands. The functions of the systems have been centred around monitoring the values

of the telemetry parameters and issuing telecommands. Considerable effort has been invested over the years in ad hoc attempts to derive actual and desired spacecraft status from this collection of isolated measurement and control items and a certain level of sophistication has been reached, however at a considerable cost.

The SCOSII design team has recognised that it is necessary to make a concerted effort to improve the situation. To this end the approach to the fundamental database of information which is used to drive the control system software has been completely changed in order to allow the user to concentrate more on the characteristics of the subsystems or devices being controlled (e.g. Attitude and Orbit Control Subsystem, thrusters, batteries etc) and less on the transport mechanisms used to view these devices (packets, frames, parameters, sampling rates, command frames etc).

It is not sufficient to provide a description of the devices; the system must be able to make appropriate use of this information! Traditionally, a single model or processing technique has been applied to the whole spacecraft. Thus telemetry parameters are described in tables, including for example limits on their values. Equally, telecommands are described in tables which include among other information the expected effects on telemetry values. These tables may be administered via a database system. A single data processing "engine" will scan each entry to carry out certain prescribed checks (e.g on limits).

SCOSII will allow (although not require) each item described in the database to provide its own engine to interpret its database, telemetry and telecommand data in its particular way. These engines may be shared; it is possible, for example, that all heaters on a particular spacecraft will have the same behaviour and will differ only in the specific details of their telemetry and telecommand data.

As a result of all these modifications the monitoring functions of a SCOSII system are best seen as a collection of independent models of various parts of the spacecraft which act in concert to maintain a view of the spacecraft (as opposed merely to a list of the

current values of the telemetry parameters) using specially chosen methods appropriate to each model. These models form a sort of "ghost" copy of the spacecraft communicating with the real spacecraft using the telemetry and telecommand links.

Model the Ground systems too

A Mission Control system must not only monitor and control the spacecraft but also the ground segment. Previously this has been done by a collection of specific utility programs which have been only loosely integrated with each other and with the spacecraft monitor and control facilities. This was identified as an area for improvement, given that many aspects of operations require a close coordination of ground facilities with spacecraft operations (ranging operations or command uplink acquisition for example).

To do this, we can take advantage of the removal of the restrictions imposed by the need to be completely data driven and interpretable by a single engine. Thus we can employ the same modelling techniques for ground segment monitor and control as for the spacecraft the ground segment facilities being represented by additional models. Thus in a typical SCOSII based system there could be items in the database representing such things as the X.25 network, the telecommand and telemetry equipment at each of the stations, the station antenna and even the various components of the SCOSII system itself. Each of these models will monitor and control the item which it represents using an appropriate access channel (for example the programmers interface to the X.25 network will provide the network model with information, a link to the equipment controlling the ground station antenna will support the antenna model, Local Area Network monitoring facilities will contribute to the model of SCOSII itself).

One of the major advantages of such an integrated database is that all of the functions foreseen for spacecraft control can be used for ground segment control. Future SCOSII based systems will contain automated procedures which cover more than just spacecraft operations. An example would be the acquisition of the telemetry and telecommand links at the start of a pass. Today this

requires a carefully orchestrated sequence of operations involving several systems and several independent operations staff, thus offering many possibilities for human error.

In a similar way the data display and analysis tools originally conceived for spacecraft related use can be applied to ground segment data as well. A typical monitoring window might contain station related items (transmitter mode and power, received signal strength and noise levels for example) together with the equivalent spacecraft data and would provide an integrated "Up- and Down-link" monitoring capability.

Building Blocks for Models

As the full use of the SCOSII infrastructure requires extensive creation of models of various elements of the space and ground segments some effort must be made to ease the task of preparing a system for use in a particular mission. It is obviously not feasible to expect each mission team to prepare from scratch all of the models required.

SCOSII will provide a library of "building blocks" which can be combined in various ways to produce the overall spacecraft and ground system model. To allow this to be done easily, object-oriented software engineering technology has been updated for analysis and implementation of SCOSII. Specifically the Coad/Yourdan method and the C++ programming language) have been chosen. Correctly used, this technology and its supporting tools should ensure the clarity of interface definition and flexibility of implementation essential for a building block approach.

Extension of Systems by specialising Building Blocks

Not all missions are the same, which, as remarked earlier, led to large costs on earlier infrastructure systems. In many cases it will be necessary to make modifications to the library building blocks to be used in a specific mission. The object oriented approach to the system has an advantage in this area as well.

Using an object oriented technique known as inheritance it will be possible to provide a customised

building block for, say, the batteries of a given mission by specifying (and implementing) only the differences between the batteries and those represented by the generic building block. This avoids a proliferation of similar, but subtly different, models and the resulting software and operational configuration control issues which would consequently arise. It should also save manpower by avoiding such multiple implementations. Finally, the use of models which differ only where absolutely necessary should promote the use of similar, if not identical, operational procedures. This should help to reduce the cost of preparing operations and should also contribute to the safety of mission operations by ensuring that new (and potentially faulty) procedures are only created when strictly required rather than in all cases, as at present.

Separation of user interfaces from implementation machinery

Each of the models discussed above will provide an interface to a human operator. These interfaces may be grouped into "windows" which will be located and managed on a "desktop" following the well established techniques of Graphical User Interfaces.

In contrast to current implementations in which applications and interfaces are inextricably linked the choice of grouping and the layout of these windows will be separated from the models themselves and will be easily modifiable by the users of a specific mission. This means that it will be quite possible to have, say, network status information in the window of the manual commanding interface for mission X while replacing or augmenting it with spacecraft power status information for mission Y.

What kind of hardware and software does this imply?

Distributed Systems

The demands placed on the computing environment by such a flexible and ambitious set of system functions will be considerable. The hardware concept for SCOSII must be flexible enough to provide configurations to deal with the differing demands of

the specific Mission Control systems while not requiring software modifications to cope with them.

In view of this, and in view the strategic objective of vendor independence discussed earlier, SCOSII system will be hosted on a Local Area Network of Unix workstations. Each operational user will be provided with at least one processor at their workstation to cope with the processing load of supporting his or her user interface elements. A set of overall coordination functions will be embedded within the SCOSII system software to ensure consistency between the spacecraft models located on these workstations and to provide a relocation service allowing system functions to be distributed over the physical hardware as mission needs require.

Some services of the system will be provided by "server" processors which are not dedicated to any particular user but which provide a service to the system as a whole. A typical example of such a server would be a database server, containing the basic representation of each of the models used in a particular mission and which would be copied to each active workstation which required to monitor the item in question. Such use of centralised services by applications software is commonly referred to as the "client-server" concept.

It is also planned that a minimum SCOSII system should be capable of running on a single workstation should it be necessary to install mission control facilities at remote sites (typically in ground stations). In this case the servers and their clients would be physically located on the same processor.

The use of such a distributed system also offers advantages in terms of system availability and failure tolerance. By careful planning and design (particularly of redundant servers) we expect to achieve resilience of SCOSII based systems to most failures (although a user may be required to move to an alternate workstation in some cases).

Performance Goals

As SCOSII is intended to be the basis for systems until the early part of the next century we have adopted some fairly ambitious performance goals;

these include real-time data rates (for spacecraft housekeeping data) of 2-3 Mbits, display update rates exceeding 10 per second (particularly during retrieval of non real-time data, a problem of existing systems) and user communities of up to 50 workstations. The first release of SCOSII is not required to achieve such levels of performance. Despite this we are paying great attention to performance factors in the design of the system rather than relying on the ever increasing performance of workstation hardware and software.

Adaptive processing

In typical mission control systems there are two basic usage scenarios which must be supported - the "normal" case and the "critical operations" case. A normal case scenario is characterised by a small number of users at any one time and by limited and fairly repetitive user activities. A critical operations scenario usually involves a larger number of users and a more varied set of activities. The critical operations case is the more difficult one, but it has a number of peculiarities which can be used to advantage when designing the system. These are as follows:

- The users will be working with a relatively small amount of data; this will be related to the procedures being executed to the time period of the anomaly. The SCOSII infrastructure should allow adaptation to this situation at the cost of degraded response for those requiring other data (ie. not involved in critical operations).
- A particular user will only be looking at only some subset of the full data set within the time window.

In order to take proper advantage of these two characteristics, each user workstation will be provided with a local "cache" store where telemetry and model data is stored and retrieved without effect on other users of the system. The algorithms which determine which data is to be kept in the cache and which will have to be retrieved from the system server can be tuned as usage patterns for the system become more obvious. An initial version of the system will apply a simple "most recently used"

approach combined with a filtering, to eliminate types of data not required by that user.

Status & Future plans

The User Requirements for the first major release of SCOSII are currently under review; together with this the matching OOA model has been produced and documented in a Software Requirements Document. This will be reviewed as soon as the User Requirements review has been completed. In addition proof of concept prototyping of the technology was carried out in 1992, and considerable prototyping has been done in support of the user requirements definition.

An initial delivery of Release 1 is foreseen for autumn 1994. It will contain basic functions of the system and will provide equivalent capability to that of existing SCOSI based systems.

Acknowledgments

The authors would like to acknowledge the enormous effort and enthusiasm of all of the ESOC SCOSII team members, past and present; many of the concepts mentioned here are directly attributable to their efforts, vision and dedication.

THE ROSAT TELECOMMAND SYSTEM From Command Generation to Command Verification

Norbert Jansen
DLR - GSOC
Münchener Straße 20
D-82234 Weßling
Germany
Tel. +8153 - 28 2743
FAX: +8153 - 28 1454
E-Mail: JANSEN@GSOCMAIL.RM.OP.DLR.DE

Abstract

This paper discusses the major system components and features of the ROSAT Telecommand System which has now been in operational use since June, 1990.

Due to the nature of the mission a large number of telecommands must be sent and verified as reaching the spacecraft each day. Special off-line processing software has been developed in order to atomise the command generation process as far as possible. Other ground support tools assist the operator to create command sequences and their schedule specifying which particular sequences have to be radiated to the spacecraft during a specific contact period.

The on-line processing software - the telecommand transport system - has been designed to operate at the high bitrates required and in addition provides suitable features to verify the correct reception of telecommands on-board the spacecraft.

Keywords: Automation of command generation, Command sequencing and scheduling, High throughput commanding, Command verification.

1. Mission Overview

The ROentgen SATellite - ROSAT - mission is a space research project sponsored by the German "Bundesministerium für Forschung und Technologie (BMFT)", in co-operation with NASA and the Science and Engineering Research Council of Great Britain (SERC). The spacecraft was launched from Cape Canaveral on June 1st, 1990 into a low earth circular orbit (580 km) with an inclination of 53 degrees.

NASA provided the launch vehicle, a Delta II, and the High Resolution Imager (HRI), an X-ray detector

developed by the Smithsonian Astrophysical Observatory (SAO).

SERC provided the Wide Field Camera (WFC), a second imaging telescope, which was built by a British consortium of universities and laboratories under the leadership of Leicester University.

German industry (DASA) was responsible for development, manufacturing, integration and test of the spacecraft.

The scientific management and the responsibility for developing the focal plane instrumentation of the X-ray telescope is with the "Max Planck Institut für Extra-terrestrische Physik (MPE)" at Garching north of Munich. The science data centre for analysis and interpretation of all scientific data is also located here.

During all phases of the mission, operations are performed by the German Space Operations Centre (GSOC) at Oberpfaffenhofen near Munich. GSOC is the multimission operations centre of the German Space Research Organisation DLR. The prime ground station is at DLR's ground station complex located in Weilheim, 40 km south of Munich. In emergency cases additional station support from the NASA Deep Space Network can be scheduled at short notice.

The scientific objective of the mission is the investigation of X-ray emissions from almost all celestial objects. For this purpose the mission is split into two phases:

- The "Scan Phase" during which the first all-sky X-ray survey in the soft X-ray (0.07 - 2.4 keV; 100 - 5 Å) and the extreme ultraviolet (0.025 - 0.2 keV; 500 - 60 Å) bands using high-resolution imaging telescopes was performed. This mission phase was successfully completed by

end of January 1991, more than 60.000 new X-ray and 400 new XUV sources have been detected [1].

- The "Pointing Phase" during which selected sources are observed with respect to spatial structure, spectra and time variability. The location of the sources can be determined with an accuracy better than 10 arcsec. The instruments are twice as sensitive as those used in previous missions.

This second mission phase can also be considered as extremely successful; first analysis of the scientific data showed that the images are of a high quality and resolution.

2. ROSAT Mission Operations Some Implications for Commanding

Mission Operations for ROSAT is characterised by the high degree of automation, optimising the utilisation of the available on-board computer power and data storage capabilities in conjunction with complex operations support tools. The reason for this is given by the two mission specific issues:

- The Mission Operations Scenario
and
- The Onboard Data Processing System

2.1 Mission Operations Scenario

Routine mission operations are performed via one ground station only and due to the low orbit, contacts are very short (6 to 8 minutes) and occur only in the course of six consecutive orbits per day resulting in telecommunication gaps of about 15 to 18 hours each day.

Due to the nature of the mission, frequent changes of instrument pointing direction, detector and filter switching are necessary. Consequently a large number of telecommands (up to 6000 per day) have to be uplinked and stored on-board the spacecraft together with time tags specifying the time of command execution. If all commands were to be radiated contiguously with an uplink bitrate of 1 kbps approximately 10 minutes of the available uplink time would be taken through this activity alone. This is ignoring the time required for protocol handling between ground station and control centre and the time needed for command verification. As a result

very little time is left during telecommand radiation for interactive operations. Therefore all the planning and command scheduling must take place either prior to or between the contacts.

The ROSAT Sciences Data Centre (RSDC) at MPE, Garching plays an important role in the command generation process as it is actively involved in experiment operations and control. MPE issues "Test, Observation and Calibration Requests" which represent the desired spacecraft activities. These requests and an orbit prediction are taken as input by the Mission Planning System [2] - also called ROSAT Timeline Generator (RMTG) - which generates once per week an optimised short term timeline (STL) - the master plan of all spacecraft operations. This timeline is the prime source for telecommands as it contains high level descriptions ("keywords") of the onboard activities required during a mission day. These keywords have to be translated into command macros which vary with the additional parameters accompanying the keywords.

Since - for cost reduction purposes - routine spacecraft operations must be handled by a single Spacecraft Operator only, it is obvious that the command generation and scheduling process has to be automated as far as possible. Real-time operations have to concentrate on radiation and verification of pre-processed command files, verification of the expected satellite status and dump of the science data which are stored on the on-board tape recorder, while all other processes such as command generation and scheduling, data analysis, trouble-shooting etc. have to be performed off-line.

2.2 The Onboard Data Processing System

The difficulties in meeting the demands of such a mission profile are determined by the complexity of the communications and commanding functions of the spacecraft. For ROSAT the command data handling by the on-board processing system can be logically subdivided into the following four elements:

- The Data Handling System (DHS) of the spacecraft bus receives telecommands via one of two redundant ESA-Standard Telecommand Decoder Chains [3] at 1kbps which results in about ten commands per second. The Command Decoder ensures that corrupt frames are not processed on-board.
- The Attitude Management and Control System

(AMCS) - based on a dual-redundant microprocessor system which implements the complex control laws required to maintain safety constraints and the desired observation direction.

- The data processing system of the Focal Instrumentation (FI) of the X-ray telescope which handles time-tag and status buffer management.
- The data processing system of the Wide Field Camera (WFC) which handles absolute and relative time-tag buffer management .

has consequently to be handled in a different way especially concerning:

- capacity of the time-tagged command buffers which must not overflow or become corrupt
- buffer type (linear or ring buffer)
- buffer management methods
- methods of dealing with omitted / missing data
- availability of verification parameters
- verification methods

The design of the ROSAT Command System has been considerably influenced by the fact that each subsystem has its individual design and layout and

The following table lists all major constraints and capabilities which had an impact on the command system design:

Subsyst	Buffer Type	Capac.	No. of Cmd's / day	Time Tag	Verification	Constraints
S/C Bus	linear	2 TTC's	6 * 2 TTC's	16 bits	Cmd Decoder Counter	Cmd Counter is transmitted every ten seconds only
AMCS	linear + ring	2000 / 1001	2000 / 1250	32 bits	Star Counter; Number of used bytes	Star Cat. must be loaded within 1 contact; TTC's must be in chronological order; no insertion/deletion of cmd's is possible
FI/HRI	Ring / linear	478 / 34	1000	32 bits	CMD block counter; CRC Polyn.	availability of verification parameters is mode dependent; CRC is transmitted only once per command
WFC	Ring / linear	256 / 128	2000	16 / 8 bits	Read and Write Pointer; Execution Pointer	TTC's must be in chronological order; Write Pointer must be controlled from ground;

Table 1: Subsystem Characteristics

As can be seen from the table above four different procedures had to be developed for command buffer loading and maintenance, verification of the correct command reception, and time-tag generation.

3. Telecommand System Overview

GSOC provides support for a variety of space flight missions and mission profiles. During the time of the ROSAT design phase several other missions were also under development. To keep the costs to a minimum it was decided to develop a multi-mission kernel real-time system capable of supporting all current and perceived system requirements. The advantages of this method were cost reductions in spacecraft operator retraining, system implementation and maintenance.

Due to the extremely short contact cycles it was necessary to minimise the workload of the spacecraft operator during the contacts. To this end a suite of off-line tools were designed and developed to optimise performance for the ROSAT mission.

The system was functionally broken down into a number of components based on the functions to be performed from command generation to command verification.

3.1 Off-line activities -

The off-line contact scheduling [5] has been divided into two operational packages which reflect the logical sequence of operations that the operator is required to perform during a nominal ROSAT day.

These packages being

- Telecommand generation:-
Timeline and Directive Access (TDA) package
- Telecommand Scheduling
Directive Editing and Scheduling (DES) package.

The data flow and functions of these packages are illustrated in fig. 1.

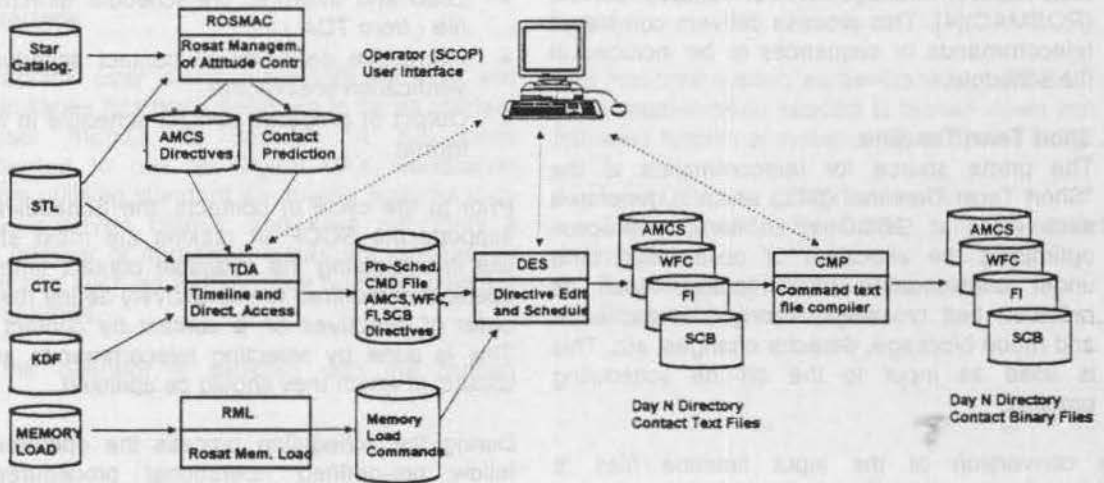


Fig. 1: Command Scheduling

3.1.1 Telecommand Generation

During the course of an operational day between 2000 and 6000 telecommands must be transmitted to the spacecraft. The individual telecommands or sequences originate from a number of varying sources. These can be listed as follows:

1. Operator inputs

As one of the features of the system the operator always has the ability to generate sequences which can be used during real-time activities to cater for anomalous or erroneous conditions.

2. On-board memory loads

To provide the capability to modify and enhance the on-board software the spacecraft / instrument manufacturer and scientists produce memory load files. These have to be parsed and converted into a series of telecommands to be radiated to the spacecraft. The requirement for these memory loads depends considerably on the state of the satellite and the on-board systems, therefore they tend to be irregular in frequency.

3. Attitude control telecommands.

The complex task of defining the correct attitude parameters for the AMCS during a particular observation cycle is performed by a specific task ROSAT Management of Attitude Control (ROSMAC)[4]. This process delivers completed telecommands or sequences to be included in the schedule.

4. Short Term Timeline.

The prime source for telecommands is the "Short Term Timeline" (STL) which is generated each week at GSOC in an iterative process optimising the allocation of observation time under consideration of constraints such as radiation belt crossings, strong sources, earth and moon blockage, detector changes, etc. This is used as input to the off-line scheduling process.

The conversion of the input timeline files is performed by the Timeline Directive Access software (TDA). The purpose of the TDA is to provide the following main functions:-

- Load of ROSMAC and RMTG Telecommand and Timeline file products.
- Create and access Keyword definition database
- Access and freeze Short Term Timeline.

- Creation of pre-schedule directive file which forms the input to the "Directive Editing & Scheduling Software" (DES) package.

The primary task of converting the spacecraft activities as represented in keyword form into completed command mnemonics, is accomplished using a Keyword database. During the translation process, all relative times, defined as offsets are recalculated and allocated an absolute execution time.

In parallel, any outstanding memory load files are translated using the Memory load pre-processor that reads the hexadecimal load data and converts it into the sub-system specific memory load telecommands.

The output files generated by the above processes are then used as input to the scheduling process.

3.1.2 Command Scheduling

The intention of the off-line Directive Editing and Scheduling (DES) S/W is to provide the Spacecraft operator (SCOP) with an interactive tool to assist him in preparing the command sequences that are required to be uplinked during a ROSAT day.

The DES has the following main functions:-

- Load and interpret pre-schedule directive text file (from TDA).
- Interactive definition of contact schedule with verification breakpoints.
- Output of prepared contact schedule in text file format.

Prior to the cycle of contacts, the Scheduling S/W supports the SCOP in making the most effective use in optimising the available contact times. The operator is required to interactively define the uplink order of directives on a contact by contact basis. This is done by selecting telecommands and the contact in which they should be uplinked.

During the scheduling process the operator must follow pre-defined operational procedures and constraints, these determine the sequence/contact allocation, the sub-system priorities and the utilisation of the on-board time-tag buffers.

When the current day's directives are loaded the DES will calculate the changing states of the onboard buffers (the amount of free space available in the four Time tagged Telecommand Buffers) for

each of the current day's contact times. It carries out checks to warn the operator if schedule rules or bounds are violated. Subsystem dependant checks include correct chronological ordering of directives in each of the contacts, avoidance of Time tag buffer overflow and the scheduling of more commands in a contact than there is time allowable. Similarly it will prevent commands being scheduled for contacts beyond the expiry of the pre-defined execution time.

Due to the limited capacity of the on-board buffers it may be possible that there are more directives planned for the current day activities than there are buffer slots available. Such leftover directives will be automatically included when loading the following days directives.

The DES and real-time systems have been designed to deal with anomalous conditions and allow rescheduling activities to take place. This function utilises output from the real-time command system to update sub-system buffer models and will highlight any discrepancies between a previously scheduled number of commands and those actually transmitted and received by the satellite.

Once the initial processing of the schedule has been completed, contact times, time tagged buffer loads and directives are displayed to the operator on the user interface.

The graphical user interface for both the TDA and DES packages has been designed to be as efficient and user friendly as possible. It has been implemented to run on Digital VAX workstation platforms utilising standard windowing features such as mouse driven menus, soft keys etc. Only a limited number of numerical inputs are required by the operator such as ROSAT day number, print log start/end times.

Once the operator is satisfied with the contact

coverage of scheduled directives, the remaining transmission time can be allocated for placing verification breakpoints at the start and end of ranges of telecommands ("Verification Groups") for a particular subsystem. The start and end of a verification range is recognised by the PREPARE - BREAKPOINT directive pair.

Having completed the scheduling for the current ROSAT day a set of post schedule text files is produced which contain the telecommands and verification breakpoints for the various sub-systems in scheduled order for each contact.

The text files are then compiled into binary files to be used by the real-time ROSAT Command System. This not only improves the throughput rate during the pass, but also allows any syntactic checks to be performed prior to the contacts, thus ensuring telecommand data consistency.

4. Real-time Activities

The real-time system is primarily responsible for the successful transmission of the telecommands to the appropriate ground station and hence to the satellite. In addition to the standard uplink features the ROSAT system provides complex closed-loop verification functions utilising real-time telemetry to validate the correct reception of commands on-board.

The real-time system as developed for ROSAT and other multi-mission support is broken down into the following functional systems [6], as shown in fig. 2:

- Input Directive Interpreter module.
- Telecommand Execution and Verification modules
- Telecommand Transmission module.
- General Logging module.

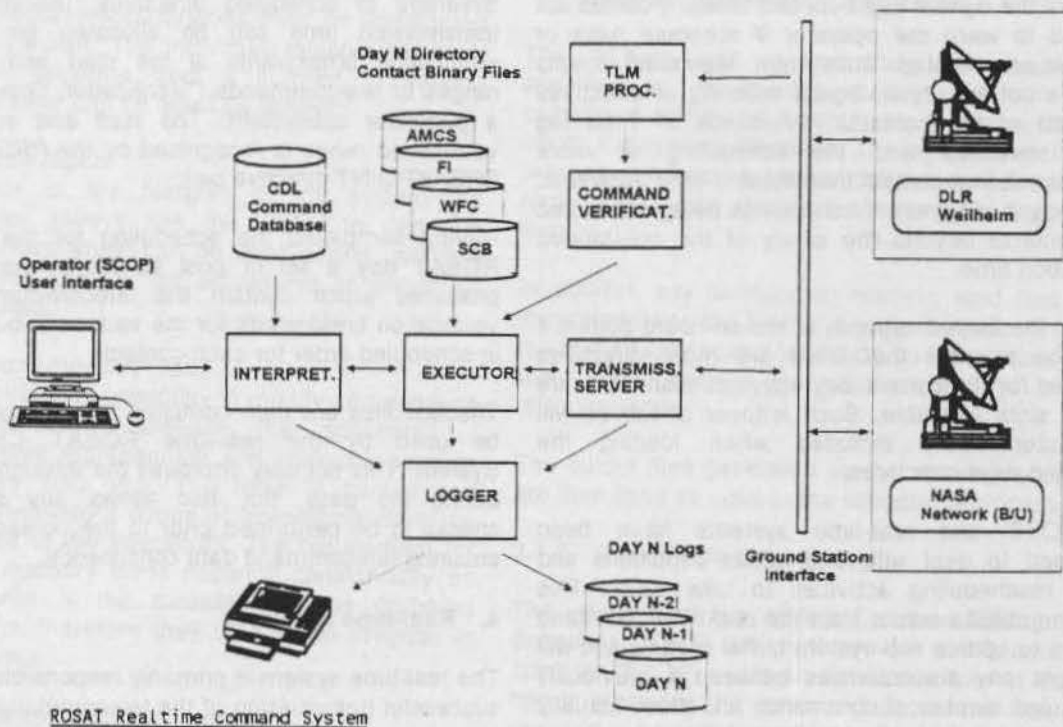


Fig. 2: Real-time Command System

4.1 Input Directive Interpreter Module

This module handles all the user interaction with the command system, interpreting input directives as they are entered into the system. The directives contain instructions to the system to perform certain predefined functions. These functions are subdivided into those associated with the overall control and configuration of the system and the ground station interface and those allowing the definition and loading of timeline sequences or individual telecommands.

To guarantee the required performance, this module has been decoupled from the time-critical modules to ensure that operator input does not directly affect ongoing telecommand transmission.

4.2 Telecommand Executor and Verification Module

This module is the central hub of the command system and deals with the execution and manipulation of telecommands which are maintained in queues or sequences. The executor

allows multiple queues or sequences to be defined, thus optionally allowing command radiation to be performed on a sub-system basis. The operator may instantly switch between these sequences to maximise the use of the uplink time in the event of sub-system anomalies.

Telecommands are entered into the system, via directives to the interpreter, either from the generated contact schedule files or for contingency purposes as individual commands.

Timing constraints defined in the timeline sequence determine when telecommands are sent for transmission. Once released for transmission they pass through the Transmission module to the ground station which will respond with an uplink confirmation.

Although the ROSAT real-time command system is based on the GSOC kernel system it has also to accommodate fairly detailed mission specific requirements. The functions to support these requirements are defined in separate control procedures which are implemented as removable modules which can be linked into the real-time

system. This allows the system to maintain a base level functionality applicable to all projects while allowing it to be configured to suit the requirements of individual projects.

Features that are provided as 'extra' for ROSAT are:-

- multi-sequence option for individual sub-systems. This allows sequences to be allocated on a sub-system or function basis. Nominally each sub-system is loaded into an individual sequence with an additional sequence for contingency procedures.
- data block packing algorithm for throughput optimisation. This is necessary to support the requirement of an uplink rate of 10 command per second and reduce ground station protocol overheads.
- telemetry interface to access spacecraft clock and verification parameters.
- external modules for time-tag generation and spacecraft clock correlation. These use the actual values as delivered in telemetry to correlate all time-tags.
- modules to support the various sub-system verification methods.

4.2.1 Telecommand Verification

As with other projects supported at GSOC, ROSAT supports command verification using real-time telemetry. However, in comparison with other projects, the methods defined to support verification are significantly more varied and complex.

As most of the telecommands will be executed outside the contact period, full execution verification cannot be performed. For example with geostationary missions this allows the operator/system to validate that the command has correctly performed its designated function on-board the satellite. Verification for ROSAT is therefore restricted to reception verification only, albeit fairly detailed.

Due to the short contact periods and the necessity to provide maximum uplink capability, verification cannot be performed on an individual telecommand basis. As stated earlier, during the scheduling process the operator defines verification groups. These are series of telecommands which will be verified together rather than individually.

As a result of the satellite design, each sub-system has its own buffer management system and therefore requires separate method(s) of

verification. The verification method to be applied to the next verification group is specified by the use of the "Prepare" directive and an associated parameter.

4.2.2 Verification Process

The verification process is performed in three well defined stages:-

1. Prior to the transmission of a verification group, the actual stable values of critical telemetry parameters are stored in a sub-system model.
2. During the transmission of telecommands within a particular group, the model is updated in relation to the number and type of telecommands transmitted.
3. Following successful transmission of all telecommands within the group a new set of actual telemetry values is compared with those stored in the command system model. If the model matches the current status of the telemetry then transmission will continue. If however, an error is detected due to a mismatch, then the system reacts to the failure as defined by the corresponding breakpoint. This may be an abort of the current sequence, enabling a switch to another sub-system or in certain circumstances a retransmit of the previous verification group.

To prevent an indefinite interruption to the telecommand uplink, timing limits on the updates to required telemetry values can be specified. Time-outs on these updates will also cause verification to fail.

4.3 Transmission Server Module

This module handles the asynchronous interface to the ground station(s), dealing with the various data protocols associated with the different networks. It ensures that the telecommand sequence once released for uplink is transmitted in the correct order and is complete and error free. Where applicable it maintains a status of the ground station equipment and will prevent transmission in the event of a serious anomaly.

4.4 General Purpose Logger Module

This module has an active interface to all the other modules in the system receiving all logging information. Its prime task is to tag and log to disk all the activities performed by the command system. To prevent the large amount of disk I/O influencing the real-time functions it was also decided to

decouple the logging task.

Logging activities are classed according to their type, e.g.:-

- Operator activity.
- Telecommand transmission/verification
- System anomalies.

Each of these types may be subsequently selected for off-line analysis and rescheduling.

5. Conclusion

Experience has shown that the development of kernel system has been of significant benefit to GSOC, who have since support over 10 missions with the system. In each case the base level functionality which is applicable to all projects has been enhanced by a small amount of spacecraft specific processing. Where applicable this has been subsequently added to the kernel system functions.

During the requirements phase an initial investigation took place into a fully automated system to create an all encompassing mission planning system. However it was concluded at that time, that the development costs would have been too high for the project. Therefore a compromise was reached whereby although the systems were given a slightly reduced level of scheduling functionality, sufficient processing and decision making was built-in to provide the operator with sufficient assistance to perform his duties.

In addition, 3 years of mission operations have shown that with this level of functionality it is possible to operate complex satellites with a minimum of operations personnel.

As explained throughout the paper, one of the major problems associated with the development and implementation of the ground systems for ROSAT was the varying and complex designs of the on-board systems. It would certainly have been a great deal simpler and perhaps more cost effective, had standards, such as recommended by CCSDS, been implemented by all those involved with the ROSAT project.

6. Acknowledgement

The author would like to thank Mr. Simon Maslin and Mr. Ian Lunn, Cray Systems, for their invaluable assistance with the preparation of this paper. Both are members of the software development team in charge of the design and implementation of the

ROSAT Telecommand System at DLR - GSOC.

References

- [1] Proceedings of the "European International Space Year Conference"
Munich, 31 March - 2 April 1992
- [2] H. Frank, DLR/GSOC & D. Garton, CAM
"ROSAT Mission Planning and its Perspectives for Future Scientific Missions", Paper AIAA-90-5092-CP,
Proceedings of the AIAA/NASA Second International Symposium on Space Information Systems,
Pasadena, Cal., 17 - 19 September 1990
- [3] PCM Telecommand Standard, ESA PSS-45 (TTC-A-01),
Issue 2 (1982)
- [4] M. Bollner, U. Feucht, DLR/GSOC
"Ground Operations to Support the Attitude Control System of the ROSAT Spacecraft", Paper 89/113, Proceedings of the International Symposium on Space Dynamics,
Toulouse, Nov. 1989
- [5] P.C. James & I.D.S. Lunn, "ROSAT Telecommand Scheduling", JBIS, 44, 328-336, 1991
- [6] P.C. James & S. Maslin, "The Core Command System at the German Space Operations Centre", JBIS, 42, 213-220, 1989

ISACS OF ISAS - AN INTELLIGENT SATELLITE CONTROL SOFTWARE -

Kuninori Uesugi*, I. Nakatani*, T. Mukai*, M. Hashimoto*, T. Obara* and N. Nishigori**

* Institute of Space and Astronautical Science (ISAS)
3-1-1 Yoshinodai, Sagami-hara, Kanagawa, 229 Japan
e-mail: tonon@net202.newslan.isas.ac.jp

** Fujitsu Limited
1-9-3 Nakase, Mihama-ku, Chiba-shi, Chiba, 261 Japan

Abstract

An Intelligent Satellite Control Software (ISACS) system, which was developed by Institute of Space and Astronautical Science (ISAS) to overcome the difficulties to carry out complicated satellite ground control and mission operations by a small number of ISAS personnel, is discussed. The ISACS system applies the Artificial Intelligent (AI) technology including the EXPERT system and it has been successfully utilized for the ground operations of the GEOTAIL spacecraft, which was launched in July, 1992, as one of the ISTP (International Solar-Terrestrial Physics) fleet.

Keywords: Artificial Intelligence, EXPERT System, Satellite Ground Control and Mission Operations.

Introduction

ISAS (Institute of Space and Astronautical Science) has launched 22 satellites since 1970 and five of them are currently in operation. Among them, the GEOTAIL spacecraft (Fig. 1), launched in July, 1992, is the biggest scientific satellite ISAS has ever developed. As one of the ISTP (International Solar-Terrestrial Physics) fleet, GEOTAIL is exploring the distant geomagnetic tail region by taking the double lunar swingby trajectory as shown in Fig. 2.

As one of the international cooperation projects between ISAS and NASA, the whole GEOTAIL spacecraft system including five scientific instruments aboard was developed by ISAS, and NASA provided two scientific instruments and took charge of the launch by

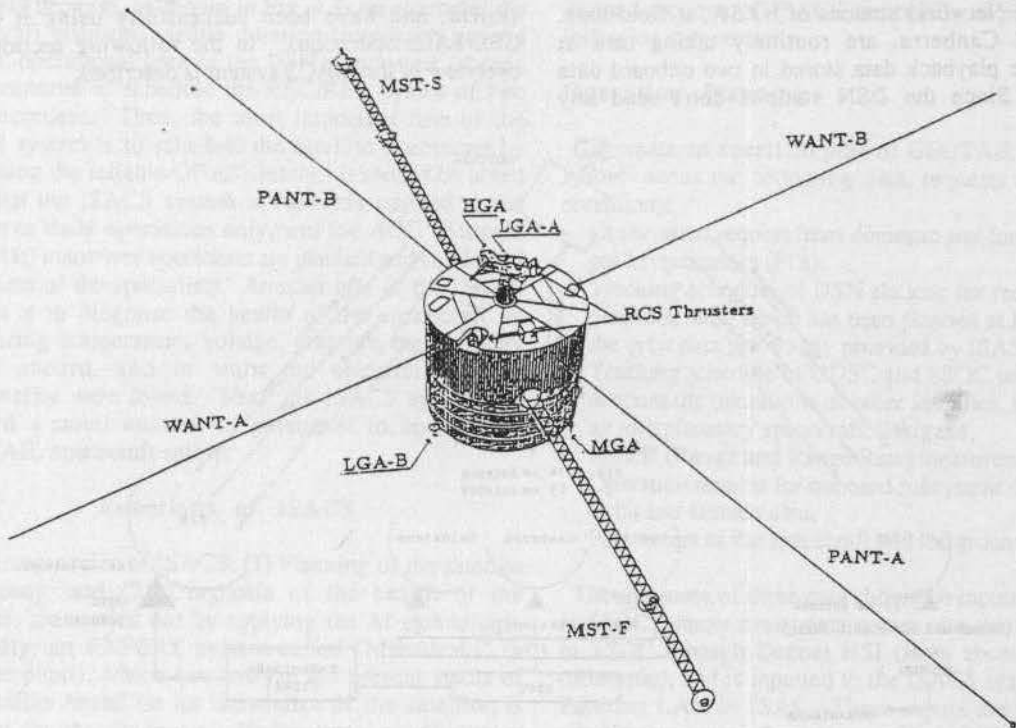


Figure 1: GEOTAIL spacecraft

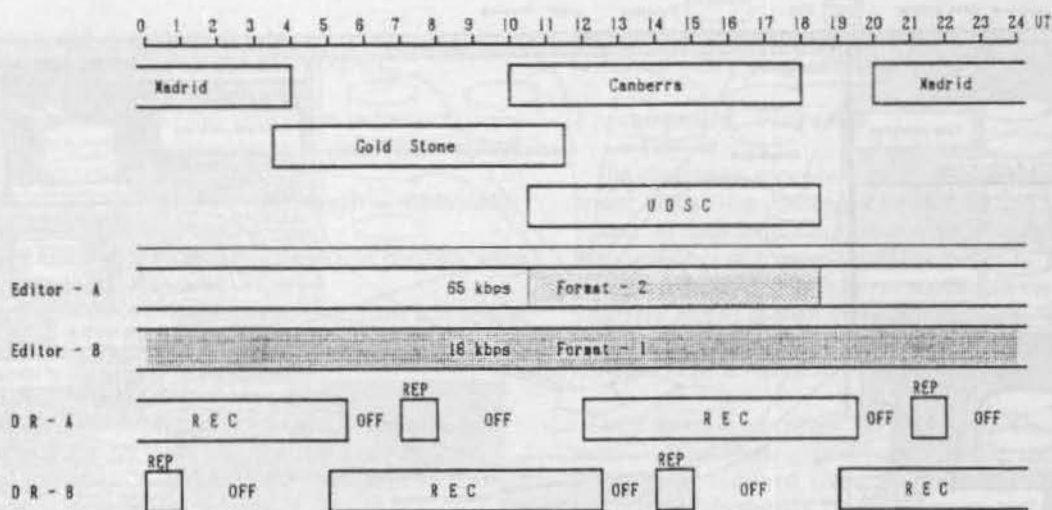


Figure 4: DR REC/REP cycles in GEOTAIL operations

Roles of ISACS

Basically, the GEOTAIL spacecraft is controlled and operated by the Operation Program (OP) which consists of a stream of up-link commands. Once an OP is transmitted to the spacecraft from SSOC via 64 m antenna at UDSC, GEOTAIL can work autonomously for approximately a week. The OP contains many commands to govern the record (REC) / replay (REP) cycles of the data recorder (DR), pointing of the high gain mechanical despun antenna to the Earth, control of the scientific instruments according to their observation plans and so on. It would be a heavy load to the operators at SSOC if they had had to generate an OP manually and routinely because, as shown in Fig. 4 as an example, the spacecraft position, visible duration from each ground station, operational time of the DSN stations etc. should be considered to schedule the REC/REP cycles of two data recorders. Then, the most important role of the ISACS system is to schedule the satellite operations by generating the reliable OP efficiently. It should be noted here that the ISACS system is currently applied to the routine or daily operations only, and the AOC (Attitude and Orbit) maneuver operations are planned and conducted by a team of the specialists. Another role of the ISACS system is to diagnose the health of the spacecraft by monitoring temperature, voltage, pressure etc. at many points aboard, and to warn the operators if any abnormality were found. Thus, the ISACS system has enabled a small number of personnel to operate the GEOTAIL spacecraft safely.

Functions of ISACS

Both major roles of ISACS: (1) Planning of the satellite operations, and (2) Diagnosis of the health of the satellite, are carried out by applying the AI technology. Specially, an EXPERT system called "Manadeshi" (a favorite pupil), which can analyze the present status of the satellite based on its knowledge of the satellite, is utilized for the diagnosis. Under many conditions or

restrictions concerning thermal, power, communication links etc. which are sometimes fuzzy or conflict with each other, the ISACS can find the best solution for the satellite operations through the simulation of possible operation plans and the stochastic analysis of them. Even when these conditions should be changed, any complicated and tedious works to modify the software itself are not necessary. The knowledge of the satellite and its environment has been previously inputted by human experts into the database, and it can be increased or updated at any time. Then, as the ISACS system is getting more knowledgeable, the satellite operations can be more improved and sophisticated. In Fig. 5, the structure of the ISACS system is illustrated, and two major functions of ISACS are briefly explained in the following sub-sections.

Operation Planning

To create an operation plan of GEOTAIL, the ISACS system needs the following data, requests or boundary conditions:

- Observation request from domestic and foreign Principal Investigators (PI's),
- Tracking schedule of DSN stations for receiving DR's playback data, which has been planned at JPL based on the orbit data previously provided by ISAS,
- Tracking schedule of UDSC and SSOC taking into account the operations of other satellites, specially of an interplanetary spacecraft, Sakigake,
- R&RR (Range and Range Rate) measurement plan,
- Operation request for onboard subsystem if any,
- Orbit and attitude data,
- Parameters of the spacecraft and the ground stations.

Though some of these data should be inputted manually at SSOC, almost every data comes into the work station in SSOC through Decnet NSI (from abroad) or TISN (domestic), and is inputted to the ISACS system through Ethernet LAN in ISAS. These inputs are written in a simple computer language called ORL (Operation Request Language).

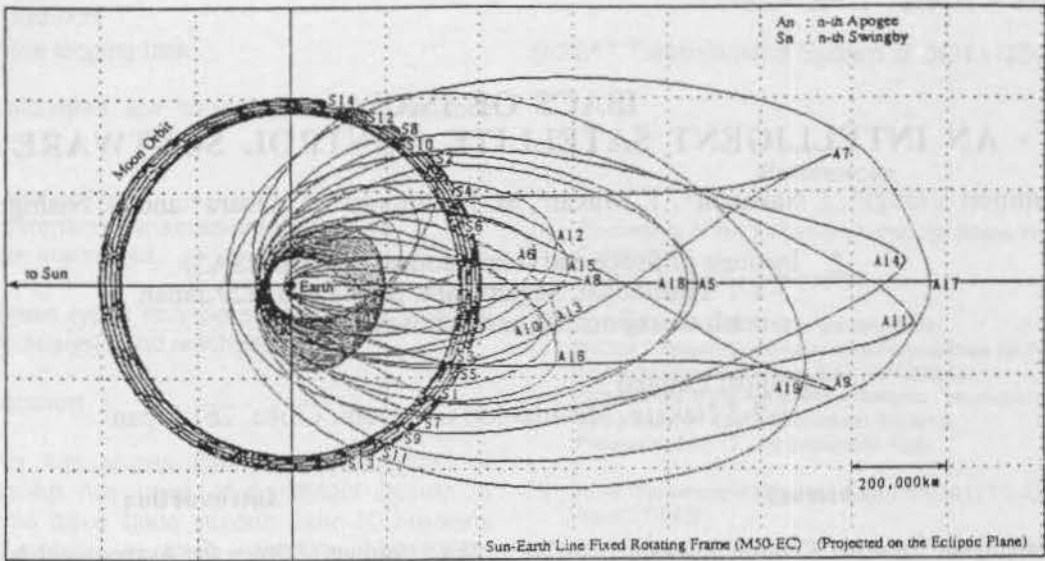


Figure 2: Trajectory of GEOTAIL

a Delta-II rocket. After the launch, ISAS has been responsible for its entire ground control and mission operations. In addition to the precise trajectory control maneuver (TCM) operations to keep the spacecraft flying on the double lunar swingby orbit, GEOTAIL's daily mission operations require the quite complicated procedure. As shown in Fig. 3, GEOTAIL is controlled by a lot of up-link commands sent out from Sagami Space Operation Center (SSOC) in ISAS through a 64 m dish antenna at Usuda Deep Space Center (UDSC), Nagano, Japan. The scientific data are received by the antenna at UDSC in realtime manner, and three DSN (Deep Space Network) stations of NASA, at Goldstone, Madrid and Canberra, are routinely taking turn at receiving the playback data stored in two onboard data recorders. Since the DSN stations don't send any

commands up to the GEOTAIL spacecraft in order to make SSOC the sole station which can control the spacecraft, ISAS has to create routinely the Operation Program (OP), which consists of a stream of commands including the record/playback cycles of the data recorders. However, ISAS is one of the national inter-university joint research institute in Japan, and its resources are limited. To overcome the difficulties to carry out such complicated mission operations by a small number of ISAS personnel, we developed an Intelligent Satellite Control Software (ISACS) system by applying the AI (Artificial Intelligence) technology including EXPERT system, and have been successfully using it in the GEOTAIL operations. In the following sections, an overview of the ISACS system is described.

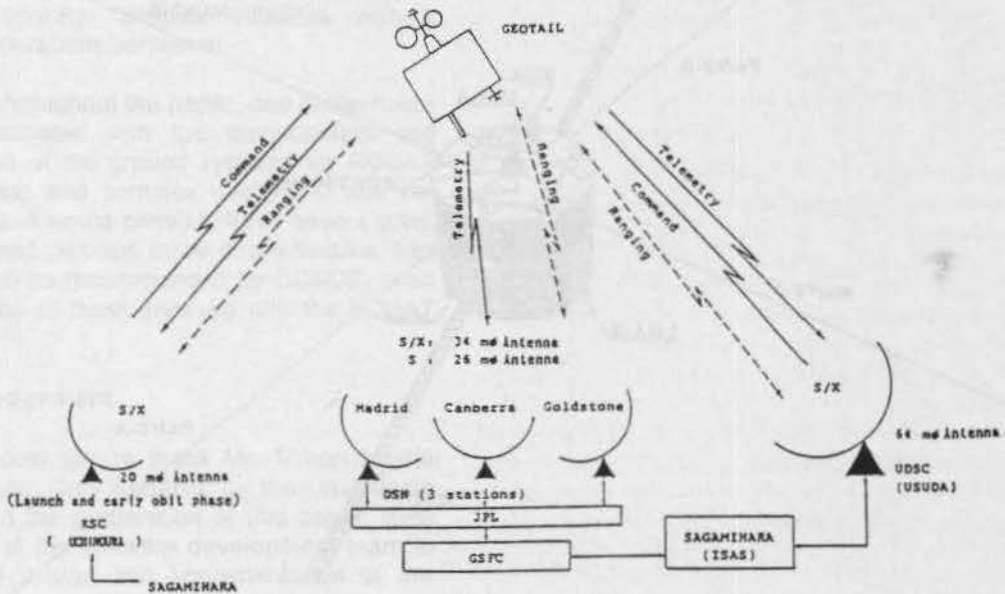


Figure 3: Communication links between GEOTAIL and the ground stations

monitors and diagnoses the health of the satellite, is introduced into the operations of GEOTAIL.

The design criteria of this system are as follows:

- To provide tools to the operator to check the health of the spacecraft,
- To warn the operator when a symptom of abnormality is found in the spacecraft,
- To recommend a "first aid" action to the operator when the abnormality is found,
- To provide tools to human experts to create and update the knowledge database easily.

And the following conditions are assumed:

- The information necessary for the diagnosis can be obtained directly from the telemetry data, from the computer at SSOC and from the knowledge database of its own.
- This system does not diagnose the status of the spacecraft during the AOC maneuvers, since it cannot predict how the status would change in these maneuvers conducted by a team of specialists.

This system is developed on a personal computer system using a commercially available diagnostic domain shells, "Manadeshi" (a favorite pupil). It has four major components called "System Manager", "Knowledge editor", "Inference Engine" and "Knowledge Database" as shown in Fig. 6, and it has the following functions:

Creation of Knowledge Database

The knowledge database is created by the conversations between the knowledge editor and human experts. The editor classifies the knowledge for diagnosis into the tree formation, and each node of the tree is defined by a set of a question and an answer. The system can control the procedure of editing such as issuing several questions related with each other at once or skipping some questions to which answers have been already obtained. In case that the human expert could not give a unique answer, or a criterion of the diagnosis should be fuzzy, the editor provides a table in which a causal relationship

between the given knowledge and the result of diagnosis is defined with a weighed number.

Execution of Diagnosis

The diagnostic procedure is conducted by tracing the nodes of the tree formation created by the knowledge editor. At each node, the inference engine judges whether the satellite is in normal condition or not by comparing the data representing the current status with the criteria of diagnosis stored in the knowledge database. These data are inputted from the consoles monitoring telemetry, attitude, AGC levels of receiving signals and so on.

The diagnostic procedure can be done in "Online Mode" or in "Manual Mode". In the online mode, the necessary information obtained from the telemetry data can be inputted automatically from the telemetry monitoring console via Ethernet LAN. Though the other information not included in the telemetry data should be inputted manually by an operator at the present time, it is now planned to input every necessary data through the computer network and then to make the diagnostic procedure fully automatic in realtime manner.

To the contrary, in the manual mode, an operator has to answer to the questions by inputting data manually at each node of diagnosis. However, even in this operational mode, approximately 80 % of information can be inputted automatically if the operator orders Manadeshi to get telemetry data through Ethernet LAN.

On tracing the nodes of the tree, the ground segments at SSOC and UDSC are checked at first, and then the onboard subsystems, which are called as Common Instruments (CI's), such as power supply, communications, thermal control, house keeping, AOC, RCS (Reaction Control System) etc., are diagnosed in order on the assumption that the ground segments are healthy. It is followed by the diagnosis of the Scientific Instruments (SI's), also assuming that the ground segments and the common instruments have been certified as normal. Table 1 shows capacity of the diagnostic knowledge database for CI's and SI's, and the general flow of the diagnosis process for CI's and SI's is shown in Fig. 7.

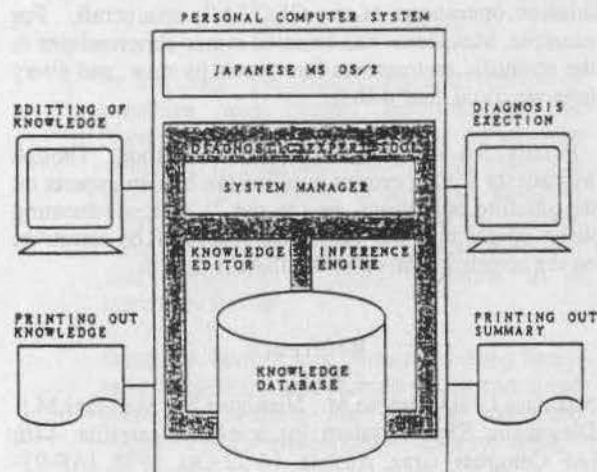


Figure 6: Structure of the diagnosis system

The results of diagnosis are displayed and printed out with detailed explanations so as to be easily understood by the personnel who is not familiar with the spacecraft system. Fig. 8 shows an example of the display. In case that Manadeshi judges the emergency measures should be taken, it recommends a minimum number of commands (the first-aid commands) to be sent so as to save the spacecraft from the catastrophe, and outputs a list of telephone numbers of senior engineers or scientists who can supervise the further contingency operations if necessary.

The log of diagnoses is kept in a file and it can be reproduced in any time. It is also possible to remake the diagnostic procedure by giving different answers to the reproduced log.

Table 1: Capacity of the diagnostic knowledge database for the common and scientific instruments

	Common Instruments				Scientific Instruments						
	BCM* ¹	BAO* ²	BPS* ³	BDC* ⁴	LEP	EFD	MGF	HEP	PWI	EPIC	CPI
TREE NODES	121	53	5	0	20	36	10	18	8	6	9
QUESTIONS	99	69	51	101	1	29	1	1	1	1	4
TABLES	3	0	2	0	0	0	0	0	0	0	0

- *¹ BCM: Operation Control and Data Processing System
- *² BAO: Attitude and Orbit Control System
- *³ BPS: Power System
- *⁴ BDC: General Questions for Operation Summary

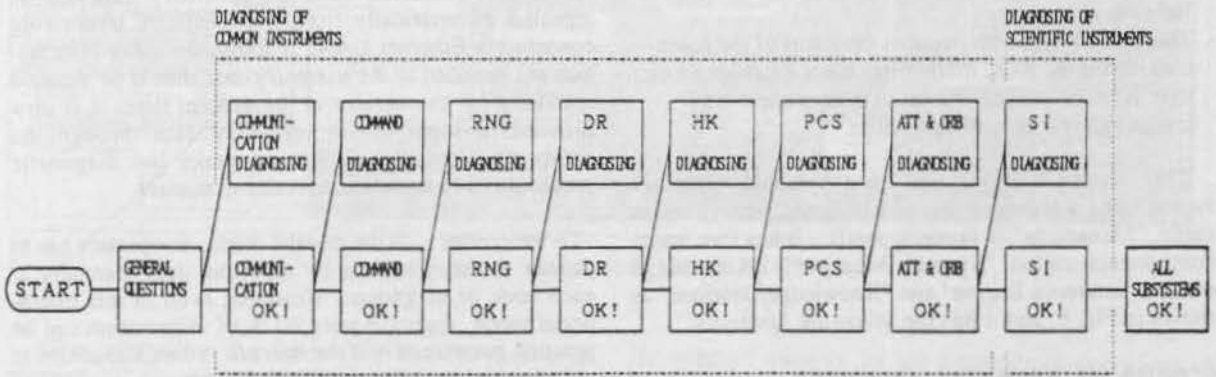


Figure 7: General flow of diagnosis of space segments for the common and scientific instruments

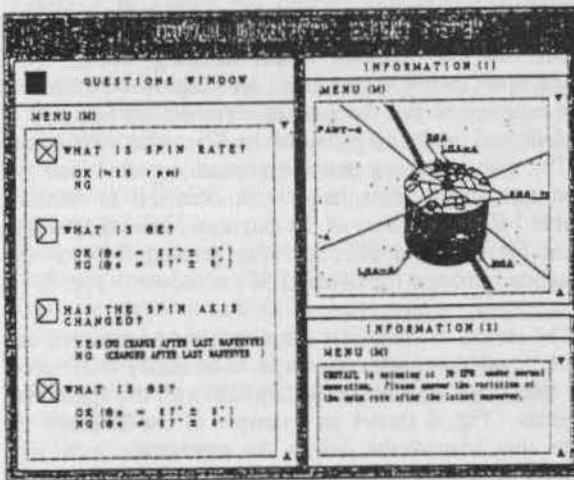


Figure 8: Example of the diagnosis display

ances for home use etc., because it is easy to create a diagnosis system applying the stochastic analysis based on many sample data from troubles in the mass-production lines. However, though some cases of success have been reported, it is difficult to apply the AI technology to the operations of a satellite, specially of a tailor-made scientific satellite.

We challenged this difficulty, and so far the ISACS system has been working well in the ground control and mission operations of the GEOTAIL spacecraft. For example, Manadeshi has detected minor abnormalities in the scientific instruments four times by now, and every time we could deal with it.

Finally, we would like to show an episode. Though Manadeshi is the favorite pupil of the human experts on the satellite operations, he (or she ?) is now educating junior operators of the GEOTAIL spacecraft by narratives on the screen displayed in the ISACS system.

Conclusion

An overview of the ISACS system was described. The AI technology and the EXPERT system have been getting applied in many fields. For example, the EXPERT diagnosis system is broadly utilized in the mass-production lines for automobiles, electric appli-

Reference

Nakatani, I.; Hashimoto, M.; Nishigori, N.; Mizutani, M.; Diagnostic Expert system for scientific satellite, 44th IAF Congress, Graz, Austria, 16-22 Oct. 1993, IAF-93-U.2.547.

THE ESA PACKET UTILISATION STANDARD P.U.S.

J.-F. Kaufeler, P. Kaufeler ESA/ESOC, D-64293 Darmstadt, Germany
A. Parkes NOVA Space Associates Ltd., Bath, U.K.

ABSTRACT

ESA has developed standards for packet telemetry (Ref.2) and telecommand (Ref.3), which are derived from the recommendations of the Inter-Agency Consultative Committee for Space Data Systems (CCSDS). These standards are now mandatory for future ESA programmes as well as for many programmes currently under development. However, whilst these packet standards address the end-to-end transfer of telemetry and telecommand data between applications on the ground and *Application Processes* on-board, they leave open the internal structure or content of the packets.

This paper presents the *ESA Packet Utilisation Standard (PUS)* (Ref.1) which addresses this very subject and, as such, serves to extend and complement the ESA packet standards. The goal of the PUS is to be applicable to future ESA missions in all application areas (Telecommunications, Science, Earth Resources, microgravity etc.). The production of the PUS falls under the responsibility of the ESA Committee for Operations and EGSE Standards (COES).

Keywords: Packet Utilisation, Packet Structure, COES.

1. INTRODUCTION

In the past, the monitoring and control of satellites was largely achieved at the "hardware" level. Telemetry parameters consisted of digitised read-outs of analogue channels and status information sampled from registers or relays. These parameters were sampled according to a regular pattern and appeared at fixed positions in a telemetry format.

Similarly, control was performed using fixed-length telecommand frames which contained basic instructions for loading on-board registers or for enabling/disabling switches.

Moreover, the associated space-ground communications techniques guaranteed

neither a reliable nor a complete transmission of telemetry and telecommand data.

Through the 1980s, there was a progressive increase in the use of on-board software to implement functions which should logically be performed on-board the satellite rather than on the ground e.g. control loops with short response times, data compression prior to downlink etc. However, this software had to be remotely monitored and controlled using the traditional hardware-oriented techniques.

This imposed significant constraints on the on-board software implementation, limiting its flexibility and consequently hampering the trend towards more on-board intelligence and autonomy.

In order to overcome these problems, the CCSDS recommended the use of telemetry and telecommand packets (Refs. 4 & 5) which provide a high quality space-ground communication technique enabling a flexible exchange of data between an on-board *Application Process* and a ground system. An *Application Process* is a logical on-board entity capable of generating telemetry packets and receiving telecommand packets for the purposes of monitoring and control. It is uniquely identified by an *Application ID*, which is used to establish an end-to-end connection between the *Application Process* and the Ground. Many different mappings can be envisaged between *Application Processes* and on-board hardware. At one extreme, each platform subsystem or payload (or part of thereof) could contain its own *Application Process*. In a more modest design, a single *Application Process*, say within the OBDH, could serve many, or even all the on-board subsystems and payloads.

The door was now open to implement a "message-type" interface between ground and space-based applications and thus to move towards the realisation of "process control" techniques.

In 1987 ESA set up the Committee for Operation and EGSE Standards (COES). The primary objective of this group was to define those functions which are common

between a satellite checkout system (EGSE) and a satellite control system. Even though these systems are used for different objectives and in different project phases, the logical interface to the satellite is identical and many of the functions are similar. Therefore, a *common system* could be used for the pre-launch checkout and post-launch mission operations both within a given project and also across different projects (see Fig.1).

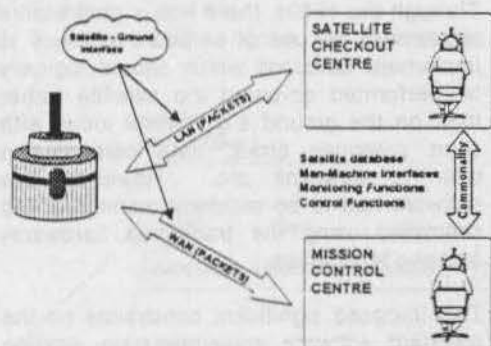


Fig.1 Check-out / Operations Commonality

COES decided to define such a common system for missions using the newly defined ESA Telemetry and Telecommand packets. However, the flexibility introduced by the use of packets leads to the possibility of implementing a given control function in many different ways. It soon became clear to COES that its task was only feasible if a clear satellite-ground interface existed, based on the use of packets.

Consequently, the first task of the COES was to produce a standard which defined precisely *how* telemetry and telecommand packets should be used.

2. SCOPE OF THE PUS

The term "Utilisation" is used in the title of the standard, since the intention is that the PUS should address all aspects relating to the use of packets i.e. the circumstances under which they are generated and the rules for their exchange, as well as their structure, format and content.

The PUS can therefore be seen as an interface document defining the relationship between space and ground.

The PUS contains the following elements:

- ↓ operational requirements relating to satellite monitoring and control functions and to testability;
- ↓ standards for the secondary data header of telemetry and telecommand packets;
- ↓ the definition of a set of PUS Services which respond to the operational requirements. A Service specification includes the corresponding on-board Service model and a full definition of all the Service Data Units (SDUs) supported by the Service i.e. the telemetry and telecommand packets;
- ↓ standards for the data structures and parameter encoding types allowable within packets.

The Operational Requirements cover all aspects of Nominal and Contingency Operations for the full spectrum of mission types and classes. They include generic requirements for:

- ↓ the different classes of telemetry data to be transmitted to the ground and the circumstances under which the data shall be generated;
- ↓ the provision of different levels of telecommand access to the satellite to ensure the maximum degree of controllability;
- ↓ telecommand verification;
- ↓ the control of on-board software;
- ↓ the loading and dumping of on-board memories.

In addition, requirements are identified for a number of "advanced" on-board functionalities, which may only be required for particular classes of mission:

- ↓ on-board scheduling of commands for later automatic release;
- ↓ on-board parameter monitoring;
- ↓ on-board storage and retrieval of data;
- ↓ transfer of large data units (e.g. files) between space and ground and vice-versa.

The requirements for Contingency

operations cover the setting up of a "diagnostic" mode, wherein the ground can oversample selected telemetry parameters for ground evaluation purposes. Also, it should be possible to by-pass on-board functions by ground command and to operate a function in an off-line mode in order to isolate hardware faults.

The Packet Data Field Header (PDFH) is left undefined within the ESA packet standards. However, the PUS identifies a fixed structure for this header for both telemetry telecommand packets, which is shown in Figure 2 below

Version Number	Checksum Type	Ack	Service Type	Service Sub-type
3 bits	1 bit	4 bits	8 bits	8 bits

Telecommand Packet Data Header

Version Number	Checksum Type	Spere	Service Type	Service Sub-type	Time
3 bits	1 bit	4 bits	8 bits	8 bits	Variable

Telemetry Packet Data Header

← Mission Optional →

Fig. 2 : Packet Data Field Headers

The PDFH for telemetry and telecommand packets is identical, with the exception that that a telemetry packet may (optionally) contain a time field for datation purposes.

The version number allows for future versions of the data field header and possibly of other aspects defined by the PUS. For example, a new version could be defined for packets containing multiple Service Data Units, as proposed by NASA/JPL for deep-space missions.

The two most important fields in the PDFH identify the *Service Type* and the *Service Subtype* to which the packet relates. The specification of the "standard" Services provided by the PUS constitutes the bulk of the standard and these Services are covered in more detail in the next section.

In principle, 256 Services and, for each Service, 256 Service Subtypes can be defined. The range from 0 to 127 is reserved for the PUS, in both cases, whilst the range from 128 to 255 is denoted as "mission-specific". The PUS thus has considerable growth capability for the later introduction of new Services or new Service

Subtypes within an existing Service.

3. PUS SERVICES

At present, 17 PUS Services have been defined and these are listed in Table 1 below.

Type	Service Name
1	Telecommand Verification
2	Device Command Distribution
3	Housekeeping & Diagnostic Data Reporting
4	Statistical Data Reporting
5	Event Reporting
6	Memory Management
7	Task Management
8	Function Management
9	Time Management
10	Time Packet
11	On-Board Scheduling
12	On-board Monitoring
13	Large Data Transfer
14	Packet Transmission Control
15	On-Board Storage and Retrieval
16	On-Board Traffic Management
17	Test

Telecommand Verification Service

Whilst none of the PUS Services is mandatory, it is expected that all Application Processes would implement this particular Service. Depending on the operational requirements and the on-board capabilities, commands can be verified at all stages: acceptance, start of execution, intermediate stages of execution and completion of execution. The selection of verification stages and whether positive as well as negative acknowledgement packets shall be generated can be done at the level of each individual command which is uplinked.

Device Command Distribution Service

There are 3 sub-services for the distribution of hardware-level commands:

↓
distribution at Telecommand Segment level; these commands require no software for their execution and would be used e.g. for unblocking or resetting the on-board Packet Assembly Controller (PAC);

↓ distribution by the CPDU (Command Pulse Distribution Unit) within the decoder. These are high priority on/off commands which are distributed directly (hardwired) to on-board devices;

↓ distribution by other Application Processes to devices, for example over an internal bus. Such commands may be used for normal operations or in a contingency situation e.g. where the normal higher-level control of the device is not to be, or cannot be, used.

Housekeeping and Diagnostic Data Reporting Service

The *housekeeping* sub-service covers the reporting of engineering data to the ground for monitoring and evaluation purposes. In order to adapt to changing operational conditions, the capability exists to define new housekeeping packets (or to re-define the contents of existing packets). Also, instead of systematically transmitting the housekeeping data to the ground, an optional "event-driven" mode is available. Event-driven means that the housekeeping packet is only generated if the value of a parameter within it varies by more than a prescribed threshold.

The *diagnostic* sub-service is used to support ground-based troubleshooting, where high sampling rates may be required for selected parameters

Statistical Data Reporting Service

In addition to the direct reporting of engineering data to the ground, summary *statistical* data may also be provided, consisting of the reporting of maximum, minimum and mean values of specified parameters over a time interval.

Event Reporting Service

This Service covers reports of varying severity from "normal" reports (e.g. progress of operations) to the reporting of serious on-board anomalies. This provides the mechanism for on-board functions to report to the ground autonomous actions they have taken or events they have detected.

Memory Management Service

This covers all aspects of loading and dumping of on-board memory blocks, as well as performing checksums on specified memory areas on ground request.

Task Management Service

This Service allows the ground to exercise control (e.g. start, stop, suspend etc.) over on-board software tasks managed by an Application Process. For many missions, this level of control may only be exercised in contingencies.

Function Management Service

This Service provides the "normal" mechanism for control of the functions executed by an Application Process (e.g. activate, deactivate, pass parameters etc.)

Time Management Service

This service permits control over the on-board generation rate of the Time Packet. In the future, this may be extended to cover the use of GPS.

Time Packet Service

This service is constituted solely of the Time Packet which is defined at the higher level of the ESA Packet Telemetry Standard (Ref.2).

On-Board Scheduling Service

For many missions, it will be necessary to load telecommands from the ground in advance of execution, for release on-board at a later time. For example, LEO missions, where operations must be conducted whilst outside of the limited ground passes.

This Service provides the capability for loading, deleting, reporting and controlling the release-status of telecommands in an On-board Schedule. Telecommands may also be time-shifted, without the necessity of deleting and re-loading them with new times.

A telecommand may also be "interlocked" to another telecommand, released earlier in time from the Schedule. That is to say, the release of the telecommand will be dependent on the success (or, alternatively, the failure) of the earlier command.

On-Board Monitoring Service

This Service provides some of the basic telemetry monitoring functions which are normally implemented on the ground i.e. mode-dependent limit, trend and fixed-status checking. Out-of-limit conditions are automatically reported to the ground.

Large Data Transfer Service

For many mission, it is anticipated that the largest desirable packet size may be much smaller than the maximum allowed by the ESA standards. This Service provides for the reliable transfer of a large Service Data Unit of any Type (e.g. a file, a large memory load block or a large report) by means of a sequence of smaller packets. The Service may be invoked either for the uplink or the downlink of a large Service Data Unit.

Packet Transmission Control Service

This Service permits the enabling and disabling of the transmission of packets (of specified Type/Sub-type) from an Application Process.

On-Board Storage and Retrieval Service

This Service allows for the selective storage of packets for downlink at a later time under ground control.

In principle, a number of independent stores may exist, which may be used for different operational purposes. For example, for missions with intermittent ground coverage, packets of high operational significance (e.g. anomaly packets) could be stored in a dedicated packet store so that they may be retrieved first during the next period of coverage.

A "lost packet recovery" capability may also be achieved by systematically storing all event-driven packets on-board.

On-Board Traffic Management Service

This Service provides the capability to monitor the on-board packet bus (e.g. its load, the number of re-transmissions etc.) and to exercise ground control over on-board traffic and/or routing parameters or problems.

Test Service

This Service provides the capability to activate test functions on-board and to report the results of such tests in the telemetry. A standard Link Test ("Are you

alive?") Sub-service is provided.

4. MISSION-TAILORING

An important aspect for the wider acceptance of the PUS is that it should be easily tailored to the specific requirements of a given mission.

This consideration has been at the forefront whilst developing the standard and is achieved by the following measures:

↓
a mission may choose to implement only that sub-set of the PUS Services (and/or Sub-services) which it deems appropriate to its requirements;

↓
the structures defined for the Service Data Units (the telecommand and telemetry packets) identify "mission-optional" fields. These correspond to the "optional" capabilities within a Service (the so-called *Capability Sets*). If a capability set is not implemented for a particular Service, then the corresponding mission-optional fields may be omitted;

↓
for the data type of each field of the Service Data Units, the PUS only specifies the *encoding type* (e.g. real or integer) with the *encoding length* being specified at mission-level;

Thus, a mission may remain fully compliant with the PUS whilst incurring no detrimental impact on its packet overhead as a consequence.

5. VALIDATION

Prior to approval of the PUS, and before implementing supporting infrastructures, it was necessary to ensure the correctness, practicability and operational usefulness of the standard. This was achieved by means of a prototyping exercise completed in 1992, which both validated the standard and, at the same time, provided some indicators for possible implementation techniques.

The packet communication techniques were not addressed in this prototype since these have already been independently demonstrated. Instead, the prototype concentrated on the end-to-end application-

level aspects, emulating the on-board behaviour in response to the Ground control system.

This prototype (called PUSV) runs on one or two SPARC workstations and at the same time allows modelling of different on-board Application architectures. A reference satellite model (called PUSSAT) was implemented for validation and demonstration purposes.

6. FUTURE PERSPECTIVE

The draft Issue of the PUS has been exhaustively reviewed at Agency level during the course of 1993 and is currently being updated to reflect this review process. It is expected that the PUS will become an approved Agency standard in the first half of 1994.

The PUS is expected to evolve in the future, in an incremental manner, as new monitoring and control Services become sufficiently mature to be generalised and thus standardised.

ESOC is currently undertaking a major mission control infrastructure development, the so-called SCOS-II, which is a distributed system based on SUN workstations. SCOS-II will provide full application-level support to missions conforming with the PUS.

COES is also specifying the functional requirements for a generic system to be used for checkout and operation across different projects.

7. REFERENCES

1. Packet Utilisation Standard (PUS), ESA PSS-07-101 Issue 1, Draft October 1993.
2. Packet Telemetry Standard, ESA PSS-04-106, Issue 1, January 1988.
3. Packet Telecommand Standard, ESA PSS-04-107, Issue 2, April 1992.
4. (CCSDS) Packet Telemetry, 102.0-B.2, Blue Book, January 1987.
5. (CCSDS) Telecommand: Part 3, Data Routing Service, 203.0-B.1, Blue Book, January 1987.
6. (ESA) EGSE & Mission Control System (EMCS) Functional

Requirements Specification, ESA PSS-07-401, Issue 1, Draft 8 November 1992.

GROUND SYSTEMS I

1. Keyte, K. (Vitrociset-Italy):
"SCOS II - A Distributed Architecture for Ground System Control" 319
2. Carrou, J.P.; Campan, G.; Fourcade, J. and Foliard, J. (CNES-France):
"The Technical Evolution of Ground Flight Dynamics System Utilized for Spacecraft Operations" 327
3. Kruse, W. and Pilgram, M. (DLR-Germany):
"Inter-Agency Cross-Support: A Decade of Experiences by GSOC" 335

The ground system architecture for the SCOS II is a distributed architecture for ground system control. It is based on a central computer system which is connected to several remote computers. The central computer system is responsible for the overall control of the ground system, while the remote computers are responsible for the control of the individual spacecraft operations.

The ground system architecture for the SCOS II is a distributed architecture for ground system control. It is based on a central computer system which is connected to several remote computers. The central computer system is responsible for the overall control of the ground system, while the remote computers are responsible for the control of the individual spacecraft operations.

The ground system architecture for the SCOS II is a distributed architecture for ground system control. It is based on a central computer system which is connected to several remote computers. The central computer system is responsible for the overall control of the ground system, while the remote computers are responsible for the control of the individual spacecraft operations.



Figure 1 - SCOS II Ground System Architecture

SCOS II - A DISTRIBUTED ARCHITECTURE FOR GROUND SYSTEM CONTROL

Karl P. Keyte
Vitrociset S.p.A., Rome, Italy
c/o ESOC
Robert-Bosch Straße 5
D-64293 Darmstadt
Germany
E-mail: KKEYTE@ESOC.BITNET

Abstract

The current generation of spacecraft ground control systems in use at ESA/ESOC is based on the SCOS I. Such systems have become difficult to manage in both functional and financial terms. The next generation of spacecraft is demanding more flexibility in the use, configuration and distribution of control facilities as well as functional requirements capable of matching those being planned for future missions.

SCOS-II is more than a successor to SCOS-I. Many of the shortcomings of the existing system have been carefully analysed by user and technical communities and a complete redesign was made. Different technologies were used in many areas including hardware platform, network architecture, user interfaces and implementation techniques, methodologies and language. As far as possible a flexible design approach has been made using popular industry standards to provide vendor independence in both hardware and software areas.

This paper describes many of the new approaches made in the architectural design of the SCOS-II.

Key words: Ground System Control, Distributed Architecture, SCOS.

Past Shortcomings

The shortfalls of the current system are manyfold. The architecture of SCOS-I is based around a central VAX processor with connected user terminals or workstations. SCOS I-A uses custom built workstations based on Intel 8086 CPUs. SCOS I-B uses Sun workstations which perform only user-interface related tasks. The lack of distribution of the

workload places high demands on the central VAX system which is often stretched to provide the processing power for the spacecraft control as well as the communication with the workstations. Response times are poor, retrieval performance suffers as more users access historical data and the flexibility of the services offered is limited.

SCOS-I also suffers a maintenance problem in that nearly no two operational missions have used the same version of the control software, making the job of the maintenance team very difficult as they struggle to support multiple versions of the system.

Perhaps the largest shortcoming of the existing system is the lack of support for many features common to all spacecraft. Whilst much of the telemetry processing is handled within the SCOS-I, telecommanding is left to custom mission software. This is also the case for data reception, command verification and spacecraft database maintenance. Large amounts of manpower have been required for development of custom mission software to provide these essential tasks. Figure 1 shows the depend-

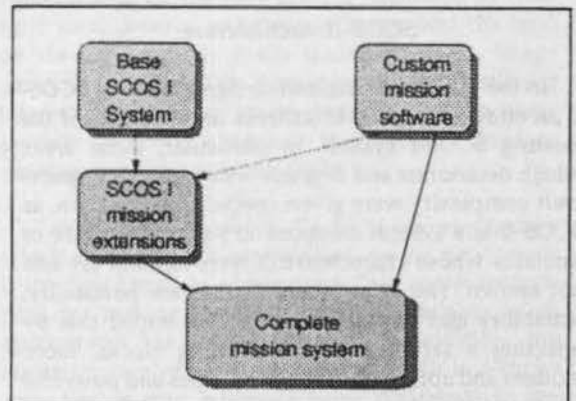


Figure 1 - SCOS-I Mission System Construction

encies in the construction of a mission system based on SCOS-I. As can be seen, it is not only the custom mission software which must be written but typically also a number of modifications to the SCOS-I kernel software. The combination of the two are then used to generate the final mission software.

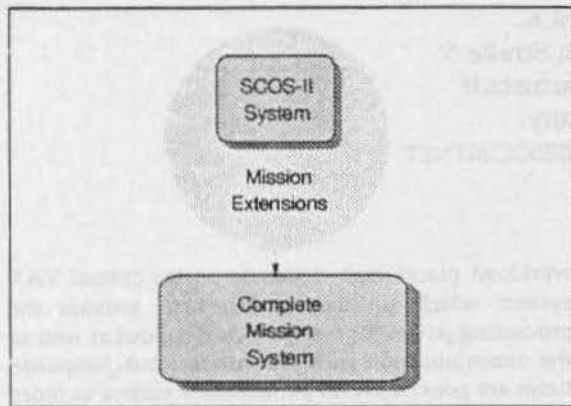


Figure 2 - SCOS-II Mission System Construction

In contrast to the SCOS-I philosophy, SCOS-II aims to provide mission teams with a *customisable* system, functional in its own right, with which the teams *extend* the system at the interface points provided by SCOS-II. Figure 2 shows how a mission system is constructed by building extensions to the provided interfaces of SCOS-II. This system allows much tighter control of the interfaces provided and enables the SCOS-II maintenance team to support only a single version of the system. If a mission identifies a need for unforeseen interfaces, it is provided for all missions and may be used if required. The use of *Object-Oriented* technology greatly assists in the process of *extending* the system through these provided interfaces.

SCOS-II Architecture

In the initial analysis and design phases of SCOS-II an effort was made to address the shortfalls of the existing SCOS-I system. In particular, those areas which deteriorate and degrade with increasing spacecraft complexity were given special consideration, as SCOS-II is a system designed to support a future of satellites whose characteristics were not and are still not known. The chief design goals were portability, scalability and flexibility. It was also hoped that by selecting a set of standard building blocks, more modern and appropriate methodologies and powerful workstation technology, that cost-effectiveness would be increased in terms of providing greater

functionality for a similar investment to that made traditionally.

Basic Network Architecture

In contrast to the previous generations of ESA's ground-control systems, the SCOS-II architecture leaves behind the concept of centralised processing of spacecraft data. The original approach was clearly made for financial reasons, though the current availability of high-powered personal workstations offers the possibility of distributing processing to the users or locations where it is most needed. A SCOS-II system is based around a local-area network with workstations connected in a number appropriate for the mission being undertaken. The philosophy of the design is such that workstations should be made sufficiently independent to allow the addition and removal of user-workstations without a functional impact on operations.

Each SCOS-II workstation comprises a high-performance Unix system (currently baselined as a Sun Sparc-10 machine) with one, two or three high-resolution colour monitors, large local disk capacity and a network connection. At present a 10Mbit

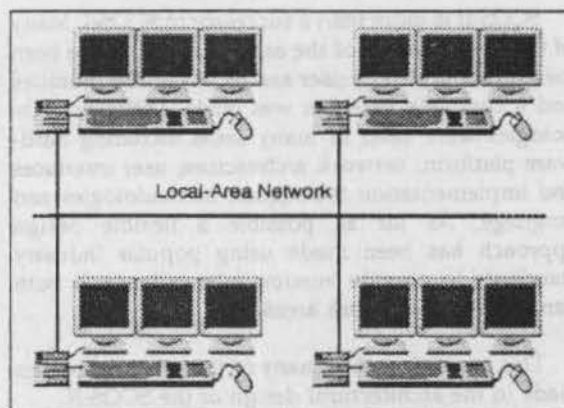


Figure 3 - Section of typical SCOS-II configuration

Ethernet network is used to connect all machines. Figure 3 shows a partial configuration of four typical workstations connected together on the local-area network.

The network architecture together with the independent control software of each workstation provides much fault tolerance at the workstation level. If a single workstation malfunctions it may be removed from the network for repair or replacement without undue impact on users at other workstations. A replacement workstation may be connected directly to the network in its place to provide a continued

service for the user suffering the interruption.

Telemetry Distribution

One of the more novel aspects of SCOS-II, and of particular importance in providing the required performance on a possibly large network, is the manner in which telemetry from the spacecraft is received and distributed. Since no single computer on the network is responsible for processing data received from the satellite, a means of providing each workstation with the required telemetry is required. SCOS-II chose to *broadcast* all housekeeping telemetry on the local-area network, allowing any workstation to gather the data it requires. Each workstation is therefore free to select the type of data it wishes to process and ignore any in which it has no interest. As telemetry arrives at each workstation it is stored in a shared memory area and applications running locally are notified of the arrival of the new data.

Usually associated with the broadcast of data on a network rather than a point-to-point transmission is the unreliability of delivery. This is because the sender has no knowledge of the potential recipients and can make no attempt to verify that the data has been correctly delivered. This is synonymous with all broadcast transmissions such as radio and television. In the SCOS-II system however, there are occasions where a greater level of reliability is required. It would be possible for recipients to register their intent to receive with a central manager and leave the responsibility of ensuring safe delivery to that management function. This would create an unwanted single point of failure which is against the design philosophy of the SCOS-II system.

To provide a high-level of reliability within the broadcasting system, SCOS-II designed and build a custom Inter-Process Communications (IPC) library based on the Internet Protocols (IP). As well as supporting the common TCP/IP and UDP/IP protocols, the SCOS-II IPC supports an extension, UDP+. UDP+ may be used for reliable delivery of point-to-point or broadcast data, thereby avoiding the potentially dangerous limitation. The system does not and, due to inherent network limitations, can not guarantee 100% reliable data delivery but it provides both the sender and receiver of data the knowledge of any failure to complete the transaction.

The current use of an Ethernet network has been selected for the medium term and is expected to be adequate for telemetry rates of satellites over the next 5 years. Extending SCOS-II to use fibre-optic technology such as FDDI in no way affects the logic of the design and it is envisaged that this direction will be

taken at some time in the future.

The means with which telemetry arrives in the system is mission specific and SCOS-II will deliver a basic telemetry reception and broadcast service for mission teams to extend. The telemetry receiver must handle non-standard protocols, multiple data sources, etc. SCOS-II currently works with packetised telemetry according to ESA's Packet Utilisation Standard and the telemetry broadcast service expects packets to conform to that standard.

Network Cache & Retrievals

One of the most challenging requirements made on ESA's ground control systems is that of data *retrieval*. All housekeeping data must be stored and maintained for the full duration of the mission. A user must have the capability to request a retrieval of any period of data over the lifetime of the mission. Traditional systems have maintained only a small subset of mission data on line and have had to resort to a very slow off-line tape or cartridge service to examine data which has migrated out of the control system. Data recovered in this fashion may not be viewed at the control workstation.

SCOS-II aims to provide mission controllers and spacecraft engineers with the tools to retrieve data from *any* period of operations efficiently and using the same tools and applications to view the data as they use to examine real-time data. This is achieved using a two-level storage scheme for data packets. All packets broadcast on the network are received and stored by a *History File Archive* (HFA) application running nominally on a dedicated workstation. The existence of the HFA allows all applications on any workstation to make network retrievals. This scheme however, loads the network with retrieval data for *each* user retrieval as well as the real-time telemetry transmissions. With an increase in the number of workstations on the network the likelihood of multiple simultaneous retrievals increases and the load on the network may reach saturation levels. Usage patterns also show that during a period of particular interest, many users make retrievals for the same periods. SCOS-II addresses this network loading problem with the *Network Cache*.

The SCOS-II Network Cache is an application which exists on each workstation on the network. It is the only recipient of telemetry data and is responsible for making the data received available to all applications via shared memory. In addition, the telemetry received is stored on local disk in a cache area. Rather than retrievals being addressed to the HFA they are directed to the Network Cache. Should

the data covering the period of the retrieval be found in the cache it is returned to the application with no network communication whatsoever. Since the size of the local disk is large (typically between 1GB and 4GB), the cache is able to store a large amount of data locally. Most retrievals relate to recent data and only rarely will data not be found in the local cache.

Should a retrieval request be made for data which is no longer resident in the cache, then the responsibility is on the Network Cache to request the data from the HFA, returning it to the application in the usual manner. This allows applications to make

real-time telemetry and retrieval data. It should be noted that the data passed from the Network Cache to the applications (data users) consists only of memory addresses from which the application may access the actual data. This allows read-only access of the data without any additional copying between process contexts. Services exist to ensure that the applications cannot address incorrect data should the original data have been dropped by the cache by the time the application is ready to examine it.

An extension of cache policies is currently being examined to further optimise performance. Since

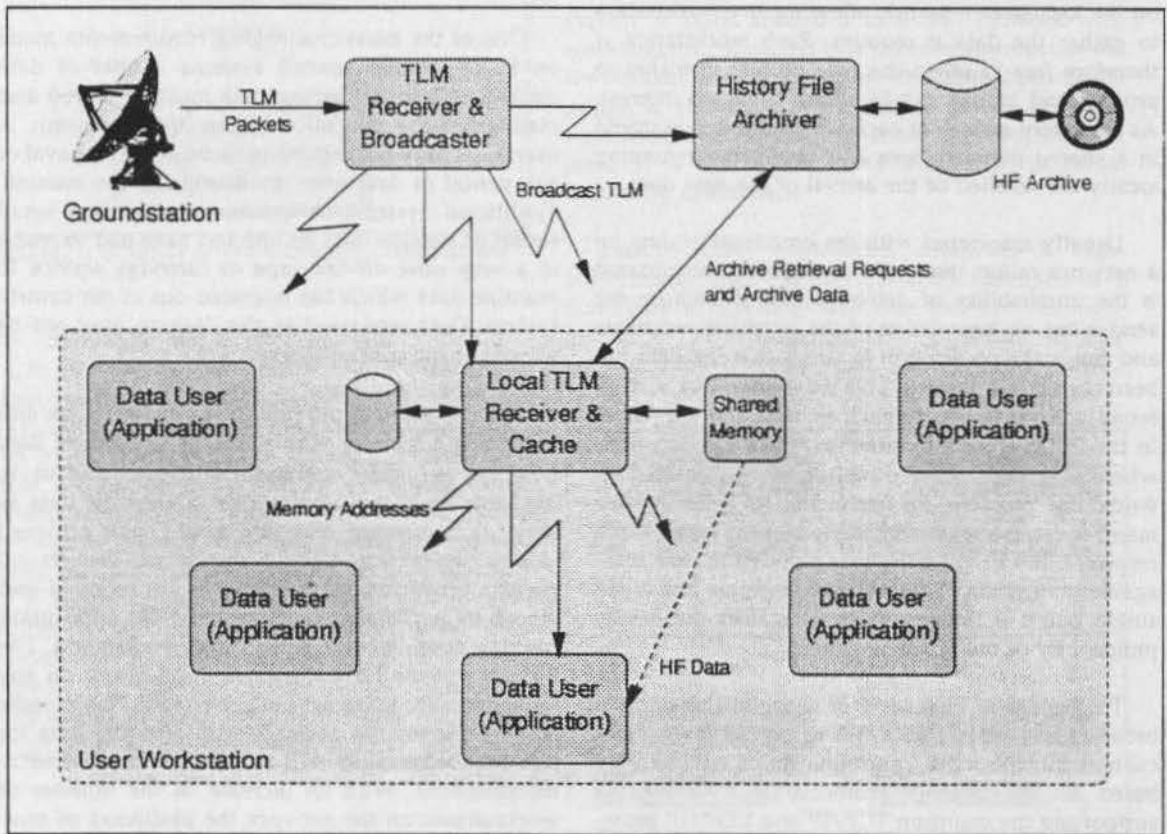


Figure 4 - Internal architecture of the SCOS-II kernel

retrieval requests covering any period in a consistent way, keeping the actual location of the data transparent to the requester.

Additional services are available to the application to examine the time span of data without necessarily retrieving the full content. This provides facilities to browse the index of available data without incurring the penalty of handling the full data volume.

Figure 4 shows the architecture of the SCOS-II kernel, identifying the elements involved in handling

usage patterns indicate that users tend to retrieve similar periods of data, a predictive retrieval algorithm may be used to *pre-load*, via broadcast, the caches at workstations other than the one making the request. This is only the case when data must be obtained from the HFA server. Using this scheme will allow all users to view the same historic data with only a single request to the archive server being made from the first initiator of the request. Currently, however, local cache disk capacities are of adequate size to provide a high percentage of retrieval requests with data directly from the cache.

Long-Term Archiving

In the discussion on the SCOS-II Network Cache it was indicated that the History File Archive (HFA) maintains all historic data for the duration of the mission. The volume of data involved is clearly very large, particularly for a spacecraft with high data rates and/or long operational lifetime. It is not entirely true to say that the HFA will keep the full mission data in all cases. The mission requirements dictate the configuration of the long-term storage medium. In the simplest (and most economical) case the history archive will be maintained as a circular history on disk, much like the Network Cache. At the other extreme the configuration may comprise a migratory "infinite" storage system as shown in Figure 5. Such a configuration provides a huge volume of data via re-writable optical disk. Access

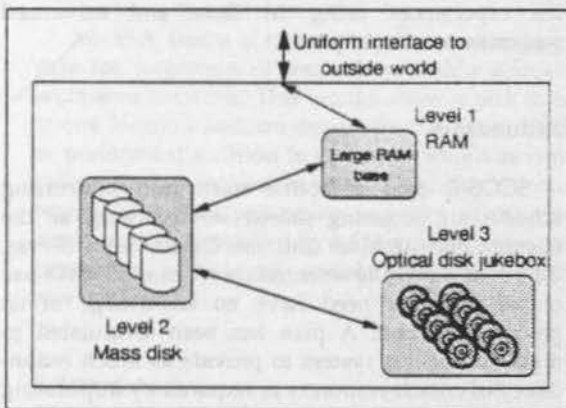


Figure 5 - Migratory "infinite" storage system

speeds are optimised by using magnetic disk and RAM as lower-level caches. Data is initially buffered in RAM (and written through to magnetic disk). As the data is not accessed it quickly disappears from the RAM. If it is still not accessed for some pre-determined time it is copied to optical disk and dropped from magnetic disk. When it is re-accessed, the data follows the opposite direction, being held in RAM for the time it is required to increase access time.

Since retrieval requests to the HFA may vary dramatically in frequency and volume of data requested, a policy of scheduling and prioritisation is needed. The SCOS-II HFA uses an interleaving technique to provide each request in its request queue with a configurable volume of data before moving on to the next request. Requests are thus handled in a *round-robin* manner to prevent unacceptable response times in cases where a large retrieval request arrives before subsequent requests. In addition to this simple scheduling algorithm a priority

may be associated with each request to influence either the frequency in which the request receives attention or the volume of data retrieved each time attention is received. The algorithms are not unlike the CPU sharing algorithms of multi-tasking and time-sharing operating systems.

Retrieval requests fall into two broad categories: on-line requests or batch requests. The first category typically includes all retrievals made by spacecraft controllers and engineers at user workstations. They are normally of low-volume with a demand for a high response time. The batch requests are made by applications performing such tasks as spacecraft performance monitoring, where a large volume of data may be required to identify parameter trends and variances. The scheduling and particularly the prioritisation algorithms greatly assist in satisfying these different demands.

To optimise the use of workstations' local network cache it is possible to configure a workstation as being used predominantly for a specified task. For performance monitoring tasks as described above, for example, it may be appropriate to increase the size of the network cache space by adding disks and to disable the caching of data other than that being examined. This greatly increases the chance of a cache *hit* and reduces the number of accesses made to the HFA.

Sharing Data between Applications

With the introduction of a distributed architecture the sharing of data between applications becomes more difficult. Applications may be resident at any location on the network and the integrity of common data must be maintained. SCOS-II uses two schemes for making the sharing of data possible. The first provides facilities for sharing *object hierarchies* across the network in a distributed manner. The second addresses the sharing of data local to a workstation where performance demands are more challenging.

• Object Store

The configuration of the spacecraft and the control system is maintained in the Mission Information Base (MIB). The MIB must be available at all workstations and sections may be modified locally to test new configurations. SCOS-II looked at a number of commercial Object-Oriented database systems during the analysis phase, but rejected this option in favour of a system built in-house.

The SCOS-II Object Store maintains a central base of objects which may be accessed from any appli-

cation, anywhere in the network. The Network Cache is once again used to optimise access to frequently referenced data. Any changes to the centrally maintained information base override the MIB by being held locally. After testing changes users (subject to authorisation checks) may make the changes available to either a selection of users (by direct transmission to individual workstation Object Stores) or all users (by returning changes to the central MIB).

wide *semaphore* system is available to provide mutual exclusion to any resource on the network without invalidating the integrity of that resource.

Future Issues and Directions

SCOS-II is planned in three main phases. The *Basic System* provides functionality comparable to existing control systems in ESA but with much increased performance and extended flexibility in the user interfaces. The *Advanced System* adds considerable functionality to the area of spacecraft modelling and the manner in which users may view the model. A Release 2 of the system is planned for the future which will extend the services of the control system in other areas. Some of these areas have been provisionally outlined - others will be decided based on the experiences using the Basic and Advanced systems operationally.

Redundancy

SCOS-II uses a *location-independent* addressing scheme for accessing shared services such as the History File Archiver and the Object Store Server. This means that the workstation wishing to make use of the resource need have no knowledge of its physical location. A plan has been formulated to make use of this system to provide as much redundancy of critical resources as required by duplicating the services. The location independency allows the switching of the prime service without the need to inform the users of that service. Automatic switching of redundant units in the event of a prime unit failure will provide users with an uninterrupted service.

Increasing Autonomy

Current control systems require much intensive and attentive support from spacecraft controllers. As spacecraft become more and more complex, the job of such individuals becomes not only corresponding complex but also more critical. It is rapidly reaching the stage where spacecraft controllers are unable to monitor all attributes of the health of the system. It is often not possible to extend the on-board autonomy adequately to augment the work of the controllers.

ESA is currently undertaking studies and prototype programmes to maintain flight operations plans electronically. This not only reduces the likelihood of error in producing and updating the plans but also offers the possibility of interfacing the flight plan

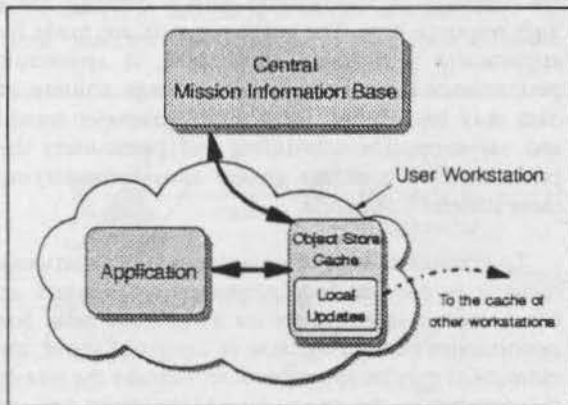


Figure 6 - Object Store Data Routes

Figure 6 shows the paths of the data between application and Object Store. Note that the central information base is managed by an Object Store server and the local caches are managed by an Object Store client. This scheme follows a conventional client/server relationship common in distributed systems.

Locally Shared Objects

In contrast to the distributed nature of the Object Store where data must be made available to applications running at different locations on the network, SCOS-II also provides a highly efficient means of sharing data locally at any one workstation. Shared memory is used to store objects of data managed by the shared object control services. These services are required to provide applications with the appropriate addresses (which may be different for the same object for each application) and to protect the data from concurrent modification by more than one application. Performance is enhanced by using cooperative rather than mandatory locking and by offering access to the data without copying to the processes own context.

Further services are provided by the SCOS-II control system to allow applications to make use of shared resources at their own discretion. A network-

with the control software. This would allow the spacecraft controllers to refer to procedures directly relating to any situation which the control system has detected. Recovery procedures such as command sequences may be automatically prepared and, if not sent directly, given to the controllers for authorisation prior to transmission.

Process Context & Migration

Although the current SCOS-II system distributes control services within the network, it does so by coordinated replication rather than optimising and dividing the workload between workstations. To a degree this approach promotes the safety of the system by allowing each workstation to operate in an independent manner, but there are foreseeable cases where a sharing of processing may be desired.

An ESA study is currently underway to investigate the migration of processing within a local- or wide-area network. This would allow a task to start at one location and, on detection of a more efficient or performant location to continue, would automatically transfer to the new location. Such features would allow the processing capacity of the whole network to be expanded by adding high performance processors without any reconfiguration of existing workstations.

External Access

There is a growing demand for visibility of operations from sites other than the prime controlling location. SCOS-II has been designed to be highly configurable (in network size) and highly portable (in terms of location of operation). For these reasons it is not unreasonable to expect the system to be employed at sites closer to users of payload data, groundstations, etc. This, and an increasing interest in a diversity of user communities in spacecraft data, leads to a recognised need for the provision of external access to the system. There have been very justifiable concerns in the past about the safety and security of a spacecraft into whose control system access to the outside world is provided. Although it is impossible to eliminate attempts at unauthorised access it is also possible using modern networking technology to greatly reduce the likelihood of such access.

The inter-process communication services within the current SCOS-II have facilities to add data compression, encryption and authorisation. All of these services would be of considerable importance in any provision of external access. It is not however cur-

rently envisaged that control services will be made readily available outside the control centres but rather the services relating to viewing and monitoring spacecraft data.

Conclusions

The design of ESA's new generation control system has been made with a much greater degree of modularity and flexibility than before. Use of modern workstation and network technology have greatly assisted in providing the hardware flexibility while the object-oriented approach to the software definition and implementation has speeded up realisation of the system.

It has not been possible to entirely eliminate central provision of services due to costs and convenience, but SCOS-II offers a highly distributed architecture with provision for vastly different configurations. The smallest control system configuration is the so-called "SCOS-II-in-a-box" where the complete system operates on a single workstation with no network. At the other extreme is a system with many dozens of workstations, archive and database servers.

Performance considerations were of very high priority during the design phase of SCOS-II. Because of the anticipated large configurations of the system individual workstation performance was not to be a function of the number of workstations on the network. The design of the telemetry distribution system, together with the network cache, allows workstations to be added without degradation in performance. Although the system is not yet fully tuned and optimised for operational use, the performance so far attained is an order of magnitude better than existing systems in use by ESA. Figure 7 shows the approximate data and packet rates of the

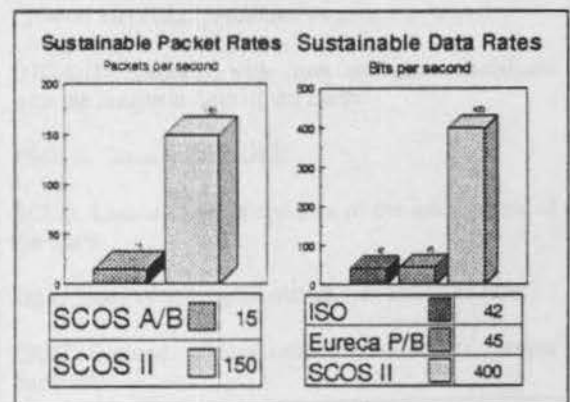


Figure 7 - Comparative performance of SCOS-II

THE TECHNICAL EVOLUTION OF GROUND FLIGHT DYNAMICS SYSTEM UTILIZED FOR SPACECRAFT OPERATIONS

J.P. CARROU, G. CAMPAN, J. FOURCADE, J. FOLIARD

CNES, Toulouse, France
18, avenue E. Belin

31055 TOULOUSE CEDEX

Abstract

Since 1964, the CNES activity, as regards space mechanics systems ground control, has been increasing substantially. Originally, it started with numerous small scientific or application satellites which enabled to cope with theoretical problems (orbit modelization), tracking datas from ground stations and the first utilizations of computers.

Later on, this activity was reinforced to give way to preoperational systems, genuine prototypes of exploitable space. Together with the specializations of missions Telecommunication and Earth observation satellites, the new ground station networks were developed while improved algorithms were using more efficient computers.

Lastly, nowadays the commercial and operational space industry uses well-itemized families of satellites, efficient ground station networks and moreover computer facilities based on the advent of a particularly exhilarating computer science: workstations. The latter allowed a good match between computer facilities and space mechanics and above all an efficient utilization of renewed algorithmics using adaptable, reliable and easy to extend informatics.

1. CNES experiences

These experiments are described in three stages:

1.1. Introduction of space activities 1965-1974

French space activity began on 26 november 1965 with the launching of the Diamant rocket from HAMMAGUIR. Space mechanics activity, started with the launching of FR1 (6 december 1965 by a SCOUT), DIA (17 february 1965 by a Diamant A) which allowed the passage from theory to application.

Later on this activity expanded rapidly thanks to a great number of experimental or scientific satellites, thanks to the participation of CNES to international

tracking campaigns (TRAPOL, ISAGEX, GRI, ...) or to satellite programs in varied fields: telecommunication, localization, meteorology, geodesy.

At the time the aims were concerning three types of activities:

- the operational aspect based on orbit determination and station visibilities, on satellisation diagnosis of national satellites, on attitude determination and lastly on position and velocity orientation at each telemetry time;
- the theoretical aspect to study new problems, the upgrading of the issues in the light of experiences, the study of new algorithms of fitting orbital parameters in estimation theory;
- the mission analysis aspect covering the study of various parameters (orbit, attitude, date and launching conditions) according to the satellite and launcher characteristics.

MAIN SATELLITES PROCESSED DURING THE PERIOD 1965-1974

- FR1 (62 kg): Study of ionosphere. Very low frequency.
- DIA (19 kg): Geodesy with doppler measurements on 150-400 MHz link. Stabilized by spin.
- D1C-D1D: Geodesy with laser reflectors. Stabilized with the magnetic field of the Earth.
- PEOLE: Training for EOLE.
- EOLE: Localisations of balloons in the atmosphere of the Earth.
- D2A: Study of hydrogen distribution and solar rays.
- SRET: Evolution of solar cells in relation with charged particles.

GEOS B, BEACON B, BEACON C.

AL1, AL2, ISIS for the GRI (Groupe de Recherches Ionosphériques).

ESR 01, HEOS A1, IMP 4, INTELSAT 2/F1, INTELSAT 2/F2 for the preparation of the French/German telecommunication program SYMPHONIE.

SOLAR 9, NIMBUS 2, ESSA 5-6-8, IRIS, OSO 3, OGO 4-5, OAO 2, etc...

Ground segment:

- The measurements:

- . Interferometers 135-138 MHz (HAMMAGUIR, PRETORIA, REDU, minitrack networks).
- . Doppler 150-400 MHz and 136 MHz (DIANE, IRIS (1969)).
- . Optical measurements.
- . Laser measurements.
- . Radar measurement.

The rough measurements were transmitted by punched tapes and telex together with corrections and meteorological measurements. Thus kilometers of tape were handled.

- Computer and software:

The first application programs were realized in FORTRAN on IBM computers (1401, 7040, 360/40, 360/65) whose central memories and computation speed are far from today's PC computers performances!

Later on in the seventies, CDC (CONTROL DATA CORPORATION 6200 and 6600) were used.

- Application software:

They were divided into four classes:

. Measurement preprocessing:

The phase measurements of interferometers are turned into cosines after different corrections (internal and external calibration, datation...).

Then more efficient methods were carried out for phase determination with ambiguity problem but will always remain difficult for false measures.

. Orbit determination:

The first operational software was adapted to the specific case of DIA (orbit 500-2700 km) and B (orbit 600-1350 km). Its main characteristics are the

use of the adapted analytical theory of Brouwer (short and long terms periods and secular terms..., with Earth potential limited to the fourth harmonic), the use of numerical integration to take into account the drag effect, and finally the least squares method for differential corrections.

LIDO program (Brouwer theory) and GIN (Cowell numerical method) were mainly used.

Specific programs were created to fit particular demands (ISAGEX campaign) or (BANCO) to save computer resources (memory and time processing).

Ground station forecasts:

They have a content and presentation adapted to their utilisation. The orbit extrapolation theory depends on the required precision: Cowell for accurate forecast (about 1 km along track within a few hours), LIDO for gross forecast (some 10 km along track within a few hours).

Attitude determination:

Satellite attitude stabilization was rudimentary (Earth gravity, Earth magnetic field).

The attitude determination was used by the scientist to know, within an accuracy of about 1° in the best case, the line of sight of their onboard instruments.

All the application software was developed in the form of monolithic programs, including subroutines, but without any link between them.

As the inputs of some were the outputs of the others, it was quite usual to punch or type again and again all the values of orbital parameters.

How incredible it is, for our young engineers, to imagine these old punched cards, one measure corresponding to one card! The suppression of false measures was really a manual operation! In a more sophisticated version, its weight was merely put to zero in the computation process.

The classical sketch for the orbit determination group included one card reader, one card puncher, one printer and one punched tape generator.

Work exploitation began by the reading of punched cards set..., and sometimes this required some juggling in order to avoid the loss or melting of information.

Station designation was done by telex from punched tapes. The more efficient operators did manage to recognize synchronization words in the binary file, but couldn't avoid the tapes to mix themselves from time to time! and the result was they had to restart their job from the very beginning!

The software development (we say so now) was quite anarchical: no comment in the code, no subroutine, no well-defined structure.

The results:

They were always satisfactory and allowed us to be knowledgeable and competent in systems considered today as simple.

In order to illustrate this remark, let us quote the following examples:

- During an orbit determination, very important and unusual residuals were noticed. Contact with antennas specialists allowed, after investigations, to conclude on a first occasion that it was an antenna asservissement problem and on other occasion that there was snow in the antenna dish.
- The first orbital periods were accessed by the acquisition and loss of signal by ground stations. Although it was not accurate, this method allowed us to have a first gross diagnosis of orbit injection.
- Antenna tracking designation, easier by large antenna patterns (some 10°) allowed the staff to get familiar with the specificities of space activity and to become very competent.

1.2. Preoperational phase 1975-1986. Beginning of "commercial space"

Right from the start of this period, a sensible decrease in number of scientific and experimental satellites took place.

We worked then on missions of telecommunication (SYMPHONIE, TELECOM), direct broadcasting (TDF), Earth observation (SPOT).

The first complete experience in space flight mechanics was realised with the two German/French satellites SYMPHONIE. These satellites were the first European satellites with billyquid apogee motor, spin stabilized in transfer orbit, and three axes stabilized during their operational life. During the station keeping maneuvers the bi-propellant system was used for the orbit corrections and a cold gas system for the attitude control.

The various actions previously described have, of course, been carried on, but other very new tasks were developed. It was a matter of taking into account the satellite attitude and orbit maneuver strategy in order to pass from the transfer orbit to the in station longitude (in station window: 0.2°).

The following improvements were made:

- The use of interferometric measurements from KOUROU and WEILHEIM and angular measurements from TOULOUSE.

- A better computer organization:

A CDC 6600 was always used for the orbit determination. The software improvement was based on good sense and on the very first rules of good programming. The orbit determination software was a big one, GIN, requiring the overlay method.

- Progress in theoretical methods:

Use of adapted parameters, mean element parameters, adjustment of integration steps depending on orbit type (90 s for transfer orbit, 15 mn for drift orbit for numerical integration method).

A second step, particularly important, was achieved for the satellite TC1-A.

Three new elements were to be taken into account:

- The satellite was one of a new generation: spin-stabilized in transfer orbit with a solid apogee boost motor, and three axis stabilized with rotating solar panels in final orbit.
- The ground tracking stations was new (2 GHz).
- It was the first launch (V10) of Ariane III with two solid propellant boosters.

The new definitions, presently used, were developed at this time:

- mission analysis in space mechanics,
 - ground segment configuration,
 - launcher interfaces,
- associated with operational organization.

During station acquisition, orbit determination programs were run on a big computer (CDC 750), while all others were run on mini computers (SOLAR): attitude determination, orbit and attitude maneuvers, data monitoring and displaying in real time satellite parameters.

We have improved the security, trying to install laws of organizations of work, people and global redundancy. The results were not always as expected. We can talk about the hot redundancy we tried to get with two mainframes CDC doing the same job (orbit determination) at the same time. This kind of machine is not synchronisable: the files of measurements taken into account by each computer were not the same at a time... and the results were not identical! the medicine was worst than the disease!

All the operations went off correctly with the SOLAR computers, but we could notice the heaviness of task linking, the difficulty of telemetry play-back for expert evaluation and à too great number of participants to these operations (computer specialists, space mechanics specialists...).

Attitude determination, although well prepared, caused some problems for the first TC1A. The choice of the good solution (confirmed by the apogee boost) was done thanks to the great competence of specialists in space mechanics; during attitude determinations, they were able to think calmly, relying on their experience which had grown during trainings of technical and operational qualifications.

An important effort had been made in the following fields:

- automatic acquisition of telex.
- automatic 2 GHz ground station designation.
- linking of orbit computation on CDC computer.

If the two first points were satisfactory, the third one was not very easy to use and not adaptable during operations.

As a consequence this task was completely rebuilt for future applications.

In that case too, accumulated experience was beneficial to CNES to define more flexible and outstanding systems.

1.3. Operational and commercial space (from 1987)

CNES activities, then increased with the following programs:

- Earth observation SPOT 2-3-4, HELIOS 1.
- telecommunications TC1 B-C, TC2 A-B, INMARSAT 2 F1-2-3-4, ARABSAT 1C.
- direct broadcasting TELE X, TDF1, TDF2.

All the launching activity is to be preceded by intensive preparations.

For geostationary satellites station acquisition, an assesment of the experiences was done and only some key points are rapidly enumerated here after:

- Operational progress is mainly due to theoretical progress in space mechanics.

- The new theoretical methods must be converted rapidly in software application easily usable during the operations. The software must be easily extendable.

- The security is obtained by:

- good command and simplicity of the system,
- good knowledge of the users.

The informatic process aims at helping decision, as well as executing defined or rigid applications.

- People and system must be adaptable to new problems occuring during operations.

CNES, then has developed a new software system called MERCATOR, specially well adapted and performant for acquisition and on station phases of geostationary satellites.

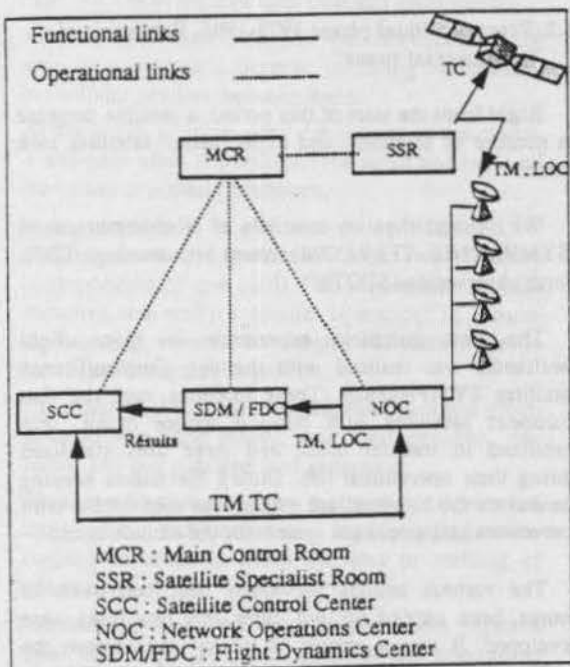


Figure 1: Functional scheme - MERCATOR is the informatic system of SDM

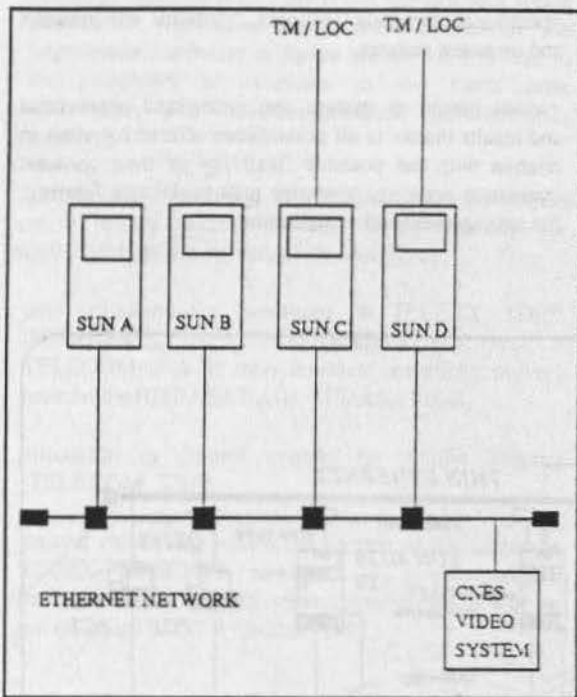


Figure 2: Functional scheme of MERCATOR

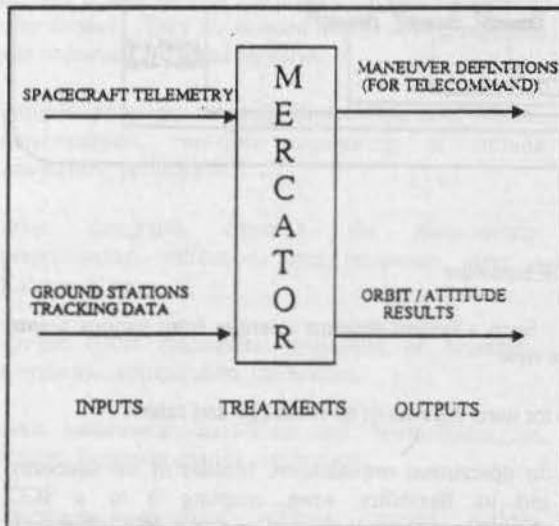


Figure 3: Inputs and outputs of MERCATOR

MERCATOR (Méthodes et Réalisation pour le Contrôle de l'Attitude et de l'Orbite des satellites) is the informatic structure of the "Service de Détermination des Manoeuvres" (SDM).

This service is part of the ground system for geostationary satellites, in Toulouse Space Center (see Figure 1). Responsible for space mechanics aspects, it is an autonomous entity which receives information directly from satellite via the telemetry link and from the tracking stations via the ground connecting network. Its results are transmitted to the other components via video transmissions (see Figure 3).

The SDM is composed of two parts:

- the software system,
- the space mechanics applications.

The software system:

We are going to deal more particularly with the informatic system called Mercator. It is a system based on a distributed architecture as well as on hardware and software aspects.

The operational system for station acquisition is composed of four similar workstations (SUN) connected together by an ETHERNET network. The video, graphical and alphanumeric displays are distributed via PC or terminals (see Figures 2 and 4).

The software of the operational system is composed of three parts:

- link acquisition and data preprocessing,
- system supervision,
- man machine interface and process monitoring.

Each workstation runs the same software. The system may be run on a single computer; the choice of the four workstations is due to backup considerations and occasionally to run many tasks at a time.

It corresponds in fact to an applications structure for space mechanics programs.

This structure has been developed in order to minimize the integration effort for a new application, the maximum effort has to be done on the application itself.

Another aspect is the easiness to switch from a mission to another: about half an hour to configure the computer for a new mission.

During the development and training phases, we can run different missions on each computer.

When the space mechanics applications are integrated in the Mercator system, it allows the following tasks:

- data acquisition preprocessing (telemetry, localisation).
- real time orbit determination.
- maneuvers computation and real time monitoring for orbit and attitude.

- real time attitude determination.
- operational forecasts (eclipses, visibility for stations and on board sensors, ...).
- various means to analyse and understand phenomena and results thanks to all possibilities offered for users in relation with the possible flexibility of their choices: interactive drawing, telemetry play back, data filtering, file management and visualisation.

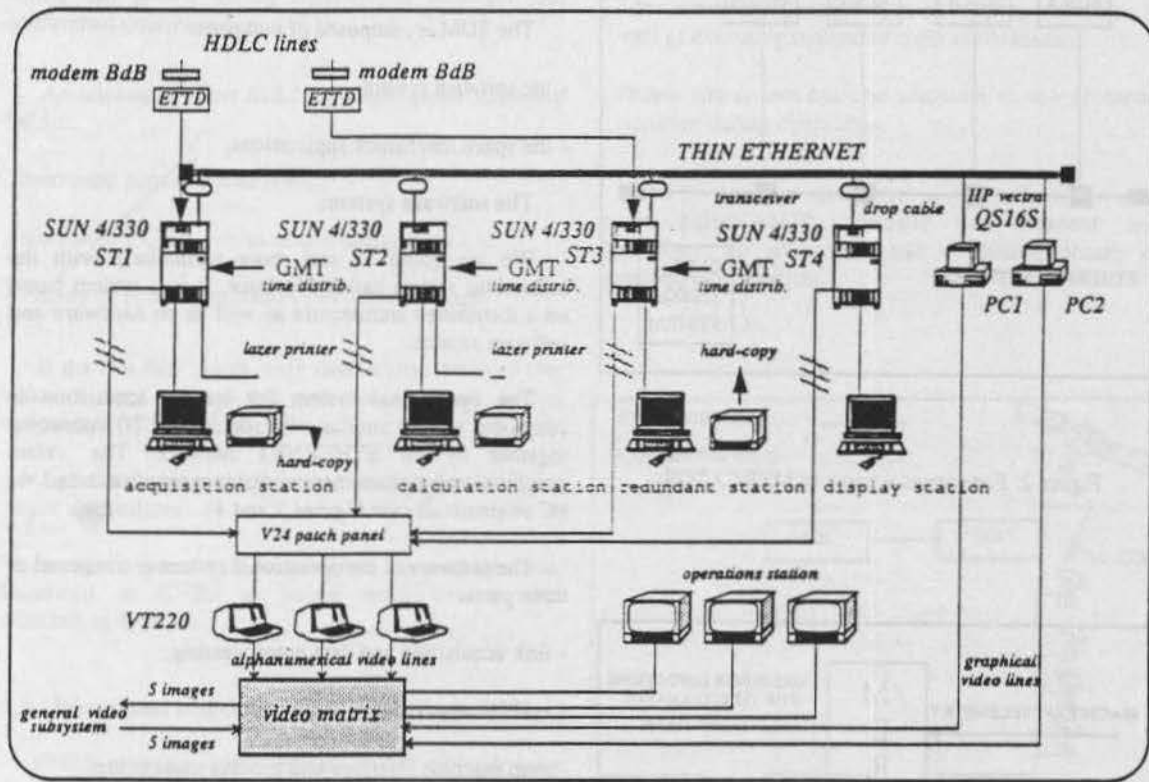


Figure 4: MERCATOR hardware

The performances of the system obviously works towards the good quality of the man machine interface.

Besides the compatibility of Mercator to UNIX commands and multi windows, we have at our disposal a great number of possibilities of extra analysis.

It is worth noticing that all the applications (mission analysis included) are nowadays developed on SUN; therefore the computer working interface, from preliminary studies to operation, is the same.

Such a system presents interests from various points of view:

- for users because of its flexibility and safety,
- for operational organisation, because of its autonomy and its flexibility when coupling it to a SCC (Specialized Control Center) and to a NOC (Network Operation Center: junction of data links, video, voice and ground stations coordinator).

- for the possibility of adaptation for the mission. As a matter of fact, MERCATOR is not devoted to a single mission; it will cover the mission defined by the implemented software of Space Mechanics and lead to the possibility of extension to low Earth orbit observation and telecommunication (constellation) satellites.

Numerous operational utilisations already performed turn it into a reliable product, facing perfectly the requirements of the operation: mission first!

- past utilisation for operations on TELE X, TDF2, INMARSAT 2 F1-F2-F3-F4, ARABSAT 1C, TELECOM 2 A-B; then foreseen operations in very near future HISPASAT A-B, TURKSAT A-B, ...

- utilisation in control centers for station keeping (TELECOM, TDF),

- ground validation, within the context of the launch of TOPEX-POSEIDON satellite, of an embarkable navigator using DORIS measurements which will be put on board SPOT 4 satellite (1995).

Space mechanics software:

About fifty space mechanics programs are implemented in the MERCATOR system for one mission of station acquisition. These softwares enable to cover all the nominal and foreseen non nominal cases of functioning of the satellite. They represent roughly about 60000 code lines in FORTRAN language. The C language is also used for the interface (graphics purpose: faster display). They are divided into several groups; the most important are listed hereafter:

- attitude: programs covering all the aspects of attitude determination, real-time monitoring of attitude maneuvers, calibration.
- orbit: programs covering the measurement preprocessing, validation, orbit restitution using a Kalman filter...
- apogee boost maneuvers: definition of strategies, simulation, optimization, calibration,
- orbit maneuvers: East-West and North-South, on station, longitude change, calibrations,
- operational forecasts: eclipses, ground stations visibilities, sensors visibilities and dazzlings...
- monitoring and computation for the three-axis acquisition phase for normal mode,

- genral tools: programs providing facilities to help for computations and decisions.

Two main points made it possible to imagine and realize the MERCATOR system:

- CNES engineer experience in spacecraft operations,
- workstations whose power and flexibility allow a dispatching of the tasks and a more secure development and exploitation.

Therefore the marriage of the two basic techniques: informatics and space mechanics ensure the success of such a product.

Today, MERCATOR works perfectly well not only for transfer orbit operations but also for informatic structures for the station keeping of the satellites whose exploitation is ensured by the CNES.

2. Present strategy

The real commercialisation of space applications occurs, till now, only for geostationary satellites.

This justifies the choice of the CNES: developing the MERCATOR system working for a given application at the beginning point. This system is entirely exportable: it will work for the operations of the two spanish satellites HISPASAT. At the moment, MERCATOR is being installed in Madrid and will be processed by the CNES during autumn 92 and spring 93.

Today, facing the total success of the operation, the CNES is developing OREMUS (Orbite, Restitution, Extrapolation, Manoeuvres, Utilitaires, Simulations) which is a generalization of MERCATOR for the following aspects:

- handling all kinds of space mechanics applications for a ground control segment,
- independence with the builders of workstations. OREMUS is a new informatic structure able to handle all the functionalities of space mechanics necessary for the different missions of the satellites.

That means a significant cut in cost if we consider the various MMI (Man Machine Interface) which are always redefined and realized by the new projects; now they can be developed with OREMUS.

The CNES is in a good position to enforce this policy: today several MMI of space mechanics were developed or are on development: MERCATOR, orbital operational center, SPOT 1-2-3, HELIOS 1.

- station acquisition of geostationary satellites,
- station keeping of geostationary satellites,
- station acquisition and keeping of low Earth orbiting satellites,
- station acquisition and keeping of constellations of satellites,
- flight control center for HERMES or space stations,
- interplanetary navigation.

OREMUS applications

It is urgent to complete the development of OREMUS in order to avoid an increase of the number of MMI which would be imposed by new projects (HELIO 2, S 80, ...).

OREMUS will be operational by mid 93. Afterwards this structure will be advised to projects managers to reduce the cost of development and maintenance.

Of course the development of space mechanics software, peculiar to missions, is not taken into account. It is worth noticing that these software programs will be introduced in a library which will be used by OREMUS. This is a guarantee of consistency and safety of development, of respect of programming standards, of software quality, of fast assembling and tests for the new developments.

For the realisation of a ground segment for Space Mechanics, thanks to OREMUS, we consider that the informatic development will be from five to ten times less expensive. Naturally this factor of reduction may only be applied to two parts: on the one hand the sequencing of tasks (which represents between 100000 and 200000 code lines) and on the other hand the unitary and global tests.

The further asset of OREMUS is the capitalisation and transmission of knowledge; every new group in charge of informatic development gains a precious time by reusing an operational reliable product.

In space mechanics, theoretical studies carried out today on orbit control deal mainly with analytical theories using mean parameters for restitution and long term prediction so as to cope properly with the problems connected to constellations. Moreover the matters of relative orbit control of several satellites will be soon studied.

3. Future

Together with the realisation of OREMUS, CNES is interested in two thematic aspects:

- The introduction of expert systems to help expertise and decision. A first realisation (CORTEX) within the context of orbit determination leads us to take this possibility cautiously. For us an expert system can only

be used in limited conditions that is to say in a case of well defined routine (for example orbit restitution of a given satellite).

A second realisation is in progress within the context of space mechanics mission analysis of HERMES. It will help defining and taking into account the sensitive parameters in order to work out the first phases of the rendezvous strategies (handling constraints of final fuel budget, duration of phases, crew life, ...).

The purpose of this realisation is to help the control center to take account of new conditions and constraints.

More generally, as far as OREMUS is concerned, an analysis is performed now to specify the themes for which the expert systems could help us in interpreting and taking decisions.

- Autonomous navigation of satellites.

In order to simplify ground operations, several organisations or industrials are proposing onboard autonomous navigation systems. Within the frame of the R & T (Research and Technology) program, the CNES decided to embark in the SPOT 4 satellite, whose launch is planned in 1995, a real time orbit determination system (utilisation of doppler DORIS measurements). The identification of orbital parameters using a Kalman filter leads to the insertion of the orbital results in the image telemetry of the SPOT 4 satellite.

Afterwards more complete realisations may be developed making it possible to compute and realize genuine on board orbit corrections and maneuvers.

An economic survey is in progress now: the CNES has chosen a contractor to study the economical conditions of the world-wide market of autonomous navigation of satellites.

It is proper to notice that whatever the level of automatism accepted on board is, the ground center for mechanics aspects will have to adapt itself to the best compromise board-ground. Moreover any extra automatism will increase, at the very beginning and during many months, the monitoring and redundant computations. This points out the advantages of OREMUS whose characteristics allow a very easy adaptation in regards to the specification changes without requiring prohibitive costs of development.

The authors want to thank Roger Laurat, Colette Aubert and Magali Tello for their contribution and Françoise Foliard for her help in the translation.

INTER-AGENCY CROSS-SUPPORT A DECADE OF EXPERIENCES BY GSOC

Wilfried Kruse, Martin Pilgram
DLR - GSOC
Münchener Str. 20
D 82234 Wessling
Germany
email: Pilgram@GSOC0007.rm.op.dlr.de

Abstract

Inter-agency cooperation in the support of space missions is known as cross-support. The advantages of cross-support include an extended ground station network for space missions and a reduction of costs by a more intensive utilization of existing resources. GSOC has gained much experience in the area of cross-support for several missions with various space agencies. In each case GSOC implemented Gateways in order to obtain access to the foreign space data networks. The function of the gateway is the communication protocol transformation and conversion of data formats. With gateways GSOC is capable of linking different foreign space agencies together.

While cross-support for telemetry data is not too difficult, problems arise for command and for tracking data.

CCSDS is chartered with developing a standardized solution to make cross-support easier to realise.

Key words: Cross-support, Communication, Gateway

between centers.

5. More intensive utilization of existing resources (Equipment, Manpower) reduces costs.

The major problem of cross-support between different international spaceflight agencies is the lack of an existing standard for these services.

Neither the quality nor the amount or level of service is standardized. The data transfer protocols and data types are also not defined.

In a situation where only two agencies are involved, one agency needs to adapt to the type of service which is delivered by the other. This type of support has been given many times by various agencies to external space missions during previous years.

If for a certain space mission more than two agencies are involved, and not all of them are prepared for mutual cross-support, the problem can be solved by a foreign ground station supporting the designated control center via a third agency as nodal point.

With this type of support the amount of communication equipment, number of data links, and the number of communication interfaces can be reduced.

General

Agency internetworking in the support of space missions is known as cross-support. This type of support is not only needed for Launch and Early Orbit Phases (LEOP) but also during standard satellite and spacecraft operations. Joint projects involving more than one agency usually require as well inter-agency cross-support.

There are many benefits derived from cross-support cooperation. Some of the advantages include:

1. Additional tracking stations provide a better coverage for the spacecraft control and operations.
2. Launch and transfer orbit support from an extended ground station network.
3. More ground stations provide redundancy for station support in critical phases.
4. Exchange of data for co-operative space missions

Cross-Support Scenarios

In a typical cross-support situation one agency usually acts as consumer of services while the other partner acts as service provider.

A. The service consumer agency requires the following services:

1. Usage of ground stations from an external agency for support of satellites controlled by their own with real-time telemetry, commanding capabilities, and tracking services.
2. Off-line telemetry data transmission from the station and orbit information from external agencies.

B. In response the service provider agency is providing the following services:

1. Real-time support of a spacecraft from an external

agency with telemetry, tracking data, and also telecommand capabilities via the ground station.

2. Off-line telemetry transmission and orbit information for the foreign spacecraft.

C. In some situation an agency is requested to act in a bridging function as service consumer and provider at the same time. The agency is acting as intermediate contact and routing node to connect a foreign spacecraft control center with a ground station or control center of a third agency.

While cross-support of the first two types have already been practiced by several spacecraft agencies, the third support type would appear to be a unique capability of GSOC.

Supported Missions

GSOC has gained experience over more than 10 years with cross-support services for a number of different space missions.

Support from foreign ground stations for GSOC controlled satellites.

Scientific Satellites:

AZUR
AEROS-A,B
AMPTE
HELIOS-A,B
ROSAT

Geostationary Satellites:

SYMPHONIE-A,B
TV-SAT 1,2
DFS KOPERNIKUS 1-3
EUTELSAT F II Series 1-5 (LEOP)

Support of satellites from other agencies by the DLR ground station (Weilheim) for spacecrafts:

VOYAGER-1,2
TDF 1-2
IRS-1A,1B
GIOTTO
GALILEO
ULYSSES
EUTELSAT F II Series (Operations)

Support as a third agency nodal point for satellites:

IRS-1A,1B (ISRO - GSOC - NOAA)

IRS-1A,1B (ISRO - GSOC - ESA)
TDF-1,2 (CNES - GSOC - ESA)

Telemetry and telecommand data services with spacecraft Electrical Ground Support Equipments (EGSEs) at integration sites or the spacecraft simulators satellites:

EUTELSAT F II (ASCA)
ROSAT (DORNIER)
TV-SAT (MBB)
DFS KOPERNIKUS (NASA/KSC)
D-2 Spacelab (SIMULATOR, MBB/ERNO)

Cross support with NASA for the Spacelab missions:

FSLP (SPACELAB-1)
D-1
D-2

Support for remotely located User Support Centers during the D-2 mission.

Microgravity User Support Centre (COLOGNE)
Microgravity Advanced Research and Support Centre (NAPLES)

Gateways

A gateway is a computer or switching device for translation of protocols, logical sets, voltage levels, etc. from one network to another. For a cross-support gateway the two major tasks are the handling of two different communication protocols and the transformation of the data type structures from one standard to the other.

While the communications protocol handling can be done without major difficulty, problems arise for the transformation of data blocks. The different data structures are often not totally compatible. In addition problems also occur from different procedures for station commanding, if requested.

A gateway is sometimes required for obtaining access to a software simulator located in-house, when the simulator does not use the standard local agencies interface.

In some special situations cross-support can be provided without using a gateway. The external user of a ground station might bring its own communication equipment to the ground station and connect it to a public line. In this case the station looks to the agency as a remote entity of its own network.

This method has been used for commanding of GSOC controlled satellites via the Indian ground

stations at Bangalore, India.

In very seldom cases network characteristics are closely compatible and the role of a gateway is then very simple.

(NASA - NOAA - CNES), (ESA - EUTELSAT)

Network Characteristics

GSOC implemented Gateways to the space data networks of CNES, ESA, EUTELSAT, ISRO, and NASA. The networks have the following characteristics:

	Data-Unit Standard Used	Communication Protocols
CNES	NASCOM-var.	NASCOM/HDLC
DLR	DATANET	DECnet
ESA	ESA-Stand.	X.25 Level 3
ISRO	ISRO-Stand.	X.25 Level 2
NASA	NASCOM/GCF	NASCOM
NASA	CCSDS	D-2 specific
EUTELSAT	ESA-var.	X.25 Level 3

In comparison to NASA, ESA, and CNES, DLR is a smaller agency, and had to adapt all the external procedures and protocols for cross-support in order to obtain support from the other agencies.

As a result of this GSOC is in a situation to interwork with quite a number of different agencies and companies. These capabilities are not only necessary for DLR projects but can also be offered to other agencies to enable them, within a short time frame, to interconnect to another agency where no cross-support service exists.

Gateway Problems

While external ground station cross-support for a control center with telemetry is relatively easy, the support with commanding capabilities is more complex due to the different procedures and protocols for spacecraft commanding at different agencies. Also cross-support with real-time navigation data is rather complicated and has been achieved only in individual cases.

The specific problems for the different services are listed below.

Communication Procedures

Some communication protocols require procedural agreements to establish the network connection in MASTER - SLAVE relationship. In general control

centers act as master (Client) while ground stations act as slaves (Server). For cross-support the gateway must act as a client if a foreign ground station is used but it has to act as a server if a foreign control center asks for station support. To support both cases it might be necessary to implement two different types of gateways, one as server, the other as client.

Different spacecraft, source, and destination codes within the network data block header fields require a transformation of codes by the gateway. This transformation is usually table driven and has to be updated for any new mission or ground station.

Another problem occurs if the control center uses procedures as Subsystem Alive Requests or Station Commanding which is not supported by the foreign ground station. In this case these procedures must be disabled at the control center, or the gateway has to simulate the station response with a fixed message that says "everything ok".

Telemetry support

A frequent problem for cross-support with telemetry data occurs if one partner is using frame synchronized data and the other is not. While many ground station do already frame synchronize their telemetry data by hard- or firmware, a gateway has to frame-synchronize the data by software due to the asynchronous data input and the transport frame overhead. Conversely a "frame desynchronizer" is sometimes required.(Ulysses telemetry support from DLR ground station Weilheim)

In addition the Earth receive time must be recalculated for transmission in either directions.

Status information about Frame Sync is sometimes incompatible between different agencies, and station equipment configuration parameters are very often either incompatible or unavailable. Parameters such as AGC or SNR are sometimes not supported either.

Stations which have been more or less automated are unable to retrieve stored telemetry data from archive without a request from the client over the space network. This is not usually a built-in feature for the foreign agency gateway.

Commanding Support

Cross-support for spacecraft commanding is relatively easy to implement in a gateway for commanding in "Throughput Mode" without response messages. If station reponse messages are required, the messages are handled differently for each network protocol. For example CNES responds by sending a copy of the forward command block, while ESA returns detailed information about the transmission

status.

The conversion of status information from protocol to protocol is not uncomplicated and sometimes cannot be exactly mapped to the original protocol format.

For a "Store and Forward" commanding mode very sophisticated procedures must be implemented as part of the command system.

Tracking Support

Due to different station equipment and measurement procedures real-time tracking support has only been done without transformation of the tracking data format. In some cases the network header had to be transformed for transmission purposes. The tracking data formats from different agencies are very dissimilar and no attempts have been made for format conversions. The real-time data is usually directly processed by preprocessing software in front of the flight dynamics system. Even DLR uses two different tracking systems, the data is processed offline to a unique data format.

Off-line state vectors (ICV's) are usually formatted in ASCII and therefore more a standard type, so only the network headers need to be converted.

An often used procedure for off-line tracking data transmission is the sending of text messages by facsimile or by text data messages within the space data networks.

Text Data

Some space networks include the possibility of off-line text data transmission. Because this is usually data encoded in ASCII the data transformation is not necessary and only changing of network headers is required.

CONCLUSIONS

As a result of the issues described above a need of an international cross-support standard is evident, while in future a stronger demand for this type of support is to be expected.

The final goal should be the definition of standards for real-time and off-line services for cross-support. As this requires the implementation of general service standards, it may take a long time before these standards are available. An intermediate solution would be an inter-agency cross-support standard that could reduce the number of different gateways to one and also enable the usage of ground stations where no cross-support standard has been implemented.

A simple first step could be a coordination of all agencies to use unique spacecraft, source, and destination codes.

CCSDS, an international standardization organization, is chartered with developing standardized solutions to common problems in the handling of operational and scientific data from space missions. The goal of this standardization is to help foster an environment whereby different space agencies can more easily cooperate with each other in inter-agency support of space missions.

Therefore, CCSDS is producing recommendations for defining the way that selected data services are handled between space agencies.

All space agencies should be called upon to participate in this endeavour.

GROUND SYSTEMS II

1. Suard, N. and Durand, J.C. (CNES-France):
"A Processing Centre for the CNES CE-GPS
Experimentation" 341
2. Garlick, D. (Utah State University-USA):
"A Distributed Ground Based Data Processing System
for a Scientific Satellite" 346
3. Gremillon, P. and Gaullier, F. (Matra Marconi Space-
-France):
"Turnkey Solutions for Satellite Operations" 353
4. Kehr, J. (DLR-Germany) and Salter, W. (Cray Systems-
-U.K.):
"The Planned European In-Orbit Infrastructure and
the Role of the DLR Manned Space - Laboratories
Control Center (MSCC)" 361
5. Fournier, D.; Boutonnet, G.; Orsal, E. and Piéplu,
J.L. (CNES-France):
"The French Scientific Mission Centre for the Mars
94/96 Mission" 369
6. Lundin, S.; Grahn, S. and Holmqvist, B. (SSC-Sweden):
"A Reliable High Performance Control Centre for
Scientific Satellites Using Personal Computers" 376

A PROCESSING CENTRE for the CNES CE-GPS experimentation

Norbert SUARD - Jean-Claude DURAND

C.N.E.S. - CT/TI/PS/AP & SDS/SM/ES
18 av. E. Belin
31055 TOULOUSE Cedex - FRANCE

Abstract

CNES is involved in a GPS (Global Positioning System) geostationary overlay experimentation. The purpose of this experimentation is to test various new techniques in order to select the optimal station synchronization method, as well as the geostationary spacecraft orbitography method. These new techniques are needed to develop the Ranging GPS Integrity Channel services.

The CNES experimentation includes three transmitting/receiving ground stations (manufactured by IN-SNEC), one INMARSAT II C/L band transponder and a processing centre named STE (Station de Traitement de l'Expérimentation).

Not all the techniques to be tested are implemented, but the experimental system has to include several functions; part of the future system simulation functions, such as a servo-loop function, and in particular a data collection function providing for rapid monitoring of system operation, analysis of existing ground station processes, and several weeks of data coverage for other scientific studies.

This paper discusses criteria for the distribution of software functions between ground stations and the processing centre and between the processing centre and different processing centres for scientific data, as well as system architecture, the approach used to develop a low-cost and short-life processing centre in collaboration with a CNES sub-contractor (ATT-DATAID), and some STE project results.

Keywords : Ground System, Architecture, Software.

1. Introduction

The GPS system offers exceptional qualities (accuracy and worldwide coverage). But for civil aviation (see (1)), this system has three major drawbacks :

- insufficient integrity,
- limited availability,
- voluntary spatio-temporal degradation.

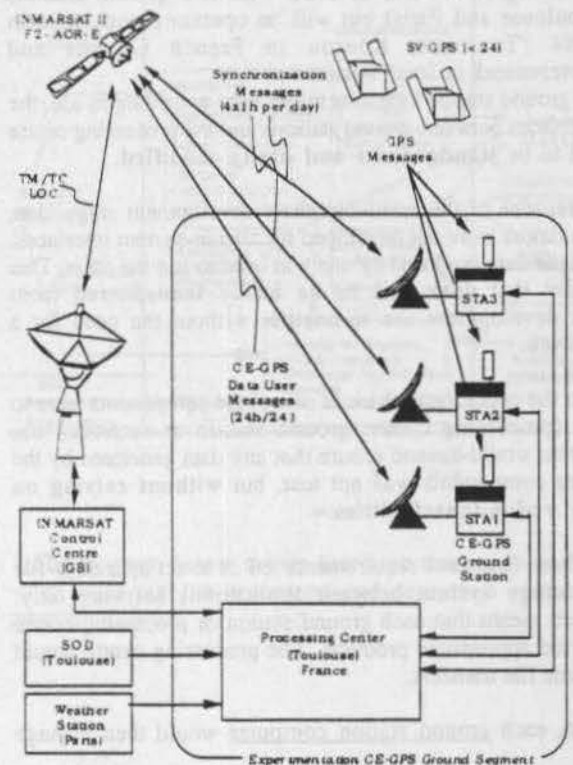
Ranging GPS Integrity Channel services (RGIC) should

enable GPS to be used by civil aviation.

The experimentation prepared by CNES (see (2)) is dedicated to the technical validation of the Ranging GPS Integrity Channel concept that always needs :

- station synchronization better than 10 ns,
- GPS-type signals transmitting,
- geostationary spacecraft orbitography better than 10 meters.

The CE-GPS (European complement to GPS) experimentation includes a master ground station transmitting a GPS-type signal to an INMARSAT 2 geostationary satellite. The repeater broadcasts this signal in L-band to the master station and to the other stations. These also have receiving and transmitting facilities for GPS-type signals.



Each ground station includes a computer and software to :

- record broadcasted and raw data from several facilities,
- process some of the data in a real time loop (0.6 seconds) to generate transmitting signals correctly,
- control and monitor equipment,
- make some of the data available to the processing centre.

Other data (such as orbital and some weather parameters) required to drive the system or for various scientific studies are centralised at the processing centre.

The functions of the processing centre (STE) are to :

- prepare data for ground operation control station schedules,
- collect data from ground stations and other sources,
- archive and distribute these data to different scientific teams, sometimes after specific processing,
- monitor ground station operations.

2. Context and criteria for the distribution of software functions

2.1. Distribution between ground stations and processing centre

The system may use different configurations, with one, two or three ground stations. For example, this system was operating at the end of 1993 with two ground stations (Toulouse and Paris) but will be operating with three in 1994 (Toulouse, Kourou in French Guyana and Hartebeesoek in South Africa).

As ground station locations might vary according to use, the interfaces between ground stations and the processing centre had to be **standardised and easily modified**.

Because of the relatively short development stage, data simulators were not developed for all sub-system interfaces, and the data produced by one was used to test the other. This meant that **data had to be easily transported** from one development site to another without the need for a network.

In the operational phase, if one of the components were to fail (processing centre, ground station or network), the system would have to ensure that any data generated by the other components was not lost, but **without relying on any redundant facilities**.

These first three requirements led us to set up a **data-file exchange system** between applications software only, which meant that each ground station or processing centre needed appropriate products. The processing centre would initiate file transfers.

So, each ground station computer would then manage

short-term file-saving (over a few days), while the processing centre would manage long-term archiving for all ground stations and all system configurations used.

As ground stations include a real-time loop to generate GPS-type signals, it was decided that the main processing system in each ground station should collect all data from all facilities through RS232 or IEEE links, even though the processing centre would be able to obtain data through a different link. This provided an **uniform means of data exchange** between any ground station and the processing centre.

One of the aims was to cut down manual operations in ground stations so that they would not need to be staffed on a permanent basis. All operations where data has to be **keyed in manually** are carried out in the **processing centre**, and the results file is then transmitted to the ground station (before the operational phase, data may be input with a text editor as the data in these files is in ASCII format).

NB : The only manual operation needed under normal station operating conditions is a twice-weekly cartridge change.

Another point we observed was to **avoid allocating to ground stations any processing occurring at irregular intervals** as site and azimuth angles processing, so that real-time loops would not be affected by a random load peak. Any such processing is carried out at the processing centre and gives results files that are valid over the whole operational period and transmitted. The ground station software only uses indirect time and date addressing to retrieve data when needed.

The final point was to provide for monitoring of station operation. **Station monitoring** from the processing centre is **not carried out in real time**, for two reasons :

- 1) equipment is more and more reliable :
- 2) the loss of a few data-days is not a problem, but when the data collection function is operating, we have to be certain that the data is correct.

To meet this requirement, ground station software stores three types of data in monitoring files.

The first type is made up of raw data extracts, the second of extracts of equipment command data received and distributed by the servo-loop mechanism, while the third type consists of monitoring indicators generated on ground stations (watchdog function for the various flows of expected data, quality indicators for INMARSAT 2 satellite links as bit error rates, etc.).

These monitoring files are processed by dedicated software at the processing centre using simplified equations to describe observable phenomena. The operator can then display the resulting parameters in graph form. The curves change colour if values exceed monitoring thresholds, which take into account the simplifications in the equations.

2.2. Distribution between STE processing centre and scientific processing centres

The first criterion was to avoid imposing specific types of equipment on scientists configuration. Hardware for data exchange was defined for each processing centre for scientific data, STE processing centre which would be responsible for setting up a hardware and software configuration based on existing facilities at CNES.

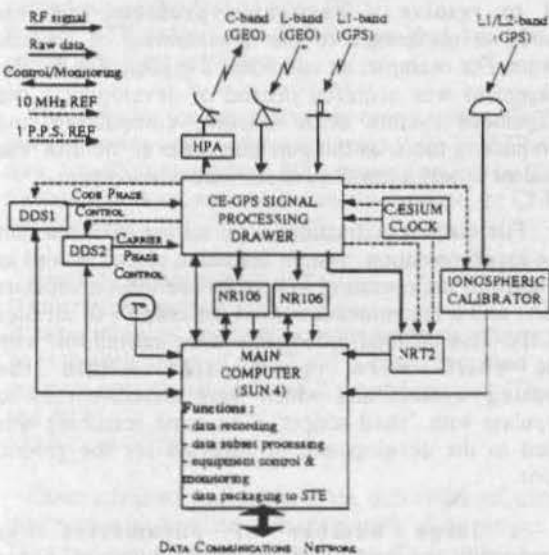
The second criterion was to develop and operate at the processing centre any data pre-processing software which would be common to at least two scientists.

The third criterion was to keep options open for specific software to be set up within the processing centre to enable the operator to pre-process also scientific data, as the processing of raw data to obtain interpretable results can otherwise be very time-consuming for the scientists using them.

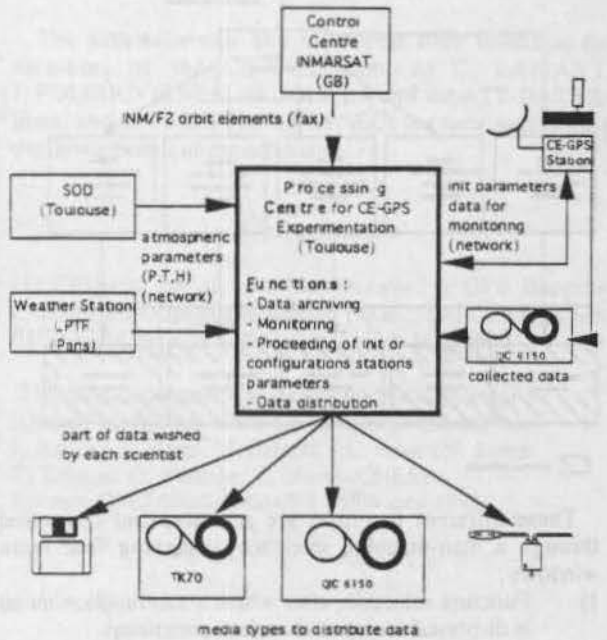
3. Architecture

In this chapter, the architecture of the ground station and of the STE are presented. The first diagram gives an overview of the ground station architecture. The others detail the processing centre architecture.

3.1 Ground stations architecture

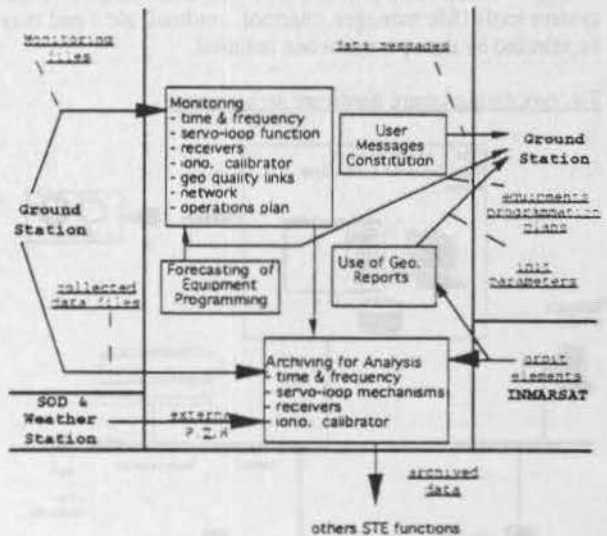


3.2. processing centre architecture : external links

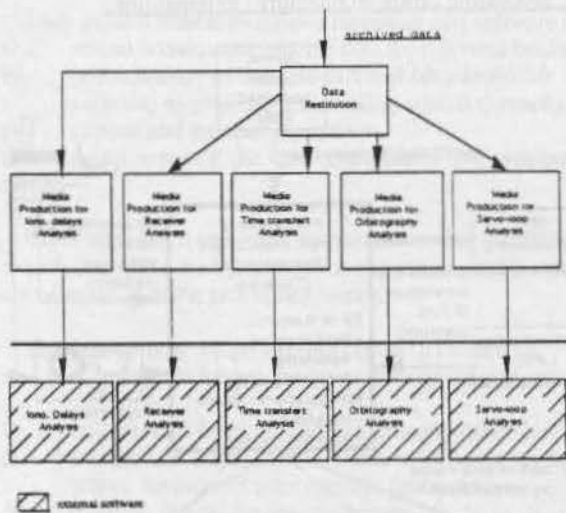


3.3. processing centre software architecture

The diagram below shows functions that are only used when data are collected.



The diagram below shows functions that are only used when data are pre-processed and sent to a scientific processing centre.

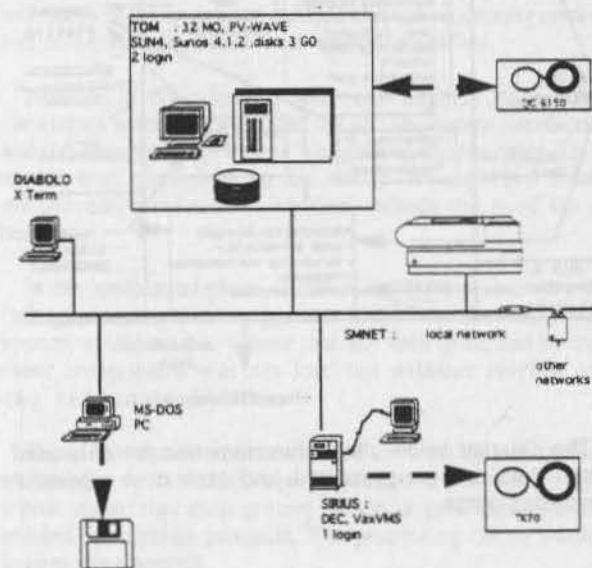


These different functions are activated and controlled through a man-machine interface displaying four main windows :

- 1) Function selection, after which a sub-function menu is displayed for input of various parameters.
- 2) Display of the number and type of tasks currently running.
- 3) Output of task messages.
- 4) System message output (console).

Other windows are available with OPENLOOK SUN system tools (file manager, calctool, cmdtool, etc.) and may be selected by the operator when required.

3.4. processing centre hardware architecture



4. Approach used in STE development

The processing centre software was to be written by a specialised firm, and to have it ready on schedule (development began in November 1992 for partial implementation at the end of March 1993), without the constraints involved in managing too large a team, the following considerations were applied.

1) As the processing centre would be operating for no more than 2 years, the **normal rules of management were made more flexible**. The alterations mainly concerned reviews at the end of each development phase and the documents to be managed within the configuration. For this processing centre, key-points with only the CNES and ATT-DATAID technical managers present were substituted for all reviews. This rule remained valid as long as no major differences arose between ATT-DATAID and CNES.

2) A study was carried out before the contract was signed, to assess the possibility of **including existing products** to meet requirements for all or some of the functions needed. Such products would be incorporated by adapting the new software packages to the interfaces. The functions delivered to ATT-DATAID thus included graph-plotting (developed in PV-WAVE command language), orbit computation functions for the geostationary and GPS satellites and computing routines for tropospheric delay factors.

3) Whenever existing **low-cost hardware could be used to resolve a particular problem**, this was acquired in preference to the development of specific software. For example, an additional 2 gigabit disk for file management was acquired instead of developing a file management system with existing compacting and decompacting tools, as the purchase price of the disk was equivalent to only a few days of software development.

4) File name specifications were set out from the start of the experimentation system definition phase, as well as the choice of the operating system for the main computers (UNIX) and a recommendation on the content of all files (ASCII). This enabled processing to be carried out with **tools which were incorporated within the operating system** and which were therefore easy to manipulate with "shell-scripts". The same reasoning was applied to the development of software for the ground stations.

5) A **large number of parameters** was incorporated into the processing centre software, either within configuration files to be handled by the text editor or as data to be keyed in through the man-machine interface. This last solution does not affect costs as the centre is permanently staffed (except at weekends) during system use.

6) In order to maintain autonomy between functions and to avoid over-automation of the processing centre, some data input is carried out by the operator even where such data can be deduced from available data in the processing centre.

7) The software for the processing centre was delivered in several stages :

- Stage 1 : man-machine interface ;
- Stage 2 : all data collection functions (see first diagram in 3.3) ;
- Stage 3 : all data distribution with scientific data pre-processing ;
- Stage 4 : incorporation of specific processes when requested by a scientist.

This method enabled real progress in processing definition to be monitored without the need to program everything in advance.

Tasks were therefore not scheduled in the usual sequence for this type of development (definitions - specifications - realization).

This is not always advantageous (project management is more demanding), but the final product is better matched to the real needs of different users.

5. Some results

ATT-DATAID supplied 230 working days to write the processing centre software, starting on the 2nd November 1992 and ending with Stage 3 acceptance tests which were carried out on the 21st of April 1993.

For the STE project, the CNES work-load over the same period amounted to 70 days.

The software for this processing centre comprises 17 000 lines of source code without annotations (in FORTRAN, C, awk, shell), of which 4 000 were supplied by CNES. Certain functions were also directly supplied by CNES as binary codes.

Anomaly report number was :

- 16 after acceptance testing ;
- 29 after technical approval from the processing centre ;
- 34 at the beginning of the CE-GPS experimentation ground segment operational use with 2 ground stations (Toulouse and Paris) ;
- 47 on close of this operation.

Other scientists had access to the data collected, although they were not identified at the beginning of the project. They required no specific processing. To enable the system to produce and distribute their data, declarative instructions were input into the parameter files then tested (1 day work load).

Acknowledgments

The authors would like to express their thanks to the members of the CE-GPS team, to C. LAMANT, J. FOLIARD (CNES), H. JOUCLA and the ATT-DATAID team, and to F. SAFFRE (IN-SNEC) for their help during the development of the software.

Bibliography

(1) Proposal for an interface between a GPS Integrity Channel with Ranging capability (RGIC) and GPS receivers EUROCAE WG 28 Sub-Group 2, 13th May 1992

(2) *Définition détaillée de l'expérimentation CE-GPS* (Detailed definition of the CE-GPS experimentation)
J. Barbier, P. Brun, M. Brunet, J.L. Issler, N. Suard, T. Trémas, C. Valorge, C. Yven (CNES)
Ref note CNES/190/SDS/SM/ES - 15th april 1992

A DISTRIBUTED GROUND BASED DATA PROCESSING SYSTEM FOR A SCIENTIFIC SATELLITE

Dean S. Garlick

Space Dynamics Laboratory / Utah State University

1847 North Research Parkway

Logan, UT USA

dean@sd.l.usu.edu

Abstract

The SPatial InfraRed Imaging Telescope (SPIRIT III) is a cryogenically cooled, long-wave infrared (LWIR) five color band radiometer and interferometer space sensor that is the primary science data gathering instrument on board the Midcourse Space Experiment (MSX) spacecraft. The ground data processing of the SPIRIT III data is a key element in the success of the mission. The ground processing hardware consists of a distributed system of high performance workstations connected via a fiber optic network. The ground processing software performs automated monitoring functions, utilizes a relational database management system, and includes data visualization and data analysis tools. A key component in the ground data processing is the instrument pointing calculation. The complete process and the included errors are based on the instrument calibration, point source extraction, instrument to spacecraft alignment, and spacecraft attitude estimation. An automated method to monitor the parameters associated with the sensor pointing is presented in this paper.

Introduction

The algorithms, data processing, and technical applications of the principles discussed in this paper are focused on the SPIRIT III instrument. SPIRIT III is a cryogenically cooled infrared five color band radiometer and interferometer space sensor that is the primary science data gathering instrument on board the Midcourse Space Experiment (MSX) spacecraft, a U.S. government sponsored spacecraft that is scheduled for launch during 1994. The MSX spacecraft will provide state-of-the-art infrared radiometric and goniometric data for the scientific community. MSX is primarily a data collection experiment. The mission objective is to measure the spectral, spatial, and radiometric parameters of various objects, celestial sources, zodiacal emissions, the earth's airglow, the aurora, and other upper atmospheric phenomena. Contamination and background data pertaining to celestial earthlimb phenomena will also be collected.

Figure 1 shows the instrumentation aboard the MSX spacecraft, including the SPIRIT III sensor.

SPIRIT III is a long-wave infrared (LWIR) instrumentation package consisting of an extremely high-off-axis-rejection telescope; a five-color, high-spatial-resolution 4.2 to 26 micrometer multi-spectral radiometer; and a six-channel, high-spectral-resolution 2.5 to 28 micrometer interferometer-spectrometer, all of which are cooled to cryogenic temperatures by a solid hydrogen-filled cryostat/heat exchanger. Supporting the telescope, radiometer, and interferometer assemblies are a number of ancillary/diagnostic instruments, including an autocollimator for pointing corrections, various internal stimulation sources for calibration monitoring and updates, and other associated monitors and telemetry. The instrument telescope uses a scan mirror to provide the full field of regard coverage for the five color band (colors labelled A-E) radiometer with the instantaneous field of view being 1 degree x 720 micro-radians maximum for each color. Colors A, D, and E are coaligned and colors B and C are coaligned. The radiometer employs 3,840 detectors which are capable of imaging a 1 x 3 degree field of regard with a 90 micro-radian resolution at four samples per dwell in the in-scan direction and 2 samples per dwell in the cross-scan direction.

Ground Data Processing Overview

As with most scientific satellites, the ground data processing is a critical and an integral part of the mission success. The data processing task can be separated into two categories: 1) scientific data analysis, and 2) instrument performance assessment. Although the tools to perform both data processing tasks are similar, the primary focus of this paper is the instrument performance aspects of the task. Key elements in the performance assessment processing are data verification, instrument calibration, instrument parameter validation, pointing reconstruction, and instrument attitude uncertainty estimation. Since the instrument is collecting data on-orbit every day, verifying the operational boundaries and characterizing the instrument performance are critical tasks required to be conducted in a rapid manner. The required timely turn-around of the data analysis team necessitates a wide variety of data processing tools to quickly diagnose the health and performance of SPIRIT III, as well as provide a rapid assessment of the validity of the scientific data collected.

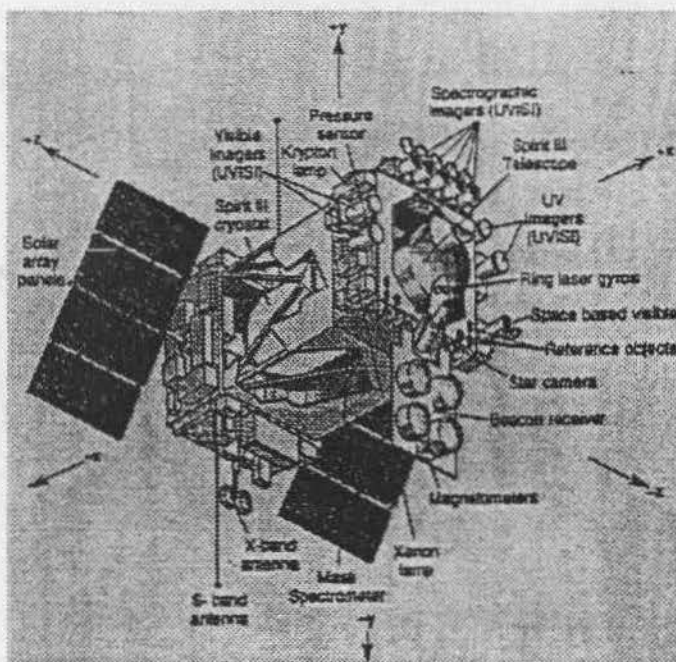


Figure 1. MSX Spacecraft

The data from SPIRIT III will be processed at the SPIRIT III Data Processing Center (DPC) located in Logan, Utah, USA. The flight data processed will consist of radiometer images, interferometer data, and housekeeping parameters, totalling approximately 8 Gigabytes of data per day, 7 days per week for 20 months. This results in an estimated total of 5 Terabytes of raw data for the entire mission.

Due to the complexities of the algorithms used in software development and the massive amounts of data to be processed, high performance computing capabilities were needed to meet the system requirements. Since large scale computers (e.g., Cray) are extremely expensive, additional hardware and software options were investigated. The final design of the DPC was based on a distributed system of high-end workstations with sophisticated custom designed and built software. This option provides the power, flexibility, and robustness of a classical high performance computing center at greatly reduced costs and much less expense to upgrade and maintain.

The main software functions in this distributed system consist of:

- Automated Processing Chain
- Relational Database
- Data Visualization
- Data Analysis Tools

Figure 2 outlines these components and demonstrates the interaction and interface between them. Each of these components is described in a subsequent section.

Hardware Configuration

The hardware configuration consists of a cluster of several high end workstations networked via a fiber optic connection as shown in Figure 3. This distributed system takes advantage of the high speed network and the distributed processing capabilities, and is designed to meet the processing requirements of the DPC. In the case of most hardware failures, a graceful degradation of the performance of the system will result as opposed to an immediate shutdown with loss of data processing, demonstrating the robustness of the system.

Furthermore, the system is easily to upgrade by adding additional nodes. There are several other advantages to this system such as maintainability and heterogenous system capabilities. The disadvantages are that the software must be "smart" enough to distribute the data to the various compute nodes in the system. Another disadvantage is the network and the possibility of it becoming a bottleneck in the system.

Automated Processing Chain

The automated processing chain in the DPC has the ability to perform several satellite data processing functions.

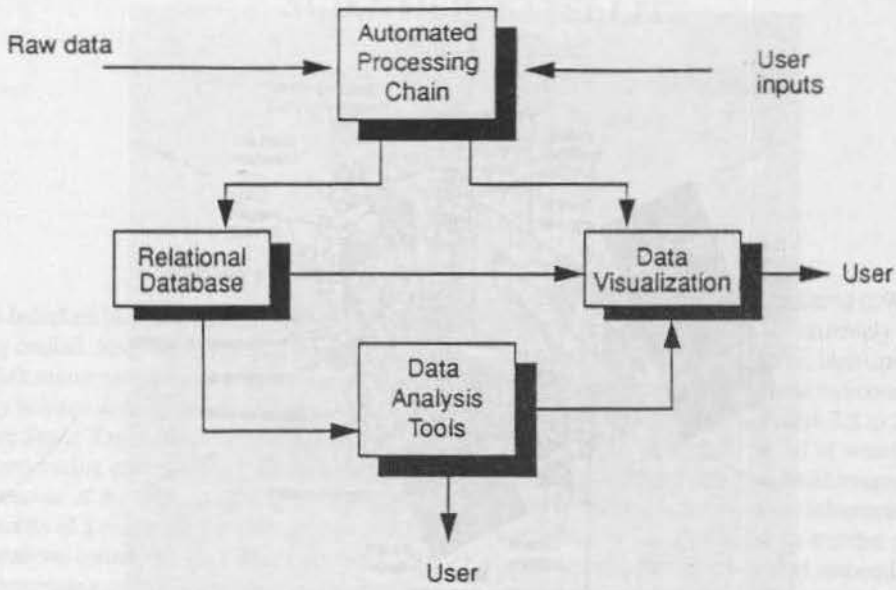


Figure 2. SPIRIT III DPC Software Components

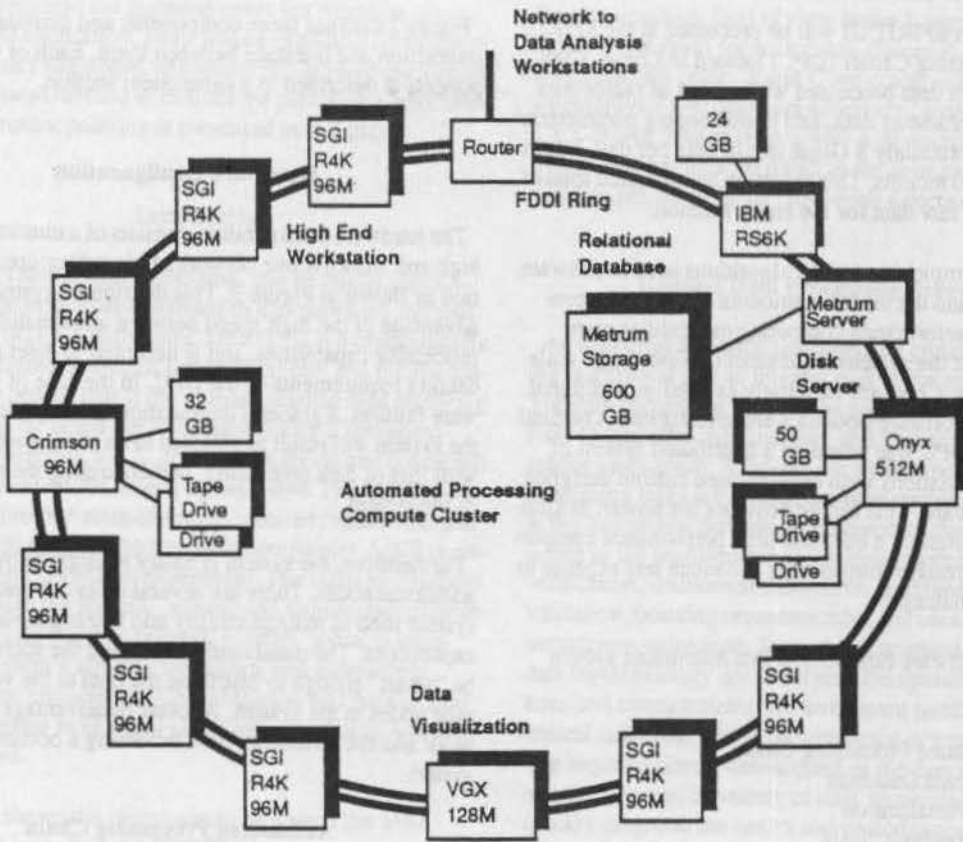


Figure 3. DPC Hardware Configuration

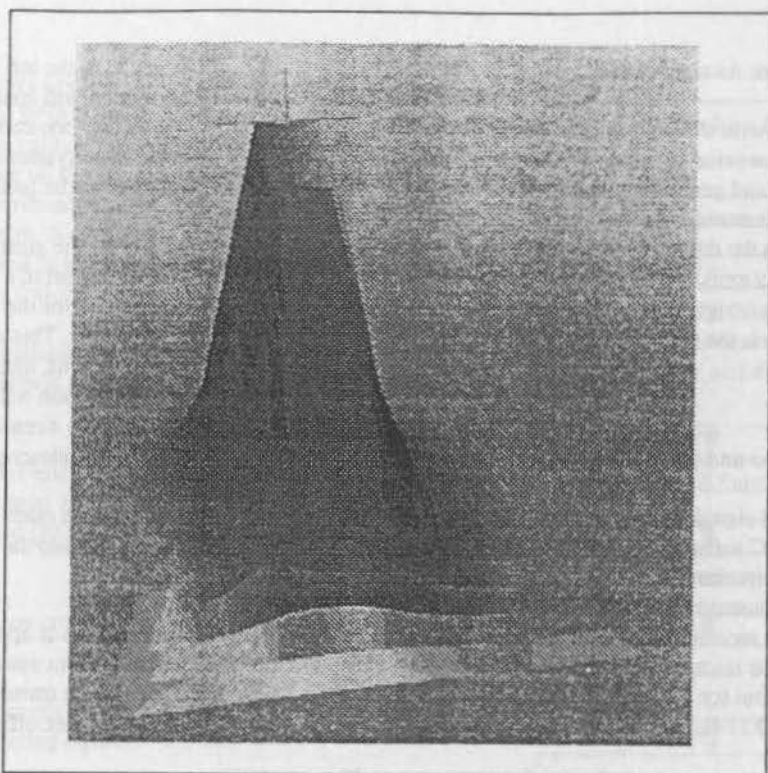


Figure 4. Radiometer Surface Plot with Point Source

These functions including the following:

- Automated monitoring and anomaly identification
- Data decoding and decommutation
- Spike detection and removal
- Statistical computations
- Conversion of raw data to idealized (calibrated) counts
- Point source extraction
- Attitude computations
- Automated star processing
- Other remote sensing and satellite processing functions.

The software that performs the automated processing was developed to support distributed hardware configuration described above. The unprocessed, or raw, data is broken into "images" and dispatched to one of the compute nodes with a corresponding task assignment. After the processing is complete on the compute node, the results are sent via the network to a common disk to be imported into the relational database for investigation and further processing with the analysis tools.

Relational Database

Due to the complexities of the SPIRIT III instrument and the massive amounts of data collected, a relational database program is required to analyze the results of the processing

and manage the data. The management of data sets of this size can become a significant, if not the most foreboding technical issue facing a data processing center of this type.

In addition to managing the data, long and short term trending and tracking are provided by the relational database. Query capabilities to analyze any correlation between instrument parameters and performance or to diagnose on-orbit problems make the relational database a critical element in the DPC. The details of the design, implementation, and operation of the relational database are beyond the scope of this paper.

Data Visualization

After the raw data is processed, data visualization is used to display the results of the automated processing chain. Visualization techniques are required to analyze the collected data sets mainly because of the massive amounts of data. The variety of processing tasks, high-performance computing capabilities, and the multiple outputs of the data processed lends itself naturally to a wide variety of data visualization techniques. Examples of the type of data visualization used in processing SPIRIT III data are shown in Figure 4.

Data Analysis Tools

Since most problems with the performance of the instrument cannot be foreseen prior to launch, the analysis tools developed are flexible and general in nature with some specific input and output formats and the ability to quickly interrogate and process the data in a variety of ways. A key element for the analysis tools is a seamless interface with the relational database. A significant effort was made in developing this software, the details of which are beyond the scope of this paper.

Key Algorithms and Processing Approach

Several important and significant algorithms have been implemented in the DPC software and hardware. One of the more interesting and important aspects is the pointing solution for the SPIRIT III instrument. As with most spacecraft, "after the fact" attitude reconstruction is essential to mission success. Not only is it important to reconstruct the attitude of the spacecraft, but for a science gathering instrument such as SPIRIT III, the pointing reconstruction of the sensor itself is critical. The SPIRIT III pointing reconstruction algorithm consists of those functions required to take a point source position in focal plane coordinates in one of the SPIRIT III color bands and compute the same position in SPIRIT III coordinates (boresight of SPIRIT III instrument), body fixed (MSX spacecraft) coordinates, or Earth Centered Inertial (ECI) coordinates. The algorithm to perform this calculation is shown in the equation below.

Given a point source position in instrument focal plane coordinates, $\vec{\rho}_{FPC}$, this equation will compute the same position in ECI coordinates, $\vec{\rho}_{ECI}$

$$\vec{\rho}_{ECI} = \mathcal{R}_{DAF}(t) \times \mathcal{R}_2 \times \mathcal{R}_{ac}(t) \times \mathcal{R}_1 \\ \times M_{distortion}(M_{coalignment}(\vec{\rho}_{FPC}, i))$$

Where:

$\vec{\rho}_{FPC}$	point source position in a specific color in the SPIRIT III radiometer
i	radiometer color band
$M_{coalignment}$	Colors A, D, and E are oriented to look to the right of the SPIRIT III boresight, and

B and C to the left of the same. This correction will coalign the radiometer colors into one common SPIRIT III coordinate system and adjust for any "tilting" of the focal planes.

$M_{distortion}$	As part of the ground calibration, and verified on-orbit, a curve fit will be determined for the optical distortion components. This assumes a K-order polynomial fit, distinct for each color. This correction will remove any distortion as a result of the optics in the SPIRIT III telescope.
\mathcal{R}_1	This rotation maps the SPIRIT III sensor frame data into the autocollimator coordinates.
$\mathcal{R}_{ac}(t)$	This rotation is applied from the frame for the current autocollimator offset angles to the frame existing when the autocollimator offset angles are (0,0).
\mathcal{R}_2	From the nulled autocollimator frame, the data is rotated via this rotation matrix to the spacecraft body-fixed frame. This function is the final step in aligning the SPIRIT III instrument with the spacecraft.
$\mathcal{R}_{DAF}(t)$	Rotation matrix from body fixed to ECI, which actually is the definitive (refined) attitude of the MSX spacecraft.
$\vec{\rho}_{ECI}$	Point source position in ECI coordinates.

Error Descriptions

The system uncertainty requirement for positional knowledge of a point source on the SPIRIT III focal plane arrays must be less than 9 microradians. To compute a point source position in ECI from the SPIRIT III instrument, errors will be introduced at the following points in the processing and data collection:

- Calibration uncertainty errors
- Point source extraction errors
- Instrument alignment errors
- Spacecraft attitude errors

Each type of error is discussed below.

Calibration uncertainty errors

The calibration of the SPIRIT III sensor is a very complex task. A majority of the calibration will be accomplished in the calibration chamber on the ground, but a few significant steps and some verification of the ground calibration will be executed on orbit. A condensed summary of the products to be generated as a result of the calibration of SPIRIT III include the following:

- Calibration equations and coefficients to compute idealized instrument counts from raw SPIRIT III counts.
- Point Response Function (PRF) characterization. The PRF is defined as the convolution of the Point Spread Function (PSF) with the detector response function.
- Optical distortion corrections across the Field Of Regard (FOR).
- Color to color coalignment. This provides the first term of the pointing equation (1).

Point source extraction errors

The steps for the point source extraction algorithm are shown in Figure 5. Each step is explained below:

1. Compute idealized (calibrated) counts using calibration equation and calibration generated coefficients.
2. Construct image using scan mirror position, spacecraft attitude velocity and, data time tags.
3. Using rolling ball filter to remove background of image.
4. Blob identification. Given some constant a , determine the average, μ , and standard deviation, σ , to compute a threshold T , where $T = a\sigma + \mu$. Select samples with amplitude greater than T and organize them into "blobs", defined as a set of pixels which are within some radius of another pixel within the blob. Additional blob discrimination is done using size, shape, amplitude, etc. to determine which blobs are likely to be responses from point sources.
5. Perform local background subtraction using a polynomial fit on the original data.
6. The point source extraction is performed by fitting a model PRF to the data. This is done by computing the maximum of the cross-correlation as determined by a maximization technique.

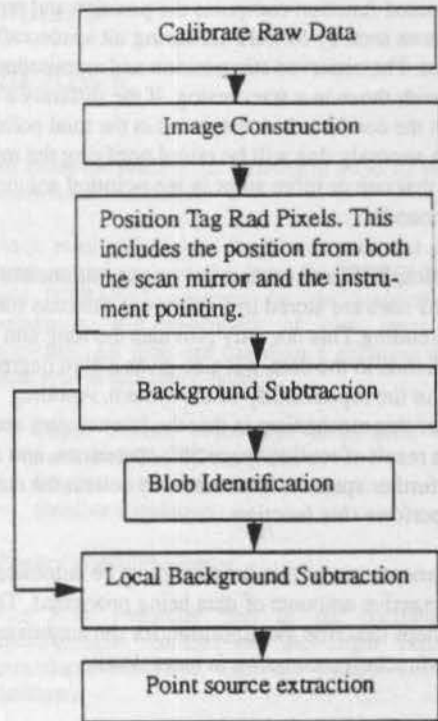


Figure 5. PSE Algorithm

Instrument alignment errors

The SPIRIT III instrument will be aligned with the spacecraft optical bench on the ground prior to launch. Since this alignment will most likely change after launch, several alignment experiments viewing clusters of known stars will be executed after launch to determine the updates necessary to the sensor alignment matrices.

Spacecraft attitude errors

There are several aspects of the attitude determination which can introduce errors. A complete discussion of the attitude determination is beyond the scope of this paper.

Automated Pointing Monitoring Function

There is a high probability that due to thermal gradients, spacecraft flexure, contamination, and other effects, the various components of the total pointing solution will change over time. To aid in the monitoring of the errors and calibration of the SPIRIT III instrument, an automated monitoring function was developed. Due to the large amount of data, the spacecraft schedule constraints, and the stringent after-the-fact pointing knowledge requirements, this method was needed to autonomously monitor the end-to-end pointing solution errors.

The automated function computes the position and amplitude of stars as seen by SPIRIT III during all spacecraft observations. The observed star position and amplitudes are compared with those in a star catalog. If the difference is greater than the combined uncertainties in the total pointing solution, an anomaly flag will be raised notifying the instrument team that one or more steps in the pointing solution are out of bounds.

The statistics, PRF, and other point source parameters of the observed stars are stored in a relational database for long term trending. This not only provides the long and short term trends in the data, but also gives a high degree of confidence in the repeatability of the system. Another advantage of this mechanism is that the known stars are viewed as a result of routine spacecraft operations, and thus require no further spacecraft resources to collect the data needed to perform this function.

The implementation of this function must be automated due to the massive amounts of data being processed. The following steps describe the algorithm for the automated monitoring function processing in more detail:

1. Apply calibration corrections to one scan of raw radiometer and housekeeping data.
2. Given one SPIRIT III scan, compute the ECI positions of the four corners of the image to generate the image boundaries.
3. Using spacecraft attitude and scan mirror position, determine the area of the celestial sphere seen in the image.
4. Interrogate the star catalog for candidate infrared (IR) stars that are located in the area computed in the previous step. If there are no stars in the area skip to step 10.
5. Compute the irradiance values and position of the stars in the radiometer image data.
6. Perform star matching with the observed stars and the catalogued stars to compute a rotation matrix for a given scan. Store the rotation matrix for trending.
7. Compare the position and irradiance of the observed data with the position and irradiance of the identified stars. Store the data and the differences for long term trending and repeatability.
8. If the position and or irradiance of the star is not in the catalogue, store the results for future observations and to trend repeatability.

9. If the difference between the observed stars and the catalogued stars in irradiance or position is greater than the combination of the calibration, attitude, and star catalog errors, raise an anomaly flag in the automated processing chain.

10. Repeat from Step 1 until all data from the observation is processed.

This algorithm provides the ability to process the data and autonomously monitor the performance and uncertainty estimates of the SPIRIT III instrument.

Conclusion

The SPIRIT III instrument will provide state-of-the-art LWIR radiometric and goniometric data for the scientific community. The ground data processing, error analysis, and automated monitoring of the system performance are critical elements to ensure mission success. As demonstrated in this paper, the SPIRIT III pointing solution has a particularly interesting and important role in achieving the mission goals. The approaches and algorithms devised will not only benefit the analysis of the SPIRIT III sensor and its data, but will certainly be useful for similar programs and data processing challenges.

References

- Wertz, J.R. "Spacecraft Attitude Determination and Control", Kluwer Academic Publishers, 1978, Appendix D.
- Space Dynamics Laboratory/Utah State University. "SPIRIT III DPC Convert User's Manual", Omega Release, SDL/92-113, August 1993.
- Space Dynamics Laboratory/Utah State University. "SPIRIT III DPC Pointing Convert User's Manual", Omega Release, SDL/93-042, January 1994.

TURNKEY SOLUTIONS FOR SATELLITE OPERATIONS

PHILIPPE GREMILLON
FRANCOIS GAULLIER

MATRA MARCONI SPACE

Abstract

A unique expertise has been developed by MMS in satellite operations covering all aspects of operations activities from mission design up to routine on station operations.

This paper describes the various aspects of MMS involvement in satellites operations with emphasis on satellite operations services which can be tailored to customer requirement in order to provide safe operations at low cost.

For mission design and operation engineering specific tools and methods have been developed in order to reduce operation costs, perform early validation of satellite procedures and ensure that return form in orbit experience is used as input for the design of next programs.

MMS has developed enhanced ground control system based on modern architecture and using multifunction satellite operator workstations as well as orbitography function for collocated satellites and now in use for Hispasat and Telecom 2 and at MMS Customer Support center. Within MMS a Customer Support Center (CSC) has been set up based on this modern Satellite Control Center and connected to advanced AI tools. From the CSC, MMS is able to propose a full range of operation services to the EUROSTAR Customer from early satellite operations training up to LEOP support and back up control center capability.

This overall system allows MMS to provide a set of turnkey solutions which make satellite operations for EUROSTAR customers :

Simple, Safe and Low cost

1 - Mission design and operation engineering

The operational documentation and its quality has been recognised by MMS has one the key of success for satellite operations simplicity and safety.

The volume of data that have now, to be manipulated from satellite design up to end of in orbit life has significantly increased in the recent years, this raises the problem of the access and validity of the essential and adequate informations

all along the satellite life (having in mind 10 to 15 years in orbit lifetime).

As a result MMS has developed, validated and used several tools in the frame of TELECOM 2 and HISPASAT program for the preparation, validation and execution of the operation activities. All tools are based on a common data base system and cover mainly :

- Flight Control procedures preparation and associated TM/TC data base
- Satellite description
- Satellite simulation

Flight Control Procedure

The most important part of the operational documentation consists of the flight control procedures associated with the related TM/TC database.

The flight control procedures define the operations to be done on the satellite within its exploitation phase (Launch and Early Orbit phase and On-station phase). They cover both nominal and foreseen contingency cases. Procedures are mainly based on the Operation requirement Handbook (descriptive part). Other sources are also necessary such as Mission Analysis, switching Diagrams, ground Software specifications, TM/TC Database, etc...

Each procedure consists in a set of actions which can't be dissociated (so-called steps). These steps specify commands, controls and monitoring which shall be done sequentially and in well-defined conditions i.e. according to specific constraints.

The procedures are not fixed documents, but, in the contrary, have to be modified several times before and during the satellite operational life :

- Before launch, they will be modified due to the ORH updates and due to the difficulties or errors encountered while the validations on the satellite simulator.
- During the operational phase, the document will be modified for clearness improvement or to answer to in-orbit anomalies or satellite failures.
- All these modifications are as much hazards to introduce inconsistencies into the document (two levels of coherence : satellite level and procedure level).

The document updating can only be performed by a staff having a complete knowledge of all the procedures, a large system knowledge and whose availability is required during all the operational phase. Therefore, it appears that the structure of the procedures has to be formalised to make easier creation, updating and procedural knowledge access. This authorizes also to develop a tool insuring procedure consistency and reliability during updating phase. It allows an improvement of constraints processing at procedure, function and telecommand levels.

For that purpose a tool so called "POM" tool has been developed by MMS within a CNES R&T contract.

The tool is implemented on Macintosh IICx apple Computer with a 21 inches screen. All the data are managed by the Relational Database Management System ORACLE. The queries of command execution are written in SQL*PLUS language. The man machine interface is made with SUPERCARD software.

The Super-Card functioning is based on the used of buttons and fields, easily accessible, associated to scripts allowing the execution of the different tool functions (searching, browsing,...).

The aims of the tool for operational procedure creation and utilisation are :

- to allow easy manipulation of procedure in creation or updating
- to provide the user with powerful operating modes of information searching
- to insure information integrity
- to provide the user with satisfying ergonomny making easier information access

The tool has been successfully used on TELECOM 2 and HISPASAT program from 1989.

Based on this successful operational experience, an enhanced version of the tool is now under finalisation based on OPSWARETM and will include an enhanced version of procedures tool (OPSAT) as well as computerised management of descriptive part of Operation Requirement handbook (ORH).

Those tools can be run from a UNIX workstation and are based on standard software as ORACLE, Framemaker and Open Interface.

The common software language is C.

the basic functions provided by OPSAT are :

- a procedure editor
- a procedure compiler
- a procedure formatter
- a procedure checker

The procedure editor allows the user to quickly set-up a new procedure according to the predefined procedure form. The editor is syntax driven then ensuring consistency between all the procedures presentation and vocabulary.

An on-line link to the Telemetry/Telecommand database is permanently available to help the operator to build-up his procedure. In the procedure file, only the TM/TC identifiers are input and the relevant data are then up-to-date at the time of either consultation or printing according to the TM/TC database latest modifications.

The procedure compiler generates an internal, formal representation of the procedures and, when applicable, detects errors.

An advanced procedure formatter is provided for printing the procedure manual based on FrameMaker.

A procedure checker provides a rich set of verifications : temporal, logical and quality checks. The logical verifications are based on process modelling to compute the satellite state all along the procedure execution and detect missing, dangerous or wrong commands. These checks may speed-up the procedure validation process : simple errors are detected early before starting detailed simulations.

Satellite description

To allow the management of the descriptive part of the Operational Requirement Handbook, ORH has been developed. It's an advanced computer integrated tool which includes all parts of the document : text, tables, graphics, databases and procedures.

The documents can be visualised, modified and printed.

A Full text parser is used to "tag" some predefined elements of the Framemaker files such as TM/TC identifiers, acronyms, keywords and procedure identifiers. This gives the operator a direct access to the relevant complementary information (database sheet) by just doing a mouse operation.

ORH can easily be expanded to other documents by just adding branches to the generic access tree. Any kind of information (docs, plans, notes, graphs, reports...) can be added by just mentioning the file name, the path and the associated kind of process. This is very helpful during the spacecraft on-station phase to centralise the technical memory by using a unique software entry point.

Satellite Simulator

In order to perform early validation of satellite procedures MMS has developed enhanced dynamic satellite simulator for TELECOM 2 and HISPASAT programs : the utilisation of such simulator is of great benefit for operational preparation : flight control procedures and operational data base validation, satellite control center validation and for operational staff training.

The satellite simulator is operated via a colour graphic workstation of the Satellite Control Center. The simulator is easily controlled, and no computer expertise is required for running simulations.

Appropriate analysis and control facilities are provided for the simulator operator. :

- Simulation log of important events,
- Mimic displays and displays of groups of selected variables,
- TM archiving
- Failure case

Software utilities are developed to enable interface with the satellite data base (TM/TC parameters) and mimic creation.

The simulator operator can activate the simulation functions through specific statements which can be chained and executed automatically.

A specific function simulates the up and down links with the satellite operational control centre through a LAN interface.

All the platform subsystems which entail ground interface (telemetry and command) are given a

representation ; moreover, the dynamic evolutions of the satellite orbit, attitude and ground station visibility are modelled. It allows a closed loop between the ADCS equipment and the satellite environment. The dynamic behaviour of the sensors and the actuators is therefore modelled and the configuration of the switchable elements is taken into account.

The environment model refers to the elements which either influence or are affected by the spacecraft but which are external to the spacecraft subsystems ; it concerns the rotational dynamics (rotate vector and attitude of the satellite), the transitional dynamics (satellite position in orbit), earth and Sun position towards the satellite.

For each subsystem, there are two type of simulation :

- simulation of equipment configuration, i.e treatment executed at ON/OFF command and, functional simulation which affects the parameters which dynamics change
The simulation of equipment configuration follows the following general principles :
 - validity of command electronics configuration,
 - simulation of the unit switching,
 - validity of acquisition electronics configuration.
- The functional simulation mainly concerned the following subsystems :
 - attitude determination and control subsystem (ADCS) : simulation of sensors, actuators and control law as described in figure
 - power supply subsystem : simulation of battery current and state of charge,
 - central intelligent unit (CIU) : simulation of the mission functions of the CIU.

2 - SATELLITE CONTROL CENTER

In order to define a global system approach for EUROSTAR operations MMS has developed a new generation satellite control center software which is now in use for HISPASAT and TELECOM 2 and has been installed at MMS customer support center.

The Spacecraft Control Center (SCC) developed by MMS is based on modern and distributed hardware and software architecture able to run on the latest products such as Dec Alpha AXP series. All the SCC components are linked by an Ethernet local area network.

The main features of the SCC are :

- a simple, homogenous, highly available and modular architecture designed with built-in of robustness and simplicity to ease and secure the operational use and maintenance.
- extensive use of efficient and fully proven proprietary software such as Open VMS, Decnet, Decwindows.... that are now "de facto" standards.
- architecture based on modern HW components providing in particular user friendly man machine interface and large CPU power in a very short volume.
- automatic capability of H/W failure detection and recovery minimising operator actions in case of contingency situation.
- high extension capability such as an additional satellites could be easily taken into account and additional operator positions could be transparently added.
- high flexibility in its operational use in particular through an extensive standardisation of the operator position that can be used for different purpose.
- broad access capability through access to display and analyses functions by PCs.

The architecture includes :

- Two AXP 3000/800 servers in charge of most of the data acquisition and processing.
- A set of two screens AXP 3000/800 workstations mainly devoted to TM display both on line and off line, TC preparation and sending, data base management, satellite simulator.

- A set of single screen AXP 3000/300 workstations dedicated to TM displays both on-line, TM analysis and data base management.
- A set of PCs with the same capabilities as the single screen workstation.
- Two network nodes, in redundancy, to connect the SCC with TT&C network

At any time, each computer runs two different sets of application software according to whether it is the main computer or not. An automatic failure detection and recovery mechanism is in charge of switching from the main computer to the redundant one triggering/stopping the related set of application software.

The design is flexible so that any function (telecommand, telemetry, orbitography) can be performed from any workstation on any satellite :

The software has been developed using the latest technology of Man Machine Interface and through a close collaboration between the operation teams and the software development team so as to obtain a product which provides an adequate level of safety and confort.

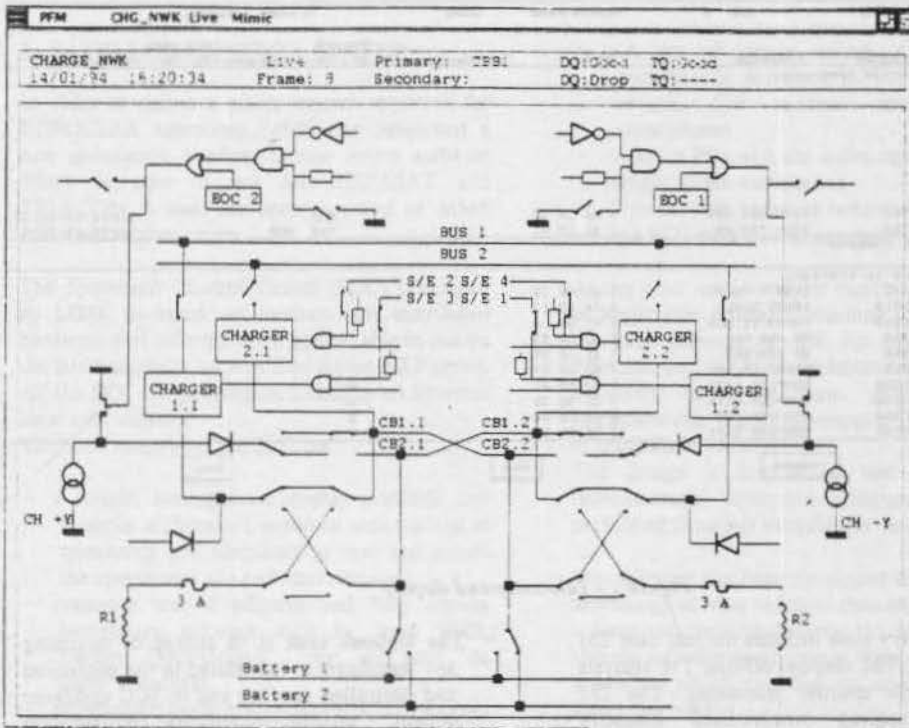
The main tasks performed by the control center are :

- **The telecommand task** is highly secured and minimises the amount of data to be manipulated by S/C controllers. For a given flight control procedure a dedicated telecommand plan is selected from the data base and activated. All necessary verifications to be performed at ground or satellite level before or after a telecommand is uplinked are performed automatically by the system. if an anomaly is detected, the telecommand process is stopped automatically and a self content message is sent to the controller. For a given procedure the operator has only to modify or confirm variable telecommand profiles such as manoeuvre duration, manoeuvre dates... At any time the operator has a knowledge of the status of the current TC in progress as well as the list of all the previously sent commands and the list of the remaining command to be sent. Under the occurrence of specific TM events, dedicated telecommands can be sent automatically.

PPH Command Trace									
Session	EDR	Options							
Echo:	ENABLED	CRZ: A	SECURE mode:	CLEAR	TC mode:		MANUAL		
Identifier	Description	Pr/Fls	Execution Time	Pre-verts	Post-verts	Valid Date			
Transmitted commands:									
1781	GTP1 INT OFF	3 A1	10 00			21/12 15:56:32			
1780	GTP1 INT ON	3 A1	10 01			21/12 15:57:57			
Current Command:									
Commands to transmit:									
001	1920	IRRM 1 CORP.	3 A1	41 58					
002	11018	RESET DWELL	3 01	00 12	U				
003	11019	RESET TT QUR	3 01	00 10					
004	1950	SH SRM PAR	3 A1	08 88					
005	1946	SH WTK SRM	3 A1	08 09					
006	1919	RESET IN SRM	3 A1	08 81					
007	11050	COMPLEX DATA	3 02	00 00	U				
008	11050	COMPLEX DATA	3 02	00 00	U				
009	11050	COMPLEX DATA	3 02	00 00	U				
010	11050	COMPLEX DATA	3 02	00 00	U				

Figure 1 - Telecommand display

- The telemetry task includes the real time TM processing, TM display, off-line TM analysis and mission specific processing. The TM process receives synchronised telemetry frames from the TT&C baseband equipment and performs the classical functions of decommutation, engineering value conversion, limit checking and data display. The system is able to perform the computation of derived parameters with up to 64 operators and operands. Four types of display are available to the operator : alphanumeric pages, graphic pages, animated synoptic and strip chart recorders. A specific "out of limits" page is also available, it includes all the parameters which currently violate the specified limits and status checks. For graphics, parameters can be plotted against time or against another parameter. Historical telemetry data may be replayed on a workstation. The operator has full control over the telemetry replay, with the following options available : pause, single step, continue, change replay speed (nominal, slow or accelerated). off-line analysis are also available and can be used to perform statistics, plots and printout of telemetry.
- The logbook task is in charge of recording any significant event related to the monitored and controlled satellite and to SCC computer system : satellite monitoring configuration change, TM alarm, telecommand history, SCC computer system failure and recovery, operators activities, archiving session start/end, etc...
- The database task is in charge of all operational data management to offer the required level of security for operations and also rapid reconfiguration to support different satellites or operational requirements. When a new version of the data base is under preparation validity checks are performed automatically at several levels.
- The orbitography task provides through a user friendly man machine interface all functions necessary for orbit restitution, orbit propagation, manoeuvre computation, manoeuvre evaluation and full consumption computation. The system has been design to avoid manual data manipulation and all necessary input data are automatically loaded from results of previous application process. The orbitography software includes collocation modules compatible with a deadband of $\pm 0.05^\circ$ in E/W and N/S.



PFM A_SKM2 Live

SKM2 Live Primary: T8B1 DQ:Good TQ:Good
 23/12/93 09:57:43 Frame: 3 Secondary: DQ:Drop TQ:----

ARE	CPE FUNCTIONS	
M090 ARO MEMO = NO	M042 MODE ST = NM	M054 MAN GAIN = HIGH
M117 ARM2/3 FLG = ARM2	M048 SUBMODE ST = SOSA	M078 WTM CONV = REACHED
M095 ARE EP CR = ENAB	M083 THMOD FLAG = ENAB	M079 WTM GAIN = LOW
M097 ARE GYP CR = INHIB	M507 MAN TIMER 217.0s	M053 NM COMP K = INHIB
M104 ARE RCTSUM = INHIB	SADE	IRES ON LINE
ATTITUDE		M077 SADE MODE = SOSA
B122 IRONL ROLL -0.022°	B071 SASS S ANG -5.13°	B100 IRES ONL = IRES 2
B089 YAWGYP RAT	B072 SASS N ANG 2.74°	B104 IRONL TRC1 = ENAB
B090 YAWGYP ANG 0.042°	TANKS PRESSURE	
B123 IRONL PTCH -0.100°	B176 NTO U PT 16.83bar	B106 IRONL RATE = 1.25 Hz
B181 WHL MEASKM -43.630Nms	B177 MMH U PT 17.43bar	GYP
FCV SUM		B079 GYP 1 = OFF
B148 FCV 1 SUN2 0.000s	B178 NTO D PT 16.84bar	B080 GYP 2 = OFF
B149 FCV 2 SUN2 0.000s	B179 MMH D PT 17.42bar	B082 GYP2 INTG
B150 FCV 3 SUN2 0.000s	THRUSTER CURRENT	
B151 FCV 4 SUN2 0.000s	B154 THRUSTA I -0.005A	B083 GYP1 INTG
B152 FCV 5 SUN2 0.000s	B155 THRUSTB I -0.015A	B085 GYP 1 TEMP 5.00°C
B153 FCV 6 SUN2 0.000s	GROUP FCV TEMP	
	G006 FCV123 TP 0 0	B086 GYP 2 TEMP 5.00°C
	G007 FCV456 TP 0 0	B084 GYP1/2 TP = ON
		B081 GYP ONLINE = GYP 2
		M045 GYP MONITG = GYP 1

Figure 2 - Telemetry displays

3 - OPERATION SUPPORT TOOLS

The SCC can be connected to a set of advance tools for operations support. All the tools are based on Sun/spark workstation with Oracle database, Framemaker and Open interface and can be access from any X-terminal.

- SAT-analyst is able to perform systematic trending analysis on satellite telemetry and to issue automatic reports : the tool is used to detect abnormal evolution or behaviour of satellites which can not be detected by simple GO/NOGO criteria such as limit checking. The user is able to define through a dedicated interface the content of the report as well as the processing to be performed (comparison with previous plots, FFT, derived parameters computation...).
- SAT-Diagnostic is used as a support for failure diagnosis and is based on A.I. technology, it covers all platform subsystems and its knowledge database can be improved through the in orbit experience. The tool is used as a support by S/C controllers for failure localisation and as a training system.

SAT-Diagnostic is based on a generic kernel which address two main knowledge representation levels :

- the behaviour level : decision trees implement the failure first analysis procedures, and knowledge about the predictable effects of equipment/component failure on the dynamic behaviour of the spacecraft.
- the functional level : functional representations of the on-board equipments are used to discriminate among possibly faulty component by using the available telemetry.

An operational version is now in used at TELECOM 2 satellite Control Center and at MMS CSC.

4 - CSC AND MMS OPERATION SERVICES

MMS is used to support EUROSTAR customers for the in orbit phase. This support starts by the delivery of a complete and fully validated operational documentation and associated operation support tools as described before, but includes also the provision of very attractive operation services. From 1989 MMS has been largely involved in all LEOP services of EUROSTAR satellites (8 successful LEOP up today). MMS has been in particular fully responsible for satellite operations activities for INMARSAT 2 F1, F2, F3, F4 and HISPASAT PFM and FM2. This includes preparation, validation of the satellite flight control procedures and associated TM/TC data base. During LEOP operations MMS was on charge of satellite operations. Based on this experience which covers also Network assembly and flight dynamics activities, MMS can propose LEOP services tailored to customer requirements. As an example HISPASAT LEOP was performed with CNES cooperation under full contractual responsibility of MMS from the customer control center set up in Spain by MMS. Mission preparation was performed in less then 12 months using a MMS in house multimission facility called CSC for customer support center.

The CSC major functions are :

- processing of up to 9 different Spacecraft
- real time monitoring and commanding of Spacecraft
- off line analysis/replay, trend analysis, report, by using SAT-analyst
- use of expert system for trouble shooting (SAT-Diagnostic)
- training and simulation of Eurostar operations
- telemetry dissemination on MMS network (for quick engineering support)
- back-up satellite control center (TC capability)
- Orbitography support for on station and LEOP

The present implementation at MMS Toulouse is composed of :

- 3.1 m C band antenna
- 3.7 m ku band (TM and TC) antenna
- 0.9 m ku band antenna
- baseband equipment for TM and TC functions
- satellite control center
- telemetry dissemination on MMS network

- EUROSTAR spacecraft simulator
- OPSAT, ORH, SAT-analyst and SAT-diagnostic
- capability for connection to external network (CNES, NASA, HISPASAT, ...)
- flight dynamic center

The CSC can be used for various activities according to customer requirements :

mission preparation, validation and training of customer operational staff : The C.S.C. is equipped with the POM, OPSAT and ORH tool as presented before as well as with the EUROSTAR dynamic satellite simulator. This allows to perform an easy and early validation of Flight Control procedures during the satellite design phase. In addition Customers can be trained using these flight control procedures with the CSC ground system which is equivalent (functionally and as far as Man Machine Interface is concerned) to the Satellite Control Center which will be delivered at Customer site : this allows for Customer Staff a parallel development of Ground Control System and Operational preparation and guarantee his ability to operate safely the satellite after its in orbit delivery.

LEOP support for operation team and specialist team : The CSC facilities have been used during HISPASAT Leap for satellite specialist monitoring : allowing to have quick answer to in orbit unforeseen behaviour. The CSC was also able to be used a back up site in case of main center at ARGANDA (Spain) unavailability. Depending on customer requirements various type of services can be proposed including full Leap services from CSC.

back-up control center : as example the CSC was used as a back up control center for HISPASAT during 9 months and MMS was able to take full responsibility of satellite operations in less than 2 hours notices. Depending on Customer requirement and existing Ground Control System the back up control center services can be adapted (2 hours time notice, 48 hours time notice...) to avoid unnecessary customer investment. The availability at CSC facilities of MMS EUROSTAR operation experts guarantee that the satellite will be operated safely until the recovery of nominal conditions of customer ground control center.

in orbit support to customer : for satellite health assessment and mission optimisation. A team of more than 50 highly expertise engineers is available to perform systematic satellite health assessment and provide support to real time operations if anomaly occurred.

The in orbit support generally include :

- improved satellite monitoring with trend analysis in complement of satellite control center analysis
- analysis and processing of in-orbit anomalies :
 - component alert processing
 - system evaluation such as propellant or power evaluations
 - particular equipment monitoring
 - elaboration of contingency procedures
 - update of satellite operation handbook
 - modification, validation and improvement of operational procedures

(through this activity a continuous process of improvement of satellite flight control procedure is performed)

- knowledge maintenance of in-orbit satellite behaviour
- design knowledge maintenance

The CSC is connected to the set of enhanced operation support tools presented before (OPSAT, ORH, SAT- analyst, SAT-diagnostic) :

This allow the operation and subsystem experts to have instantaneous access to all the necessary informations (from design, development, integration and test phases) as well as to real time or archived in orbit telemetry (Thanks to CSC capabilities, the satellite telemetry, real time or off line is available on specialist desk top PCs as well as SAT-analyst functions and ORH functions through MMS Local Network).

The CSC when used with its associated services is the right answer at customer level :

- to reduce at minimum the operations cost
- to safe the in orbit satellite
- to maximise the mission availability and customer revenue.

THE PLANNED EUROPEAN IN-ORBIT INFRASTRUCTURE AND THE ROLE OF THE DLR MANNED SPACE-LABORATORIES CONTROL CENTER (MSCC)

Dr. Joachim Kehr
Wayne Salter

Deutsche Forschungsanstalt für Luft-und Raumfahrt (DLR)
82230 Weßling, Germany
(KEHR@GSOCCMAIL.RM.OP.DLR.DE)

Cray Systems Ltd.
DAS House, Temple Way, Bristol, BS1 6NH, England
(SALTER@GSOCCMAIL.RM.OP.DLR.DE)

ABSTRACT

This paper describes the In-Orbit Infrastructure Ground Segment (IOI GS) required to support the Columbus Laboratory payload operations and system control functions as part of the Columbus Program. The Columbus Program and the corresponding ground infrastructure have changed significantly since the Program was first initiated. However, this paper concentrates on the IOI GS in the configuration which was defined at the European Space Agency (ESA) council meeting at Ministerial level held in Granada in November 1992 - the "Granada Scenario", and the developments that have taken place since then. The facilities that comprise the IOI GS are introduced and a high level description of the role of each facility is given. However, throughout this paper particular emphasis will be placed on the role of the Columbus Laboratory Control Center (CL-CC) which includes the European payload operations co-ordination function and will be located in the MSCC on the site of DLR in Oberpfaffenhofen, Germany. Furthermore, the impact of the re-design of the Space Station Freedom, as initiated by the Clinton Administration, on the IOI Ground Segment is fully detailed.

The development of the MSCC and its operational involvement firstly for the highly successful Spacelab D-2 mission in April/May '93, subsequently for the coming Columbus Precursor Missions and finally up to and including the Columbus era is described.

The role of the CL-CC, and its interaction with the NASA centres as well as the other IOI Ground Segment facilities, is then described in more detail. Particular emphasis is placed on the services provided by the payload operations co-ordination function for the European users with experiments located in the Columbus Laboratory.

The Architectural Design of the CL-CC resulting from the functional analysis of the tasks to be performed for

payload operations co-ordination is presented, and this forms the main body of the paper. The interesting/novel aspects of the proposed physical architecture are addressed, together with the corresponding advantages. In particular, the largely distributed nature of the architecture, whereby tasks are generally allocated to multiple workstations rather than being hosted by a large mainframe, is discussed. This discussion has not previously been published.

Key Words: Columbus Laboratory, In-Orbit Infrastructure, Columbus Laboratory Control Center, Space Station, Attached Pressurised Module

OVERVIEW

The Columbus Program was initiated at the ESA Council meeting at ministerial level in January 1985 with the aim of establishing an autonomous capability in the field of manned space flights, and to accept the offer from the United States to participate in the Space Station Program. The Columbus Program definition has undergone much change since its initiation, but the basic aims have been continually re-instated. The last occasion on a ministerial level was the meeting in Granada in November 1992. The Columbus Program defined at this ESA Council meeting (Reference: ESA/PB-COLUMBUS(92)18, rev.7) comprised the following elements:

- A pressurised module to be permanently attached to the Space Station (SSMB), the Columbus Attached Laboratory (APM), and the associated In-Orbit Infrastructure Ground Segment (IOI GS)
- A free flying Columbus Polar Platform and the associated ground segment
- Columbus Precursor flights (presently one Spacelab flight, 2 ESA MIR missions and one Eureka re-flight) to prepare for the exploitation of the APM

The APM would be launched by the Shuttle and would form a permanent part of the Space Station, from which

it would receive its resources (power, heating, cooling, water, etc). The Space Station Control Centre (SSCC) would be located at the Johnson Space Center (JSC), which would be responsible for the Space Station as a whole and for all system aspects. The co-ordination of the payload operations would be handled by the Payload Operations Integration Center (POIC) at the Marshall Space Flight Center (MSFC). The European payload operations co-ordination would be the responsibility of the European Payload Operations Co-ordination Center (E-POCC), as it was then called, which would interface to the POIC to provide consolidated European inputs which would then be integrated by the POIC with all other inputs from the international partners into overall Space Station products.

The IOI GS as defined during the Granada Meeting comprised the following elements:

- E-POCC responsible for the payload co-ordination for all European experiments located in the APM or elsewhere in the Space Station
- Multiple User Support Operations Centre's (USOC's) to support the users, both technically and scientifically, in the preparation and execution of their experiments and further in the interpretation of the results. Most users will also be located at the USOC's during their experiment execution
- APM-Centre (APM-C) to perform payload integration and to provide system engineering support and logistics services for the APM and its on-board systems
- Tactical Operations Planning and Increment Management Centre (TOPIC) which will carry out the European tactical operations management and planning and will have a direct interface to the internationally staff Integrated Tactical Operations

Organisation (ITOO) responsible for the implementation of all tactical level activities

- Interconnection Ground Subnetwork (IGS) is the ground network to support the APM operations, that will allow the transmission of data, voice and video between the USA and Europe and will handle all operations communication between the IOI GS facilities in Europe. As part of the IGS will also be:
 - Network Management Centre (NMC) responsible for planning and co-ordinating all communications resources/requirements and for managing the European communications infrastructure
 - ESA Relay Facility located in the USA responsible for providing the interface between the NASA and IGS communications networks

Figure 1 gives an overview of the IOI GS and its interface to the NASA facilities and the space element.

IMPACT OF THE SPACE STATION RE-DESIGN

Due to financial problems at NASA and due to significant political changes, the newly elected Administration under President Clinton decided to initiate a "global" space station design involving Russia as a partner. The re-design process was completed in November 1993 and the resulting station, the so-called "α-Station", see Figure 2, includes significant Russian elements.

Also due to financial problems in Europe, ESA revisited the "Granada Scenario" in the light of the above NASA decisions with the following result: A Columbus Laboratory still constitutes the European provided element for the global space station manned base.

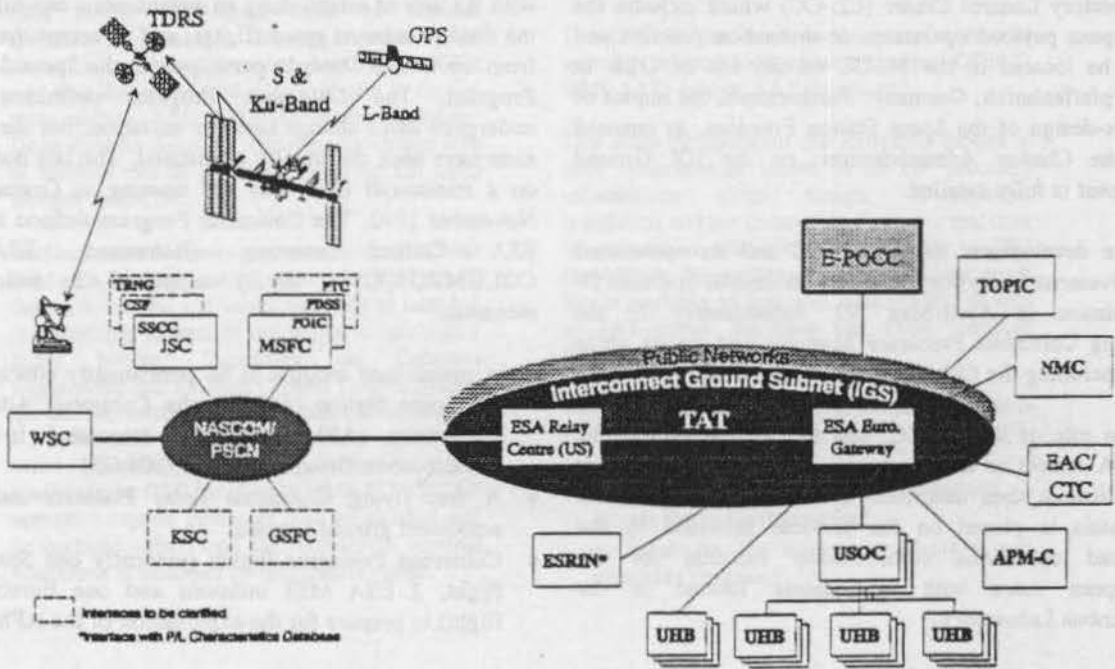


Figure 1: Overview of the In-Orbit Infrastructure Ground Segment ("Granada Scenario")

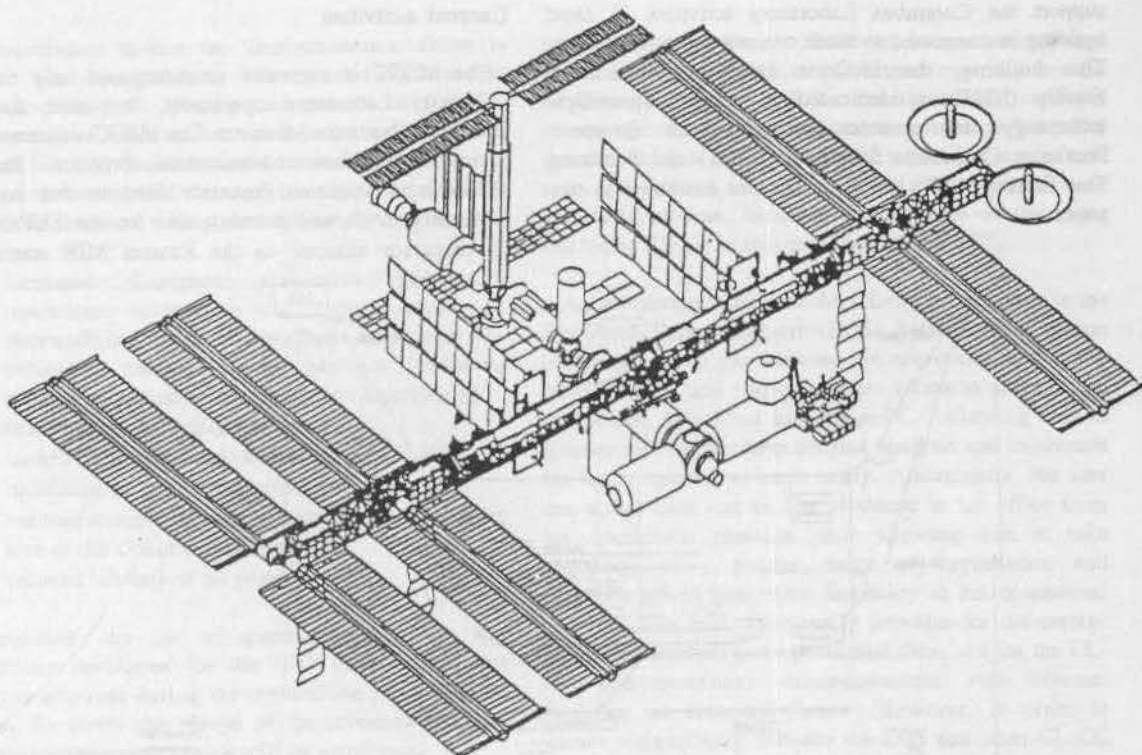


Figure 2: α -Station Configuration

The Columbus Laboratory is to be:

- Launched by Ariane 5 and manoeuvred to the Space Station by the European provided Automatic Transfer Vehicle (ATV)
- Attached to the Space Station as part of a permanently manned capability provided by the Space Station partners in a 51.6° orbit, allowing the installation of 4*5 standard double racks
- Targeted for a 2002 launch date with a lifetime of 10 years (previously 30 years)

In addition, the European Data Relay Satellite (DRS) will be exploited as necessary to support the Columbus in-orbit/ground communications requirements. With the introduction of the DRS communication system a more independent approach for the operation of the Columbus Laboratory was proposed by ESA. The E-POCC as described in the previous section would be designed to perform payload operations co-ordination for all payloads within the Columbus Laboratory and all "non-safety critical" system control functions for the Columbus Laboratory becoming the "Columbus Laboratory Control Center". The revised IOI GS (compared to the "Granada Scenario") is now:

- Columbus Laboratory Control Center (CL-CC) in Oberpfaffenhofen, performing laboratory "non safety critical" system control functions for operations and all tasks for co-ordinating European and non-European user operations. Safety critical operations are to be performed by the Space Station Control Center in Houston.
- Multiple USOC's as described above

- A significantly reduced APM-C (now called "Laboratory Engineering Center")
- A significantly reduced TOPIC (possibly integrated with the CL-CC)
- IGS which now includes a DRS Earth Terminal (possible integration of the NMC and the DRS Earth Terminal into the CL-CC)

Figure 3 gives an overview of the revised IOI GS.

DEVELOPMENT OF THE MSCC

Initial Development and Previous Missions

DLR with the aid of national funding has established the MSCC on its site at Oberpfaffenhofen near Munich. The MSCC is an extension to the existing German Space Operations Center (GSOC) facilities already located on this site. The MSCC, completed in 1989, consists of two buildings; the first housing the Mission Control Facility and the second the Operations Missions Sequence Simulator (OMSS). The Mission Control building provides four large fully equipped control rooms, multiple rooms to accommodate further operational personnel and users involved in both real time and off-line activities, areas to accommodate all computer equipment and two levels of office space. Access is available to the MSCC in-house voice, video and data processing systems in all operational areas. The OMSS building provides a large area to house an Columbus Laboratory mock-up and other simulation or training tools, computer rooms and office space. The OMSS will accommodate all MSCC Training, Qualification & Validation (T, Q & V) tools and simulations facilities to

support the Columbus Laboratory activities. A third building is connected to these two via a common foyer. This building, the In-Orbit Operations Simulation Facility (IOSF), is dedicated to manned spaceflight technology developments including the European Proximity Operations Simulator (EPOS) and Servicing Test Facility (STF) but is not further addressed in this paper.

Current Activities

The MSCC is currently preparing not only for the Columbus Laboratory operations, but also for the Columbus Precursor Missions. The MSCC will house the payload operations co-ordination function for an international Spacelab Precursor Mission due for late 1996/early 1997, and possibly also for the EUROMIR '95 precursor mission on the Russian MIR station in

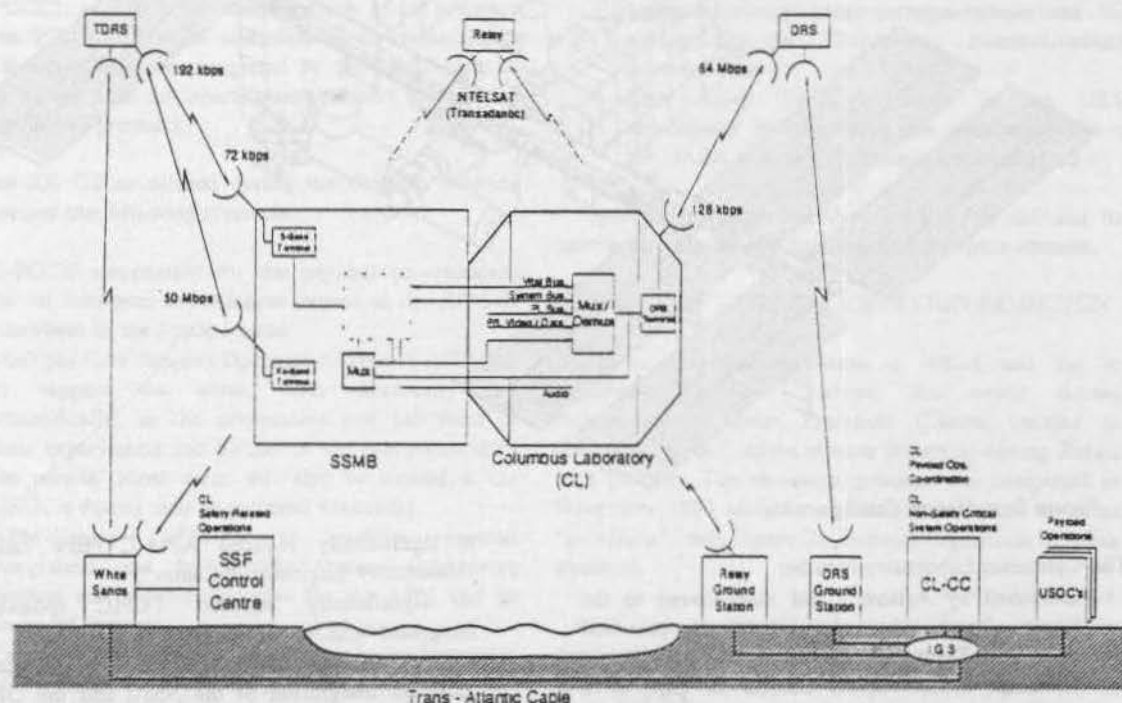


Figure 3: Revised Columbus Laboratory Communications Concept

The DLR has gained much valuable experience in manned space operations through its involvement in the Spacelab 1, D1, MIR '92 and D-2 missions. The latest of these mission, the highly successful second German Spacelab Mission D-2 (Mission Duration: 26.4.93-6.5.93), was the first mission to be performed from the MSCC configured as the Payload Operations Control Centre (POCC). The payload operations were controlled from the POCC, where the majority of the users were also located for the duration of the mission. The Spacelab data was transferred to roof top terminals at the POCC from the USA via satellite. The data was processed by the POCC systems and then distributed to the users in the POCC user rooms. Furthermore, a dedicated POCC position was responsible for co-ordinating all payload commanding. Additionally, Spacelab video and air-to-ground voice were made available to the operational personnel via the POCC in-house systems.

The MSCC, through its participation in this mission, has confirmed its position as Europe's POCC for manned missions.

1995. The implementation phase for these missions is expected to start in 1994. These missions will provide an important stepping stone towards Columbus and particularly the Columbus Laboratory operations. Two important Columbus operations concept features are likely to be utilised for these missions. Firstly, many of the users will be located in USOC's dispersed throughout Europe and will be able to perform telescience operations. This will allow the users far more flexibility with the execution of their experiments. In order to make this decentralised operations concept work, it is important that these users are adequately supported by the payload operations co-ordination function, which will be responsible for co-ordinating all payload commanding, for co-ordinating the experiment timing and replanning, and for ensuring the end-to-end data transfer. Secondly, a forerunner of the Columbus communications network, the IGS, is likely to be employed for all operational communications between the ground facilities, covering data, voice and video, and to provide direct interconnections between the NASA communications network, the MSCC and the USOC's.

The IOI GS studies Design Consolidation Phase (DCP), which as the name suggests is intended to ensure that all aspects of the IOI GS design and definition are

fully established before the Implementation Phase is entered, was completed in December 1993 for the "Granada Scenario". During this phase the IOI GS architecture and requirements, including subsystem level and with full interface definitions, were finalised.

Due to the introduced changes, the results of the DCP have to be revised taking the following aspects into account:

- increased European Columbus Laboratory operations autonomy, i.e. system operations responsibility and the payload operations co-ordination function for all payloads (including partner utilisation of the Columbus Laboratory)
- launch delay until 2002
- launch by Ariane 5 and utilisation of the ATV
- utilisation of DRS for communications
- reduced number of experiments due to the smaller size of the Columbus Laboratory
- reduced lifetime of 10 years

In addition, the use of space segment tools and applications developed for the C/D phase to support operation activities during the exploitation phase is to be studied. To verify the results of the investigation, low cost development/prototyping will be employed.

The above activities will result in firm procurement and integration plans for the CL-CC subsystems by the end of 1994. Before proceeding into the implementation phase, a decision from a future ESA Council meeting in 1995, will be required.

CL-CC/MSCC Architecture for Columbus

Figure 4 shows the CL-CC architecture to support the Columbus Laboratory Payload Operations. The following description concentrates on the payload operations co-ordination function of the CL-CC. The "non safety critical" system operations aspects have yet to be analysed in detail. However, the described architecture will also be able to accommodate these tasks. The architecture shown follows the trend towards distributed processing, and takes advantage of the recent advancements in work station technology. Instead of the functions being concentrated on large central mainframe computers, many of the functions are distributed to smaller, but nonetheless powerful work stations. The resulting balance between centralised and distributed processing shown in Figure 4 was an outcome of the functional analysis of the payload operations co-ordination requirements.

Each subsystem is comprised of multiple assemblies each performing a subset of the overall subsystem tasks. The assemblies are typically based on one or more work stations, provide local storage and possibly other peripherals, and are linked by subsystem Local Area Network(s) (LAN's). Following the distributed approach, each subsystems holds a database containing the information required to carry out all subsystems tasks. Additionally, each subsystem provides its own

local short term storage. However, longer term storage of all operational data is performed centrally by the Archiving Subsystem (ARS), which provides two types of storage. Firstly, a medium term storage up to 3 months which is held on-line and accessible in near real time. The second is the long term archive and is only accessible off-line. Medium term storage of the voice and video signals is also provided by the ARS.

An interesting feature of the CL-CC architecture is the Electronic Office Support (EOS) System. This system bridges the usual gap between the operational and office environments, and allows its users access to much of the operational data from his office PC, allowing him to prepare reports, perform off-line analysis and to prepare for future operations more easily. Additionally, the user can access data that he has produced in his office from his operational position, thus allowing him to take advantage of a greater range of applications and therefore afford him extra flexibility at his operational position. The EOS additionally provides for the storage and retrieval of all non-operational data, and for the CL-CC non-operational communications with external facilities, as described below. However, in order to ensure compatibility between the EOS and other CL-CC subsystems, the design of the EOS front-end and archiving features is being performed by the appropriate subsystem (CIS or ARS) designers.

All operational communications to and from the CL-CC are handled by the Communications and Infrastructure Subsystems (CIS), and all non-operational communications by the EOS, via one of two interfaces. The first, and most important, is to the IGS. The IGS provides two communications networks; the operational and administrative networks. The operations network, as the name suggests, is for all operational data, voice and video distribution, both space-to-ground and ground-to-ground regardless of the transportation means (TDRSS or DRS), and this data exchange is subject strict latency and security requirements. The administrative network is for general information exchange with lesser latency and security constraints. The MSCC also supports an interface to the local Public Telephone and Telegraph (PTT) network for electronic data exchanges and normal telephone and telex capabilities as general infrastructure. These connections will supplement the IGS administrative network.

The CL-CC subsystems themselves are connected by two backbone LAN's each based on the Fibre Distributed Data Interface (FDDI) standard allowing data rates up to 100 Mbps. The first LAN, the Operations LAN, is the safety critical LAN supporting the interfaces between assemblies involved in the realtime payload and ground operations with the operational IGS to the NASA control centers and the SSMB. Further, this Operations LAN consists of two physical LAN's, the Routine Operations LAN for on-line data, and the Extended Operations LAN used during high activity phases and for simulations data/playbacks,

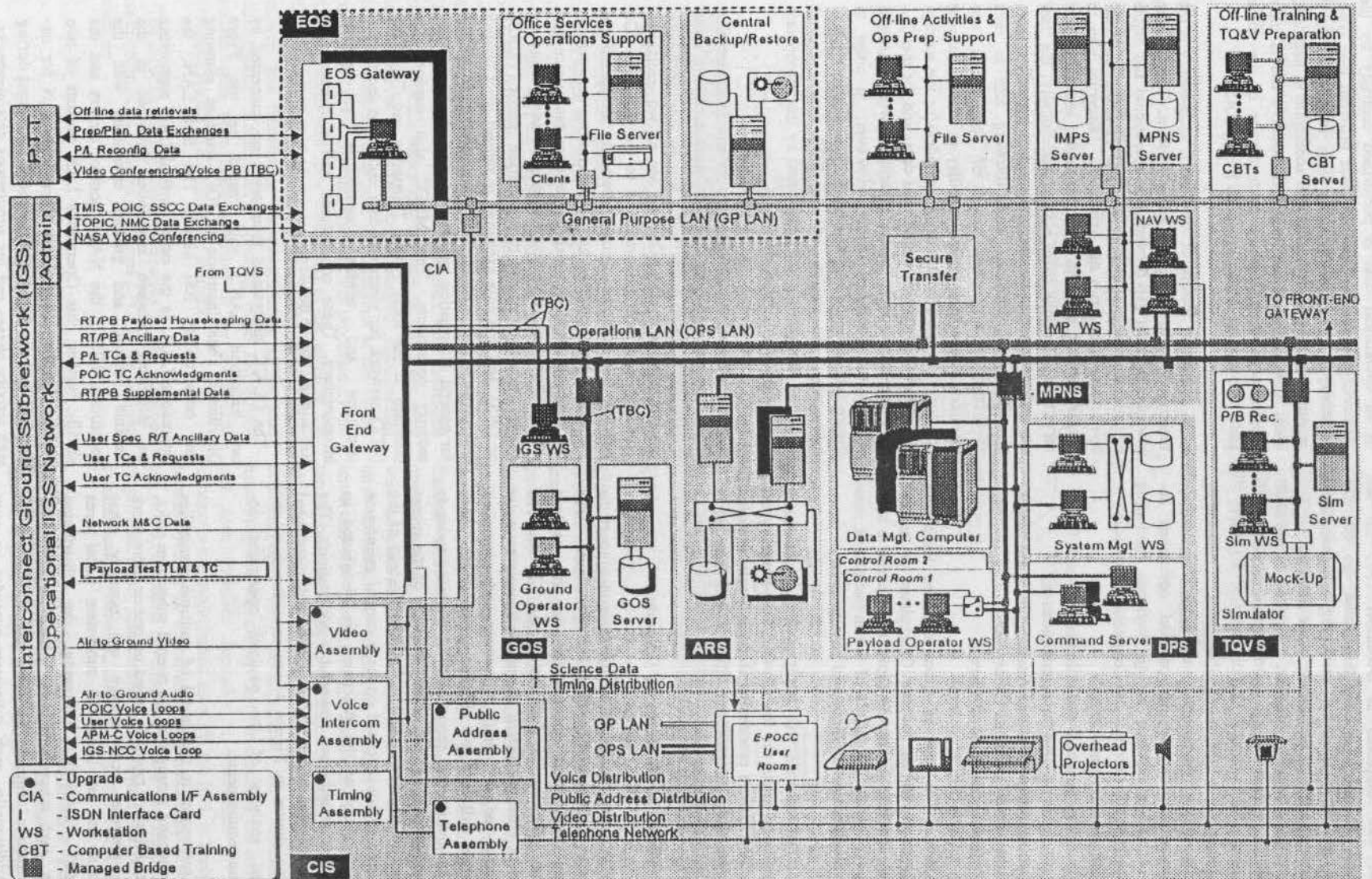


Figure 4: MSCC Functional Architecture

which can also carry traffic from the Routine Operations LAN in the case of malfunctions. The second LAN, the General Purpose LAN, is used to interface between all other assemblies necessary in the CL-CC infrastructure for supporting payload and ground operations and to the external world via PTT and the IGS administration network. For safety and security requirements the Operations and General Purpose LAN's are isolated from each other. The connection of all subsystems via these LAN's allows for easy and reliable data exchange, and therefore, the ability for the subsystems to interact more easily.

In addition to the data distribution LAN's, there are also voice, video, timing and public address distribution systems, which allow the distribution of these signals to all operational areas, and to selected non-operation areas, of the MSCC.

The Monitor and Control (M&C) concept for the CL-CC has two levels. Each subsystem provides its own local M&C capabilities, which are in turn provided centrally to the Ground Operations Subsystem (GOS), in order to allow an operator to monitor and control all on-line subsystems from a central location. The GOS is therefore the central point of monitoring, control and co-ordination for ground operations within the CL-CC. Health and status data from the on-line ground operations subsystems and assemblies are brought together at the GOS. These data are expected to already be calibrated or quantified in the originating system, therefore processing at the GOS will primarily be concerned with preparing the data for display, performing extended processing to derive additional parameters or information, and checking parameters for limit and configuration violations. Control of subsystem and assembly functions and equipment from the GOS is based on the criticality of the function, the amount of co-ordination or insight into other system configurations required to perform the function, and the ease in which the remote control of the function can be implemented.

Columbus Laboratory Payload Operations Co-ordination Function

The CL-CC will be responsible for the co-ordination of all payload activities taking place within the Columbus Laboratory. Specifically the CL-CC will perform the following functions:

- Act as single point of contact for Columbus Laboratory utilisation co-ordination
- Co-ordinate and integrate the formalised user requirements for the entire Columbus Laboratory
- Generate the Columbus Laboratory timeline
- Perform Columbus Laboratory replanning
- Ensure the resource availability to the Columbus Laboratory during the planning phase
- Enable/disable the Columbus Laboratory command capability for European and other users, and validate

all commands according to plans or on requests, in close co-operation with the SSCC

- Monitor and control experiment resource envelopes during mission operations
- Ensure health and safety of the Columbus Laboratory payloads and take appropriate steps in the event of anomalies
- Co-ordinate and ensure end-to-end data handling for all experimentation taking place in the Columbus Laboratory
 - Co-ordinate voice communication between the crew and authorised users
 - Co-ordinate real time and off-line data dissemination
 - Provide data storage for low rate data, voice and video as well as high rate data in the backup case
 - Distribute recorded data off-line
- Provide post increment reports
- Accommodate users which are not supported by a USOC

For Columbus the main goal is to achieve good science. To this end the services provided to the users in order to achieve this are of paramount importance. Most of the European users for the Columbus Operations will be located in appropriate USOC's.

The services provided by the CL-CC to the users are given below:

- Operations Preparation
 - Columbus Laboratory Execution level planning and replanning by integration of harmonised requests from the USOC's
- Operations Execution
 - Columbus Laboratory payload resource monitoring and control
 - Columbus Laboratory payload health and safety control
 - Columbus Laboratory payload command co-ordination / validation, incl. telepresence throughput co-ordination
 - End-to-end communication co-ordination
- User Data Services
 - User data service co-ordination
 - Data quality monitoring
 - Data accountability
 - Intermediate data recording and data product generation and distribution

In addition, users will also be accommodated at the MSCC in internal user rooms during the missions. In such cases, the user interfaces will be treated identically to those located externally.

CONCLUSION

The rescoping of the Space Station Freedom with the inclusion of the Russian Space Agency as a partner and the re-definition of the European Columbus Program has yielded a more cost effective approach for both the

American and European space agencies. This has meant a significant increase in the responsibilities of the MSCC within the Columbus Program, reflecting a more centralised and autonomous European approach. With modern design methods being employed for the MSCC, the facility architecture has proven to be flexible enough to cope with a significant variety of changes for the benefit of the manned space program and in particular for the benefit of the experimenters and their scientific investigations.

TAT Trans-Atlantic Optical Cable
 TDRS Tracking and Data Relay Satellite
 TOPIC Tactical Operations Planning and Increment Management Centre
 T, Q & V Training, Qualification and Validation
 UHB User Home Base
 USOC User Support Operations Centre
 WS Work Station
 WSC White Sands Complex

ABBREVIATIONS LIST

APM Attached Pressurised Module
 APM-C Columbus Laboratory-Centre
 ARS Archiving Subsystem
 ATV Automatic Transfer Vehicle
 CBT Computer Based Training
 CIA Communications Interface Assembly
 CL-CC Columbus Laboratory Control Center
 CIS Communications and Infrastructure Subsystem
 CSF Columbus Simulations Facility
 CTC Crew Training Complex
 DCP Design Consolidation Phase
 DLR Deutsche Forschungsanstalt für Luft- und Raumfahrt
 DPS Data Processing System
 DRS Data Relay Satellite
 EAC European Astronaut Centre
 EOS Electronic Office Support
 CL-CC European Payload Operations Co-ordination Center
 EPOS European Proximity Operations Simulator
 ESA European Space Agency
 FDDI Fibre Distributed Data Interface
 GOS Ground Operations Subsystem
 GPS Global Positioning System
 GSFC Goddard Space Flight Center
 GSOC German Space Operations Center
 IOI GS In-Orbit Infrastructure Ground Segment
 IOSF In-Orbit Operations Simulations Facility
 ITOO Integrated Tactical Operations Organisation
 JSC Johnson Space Center
 KSC Kennedy Space Center
 LAN Local Area Network
 M&C Monitor and Control
 MP Mission Planning
 MPNS Mission Planning and Navigation Subsystem
 MSCC Manned Space-Laboratories Control Center
 MSFC Marshall Space Flight Center
 NAV Navigation
 NMC Network Management Centre
 OMSS Operations Mission Sequence Simulator
 PDSS Payload Data Services System
 POIC Payload Operations Integration Center
 PTC Payload Training Complex
 PTT Public Telephone and Telegraph
 SSCC Space Station Control Center
 SSMB Space Station Manned Base
 STF Servicing Test Facility
 STP Short Term Plan

THE FRENCH SCIENTIFIC MISSION CENTRE FOR THE MARS 94/96 MISSION

Denis Fournier

Guy Boutonnet, Evelyne Orsal, Jean-Louis Piéplu

French Space Agency

CNES, CT/TI/PS/AP

18 avenue Edouard BELIN

31055 Toulouse Cedex

France

fournier@melies.cnes.fr

Abstract

France is cooperating extensively with the Russian MARS 94/96 mission by providing scientific instruments. CNES (the French Space Agency) has decided to establish a mission centre at Toulouse so that the scientific community will be able to use its instruments under the best possible conditions.

Even though it will be decentralized at Toulouse, the centre will be part of the global ground segment, for which the most important parts are to be under Russian responsibility. This centre should enable scientists to control and program the functioning of their experiments while at the same time providing facilities for processing, distributing and archiving data and results. This objective will require the development of communications facilities between the different partners and of processing systems for telemetry, operations management and mission analysis.

This paper describes the general organization and architecture of the centre as well as the various strategies and means to be employed to carry out the different functions.

Foreword

For several years now the international scientific community has expressed an increasing interest in the planet MARS. Following on the analysis of data from the MARINER programme and the VIKING mission and the contribution made by PHOBOS 2, the Russian MARS 94/96 mission will enable more thorough research based on the previous discoveries. This programme will be articulated around 2 centres of interest, namely remote sensing (cartography, studies of the atmosphere, geology, mineralogy, gravitational and magnetic fields) and study of the ground by means of a network of fixed stations.

France has a privileged role to play in this programme of international cooperation not only because of the scientific instruments which it is providing, but also because it is responsible for the vehicle-related aspects (telemetry relay, Aerostat and Rover navigation system). The MARS 94 mission, due to be launched in

October 1994, will consist of an orbiter, two stations and two penetrators. During this first mission, France will be participating in 11 scientific experiments.

To cope with the diversity and complexity of the required supplies, CNES set up a project group at the Toulouse Space Centre in 1988. This group is responsible for the technical, budgetary and scheduling aspects for all of the French services to be provided. Given the extent of French participation in this mission, CNES deemed it necessary to develop a specific mission centre to manage flight experiments and process information. For this purpose a ground segment project group was set up to act as prime contractor for developing such a centre.

The centre's functions

The French Scientific Mission Centre or C.M.S.F. (*Centre de Mission Scientifique Français*) fits into the global control and processing system for the MARS 94/96 mission, which is being coordinated by the Russians. It should enable the French scientific community to get the most out of the equipment carried on the mission, by providing scientists with facilities for managing and controlling experiments, for defining measuring plans and for processing and distributing information. The centre will coordinate all work on the French part of the mission and will be the sole interface with the Russian control and mission centres throughout the operational part of the mission (exchanges of TC (telecommand) proposals, reception of TMs (telemetry), etc.)

The scientists have made it clear that priority should be given to rapid data retrieval in France thus enabling them to quickly interpret on-board measurements and thus plan work sessions for subsequent orbits. In general they have asked that special attention be paid to problems to do with exchanges of information between the different partners (Russian centres, laboratories, etc.)

The primary functions of this centre will be:

- recovery, archiving and management of telemetry and ancillary data.

- preparation of programming for flight experiments, operations control and technological monitoring,
- processing of information and distributing of results,
- elaboration of forecasts and determination (orbits,

attitude, pointing, visibilities, location of stations).

The specified time limits require that the centre be equipped for real-time (or approximately real-time) processing of information received by stations.

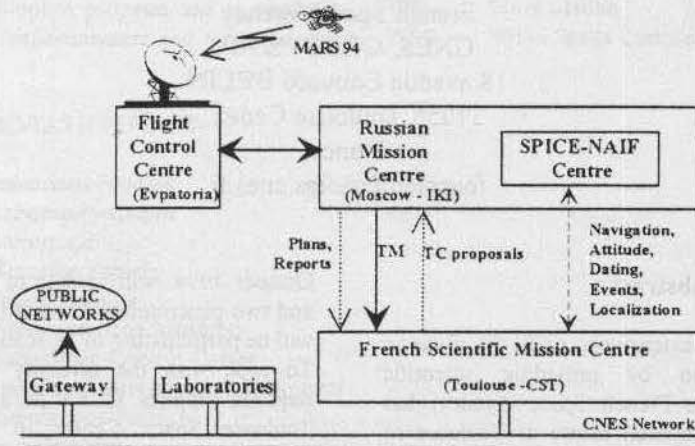


Figure 1

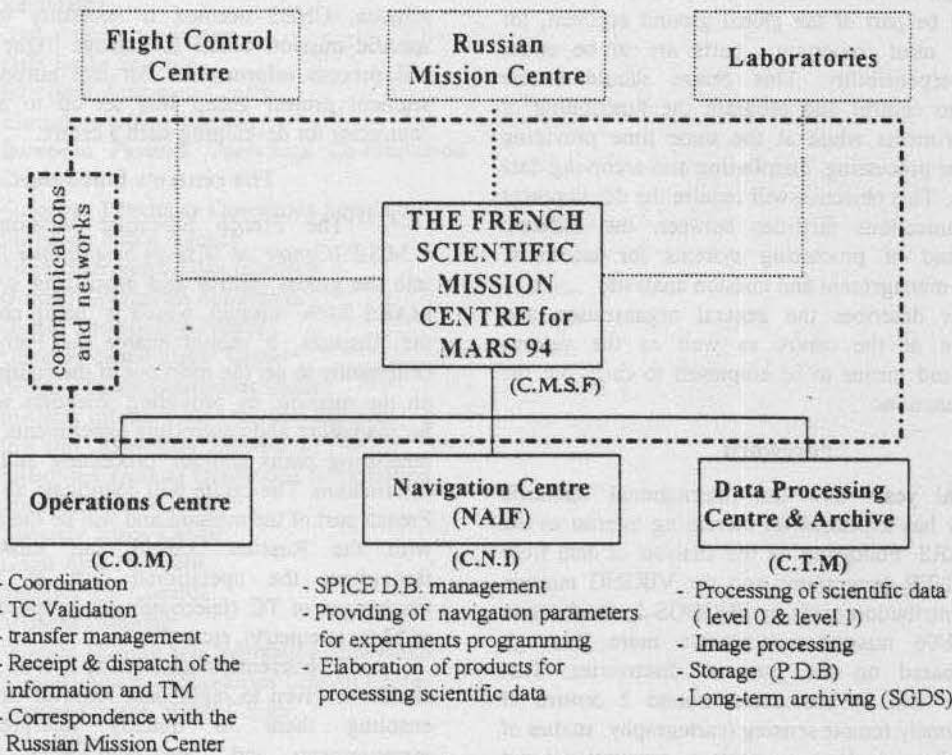


Figure 2

General organization

The C.M.S.F. will centralize all of the management and processing functions and will be closely interlinked with the mission and control centres in the CIS and the French laboratories. The flight control centre and the

principal receiving station are located in the Ukraine (Evpatoria). The Russian mission centre is in Moscow, and there are nine French laboratories located at different areas in France. Figure 1 shows the general organization of the ground segment for the MARS 94/96 mission.

In functional terms the C.M.S.F. can be divided into 4 sub-systems for carrying out the 4 major tasks, which are:

- operations management,
- navigation and processing of ancillary data (attitude, dating, etc.),
- data processing and archiving,
- communications and networks

The C.M.S.F. will consist of 3 centres, the Operations Centre or C.O.M. (*Centre des Operations Mars*), the Interplanetary Navigation Centre or C.N.I. (*Centre de Navigation Interplanétaire*) and the Mars Processing Centre or C.T.M. (*Centre de Traitement Mars*), which will rely on a communications and network system to provide all of the internal and external links. Figure 2 shows the organizational diagram for the C.M.S.F.

The communications system

The conception of a decentralized mission centre required the development of a communications system to meet the specific constraints of such a project. Since the operational functions practically require real-time reception of telemetry and a high degree of integrity for exchanges, the network architecture had to be organized around our own facilities, dedicated to the different links with centres located in the CIS. Public networks do not offer a sufficient level of reliability and

availability to guarantee the necessary security and efficiency for exchanges.

The network architecture

The telemetry will mostly be acquired by the Evpatoria station located in the Ukraine. Communications sessions with the probe will take place every 2 days and will last for 6 hours during which the various memories aboard the spacecraft will be emptied at a rate of 64 Kb/s.

This data will be received and processed in real-time at the Toulouse Space Centre by the scientific teams, using their test and control equipment (GSE).

Given the decentralization of centres in the CIS (Evpatoria, Moscow, Khimki), it will be necessary to have an efficient communications system enabling all types of exchanges between the different centres. The principle chosen is to interconnect the different computer networks of the various centres by means of digital channels with high transmission rates. A first satellite link (Eutelsat or Gorizont at 64Kb/s) will connect the acquisition system of the Evpatoria station with the Russian mission centre at Moscow (IKI). The communications protocol to be implemented on this section will be of the IPX type used for interconnecting two NOVELL networks.

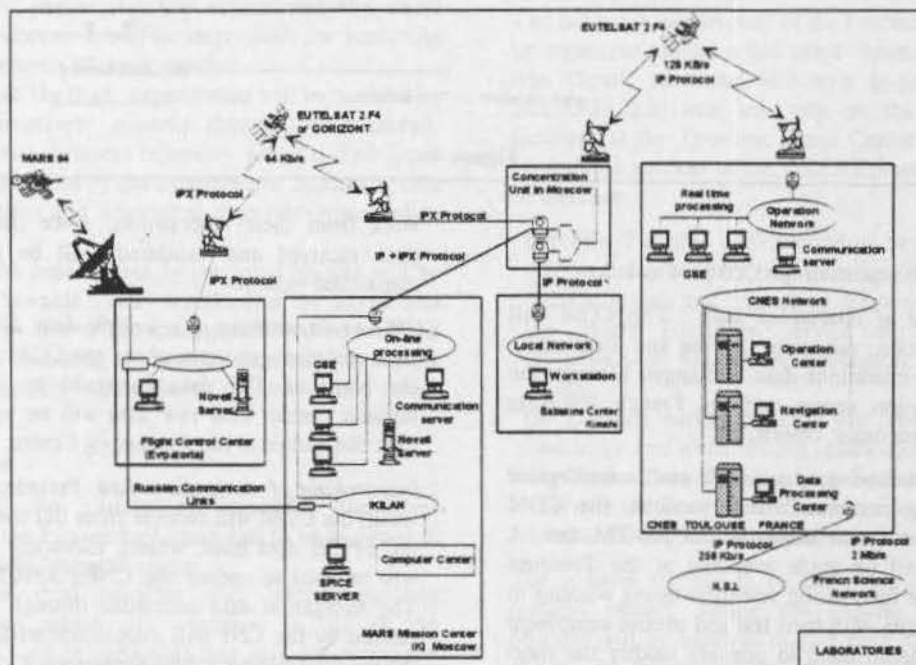


Figure 3

A second satellite channel (Eutelsat at 128 Kb/s) will connect the computer networks of the different Moscow centres to the CMSF's operations network. This connection will accept the IP protocol for the exchange

of digital data, but will also carry telephone and fax channels, both of which are absolutely necessary in order to enable flight control operations to be carried out from French territory.

All of the communication lines connected to CNES, and on the CIS' territory, will be centralized by a concentration station installed by CNES in Moscow. All of the multiplexers and routers installed will be directly monitored by the telematics management department at the Toulouse Space Centre.

At the CMSF level a dedicated network will be established (Operations Network) to handle supervision of information exchanges, and real-time reception and dispatching of data to the GSE (Ground Station Equipment).

The other elements of the French mission centre (the centres for navigation, operations coordination and processing) have been organized around the internal optical fibre network at the Toulouse Space Centre. This network is moreover linked to the national research network and to the NSI (via a specialized 256

Kb/s line). The general architecture of the communications system is shown in Figure 3. Such a system will enable all of the information to be processed in France, while ensuring close cooperation with the Russian centres responsible for controlling the satellite and avoiding permanent assignment of scientific teams to the CIS.

The Operations Centre

As the sole correspondent of the Russian Operations Centres, the Mars Operations Centre (COM) has to coordinate and handle operations for the French part of the mission. It will be responsible for all of the information exchanges between the Russian centres and the different participants in France (laboratories and navigation and processing centres).

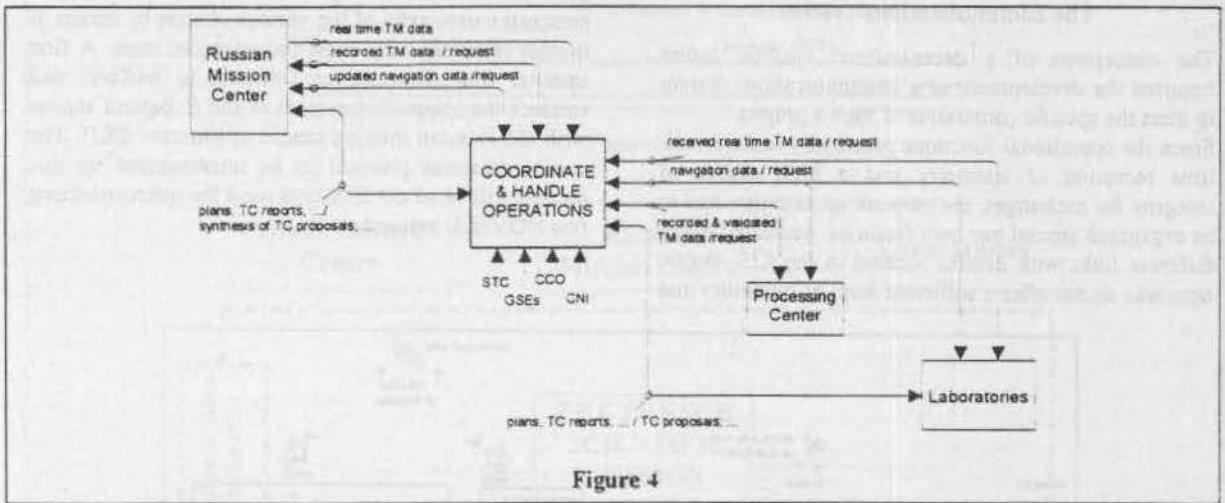


Figure 4

Functions

The principal functions of the COM are as follow.

- **Management of operations data :** The COM will handle reception, validation, storing and dispatching of all of the operations data exchanged between the Russian mission centre and the French scientists (plans, TC proposals, reports, etc.)
- **Real-time monitoring of scientific and technological data:** During communications sessions, the COM will handle real-time acquisition of the TM data. A laboratory will be made available at the Toulouse Space Centre for visiting scientific teams wishing to analyze the data with their test and control equipment (GSE), to enable them to possibly modify the short term programming for their experiments. This organization will enable scientists to conduct flight operations from Toulouse without having to be present in Moscow in the Russian mission centre. However, for routine stages, the experimenters will be able to do all of their control and programming

work from their laboratories, since the telemetry, once received and validated, will be immediately dispatched to them.

- **Off-line dispatching of scientific data:** 24 hours after each communications sessions the COM will recover the real-time TM data corrected by the Russian mission centre. This raw data will be validated and then dispatched to the Processing Centre.
- **Dispatching of navigation data:** Periodically (once a week) the COM will recover from IKI the updates for the SPICE data base, which, following verification, will be used to update the CNES SPICE data base. The navigation data accessible through the services offered by the CNI will enable scientists to prepare the programming for their experiments.

Figure 4 shows the exchanges of data between the COM and the other centres: the Russian mission centre, laboratories and the processing centre.

Facilities

The COM is the CMSF's operations control body. In functional terms it will consist of 2 sub-systems: the Operations Coordination Centre or CCO (*Centre de Coordination des Opérations*) and the GSE (Ground Station Equipment).

In addition, it will rely on the multi-mission facilities at the Toulouse Space Centre which are:

- the Telecommunications Server or STC (*Serveur de TéléCommunication*) for all information exchanges (digital data, fax, phone links) between the Toulouse Space Centre and the CIS;
- the Interplanetary Navigation Centre for updating and consulting of the SPICE data base.

The hardware architecture planned for each of these sub-systems developed and operated by CNES (CCO, CNI, STC) will consist of dedicated computers of the SUN/SOLARIS type. The GSE provided and operated by the laboratories will be PC/DOS type computers.

The Processing Centre

The Processing Centre which is a part of the CMSF has been designed to process information so that it may be exploited by scientists.

Its functions are management, processing and archiving of telemetry data relative to all of the French experiments, or experiments involving French participation, concerning the orbiter and the small stations. Moreover, it will be responsible for analyzing the relay telemetry (French supply).

The data from the flight experiments will be handled by several management systems aboard the spacecraft, which generate different telemetry formats. Two types of data are provided by the experiments: numerical data (scientific data) and analogical data (servomechanism data).

Data from the experiments on the small stations will be transmitted towards a relay installed on the orbiter and then stored by one of the management systems aboard the orbiter. Processing of the relay data will require the use of decoding techniques (Viterbi and Reed-Solomon).

Organization

Because of the variety of scientific disciplines concerned, the Processing Centre had to be designed to fit into a global "project" vision.

At first we shall consider only information and characteristics which are common to all of the experiments, and in particular that used for extracting and dispatching raw data and for archiving it. This level of processing will be referred to as level 0.

During the second stage, the Centre will handle specific and systematic processing of experiment data. This processing does the ground work for later scientific exploitation which will be done in laboratories. It

basically consists in decommutating data, in reconstituting spectra and sometimes in transforming raw values into physical values. This processing is accompanied by the production of quick-look images which will be widely circulated to scientists by means of interactive media.

To fulfil the specific needs relative to the video cameras in the small stations, an Image Processing Centre will be established; this centre will work closely with the scientific laboratories involved. Computing techniques for digital elevation models will be used.

Since the experiments are often conducted within the framework of national and international cooperation on a large scale, the raw or processed data will have to be dispatched to a great number of laboratories; this will be done by generalizing distribution of information on CDs and via high transmission rate computer networks.

To provide efficient access to the data, it will be archived in two stages. The first level of archiving will be a medium term storage of the data to enable experimenters to have access to their raw or pre-processed information (Project data base). The second level of archiving will be done with a long term goal of ensuring the integrity and durability of the data (as an inheritance) and of making this data available to the entire national and international scientific community. Figure 5 shows the general organization of processing to be done by the centre.

The hardware architecture of the Processing Centre will be organized around a dedicated computer of the SUN type (Spark 10 model 402 with bi-processor, under SOLARIS 2.3) and will rely on the multi-mission facilities at the Toulouse Space Centre. The different centralized services of the CNES Computing Centre to be used are:

- the File Transfer and Archiving Service or STAF (*Service de Transfert et d'Archivage de Fichiers*) for archiving data and organizing the project data base.
- the Media Exchange Service or SEM (*Service d'Echange de Media*) for circulation of data on CD ROM.
- the graphics workshop which will produce the colour and black and white images (quick-looks).
- the Space Data Management Service or S.G.D.S. (*Service de Gestion des Données Spatiales*) for long term archiving and preservation of this data.

The volume of data to be processed depend on the mission phases: during the transfer phase, a few Moctets will be received during each communications session, on the other hand, during orbital phases, the volume of data could be as high as 30 Mbytes per day. Since pre-scientific processing will only be done for a few experiments, the volume of output data will only be slightly higher than the input data. Archiving of all of this data, raw or processed, should amount to an overall volume of 50 Gbytes for the mission.

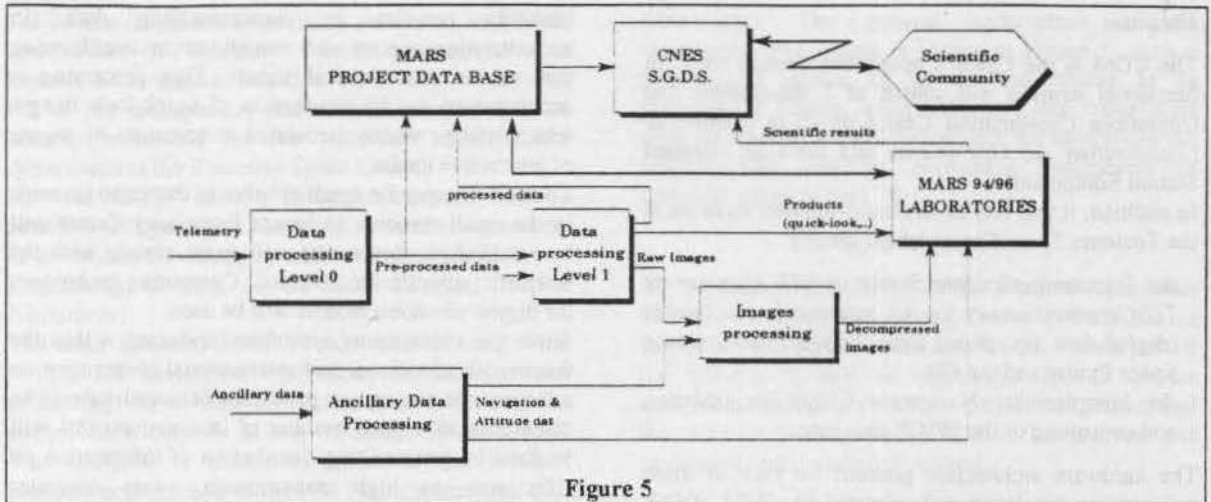


Figure 5

The navigation centre

Plans for the Mars 94 ground segment, include the development of an interplanetary navigation centre or C.N.I. (*Centre de Navigation Interplanetaire*) whose role will be :

- to handle the mission's analytical work (minimization of masses, optimization of visibilities),
- to participate in navigation and location operations for the probe and the stations jettisoned onto the Martian surface,
- to provide support to the French scientific community in the field of space mechanics,
- to compute and provide all of the parameters (attitude, navigation, dating) necessary for the scientific processing, the image processing and the operations done within the CMSF framework.

However the centre envisaged will be developed within a multi-mission perspective (this system will be used for the CLEMENTINE project).

Location process

CNES personnel have developed a Kalman filter by upgrading the initial version used for the Phobos optical navigation. This software, named FILON (*Filtering for Location and Navigation*) is a multi-purpose software package for locating objects on the surface of a planet by means of relative measurements taken by a spacecraft. It is currently being used for Mars 94/96, for the VAP project (the French rover studies), for the TAOS and S80T projects (mini earth satellite for location of mobile targets). In the current version the state vector has up to 20 components, 6 for the mobile, 7 for the spacecraft and others for bias, drift, ionosphere and error measurements. In the case of the Mars 94 project, the only measurements which are processed by the software are relative measurements, for instance, 1 way Doppler measurements from the

landers to the spacecraft. More precisely, no ground based measurements are currently being processed.

Consequently, the initial state vector for the spacecraft is computed by the Russian ballistic centres (IPM, TSOUP).

The location process for the small stations and penetrators will involve different partners in different countries:

. Russia:

Ballistic Centres: TSOUP, IPM, Babakine, Flight Control Centre (Evpatoria).

IKI (Institute for Cosmic Research): which will receive the telemetry relayed by M94.

. France: CNES Toulouse.

It has been decided that all information concerning the Spacecraft state vector will be sent via the SPICE system (navigation ancillary information data base) developed by JPL. As far as Mars 94 is concerned, IKI is responsible for the SPICE data base. The proposed data flow exchange is shown in Figure 6.

Support to French scientists

Another part of the navigation tasks is to help scientists prepare their telecommands and analyze their results. This consists mainly in predicting events, with limited accuracy, for telecommands. These predictions will then be updated and re-computed with greater accuracy in order to analyze results.

This task will be done using the SPICE system. The main scientific experiments aboard the Mars 94 S/C or landers are:

SPICAM: (solar and stellar occultation).

Specific requests: prediction and reconstruction of the occultations.

ELISMA: (plasma studies)

Specific requests: prediction of the duration of stay in the Ionospheric region; ephemeris and the closest approach to Phobos and Deimos

OMEGA: (infrared spectrometer)
 Specific request: Nadir pointing coordinates
DYMIO: (ionospheric studies)
 Specific request: crossing into the Martian magnetosphere
OPTIMISM: (seismology experiments on the small stations)

Specific requests: location of small stations and reconstruction of the landing trajectory
METTEG: (meteorology on small stations)
 Specific request: location of the small stations.

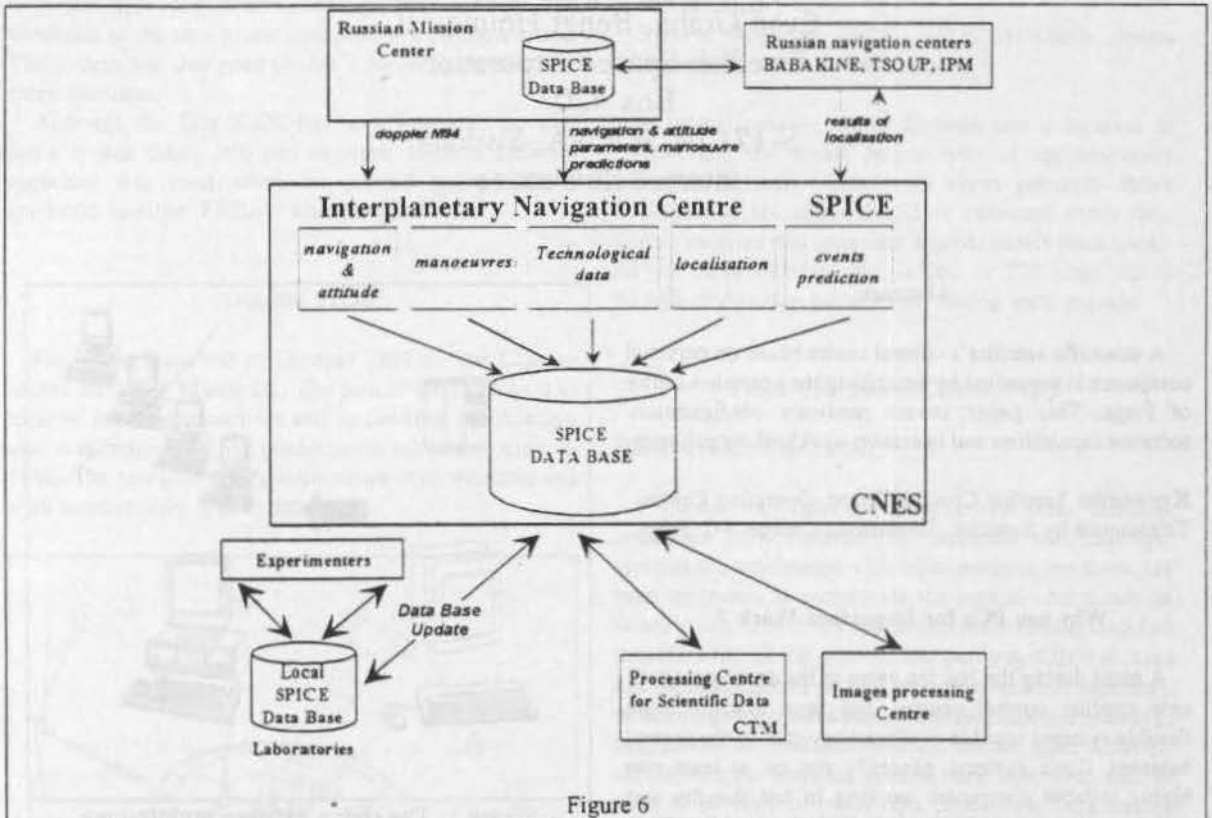


Figure 6

On the Russian side, IKI is responsible for maintaining and updating the SPICE Space Data base. For example, the spacecraft ephemerides will be updated on a weekly basis. Once a week, a new file will be catalogued, thus covering a 15 day period: 7 days reconstruction, 7 days extrapolation.

This SPICE Data base will be copied in Toulouse, as soon as any change occurs, and updated by France with French results (such as the lander location). The SPICE toolkit will be installed in every French laboratory involved in the mission along with special routines developed by our department, if these prove necessary. The Mars 94 SPICE data base will be catalogued in Toulouse and updated as frequently as is necessary. Scientists will have access to this data base and will be able to copy any files they want by means of FTP.

Conclusion

The French mission centre established within the framework of the MARS 94/96 mission has been designed in such a way as to provide the scientific

community with support in programming their experiments and to create a centralized system for processing and managing scientific data. Apart from its architecture and the means used to construct it, the centre was developed using a new approach to its definition for the purpose of scientific missions to be undertaken jointly with the Russian space agency. Moreover, special care has been taken to provide for multi-mission facilities (navigation centre, communications systems, general architecture, Space Data Management Service), in order to be able to re-use the systems to be developed and also the organizing principles, for future missions.

A RELIABLE HIGH PERFORMANCE CONTROL CENTRE FOR SCIENTIFIC SATELLITES USING PERSONAL COMPUTERS

Stefan Lundin
Sven Grahn, Bengt Holmqvist
Swedish Space Corporation
Box 4207
S-171 04 SOLNA, Sweden
internet:slu@ssc.se

Abstract

A scientific satellite's control centre based on personal computers is presented by describing the operation centre of Freja. This paper covers hardware configuration, software capabilities and operation workload organisation.

Keywords: Satellite Control Centre, Operation Centre, Telescience by Satellite, Scientist-In-Charge, PC, Freja.

Why use PCs for Important Work ?

A trend during the last ten years in the development of new satellite control centres, has been towards more flexible systems capable of almost any task in the control business. Such systems generally run on at least two highly reliable computers working in hot standby and with several terminals or workstations connected to them. By using a mouse or joystick, a privileged operator may monitor, adjust a parameter or simply exchange any part of the ground or space segment systems, using anyone of the connected terminals or workstations. From the same desk, all tasks could easily be performed as long as the operator knows what to do.

For associations with several satellites with similar characteristics, this gives possibilities to concentrate the control of satellites to the same unit which could be a building, a floor or even the same control room. This possibility of course allows operators in a very natural way to share achieved experience effectively and also to become backup for each other.

For organisations with few satellites, perhaps with very different missions, these flexible workstations "capable-of-everything" may not always be the optimal solution. Instead a system with several dedicated computers, each handling one specific task, could very well better suit the requirements of a specific mission. This is the case if several tasks are to be performed sequentially by the

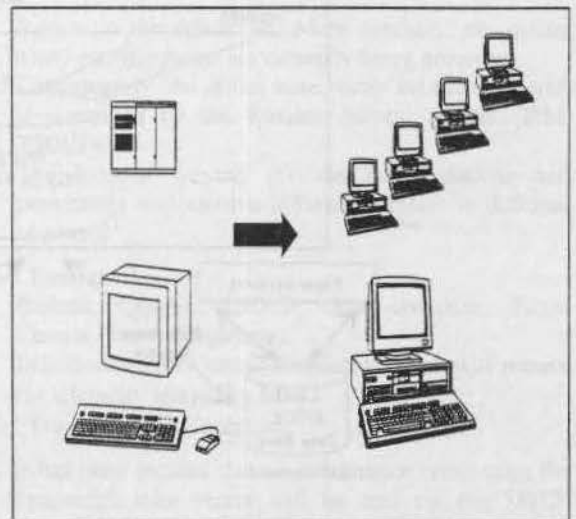


Figure 1: The choice between multitasking workstations or cheaper PC-based control centres.

same person at different locations. If the tasks are possible to define in such a way that standard personal computers can be used, a non-negligible cost reduction may be encountered. Such computers are truly mass produced off-the-shelf equipment and for a reasonably large organisation the maintenance could probably be performed in-house, avoiding expensive and time-consuming maintenance and support contracts. Also development cost may decrease, as plenty of PC software support packages for data presentation, communication etc are available on the market.

In this scenario it is important to keep in mind that the different computers must be capable of substituting each other. Personal computers are still said to be less reliable than the best workstations and the most important control tasks must be possible to reinstall on a new computer rapidly.

Previous Control Centre Experience

The Swedish Space Corporation (SSC), also strove for expandable, flexible systems when we specified the control centre (CC) for the Direct Broadcasting Satellite "Tele-X". Two main and two front-end computers, working in hot standby, are in this system controlled by a switch-over unit which changes the monitors and terminals to the new prime computer if a problem arises. The system was designed so that it could be extended for three satellites.

Although the Tele-X CC has been working very well since it was taken into use in April 1989, a different approach was used when the ground segment for a scientific satellite, FREJA, was designed.

Satellite Facts

Freja was launched in October 1992 by the Chinese rocket the Long March 2C. The aim of the satellite is to explore the magnetosphere and to continue the research that was started by its predecessor satellite Viking in 1986. The research now continues on other altitudes and with substantially higher data rate.

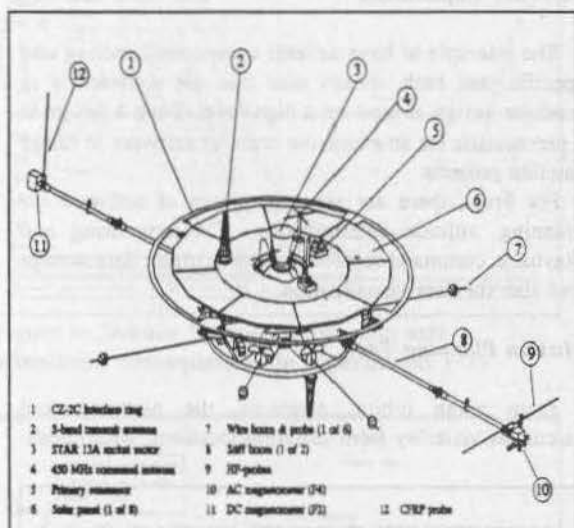


Figure 2: The design of the scientific satellite Freja

Freja is a sunpointing spinner with a 2.2 m diameter and a 214 kg mass. Its orbit is between 600 and 1750 km with an inclination of 63°. The satellite images the aurora and measures particles and fields in the upper ionosphere and lower magnetosphere. Swedish, German, Canadian and U.S. instruments are flown as eight separate payload experiments, each one exploring their specific area of interest.

Three data receiving stations are used, one of them also capable of sending commands. They are:

- Esrange Space Centre in Sweden (67°54'N, 20°04'E), where excellent passage coverage (9 out of 13 passages) is achieved due to the extreme latitude. This is the location of the control centre,
- Prince Albert Satellite Station, PASS, in Canada (53°21'N, 105°93'W) ideally located to receive real-time data from magnetic oval crossings at these altitudes and
- Syowa, Antarctic (69°S, 39°25'E) which covers phenomena at the lower altitudes.

A typical passage above Esrange has a duration of 20 min and the nodal period time is approximately 109 min. Normally, data from seven passages above Esrange and six above PASS is collected every day. Syowa receives real time data approximately once-a-day. As the downlink data rate is 262 or 524 kbps, up to 80 MB of data can be collected during each passage.

Freja Operations Centre, FOC

Hardware Configuration

Freja has very little in common with other satellites controlled from Esrange. RF antennas and baseband systems are timeshared with other projects but there has been no reason to incorporate the control centre into an existing one. The Freja operations team should take full responsibility of the satellite and perform different tasks like passage control (ie data storage overview, telemetry monitoring and commanding), detailed mission planning, data production and maintenance. As the tasks differed, several natural working places were identified and as there is no need to reach data production tools during satellite passages, no special interest of a multitasking, flexible workstation existed. Besides, the project had to save money and therefore it was decided to choose a PC based solution.

The control centre is built up by six off-the-shelf 80386 based personal computers, connected by Ethernet into a minor local area network. Each computer handles one specific task but may share data with the others. The different computers' tasks could be described as:

- a Command generator, manned during passages,
- a Telemetry monitor, simultaneously manned during passages by the same operator,
- a Saver, used for automatic storage of received TM,
- a Data Summary Plot generator, used after the passages,
- a DAT cassette copier, used to produce one DAT tape for each scientific group and
- a File server, used to control the local area network.

Mechanical devices like disks and DAT recorders are of higher quality and placed in external cabinets for easy

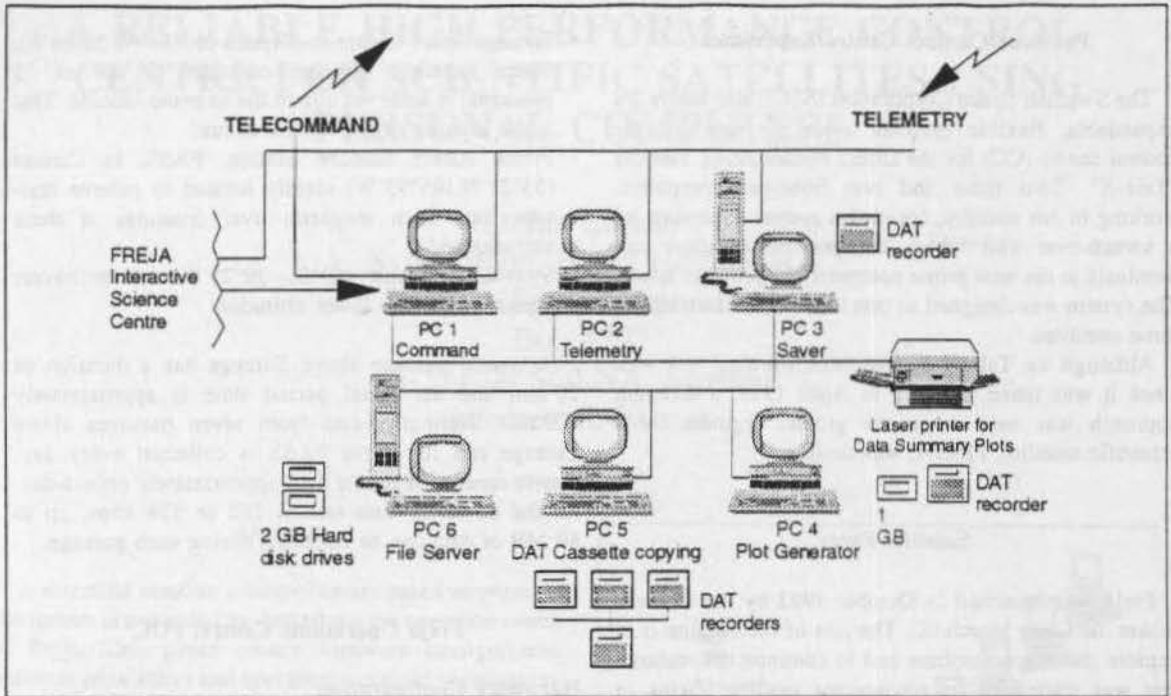


Figure 3: Computer system configuration of the Freja Operation Centre

maintenance. Three disks of 1 GB and six DAT recorders are used simultaneously while two recorders are stored as spare parts. The whole control centre uses uninterruptible power supply. So far the system has been working far more than 10,000 hours.

During periods without contact, planning may be performed at anyone of these six computers. In practice however, planning is performed at the Satellite Operation Manager's Office on a separate computer excluded from the network.

Three computers inside FOC have direct access to telemetry: one for commanding, one for monitoring and the data saver. For this purpose they are equipped with a commercial product, the "Bit and Format Synchronizer"-board, that allows direct access of the PC to a biphase or NRZ signal. These three computers are also the only critical ones. The computer that generates plots also contains the "Bit and Format Synchronizer"-board and could consequently be used if one of the others suddenly fails.

Prince Albert Satellite Station is equipped with one redundant saver computer while Syowa records received data on tape for later evaluation. The reception of data above Syowa was organized after launch when it was clear that it had some spare time for data reception. Due to the simple hardware requirements, the station could rather fast be taken into operation also for Freja!

Software Capabilities

The principle to have several computers handling one specific task each, makes sure that the software is in modular design at least on a high level. Such a design is a prerequisite for an extensive reuse of software in future satellite projects.

For Freja, there are separate pieces of software for planning, attitude determination, TM monitoring and playback, command selection and execution, data storage and also for data visualization.

Mission Planning Tool

From given orbital elements, the planning tool calculates visibility from different locations, determines

OPERATIONS SUPPORT SOFTWARE FOR THE FREJA SCIENTIFIC SATELLITE v.1.9		
Utilities Today is 1994/01/18 - day number 18		
VIEW TEXT FILES	SCREEN PRINTER	BULLETIN BOARD I/F
Attitude Control 409 days since launch		
MANOEVRE PLANNING	ATTITUDE/TARGET	CREATE SLEW RATES
SPIN MANOEVRE	SIMULATE PRECESSION	GENERATE COMMANDS
Operations Support		
SCIENCE PLANNER	ATT.DATA COLLECTION	GRAVITY GRADIENT
PLANNING FILE	GEOCENTRIC DATA	PLOT GEOCENTRIC DATA
INERTIAL ORBIT	GROUND SITES	REALTIME TRACK
ELEMENT DATABASE		ECLIPSE PREDICTIONS
EXIT		

Figure 4: Planning Selection Menu

the attitude, generates attitude correction command sequences, visualizes spin direction consequences for the experiment etc. Examples of the choices and its output are given in figure 4 to 7.

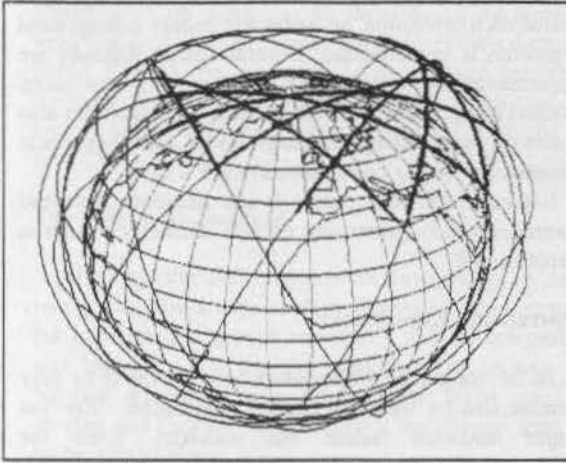


Figure 5: Visibility of the satellite from its control centre.

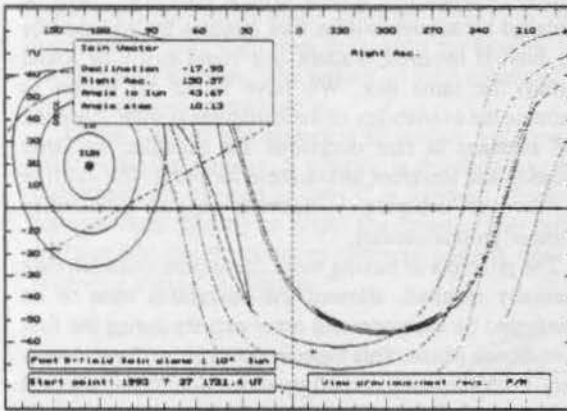


Figure 6: Science Planner shows spin axis orientation consequences on experiments FOV

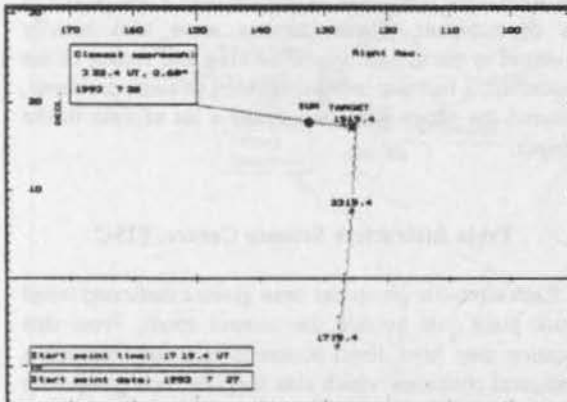


Figure 7: Simulation of attitude corrections based on the quarter-orbit magnetic torquing method

Command Generation

The command generator executes preprogrammed command sequences selected by the operator on duty. Depending on received telemetry (if such conditions are defined) and the interaction of the operator, the chosen command sequence performs its checks and issues predefined commands.

Command sequences are organized by mission phase, subsystem and function, and most of them contain timing information when to execute the command on-board the satellite.

Telemetry Monitor

Telemetry may be monitored in realtime or playback, as analogue bars as well as digital values. The Freja project by purpose avoids windows with flexible sizes and positions to simplify fast recognition of displays and to identify the occurrence of unusual values. The system itself supports the operator with value validity check and signals for alarm condition. Telemetry monitoring is exemplified in figures 8 and 9.

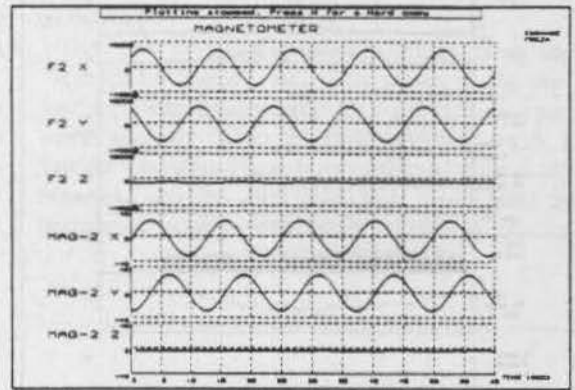


Figure 8: Signal evaluation for trend analyses

CD	Class name	Value	CD	Class name	Value
PT10	WALL SW	27.3	PT12	spin	0.32
PT16	WALL SW	1.60	AT10	Magnetometer 1	WALL
CT18	SWITCH 1	WALL	AT16	Magnetometer 1	SW
CT19	SWITCH 2	WALL	AT20	Magnetometer 2	WALL
CT21	SWITCH 1	AMP	AT21	Magnetometer 2	SW
CT23	SWITCH 2	AMP	PT23	DATA SWITCH	SWITCH
HW1	TORQUE S/C Power *	20.73	AT28	Powermeter 1	WALL
PT21	AMP WIND SWCH 1	1.86	AT13	Powermeter 1	SW
PT23	AMP WIND SWCH 2	-0.28	AT20	SW 1 DATA CHOOSE	CHOOSE
PT14	ALL DATA SWITCH	SW	CH20	SW 2 DATA CHOOSE	CHOOSE
PT11	DATA TYPE	1	CH24	SW 1 DATA CHOOSE	CHOOSE
PT12	PT FULL ORBIT Dump	1	AT18	Powermeter 2	WALL
PT18	SWCH CLASS DATA	1	AT24	Powermeter 2	SW
PT25	MAGNETIC CLASS NEW	10279	AT28	SW 2 DATA CHOOSE	CHOOSE
PT26	MAGNETIC CLASS OLD	56795	CH21	SW 2 DATA CHOOSE	CHOOSE
PT10	COMMAND IN QUEUE	311	CH21	SW 2 DATA CHOOSE	CHOOSE
PT28	COMMAND PACKET CAC	128	CT28	SW 1 DATA CHOOSE	CHOOSE
PT29	SWCH SWCH	2	CT29	SW 1 DATA CHOOSE	CHOOSE

Figure 9: Telemetry monitoring of the most essential signals.

Data Products

Freja transmits real-time telemetry data with the speed of 262 or 524 kbps during passages. Each experiment has its own data set and its own software for fast evaluation. These programs are written by the scientists themselves and merged into "Data Summary Plots", a data product that gives an overview of the achieved results. The DSP:s are stored in PostScript format and distributed to the scientists by e-mail. Normally the plots are available within six hours after a passage above Esrange.

For further analyses, raw data is stored on DAT cassettes and sent by mail approximately once-a-week. An example of a DSP (1 out of 3 pages only) is given in figure 10.

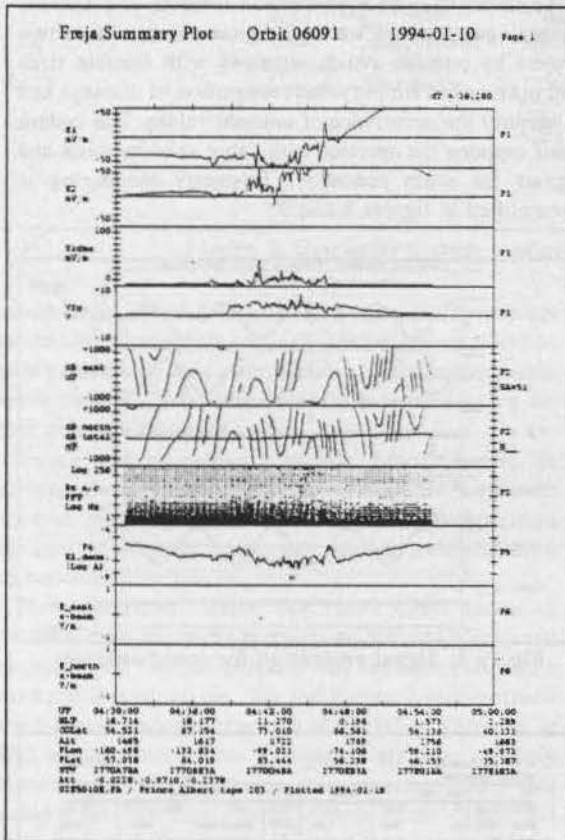


Figure 10: Data Summary Plots quickly give an overview of achieved results.

On-board Software

To secure the satellite in case of temporary ground segment outage and to reduce the amount of necessary operations, certain basic platform management functions have been implemented in the satellite's on-board controller software. Commands to reconfigure the payload experiments into suitable measurement modes as well as S-band transmitter handling are executed on-board at a predefined time by so called timetagged

commands. By this principle, measurements above all three receiving stations could be performed without having both transmitter and experiments turned on throughout an orbit.

As Freja normally encounters a 30 minutes eclipse period each revolution, an automatic battery management algorithm is implemented. Several charge methods are implemented but the selected one is an amp-hour meter method using a charge factor of 1.05. The algorithm also reacts on high battery discharge levels and disconnects unnecessary power consumers in such a case.

Naturally, software to decode and distribute command messages and to gather and encode telemetry signals is implemented.

Operational Experience

So far, the personal computers have proven to be very reliable also for the Freja control application. Only one major hardware failure has occurred, when the motherboard in the DATA copy machine suddenly failed. It was repaired during the day although if necessary, it could have been done faster.

It is believed that a time critical computer could be replaced by another within five minutes by the operator on duty. If required, a spare one could easily be found during the same day. We have found no reason to increase the availability of the computer system, since the RF antennas at rare occasions are occupied by other projects and therefore unavailable for Freja. The satellite is however designed to survive several revolutions without ground contact.

The principle of having more computers available than normally required, allowed the operations team to be reinforced by designers and other experts during the first post-launch phase. This support could be performed with very little hardware reconfigurations due to the selected architecture of the system.

The CC uses the same software that is used in the EGSE test equipment. This combined and thereby limited software made it possible to involve only a few people in its development. These persons were also heavily involved in the design, manufacturing and testing of the spacecraft, a fact that probably spared us some problems, reduced the paper work and saved a lot of time in the project.

Freja Interactive Science Centre, FISC

Each scientific group has been given a dedicated small work place just outside the control room. From this location they have direct access to telemetry through a dedicated connector which also supplies each group with power, telephone connection etc. During the period directly after launch this lobby was rather crowded as more and more scientists arrived to observe how their experiment was doing.

Organisation

Control Centre Personnel

The control centre is run by a small team consisting of a satellite operation manager and three operators. Their tasks are to determine the orbit and attitude, operate the satellite during Esrange passages, produce different data products and to plan operations for the next revolutions using actual orbit, power budget and scientific demands and preferences. All four are capable of doing each task.

The Freja Operation Centre is incorporated in the control room of Tele-X, which is manned around-the-clock. To support the Freja team the Tele-X operators have been taught to take care of routine operation of the Freja satellite during passages outside office hours.

The Scientist-In-Charge Concept

Freja's eight scientific groups measure different parameters of the same phenomena. As they have partly different interests, arguments concerning coordination, satellite pointing, passage priority, allocation of available power etc could cause long discussions and thereby large problems.

Our way of avoiding such problems is to use a "Scientist-In-Charge", SIC. This person is the one to produce planning instructions for the next coming period which normally covers the following two weeks. The Satellite Operation Manager, responsible for the platform behaviour and the data production, could from these instructions produce detailed revolution-per-revolution

Through one multiplexed line, the scientists are able to send telecommands to their own experiments. Only one group at a time can use this line and precaution against erroneous stimuli of the platform or the other experiments are taken care of. By allowing the groups to send commands, the engineers who built the experiment could also do the commanding to evaluate behaviour, perform calibration procedures etc. The operator on duty simply turns on the experiments and then opens the line for FISC commands.

Telescience by Satellite

Although the FISC room has been useful in many ways, it is now-a-days seldom manned. Instead, some of the experimental groups have put a transfer computer at this location. The transfer computer can receive and forward telemetry from Freja to the home site, and receive and forward telecommands transmitted from the home site to Freja.

By addressing this remote computer through Internet, scientists in United States, Canada, Germany and Sweden receive fresh Freja telemetry at their offices. They may also transmit commands (Walker 1993) to their experiments from their own desk when the satellite is in contact with Esrange. The impact of their command can then be studied immediately.

As the satellite sometimes is in contact with both its main receiving stations, a scientist in America may send commands via Internet to the CC in Sweden, which will forward them directly to Freja. The scientist may then in realtime observe the result as telemetry coming from the receiving station in Canada.

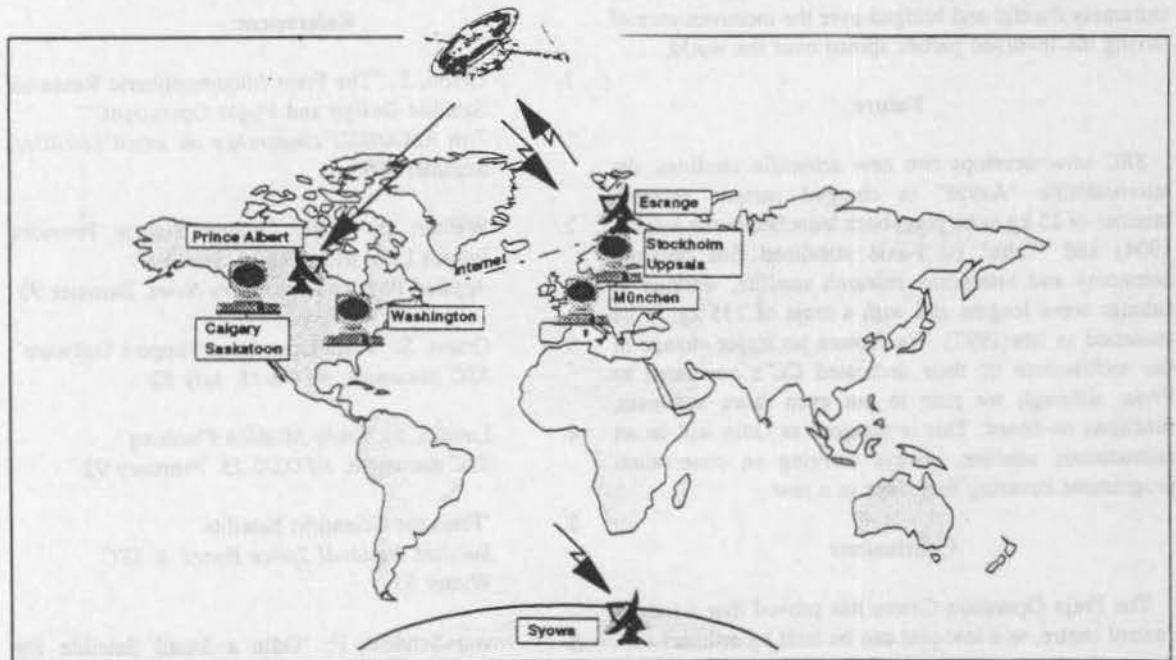


Figure 11: By world-wide telescience, scientists may command their experiment whenever the satellite is in contact with its control centre.

plans and exactly plan what to do during the next passage above the control centre.

The honour of being SIC is alternating among the different scientific groups.

Scientific Data Library

Another time consuming and important task is to keep track of all gathered data. Although data is spread to all Principal Investigators on DAT cassettes, a library with all relevant data concerning Freja available on disk is most effective. The Department of Plasma Physics at the Royal Institute of Technology in Stockholm, Sweden is taking care of this task. In this way data is where it belongs; at the scientists with easy access to other groups. A master copy is also stored at Esrange.

So far (December 1993), approximately 280 GB of data spread on 400 DAT cassettes of 700 MB each has been produced. As the whole project, including launch and experiments, cost approximately 20 MS each received byte has cost only 0.00007 \$.

Communications Between Participants.

Since launch, four Freja Science Meetings have been organised where different scientific groups present their research and compare results. On a more regular basis, discoveries, opinions and SIC instructions are spread by e-mail to every subscriber of the so called "FrejaInfo".

During normal conditions approximately five e-mail messages per day are issued, most of them from FOC giving information about orbital elements, DAT-cassette contents etc. During special events a lot more messages are distributed. The good communications have been extremely fruitful and bridged over the inconvenience of having the involved parties spread over the world.

Future

SSC now develops two new scientific satellites: the microsatellite "Astrid" (a charged particle research satellite of 25 kg to be piggyback launched in the autumn 1994) and "Odin" (a 3-axis stabilized fine pointing aeronomy and astronomy research satellite, working in submm wave lengths and with a mass of 235 kg, to be launched in late 1997). We foresee no major change in the architecture of their dedicated CC's compared to Freja, although we plan to put even more automatic functions on-board. This is required as Odin will be an autonomous satellite, always carrying an observation programme covering four days in a row.

Conclusions

The Freja Operation Centre has proved that a simple control centre, to a low cost can be built by ordinary off-the-shelf personal computers and still handle a considerable amount of data.

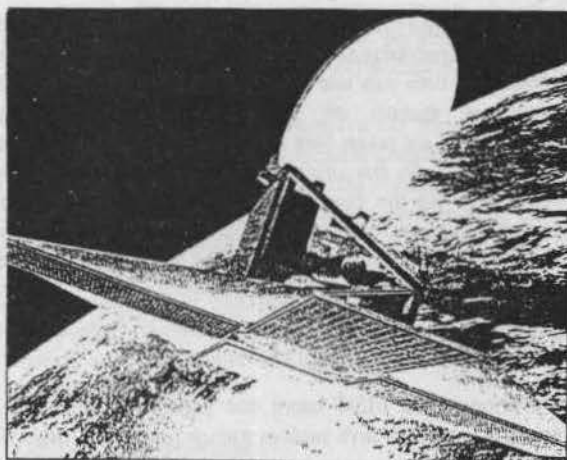


Figure 12: Odin - a future fine pointing aeronomy and astronomy research satellite.

To give authority and full safety responsibility to the operations team while leaving mission objectives and data storage to the users has been very powerful. Scientific trade-offs are now discussed and assessed by the users while the operations team concentrate on more basic platform management.

By allowing the satellite users to perform telescience on their own experiments, increased flexibility for the scientific groups is achieved. At the same time the workload on the operation team is reduced. We knew everybody is pleased by it and believes that better science is achieved with this philosophy.

References:

1. Grahn, S; "The Freja Magnetospheric Research Satellite Design and Flight Operations." *7:th AIAA/USU conference on small satellites*, Summer 1993.
2. Walker, B; "APL Ground Station Provides Instant Link with FREJA Satellite." *Applied Physics Laboratory News*, Summer 93.
3. Grahn, S; "Freja Operations Support Software" *SSC document, RFO3-15*, July 92
4. Lundin, S; "Daily Mission Planning" *SSC document, RFO2/2-23*, February 92
5. "Freja the Scientific Satellite" *Swedish National Space Board & SSC*, Winter 93
6. von Schéele, F; "Odin a Small Satellite for Astronomy and Atmosphere Research" *SSC document, RAC21-1*, October 1993

OPERATIONS I

1. Leconat, F.; Saint Vicent, A.; Brenot, J.M.;
Darroy, J.M.; Gaullier, F.; Pham, P. and
Pessah, P. (Matra Marconi Space-France):
"Improving the Management of Operational
Information for Safer and More Efficient
Spacecraft Operations" 385
2. Hardsten, G. and Jarnmark, J. (SSC-Sweden):
"Operational Training for the Flight Crew of the
Tele-X Satellite" 395
3. Sitruk, F. (CNES- France):
"Improvement of Operational Activities
Efficiency" 399
4. Gaullier, F. and Limouzin, G. (Matra Marconi Space-
-France):
"The Eurostar Operational Concept" 404
5. Booty, K.; Haire, A.G. and Mara, S. (Cray Systems-
-U.K.):
"VISIM-Graphical Support for Spacecraft Operation
and Simulation" 412

IMPROVING THE MANAGEMENT OF OPERATIONAL INFORMATION FOR SAFER AND MORE EFFICIENT SPACECRAFT OPERATIONS

F. Lecouat, A. De Saint Vincent, JM. Brenot, JM. Darroy
F. Gaullier, P. Pham, P. Pessah

MATRA MARCONI SPACE
31, rue des Cosmonautes
31077 Toulouse, France

Abstract

Spacecraft control centers are getting more and more sophisticated over time. A lot of advanced software is installed to improve operations safety and efficiency. The data bases required by the control center software tools together with the technical documentation used by operators, is called the Operational Information in this paper. The effectiveness of operations not only depends on the functions of the control center but also on the quality and completeness of the Operational Information. It is thus necessary to develop new methods and tools so that the information generated during spacecraft development is adapted to new operations requirements. In the same time these tools can also improve the spacecraft development process itself by facilitating information access and validation. This is illustrated by MATRA MARCONI SPACE (MMS) experience on recent spacecraft development projects where OPSWARE tools are used both for operations preparation and operations execution.

Introduction

A huge amount of information is generated during the lifetime of a satellite project and this amount keeps increasing. For instance, in the field of the telecommunication satellites, the number of telecommands and telemetries has been multiplied by three between the TELECOM 1 generation and the TELECOM 2 one. The amount of information generates problems of access, of validation, of consistent sharing between different the teams involved in a satellite project, and of maintenance during the whole operational life that can last up to 15 years for some telecommunication satellites.

To deal with these problems it is necessary to introduce new methods and associated tools to normalize the information available during the development of the project, to help its validation, and to make it available during the exploitation phase of the satellite. In doing so, the objective is also to make this information directly usable by advanced software tools dedicated to operations support (e.g. procedures execution, diagnosis, ...), this being a key to their deployment in satellite control centers.

This paper is structured as follows. First, the different sources of information as they exist in a typical satellite

project, and the relations between the various pieces of information are presented in Chapter 1. Then, Chapter 2 introduces the OPSWARE tools, developed by MMS, together with European partners, describes how some of them are used for preparing the Operational Information during spacecraft development (operations handbook, procedures, timelines, and various knowledge bases). The same tools can also be used at the control center for maintaining the Operational Information. Chapter 3 describes OPSWARE tools that are using the Operational Information at the control center for conducting operations tasks. They provide support to procedure execution, real-time or near real-time spacecraft monitoring and diagnosis, long-term trend analysis, mission planning, and operators training.

1 INFORMATION FLOW DURING SPACECRAFT DEVELOPMENT

The requirement for information sharing is obvious when analysing the relations between the different entities involved in a satellite project. For example, the operations procedures developed by the operations team can be useful for the validation tests of the Attitude Control and Determination Subsystem (ADCS), and for the Assembly Integration and Validation (AIV) activities. In the same way, the dynamic simulator development team, AIT and operations are concerned by the functional description of the satellite subsystems.

A large part of these shared informations could be easily formalized and managed under a database - this is of course the ideal objective -, while some can only be managed under paper format. Today, for the satellite development at MMS, several tools have been already developed to centralize the information that were usually managed under paper format. The description of these tools is the purpose of the ch. 2 and 3 of this paper.

In this first chapter, we review the main stages of the information flow during the complete life of a satellite (development and exploitation), which are :

- The requirement specifications
- The design, the simulation and the subsystems tests
- The preparation of the operational documentation
- The satellite integration
- The simulation at system level
- The operations and the follow-up of the in-orbit satellite

1.1 System requirements

At the very beginning of the project, the system team defines a strategy to put the satellite in orbit (LEOP) and to maintain it during its operational lifetime (Station-Keeping). This strategy, defined in cooperation with the different entities involved in the project, must be compliant with the requirements of the customer. Different types of requirements are also generated: S/S design constraints, observability requirements and principles (type of information, type of sensor), etc...

1.2 Design, simulation and subsystem tests

On the basis of the design requirements, design analysis is performed for each subsystem. This results into the following outputs:

- A *telemetry plan* that describes all the nominal and non-nominal modes of each equipment, and the telemetries associated to the monitoring of these different modes. This kind of information exists since the TELECOM 2 project and should now be systematically applied on every project. In the future, the telemetry plan for all sub-systems should be consistently formalized and made available under data management facilities. It could then be used for the FMECA analysis and before the creation of the TM-TC database.

- A *functional description* of the subsystem as part of the operation handbook delivered by the subsystem supplier. It is used by the reliability engineers for the realisation of the FMECA. This description should also be formalized and stored under a data management facility, to make it usable by a diagnosis tool (§3.3) or by operational information management tool.

- *Subsystem procedures*: The operational procedures must be defined as soon as possible, so that they can be used and validated at the different steps of the development of the satellite. The procedures are written under a database tool. They can then be used for the subsystem validation tests (in this case, this is directly the operational sequence that is validated), and by the AIV. Little by little, the procedures files are enriched by the different users. At the end of the process, the procedure files are transferred to the operations team that takes the benefit of all the experience gained during the different steps of the project.

1.3 Preparation of the operational documentation

The operations handbook is the synthesis of the subsystems documents (S/S operation handbook, design review reports) with other documents (mission analysis, the on-board / ground interface or the FMECA), and additional system-level informations that were not available in the previous phases. The operation handbook is structured in a way consistent with the logic of the production of these informations, and usually as follows for a telecommunication satellite:

- Functional description of the different subsystems
- TM-TC list

- Board/ground interface
- Nominal operational procedures
- Contingency procedures and failure analysis trees
- Some test and simulation results
- The specification of some ground software required for the operations

1.4 Satellite integration (AIV)

1.4.1 Non-compliance reports

All along the integration process, the performances of the equipments and subsystems are checked with respect to their specifications. Any non-compliance, or any anomaly occurring during integration is recorded in an Anomaly Form (AF) and transmitted to the project team.

After investigation, if the actions undertaken to correct the anomaly lead to a degradation of the performances or to a modification of the equipment, a Non-Compliance Report (NCR) is issued. Such a non-compliance may have some operational impact (in the use of an equipment, or in the sequence of a procedure). Thus, the Non-Compliance Reports are an important input of the operation handbook. They are also an important source of information for future investigation of the in-orbit anomalies: one of the first investigations performed for troubleshooting is to search for a similar problem occurred during test and integration phases.

In this context, it would be very helpful to generalise the management of the anomalies to the ones having occurred before the integration of the satellite, at component or equipment level. These informations can be very helpful for the AIV or for in-orbit troubleshooting.

1.4.2 Interaction with the TM-TC database

The TM-TC information used by the AIV are provided by the operation database. During the AIV tests, the validity of the information and its consistency is checked. The operation handbook and the TM-TC database are updated consequently.

1.4.3 Validation of the operational procedures

The purpose of the AIV activities is to integrate the satellite and to check that it is compliant to the specifications. For this the satellite is submitted to functional, performance and environmental tests. Even if it is not the main objective of this phase, it is very interesting to take the opportunity of this first complete satellite configuration to validate the operational flight procedures. This approach has been followed on TELECOM 2. Important procedures such as the initial configuration setting of the ADCS have been played on the satellite. This allowed an early identification and correction of some procedure anomalies.

1.5 Simulation and system validation

1.5.1 The satellite simulator

The aim of the simulator is to validate the operational procedures before the launch, and to help for the training of the satellite operator in local mode or in line with the ground segment. The development of the simulator is based on the functional description of the satellite. In some projects, the framework of the simulator is automatically generated on the basis of the functional description. Here again, one can notice that the workload could be minimised, to some extent, by a normalisation of the functional description. Another line of improvement would be a connection to hardware equipments, or to accurate simulator coming from the subsystems analysis.

1.5.2 Validation of the procedure by the satellite control center.

The satellite procedures as delivered by the operation handbook are enriched with all the aspects that are specific to the ground resources. The modified procedures are then validated on the satellite simulator. When this validation is completed, the procedures are one more time tested on the satellite. The control center is connected via a TM-TC modem to the satellite. The operational sequence are for the very last time executed and validated on the satellite. This compatibility test allow to perform a final test on the coherency of the TM-TC database including all the data processing means of the ground segment.

2 PREPARING OPERATIONAL INFORMATION WITH ADVANCED SOFTWARE TOOLS

2.1 OPSWARE tools

Usually a control center provides basic software functions to support the fundamental tasks related to spacecraft operations. However there is a need to develop advanced software functions to partly automate some tasks in order to improve reliability and efficiency in the context of more complex satellites. A new generation of operations assistance tools which is now emerging, will deeply affects the performances and the economics of space operations.

In particular, MMS has been developing for several years the OPSWARE concept and the associated generic tools to support space operations [6,7,8]. The OPSWARE concept is a view of the activities centered around conventional control centers, as a consistent set of well defined tasks that can be automated thanks to software applications providing intelligent assistance :

- scheduling the operations
- spacecraft monitoring through telemetries.
- spacecraft commanding based on operations procedures.
- diagnosis and quick reaction to anomalies
- thorough analysis of anomalies and study of spacecraft aging

- maintenance of operational information
- knowledge preservation and training of new staff

These tools are the basis of several operational applications that have already demonstrated very significant pay-offs. They are based on advanced technologies and concepts from computer science: artificial intelligence and knowledge based systems (KBS), knowledge acquisition, computational linguistic, human factors engineering, operations research, object oriented programming, hypertext techniques... Each application has been developed in close cooperation with operations engineers of MMS and with MMS customers at ESA, CNES, ARIANESPACE...

One of the main lessons learnt through the development of OPSWARE is the importance of a correct integration of this kind of tools with the satellite life-cycle. This is why the scope of the OPSWARE tools concerns both the preparation and the execution of operations, with the aim of providing a continuous "information chain" taking its roots in the spacecraft design and mission preparation phases.

More precisely, the OPSWARE tools can support mission preparation tasks in four main areas :

- preparation of the Operations Requirement Handbook (ORH)
- preparation and verification of operational procedures
- preparation and verification of timelines
- preparation of other types of spacecraft knowledge, such as diagnostic and performance evaluation knowledge.

2.2 Operations Handbook preparation

MMS has implemented a system for editing and browsing the operations handbook of the HISPASAT satellite, the ORH Browser, with the following characteristics:

- browsing and navigating through distributed text documents, usually written separately : through an active table of contents, the user can select a document or a chapter, the tool finds the corresponding file on the file system and opens it at the selected paragraph. Hypertext links permit to jump to a specific point of interest.
- access to databases and non-textual data : an important part of the information relative to a satellite is stored in databases. The ORH Browser offers several access modes to those bases (predefined queries in menus, indirect requests through hypertext markers, etc. It can also activate dedicated editors or display tools for the access to graphics or other media.
- full text search : a search mechanism has been implemented to analyse a full text request and compare it to the components of the documents to propose the best matches.

The ORH Browser is based on the ODIN kernel that has already been used in another context (on-line documentation of an engineering design environment).

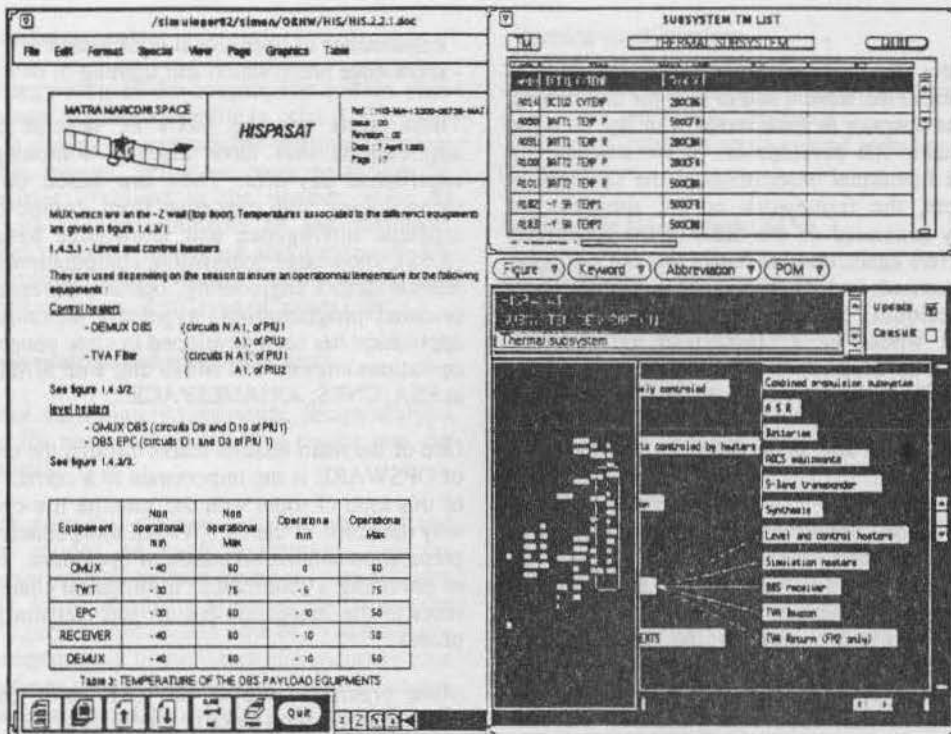


Fig 2.2, a screen of the HISPASAT ORH Browser

2.3 Procedures preparation

As seen in §1, one of the most important tasks to be carried out during mission preparation is the preparation and validation of operational procedures. This is a complex and costly task, which concerns many entities in a project. This has motivated the development of several applications dealing with procedures preparation support.

The POM tool has been developed by MMS to support the generation and maintenance of satellite ground control procedures, and to facilitate their use during operations thanks to a procedure browser. POM is now used operationally for the procedures of the Telecom 2, HISPASAT and SOHO spacecrafts. Savings that can be credited to POM during the procedure elaboration phase at MMS were estimated at 50%. Another fine result was the increase of procedure quality.

From the experience of the various procedures management tools developed in the last four years (including the POM, EOA and CSS projects [10]), MMS has derived OPSMAKER, a generic tool for procedure elaboration and validation. It has been applied to quite different types of missions, ranging from crew procedures (PREVISE system [12]), ground control centers management procedures (PROCSU system), and - most relevant to the present paper - satellite operational procedures (PROCSAT developed for CNES, to support the preparation and verification of SPOT 4 operation

procedures, and OPSAT for MMS telecom satellites operation procedures). Moreover OPSMAKER should probably be applicable to *integration procedures* used in spacecraft AIV that have a lot of common aspects with operations procedures.

The basic functions provided by such procedures preparation applications are :

- a procedure editor which supports "assisted editing" (eg: on-line access to system data) for more efficient procedures writing;
- a procedures compiler, which generates an internal, formal representation of the procedures (and, when applicable, detects syntactic errors);
- a procedures formatter, which generates automatically a high-quality document (FOP, Flight Data File);
- a procedures checker, based on qualitative simulation, which provides for a rich set of verifications to speed up procedure development : simple errors are detected early before starting detailed simulations.

The procedures can include additional information (text and graphics) extracted from data bases. Formalisation of procedures and modelling of actions facilitate team work by guarantying homogeneous procedures manuals. Everybody works at the same level of detail, with the same language. Maintenance of procedures is facilitated since information is never duplicated and powerful search functions are provided. Formalised procedures are ready for use in assisted execution tools (§3.1), and in training tools to prepare future operators (§3.3).

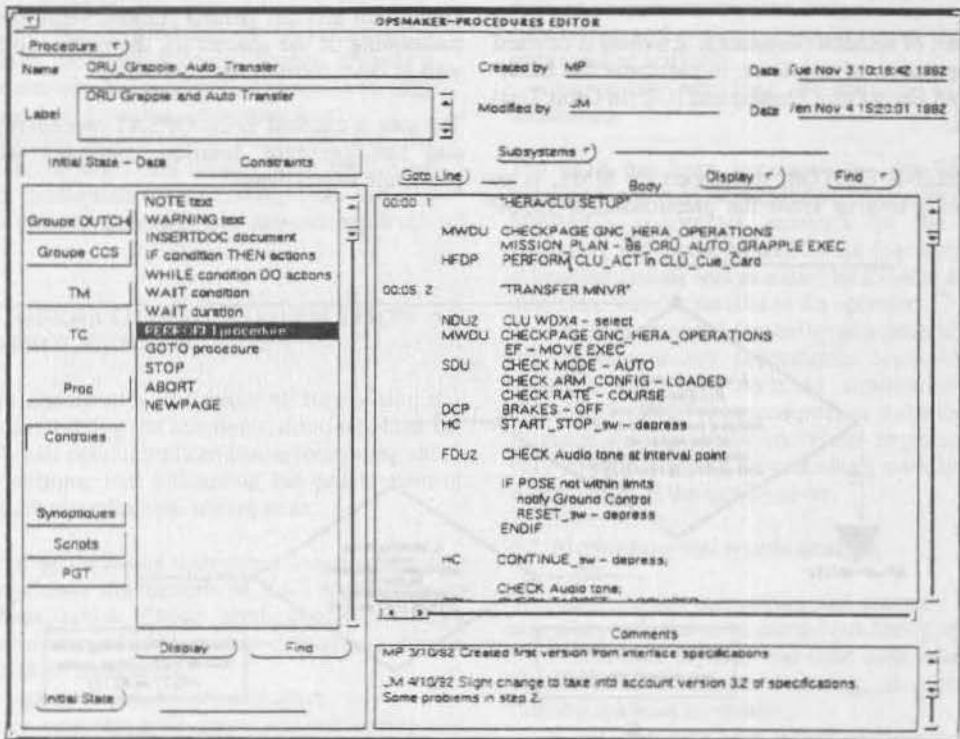


Fig. 2.3, an OPSMAKER procedure editor: once a procedure has been entered, it can be verified by the system and then automatically formatted to a high quality document.

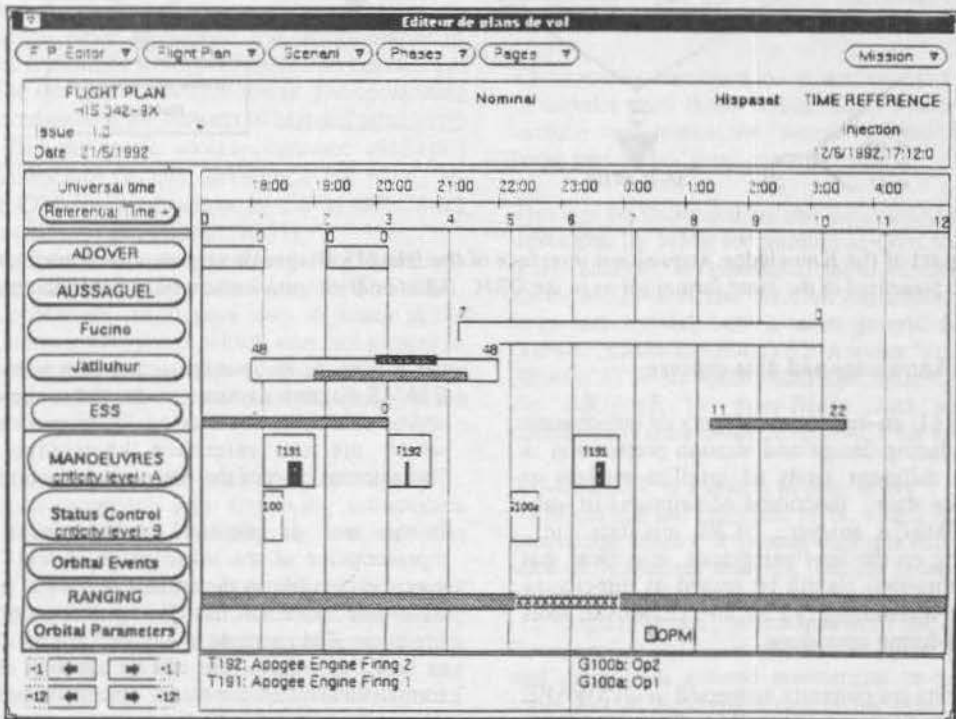


Fig. 2.4, User interface of the TIMELINE EDITOR, for preparing LEOP timelines.

2.4 Timelines preparation

Another part of mission preparation activities is devoted to the preparation of timelines, in particular for LEOP (Launch and Early Orbit Phases) and IOT (In Orbit Test) operations.

The TIMELINE EDITOR, developed by MMS, is an example of a tool to assist the preparation of LEOP

timelines (procedures and manoeuvres scheduling), taking into account ground stations visibilities, relative positioning of the spacecraft, the earth and the sun, as well as other constraints.

The tool is coupled to the OPSAT procedures data base and can generate detailed timelines where each procedure step is dated.

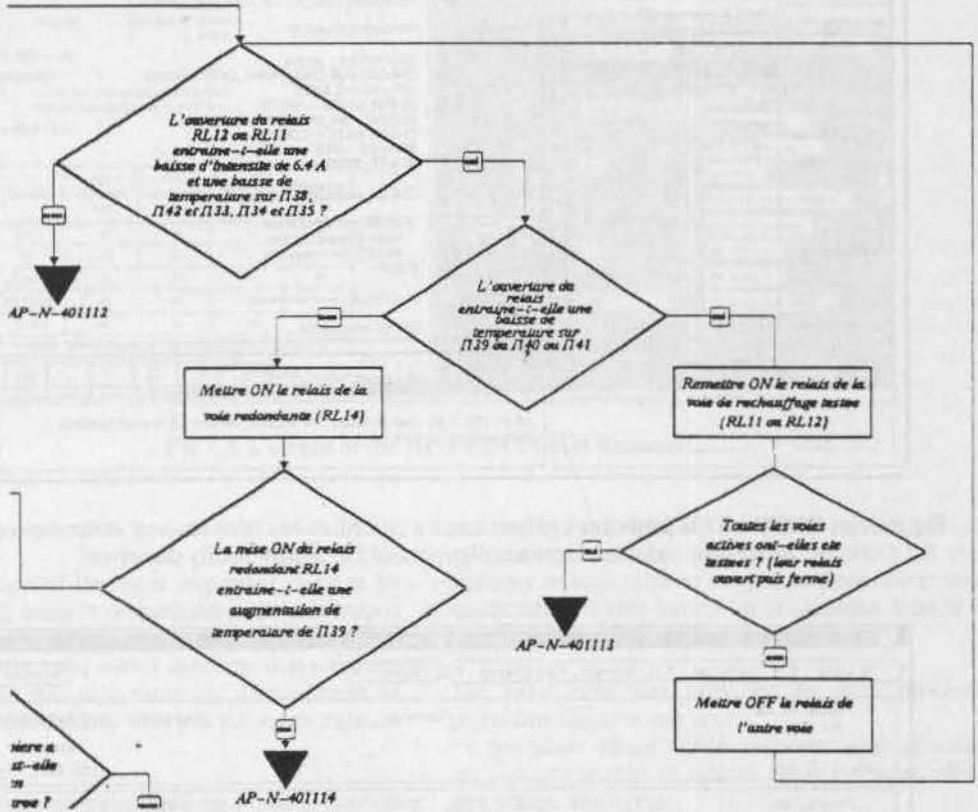


Fig. 2.5 : part of the Knowledge Acquisition interface of the DIAMS Diagnosis system: discrimination procedures are presented in the same formalism as in the ORH. Additional information can be attached to objects.

2.5 Design knowledge and data capture

As seen in §1, an important category of information generated during design and mission preparation is related to different kinds of satellite models or performance data : functional descriptions of sub-systems, FMECA analyses, NCRs, test data, etc... Anticipating on the next paragraphs, it is clear that these informations should be reused as directly as possible in Monitoring (§3.2) and Diagnostic tools (§3.3) used during operations.

These aspects are currently addressed in OPSWARE systems through specific Knowledge Editing modules. For instance, figure 2.5 shows the user interface for

the part of the knowledge acquisition module of the DIAMS diagnosis system, dedicated to the definition and/or editing by the user of "discrimination trees", which are the reference knowledge for the "behavioural" part of the diagnosis process (see §3.3).

In this area, an essential requirement is that the representation of the information should "stick" as much as possible to the formalizations in use during the whole spacecraft design and mission preparation life-cycle. The example of figure 2.5 is an illustration of how this requirement can be handled; indeed, the formalism selected for these "discrimination trees" is the same as the one which was "conventionally" used in the Operations Requirement Handbook.

However, significant progress remains to be made in this area, in particular:

- to improve the methodologies of information transfer during the satellite design phases, towards a direct capture of the relevant informations (eg: functional models) from the sub-system level;
- to support the capture (and, when relevant, the formalization) of more data coming from the design phases (eg: performance data coming from test and integration phases, anomalies at sub-system level, etc...).

3 USING OPERATIONAL INFORMATION AT THE CONTROL CENTER

For modern spacecrafts, the tasks of supervising the spacecraft, interpreting the telemetry, deciding about the correct on-board operational conditions, reasoning about proper corrections, and evaluating the proper control procedures, are complex operational tasks.

A number of applications developed over the last few years have shown the benefit of KBS techniques to support these tasks. These applications, although showing some amount of functional overlapping, can be classified in three main areas :

- real-time support to procedures execution
- real-time or near real-time spacecraft monitoring and diagnosis
- long-term trends analysis

3.1 Procedures Execution

Requirements for the improvement of operations safety and efficiency have motivated the development of several prototype tools, to support spacecraft operators in real-time for the spacecraft monitoring and controlling tasks, centered around the concept of assisted procedures execution. This category of tools is illustrated the Expert Operator Associate (EOA), developed for ESOC by MMS and CRI for application to the MARECS-B2 spacecraft command and control [10,11].

EOA is based on a formal representation of operations procedures such as those produced by OPSMAKER. The EOA procedure language allows to attach to the procedure some informations which were not present in the "conventional" procedures : goal, context of applicability, and a more complete description of the execution constraints.

EOA basic functionalities are to assist the operator by :

- receiving, interpreting and displaying information regarding the state of the S/L; filtering non important alarms
- proposing selected procedures based on the current operating state of the S/L and the indication of the desired state by the user, presenting the chosen procedure to the user in both textual and graphical form, and dynamically reflecting on the display the status of execution of the procedure;

- preparing the various command sequences needed for the execution of the operational procedure, and uplinking them on acceptance from the user;
- receiving and evaluating reports from the MSSS on commanding activity;
- continuously verifying the validity of operations constraints.

The EOA has been interfaced to the ESOC Multi-Satellite Support System (MSSS), and experimented with MARECS spacecraft analysts on the MARECS simulator, and on the MARECS B2 spacecraft, where an eclipse operations was executed by EOA in a completely automatic way (in parallel to the operator).

This demonstrates the feasibility of a generic mechanism for semi-automated procedures. Moreover a lot of progress has been made in applications such as PROCSAT (SPOT 4 procedures) to make the procedure language easy to use by operations engineers. This is a very important aspect for procedure maintainability and acceptability of the tool by users.

3.2. Monitoring and trends analysis

Spacecraft health monitoring and anomaly detection is also a key function to be carried out during operations:

- 1- real-time or near real-time data monitoring and first-level interpretation : aiming, as a minimum, at filtering spurious anomalies;
- 2- off-line, long-term trends analysis for spacecraft and payload performance evolution analysis.

Conventional monitoring systems (such as those used within current satellite control centers) have well-known limitations : false alarms upon inter-modes transitions, inability to detect progressive degradations, etc...

KBS systems developed in the last few years have shown to address well these issues. Such systems can thus usefully complement the "simple" monitoring functions being part of the "core" control center.

This can be illustrated by the SAT-ANALYST system developed by MMS for satellite in-orbit follow-on and trends analysis, in operational use at MMS for one year for the HISPASAT and Telecom 2 satellites. This system is in fact derived from a more generic data analysis "kernel", called X-ANALYST. Another "instance" of X-ANALYST is the ARIANEXPERT system, dedicated to the ARIANE IV post-flight data exploitation, operationally used at ARIANESPACE for two years.

X-ANALYST is a system in two "layers" :

- a numerical and graphical layer, which is basically an expandable library of general data processing functions such as : statistical analysis, filtering functions, Fourier analysis, etc... ;
- a "logical" layer, which provides the user with a "language" to define or edit data analysis "procedures", and includes a general mechanism to automate the application of these procedures on the data.

An associated knowledge acquisition tool allows to interactively define / edit these two models. Specific graphical tools enable the design engineer to encode himself these schemas.

DIAMS is now installed in the TELECOM 2 satellite control centre, and used operationally. A first complete version of the system has been available since June 1992, and the system has been formally delivered to CNES in January 1993 and in April 1993.

This system is also considered by CNES as an efficient training tool, thanks to the embedded deep knowledge of the spacecraft and thanks to the possibility of session replay. It is also viewed as generating a mission technical memory, allowing the integration of in-orbit experience. Its main benefits are related to expertise transfer from spacecraft designers to spacecraft operators, and to in-orbit experience capture (a critical point, if we consider the important turnover in operations staff).

3.4 Operator Training

Operators training in a spacecraft control center is a recurrent activity, which is going to take an increasing importance with the growing complexity and increasing life duration of modern spacecrafts.

In this perspective, it appears essential to develop new training environments/tools allowing to make this task easier and less demanding on instructors availability.

This is the idea of the on-going ATIS project, carried out by CISE and MMS for ESA/ESTEC [3]. This system is applied to the case of astronauts training to the operation of a microgravity payload (RAMSES), but is based on widely applicable concepts and mechanisms which are :

- tutoring functions/modes : in these modes, the user can access to and navigate in technical / operational documentations, either in a free manner, or being guided by the system following an initially specified "training objective";

- procedural training functions/modes : in these modes, ATIS is connected to a simulator. The session is started by specifying an initial scenario (possibly a contingency case) ; the user (operator) executes an operational procedure as in "traditional" simulation session, but is constantly monitored by ATIS which in parallel tracks the procedure to be executed. In case of error, the operator is given corrective guidance. He also has contextual access to the relevant informations.

Such functionalities could be usefully integrated to a Mission Control Center. A key point - and this shows the advantage of interoperable tools and data/knowledge - is that such tool can reuse a large part of knowledge already produced by other advanced tools (in particular : formal procedures definition produced by procedures preparation tool), and information access functionalities such as the ORH browser described in §2.1. Having a unique source of information for training and operations will enforce the representativity of training.

Conclusion

The amount of information generated in spacecraft project raises three main concerns:

- access to the information all along the lifetime of the project.
- validation of the operational information so that it is always consistent with the spacecraft.
- maintenance of the operational information since is the basis of the in-orbit follow-up that can last up to 15 years for some telecommunication satellites.

MMS is implementing methods and their dedicated tools to address these problems, to normalize the information available during the development of the project and to make it available during the exploitation phase of the satellite.

The quality of the Operational Information (technical documentation, data bases and knowledge bases) delivered to the operations team is essential. This makes possible the use of advanced software such as OPSWARE tools to improve the safety and efficiency of operations.

The early formalization of the Operational Information reduces the cost of knowledge acquisition and improves the spacecraft development process itself though a better communication between the project teams.

References

- [1] M.Arentoft, J.Fuchs, Y.Parrod, A.Gasquet et al., *OPTIMUM-AIV, A Planning and Scheduling System for Spacecraft AIV*, ESA Workshop on Artificial Intelligence and KBS for Space, Noordwijk, The Netherlands, May 1991.
- [2] C.Bastien-Thiry, J.C.Maurize, *SE-TC2: The first expert system in a CNES Satellite Control Center*, ESA Workshop on Artificial Intelligence and KBS for Space, Noordwijk, The Netherlands, May 1993.
- [3] A.Bertin, L.Bertotti, F.Buciol, A.De Saint Vincent, P.Caloud, J.Kaas, F.Allard, *An Intelligent Tutoring System for System and Procedural Training of Astronauts*, 4th ESA Workshop on Artificial Intelligence and KBS for Space, Noordwijk, The Netherlands, May 1993.
- [4] J.M.Brenot, P.Caloud, L.Valluy, *The development of an operational expert system for the Telecom2 satellite control centre*, ESA Workshop on Artificial Intelligence and KBS for Space, Noordwijk, The Netherlands, May 1991.
- [5] J.M.Brenot, Y.Parrod, D.Aubin, C.Parquet, *ARIANEXPERT: a Knowledge Based System to analyse ARIANE's mission data*, ESA Workshop on Artificial Intelligence and KBS, Noordwijk, The Netherlands, May 1991.
- [6] J.M.Darroy, *Knowledge-Based Systems for Spacecraft Control*, keynote address, First

An essential feature of X-ANALYST is that the user can specify (off-line) data analysis procedures, using a dedicated knowledge acquisition tool. This flexibility allows experts to progressively refine the exploitation of telemetry data, based on their experience acquired throughout flights : this is typically a function which is part of the mission preparation (§2.5) and/or maintenance phases to preserve the technical memory.

During a data exploitation session, X-ANALYST automatically executes the "exploitation procedures" specified by the user. Built-in mechanisms allow to correlate the currently analysed data with the ones of former analyses. Thus X-ANALYST helps to manage the in-orbit experience. At the end of a session, a report is automatically generated in a desktop publishing tool format (FrameMaker).

SAT-ANALYST is currently used for long term data analysis although real-time applications of this tool are possible for instance analysing the performance of a low earth orbit spacecraft once it has left the visibility window.

3.3 Diagnosis

Failure diagnosis is a traditional application domain of Expert Systems, and this is also true in the space domain where a number of mock-ups and prototypes have been developed.

The "DIAMS" system developed by MMS for the TELECOM 2 satellites [2,4] combines two

complementary reasoning paradigms (and types of knowledge):

1) The behavioural model describes the discrimination strategies which allow at the beginning of the reasoning process to focus the attention on definite parts of the S/L. This model essentially corresponds to experimental or shallow knowledge which is explicitly derived by the operations engineers during mission preparation in order to prepare the Contingency Operations section of the ORH, or which is derived from the anomalies experienced during the S/L operation. The experimental knowledge become richer all along the life of the system. It is represented as decision trees whose nodes are either binary tests (e.g. "is parameter abnormal") or actions on the satellite (i.e. send command). See Figure 2.5 above for an example of discrimination procedure.

2) The functional model corresponds to the TM/TC plan which describe the internal functional interactions inside the system and allows to locate the system basic commands (TC) and observables (TM). The model is hierarchically decomposed into blocks having well-defined functions (subsystems, functional units,...) until the appropriate level for diagnosis is reached. The fault propagation paths from the faulty components to the observables can be directly derived from the model using generic reasoning mechanisms. Figure 3.3 partly shows a block of the TELECOM 2 functional model.

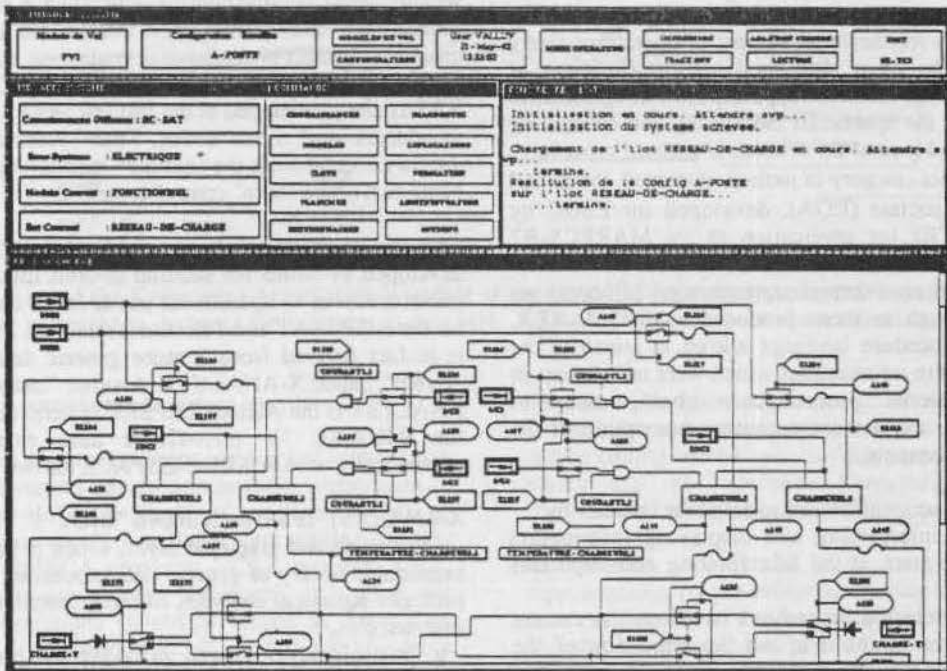


Fig 3.3, a screen of the DIAMS failure diagnosis tool: This shows the functional model of an equipment that is animated during a diagnosis session.

International Symposium on Ground Data Systems for Spacecraft Control, Darmstadt, FRG, 1990.

- [7] J.M.Darroy, *Influence of a New Generation of Operations Support Systems on Current Spacecraft Operations Philosophy: the user's feedback*, Second International Symposium on Ground Data Systems for Spacecraft Control, Pasadena, California, 1992.
- [8] J.M.Darroy, F.Lecouat, J.M.Brenot, A.de Saint Vincent, *OPSWARE : A new generation of software tools for making space operations faster, better and cheaper*, 44th Congress of the International Astronautical Federation, Graz, Austria, Oct. 1993.
- [9] J.Fuchs, A.Gasquet, J.Muller, P.Viau, *The Expert Planning System Prototype: Experience and Users Feedback*, ESA Workshop on Artificial Intelligence and KBS, Noordwijk, The Netherlands, May 1991.
- [10] F.Lecouat, M.Nielsen, K.Grue, *Knowledge-Based Assistance for Generating and Executing Space Operations Procedures*, ESA Workshop on Artificial Intelligence and KBS for Space, Noordwijk, The Netherlands, May 1991.
- [11] M.Nielsen, K.Grue, B.Olalainty, F.Lecouat, J.Wheadon, *Expert Operator's Associate: an Expert System for Spacecraft Control*, First International Symposium on Ground Data Systems for Spacecraft Control, Darmstadt, FRG, June 1990.
- [12] A.De Saint Vincent, F.Lecouat, G.Leonis, F.Allard, *PREVISE: a KBS to Support the Preparation and Verification of Crew Procedures*, 4th ESA Workshop on Artificial Intelligence and KBS for Space, Noordwijk, The Netherlands, May 1993.

OPERATIONAL TRAINING FOR THE FLIGHT CREW OF THE TELE-X SATELLITE

Gunnar Hårdsten
Jonny Järnmark
Swedish Space Corporation, Erange
Box 802
S-981 28 KIRUNA, Sweden
gha@esrange.ssc.se (Internet)

Abstract

There are several advantages in training the flight crew in routine operations and solving problems regularly. The flight crew achieve high competence and becomes motivated in their work, flight instructions are verified, new operations can be verified before implementation. It is also important that the training is performed in the same environment as for the real operations. The training program has proven to be an excellent tool for system quality improvements.

This paper will present the operational training for the flight crew of the Swedish telecommunication satellite Tele-X.

Keywords: Operational training, Quality improvements, Flight instruction verification, Operational responsibility, Operational procedure implementation.

History

Tele-X

On 2 April 1989, the Swedish telecommunication satellite Tele-X was successfully launched by an Ariane2 rocket from Kourou at French Guyana. Two weeks later, orbit acquisition in the geostationary position 5° east $\pm 0.1^{\circ}$ was accomplished.

Tele-X is a direct broadcasting communication satellite. It provides a variety of interesting services to users in the northern part of Europe. The services include:

- direct broadcasting of TV to home receivers
- business communication between small, inexpensive terminals
- high speed and high volume data transmission
- video conferences
- tele-education
- distribution of cable TV programs
- collection of event television
- distribution of digital and analogue radio.

Satellite control

Satellite Control Facility

All satellite control functions, including Payload Configuration, Traffic Monitoring & Control and Orbit Monitoring & Control are done by one ground station at Erange. Erange is located close to the Swedish town Kiruna, north of the Arctic Circle (see Figure 1).



Figure 1: Location of Erange

Figure 2 shows the Satellite Control Facility computer configuration in normal operations. Two computers are used for monitoring and control of the satellite and ground system. The third computer is used for off line data processing, for orbit determination and as a ground station simulator during operational training.

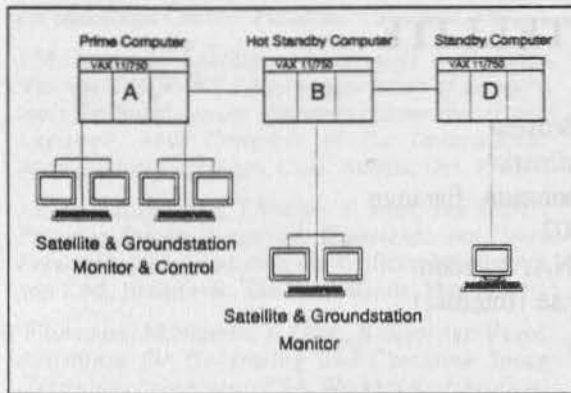


Figure 2: Computer configuration in the Satellite Control Facility

Personnel

The ground station is organized in three groups according to Figure 3.

Satellite & Orbit Control group consists of one group leader and two technicians. System Support group consists of one group leader and two technicians. Flight Control group consists of one group leader and ten flight crew members working in three shifts. The flight crew are recruited from technicians who has been studying at least three years of an upper secondary school.

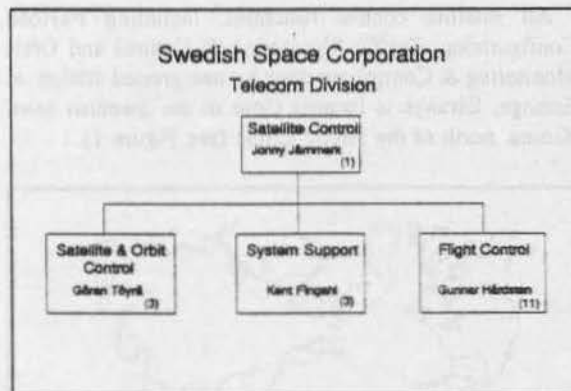


Figure 3: Satellite Control Organization

Responsibility of the flight crew

The flight crew, in action 24 hours/day around the year, closes the control loop for the entire satellite system. The organization at the control centre is such that each member of the flight crew is allotted a high degree of responsibility. This responsibility must be matched with good system knowledge to ensure a safe and reliable operation, especially during situations deviating from the normal pattern. This is accomplished by regular training of contingencies and new or changed operational procedures.

For each subsystem onboard the satellite or in the ground station, "subexperts" are nominated within the flight crew members, having at least one year of operational experience.

The "subexpert" evaluates his/her subsystem and provide recommendations for improvements of operations or documentation to the Satellite & Orbit Control group or the System Support group.

Training programme

Training objectives

The training programme teaches the flight crew how to operate the Tele-X satellite and the ground equipment in normal and contingency operations with a minimum of help from the subsystem experts.

An important part of the program is simulation of experienced events and anticipated events, as derived from FMECA analysis. The training also handles problems that have occurred on similar satellites as Tele-X.

The objective of the training programme is to:

- maintain a high competent and a highly motivated personnel
- verify that all our flight control documentation gives the flight crew correct and understandable instructions
- verify new and changed operational procedures
- realize system quality improvements

Training instructions

At present there are about one hundred different cases that can be simulated. These cases are assembled in a "training cover". Each cases contain an instruction how:

- the teacher should induce the case
- what important information that the flight crew shall check before performing an operation
- what the flight crew are supposed to do
- how long time it should take to find the problem and to correct it

There are also instructions how to train the flight crew on periodical operations, such as eclipse operations and station keeping manoeuvres, with and without malfunctions.

All new or changed operation procedures are tested in the satellite and ground equipment simulators, before approval by the Satellite & Orbit Control group. After approval of the operational procedures all flight crew members undergoes a dedicated training program in the simulators before operational commissioning.

Training schedule

Each flight crew member gets at least ten days of operational training every year. They are trained two at a time in the Satellite Control Facility for Tele-X during one week in the spring and one week in the autumn. The training is performed during day shift, in parallel with the normal satellite and ground station operation.

All new employed flight crew members get a theoretical training of at least two weeks followed by a practical training during two weeks with the simulators. The training covers how to operate the satellite and the ground equipment in normal and contingency operations.

Occasionally, personnel from other groups working with Tele-X participate in the operational training with the simulators.

Training conduction

Figure 4 shows how the computers in the satellite control facility are configured for training. The computer (A) is configured for normal satellite and ground station operations. The computer (B) is configured for training purpose and connected to the ground station simulator (disconnected from the normal operations). The ground equipment simulator is started in the computers (D) and the satellite simulator is started in the personal computer (PC).

The flight crew are placed behind the control desk for the satellite and ground station simulators. They are now ordered by the teacher to monitor and operate the simulators. The teacher chooses an exercise from the training cover, introduce a problem and/or asks the flight crew to perform an operation. To get a more complex situation, the teacher sometimes introduces another different problem, while the flight crew are solving the original one.

During the exercise the teacher makes notes how the flight crew solves the case. After each exercise the teacher together with the flight crew, discuss how the case was solved, and if there should be any improvements in the flight crew operations. They also discuss if there are any errors or misunderstandings in the flight control documentation.

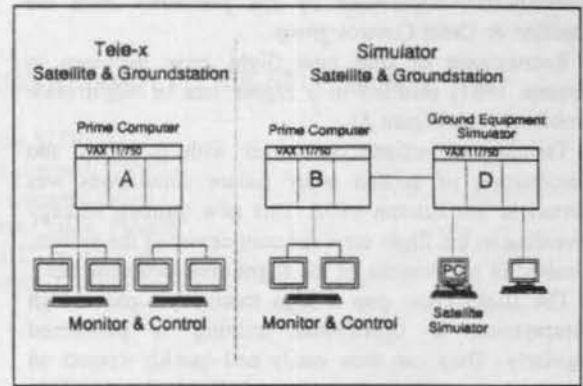


Figure 4: Simulation configuration

Evaluation

Every six months the teacher issue an evaluation report describing the previous six months training. The report includes:

- number of training days for each flight crew member
- number of trained cases for each subsystem
- operational problems encountered by the flight crew (see next paragraph)
- number of misunderstandings of the flight control documentation
- number of errors in the flight control documentation

An operational problem by the flight crew is encountered when:

- a subsystem expert is required to solve the problem
- it takes too long time to solve the case
- the flight crew forgets to check for vital information
- the flight crew perform an incorrect operation

Cases that caused problem by the flight crew are identified and evaluated. There is also a general part of the evaluation report describing what type of strategy that have been used. This part of the report is used as a feedback to select the type of cases that must be trained in the next training period.

Lessons learned

After the first training period it was found that the flight crew, in many cases had difficulties to read and understand the flight control documentation. In some cases the flight crew even misunderstood the instructions (see - Instruction problems - in Figure 5). For that reason, a revision of all our documentation was started in the autumn 1991. This work was done mostly by the

"subexperts", supervised by the personnel from the Satellite & Orbit Control group.

Recruitment of four new flight crew members in autumn 1991, resulted in a higher rate of flight crew problems (see Figure 5).

Training of eclipse operations with problems and introduction of second order failure simulations was started in the autumn 1992. This new training strategy revealing to the flight crew the complexity of the system, resulted in an increase of the flight crew problem rate.

The flight crew gets a high motivation and a high competence, if operational training is performed regularly. They can then easily and quickly correct an error situation. The training is a challenge for the flight crew and they all look forward to participate.

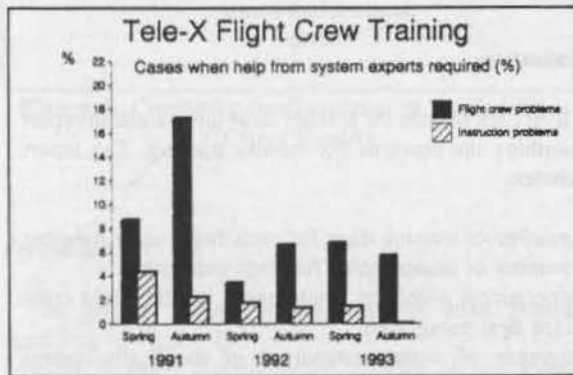


Figure 5: Evaluation from three years of operational training

Operations training tools

System operation tools

Simulation tools for the satellite and ground equipment training has been developed to support this effort. The satellite simulator is a dynamic simulator consisting of a personal computer with an HDLC interface to communicate with the ground station simulator. The ground station simulator consists of application programs in one of our control centre DEC computers (D). The man-machine interface during operations is one of the DEC computers (B) disconnected from the normal satellite and ground control operations and configured for education. The environment for the flight crew is identical to the interface used during operations.

Integration of simulators

The computer with the satellite and ground system control program loaded (B) is connected to the ground system simulator computer (D) through a DEC-net connection. Telecommands (TC), telemetry (TM),

groundcommands (RC) and ground monitoring data (RM) is routed through the DEC-net. The ground system simulator computer (D) is connected to the satellite simulator through an HDLC interface. Telecommands (TC), telemetry (TM), information of uplink (UL) and information of downlink (DL) is routed through the HDLC interface (see Figure 6). UL block contains status information about the ground equipment to inform the satellite simulator if uplink is possible, and DL block contains information about the attitude and TT&C status to inform the ground station simulator if downlink is possible.

The teacher can command the satellite simulator from the keyboard of the personal computer and command the ground station simulator from the keyboard of a VT420 terminal.

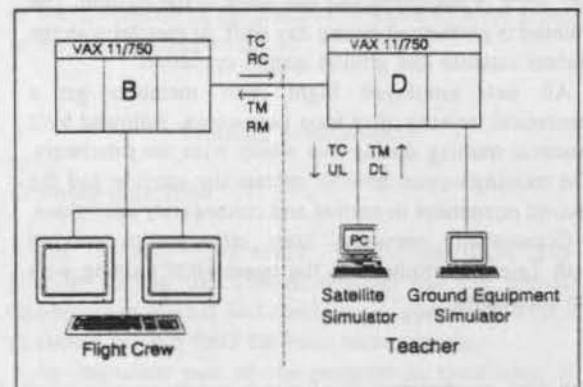


Figure 6: Simulations integration

Conclusions

The operational training program for the flight crew of the Tele-X satellite has proven to be an excellent tool for system quality improvements by:

- giving each flight crew member the system knowledge and experience needed for a safe and reliable handling of anomaly situations
- stimulating all personnel at the Satellite Control Facility to operational commitment
- supporting the activities for improvements of operational procedures with detection of ambiguities and errors in the flight control documentation
- supporting verification of new and changed procedures before operational commissioning

IMPROVEMENT OF OPERATIONAL ACTIVITIES EFFICIENCY

Mr Fabien SITRUK
French Space Agency, CNES
18 Avenue Edouard Belin
31055 Toulouse Cedex, France
Tel: 61 27 46 67
Fax: 61 28 22 84

ABSTRACT

This paper presents the methods used by the Toulouse Space Centre (CNES) to minimise the risk of deterioration in service during flight mission operations. It also presents planned improvements following recent analyses.

1. INTRODUCTION

Up until 1991/1992, Quality Assurance activities in the operation of space systems were mainly dedicated to the definition and application of general rules designed to control the availability of ground support facilities (both hardware and software) used to control satellites and operate their payloads.

Over the last few years, application missions for Telecommunications, Earth observation etc. have become increasingly critical in a context of heightened competition (due to the commercial consequences, sensitivity of data processed etc.). Ensuring service continuity has become an additional objective to be attained in the area of RAMS (though saving the satellite itself remains the greater priority). It has therefore been necessary to guarantee, as far as is possible, the correct execution of operational activities, i.e. the safety of operations.

2. CONTROLLING OPERATIONAL AVAILABILITY

In order to attain this objective, general operating rules applicable to satellite control facilities were defined then applied under the control of the Quality Assurance department. These rules are contained in a Quality Manual specific to operational activities and mainly cover the following four areas:

- First using new operational facilities
- Anomaly processing procedure
- Configuration management procedure

■ Maintenance procedure

2.1 The rationale behind first using new operational facilities

This concerns:

- The definition as early in the project as possible then, at the end of development, delivery of operational support items (documentation, test and training means, replacements etc.)
- A technical qualification process to check that specifications have been complied with
- The identification of the reference configuration at the beginning of operations

2.2 Anomaly processing procedure

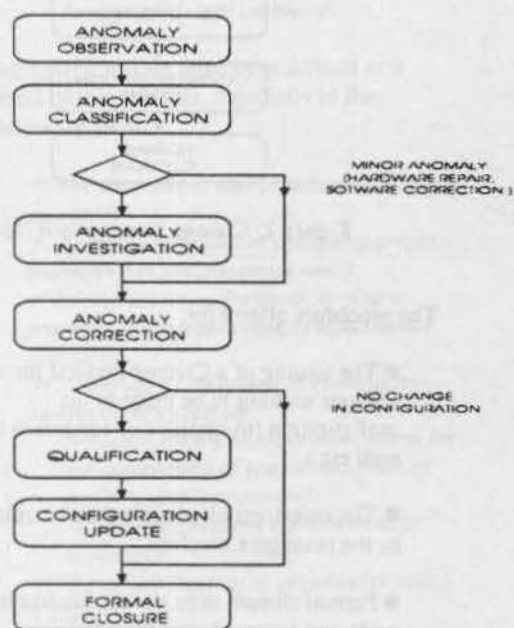


Figure 1: Anomaly management logic

The procedure allows for:

- The investigation and classification of all anomalies affecting all operational means
- The investigation of the anomaly after correction (acceptance of current state, possibly despite non conformance)
- Formal closure once the change has been made and accepted, and the reference configuration updated

2.3 Configuration management procedure

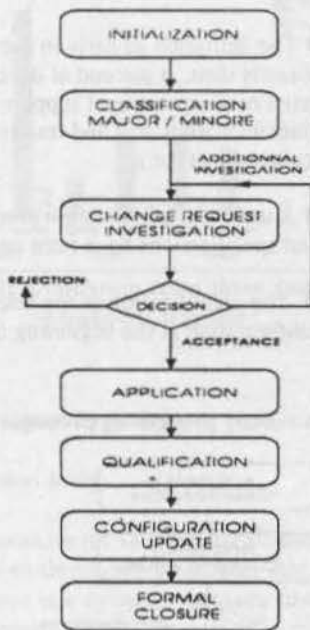


Figure 2: Change management logic

The procedure allows for:

- The issuing of a Change Request for any changes wishing to be made to the configuration (to improve or adapt it to a new need etc.)
- The investigation process then acceptance by the managers involved
- Formal closure once the change has been made and accepted, and the reference configuration updated.

2.4 Maintenance procedure

This concerns:

- The organisation and planning of maintenance activities
- The management of maintenance operations (monitoring availability, analysing trends, managing replacements and resources etc.)
- Quality requirements, in particular those relating to software maintenance (non-regression tests, archival, software quality factors etc.)

3. THE SAFETY OF OPERATIONS

The risks to be controlled in this area mainly concern two aspects:

- The incorrect performance of a nominal operation (the operation usually being repetitive in nature)
- The appearance of an anomaly in a satellite or ground support facilities requiring fast and often critical action by the operational teams

Consequently, the dependability of operations is based both on compliance with an operational methodology and the reduction of the number and effect of human errors during the operational phase.

3.1 Operational methodology

Operational rules have been set up within CNES and improved with feedback from programmes currently in operation. These rules concern:

- The formal preparation of operations before the operational phase
 - Training operators
 - Defining then validating the operational organisation
 - Writing and qualifying operational procedures
 - Simulating operations (checking time constraints)
- Keeping teams operational throughout the utilisation phase
 - Keeping up skills

- ☞ *Practical training in operation proceedings*
- ☞ *Training new controllers*

■ The systematic processing of anomalies arising from operations by the operational teams involved so as to avoid similar anomalies occurring. The following are just some of the measures already taken in this area:

- ☞ *The automation of certain preparatory tasks which could lead to typing or reading errors (such as computing an orbit correction manoeuvre)*
- ☞ *An in-depth analysis which has identified those telecommands critical for the mission (possibly requiring a double-check before transmission)*

3.2 Reducing human errors

Three main actions were carried out in CNES in 1992 and in 1993:

- **In-depth risk analysis based on operating errors already committed**
- **Risk analysis of procedures used in operational centres**
- **Risk analysis about contingency cases**

3.2.1 Analysis of operating errors

This analysis was performed by a group of experts representative of the various areas of activity involved in a space programme (operational managers, satellite design authority, reliability experts, Quality Assurance manager). The input data for this study was as follows:

- ☞ *Existing files describing the significant operating errors committed*
 - ⇒ *45 such files since 1984*
- ☞ *Additional information provided by the operational teams*
 - ⇒ *Context and concrete consequence(s) of the anomaly*
- ☞ *Experience from other areas (e.g. launch vehicles or manned flights), and from exchanges with other organisations outside the field of space (EDF)*

EDF: French national agency in charge of the production and the distribution of electrical power.

The study's main results are as follows:

- ☞ *Characterisation of anomalies, as regards the context in which they occurred:*
 - ⇒ *75% of anomalies occurred during the completion of nominal or routine operations*
 - ⇒ *15% of anomalies occurred after the satellite entered a contingency case*
 - ⇒ *10% were committed in other contexts (positioning, in-flight acceptance)*
- ☞ *Characterisation of anomalies, as regards the root causes:*
 - ⇒ *65% of anomalies were due to so-called "elementary" errors (error in preparation, reading or real time telecommand typing)*
 - ⇒ *25% of anomalies were due to incomplete or ambiguous procedures*
 - ⇒ *10% were due to the nominal process not being respected (non conformance as regards an instruction or had estimation of time constraint)*
- ☞ *Identification of factors favourable (in the operators' opinion) to the occurrence of a human error*
 - ⇒ *Paradoxically, the situation considered the most critical is very long process whereby the control centre returns a satellite to its nominal situation following the satellite's automatic reconfiguration due to a downgraded case on board*

Preventive actions have been defined as a result of this analysis, especially in the following areas:

- ☞ *The theoretical and practical training of operators*
- ☞ *A wider collection of operating errors (including inconsequential ones)*
- ☞ *Improvement of feedback to future projects in the framework of operational activities*
- ☞ *A seeking of solutions to elementary human errors such as:*
 - ⇒ *Generalising telecommand plans for the completion of operations (risk of omitting a telecommand)*
 - ⇒ *Double-checking certain critical sequences*
- ☞ *The reliabilization of procedures (see § 3.2.2)*
- ☞ *Prior analysis of satellite contingency cases (see § 3.2.3)*

A table has been drawn up to summarise the anomalies according to their context, cause and consequence.

CONTEXT	ROUTINE	Critical (manoeuvre)
	ACTION	Not critical (maintenance)
	CONTINGENCY CASE	Serious and unforeseen
		Serious but foreseen
	OTHER	Elementary error (use of a backup) (Acceptance, Positioning)
CONSEQUENCE	LOSS OF SATELLITE	
	FAILURE OF MISSION	
	MISSION DOWNGRADED	
	LOSS OF BACKUP (WITH NO CONSEQUENCES ON THE MISSION)	
	NEGLECTIBLE	
	EXCESSIVE WORKLOAD	
TYPE OF ERROR	INCORRECT COMPLETION OF A PROCEDURE	Preparatory task error
		Omission of a step
		Typing error
	WRONG PROCEDURE	Incomplete
		Ambiguous
	NORMAL DECISION-MAKING	Training problem
		No procedure
	PROCESS NOT COMPLIED WITH	Process unsuitable
		Poor assessment of the emergency
		Instruction not complied with
NO DECISION-MAKING AID	Unforeseen contingency case	

Figure 3: Anomaly classification table

The Quality Assurance service is responsible for keeping this table permanently up-to-date so that the efficiency of the measures taken may be confirmed and new lines of improvement followed if necessary.

3.2.2 Reliabilizing procedures

The most critical procedures were analysed using a two-stage methodology:

- A detailed study of each procedure, looking at the rationale behind the sequencing of actions (exhaustiveness of information and coherence with proceedings) without calling the technical content of the procedure into question
- Identification of the risks of drifting away from the procedure (in collaboration with the operational personnel involved).

This analysis led to the drawing up of risk-reducing recommendations specific to each procedure or more generally to all the procedures. The generic recommendations cover the following aspects in particular:

- Principles behind procedure structuration
 - ⇒ Initial checks
 - ⇒ Completion
 - ⇒ Final checks
- Codification rules for basic actions
 - ⇒ According to their importance
 - ⇒ According to their nature
- Decision-making logic in the event of an anomaly

3.2.3 Taking contingency cases into account

Downgraded cases (whether onboard or ground) to be considered as a matter of priority are those requiring the operational teams to act quickly. With this in mind, such types of contingency situation and the events leading up to them have been identified either through detailed analysis by satellite experts or through feedback from a similar programme.

The corresponding procedures have been written up, qualified then introduced into the plan designed to keep ground teams operational.

4. CONCLUSION

The improvement highlighted above have been taken into account after consultation with the operational teams: they have given first quantifiable results; in particular for the duration of loss of (Telecommunication) mission with a human error origin:

- ☛ In 1991 : >2 Hours
- ☛ In 1992 : >2 Hours
- ☛ In 1993 : < 10 Minutes

Nonetheless, more effective results also require additional actions further upstream in the development of space programmes, in particular within the following areas:

- An operational analysis of the constraints involved in the utilisation phase needs to be carried out at the time of vital choices (preliminary and final design phase).

☛ In the light of this, teams must draw up their operational requirements specifications very early on in the process

- The drawing up of a design methodology for operational procedures (structure, ergonomic, reliability etc.).

- The definition of simulation means sufficiently representative to keep teams operational (simulation of nominal and downgraded cases)

The human operator is a dimensioning factor in the safety of operations. Through his own initiative, he can avoid a downgraded situation which could otherwise have led to a break in service; similarly, he can create an anomaly following an error on his part. The latter possibility explains why the reduction of human errors remains a primordial objective.

THE EUROSTAR OPERATIONAL CONCEPT

F. GAULLIER
G. LIMOUZIN

MATRA MARCONI SPACE

Abstract

On July 22nd 1993, the HISPASAT 1B spacecraft was launched from Kourou (French Guiana) to provide telecommunication services to Spain. It was the eight of the EUROSTAR series, accumulating 14 years in orbit without any operational problems. Selected so far by INMARSAT for their four spacecraft of the Inmarsat 2 serie, by HISPASAT (2 satellites), by FRANCE TELECOM (4 satellites) and by ORION Satellite Corporation (1 satellite) making 11 the total number of EUROSTAR ordered, the design has been proved easy to operate, highly reliable and secure in all phases of the mission.

The EUROSTAR operational concepts are reviewed from the Launch and Early Operational Phase when the body is spun about its inertial axis, up to the On-Station position, when it is 3 axis stabilized. To reach safely its on-station location, the spacecraft combines on-board security and ground centres monitoring.

From INMARSAT to HISPASAT, improvements in on-board memory sizes and software developments have modified - sometimes in great extent - the operational approach, leading to an increasing on-board autonomy. Emphasis will be made on these evolutions.

Key words: EUROSTAR, safe and low cost operations, autonomy and reliability

1- Introduction

The EUROSTAR platform has been developed by MATRA Marconi Space and British Aerospace to cover the full range of 1 000 kg to 3 000 kg class of telecommunication spacecraft. Beginning of the development took place in 1984 and since then, it has been constantly improved. The first four spacecraft based on the platform were the Inmarsat II serie: the platform used was the EUROSTAR.1000 bus (weight \approx 1 400 kg).

The last to date to be put in orbit were the HISPASAT telecommunication spacecraft which have benefited from the latest developments. They are based on the EUROSTAR 2000 bus.

This class of spacecraft favors a spin stabilization platform in transfer orbit and is 3 axis controlled once on-station. It is the purpose of this paper to describe first the operations to position the spacecraft on its orbital location and eventually, the evolutions in terms of operational concepts from the INMARSAT to the HISPASAT spacecraft.

2- Launch and Early Orbit Phase

2.1 Operations in transfer orbits

The EUROSTAR platform is fully compatible with the current commercialized launchers (2 of the 4 Inmarsat spacecraft have been launched with Delta II rockets and were compatible with an STS launch). We will however only present hereafter typical operations based on an Ariane launch.

At launcher separation, the spacecraft is injected into a geosynchronous orbit - a low perigee of about 200 kilometers high and an apogee at geostationary altitude. On this orbit, the spacecraft is, spinning at 5 rpm. Separation with the launcher triggers an on-board automatic sequence to switch on the telemetry transmitter allowing on ground telemetry reception. The telecommand receivers are on throughout the launch.

Once the ground centre has assessed the status of the spacecraft, the control and the propulsion subsystems are initialized through ground commands. The potential appendices (stabilization booms, lateral antennas,...) are then deployed and the satellite spun at 13 rpm to further improve the stabilization of the spinning body.

The satellite remains in this configuration throughout the transfer orbits - besides the manoeuvre preparation and execution. It is a safe configuration which requires a small amount and then reduced and simple operations.

Attitude Control and Orbit circularization subsystem

The kinetic momentum provided by the 13 rpm spin rate, induces a gyroscopic stiffness and hence, a very strong stability to the body. The attitude of the spacecraft is then only modified by ground commanding.

Otherwise, the attitude control is purely passive and the propulsion subsystem remains inhibited.

In transfer orbits, only three types of manoeuvres are commanded: the slew or spinning axis re-orientation to optimize the apogee manoeuvres, the apogee manoeuvres themselves and the spin or despin manoeuvres to adjust the spin rate to 13 rpm.

The excellent mass balance of EUROSTAR allows a very good stability during all these thrust phases (see figure 1).

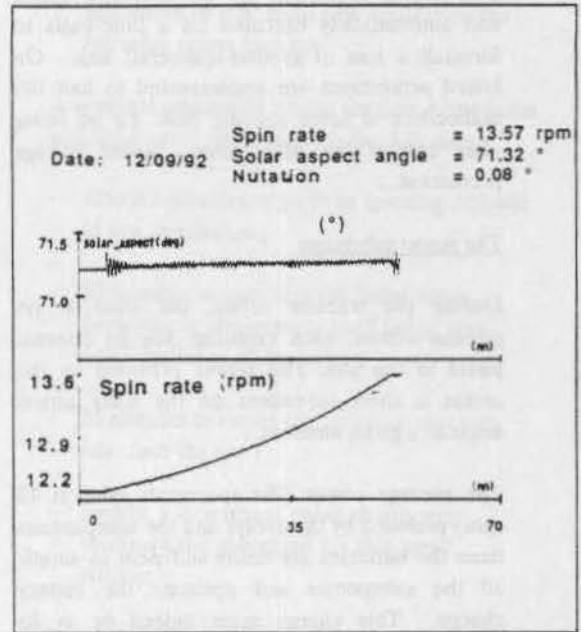


Figure 1 - Attitude of the S/C during an apogee manoeuvre

Concerning the slew or spin/despin manoeuvre, the knowledge of the thruster characteristics minimizes the number of these manoeuvres and optimizes their amplitude. The resulting error is always very small and well under the 3σ range permitted.

The classical strategy in three apogee burns is applied to reach the geostationary orbit. After each firing, the performances of the apogee engine are better known, until the third manoeuvre which, by its short duration and the required precision, optimizes the propellant consumption and the positioning of the spacecraft on the geostationary orbit.

All the manoeuvre phases and most specifically the apogee burns are carried out when at least one ground station is in visibility with the spacecraft.

The critical sequences are however pre-loaded and automatically executed on a time-basis to forestall a loss of ground-spacecraft link. On board protections are implemented to halt the manoeuvre in some specific case: e.g no firing after end of the manoeuvre, under voltage protection,...

The power subsystem

During the transfer orbits, the solar arrays remain stowed, each exposing only its external panel to the sun. The power provided by the arrays is then dependent on the solar aspect angle at a given moment.

The average power (the spacecraft spins at 13 rpm) provided by the arrays and the complement from the batteries are easily sufficient to supply all the subsystems and optimize the battery charge. This charge must indeed be at its maximum for the demanding sun acquisition.

Operationally, the power subsystem is nominally fully automatic. Configuration of the charge/discharge network is checked prior the launch and is not modified until the drift orbit.

The thermal subsystem

The concept of the spinning body provides a fairly homogeneous distribution of the thermal fluxes within the spacecraft (Solar Aspect Angle is never very far from 90°). The power required to heat the "coldest" parts is then minimized, and thus, the thermal design for this phase is simplified. The thermal subsystem does not require any specific operation during the transfer orbit. It is again a fully automatic subsystem.

The propulsion subsystem

Mention was made of the three types of manoeuvres, the spacecraft had to perform in transfer orbits. Only these manoeuvres require a propulsion subsystem enabled. The rest of the time (corresponding to about 90 % of the total time) this subsystem is inhibited, thus reducing

the risks associated to the use of any equipment and in particular of the propulsion devices.

Summary of the transfer orbits operations

As seen, the ground centre is practically, only actively involved when during the manoeuvre phases. The rest of the LEO Phase is spent in monitoring the downlinked data and analysing them to check the spacecraft for any anomaly.

Duration of the transfer phase is roughly 4 days until beginning of the next phase, the drift orbit phase.

Sequences of commands are simple and organized in a way to fully safeguard the operations in case of loss of the ground/spacecraft link. They concern almost exclusively commands related to the Attitude and Control subsystem and the configuration of the propulsion subsystem. The other subsystems behave autonomously.

3 - Drift Phase

Once the third apogee burn is completed, the satellite drifts slowly towards its final orbital position. This last burn, as stated above is dimensioned to optimize the drift and minimize the manoeuvres to perform for the satellite to reach its on-station position. The spacecraft is from now always in visibility from at least one ground station although TTC link depends on the attitude of the body.

3.1 Sun Acquisition and Solar Array Deployment.

The first part of this phase consists in spinning down the spacecraft to allow the Sun Acquisition on board closed loop control system to converge. The spin down is ground commanded on the same basis as the spin adjustments during the transfer phase.

Once the spin reduction is completed, the ground centre can actively prepare what is considered as the most exciting part of a launch phase: the sun acquisition followed by the Solar Array deployment.

It is indeed the most interesting part due to several aspects:

- The spacecraft attitude changes based on an on-board closed loop ;
- Power budget is modified because of the attitude change ;
- Thermal balance is modified for the same reason. The spacecraft is not spinning anymore, thus showing the same face to the sun.
- The propulsion subsystem is used with nearly all its nominal thrusters -5 out of 6 and among the 5, 2 have not yet been used ;
- The sun acquisition is followed by the Solar Array deployment thus allowing the power

subsystem to rely from now entirely on the full solar arrays capacity.

A nominal sequenced timing for Sun Acquisition and Solar array deployment is the following:

- About 3 minutes to go from spinning attitude to sun acquisition ;
- 30 minutes to complete the Solar Array deployment, deployment itself being very quick (order of 30 seconds) ;
- 20 minutes to rotate the arrays so that they can face the sun ;
- Finally, a 20 minutes phase to properly configure the spacecraft for this "new" attitude.

From now, the spacecraft is ready for the Earth acquisition and 3 axis stabilization at the next Earth orthogonality. This phase ends usually the launch operations. The spacecraft is then in a configuration which allows the commissioning phase to begin.

3.2 Summary of the Drift Orbit operations

We can imagine that time of the ground controllers could be largely booked during the sun acquisition and the array deployment sequence.

Actually, there is a good deal of work to prepare the sequences and insert them in the on-board time-tagged queue before the expected sun acquisition starting time. During the execution, time is only spent in monitoring carefully the spacecraft.

The commands are loaded in a way which fully secures the execution of the sequence in case of ground spacecraft link interruption, the actual sun acquisition order being loaded at the end. On the other hand, on-board monitorings are implemented to automatically trigger a reconfiguration of the spacecraft in case of criteria violation. The idea is then to put the

satellite in a safe configuration waiting for the ground to recover the situation.

MMS never had to experience the triggering of this protection, all the Sun acquisitions on EUROSTAR having been performed very smoothly.

The Earth acquisition as well as the 3 axis stabilization sequence are straight forward operations which do not require as much care as the sun acquisition. They are secured by on-board monitoring and reconfiguration triggering in case of criteria violation. Once the spacecraft is 3 axis stabilized, all the on-board protections are enabled and stay as such throughout its life time.

4- The On-station Phase

The EUROSTAR platform operational concepts emphasize a lot the on-station phase. The reasons is that the phase is the one which lasts the longest and requires the quasi-permanent presence of ground controllers. The objectives are to limit the number of operations to be performed from the control centres and hence to implement on board most of them. Nominal and anomaly management are part of this implementation, thus procuring a high level of safety and optimizing the communication service.

4.1 - Autonomy

Before going into the details of the operational concepts of the EUROSTAR platform, let us define what we understand by autonomy: this concept was developed in the frame of the TELECOM2 program :

- the satellite is able to maintain the nominal performances of the mission even in case of a ground unavailability, and this during periods up to 24 hours.
- In case of on-board failure, the on-board software secures the spacecraft either in passivating the failure or in configuring safely such that no failure propagation can occur. In this last case, the mission may be interrupted depending on the failure type. The spacecraft waits for a ground intervention to fully and safely recover the situation.

Such a definition has led to the implementation of on-board automatic control systems to manage most of the spacecraft subsystems.

Power subsystem

This subsystem does not require any ground intervention in the nominal case. It manages:

- The connection of the necessary solar array sections in function of the requested power ,
- The configuration when during the eclipses switching from the arrays to the batteries and vice-versa ,
- The optimization of the battery recharge after eclipse,
- The unlatching of non-vital equipment or depth of discharge on ampere-hour criteria.

At the operational level, this autonomy gives:

- The assurance that whatever the satellite configuration is, nominal or contingency, the necessary power is available.
- Ground intervention reduced to seasonal activities.

Thermal subsystem

The thermal control is also very much autonomous. The thermal configuration is automatically adapted to the level of utilisation of the payload (no-drive, back-off or saturation).

The only operations are:

- Thermal reconfiguration due to the season (4 times a year) ;
- Reconfiguration linked to the modification of the repeaters configuration (TWTA on or off).

Orbit Control Subsystem

This subsystem requires a great involvement from the ground during the SK manoeuvres. The idea behind a more important on board autonomy for this subsystem is not so much to reduce this involvement than to lighten the workload control of the operators. To reach this goal, automatic sequences of operations are implemented on board for example to return to normal Solar Sailing control after each station keeping manoeuvre. These sequences can obviously be modified by the ground if needed, are triggered by so called "macro-commands", their correct execution being controlled by the on board software.

4.2 Safety of the attitude control

The normal mode for the attitude control of the EUROSTAR satellite is based on the "Solar Sailing" concept developed by Matra Marconi Space.

This type of control, based on the solar arrays as "actuators", has a major impact on the ground operations because it does not use the propulsion subsystem outside of the Station Keeping manoeuvres. It minimises the potential risks associated to the continuous use of the thrusters.

The solar sailing concept provides smooth and accurate roll-yaw control of a bias momentum stabilized satellite. It uses the solar pressure forces to generate control torques involving the thrusters. The main components of solar pressure is applied on the solar arrays by depointing them from their nominal sun-pointed position.

With the 8 EUROSTAR in orbit, the Solar Sailing control has made the demonstration of its capability and its performance.

The figure 2 shows the roll performances over a day with the associated commanded biases on the solar arrays.

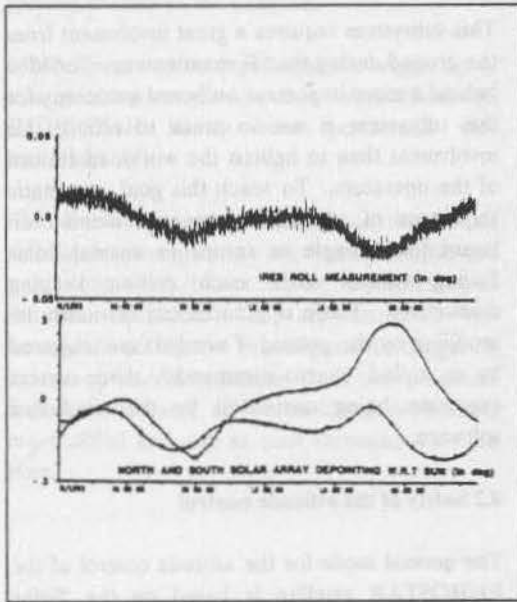


Figure 2 - Solar Sailing Performances

4.3 Failure Detection and Recovery

The attitude control subsystem performs its own monitoring through the so-called "Automatic Reconfiguration Mode" logic (ARM logic).

This logic takes into account subsystem parameters acquisition (such as depointing, voltages, temperatures, earth presence) to detect the occurrence of an anomaly. When a detection takes place, the logic triggers an automatic reconfiguration of all the equipments of the subsystem to their redundant one.

The logic has been tested several times during the commissioning phases of the 8 EUROSTAR platforms. It has been proved highly efficient to recover the anomaly without perturbation of the mission. Figure 3 shows the pointing performances in this mode. Let us mention that those performances are still compatible with the mission requirements, thus increasing the high rate of availability of the different communication mission.

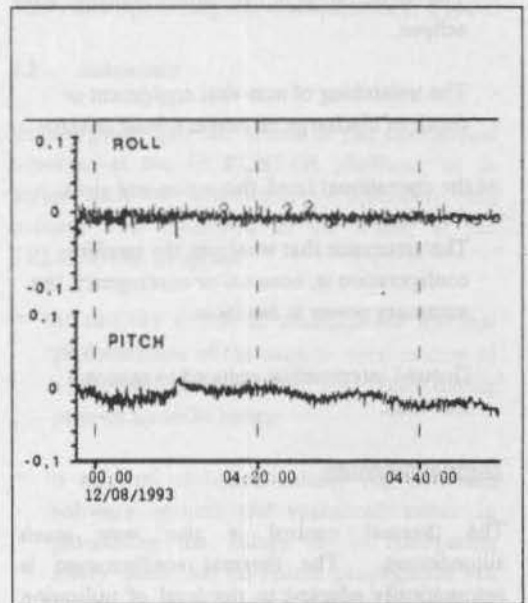


Figure 3 - Control Performances when a reconfiguration order is sent - Commissioning phase -

4.4 Summary of the on-station operations

The nominal Station Keeping operations are usually based on a 2 weeks-cycle. Figure 4 summarizes the set of operations to perform first during the 2 weeks-period and then those due to the seasonal effect.

Operation name	Duration	Periodicity
South station keeping manoeuvre	3 hours	1 every 2 weeks
East/West station keeping manoeuvre	3 hours	1 or 2 every two weeks
Thermal reconfiguration	20 minutes	4 times per year
IRES configuration	20 minutes	4 times per year
IRES autocalibration	1 hour	1 time per year
Tanks swapping	30 minutes	2 times per year
Moon interference	30 minutes	4/5 times per month
Battery reconditioning	30 minutes	2 times per year

Figure 4 the EUROSTAR nominal operations cycles

All the concepts detailed above have a direct impact on the operations and their simplicity:

When the on-board safety of the satellite increases the ground operations get more secured. We have indeed noted that most of the in-orbit "problems" were related to ground operations. Hereafter are listed all the satellite operations that do not require the intervention of the ground:

Power subsystem:

- Eclipses,
- Battery charge,
- In case of anomaly, unlatching of non-vital equipments when the available power is not sufficient.

Thermal subsystem:

- Adaptation of the thermal configuration with respect to the utilisation of the payload (back-off, no drive or saturation).

Attitude control subsystem:

- Earth sensor configuration before and after each eclipse.
- Return to normal mode after a manoeuvre (automatic on-board sequence).

5 - Conclusion

The capacity for the on-board software to execute sequences of monitoring and commands is a new approach in the telecommunication satellites.

For a geostationary satellite the constant visibility of a ground station added to the minimum required cost were preventing the on-board software to be developed in the same way as the low earth orbiting platforms. The availability of powerful and lower costs processors and the increasing workload of the ground controllers provide opportunities to greatly increase the on-board capacities.

In a close cooperation with the to-days users of EUROSTAR, MMS develops the new concepts for the next generation of platforms : towards an increasing autonomy, which also means the greater security and reliability.

VISIM - GRAPHICAL SUPPORT FOR SPACECRAFT

OPERATIONS AND SIMULATION

K. Booty, A.G. Haire, S. Mara

Cray Systems, DAS House, Quayside, Temple Back, Bristol, BS1 2NH

ABSTRACT

Over the last decade, the increasing power of the microprocessor has led to operational spacecraft simulators moving away from powerful mainframe computers towards desktop workstations. These workstations allow a single user great flexibility in the presentation of information including graphical displays. Previously, spacecraft simulation experts have often relied on little more than alpha-numerical displays to present their information. However, recent simulator developments, notably ESA's ISO simulator, have taken advantage of the workstation environment used, in particular Digital's flexible X-windows interface, to greatly enhance the quality of data presentation.

The result is Cray Systems' product VISIM - a visualisation tool for spacecraft simulations. The key feature of VISIM is that it provides information enhancement in a non-interventive manner, i.e. it can be easily engineered into existing applications. It is this feature which has now resulted in VISIM being integrated into operational systems (VISOPS). For example, VISOPS was used during the DFS/Kopernicus launch to enhance the downlinked telemetry from the spacecraft and show such critical early mission events as array deployment and ABM firing. These events were displayed on a projection screen in the main control room at DLR in Oberpfaffenhofen, Germany. This was performed without any modification to the control centre software system.

VISIM was originally developed for ESA's ISO program, other users of VISIM now include the Italian Space Agency's SAX project and DLR's Rosat mission.

Key Words: Visualisation, Spacecraft, Simulation, Operations

1. INTRODUCTION

VISIM is a software package running on a workstation to display, in 3-D colour graphics, the attitude and dynamical behaviour of a spacecraft. It has several types of display including views from the spacecraft's sensors which can show either which stars (including the sun) or which region of the Earth, the

spacecraft is pointing at. The unique feature of VISIM is the way it can be easily configured to cope with different types of spacecraft e.g. astronomical, telecommunications, Earth Observing and even NASA's Space Shuttle. The graphical displays respond to incoming data (telemetry) either from a spacecraft simulator or the satellite itself via a control centre. VISIM can therefore be used in both a training and an operational role.

In simple terms, it allows a user to see changes in a spacecraft's orbit and attitude as it receives commands from the control centre, or as the spacecraft's on-board software performs manoeuvres.

2. HISTORY OF DEVELOPMENT

Back in 1990, Cray Systems were awarded a contract by the European Space Operations Centre (ESOC) in Darmstadt, Germany, to develop the spacecraft simulator for the Infra-Red Space Observatory (ISO). This is an astronomical spacecraft designed to examine the stars for infra-red radiation. Therefore the sensors inside the telescope are particularly sensitive to heat and so the payload is contained within a thermal jacket of liquid helium to keep the temperature of the sensors down to just a few degrees Kelvin. ISO has a sophisticated on-board Attitude and Control System (AOCS) to ensure that:

- 1) The solar panels always face the Sun (These panels as well as providing electrical power also act as a shield for the body of the satellite)
- 2) The telescope aperture of the satellite never looks directly at a "hot" object such as the Sun, Earth or Moon.

The design of the simulator included incorporating the actual flight software into the AOCS subsystem model. Thus the simulator provided identical responses to attitude control commands as the real spacecraft. So, for example, as pointing commands were sent to the simulator, it responded by producing telemetry attitude data showing the complicated movements the spacecraft had to perform to obey both the pointing command and

the constraints imposed to avoid damaging the instruments by pointing the telescope at "hot" objects (e.g. Sun, Earth and Moon).

These complicated manoeuvres were difficult to visualise in the user's mind and so Cray Systems decided to build a simple graphical tool which responded to the attitude quaternions contained in the ISO telemetry by rotating the image of the spacecraft seen on a workstation display.

This simple visualisation caught the imagination of both the Cray developers and the ESOC staff who came up with other displays that could be shown. Cray Systems realised the potential of this tool and so have extended it and developed it to become a product in its own right - VISIM.

3. DESIGN PHILOSOPHY

The main design principles in the development of VISIM were: low cost, portability and ease-of-use.

VISIM is written in FORTRAN and C and contains no third-party commercial graphics packages. It utilises the industry-standard X-Windows and Motif products. This provides a mouse-driven windows interface to allow a user to expand windows to any size, display as few or as many views as he wants and either have the windows tiled or overlapping on the workstation screen and providing a standard look-and-feel.

VISIM was developed on standard factory-installed DEC workstations (3100, 4000) under the Digital operating system VMS. Because of its construction, VISIM has recently been effortlessly ported to a Digital Alpha AXP workstation running under Open-VMS. The combination of X-Windows, Motif and C will make a port to UNIX workstations straightforward.

Cray Systems close links with Digital have allowed both companies to promote the new Alpha workstation and VISIM concurrently. VISIM has been demonstrated on the Alpha at presentations in Madrid, at the 1992 Simulations conference in ESTEC and the 1992 Space Operations conference in Pasadena.

4. VISIM FUNCTIONS

The current list of VISIM's features and functions include:

Spacecraft Display

The main display shows a user-defined representation of the spacecraft, oriented correctly in inertial space. The Sun, Moon and Earth vectors may be shown as well as the three spacecraft axes.

Elementary spacecraft generation

The spacecraft "model" seen on the screen is constructed from simple, elemental building blocks: cylinders, cubes, planes, lines etc. By specifying their position on the screen a user can build up a

representation of the spacecraft. This representation can be as accurate as required. For example, if one is just interested in the spacecraft's attitude to the Sun, a basic model showing the top & bottom could be built. On the other hand, it may be desirable to see solar panels deploy or when certain thrusters fire. These are known as "conditional-draw" objects and are easily added. They are further described below.

Efficient spacecraft drawing

The main display uses a simple algorithm to rapidly draw the spacecraft image. Known as Painter's Algorithm this determines the order of the 2-dimensional faces that are to be drawn and filled in. This order changes as the spacecraft rotates and the surfaces are drawn with the furthest from the viewpoint being drawn first.

Accurate Rendering

Rotation of the spacecraft is shown by the shading of each face, the colour being darker, the greater the angle to the Sun. Cylindrical objects are approximated as having a discrete number of sides (typically 16, although this is user-configurable).

Conditional Draw

The spacecraft image is a collection of many objects. Some of these objects (spacecraft body, instrument etc) are drawn on every update. But some only need to be drawn under special conditions (e.g. thruster plumes, antenna deployment etc). Thus the facility exists to draw portions of the display only where a certain condition is met. This condition can be described, for example, by a status parameter in the telemetry. These parameter values are sampled on every update before drawing of the associated object. Thus the image provides a useful visualisation of the change in spacecraft configuration and status as contained in the telemetry.

Secondary Transformations

For deployments, the update of the object position is not calculated from the previous position but is calculated from the original data in the Object Definition File entry for the object. A transformation calculation is made on this data up to the current extended point that is to be drawn, then a second transformation is made using the current attitude matrix as output by the "In-Betweening" function.

"In-Betweening"

This refers to the process whereby the attitude and orbit are maintained correctly between data updates. Typically the image or orbit depiction has to be updated many times in between the arrival of the data (either from the simulator or the satellite) that drives it. Thus the spacecraft attitude motion is updated smoothly between data arrivals using the standard Euler equations of

motion and Keplerian dynamical equations are used for the calculation of intermediate orbit positions.

Viewpoint modification

It is possible to alter the viewing position of the spacecraft image by altering the elevation and azimuth point of the viewer. This allows the viewpoint to move around the spacecraft. Also the field of view as represented by the display image and the distance of the viewer from the spacecraft are modifiable.

Startracker and Star Map Display

The VISIM configured for astronomical satellites (e.g. ISO and ROSAT) has a special Startracker view which shows the actual star constellations that the spacecraft is observing. Currently, the star coordinates (right ascension and declination) are taken from the star catalogue being used for the ISO mission at ESOC. The user sees the complete celestial sphere with the Startracker field-of-view superimposed upon it. The user can then select a region of sky and zoom in as often as he wishes. He can also remove "clutter" by only displaying stars below a specified magnitude.

Earth Projection

A view of the Earth is provided showing the major continents. A plot of the groundtrack of the spacecraft is displayed along with night/day shading and the coverage zones of specified ground stations. The groundstation symbol flashes when the spacecraft is in range. The user can select and zoom into any portion of the display.

Orbit and Ground Station Visibility

A view of the spacecraft orbit is provided showing the orbit path around the Earth and spacecraft position in the orbit. Groundstation positions are depicted on the earth image. These flash when the spacecraft is in range of the particular groundstation. The subsatellite point is also shown on the earth image.

User-Configurable

The spacecraft model, user-text and all displays are fully user-configurable in a text file. This Object Definition File (ODF) is read at program start-up but can be edited on-line using the provided forms-based editor. All changes take place immediately. Different ODFs can be selected at runtime thus different spacecraft can be viewed without restarting VISIM. All displays that may be running are changed according to the spacecraft ODF requested.

Communications Flexibility

The visualisation and calculation functions are isolated as much as possible from the data source. Thus coupling to a simulator telemetry source or to a spacecraft telemetry source is transparent to the visualisation functions processing the received data.

Currently, the required data is obtained via either a mailbox connection or over DECnet from a separate process. This de-coupling of communications links from the visualisation offers wide flexibility and is vital for the range of applications areas in which VISIM will be used.

For example, although originally planned to work alongside a spacecraft simulator, it is possible (and has been done for DFS-3 Kopernicus and ROSAT) to acquire data from an operational spacecraft control system. This allows spacecraft operators in an Operational Control Centre to see a representation of the actual spacecraft as it performs manoeuvres.

5. CONFIGURATION

All details of the spacecraft model, as well as sensor fields of view and all text seen on the screen is held in an ASCII file which is read-in by VISIM at program start-up. This ODF is a key part of VISIM's flexibility. It allows a user to have full control of the spacecraft colours, perspective views, zoom factor, update rate and rendering definition. This last attribute is particularly important because it allows a user to tailor the display to the workstation he is using. For example, to represent a cylinder, a multi-faceted figure of typically 16 sides is used. If a user wants a better representation this figure can be increased: however the more faces, the more processing required and the greater the load on the workstation processor.

VISIM typically uses 25% of a VAX Station 4000/60 when configured for an update rate of 10 Hertz. Altering the screen- update rate or number of sides per shape can increase or decrease this quite dramatically.

Because the ODF is such a key component, there is an ODF editor built into VISIM. This editor allows a user to make on-line changes and save the ODF under the same or a different name. Therefore, a user can have many different configurations (perhaps different screen-update rates or magnification factors) stored in different ODFs. Using the VISIM editing functions the appropriate display can be called-up whenever the user wishes.

The ODF also allows us to offer language-independence. All text seen on the VISIM displays, including menu titles and help messages, are stored in the ODF. It is therefore easy to produce, say, a German or French version, and switch between them on-line. All changes take place immediately.

6. SENSORS

Of particular interest to the user is the capability to observe what is visible in the FoVs of the various sensors a particular spacecraft may be carrying. VISIM supports rectangular and circular FoVs of varying dimensions and

allows users to observe whether any of the major bodies (Earth, Moon, Sun) appear.

The position of the major bodies at a particular epoch are calculated using the standard Low Precision Almanac formulae. Since the current spacecraft attitude is known and with the exact position of the sensor on the spacecraft together with its FoV, it is possible to generate a graphic which can show whether the object appears in the FoV.

The positions of the major planets (Venus, Mars, Jupiter and Saturn) are also calculated and these can be seen crossing FoVs. In future developments of VISIM it is hoped that the resulting image of the FoV, which currently only depicts the major body or planet, will be upgraded to include a depiction of the star field.

7. OPERATIONAL VISIM

VISIM was originally written to form the visualisation part of the European Space Operations Centre's (ESOC) training simulator Man-Machine Interface (MMI). Its place in this product means that VISIM can be used for all future spacecraft for which ESOC procures a simulator (e.g. Cluster and Envisat).

From a simulation tool, VISIM has grown to become an operational one. It has already been used at the launch of DFS-3 Kopernicus at the German Space Operations Centre (GSOC) to demonstrate the deployment of the spacecraft's solar arrays and the firing of the main engine (always a critical phase in the life of a satellite).

Its success at the launch (the display was projected on the main control screen to all the visiting dignitaries) has led to VISIM being fitted into the ROSAT control centre displays. Cray Systems has also been invited to quote for installing VISIM at the control centres for the Eumetsat V and Eutelsat V and are presently preparing VISIM for the German Spacelab D2 (utilising the European laboratory fitted to NASA's Space Shuttle) launch and operations.

To adapt VISIM to receive operational telemetry was a straightforward task. A crucial design decision taken at an early stage was to separate the main pieces of VISIM into self-contained modules as much as possible. These modules are:

Drawing	Communicates with the screen and draws the graphics.
Transformations	Decides where each part of the image should be drawn
Communications	Receives the incoming telemetry.

Originally the telemetry was produced by a spacecraft simulator. Since a spacecraft simulator is designed to mimic the operation of a spacecraft as closely as possible, the telemetry it produces is identical to that of the real spacecraft. As VISIM was designed to process telemetry, it was a simple task to get the program to interpret operational telemetry.

The data required by the drawing routines are:

- Attitude matrix
- Spacecraft Rates
- Earth Sun and Moon vector
- Apparent radii of celestial bodies
- Conditions (e.g. Thruster firing on/off)

For this operational scenario, the data is acquired via a VISIM mailbox. A VISIM process waits at the mailbox for messages to arrive from either a simulator or the actual spacecraft. On arrival, the message is validated and the data values preserved in local, VISIM variables. VISIM performs all transformations on the local variables.

The display is updated according to the transformation information. The screen re-draw rate is user-configurable and completely separate from the data telemetry rate.

The contents of spacecraft telemetry are dependent on many factors such as subsystem design and mission objectives. A science satellite such as ROSAT or ISO is designed to be pointed at different stars and so precise pointing information is sent to the spacecraft and accurate positional and movement data returned in the telemetry stream. However, communications satellites do not need to be realigned as often and so their telemetry contains less information on the spacecraft attitude. To accurately model DFS-3 therefore required the computation of additional orbit parameters. Fortunately, Cray's experience in writing many spacecraft simulators allowed us to use existing algorithms to generate the required data.

8. VISIM AND THE INFRA-RED SPACE OBSERVATORY

To illustrate the power and use of VISIM, let us consider a particular implementation: the Infra-Red Space Observatory (ISO) satellite simulator completed by Cray Systems in July 1992.

The particular pointing constraints on ISO have already been explained in section 2 of this paper. To help ISO cope with these constraints, it has four key sensors:

- Sun Acquisition Sensor +Z
This sensor is placed on the back of the satellite with its boresight parallel to the +Z spacecraft axis. It has a FoV of greater than 180 degrees.
- Sun Acquisition Sensor -Z
This sensor is placed on the other side of the spacecraft. If the AOCS detects that the Sun is being recognised by this sensor it knows it must turn the spacecraft around.
- Fine Sun Sensor

This sensor is again placed to view parallel to the +Z axis. It provides very accurate alignment by covering the low resolution portion of the SAS +Z FoV.

- **Earth Limb Sensor**

This sensor will recognise any hot objects in its FoV and is positioned on the Sun-Shield at the opening to the telescope. Its role is to warn the AOCS if there is a danger of any hot objects shining directly into the telescope.

- **Star Tracker**

To help accurately align the telescope before the main instruments are activated, the operators use one of two Startrackers. These instruments are co-aligned with the spacecraft X axis which runs along the telescope boresight.

As with all spacecraft simulators, the movement, momentum and inertia of the spacecraft body were accurately modelled. Also included was the actual AOCS code flown on-board ISO. By sending the appropriate telecommands from a console and watching the VISIM display many of the decisions made by the AOCS could be observed. For example:

- Manoeuvres performed after separation from the launcher (in ISO's case this will be Ariane)
- Change of spacecraft orientation as it approached perigee to avoid the Earth or Sun "shining" directly into the telescope.
- Thruster firings to accurately align the spacecraft.

A spectacular simulation could be observed by applying an impulse to one side of the spacecraft (simulating a meteorite impact). This initially causes the spacecraft to tumble wildly until the AOCS, by firing thrusters, brings the spacecraft back to a stable, steady state. It is particularly impressive to see the AOCS cycle the thrusters on and off very quickly to achieve fine pointing and reaction-wheel off-loading.

9. VISIM AND ITS FUTURE

As previously mentioned, VISIM is now an established part of ESOC's simulator MMI. As such it is in use for the ISO simulator campaign and is expected to be used on future simulators by Cray Systems.

One future project, Cluster, will provide a new challenge for the VISIM designers as the mission uses four spacecraft which orbit together. VISIM's current "eye-point" is at a pre-determined point in space. For Cluster, displays will have to be written which allow the user to "fly" the eye-point through and around each of the four spacecraft. This will allow, for example, a user to "sit" on one of the spacecraft and observe what the other three are doing. Cluster will therefore be the first multi-spacecraft display for VISIM.

Following VISIM's successful launch at the 1992 Farnborough Air-show (where it was filmed and

broadcast by the BBC), VISIM was enhanced to receive operational telemetry, as previously stated, for the DFS-3 Copernicus launch and ROSAT on-going mission. It is expected that other satellite operators to whom Cray have issued quotes will soon have their own VISIM system.

The VISIM system is continually being enhanced with ideas from Cray's own engineers and from users at ESOC and GSOC. We are now currently working towards the third generation of this product. However, the original design aims of ease-of-use and user-configurability will always be adhered to. For example, functions that are currently undergoing beta-testing are:

- Spacecraft orbits around other planets.
- Improved shading algorithms to be provided as a configurable option
- Depiction of communications contact zones with Ground Stations and other satellites e.g. the Data-Relay Satellites: DRS and TDRSS.
- Addition of sensor swathes to the Earth projection so that operators and users can see precisely what instruments are operating at any one time and what part of the globe is being scanned.

This last display will be of interest to the Earth Observation community and particularly the operators of ERS-1.

Cray Systems are also aware of a user's processing resources and costs. Therefore, it is always looking for ways to reduce the processing overhead on the workstation whilst improving the quality and fidelity of the displays.

Although VISIM was written for the Digital-VMS environment (as this is the host for simulators at ESOC and GSOC); since UNIX is a popular alternative, Cray are ensuring that a port to UNIX will be straightforward and low cost.

10. CONCLUSION

VISIM is now a tried and tested facility used for operations and simulations on several missions. Its use has demonstrated that the users of spacecraft simulators and operation teams benefit from an accurate, easy-to-use graphical display package.

There is no doubt that a major attraction of VISIM is its low-cost and ability to run on standard workstations with no special graphical-accelerator boards or expensive graphics software libraries being required.

With the high costs involved with the space and ground segments, any product that provides or enhances received information at a low cost will always be welcomed. As Dave Wilkins, head of the Flight Control Systems Department at ESOC said recently: "VISIM will be a vital part of our simulation system because the complete visualisation of complex spacecraft

manoeuvres, together with a celestial environment, is now available"

11. ACKNOWLEDGEMENTS

The authors would like to thank ESOC staff members J.J. Gujer and J. Miro; Digital Equipment Corporation; and members of Cray Systems simulations staff in Bristol, ESOC and GSOC for inspiration in the development of VISIM and help in the preparation of this paper.

12. LIST OF ABBREVIATIONS

AOCS Attitude and Orbit Control System
DRS Data Relay Satellite

ERS-1 Earth Resources Satellite 1
ESA European Space Agency
ESOC European Space Operations Centre
ESTEC European Space Technology Centre
FoV Field-of-View
GSOC German Space Operations Centre
ISO Infra-Red Space Observatory
MMI Man-Machine Interface
NASA National Aeronautics and Space Administration
ODF Object Definition File
ROSAT Roentgen X-Ray Telescope satellite
TDRSS Tracking and Data Relay Satellite
VMS Digital Equipment Corporation's Operating System

OPERATIONS II

1. Rozenfeld, P.; Orlando, V. and Schneider. E.M. (INPE-Brazil): "Overview of INPE's Satellite Tracking and Control Center and Main Aspects of its Debut in Satellite Operations"	421
2. Pacholczyk, P. (CNES-France): "In-Orbit Storage of SPOT 1 Satellite"	426
3. Hechler, M. (ESOC-ESA): "ROSETTA Interplanetary and Near Comet Navigation: A Challenge for Ground Operations"	432
4. Campan, G. and Brousse, P. (CNES-France): "Experience of Eight Geostationary Satellite Positionings"	440
5. Brittinger, P. (DLR-Germany): "DLR/GSOC Experience in the Field of Geostationary Communication Satellites"	447
6. Donat, H. (CNES-France): "Positioning of Geostationary Satellites at CNES: Facilities Operational Organization and Documentation"	451

OVERVIEW OF INPE'S SATELLITE TRACKING AND CONTROL CENTER AND MAIN ASPECTS OF ITS DEBUT IN SATELLITE OPERATIONS

Pawel Rozenfeld

Valcir Orlando[†]

Etiene Monteiro Schneider

Instituto Nacional de Pesquisas Espaciais - INPE

Caixa Postal 515

12227-010 - Sao Jose dos Campos - SP - Brazil

[†]E-Mail: valcir@dem.inpe.br

Abstract

The Satellite Control Center (SCC), located in Sao Jose dos Campos, together with the Cuiaba and Alcantara ground stations, which are linked by a data communication network (RECDAS), constitute the Satellite Tracking and Control Center (CRC) of the Brazilian Institute for Space Research (INPE). The CRC has the responsibility of operating in orbit the satellites developed by INPE or in cooperation with other organizations. This work presents an overview of the CRC system architecture, hardware and software, its operational structure and the activities undertaken in preparation of the whole system to support its first space mission. Relevant aspects of the CRC satellite operations activities, since its debut, on February 9, 1993 with the launch of the SCD-1 (Environmental Data Collecting Satellite), the first satellite designed, manufactured and operated in orbit by INPE, are briefly explained. Some parameters showing the present functional performance of the SCD-1 after a year in orbit are presented and discussed.

Key words: Satellite Tracking and Control Center, Ground System Architecture, Brazilian SCD-1 Satellite, LEOP operations.

Introduction

The INPE's Satellite Tracking and Control Center (CRC) is responsible for the planning, management and performance of its satellite operations activities. During four years since its creation, the CRC main activities was to participate in the establishment of the INPE's ground control system, to plan the operations activities for the INPE's first satellite, to provide and

train satellite operations personnel¹, to develop operational procedures and to set-up the ground control system for mission operations.

The paper presents an overview of the CRC system architecture, its operational structure, and the activities undertaken for the preparation of the whole system to support its first space mission. The relevant aspects of CRC debut in satellite operation activities on February 9, 1993 with the launch of the SCD-1 (Environmental Data Collecting Satellite), the first satellite designed, manufactured and operated in orbit by INPE, are also explained.

The next section is dedicated to a brief presentation of the SCD-1 satellite and its mission. In the following section an overview of the whole INPE's Ground Control System is presented, including a brief presentation of the CRC operational structure. The main aspects of the INPE's debut in satellite operations activities are presented afterwards. In conclusion an evaluation about system performance is done.

The Environmental Data Collecting Satellite (SCD-1) and its Mission

The Data Collecting Satellite (SCD-1) is a relay satellite which receives the data collected by the automatic platforms (DCP's) in UHF-band and transposes them in real time to the S-band. When DCP's, the satellite and the Cuiaba Ground Station are in mutual visibility the collected data are received by the Ground Station. These data are stored at the Station and after satellite pass are transferred to the Data Processing and Distribution Facility (DPDF) by means of Data Communication Network. The DCP's users receive the processed data from the DPDF.

The DCP's are mainly of meteorological kind which means that they collect information such as local tem-

perature, precipitation, wind speed and so on.

Some of the DCP's are used for river level monitoring (flood control). Some others are used for forest fires monitoring by measuring the seasonal variations of the CO, CO₂ and O₃ component in the air. There are 10 DCP of this kind located at 10° S latitude from east to west of Brazil.

Still other DCP's are dedicated to monitor the Amazon rain forest regeneration by monitoring at three sites (deforested site, new forest and old forest) several parameters which allows to determine the forest regeneration rate.

SCD-1 is a low earth orbiter with nominal altitude of 750 km and with orbit inclination of 25°.

The satellite is an octogonal prism with 1m base diameter and 1.055m height. Its weight is 115 kg. Satellite's all faces but one are covered by solar cells. The remaining face is used as a heat sink in its passive thermal control. It should not be directed to the sun. In order to avoid this problem an attitude maneuver has been foreseen after satellite 6 month life in orbit. No other maneuvers has been planned during satellite one year nominal life.

The attitude subsystem is constituted by a magnetometer and two sun sensors, a nutation damper and a spin axis torque coil. The satellite stabilization is achieved by spin, initially at 120 rpm.

The TT&C antennas of same polarization are located on the opposite bases. Because of their radiation patterns, silence zones were expected to occur depending on the satellite attitude ($80^\circ < \phi < 100^\circ$), where ϕ is the solar aspect angle) during the passes over the Ground Stations.

The INPE's Satellite Tracking and Control Center

INPE's Ground Control System is constituted by a Satellite Control Center (SCC) located in Sao Jose dos Campos (23° 12' S; 45° 51' W), a Ground Station located in Cuiaba (15° 33' S; 56° 04' W) and another Ground Station located in Alcantara (02° 20' S; 44° 24' W). Connecting all three sites there is a Data Communication Network. This system constitutes the Satellite Tracking and Control Center (CRC). The Fig. 1 shows the geographic location of the SCC and the ground stations on the Brazilian map.

The Cuiaba site has been chosen for the Ground Station location because it has a very good coverage of whole South America and because INPE already had a LANDSAT-SPOT-ERS1 receiving station at this site.

The Alcantara Ground Station, which is located at a new Brazilian Launch Center, allows to track a satellite launched from the Center since the satellite injection into orbit.

The Ground Stations up and down links are in S-band. The Stations are almost identical in their hardware. The only difference is that the DCP data receiver



Figure 1: SCC and Ground Stations Locations

is located at Cuiaba Ground Station making it a TT&C and payload receiving station. The Alcantara Ground Station is a TT&C station and it has an acquisition antenna mounted on the rim of the main dish. This feature was very useful for initial acquisition of SCD-1. Both stations have a computer system (microVAX II) which, besides performing monitor and control function of the station equipment, host, also, the real time software identical to that of SCC. In this way each Ground Station can assume, in degraded mode, satellite operation, a feature which proved to be very useful after SCD-1 launch. The Telecommand, Telemetry and Ranging functions are performed according to ESA PCM standarts.

The Satellite Control Center hardware is composed of DEC computers. There are two VAX 8350 in cluster arrangement for mission operation and a VAX 11/780 for software development. The communication between real time software and the Ground Station equipment is done according to ESA SDID protocol.

The data communication network is a private packet switching one which implements X.25 access protocol. Its bit rate is 9600 bps. It has star configuration with the network management center located in SCC.

The Fig. 2 illustrates the basic architecture of the INPE's ground control system for the SCD-1 satellite. By using the in-house developed Flight Dynamics software, files containing pass predicts of the satellite over the ground stations are generated. These files are sent to the ground stations where they are used as input data to a tracking antenna control software, which au-

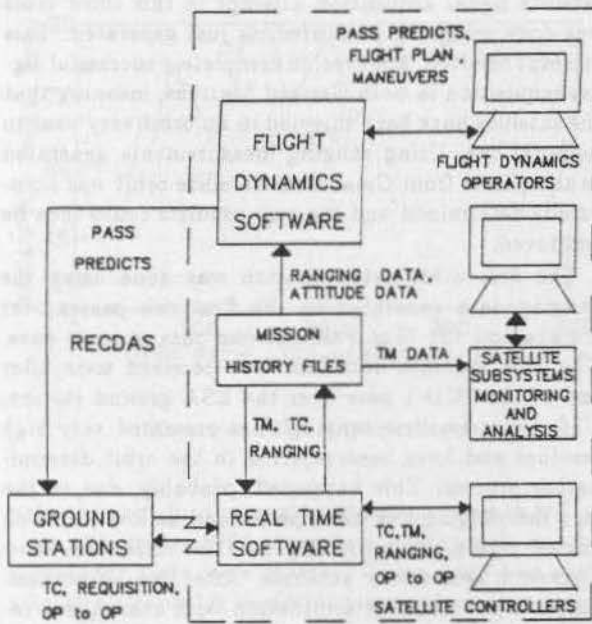


Figure 2: Ground System Basic Architecture

tomatically positions the antenna for acquisition of the satellite signal at pass beginning. In the case of a signal loss during a pass, the software generates, by means of a local orbit propagation process, data used to automatically point the antenna according to the expected direction of the satellite orbit track. This maintains the antenna pointed to the satellite until the signal re-acquisition happens. In the SCC, the pass predicts files are used to periodically generate the flight operations plan for the satellite routine phase. For this task a specific software which automatically generates the flight plan is used. Its input data are the most recently generated pass predicts.

The real time tasks are the well known functions of TM data acquisition, storage and display; TC transmission; ranging measurements, ground station monitoring and SCC to ground station operators communication. All these tasks are done with help of an in-house developed real-time application software.

The software for satellite subsystem performance evaluation operates only in non-real time from the history files of the mission.

Operationally, the CRC is divided into two areas: the Space Operations Area and the Ground Operations Area. The Ground Operations Area is responsible for all activities required to maintain the ground control system (SCC and ground stations) in operational working condition. This area comprises two branches: the Ground Operations Branch and the Technical Support Branch. The Ground Operations Branch is responsible for the coordination of the activities related to the

whole ground system operation (SCC, ground stations and data communication network). The Technical Support Branch is responsible for the execution of the activities related to the communication services and ground system equipment operation and maintenance. The Space Operations Area is responsible for the activities related to the in-orbit control of the INPE's satellites. This area is divided into three branches: the Control System Branch, the Satellite Operations Branch and the Rehearsal and Simulations Branch. The Control System Branch is responsible for the operation of the SCC computer system and for the configuration of the SCC application software. The Satellite Operation Branch is responsible for the coordination and execution of all activities directly related to satellite in-orbit control. Finally, the Rehearsal and Simulations Branch has the function of developing the activities related to the training of the satellite operations personnel and coordinating the mission rehearsals. It is also responsible for: specifying user requirements, following the development, testing and operating high fidelity real time satellite simulators².

The operation of the whole ground control system runs 24 hours a day in four 6-hours shifts.

The INPE's Debut in Satellite Operations

On 9 February 1993 at approximately 14:42:20 GMT SCD-1 was injected into orbit with 2 hours delay relatively to nominal injection time. The launch was performed by the north-american launcher Pegasus manufactured by OSC. The Fig. 3 shows initial orbit traces, displaying the visibility circles of Brazilian Alcantara and Cuiaba Ground Stations and of the European Space Agency (ESA) Mas Palomas ground station. ESA had agreed to perform SCD-1 ranging measurements from this station during SCD-1 first pass over it. These measurements would be sent to INPE by fax in compact form after pre-processing. It must be noted that only from the third orbit on the satellite was visible by Cuiaba Ground Station.

Approximately 1 minute after the separation, OSC should inform INPE the time instant when satellite injection into orbit has effectively occurred. About 15 minutes later, INPE should receive from OSC satellite orbit and attitude state data at the injection point. These data should be used to generate pass predicts and antenna pointing angles for satellite second pass over Alcantara. After satellite second pass over Alcantara, OSC should send to INPE satellite orbital state estimate determined by NORAD (USA). These data should be used as initial conditions in the updated pass predicts generation as well as used as initial condition for the orbit determination process. The orbit determination would be accomplished by processing ranging data generated by Alcantara and Cuiaba Ground Stations. The first orbit determination would occur after satellite second pass over Alcantara. New orbit deter-

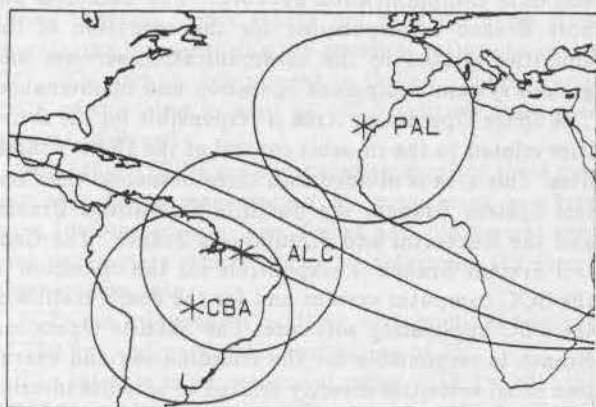


Figure 3: Initial Orbits

minations would be performed successively after each pass over Cuiaba up to the ninth orbit when the first cycle of the successive satellite passes over Ground Stations would end up and 11 hours out-of-visibility period would start.

The Satellite signal acquisition by the Alcantara Ground Station happened at 14:42:24 GMT by using acquisition antenna and then switching to the main one. It was verified by telemetry that the satellite was operating normally in the nominal configuration. The definitive satellite orbit determination was, however, a hard task due to some problems which occurred:

- shortly before the launch a failure in the Alcantara ranging system occurred and the stations could not perform the required ranging measurements,
- required information expected from Wallops Launch Center on the injection instant and related orbital elements could not be provided by OSC due to a technical problem occurred in the launch center,
- orbit data determined by NORAD, expected to be provided after the second pass of the satellite over Alcantara, was provided only two days after launch.

Due to these problems the second pass over Alcantara was lost. In spite of the lack of information, the Flight Dynamics group performed the computation of an estimate of the in-orbit injection time. A new orbit propagation was then done from this estimate of the injection time, using the nominal state vector of the injection point as initial condition. New pass predicts was then generated for Alcantara and Cuiaba. In case Wallops information on injection point or NORAD information, expected by then, would arrive on time, the new pass predicts would be generated in order to substitute the just generated ones. No information,

however, have been received in such a way that a new satellite signal acquisition attempt in this third orbit was done using the pass predicts just generated. This attempt resulted, however, in completely successful signal acquisition in both Ground Stations, meaning that the satellite have been injected in an orbit very near to nominal one. Using ranging measurements generated in the passes from Cuiaba the satellite orbit was accurately determined and the pass predicts could then be improved.

The first orbit determination was done using the ranging data generated in the first two passes over Cuiaba and the Mas Palomas one pass ranging data. The Mas Palomas data has been received soon after end of the SCD-1 pass over the ESA ground station. Unfortunately these ranging data presented very high residues and have been rejected in the orbit determination process. This happened, probably, due to the fact the ranging has been performed at low elevation angles, where the modelling used for refraction error correction is not very accurate. After two subsequent passes a new orbit determination with consequent refinement of the pass predicts was done. The last pass predict was satisfactory for Cuiaba tracking up to the ninth pass with no problem in the satellite signal acquisition. This ended up the first cycle of satellite consecutive passes over Brazilian station. A time interval of roughly 11 hours with no Cuiaba visibility followed. During this time the fourth orbit determination was performed. The results of this orbit determination was used to generate pass predicts for the next visibility pass cycle over Cuiaba. From that point on there were no more problems, related to orbit determination, to acquire the satellite by the Cuiaba ground station.

As far as the attitude determination is concerned, some initial problem have occurred due to reception of a large quantity of the invalid telemetry frames. It was necessary to introduce small modifications in the pre-processor in order to avoid that valid data were rejected altogether with the bad ones. The problem of the reception of the invalid frames was later eliminated by lowering the transmitted power at Cuiaba, which was interfering on the SCD-1 downlink. Despite having some problems before getting the first attitude determination, the results have been satisfactory ones. The first attitude determination resulted in the value of 64.73° for the solar aspect angle and spin rate of 119.18 rpm at 18:00 GMT of the launch day. These results have been confirmed later by OSC. Good quality of the results have been confirmed by the communication silence zone predicts during satellite passes over Ground Stations. Nominally these silence zone should occur when the angle formed by the satellite-station direction and satellite spin axis had values between 80° and 100° . Besides confirming the foreseen time instant when there should be silence zone with their actual occurrence, it was noted that the 80° to 100° degrees range was over-estimated. In practice the TM bad frames

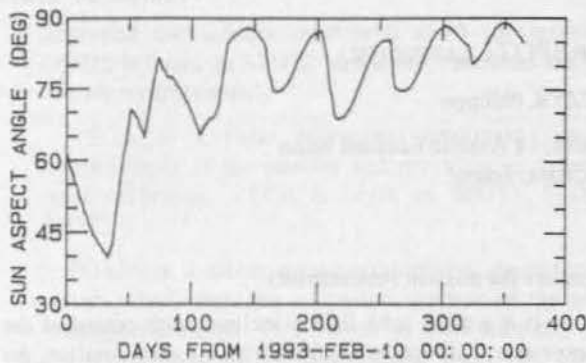


Figure 4: Solar Aspect Angle

only occurred for the angle values very near to 90° .

On 12 february 1993, three days after launch, in-orbit acceptance tests were started. These tests had show a totally acceptable performance of all satellite essential subsystems. Only the operational software of the satellite on-board computer (OBC) loaded from the ground by means of telecommands presented a non-satisfactory performance. But OBC is an experimental subsystem. Nowadays the problem have been completely solved. A new software version loaded to the computer allows all OBC functions to be realized successfully.

The solar aspect angle, which was of the order of 39° , should be rised to near 90° by using the satellite torque coil. The PCD transponder reaches lower maximum temperature values in an orbital period for solar aspect angle of 90° . This value should be avoided, however, because above this value the sun rays would incide on the lower panel. This could cause thermal problems. After finishing the maneuvers, the solar aspect angle was elevated to 72° . With this PCD transponder temperature dropped to variation range with maximum value of order of 20° C. At present days, new spin axis maneuvers have been performed, leaving the solar aspect angle near to 90 degrees. Fig. 4 shows the behavior of the solar aspect angle from the begining of the operation to the present day. After one year of the launch the satellite spin rate is of the order of 69 rpm.

From the launching to the present time the satellite does not present any hardware problem and it is expected to have 2-year in-orbit operational life instead of nominal 1-year.

Conclusion

The paper presented an overview of the INPE's Satellite Tracking and Control Center. The Center had its debut in real satellite operations activities with the launch of the SCD-1 satellite. In spite of the occurrence of some operational problems during the SCD-1

LEOP the CRC operations personnel has showed to be well prepared to overcome them and to conduct the operations to a successful routine phase. Although the Ground Control System has presented some hardware problems its characteristics of robustness allowed a safe conduction of the SCD-1 operations activities.

After one year of the SCD-1 launch its telemetry shows an excellent performance of all satellite systems which did not present any malfunction since launch. It is now expected that the satellite operational life will be increased by one year more.

References

¹ Rozenfeld, P. "Operational Training for the Mission Operations at the Brazilian National Institute of Space Research (INPE)." *2nd International Symposium on Ground Data Systems for Space Mission Operations - SPACEOPS 92*, Pasadena, CA, USA, November 16 - 20, 1992, p. 667-671.

² Orlando, V.; Rozenfeld, P.; Miguez, R. R. B.; Fonseca, I. M. "Brazilian Data Collecting Satellite Simulator." *Eighteenth International Symposium on Space Technology and Science*, Kagoshima, Japan, 1992.

IN-ORBIT STORAGE OF SPOT1 SATELLITE.

Mr PACHOLCZYK Philippe

Centre National d'Etudes Spatiales, 18 Avenue Edouard Belin
31055 Toulouse Cedex, France

Abstract

SPOT sun-synchronous remote sensing satellites are operated by CNES since February 1986. Today, the SPOT mission and control center operates SPOT1, SPOT2 and SPOT3.

The eight years old SPOT1 satellite is still able to transmit in real time the images acquired. In 1992, CNES decided to store it in orbit as a back-up satellite in case of major failure on SPOT2 or SPOT3.

The storage is based on an entire in-orbit autonomy of the satellite for orbit and attitude control, and a reduced using of the ground equipments. With two visibilities per day used only for telemetry monitoring and orbit computation, the ground control workload decreases to a low cost operating.

Obviously, in case of satellite anomaly, all the mission and control center can be reactivated in order to repair the failure.

Key words: satellite storage, in-orbit autonomy, operations

SPOT satellite mission

The decision of SPOT earth remote sensing program was taken by the French government in 1978.

Designed by CNES (Centre National des Etudes Spatiales) and built by France with Belgium and Sweden cooperation, the SPOT system is operational since 1986. It is composed of an image receiving and processing ground segment, a mission and control ground segment and the Spotimage commercial company, which is in charge of earth images selling. See Fig. 1.

Primary Mission

The aim of SPOT satellites is to perform images of the whole earth. Equipped by two optical instruments and two magnetic recorders, the satellites can transmit two images of 10 or 20 meters resolution at the same time, in four visible wave bands. Each image requests a 25 Mbits per second data link. These images can be recorded on board for further transmission or directly transmitted down to ground by using a X band (8 GHz) downlink.

The SPOT satellites orbit has been precisely defined to

insure the mission requirements:

- it is a polar orbit lightly inclined with regard of the pole axis. This feature enables, with the earth rotation, the whole earth observation.

- the orbit phase is 26 days long and enables a repetitive image taking. As a matter of fact the side angle viewing capability offers stereoscopic images capability and a 5 days long accessibility delay.

- the orbit is roughly circular (830 kms) and the images have the same characteristics whatever the observed point is.

- the orbit is sun-synchronous and implies the overflight of the same point at the same date (1030Z). Then, the images have the same lighting conditions.

These orbit characteristics imply a ground segment rhythm with two visibility groups, one in the morning (about 1030Z) and the other in the evening (about 2230Z).

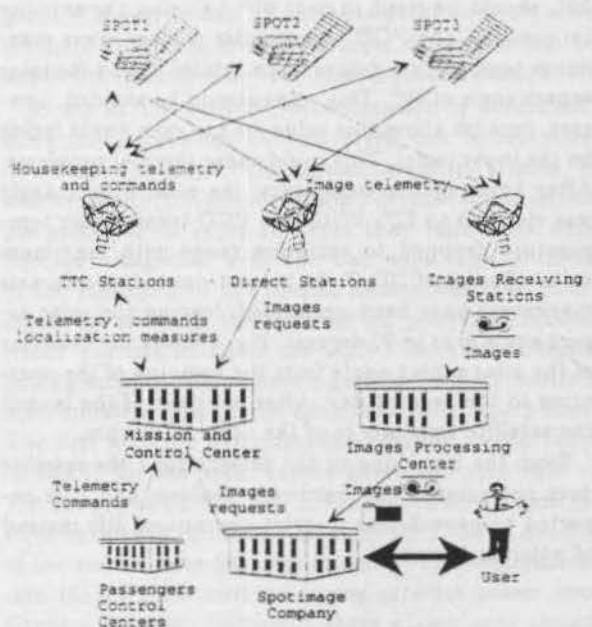


Figure 1: SPOT system organization

Secondary Missions

Since the beginning, SPOT satellites include several passengers which perform secondary missions:

DORIS is a doppler measurement instrument used to

determine the satellite orbit with a 10 cm accuracy. DORIS is board on SPOT2 and SPOT3 satellites and has its own control center.

VEGA is a radar responder instrument running independently of the satellite and providing an accurate radar calibration. VEGA is board on SPOT1, SPOT2, SPOT3.

POAM is a polar ozone atmospheric measurement system which performs a spectral analysis of the polar stratospheric clouds. POAM has its own telemetry link and is monitored by the Consolidated Space Test Center in Sunnyvale, CA. POAM is board on SPOT3.

Ground Segment General Organization

The SPOT ground segment is subdivided into three parts. See Fig. 1 and 2.

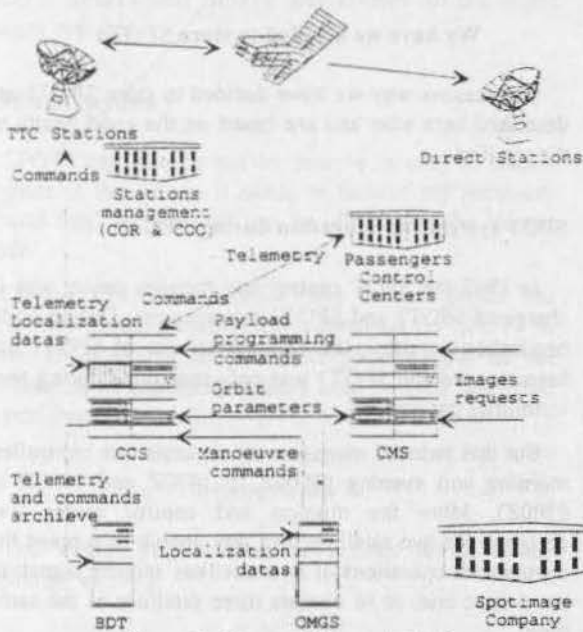


Figure 2: One satellite organization

The first part is the TT&C stations network which enables housekeeping telemetry reception, commands transmission and satellite tracking. The stations are situated near Toulouse in France, Kiruna in Sweden, Pretoria in South Africa, Kourou in Guyana and use the 2 GHz band. They are managed by the network operation center (COR) and the orbitography and ephemerides center (COO).

The second part is the image ground segment which includes:

- the image receiving stations which can receive direct or recorded images. These stations are situated near Toulouse and Kiruna.
- the image processing centers which process, archives

and produces the satellites images on film or magnetic tape. These centers are settled in Toulouse and Kiruna.

- the direct receiving stations which can only receive direct image telemetry. Today they are twelve spread all over the world.

The third part is the mission and control center (CCM) which is in charge of satellite monitoring and commanding, payload programming, orbit processing and ground facilities coordination.

CCM interfaces with the passengers control centers for passengers monitoring and commanding.

CCM organization

Designed at the beginning of the 80's for the control of one satellite, the ground equipment and/or software have been duplicated for each satellite. See Fig. 2 and 3.

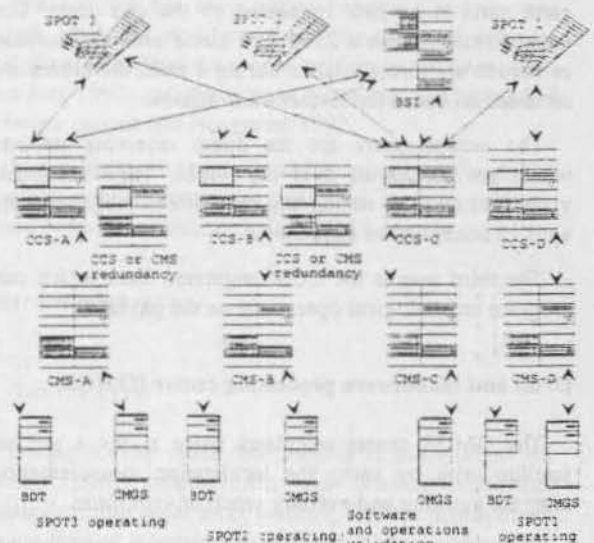


Figure 3: Three satellites organization

Two additional computers (CCS and CMS) are used during launch for redundancy and during operating for software and operations validation.

CCM includes the following parts, duplicated as needed for three satellites.

Control center (CCS)

During a satellite visibility on a 2 GHz TT&C station, the CCS is in a real-time mode and performs the following functions:

- real-time monitoring of the telemetry parameters.
- commands transmission to the satellite.
- localization measurements reception from the TT&C station.

Between two visibilities, the CCS is in a postponed mode and performs the following functions:

- preparing the commands plan for the next visibility.
- postponed monitoring of the satellite telemetry: on-board configuration, thermal and power monitoring, trend analysis, etc.

The CCS can also play back the telemetry in case of precise investigation and interfaces with passengers control centers for passengers housekeeping telemetry providing and passengers commands transmission.

Mission center (CMS)

The CMS daily performs automatically the payload work schedule to be send to the CCS by taking into account the requests of the following users.

The first user is Spot Image company which sends the earth parts to be shot requested by the end users. The images situated into a 2500 kms circle around Toulouse or Kiruna are directly taken during a pass, the others are recorded on board for further transmission.

The second users are the direct receiving stations which are spread all over the world. They can book visibilities on their station and send direct image requests until 12 hours before executing.

The third user is the CCM engineers team which can program technological operations on the payload.

Orbit and manoeuvre processing center (OMGS)

The OMGS center calculates twice a day a precise satellite orbit by using the localization measurements, after the morning and evening group of visibilities.

It determines a predicting orbit which is used for the payload programming, the TT&C visibilities prediction and the management of on-board attitude events (earth or sun sensors, in orbit position, ...). It also calculates and generates the commands to be send for a manoeuvre, in order to insure a right orbit.

Technological database (BDT)

All the data related to the CCM and satellite status are daily archived in the technological database: telemetry, sent commands, orbit parameters, ...

These data can be retrieved and reported on display, paper or plotter. Today, the BDT manages more than 20 Gigabytes which represents all the status data of CCM and SPOT satellites since their launch.

Satellite simulator (BSI)

The satellite simulator includes a real on-board computer which runs the satellites on-board software. The other equipments and the environment are simulated. The BSI is used for operations and on-board software releases qualifications.

Human organization

More than forty people are working in the control and mission center. They are in charge of satellites or ground facilities management (engineers and controllers).

SPOT2 and SPOT3 CCM are managed from 0500Z to 0200Z by four controllers.

SPOT1 CCM is only managed during the two visibilities by one of the four controllers.

Wy have we decided to store SPOT1 ?

The reasons why we have decided to store SPOT1 are described here after and are based on the good health of the satellite.

SPOT system configuration during 1992

In 1992 the SPOT control and mission center was in charge of SPOT1 and SPOT2 management. During north hemispheric winter, the commercial use of SPOT1 has been stopped and SPOT1 was only controlled during four visibilities par day.

But this reduced management requests one controller, morning and evening (0600Z to 1430Z and 1830Z to 0200Z). More the mission and control center was designed for two satellites and was unable to support the commercial operations of two satellites and the launch of the a third one, or to operate three satellites at the same time.

SPOT1 state in 1992

SPOT1 has been launched during February 1986 and was designed for a two years lifetime. Of course it is a eight years old satellite which has lost some redundancies. Both on-board recorders are no longer available for several years and the nominal travelling wave tube has been lost four years ago. But the redundant one is operational for images transmission, the satellite is still able to acquire direct images and can be used either by Spotimage company with the image receiving stations or by foreign countries with the direct receiving stations. See Fig 1.

There was no problem on the other equipments of the payload or the platform and the calibrations had shown a

good performance of the payload. After seven years, we were still confident in the robustness of the satellite and foreseen several more years of use.

SPOT1 schedule between 1992 and 1994

In 1992, it was foreseen to use commercially SPOT1 only until October 1992 and between April and July 1993. After this date, SPOT1 will be store in orbit several months during SPOT3 launch and in flight acceptance tests.

Due to its good health, SPOT1 can be used as a backup satellite.

On the first hand, in case of major failure on SPOT2 which would imply a loss of its commercial activity, SPOT1 can continue the mission.

On the other hand, in case of unsuccessful launch of SPOT3, SPOT1 and SPOT2 can assume all the direct images mission.

1995 and beyond

SPOT1 can also be put by reserve in case of market upgrade in the future. It needs to foreseen the necessary ground facilities but they can be idle during the storage mode.

During 1991, the mission and control center has performed some technological operations on SPOT1 in order to determine the in orbit performances of the satellite. Some experiments have been delayed and could be performed later.

Storage aims

The storage requirements have been settled at the beginning of 1992.

Safety of the satellite

During the storage mode, the satellite must be maintained in working order.

It implies that the satellite must be autonomous for electric power management and thermal regulation.

It means also that we shall be able to perform the satellite maintenance procedures: unused gyroscopes reactivation and electrostatic cleaning of the momentum wheels.

Workload and cost

We wanted also to decrease the operations workload and cost.

Without payload programming, the on-board attitude control needs only attitude datas refreshing twice a day and the orbit control a manoeuvre programming roughly every month.

The aim was to suppress all these ground control commands in order to perform only telemetry monitoring, during visibilities as few as possible. The goal was to decrease the ground monitoring to one visibility per day.

Return to commercial mode

Lastly we wanted to setup simple procedures for storage and return to the nominal mode. Indeed, in case of SPOT1 activation after the failure of another satellite, the commercial activity break must be as short as possible.

Storage solution

The solution has been settled between February and March 1992, the modifications of the on-board software and ground facilities have been performed between April and July 1992, and the storage mode has been qualified between August and November 1992.

Matra Marconi Space is prime contractor for SPOT satellite manufacturing and has been in charge of on-board software modification for SPOT1 storage.

Board configuration

Satellite safety

During routine mode, the satellite is autonomous for electric power management and thermal regulation. Battery cycling, solar array pointing, heaters management are performed automatically by the on-board software. A ground control is only done every month to prevent a drift of the system.

The on-board software performs also the monitoring of all equipments, and recovery procedures execution in case of anomaly detection. After a recovery, the satellite is in a safe mode but the return to a nominal mode needs a ground intervention.

After seven years, we were confident in the robustness of the software and we decided to let it manage and monitor the satellite as previously. We decided also to relax the ground intervention delay in case of board anomaly to the next working day for the worst case.

At last, after a use of seven years, we were confident in the robustness of the payload during the standby mode. That's the reason why we choosed a sucess oriented strategy: the payload performances will be verified and calibrated during the return to the commercial mode.

Satellite autonomy

During nominal mode, the on-board attitude control needs an update of its datas twice a day, necessary for the adjustment of the earth and sun sensors measurements around the year.

With default predefined data, the attitude control accuracy is a little bit degraded but without impact on the geocentric pointing monitoring. Thus, there is no more update of the attitude control datas by the ground control center. Of course this degraded mode is inconsistent with the image mission.

During nominal mode, the on orbit position is maintained by the on-board software but the algorithm must be adjusted twice a day by the ground center. This on orbit position is counted from the ascending node and, due to the pole axis obliquity, must be updated all year long.

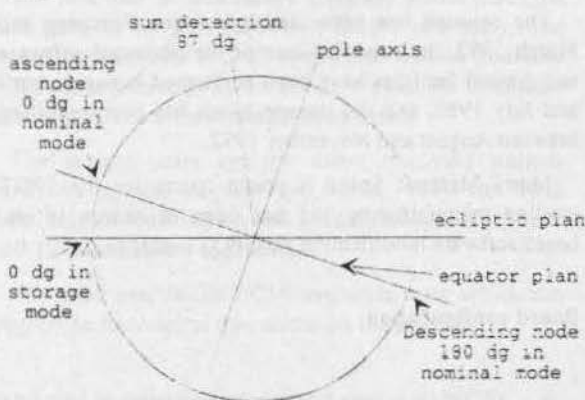


Figure 4: On orbit position counting during storage

The sun sensor has been designed to see the sun at the same position (87 degrees) with regard to the ecliptic plan. The sun detection is used by the a new on-board software module to adjust the on-orbit position counter. See Fig 4.

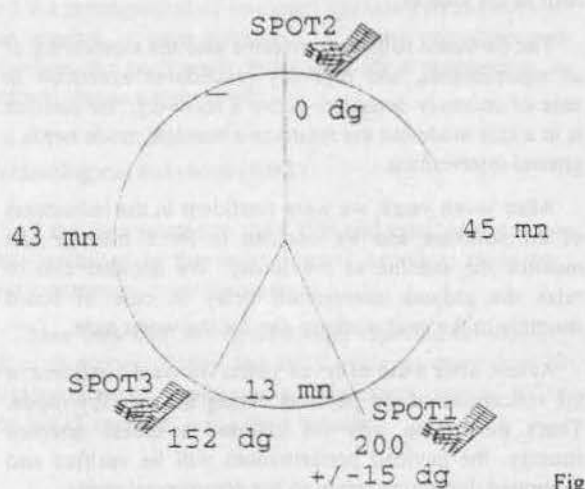


Figure 5: On orbit position of the satellites

Without payload using, the on orbit position accuracy can be released roughly ten times (± 15 dg), without conflict with SPOT2 or SPOT3 satellites. In this way, the orbit correction manoeuvres can be rare and short. See Fig. 5.

Manoeuvres programming requests a several days long setup of the ground facilities. That's why we have decided to add an automatic manoeuvre programming module in the on-board software. The delay between two manoeuvres and the trust power can be adjust by the ground control center.

Ground configuration

Regarding the ground facilities, they have been settled as follow.

The telemetry, tracking and command stations are managed by a multiproject center. This one is in charge of orbit and station ephemerides computation and needs at least two visibilities per day.

The satellite monitoring and maintenance needs only a control center for telemetry monitoring and commands transmission, during one visibility per day. But due to the ephemerides computation request, the satellite is controlled during two visibilities per day, morning and afternoon.

Nevertheless the satellite database is filled with the telemetry of one visibility per day.

The mission center, in charge of payload programming, and the orbitography center, in charge of accurate orbit computation and manoeuvres programming, are stopped.

So, the workload is decreased to one hour per day.

The commercial operation of one satellite needs two controllers, twenty hours per day, and the full capabilities of the control and mission center. SPOT1 and SPOT2 are operated from the same room and their ground station passes are choosed to avoid schedule conflict. Therefore, one of the SPOT2 controllers can assume the management of SPOT1 visibilities.

According to the kind of on-board anomaly, the correcting procedure needs only either the use of the control center or requests the utilization of the orbitography center. Except for survival mode, which is the worst anomaly case, the known procedures are five days long at the maximum. They can generally be performed with two visibilities per day.

Lately, the return to a commercial mode needs to warm up the mission and orbit centers and, if necessary, to perform a rendez-vous manoeuvre in order to place SPOT1 at the right orbit position. It could be two to five weeks long, depending on the drift of SPOT1 satellite inside the 15 degrees window.

In orbit storage review since December 1993

First storage

We have performed the first in-orbit storage of SPOT1 at the beginning of December 1992. The satellite has been stored two weeks in order to qualify the operations.

The storage procedure has been executed on December 1st and the return procedure on December 15th. The satellite was autonomous during 13 days without problem.

Second storage

After this storage qualification, we wanted to store SPOT1 as quick as possible, on December 16th. During the storage operation, there was a conflict between the sun sensor monitoring by the on-board software and the ground segment commands. This conflict has implied a safe mode of the satellite and a heavy recovery workload for the ground facilities.

So, the second storage has really started on February 2nd 1993 and was 6 weeks long, ending on March 17th. After this date, SPOT1 has been commercially used until August.

During this second storage, the on-board software has performed automatically and successfully 3 semi-major axis correction manoeuvres of 20 meters each.

Third storage

Due to the SPOT3 launch, SPOT1 satellite has been stored again on August 4th 1994 and is always stored today.

During these 7 months, the satellite has performed successfully 2 manoeuvres, with a 85 meters correction for the last one.

During December, the on-board software has detected 2 memory bit latch up due to heavy ions. The on-board safety procedure has been performed by the software but this kind of anomaly needs a ground facilities intervention for recovering.

These operations have been performed with two visibilities per day but were 5 days long each.

Results

First of all, the platform functioning and the payload standby mode are nominal.

The satellite maintenance procedures have been performed during storage visibilities without any problem.

Some memory bit latch up have been detected by the on-board software and corrected by the ground facilities without problem. On the whole, these anomaly corrections have been two weeks long. They have shown that the setup of the necessary ground facilities is easy but the operation implies a weighty human workload. Indeed preparation and execution of the operations need a work of several hours per day for an engineer and a controller.

The on-board software has performed successfully five automatic manoeuvres. On the whole, these manoeuvres have corrected 165 meters on the semi-major axis and used 450 grammes or 0.4 percent of the remaining fuel.

Compared with a commercial one, the storage mode cost is very low: quite no controller rather than six per day and two visibilities per day rather than six. The storage cost for the control and mission center is roughly 10 to 20 % of the operational cost.

Last of all, with some adjustments, this storage mode could be used on the others SPOT satellites and increase the flexibility of the SPOT system with respect to the commercial load or satellites contingency.

References

1. Pacholczyk, P. SPOT satellites family: past, present and future of the operations in the mission and control center. In SpaceOps 92, Pasadena, JPL.

ROSETTA INTERPLANETARY AND NEAR COMET NAVIGATION A CHALLENGE FOR GROUND OPERATIONS

M. Hechler

European Space Operations Centre (ESOC)
Robert-Bosch-Str. 5, 64293 Darmstadt, Germany

Abstract

The prime objective of the ROSETTA Comet Rendezvous Mission is insitu analysis of cometary matter. Launched by ARIANE 5 in July 2003, the ROSETTA spacecraft will reach comet Schwassmann - Wachmann 3 in 2008 utilising (powered) gravity assists at Mars and Earth and also passing by an asteroid. It will enter into orbits around the comet and observe the nucleus through its perihelion passage in 2011. ROSETTA mission operations will be performed by ESOC. A major task will be to navigate the spacecraft healthily and safely towards and near the comet. The navigation during the interplanetary cruise, the planetary and asteroid flybys and the comet approach will utilise conventional range and Doppler tracking and some 'classical' optical navigation, imaging the targets as point sources against the star background. Finally when the spacecraft is near the comet, imaging of landmarks on the surface of the cometary nucleus will provide the necessary spacecraft position and comet rotational state knowledge.

Key words: Interplanetary Navigation, ROSETTA Comet Rendezvous Mission.

Introduction

Project Evolution

Following the definition of the 'Planetary Cornerstone' in the long term plan of Scientific Projects of ESA in 1984 (*Horizon 2000*¹), ROSETTA had originally been conceived as a Comet Nucleus Sample Return Mission. To this objective the mission concept had evolved from 1984 to 1991 through a series of scientific and engineering efforts. Since 1988 it had been envisaged as a joint ESA/NASA project. Sample return mission and spacecraft concepts, based on a Mariner Mark II carrier spacecraft, had reached a considerable level of sophistication during a System Definition Study (1989 to 1990). In 1991 it became clear that programmatic incompatibilities between ESA and NASA made it difficult for ROSETTA to compete for the ESA Cornerstone 3 selection in 1993 as a joint project. The cancellation of the NASA Comet Rendezvous and Asteroid Flyby Mission (CRAF) in early 1992 further changed the programmatic situation. Under these circumstances ESA decided to investigate a mission concept which could be realised by ESA alone. Recent evolution in space experiment capabilities opened the possibility of 'taking the laboratory to the comet' rather than bringing a sample back to Earth, and still coming close to the original scientific objective of the planetary cornerstone as stated in *Horizon 2000*¹,

and remaining within the budget limitations. In parallel to the discussions in the scientific community, mission analysis and engineering studies proved the feasibility of a comet rendezvous mission, based on a communications spacecraft bus with solar arrays, launched by ARIANE, including an experiment package to be dropped by the spacecraft onto the surface of the comet. In November 1993 ROSETTA has been selected as 'Cornerstone 3' of the ESA Scientific Program.

Mission Objective

Cometary Nuclei and - to a lesser extent - asteroids represent the most primitive solar-system bodies. They are assumed to have kept a record of the physical and chemical processes that prevailed during the early stages of the evolution of the solar system. Analysis of comets and asteroids as a whole and of cometary material in particular, is expected to provide essential information on the provenance of meteorites and interplanetary dust and to improve our current understanding of the formation of the solar system².

To this objective the ROSETTA mission will:

- perform in-situ investigations of the chemical, mineralogical and isotopic composition, and the physical properties of volatiles and refractories in the nucleus,
- study the development of cometary activity, and its link with the characteristics of the nucleus (active areas; mantled areas),
- acquire complementary information on the diversity of asteroids from selected fly-bys.

Mission Opportunities

For the required launch time from mid 2002 to end 2004, ten mission opportunities have been found. For an ARIANE 5 launch and for the spacecraft as designed (about 1000 kg dry mass) the utilisation of gravity assists of Venus or Mars combined with at least one Earth gravity assist is necessary to reach comet rendezvous conditions. The mission duration from launch to the comet rendezvous manoeuvre may thus take from 5 years up to 9 years. All missions contain at least one asteroid flyby.

As reference a mission to the comet Schwassmann - Wachmann 3 has been selected, with a launch in July 2003. This mission is near the limit of tank filling and also launch mass, but it has a particular

short duration. Short mission duration was a major selection criterion to save operations cost.

An orbit plot (ecliptic projection) of the reference mission is shown in Figure 1. The maximum sun distance is 5.2 AU, the maximum communications distance is 6.2 AU. The total ΔV for nominal orbit manoeuvres is 1924 m/s.

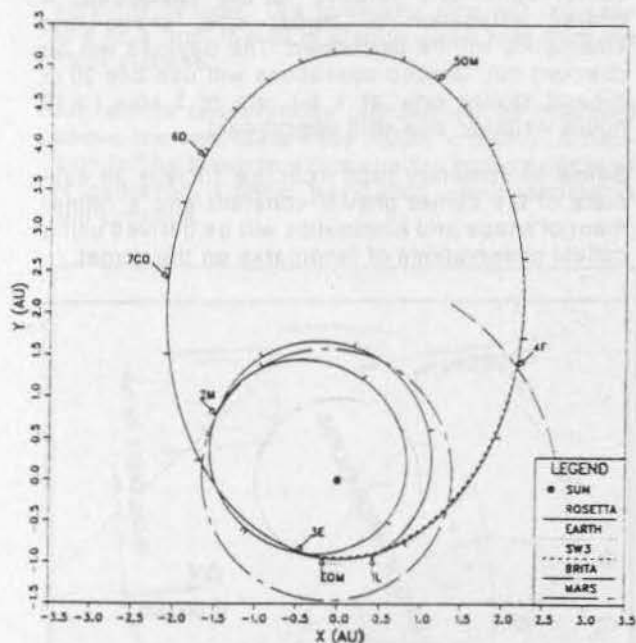


Figure 1. ROSETTA Interplanetary orbit

The Navigation Task

A central task in ROSETTA operations will be to navigate the spacecraft towards the comet and finally near the comet. This means to determine the spacecraft orbit from different types of tracking data, to calculate the necessary orbit manoeuvres and finally to implement those manoeuvres such that the target conditions are reached. To some extent a similar task has been performed by ESOC for the GIOTTO mission, for two fast comet flybys at a rather close distance and one Earth gravity assist. Nevertheless the ROSETTA navigation will comprise several features which will be new, not only to ESOC.

- powered gravity assists at Earth and possibly Venus or Mars,
- optical navigation during Asteroid flybys and comet approach,
- landmark navigation near the comet,
- surface package delivery.

The ROSETTA spacecraft development (phase B) will start in 1996. At about the same time ESOC will start the implementation of the ground operations systems. Before that time some of the concepts invented during the mission analysis have to be refined such that actual system development

can be based on them. This paper is intended to outline these concepts and the demanding operational challenges of the ROSETTA navigation to a wider audience, and hopefully to create interest in support of further studies and to foster ideas for new concepts.

Mission Operations

Mission Schedule

The description of the ROSETTA operations for the different mission phases given below indicates the central role of navigation.

Launch (2003/07/18)

ROSETTA will be launched by ARIANE 5 from Kourou. After burnout of the lower composite the upper stage (L9.7) with the spacecraft will remain in an eccentric coast orbit for about 2 hours. Before perigee passage the upper stage will be ignited and will inject the ROSETTA spacecraft into the required escape hyperbola towards Mars (escape velocity = 3.37 km/s). The spacecraft will separate from the launcher upper stage and will autonomously acquire its 3-axis stabilisation.

Early Orbit (3 months)

Ground operations will acquire the downlink in S-band using the ESA network, and deploy the solar arrays and the high gain antenna. The spacecraft will immediately enter the sun pointing cruise configuration and communications will be via the high gain antenna in X-band. Ranging, orbit determination, attitude determination will be performed and the departure trajectory will be verified and corrected. All spacecraft functions required during the cruise to the comet, in particular autonomous cruise functions, hibernation and reactivation functions, will be checked out.

Earth to Mars to Earth cruise (380 + 658 days)

The spacecraft remains in a sun pointed cruise configuration. The S/C health and attitude are to a large extent maintained by autonomous functions, without ground intervention. During one communications pass of 8 hours every two weeks the spacecraft health will be verified. The ground control system will resume control only in case an anomaly on the spacecraft is detected.

Mars flyby

Daily operations will be resumed 3 months before arrival at Mars. Tracking will be performed using two ground stations. Several re-targeting and correction manoeuvres will be executed before and after the Mars flyby.

Earth flyby (Perigee height 200 km)

Operations will be mainly related to tracking and orbit maintenance from 3 months before flyby until 1 month after as for the Mars flyby. A large orbit manoeuvre (730 m/s with constant attitude, 1 hour duration) near the pericentre of the flyby hyperbola will be necessary. Several orbit correction manoeuvres before and after the flyby will be executed.

Earth to comet cruise (750 days)

The Earth to comet cruise will be interrupted by an asteroid flyby (on day 229 from Earth in the reference case). For the rest of the time the spacecraft will be in the quiet cruise mode as described above for the Earth-Mars-Earth interplanetary arcs with one ground contact every two weeks. The comet and asteroid ephemeris will be continuously improved by ground based astrometry.

Asteroid flyby

Flyby operations will last from 3 months before the flyby to one month after. Parallel to the daily tracking from the two ESA X-band stations with orbit determination and corrections, the flyby payload will be checked out.

Detection of the asteroid by the spacecraft narrow angle camera is expected about 8 days before the flyby. The flyby point is chosen such that the asteroid to sun line is in the relative orbit plane. The nominal flyby distance is ~ 500 km sunward, which is the limit of the turning rate for the viewing instruments mounted on the spacecraft body. The payload will be operated within 500 000 km from the asteroid. The solar array and the high gain antenna will be fixed over a short time interval at the flyby when the steering systems are not capable to follow the spacecraft turning rate. Science data will be stored in memory for later transmission. Immediately after the flyby sun pointing of the arrays and Earth pointing of the high gain antenna will be reacquired. About 1 day later, a major orbit manoeuvre will re-target the spacecraft to the comet. The flyby phase will end with an orbit correction 1 month after the flyby.

Near comet drift (700 days)

The major orbit manoeuvre which puts the spacecraft in rendezvous conditions with the comet except for a residual drift rate (960 m/s ~ 100 m/s) will be performed before comet detection by the spacecraft camera, using ground astrometry knowledge of the comet orbit only, at a sun distance of 4.95 AU and an Earth distance of 5.97 AU for the reference mission. The comet distance will be of the order of 5×10^7 km.

The spacecraft will drift towards the comet. Ground operations will return to the quiet cruise mode, waiting until the spacecraft reaches a sun and a communications distance which allows comet detection operations.

Comet recovery and approach (up to 90 days)

The initial targeting will be to a point 100 000 km from the comet towards the sun, with a relative velocity of ~ 100 m/s.

Approach operations starts at a distance of 500 000 km at which the high resolution camera can be expected to detect the comet. At 300 000 km distance, after about 20 days, the trajectory bias will be moved closer to the comet (30 000 km) and the relative velocity will be reduced to 70 m/s. The approach manoeuvre sequence will reduce the rela-

tive velocity to finally 10 m/s at day 90 from the start of the approach. The final targeting bias at 1000 km distance will be 100 km.

Image processing on the ground will primarily derive S/C comet directions in the inertial reference frame which will improve the spacecraft orbit knowledge relative to the comet, or better the comet ephemeris relative to the spacecraft. A coarse estimation of comet size, shape and kinematics will be performed. The payload will be checked out. Ground operations will use one 30 m X-band station only at a bit rate of 2 kb/s (> 12 hours visibility, one shift operations).

Below 50 cometary radii from the nucleus an estimate of the comet gravity constant and a refinement of shape and kinematics will be derived using optical observations of landmarks on the comet.

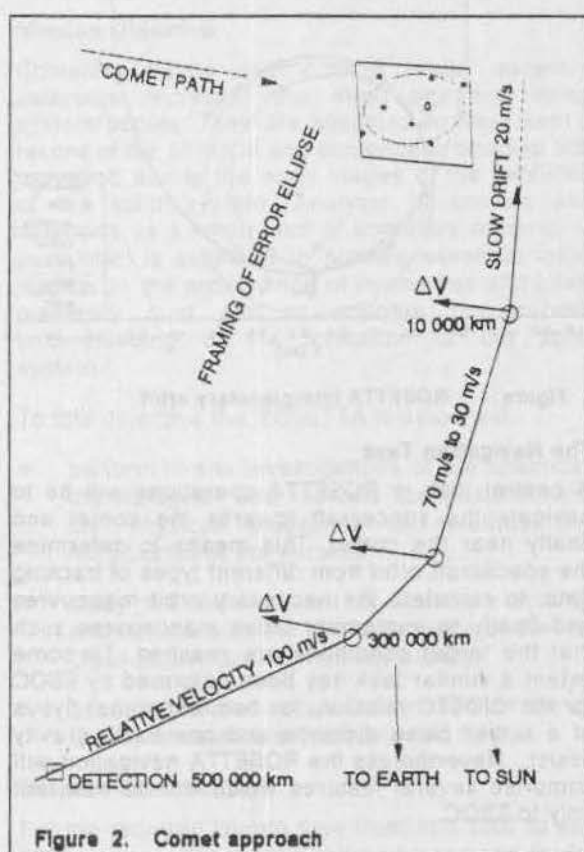


Figure 2. Comet approach

Global mapping (up to 70 days)

The link from the 15 m X-band stations at 1 kb/s is reacquired, the telemetry bitrate from the 30 m station increases to 4 kb/s. Two shift ground operations will commence.

Mapping will be done from eccentric orbits around the comet (5 to 25 comet radii), with orbit parameters depending on comet size and spin properties. Usually the orbit plane will be chosen to contain comet spin axis and the comet sun line. Comet shape and surface properties (physiography, roughness) will be determined, and a detailed

kinematic and gravitational model using optical landmark observations will be derived. Areas on the surface will be selected for close observation.

Close observation (up to 30 days)

Eccentric orbits will be acquired to fly over up to five selected sites at altitudes below 1 nucleus radius. At least two orbit manoeuvres will be necessary per fly-over. The telemetry rate will increase to 8 kb/s from the 30 m station and 2 kb/s from the 15 m stations.

All remote observations payload will be operated above the candidate sites (500m x 500m). A decision will be taken to which site the surface package is delivered. Optical navigation using landmarks will continue.

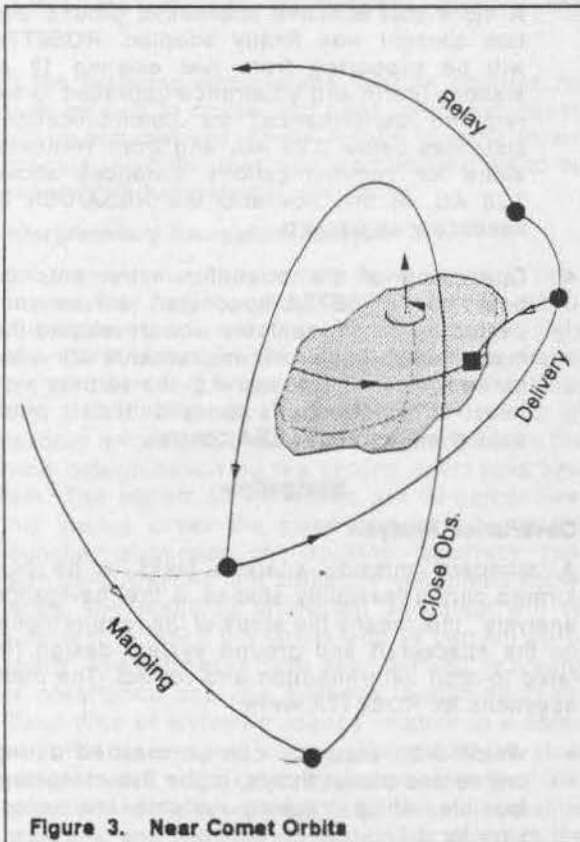


Figure 3. Near Comet Orbits

Surface package delivery and relay (20 days)

The spacecraft will transfer to surface package delivery conditions, typically into an eccentric orbit with a 1 km pericentre altitude passing over the desired delivery site. The time and direction of the surface package separation will be chosen such that the package arrives at the surface with a spin axis orientation along the surface normal and with minimum vertical and horizontal velocity components. A spin eject mechanism will separate the surface package with a relative velocity of 2 m/s. The package will reach the surface without any active control of orbit or attitude and without communications. Damping devices will avoid a re-

bound at impact. After delivering the surface package, the spacecraft is manoeuvred to an orbit which is best suited to receive the data transmitted from the surface package and to relay them to Earth.

Extended monitoring (240 days through perihelion)

After the end of the activities related to the surface package science, the spacecraft will spend at least 8 months in orbit around the comet until after perihelion passage. The science goals of this phase are to monitor the nucleus (in particular active regions), dust and gas jets, and to analyse dust, gas and plasma in the inner coma from the onset to peak activity. Spacecraft orbits will be selected according to these scientific goals and spacecraft safety considerations. Mission planning will therefore depend on the result of previous observations, such as the activity pattern of the comet. The ground support activity will continue with two shifts of operations using two 15 m ground stations.

Spacecraft

The ROSETTA spacecraft design⁴ has been derived from a three-axis stabilised communications bus. The main configuration features, tanks size, solar array mounting and basic structure, of such a 'standard' bus were surprisingly well suited for the deep space mission. To cope with the large variations in sun and Earth distance and pointing directions which the spacecraft has to pass before arriving at the comet and in the orbit around the comet, the ROSETTA spacecraft uses solar arrays with a newly developed type of Low Intensity Low Temperature (LILT) cells with the usual one degree of freedom mounting in two wings. The 2 m high gain antenna dish is mounted on a two degrees of freedom mechanism, all payload and the navigation equipment (cameras, star sensors, gyros, accelerometers) are body fixed. The configuration is shown in Figure 4.

Of particular interest to ground operations is the Data Handling system design in which attention has been given to the necessity of allowing autonomous spacecraft functioning also in cases without active ground intervention for extended periods. The ground activity during these mission phases can be reduced to monitoring of the spacecraft health every two to three weeks and reactivation in case of an autonomous reconfiguration at the occurrence of a failure during the period without contact. Special on board features for reacquisition of ground control after failures will be implemented. For mission periods under ground control the data handling system will provide an On Board Master Schedule function. This means a sequence of commands can be stored on board and sequentially modified and extended, for time tagged execution over time intervals up to 30 days ahead.

The baseline payload to be accommodated on the ROSETTA spacecraft for remote sensing consist of a set of 5 complementary instruments. The two camera systems ('narrow' angle 3.5x3.4° FOV and

wide angle $17.2 \times 17.2^\circ$ FOV) will be used for the scientific observations and for spacecraft navigation in conjunction with a dedicated star and target tracker. Another 7 instruments will be mounted on the surface package which will have to be brought into immediate contact with the comet nucleus.

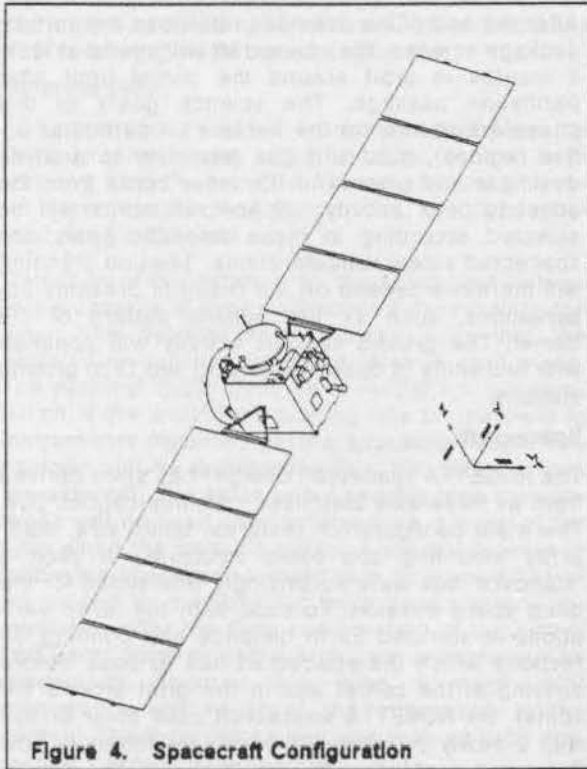


Figure 4. Spacecraft Configuration

Ground Segment Concept

As indicated above the cost of mission operations for the required mission duration of up to 10 years was one of the major concerns during mission and spacecraft design. To obtain a cost effective operations support for ROSETTA the following concepts have been adopted³:

- All ROSETTA Operations will be performed by ESOC according to procedures defined in the *ROSETTA Flight Operations Plan*, a comprehensive document prepared well in advance of mission execution.
- Spacecraft Operations during all mission phases will be 'off line'. The communication turnaround between ground and the ROSETTA spacecraft will be up to 2 hours, real time monitoring and control on the ground is therefore excluded. The spacecraft has to provide the on-board capabilities for monitoring itself and also the necessary reconfiguration and correction logics in case of anomalies. Contacts between the Mission Control Centre (MCC) at ESOC and the spacecraft will not be continuous and will be primarily used for pre-programming of those autonomous operations on the

spacecraft, and for data collection for off line status assessment. Anomalies will normally be detected with a delay.

- Availability of at least two ground stations throughout all critical phases of the ROSETTA mission operations was found to be mandatory, to guarantee the required reliability. Preferably the ground segment should therefore comprise two 30 m ground antennae with complementary coverage. The only station owned by an ESA member state which is currently suited for ROSETTA operations throughout the mission is the 30 m antenna located at Weilheim in Germany. Therefore it was initially intended that ESA would build a 30 m S/X-band station on the hemisphere opposite to Weilheim.

A more cost effective alternative ground station concept was finally adopted. ROSETTA will be supported from two existing 15 m stations (Perth and Villafranca upgraded to the required performance) for communications distances below 3.25 AU, and from Weilheim alone for communications distances above 3.25 AU. In this scenario the NASA/DSN is necessary as backup.

- Operations of the scientific instruments on board the ROSETTA spacecraft will be conducted by the PI institutes who developed the instruments. If scientific instruments are used for operational purposes, e.g. the camera systems for navigation, its operational data processing will be under ESA control.

Navigation

Covariance Analysis

A 'standard' mission analysis tasks to be performed during feasibility studies is the 'navigation analysis', this means the study of the requirements on the spacecraft and ground system design related to orbit determination and control. The main questions for ROSETTA were:

- Which orbit accuracy can be reached during cruise and planet flybys, is the flyby targeting feasible, which tracking systems are necessary for it?
- How much propellant is required to compensate the launcher dispersion and any other stochastic influences on the orbit?
- Which delivery accuracy can be obtained for the surface package, how accurate can the comet kinematic and gravitational model be determined, which data types are necessary for this?
- Which is the influence of spacecraft and ground system performance parameters on orbit determination, propellant allocation and manoeuvre errors (e.g. camera and star sensors resolution and pointing accuracy, thruster

alignment and attitude error, accelerometer error, radiation pressure effects, ground system tracking errors, station coordinates etc.)?

- Which algorithms are necessary in ground and on board software, how does the overall navigation system have to be organised?

A 'standard' method to handle above questions is covariance analysis. For orbit determination the statistical properties of the deviation of the estimated spacecraft state \hat{x} from the real state x have to be derived. For manoeuvres the stochastic deviation of the real state x from some desired or reference state \bar{x} , or better the deviation of the predicted real state from some final reference conditions has to be investigated. The statistical manoeuvre properties, e.g. the propellant estimates, thus depend on statistics of $\hat{x} - x$ and $x - \bar{x}$.

In the following some of the mission analysis results related to cruise and near comet navigation will be summarised. These results to some extent indicate the difficulties and the complexities to be expected in navigational operations.

Interplanetary Navigation Analysis

On the way to the comet several large orbit manoeuvres will be required. In addition, small correction manoeuvres are necessary immediately after Earth departure, before and after the planetary and asteroid flybys and during the interplanetary cruise. Their size and direction depend on random errors and they will be calculated from the orbit determination by the ground operations system. The stated ΔV estimates are 99-percentiles, this means under the given assumptions on the launcher dispersion, the tracking accuracy, random perturbations and planetary ephemeris knowledge, the resulting propellant allocation will be sufficient to reach the target with 99 percent probability. The estimates have been derived by means of covariance analysis methods, assuming linear (fixed time of arrival) guidance relative to a nominal orbit as outlined above. The estimated state variables are augmented by parameters to model coloured noise processes, e.g. due to radiation pressure, and considering systematic errors in the tracking system, e.g. station coordinate and ranging biases. The propellant statistics assumes that for larger corrections the spacecraft main engine is turned into the required direction.

The largest orbit correction will be necessary as soon as possible after launch. The orbit into which the launcher will deliver the spacecraft will deviate from the nominal orbit, this means from the orbit which the launch conditions have been calculated for. This deviation has to be estimated by range and Doppler tracking. The ARIANE 5 launcher dispersion for delayed ignition of the upper stage to reach an escape orbit is not precisely known at the current time, it mainly depends on the per-

formance of the upper stage guidance system. Therefore pessimistic assumptions have been derived from the known dispersions for an injection into geostationary transfer orbit. Under these assumptions an allocation of 40 m/s for the first orbit correction has been made (99-percentile, execution at the latest after 10 days).

Other mission phases which require statistical orbit correction above the 1 m/s level are the planetary gravity assists and the asteroid flybys. In the reference case the Mars flyby is about 2.6 AU from Earth, so the orbit determination accuracy is worse than near Earth. Nevertheless an accuracy of less than 20 km (3σ) can be reached at the flyby pericentre which is at an altitude above 2000 km, such that there is no risk of a Mars encounter. The error in the flyby altitude will introduce an error in the hyperbolic deflection angle. This error will be detected by the Doppler and range tracking after the flyby and has to be corrected as soon as possible.

The Earth flybys are not critical in terms of targeting accuracy, as the ground tracking provides an extremely precise orbit prediction. The orbit correction after the Earth flyby in the reference case requires 12 m/s which is mainly due to the execution error of the large manoeuvre at the flyby (727 m/s).

The navigation process during the planetary flybys is assumed to rely on conventional tracking only. The flyby accuracies could be enhanced by means of optical navigation, this means by using images of Phobos or the Moon with respect to the star background to locate the spacecraft relative to the target planet.

For the reference mission there will be only one asteroid flyby with (1071) Brita. It will be at a sun distance of 2.52 AU, the flyby velocity will be 15.8 km/s and the sun-asteroid-spacecraft (illumination) angle during approach will be 16.7°. These conditions are typical for an asteroid flyby on the final arc from Earth to the comet.

Before the spacecraft camera detects the asteroid, the navigation error, in this case in terms of targeting error at the flyby, will be dominated by the asteroid ephemeris error, which can be reduced by ground astrometry at the best to a few 100 km in position. The spacecraft narrow angle camera (field of view of $3.5 \times 3.5^\circ$) will be able to detect the asteroid when it reaches magnitude 13, more than 8 days before the flyby in the reference case. The observations of the target against the star background will improve the knowledge of the position of the spacecraft relative to the target, and thus the flyby error can be reduced to less than 20 km (3σ) by means of a sequence of correction manoeuvres performed between 5 and 0.2 days before the flyby. Immediately after the flyby at Brita, a manoeuvre of 219 m/s has to be executed to re-target the spacecraft towards the comet.

Near Comet Navigation Analysis

The orbit determination near the comet will be primarily based on observations of natural landmarks on the surface by the wide angle camera. Together with the range and Doppler measurements from Earth, this will allow to simultaneously estimate 19 dynamical state variables, namely to

- spacecraft position and velocity relative to the comet (6), and comet position and velocity relative to the sun (6),
- quaternions to define the axes of the comet nucleus relative to inertial (ecliptic) axes (4), and angular rates of the nucleus in body axes (3).

In addition, for a typical case using five landmarks, there are 19 constants to be estimated, which are equivalent to

- principal gravitational constant of the comet and elements of the inertia matrix (7)
- positional coordinates of the landmarks (12).

The moments of inertia will be related to the third order harmonics of the gravity field. In the simulations higher order terms of the gravity field have been included.

A variety of parametric simulations^{4,5} have been performed for different phases of the near comet sequence, comparing theoretical standard deviations produced by covariance analysis with simulated errors. A wide range of assumptions on the dynamic and kinematic properties of the cometary nucleus, its size and shape and its orientation in space, has been covered and many different assumptions on the available observables (optical and ground tracking) have been simulated. The following mission analysis conclusions could be drawn:

- Starting from approach, excellent improvement of the spacecraft orbit relative to the comet is obtained from the optical measurements.
- The preferred sensor for optical navigation has a field of view of typically $20^\circ \times 20^\circ$ with 1000×1000 pixels.
- The orbit manoeuvres near the comet need to be well calibrated by means of high precision (0.001 g) accelerometers.
- A (predicted) accuracy of 200 m (3σ) in position relative to the centre of gravity of the comet can be reached at the pericentres during the close observation orbits.

Figure 5 shows the spacecraft position error as function of time for a typical overall simulation from approach to close observation.

The statistical properties of the surface package delivery, the relation of tip-off errors, spacecraft

orbit determination errors and errors at impact are currently investigated.

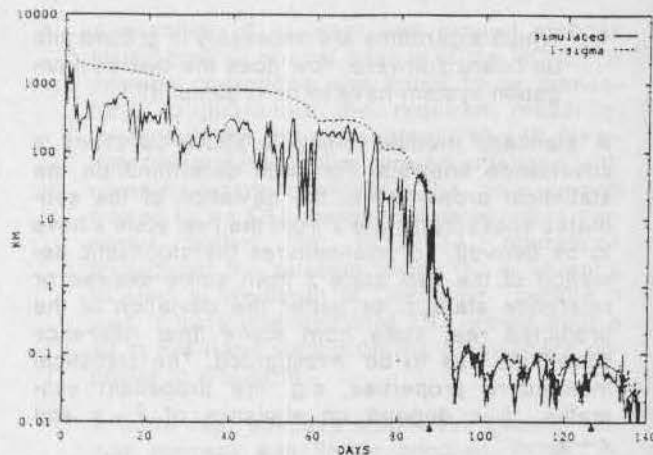


Figure 5. Spacecraft Position Determination from Landmark Tracking: Root-square-sum of the simulated spacecraft relative position error (km, continuous line) versus the error estimate (1σ , dashed line).

An indicator for the difficulties to be expected when designing the operational software was the need to tune the estimation filter utilised in the mission analysis by addition of fictitious noise to avoid divergence, as a function of the simulated case. E.g. for a large fast spinning comet for which the angular momentum is aligned with a principal body axis (no tumbling), the comparison of the simulated data representing the 'true' state displayed that the estimated covariance was not representative for the deviation of the estimated from the simulated state. Mission analysis will conclude that the linearised estimation procedure is not adequate or that there may be observability problems for the dynamical system in some cases. The results obtained by adding the artificial system noise may serve as bounds on the reachable accuracies. Operations will not know a 'true' state to compare with. The estimation must converge in any case. Possibly, different methods must be made ready depending on the phase and the actually prevailing conditions near the comet. These methods can be developed with support of the tools prepared during the mission analysis.

Navigational Operations System

The navigation process during mission execution will consist of all activities related to orbit determination and orbit control. For orbit determination this comprises:

1. Cruise and planet flyby orbit determination from ground tracking
2. Optical navigation during asteroid flybys
3. Approach orbit determination using ground tracking and on-board observables

4. Comet orbit determination from ground astrometry and from on-board observables
5. Near comet orbit determination based on landmark tracking
6. Determination of the kinematic motion of the cometary nucleus
7. Comet gravity field determination, including moments of inertia and the related harmonics
8. Navigational image processing

With respect to manoeuvre calculation the following tasks have to be performed:

9. Mission optimisation for cruise and planet flybys
10. Dynamic re-optimisation of the interplanetary mission schedule
11. Calculation of stochastic deep space orbit corrections
12. Calculation of manoeuvres near planetary flyby pericentres
13. Optimisation of rendezvous manoeuvre and near comet drift
14. Comet approach manoeuvre scheduling
15. Mapping strategy and optimisation of transfer to mapping
16. Orbit strategy for close observations
17. Surface package delivery strategy, acquisition of delivery corridor and separation attitude

Other tasks in which the navigation team has to participate are:

18. Preparation of auxiliary data for payload, e.g. for camera pointing, S/C pointing
19. On-board software maintenance for near comet contingency orbit and attitude maintenance software algorithms

None of above tasks is completely identical to work previously performed e.g. for GIOTTO. The areas which will require most new (software) development are the manoeuvre strategies and the orbit determination using landmark observables near the comet. Mission analysis and spacecraft system studies have spent considerable effort on these subjects because they were found to be critical for the feasibility of the mission, but this may be of limited usefulness for the preparation of the operational software.

Summary: The ROSETTA Navigation Challenge

The navigation work performed during the feasibility studies up to now was dedicated to prove the feasibility of the mission and in particular to support the spacecraft design by deriving the major

requirements on propulsion and tracking systems. To consider the concepts of the ground operations system was a secondary objective. The complexity of the ROSETTA navigation system is beyond that of similar tasks done before, like the GIOTTO navigation. To perform cost effective operations and to develop the necessary ground infrastructure in a cost effective manner will be a particular challenge for ESOC.

The ROSETTA development schedule gives the chance to bridge the gap from mission analysis studies to the design of the operational navigation system. Therefore a study has been initiated to cover the near comet orbit strategy and navigation aspects beyond conventional mission analysis, namely

- perform a detailed analysis of the related algorithms,
- complete the navigation concepts for a wide range of cases (contingencies etc.),
- document the algorithms in a form which allows transfer into the operational software.

The study will concentrate on the concepts, it will not comprise much model refinements. E.g. it must be clear beforehand which estimation method can successfully be used in operations, without any danger of failure or divergence. The gravity and kinematic models for which this method is studied need not cover all details which are necessary in the operations.

Based on the output prepared by this study a better definition of the related critical operational software should be possible, and this should improve the development schedule. The next three years should be used to extend the 'data base of ideas' on how to perform the near comet navigation. Any input will be welcome.

References

1. Horizon 2000, ESA SP-1070, Dec. 1984
2. ROSETTA Comet Rendezvous Mission, ESA SP-1165, Jan. 1994
3. M. Hechler, ROSETTA Mission Assumptions Document - Issue 1, Operations and Ground Segment Concept, ROS-MAD-004, 93-07-21, ESOC/MOD/MAS
4. M. Noton, Orbit Strategies and Navigation Near a Comet, ESA Journal, Vol 16/3, 1992, pp. 349-362
5. E. Gonzalez-Laguna, ROSETTA Navigation Near a Comet, MAS Working Paper No. 344, Sept. 1993, ESOC
6. ROSETTA System Definition Study Rider 2, Matra Marconi Space, Contract Report CNSR/FF/128.93, August 1993

EXPERIENCE OF EIGHT GEOSTATIONARY SATELLITE POSITIONINGS

Geneviève CAMPAN

Pascal BROUSSE

CNES, Toulouse, France

Abstract

Between October 1990 and August 1993, CNES has been involved in several geostationary Launch and Early Operations Phases (LEOP) of telecommunication satellites among which eight were based on the EUROSTAR platform: INMARSAT-2 F1, F2, F3 and F4, TELECOM 2A and 2B, HISPASAT 1A and 1B.

During these operations, successfully performed in 34 months, the Flight Dynamics Center (FDC) faced various situations including:

- two different kinds of geostationary transfer orbits delivered by ARIANE IV and DELTA II launchers,
- different ground station networks: INTELSAT C-band network for INMARSAT-2 and CNES and NASA S-band networks for TELECOM 2 and HISPASAT, and the customer specific stations for the end of LEOP,
- simultaneous LEOP of two satellites: INMARSAT-2 F3 / TELECOM 2A (Ariane V48) and INMARSAT-2 F4 / TELECOM 2B (Ariane V50),
- duplication of the FDC in Madrid to perform LEOP on customer's premises for HISPASAT LEOP,
- different spacecraft launch masses from 1,2 tonnes up to 2,2 tonnes,
- different LEOP durations from 6 days to 2 months,
- different attitude determination accuracy requirements,
- contingency cases.

After a brief description of each mission, this paper will give an analysis of the space dynamics results in the fields of:

- the orbit determination showing the impact of different networks and the maximal exploitation of the available measurements in particular for the maneuver diagnosis,

- the attitude determination for which a large set of software was developed allowing a maximum coverage of contingency cases,

- the computation, monitoring and calibration of attitude and orbit maneuvers. For the apogee maneuvers, original methods were fit, as well as a computer interface between the operation manager who prepares the operational documentation like flight plan or timeline and the flight dynamics activities allowing an almost automatic preparation of Flight Plan.

This paper will also examine the lessons learned in areas such as operational preparation and organisation and will suggest improvements for the two upcoming missions TELECOM 2C and 2D, also based on EUROSTAR platform or for other similar missions.

Moreover, all the experience acquired during these eight LEOP allowed us to tune our software, to develop our engineer's know-how. This know-how and the numerous methods and software developed in CNES FDC were or will be also used for others LEOP as ARABSAT1C or TURKSAT LEOP. In addition, during all these LEOP the operational system and now the mission analysis system were based on the MERCATOR data processing system which by its redundancy, its modularity and its flexibility allows to a team of only four engineers to handle the space mechanics aspect of a complete geostationary positioning from injection in transfer orbit to the final manoeuvres in the station keeping window.

1. Introduction

Since 1974, CNES, the french national space agency, has been involved in seventeen geostationary launch and early operations phases (LEOP) of moving satellites from a transfer orbit delivered by a launcher to a geostationary point.

For these operations and their preparation the Flight Dynamics Center (FDC), part of CNES LEOP facilities is in charge of all the space mechanics aspects.

Among these spacecrafts positioned by CNES, between October 1990 and August 1993, eight were based on the same Satcom International EUROSTAR bus designed and built by Matra Marconi Space and British Aerospace.

Even if the platform is the main guide of the operations every time some particularities either in the mission on the orbit delivered by the launcher or even the spacecraft prevent to have a complete reproductibility in terms of operations and also methods and software.

After a brief description of each project, highlighting their specific points with regard to a general mission, this paper shows the CNES solution to achieve its mission as efficiently as possible, the solutions are expressed in terms of processing and also flight dynamics point of view.

To conclude some main operational results are presented and ideas of improvement (in progress or to be done) are suggested.

2. Spacecraft and missions

2.1. EUROSTAR platform description

Two EUROSTAR platform configurations exist

- the EUROSTAR 2000 for satellites around 2000 kg launch mass and the EUROSTAR 1000 for smaller satellites.

The main EUROSTAR characteristics that influence mission analysis and space mechanics calculations are the following:

- Combined propulsion system: the propulsion system used for apogee maneuvers, attitude and orbit control is a combined propulsion system (CPS), that is to say a 500 Newton apogee engine and six pairs of 10 Newton thrusters fed by the same tanks.
- Spin stabilization: during the transfer orbits, a 13 rpm spin rate is maintained, providing the satellite a passive stability particularly during the apogee firings. During the transfer phase it is then necessary to determine the orientation of the angular momentum with regard to an inertial reference frame while taking into account the wobble angle.
- Three axis stabilization on station: after the last apogee firing, the satellite attitude is established in its normal three axis configuration with the communication antenna directed towards the earth.
- Five types of sensors:
 - the Earth and Sun Sensor (ESS) is used only during transfer orbit to perform attitude determination with

two slits detecting the sun and two infra-red earth sensors detecting the earth,

- two Sun Acquisition Sensors (SAS) are used during sun acquisition between transfer mode and station-keeping mode,
- two redundant IRES used only during earth acquisition and station keeping,
- two redundant gyroscopes giving information on yaw angle and yaw speed during station keeping maneuvers,
- two Solar Arrays Sun Sensor (SASS) positioned on north and south solar arrays and used for the orientation of the solar panels.

2.2. Mission description

Even though the platforms are identical the missions INMARSAT2, TELECOM2 and HISPASAT are different.

INMARSAT2 mission:

The space segment of the INMARSAT2 system is composed of four identical telecommunication satellites (INMARSAT2, F1, F2, F3, F4) built by British Aerospace as main contractor and provides mobile communications world wide (sea, air and land).

INMARSAT2 F1 launched on October 30, 1990 was the first satellite to use the Eurostar platform.

A unique element of the Inmarsat mission is that the targeted orbit was an inclined orbit (with a maximum of inclination of 2.7 deg). Each of the four satellites had to reach a specific window of ± 1 deg in longitude with only 159 hours in sun phase.

The requirement in attitude determination was very strict 0.8 deg (3σ) what needed sound work on the subject (to analyse and to take into account the wobble angle, to analyse the impact of the moon presence in ESS sensor).

The two first satellites INMARSAT2 F1 and F2 were launched by DELTA II. The DELTA II dispersions on the semi major axis and on the argument of perigee were announced so large (± 1600 km (3σ) on the semi-major axis and $\pm 1^\circ$ (3σ) on the argument of perigee) that the apogee manoeuvre strategy had to be computed in real time taking into account the actual orbit at injection.

An interface between the operation manager who prepares the operational documentation and the flight dynamic center has been then developed to supply almost automatically the flight plan. This interface has been used again for the INMARSAT2 F3 and F4 launches to save time in the operation preparations.

An other INMARSAT2 LEOP innovation was to use a new station network. Indeed INMARSAT2 LEOPs were performed with INTELSAT and INMARSAT networks in the 6-4 GHz C-band instead of the 2 GHz CNES network usually used.

TELECOM2 mission:

TELECOM2 is a French satellite system composed of four identical satellites built by Matra Marconi Space as main contractor and used for direct TV broadcasting, telephone and military transmissions.

TELECOM 2A and TELECOM 2B were launched by Ariane on the same flights as respectively INMARSAT2 F3 and INMARSAT2 F4.

TELECOM 2C launch is scheduled in 1995 and TELECOM 2D launch around 1997.

For both dual launches two FDCs were installed, one for TELECOM2 and one for INMARSAT2 with the same configuration. For TELECOM2 the network used was the 2 GHz CNES network [ref 6].

Due to different launch window constraints and different target orbits, (TELECOM2 had to reach a very small inclination (less than 0.05 degree) and a longitude window of ± 0.08 deg), the INMARSAT2 and TELECOM2 FDC team worked together to determine the best common launch window.

HISPASAT Mission:

HISPASAT is a Spanish space system, built by Matra Marconi Space as main contractor and composed of two telecommunication satellites located in the same window. HISPASAT 1A was launched by Ariane 4 on September 1992 and HISPASAT 1B on August 1993.

On the one hand the positioning mission of HISPASAT was significant because all the LEOP operations were performed in Madrid Spain, using HISPASAT Satellite Control Center, and the FDC was duplicated and integrated with other Spanish entities.

On the other hand the HISPASAT LEOP used the same 2 GHz network and almost the same manoeuvre strategy as TELECOM2 mission (the most different parameter being the targetted station longitude).

3. The FDC

The FDC is the operational entity in charge of all space mechanics aspects. The work of the corresponding team starts at the beginning of the project by issuing the flight dynamics mission analysis to prove the feasibility of the positioning in 99,73% (3σ) of the cases of

dispersions while fulfilling the satellite and mission constraints and minimizing the propellant consumption, then before operations FDC team technically prepares the FDC with all the software necessary to safely perform operational computations. The last phase corresponds to the operations themselves.

For all these phases a team of four engineers is progressively formed with one or two people at the beginning of the project up to four for the operations. Depending on the phase and the work to do the working time is either partially dedicated to a mission or completely dedicated.

To succeed with such a limited team, a policy at used tools level is imperative and in CNES FDC it was emphasized in two main fields:

- Mercator software package,
- Flight dynamics methods and software.

3.1. Mercator software package

Mercator means M^Ethod and R^Ealization for the C^Ontrol of the A^Ttitude and the O^Rbit of spacecraft. It is a data processing system used by the Flight Dynamics Center (see reference 1 to 4).

It is in fact a flight dynamics support system, i.e. a software structure providing:

- elementary functions (general communication facilities for external data interfaces, data preprocessing, system monitoring, time synchronisation, interactive displays, edition, ...),
- shells and state of the art man machine interface for implantation, modification and implementation of applications, software (chaining functions, filters on data, deferred time executions, ...).

It allows the flight dynamics engineer using it to concentrate his work on the space mechanics software offering him various analysis tools:

- real time or batch mode data processing,
- synchronization of space mechanics modules,
- dynamic displays and plots,
- powerful control of input data and results.

By a real time acquisition and first preprocessing, of data coming from stations (and storage). Mercator also allows any workstation connected to the FDC network to have access to the data and to use them with the Mercator mechanisms. The choice of the data origin machine is done by MMI when opening the Mercator application and can be very easily change at any time (2 UNIX commands).

So with the above description it is easily seen that for a given mission the flight dynamics engineers have a lot of capabilities to prepare and perform their tasks whatever the phases are.

With a positioning schedule such as described at the beginning, the multimission aspects were also primordial for two reasons:

- the adaptation time from one mission to another one has to be as short as possible,
- the missions follow each other implying a preparation in parallel on the same computer.

To meet these both constraints an architecture was designed allowing:

- to quickly configure Mercator software for a mission,
- to change or adapt the flight mechanics software very easily,
- to have the capability to prepare several missions in parallel.

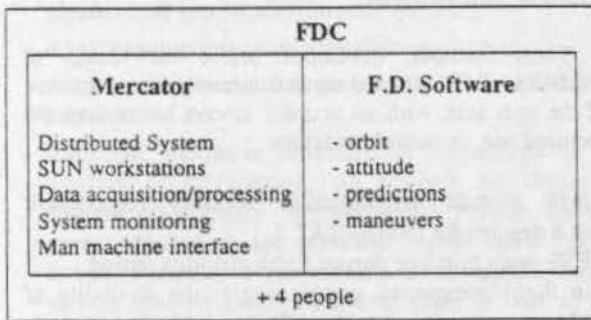


Figure 1 : FDC

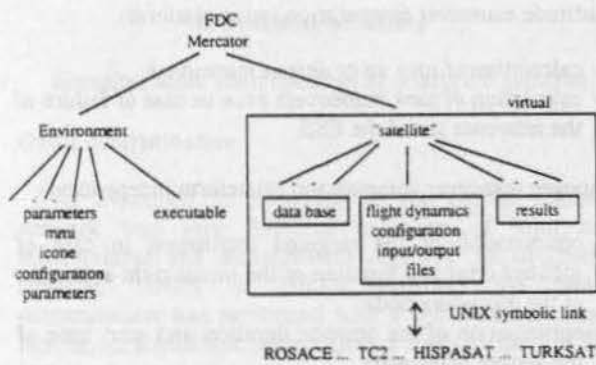


Figure 2 : Mercator directory hierarchy

This architecture is graphically represented as figure 2. Each level corresponds to a directory or subdirectory with UNIX meaning.

The "environment" branch is the less variable of the system.

It corresponds to Mercator software with its executable codes and its configuration parameters (man machine interface, icone, data interfaces).

The major changes in this part would be the addition of a new ground station network or the addition of a new protocol for data acquisition. At the time being Mercator can process data acquired with HDLC protocol and asynchronous RS232 transmissions, and process data from CNES 2 GHz, NASA, Intelsat, Telesat, INMARSAT, Arabsat, Turksat ground stations network.

Nota: The telemetry processing is quite generic and defined later in the satellite part.

Such modifications were not necessary for the eight concerned positionings and consequently this part was exactly the same.

The "satellite" branch is the heart of the system. All the "data" corresponding to the mission are gathered in it.

Three main groups compose this set: data base, executable codes, results.

The data base is defined in different files (ASCII files):

- spacecraft technological file,
- decommutation table or plan to extract binary values from the telemetry flow. With an adequate parameter several telemetry formats are processed without code modification,
- telemetry transfer functions to convert binary values into physical values,
- ground stations file,
- state file living with the mission, representing the state of the satellite at a given time (orbit, attitude ...). All its data are computed by some applications and used by others one. This file is organized so as to preserve the historical record of the positioning.

The executable directory corresponds to the set of flight dynamics software necessary for the mission devoted to the FDC.

For each, some input and output configuration files (ASCII files) allow to interface Mercator and the flight dynamics software.

The "result" directory corresponds to files got after processing by a software: either Mercator after data

acquisition and preprocessing or flight mechanics software. All these files are also text files.

The link between Mercator and the "satellite" to process is done by a UNIX symbolic link. Each "satellite" is completely defined in a directory which always has the same structure. Hence it is possible to have on the same machine several mission in parallel.

This can be improved by using UNIX environment variables allowing to remove the fixed structure constraint. To summarize:

- the change from a mission to an other is obviously done by adaptations of flight dynamics software and by only text file modification which is a great advantage (readability, flexibility),
- due to architecture several missions can be prepared in parallel,
- a flight dynamics center is easily portable since with
 - o 1 magnetic tape for Mercator,
 - o 1 magnetic tape for application
 - o or 1 magnetic tape for bothflight dynamics center can be implanted and carried out on any Sun workstations: it was already operationally done for HISPASAT LEOP (see Ref. 5), and for demonstrations (see Ref. 4).

3.2. Flight dynamics software

These software are used to compute all flight dynamics aspects, even in contingency cases.

Some of them are Eurostar specific software that is to say that they have been developed taking into account platform particularities, some of them are platform independent and can be used for any other kind of satellite.

Only few software are satellite specific software, they have been developed to achieve a specific mission problem or requirement.

The software are organized in different groups. Each groups of software, described herebelow, support a basic tasks during the LEOP:

orbit determination (platform independent):

- pre-processing and processing of localization data.
- phase coherence control for INTELSAT ranging measurements,
- least square filter and Kalman filter for real-time orbit determination,
- residues processing after or before orbit calculation,
- orbit extrapolation;

operational predictions (platform independent):

- prediction of apside time,
- prediction of visibilities,
- prediction of eclipses by the moon or by the earth,
- prediction of sensor events (from one platform to another the sensor definition must be updated);

attitude determination (Eurostar specific but this piece of software can be used for any satellite equipped with an Earth Sun Sensor):

Two different methods are used:

- attitude determination taking into account a differential correction of the wobble angle. This method, used in real time to monitor the spacecraft attitude, gives good results but only when wobble angle is lower than 5 degrees,
- the second method based on analytical equation formulation is used in contingency case for high value of the wobble angle.

Statistical tools are also implemented to analyze the results of both methods.

These methods, developed before the launch of INMARSAT F1, allowed us to determine the orientation of the spin axis, with an accuracy always better than the required one, in various situation:

- high attitude determination accuracy requirement (0.8 deg 3σ) for INMARSAT 2,
- ESS moon blinding during Earth visibility period,
- in flight unexpected wobble angle: the flexibility of Mercator system and the efficiency of the methods enabled us to verify and sometimes correct the wobble angle during the operations.

attitude maneuver computation (spun platform):

- calculation of spin up or despin maneuvers,
- calculation of slew maneuvers even in case of failure of the reference slit of the ESS,

apogee maneuver computation (platform independent):

- optimization of the targeted inclination in case of inclined orbit as a function of the initial right ascension of the ascending node,
- optimization of the attitude duration and start time of the apogee maneuvers.

The optimization method used is based on the Simplified Nodal Transfer (SNT) [ref 7]. The SNT was well fitted to secure the maneuver strategy before the operations through Monte Carlo Simulation and to automate the

AEF strategy determination during the operation whatever the satellite mission was:

- INMARSAT mission that targeted an inclined drift orbit ($2,7^\circ$) in order to extend the lifetime,
- TELECOM2 and HISPASAT missions that targeted a very small window of ± 0.05 deg in inclination and ± 0.08 deg in longitude,
- simulation of apogee maneuvers,
- calibration of apogee maneuvers by comparison of orbits before and after the maneuver ;

station-keeping maneuver computation (platform independent):

- calculation and simulation of inclination, semi-major axis, eccentricity and longitude maneuver,
- geosynchronous orbit prediction with semi-analytical evolution model,

and various software,

- analysis of Ariane telemetry (platform independent),
- satellite technological parameter monitoring on request of spacecraft specialists (Eurostar specific),
- mass consumption calculation (Eurostar specific),
- thruster characteristic calculation as a function of tanks pressure,
- spacecraft mechanic characteristic calculation as a function of fill fraction. As example for Hispasat mission 60 software (around 60000 Fortran source lines) installed in the Mercator system allow flight dynamics experts to use within a short response time, various analysis tools in nominal cases as well as in degraded cases.

4. Operational results

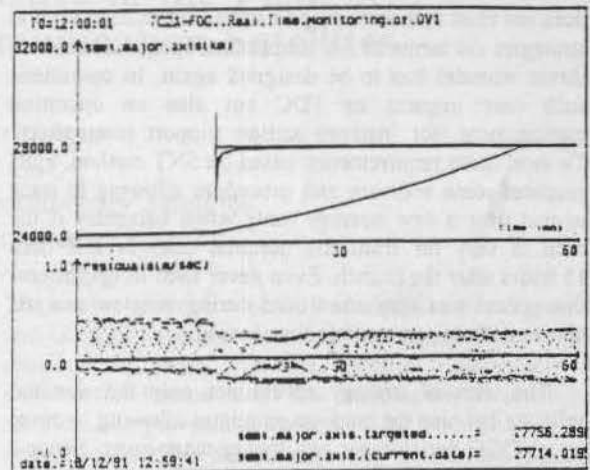
Hereafter some main operational results are gathered.

Orbit determination

As explained in paragraph 2, the ground station network was very different in terms of kind of measurement and measurement accuracy. In all cases (Intelsat, CNES or NASA network) the orbit determination was performed with a sufficient accuracy having no significant impact (less 1 m/s) on the LEOP cost.

However in some cases the available data allowed to monitor (with orbit point of view) the apogee maneuver with a good accuracy. These diagnosis are very useful in operations.

An example of Telecom 2A first apogee manoeuvre is given in the following figure.



Continuous doppler measurements from the different stations were available.

This monitoring enables us to follow the progress of the orbital parameters during any orbit maneuver when the measurements are available.

The accuracy reached a few minutes after the maneuver is of a few kilometers on the semi major axis what is a great positive point in the operations management increasing their reliability by a quicker reaction to a new situation.

Attitude determination

For the spun satellites, the most delicate point in attitude determination concerns the wobble angle impact. According to the phases and the geometrical configuration it is more or less important on the right ascension or declination.

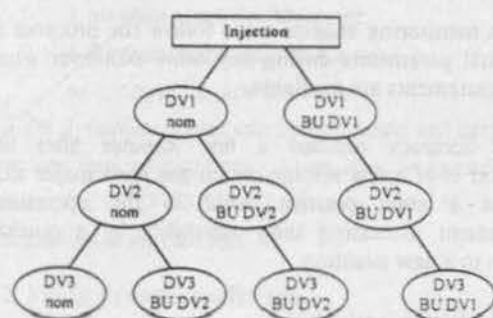
The attitude group set in the CNES FDC includes 10 software covering nominal and contingency cases. Among the eight LEOP and more than 30 attitude determinations the obtained accuracy was always less than 0.5 deg which is totally compliant with the specification. These results show the well founded method but also the good prediction of the wobble angle versus the satellite mass. An other important consequence of such accuracy is the fuel saving with regard to the worst case fuel budget.

Orbit maneuver

For the orbit maneuver aspects, the INMARSAT2 heritage was very strong. Indeed in case of Delta II launcher, the semi major axis dispersion may be large (see paragraph 2). Beyond the cost problem, these dispersions induce difficulties in the operation preparation. Indeed the mission analysis has to prove the

mission feasibility in 3σ cases of dispersions. However when the dispersions are so large one unique solution does not exist and according to actual dispersions several strategies (in terms of ΔV amplitude, apogee number or thrust attitude) has to be designed again. In operations such case impacts on FDC but also on operation management (for instance station support reservation). To meet these requirements, based on SNT method, FDC prepares some software and procedure allowing to issue in real time a new strategy (only when necessary if the orbit is very far from the nominal one) in less than 15 hours after the launch. Even never used in operations, this system was very often used during mission analysis phases with an appreciable time saving.

The term of strategy covers not only the nominal splitting but also the back-up strategies allowing to cover up a NOGO decision per any apogee manoeuvre. Hence a strategy in 3 main thrusts with its back-up solutions is relatively complex to search. It can be represented by a tree.



Conclusion

The eight Satcom platforms positioning missions were very successful. From the space mechanics point of view this was due to the correct design and behaviour of the Eurostar platform, the quality of the flight dynamics software, the flexibility and simplicity of the Mercator system.

Originally designed to perform FDC space mechanics tasks related to geostationary positioning Mercator has already been extended to other applications:

- TOPEX/DORIS on board orbit determination simulation,
 - MEPHISTO experiment, part of United States Microgravity Payload (USME),
 - mission analysis purposes,
- and is going to be extended in the next future to:
- low earth orbit satellites and mini satellites ground segments,
 - any space mechanics center...

For this purpose some improvements are already studied to automate repetitive tasks such as regular orbit determination and operational predictions (geometric and radiofrequency station visibilities sensors visibilities, solar eclipses by the earth or the moon). Moreover Mercator is going to be compatible with the new UNIX Operating System Solaris 2X and other kinds of workstation (HP9000 and IBM Rix 6000).

From flight dynamics point of view there are now studies to develop a modular software package as flexible as possible even in the field of the orbit maneuver computation and optimization to face any type of transfer on orbital maneuvers. All these modules will be written using all the capabilities of the new processing language C++. For the orbit determination the objective of the software and methods improvements is to enable us to perform orbit diagnosis after launcher separation or orbital maneuvers with less measurements than today.

References

- [1] MERCATOR, a new ground system for orbit and attitude control - B. Belon, J.C. Berges, G. Campan, P. Legendre - Second International Symposium on Spacecraft Flight Dynamics - 20-23 Oct. 1983.
- [2] MERCATOR, a distributed ground control system for geostationary satellite positioning - H. Secretan, P. Vielcanet - ESA, International Symposium, Ground Data Systems for spacecraft control - June 90.
- [3] Mise à poste INMARSAT 2/F1 - G. Campan - IVth European Aerospace Conference EAC 91, Paris, France.
- [4] MERCATOR: Methods and realization for Control of the Attitude and the Orbit of spacecraft - G. Tavernier, G. Campan - Space Gps 1992, JPL, Pasadena, USA.
- [5] Hispasat Launch and Early Operations Phases Computation and monitoring of geostationary satellite positioning - P. Brousse, A. Desprairies - Space Ops 1992, JPL, Pasadena, USA.
- [6] Launch and early operations phase for the dual launch of Telecom 2A and INMARSAT 2 F3 - B. Lazard - IAF 43 rd - 1992, Washington, USA.
- [7] Apogee maneuver strategies for the INMARSAT 2 spacecraft - E. Cazala-Hourcade - AIAA, Astrodynamics, 1991, Durango, Colorado, USA.

DLR/GSOC Experience in the Field of Geostationary Communication Satellites

Peter Brittinger

DLR / GSOC

Project Manager Geostationary Satellites
82230 Oberpfaffenhofen - Germany

Abstract

During the past 25 years the DLR-German Space Operations Center (GSOC) has operated an extensive variety of satellites. In particular, GSOC has specialized in the positioning and operation of Geostationary Communication Satellites and has successfully delivered and maneuvered eleven geostationary satellites to their on-station positions.

This paper discusses GSOC's operational activities and focusses on the following major topics:

1. The role of GSOC within the DLR and its responsibilities in the preparation and execution of national and international spaceflight projects.
2. The current track record in the field of communication satellites discussing the specific features of the different missions and the special requirements that these missions put on the ground segment facilities and staff.
3. Experience accumulated during successive missions has resulted in a generic approach to the procedures and methodologies used for positioning of Geostationary satellites. Starting with SYMPHONIE A, GSOC has continuously and systematically reviewed and updated the operational methods from project to project. The paper shows how the GSOC operations concept can be used in this generic fashion.

The remit of the GSOC

The German Aerospace Research Establishment (Deutsche Forschungsanstalt fuer Luft- und Raumfahrt - DLR) is the Federal Republic of Germany's largest research institution for the engineering sciences and employs over 4.000 people at six Research Centers.

Situated on the DLR site at Oberpfaffenhofen near Munich, the German Space Operations Center (GSOC) has over the past 25 years provided services for the operation and support of a wide variety of space missions. Currently the GSOC is responsible for the German National space programme and in addition supports both ESA and NASA activities.

The current generation of DLR spacecraft control systems and facilities have been developed and maintained over the previous 10 years with the specific requirements of multimission functionality. The implementation which has resulted, has proven the strategy to be both flexible and cost effective. This has subsequently enabled the DLR to use essentially the same software, systems and facilities to support a wide variety of spacecraft including manned missions, scientific missions and telecommunications spacecraft both in LEOP and routine mission phases.

The experience available through the GSOC is reflected in the wide variety of space missions which have been supported since its establishment and include:

- Geostationary Satellites (SYMPHONIE, TV-SAT, DFS & EUTELSAT II);
- Interplanetary Missions (HELIOS, GALILEO);
- Earth-Orbiting Scientific Missions (AZUR, AEROS, AMPTE, ROSAT);
- Manned Spaceflight Missions (FSLP, SPACELAB D1 and D2, COLUMBUS);
- Ground Station Support (e.g. GIOTTO, EUMETSAT);
- Sounding rocket programs (ARIES, TEXUS, MAXUS).

Currently the GSOC operates eight control rooms at the Oberpfaffenhofen site. This includes the original facilities and a new complex equipped with modern facilities. To date this new facility has been used successfully for the D2 mission in May 1993. The new complex will also be available and utilised for un-manned projects, i.e. conducting LEOPs, routine operations and for the support of scientific missions.

At the DLR ground station in Weilheim the GSOC also operates two 15 meter S-Band Antennas and one 30 meter X-Band Antenna. In 1996 the facilities will be enhanced by the addition of a Ku-Band Antenna.

Communication Satellite Track Record

GSOC has specialized in the positioning and operation of geostationary communication satellites and has successfully positioned eleven satellites on station since 1974. GSOC has been involved in Communications Satellite Operations since the beginning of European efforts in this area, beginning with the German-French SYMPHONIE Programme.

Between 1987 and 1993 GSOC was awarded various contracts to position satellites in geostationary orbit, to perform early operations, routine operations and also to support so called "Hot Standby"-operation phases. The individual LEOPs (Launch and Early Orbit Phase) are described below, with short explanations of the project specific characteristics.

- **SYMPHONIE A, Launch 19.12.74 on DELTA**
SYMPHONIE B, Launch 27.08.75 on DELTA

Following the launch, GSOC was responsible for the operations required to place the satellite at its dedicated position in the geostationary orbit. For the first time in Europe, procedures for positioning a 3-axis stabilized geostationary satellite with optimized fuel consumption for routine operations and station-keeping were developed and successfully implemented. The on-station operation was executed by time and work sharing with CNES over a period of 10 years (the Satellite's designed lifetime was 5 years). Another significant first for these missions was the fact that SYMPHONIE A/B were the first geostationary communication satellites to be brought into the so called "graveyard orbit" by use of the remaining fuel.

- **TV-SAT 1, Launch 21.11.87 on ARIANE 2**

After the positioning phase was successfully completed the problems with the deployment of the solar panel prevented the operating ability of the Ku-Band TX-antenna and subsequently any routine spacecraft operation in Ku-Band. Extensive tests and error analysis was performed. The complexity and size of the actual program undertaken was possible only because of GSOC's existing engineering know how, the flexibility of the equipment used, and the ability to undertake quick software- and configuration changes. At the beginning of March 1989, when the test phase was terminated the TV-SAT I was moved into a safety orbit ("Graveyard"), 340 km above the geosynchronous orbit.

- **DFS-1 Kopernikus, Launch 5.6.89 on ARIANE 44L**

Successful positioning of the satellite by means of the classical 3-impulse method into its planned position of 23.5°E. After termination of the in-orbit tests GSOC was responsible for all satellite operations (routine and other). In August 1990 the operational responsibility for DFS-1 was transferred from GSOC to the Deutsche

Bundespost TELEKOM Control Center at Usingen in August 1990. For an additional three months the GSOC operations team remained in so-called "Hot Standby", i.e. being capable at any time to take over the operation if necessary.

- **TV-SAT 2, Launch 8.8.89 on ARIANE 44L**

Utilizing experienced operation planning and optimized procedures, the satellite was placed into its planned position within a record time of 11 days. The operational responsibility for routine operation was transferred stepwise up to mid of 1990 to the Deutsche Bundespost TELEKOM.

- **DFS-2 Kopernikus, Launch 24.7.90 on ARIANE 44L**

This satellite was positioned in its geostationary location and made available to the TELEKOM for telecommunication operations within record time. GSOC was responsible for routine satellite operation until March 1991.

- **EUTELSAT II-F1, Launch 30.8.90 on ARIANE 44LP**

The high level of EUTELSAT standard requirements were met utilizing a positioning procedure especially developed by DLR/GSOC. The mission operations experience gained from earlier positioning activities (SYMPHONIE, TV-SAT and DFS) were used effectively. The satellite was positioned within the shortest possible time, and additionally, due to specially developed optimizing programmes, the fuel consumption could be minimized, thus extending the operational life time of the satellite. 17 days after launch the EUTELSAT II-F1 satellite was handed over to the EUTELSAT Satellite Control Center in Paris for utilization. For a further 4 weeks GSOC was available for "Hot Standby" operations.

- **EUTELSAT II-F2, Launch 15.1.91 on ARIANE 44L**

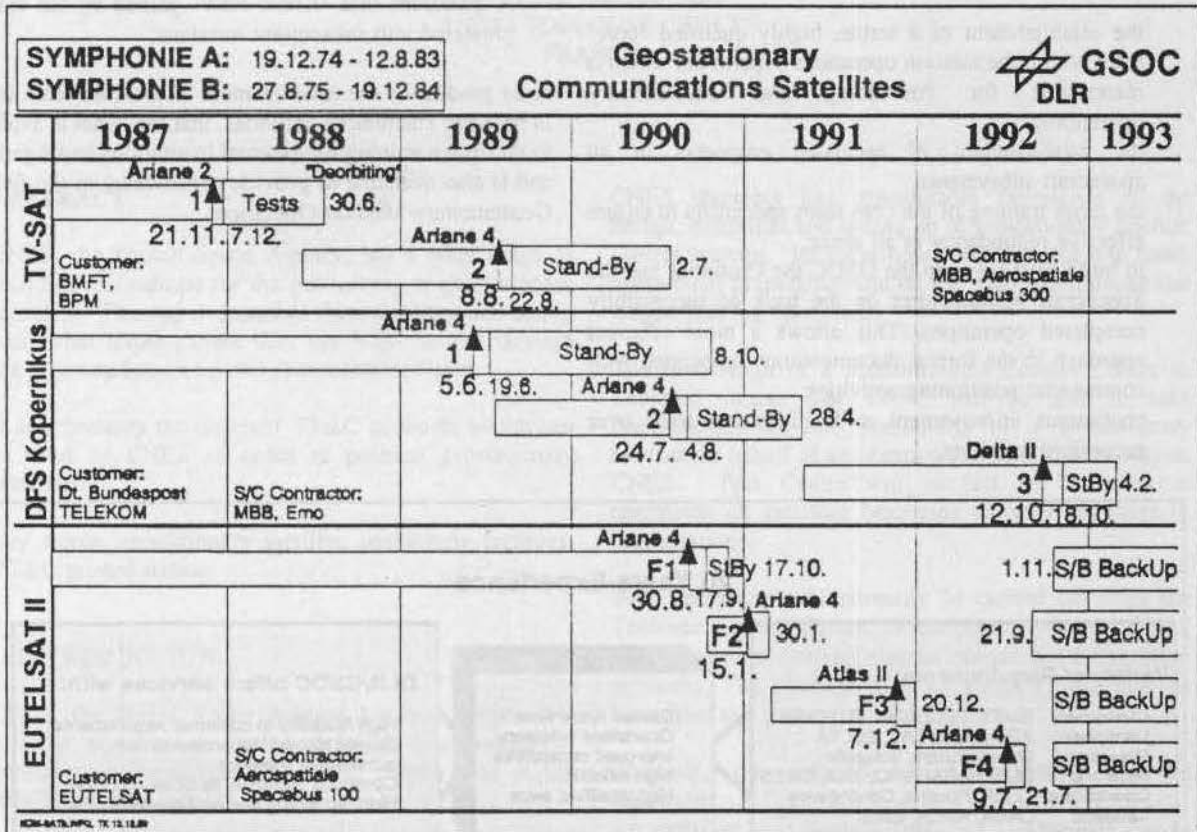
During the "Station Acquisition Phase" of the positioning of EUTELSAT II-F2, new strategies and maneuvers were performed (using specially developed colocation software) in which the satellite flies around the operational control boxes of other geostationary satellites to avoid collisions.

- **EUTELSAT II-F3, Launch 7.12.91 on ATLAS II**

The launch of EUTELSAT II-F3 using an ATLAS II rocket meant a new challenge for GSOC. The satellite was launched into an orbit outside the geostationary orbit (42.000 km). An additional perigee orbit maneuver was necessary, and was performed for the first time. The development of new operational procedures and the continuous development of the maneuver software allowed the GSOC operations team to meet the customer's request to position the satellite within two weeks.

- EUTELSAT II-F4, Launch 9.7.92 on ARIANE 44L After normal routine positioning the satellite was handed over to the EUTELSAT Satellite Control Center in Paris after 11 days.

- DFS-3 Kopernikus, Launch 12.10.92 on DELTA II The Launch of this satellite with a DELTA II Rocket symbolized another new mission profile when compared with the launch orbits of ARIANE and ATLAS. Further development of existing maneuver strategies allowed a fast maneuver sequence which enabled GSOC to position the satellite in the record time of only 6 days.



To summarize the activities performed by the DLR in this area the following facts are of particular significance :

- during the period from mid of 1989 until end of 1992 eight geostationary communication satellites were successfully positioned and serviced, i.e. an average of one LEOP every 5 months;
- within a period of 3 months from June 1, 1990 to August 31, 1990, GSOC launched and serviced three missions - ROSAT, DFS-2 and EUTELSAT II-F1;

as a special capability in the sector of communication satellites it is significant that GSOC can handle launches and transfer orbit injections with any kind of launcher. To date this includes EUTELSAT II-F3 on ATLAS II, EUTELSAT II-F4 on ARIANE and DFS-3 Kopernikus on a DELTA II.

Operations - The Generic Approach

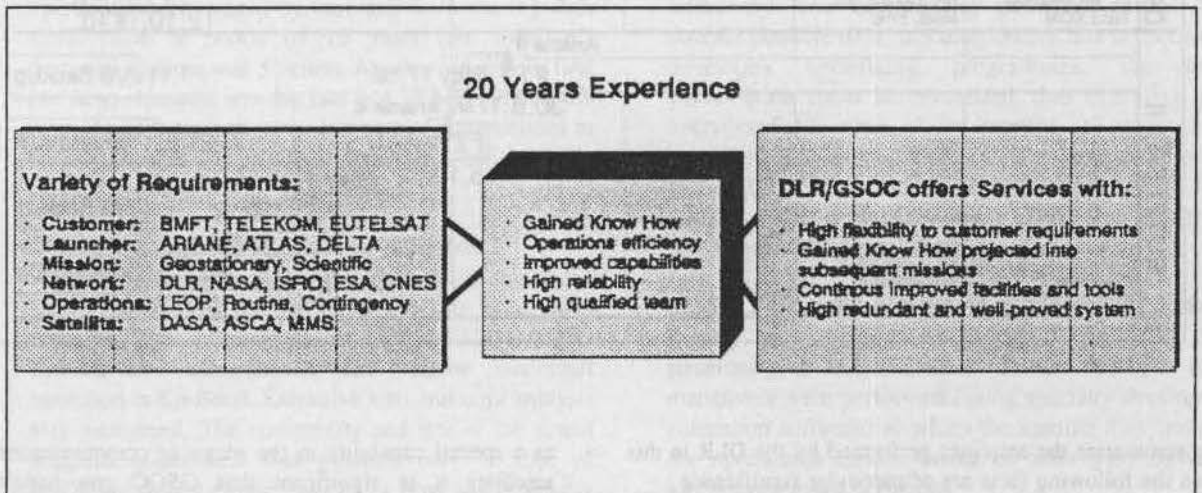
Starting with SYMPHONIE, GSOC has been careful to systematically review and update the operational and management procedures and methods applied to positioning projects. This approach has allowed the development of a set of standard geostationary positioning procedures and working methods which are optimised for modern communication satellites. Of particular significance are the following points:

- the establishment of a stable, highly qualified "core" team within the mission operations department which is responsible for Positioning and Geostationary operations;
- the establishment of specialist engineers in all spacecraft subsystems;
- the cross training of the core team specialists to ensure effective redundancy in all areas;
- to build trust between the GSOC the Customer and the Spacecraft Manufacturer on the back of successfully completed operations. This allows a more efficient approach to the formal documentation associated with commercial positioning activities;
- continuous improvement to facilities and tools over successive missions.

The Project Management Procedures developed and improved over the years and as they are applied by GSOC for the EUTELSAT II project have demonstrated:

- A high degree of flexibility so that all customer requirements may be fulfilled;
- The capability to support both normal and contingency operations;
- A guarantee that "Know-How" gained by the team is projected into subsequent missions.

A by product of the establishment of the core team is that in between Positioning activities, that this team is available to undertake training for external Institutions and Agencies, and is also available to provide consultancy in the field of Geostationary Mission Operations.



Conclusion

Starting with SYMPHONIE and extending to the current series of Eutelsat II spacecraft, the experience gained and retained over many years has been continuously used to both improve the ground operations facilities and also to enhance the operational capacity of GSOC specifically in the domain of geostationary satellite operations.

The LEOP team at GSOC is able to react quickly and effectively to the most varied customer requests in a responsive and unbureaucratic fashion.

GSOC has proved its capability to adapt a variety of technical and management constraints as well as different contractual relationships. In this way the GSOC is enviable in the position of being able to adapt its systems and operations to support practically any customer and any spacecraft manufacturer.

**POSITIONING OF GEOSTATIONARY SATELLITES AT CNES:
FACILITIES, OPERATIONAL ORGANIZATION AND DOCUMENTATION**

H. DONAT

Centre National d'Etudes Spatiales (CNES)
French Space Agency
18, Avenue Edouard Belin
31055 - TOULOUSE CEDEX
FRANCE

ABSTRACT

CNES, the French Space Agency, has a wide range of facilities in Toulouse for the positioning of geostationary satellites. This paper describes these facilities and shows with what thoroughness they are implemented through the organization set up and documentation used.

It also presents the different TT&C networks which can be used by CNES in order to position geostationary satellites.

Key words: geostationary satellite, positioning facilities, TT&C ground station

1. INTRODUCTION

CNES, the French Space Agency, has been responsible for the positioning, station keeping and control of geostationary satellites since 1974, launch date of the first Symphonie satellite.

Since, CNES has successfully brought 15 operational geostationary satellites on station, with a peak activity between December 1991 and April 1992 (five LEOPs in five months with two dual LEOPs):

Satellite	launch date	Operator
TELECOM 1A	4 Aug 84	FRANCE TELECOM
TELECOM 1B	8 May 85	FRANCE TELECOM
TELECOM 1C	11 Mar 88	FRANCE TELECOM
TELE-X	2 Apr 88	Swedish Space Corp.
TDF 1	28 Oct 88	TDF (France)
TDF 2	24 Jul 90	TDF
INMARSAT 2 F1	30 Oct 90	INMARSAT
INMARSAT 2 F2	8 Mar 91	INMARSAT
INMARSAT 2 F3	17 Dec 91	INMARSAT
TELECOM 2A	17 Dec 91	FRANCE TELECOM
ARABSAT 1C	27 Feb 92	ARABSAT
TELECOM 2B	15 Apr 92	FRANCE TELECOM
INMARSAT 2 F4	15 Apr 92	INMARSAT
HISPASAT 1A	10 Sep 92	HISPASAT (Spain)
HISPASAT 1A	22 Jul 93	HISPASAT

CNES therefore has considerable experience in the design, definition and setting up of geostationary satellite control systems. Its know-how covers, on the one hand, operational preparation and on the other, positioning and station keeping operations.

The installation of a Multimissions Control Centre in Toulouse means that CNES will be able to take responsibility for the positioning of a geostationary satellite on behalf of an organization or customer outside CNES. This Centre will in fact be dedicated to operations on satellites belonging to other countries or organizations.

Such operations will normally be carried out from the Toulouse Control Centre, in association with the CNES 2 GHz stations, but can also be carried out using other networks. The customer's own Control Centre may be associated to a greater or lesser extent.

Presently, the planned LEOP operations are the following:

Satellite	launch date	Operator
TURKSAT 1B	Jul 94	TURKISH TELECOM
TELECOM 2C	Jan 95	FRANCE TELECOM
ARABSAT 2A	Feb 96	ARABSAT
TELECOM 2D	Dec 96	FRANCE TELECOM

2. DESCRIPTION OF THE SATELLITE POSITIONING GROUND SUPPORT SYSTEM

CNES ensures the setting up, testing and implementation of the following ground support equipment for the positioning of geostationary satellites:

- a Satellite Control Centre (SCC),
- the Flight Dynamics Centre (FDC),
- the Network Operations Centre (NOC),
- the Orbit Computation Centre (OCC),
- the Main Control Room (MCR),
- the Satellite Specialists Room (SSR),

- a network of TT&C ground stations composed of either the CNES S-band network completed by some NASA or

ESA stations, the INTELSAT C-band network, or the TELESAT KU-band network.

2.1 The Toulouse Control Centre

The Toulouse Control Centre is made up of several different operational entities (figure 1).

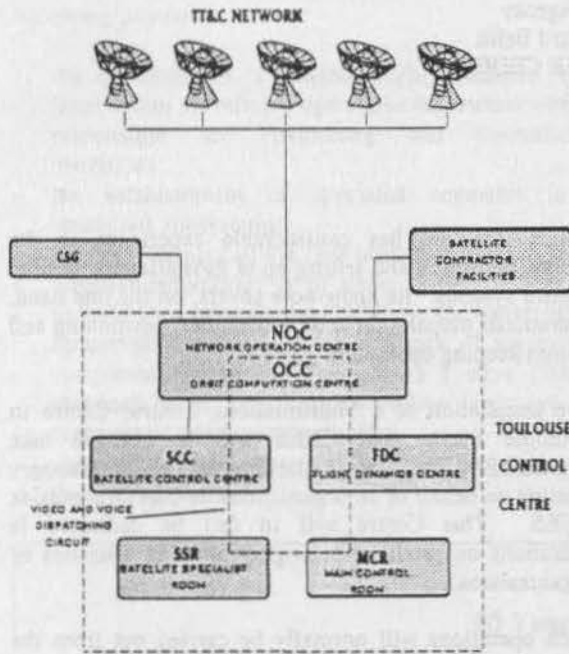


FIGURE 1: THE LEOP GROUND CONTROL SYSTEM

2.1.1 The Satellite Control Centre (SCC)

During the positioning phase, the Control centre takes part in satellite monitoring and technological control operations. It uses the following functions to do so:

- acquisition, processing and exploitation of telemetry data,
- the preparation and sending of telecommands.

The SCC comprises:

- two redundant workstations performing:
 - . Telemetry (TM) acquisition, frame verification and synchronization,
 - . TM storage (more than 12 days on line),
 - . TM distribution towards personal computers (PC) in SCC, MCR and SSR,
 - . Command (TC) preparation and sending with X terminal displays.
- three PC performing:
 - . Acquisition and processing of TM coming from workstations,
 - . Display TM parameters pages and plots,
 - . Monitoring of analogic and status parameters,

Storage of the last 48 hours of TM, in order to replay.

Three others PC permit to generate video pages showing both the latest telecommands sent and those being prepared to television standards; these images are distributed to other CNES facilities by the videofrequency system. It can also receive, via this same channel, images generated by other facilities.

2.1.2 The Flight Dynamics Centre (FDC)

a) Function:

The FDC is responsible for the space mechanics part of operations. In particular, it:

- restitutes the satellite's attitude,
- prepares and monitors attitude manoeuvres,
- determines the orbit,
- prepares, monitors and diagnoses orbit manoeuvres.

It has at its disposal facilities managed strictly and thoroughly for all nominal operations, but a much more flexible management approach to their use for contingency cases, even when unforeseen.

In order to carry out these functions, the FDC:

- receives the satellite's telemetry signals from the NOC and tracking measurements from the TT&C stations,
- provides its results either in the form of video pages distributed by the Toulouse Centre's video system (pages of manoeuvres and graphic monitoring of manoeuvres) or on listing paper (operational forecasts).

b) Description:

The system is composed of 4 workstations connected by an ETHERNET local area network (LAN):

- Two redundant workstations performing the orbit and attitude computations,
- Two redundant workstations performing the telemetry and tracking measurements acquisition and the broadcasting of alphanumeric video outputs,

Two redundant microcomputers designed to control the graphic video outputs are also connected to the LAN.

2.1.3 The Orbit Computation Centre

a) Function:

The OCC's task is to determine the satellite's orbit during both transfer and drift orbits so as to draw up the pointing data for the TT&C stations.

It receives the tracking measurements from the stations (ranging, doppler and angular data if available).

During the launch, it also receives both the initialization data from the French Guiana Space Centre (CSG) and the data contained in the launch vehicle telemetry signals.

Once the tracking measurements have been processed, the OCC determines:

- the satellite's orbit
- the stations' visibility and the ephemerides used to the stations pointing.

b) Description:

The OCC's computing means are as follows:

- 2 redundant workstations used to acquire the location measurements ,
- 2 redundant workstations performing orbit calculations,
- 2 redundant workstations performing graphics,
- 2 redundant workstations performing data storage,
- 2 redundant PC used to send ephemerides to the stations,
- 1 ETHERNET LAN linking all the computers.

2.1.4 The Network Operations Centre (NOC)

a) Function:

The NOC is a technical and operational interface acting as a switching centre between the Toulouse Control Centre and outside facilities:

- the CNES network,
- the ESA network,
- the NASA network,
- the INTELSAT network,
- the TELESAT network,
- the Launch Centre.

It receives:

- the telemetry signals from the TT&C stations, which it then distributes to the SCC and FDC,
- the tracking measurements from the TT&C stations, which it then distributes to the FDC and OCC,
- the commands from the SCC, which it then transmits to the TT&C station.

b) Description:

The NOC was designed as a redundant system including:

- a data transmission system for permanent links between stations in the CNES network (and other networks) and the Toulouse Control Centre.

- a processing system to ensure the routing and supervision of traffic.

2.1.5 The Main Control Room (MCR)

The mission's general management (the Mission Director, Customer and CNES authorities) involved in the mission are all found in this room.

The equipment of MCR are:

- 4 PC for TM monitoring,
- 11 video screens to receive video pages distributed by:
 - .SCC (commands history),
 - .FDC (manoeuvre pages and attitude graphics),
 - .OCC (orbit parameters),
- 3 voice conference devices,
- 3 video wall screens,
- a video text camera,
- universal time (UT) and count down display,
- a fax and telephone sets for each position.

2.1.6 The Satellite Specialists Room (SSR)

The satellite specialists are located in a room next to the MCR which is doted with display facilities so that they may:

- monitor the satellite's status,
- ensure the mission is successfully accomplished,
- intervene in contingency cases.

The SSR is equiped of several desks for : the Satellite Team Leader (STL) and AOCs, propulsion, power, thermal and TT&C subsystems teams.

Each desk is equiped with:

- a PC for TM monitoring and display TM pages and plots,
- a video screen to display video pages from SCC, FDC and OCC,
- voice conference devices and telephone sets.

2.2 The S-band network

The 2 GHz network used in the positioning of geostationary satellites is composed of the CNES network complemented by NASA or ESA stations so as to ensure the coverage of all transfer orbits with active redundancy during the critical phases.

2.2.1 The CNES network

The CNES network comprises the following stations:

- AUSSAGUEL (AUS), near TOULOUSE,
- KOUROU (KRU), in French Guiana,

- HARTEBEESTHOEK (HBK) near PRETORIA (South Africa),
- KERGUELEN (KER) in KERGUELEN Island (South Indian Ocean).

2.2.2 The ESA network

In order to improve the coverage of transfer orbits, it is possible to use ESA's station in PERTH (PTH), Australia, and that in KOUROU (KRU), French Guiana.

The compatibility of CNES and ESA networks has already been investigated. Interface equipment has been set up and already used operationally.

2.2.3 The NASA network

The NASA network, and specifically the stations of GOLDSTONE (GDS) California (USA) and CANBERRA (CAN) in Australia, is also used to complete the coverage of transfer orbits.

As is customary, these facilities are subject to one limitation, that of NASA's own activities having a greater priority.

2.3 The C-band network

The INTELSAT network is composed of the following stations:

- CLARKSBURG (USA)
- RAISTING (Germany)
- FUCINO (Italy)
- BEIJING (China)
- PERTH (Australia)
- PAUMALU (Hawaii)

The Intelsat Satellite Control Centre (ISCC) is in WASHINGTON. It is connected to the Toulouse NOC by two redundant links.

2.4 The KU-band network

The TELESAT network is composed of the following stations:

- ALLAN PARK (Canada)
- PERTH (Australia)

It may also be complemented by the following stations (with which TELESAT has agreements):

- CHILWORTH near Southampton (Great Britain - BSB),
- SYDNEY (Australia - AUSSAT).

The Operations Centre is in Gloucester, ONTARIO (Canada). It is connected to the Toulouse NOC by two redundant links.

3. OPERATIONAL DOCUMENTATION AND ORGANIZATION

3.1 Operational documentation

Operational documentation groups all the documents and data used for the operational qualification and completion of the mission itself.

We shall look at three levels of documentation (figure 2).

Level 1: reference documents

These documents do not form part of operational documentation but constitute the reference documentation for it. They are:

- The Satellite Operations Handbook, including Satellite Control Procedures, produced by the satellite manufacturer.
- The Ground/Spacecraft Interface Document comprising the documents produced by the manufacturer. These are:
 - * Satellite/Ground Interface Specifications,
 - * Telemetry and Telecommand files,
 - * The satellite's Technological file (including the data necessary for mission analysis),
 - * The ground software specifications.

- The Ground System Definition.

The purpose of this document is to give a complete definition of the Ground Control System used for positioning operations.

- Mission analysis.

A mission analysis document is prepared prior to the mission by the satellite manufacturer; the final mission analysis document is produced by CNES.

- Handover plan.

The handover plan defines the conditions of the transfer of the control of the satellite from CNES to the Customer.

Level 2: General execution and coordination documents

- the General Operation Plan,
- the Flight Plan,
- the Sequence Of Events (SOE),
- the Decision Authority Plan,
- the Flight Control Procedures,
- the Simulation and Rehearsal Plan.

Level 3: Specialized execution documents

These are in-house documents prepared by CNES for the completion of operations. They are:

- the Specialized Operation Plans,
- the Operations Support Plans,

- the Launch Operation order,
- the Rehearsal Operations order,
- the Operational Interface Specifications.

3.1.1 Presentation and management of documentation

- Presentation of documents

For the purposes of homogenization and to facilitate the identification, use and management of operational documentation, the documents respect requirements in force at CNES.

- Application of documents

The application of these documents comes under the responsibility of the operations manager. They are applied for each simulation and all operations.

- Qualification of documents

Documents are qualified during simulation and rehearsals. Documentation is configuration-managed. Change requests are dealt with at project management level.

- Management of documents

Operational documentation is configuration-managed according to the procedures in force within CNES and defined in the Quality Plan.

The configuration file for the operational system identifies the state of all operational documents, and constitutes the reference configuration. This file is drawn up when the full and definitive version of the documentation is created (before qualification tests).

Configuration management consists in controlling the modifications which will affect the reference configuration so that the state of the configuration may be known at any point in time.

3.1.2 Description of operational documentation

- Mission Analysis

The mission analysis document covers the following points:

- * Data, constraints and optimization criteria used for the mission analysis and strategy determination,
- * Launch window determination,
- * Optimization of the positioning strategy (apogee manoeuvres and attitude reorientation) including:
 - . optimization of fuel consumption,
 - . optimization of the orbit acquisition duration,
 - . optimization of the global safety of operations.
- * Analysis of the first acquisition by the TT&C network,

- * Determination of TT&C stations visibilities and redundancies,
- * Definition of orbit determination accuracy,
- * Prediction and analysis of problems related with possible sun eclipses or sun and moon interference with attitude sensors,
- * Analysis of the strategy proposed for final attitude acquisition: definition of possible specific software or of computer aided procedures to carry out the operations,
- * Establishment of the sequence of events: chronology, dates of nominal and back-up events, their duration and methods used.

- The General Operation Plan

This document contains all the general information needed for each operational entity to organize itself in accordance with mission needs, i.e.:

- * the project's operational organization,
- * the ground system configurations and functions,
- * the synthesis of operation proceedings in chronological order,
- * the contribution made by each entity (contributions, operational interfaces, support).

- The Flight Plan

This is a graphic synthesis of the Sequence Of Events (SOE). Each orbit is represented on a page which shows:

- * TT&C station visibilities with an indication of the main station,
- * periods when it is possible to acquire attitude data,
- * periods of tracking data acquisition,
- * the Flight Control Procedures (FCP) carried out,
- * time of orbital parameters delivery,
- * any useful information about the orbit: time constraints, intermittent TM or TC coverage, etc...

- The Sequence Of Events (SOE)

The SOE is the document along which entity proceed during mission execution,

It covers the period of time stretching from the readiness system check launch, to the beginning of on-station operations.

It gives, in chronological order, the sequence of events, the operations and controls to be performed. Each operation consists of synchronized actions with "GO/NO GO" steps, actions to be carried out in the ground system.

The SOE refers back to the FCPs for details on actions, particularly for the commands to send. The chronology takes into account nominal operations and some non nominal events that could arise (back-up operations for apogee manoeuvres, for example).

The SOE is validated during the simulation and rehearsal phase and updated thereafter if necessary.

- The Decision Authority Plan

This document describes the working organization and the role of Customer and CNES authorities during the mission.

It defines the decision process in the event of unforeseen anomaly.

It describes the staffing and the available facilities in the Main Control Room (MCR) and in the Satellite Specialists Room (SSR).

- Flight Control Procedures (FCPs)

There is one procedure for each satellite operation.

Each procedure describes with the most possible details the commands to be send, the parameters to be check before and after each command, the time constraint for the operation, the GO/NO GO steps for manoeuvres, the description of the required status of the satellite before the procedure, the expected status of the satellite after the procedure.

The procedures are derived from Satellite Operations Handbook by adding the parameters involving the LEOP ground system when necessary, for instance introduction of parameters issued from manoeuvres preparation.

These procedures apply in nominal and back up cases. Procedures are also foreseen for some contingency cases that might occur.

- The Simulation and Rehearsal Plan

The Simulation and Rehearsal Plan is a document which fixes the framework for, and presents the principles of, the operational qualification of the ground support system:

- * the aim of qualification exercises,
- * checkout criteria on ground support system specifications,
- * facilities used (including simulators),
- * the personnel required,
- * the schedule for the exercises,
- * the differences with respect to the General Operation Plan specific to the exercises.

- Specialized Operation Plans

Each entity (SCC, FDC, NOC and OCC) shall produce a Specialized Operation Plan to provide a description of its internal organization and how it works to reach the mission requirements.

These documents mainly contain:

- * general synoptics of the whole facility (with redundancies),
- * interfaces with other entities,
- * the list of procedures,
- * the detail of tasks performed along the mission,

- Operations Support Plans

Operational entities benefit from the support of various CNES departments. Each department which provides support must draw up an operations support plan.

The different kinds of support apply to the following technical areas:

- * hardware and software maintenance,
- * power supply and air conditioning,
- * data link maintenance,
- * general support,
- * security.

- Operational Interface Specifications

This type of document defines the operational interfaces which exist between two entities. There are as many documents as necessary.

- Launch Operation Order

This document provides general information such as:

- * the launch date, launch window and consequence on the mission plan,
- * readiness system check and criteria for decision,
- * staffing of the MCR and SSR,
- * appointments for briefings, reports.,

- Rehearsal Operations order

Rehearsal consist of several tests. For each one, an Operations order gives the general information necessary to perform the test such as:

- * purpose of the test,
- * facilities and equipment involved,
- * configuration of the ground system,
- * simulation,
- * procedures,
- * schedule,
- * briefings and debriefings reports.

3.2 Operational Organization

3.2.1 Principles

During the preparation phase for satellite positioning, the project team is organized as shown in figure 3.

During the positioning and operational qualification phases, a special organization, known as operational

organization, is set up. It is based on the project organization and includes two main levels of responsibility, as shown in figure 4.

This organization has already been put into practice and validated during successive launches under the Toulouse Control Centre's responsibility. It has reached a high level of efficiency and safety, particularly in contingency situations.

The organization is such that the work schedule covers 24 hours a day and includes all the entities of which the LEOP Ground System is composed.

3.2.2 Execution activity

The execution activity is managed by the Operation Manager. He coordinates the operational entities in accordance with the Sequence Of Events. He is located in the Satellite Control Centre room.

This activity implies careful operation execution following, without deviation, the operational documentation:

- the SOE coordinated by the Operations manager,
- the Flight Control Procedures carried out by the Satellite engineer,
- the Specialized Operation Plans executed by each entity.

The Operations manager reports to the Mission Director in the following cases:

- at "GO/NO GO" rendez-vous steps prepared, in the SOE, to get authorization to further proceed,
- when the situation appears to be non nominal, to get approval of the envisaged back-up procedure in a foreseen case or instructions in an unexpected case.

3.2.3 Control and Decision activity

The control and decision activity is managed by the Mission Director, located in the MCR. This activity involves:

- Satellite system and subsystem specialists who:
 - . verify and confirm that the satellite's behaviour is nominal,
 - . give an alarm when they detect a non nominal situation,
 - . approve, when necessary, the decision to switch over to a satellite contingency procedure or to come back to the normal situation.
- Customer Mission Manager: he is requested to give their approval at the most important steps of the mission (launch decision, firing the apogee motor, etc.).

In addition, and assisted by Satellite Specialists, he is in charge of providing the Mission Director with satellite contingency procedures in case of unforeseen satellite situations.

ORBIT DETERMINATION I

COMPARISON OF FOUR EUROPEAN

1. Alby, F. (CNES-France); Bianco, G. (ASI-Italy);
Fourcade, J. (CNES-France); Gill, E.
(DLR-Germany); Kirschner, M. (DLR-Germany);
Luceri, V. (Telespazio-Italy); Mesnard, R.
(CNES-France), Montenbruck, O. (DLR-Germany);
Schneller, M. (DLR-Germany) and Schoemaekers, J.
(ESA):
 **"Comparison of Four European Orbit Determination
 Systems"** 461
2. Kuga, H.K. and Rao, K.R. (INPE-Brazil):
 **"SCD1 Orbit Determination System: Pre-Launch
 Preparation, LEOP Performance and Routine
 Operations"** 472
3. Maisonobe, L.; Campan, G. and Brousse, P.
(CNES-France):
 **"ROSACE Orbit Determination Using Telescope
 and CCD"** 478
4. Pallaschke, S. (ESOC-ESA):
 "Review of INPE/ESA Orbit Determination for SCD1" 485
5. Pinheiro, M.P. (Hughes-USA):
 **"Transfer Orbit Determination Accuracy for Orbit
 Maneuvers"** 494
6. Nazirov, R.R. and Timokhova, T.A. (IKI-Russia):
 **"Comparison of NORAD and RCSC Element Sets for
 Near-Earth Space Object"** 498

COMPARISON OF FOUR EUROPEAN ORBIT DETERMINATION SYSTEMS

F. Alby (CNES), G. Bianco (ASI), J. Fourcade (CNES), E. Gill (DLR),
M. Kirschner (DLR), V. Luceri (Telespazio), R. Mesnard (CNES),
O. Montenbruck (DLR), M. Schnelller (DLR), J. Schoemaekers (ESA)

ABSTRACT

The objective of this paper is to present the activities and the main conclusions of the IOI (In-Orbit Infrastructure) Flight Dynamics Working Group. This IOIFDWG is an inter-agency working group composed of flight dynamics experts coming from the following space agencies: ASI, DLR, ESA and CNES.

These agencies are in charge of elements of the future European orbital infrastructure such as the space station, the launcher, the vehicles, relay satellites or the ground control centre. During the operations they will have to exchange flight dynamics data; therefore the main objective of the group was to analyze the compatibility of the orbit determination systems at the participating agencies.

In order to identify the origin of possible discrepancies in the complex orbit determination process, the comparisons have been performed in three successive steps: first the orbit propagation software modules have been compared, then the tracking measurements modules and, finally the orbit estimation software modules themselves.

After a short description of the software systems used at each agency, with their main features, this paper presents, for each step, the description of the tests and the main results. Then, the significant differences are discussed and in particular, the major contribution due to the atmospheric drag

modeling is shown; finally, the main conclusions are summarised and recommendations for the exchange of state vectors are proposed including a list of data to be harmonised between agencies.

1. INTRODUCTION

The future European In - Orbit Infrastructure (IOI) will be made up with several elements such as a space station to be visited, a launcher, vehicles to carry crew and cargo up and down, relay satellites, ground tracking stations and control centers.

During the operations, and also before, during the studies and the preparation phases, the space agencies in charge of this IOI elements will have to exchange flight dynamics data; these data have to be compatible and accurate enough in order to perform proximity operations.

To cope with this problem, the IOI Flight Dynamics working group has been established in August 1990. This group, composed of flight dynamics experts from ASI, DLR, ESA and CNES, had the following objectives:

- to stimulate a continuous exchange of know-how relevant to flight dynamics operations of the IOI,
- to exchange results of relevant preparatory studies,

- to coordinate preparatory studies and undertake joint studies
- to address issues of IOI-wide relevance in the flight dynamics area and recommend standards.

Experience with past cooperative projects (e.g.: Giotto, Ulysses, Phobos, Eureka) have demonstrated the importance to guarantee compatibility between the different Flight Dynamics sub-systems involved. It was therefore decided to analyse the compatibility of the orbit determination systems at the participating agencies. The purpose is to identify differences in models, that lead to significant differences in results and to quantify these differences. This is done by running the orbit determination programs or parts of them with compatible input parameters and analysing the differences in results.

The main work was carried out between August 1990 and spring 1992. During this period five meetings were held, including a preparatory meeting, to exchange results and take decisions for further actions. The major activity concentrated on a detailed software compatibility test of the orbit determination and propagation software available at the participating agencies.

In addition to this synthesis, a technical report has been edited by J. SCHOENMAEKERS (ESOC/OAD, 18/12/92), which contains a detailed description of the test parameters and test results and should allow other agencies to execute the tests and compare their data with those contained in the report.

2. METHOD

The approach is first to reach compatibility in the basic functions, i.e. orbit propagation,

measurement models and estimation method. Only after an acceptable level of compatibility is reached in these basic functions, the compatibility of the orbit determination as a whole is analysed.

This approach leads to the following sequence of tests:

- Orbit propagation tests
- Measurement model tests
- Estimation method tests
- Full scope orbit determination tests

The measurement models can reasonably only be tested using an orbit propagation. In order to minimize the effect of orbit model differences on these tests, they are executed using a simple orbit model and only after sufficient compatibility is reached for this simple model.

The estimation method can only be tested using an orbit propagation and a measurement model. In order to minimize the effect of orbit and measurement model differences on these tests, they are executed using a simple orbit and measurement model and only after sufficient compatibility is reached for these simple models.

Apart from one test, which uses real ERS-1 data, all tests are assuming a space station type orbit (Approximately circular with an altitude of 480 km and an inclination of 28.5 deg).

All orbits defined in the test plan or generated as a result of the tests are referred to the **True of epoch date reference system**. This is an inertially fixed system, its X/Y-plane and X-axis coincide with the true equator and equinox at the time for which the orbit is given and assuming the precession and nutation adopted in the IAU J2000 system.

All times used in the test plan are referred to UTC.

3. ORBIT PROPAGATION

3.1. COMPARISON OF ORBIT PROPAGATION PROGRAM

Orbit input

	ASI	CNES	DLR	ESOC
Coordinate system	True of date Mean of date Mean of B1950 Mean of J2000	True of date	True of date Mean of date Mean of B1950 Mean of J2000	True of date Mean of date Mean of B1950 Mean of J2000
Time reference	UTC	UTC	UTC	UTC
Orbit representation	Position/Velocity Oscul. Kepler elements Non sing. Kepler elements	Position/Velocity Oscul. Kepler elements	Position/Velocity Oscul. Kepler elements	Position/Velocity Oscul. Kepler elements

Orbit output

	ASI	CNES	DLR	ESOC
Coordinate system	True of date Mean of date Mean of B1950 Mean of J2000	True of date	True of date Mean of date Mean of B1950 Mean of J2000	True of date Mean of date Mean of B1950 Mean of J2000
Time reference	UTC	UTC	UTC	UTC
Orbit representation	Position/Velocity Oscul. Kepler elements	Position/Velocity Oscul. Kepler elements	Position/Velocity Oscul. Kepler elements	Position/Velocity Oscul. Kepler elements

Integration

	ASI	CNES	DLR	ESOC
Coordinate system	True of date	VEIS	Inertial true of reference epoch	Mean of J2000
Time reference	A1	UTC	A1	TAI
Method	Variable order predictor-corrector Cowell	8th order Cowell	11th order multistep predictor-corrector Stoermer-Cowell (position) and Adams-Bashfort Adams-Moulton (velocity)	8th order multistep predictor-corrector Cowell

Geopotential

	ASI	CNES	DLR	ESOC
Coefficients	Variable degree and order	Variable degree of zonal, degree of tesseral, and order of tesseral terms (deg/order < 37)	Variable (< 25) degree and order	Variable (< 37) degree and order
Precession	Newcomb	Lieske	Lieske Newcomb	Lieske
Nutation	Woolard(DE96) Wahr(DE118) Wahr(DE200)	Wahr (J2000)	Wahr (DE118) Wahr (DE200) Woolard (DE96)	Wahr (DE200)
Polar motion	IERS	No	No	IERS
UTC-UT1	IERS	IERS	IERS	IERS
Sidereal time	IAU(1961) IAU(1984)	VEIS	IAU (1984) IAU (1961)	IAU (1984)

Air drag

	ASI	CNES	DLR	ESOC
Density model	Jacchia (1971)	DTMH	Modified Jacchia (1971)	MSIS (1977) Jacchia (1971)
Winds	No	No	No	No
Satellite model	Constant body cross section	Constant body cross section	Constant body cross section	Complex geometry + Attitude profile considered for cross section

Solar pressure, sun and moon attraction

	ASI	CNES	DLR	ESOC
Ephemeris	DE96 DE118 DE200	Analytical Sun: Newcomb Moon: Brown	DE96 DE118 DE200	DE 200
ET/TBD-UTC	IERS		IERS	IERS
Satellite model	Constant body cross section	Constant body cross section	Constant body cross section + Solar panels	Complex geometry + Attitude profile considered for cross section

3.2. TESTS OF THE ORBIT PROPAGATION PROGRAMS

A total of 7 orbit propagation tests are executed, each with a different orbit model.

They consist in propagating the following orbit:

- Semi-major axis	= 6858.140 km
- Eccentricity	= 0.00001
- Inclination	= 28.5 deg
- Ascending node	= 0.0 deg
- Arg. of perigee	= 0.0 deg
- True anomaly	= 0.0deg

from an initial epoch of 2 July 1990 00:00 UTC to a final epoch of 9 July 1990 00:00 UTC.

The following tests are executed (the referred orbit models are used as far as they are supported by the orbit determination S/W):

Test P1	Uses a pure Kepler orbit i.e. the only force acting on the S/C is the attraction of the earth, where the earth is assumed to be a point mass.
Test P2	Uses a Kepler orbit + geopotential perturbation.
Test P3	Uses a Kepler orbit + air drag.
Test P4	Uses a Kepler orbit + solar radiation pressure.
Test P5	Uses a Kepler orbit + sun attraction.
Test P6	Uses a Kepler orbit + moon attraction.
Test P7	Uses a Kepler orbit + geopotential perturbation, air drag, solar radiation pressure, sun and moon attraction.

For each test, the orbit is compared at the end of the propagation period. In addition, for test P2, the orbit is also compared during the propagation with

15 minutes interval, starting at the initial epoch and ending at the final epoch.

3.3. ORBIT PROPAGATION TESTS RESULTS

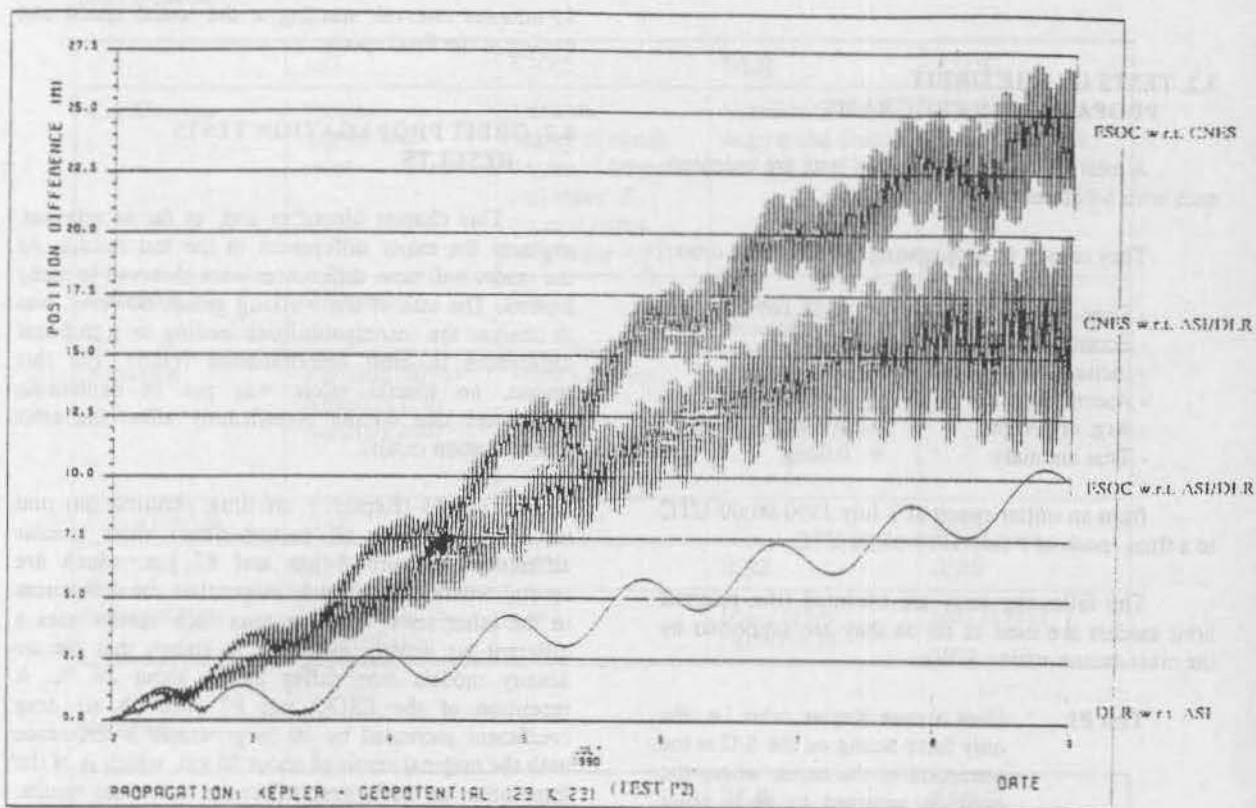
This chapter identifies and, as far as relevant, explains the major differences in the test results. As the reader will note, differences were observed in many aspects. The task of the working group, however, was to analyse the incompatibilities leading to significant differences in orbit determination results. For this reason, no special effort was put in explaining differences that do not significantly affect the orbit determination results.

Test P3 (Kepler + air drag perturbation) and test P7 (Kepler + all perturbations) show similar differences between 8 km and 87 km, which are several orders of magnitude larger than the differences in the other tests. In these tests each agency uses a different air density model. It is known that the air density models may differ up to about 20 %. A repetition of the ESOC test P3 with an air drag coefficient increased by 20 % generated a difference with the original result of about 56 km, which is of the same order as the largest difference in the test results. From this all, it can be concluded that in the orbit propagation the modelling of the air drag is the dominant source of differences. The large differences can be explained by the use of different air density models.

The relatively small difference of about 10 km between ASI and DLR is due to fact that, while ASI uses the original Jacchia 1971 air density model, DLR uses a variation of this model that differs from it by maximum 11 %. It should be noted that the input parameters to the density models, such as solar and magnetic values had been harmonized in the tests.

In test P1 (Kepler propagation only) one should expect very small differences. It is therefore worthwhile noting the difference of about 22 m between CNES and the other agencies. This is due to the use, by CNES, of the non-inertial VEIS coordinate system for integration, without modelling the acceleration of the system.

As an example, the comparison of the positions at 15 minutes interval for test P2 is given below:



4. MEASUREMENTS

4.1. COMPARISON OF MEASUREMENT MODELS IN THE SOFTWARES

	ASI	CNES	DLR	ESOC
Measurement types	Range Range-rate Azimuth/Elevat. X/Y angles	Range Range-rate Azimuth/Elevat. X/Y angles	Range Range-rate Azimuth/Elevat. X/Y angles (E/W and N/S mount)	Range Range-rate Azimuth Elevation Interferometer Altimetry
Datation time	UTC	UTC	UTC	UTC
Precession	Newcomb	Lieske	Lieske Newcomb	Lieske
Nutation	Woolard(DE96) Wahr(DE118) Wahr(DE200)	Wahr (J2000)	Wahr (D118) Wahr (DE200) Woolard (DE96)	Wahr (DE200)
Polar motion	IERS	No	IERS	IERS
UTC-UT1	IERS	IERS	IERS	IERS
Sidereal time	IAU(1961) IAU(1984)	VEIS	IAU (1984) IAU (1961)	IAU (1984)

Light time correction	Iterative	Iterative	Iterative	Iterative
Ionosphere	No	No	No	Rawer-Bent Willman
Troposphere	Hopfield Marini-Murray (laser)	TBD	Hopfield (1974)	Hopfield/ Yionoulis Saastamoinen Marini Murray- Marini laser

4.2. TESTS OF THE MEASUREMENT SOFTWARES

The tests cover the following measurement types

- **Range measurement:** corresponding to the propagation time of a signal from the station to the satellite and back to the station, divided by 2 and multiplied by the speed of light. The measurement time tag refers to reception time.
- **Range-rate measurement:** corresponding to the variation in range measurement during a given count interval divided by the count time. The datation time corresponds to the end of the count interval.

A total of 6 measurement model tests are executed, each with a different measurement model.

They consist in propagating a nearly circular orbit (480 km altitude, 28.5 degrees inclination) using a Kepler orbit model, then in computing the residuals w.r.t. theoretical measurements simulated for the PERTH ground station.

The following tests have been executed.

- Test M1** The measurement model includes the earth rotation, earth precession, earth nutation, light time correction and UT1-UTC correction. Not included are ionospheric delay, tropospheric delay, station/transponder delays/biases and polar motion.
- Test M2** Test M1, but now including polar motion.
- Test M3** Test M1, but now including ionospheric delay.

Test M4 Test M1, but now including tropospheric delay.

Test M5 Test M1, but now including station/transponder delays.

Test M6 Test M1, but now including ionospheric delay, tropospheric delay, station/transponder delays and polar motion.

For each test, the residuals w.r.t. the simulated measurements are compared.

4.3. MEASUREMENTS TESTS RESULTS

In test M2 (including polar motion if possible) CNES differs from the other agencies of up to 14 m for the range measurements and 5.5 cm/s for the range-rate measurements. This is because CNES does not model the polar motion.

In test M3 (including ionospheric delay if possible) ESOC differs from the other agencies up to 1.7 m for the range measurements and 0.6 cm/s for the range-rate measurements. This is because only ESOC models the ionospheric delay.

In test M4 (including tropospheric delay if possible) the differences go up to 1.3 m for the range measurements and 0.8 cm/s for the range-rate measurements. This is due to the use of different tropospheric models or at least implementations of these.

In test M5 (including delays) the results are affected by the accuracy limitation for out-putting the range residuals in the ESOC/BAHN S/W. The digits after the comma can not be provided, and therefore the results are containing a rounding error up to 1 m.

The previously mentioned differences are also apparent in the results of test M6, where the full measurement model was used.

5. ESTIMATION

5.1. COMPARISON OF ESTIMATION SOFTWARES

	ASI	CNES	DLR	ESOC
Estimation method	Bayesian least squares	Bayesian least squares	Bayesian least squares	Bayesian least squares

5.2. TESTS OF THE ESTIMATION SOFTWARES

A total of 5 estimation method tests is executed, each with different measurement types, arcs and/or accuracies.

They consist in estimating the osculating Kepler elements from simulated range and/or range-rate measurements using the same simplified orbit and measurement model as used for simulating the measurements.

The following tests are executed:

- Test E1** Uses a 3 days arc of bias and noise free range and range-rate measurements.
- Test E2** Uses a 1 day arc of bias and noise free range and range-rate measurements.
- Test E3** Uses a 1 day arc of bias and noise free range measurements.
- Test E4** Uses a 1 day arc of bias and noise free range-rate measurements.
- Test E5** Uses a 1 day arc of biased and noisy range and range-rate measurements.

The orbit propagation uses a Kepler orbit model extended with the perturbation of the earth geopotential only. In the transformation of the geopotential perturbation from earth fixed to inertial coordinates, the earth rotation, earth precession, earth nutation and UT1-UTC correction are included. The polar motion is not included.

The measurement model includes the earth rotation, earth precession, earth nutation, light time correction and UT1-UTC correction. Not included are the ionospheric delay, tropospheric delay, station/transponder delays biases and polar motion.

The following results are compared:

- the orbit and its covariance at different dates,
- the measurement residuals.

5.3. ESTIMATION TESTS RESULTS

The differences in test E1 between CNES and the other agencies of about 2.5 m for the estimated position at epoch and 4.5 m for the propagated orbit are probably related to the differences in the Kepler propagation.

In test E2, E3 and E4 the observation geometry is deteriorated w.r.t. test E1. In these tests the differences between ESOC and the other agencies increase by about 7 m for the estimated state and 10 m for the propagated state. This indicates that a reduction of the observation geometry is not handled in the same way by the different agencies.

Test E5 differs from test E2 in that a slowly varying bias and noise were added to the measurements. In this test no significant increase was observed in the differences. Also the residuals show a compatible behaviour. This indicates that biased and noisy measurements are handled in the same way by the different agencies.

6. FULL SCOPE ORBIT DETERMINATION TESTS

A total of 3 full scope orbit determination tests are executed.

They consist in estimating the osculating Kepler elements and eventually the air drag coefficient from simulated or real range and range-rate measurements.

The following tests are executed :

- Test F1** Uses a 1 day arc of biased and noisy simulated range and range-

rate measurements from the stations Maspalomas and Perth. Only the osculating Kepler elements are estimated.

Test F2 Uses a 1 day arc of biased and noisy simulated range and range-rate measurements. The osculating Kepler elements and the air drag coefficient are estimated.

Test F3 Uses a 1 day arc of real ERS-1 range and range-rate measurements collected at the Kiruna ground station. The osculating Kepler elements and the air drag coefficient are estimated.

The orbit model used includes, as far as possible, the perturbation due to the earth geopotential, air drag, solar radiation pressure, sun and moon attraction.

The measurements model used includes, as far as possible, the earth rotation, earth precession, earth nutation, light time correction, UT1-UTC correction, ionospheric delay, tropospheric delay, transponder delay and polar motion.

The simulated measurements were generated with the above defined orbit and measurement models.

The following results are compared :

- the orbit and its covariance at different dates,
- the air drag coefficient and its standard deviation,
- the measurement residuals.

The osculating Kepler elements calculated by each agency are contained in the next table:

RESULTS OF FULL SCOPE ORBIT DETERMINATION TESTS

		SEMI-MAJOR AXIS (KM)	ECCENTRICITY	INCLINATION (DEG)	ASCENDING NODE (DEG)	ARGUMENT OF PERIGEE (DEG)	ARGUMENT OF LATITUDE (DEG)
TEST =F1	ASI	6858.1290956	0.000021188400	28.494195201	159.953016317	29.292940329	50.03954322641
EPOCH=90/07/02	CNES	6858.1336183	0.000010600000	28.499020900	159.994323500	5.126444100	50.00459980000
00:00:00	DLR	6858.1306073	0.000019888406	28.494730068	159.957600222	27.757472306	50.03570082200
	ESOC	6858.1400100	0.000009765000	28.500091385	160.000763734	359.319712424	49.99933707500
TEST =F1	ASI	6858.2519670	0.000842960140	28.497246243	139.479540249	358.442671730	46.34508813038
EPOCH=90/07/05	CNES	6858.2303163	0.000838700000	28.502075600	139.521541100	357.643220200	46.33762410000
00:00:00	DLR	6858.2442910	0.000842423400	28.497774491	139.484196530	358.343945450	46.35137934500
	ESOC	6858.1966970	0.000834776000	28.503093102	139.528202074	357.558568816	46.37741150300
TEST =F2	ASI	6858.1426766	0.000009759300	28.499778212	159.999109000	1.728556725	50.00078369664
EPOCH=90/07/02	CNES	6858.1417306	0.000009900000	28.499615300	159.999163100	359.152568600	50.00072430000
00:00:00	DLR	6858.1428001	0.000009778008	28.499737128	159.998921471	1.446938748	50.00095243600
	ESOC	6858.1401790	0.000009651000	28.500167291	160.001387302	358.509595272	49.99881232700
TEST =F2	ASI	6858.1822390	0.000836896630	28.502768058	139.526433071	357.494092265	46.39773808431
EPOCH=90/07/05	CNES	6858.1854028	0.000835400000	28.502631500	139.526324000	357.578663700	46.39163180000
00:00:00	DLR	6858.1817170	0.000837009860	28.502726636	139.526235216	357.494035175	46.39867884300
	ESOC	6858.1958340	0.000834688000	28.503166246	139.528836846	357.546081910	46.37801857300
TEST =F3	ASI	7147.0838488	0.000830072900	98.514209042	28.367637460	173.605854146	65.73218689000
EPOCH=91/11/12	CNES	7147.0837483	0.000830700000	98.514222800	28.367384200	173.615333800	65.73224610000
06:40:00	DLR	7147.0837901	0.000830321269	98.514206995	28.367665467	173.600809258	65.73217638800
	ESOC	7147.0833130	0.000832136000	98.514220134	28.367696869	173.547145501	65.73208132700
TEST =F3	ASI	7147.0008940	0.000825648560	98.514321053	31.321232264	174.298043173	66.01768407630
EPOCH=91/11/15	CNES	7147.0003424	0.000826900000	98.514335800	31.320974000	174.150170400	66.01772570000
06:40:00	DLR	7147.0014420	0.000825907850	98.514318930	31.321259203	174.289129290	66.01711421000
	ESOC	7147.0050060	0.000827588000	98.514331974	31.321293264	174.196913735	66.01340084300

The large differences in test F1 up to 1.3 km for the estimated orbit at epoch and 9 km for the propagated orbit are due to the use of different air drag models which could not be compensated since the drag coefficient was not estimated.

Differences smaller than 50 m, hence compatible with usual orbit determination accuracies, are obtained in test F2 and test F3 as regards the estimated state. For the propagated state ESOC differs of about 2 km (test F2) and 500 m (test F3) from the other agencies. This difference is due to a lower estimation of the air drag by ESOC, which finds its explanation in the use of the ionospheric correction by ESOC only. In both tests the ionospheric delay was larger at the start of the measurement arc than at the end. On the range measurement this has the same effect as the decay due to air drag. ESOC attributed this effect partially to the ionospheric delay and partially to the air drag. The other agencies attributed it all to the air drag and therefore obtained larger values for the drag coefficient. Since the ionospheric delay has basically a period of one day, the difference is expected to disappear when measurement arcs of e.g. 3 days would be used.

7. CONCLUSIONS AND RECOMMENDATIONS

When propagating a 480 km altitude circular orbit with different softwares, starting at the same epoch with an identical state vector and harmonized planetary and geophysical constants, unacceptable deviations may occur. A propagation period of one week can lead to differences of about 87 km in the final state vector. The differences are mainly due to the use of incompatible air drag models.

The possible solutions of this problem are the following:

- a. When an agency needs propagated states, it has to estimate the states of both IOI elements and then to propagate them by itself. In this case no states have to be exchanged between the agencies. This requires an orbit determination capability at the corresponding agency.
- b. For a particular IOI element only one agency estimates and propagates the state and makes the results available for the other agencies. This can be implemented by transmitting the required state on request or by distributing a file with the propagated orbit each time an orbit determination has been performed.

- c. For a particular IOI element only one agency estimates the state. It then performs a long term propagation that will contain propagated states in long term intervals of e.g. 6 hours. On the basis of this information the other agencies then only perform short term propagation to the required epoch.
- d. Identical air drag models are used. This would allow all agencies to propagate states from all sources over long time periods.

For the orbit determination software at the different agencies, the differences turned out to be much smaller - for a full orbit determination process they have been in the order of 50 m; but if this estimated orbit is propagated 2 days beyond the data the differences increase up to 2 km. The deviations in this case are again dominated by the use of different air drag models. Nevertheless a list of constants to be harmonised has been set up:

- Gravitational constant of the sun
- Gravitational constant of the moon
- Gravitational constant of the earth
- Earth equatorial radius
- Geopotential coefficients
- Polar motion parameter X
- Polar motion parameter Y
- Sun/Moon ephemeris file (= DE200)
- Effective solar radiation pressure at mean earth distance from the sun
- UT1-UTC correction value
- Inverse earth flattening coefficient
- Speed of light
- Geomagnetic values (air drag model)
- Solar flux values (air drag model)

In fact, the polar motion and the UT1-UTC correction vary slowly in function of time, but, considering the duration of the mission (a few weeks) and the level of accuracy to be obtained, these corrections can be considered as constants.

One can therefore conclude that the orbit determination programs of the participating agencies are sufficiently compatible in producing an orbit estimate close to the data arc for space station type orbits. Whenever a propagation away from the data arc is performed significant differences may occur.

Finally, considering that the constant model coefficient have been harmonised before the operations, the document for the standardised exchange of orbit parameters between agencies should contain only the following information:

- Coordinate system to be used: this depends on the programs that will actually be used. With the present programs the true of reference date earth equator and equinox coordinate system would be suitable.
- The orbit elements to be exchanged.
- The epoch of orbital elements.
- Air drag information: Drag coefficient * Cross section area/Mass.
- Solar radiation pressure information: Solar radiation pressure coefficient * Cross section/Mass.
- Manoeuvre information.

REFERENCES:

[1] Schoenmaekers, J.; ESOC/OAD: IOI FDWG Orbit Determination Compatibility; Final report; 18. December 1992

[2] Schneller, M.; GSOC: IOI FDWG Recommendations to the Columbus/Hermes project; 12. February 1993

SCD1 ORBIT DETERMINATION SYSTEM: PRE-LAUNCH PREPARATION, LEOP PERFORMANCE AND ROUTINE OPERATIONS

Hélio Koiti Kuga[†]

Kondapalli Rama Rao[‡]

INPE - Instituto Nacional de Pesquisas Espaciais

CP 515 - São José dos Campos - SP

CEP 12201-970 BRAZIL

E-Mails: [†]HKK@DEM.INPE.BR, [‡]KRR@DEM.INPE.BR

Abstract

This paper presents a complete overview of the Orbit Determination System (ODS) software developed by the flight dynamics group of the Division of Space Mechanics and Control (DMC) of INPE, for the first Brazilian satellite SCD1. The paper is divided into four parts. The first part explains in brief the SCD1 mission, its ground and space segments and the principal characteristics of its launch system. The second part, i.e. the pre-launch preparation of the software, describes the structure of the ODS adopted for SCD1, and includes a brief history of its development, of its testing with real data of foreign satellites, and of its assessment through the comparison of accuracies obtained. The third part, i.e. the Launch and Early Orbit Phase (LEOP) performance, narrates the experience of the flight dynamics group on the fateful day of the launch: all the odds against the process of orbit determination in terms of lack of enough tracking data, failure of the launch vehicle staff in providing the injection information, last minute modifications of the flight plan, and a few hours of anxiety which preceded the successful follow-up of the mission. The fourth part, i.e. the routine operations part, explains the methodology adopted for using the ODS in day-to-day operations, the accuracy in extended pass-predictions for the Brazilian tracking stations, and the overall performance of the ODS for SCD1. In addition, one also comments about the necessary modifications made during the routine operations along time and possible future improvements to be introduced in the software for the upcoming missions.

Key words: Orbit Determination, Flight Dynamics Operations, SCD1 Orbit Computations.

Introduction

Under the "Complete Brazilian Space Mission (MECB)" project, the first Brazilian satellite SCD1 was designed and manufactured by the Brazilian National Institute for Space Research (INPE), and was successfully launched by the Pegasus rocket of Orbital Sciences Corporation (OSC), USA on 9th February 1993 at 14:42:20 UTC. Since the conception of the project until this debut of Brazil into the space club consisting of very few countries, it has been a long journey for INPE, in general, and for the flight mechanics personnel, in particular. Amongst many others, one of the main responsibilities of the INPE's flight mechanics group was the development of the complete Orbit Determination System (ODS) for SCD1. Starting from the pre-launch preparation of the software¹ where it was tested with real data of foreign satellites, through the Launch and Early Orbit Phase (LEOP) usage, where the problems arisen were dealt with extreme efficiency by the software², until the routine operations in the Satellite Control Center (CCS), where extended pass-predictions are made regularly for the Brazilian tracking stations, the ODS of SCD1 has a long history. Dividing into four parts, the whole development of the ODS - the history as well as the technical details - is described here, after summarizing in brief the details of the SCD1 mission, its ground and space segments and the SCD1 launching system.

SCD1 Mission

SCD1 is an experimental low Earth orbit satellite for real time reception and retransmission of weather data collected by various data collecting platforms (PCDs) spread over the Brazilian territory. The weight and height of the spacecraft are 108 kg and 0.7 m, respectively, and its shape is a right octogonal prism whose base fits within a circle of 1 m diameter. The nom-

inal orbit was planned to be a 750 km circular at an inclination of 25° so as to cover the entire Brazilian territory. Everytime when the satellite is in the visibility circle of Cuiabá, any PCD within the coverage angle of the satellite payload antennas would have its VHF signal relayed by the satellite to Cuiabá in S-band. In addition to the primary mission of the data relay, the satellite is planned to carry two more payloads: one to flight-test solar cells made by Brazil and the other to flight-qualify an on-board computer.

SCD1 Ground Segment

The Satellite Control Center (CCS) situated at São José dos Campos, in São Paulo state, where the INPE head office is located, is the main component of the ground segment, whence the SCD1 and also all other future Brazilian satellites are planned to be controlled. The engineers and the scientists of INPE have developed the complete software package to be used in the CCS during the operational phase of the satellite SCD1. The TT&C S-band stations located at Alcantara (ALC) and Cuiabá (CBA) are intended to be used during the various phases after launch, the former to be used also during the acquisition phase of the satellites. Currently, Cuiabá has the capability of performing ranging and angle measurements, and is provided with a system of automatic acquisition and tracking of satellites with the help of an antenna of 11 m diameter. It is the master station and receives the payload data as well. Alcantara, located nearby the future satellite launch base, has ranging capability, besides TT&C, and is mostly used during the LEOP and as a hot backup to Cuiabá. It is also provided with an additional acquisition antenna with a larger beam to facilitate the acquisition of satellites around the horizon. A tilt mechanism to deal with zenithal passes of spacecrafts is also a part of the ground station complex. Alcantara is steadily going to become fully operational and is nowadays participating in the routine tracking of SCD1. The integration and testing of the satellites are to be done at the Laboratory of Integration and Testing (LIT), which also is located at INPE, São José dos Campos, and where the satellites are to be built and ground-tested for vibration, thermal control etc. In essence, the ground segment consists of the CCS from where the satellite controlling operations are executed, and the tracking stations Cuiabá and Alcantara, all located in Brazil.

SCD1 Space Segment

One of the most important characteristics of the SCD1 space segment is that it is a spin-stabilized satellite. Its attitude control subsystem is equipped with a magnetic torque coil in order to maneuver the spin-axis orientation in space. At launch, the spin rate would

be 120 rpm which would decrease along time, mostly due to the action of eddy currents, until the spin axis becomes non-maneuverable. A useful lifetime greater than one year is expected. The subsystem equipment is mounted on three horizontal panels such that one of the principal axes of inertia coincides with the spin-axis. In normal operation, the nutation is negligible by the action of a nutation damper. The lateral panels and the upper panel are covered with solar cells which provide the primary electrical power when illuminated by sunlight. The thermal control is achieved by passive means such as the use of heat shields, disposal of the excess heat through the bottom panel which is not covered by solar cells, selective coating of the interior parts and electronic boxes, etc. The solar aspect angle with the spin-axis is required to be in the range of 0-90° in order to assure power generation. The range between 90-180° is forbidden due to thermal constraints, meaning that the bottom panel should never be illuminated by the Sun. Sun and magnetic sensors have been provided for the attitude determination.

SCD1 Launching System

INPE hired the OSC to launch the SCD1 by means of the Pegasus rocket. This launching system is somewhat different from usual launching systems. Initially, the Pegasus rocket is fixed under one wing of a B-52 airplane carrier specially adapted for this purpose. When the carrier reaches a pre-computed drop-point, it drops the rocket, which, in its turn, is ignited and rises up to the injection point. Three rocket stages are used to accomplish the final injection point. Before the release of the rocket from the carrier, the mission can still be delayed if some mal-function is found. In case the problem can be solved quickly, it would make another overfly to the drop-point for another launch attempt 25 minutes later. For this mission, due to launch window constraints, only two overflies at well-established times were scheduled so that the flight dynamics team could pre-fix the nominal orbital elements at the corresponding times. A complete scenario was set beginning few days before the departure of the B-52 carrier from the West coast (Edwards Air Force Base) until its arrival to the East coast of USA (Kennedy Space Center) at a shuttle landing facility. On the launch day, the B-52 would take-off from the facility, fly up to the drop-point located at 29°N and 79°W with around 41500 feet of altitude and release the Pegasus rocket. After 5 seconds in free fall the rocket would then follow its own programming, from first stage ignition through second stage ignition, third stage ignition, coasting and spin-up, up to orbit insertion eleven and half minutes later.

Qualification of ODS

The estimation method on which the ODS software is based upon is that of weighted least squares differential correction. The software was thoroughly tested, analyzed and qualified using the real data of various satellites from different organizations¹. GIOTTO (Halley comet encounter mission), SPOT (French Remote Sensing Satellite), HIPPARCOS (a European Star Mapper Scientific Satellite), IRS (Indian Remote Sensing Satellite), and the BRASILSATs (Brazilian Telecommunications Satellites) are the satellites whose tracking data have been used in this software qualification. In order to make the assessment of the software more reliable, different combinations of perturbation models have been employed in each test case. The test results obtained in the case of GIOTTO are given here as an example.

In the case of GIOTTO, two test cases were run in the DEC-Vax 780 digital computer. Table 1 shows the cases selected. Only range measurements with a standard deviation of 5 meters were taken into account in both the cases. For case 1, the Keplerian orbital elements of ESOC-ESA (European Space Operations Center-European Space Agency) were available for comparison, and this case was run with complete perturbation model, viz., geopotential function with zonal harmonics upto 9 and tesseral harmonics upto 6, air drag and sun-moon gravitation. For case 2, since RMS (Root Mean Square) of residuals for the three stations with various combinations of perturbation models have been supplied by ESOC for comparison, this case was run with the same combinations of perturbation models.

In the first case, the comparison of the Keplerian elements obtained by our software with those obtained by ESOC is given in Table 2. Here, one can see that the results obtained by INPE are very much in agreement with the results obtained by ESOC. Although the differences in the true anomaly u and the argument of perigee ω values are around 0.05 degrees, the difference in the sum of the argument of perigee and the true anomaly, which is more important, is less than 0.01 degrees.

Table 2: Comparison in the case 1 of GIOTTO

Orbital element	ESOC	INPE
a (km)	24477.0	24476.8
e	0.731315	0.731319
i ($^{\circ}$)	6.990	7.009
Ω ($^{\circ}$)	264.72	264.76
ω ($^{\circ}$)	177.95	177.89
u ($^{\circ}$)	354.62	354.67

In the case 2, the comparison is done between the RMS of residuals for the three stations with various combinations of perturbation models: (1) zonal har-

monics upto 6 and air drag, (2) model (1) plus lunar attraction, (3) model (2) plus tesseral harmonics upto 6, (4) same as model (3) except that the zonal harmonics are taken upto 9, and (5) model (4) plus solar gravitation. The corresponding results are given in Table 3.

The comparison in Table 3, where the RMS of residuals are given in meters, shows that the results of INPE are reasonably good and comparable to a very great extent with those obtained by ESOC. The slight deviations that exist may be due to the modes of correction, probable differences in some constant values, the very manner of programming etc.

LEOP Performance of ODS

The primary task of the flight mechanics group during the LEOP phase was to assure the acquisition and tracking of the satellite from the injection time on, by estimating the orbit and sending the tracking schedule to the ground tracking stations. However, this simple-looking task turned out to be a breath-taking experience for the group because of various problems surfaced along time², since fixing the first launch date. Postponement of the launch not only by few days and weeks during a period of nearly two months but also by few hours and minutes on the day of launch forced the flight mechanics team to recompute and reconfigure several computer files in accordance with the launch dates, times and launch window constraints. Failure of the ranging equipment at Alcantara due to a power shortage restricted the group to use, for orbit determinations, only the tracking data of Mas Palomas for the first orbit and that of Cuiabá from the third orbit onwards. The most shocking event occurred when an 'abort' command was given by one of the Wallops Control Center operators as the B-52 arrived at the drop-point, and especially, when it was not obeyed and the rocket was launched. The next eleven minutes of second-stage ignition, third stage ignition, spin-up and separation was accompanied by the group, as well as the systems group, dumb-founded. Acquisition Of Signal (AOS) immediately by Alcantara station confirmed a successful launch but the problems were not yet over. The climax came when OSC could not provide the correct injection time due to a clock failure and the group was in a real fix. However, having Alcantara AOS time, the group estimated quickly through some backward extrapolation that the injection time should be most probably around 14:42:20 UTC. After fixing our estimate of injection time, new injection orbit elements were computed, tracking predictions were generated and sent to the ground stations. Unfortunately, however, Alcantara could not track the second orbit pass due to the delay in correcting this erroneous synchronization. Moreover, the very low elevation ranging data combined with very few observations from Mas Palomas made the OD process to diverge and pro-

Table 1: Test cases of GIOTTO

Case	Initial Time	Final Time	Reference Epoch	Amount of Data
1	85-Jul-02 12:24	85-Jul-02 13:17	85-Jul-02 11:38	23
2	85-Jul-02 18:14	85-Jul-03 10:10	85-Jul-02 18:00	87

Table 3: Comparison in the case 2 of GIOTTO

Force model	Malindi		Kourou		Carnarvon	
	ESOC	INPE	ESOC	INPE	ESOC	INPE
1	430	459	150	148	180	173
2	95	135	45	38	35	35
3	80	116	40	37	30	30
4	75	115	40	37	30	30
5	40	45	15	16	35	37

vided an unreliable orbit determination. And also the NORAD orbit elements which were expected to come within three hours of satellite injection into its orbit did not arrive on that day and there was no way to confirm our orbit determinations other than waiting for more tracking data. Anyhow, although the orbit determination schedule planned in advance by the flight mechanics group was completely upset with all these problems, it was reset again along time as the new data arrived and the tracking confirmed our injection time estimate and orbit determinations.

In order to analyze the accuracy of the successive ODs as well as the impact of the ODs in the tracking operation, the results of several ODs carried out during LEOP are shown in the Table 4.

The OD using single-pass ranging data from PAL was considered unreliable due to the fact of using few data points at very low elevations, less than 4°. PAL provided ranging only for the very first orbit.

The PAL+CBA₁ result used ranging from the PAL and the first pass over CBA. A poor and bad fit was accomplished and the OD result was not used at all. We see a very large difference compared with the nominal and the PAL solution, mainly in terms of the semi-major axis and eccentricity components. The sum $\omega + M$ was also somewhat misleading and undefined.

The OD-0 result used solely 2-pass ranging taken from CBA. The prospect seemed a lot better than the former ones with a fair fitting to the measurements. Nevertheless, we decided to wait for an additional pass of SCD1 over CBA to get more confidence in the result.

The OD-1 result used 3-pass ranging data from CBA and confirmed the OD-0 orbit parameters. Then, the first update of the tracking schedule was generated and sent to CBA and ALC stations.

The OD-4 result used 1-day ranging data from CBA (7 passes), and OD-6 used 2-day data (around 14 passes). The OD-6 result was considered the definitive OD of the injection orbit.

Afterwards, daily ODs were performed during 5 days

and once confirmed the good performance of the tracking schedule from the ground stations the ODs started to be performed on weekly basis.

Table 5 presents the actual pointing error on the AOS (Acquisition Of Signal) region of the CBA antenna, if the results corresponding to the listed ODs were used. The error analysis is made possible by direct comparison with the acquisition angles measured by the CBA antenna. The listed errors correspond to several orbits, namely the orbits O-4, O-5, O-6, O-8, O-17, O-22, and for 3 days (+3d) and 1 week (+7d) after the injection time. Together with the orbit number, in parenthesis are the elevations at which the errors were computed. The main aim of this analysis is to depict the possibility of acquiring or losing the rising satellite near the horizon, causing the tracking to be unfeasible by the CBA ground station antenna.

The pointing errors were computed by comparing, at the listed elevations, the collected azimuth and elevation measurements of CBA with the estimated azimuth and elevation generated by the corresponding ODs. The measured azimuth and elevation were smoothed beforehand and pre-processed, presenting certainly an accuracy better than 0.1°.

We can see that the use of the nominal orbit parameters would cause some troubles in the AOS and after orbit 6 (O-6) would make the AOS virtually impossible. The flight mechanics team was aware of possible large injection errors and set up the CBA antenna to make a large scan, with 6° by 4° amplitudes at the AOS region around 4° elevation, in order to acquire the satellite. Fortunately this facility proved very handy because it permitted the nominal orbit parameters to be used up to the orbit 4 (O-4). It was also by chance that the team obtained the OD-1 result on O-4 and sent the updated tracking schedule to be used from O-5 until O-8 inclusive.

Use of PAL solution would cause the AOS to be unsuccessful throughout. On the other hand, use of PAL+CBA₁ solution would be possible only until or-

Table 4: LEOP OD Results

Parameters	Nominal	PAL	PAL+CBA ₁	OD-0	OD-1	OD-4	OD-6
a (km)	7132.06	7241.31	7135.72	7140.00	7139.40	7138.12	7138.80
e	0.0018	0.0149	0.0153	0.0042	0.0044	0.0037	0.0039
i (°)	25.00	25.09	24.80	24.66	25.04	24.92	24.96
Ω (°)	185.42	185.03	185.69	186.70	186.58	186.24	186.17
ω (°)	284.76	142.07	50.85	120.45	98.76	9.84	351.51
M (°)	191.72	335.44	64.16	355.01	16.79	106.28	125.02
$\omega + M$ (°)	116.48	117.51	115.01	115.46	115.55	116.12	116.53

Table 5: Impact of OD accuracy on CBA tracking schedule

OD	CBA pointing error (°) at AOS region							
	O-4	O-5	O-6	O-8	O-17	O-22	+3d	+7d
Used	(8.6°)	(6.4°)	(8.1°)	(9.4°)	(8.0°)	(12.4°)	(5.4°)	(11.7°)
Nominal	2.2	4.0	5.8	7.6	16.0	35.9	85.1	147.9
PAL	27.6	34.1	40.7	47.2	85.1	106.9	13.0	49.8
PAL+CBA ₁	1.6	1.3	1.3	1.1	6.9	5.6	18.9	107.4
OD-0	1.1	0.9	1.1	0.8	3.3	2.3	5.2	14.3
OD-1	0.4	0.1	0.2	1.4	2.1	1.9	3.3	9.7
OD-4	0.1	0.2	0.3	0.2	1.0	1.5	2.7	11.6
OD-6	0.2	0.2	0.2	0.2	0.2	0.2	0.2	0.3

bit O-8. For the subsequent orbits the AOS would be doubtful.

We verify that OD-0 solution could be used until the orbit O-22, 2 days after the launch. The OD-1 solution is clearly not more accurate than the OD-0. The OD-4 solution, using 1-day of accumulated data, could be used a bit longer but was also not much more accurate than the OD-0.

The definitive solution OD-6, using 2-days of accumulated data, could even be used without problems for one-week tracking predictions. The level of errors are in the order of 0.2° compared to the measured pointing angles, which are accurate to better than 0.1°. This is an excellent outcome which describes the overall performance of the ground station tracking equipment in conjunction with the flight dynamics software.

Routine Performance of ODS

The OD in the Control Center is executed nowadays on weekly basis routinely. The accumulated 7-days ranging data are processed to produce the best orbit estimate. Based on this OD result, the normal procedure has been to generate long period Orbit Predictions (OPs) sometimes spanning up to 02 months duration. The main aim of the long period predictions is to use them in the attitude system software in order to predict and schedule the need of future attitude maneuvers.

To show the accuracy of extended OPs made weekly at the Control Center, at first, we exercised an Orbit

Determination (OD) based upon one week of accumulated ranging data from 01 to 07 December 1993 and generated OPs for the period from 08 to 21 December 1993.

Then, we performed several ODs, also based upon 07 days ranging, one for each day for the first week of the OP (08-14 Dec.). This sequence of ODs, considered as the reference, was compared with the OPs of the same period. Figure 1 shows how the OP deviates from the sequence of ODs used as reference. Position errors in the cross-track direction are not distinguishable, the radial-track direction seems to have a cyclic behaviour, and the along-track direction seems to grow up steadily as expected. Surprisingly the position error is not very pronounced, meaning that the OP is not degraded in one week of prediction.

Another test was to compare the antenna pointing angles, computed on basis of 02 weeks prediction (08-21 Dec.), with the angles effectively measured by the Cuiabá (CBA) ground station. The angle measurements, pre-processed and smoothed, are considered as having an accuracy better than 0.1°, as stated formerly. Figure 2 shows the shape of the pointing deviation between measured and predicted angles. As expected, the cloud of points shows clearly a trend of becoming larger and larger, but still accurate enough to allow tracking of SCD1 by the ground station, at least for the 02 weeks of OP of this test.

Therefore, generally speaking, the overall routine performance of the ODS has been completely satisfactory. A single OD every week is executed at the

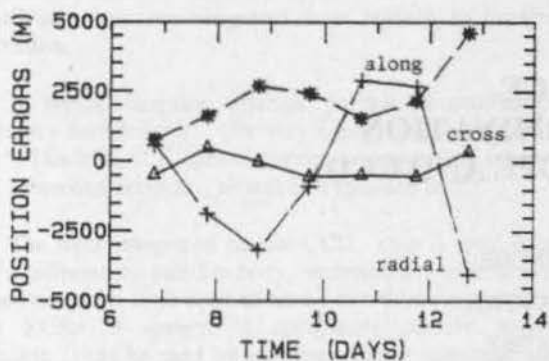


Figure 1: Orbit accuracy for one week prediction

beginning of the week and the OP file update follows. For the very few losses of the satellite passes none is reported to be credited to the ODS.

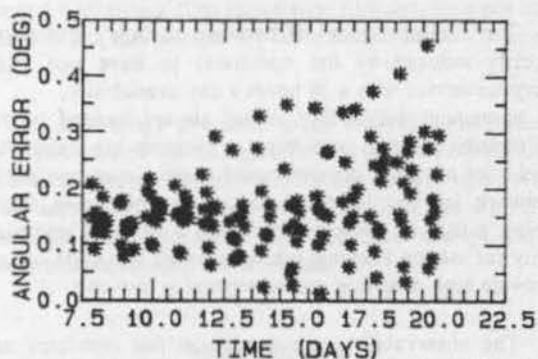


Figure 2: Antenna pointing accuracy for 02 weeks prediction

Modifications for Future Missions

For the upcoming SCD2 mission no major modifications in the present software are expected. A version to estimate the C_d (drag coefficient) and C_r (Solar radiation pressure coefficient) is almost ready for use, although this kind of perturbations can be considered very small for the SCD1 or SCD2 missions (750 Km altitude). We have been using the theoretical values calculated for these parameters and preliminary tests show that they are very badly observable in the SCD1 mission.

For the Remote Sensing Missions (SSR1 and SSR2), an extended ODS is being thought of. It should include the capability of considering station coordinate errors, measurement biases, alternative formulations of the orbit Differential Equations for improved accuracy, and numerically reliable algorithms for the estimation processes. Another "wishful thinking" is a real time

ODS including impulsive maneuvers estimation which could be used for the SSR satellite series. In this connection, some experience has been obtained from technological cooperations with other space agencies, viz. ESOC-ESA and GSOC-Germany.

Comments

It can be seen, from the experiences narrated in this paper, that the debut of INPE's flight mechanics group into actual spacecraft flight operations world is a great accomplishment. Firstly, a big effort was made to qualify the ODS beforehand by obtaining the real data of various satellites from different organizations. Secondly, considering the pressure exerted on the day of launch, the team proved to be very much experienced to overcome the adverse circumstances, which is very crucial. Despite the appearance of problems like the unavailability of ranging data from one of the two local ground stations, failure of launcher clock which made the injection time an incognita, lack of NORAD data in a critical time etc. one by one, it can be seen that everything worked fine. Although luck favoured a little bit as the launcher lofted the satellite in a near-nominal orbit and the preliminary ODs were useful, the right decisions taken at right times by the flight mechanics team gave excellent results during LEOP. Last but not the least is the wonderful performance of the ODS software in routine operations. All this together proves that the Orbit Determination of the SCD1 mission as far as the flight mechanics group operations are concerned, is a grand success.

Acknowledgements

We are very much indebted to Mr. S. Pallaschke of ESOC-ESA for providing the ranging measurements from Mas Palomas ESA ground station during the first orbit of SCD1, for the support and advices during the Orbit Determination software development, and for the help in calibrating the S-band ranging system of the Cuiabá and Alcantara Brazilian ground stations.

References

- ¹Kuga, H.K.; Kondapalli, R.R. "Analysis, Testing And Assessment Of The OD System For The First Brazilian Satellite." *3rd. International Symposium on Spacecraft Flight Dynamics*, Darmstadt, Germany, 30 Sep.-04 Oct. 1991, p. 149-153. ESA SP-326.
- ²Kuga, H.K.; Kondapalli, R.R. "Satellite Orbit Determination: A First-Hand Experience With The First Brazilian Satellite SCD1." *14th. Congress of the International Astronautical Federation*, Graz, Austria, 16-22 Oct. 1993, Paper IAF-93-A.5.43.

ROSACE ORBIT DETERMINATION USING TELESCOPE AND CCD

Luc MAISONOBE

Geneviève CAMPAN

Pascal BROUSSE

CNES, CT/TIMS/SG, Bpi 1214

18, avenue E. Belin

31055 TOULOUSE CEDEX

Email: luc @ kaula.cnes.fr

Abstract

This paper describes the ROSACE system, a low cost ground system using optical devices (telescope and CCD) in order to achieve high precision orbit determination. The elementary measurements are angular separations between the satellite spot and the dotted path of a known star. Those measurements are performed without any onboard equipment, thus allowing ROSACE to be used in contingency cases with non-cooperative satellites.

The layout of the various components of a ROSACE station is described. The results of the preliminary studies presented here show that even with a pessimistic measurements rate, ROSACE can reach the level of accuracy of the best and expensive systems already in use in the field of geostationary satellites.

An overview of the space systems that could benefit of ROSACE stations ranges from high precision needs (for colocated satellites cluster control or station calibration) to small budget mission, including emergency localization of dead satellites or debris.

Keywords: orbit determination, high accuracy, low cost, optical measurements, CCD, geostationary satellites, telescope.

Cost/accuracy trade-off

Ground stations are expensive. If both high precision angular measurements (for station keeping needs) and fast pointing capabilities (for station acquisition needs, near the perigee of a transfer orbit) have to be covered by the same large antenna (for example a 9m diameter Ku band antenna), this single antenna will play a major role in the overall cost budget.

The common trade-off between accuracy and cost is greatly induced by the constraint to have one multi-purpose device with a 24 hours a day availability.

A permanent availability is not always needed (station calibration systems and backup systems are examples), and a lot of space systems could share a common station network for day to day localization, their own station being a part of the network. Such a network optimized only for station keeping sake can break the trade-off and provide high precision measurements at low cost.

The observability rate needed in this restricted area allows the use of optical wavelengths, since a sufficient number (say about 3) of well chosen stations reduces the risk of bad weather over every station simultaneously.

Optical wavelengths are several orders of magnitude smaller than radiofrequency ones (0.6 μm versus 2 to 15 cm), hence the diffraction pattern of the image of a point is far much smaller in the focal plane of a telescope mirror than in the center of phase of an antenna dish. A localization antenna has only one detector at the center of phase, and measurements are performed by moving the antenna. A telescope has a detector mosaic (human eye, photographic plate, CCD chip) that extracts an image from all field of view, without any motion.

The stars in the image can be used as position references. It is therefore possible to extract angular information from image data only. This is the principle used in ROSACE stations.

Using a celestial reference within the image itself prevents various errors from perturbing the measurements. Those errors are: pointing errors, optical and mechanical axis misalignments, axis torsion, wind effects, orientation readings, radioelectrical pattern modelling. Another error, even if not removed, can be drastically reduced: the refraction effects. Since the reference is close to the

measured point, the refraction model is used only inside a small area, and not integrated from horizon to satellite elevation.

A typical angular antenna provide measurements accuracy between 0.01° (for very expensive antennas) and 0.1° . The ROSACE optical system is expected to achieve a 1 arcsecond accuracy, as will be explained later.

The light integrated on the CCD chip is only solar light reflected by satellite body, antennas and solar arrays. Therefore there is no need to have any onboard equipment, the ROSACE system is completely passive versus satellite. It can be used for satellites already launched, and for non-cooperating satellites during contingency phases.

The high accuracy of optical system is known from a long time ago, and was used for example with the Baker-Nunn cameras. Those camera were Schmidt wide field telescopes ($5^\circ \times 30^\circ$) and did use photographic film. The operational and technological constraints on such systems (manual operations, film sensitivity, film development and analysis) led this system to be forsaken about 20 years ago.

The technology available today reduces considerably the drawbacks of optical systems. Powerful workstations are able to perform most of the routine control operations of an automated telescope, and CCD detectors converts faint light level into measurable electrical charge, those measurements feeding the workstation.

Measurements

As explained above, ROSACE elementary measurements are angular separations between satellite spot and position references given by stars in one image of a field of view around the satellite.

Geostationary satellite reflected light is rather low, as an example HISPASAT magnitude is around 9.5 and METEOSAT magnitude is around 14.5 (solar time dependant); on the other hand, there are a lot of stars brighter than those satellites, a common estimation being 1000000 stars brighter than 11^{th} magnitude.

Those figures have led us to decide ROSACE station will nominally track the satellite if its angular velocity is above a threshold depending on its magnitude (for example small satellites in inclined orbits or satellites far below geostationary arc), and will be completely motionless if velocity stays below this threshold.

During the light integration period, stars images will travel across the detector mosaic and draw a bright line. The chosen detector is a CCD chip, 512×512 pixels wide for the prototype. CCD chips are extremely sensitive with a quantum efficiency between 40% and 80%, versus 2% to 4% for photographic plates, furthermore CCD chips are electronic devices and hence can be directly inserted into

an electronic measurements bed. An early experiment showed that a 500 mm diameter, 2 m focal length telescope and a classic CCD chip would allow stars down to magnitude 10.7 to be detected even if they stay only 0.13 second over each pixel (that is to say if they travel at 15 arcsecond per second, which is earth motion).

Each star brighter than magnitude 10.7 will draw a detectable line, giving position information. A shutter will split those lines into several dots, giving time information with the help of a precise clock connected to it. One star path is enough to compute the direction of the satellite at a given date, since the path give both a point on the unit sphere and the East/West direction, the measurement is not a traditional astrometric reduction, which requires at least three stars.

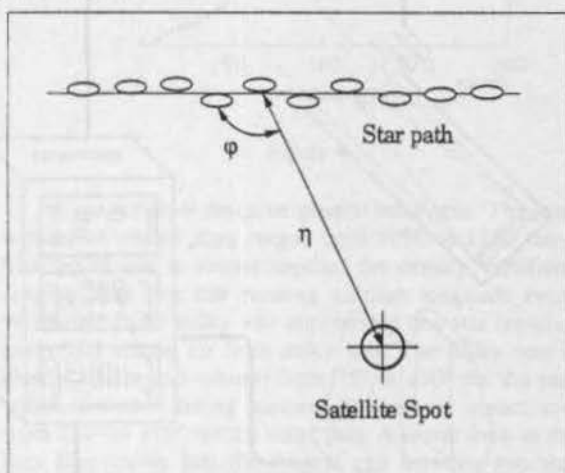


Figure 1: Elementary measurement

Data extraction

The image analysis involve several steps.

First of all, once image is acquired, some calibration is realized to correct any offset or gain biases of the photometric response of each pixel of the CCD detector. Some abnormal pixels can be detected at this step, due for example to high energy gamma rays.

The second step is the extraction of the spots from the background and the computation of some statistics about each spot (centroid position, global brightness, size, ...). After this step the information is not an image anymore but a collection of individual objects.

The third step is the analysis of the individual spots in order to identify the dotted lines of the stars, the satellites and the eventual planes and meteoroids which pollute the field of view. The identification uses both the object collection, a precise star catalog, and some coarse information about the orbit of the target satellite and the telescope pointing.

The last step is the true measurement. First the refraction effect is computed for each individual spot, and then the star path is precisely adjusted against a theoretical model to remove atmospheric turbulence effect, the satellite spot position is computed according to each star line, producing a measurement that can be weighted with the turbulence noise estimated from image data, this information being transmitted to the end user who can use it if his orbit determination system supports it. The measurements can be presented as dated azimuth elevation data, thus allowing their use in most existing systems.

Station layout

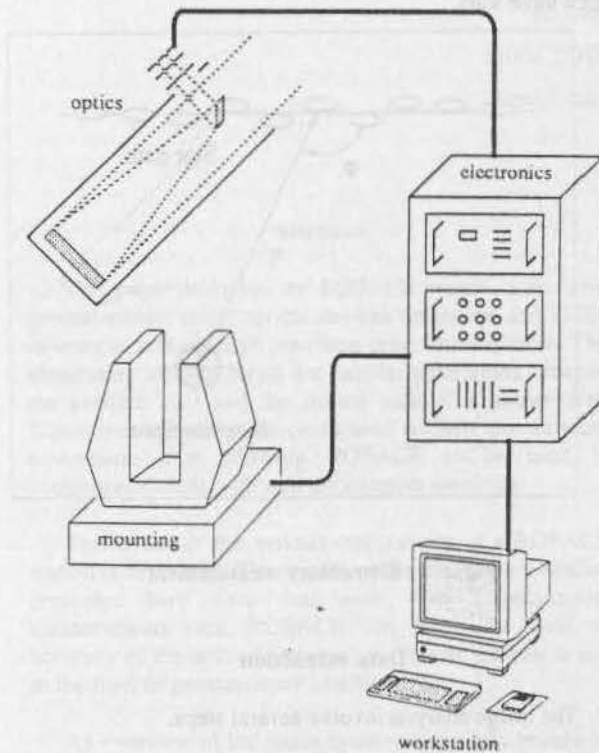


Figure 2

The main device of the ROSACE station is the telescope. Considerations of field of view, limit magnitude, insensitivity to light interferences, and cost have led to choose a traditional Newton design with a 500 mm diameter and 1900 mm focal length.

The CCD detector is a commercially available 512x512 MPP chip that doesn't need much cooling during use (cooling greatly reduces thermal noise for long integration time but need heat evacuation systems : MPP chips are less sensitive to thermal noise than older chips). The CCD camera produces a 12 bit deep numeric image.

Between the telescope and the CCD detector at focal plane, one would find focusing and field orientation mechanisms, a field corrector, a filter and a shutter.

The field orientation mechanism allows the use of rectangular CCD chips and optimization of field of view depending on star-satellite predicted distance.

The focusing system can defocus the telescope when bright stars are to be used as reference, since the light can be spread over several pixels thus increasing centroid position accuracy. Both orientation and focusing data are computed before image acquisition, during a planification phase.

The field corrector is used to reduce coma aberration that affects wide aperture telescopes. This correction is especially important if one is to observe a spot near the field border with a wide CCD chip, and depends on the telescope aperture.

The filter prevents waves shorter than 650 nm to hit the detector, it is a red filter. This is used to reduce two atmospheric effects. The first one is the chromatic dispersion at low elevation, this effects spreads vertically the image with red light at top and blue light at bottom. The chromatic dispersion effect induces an error in photometric centroid position and should be corrected, hence the red filter.

The second effect the filter counteracts is the Rayleigh diffusion of sky background, this effect enhances sky intensity near the moon, reducing it allows to perform observations closer to the moon disk.

The shutter is used to introduce time information into star paths, this information will be used both for path modelization and for measurement precise datation.

The telescope is supported by an altazimuth mounting. Very precise stepper motors drive the high precision wheel and worm devices that control mounting orientation.

The electronic set includes all controlling cards involved in the stepper motors, shutter, and CCD camera use, as well as some acquisition cards for external data such as meteorological and time data. One important design choice was to use as much as possible commercially available packages.

As an example, shutter datation is performed by an easily designed card that uses the shutter electronics pulse and the PPS pulse of a standard GPS receiver.

All electronic devices are controlled by one UNIX workstation. The software architecture is implemented under the Mercator environment that provides general purpose mechanisms for data stream acquisition and use, both in real time and on a postponed basis.

Mercator software insertion facility was used to include software specifically developed for ROSACE needs into an homogeneous system. All software packages are included in the controlling workstation, therefore the

station can operate as a standalone localization station, performing all measurements scheduling, acquisition and analysis, up to orbit determination. The standard wide area network facility can also be used to download all measurements priorities from a main control center, and to send it back all measurements data after completion, should the station be a part of a more general system.

Preliminary studies results

One of the most important question that has arose during feasibility studies was: what are the elementary measurements rate and accuracy? Despite a very poor star catalog (less than 260000 stars down to 11th magnitude), the statistics were good enough to allow the "small" telescope described earlier to be chosen.

The repartition of the stars in the available catalog are shown on figure 3. One can see that there is a cutoff between magnitude 10 and 11. This cutoff is due to the catalog small size, the omitted stars being mainly faint stars. Therefore, the rates given in the following paragraphs are pessimistic.

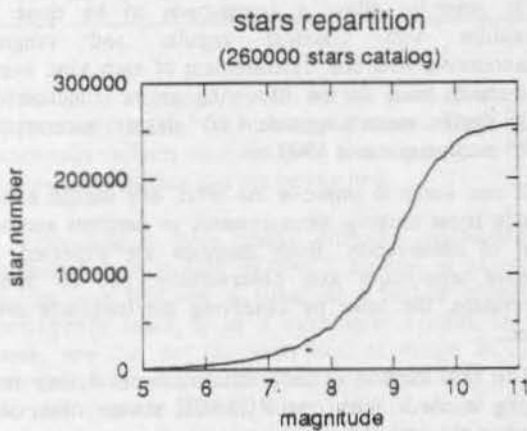


Figure 3

An amateur astronomer using a telescope and a CCD camera very similar to those foreseen kindly took a test picture of an open cluster without any star tracking. This test picture has been analyzed and showed that stars as faint as 10.7 magnitude could be used as reference stars. There are about 255000 such stars in our small catalog, and the real number is certainly much more important. This number is very large, but stars repartition in the sky is not uniform.

Figure 4 gives more reliable informations about measurements rates. Given an observation geometry (station latitude, station/satellite longitude difference), the earth rotation leads the satellite to be seen at a fixed declination. For example a 45° north station sees the satellite at same longitude at -6.83° declination. Taking into account the field of view height, all stars inside a

known declination band can be used as reference stars. Figure 4 shows the repartition of all those stars according to their right ascension. Each curve corresponds to a specific station latitude (between -45° and +45°).

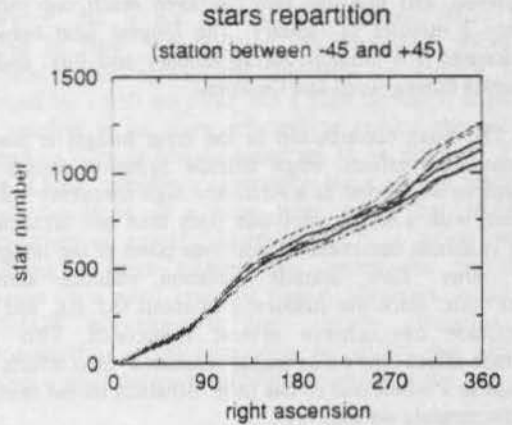


Figure 4

All curves show the same general behaviour. The total number of visible stars ranges from 1050 to 1250 stars. The repartition is almost regular, the density variations ranging from one star crossing satellite longitude every 46 second inside milky way regions and one star crossing every 103 second far from milky way. The milky way is clearly visible and extends from 75° to 130° for the part which is visible during northern hemisphere winter, and from 270° to 310° for the other part. A closer look to the data files shows that the longest gap between two star crossings is always between 10 and 14 minutes. During those moments the telescope could be pointed to other station keeping slots where measurements are possible.

Figure 5 shows for several station latitudes the holes repartition for holes leading to more than 5 minutes without any star crossing. The total number of holes lies between 24 and 35. As could be expected there are less wide holes near milky way than far from it.

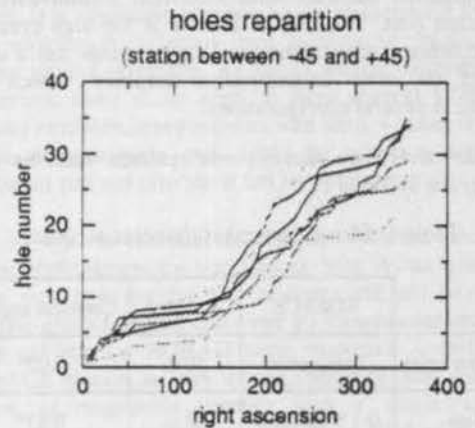


Figure 5

Taking into account all stars and holes repartition effects and using a simulation including operational constraints (time between picture acquisitions, field of view pointing, ...) we can conclude that at least a mean rate of one picture every 3 minutes all year long can be achieved, and that this rate can even reach one picture every 2 minutes in January. The longest time between exposures is 8 minutes during January and July, and 14 minutes during April and October.

The main contribution to the error budget is due to atmospheric effects. High altitude agitation causes the image to be blurred at a relatively high frequency (about 1 Hz), with a small amplitude (less than one arcsecond) and is almost decorrelated from one point of the image to the other. Low altitude agitation induces another behaviour, since the frequency is about 0.1 Hz, and the amplitude can achieve several arcseconds. This low altitude effect (known as casual refraction) also affects the image as a whole and so has little influence on the relative measurements we use.

The other contributions to the error budget are pixel size (center of each spot is positioned with a 0.2 pixel error), time resolution (limited by both shutter speed and clock ticks), references knowledge (star catalog and station position), and refraction modelization.

A reasonable estimation of all these error factors have been realized, the overall error budget stays below 1 arcsecond. Keeping in mind the fact that each observation site have their turbulence peculiarities that could greatly affect the turbulence figures given above, we have chosen 1 arcsecond as the target accuracy for elementary measurements.

Orbit determination with ROSACE system

ROSACE provides true angular measurements. Simple geometry is sufficient to transform the separation and phase angle between satellite and stellar reference into elevation-azimuth angles. The main advantage of this transformation is the possibility to feed existing orbit determination software with ROSACE measurements at minimum cost. The only difference is the high precision of elementary measurements. This precision has a direct impact on orbit determination accuracy, which was studied in several configurations.

The covariance analysis was realized with the input data given in Table 1:

Table 1: Elementary measurements accuracy

	ROSACE	Ranging	Classical angular
Random error	1 arcsecond	10 m	0.02°
Bias	0.1 arcsecond	30 m	0.03°
Datation error	1 ms	1 ms	1 ms

For all simulations, a rate of one picture every 30 minutes was chosen for ROSACE measurements, far under the limit our small star catalog gave. This choice corresponds to the fact it allows one telescope to be used on several orbital slots during the same night. The best accuracy is achieved when the telescope keeps switching between the slots all over the night, thus distributing measurements over the orbit. This distribution increases observability of semi-major axis, which is the least observable parameter from the point of view of angular measurements.

The first result was obtained with only ROSACE measurements covariance analysis. Inclination is very easy to observe (we perform angular measurements). Longitude is also accurately determined, despite the gain is less important. Even with only one station and a short six hours night, remaining uncertainties are $2 \cdot 10^{-4}$ degree for inclination and $3 \cdot 10^{-3}$ degree for mean longitude¹. Eccentricity is more difficult to determine, since the residuals are $3 \cdot 10^{-5}$ with one station during one short night, and since we need two stations to reduce it below 10^{-5} . Semi-major axis is quite unobservable. Even with three widely separated stations, there is still a 300 m uncertainty.

In order to allow a comparison to be done, a simulation with classical angular and ranging measurements with one measurement of each kind every 30 minutes leads to the following errors : inclination $4 \cdot 10^{-2}$ degree, mean longitude $4 \cdot 10^{-2}$ degree, eccentricity $1 \cdot 10^{-4}$, semi-major axis 1300 m.

If one wants to improve the orbit, one should either include some ranging measurements or perform another night of observation. Both methods are expected to improve semi-major axis observability, one by direct observation, the other by observing the longitude drift effect.

The first method is very efficient even if very few ranging is used. With one ROSACE station observing during night and three classical ranging measurements (noon the day before, midnight, noon the day after), semi-major axis error drops to a little more than 70 meters.

Eccentricity is also best determined ($8 \cdot 10^{-6}$) and longitude accuracy is slightly decreased. Care should be taken with the weight of distance measurements (they are less accurate than ROSACE measurements). With badly chosen weights, semi-major axis will be good, but other parameters can be very badly influenced with too much confidence to ranging.

The second method is even more efficient. The semi-major axis error lies between 5 and 10 meters, and the other parameters are either not influenced (inclination residuals are just below $2 \cdot 10^{-4}$ degrees) or enhanced ; eccentricity uncertainties is $4 \cdot 10^{-6}$ and longitude is accurate to $4 \cdot 10^{-4}$ degree. These results are achieved with

¹ All results given here are 3σ errors.

only one station. Using three widely separated stations surprisingly does not increase much the overall accuracy.

The influence of elementary measurements accuracy was evaluated in the configuration with one station during two nights. Table 2 shows the results:

Table 2: Influence of elementary accuracy upon orbital parameters

Elementary measurements (arc seconds)	1.0	1.5	2.0	2.5	3.0	3.5	4.0	4.5	5.0
Semi-major axis (meters)	6.5	9.7	12.9	16.1	19.3	22.6	25.8	29.0	32.3
Eccentricity vector (10^{-6})	3.7	5.5	7.3	9.1	10.9	12.8	14.6	16.4	18.2
Inclination vector (10^{-4} deg)	1.5	2.1	2.8	3.4	4.0	4.6	5.2	5.8	6.4
Longitude (10^{-4} deg)	3.9	5.7	7.6	9.4	11.2	13.0	14.9	16.7	18.5

As could be expected with such a level of accuracy, we are still inside the linearity domain. There is no exponential effects and we have some margins event if elementary accuracy can not be reached.

According to those results, differing approaches can be followed to include ROSACE stations in an ground system. The first one is either as a backup system for contingency cases or as a calibration system. In both cases, one can not (or want-not) to merge ROSACE measurements with classical ranging, ROSACE is to be the reference. In such a case, one six hours night is sufficient for a first guess and two nights are sufficient even for very high confidence levels. The second approach is as a common low cost day to day operations system. The best thing to do there is to include ranging measurements (they are also very cheap) and to limit the measurements duration.

The second result is that the number of ROSACE stations can hardly be used as an accuracy enhancer. However, increasing stations number and distributing them over the world would greatly increase the availability of the system. This is due to the fact that optical measurements can not be performed at all if clouds are covering the sky. Since one station is sufficient for orbit determination, even if one switches from one longitude slot to the other and return on the same satellite only twice per hour, it is possible to constitute a network where each station is nominally dedicated to one satellite but still can perform measurements to other satellites and provide them to stations covered by clouds.

Atmospheric effects

The main drawback of optical measurements is the need for clear nights. Station implantation sites are to be chosen according to the average number of clear nights. However, this is not the only atmospheric effect that should be taken into account. As explained before, a chromatic effect spreads the light near the horizon. It is reduced by a 650 nm filter, but a high elevation angle of the satellite is far more efficient to reduce this effect. Therefore sites at low latitudes are to be preferred. Last effet is local turbulence sensitivity, but a precise study of local turbulence is a long term study that requires installation of specific instruments. It is worth when installing a large astronomical instrument, but less obvious for a small low-cost station. However, installing ROSACE telescopes at sites already identified by astronomers is a very interesting possibility that will be analyzed when network installation will be on the run.

Potential users

As explained before, ROSACE system main advantages are high accuracy, low cost, and passivity with regard to satellites. Therefore, several different ground systems could benefit of it.

High precision measurements can increase confidence upon determined orbits of colocated geostationary satellites. The safety margins applied to separation strategies can be reduced thus reducing the eccentricity control cost. Another feature that could be of interest in the field of colocated clusters is the ability to perform relative measurements, without any star in the field of view. Those measurements are used to determine directly the separation parameters which are of interest for coordinated station keeping strategies.

High precision measurements is also the key feature to be used in the case of station calibration. As ROSACE uses a technic very different from classical antennas, its use as a calibrator allows a more precise crosscheck of all effects. It is absolutely independant of transponder delays, uses wavelength differing from localization bands, and has no ground reference. As far as station calibration is concerned, there is no need to have several ROSACE stations available, since one can wait until weather is clear above the telescope and since the accuracy increase additional stations provide is not very important.

Low cost is essential for backup systems, and is a major improvement for operational ones. As an example, some very light budget past missions did not have any specific ground station and even no transponder onboard (they did rely on NORAD radar systems). A dedicated ROSACE station is very cheap (between one and two orders of magnitude cheaper than a single angular antenna), and measurements sold by a ROSACE based network would reflect this fact.

Passivity is an outstanding advantage in contingency cases. Even when the nominal system does not include any ROSACE station, measurements can be performed by an external ROSACE network or station. Measurements can either be directly provided to the nominal orbit determination system using simple file transfers, or the orbit can be determined by the ROSACE network. ROSACE external interface is a traditional dated azimuth/elevation ephemeris which is very easy to translate into a format emulating classical antenna localization file with simple text editing scripts. Every space system, either already existing or still to come, could benefit of this facility.

Scheduling

ROSACE project is still under development. It is already protected by a french patent, and international patents are on the run. Both hardware and software development have begun, and the integration of the prototype is scheduled at the end of 1994. Year 1995 will be dedicated to prototype validation.

Conclusion

Available technology has allowed to revive optical measurements system, which are very accurate, cheap, and do not need anything onboard. Studies have shown that one ROSACE station can reach the accuracy level much more expensive system provide (like turn-around), as soon as you can wait two nights. Should a quicker response be needed, ROSACE measurements and even scarce ranging measurements can be associated for orbit determination, with some care concerning the weight of each measurement. A global network can be used to increase system availability, but has little impact on overall accuracy. ROSACE system can be used for operational orbit determination only if permanent availability is not required, and can be efficiently used as calibration or backup system. ROSACE can also track satellites not specifically designed for that, for example satellites already launched. The system is to be operationally validated during year 1995.

References

- [1] Lunettes et télescopes - A. Danjon - A. Couderc - Ed. Blanchard - 1983
- [2] Astronomie générale - A. Danjon - Ed. Blanchard - 1980
- [3] Astronomie CCD - Ch. Buil - Société d'astronomie populaire

- [4] Photographic observations of the colocated spacecraft at 19 deg West - H. Boehnhardt - 3rd International Symposium on Spacecraft Flight Dynamics - Darmstadt - 1991
- [5] Les mesures en orbitographie - A. Cariou - Cours de technologie spatiale - CNES - 1980
- [6] ROSACE Autonomous orbit determination system using deviation on CCD - L. Maisonobe - B. Lazard

REVIEW OF INPE/ESA ORBIT DETERMINATION FOR SCD1

S. Pallaschke

European Space Operations Centre, Flight Control Systems Department,
Robert-Bosch-Str. 5, 64293 Darmstadt, Germany

ABSTRACT

The support provided by ESA/ESOC to INPE concerning orbit determination aspects commenced in 1987, when INPE started with the development of their orbit determination system for the satellite SCD1. SCD1 is the first Data Collection Satellite of the Brazilian Space Mission MECB. The envisaged launch date was January 1989.

The launch preparation of the orbit related part included the following areas:

- development of orbit determination software
- analysis of the early orbit phase; external support, in particular, was envisaged because of the rather late acquisition of SCD1 by the INPE ground stations
- calibration of tracking facilities.

The ground facilities included the two stations Cuiaba and Alcantara. Both stations have been equipped with S-Band ranging systems, and in order to ease the exchange of tracking data between the two agencies the format of the ESA LCT ranging has been adapted by INPE.

Various tracking campaigns were organised for the validation of the INPE tracking systems. The station Cuiaba tracked the ESA satellite HIPPARCOS (geostationary transfer orbit type) in November 1991 and May 1992. Because of the nature of the orbit, these tests were considered as preliminary ones and precise ranging calibrations could not be carried out. Further tracking campaigns were organised with the ESA satellite ERS-1 (close earth, polar), i.e.: Cuiaba tracked ERS-1 in September/October 1992 and Alcantara performed ranging with ERS-1 in January 1993 shortly prior to the launch of SCD1.

The launch of SCD1 took place on 9 February 1993, and the satellite was also tracked during one pass from the ESA station Maspalomas. The ranging measurements of Maspalomas and of the first few days of Cuiaba were exchanged between the two agencies.

1. INTRODUCTION

The collaboration between INPE and ESA/ESOC in the field of orbit determination began in 1987 with some general coverage analysis for the launch of SCD1, the first Data Collection Satellite of the Brazilian Space Mission MECB. INPE planned to launch the satellite with a Brazilian launcher from Alcantara into a close earth orbit (height of 750 km, inclination of 25°). The envisaged launch date was January 1989.

The activities were split up into 3 areas:

- Orbit Determination Aspects
Provision of satellite tracking data (S-Band) by ESOC to INPE for tests of the INPE orbit determination software and comparison of the results.
- Orbit Analysis
Parametric study of the acquisition sequence for the launch phase of SCD1 taking into account launcher dispersion and the non-readiness of the Alcantara antenna system. For the latter case external support was considered, since the analysis showed that the other ground station, Cuiaba, would only acquire the satellite about 12 hours after launch (see Figure 1). Different scenarios were looked at, use of ESA ground stations, in particular Maspalomas, or support from ISRO, India.
- Station Calibration
Performance assessment of the tracking systems installed at the stations

Alcantara and Cuiaba by means of tracking ESA satellites.

The ESA satellites HIPPARCOS and ERS-1 were used for this assessment. The tracking data performed at the INPE stations were evaluated within the regular orbit determination at ESOC.

The collaboration between INPE and ESOC required a few visits. The dates and the purposes of these visits and the names of the persons involved are listed in order to provide an overview of the activities.

July 1987: H. Kuga at ESOC for SCD1 coverage and orbit determination analysis. An internal paper was issued (1).

Dec. 1987: S. Pallaschke at INPE for discussions on orbit determination software.

May 1988: P. Rozenfeld, S. Pallaschke at Bangalore, India for discussions concerning external tracking support for SCD1 from ISRO ground stations.

April/May 1990: H. Kuga, Kondapalli Rama Rao at ESOC in order to study the orbit determination software and to obtain some practical experience in this area. Two internal notes were written, one on the orbit determination software (2) and the other on orbit accuracy aspects of HIPPARCOS (3).

After the visit in Spring 1990 work still continued, in fact the most significant part, the station calibrations, were carried out after this date. The ground station calibrations were split up into two parts, the first in Nov. 1991 and May 1992 with the satellite HIPPARCOS to check out the tracking equipment and afterwards in Oct. 1992 and Jan. 1993 to calibrate the ground tracking systems with the satellite ERS-1.

Because of the delay in the development of the Brazilian launcher, INPE decided to launch SCD1 by a Pegasus rocket of the Orbital Sciences Cooperation, USA. The launch took place on 9 February 1993 and the satellite was successfully injected into the nominal near circular orbit with a mean altitude of 760 km and an inclination of 25° (4). Maspalomas provided tracking support during the first pass (see Figure 2).

The subsequent paragraphs summarise the activities and results of the INPE/ESOC collaboration concerning orbit determination aspects.

2. ORBIT DETERMINATION SOFTWARE

The set-up of the orbit determination software of INPE followed very closely the standard principles, which have been used for the various orbit determination packages at ESOC. The typical elements of the orbit determination are briefly described.

The orbit determination is normally based on tracking measurements carried out by various ground stations. Very often these raw tracking data are not directly suitable for the orbit determination and some preprocessing is necessary. An essential part of the preprocessing consists of proper smoothing by means of suitable mathematical functions, which also permit the rejection of incorrect measurements. The subsequent orbit determination is based on the resulting observations (range, range rate, angular data). The program could, for example, use a weighted least squares method to apply differential corrections to an a priori estimate of orbital parameters and to other parameters such as measurements bias, station coordinates etc. Two essential parts observe particular attention:

- Generation of satellite movement: The usual perturbing accelerations have to be included in the equations of motion, e.g. atmospheric drag, higher harmonics of Earth's gravity field, Sun and Moon gravitational attraction, solar radiation pressure and thrusts from orbit and attitude manoeuvres.
- Observations handling including the necessary corrections due to station position, atmospheric effects, Doppler shift, propagation delay, etc.

The determination of the orbit is followed by an updating of the satellite positional predictions, the accuracy of which depends on the quality of the orbit generator and the predictability of the parameters.

The last part, the scheduling and station visibility prediction part, is executed subsequently.

3. TRACKING SYSTEM

For the tracking of the satellite SCD1 a Tone Ranging System was implemented at the ground stations Alcantara and Cuiaba. The Tone Ranging System is, to some extent, compatible to the ESA LCT ranging system (5). The system employs a major tone with

a frequency of 100 kHz and a few minor tones with lower frequencies in order to establish a correspondence between the transmitted and received signals.

For reasons of compatibility with the ESA system, the generated output message is according to the SDID layout (6).

The total measured delay is the sum of

- the two-way distance between the ground station and the spacecraft,
- the delay in the signals through the station,
- the delay in the transponder onboard the satellite, and
- the additional delay due to atmospheric diffraction of the transmitted and received signals.

The calculated distance should refer to a point of the antenna which is constant and hence independent of the direction of the antenna. Such a point is the intersection of the azimuth-and elevation axis. For this reason, the ground calibration loop measurement has to be corrected.

The ground calibration loop measures the delay between the ranging equipment and the antenna (reflective converter). This delay includes various parts beyond the axis intersection point. Therefore a further ground calibration correction has to be included.

A further important point is of course the time tagging of the measurements. In case of the ESA LCT ranging system it refers to the transmission of the signal.

The station parameters are:

	ALCANTARA	CUIABA
Longitude (WGS72)	-44.404 273°	-56.069 801°
Latitude	-2.338 588°	-15.555 000°
Height	50.760 m	235.682 m
Calibration Loop	39088620 nsec	39148480 nsec
Correction	-18.54 nsec	-14.84 nsec

Various calibration campaigns were conducted during the years 1991 through 1993 in order to validate the tracking system and to verify the above quoted calibration figures. For this analysis the tracking data was exchanged between INPE and ESOC. The following procedure was applied:

INPE to ESOC: Transmission of raw tracking data in form of binary files via E-mail

ESOC to INPE: Transmission of preprocessed observations via telex.

4. CALIBRATION CAMPAIGNS

The calibration campaigns had in fact two goals, first to check out the ranging system and secondly to calibrate the tracking equipment at the ground stations Alcantara and Cuiaba. For this reason two types of campaigns were conducted, one with HIPPARCOS for the ranging check-out, and the other with ERS-1 for the calibration of the tracking equipment. The satellite HIPPARCOS stayed in an almost geostationary transfer orbit, and was therefore visible for longer periods, which offered better possibilities for repetitive ranging operations. However the satellite orbit could not be determined accurately because of the unmodelled effects of the attitude control around perigee. This attitude control mode was necessary to compensate the disturbing torques.

ERS-1 has a low Earth polar orbit and the satellite position has to be determined with an accuracy of better than 100 m. The ERS-1 orbit determination is based on precise altimeter data plus ranging measurements from Kiruna, Sweden. Because the ERS-1 orbit is known precisely, this satellite was used to calibrate the INPE ranging systems.

Within the past few years the following campaigns were conducted:

Date	Satellite	INPE Station	ESA Stations
11-13/11/91	HIPPARCOS	Cuiaba	Odenwald, Perth
05-07/05/92	HIPPARCOS	Cuiaba	Odenwald, Perth
29/09-02/10/92	ERS-1	Cuiaba	Kiruna (+ altimeter)
05-07/01/93	ERS-1	Alcantara	Kiruna (+ altimeter)
09-11/02/93	SCD1	Cuiaba	Maspalomas
17-20/12/93	ERS-1	Cuiaba	Kiruna (+ altimeter)

Only one calibration campaign was performed with Alcantara, the last one in Dec. 1993 was supposed to have Alcantara included as well, but the station was not available.

4.1 HIPPARCOS Campaigns

The satellite HIPPARCOS was launched in August 1989 in a transfer orbit with the aim of placing it subsequently in a geostationary orbit. Because of the failure of the apogee boost motor the satellite was manoeuvred into a modified transfer orbit with the following characteristics:

Height of perigee:	520 km
Height of apogee:	35740 km
Inclination:	6.8°
Period:	636.5 min.

In this configuration the attitude of HIPPARCOS was perturbed significantly around perigee due to the effects of gravity gradient and atmospheric drag. In order to maintain the attitude, a strong perigee control mode was necessary. Because this effect could not be modelled, the orbit determination of HIPPARCOS degraded significantly and the S-Band range measurement residuals from Odenwald and Perth increased from the expected 10 m to about 100 - 150 m. The satellite was operated up to August 1993.

Although HIPPARCOS had a degraded orbit determination performance, it was used for the initial check-out of the INPE ranging facilities. Two campaigns were conducted from Cuiaba in Nov. 1991 and in May 1992.

The essential figures of the two campaigns are summarised in Table 1.

The measurements performed during the first campaign had a nominal noise. However the residuals of the various passes showed a significant slope which was caused by a station timing problem.

During the second campaign the initial check-out of the ranging system was successfully completed. The residuals of the range measurements were in the order of 60 m, which compared well to the range residuals from Odenwald and Perth. However two parameters had to be estimated in addition, i.e.

time offset of -.08 sec
range bias of about -450 m.

Because of the degraded HIPPARCOS orbit determination performance it was not clear

whether these determined offsets were caused by the Cuiaba ranging system or not.

4.2 ERS-1 Campaigns

The satellite ERS-1 is the first ESA remote sensing satellite and it was launched in July 1991. The satellite orbit has the following characteristics:

Height	780 km
Inclination	98.5°
Local time of descending node	10:30

In routine phase ERS-1 is tracked from Kiruna, Sweden using range, Doppler and altimeter data (7). An orbit determination is carried out on a daily basis and uses tracking measurements over the past 3 days. Several hundred measurements are accumulated over a 3-day period and the mean residuals obtained are for

Range	better than 10 m.
Doppler	better than 3 cm/s and
Altimeter	better than 3 m.

With this amount of accurate tracking an orbit determination can be achieved which fulfills the positional requirement of about 70 m in total.

As the ERS-1 orbit is known precisely, this satellite was used for further calibration campaigns from the INPE ground stations Alcantara and Cuiaba.

Three campaigns were conducted during the years 1992 and 1993. The essential figures of the campaigns are summarised in Table 2.

Because the three campaigns were spread over more than a year, different station parameters were considered within the evaluation. For the first campaign in Oct. 1992 the station coordinates of Cuiaba had to be estimated as well, as the final information on the station locations was not available at that time.

In order to obtain small residuals of the INPE range measurements, a range bias and a time bias had to be estimated. Especially the estimation of the time bias improved the solution significantly.

The estimated bias figures were:

Date	Station	Time bias (sec)	Range bias (m)
Oct. 1992	Cuiaba	-232 sec	-31.9 m
Jan. 1993	Alcantara	.200 sec	5.7 m
Dec. 1993	Cuiaba	.203 sec	-36.1 m

The interpretation of these results is difficult, since not all the figures are consistent. The range bias of Cuiaba is similar for the two campaigns, but the time bias is not. A modification could have been introduced in the ranging system in late 1992, since both stations have almost the same time offset of .200 sec for the campaigns conducted in 1993.

5. SCD1 LAUNCH

The launch of SCD1 was planned initially for the 7 January 1993 and the Maspalomas ground station has been set-up to provide tracking support during the first pass shortly after the injection of the satellite. The launch was postponed several times. The satellite was then launched successfully with a Pegasus rocket on 9 February 1993 and was injected into the nominal orbit at 14:42:20 GMT (4).

The essential figures of the SCD1 launch phase are summarized in Table 3.

Unfortunately Alcantara was not available for tracking during the launch and early orbit phase, so that the ranging from Maspalomas became more important. A few range measurements were performed during this first pass around 14:57 GMT. The tracking data from Maspalomas as well as from Cuiaba were exchanged and an orbit determination was carried out at ESOC.

Because few measurements were taken from Maspalomas, compared to the high number taken at Cuiaba, this orbit determination could not be used for any calibration purposes.

The orbit determination showed nominal range residuals for Cuiaba, however several measurements had ambiguity errors of some minor tones (primarily 160 Hz tone, 55 measurements out of 323 measurements).

6. SUMMARY

A successful collaboration between ESA/ESOC and INPE in the field of orbit de-

termination was carried out during the past years. It commenced in 1987 with some preliminary coverage analysis for SCD1, it included support for the INPE orbit determination software and ground station tracking calibration and it concluded with the tracking support from Maspalomas during the launch phase of SCD1 in February 1993.

The INPE tracking facilities and the orbit determination system were ready in time for the successful operation of SCD1.

During the tracking campaigns conducted with ERS-1 and to some extent with SCD1 a few minor problems were discovered, e.g. time bias of .200 sec and occasional ambiguity errors of the minor tones.

A further tracking campaign with ERS-1 is recommended involving both INPE stations, Alcantara and Cuiaba, in order to establish full coherence between the INPE- and the ESA tracking systems.

ACKNOWLEDGEMENT

Messrs. S. Martin (LOGICA), O. Mikkelsen (CRI) and R. Zandbergen (LOGICA) were deeply involved in the evaluation of various tracking campaigns and this contribution is highly appreciated.

7. REFERENCES

- (1) Orbit Determination Analysis for SCD1, Internal paper, H. Kuga, O. Mikkelsen, S. Pallaschke, July 1987.
- (2) An Overview of the Multi-Purpose Orbit Determination and Prediction Software at ESOC/ESA, Internal Paper, Kondapalli Rama Rao, H. Kuga, S. Pallaschke, April 1990.
- (3) Preliminary Analysis of Perigee Attitude Control on HIPPARCOS, Internal Paper, Kondapalli Rama Rao, H. Kuga, S. Pallaschke, April 1990.
- (4) Satellite Orbit Determination: A First-Hand Experience with the first Brazilian Satellite SCD1, H. Kuga, Kondapalli Rama Rao, IAF-93-A.5.43, Graz, Oct. 1993.
- (5) Review of ESA Tracking Facilities and their Contribution to the Orbit Determination, S. Pallaschke, M. Schaefer, O. Mikkelsen, Flight Dynamics Symposium, Darmstadt, Oct. 1986 (ESA-SP-255).

(6) Station Data Interchange Documents, Chapters SDID 0230 and 0403, ESOC

(7) ERS-1 Operational Orbit Determination and Prediction at ESOC, R. Zandbergen, J. Dow, S. Martin, Journal of the British Interplanetary Society, Vol. 45, pp 117 - 120, 1992.

Table 1: HIPPARCOS CALIBRATION CAMPAIGNS

<u>Satellite data</u>	uplink frequency	2063.5875 Mhz
	downlink frequency	2241.0000 Mhz
	2way transponder delay	1334.2 nsec

Nov. 91 campaign

Orbit determination interval

91/11/11 00:00 - 91/11/14 06:00 GMT

Tracking measurements

Operational: Odenwald, 25 measurements with 160 m rms
 Perth, 37 measurements with 90 m rms

Cuiaba (all passes around perigee with a distance of less than 7000 km)

91/11/11 14:03 - 14:09 GMT
 91/11/12 11:05 - 11:19 GMT
 91/11/13 19:41 - 19:45 GMT

May 92 campaign

Orbit determination interval

92/05/04 00:00 - 92/05/10 00:00 GMT

Tracking measurements:

Operational: Odenwald, 55 measurements with 110 m rms
 Perth, 58 measurements with 100 m rms

Cuiaba (all passes around perigee with a distance of less than 9000 km, measurement rms of 60 m)

92/05/05 16:51 - 17:09 GMT, 80 measurements
 92/05/06 14:01 - 14:20 GMT, 70 measurements
 92/05/07 11:14 - 11:15 GMT, 4 measurements

Table 2: ERS-1 CALIBRATION CAMPAIGNS

<u>Satellite data</u>	uplink frequency	2048.8534 Mhz
	downlink frequency	2224.9992 Mhz
	2-way transponder delay	3198 nsec

Sept./Oct. 92 campaign

Orbit determination interval 29. Sept. - 03 Oct. 92 using
 Kiruna range data, 830 measurements with 8 m rms
 Altimeter data, 1000 " with 2 m rms

Cuiaba measurements (ranging with 12 m rms)

92/09/29	14:16 - 14:21 GMT	18 measurements
92/10/01	02:06 - 02:16 "	27 "
	14:50 - 14:57 "	28 "
92/10/02	01:37 - 01:43 "	22 "

Estimated parameters: Cuiaba station location
 Cuiaba timing bias of -.232 sec
 Cuiaba range bias of -31.9 m

Jan. 93 campaign

Orbit determination interval 05 - 07 Jan. 1993 using

Kiruna range data	500 measurements with	7 m rms
Doppler data	510 "	" 2 cm/s rms
Altimeter data	860 "	" 2 m rms

Alcantara measurements (ranging with 9 m rms)

93/01/05	14:28 - 14:32 GMT	18 measurements
93/01/06	12:18 - 12:23 "	23 "
93/01/07	00:53 - 00:57 "	20 "
	13:25 - 13:33 "	35 "

Estimated parameters: Alcantara timing bias of .200 sec
 Alcantara range bias of 5.7 m

Dec. 93 campaign

Orbit determination interval 17. Dec. - 21. Dec. 93 using

Kiruna range data,	870 measurements with	9 m rms
Doppler data,	890 "	" 2.5 cm/s rms
Altimeter data,	2050 "	" 2 m rms

Cuiaba measurements (ranging with 11 m rms)

93/12/17	13:17 - 13:25 GMT	30 measurements
93/12/18	12:49 - 12:51 "	10 "
93/12/19	13:56 - 14:02 "	30 "
93/12/20	13:23 - 13:31 "	30 "

Estimated parameters: Cuiaba timing bias of .203 sec
 Cuiaba range bias of -36.1 m.

Table 3: SCDI LAUNCH PHASE

<u>Satellite data</u>	uplink frequency	2033.2 Mhz
	downlink frequency	2208.0 Mhz
	2way transponder delay	1803.0 nsec
	(back-up)	1869.0 nsec

Ground station visibility (Injection time 93/02/09 at 14:42:20 GMT)

Rev. no.	Maspalomas max el.	Cuiaba max el.	Alcantara max el.
1	14:46-14:58 12°		14:42-14:53 7°
2			16:27-16:42 24°
3		18:14-18:26 13°	18:13-18:29 84°
4		19:58-20:14 46°	20:01-20:15 25°
5		21:45-22:01 60°	21:49-22:01 8°
6		23:32-23:47 32°	23:39-23:47 4°

Tracking passes

Maspalomas 93/02/09 14:56 - 14:58

Cuiaba 93/02/09 18:20 - 18:24
20:02 - 20:11
21:48 - 21:59
23:35 - 23:45

93/02/10 01:21 - 01:32
03:09 - 03:20
04:55 - 05:07
17:34 - 17:37
19:17 - 19:26
21:04 - 21:14
22:52 - 23:01

93/02/11 00:37 - 00:45
02:25 - 02:35
04:12 - 04:20

ambiguity errors

"

"

"

"

bad measurements

"

"

"

"

"

"

TRANSFER ORBIT DETERMINATION ACCURACY FOR ORBIT MANEUVERS

Mery Passos Pinheiro
Hughes Aircraft Company
MCC - Mission Analysis Department
S67 D457 - PO Box 92919
Los Angeles - CA 90009
Tel. (310)607-8623
Fax.(310)607-8700

Abstract

This work intends to show the accuracy of the orbital elements determined during transfer orbit as a function of data span, as well as the feasibility of performing maneuvers. The orbit estimator used is a weighted least squares algorithm. The observation vector is composed of angle data (azimuth and elevation) and range data and are from the Asura 1C mission. The state vector is either propagated by Brower model or numerical integration (for small eccentricities and inclination). The complete software to determine the orbit has been developed by Hughes Aircraft and been used for all Hughes satellite mission.

Key Words: Geostationary Satellite, Vernier

Introduction

The affirmation of "this formula gives excellent results over short observational time spans" can be found in P. Escobal's book "Method of Orbit Determination"¹, and that refers to an orbit determination method by Herrick-Gibbs using range and angle data.

At Hughes Aircraft it can be observed that the term "short" may be defined depending on the objectives one wants to reach. Since 1983 J. Salvatore has successfully been using a technique called Vernier, which consists of performing a small maneuver using a short observational data span to determine the orbit after a big maneuver.

Having many satellites in geostationary orbit creates very difficult constraints when designing a mission. Sometimes the mission design asks for burns in a very crowded area with longitudinal separations of 2 or less degrees. In these cases to avoid interference, as well as to reach the final longitude, the Vernier technique has become almost indispensable.

A study was performed² on Palapa B4 and Galaxy 5 transfer orbits to analyze the orbital element's standard deviations as a function of the span of time over which the data was collected. In this article the elements themselves are presented and an analysis is performed on the drift rate and its standard deviations to show the feasibility of performing Verniers.

1 - Orbit Determination Method

Orbit determination is a process which involves the state vector propagation, the estimation method and the observation data. In this work the orbit is determined by a method described in³.

1.1 - Transfer Orbit Propagation

The state vector is propagated by a semi-analytical method⁴. The classical elements semi-major axis(a), eccentricity(e), inclination(i) mean anomaly(M), argument of perigee(ω), right ascension of the node(Ω), are propagated from a set of constants through time t , without using numerical integration.

The perturbations considered are due to the first and second zonal harmonics of earth's potential. The secular terms for M , ω and Ω vary linearly with the time. Long period terms have sine arguments in mean argument of perigee. Short periods terms contain the mean anomaly in their arguments.

1.2 - Drift Orbit Propagation

The near synchronous orbit is propagated by a numerical integration method due to Encke, in which the equations of motion for a two body problem subjected to perturbations are integrated. The perturbations result from earth non uniformity (a_e), solar potential(a_s), lunar potential(a_l) and solar radiation pressure(a_r). The equation of motion is written as:

$$\frac{d^2 \vec{r}}{dt^2} + \mu \frac{\vec{r}}{r^3} = \vec{a}_e - \vec{a}_s + \vec{a}_l - \vec{a}_r = f(\vec{r}, \vec{v}, t) \quad (1)$$

1.3 - Observation Data

The observation data used are azimuth, elevation and range. The relation between these data and the inertial position vector can be easily understood using the following equations⁵.

$$A = \arctan \left[\frac{-\rho_x \sin \alpha + \rho_y \cos \alpha}{-(\rho_x \cos \alpha + \rho_y \sin \alpha) \sin \zeta - \rho_z \cos \zeta} \right]$$

$$E = \arcsin \left(\frac{-\rho_x \sin \alpha + \rho_y \cos \alpha}{\rho} \right) \quad (2)$$

$$\rho = \left[\begin{aligned} &(-\rho_x \sin \alpha + \rho_y \cos \alpha)^2 + \\ &(-(\rho_x \cos \alpha + \rho_y \sin \alpha) \sin \zeta - \rho_z \cos \zeta)^2 + \\ &((\rho_x \cos \alpha + \rho_y \sin \alpha) \cos \zeta + \rho_z \sin \zeta)^2 \end{aligned} \right]^{1/2}$$

$$\rho_x = x - x_{sta}$$

where $\rho_y = y - y_{sta}$

$$\rho_z = z - z_{sta}$$

and x, y, z

$$x_{sta}, y_{sta}, z_{sta}$$

are the satellite and ground station coordinates respectively in the geocentric inertial system. α, ζ , are the ground station right ascension and geodesic latitude.

1.4 - Orbit Estimator

The orbit estimation method computes iterative corrections and adds them to the initial state vector in order to converge on the orbit which best fits the angle and range data.

The estimator computes the corrections by a weighted least square method. Consider the model to fit the data is:

$$f(t) = x_1 g_1(t) + x_2 g_2(t) + \dots + x_n g_n(t) \quad (3)$$

where g_1, g_2, \dots, g_n are arbitrary functions of t , then the least square solution for x is the one for which

$$\sum_{i=1}^6 (y_i - f(t_i))^2 \quad (4)$$

is minimum.

A first order approximation, given a good initial estimate \bar{x}^0 , is written as:

$$y_i - f_i(\bar{x}^0) \cong \sum_{j=1}^6 \left. \frac{\partial f_i(t)}{\partial x_j} \right|_{\bar{x}^0} (x_j - x_j^0) \quad (5)$$

The solution is thus

$$\Delta x = (U^T W U)^{-1} U W \Delta y^2 \quad (6)$$

where Δx is the correction state vector, Δy is the vector data residuals, W is the $m \times m$ weight matrix of partial derivatives and U is the $m \times 6$ matrix of partial derivatives.

2 - Summary of Results

The classical orbital elements as well as the drift rate and its standard deviation are presented in the following tables. The angle and range data were provided by the following 3 ground stations:

- Perth (P) in Australia
- Allan Park (A) in Canada
- Betzdorf (B) in Luxembourg.

Table 1 - Post Maneuver 1 (Lam Test 1)

Time Span	a (km)	e	i (°)	M (°)	ω (°)	Ω (°)	d (°/rev)	σ_d (°/rev)
A(30min)	24467.7	0.73093	4.99	112.82	59.11	59.11	-200.945	0.023

Table 2 - Post Maneuver 3 (11h orbital period)

Time Span	a (km)	e	i (°)	M (°)	ω (°)	Ω (°)	d (°/rev)	σ_d (°/rev)
P(40 m)	24485.7	0.72919	4.98	211.40	179.87	57.41	-200.767	0.0119
P(3h) A(1h)	24480.7	0.72974	5.01	211.34	178.60	58.63	-200.817	0.0008
P(7h) A(1h)	24480.3	0.72976	5.02	211.34	178.63	58.60	-200.820	0.0001

Table 3- Post Maneuver 5 (12h orbit period)

Time Span	a (km)	e	i (°)	M(°)	ω (°)	Ω (°)	d(°/rev)	σ_d (°/rev)
A(1h)	27059.2	0.56482	2.83	182.69	178.97	58.34	-174.960	0.0021
A(1h)P(9h)	27059.1	0.56489	2.86	182.68	179.16	58.14	-174.960	0.0004

Table 4 - Post Maneuver 6 (15h orbit period)

Time Span	a (km)	e	i (°)	M(°)	ω (°)	Ω (°)	d(°/rev)	σ_d (°/rev)
P(1h)	30706.7	0.37911	1.56	181.85	178.37	58.84	-136.291	0.0090
P(2h) A,B(30m)	30703.8	0.37908	1.55	181.83	178.79	58.36	-136.322	0.0016
P(14h) A,B(30m)	30704.8	0.37907	1.56	181.83	179.31	57.85	-136.285	0.0000

Table 5 - Post Maneuver 8 (20h orbit period)

Time Span	a (km)	e	i (°)	M(°)	ω (°)	Ω (°)	d(°/rev)	σ_d (°/rev)
A(25m)	36972.9	0.14520	0.62	180.47	174.19	62.82	-64.395	0.0731
A(50m)	36973.9	0.14518	0.61	180.48	174.31	62.70	-64.383	0.0129
A(9h)	36974.6	0.14531	0.61	180.49	179.24	57.58	-64.375	0.0007
A(11h)	36973.9	0.14529	0.60	180.49	178.68	58.31	-64.381	0.0009

Table 6 - Post Maneuver 12 (23h orbit period)

Time Span	a (km)	e	i (°)	M(°)	ω (°)	Ω (°)	d(°/rev)	σ_d (°/rev)
B(30min)	41028.3	0.03234	0.16	172.82	186.24	55.21	-14.449	0.0573

Table 7 - Post Maneuver 13 (23h orbit period)

Time Span	a (km)	e	i (°)	M(°)	ω (°)	Ω (°)	d(°/rev)	σ_d (°/rev)
B(13h)	41307.7	0.02522	0.13	198.33	175.24	64.61	-10.913	0.0001
B(20h)	41307.7	0.02522	0.13	198.34	176.08	63.71	-10.913	0.0001

3 - Analysis of Results and Conclusion

3.1 - Classical Elements

Tables 3,4 and 5 show that the uncertainty in the argument of perigee and the right ascension of the node increase as the inclination magnitude decreases, as listed below

i(°)	$\Delta\omega$ (°)	Data Span	$\Delta\Omega$ (°)
2.8	+0.2	1 and 9h	-0.2
1.6	+0.5	1 and 14h	-0.5
0.6	+5.0	50 min and 9h	-5.0

The uncertainty increasing can be associated with the fact that for small inclinations the argument of perigee and the

right ascension of the node are not well defined. Therefore the best estimation for those elements is the one considering a span data covering bigger orbit arcs. Although $\Delta\omega$ and $\Delta\Omega$ exhibit 5 deg values, the angle resultant by adding the mean anomaly to the argument of perigee and right ascension of the node shows an maximum 0.2 deg uncertainty.

The eccentricity is very well determined in transfer orbit phase. For *quasi-circular* orbits, (table 4 - 14 h orbit period) very good accuracy is achieved when 2 stations are used. However, in a single station situation (table 5 - 19 h orbit period) a 50 min span data would generate an uncertainty of 0.015 deg in the longitude.

The semi-major axis and the drift rate are redundant elements. Since the drift rate is the key element for Vernier maneuvers, its uncertainty will be analyzed instead of semi-major axis.

3.2 - Vernier Maneuver

In a liquid propellant mission scenery, the final geostationary orbit is achieved with multiple burns. A good design for this kind of mission has to take into account others satellites in the geostationary altitude in order to avoid communication interference. Therefore the orbital maneuver burns should occur in clean areas. However the geostationary altitude has become very crowded which makes that a difficult constraint. In real time orbit operation situations, one must also consider the maneuver performance as well as reaching the on-station longitude.

The initial position vector is well known at the time a big orbital maneuver is performed. It becomes clear then, after an orbit maneuver, the drift rate is the key element in order to assure the satellite will be in the right longitude for the next big maneuver.

The Vernier technique consists of performing 95 to 98% of a big maneuver, collecting data for a minimum amount of time and then performing a small maneuver (Vernier) in the same apse.

Tables 1 and 5 shows worst cases for drift standard deviation using a 30 and 25 min span data. After 50 min data collection from a single station (table 5....) the drift rate standard deviation is such that the longitude uncertainty for the next burn, in the following apogee, is within 0.03 in a $3\sigma_d$ situation.

Acknowledgments

The author wishes to thank J. Salvatore for illuminating discussions, C. Shallon for important comments, the Astra 1C Orbital Operations Team for orbit data and Hughes Aircraft for supporting this work.

References

- 1 Escobal, P.R.:1965, "Methods of Orbit Determination", Robert E. Krieger Publishing Co., Inc - Malabar, Florida
- 2 Gingiss, A; Noel, J; Pinheiro, M.P; Gutierrez, J.: 1992, "A Study of the Dependence of Orbit and Attitude Accuracies on Data Span", Technical Memo, Hughes Aircraft - El Segundo - CA
- 3 Shallon, C. R. :1983, "Synchronous Satellite Dynamic Analysis and Operations", Ref. F1532SCG NO 8410068 - Hughes - El Segundo, CA
- 4 Brower, D.; Clemence, G.:1959 "Methods of Celestial Mechanics"
- 5 Pinheiro, M.P.:1989, "Determinação de Orbita Geoestacionaria em Tempo Real" Doctorate Thesis - Observatorio Nacional - Rio de Janeiro, RJ

COMPARISON OF THE NORAD AND RCSC ELEMENT SETS FOR NEAR-EARTH SPACE OBJECT

Dr. Nazirov R.R., dr. Timokhova T.A.
Space Research Institute
Russian Academy of Sciences
Profsoyuznaya Str. 84/32
117810 Moscow Russia GSP-7
Telephone: (7)(095) 333-50-89
Fax: (7)(095) 310-70-23
E-Mail: RNAZIROV ESOC1.BITNET
E-Mail: TTIMOKHO ESOC1.BITNET

Abstract

This paper gives results of the comparison of the general perturbations element sets generated by NORAD with element sets generated by RCSC (Russian Centre of Space Control) and MCC (Mission Control Centre) for near-Earth (period less than 225 minutes) satellites "Active", "Magion-1", "Apex".

Consistency of the positions obtained from NORAD element sets and RSCS, MCC element sets for above satellites at the same time has been checked. Analysis of the accuracy of the above satellites prediction by program applied to the NORAD element sets has been made. The method of calculation of the initial parameters for motion integration calculation is proposed.

Element sets

Russian Centre of Space Control and Mission Control Centre generate orbital data in the form of well known osculating elements which are in one-to-one mapping (according to the Kepler law) with position and velocity at the moment of passing over orbit ascending node. Note them RES1 (Russian Element Sets generated by MCC) and RES2 (Russian Element Sets generated by RCSC).

The NORAD element sets are "mean" values obtained by removing periodic variations in a particular way. In order to obtain good predictions or to calculate position and velocity at the same moment, these periodic variations must be reconstructed (by the prediction model) in exactly the same way they were removed by NORAD. These element sets are called TLE (Two Line Elements). For near-Earth (period less than 225 minutes) satellites: "Active", "Magion-1", "Apex", which are under consideration, one must use applied to NORAD element sets program SGP4.

There are orbital data on following period of the time: from Sept. 1989 to Apr. 1992 (73 points of RES1) and from Oct. 1989 to Nov. 1989 (37 points of RES2) for satellite "Active"; from Oct. 1989 to Mar.

1991 (31 points of RES1) and from Oct. 1989 to Feb. 1990 (122 points of RES2) for satellite "Magion"; from Apr. 1992 to Dec. 1992 (49 points of RES1) for satellite "Apex" TLE data which cover above periods of time with frequency three time per day or one time per three days.

Above satellites have the similar orbits with the semimajor axis ~ 8 000 km, eccentricity ~ 0.14, inclination ~ 82 deg.

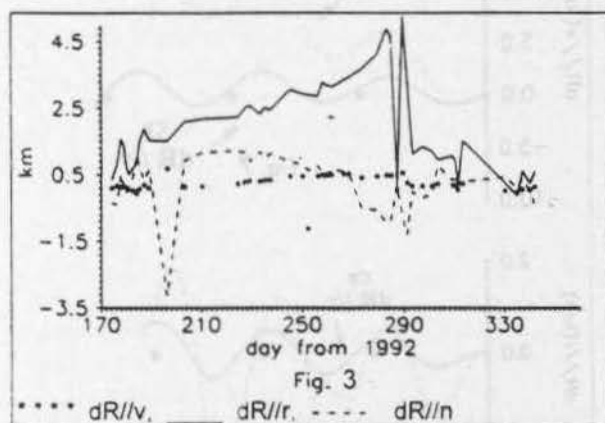
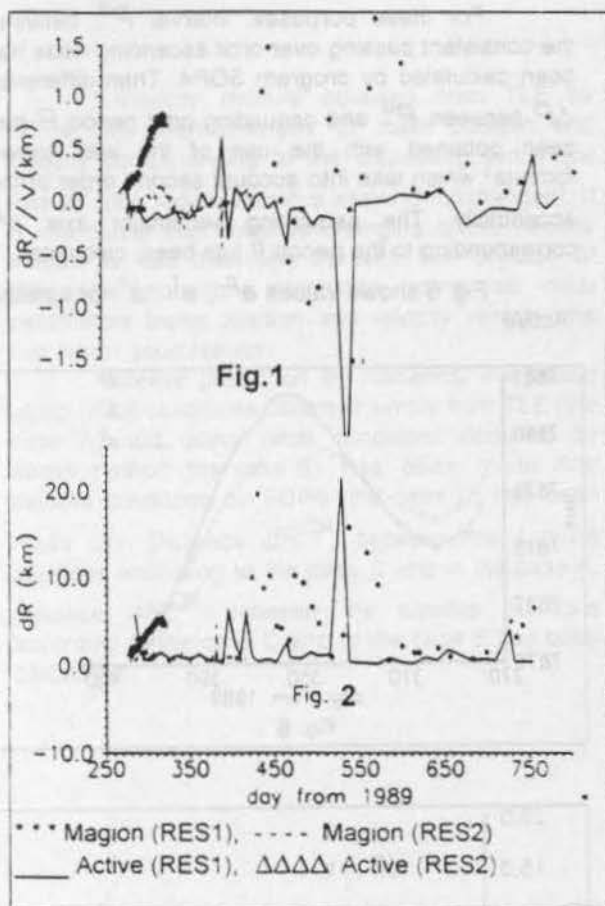
Comparison of the satellite position.

Consistency of the positions obtained from TLE element sets and RES1, RES2 element sets for above satellites at the same time has been checked. Orbit elements are given in the different moments of time. RES1 and RES2 correspond to the moment of the passing over orbit ascending node and are sufficiently seldom. Therefore it was necessary to obtain satellite position from TLE on the same moments of the time.

For these purposes TLE prediction has been made on the nearest moment of the passing over orbit ascending node. Then osculating elements has been obtained from position and velocity (according to the Kepler law) and linear interpolation to the moments corresponding to RES1 and RES2 data moments has been made. Linear interpolation is suitable in this case because of the time difference between neighbouring TLE data is small, osculating elements are constant in the Kepler case and influence of the Earth field at the moment of passing of the ascending node is approximately the same.

Distance (dR) between the satellite positions according to TLE and RES1, RES2 data has been calculated. Graphs and statistical characteristics of the projections of the distance (dR) to the velocity vector (dR/v), radius vector (dR/r) and normal to the orbit (dR/n) has been obtained.

Figures 1,2 show dR/v , dR separately for satellites "Active" and "Magion", but figure 3 shows all values dR/v , dR/r , dR/n for satellite "Apex". Abscissa corresponds to number of day from beginning of the year.



E	σ				n
	km	km	km	km	
dR/v	0.1	0.3	2.8	1.7	5
dR/r	0.4	2.4	6.6	20.	9
dR/n	0.7	2.2	21.	6.5	2
dR	2.1	2.6	0.1	22.	6

All above data (122 items) was processed statistically. Statistical mean (E), square deviation (σ), minimum value (mn), maximum value (mx) and number of deviation getting out three σ (n) are showed on the table

Results show that consistency of the TLE and RES1, RES2 satellite position is good. But there are anomalous points

3. Accuracy analysis of the orbit prediction by program SGP4

Analysis of the accuracy of the above satellites prediction by program SGP4 from TLE data has been made. Prediction results have been compared with TLE data at the same moment. It was shown that the prediction results may be improved by selecting of the coefficient $BSTAR$, which is one element of the TLE and depends from atmospheric drag effect.

Element $BSTAR$ selecting method has been proposed. That is

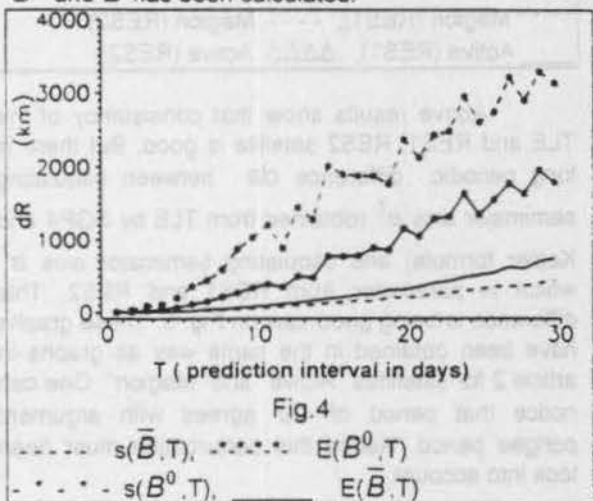
Let element $BSTAR$ from element set TLE2, corresponding to the moment t_2 , must be improved. Note $BSTAR(t_2) = B^0$. Element set TLE1, corresponding to the moment t_1 , is selected. Time difference $\Delta t = t_2 - t_1 > 0$ may be different. Here it equals 30 days. It is close to optimal one. Orbit periods $P_1(t_1)$ and $P_2(t_2)$ are calculated by program SGP4. Minimum of the function

$$(P_1 - P_2) \cdot n - F(BSTAR)$$

over parameter $BSTAR$ is calculated. Here n is number of the orbits between moments t_1 and t_2 . function F equals to the modification of the orbit period, which is calculated by program SGP4 as difference between periods of the consistent orbits.

Minimum argument is equal to improved value \bar{B} of the parameter $BSTAR$.

Consistency of the prediction accuracy with B^0 and \bar{B} has been checked. For above satellites 1350 element sets have been possessed. For each point prediction on interval T by program SGP4 with B^0 and \bar{B} has been calculated.



Distance (dR) between the satellite positions according to the TLE and orbit prediction has been calculated. Statistical characteristics of the projections of the distance (dR) to the velocity vector (dR/v), radius vector (dR/r) as a function of the interval T has been obtained.

Results show that prediction accuracy with \bar{B} is significant better than prediction accuracy with B^0 .

Fig. 4 shows statistical means $E(B^0, T)$, $E(\bar{B}, T)$ and square deviations $s(B^0, T)$, $s(\bar{B}, T)$ of the value dR for satellite "Active". Results for satellites "Magion" and "Apex" are the similar.

Method of calculation of initial condition from TLE for numerical integration.

As it has been said above, to obtain good predictions, TLE must be reconstructed (by the prediction model) in exactly the same way they were removed by NORAD. Hence, inputting TLE into a different model (even though the model may be more accurate) will result in degraded predictions. The problem is to calculate initial condition from TLE for numerical integration.

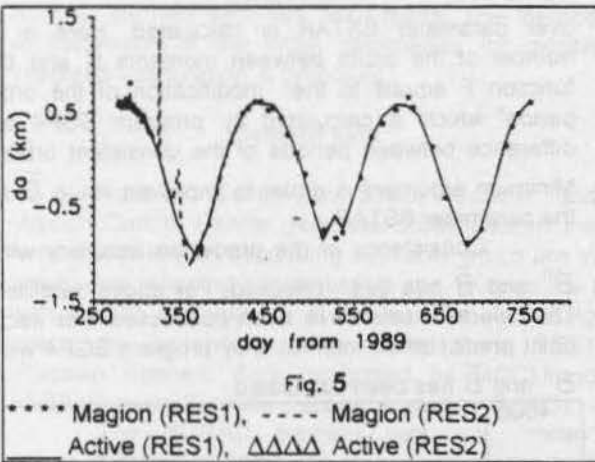


Fig. 5

Above results show that consistency of the TLE and RES1, RES2 satellite is good. But there is long periodic difference da between osquating semimajor axis a^t (obtained from TLE by SGP4 and Kepler formula) and osquating semimajor axis a^r which is parameter from RES1 and RES2. This difference is being good saw on Fig. 5. These graphs have been obtained in the same way as graphs in article 2 for satellites "Active" and "Magion". One can notice that period of da agrees with argument perigee period. Hence this perturbation must be taken into account.

For these purposes, interval P^d between the consistent passing over orbit ascending node has been calculated by program SGP4. Then difference ΔP between P^d and osquating orbit period P has been obtained with the use of the well known formula¹ which take into account second order of the eccentricity. The osquating semimajor axis a^p corresponding to the period P has been calculated.

Fig. 6 shows values a^p , a^t , a^r for satellite "Active".

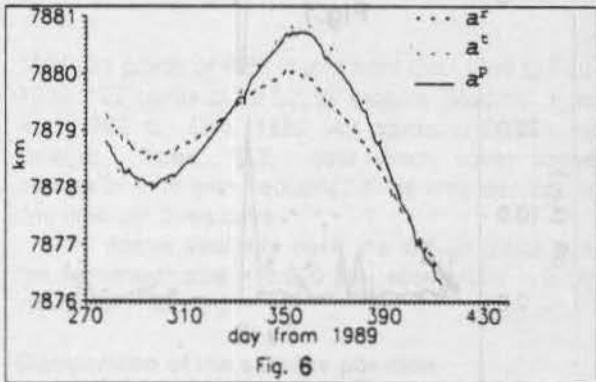


Fig. 6

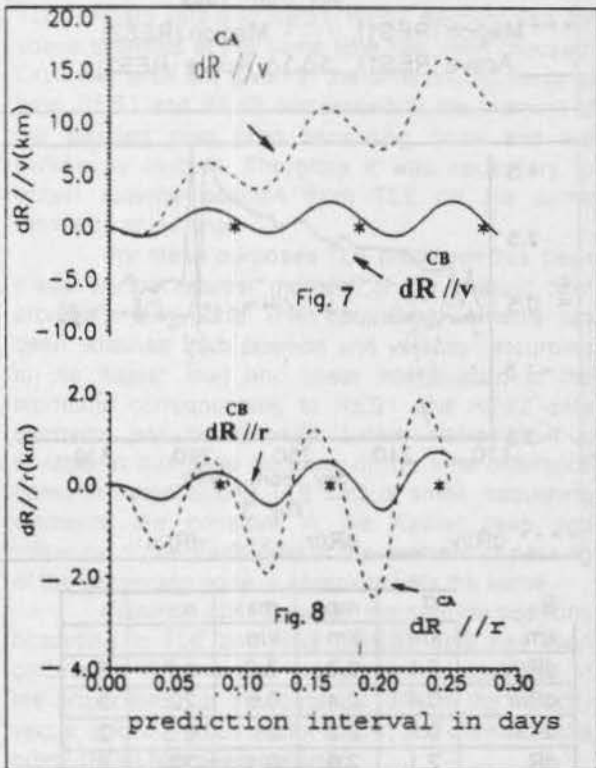


Fig. 7

Fig. 8

¹ Eliasberg, P.E.: 1965, Introduction into the Flight Theory of the artificial Earth Satellite, Nauka, Moscow.

Velocity module obtained from TLE by SGP4 has been changed to make position and velocity corresponding to the osculating semimajor axis a^p (the radius vector is keeping unchanged). It is interesting that obtained changing of the velocity module is less than one percent, but for case of differential equation integration using as initial parameters these position and velocity vectors one can obtain good results.

Satellite prediction by numerical integration using initial conditions obtained simply from TLE (the case A) and using initial conditions obtained by above method (the case B) has been made. And satellite prediction by SGP4 (the case C) has been made too. Distance dR^{CA} between the satellite positions according to the case C and to the case A, distance dR^{CB} between the satellite positions according to the case C and to the case B has been calculated.

Fig. 7.8 show graphs of the projections of the distances dR^{CA} , dR^{CB} to the velocity vector ($dR^{CA} // v$, $dR^{CB} // v$), radius vector ($dR^{CA} // r$, $dR^{CB} // r$) for satellite "Active". Stars on the graphs correspond to the moment of passing over orbit ascending node.

Results show that above method allows to use changed initial conditions for numerical integration with sufficient accuracy.

Then, the following conclusions exist. The satellite orbit element sets generated by NORAD may be used successfully.

ORBIT DETERMINATION FOR GEOSTATIONARY SPACECRAFT USING ION PROPULSION

Karlheinz Spindler
 MBP Informationstechnologie GmbH:
 currently based at the
 European Space Operations Centre (ESOC)
 Robert-Bosch-Straße 5
 D - 64293 Darmstadt
 Phone: (06151) 90-2025
 FAX: (06151) 90-2271
 Electronic mail: kspindle@esoc.bitnet

Abstract

The Advanced Relay and TEchnology MISsion (ARTEMIS) will be ESA's next geostationary communications-technology demonstration satellite¹. The inclination station keeping of this spacecraft is foreseen to be carried out by an ion propulsion system performing twice-daily low-thrust manoeuvres, each with a duration of typically 3 hours. Therefore, orbit determination software had to be developed which can estimate, among other parameters, the performance of nonimpulsive manoeuvres. It is the purpose of this paper to describe the theoretical basis underlying this software.

Keywords: Orbit Determination, Geostationary Spacecraft, Nonimpulsive Manoeuvres, Ion Propulsion

Estimation algorithm

The algorithm employed is an iterative weighted least squares method. In general, the goal of such a method is to find optimal estimates for M state parameters p_1, \dots, p_M from N measurements q_1, \dots, q_N under the assumption that there is a nonlinear relation $q = f(p)$; here an estimate \bar{p} is considered optimal if it minimizes a functional of the form

$$(q - f(\bar{p}))^T W (q - f(\bar{p})) + (\bar{p} - p^{(0)})^T W_{init} (\bar{p} - p^{(0)})$$

where the weighting matrices $W \in \mathbb{R}^{N \times N}$ and $W_{init} \in \mathbb{R}^{M \times M}$ are positive definite and where $p^{(0)}$ is an initial estimate to start an iteration with. In order to improve this initial estimate, one successively constructs a new estimate $p^{(k+1)}$ from a previously determined estimate $p^{(k)}$ by carrying out the following four steps.

- Determine the partial derivative matrix.

$$Q(k) = \frac{\partial q}{\partial p}(p^{(k)}) = \left(\frac{\partial q_i}{\partial p_j}(p^{(k)}) \right)_{\substack{1 \leq i \leq N \\ 1 \leq j \leq M}} \in \mathbb{R}^{N \times M}$$

- Determine the measurement values which are theoretically expected from the current best estimate.

$$q^{(k)} = f(p^{(k)})$$

- Solve the normal equation.

$$\begin{aligned} (Q(k)^T W Q(k) + W_{init}) h = \\ Q(k)^T W (q - q^{(k)}) + W_{init} (p^{(0)} - p^{(k)}) \end{aligned}$$

- Update the parameter estimate.

$$p^{(k+1)} = p^{(k)} + h$$

The crucial step in each iteration is to find the partial derivatives of the measurement variables with respect to the parameters to be estimated. It is well known² that the least squares determination is rather insensitive to errors in these partial derivatives. Therefore, a linearized model for the motion of a geostationary spacecraft will be derived which is too crude to be used for the prediction of the spacecraft orbit but which is accurate enough to yield reasonable values for the partial derivatives of the tracking measurements (range, azimuth and elevation[†]) with respect to the dynamical parameters to be estimated (initial state, manoeuvre parameters, effective cross section/mass ratio). This model will allow one to explicitly write down the geocentric distance r , the latitude θ and the longitude λ of the spacecraft as functions of its sidereal angle s and of the dynamical parameters. Then the chain rule in the form

$$\frac{\partial(i\text{-th measurement})}{\partial(j\text{-th parameter})} = \frac{\partial(i\text{-th measurement})}{\partial(r, \lambda, \theta)} \frac{\partial(r, \lambda, \theta)}{\partial(j\text{-th parameter})}$$

will allow us to explicitly write down the desired partial derivatives.

[†] Thus we exclude range-rate measurements even though their discussion would not cause any additional difficulties.

Notation

The following notation will be used:

- ψ = earth's angular velocity;
- μ = earth's gravitational constant;
- $R = \sqrt[3]{\mu/\psi^2}$ = geostationary radius;
- P = solar radiation pressure near earth;
- $G(t)$ = Greenwich sidereal angle at time t .

To describe the motion of a geostationary spacecraft the *classical orbital elements*

- a = semimajor axis,
- e = eccentricity,
- i = inclination,
- Ω = right ascension,
- ω = argument of perigee,
- ν = true anomaly

are less convenient than the *synchronous elements*. To define these elements we fix an arbitrary epoch t_0 and denote by $\nu_0 = \nu(t_0)$ and $G_0 = G(t_0)$ the true anomaly and the Greenwich sidereal angle at time t_0 ; then $G(t) = G_0 + \psi(t - t_0)$ at any time t . Now the synchronous elements are defined as follows:

$$D := -\frac{3}{2R}(a - R) = \frac{\text{mean longitude drift rate}}{\psi};$$

$$\lambda_0^m := \Omega + \omega + \nu_0 - 2e \sin \nu_0 - G_0$$

= mean subsatellite longitude at time t_0 ;

$$\begin{bmatrix} i_x \\ i_y \end{bmatrix} := \begin{bmatrix} i \sin \Omega \\ -i \cos \Omega \end{bmatrix} = \text{inclination vector};$$

$$\begin{bmatrix} e_x \\ e_y \end{bmatrix} := \begin{bmatrix} e \cos(\Omega + \omega) \\ e \sin(\Omega + \omega) \end{bmatrix} = \text{eccentricity vector}.$$

Note that all synchronous elements except λ_0^m are constant and small for an unperturbed Keplerian motion and hence will remain small throughout the motion of a geostationary satellite.

Unperturbed Keplerian motion

Since we will be interested in geostationary orbits for which e and i are small and for which a differs only slightly from the geostationary radius R , we will linearize the system dynamics around $e = 0$, $i = 0$ and $a = R$. The position vector of a spacecraft in unperturbed Keplerian motion with respect to a Cartesian inertial system is then given by $\vec{r} = r\vec{e}_r$ where

$$r = \frac{a(1 - e^2)}{1 + e \cos \nu} \approx R \left(1 - \frac{2D}{3} - e \cos \nu \right)$$

and

$$\begin{aligned} \vec{e}_r &= \begin{bmatrix} \cos \Omega \cos(\omega + \nu) - \sin \Omega \sin(\omega + \nu) \cos i \\ \sin \Omega \cos(\omega + \nu) + \cos \Omega \sin(\omega + \nu) \cos i \\ \sin(\omega + \nu) \sin i \end{bmatrix} \\ &\approx \begin{bmatrix} \cos \Omega \cos(\omega + \nu) - \sin \Omega \sin(\omega + \nu) \\ \sin \Omega \cos(\omega + \nu) + \cos \Omega \sin(\omega + \nu) \\ i \sin(\omega + \nu) \end{bmatrix} \\ &= \begin{bmatrix} \cos(\Omega + \omega + \nu) \\ \sin(\Omega + \omega + \nu) \\ i \sin(\omega + \nu) \end{bmatrix} \end{aligned}$$

so that

$$\vec{r} \approx R \left(1 - \frac{2D}{3} - e \cos \nu \right) \begin{bmatrix} \cos(\Omega + \omega + \nu) \\ \sin(\Omega + \omega + \nu) \\ i \sin(\omega + \nu) \end{bmatrix}.$$

Comparing this with spherical polar coordinates

$$\vec{r} = r \cdot \begin{bmatrix} \cos \theta \cos s \\ \cos \theta \sin s \\ \sin \theta \end{bmatrix}$$

we get the following approximations:

$$\begin{aligned} r &\approx R \left(1 - (2D/3) - e \cos \nu \right); \\ \cos \theta \cos s &\approx \cos(\Omega + \omega + \nu); \\ \cos \theta \sin s &\approx \sin(\Omega + \omega + \nu); \\ \sin \theta &\approx i \sin(\omega + \nu). \end{aligned} \quad (1)$$

The last three of these equations imply that $\sin \theta \approx \theta$ and $\cos \theta \approx 1$; hence (1) can be simplified to

$$\begin{aligned} r &\approx R \left(1 - (2D/3) - e \cos \nu \right); \\ s &\approx \Omega + \omega + \nu; \\ \theta &\approx i \sin(\omega + \nu). \end{aligned} \quad (2)$$

The first and the last equation in (2) immediately yield r and θ as functions of the sidereal angle and the synchronous elements; in fact, we have

$$\begin{aligned} r &\approx R - \frac{2}{3}RD - Re \cos(s - (\Omega + \omega)) \\ &= R - \frac{2RD}{3} - Re \cos s \cos(\Omega + \omega) \\ &\quad - Re \sin s \sin(\Omega + \omega) \end{aligned} \quad (3)$$

and

$$\begin{aligned} \theta &\approx i \sin(s - \Omega) \\ &= i(\sin s \cos \Omega - \cos s \sin \Omega) \\ &= -i_y \sin s - i_x \cos s. \end{aligned} \quad (4)$$

To obtain an analogous formula for λ we need to express the true anomaly in terms of the sidereal angle and the synchronous elements. The function $t \rightarrow \nu(t)$ can be found by integrating the equation

$$\dot{\nu} = \frac{\sqrt{\mu a(1-e^2)}(1+e \cos \nu)^2}{a^2(1-e^2)^2}$$

and is implicitly given by the formula

$$\frac{2}{\sqrt{1-e^2}} \arctan \left[\frac{(1-e) \tan(\nu/2)}{\sqrt{1-e^2}} \right] - \frac{e \sin \nu}{1+e \cos \nu} = \frac{\sqrt{\mu a(1-e^2)}}{a^2(1-e^2)} t + \text{const.}$$

where the constant can be determined by plugging in $t = t_0$. Linearizing this formula about $e = 0$ and $a = R$ (i.e., $D = 0$) we find that

$$\nu(t) \approx (\psi + \psi D)(t - t_0) + 2e \sin \nu(t) + \nu_0 - 2e \sin \nu_0.$$

Replacing ν as an argument of the sine function by the right-hand side of this equation and linearizing further, we obtain

$$\nu(t) \approx (\psi + \psi D)(t - t_0) + 2e \sin(\psi(t - t_0) + \nu_0) + \nu_0 - 2e \sin \nu_0.$$

Since

$$\begin{aligned} s - s_0 &= s(t) - s(t_0) \\ &= (\lambda(t) + G_0 + \psi(t - t_0)) - (\lambda(t_0) + G_0) \\ &= \psi(t - t_0) + \lambda(t) - \lambda(t_0) \\ &= \psi(t - t_0) + \text{small term} \end{aligned}$$

this yields

$$\begin{aligned} \lambda &= s - G \\ &\approx (\Omega + \omega + \nu) - (G_0 + \psi(t - t_0)) \\ &\approx \Omega + \omega + \psi D(t - t_0) + 2e \sin(\psi(t - t_0) + \nu_0) + \nu_0 - 2e \sin \nu_0 - G_0 \\ &\approx (\Omega + \omega + \nu_0 - 2e \sin \nu_0 - G_0) \\ &\quad + D(s - s_0) + 2e \sin(s - s_0 + \nu_0) \\ &\approx \lambda_0^m + D(s - s_0) + 2e \sin(s - \Omega - \omega) \\ &= \lambda_0^m + D(s - s_0) + 2e \sin s \cos(\Omega + \omega) \\ &\quad - 2e \cos s \sin(\Omega + \omega) \\ &= \lambda_0^m + D(s - s_0) + 2e_x \sin s - 2e_y \cos s. \end{aligned} \tag{5}$$

In the above equations we have expressed r , θ and λ as functions of the synchronous elements and of the sidereal angle s . Combining (3), (4) and (5) and taking

the derivatives with respect to s in these equations, we obtain the following formulas³ which express the unperturbed spacecraft motion in linearized form.

**Formula (A):
Linearized unperturbed orbital evolution**

$$\begin{aligned} r(s) &\approx R - 2RD/3 - R(e_x \cos s + e_y \sin s) \\ \theta(s) &\approx -i_x \cos s - i_y \sin s \\ \lambda(s) &\approx \lambda_0^m + D(s - s_0) + 2e_x \sin s - 2e_y \cos s \\ r'(s) &\approx R(e_x \sin s - e_y \cos s) \\ \theta'(s) &\approx i_x \sin s - i_y \cos s \\ \lambda'(s) &\approx D + 2e_x \cos s + 2e_y \sin s \end{aligned}$$

To see how derivatives with respect to s are related to time derivatives we observe that the equation $s(t) = G_0 + \psi(t - t_0) + \lambda(s(t))$ implies $\dot{s} = \psi + \lambda'(s)\dot{s}$ so that

$$\dot{s} = \frac{\psi}{1 - \lambda'} \approx \psi(1 + \lambda')$$

where λ' is small and hence can be neglected if \dot{s} is multiplied by a small quantity.

Effect of an impulsive manoeuvre

We now use Formula (A) to determine the increments in the synchronous elements caused by an impulsive manoeuvre. Since such a manoeuvre has no instantaneous effect on the spacecraft position we have

$$\begin{aligned} 0 &= \Delta r \sim -R(\frac{2}{3}\Delta D + \Delta e_x \cos s + \Delta e_y \sin s); \\ 0 &= \Delta \theta \sim -\Delta i_y \sin s - \Delta i_x \cos s; \\ 0 &= \Delta \lambda \sim \Delta \lambda_0^m + \Delta D(s - s_0) \\ &\quad + 2\Delta e_x \sin s - 2\Delta e_y \cos s \end{aligned} \tag{6}$$

where $s = s_{\text{burn}}$ is the sidereal angle at the time of the manoeuvre. Note that the formulas (6) can be read as equations in zero-th order approximation only. (Hence we use the notation \sim rather than the symbol \approx which denotes linear approximation.) In fact, the increments of the synchronous elements are not small quantities in terms of our linearization, but have finite magnitude since we are modelling an impulsive manoeuvre. The velocity increment caused by the manoeuvre is usually expressed in a different coordinate system which we will now define. At any time t a right-handed ortho-

normal system $(\bar{e}_1, \bar{e}_2, \bar{e}_3)$ is given by

$$\begin{aligned}\bar{e}_1 &= \begin{bmatrix} \cos \theta \cos s \\ \cos \theta \sin s \\ \sin \theta \end{bmatrix} \sim \begin{bmatrix} \cos s \\ \sin s \\ 0 \end{bmatrix}, \\ \bar{e}_2 &= \begin{bmatrix} -\sin \theta \cos s \\ -\sin \theta \sin s \\ \cos \theta \end{bmatrix} \sim \begin{bmatrix} 0 \\ 0 \\ 1 \end{bmatrix}, \\ \bar{e}_3 &= \begin{bmatrix} \sin s \\ -\cos s \\ 0 \end{bmatrix}.\end{aligned}$$

Moreover, we define the *body system* $(\bar{e}_R, \bar{e}_T, \bar{e}_N)$ at time t as follows:

$$\begin{aligned}\bar{e}_R &:= \frac{\bar{r}}{r} = \bar{e}_1; \\ \bar{e}_T &:= \frac{\bar{v} - \langle \bar{v}, \bar{e}_R \rangle \bar{e}_R}{\|\bar{v} - \langle \bar{v}, \bar{e}_R \rangle \bar{e}_R\|} = \frac{\dot{\theta} \bar{e}_2 - \dot{s} \cos \theta \bar{e}_3}{\sqrt{\dot{\theta}^2 + \dot{s}^2 \cos^2 \theta}} \\ &= \frac{\theta' \bar{e}_2 - \cos \theta \dot{s} \bar{e}_3}{\sqrt{(\theta')^2 + \cos^2 \theta}} \sim -\bar{e}_3; \\ \bar{e}_N &:= \bar{e}_R \times \bar{e}_T = \frac{\dot{\theta} \bar{e}_3 + \dot{s} \cos \theta \bar{e}_2}{\sqrt{\dot{\theta}^2 + \dot{s}^2 \cos^2 \theta}} \\ &= \frac{\theta' \bar{e}_3 + \cos \theta \dot{s} \bar{e}_2}{\sqrt{(\theta')^2 + \cos^2 \theta}} \sim \bar{e}_2.\end{aligned}$$

Then we have

$$\begin{aligned}\Delta \bar{v} &= \Delta_R \bar{e}_R + \Delta_T \bar{e}_T + \Delta_N \bar{e}_N \\ &\sim \Delta_R \bar{e}_1 + \Delta_N \bar{e}_2 - \Delta_T \bar{e}_3 \\ &\sim \begin{bmatrix} \Delta_R \cos s - \Delta_T \sin s \\ \Delta_R \sin s + \Delta_T \cos s \\ \Delta_N \end{bmatrix}.\end{aligned}\quad (7)$$

On the other hand the fact that $\bar{r} = r \bar{e}_1$ implies that

$$\begin{aligned}\bar{v} &= \dot{r} \bar{e}_1 + r \dot{\bar{e}}_1 \\ &= \dot{r} \bar{e}_1 + r \dot{\theta} \bar{e}_2 - r \dot{s} \cos \theta \bar{e}_3 \\ &= r' \bar{e}_1 + r \theta' \bar{e}_2 - r \dot{s} \cos \theta \bar{e}_3 \\ &\approx r' \bar{e}_1 + r \theta' \bar{e}_2 - r \dot{s} (1 + \lambda') \bar{e}_3 \\ &\approx \begin{bmatrix} -\psi R(e_y + \sin s + (D/3) \sin s) \\ \psi R(e_x + \cos s + (D/3) \cos s) \\ \psi R(i_x \sin s - i_y \cos s) \end{bmatrix}\end{aligned}$$

so that

$$\Delta \bar{v} \sim \psi R \begin{bmatrix} -\Delta e_y - (\Delta D/3) \sin s \\ \Delta e_x + (\Delta D/3) \cos s \\ \Delta i_x \sin s - \Delta i_y \cos s \end{bmatrix}.\quad (8)$$

Comparing (7) and (8) we find that

$$\begin{aligned}-\psi R((\Delta D/3) \sin s + \Delta e_y) &= \Delta_R \cos s - \Delta_T \sin s, \\ \psi R((\Delta D/3) \cos s + \Delta e_x) &= \Delta_R \sin s + \Delta_T \cos s, \\ \psi R(\Delta i_x \sin s - \Delta i_y \cos s) &= \Delta_N.\end{aligned}\quad (9)$$

Denoting by $A(s)$ the matrix

$$A(s) = \begin{bmatrix} 1 & s - s_0 & 2 \sin s & -2 \cos s & 0 & 0 \\ 0 & 2/3 & \cos s & \sin s & 0 & 0 \\ 0 & (\cos s)/3 & 1 & 0 & 0 & 0 \\ 0 & -(\sin s)/3 & 0 & -1 & 0 & 0 \\ 0 & 0 & 0 & 0 & \cos s & \sin s \\ 0 & 0 & 0 & 0 & \sin s & -\cos s \end{bmatrix}$$

we can combine equations (6) and (9) to a system of linear equations which relate the increments in the synchronous elements with the manoeuvre parameters Δ_R, Δ_T and Δ_N by writing

$$A(s) \begin{bmatrix} \Delta \lambda_0^m \\ \Delta D \\ \Delta e_x \\ \Delta e_y \\ \Delta i_x \\ \Delta i_y \end{bmatrix} = \frac{1}{\psi R} \begin{bmatrix} 0 \\ 0 \\ \Delta_R \sin s + \Delta_T \cos s \\ \Delta_R \cos s - \Delta_T \sin s \\ 0 \\ \Delta_N \end{bmatrix}.$$

This system can be easily solved by explicitly inverting $A(s)$; the result is the following formula which yields the increments in the synchronous elements due to an impulsive manoeuvre at sidereal angle $s_b = s_{\text{burn}}$ as a function of the manoeuvre parameters.

**Formula (B):
Effect of an impulsive manoeuvre**

$$\psi R \begin{bmatrix} \Delta \lambda_0^m \\ \Delta D \\ \Delta e_x \\ \Delta e_y \\ \Delta i_x \\ \Delta i_y \end{bmatrix} = \begin{bmatrix} -2 & 3(s_b - s_0) & 0 \\ 0 & -3 & 0 \\ \sin s_b & 2 \cos s_b & 0 \\ -\cos s_b & 2 \sin s_b & 0 \\ 0 & 0 & \sin s_b \\ 0 & 0 & -\cos s_b \end{bmatrix} \begin{bmatrix} \Delta_R \\ \Delta_T \\ \Delta_N \end{bmatrix}$$

Note that, strictly speaking, the increments in the synchronous elements are functions of the current sidereal angle \bar{s} whose values are zero if $\bar{s} < s_b$ and whose values are given by Formula (B) if $\bar{s} > s_b$.

Effect of a nonimpulsive manoeuvre

We consider a nonimpulsive manoeuvre over the arc $s_1 \leq s \leq s_2$ as a continuous family of infinitesimal impulsive manoeuvres with velocity increments

$$\begin{bmatrix} \Delta_R \\ \Delta_T \\ \Delta_N \end{bmatrix} = \begin{bmatrix} a_R \\ a_T \\ a_N \end{bmatrix} dt = \begin{bmatrix} a_R \\ a_T \\ a_N \end{bmatrix} \frac{1 - \lambda'}{\psi} ds \approx \begin{bmatrix} a_R \\ a_T \\ a_N \end{bmatrix} \frac{ds}{\psi}$$

where a_R , a_T and a_N are the accelerations in radial, tangent and normal direction. Then the corresponding increments in the synchronous elements are obtained by adding up the contributions of all these infinitesimal impulsive manoeuvres. We assume that the accelerations a_R , a_T and a_N are constant throughout the manoeuvre. Then Formula (B) shows that for any sidereal angle $\bar{s} \geq s_1$ the incremented vector

$$[\Delta\lambda_0^m, \Delta D, \Delta e_x, \Delta e_y, \Delta i_x, \Delta i_y]^T$$

is in zero-th order approximation equal to

$$\begin{aligned} & \frac{1}{\psi^2 R} \int_{s_1}^{\min(\bar{s}, s_2)} \begin{bmatrix} -2 & 3(s-s_0) & 0 \\ 0 & -3 & 0 \\ \sin s & 2 \cos s & 0 \\ -\cos s & 2 \sin s & 0 \\ 0 & 0 & \sin s \\ 0 & 0 & -\cos s \end{bmatrix} \begin{bmatrix} a_R \\ a_T \\ a_N \end{bmatrix} ds \\ &= \frac{1}{\psi^2 R} \begin{bmatrix} -2s & \frac{3}{2}(s-s_0)^2 & 0 \\ 0 & -3s & 0 \\ -\cos s & 2 \sin s & 0 \\ -\sin s & -2 \cos s & 0 \\ 0 & 0 & -\cos s \\ 0 & 0 & -\sin s \end{bmatrix} \begin{bmatrix} a_R \\ a_T \\ a_N \end{bmatrix} \Big|_{s=s_1}^{\min(\bar{s}, s_2)} \\ &= \frac{1}{\psi^2 R} \begin{bmatrix} -2sa_R + \frac{3}{2}(s-s_0)^2 a_T \\ -3sa_T \\ -a_R \cos s + 2a_T \sin s \\ -a_R \sin s - 2a_T \cos s \\ -a_N \cos s \\ -a_N \sin s \end{bmatrix} \Big|_{s=s_1}^{\min(\bar{s}, s_2)} \end{aligned}$$

Thus given a nonimpulsive manoeuvre over an arc $s_1 \leq s \leq s_2$, the following formula expresses the increments in the synchronous elements at some sidereal angle $\bar{s} \geq s_1$ due to this manoeuvre.

**Formula (C):
Effect of a nonimpulsive manoeuvre**

$$\psi^2 R \begin{bmatrix} \Delta\lambda_0^m \\ \Delta D \\ \Delta e_x \\ \Delta e_y \\ \Delta i_x \\ \Delta i_y \end{bmatrix} = \begin{bmatrix} -2sa_R + \frac{3}{2}(s-s_0)^2 a_T \\ -3sa_T \\ -a_R \cos s + 2a_T \sin s \\ -a_R \sin s - 2a_T \cos s \\ -a_N \cos s \\ -a_N \sin s \end{bmatrix} \Big|_{s=s_1}^{\min(\bar{s}, s_2)}$$

Note that these increments are functions of \bar{s} which are constant for $\bar{s} \geq s_2$ (and constantly zero for $\bar{s} \leq s_1$).

Effect of solar radiation pressure

The sun's electromagnetic radiation is taken into account by treating it as a nonimpulsive manoeuvre. We

assume that the force \vec{F} exerted by solar radiation points in the direction from the sun to the spacecraft and has the magnitude

$$F = P \cdot C \cdot (1 + \varepsilon) \cos \alpha$$

in the vicinity of the Earth where C is the cross section of the spacecraft, where $\varepsilon \in (0, 1)$ is the reflectivity coefficient of its surface and where α is the angle between the normal of the reflecting surface and the direction of the incoming sun rays. Since different surfaces with varying reflectivities and cross sections are exposed to the sun as the spacecraft follows its path, it is very difficult to accurately model the acceleration due to solar radiation. We will use a rather crude model with one single parameter

$$\sigma := \frac{C}{m} (1 + \varepsilon)$$

which is called the *effective cross section/mass ratio*; here m denotes the spacecraft mass whereas C and ε represent typical values for the cross section and the reflectivity during the tracking interval. Then the acceleration of the spacecraft due to solar radiation is

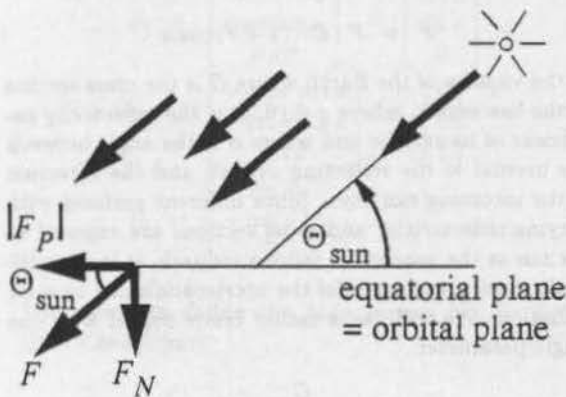
$$\vec{a} = \frac{1}{m} \vec{F} = \sigma P \cos \alpha \frac{\vec{r} - \vec{r}_{\text{sun}}}{\|\vec{r} - \vec{r}_{\text{sun}}\|} \quad (10)$$

Here \vec{r} and \vec{r}_{sun} denote the geocentric position vectors of the spacecraft and of the sun, respectively. To make the computations tractable we assume that the tracking interval is so short that we can imagine the sun as having a constant position

$$\vec{r}_{\text{sun}} = r_{\text{sun}} \begin{bmatrix} \cos \theta_{\text{sun}} \cos s_{\text{sun}} \\ \cos \theta_{\text{sun}} \sin s_{\text{sun}} \\ \sin \theta_{\text{sun}} \end{bmatrix}$$

Then it is straightforward from (10) to express the acceleration \vec{a} with respect to the body system so that $\vec{a} = a_R \vec{e}_R + a_T \vec{e}_T + a_N \vec{e}_N$; then the effect of solar radiation pressure on the synchronous elements can be determined by plugging in the obtained values for a_R , a_T and a_N (which are functions of s) into the integration formula used to determine the effect of a nonimpulsive manoeuvre. This, however, leads to intractable integrands. Therefore we simplify our model somewhat. First, we assume that, due to the great distance of the sun, the sun rays are all parallel when they intersect the orbital plane. Second, we identify the orbital plane with the equatorial plane. Third, we assume that the solar paddles (which are mostly affected by solar radiation) are orthogonal to the orbital plane and oriented towards the sun throughout the motion of the spacecraft. Under these assumptions we have $\alpha = \theta_{\text{sun}}$ and hence $F = m\sigma P \cos \theta_{\text{sun}}$. We can then easily split the

force \vec{F} into its component \vec{F}_N perpendicular to the orbital plane and its component \vec{F}_P in the orbital plane.

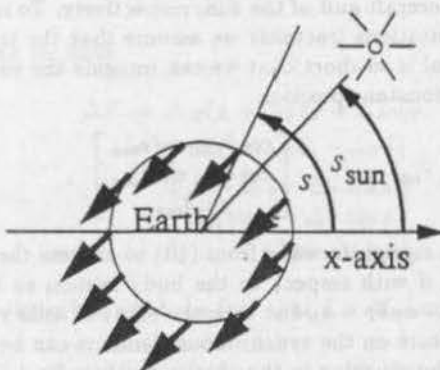


$$F_N = -F \sin \theta_{sun} = -m\sigma P \cos \theta_{sun} \sin \theta_{sun}, \quad (11)$$

$$|F_P| = F \cos \theta_{sun} = m\sigma P \cos^2 \theta_{sun}.$$

The in-plane component is further decomposed into its radial and tangent component. To find this decomposition we denote, at any point on the orbit, by \vec{e}_{sun} the projection of the vector from the Earth to the sun; then the in-plane component of the force \vec{F} is given by

$$\vec{F}_P = -|F_P| \vec{e}_{sun}.$$



Since

$$\begin{aligned} \vec{e}_{sun} &= (\vec{e}_{sun}, \vec{e}_R) \vec{e}_R + (\vec{e}_{sun}, \vec{e}_T) \vec{e}_T \\ &\approx \begin{bmatrix} \cos s_{sun} \\ \sin s_{sun} \end{bmatrix}, \begin{bmatrix} \cos s \\ \sin s \end{bmatrix} \vec{e}_R \\ &+ \begin{bmatrix} \cos s_{sun} \\ \sin s_{sun} \end{bmatrix}, \begin{bmatrix} -\sin s \\ \cos s \end{bmatrix} \vec{e}_T \\ &= \cos(s - s_{sun}) \vec{e}_R - \sin(s - s_{sun}) \vec{e}_T \end{aligned}$$

this yields

$$\begin{aligned} F_R &= -|F_P| \cos(s - s_{sun}); \\ F_T &= |F_P| \sin(s - s_{sun}). \end{aligned} \quad (12)$$

Combining equations (11) and (12) and dividing by the spacecraft mass m , we see that the acceleration of the spacecraft due to solar radiation pressure has the following body coordinates:

$$\begin{bmatrix} a_R \\ a_T \\ a_N \end{bmatrix} = \frac{1}{m} \begin{bmatrix} F_R \\ F_T \\ F_N \end{bmatrix} = \sigma P \cos^2 \theta_{sun} \begin{bmatrix} -\cos(s - s_{sun}) \\ \sin(s - s_{sun}) \\ -\tan \theta_{sun} \end{bmatrix}.$$

(Note that in contrast to our assumption concerning nonimpulsive manoeuvres the accelerations a_R , a_T and a_N are here not constants, but functions of the sidereal angle s .) Since θ_{sun} and s_{sun} are treated as constants during the tracking interval, we obtain the following increments of the synchronous elements between the epoch s_0 and a sidereal angle \bar{s} at some later time during the tracking interval:

$$\begin{aligned} &\frac{\psi^2 R}{\sigma P \cos^2 \theta_{sun}} [\Delta \lambda_0^m, \Delta D, \Delta e_x, \Delta e_y, \Delta i_x, \Delta i_y]^T = \\ &\int_{s_0}^{\bar{s}} \begin{bmatrix} -2 & 3(s - s_0) & 0 \\ 0 & -3 & 0 \\ \sin s & 2 \cos s & 0 \\ -\cos s & 2 \sin s & 0 \\ 0 & 0 & \sin s \\ 0 & 0 & -\cos s \end{bmatrix} \begin{bmatrix} -\cos(s - s_{sun}) \\ \sin(s - s_{sun}) \\ -\tan \theta_{sun} \end{bmatrix} ds \\ &= \int_{s_0}^{\bar{s}} \begin{bmatrix} 2 \cos(s - s_{sun}) + 3(s - s_0) \sin(s - s_{sun}) \\ -3 \sin(s - s_{sun}) \\ \sin(s - s_{sun}) \cos s - \sin s_{sun} \\ \sin(s - s_{sun}) \sin s + \cos s_{sun} \\ -\tan \theta_{sun} \sin s \\ \tan \theta_{sun} \cos s \end{bmatrix} ds \\ &= \begin{bmatrix} 5 \sin(s - s_{sun}) - 3(s - s_0) \cos(s - s_{sun}) \\ 3 \cos(s - s_{sun}) \\ -(3/2)s \sin s_{sun} - (1/4) \cos(2s - s_{sun}) \\ (3/2)s \cos s_{sun} - (1/4) \sin(2s - s_{sun}) \\ \tan \theta_{sun} \cos s \\ \tan \theta_{sun} \sin s \end{bmatrix} \Big|_{s=s_0} \end{aligned}$$

Thus the increments of the synchronous elements at the sidereal angle $\bar{s} \geq s_0$ due to solar radiation pressure are as follows.

Formula (D):

Effect of solar radiation pressure

$$\begin{aligned} &\frac{\psi^2 R}{\sigma P \cos^2 \theta_{sun}} [\Delta \lambda_0^m, \Delta D, \Delta e_x, \Delta e_y, \Delta i_x, \Delta i_y]^T \\ &= \begin{bmatrix} 5 \sin(s - s_{sun}) - 3(s - s_0) \cos(s - s_{sun}) \\ 3 \cos(s - s_{sun}) \\ -(3/2)s \sin s_{sun} - (1/4) \cos(2s - s_{sun}) \\ (3/2)s \cos s_{sun} - (1/4) \sin(2s - s_{sun}) \\ \tan \theta_{sun} \cos s \\ \tan \theta_{sun} \sin s \end{bmatrix} \Big|_{s=s_0} \end{aligned}$$

Linearized orbital dynamics

We now study the motion of a geostationary spacecraft under the influence of a Keplerian force which is perturbed by arbitrary sequences of impulsive and non-impulsive manoeuvres and by solar radiation pressure. More specifically, assume that there are I impulsive manoeuvres at sidereal angles $s^{(i)}$ with velocity increments $\Delta_R^{(i)}$, $\Delta_T^{(i)}$, $\Delta_N^{(i)}$ (where $1 \leq i \leq I$) and that there are K nonimpulsive manoeuvres over the arcs $[s_1^{(k)}, s_2^{(k)}]$ with the constant accelerations $a_R^{(k)}$, $a_T^{(k)}$, $a_N^{(k)}$ (where $1 \leq k \leq K$). Let

$$\begin{bmatrix} (\Delta \lambda_0^m)^{(i)} \\ (\Delta D)^{(i)} \\ (\Delta e_x)^{(i)} \\ (\Delta e_y)^{(i)} \\ (\Delta i_x)^{(i)} \\ (\Delta i_y)^{(i)} \end{bmatrix} (\bar{s}), \quad \begin{bmatrix} (\Delta \lambda_0^m)^{(k)} \\ (\Delta D)^{(k)} \\ (\Delta e_x)^{(k)} \\ (\Delta e_y)^{(k)} \\ (\Delta i_x)^{(k)} \\ (\Delta i_y)^{(k)} \end{bmatrix} (\bar{s}) \quad \text{and} \quad \begin{bmatrix} (\Delta \lambda_0^m)^{\text{sun}} \\ (\Delta D)^{\text{sun}} \\ (\Delta e_x)^{\text{sun}} \\ (\Delta e_y)^{\text{sun}} \\ (\Delta i_x)^{\text{sun}} \\ (\Delta i_y)^{\text{sun}} \end{bmatrix} (\bar{s})$$

be the increments in the synchronous elements due to these manoeuvres and due to solar radiation pressure, respectively, at some sidereal angle $\bar{s} \geq s_0$. (These increments can be obtained from the formulas (B), (C) and (D) above.) Since we are considering a linearized model, the overall effect of several manoeuvres can be handled by superposition of the individual effects from each single manoeuvre. Thus at any sidereal angle $\bar{s} \geq s_0$ the instantaneous value of a synchronous element $\xi \in \{D, \lambda_0^m, i_x, i_y, e_x, e_y\}$ is given by

$$\begin{aligned} \bar{\xi}(\bar{s}) &= \xi + \sum_{i=1}^I (\Delta \xi)^{(i)}(\bar{s}) \\ &+ \sum_{k=1}^K (\Delta \xi)^{(k)}(\bar{s}) + (\Delta \xi)^{\text{sun}}(\bar{s}) \end{aligned} \quad (13)$$

where ξ is the value of the element at the epoch.

We now assume that the manoeuvres are so weak that even under their influence the motion of the satellite can be considered geostationary and hence can be reasonably described by the above linearization about $e = 0$, $i = 0$ and $a = R$. This means that the evolution formula (A) is still valid if the synchronous elements in this formula are augmented by the appropriate increments. In other words, we assume that the linearized model is valid throughout the spacecraft motion as long as the values for the synchronous elements are properly updated. Then the orbital evolution of the satellite is

given by the formulas

$$\begin{aligned} r(s) &\approx R - (2R/3)\bar{D}(s) - R(\bar{e}_x(s) \cos s + \bar{e}_y(s) \sin s); \\ \theta(s) &\approx -\bar{i}_x(s) \cos s - \bar{i}_y(s) \sin s; \\ \lambda(s) &\approx \bar{\lambda}_0^m(s) + \bar{D}(s)(s - s_0) + 2\bar{e}_x(s) \sin s - 2\bar{e}_y(s) \cos s; \\ r'(s) &\approx R(\bar{e}_x(s) \sin s - \bar{e}_y(s) \cos s); \\ \theta'(s) &\approx \bar{i}_x(s) \sin s - \bar{i}_y(s) \cos s; \\ \lambda'(s) &\approx \bar{D}(s) + 2\bar{e}_x(s) \cos s + 2\bar{e}_y(s) \sin s. \end{aligned}$$

Plugging in (13) and using the formulas (B), (C) and (D) for the increments $(\Delta \xi)^{(i)}$, $(\Delta \xi)^{(k)}$ and $(\Delta \xi)^{\text{sun}}$, we arrive at the following final result:

$$\begin{aligned} \bullet \quad r(s) &\approx R - 2RD/3 - R(e_x \cos s + e_y \sin s) \\ &+ \sum_{i=1}^I (A_i(s)\Delta_T^{(i)} + B_i(s)\Delta_R^{(i)}) \\ &+ \sum_{k=1}^K (\bar{A}_k(s)a_T^{(k)} + \bar{B}_k(s)a_R^{(k)}) \\ &- \frac{3\sigma P \cos^2 \theta_{\text{sun}}}{2\psi^2} (s - s_0) \sin(s - s_{\text{sun}}) \\ &+ \frac{\sigma P \cos^2 \theta_{\text{sun}}}{4\psi^2} (\cos(s - s_{\text{sun}}) - \cos(2s_0 - s - s_{\text{sun}})) \\ &+ \frac{2\sigma P \cos \theta_{\text{sun}} \sin \theta_{\text{sun}}}{\psi^2} (\cos(s - s_{\text{sun}}) - \cos(s_0 - s_{\text{sun}})); \\ \bullet \quad \theta(s) &\approx -i_x \cos s - i_y \sin s \\ &+ \sum_{i=1}^I C_i(s)\Delta_N^{(i)} + \sum_{k=1}^K \bar{C}_k(s)a_N^{(k)} \\ &- \frac{\sigma P \cos \theta_{\text{sun}} \sin \theta_{\text{sun}}}{\psi^2 R} (1 - \cos(s - s_0)); \\ \bullet \quad \lambda(s) &\approx \lambda_0^m + D(s - s_0) + 2e_x \sin s - 2e_y \cos s \\ &+ \sum_{i=1}^I (D_i(s)\Delta_T^{(i)} + E_i(s)\Delta_R^{(i)}) \\ &+ \sum_{k=1}^K (\bar{D}_k(s)a_T^{(k)} + \bar{E}_k(s)a_R^{(k)}) \\ &- \frac{3\sigma P \cos^2 \theta_{\text{sun}}}{\psi^2 R} (s - s_0) (\cos(s - s_{\text{sun}}) + \cos(s_0 - s_{\text{sun}})) \\ &+ \frac{\sigma P \cos^2 \theta_{\text{sun}}}{2\psi^2 R} (\sin(s - s_{\text{sun}}) - \sin(2s_0 - s - s_{\text{sun}})) \\ &+ \frac{5\sigma P \cos^2 \theta_{\text{sun}}}{\psi^2 R} (\sin(s - s_{\text{sun}}) - \sin(s_0 - s_{\text{sun}})). \end{aligned}$$

Here D , λ_0^m , e_x , e_y , i_x and i_y are the synchronous elements at the epoch. The functions A_i, \dots, E_i are de-

defined as follows:

$$\begin{aligned}
 A_i(s) &:= \frac{2}{\psi} \cdot \begin{cases} 0, \\ 1 - \cos(s - s^{(i)}), \end{cases} \\
 B_i(s) &:= \frac{1}{\psi} \cdot \begin{cases} 0, \\ \sin(s - s^{(i)}), \end{cases} \\
 C_i(s) &:= \frac{1}{\psi R} \cdot \begin{cases} 0, \\ \sin(s - s^{(i)}), \end{cases} \\
 D_i(s) &:= \frac{1}{\psi R} \cdot \begin{cases} 0, \\ 4 \sin(s - s^{(i)}) - 3(s - s^{(i)}), \end{cases} \\
 E_i(s) &:= \frac{-2}{\psi R} \cdot \begin{cases} 0, \\ 1 - \cos(s - s^{(i)}), \end{cases}
 \end{aligned}$$

according to whether $s \leq s^{(i)}$ or $s \geq s^{(i)}$. Finally, the functions $\bar{A}_k, \dots, \bar{E}_k$ are given by the expressions

$$\begin{aligned}
 \bar{A}_k(s) &:= \begin{cases} 0 & \text{if } s \leq s_1^{(k)}, \\ \alpha(s, s_1^{(k)}, s) & \text{if } s_1^{(k)} \leq s \leq s_2^{(k)}, \\ \alpha(s, s_1^{(k)}, s_2^{(k)}) & \text{if } s \geq s_2^{(k)}; \end{cases} \\
 \bar{B}_k(s) &:= \begin{cases} 0 & \text{if } s \leq s_1^{(k)}, \\ \beta(s, s_1^{(k)}, s) & \text{if } s_1^{(k)} \leq s \leq s_2^{(k)}, \\ \beta(s, s_1^{(k)}, s_2^{(k)}) & \text{if } s \geq s_2^{(k)}; \end{cases} \\
 \bar{C}_k(s) &:= \begin{cases} 0 & \text{if } s \leq s_1^{(k)}, \\ \gamma(s, s_1^{(k)}, s) & \text{if } s_1^{(k)} \leq s \leq s_2^{(k)}, \\ \gamma(s, s_1^{(k)}, s_2^{(k)}) & \text{if } s \geq s_2^{(k)}; \end{cases} \\
 \bar{D}_k(s) &:= \begin{cases} 0 & \text{if } s \leq s_1^{(k)}, \\ \delta(s, s_1^{(k)}, s) & \text{if } s_1^{(k)} \leq s \leq s_2^{(k)}, \\ \delta(s, s_1^{(k)}, s_2^{(k)}) & \text{if } s \geq s_2^{(k)}; \end{cases} \\
 \bar{E}_k(s) &:= \begin{cases} 0 & \text{if } s \leq s_1^{(k)}, \\ \varepsilon(s, s_1^{(k)}, s) & \text{if } s_1^{(k)} \leq s \leq s_2^{(k)}, \\ \varepsilon(s, s_1^{(k)}, s_2^{(k)}) & \text{if } s \geq s_2^{(k)}. \end{cases}
 \end{aligned}$$

where the auxiliary functions $\alpha, \dots, \varepsilon$ are defined as follows:

$$\begin{aligned}
 \alpha(s, s_1, s_2) &:= \frac{2}{\psi^2} (s_2 - s_1 + \sin(s - s_2) - \sin(s - s_1)), \\
 \beta(s, s_1, s_2) &:= \frac{1}{\psi^2} (\cos(s - s_2) - \cos(s - s_1)), \\
 \gamma(s, s_1, s_2) &:= \frac{1}{\psi^2 R} (\cos(s - s_2) - \cos(s - s_1)), \\
 \delta(s, s_1, s_2) &:= \frac{1}{2\psi^2 R} \left[8(\cos(s - s_2) - \cos(s - s_1)) \right. \\
 &\quad \left. + 3(s_2 - s_1)(s_1 + s_2 - 2s) \right], \\
 \varepsilon(s, s_1, s_2) &:= \frac{-2}{\psi^2 R} (s_2 - s_1 + \sin(s - s_2) - \sin(s - s_1)).
 \end{aligned}$$

Application to orbit determination

In the above discussion we derived a linearized model which explicitly describes the motion of a spacecraft in geostationary orbit under the influence of a Keplerian force which is perturbed by impulsive and nonimpulsive manoeuvres and by solar radiation pressure. The formulas obtained immediately yield the partial derivatives of r, λ and θ with respect to the dynamical parameters involved (state at epoch, manoeuvre parameters, effective cross section/mass ratio) as functions of the synchronous elements at epoch, the spacecraft sidereal angles at the manoeuvre times and the current sidereal angle. On the other hand, the partial derivatives of the measurement variables (range, azimuth and elevation) with respect to r, λ and θ are known offhand as functions of r, λ and θ (being obtainable from purely geometric formulas). All these partial derivatives can be effectively evaluated during the run of an orbit determination programme^{4,5}. Consequently, the chain rule allows one to determine the partial derivatives of the measurement variables with respect to the dynamical parameters: as explained above, this enables one to set up a least squares iteration to estimate these parameters. Numerical tests proved the validity of the proposed model for orbit determination purposes.

Acknowledgment

I am greatly indebted to Trevor Morley and Mattias Soop at ESOC for many valuable discussions.

References

- 1 Lechte, Bird, van Holtz, Oppenhauser, *ESA's Advanced Relay and Technology Mission*, ESA Bulletin 62, May 1990
- 2 Erik Mattias Soop, *Orbit determination by least squares iterations*, ESOC Internal Note No. 143, Darmstadt 1974
- 3 Erik Mattias Soop, *Introduction to geostationary orbits*, European Space Agency, SP-1053, Paris 1983
- 4 Karlheinz Spindler, *A linear model for the motion of a spacecraft in geostationary orbit*, European Space Operations Centre, OAD Working Paper No. 480, Darmstadt 1993
- 5 Karlheinz Spindler, *Orbit determination with non-impulsive manoeuvres*, European Space Operations Centre, OAD Working Paper No. 486, Darmstadt 1993

High-Order State Estimation for Space-Plane with Several Antennas

Shuji ONO

Engineer, System Technology Development Department, Tsukuba Space Center,
 National Space Development Agency of Japan (NASDA)
 2-1-1, Sengen, Tsukuba-city, Ibaragi-ken, JAPAN, Tel. 0298-52-2245, Fax. 52-2247

1 Abstract

The real-time flight control and safety system on the ground for a launch rocket or a return spacecraft, has often required the new tool, independent of the vehicle inner information by a telemeter, in order to evaluate the functioning of the on-board flight control system. This needs the estimation for the high-order state vector of attitude angle, angular rate, thrust, its offset, and dynamic parameters, beyond the ordinary estimation of position and velocity.

This paper presents the new algorithms of both stochastic and deterministic estimation for the high-order state vector of a space-plane equipped with several antennas, so as to distinguish each outer information (range & range rate, etc) of corresponding antenna. The simulation for a powered flight of return-to-Earth phase shows that the estimation has remarkably higher precision as the body scale becomes bigger. This paper would give one of fundamental guidelines both for the construction of the ground control system separate from telemeter data, and for the design of the on-board flight control system with the true robustness by two independent on-board logics, for the future space-plane.

2 Introduction

This analysis was started from the discussions in the concept study^{1,2} for the future flight control and safety system of HOPE (H-II Orbiting Plane), which is the first Japanese un-manned space-plane presently under considerations by NASDA (National Space Development Agency of Japan).

The present flight safety system for a launch rocket aims the real-time protection against a hazard due to a malfunctioning vehicle by the destruct command operations. For this decision, the position and velocity of a rocket is the primary information, and estimated in real-time by a sequential technique from the outer information (radar, optical system) independent of telemeter data. The rocket attitude, its rate, motor chamber pressure are monitored by a telemeter and treated to be the secondary as the vehicle inner information. On the other hand, the satellite operation is periodical as a constant visibility from the ground, and not real-time because the flight safety is not necessary for an orbiting satellite. The orbit and attitude of a satellite is determined by a batch technique from the measurement data stocked for several hours.

However in the future flight control and safety system for a space-plane, the operational configuration is prospected to be much different from the present. The flight profile of a space-plane consists of three main phases: the launch phase by a rocket, and the on-orbit phase including the rendez-vous with Space Station, and finally the Return-to-Earth phase from a de-orbit upto a landing. On the rendez-vous with the manned Space Station, the space-plane must be controlled with an extra care of safety, in order to avoid collision and contamination. Moreover the Return-to-Earth is also a new technical field in Japan. The de-orbit is one of the important maneuvers in this phase. A control is necessary to target the fixed re-entry corridor. If out-of-corridor, the vehicle will skip out or melt due to atmosphere. After skip-out, the possible point of second re-entry will spread over large area around the Earth. Then the tracking and control of spacecraft will be very much difficult, also for a flight safety.

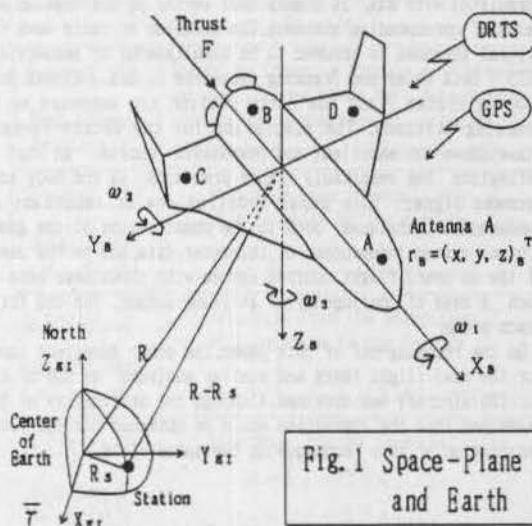


Fig. 1 Space-Plane and Earth

Although an un-manned space-plane will be maneuvered by an on-board flight control system, the flight is necessary to be judged and controlled in safety by a flight controller on the ground or in Space Station. Namely it is important that the flight controller (man) has the full-authority, and can override the flying on-board system (machine) if necessary. These require a flight control system on the ground and in Space Station with the functions: the real-time estimation of flight state (position, velocity, particularly attitude and its rate, etc), the super real-time prediction/simulation of flight state (re-entry corridor, landing point, relative conditions to Space Station), the evaluation of on-board system, the judgement of flight condition and safety, and the real-time remote control for flight correction or safety execution. As the equipment of self-destruction powder is prohibited for a space-plane of rendez-vous mission, the ordinary way and system for a rocket is not available. One of possible means against an off-nominal flight of un-manned space-plane would be the real-time remote control overrode by the flight controller for the actions: the rendez-vous stop and rapid exclusion from Space Station, and the flight safety execution by an aerodynamic destruction or by dropping in a safety area.

On the feasibility study for the construction of this flight control system, one of the same important and fundamental discussions, as the above of flight operations philosophy, was whether the on-board system can be evaluated by the separated way from the on-board information (logic and data), or not. The first key is the possibility of the independent estimation for the high-order state vector such as attitude, attitude rate, thrust, dynamic parameters, etc. The past analyses^{3,4} for the apogee motor burning phase of the geostationary satellite suggests that the high-order state vector can be estimated by a proper construction of both the dynamic and the measurement model. Moreover the winged space-plane is far much bigger than the past satellite. Therefore if several antennas are equipped on the proper locations of the space-plane, the high-order state vector was expected to be independently estimated from the outer information (range and range rate, etc) of the corresponding antennas. This idea is old, but the author could not find out the papers of excellent estimation results on the

beginning of this analysis.

Therefore the algorithms of both the stochastic and the deterministic estimation were newly constructed for the high-order state vector of a space-plane equipped with several antennas. The dynamic model is constructed with 19 dimensional state vector considering the spacecraft dynamics of powered flight. The measurement model of range, range rate, etc. is formulated with max. 24 dimensional vector to distinguish each datum of corresponding antenna. The emission of radio wave from several antennas is assumed to be simultaneous or sequential. DRTS (Data Relay and Tracking Satellite), GPS (Global Positioning System), and the Earth station are supposed as the tracking stations. The simulation for the Return-to-Earth phase shows the excellent and reasonable results, so that the estimation has remarkably higher precision as the body scale becomes bigger. This paper supplies one of important and fundamental techniques both to the construction of the ground control system independent of telemeter data, and to the design of the on-board flight control system with robustness even in such a case of contingency of attitude sensor, for the future space-plane.

On the rounding-off of this paper, the other excellent paper⁸ for the real flight tests and similar analyses by use of King Air 200 aircraft was obtained. Although the originality of this paper was lost, the conviction would be obtained for the future application of this technique in the space field.

3 Algorithm of Stochastic Estimation

This chapter outlines the algorithm of stochastic estimation for the high-order state vector of a space-plane with several antennas during powered flight. The extended Kalman filter² is adopted as one of the stochastically optimum filters. The algorithm of both the dynamic model and the measurement model is developed from the previous^{4, 5}.

Fig. 1 shows the relation between the Earth and a space-plane for a de-orbit phase. The spacecraft body coordinate and the Earth centered inertial coordinate are also defined. Four antennas are located in front and rear of the fuselage, and also on both wingtips. The motor thrust direction coincides with the body axis X_b . The tracking stations are assumed to be DRTS on a geostationary orbit, GPS on the orbits of 20000 km altitude, and the Earth station. The constructed Dynamic Model and the Measurement Model are described as follows.

3-1 Dynamic Model

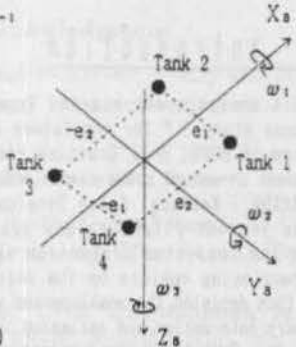
(1) State Vector X_k

The spacecraft state vector X_k is of 19 dimensions and composed of the spacecraft position, velocity, Euler angle of roll/pitch/yaw, angular rate, thrust offset as a dynamic unbalance, Moment of Inertia, mass, and motor thrust parameter.

$$X_k = (\underbrace{X, Y, Z}_{\text{Position}}, \underbrace{\dot{X}, \dot{Y}, \dot{Z}}_{\text{Velocity}}, \underbrace{\phi, \theta, \psi}_{\text{Euler Angle}}, \underbrace{\omega_1, \omega_2, \omega_3}_{\text{Angular Rate}}, \underbrace{r_1, r_2}_{\text{Thrust Offset}}, \underbrace{I_{xx}, I_{yy}, I_{zz}}_{\text{Moment of Inertia}}, \underbrace{M}_{\text{Mass}}, \underbrace{\eta}_{\text{Thrust Parameter}})^T \quad (1)$$

(2) Dynamic Model $F(X_k, t_k)$

The Dynamic Model $X_k = F(X_{k-1}, t_{k-1})$ is as follows.

$$\begin{aligned} t_k &= t_{k-1} + \Delta t \\ \Gamma_k &= \Gamma_{k-1} + V_{k-1} \Delta t + (a_{k-1} - \mu \frac{r_{k-1}}{|r_{k-1}|^3}) \frac{\Delta t^2}{2} \\ V_k &= V_{k-1} + (a_{k-1} - \mu \frac{r_{k-1}}{|r_{k-1}|^3}) \Delta t \\ \phi_k &= \phi_{k-1} + \Delta t [\omega_1 + (\omega_2 \sin \phi + \omega_3 \cos \phi) \tan \theta]_{k-1} \\ \theta_k &= \theta_{k-1} + \Delta t [\omega_2 \cos \phi - \omega_3 \sin \phi]_{k-1} \\ \psi_k &= \psi_{k-1} + \Delta t [(\omega_2 \sin \phi + \omega_3 \cos \phi) / \cos \theta]_{k-1} \\ [\omega_1]_k &= [\omega_1]_{k-1} + \Delta t [(I_{yy} - I_{zz}) \omega_2 \omega_3 / I_{xx}]_{k-1} \\ [\omega_2]_k &= [\omega_2]_{k-1} + \Delta t [(I_{zz} - I_{xx}) \omega_3 \omega_1 + r_2 F] / I_{yy}]_{k-1} \\ [\omega_3]_k &= [\omega_3]_{k-1} + \Delta t [(I_{xx} - I_{yy}) \omega_1 \omega_2 - r_1 F] / I_{zz}]_{k-1} \\ [I_{xx}]_k &= [I_{xx}]_{k-1} - \Delta t \dot{m}_{k-1} e_1^2 \\ [I_{yy}]_k &= [I_{yy}]_{k-1} - \Delta t \dot{m}_{k-1} e_2^2 \\ [I_{zz}]_k &= [I_{zz}]_{k-1} - \Delta t \dot{m}_{k-1} (e_1^2 + e_2^2) \\ M_k &= M_{k-1} - \Delta t \dot{m}_{k-1} \\ [r_1]_k &= [r_1]_{k-1} \\ [r_2]_k &= [r_2]_{k-1} \\ \eta_k &= \eta_{k-1} \end{aligned} \quad (2)$$


where

$$F_k = \eta_k F(t)$$

$$\dot{m}_k = F_k / (I_{sp} g)$$

$$a_k = \begin{pmatrix} a_x \\ a_y \\ a_z \end{pmatrix} = \frac{F_k}{M_k} \begin{pmatrix} U_x \\ U_y \\ U_z \end{pmatrix}_k$$

$F(t)$: Thrust Table
 U_x, U_y, U_z : direction cosines
 e_1, e_2 : Tanks locations.

(3) Error Propagation Matrix Φ_k

The Error Propagation Matrix Φ_k (19 x 19) is obtained by the partial derivatives of the Dynamic Model.

$$\Phi_k = \left(\frac{\partial F}{\partial X} \right)_k \quad (3)$$

3-2 Measurement Model

The measurement model is formulated so as to distinguish each datum of corresponding antenna. The emission of radio wave from several antennas is assumed to be simultaneous or sequential. The measurement vector is of range and range rate for a de-orbit phase. The measurement of angle is moreover considered for a landing phase. The algorithm for the range and range rate between the spacecraft antenna and the tracking station is as follows :

(1) Measurement Vector Y_k and Model $G(X_k, t_k)$

$$Y_k = G(X_k, t_k) = [\rho_{as}, \dot{\rho}_{as}]_k^T \quad (4)$$

$$\left\{ \begin{aligned} \rho_{as} &= [(X+X_a-X_s)^2 + (Y+Y_a-Y_s)^2 + (Z+Z_a-Z_s)^2]^{1/2} \\ \dot{\rho}_{as} &= [(X+X_a-X_s)(\dot{X}+\dot{X}_a-\dot{X}_s) + (Y+Y_a-Y_s)(\dot{Y}+\dot{Y}_a-\dot{Y}_s) \\ &\quad + (Z+Z_a-Z_s)(\dot{Z}+\dot{Z}_a-\dot{Z}_s)] / \rho_{as} \\ R_a &= [X_a, Y_a, Z_a]^T = [C][A][x_a, y_a, z_a]^T \\ \dot{R}_a &= [\dot{X}_a, \dot{Y}_a, \dot{Z}_a]^T = [C][\dot{A}][x_a, y_a, z_a]^T \end{aligned} \right.$$

where a, s : subscript of antenna number ($a=1 \sim 4$),
and of station number ($s=1 \sim 7$),
 $\rho_{as}, \dot{\rho}_{as}$: slant range and range rate between
spacecraft antenna and tracking station.
 R_a, \dot{R}_a : antenna position and velocity.
[A] : coordinate transformation matrix, defined
by (ϕ, θ, ψ) .
[A] : time derivative of [A], defined
by $(\dot{\phi}, \dot{\theta}, \dot{\psi}, \omega_1, \omega_2, \omega_3)$.
[C] : constant matrix of initial attitude.

(2) Measurement Matrix H_k

The measurement matrix H_k is defined from $G(X_k, t_k)$.

$$H_k = \left(\frac{\partial G}{\partial X} \right)_k = \left[\left(\frac{\partial G}{\partial X} \right)_{k,s} \right]_k \quad (5)$$

where the dimensions of matrix H_k is :
(24 × 19) : Simultaneous Measurement Model for
3 Stations & 4 Antennas.
(10 × 19) : Sequential Measurement Model for
5 Stations & Cyclic one of 4 Antennas.

4 Algorithm of Deterministic Estimation

The outline of this algorithm is shown in Table 1. If each of the antennas data is distinguished, each antenna position is directly determined from three range data between the antenna and three stations by the usual way. But this directly determined positions of several antennas are without the constraint that each antenna point is fixed in the instantaneous body coordinates. Therefore the antenna point on the Fixed Frame is necessary to be determined so as to be as near to the directly determined point as possible. Each antenna velocity is also determined with Fixed Frame constraint.

Table 1 Algorithm of Deterministic Estimation

Step 1 Data Smoothing	Smooth Measurement Data of Range & Range Rate by Least Square Method.
Step 2 Each Antenna Position R_a	Search an intersection point of 3 spherical surfaces with Fixed Frame constraint, from Range data between antenna and 3 stations. (Station position X_s) $\rho_{as} = R_a - X_s $
Step 3 Each Antenna Velocity V_a	Search by Cramer's formula with Fixed Frame constraint, from Range Rate data between antenna and 3 stations. (velocity V_s) $\dot{\rho}_{as} = (V_a - V_s) \cdot (R_a - X_s) / \rho_{as}$
Step 4 Euler Angle (ϕ, θ, ψ)	Determine from the positions R_a of 4 antennas by the formula : $R_{1-} - R_{1+} = [C][A](r_{1-} - r_{1+})$
Step 5 Anguler Rate ($\omega_1, \omega_2, \omega_3$)	Determine from the velocities V_a of 4 antennas by the formula : $V_{1-} - V_{1+} = [C][\dot{A}](r_{1-} - r_{1+})$
Step 6 Position R Velocity V	Determine by the formulas : $R = R_a - [C][A] r_a$ $V = V_a - [C][\dot{A}] r_a$
Step 7 The Others	($r_1, r_2, i_{xx}, i_{yy}, i_{zz}, \eta, M$) are estimated by an iteration of state propagation.

where Antenna subscript : $1 \leq a, a' \leq 4$,
Station subscript : $s = 1 \sim 3$.

4-1 Position Determination by Fixed Frame Method

The antenna position with Fixed Frame constraint of constant length among antennas points can be obtained by Six Parameters Search with S_R minimum, as shown in Fig. 2 :

$$S_R = A_0 A^2 + B_0 B^2 + C_0 C^2 + D_0 D^2 \rightarrow \text{Minimum} \quad (6)$$

where A_0, B_0, C_0, D_0 : directly determined points.
 A, B, C, D : points with Fixed Frame constraint.
 $\delta x, \delta y, \delta z, \theta_1, \theta_2, \theta_3$: Six Parameters for Position Search

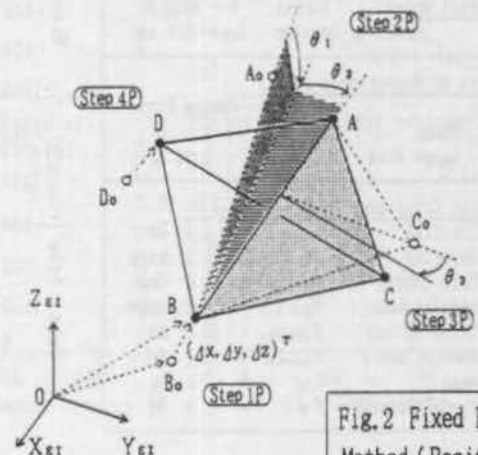


Fig. 2 Fixed Frame Method (Position)

as shown in Table 4. The equipment of several antennas was verified to be effective.

Especially the validity is well recognized in comparison with the results of one antenna in Fig. 6 (run case HB-0A). The estimation of roll and its rate is not expected because of divergence, but the others are estimated with good accuracy even in the case of one antenna. This tendency was already indicated in the past analyses*. The past target was the solid apogee motor burning phase of spinning satellite, and the roll and its rate were not necessary to be estimated.

Table 4 shows the converged variances at the simulation end $T = 150$ seconds for several different cases. The cases (HB-0A, 1A, 10A, 20A, RB-1A) are the simulations for the De-Orbit phase.

The case HB-30A is the simulation in the vicinity of a landing ground. Only RB-1A is of a rocket type body, and results a good estimation in spite of a short length between antenna C and D. The case HB-10A is the simulation by adding the attitude information (sun angle, Earth code width) to the case HB-1A.

Fig. 7 is the changes of the error variances at $T = 150$ s. in accordance with the body scale. The results indicate that the precision remarkably ameliorates as the vehicle scale becomes bigger. The purpose of this analysis is how much close the estimation from the range and range rate becomes to that with the attitude information. The possibility was thought to be technically verified.

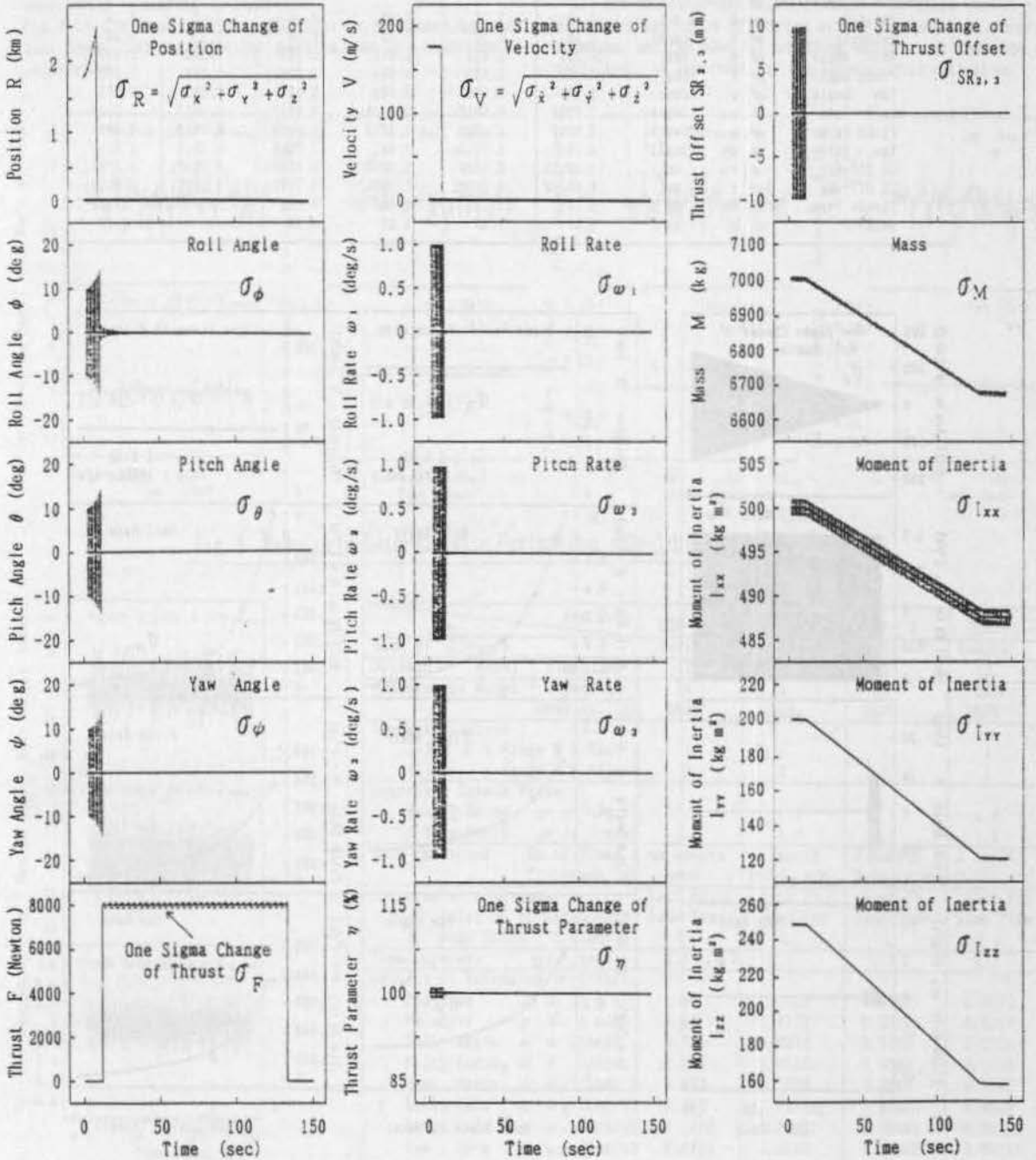


Fig. 5 Results of Stochastic Estimation (De-Orbit Phase, case HB-1A)

Table 4 Stochastic Estimation Results for De-Orbit Phase

Run Case	HB-0A	HB-1A	HB-10A	HB-20A	HB-30	RB-1A
Name of Software	Update1	Update1	Update1	RRR4	Land	Update
Dynamic Model (dimension)	19	19	19	19	19	19
Measurement Model (dimension)	10	10	14	24	17	10
(combination)	R&R	R&R	R&R& θ &EW	R&R	R&R&Az&E1	R&R
Tracking Station & Sensor :						
DRTS (Range & R.Rate)	1	1	1	1	—	1
GPS (Range & R.Rate)	4	4	4	2	4	4
Ground Station (R. & Az& E1)	—	—	—	—	3	—
ST (Sun Angle $\theta_{1,2}$)	—	—	1	—	—	—
EW (Earth Width EW $_{1,2}$)	—	—	1	—	—	—
Range Random Noise σ_R (m)	1.0	1.0	1.0	1.0	1.0	1.0
R.Rate Rand. Noise σ_{RR} (cm/s)	1.0	1.0	1.0	1.0	1.0	1.0
Location of 4 antennas & Emission of Radio Wave & Body Scale (Times)						
	Origin Sequential	Each Point Sequential	Each Point Sequential	Each Point Same Time	Each Point Sequential	Each Point Sequential
	0	1	1	1	1	1
Time Interval Δt (sec)	0.025	0.025	0.025	0.1	0.025	0.025
Results of Estimated σ Error:						
Position σ_R (m)	0.16	0.16	0.16	0.16	0.15	0.16
Velocity σ_V (cm/s)	0.50	0.50	0.50	0.50	0.50	0.50
Roll Angle σ_ϕ (deg)	150.333	0.210	0.011	0.338	0.222	0.310
Pitch Angle σ_θ (deg)	0.171	0.093	0.081	0.076	0.095	0.071
Yaw Angle σ_ψ (deg)	0.170	0.086	0.026	0.067	0.085	0.071
Roll Rate σ_{ω_1} (deg/s)	1.0000	0.0017	0.0006	0.0027	0.0017	0.0040
Pitch Rate σ_{ω_2} (deg/s)	0.0042	0.0017	0.0016	0.0018	0.0013	0.0010
Yaw Rate σ_{ω_3} (deg/s)	0.0042	0.0015	0.0011	0.0015	0.0013	0.0010
CG Off-set σ_{r_1} (mm)	0.00003	0.00001	0.00001	0.00001	0.00001	0.00001
CG Off-set σ_{r_2} (mm)	0.00002	0.00001	0.00001	0.00001	0.00001	0.00001
Thrust Param. σ_a (%)	0.149	0.149	0.149	0.143	----	0.149
Mass σ_M (kg)	3.47	3.47	3.47	3.47	----	3.47

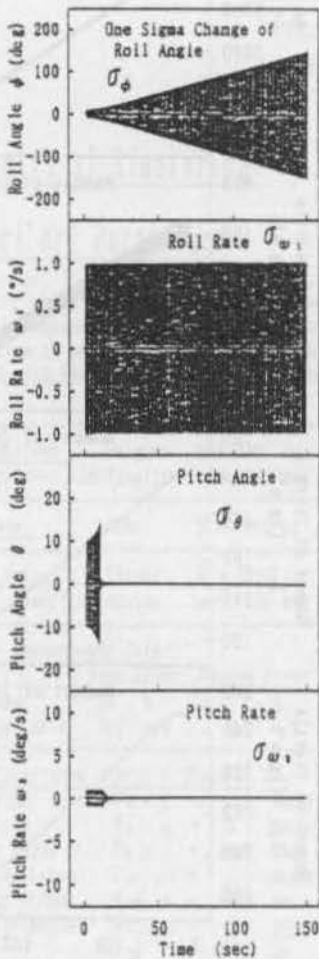


Fig. 6 Results of One Antenna (Stochastic Estimation)

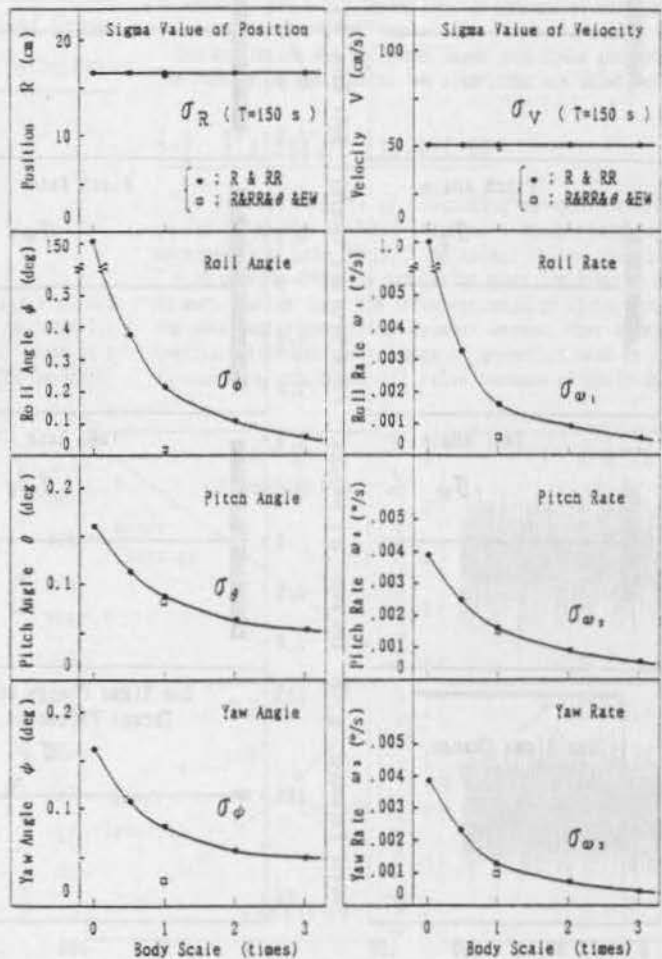


Fig. 7 Effects of Body Scale (Stochastic Estimation)

5-3 Deterministic Estimation

The results of deterministic estimation are described for the simultaneous emission model of four antennas, and also suggests high accuracy. The measurement data smoothing is necessary before the deterministic estimation, although the stochastic filter itself eliminates the random noise of raw data. Several smoothing methods were tried, but only the typical cases are mentioned.

Fig. 8 shows the results (run case HDF-12) for the De-Orbit phase. The smoothing of measurement data is twice with the criterion $|Y - Y_N| \rightarrow \min$. The estimation starts from $T = 10$ seconds. The estimated state varies very narrowly around the Nominal state change. The constructed algorithm was verified excellently to operate as expected.

Fig. 9 is the results (case HDF-02) by no smoothing, and also proves that the algorithm operates even in a condition of large noise.

Table 5 shows the standard deviations for the typical cases, which were calculated from the differences between the Nominal and the determined state over the simulation time. The standard deviation is indicated to be smaller according to the data smoothing.

Fig. 10 is the change of the standard deviation in accordance with the body scale, and also results that the precision remarkably ameliorates as the vehicle scale becomes bigger. The one antenna estimation is impossible due to the algorithm. The effect by the Fixed Frame method is shown to be remarkable as compared with the results of direct determination. The Fixed Frame method constructed for the rigid model will be developed for a flexible model by the small change of the conditions for both the relative velocity and the length between antennas.

The deterministic estimation of high-order state vector was also verified to be effective by the equipment of several antennas. And the powerful smoothing, which is not the scope of this paper, is important for the deterministic estimation.

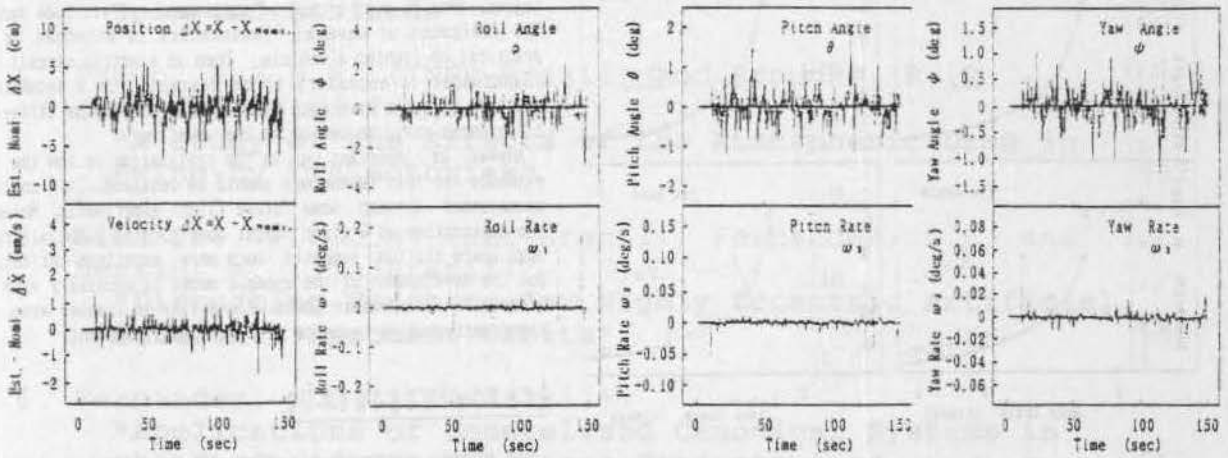


Fig. 8 Results of Deterministic Estimation (De-Orbit Phase, case HDF-12)

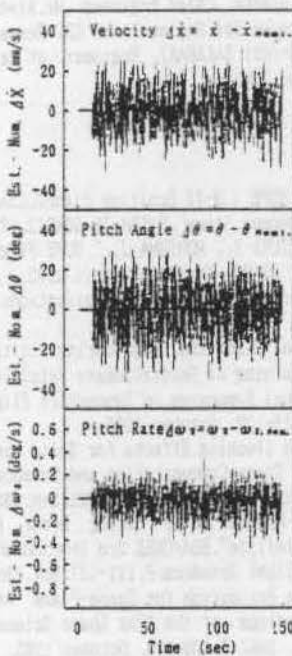


Fig. 9 Results of No Smoothing

Run Case	HDF-02	HDF-03	HDF-12	RDF-1
Name of Software	Update	Update	Update	Update
Dynamic Model (dimension)	12	12	12	12
Measurement Model (dimension)	24	24	24	24
(combination)	R&R	R&R	R&R	R&R
Tracking Station ;				
DRTS (Range & R.Rate)	1	1	1	1
GPS (Range & R.Rate)	2	2	2	2
Generated Random Noise ;				
Range Noise σ_R (m)	1.0	1.0	1.0	1.0
R.Rate Noise σ_{RR} (cm/s)	1.0	1.0	1.0	1.0
Data Smoothing (No. of Times)	no smooth	1 smooth	2 smooth	2 smooth
(Criterion)	none	$ Y - Y_N \rightarrow \min$	$ Y - Y_N \rightarrow \min$	$ Y - Y_N \rightarrow \min$
Location of 4 antennas & Emission of Radio Wave & Body Scale (Times)	Each Point Same Time	Each Pt. Same Time	Each Pt. Same Time	Each Pt. Same Time
Time Interval Δt (sec)	0.1	0.1	0.1	0.1
Results of Estimated ϵ Error:				
Position ϵ_R (m)	1.65	0.1525	0.0535	0.0536
Velocity ϵ_V (m/s)	14.42	1.4757	0.5520	0.5307
Roll Angle ϵ_ϕ (deg)	0.336	0.0292	0.0100	0.0254
Pitch Angle ϵ_θ (deg)	10.801	1.0153	0.3580	0.1788
Yaw Angle ϵ_ψ (deg)	8.439	0.7659	0.2815	0.1866
Roll Rate ϵ_{ω_1} (deg/s)	14.315	1.1342	0.49605	0.8620
Pitch Rate ϵ_{ω_2} (deg/s)	0.1082	0.0120	0.00487	0.00232
Yaw Rate ϵ_{ω_3} (deg/s)	0.0825	0.0098	0.00402	0.00224

Table 5 Deterministic Estimation Results for De-Orbit Phase

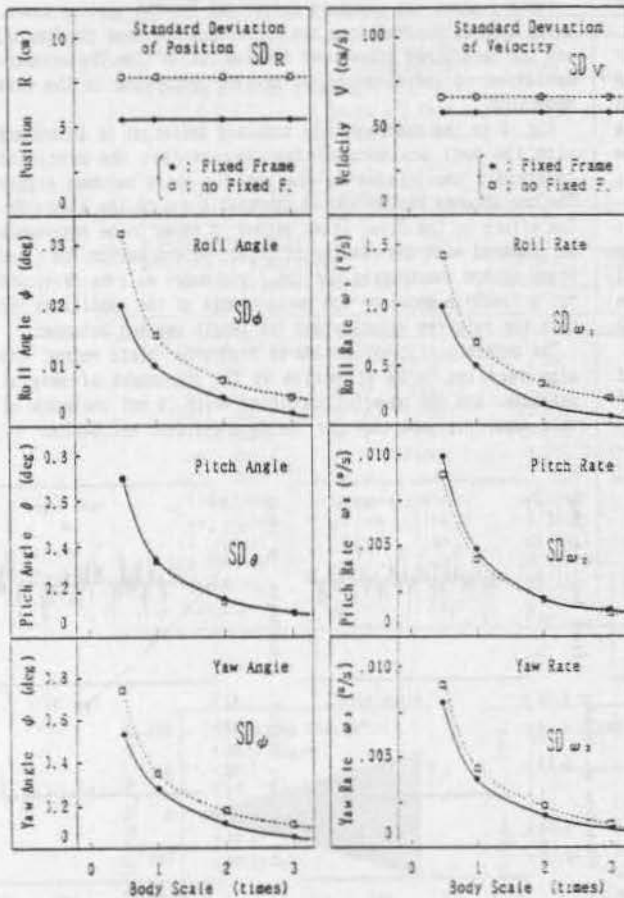


Fig. 10 Effects of Body Scale
(Deterministic Estimation)

5-4 Discussions

① Transponder :

The equipment of several transponders corresponding to antennas is ideal, but is not practical due to weight increase. Then the circuit modification of one transponder is necessary so as to emit radio wave sequentially from several antennas.

② Bias Errors :

Each bias error of corresponding antenna would be uniform from the two reasons. Each loss of the electric power supply is very little because the differences among the electric wiring lengths upto each antenna from one transponder are small of several meters. And the propagation paths of radio wave are almost the same for the long distanced spacecraft from the tracking stations. The bias error is constant for a short period, and can be estimated by the ground calibration test and the on-orbit estimation by the similar treatments in the present system for a rocket or a satellite.

Particularly, the changing tendency of the estimated state vector X_w is important on the decision of flight operations. A criterion whether the state can be estimated with a good precision or not, is the converging tendency of the estimated covariance matrix P_w . The author thinks that the influence of the bias error is not essential in the estimation of P_w for a short period. On the other hand, in the real-time system by use

of the deterministic estimation, the main information is also the changing tendency of X_w estimated by the good raw data, selected and corrected by the a priori models including the bias error model fixed by the above tests.

6 Conclusions

This paper verifies that the high-order state vector of a space-plane in powered flight can be excellently estimated by the equipment of several antennas on proper places of vehicle. Both algorithms of stochastic and deterministic are verified to be effective, also in place of attitude sensor. Especially in the flight control and safety system, the decision and action must be performed in real-time, ideally independent of the on-board information and logic. The means for this purpose has been expected, and the technical prospect for the realization is thought to be obtained. This paper would also give one of fundamental guidelines for the design of the on-board flight control system with the true robustness by two independent logics, even in such a case of contingency of attitude sensor. The equipment of several transponders to antennas is not practical to lighten a vehicle. Then an electric circuit of a transponder is necessary to be designed for a sequential emission of radio wave. Each bias error even for the difference of antennas could be set up by the usual way.

Anyway, an important key on the realization is how the real evidence for this technology should be obtained. This could be accomplished through some future flight experiments. Moreover the application to a giant flight body such as jumbo aircraft, huge space station, suggests much more excellent estimation. But the development of the dynamic model is necessary with the effects of aero-dynamic force, flexibility of slender wing, and inner perturbative resource of liquid fuel movement.

Acknowledgements

The author expresses his thanks to the following engineers for their cooperations of technical suggestions and computer runs : Mr. Takao ANZAI, General Manager, Mr. Yoshiaki SUZUKI, Chief Engineer, Mr. Yuji SIMOMURA, Engineer, of Tsukuba Space Center of NASDA, and Mr. Toshihiro HIWADA, Chief Engineer, Mr. Kiyoshi TOMOMURA, Engineer, Mrs. Katsuko Doi, Engineer, of CRC Research Institute, Inc., and Mr. Jun-ichi SAKAMAKI, Engineer, of Daiko Electronics and Communication Company.

References

- 1) NASDA, "Concept Design of HOPE (H-II Orbiting Plane), Chap. 5 HOPE Flight Operations Concept Study", NASDA-TK-S04012, 1992.
- 2) ONO S., NISHIYAMA K., SUZUKI Y., MORIUMA J., "HOPE Flight Operations Concept Study", NASDA-TK-S0410, April 1992.
- 3) IWATA T., "Estimation by Error Ellipsoid and Applications to Space Navigation", NASDA TR-7, July 1977.
- 4) ONO S., "State Estimation Algorithm Considering Attitude Motion for Apogee Motor Burning of Geostationary Satellite", ESA/CNES 2nd International Symposium on Spacecraft Flight Dynamics, ESA SP-255, P. 117-133, October 1986.
- 5) ONO S., "Spindynamics with Sloshing Effects for Solid Motor Burning Phase", Journal of Space Communication and Broadcasting, Special Issue on Spacecraft Dynamics, p. 295-321, Sep. 1987.
- 6) ONO S., "Evaluations of Apogee Motor Firing Error for Japanese Geostationary Satellite", ESA/CNES 3rd International Symposium on Spacecraft Flight Dynamics, P. 111-127, Nov. 1989.
- 7) ONO S., "High-Order State Estimation for Space-Plane with Several Antennas", Proceedings of the 37th Space Sciences and Technology Conference, 3A6, P. 429-430, October 1993.
- 8) Cohen C.E., Parkinson B.W., McNally D., "Flight Test of Attitude Determination Using GPS Compared Against an Inertial Measurement Unit", ION National Technical Meeting, P. 579-587, Jan., 1993.

SPACE DYNAMICS I

ORBITAL PERTURBATIONS OF GPS TYPE

1. Moraes, R.V. and Konemba, M. (ITA-Brazil):
"Orbital Perturbations of GPS Type Satellites" 523
2. Rodrigues, D.L.F. and Souza, M.L.O. (INPE-Brazil):
"Effects of Thrust Misalignments on Orbit Transfers" 527
3. Zanardi, M.C. (UNESP-Brazil) and Moraes, R.V. (ITA-Brazil):
"Effects of Solar Radiation Torque on Satellite Spin and Attitude" 532
4. Prado, A.F.B.A. (INPE-Brazil) and Broucke, R. (University of Texas-USA):
"A Study of the Effects of the Atmospheric Drag in Swing-by Trajectories" 537
5. Lima Jr., P.H.C.N. (EEI-Brazil); Fernandes, S.S. and Sessin, W. (ITA-Brazil):
"Disturbing Function for Highly Eccentric Artificial Satellite Resonant Orbits" 545
6. Fernandes, S.S. (ITA-Brazil):
"Applications of Generalized Canonical Systems in the Study of Optimal Space Trajectories" 552

ORBITAL PERTURBATIONS OF GPS TYPE SATELLITES

Rodolpho Vilhena de Moraes and Marcelo Konemba

CTA-ITA-IEAB

12228-900 - São José dos Campos-SP-BRASIL

FONE: (55)(123) 412211; FAX: (55)(123) 417069; E-mail: ITA@BRFAPESP.BITNET

Abstract

An analytical theory to compute orbital perturbations of GPS type satellites is briefly described. The following perturbations are considered: terrestrial gravitational field, luni-solar perturbations and solar pressure radiation. The influence of the 2:1 commensurability of the orbital period of the satellite with the period of the Earth's rotation is also presented. In order to take into account the resonance the geopotential is developed up to J_{32} terms. Hori's method and canonical transformations are used reducing the problem to the study of a dynamical system with one degree of freedom. The analytical solution is compared with a numerical integration of the equations. Some periodic effects of orbital perturbations due to J_2, J_{22}, J_{32} Moon, Sun and to the resonance, are exhibited for the semi-major axis. Within a period of about 1000 days, the resonance produces on the semi-major axis a perturbation of amplitude about 17 km.

Introduction

The space segment of the Global Positioning System (GPS) was originally conceived as a constellation of 24 satellites orbiting in near circular orbits with period of about 12 hours. Due to the characteristics of their orbits, the GPS satellites are submitted to the following main perturbations: terrestrial gravitational field, luni-solar gravitational attraction and solar radiation pressure (including the effects of the Earth's shadow). An additional perturbation arises due to the 2:1 commensurability of the orbital period of the satellite with the period of the Earth's rotation. In order to reach the accuracy needed for some specific application all these perturbations must be simultaneously considered.

Here an analytical theory is briefly presented to solve the equations of motion including the previously mentioned effects. In order to take into account the resonance the geopotential is developed up to J_{32} terms. The effects of the lunar solar attraction are studied considering terms up to L_{50} in the Moon potential and S_{30} in the solar potential. Canonical transformations are used to obtain a dynamical system which can be reduced to one degree of freedom. The

resonance is introduced. Direct solar radiation pressure is studied including the shadowing effect.

The analytical solution, based on the Lie-Hori¹ method, was compared with a numerical integration of the equations.

The effects of the orbital perturbations due to J_2, J_{22}, J_{32} , Moon, Sun and to the resonance, are exhibited for the semi-major axis. The resonance produces on the semi-major axis a perturbation of amplitude about 17 km and period of about 1000 days.

Equations of Motion

Using Delaunay variables and extended phase space, the equations of motion of an artificial Earth's satellite, taking into account the geopotential and the luni-solar attraction, can be put in canonical form as follows:

$$\begin{aligned} \frac{d(L, G, H, \Lambda)}{dt} &= \frac{\mathcal{F}}{\alpha(l, g, h, \theta)} \\ \frac{d(l, g, h, \theta)}{dt} &= -\frac{\mathcal{F}}{\alpha(L, G, H, \Lambda)} \end{aligned} \quad (1)$$

where $i = 1, 2, 3$ refers to the satellite, Moon and Sun respectively; L_i, G_i, H_i, l_i, g_i and h_i are the Delaunay variables; θ is the sidereal time and Λ is the canonical variable conjugated to θ .

The Hamiltonian F considered here is given by

$$\begin{aligned} F = & \frac{\mu}{2L_1} - n_\theta \Lambda - n_2 L_2 - n_3 L_3 - n_{g_2} G_2 - \\ & - n_{g_3} G_3 - n_{h_2} H_2 - n_{h_3} H_3 + R_{20} + R_{22} + \\ & + R_{32} + R_M + R_S \end{aligned} \quad (2)$$

Here $n_\theta, n_2, n_3, n_{g_i}, n_{h_i}$ ($i=2,3$) are the mean motion of the variables θ, l_i, g_i, h_i respectively; R_{20}, R_{22}, R_{32} denote the perturbations due to the terrestrial harmonics J_2, J_{22}, J_{32} ; and R_M and R_S represent the perturbations due to the Moon and Sun

ORBITAL PERTURBATIONS OF GPS TYPE

The potential due to the disturbing body can be expressed by²:

$$R = \frac{\mu}{a} \left(\frac{R_E}{a} \right)^2 \sum_{l=2}^{\infty} \sum_{m=0}^l \sum_{p=0}^l \sum_{n=0}^l \sum_{q=-\infty}^l \sum_{j=-\infty}^l k_{lm} \times \\ \times F_{imp}(I) F_{imp}(I^*) \times H_{lpq}(e) G_{lnj}(e^*) \times \\ \cos \left[\begin{array}{l} (l-m)\omega + (l-2p+q)M + (l-2n)\omega^* - \\ -(l-2n+j)M^* + m(\Omega - \Omega^*) \end{array} \right] \quad (3)$$

here R_E is the mean equatorial radius of the Earth and a, e, I, M, ω and Ω are the keplerian elements of the orbit of the satellite. The corresponding elements of the disturbing body are designated by asterisks e^*, I^* , etc. When the disturbing body is the Earth :

$$m(\Omega - \Omega^*) = m(\Omega - \theta - \lambda_{lm}) \quad (4)$$

The k_{lm} and λ_{lm} are characteristics constants of the disturbing body.

Neglecting terms of higher order than J_2^2 , the Hamiltonian F can be written as:

$$F = F_0 + F_1 + F_2 \quad (5)$$

where F_k is a term of the order of J_k^2 .

The period of the GPS satellite is about one half of the rotation of the Earth. This physical situation (considered resonance) can be represented by:

$$i - 2\dot{\theta} + \dot{g}_1 + 2\dot{h}_1 = 0 \quad (6)$$

The solar radiation pressure perturbations, of the order of J_2^2 , was considered in this work but, for technical reasons, it was introduced later.

Analytical Solution

The study of system (1) can be simplified after the following transformations³:

- 1) Lie-Hori transformation to eliminate short-period terms;
- 2) a "resonant variable" is introduced by

$$p_2 = l_1 + g_1 + 2h_1 - 2\theta - 2\lambda_{32} \quad (7)$$

3) a canonical transformation is given by

$$x_1 = L_1 + \frac{\Phi}{2} \quad ; \quad p_1 = l_1 + g_1 + 2h_1$$

$$x_2 = -\frac{\Phi}{2} \quad ; \quad p_2 = l_1 + g_1 + 2h_1 - 2\theta - 2\lambda_{32}$$

$$x_3 = G_1 - L_1 \quad ; \quad p_3 = g_1 + h_1$$

$$x_4 = H_1 - G_1 - H_1 \quad ; \quad p_4 = h_1$$

$$x_5 = L_2 \quad ; \quad p_5 = l_2$$

$$x_6 = L_3 \quad ; \quad p_6 = l_3$$

$$x_7 = G_2 \quad ; \quad p_7 = g_2$$

$$x_8 = G_3 \quad ; \quad p_8 = g_3$$

$$x_9 = H_2 \quad ; \quad p_9 = h_2$$

$$x_{10} = H_3 \quad ; \quad p_{10} = h_3 \quad (8)$$

Hence, the following system is obtained

$$\frac{dx_i}{dt} = \frac{\partial \mathcal{F}'}{\partial p_i}$$

$$\frac{dp_i}{dt} = -\frac{\partial \mathcal{F}'}{\partial x_i} \quad (9)$$

here $j = 1, 2, \dots, 10$. Since \mathcal{F}' doesn't depend explicitly upon $p_1, p_3, p_4, \dots, p_{10}$, the system is reduced to one degree of freedom corresponding to the pair of variables x_2, p_2 .

Inclusion of perturbation due to solar radiation pressure leads to

$$\frac{dx_2}{dt} = \frac{\partial \mathcal{F}'}{\partial p_2}$$

$$\frac{dp_2}{dt} = -\frac{\partial \mathcal{F}'}{\partial x_2} - P_2 \quad (10)$$

here $P_2 = \psi \frac{\partial \mathcal{R}_p}{\partial x_2}$, ψ is the shadow function and \mathcal{R}_p is

the potential due to the solar radiation pressure.

Let x_{20} be the value of x_2 in the condition of exact resonance (for the one degree of freedom system) i.e.:

$$\left(\frac{\mathcal{F}_0'}{\dot{\alpha}_2}\right)_{x_2=x_{20}} = 0 \tag{11}$$

Introducing a new variable $u = x_2 - x_{20}$, developing the Hamiltonian in the neighborhood of $u = 0$ and reordering the Hamiltonian, let us apply once again a Lie-Hori canonical transformation

$$(u, p_2) \rightarrow (u_2^*, p_2^*) \tag{12}$$

retaining in the new Hamiltonian only secular and resonant terms. The transformed system and the Hori auxiliary system associated to the new system are analogous to the pendulum equations and can be solved in terms of elliptic functions.

Therefore the system (10) is solved and the solution yields³⁻⁴

$$u = \frac{1}{K_1} \sqrt{A - K_3 K_1} \operatorname{cn} \left[\sqrt{-K_3 K_1} (t - t_0) \right] - \frac{K_2}{2K_1}$$

$$p_2 = 2 \operatorname{arcsen} \left[k \operatorname{sn} \sqrt{-K_3 K_1} (t - t_0) \right] + \frac{\pi}{2} \tag{13}$$

were A, K_1, K_2 and K_3 are constants depending on the initial conditions taken in the resonance condition; CN and SN are elliptic functions⁵.

Results

The Lie-Hori method extremely facilitates the analytical work to express the solution in terms of the original variables. Moreover, in the first application of this method secular perturbations due to J_2 are obtained and the generating function provides short period perturbations due to J_2, J_{22}, J_{32} , Moon and Sun. As examples Figures 1.....5, show the results for the semi-major axis. In the result for the influence of the resonance (Figure 6) is included the perturbation due to the solar radiation pressure. Numerical integration was performed (Bulirsch-Stoer method⁶) in order to check the results (Table 1).

Acknowledgments

This work was partially supported by FAPESP (90-91/0838-0), PNUD (PNUD-BRA-92/006) and CAPES.

Table 1 : Perturbations on the semi-major axis

PERTURBATION	AMPLITUDE (m)		PERIOD (h)	
	A	N	A	N
J2	1700	1700	6	6
J22	10	20	12	12
J32	25	20	12	12
MOON	70	80	6	6
SUN	25	35	6	6
RESONANCE	17000	—	1000 (days)	—
A...analytical	N...numerical			

References

¹Hori.G.I. Theory of General Perturbations with Unspecified Canonical Variables. *Publ. Astron. Soc. Japan*, 1966, 18, p.287-266

²Kaula,W.M. Development of the Lunar and Solar Disturbing Functions for a Close Satellite. *Astron. J.*, 1962, 67, p. 300-303.

³Grosso,P.R.Movimento Perturbado de um Satélite Artificial em Ressonancia 2:1. *Master Thesis*, ITA, São José dos Campos, SP, 1989.

⁴Vilhena de Moraes,R. et al..Canonical Transformations to Study GPS Satellites Orbital Motion, *to be published*.

⁵Byrd,P.F. and Friedman,M.D. *Handbook of Elliptic Integrals for Engineers and Physicists*. 1954, Springer-Verlag, Berlin.

⁶Bulirsch,R.; Stoer,J. Numerical Treatment of Ordinary Differential Equations by Extrapolation Methods. *Numerisch Mathematik*, 1966, 8, p. 93-104.

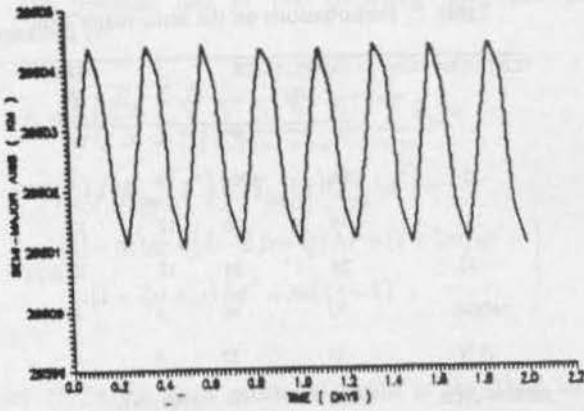


Figure 1: Influence of J_2 on the orbital motion

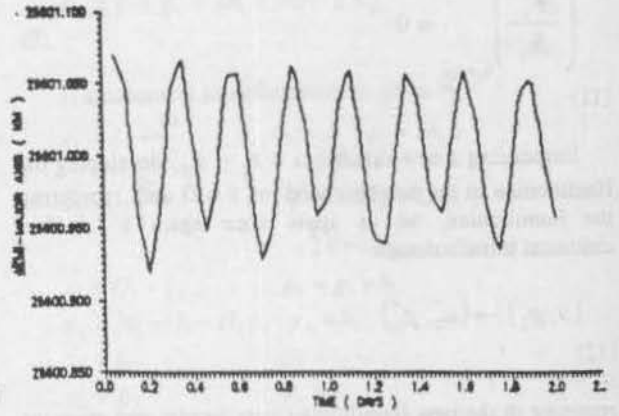


Figure 4: Influence of the Moon on the orbital motion

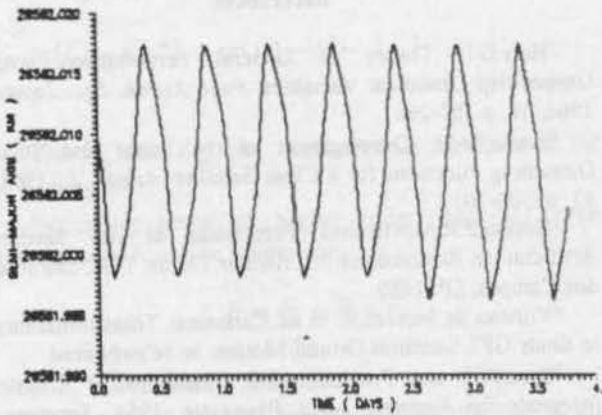


Figure 2: Influence of J_{22} on the orbital motion

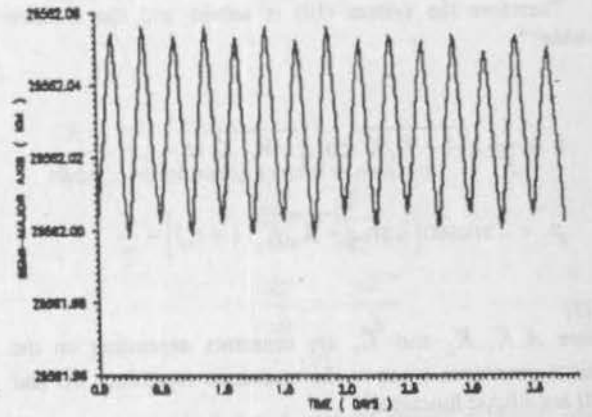


Figure 5: Influence of the Sun on the orbital motion

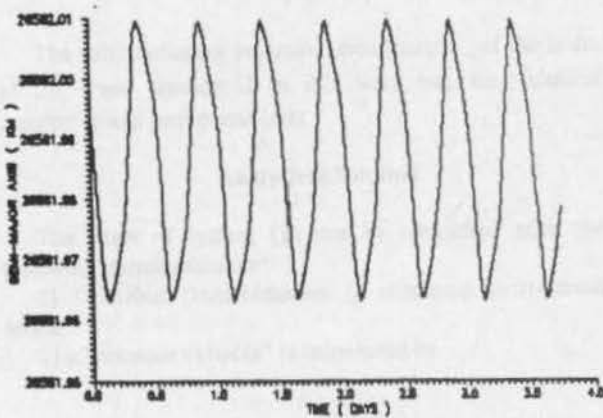


Figure 3: Influence of J_{32} on the orbital motion

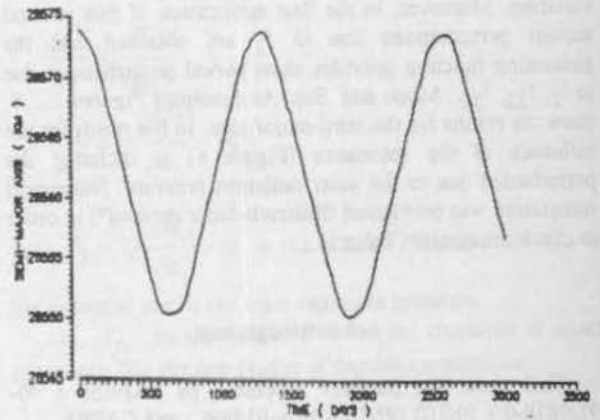


Figure 6: Influence of the resonance on the orbital motion

EFFECTS OF THRUST MISALIGNMENTS ON ORBIT TRANSFERS

Daniel Levy de F. Rodrigues and Marceio Lopes de O. e Souza

Instituto Nacional de Pesquisas Espaciais-INPE

Av. dos Astronautas, 1758-CP 515

12227-010, Sao Jose dos Campos, Sao Paulo, Brasil

Tel: 0123-418977 Fax: 0123-218743 Telex: 1233530

E-mail: Marceio@dem.inpe.br

ABSTRACT

In orbit transfers, the thrust vector must follow an orientation determined by some particular strategy. However, a disturbing torque appears during the propulsion due to unintentional misalignments of the thrust axis with respect to the center of mass. The present paper makes a simplified analytical study of the disturbing torque influences on the trajectory of the center of mass, in the absence of active attitude control. Some conclusions are drawn of this study, for example, the maximum time of propulsion actuation such as to reduce the undesirable effects.

Key Words: Thrust misalignments, orbit transfers

INTRODUCTION

Space vehicles are frequently designed to have propulsive systems capable of generating longitudinal forces with application axis passing through the instantaneous center of mass of the vehicle. However, in many practical cases, this does not occur and a disturbing torque appears, named misalignment torque. But such misalignment usually has low magnitude and is mainly due to the structural design of the vehicle, vibrations, the motion of movable parts (specially liquids) and to displacement of the center of mass originated by the fuel consumption (Ref. 1).

In general, the misalignment can be angular or linear (Figure 1). Schewende and Strobl (Ref. 2) mention as reasonable an angular misalignment less than 0.002 rad for a typical apogee motor.

In the case of orbital transfers the misalignment torque -even with small magnitude- is very important since it alters the force orientation with respect to the specified strategy and, as consequence, it produces an error with respect to the desired final orbit, thus generating the necessity of implementing an active attitude control during the orbital transfer. Longiski, Kia & Breckenridge (Ref. 3) present a control proposal which eliminates the damage caused by this misalignment during propulsive maneuvers. Their proposal consists of splitting it in two parts, intercalated by a time interval without propulsion.

The spin stabilization is a strategy that has shown very much use in apogee motors, due to the fact of canceling the torque of the transverse misalignment.

In this work we intend to verify analytically the consequences on the motion of the center of mass generated by the unintentional misalignment torques, supposing the absence of active attitude control during the propulsion. A numerical example illustrates the situation for a hypothetical vehicle. Details are in chapter 5 of Ref. 4.

A SIMPLIFIED ANALYTICAL STUDY

Consider a model constituted by a rigid and constant mass vehicle and only subjected to a unique force with a constant orientation with respect to the vehicle principal inertia axes and with its application axis not intercepting the vehicle center of mass (CM). In this way, the trajectory described by the CM remains in the plane which contains this force and the CM. Thus, we can choose a reference system OXYZ whose plane XY contains the referred trajectory (Figure 1).

The equations of motion of the center of mass and of the attitude motion with respect to the OXYZ reference system can be easily obtained, as:

$$I\ddot{\theta}(t) = F(h \sin \delta + v \cos \delta) \quad (1)$$

$$m\ddot{\mathbf{R}} = \mathbf{F}(t) \quad (2)$$

where m is the body mass (supposed constant), \mathbf{R} is the CM position vector with respect to the reference system OXYZ, \mathbf{F} is the resulting force written in terms of the OXYZ versors, h is the longitudinal distance of the force line to the center of mass, I is the inertia moment with respect to the rotation axis Z, θ is the attitude angle, v and δ are the linear and the angular misalignments of the thrust vector, respectively, and t is the time.

From equation (1) we get:

$$\dot{\theta}(t) = \frac{F_E}{I} t + \dot{\theta}(0) \quad (3)$$

$$\theta(t) = \frac{F_E}{2I} t^2 + \dot{\theta}(0)t + \theta(0) \quad (4)$$

where $\varepsilon = h \sin \delta + v \cos \delta$

Some mathematical difficulties can be avoided if we consider zero initial conditions: $\mathbf{R}(0)=0$, $\dot{\mathbf{R}}(0)=0$, $\theta(0)=0$ e $\dot{\theta}(0)=0$. This will be the situation valid from now on.

Equation (2) can be written in terms of the components of the center of mass position vector $X(t)$ and $Y(t)$:

$$m\ddot{X}(t) = F \sin\left(\frac{F\varepsilon}{2I}t^2 - \delta\right) \quad (5)$$

$$m\ddot{Y}(t) = F \cos\left(\frac{F\varepsilon}{2I}t^2 - \delta\right) \quad (6)$$

AN APPROXIMATE ANALYTICAL SOLUTION

It is possible to obtain approximate solutions to equations (5) and (6) for t near zero and for t growing without bound.

Consider initially the case where $t \rightarrow 0$. In this case the relations $\cos\theta(t)=1$, $\sin\theta(t)=\theta(t)$ hold. Normally δ is very small thus we can write $\cos\delta=1$ and $\sin\delta=\delta$. Then the equations (5) and (6) can be rewritten as:

$$m\ddot{X}(t) \approx \frac{F^2\varepsilon}{2I}t^2 - F\delta \quad (7)$$

$$m\ddot{Y}(t) \approx F \quad (8)$$

The equations (7) and (8) are easily integrable and give:

$$\dot{X}_0 \approx \frac{F^2\varepsilon}{6mI}t^3 - \frac{F\delta}{m}t \quad (9)$$

$$\dot{Y}_0 \approx \frac{F}{m}t \quad (10)$$

$$X_0 \approx \frac{F^2\varepsilon}{24mI}t^4 - \frac{F\delta}{2m}t^2 \quad (11)$$

$$Y_0 \approx \frac{F}{2m}t^2 \quad (12)$$

where subscript 0 indicates $t \rightarrow 0$.

By isolating the time in equations (9) and (10) we get:

$$\dot{X}_0 \approx \frac{m^2\varepsilon}{6FI} \dot{Y}_0^3 - \delta\dot{Y}_0 \quad (13)$$

$$X_0 \approx \frac{m\varepsilon}{6I} Y_0^3 - \delta Y_0 \quad (14)$$

This model is the simplified case of a vehicle which has a propulsive system which generates a misalignment torque. The ideal case would be without misalignments and, consequently, the vehicle CM trajectory would ideally and entirely be in the Y axis. Due to the presence of the misalignments, this trajectory degenerates, initially in the parabola described by the equation (14).

Equations (9) to (14) describe the behavior of the body CM for t close to zero. In the first instants of the propulsion the effects of the misalignments are too small, as shown by equations (10) and (12), that is, the component of the CM motion along the longitudinal axis Y follows Newton's law of the linear motion. But, gradually, the CM motion gives place to the parabolic behavior described by equation (14). This implies in degenerating the motion.

To obtain the CM behavior for very high values of t , we can integrate equations (5) and (6) from 0 to $+\infty$:

$$m \int_{t=0}^{t \rightarrow \infty} \ddot{X}(t) dt = F \int_{t=0}^{t \rightarrow \infty} \sin\left(\frac{F\varepsilon}{2I}t^2 - \delta\right) dt \quad (15)$$

$$m \int_{t=0}^{t \rightarrow \infty} \ddot{Y}(t) dt = F \int_{t=0}^{t \rightarrow \infty} \cos\left(\frac{F\varepsilon}{2I}t^2 - \delta\right) dt \quad (16)$$

$$\dot{X}_\infty = \frac{(\cos\delta - \sin\delta)}{2m} \sqrt{\frac{\pi FI}{\varepsilon}} \quad (17)$$

$$\dot{Y}_\infty = \frac{(\cos\delta + \sin\delta)}{2m} \sqrt{\frac{\pi FI}{\varepsilon}} \quad (18)$$

$$X_\infty = \frac{(\cos\delta - \sin\delta)}{2m} \sqrt{\frac{\pi FI}{\varepsilon}} t + cte \quad (19)$$

$$Y_\infty = \frac{(\cos\delta + \sin\delta)}{2m} \sqrt{\frac{\pi FI}{\varepsilon}} t + cte \quad (20)$$

where the subscript ∞ means $t \rightarrow +\infty$.

Equations (17) and (18) show that for $t \rightarrow +\infty$ the CM velocity becomes constant despite there is a non null force acting on the body. This is explained by the fact that when t becomes very large its angular velocity is so high that it almost instantaneously occupies successive opposite angular positions, cancelling the linear effects of the acting force.

By isolating t in eqs. (17) and (18) we get:

$$\dot{Y}_\infty = \frac{(\cos\delta + \sin\delta)}{(\cos\delta - \sin\delta)} \dot{X}_\infty = cte \quad (21)$$

$$Y_{\infty} = \frac{(\cos\delta + \sin\delta)}{(\cos\delta - \sin\delta)} X_{\infty} + \text{cte} \quad (22)$$

In the ideal case ($v=0$, $\delta=0$), the trajectory should describe a straight line along the Y axis with speed growing linearly with time. In the real case ($v \neq 0$, $\delta \neq 0$) the trajectory becomes straight but not necessarily along the Y axis and with constant speed, as shown by equations (17) and (18). It is interesting to note that if $\delta = \pi/4$, then the CM trajectory returns to have only the Y axis component.

The CM trajectory was determined only for the situations described ($t \rightarrow 0$ and $t \rightarrow +\infty$). But its intermediate behavior remains unknown. But some idea on this behavior can be obtained by examining equations (5) and (6). These equations show that $\dot{X}(t)$ and $\dot{Y}(t)$ present oscillatory behavior, with maximum and minimum points given by $\dot{X}(t)=0$ and $\dot{Y}(t)=0$. Eqs. (17) and (18) show that the velocity components converge to constant values. Therefore, the CM velocity behavior must be damped oscillatory. Consequently, the CM trajectory for the intermediate situation should be equally oscillatory.

It is interesting to determine the value of t for which $\dot{Y}(t)$ reaches its maximum value. Such value - here called by t^* - is important, since it indicates that, if the propulsion continues after it, the trajectory degradation will be more and more accentuated. Thus, t^* can be understood as the maximum actuation time of the propulsion system for a slightly degenerated CM trajectory. From equation (6), for $\dot{Y}(t)$ to be maximum it is necessary that:

$$t^* = \sqrt{\frac{I(\kappa\pi + 2\delta)}{F\varepsilon}} \quad (23)$$

with $\kappa = 1, 3, 5, \dots$ and the first maximum occurring for $\kappa=1$.

Approximating equation (6) by:

$$m\ddot{Y}(t) \approx F \left[1 - \frac{\left(\frac{F\varepsilon}{2I}t^2 - \delta\right)^2}{2!} + \frac{\left(\frac{F\varepsilon}{2I}t^2 - \delta\right)^4}{4!} \right] \quad (24)$$

the value of $\dot{Y}(t^*)$, denoted by \dot{Y}^* , is approximately given by:

$$\dot{Y}^* \approx \frac{F\sqrt{I(\kappa\pi + 2\delta)}}{m} \left[1 - \frac{\pi^2}{40} + \frac{\pi^4}{3456} + \left(\frac{1}{15} - \frac{\pi^2}{1512}\right)\pi\delta + \dots \right. \\ \left. - \left(\frac{\pi^2}{630} - \frac{1}{15}\right)\delta^2 - \frac{1}{945}\pi\delta^3 + \frac{16}{945}\delta^4 \right] \quad (25)$$

It is also interesting to note that the attitude angle for this situation depends of F , ε and I , and it will always be given by:

$$\theta^* = \frac{\pi}{2} \kappa + \delta \quad (26)$$

For the first maximum and for $\delta=0$, it happens that $\theta^* = \pi/2$. This result is sometimes useful to estimate how the satellite attitude will change during the burning.

A NUMERICAL EXAMPLE

Consider the hypothetical situation where we have a straight cylindrical body with basis radius r , height H , with a force F applied perpendicularly to the base, and:

$$F=10 \text{ N}, \quad v=0.01 \text{ m/s}, \quad \delta=0 \text{ rad}, \quad \varepsilon=0.01 \text{ m}$$

$$m=5 \text{ Kg}, \quad r=1 \text{ m}, \quad H=3 \text{ m}, \quad I=5 \text{ kg}\cdot\text{m}^2$$

$$R(0)=0 \text{ m}, \quad \dot{R}(0)=0 \text{ m/s}, \quad \theta(0)=0 \text{ rad}, \quad \dot{\theta}(0)=0 \text{ rad/s}$$

Figures 2-4 show the simulation results for the example in question.

From Figure 2 we observe that the approximate analytical solution is in agreement with the real solution, for small t . In this same Figure it is clear the parabolic behavior of the CM trajectory described by equation (14).

From Figures 3a and 3b we can observe that the CM velocity components have damped oscillatory behavior whose values converge to the interval of 12-14 m/s. From equations (17) and (18) we get the convergence values $X_{\infty} = Y_{\infty} = 12.53 \text{ m/s}$. The values t^* and \dot{Y}^* for this example, obtained from equations (23) and (25), are 12.53 s and 19.59 m/s, respectively. The actual value for \dot{Y}^* is 19.55 m/s, indicating a relative error in the analytic model less than 0.5% (for this example). It is interesting to note that the "ideal" value of \dot{Y}^* , given by $(F/m)t^*$, is 25.07 m/s. Thus, the application of the force during t^* seconds assures propulsive efficiency greater than 75% in that case.

From Figure 4b we note that for a very large t the CM trajectory approaches the straight line described by equation (22). In the case of $\varepsilon=0$ the CM describes a straight trajectory in the Y direction, which in fact occurs in the first instants. The misalignment causes a deviation of this trajectory (the greater is the value of ε the faster it is) which is capable of altering it substantially and capable of cancelling the effects of the force applied on it.

From Figure 5 we note that the propulsive efficiency - the relation of \dot{Y}^* and $(F/m)t^*$ - decreases monotonically with time until $\dot{Y}(t)$ reaches its first relative minimum - situation with $k=3$ in equation (23).

Despite the numerical example be specific. Figures 2 to 5 show the general behavior of the CM trajectory of a body subjected to the misalignment torque $F \times \hat{e}_z$.

CONCLUSIONS

This paper presented an analytical study of thrust misalignments.

Using some simplified approaches we got some interesting conclusions about the CM movement. Particularly, it was shown that misalignments must be important if the burning time is greater than a certain t^* - the maximum actuation time of the propulsive system to give a reasonable approximation of the ideal system (a non misalignment system).

REFERENCES

- 1 Tandon, G.K. "Modeling Torques Due to Orbit Maneuvers", *Astrophysics and Space Science Library*. Vol. 733, 1988, pp. 580-583.
- 2 Schewende, M.A.; Strobl, H. "Bi-propellant Propulsion Systems for Spacecraft Injection and Control". In: *European Space Agency. Attitude and Orbit Control Systems. Proceedings*, 3-6 Oct. 1977. Paris, ESA, 1977, pp. 405-412.
- 3 Longiski, J.M.; Kia, T. and Breckenridge, W.G. "Annihilation of Angular Momentum Bias During Thrusting and Spinning-up Maneuvers", *The Journal of the Astronautical Sciences*, Vol. 37, No. 4, October-December 1989, pp. 433-450.
- 4 Rodrigues, D.L.F. "Dynamic Analysis of Orbital Transfers". São José dos Campos, SP, Brazil, INPE, 1991 (Master Thesis, INPE-5352-TDI/461).

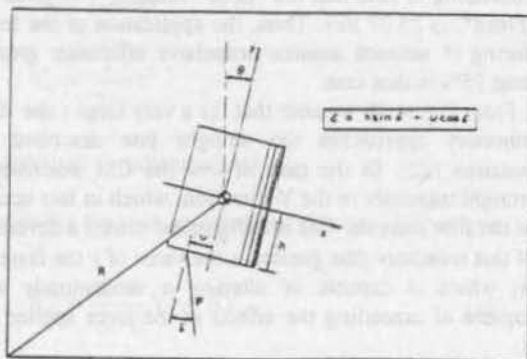


FIGURE 1

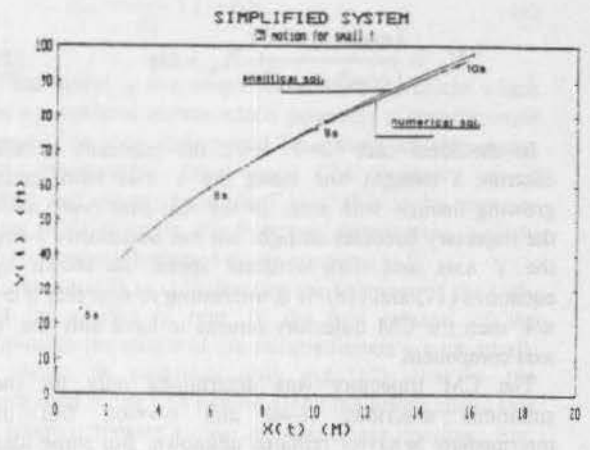


FIGURE 2

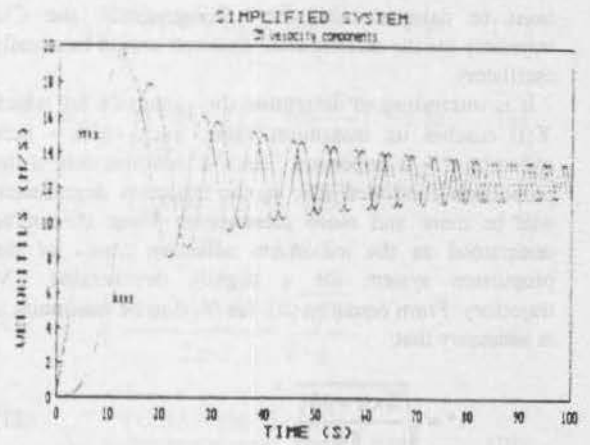


FIGURE 3a

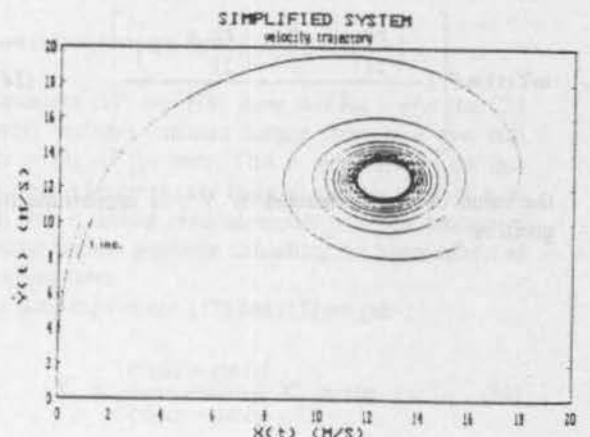
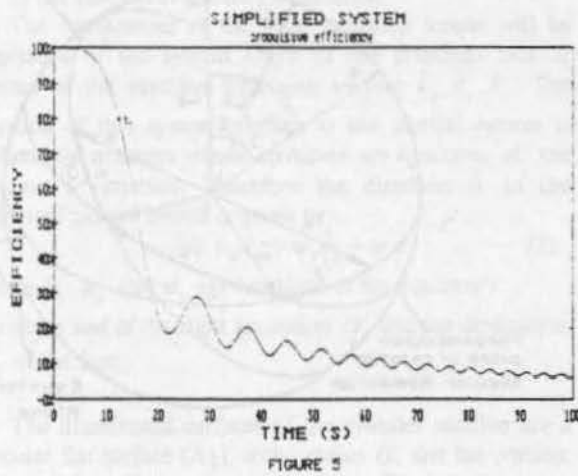
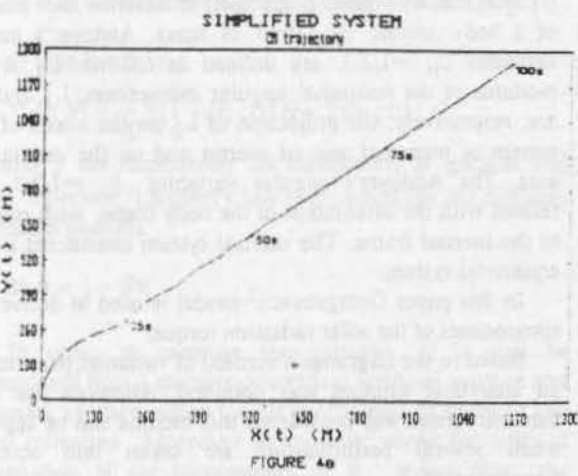
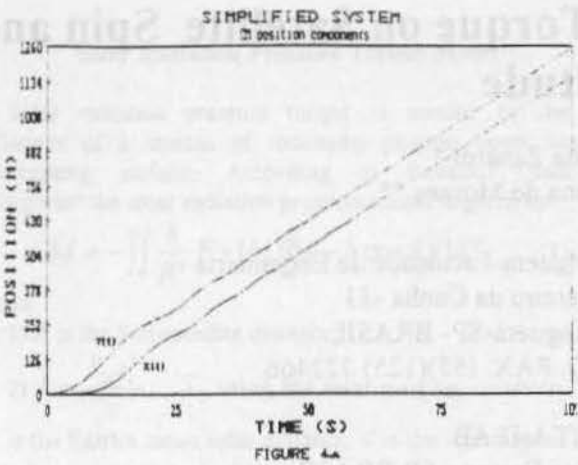


FIGURE 3b



Effects of Solar Radiation Torque on Satellite Spin and Attitude

Maria Cecilia Zanardi *
Rodolpho Vilhena de Moraes **

* UNESP-Campus de Guaratinguetá-Faculdade de Engenharia
Av. Dr. Ariberto Pereira da Cunha -33
12500-000 - Guaratinguetá-SP- BRASIL
FONE : (55)(125) 222800; FAX: (55)(125) 322466

** CTA-ITA-IEAB
12228-900 - São José dos Campos-SP-BRASIL
FONE: (55)(123) 412211; FAX : (55)(123) 417069; E-mail: ITA@BRFAPESP.BITNET

Abstract

An analytical solution for the system of equations describing the rotational motion of an artificial satellite under the influence of the direct solar radiation pressure is presented. Here is considered a satellite of cylinder circular shape and the method to obtain the analytical solution is the Lagrange's method of the variation of parameters. Andoyer's variables are used to describe the rotational motion. The analytical solution obtained shows that, due to the solar radiation, all the Andoyer's angular variables have secular and periodical variations but, the modulus of the rotational angular momentum and its projection on the z-axis of the system of principal axis of inertia vary periodically only.

In order to validate the range of the analytical solution, Bulirsch-Stoer's method is used to perform a numerical integration of the system of equations of motion. Considering a hypothetical satellite, a numerical application is exhibited.

Key words: Solar Radiation Torque, Rotational Motion, Andoyer's Variables.

Introduction

The use of artificial satellites for astronomical and geodynamics purpose has been required more and more precise orbit and attitude determination and several perturbations must be taken into account. However, besides the smallness of some perturbations, to decide which one is negligible can be not straightforward if we don't know a long time evolution of their effects

The objective of this paper is to analyze the influence of the torque due to the direct solar radiation pressure on the rotational motion of an artificial satellite. Long period and secular effects are emphasized.

Here Andoyer's canonical variables¹ (L_1, L_2, L_3) and (l_1, l_2, l_3), as in Figure 1, are used to describe the motion of a body around its center of mass. Andoyer's metric variables L_i , $i=1,2,3$, are defined as follows: L_2 is the modulus of the rotational angular momentum, L_1 and L_3 are, respectively, the projection of L_2 on the z-axis of the system of principal axis of inertia and on the inertial Z-axis. The Andoyer's angular variables l_i , $i=1,2,3$, are related with the orientation of the body frame with respect to the inertial frame. The inertial system considered is the equatorial system.

In this paper Georgevic's² model is used to derive the components of the solar radiation torque.

Based in the Lagrange's method of variation parameters an analytical solution was obtained. Although just one external torque was considered this method can be applied when several perturbations are taken into account simultaneously².

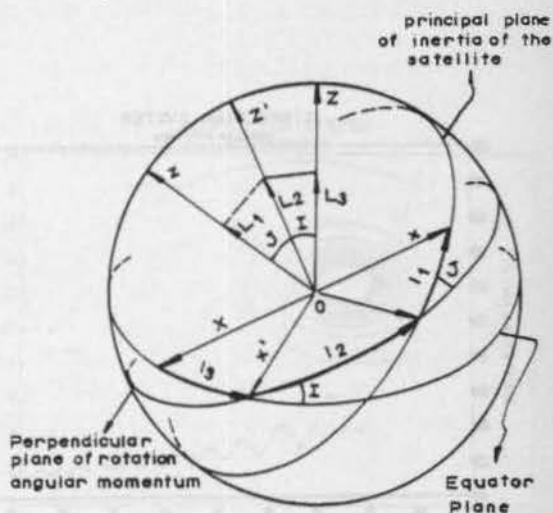


Figure 1: Andoyer's variables

Solar Radiation Pressure Torque Model

Solar radiation pressure torque is exerted by the collisions of a stream of incoming photons upon an intercepting surface. According to Beletskii³ and Georgevic⁴ the solar radiation pressure torque is given by

$$\vec{M} = - \iint \frac{k}{R^2} \vec{r} \times [b(\theta)\hat{n} + b \cos \theta \hat{u}] dS \quad (1)$$

where

1) R is the Sun-satellite distance;

2) $k = \frac{S_0 a_e^2}{c}$, S_0 being the solar constant radiation,

a_e is the Earth's mean solar distance, c is the light's speed and k assumes the value⁴

$$k = 1.01 \times 10^{17} \text{ kg m s}^{-1}$$

3) \vec{r} gives the position of the surface element dS with respect the mass center of the satellite;

4) \hat{n} is a unit vector along the outer normal;

5) \hat{u} is a unit vector along the direction of the flux ;

$$6) \cos \theta = \hat{u} \cdot \hat{n};$$

$$7) B(\theta) = \frac{2}{3} \gamma (1 - \beta) \cos \theta + 2\beta\gamma \cos^2 \theta$$

β and γ are respectively the coefficients of specular and total reflection. Lambert's law is assumed for the diffusely reflected photons:

$$8) b = 1 - \beta\gamma.$$

In order to compute the integral (1) it will be considered here a circular cylindrical artificial satellite and constant average values for the coefficients of specular and total reflection. Moreover an analysis⁵ above the order of magnitude of the components of \hat{u} shows that the following simplifications can be introduced:

1) the direction of the solar flux is given by the apparent motion of the Sun with respect to the Earth;

2) the Sun-Earth distance is constant.

The components of the solar radiation torque will be expressed in the system Oxyz of the principal axis of inertia of the satellite with unit vectors $\hat{e}_x, \hat{e}_y, \hat{e}_z$. The position of this system relative to the inertial system is defined by matrices whose elements are functions of the Andoyer's variables. Therefore the direction \hat{u} in the principal axis of inertia is given by

$$\hat{u} = u_x \hat{e}_x + u_y \hat{e}_y + u_z \hat{e}_z \quad (2)$$

where u_x, u_y and u_z are functions of the Andoyer's variables and of the right ascension α_s and the declination δ_s of the Sun.

The illuminated surfaces of the cylinder satellite are a circular flat surface (A_1), with radius σ , and the portion, of height h , of the cylindrical surface (A_2) as showed in

Figure (2). β_j and γ_j , $j = 1, 2$, are respectively the coefficients of specular and total reflection of the surface (A_j).

Using cylindrical and polar coordinates the position of the surface elements are defined with respect to the geometric center of the satellite.

After integration equation (1) remains:

$$\vec{M} = M_x \hat{e}_x + M_y \hat{e}_y \quad (3)$$

where

$$M_x = -m u_y u_z$$

$$M_y = m u_x u_z$$

with

$$m = \frac{k}{R^2} \frac{\pi \sigma^2 h}{2} (\beta_2 \gamma_2 - \beta_1 \gamma_1).$$

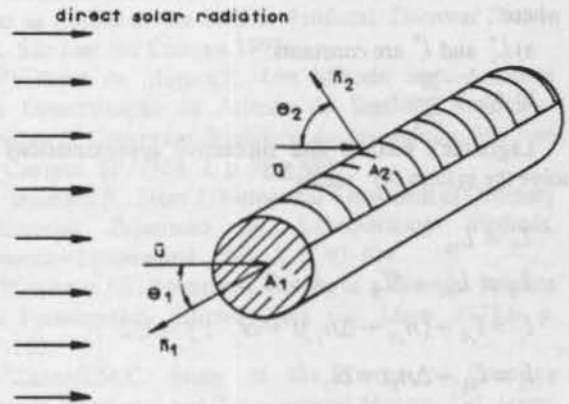


Figure 2: The Illuminated Surfaces of the Cylinder Satellite

Rotational Motion Equations

The equations describing the rotational of an artificial satellite under the influence of the solar radiation torque can written as²⁻⁷:

$$\frac{dI_1}{dt} = \frac{\partial F_1}{\partial I_1} + P_1 \quad (4a)$$

$$\frac{dL_1}{dt} = -\frac{\partial F_1}{\partial I_1} + Q_1 \quad (4b)$$

The L_i, I_i , $i = 1, 2, 3$ are the Andoyer's variables and F is the Hamiltonian of the torque free motion given by

$$F = \frac{1}{2} \left(\frac{1}{C} - \frac{1}{2A} - \frac{1}{2B} \right) L_1^2 + \frac{1}{4} \left(\frac{1}{A} + \frac{1}{B} \right) L_2^2$$

$$+ \frac{1}{4} \left(\frac{1}{B} - \frac{1}{A} \right) (L_2^2 - L_1^2) \cos 2I_1 \quad (5)$$

where

1) A, B and C are the principal moments of inertia of the satellite;

2) P_i and Q_i are functions of the components of the solar radiation torque expressed in the system of the principal axis of inertia⁵⁻⁶.

Analytical Solution

The solution of the torque free problem (P_i and $Q_i = 0$) can be put in the following form:

$$L_i = L_i^* ; l_3 = l_3^*$$

$$l_j = l_j^* + n_{j0}t$$

$$i = 1, 2, 3 ; j = 1, 2$$

where

a) L_i^* and l_3^* are constants;

$$b) n_{j0} = \frac{\partial F}{\partial L_j}$$

Lagrange's method and successive approximations to solve the system (4) yields²⁻⁵:

$$L_1 = L_{10}$$

$$L_k = L_{k0} + \delta L_k, \quad k = 2, 3$$

$$l_j = l_{j0} + (n_{j0} + \Delta n_j)t + \delta l_j, \quad j = 1, 2$$

$$l_3 = l_{30} + \Delta n_3 t + \delta l_3$$

where L_{i0} and l_{i0} , ($i = 1, 2, 3$) are constants depending on the initial conditions; δL_k and δl_j are periodic functions; n_{j0} and Δn_j are, respectively, mean motions associated with the torque free problem and the torque produced by the solar radiation pressure.

This solution shows that:

1) the solar radiation pressure doesn't influence the projection of the rotational angular momentum on the z-axis of the system of principal moments of inertia;

2) the solar radiation pressure torque produces secular and periodic variations on the angular variables l_1 but produces only periodic variations on the rotational angular momentum L_2 and in its projection on the inertial axis Z.

Numerical Application

In order to analyse orders of magnitude of the solar radiation pressure torque and validate our analytical solution, let us consider a hypothetical satellite with orbital and physics characteristic similar to the "Pegasus A" satellite⁸⁻⁹. Thus the following values will be assumed:

$$A = B = 3.9499 \times 10^5 \text{ kg m}^2$$

$$C = 1.0307 \times 10^5 \text{ kg m}^2$$

$$M = 11,550 \text{ kg}$$

$$m = 4.245 \times 10^{-5} \text{ kg m}^2 \text{ s}^{-1}$$

$$\text{orbital period} = 5778 \text{ s}$$

$$\text{rotational period} = 255 \text{ s}$$

Initial conditions for the Andoyer's variables will be taken as

$$L_{10} = 0 \text{ kg m}^2 \text{ s}^{-1}$$

$$L_{20} = 9.7307 \text{ kg m}^2 \text{ s}^{-1}$$

$$L_{30} = -2.9956 \text{ kg m}^2 \text{ s}^{-1}$$

$$l_{10} = l_{20} = J_0 = \frac{\pi}{2} \text{ rad}$$

$$l_{30} = 5.87 \text{ rad}$$

$$l_0 = 1.877 \text{ rad}$$

A numerical integration will be performed by Bulirsh-Stoer method with step of 0.1 s and simulation time of 100 000 s.

Analytical and numerical solutions agree quite well during all considered time. As an example, Figure (3) shows the result for variable l_2 for 3 distinct intervals of time. Note that after 100 000 s (about 20 orbital periods and 100 satellite revolutions) the value of the difference remains below the magnitude of the perturbation.

Table (1) shows the magnitude of the effects of the solar radiation torque on each of the Andoyer's variables. This table shows also the comparison between the analytical and numerical solution.

The small, but noticeable, differences increasing with the time can be explained by following facts:

1) in the analytical process the trigonometric functions were treated as linear functions of the time;

2) α_j and δ_j were taken as constants in the analytical solution and as a function of time in the numerical integration;

3) round numerical errors.

Conclusions

An analytical solution for the rotational motion of an artificial satellite was presented. In the analytical developments an artificial satellite of cylinder circular shape was considered. Our analytical solution was checked by comparisons with numerical integration showing to be very accurate for about 20 orbital revolutions and 400 rotations of an hypothetical satellite.

The analytical solution presents secular terms in all of the angular variables. The metric variables L_2 and L_3 contains only periodic terms. The variable L_1 is not affected by solar radiation torque.

When others torques are also considered this analytical solution can be useful as a propagation method in the optimization process of attitude determination.

A STUDY OF THE EFFECTS OF THE ATMOSPHERIC DRAG IN SWING BY TRAJECTORIES

References

- ¹Kinoshita, M. First-Order Perturbations of the Two Finite Body Problem. *Publ. Astron. Soc. Japan*, 1972, 24, p. 423-457.
- ²Vilhena de Moraes, R. A Semi-Analytical Method to Study Perturbed Rotational Motion. *Cel. Mech.*, 1989, 45, p. 281-284.
- ³Beletskii, V.V. *Motion of an Artificial Satellite About its Center Of Mass*. 1966, Israel Program for Scientific Translation, Jerusalem, Israel.
- ⁴Georgeovic, R.M. The Solar Radiation Pressure Force and Torque model. *The Journ. Astron. Sciences*, 1973, XX, 5, p. 255-274.
- ⁵Zanardi, M.C.F.P.S. Influência do Torque de Radiação Solar na Atitude de um Satélite Artificial. *Doctoral Thesis*, ITA, São José dos Campos, 1993.
- ⁶Vilhena de Moraes, R. Um Método Semi-Analítico para Determinação da Atitude de Satélites Artificiais. *Anais do 7º Congresso Brasileiro de Automática*, São José dos Campos, SP, 1988, 2, p. 986-989.
- ⁷Bulirsch, R.; Stoer, J. Numerical Treatment of Ordinary Differential Equations by Extrapolation Methods. *Numerisch Mathematik*, 1966, 8, p. 93-104.
- ⁸Cochran, J.E. Rotational Motion of a Triaxial Satellite in a Precessing Elliptic Orbit. *Cel. Mech.* 1972, 6, p. 127-150.
- ⁹Zanardi, M.C. Study of the Terms of Coupling Between Rotational and Translational Motion. *Cel. Mech.* 1986, 39, p. 147-158.

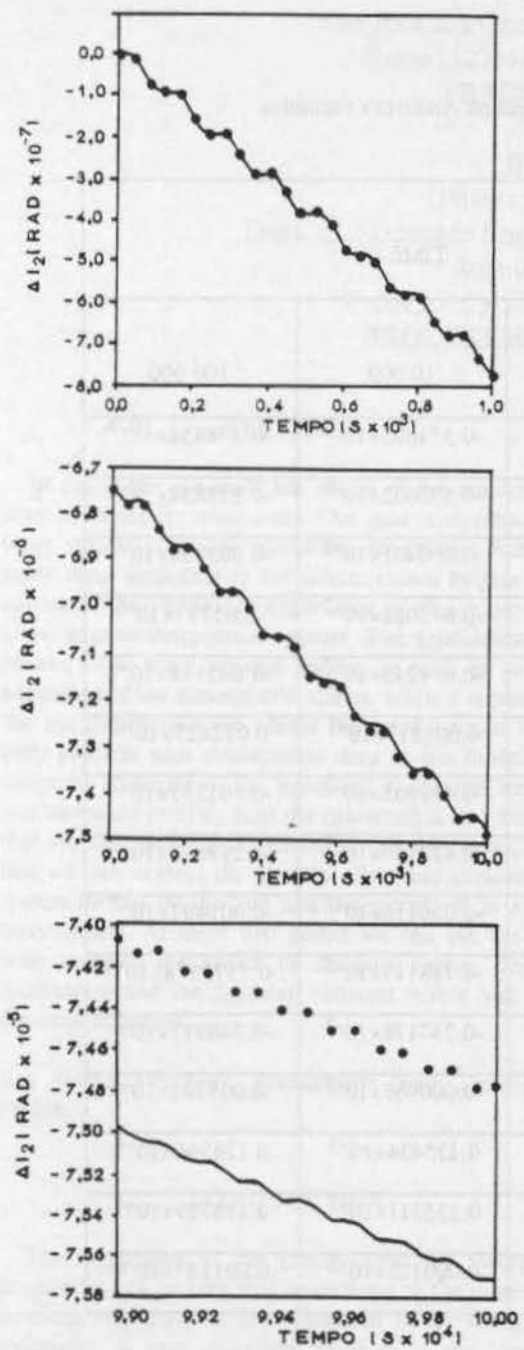


Figure 3: Secular and Periodic Variations on i_2 due to solar radiation torque
 • - numerical solution

TABLE 1: Effect of solar radiation torque on Andoyer's variables

VARIABLE	RESULTS	TIME (s)		
		1 000	10 000	100 000
ΔL_2 ($\text{kg km}^2 \text{s}^{-1}$)	ANALYTICAL	0.153389×10^{-10}	-0.574003×10^{-9}	-0.278858×10^{-9}
	NUMERICAL	0.153796×10^{-10}	-0.573602×10^{-9}	-0.278858×10^{-9}
	DIFFERENCE	$-0.000407 \times 10^{-10}$	-0.000401×10^{-9}	-0.003898×10^{-9}
ΔL_3 ($\text{kg km}^2 \text{s}^{-1}$)	ANALYTICAL	-0.663991×10^{-8}	-0.673028×10^{-7}	-0.65717×10^{-6}
	NUMERICAL	-0.664114×10^{-8}	-0.674245×10^{-7}	-0.665144×10^{-6}
	DIFFERENCE	0.000123×10^{-8}	0.001217×10^{-7}	0.012427×10^{-6}
Δl_1 (rad)	ANALYTICAL	0.381969×10^{-7}	-0.432905×10^{-7}	-0.301335×10^{-7}
	NUMERICAL	0.381982×10^{-7}	-0.432789×10^{-7}	-0.299838×10^{-7}
	DIFFERENCE	-0.000013×10^{-7}	-0.000116×10^{-7}	-0.001497×10^{-7}
Δl_2 (rad)	ANALYTICAL	-0.764686×10^{-6}	-0.748143×10^{-5}	$-0.7573178 \times 10^{-4}$
	NUMERICAL	-0.764803×10^{-6}	-0.747178×10^{-5}	-0.748017×10^{-4}
	DIFFERENCE	-0.000117×10^{-6}	-0.000965×10^{-5}	-0.009301×10^{-4}
Δl_3 (rad)	ANALYTICAL	0.108697×10^{-6}	0.135434×10^{-5}	0.136946×10^{-4}
	NUMERICAL	0.108682×10^{-6}	0.135311×10^{-5}	0.135789×10^{-4}
	DIFFERENCE	0.000015×10^{-6}	0.000123×10^{-5}	0.001157×10^{-4}

A STUDY OF THE EFFECTS OF THE ATMOSPHERIC DRAG IN SWING-BY TRAJECTORIES

Antonio Fernando Bertachini de Almeida Prado
Instituto Nacional de Pesquisas Espaciais - INPE - Brazil
Av. dos Astronautas 1758
São José dos Campos - SP - 12227-010 - Brazil
Phone (123)41-8977 - Fax (123)21-8743
PRADO@DEM.INPE.BR

Roger Broucke
University of Texas at Austin
Dept. of Aerospace Engineering and Engineering Mechanics
Austin-TX-78712 - USA
Phone (512)471-7593 - Fax (512)471-3788
BROUCKE@EMX.CC.UTEXAS.EDU

ABSTRACT

In this paper, we study the effects of the atmospheric drag in Swing-By maneuvers. Our goal is to simulate a large variety of initial conditions for those orbits and study them according to the effects caused by this close approach. The practical importance of this topic is to allow mission designers to explore close approaches with planets in a more realistic model, as well as to take advantage of the atmospheric effects, when it is possible. We use the well-known planar restricted circular three-body problem plus atmospheric drag as our model. We integrate numerically the equations of motion forward and backward in time, until the spacecraft is in a distance that we can consider far enough from the planet, such that we can neglect the planet's effect and consider the system formed by the Sun and the spacecraft as a two-body system. At these two points we can use the two-body celestial mechanics to compute energy, angular momentum and the Jacobian constant before and after the close approach.

Key Words: Swing-By, Atmospheric Drag, Three-Body Problem.

INTRODUCTION

The importance of the gravity-assist (or Swing-By) trajectories can be very well understood by the number of missions that flew or are scheduled to fly using this technique. A very successful example is the Voyager mission that flew to the outer planets of the Solar System with the use of successive Swing-Bys in the planets visited to gain energy¹. The Swing-By trajectories have a very wide range of applications, like:

1. The use of the planet Venus for a round-trip from the Earth to the Mars^{2,3,4}.
2. The use of Jupiter to make a strong plane change in a spacecraft's trajectory, to make it achieve an orbital plane perpendicular to the ecliptic to observe the poles of the Sun, like the mission Ulysses⁵.
3. The use of Swing-Bys with the Earth and/or another inner planet to reach the outer Solar System^{6,7,8,9}.
4. The use of the Moon to send a spacecraft to an elliptical or hyperbolic escape orbit around the Earth¹⁰.
5. The use of successive Swing-Bys with the Moon to keep some desirable geometry of the spacecraft's orbit around the Earth, such as satellites observing solar phenomena. More details are available in references^{11,12}.
6. The use of multiple powered Swing-Bys in the satellites of a large planet (Jupiter or Saturn) to make a tour of those satellites. Optimization methods are applied here to minimize the fuel used in the powered part of the mission^{13,14,15}. The number of Swing-Bys is usually larger than ten in this kind of mission.

All the applications above are in the field of astronautics, and they are very recent when compared with the astronomy literature. The celestial mechanics of the Swing-By is known by the astronomers for at least 150 years. It is very clear that Laplace understood the whole gravity-assist mechanism. After him, several researchers derived analytical equations for the effects of the Swing-By and/or produced numerical results in this topic, especially in the problem of escape and capture of comets by Jupiter (see references (16) and (17) for historical remarks), that is essentially the same problem.

The gravity-assist concept in the American space program appears first at JPL in the early sixties. The first explicit JPL document that we found on this subject is a memorandum (312-130) by M. Minovich¹⁸, dated August 23-1961. This document contains the formulas for the change in energy and in semi-major axis. A very detailed

account of Minovitch's activity has recently been described^{19,20}.

Among the United States activities on lunar gravity assist, another important branch of contributions is by R. W. Farquhar and his group¹¹. This work has also been well documented in a special issue of the Journal of Astronautical Sciences (Vol. 33, No. 3, 1985) in the articles by Farquhar, Muhonen, Church, Dunham, Davis, Efron, Yeomans and Schanzle^{21,22,23,24}. The ICE (ISEE-3) mission to the Moon and to the comet Giacobini-Zimmer is especially remarkable.

A recent remarkable application of gravity assist is the close encounter with the Moon of the Japanese Muses-A/Hiten spacecraft on August 5, 1990 and lunar capture on December 19. The work done at JPL by E. A. Belbruno and J. K. Miller^{25,26,27} was related to this mission or very similar in nature. A numerical study on this type of capture problems was recently published by the Japanese Researches Yamakawa and Kawaguchi²⁸. A second Japanese mission involving a lunar Swing-By is Geotail (1992).

In the future, this topic will be even more important, since the savings in fuel expenditure obtained from the gravity-assist maneuvers has a large impact in the total cost of the mission, and this is now a high-priority constraint.

In our paper, the effect of a planetary atmosphere in a close approach between a spacecraft and a planet is studied. Only planar motion is considered. The mathematical model is based in the restricted planar circular three-body problem, with the extra forces that come from the atmospheric drag included. The equations are regularized (using Lamaitre's regularization), so we can avoid the numerical problems that come from the close approach with Jupiter. The goal is to give a more realistic approach to those maneuvers and to learn more about this new tool available for mission designers.

PARAMETERS TO SPECIFY ONE TRAJECTORY

The three following parameters are used to specify each trajectory (following the paper by Broucke¹⁶):

- The angle of approach ψ ;
- The Jacobian constant J ;
- The periapse altitude (h_p), that is the distance between the periapse of the trajectory of the spacecraft around Jupiter and the surface of the planet.

The first problem to consider is the fact that those three parameters become unclear when the drag force is included in the model. J is no longer a constant and ψ and h_p are hard to define precisely. Then, it is necessary to find a method to compare those two trajectories (the one with and the one without drag). In this paper, the following procedure is used:

i) For the maneuver without drag, the spacecraft starts at periapse and numerical integration is performed forward and backward in time until the points A and B

(see Fig. 1) are reached. Then, the quantities desired are calculated at those points. This is the same procedure used in the previous section;

ii) The maneuver with drag is a little more difficult. The spacecraft starts at periapse with the same given three parameters (J , ψ , h_p) as the maneuver without drag. Then its trajectory is integrated backward in time without drag, until the point A is reached. From this point, its trajectory is integrated forward in time with the drag force active until the point B is reached.

In this way, it is possible to compare two trajectories starting with the same initial conditions in the point A and the only difference between them is the existence of the drag force when the spacecraft is close to Jupiter.

The quantities calculated to measure the influence of the atmosphere are the energy, angular momentum and Jacobian constant before and after the Swing-By. This is done with and without the drag force, so it is possible to identify its influence. The results are presented in contour-level graphs that show the variation in each quantity for each trajectory studied.

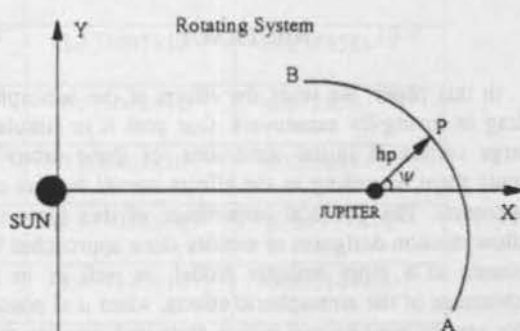


Fig. 1 - Geometry of the Close Encounter.

DEFINITION OF THE PROBLEM AND MATHEMATICAL MODEL

The problem under study here is similar to the standard Swing-By maneuver that we studied before^{29,30}. A spacecraft comes from a long distance, passes close to a planet and then leaves it again. The planet is supposed to be in a circular orbit around a central body and any type of orbit is assumed for the spacecraft (elliptic, circular or hyperbolic). Fig. 1 illustrates this situation. At the points A and B the spacecraft is supposed to be far enough from the planet, so the system can be modeled as a two-body problem (the spacecraft and the central body). The difference from the standard maneuver is that the planet is assumed to have an atmosphere and it generates a drag force in the spacecraft. The equations of motion for the spacecraft are the ones valid for the restricted circular planar three-body problem with the inclusion of the atmospheric drag. The drag force is modeled by the

standard form proportional to the square of the velocity and the density of the atmosphere is supposed to vary exponentially with the altitude. Under those assumptions, the equations of motion are:

$$\ddot{x} - 2\dot{y} = x - \frac{\partial V}{\partial x} + F_x = \frac{\partial \Omega}{\partial x} - F_x \quad (1)$$

$$\ddot{y} + 2\dot{x} = y - \frac{\partial V}{\partial y} + F_y = \frac{\partial \Omega}{\partial y} - F_y \quad (2)$$

where Ω is the pseudo-potential given by:

$$\Omega = \frac{1}{2}(\dot{x}^2 + \dot{y}^2) + \frac{(1-\mu)}{r_1} + \frac{\mu}{r_2} \quad (3)$$

and F_x and F_y are the x and y components of the drag force, that is given by:

$$F = \frac{-C_D A V^2 \rho_0 e^{-\frac{h-h_0}{H}}}{2m} \quad (4)$$

where C_D is a coefficient that depends on the form of the spacecraft, A is the area of the spacecraft, V is the velocity of the spacecraft relative to the atmosphere, m is the mass of the spacecraft, ρ_0 is the density of the planet's atmosphere at an altitude h_0 , h is the altitude of the spacecraft, H is a constant that specifies how fast the density decays with the altitude. Values for the parameters involved in those equations for the atmosphere of Jupiter are taken from Aureya, Donahue and Festou³¹.

Since the basis of our research consists of close encounters with Jupiter, we use Lamaitre's regularization³² in those equations. The reason is to avoid numerical problems during the close encounters with Jupiter, since it is one of the singularities in the equations of motion of the spacecraft.

Another important result that we need in this paper is the constant of motion known as the "Jacobian Integral", which is an invariant in the circular planar restricted three-body problem, given by the equation.

$$J = E - \omega C = \frac{\dot{x}^2 + \dot{y}^2}{2} - \frac{x^2 + y^2}{2} - \frac{1-\mu}{r_1} - \frac{\mu}{r_2} \quad (5)$$

where E is the energy, C is the angular momentum, r_1 is the distance between the spacecraft and the Sun, r_2 is the distance between the spacecraft and Jupiter and ω is the

angular velocity of the system. The expressions for the energy and the angular momentum, that will be needed later in this paper, are given by:

$$E = \frac{(x+\dot{y})^2 + (\dot{x}-y)^2}{2} - \frac{1-\mu}{r_1} + \frac{\mu}{r_2} \quad (6)$$

$$C = x^2 + y^2 + x\dot{y} - y\dot{x} \quad (7)$$

where x , y and its derivatives are the coordinates of the spacecraft in the rotating system. We emphasize the fact that E and C are the energy and angular momentum relative to the non-rotating inertial system, although the quantities x, y, \dot{x}, \dot{y} are all measured relative to the rotating system.

RESULTS

After defining and coding the mathematical model, many simulations were made. The graphs used to represent the results are contour-level plots having the angle of approach (ψ) in the horizontal axis and the Jacobian constant (J) of the spacecraft in the vertical axis. Several quantities are computed and displayed in those plots: the change in energy, angular momentum and Jacobian constant for a standard maneuver (without drag); the same quantities of the maneuver under the new mathematical model (with the drag force included) and the difference between those quantities from one model to another (to emphasize the influence of the drag force). Those variations are calculated as:

$$\Delta = (\text{Value for the maneuver with no drag}) - (\text{Value for the maneuver with drag})$$

Fig. 2 and Fig. 3 show some of the results. They do not show all the quantities for all the trajectories to save space, since many plots are similar to each other.

From Fig. 2 it is also possible to see that the graph for ΔE with drag does not cover the same region (in the plane ψ - J) as the graph for ΔE with no drag. This is due to the fact that there are some cases where the spacecraft will crash into Jupiter, as a consequence of the drag force. We can see that the crashes occur more often when ψ is close to 0° or 360° , that is the region where the variation in ΔE due to the drag is larger. The quantity of crashes also increases for lower values of J , because they have smaller velocities during the approach. Simulations with $h_0 \leq 200$ km resulted in crashes for almost all the trajectories and they are not shown here.

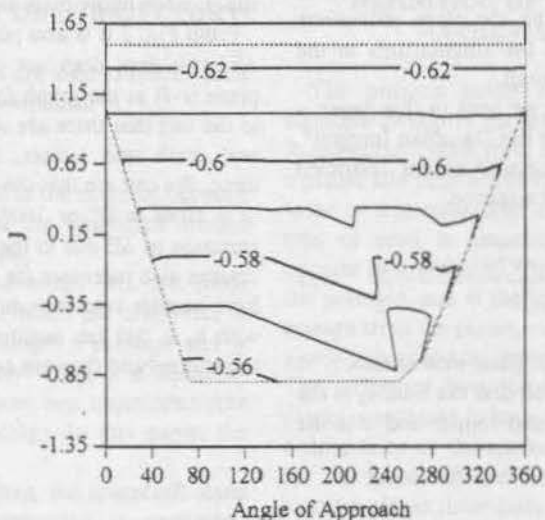
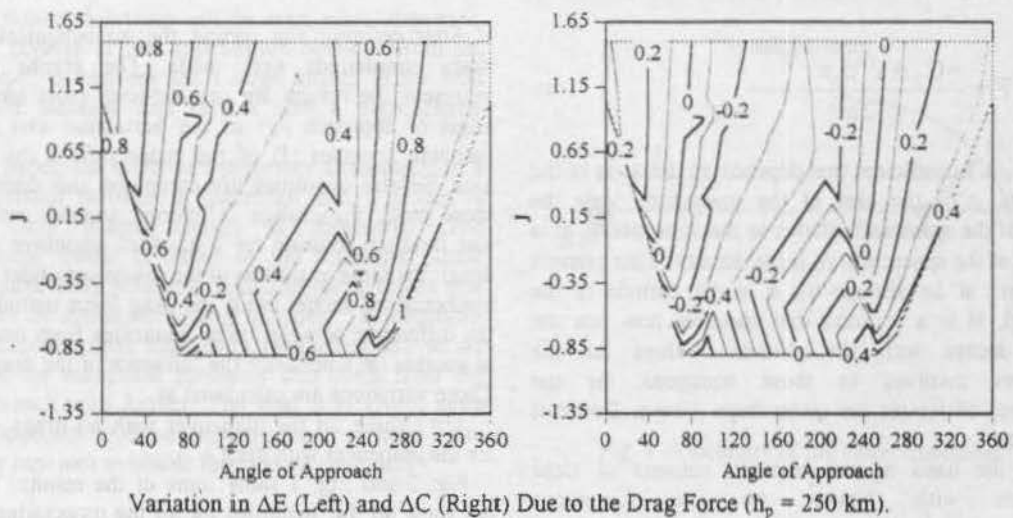
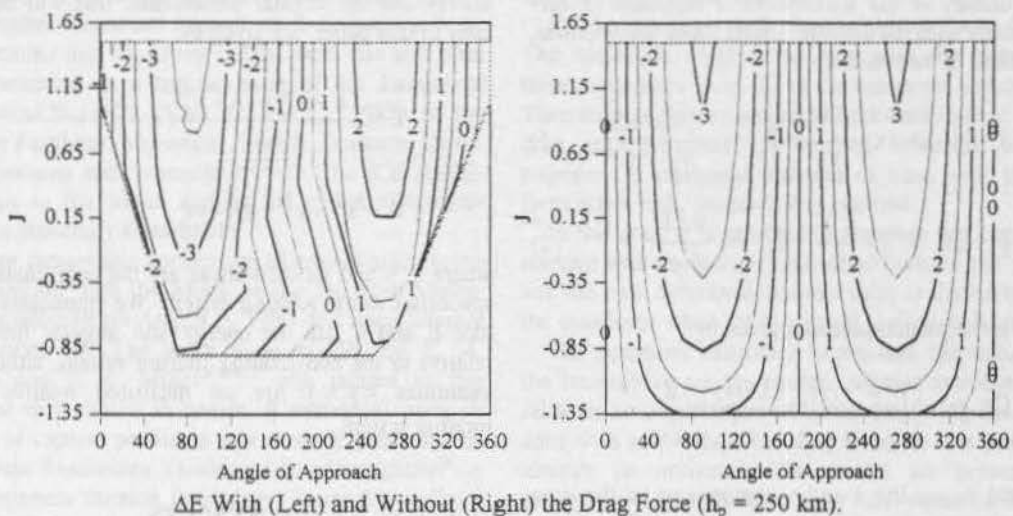
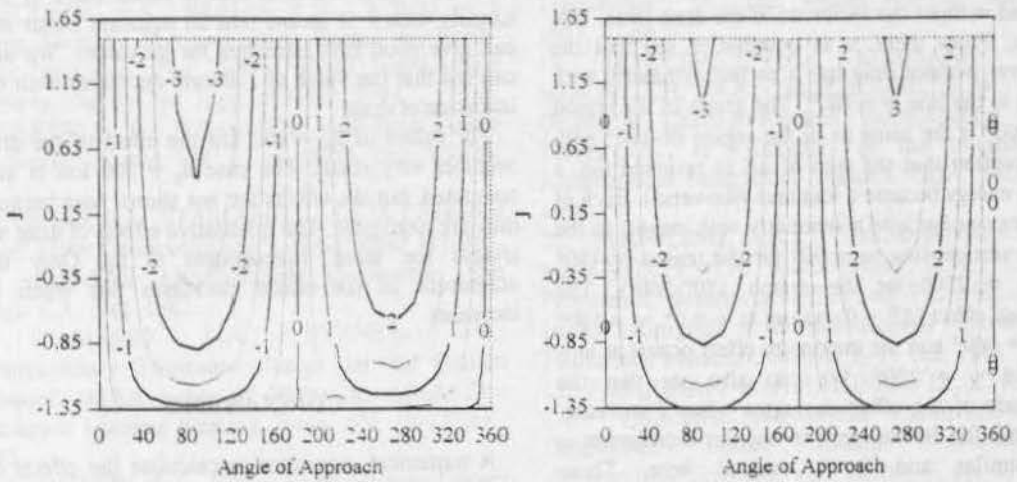
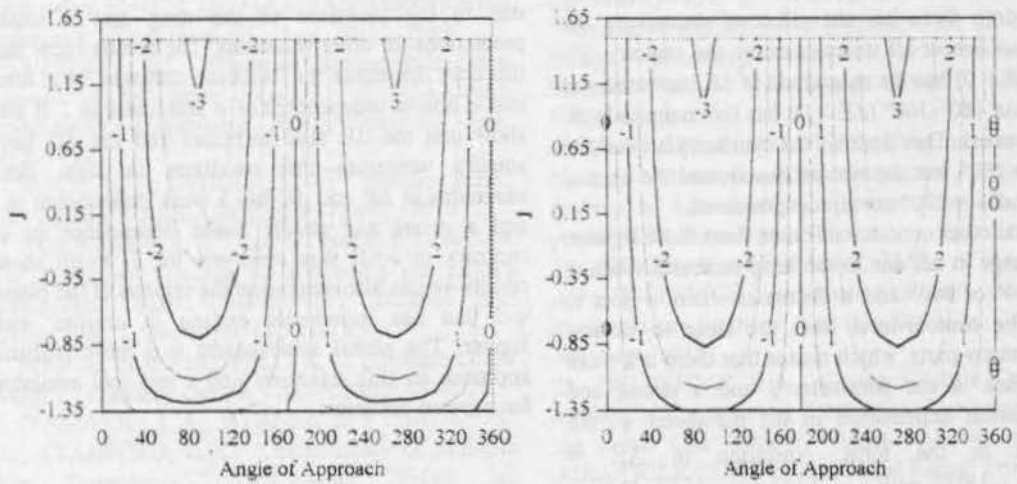


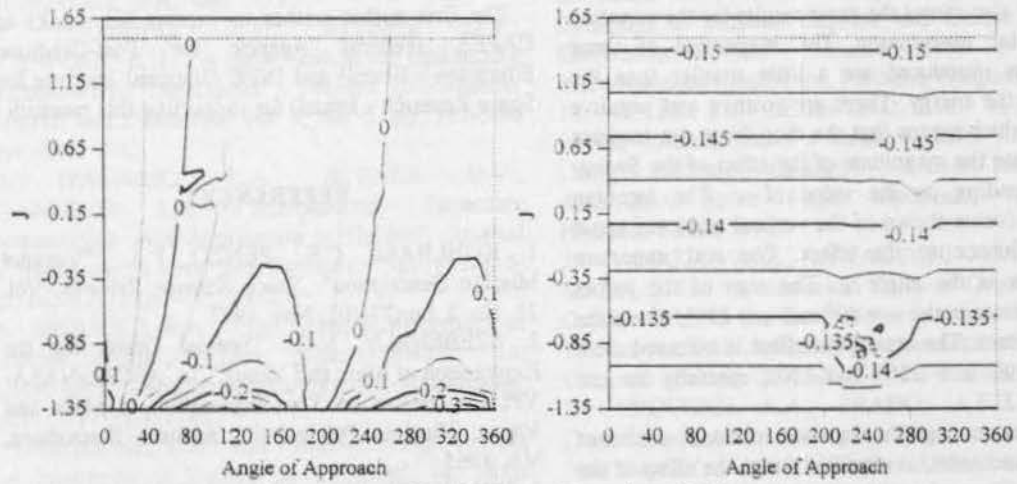
Fig. 2 - Results for $h_p = 250$ km.



ΔE With (Left) and Without (Right) the Drag Force ($h_p = 300$ km).



ΔC With (Left) and Without (Right) the Drag Force ($h_p = 300$ km)



Variation in ΔC and J Due to Drag ($h_p = 300$ km).

Fig. 3 - Results for $h_p = 300$ km

The same Fig. 2 shows a pair of graphs for ΔE with and without the inclusion of the drag force, side by side. From there, it is possible to see that the maneuver without drag has a perfect symmetry with respect to the line $\psi = 180^\circ$. The graph in the region 180° - 360° is the same as in the region 0° - 180° with the exception that the sign of ΔE is reversed (so, a gain in energy became a loss and vice-versa). Each of those regions has also a symmetry with respect to the middle vertical line ($\psi = 90^\circ$ for the region 0° - 180° and $\psi = 270^\circ$ for the region 180° - 360°). The minimum effect ($\Delta E = 0$) occurs at $\psi = 0^\circ$, $\psi = 180^\circ$ and $\psi = 360^\circ$ and the maximum effect occurs at $\psi = 90^\circ$ and $\psi = 270^\circ$. We can also see that the magnitude of the effect increases when J increase. The result for the variation in angular momentum is very similar and it is omitted here. Those characteristics are expected from the analyses of this problem in the two-body model^{16,29,30}. The inclusion of the drag force has the effect of decreasing the energy in almost all trajectories, so the region 0° - 180° ($\Delta E < 0$) has the magnitude of ΔE increased and the region 180° - 360° ($\Delta E > 0$) has the magnitude of ΔE decreased. This destroys the symmetry around the line $\psi = 180^\circ$, but the symmetries around the lines $\psi = 90^\circ$ and $\psi = 270^\circ$ are almost preserved.

Several other conclusions come from those figures. The change in ΔE due to the drag increases when ψ goes to 0° or 360° and it decreases when ψ goes to 180° . The contour-level lines are close to vertical lines in many parts, which means that there is a weak dependence in the parameter J and a strong and almost linear dependence in the parameter ψ . An equation in the form: Variation in $\Delta E = a + b|\psi - 180^\circ|$ with a and b constants would be a good first approximation for those results.

Fig. 3 also shows the same results for the variation in angular momentum. The magnitude of those variations introduced are a little smaller than the ones for the energy. There are positive and negative values, which means that the drag force can increase or decrease the magnitude of the effect of the Swing-By, depending on the value of ψ . The Jacobian constant (value shown in the vertical axis) has again little influence in the effect. The real important parameter is the angle ψ . The sign of the values changes close to the $\psi = 40^\circ$ and $\psi = 230^\circ$, where the effect is zero. The maximum effect is obtained close to the lines $\psi = 120^\circ$ and 320° , specially for low values of J .

The variation of the Jacobian constant decreases when h_p increases, as expected, since the effect of the drag force decreases with the altitude. Contrary to the other quantities calculated in this research, it is almost independent of ψ (the graphs are composed of

lines close to horizontal) and it varies more or less linearly with J . It means that an equation linear in J can give good first estimates for its values. We also can see that the value of J always decreases with the inclusion of drag.

For values of $h_p = 400$ km the effect of the drag becomes very small. The case $h_p = 500$ km is also simulated, but the effects are not shown here because they are negligible. The qualitative effects of drag are always the same, independent of h_p . Only the magnitude of the effects decreases fast when h_p increases.

CONCLUSIONS

A numerical algorithm to calculate the effects of the atmosphere in a Swing-By maneuver with Jupiter is developed. It allows us to quantify expected results due to the inclusion of the drag and to make predictions for other situations. The results show that the drag decreases the Jacobian constant in a form that is almost independent of ψ and linear in J . It also show that the ΔE also decreases and the ΔC have smaller variations that oscillates in sign. Both variations in ΔE and ΔC has a weak dependence in J and a strong and almost linear dependence in ψ , contrary to what was observed for J . From those results we can also determine the regions of the plane ψ - J that has trajectories ending in crashes with Jupiter. The global achievement is a more realistic approach for this maneuver and a new tool available for mission designers.

ACKNOWLEDGMENTS

The first author wishes to express his thanks to CAPES (Federal Agency for Post-Graduate Education - Brazil) and INPE (National Institute for Space Research - Brazil) for supporting this research.

REFERENCES

1. KOHLHASE, C.E.; PENZO, P.A.: "Voyager Mission Description". *Space Science Reviews*, Vol. 21, No. 2, pp. 77-101, Nov. 1977.
2. SZEBEHELY, V.G.: "Special Orbits for the Exploration of Mars and Venus". In: AFCRL-NASA-VPI Conference on The Exploration of Mars and Venus, Virginia Polytechnic Institute, Blacksburg, VA, 1965.
3. HOLLISTER, W.M.; PRUSSING, J.E.: "Optimum Transfer to Mars Via Venus". *Astronautica Acta*, Vol. 12, No. 2, pp. 169-179, 1966.

4. STRIEPE, S.A.; BRAUN, R.D.: "Effects of a Venus Swingby Periapsis Burn During an Earth-Mars Trajectory". *The Journal of the Astronautical Sciences*, Vol. 39, No. 3, pp. 299-312, 1991.
5. CARVELL, R.: "Ulysses-The Sun From Above and Below". *Space*, Vol. 1, pp. 18-55, Dec. 85-Feb. 86.
6. BYRNES, D.V.; D'AMARJO, L.A.: "A Combined Halley Flyby Galileo Mission". AIAA paper 82-1462. In: AIAA/AAS Astrodynamics Conference, San Diego, CA, Aug. 1982.
7. D'AMARJO, L.A.; BYRNES, D.V.: "Interplanetary Trajectory Design for the Galileo Mission". AIAA paper 83-0099. In: AIAA 21st Aerospace Sciences Meeting, Reno, NV, 10-13 Jan., 1983.
8. WEINSTEIN, S.S.: "Pluto Flyby Mission Design Concepts for Very Small and Moderate Spacecraft". AIAA paper 92-4372. In: AIAA/AAS Astrodynamics Conference, Hilton Head, SC, Aug. 10-12, 1992.
9. SWENSON, B.L.: "Neptune Atmospheric Probe Mission". AIAA paper 92-4371. In: AIAA/AAS Astrodynamics Conference, Hilton Head, SC, Aug. 10-12, 1992.
10. NOCK, K.T.; UPHOLF, C.W.: "Satellite Aided Orbit Capture". AAS/AIAA paper 79-165, 1979.
11. FARQUHAR, R.W.; and DUNHAM, D.W.: "A New Trajectory Concept for Exploring the Earth's Geomagnetic Tail". *Journal of Guidance and Control*, Vol. 4, No. 2, pp. 192-196, 1981.
12. MARSH, S.M.; HOWELL, K.C.: "Double Lunar Swingby Trajectory Design". AIAA paper 88-4289.
13. D'AMARJO, L.A.; BYRNES, D.V.; SACKETT, L.L.; STANFORD, R.H.: "Optimization of Multiple Flyby Trajectories". AAS paper 79-162. In: AAS/AIAA Astrodynamics Specialists Conference, Provincetown, MA, June 1979.
14. D'AMARJO, L.A.; BYRNES, D.V.; STANFORD, R.H.: "A New Method for Optimizing Multiple-Flyby Trajectories". *Journal of Guidance, Control, and Dynamics*, Vol. 4, No. 6, pp. 591-596, Nov.-Dec. 1981.
15. D'AMARJO, L.A.; BYRNES, D.V.; STANFORD, R.H.: "Interplanetary Trajectory Optimization with Application to Galileo". *Journal of Guidance, Control, and Dynamics*, Vol. 5, No. 5, pp. 465-471, Sept.-Oct. 1982.
16. BROUCKE, R.A.: "The Celestial Mechanics of Gravity Assist". AIAA paper 88-4220. In: AIAA/AAS Astrodynamics Conference, Minneapolis, MN, 15-17 Aug. 1988.
17. BROUCKE, R.A.; and PRADO, A.F.B.A.: "On the Scattering of Comets by a Planet". In: 181st Meeting of the AAS, Phoenix, AZ, 3-7 Jan. 1993.
18. MINOVICH, M. A.: "A Method for Determining Interplanetary Free-Fall Reconnaissance Trajectories". JPL Tec. Memo 312-130, Aug. 23 1961, 47 pp..
19. DOWLING, R.L.; KOSMANN, W.J.; MINOVITCH, M.A.; RIDENOURE, R.W.: "The Origin of Gravity-Propelled Interplanetary Space Travel". In: 41st Congress of the International Astronautical Federation, Dresden, GDR, 6-12 Oct. 1990.
20. DOWLING, R.L.; KOSMANN, W.J.; MINOVITCH, M.A.; RIDENOURE, R.W.: "Gravity Propulsion Research at UCLA and JPL, 1962-1964". In: 42nd Congress of the International Astronautical Federation, Montreal, Canada, 5-11 Oct. 1991.
21. FARQUHAR, R.; MUHONEN, D.; CHURCH, L.C.: "Trajectories and Orbital Maneuvers for the ISEE-3/ICE Comet Mission". *Journal of Astronautical Sciences*, Vol. 33, No. 3, pp. 235-254, July-Sept. 1985.
22. MUHONEN, D.; DAVIS, S.; DUNHAM, D.: "Alternative Gravity-Assist Sequences for the ISEE-3 Escape Trajectory". *Journal of Astronautical Sciences*, Vol. 33, No. 3, pp. 255-273, July-Sept. 1985.
23. DUNHAM, D.; DAVIS, S.: "Optimization of a Multiple Lunar-Swingby Trajectory Sequence". *Journal of Astronautical Sciences*, Vol. 33, No. 3, pp. 275-288, July-Sept. 1985.
24. EFRON, L.; YEOMANS, D.K.; SCHANZLE, A.F.: "ISEE-3/ICE Navigation Analysis". *Journal of Astronautical Sciences*, Vol. 33, No. 3, pp. 301-323, July-Sept. 1985.
25. BELBRUNO, E.A.: "Lunar Capture Orbits, a Method of Constructing Earth Moon Trajectories and the Lunar Gas Mission". AIAA-87-1054. In: 19th AIAA/DGLR/JSASS International Electric Propulsion Conference, Colorado Springs, Colorado, 1987.
26. BELBRUNO, E.A.: "Examples of the Nonlinear Dynamics of Ballistic Capture and Escape in the Earth-Moon System". AIAA-90-2896. In: AIAA Astrodynamics Conference, Portland, Oregon, 1990.
27. MILLER, J.K.; BELBRUNO, E.A.: "A Method for the Construction of a Lunar Transfer Trajectory Using Ballistic Capture". AAS-91-100. In: AAS/AIAA Space Flight Mechanics Meeting, Houston, Texas, 1991.
28. YAMAKAWA, H.; KAWAGUCHI, J.; ISHII, N.; MATSUO, H.: "A Numerical Study of Gravitational Capture Orbit in the Earth-Moon System". AAS 92-186. In: AAS/AIAA Spaceflight Mechanics Meeting, Colorado Springs, Colorado, Feb. 24-26 1992.
29. BROUCKE, R.A.; PRADO, A.F.B.A.: "A Classification of the Swing-By Trajectories Passing Near Jupiter". AAS 93-177. In: AAS/AIAA Space Flight Mechanics Meeting, Pasadena, California, Feb. 22-24 1993.

30. PRADO, A.F.B.A.: "Optimal Transfer and Swing-By Orbits in the Two- and Three-Body Problems". Ph.D. Dissertation, University of Texas at Austin, Austin, Texas, Dec. 1993.
31. ATREYA, S.K.; DONAHUE, T.M.; FESTOU, M.C.: "Jupiter: Structure and Composition of the Upper Atmosphere." *The Astrophysical Journal*, Vol. 247, pp. L43-L47, 1981.
32. SZEBEHELY, V.G. *Theory of Orbits*, Academic Press, New York, 1967.

DISTURBING FUNCTION FOR HIGHLY ECCENTRIC ARTIFICIAL SATELLITE RESONANT ORBITS

Paulo Henrique Cruz Neiva de Lima Jr.*
 Sandro da Silva Fernandes and Wagner Sessin**

* Centro de Desenvolvimento Tecnológico
 Escola de Engenharia Industrial
 12242-800, São José dos Campos, SP, BRAZIL

** CTA-ITA-IEAB
 12228-900 - São José dos Campos-SP-BRAZIL

Abstract

The classical development of the disturbing function in powers series of the eccentricity derived by Kaula is only valid for orbits with $e < 0.6627...$ In this paper, the disturbing function is developed in terms of Kaula's inclination functions and Hansen's coefficients, which are taken in closed-form. This development, valid for $e < 1$, is applied in study of highly eccentric resonant orbits.

Key words: Highly eccentric orbits, artificial satellites, resonance.

Introduction

The classical development of the disturbing function in power series of the eccentricity derived by Kaula¹ for the geopotential in artificial satellite theory is only valid for orbits with $e < 0.6627...$ Close to this critical value the convergence of the series becomes too slow and for larger values the series diverges. For non-resonant orbits, analytical closed-form theories exist^{2,3}; the development of the disturbing function in powers of the eccentricity is not necessary. For resonant orbits, however, the analytical theories are based on the development of the disturbing function and are limited to orbits with very small eccentricities⁴. In modern space applications, there are several artificial satellites, like Molniya and Kosmos, whose resonant orbits have eccentricities greater than the critical value^{5,6}. To develop analytical theories of the motion of such satellites, a different approach for the development of the disturbing function will be considered in this paper. The disturbing function will be written in terms of Kaula's inclination functions and Hansen's coefficients which are taken in closed form^{7,8}. This

development, valid for orbits with $e < 1$, is applied in the study of highly eccentric resonant orbits. A reduced disturbing function containing secular and critical terms is obtained neglecting short and long periodic terms in comparison to the secular and resonant ones. The integrability of the system of reduced differential equations is briefly discussed for 2:1 resonance concerning the tesseral harmonic J_{22} .

Earth's Potential

Since Kaula's development of Earth's potential in powers of eccentricity is not valid for orbits with eccentricities greater than the critical value, we will consider the following one presented by Osório⁷, involving Kaula's inclination functions and Hansen's coefficients in closed-form,

$$F = \frac{\mu}{2a} + \sum_{l=2}^{\infty} \sum_{m=0}^l \sum_{p=0}^{\infty} \sum_{q=-\infty}^{\infty} \frac{\mu}{a} \left(\frac{a_0}{a}\right)^l J_{lm} \times F_{lmpq}(I) H_q^{-(l+1)\lambda(1-2p)}(e) \cos \varphi_{lmpq} \quad (1)$$

with

$$\varphi_{lmpq} = qM + (l-2p)\omega + m(\Omega - \Theta - \lambda_{lm}) + (l-m)\frac{\pi}{2} \quad (2)$$

where a , e , I , Ω , ω and M are the classical Keplerian elements; μ is the Gaussian constant; a_0 is the mean equatorial radius of the Earth; J_{lm} is the coefficient of the (l,m) spherical harmonic; Θ is the Greenwich sidereal time; λ_{lm} is the longitude of the major axis of symmetry of the

(l,m) spherical harmonic; $F_{lmp}(I)$ are Kaula's inclination functions^{1,7}

$$F_{lmp}(I) = \frac{(l+m)!}{2^l p! (l-p)!} \sum_k (-1)^k \binom{2p}{l-m-k} \times \binom{2l-2p}{k} \cos^{2l-k} \left(\frac{I}{2} \right) \sin^k \left(\frac{I}{2} \right) \quad (3)$$

with

$$\max(0, l-m-2p) \leq k \leq \min(2l-2p, l-m)$$

$$\chi = -l + m + 2p + k$$

and $H_q^{n,m}(e)$ are Hansen's coefficients^{8,9}, defined by

$$H_q^{n,m}(e) = \frac{1}{2\pi} \int_0^{2\pi} \left(\frac{r}{a} \right)^n x^m z^{-q} dM \quad (4)$$

with $x = \exp(iv)$ and $z = \exp(iM)$, v is the true anomaly and $i = \sqrt{-1}$.

Earth's potential defined by eqn (1) with Hansen's coefficient in closed-form is valid for any orbit with $e < 1$.

Equations of motion in Delaunay variables

In order to derive some new results for resonant orbits, we will introduce Delaunay canonical variables.

Let the transformation of variables be defined by¹⁰

$$\begin{aligned} L &= \sqrt{\mu a} & \ell &= M \\ G &= \sqrt{\mu a(1-e^2)} & g &= \omega \\ H &= \sqrt{\mu a(1-e^2)} \cos I & h &= \Omega \end{aligned} \quad (5)$$

where L, G, H, ℓ, g, h are Delaunay variables.

From eqn (1) and (5) results

$$J = \frac{\mu^2}{2L^2} + \sum_{l=2}^{\infty} \sum_{m=0}^l R_{lm} \quad (6)$$

with

$$R_{lm} = \sum_{p=0}^l \sum_{q=-\infty}^{+\infty} B_{lmpq}(L, G, H) \cos \phi_{lmpq} \quad (7)$$

being

$$\phi_{lmpq} = q\ell + (l-2p)g + m(h - \Theta - \lambda_{lm}) + (l-m)\frac{\pi}{2}$$

and $B_{lmpq}(L, G, H)$ is the coefficient of $\cos \phi_{lmpq}$ in eqn (1) written in terms of Delaunay variables L, G and H .

The motion of an artificial satellite is described by the canonical system governed by the Hamiltonian function J ,

$$\frac{dQ}{dt} = \frac{\partial J}{\partial q} \quad \frac{dq}{dt} = -\frac{\partial J}{\partial Q} \quad (8)$$

where $Q=L, G, H$ and $q = \ell, g, h$.

It should be noted that the Hamiltonian function J involves the sidereal time Θ . Introducing the variable θ conjugate to Θ , we extend the phase-space. In the extended phase-space, the extended Hamiltonian function is given by

$$X = J + \omega_e \theta \quad (9)$$

where ω_e is the angular velocity of the rotational motion of the Earth. The new canonical system is given by

$$\frac{dQ^*}{dt} = \frac{\partial X}{\partial q^*} \quad \frac{dq^*}{dt} = -\frac{\partial X}{\partial Q^*} \quad (10)$$

with $Q^* = L, G, H, \Theta$ and $q^* = \ell, g, h, \theta$.

For resonant orbits is convenient to use a new set of canonical variables. Let the transformation of variables be defined by

$$\begin{aligned} X &= L & x &= \ell + g + h \\ Y &= G - L & y &= g + h \\ Z &= H - G & z &= h \\ \Theta &= \Theta & \theta &= \theta \end{aligned} \quad (11)$$

where $X, Y, Z, \Theta, x, y, z, \theta$ are modified Delaunay variables.

The motion of an artificial satellite in modified Delaunay variables is governed by the new extended Hamiltonian function X' , obtained from eqns (9) and (11),

$$X' = \frac{\mu^2}{2X^2} + \sum_{l=2}^{\infty} \sum_{m=0}^l R'_{lm} + \omega_e \theta \quad (12)$$

with

$$R'_{lm} = \sum_{p=0}^l \sum_{q=-\infty}^{+\infty} B'_{lmq}(X, Y, Z) \cos \phi_{lmq} \quad (13)$$

$$B'_{lmq}(X, Y, Z) = \frac{\mu^{l+2}}{X^{l+2}} a_e^l J_{lm} F'_{lm}(X, Y, Z) \times H_q^{-(l+1), (l-2p)}(X, Y) \quad (14)$$

$$\phi_{lmq} = (qx - m\Theta) + (l - 2p - q)y + (m - l - 2p)z - m\lambda_{lm} + (l - m)\frac{\pi}{2} \quad (15)$$

Here, F'_{lm} and $H_q^{-(l+1), (l-2p)}$ denote Kaula's inclination functions and Hansen's coefficients written in modified Delaunay variables.

Resonant Orbits

An artificial Earth satellite is in resonance with Earth's rotation when its mean motion n is commensurable with the angular velocity of Earth's rotation ω_e ,

$$qn - m\omega_e \equiv 0 \quad (16)$$

The Hamiltonian function X' , defined by eqns (12) - (15) can be greatly simplified if short and long periodic terms are neglected in comparison to the secular and resonant ones. The short periodic terms are eliminated taking the "mean" Hamiltonian \bar{X}' ,

$$\bar{X}' = \frac{1}{2\pi} \int_0^{2\pi} X' dx \quad (17)$$

It should be noted that the terms satisfying eqn (16) must remain in \bar{X}' . The secular terms correspond to $m=0$ and $l=2p$ (l is even) in \bar{X}' ; they are related to zonal harmonics of even degree. A reduced Hamiltonian function, containing only secular and critical terms, is then obtained,

$$\bar{X}' = \frac{\mu^2}{2X^2} + \omega_e \theta + \sum_{j=2}^{\infty} B'_{j0\frac{j}{2}}(X, Y, Z) + \sum_{l=2}^{\infty} \sum_{m=2}^l \sum_{p=0}^l B'_{lmp(\alpha m)}(X, Y, Z) \cos \phi_{lmp(\alpha m)} \quad (18)$$

being

$$\phi_{lmp(\alpha m)} = m(\alpha x - \Theta) + (l - 2p - m\alpha)y + (m - l + 2p)z - m\lambda_{lm} + (l - m)\frac{\pi}{2}$$

with $\alpha = \frac{q}{m}$, $m \neq 0$, $B'_{lmp(\alpha m)}$ are the same coefficients

defined by eqn (14) with $q = \alpha m$. Note that the critical terms are related to the tesseral harmonics of the potential.

Using the recurrence formulas for the derivatives of Hansen's coefficients¹¹ and the derivatives of Kaula's inclination functions¹², we can write the equations of motion for resonant orbits in closed-form,

$$\dot{X} = -\alpha \sum_{l=2}^{\infty} \sum_{m=2}^l \sum_{p=0}^l m B'_{lmp(\alpha m)}(X, Y, Z) \sin \phi_{lmp(\alpha m)} \quad (19)$$

$$\dot{Y} = -\sum_{l=2}^{\infty} \sum_{m=2}^l \sum_{p=0}^l (l - 2p - m\alpha) B'_{lmp(\alpha m)}(X, Y, Z) \sin \phi_{lmp(\alpha m)} \quad (20)$$

$$\dot{Z} = -\sum_{l=2}^{\infty} \sum_{m=2}^l \sum_{p=0}^l (m - l - 2p) B'_{lmp(\alpha m)}(X, Y, Z) \sin \phi_{lmp(\alpha m)} \quad (21)$$

$$\dot{\Theta} = \omega_e \quad (22)$$

$$\dot{x} = \frac{\mu^2}{X^3} + n_x - \sum_{l=2}^{\infty} \sum_{m=2}^l \sum_{p=0}^l \frac{\partial B'_{lmp(\alpha m)}}{\partial X} \cos \phi_{lmp(\alpha m)} \quad (23)$$

$$\dot{y} = n_y - \sum_{l=2}^{\infty} \sum_{m=2}^l \sum_{p=0}^l \frac{\partial B'_{lmp(\alpha m)}}{\partial X} \cos \phi_{lmp(\alpha m)} \quad (24)$$

$$\dot{z} = n_z - \sum_{l=2}^{\infty} \sum_{m=2}^l \sum_{p=0}^l \frac{\partial B'_{lmp(\alpha m)}}{\partial Z} \cos \phi_{lmp(\alpha m)} \quad (25)$$

$$\dot{\theta} = -\sum_{l=2}^{\infty} \sum_{m=2}^l \sum_{p=0}^l m B'_{lmp(\alpha m)} \sin \phi_{lmp(\alpha m)} \quad (26)$$

where n_x, n_y, n_z denote the frequencies due to the secular part of the disturbing function,

$$n_x = -\sum_{j=2}^{\infty} \frac{\partial B'_{j0\frac{j}{2}}}{\partial X} \quad (27)$$

n_y and n_z are similar. The partial derivatives of coefficients $B'_{lmp(\alpha m)}$ are calculated through the following equations,

$$\frac{\partial B'_{lmp(\alpha m)}}{\partial X} = -(l+2) \frac{\mu^{l+2}}{X^{l+3}} a_e^l J_{lm} \times F'_{lm}(X, Y, Z) H_q^{-(l+1), (l-2p)}(X, Y) + \frac{\mu^{l+2}}{X^{l+2}} a_e^l J_{lm} \left[\frac{\partial F'_{lm}}{\partial X} H_q^{-(l+1), (l-2p)} + F'_{lm} \frac{\partial H_q^{-(l+1), (l-2p)}}{\partial X} \right] \quad (28)$$

$$\frac{\partial B'_{\text{imp}(\alpha m)}}{\partial Y} = \frac{\mu^{l+2}}{X^{l+2}} a_e J_{\text{lm}} \left[\frac{\partial F'_{\text{imp}}}{\partial Y} H'^{-(l+1), (l-2p)}_{(\alpha m)} + F'_{\text{imp}} \frac{\partial H'^{-(l+1), (l-2p)}_{(\alpha m)}}{\partial Y} \right] \quad (29)$$

$$\frac{\partial B'_{\text{imp}(\alpha m)}}{\partial Z} = \frac{\mu^{l+2}}{X^{l+2}} a_e J_{\text{lm}} \left[\frac{\partial F'_{\text{imp}}}{\partial Z} H'^{-(l+1), (l-2p)}_{(\alpha m)} + F'_{\text{imp}} \frac{\partial H'^{-(l+1), (l-2p)}_{(\alpha m)}}{\partial Z} \right] \quad (30)$$

with

$$\frac{\partial F'_{\text{imp}}}{\partial X} = \frac{dF_{\text{imp}}(I)}{dI} \times \frac{Z}{(X+Y)\sqrt{(X+Y)^2 - (X+Y+Z)^2}} \quad (31)$$

$$\frac{\partial F'_{\text{imp}}}{\partial Y} = \frac{\partial F'_{\text{imp}}}{\partial X} \quad (32)$$

$$\frac{\partial F'_{\text{imp}}}{\partial Z} = -\frac{(X+Y)}{Z} \frac{\partial F'_{\text{imp}}}{\partial X} \quad (33)$$

$$\frac{\partial H'^{-(l+1), (l-2p)}_{(\alpha m)}}{\partial X} = \frac{dH'^{-(l+1), (l-2p)}_{(\alpha m)}}{de} \times \frac{Y(X+Y)}{X^2 \sqrt{X^2 - (X+Y)^2}} \quad (34)$$

$$\frac{\partial H'^{-(l+1), (l-2p)}_{(\alpha m)}}{\partial Y} = -\frac{X}{Y} \frac{\partial H'^{-(l+1), (l-2p)}_{(\alpha m)}}{\partial X} \quad (35)$$

$$\frac{\partial H'^{-(l+1), (l-2p)}_{(\alpha m)}}{\partial Z} = 0 \quad (36)$$

The derivatives of Hansen's coefficients with respect to the eccentricity are given by ¹¹

$$\frac{dH_i^{r,s}(e)}{de} = \frac{s}{2(1-e^2)} [H_i^{r,s+1}(e) - H_i^{r,s-1}(e)] + \left(\frac{s-r}{2}\right) H_i^{r-1,s+1}(e) - \left(\frac{r+s}{2}\right) H_i^{r+1,s-1}(e) \quad (37)$$

and the derivatives of Kaula's inclination functions with respect to the inclinations are given by ¹²

$$\frac{dF_{\text{imp}}(I)}{dI} = \left[\frac{\alpha_1}{s} c J_{\text{imp}}(c) - s \frac{\partial F_{\text{imp}}(c)}{\partial c} \right] \frac{s^{|\alpha_1|}}{2} \quad (38)$$

with

$$\alpha_1 = m + 2p - l, \quad c = \cos \frac{I}{2}, \quad s = \sin \frac{I}{2}$$

$$\text{and } J_{\text{imp}}(c) = \sum_k F_{\text{imp}}^k \sum_{r=0}^{A_1} (-1)^r \binom{A_1}{r} c^{2r+A_1} \quad (39)$$

where

$$F_{\text{imp}}^k = \frac{(l+m)!}{2^l p! (l-p)!} (-1)^k \binom{2l-2p}{k} \binom{2p}{l-m-k} \quad (40)$$

$$2A_1 = 2k + \alpha_1 - |\alpha_1| \quad (41)$$

$$A_2 = 2l - \alpha_1 - 2k \quad (42)$$

Equations (37) - (39) must be written in terms of the canonical variables X, Y, Z and then substituted into eqns (31) - (35).

The system of differential equations defined by eqns (19) - (26) has a first integral. Combining eqns (19) - (21), one gets

$$\left(1 - \frac{1}{\alpha}\right) \dot{X} + \dot{Y} + \dot{Z} = 0 \quad (43)$$

with $\alpha \neq 0$. Thus,

$$\left(1 - \frac{1}{\alpha}\right) X + Y + Z = C_1 \quad (44)$$

where C_1 is a constant of integration.

Let a canonical transformation be defined by the following equations,

$$\begin{aligned} X_1 &= X & x_1 &= x - \left(1 - \frac{1}{\alpha}\right) z \\ Y_1 &= Y & y_1 &= y - z \\ Z_1 &= \left(1 - \frac{1}{\alpha}\right) X + Y + Z & z_1 &= z \\ \Theta_1 &= \Theta & \theta_1 &= \theta \end{aligned} \quad (45)$$

The subscript "1" denotes the new canonical variables.

The reduced Hamiltonian \bar{X}' is invariant with respect to this canonical transformation. Accordingly, from eqns (18) and (45), we derive the new Hamiltonian function

$$\begin{aligned} X_1 & \\ X_1 &= \frac{\mu^2}{2X_1^2} + \omega_e \theta_1 + \sum_{j=2}^{\infty} B_{1,j,0}^{j,0} (X_1, Y_1, Z_1) \\ &+ \sum_{l=2}^{\infty} \sum_{m=2}^l \sum_{p=0}^l B_{1,\text{imp}(\alpha m)} (X_1, Y_1, Z_1) \cos \phi_{1,\text{imp}(\alpha m)} \end{aligned} \quad (46)$$

with

$$\phi_{1,\text{imp}(\alpha m)} = m(\alpha x_1 - \Theta_1) + (l-2p - m\alpha) y_1 - \phi_{1,\text{imp}(\alpha m)0} \quad (47)$$

being

$$\Phi_{1, \text{imp}(\alpha m)0} = m\lambda_{lm} + (1-m)\frac{\pi}{2} B_{l, j_0 \frac{1}{2} 0} \text{ and } B_{1, \text{imp}(\alpha m)} \text{ are}$$

the same coefficients defined by eqn (14), with $q = \alpha m$, expressed in terms of the new variables X_1, Y_1 and Z_1 . Since z_1 is an ignorable (cyclic) variable of the dynamical system governed by \mathcal{H}_1, Z_1 is a first integral, i.e. $Z_1 = C_1$.

The Hamiltonian function \mathcal{H}_1 has all critical arguments for a given resonance and can be used in a numerical investigation on the effects of overlapping of two or more resonance. On the other hand, for practical and theoretical applications, an additional hypothesis can be introduced: the critical argument is chosen a priori, i.e. m and $(l-2p)$ are fixed. In this case, the other terms in the Hamiltonian function \mathcal{H}_1 , taken as short periodic, can be eliminated. Consequently, the following critical Hamiltonian is obtained

$$\begin{aligned} \mathcal{H}_{1,c} = & \frac{\mu^2}{2X_1^2} + \omega_e \theta_1 + \sum_{j=2}^{\infty} B_{l, j_0 \frac{1}{2} 0} (X_1, Y_1, C_1) \\ & + \sum_{l=2}^{\infty} \sum_{p=0}^l B_{1, \text{imp}(\alpha m)} (X_1, Y_1, C_1) \cos \Phi_{1, \text{imp}(\alpha m)} \end{aligned} \quad (48)$$

with $k=l-2p$ and m fixed. The subscript "c" are concerned with the critical terms.

Consider the differential equations to X_1 and Y_1 variables,

$$X_1 = -m\alpha \sum_{l=2}^{\infty} \sum_{p=0}^l B_{1, \text{imp}(\alpha m)} (X_1, Y_1, C_1) \sin \Phi_{1, \text{imp}(\alpha m)} \quad (49)$$

$$\begin{aligned} Y_1 = & -(k-m\alpha) \sum_{l=2}^{\infty} \sum_{p=0}^l B_{1, \text{imp}(\alpha m)} (X_1, Y_1, C_1) \\ & \times \sin \Phi_{1, \text{imp}(\alpha m)} \end{aligned} \quad (50)$$

with $k=l-2p$ and m fixed. These equations satisfies the following relation

$$(k-m\alpha)X_1 - m\alpha Y_1 = 0. \quad (51)$$

Accordingly, the system of differential equations governed by the critical Hamiltonian function $\mathcal{H}_{1,c}$ has the first integral

$$(k-m\alpha)X_1 - m\alpha Y_1 = C_2 \quad (52)$$

where C_2 is a constant of integration.

Let the new canonical transformation be defined by

$$\begin{aligned} X_2 &= X_1 & x_2 &= x_1 + \left(\frac{k-m\alpha}{m\alpha} \right) y_1 \\ Y_2 &= (k-m\alpha)X_1 - m\alpha Y_1 & y_2 &= -\frac{1}{m\alpha} y_1 \\ \Theta_2 &= \Theta_1 & \theta_2 &= \theta_1 \end{aligned} \quad (53)$$

with $m, \alpha \neq 0$.

The new critical Hamiltonian function $\mathcal{H}_{2,c}$ resulting from this canonical transformation is given by

$$\begin{aligned} \mathcal{H}_{2,c} = & \frac{\mu^2}{2X_2^2} + \omega_e \theta_2 + \sum_{j=2}^{\infty} B_{2, j_0 \frac{1}{2} 0} (X_2, Y_2, C_1) \\ & + \sum_{l=2}^{\infty} \sum_{p=0}^l B_{2, \text{imp}(\alpha m)} (X_2, Y_2, C_1) \cos \Phi_{2, \text{imp}(\alpha m)} \end{aligned} \quad (54)$$

where

$$\Phi_{2, \text{imp}(\alpha m)} = m(\alpha x_2 - \Theta_2) - \Phi_{1, \text{imp}(\alpha m)0} \quad (55)$$

with

$$\Phi_{2, \text{imp}(\alpha m)0} = \Phi_{1, \text{imp}(\alpha m)0}$$

and $k=l-2p$ and m , fixed. Note that k assumes values such that p is an integer.

The momentum θ_2 can be straightforwardly obtained from eqn (54), since the Hamiltonian function $\mathcal{H}_{2,c}$ is a first integral in the extended phase-space, i.e. $\mathcal{H}_{2,c} = C$. On the other hand, the differential equation to variable Θ_2 is very simple,

$$\frac{d\Theta_2}{dt} = \omega_e \quad (56)$$

thus,

$$\Theta_2 = \omega_e t \quad (57)$$

with $\Theta_2(0) = 0$. Accordingly, taking Θ_2 as independent variable, the following differential equations result,

$$\frac{dX_2}{d\Theta_2} = \frac{m\alpha}{\omega_e} \sum_{l=2}^{\infty} \sum_{p=0}^l B_{2, \text{imp}(\alpha m)} \sin \Phi_{2, \text{imp}(\alpha m)} \quad (58)$$

$$\begin{aligned} \frac{dx_2}{d\Theta_2} = & \frac{\mu^2}{\omega_e X_2^3} - \sum_{j=2}^{\infty} \frac{1}{\omega_e} \frac{\partial B_{2, j_0 \frac{1}{2} 0}}{\partial X_2} \\ & - \frac{1}{\omega_e} \sum_{l=2}^{\infty} \sum_{p=0}^l \frac{\partial B_{2, \text{imp}(\alpha m)}}{\partial X_2} \cos \Phi_{2, \text{imp}(\alpha m)}. \end{aligned} \quad (59)$$

with $k=l-2p$ fixed.

The partial derivative of the coefficients $B_{2, \text{imp}(\alpha m)}$ with respect to X_2 is obtained from eqns (28), (45) and (53) by means of implicit derivation; it should be written in terms of X_2, C_2 and C_1 .

Equations (58) and (59) are valid for a given resonant orbit with $e < 1$. Note that Hansen's coefficients in the coefficients $B_{2, \text{imp}(\alpha m)}$ are taken in closed-form; they are calculated numerically through eqn (4).

An application to 12-hour artificial satellite

A brief discussion on 2:1 resonance concerning the tesseral harmonic J_{22} based on the results of the preceding sections will be presented.

For 2:1 resonance, $\alpha = \frac{1}{2}$; thus, from eqn (47), the following critical arguments are possible

$$\varphi_{1, \text{imp}(\alpha m)} = m \left(\frac{x_1}{2} - \Theta_1 \right) + \left(1 - 2p - \frac{m}{2} \right) y_1 - \varphi_{1, \text{imp}(\alpha m)0} \quad (60)$$

with $m=2, \dots, l$; $p=0, \dots, l$ and $l=2, 3, \dots$

Taking $m=2$ and $l-2p=k$, we choose the critical argument,

$$\begin{aligned} \varphi_{1, l2p1} &= (x_1 - 2\Theta_1) + (k-1)y_1 - \varphi_{1, l2p10} \\ &= (x_1 + (k-1)y_1) - 2\Theta_1 - \varphi_{1, l2p10} \\ &= x_2 - 2\Theta_2 - \varphi_{2, l2p10} = \varphi_{2, l2p1} \end{aligned} \quad (61)$$

From eqn (54), the critical Hamiltonian is given by

$$\begin{aligned} X_{2,c} &= \frac{\mu^2}{2X_2^2} + \omega_e \theta_2 + \sum_{j=2}^{\infty} B_{2, j0 \frac{1}{2}}(X_2, Y_2, C_1) \\ &+ \sum_{l=2}^{\infty} \sum_{p=0}^l B_{2, l2p1}(X_2, Y_2, C_1) \cos \varphi_{2, l2p1}. \end{aligned} \quad (62)$$

The coefficients $B_{2, l2p1}$ involve all tesseral harmonics of the general form J_{l2} and are concerned to the critical arguments $\varphi_{2, l2p1}$. For simplicity we will consider only the tesseral harmonic J_{22} , i.e. $l=2$ and we will choose $k=0$, i.e. $p=1$. Thus, eqn (62) reduces to

$$\begin{aligned} X_{2,c} &= \frac{\mu^2}{2X_2^2} + \omega_e \theta_2 + B_{2,2010} \\ &+ B_{2,2211}(X_2, Y_2, C_1) \cos \varphi_{2,2211} \end{aligned} \quad (63)$$

with the coefficients $B_{2,2010}$ and $B_{2,2211}$, given by

$$\begin{aligned} B_{2,2010} &= \frac{\mu^4}{X_2^4} a_e^2 J_{20} F'_{201}(X_2, C_2, C_1) \\ &\times H_0^{-3,0}(X_2, C_2, C_1) \end{aligned} \quad (64)$$

$$\begin{aligned} B_{2,2211} &= \frac{\mu^4}{X_2^4} a_e^2 J_{22} F'_{221}(X_2, C_2, C_1) \\ &\times H_1^{-3,0}(X_2, C_2, C_1). \end{aligned} \quad (65)$$

Note that only the secular term concerning the second zonal harmonic J_{20} appears in eqn (63); however, all secular terms can be considered.

For very small eccentricities, the dynamical system governed by the critical Hamiltonian $X_{2,c}$, defined by eqn (63) is integrable^{13,14}

Conclusion

In this paper, a new development of the disturbing function for the geopotential involving Kaula's inclination and Hansen's coefficients (in closed-form), valid for all orbits with $e < 1$, is applied in the study of highly eccentric resonant orbits. A reduced Hamiltonian function containing secular and critical terms is obtained neglecting short and long periodic terms. Since this reduced Hamiltonian has all critical arguments for a given resonance, an additional hypothesis is introduced: the critical argument should be specified a priori. A critical Hamiltonian for a given resonance is then obtained containing the specified critical argument. This critical Hamiltonian involves two arbitrary constants and the resulting differential equations must be solved numerically.

References

- 1Kaula, W. M.; "Theory of Satellite Geodesy", Blaisdell Publishing Company, Massachusetts, 1966.
- 2Brouwer, D; "Solution of the Problem of Artificial Satellite Theory Without Drag", The Astron. Journal, vol. 64, p.378-397, 1959.
- 3Kozai, Y.; "The Motion of a Close Earth satellite", The Astron. Journal, vol. 1, p. 367-374, 1959.
- 4Gedeon, G.; "Tesseral Resonance Effects on Satellites Orbits", Cel. Mech., vol.1, p.167-189, 1969.
- 5Lecohier, G. Guernonprez V. & Delhaise, F.; "European Molnyia and Tundra Orbit Control", Mecanique Spatiale, Cepadues-Editions, p.165-191, 1990.
- 6Wagner, C.A.; "Determination of Low-Order Resonant Gravity Harmonics from the Drift of Two

Russian 12-Hours Satellites", J. of Geophysical Res., vol 73, July 1968.

⁷Osório, J. Pereira; "Perturbações de Órbitas de Satélites no Estudo do Campo Gravitacional Terrestre", Imprensa Portuguesa, Porto, 1973.

⁸Plummer, H.C.; "An introductory Treatise on Dynamical Astronomy", Dover, New York, 1960.

⁹Tiserrand, F.; "Traité de Mécanique Céleste", Gauthier-Villars (reedition), Paris, 1960.

¹⁰Brouwer, D. and G. M. Clemence, "Methods of Celestial Mechanics", New York, Academic Press, 1961.

¹¹Giacaglia, G.E.O.; "The Equations of Motion of an Artificial Satellite in Non Singular Variables" AMRL 1072, Appl. Mech Res. Lab, The Univ. of Texas, Austin, 1975

¹²Canesin S.,W; "Analytical Nonsingular Theory for Geopotential Perturbations Including Resonance Effects", DFVLR -FB 82-28.

¹³De lima Jr. P.H.C.N.; MSc. Thesis, USP - Universidade de São Paulo, São Paulo, Brasil, 1988

¹⁴Grosso, P.R.; MSc. Thesis, ITA - Instituto Tecnológico da Aeronáutica, São José dos Campos, Brasil, 1989

APPLICATIONS OF GENERALIZED CANONICAL SYSTEMS IN THE STUDY OF OPTIMAL SPACE TRAJECTORIES

Sandro da Silva Fernandes
Departamento de Mecânica do Vôo e Orbital
Instituto Tecnológico de Aeronáutica
12228-900, São José dos Campos, SP, Brazil

Abstract

Some properties of "generalized canonical systems" - dynamical systems governed by a Hamiltonian function linear in the momenta - are applied in the study of optimal space trajectories. Using these properties, a systematical integration of the dynamical system governing the coast-arc is performed. The evolution of the "primer" vector along a coast arc is derived for circular, elliptical, parabolic and hyperbolic motions in Newtonian central field, and also for quasi-circular nonequatorial motion in a noncentral gravity field.

Key words: Generalized canonical systems, optimal space trajectories.

Introduction

The coast-arc problem characterizing the optimal space trajectories of a constant exhaust velocity rocket with bounded or unbounded thrust magnitude is described by a special class of dynamical systems called "generalized canonical systems"¹. These systems are governed by a Hamiltonian function linear in the momenta (adjoint variables in optimal control theory) and have intrinsic properties defined by the general solution of the system governed by any integrable part (if exist) of the Hamiltonian function. A family of Mathieu transformations is defined between the variables of the system and the arbitrary parameters of the general solution of the integrable part and, also, between two different sets of arbitrary parameters of integration (Appendix). Using such properties, a systematical integration of the canonical system governing the coast-arc is performed. The evolution of the "primer" vector along a coast-arc in Newtonian central field is derived for circular, elliptical, parabolic and hyperbolic motions. Some new relations between Lawden's constants and sets of orbital elements are presented. A

particular set of nonsingular orbital elements is used and a new expression for the "primer" vector, valid for any orbit with $e < 1$ and $I \neq \pi$ is derived. The generalized Hamiltonian formulation presented in the paper permits to study perturbative effects of additional forces (drag perturbations, oblateness of the central body, ...) by means of the canonical methods of Celestial Mechanics, in particular the ones based on Lie series or transforms^{2,3}.

The "primer" vector along a coast-arc in Newtonian central field

The evolution of the "primer" vector p_v (adjoint to the velocity vector) along a coast-arc in Newtonian central field is described by the Hamiltonian function H given by⁴

$$H = p_r \cdot v - \frac{\mu}{r^3} p_v \cdot r, \quad (1)$$

where r is the position vector, v is the velocity vector, p_r is the adjoint to r and μ is the gravitational parameter (Gaussian constant). Dot denotes the scalar vector product.

The general solution of the dynamical system governed by the Hamiltonian function H was derived in⁵ using some properties of "generalized canonical systems" and, for elliptical motion, is given by

$$r = a(1 - e \cos E) r, \quad (2)$$

$$v = \sqrt{\frac{\mu}{a(1-e^2)}} [e \sin \nu r + (1 + e \cos \nu) s], \quad (3)$$

$$p_r = \frac{a}{r^2} \left\{ 2a p_a + (1 - e^2) \cos E p_e + \left(\frac{r}{a}\right) \frac{\sin \nu}{e} p_w \right. \\ \left. - \frac{(1 - e^3 \cos E)}{e\sqrt{1 - e^2}} \left(\frac{r}{a}\right) \sin \nu p_M \right\} r + \left\{ \frac{\sin \nu}{a} p_e \right.$$

$$\left. -\frac{(\cos \nu + e)}{ae(1-e^2)} p_\omega + \frac{\sqrt{1-e^2}}{ae} \cos \nu p_M \right\} s$$

$$+ \frac{1}{r\sqrt{1-e^2}} \left\{ \sin E \left[\cos \omega p_I + \sin \omega \left(\frac{p_\Omega}{\sin I} - \cot I p_\omega \right) \right] \right.$$

$$\left. + \sqrt{1-e^2} \cos E \left[\sin \omega p_I - \cos \omega \left(\frac{p_\Omega}{\sin I} - \cot I p_\omega \right) \right] \right\} w, \quad (4)$$

$$p_v = \frac{1}{na\sqrt{1-e^2}} \left\{ \left\{ 2ae \sin \nu p_a - (1-e^2) \sin \nu p_e \right. \right.$$

$$\left. - \frac{(1-e^2)}{e} \cos \nu p_\omega + \frac{(1-e^2)^{3/2}}{e} \left(\frac{-2e}{1+e \cos \nu} \right. \right.$$

$$\left. \left. + \cos \nu \right) p_M \right\} r + \left\{ 2a(1-e^2) \left(\frac{a}{r} \right) p_a \right.$$

$$\left. + (1-e^2)(\cos E + \cos \nu) p_e + \frac{(1-e^2)}{e} \left(1 + \frac{1}{1+e \cos \nu} \right) \right.$$

$$\left. x \sin \nu \left(p_\omega - \sqrt{1-e^2} p_M \right) \right\} s$$

$$+ \left\{ \left(\frac{r}{a} \right) \cos(\omega + \nu) p_I \right.$$

$$\left. + \left(\frac{r}{a} \right) \sin(\omega + \nu) \left(\frac{p_\Omega}{\sin I} - \cot I p_\omega \right) \right\} w, \quad (5)$$

with,

$$M = E - e \sin E, \quad (6)$$

$$\tan \frac{\nu}{2} = \sqrt{\frac{1+e}{1-e}} \tan \frac{E}{2}, \quad (7)$$

where r, s, w are the unit vectors of the moving frame of reference along the radial, circumferential and normal directions, respectively; a, e, I, Ω, ω and M are the well-known Keplerian elements; $p_a, p_e, p_I, p_\Omega, p_\omega$ and p_M are the adjoint variables; ν is the true anomaly; E is the eccentric anomaly; n is the mean motion and $(r/a), (r/a) \sin \nu, \dots$ etc are known functions of the elliptical motion.

For hyperbolic motion, the general solution of the dynamical system governed by the Hamiltonian function H is very similar to the one for elliptical motion. Since the semi-major axis is negative, it should be replaced by $-a$ in equations (2)-(5). The mean motion n should be replaced by $n_H = [\mu(-a)^{-3}]^{1/2}$ and $r = a(1 - e \cosh F)$, being F the hyperbolic eccentric anomaly. Also $(1 - e^2)$ should be replaced by $(e^2 - 1)$.

For parabolic motion, the eccentricity must be taken as a constraint on the state variables (generalized coordinates) of the canonical system, i.e.

$$e(\mathbf{r}, \mathbf{v}) = 1. \quad (8)$$

Beside this, the semi-major axis becomes infinite and semi-latus rectum p should be used. Using the properties of generalized canonical systems with constraints on the coordinates one gets the general solution of the

dynamical system governed by H and subject to the constraint (8),

$$\mathbf{r} = \frac{p}{1 + \cos \nu} \mathbf{r}, \quad (9)$$

$$\mathbf{v} = \sqrt{\frac{\mu}{p}} (\sin \nu \mathbf{r} + (1 + \cos \nu) \mathbf{s}), \quad (10)$$

$$Pr = \left\{ \frac{2p}{r} p_p + \frac{\sin \nu}{r} p_\omega \right.$$

$$\left. - \left[\frac{3S}{r} - \frac{2r \sin \nu}{\sqrt{p}} - \frac{4\sqrt{\mu} p}{r^2} J \right] p_S \right\} r$$

$$+ \left\{ -2 \sin \nu p_p - \frac{1}{r} p_\omega + \left[\frac{-3S \sin \nu}{p} + \frac{4r}{\sqrt{p}} \right] p_S \right\} s$$

$$+ \left\{ \frac{1}{p} (\sin u + \sin \omega) p_I \right.$$

$$\left. - \frac{1}{p} (\cos u + \cos \omega) \left(\frac{p_\Omega}{\sin I} - \cot I p_\omega \right) \right\} w, \quad (11)$$

$$Pv = \left\{ -\sqrt{\frac{p}{\mu}} \cos \nu p_\omega + [-4\sqrt{p} J \sin \nu \right.$$

$$\left. + \frac{2 \cos \nu}{\sqrt{\mu}} r^2 \right] p_S \right\} r + \sqrt{\frac{p}{\mu}} \left\{ 2r p_p + \sin \nu \left(1 - \frac{r}{p} \right) p_\omega \right.$$

$$\left. + \left[\frac{3Sr}{p} - \frac{4\sqrt{\mu} p}{r} - \frac{2r^3 \sin \nu}{\sqrt{p^3}} (2 + \cos \nu) \right] p_S \right\} s$$

$$+ \frac{r}{\sqrt{\mu} p} \left\{ \cos u p_I + \sin u \left(\frac{p_\Omega}{\sin I} - \cot I p_\omega \right) \right\} w, \quad (12)$$

where S is the fast angular variable,

$$S = 2\sqrt{\mu}(t - \tau), \quad (13)$$

$u = \omega + \nu$, and J is defined by

$$J = \frac{1}{4\sqrt{\mu}} \left[S - \frac{D^3}{3} - \frac{D^5}{5p} \right], \quad (14)$$

being $D = \sqrt{p} \tan \nu/2$ the parabolic eccentric anomaly and τ the time of pericenter passage.

The general solution of the dynamical system governed by the Hamiltonian H , presented in the preceding paragraphs for elliptical, parabolic and hyperbolic motions, defines in each case a time independent Mathieu transformation between the Cartesian elements and the orbital ones, with respect to which the Hamiltonian function H is invariant. The new Hamiltonian function H' resulting from the Mathieu transformations is, in each case, given by

$$H' = n p_M, \text{ for } e < 1, \quad (15)$$

$$H' = n_H p_{M_H}, \text{ for } e > 1, \quad (16)$$

$$H' = 2\sqrt{\mu} p_S, \text{ for } e = 1. \quad (17)$$

Here, p_{M_H} is the adjoint variable to the fast angular variable M_H , similar to the mean anomaly in the elliptical motion.

The general solution of the new dynamical system is very simple and, for elliptical motion, is given by

$$\begin{aligned} a &= a_0 & p_a &= p_{a_0} + \frac{3M}{2a} p_{M_0} \\ e &= e_0 & p_e &= p_{e_0} \\ I &= I_0 & p_I &= p_{I_0} \\ \Omega &= \Omega_0 & p_\Omega &= p_{\Omega_0} \\ \omega &= \omega_0 & p_\omega &= p_{\omega_0} \\ M &= n(t - \tau) & p_M &= p_{M_0} \end{aligned} \quad (18)$$

The subscript "0" denotes the constants of integration. For hyperbolic motion the solution is exactly the same with n, p_M and M replaced by n_H, p_{M_H} and M_H , respectively. For parabolic motion, S is given by Eqn (13) and the other variables are constant.

Consequently, from Eqns (5), (12), (13) and (18), one gets the evolution of the "primer" vector along a coast-arc in Newtonian central field. Introducing the Lawden's constants A, B, C, D, \mathcal{E} and \mathcal{F} , and the functions I_1 and I_2 , the "primer" vector can be written as⁵

$$\begin{aligned} p\mathbf{v} &= (A \cos \nu + B e \sin \nu + C I_1) \mathbf{r} \\ &+ \left(-A \sin \nu + B(1 + e \cos \nu) + \frac{D - A \sin \nu}{(1 + e \cos \nu)} + C I_2 \right) \mathbf{s} \\ &+ \left(\frac{\mathcal{E} \cos \nu + \mathcal{F} \sin \nu}{1 + e \cos \nu} \right) \mathbf{w}. \end{aligned} \quad (19)$$

For elliptical motion,

$$A = -\frac{\sqrt{1-e^2}}{nae} p_\omega, \quad (20)$$

$$B = \frac{1}{nae} \left[\frac{2ae}{\sqrt{1-e^2}} p_a + \sqrt{1-e^2} p_e \right], \quad (21)$$

$$C = -\frac{(1-e^2)^2}{nae} p_M, \quad (22)$$

$$D = -\frac{(1-e^2)^{3/2}}{nae} p_e, \quad (23)$$

$$\mathcal{E} = \frac{\sqrt{1-e^2}}{na} \left[\cos \omega p_I + \sin \omega \left(\frac{p_\Omega}{\sin I} - \cot I p_\omega \right) \right], \quad (24)$$

$$\mathcal{F} = \frac{\sqrt{1-e^2}}{na} \left[-\sin \omega p_I + \cos \omega \left(\frac{p_\Omega}{\sin I} - \cot I p_\omega \right) \right], \quad (25)$$

$$I_1 = \frac{1}{(1-e^2)} \left[\frac{2e}{1+e \cos \nu} - \cos \nu - \frac{3e^2 M}{(1-e^2)^{3/2}} \sin \nu \right], \quad (26)$$

$$I_2 = \frac{1}{(1-e^2)} \left[\left(1 + \frac{1}{1+e \cos \nu} \right) \sin \nu - \frac{3eM}{(1-e^2)^{1/2}} \left(\frac{a}{r} \right) \right]. \quad (27)$$

For hyperbolic motion,

$$A = \frac{\sqrt{e^2-1}}{n_H a e} p_\omega, \quad (28)$$

$$B = \frac{1}{n_H a e} \left[\frac{2ae}{\sqrt{e^2-1}} p_a - \sqrt{e^2-1} p_e \right], \quad (29)$$

$$C = \frac{(e^2-1)^2}{n_H a e} p_{M_H}, \quad (30)$$

$$D = -\frac{(e^2-1)^{3/2}}{n_H a e} p_e, \quad (31)$$

$$\mathcal{E} = -\frac{\sqrt{e^2-1}}{n_H a} \left[\cos \omega p_I + \sin \omega \left(\frac{p_\Omega}{\sin I} - \cot I p_\omega \right) \right], \quad (32)$$

$$\mathcal{F} = -\frac{\sqrt{e^2-1}}{n_H a} \left[-\sin \omega p_I + \cos \omega \left(\frac{p_\Omega}{\sin I} - \cot I p_\omega \right) \right], \quad (33)$$

$$I_1 = \frac{1}{(e^2-1)} \left[\frac{2e}{1+e \cos \nu} - \cos \nu - \frac{3e^2 M_H}{(e^2-1)^{3/2}} \sin \nu \right], \quad (34)$$

$$I_2 = \frac{1}{(e^2-1)} \left[\left(1 + \frac{1}{1+e \cos \nu} \right) \sin \nu - \frac{3eM_H}{(e^2-1)^{1/2}} \left(\frac{a}{r} \right) \right]. \quad (35)$$

For parabolic motion,

$$A = -\sqrt{\frac{p}{\mu}} p_\omega, \quad (36)$$

$$B = 0, \quad (37)$$

$$C = \sqrt{\frac{p}{\mu}} p_S, \quad (38)$$

$$D = 2\sqrt{\frac{p^3}{\mu}} p_p, \quad (39)$$

$$I_1 = -4\sqrt{\mu} J \sin \nu + \frac{2r^2 \cos \nu}{\sqrt{p}}, \quad (40)$$

$$I_2 = \frac{3Sr}{p} - 4\sqrt{\mu} J \frac{p}{r} - \frac{2r^3 \sin \nu}{\sqrt{p^3}} (2 + \cos \nu). \quad (41)$$

\mathcal{E} and \mathcal{F} remain the same defined by Eqns (24) and (25), with $\frac{\sqrt{1-e^2}}{na}$ replaced by $\sqrt{\frac{e}{a}}$.

It should be noted that Eqns (4) and (5) are singular for circular and/or equatorial motions. In order to avoid these singularities a set of nonsingular elements must be used. Among several sets of nonsingular elements^{7,8} consider the following one

$$\begin{aligned} a &= \text{semi-major axis} \\ \xi &= e \cos \varpi \\ \eta &= e \sin \varpi \\ P &= \sin \frac{I}{2} \cos \Omega \\ Q &= \sin \frac{I}{2} \sin \Omega \\ L &= \varpi + \nu, \end{aligned} \quad (42)$$

with $\varpi = \omega + \Omega$.

According to Da Silva Fernandes⁸ the adjoint variables to the nonsingular elements are given by

$$\begin{aligned} p_a &= p_a \\ p_\xi &= \left[p_e - \frac{1}{\sqrt{1-e^2}} \left(\frac{r}{a} \right)^2 \sin \nu \left(\frac{a}{r} + \frac{1}{(1-e^2)} \right) \right. \\ &\quad \left. \times p_M \right] \cos \varpi - \frac{1}{e} \left[p_\omega - \frac{1}{\sqrt{1-e^2}} \left(\frac{r}{a} \right)^2 p_M \right] \sin \varpi \\ p_\eta &= \left[p_e - \frac{1}{\sqrt{1-e^2}} \left(\frac{r}{a} \right)^2 \sin \nu \left(\frac{a}{r} + \frac{1}{(1-e^2)} \right) \right. \\ &\quad \left. \times p_M \right] \sin \varpi + \frac{1}{e} \left[p_\omega - \frac{1}{\sqrt{1-e^2}} \left(\frac{r}{a} \right)^2 p_M \right] \cos \varpi \\ p_P &= \frac{2 \cos \Omega}{\cos \frac{I}{2}} p_I - \frac{\sin \Omega}{\sin \frac{I}{2}} (p_\Omega - p_\omega) \\ p_Q &= \frac{2 \sin \Omega}{\cos \frac{I}{2}} p_I + \frac{\cos \Omega}{\sin \frac{I}{2}} (p_\Omega - p_\omega) \\ p_L &= \frac{1}{\sqrt{1-e^2}} \left(\frac{r}{a} \right)^2 p_M. \end{aligned} \quad (43)$$

The new Hamiltonian function resulting from the canonical transformation defined by Eqns (42)-(43) is given by

$$H'' = ns \left(\frac{a}{r} \right)^2 p_L, \quad (44)$$

with

$$s^2 = 1 - \xi^2 - \eta^2, \quad (45)$$

$$\left(\frac{r}{a} \right) = \frac{1 - \xi^2 - \eta^2}{1 + \xi \cos L + \eta \sin L}. \quad (46)$$

Combining Eqns (5), (42) and (43), and introducing the solution of the new dynamical system governed by

the Hamiltonian function H'' , one gets a new expression for the "primer" vector, valid for $e < 1$ and $I \neq \pi$,

$$\begin{aligned} p\mathbf{v} &= (J \cos L + K \sin L + \mathcal{L}I_3) \mathbf{r} \\ &+ (-J \sin L + K \cos L + [\xi K - \eta J - (\xi^2 + \eta^2)\mathcal{M} \\ &\quad + (K - \xi\mathcal{M}) \cos L - (J + \eta\mathcal{M}) \sin L] \\ &\quad \times (1 + \xi \cos L + \eta \sin L)^{-1} + \mathcal{M} + \mathcal{L}I_4) \mathbf{s} \\ &- s^2 (1 - \xi \cos L + \eta \sin L)^{-1} ((P\mathcal{L}I_5 + \mathcal{N}) \sin L \\ &\quad + (-Q\mathcal{L}I_5 + \mathcal{O}) \cos L) \mathbf{w}, \end{aligned} \quad (47)$$

where

$$J = \frac{1}{nas} (-2a\eta p_a - s^2 p_\eta), \quad (48)$$

$$K = \frac{1}{nas} (2a\xi p_a + s^2 p_\xi), \quad (49)$$

$$\mathcal{L} = \frac{1}{nas} p_L, \quad (50)$$

$$\mathcal{M} = \frac{2}{ns} p_a, \quad (51)$$

$$\begin{aligned} \mathcal{N} &= \frac{u}{nas} \left\{ (-\eta p_\xi + \xi p_\eta) P + \frac{1}{2} [-PQ p_P \right. \\ &\quad \left. - (1 - Q^2) p_Q] \right\}, \end{aligned} \quad (52)$$

$$\begin{aligned} \mathcal{O} &= \frac{u}{nas} \left\{ -(-\eta p_\xi + \xi p_\eta) Q + \frac{1}{2} [-PQ p_Q \right. \\ &\quad \left. + (1 - P^2) p_P] \right\}, \end{aligned} \quad (53)$$

$$\begin{aligned} I_3 &= 3n(t - \tau)(\xi \sin L - \eta \cos L) \sqrt{\frac{1 + (1 - s^2)^{1/2}}{(1 - (1 - s^2)^{1/2})^3}} \\ &+ s^2 C(H \sin L - I \cos L), \end{aligned} \quad (54)$$

$$\begin{aligned} I_4 &= 3n(t - \tau)(1 + \xi \cos L + \eta \sin L) \sqrt{\frac{1 + (1 - s^2)^{1/2}}{(1 - (1 - s^2)^{1/2})^3}} \\ &+ \frac{s^2 C(FH + GI)}{(1 + \xi \cos L + \eta \sin L)}, \end{aligned} \quad (55)$$

$$\begin{aligned} I_5 &= \left(\frac{1 + (1 - s^2)^{1/2}}{1 + \xi \cos L + \eta \sin L} \right)^2 + [-(\xi^2 + \eta^2)^{1/2} D \\ &+ E(\eta \sin L + \xi \cos L - (\xi^2 + \eta^2) \cos(L - L_0))], \end{aligned} \quad (56)$$

with

$$C(L) = \left[(1 + \xi \cos L + \eta \sin L) \left(1 - (1 - s^2)^{1/2} \right) \right]^{-1}, \quad (57)$$

$$D = 2 - (\xi^2 + \eta^2)^{1/2} - (\xi^2 + \eta^2), \quad (58)$$

$$E(L) = 2 + \xi \cos L + \eta \sin L, \quad (59)$$

$$F(L) = \frac{3}{2}\xi + 2 \cos L + \frac{1}{2}\xi \cos 2L + \frac{1}{2}\eta \sin 2L, \quad (60)$$

$$G(L) = \frac{3}{2}\eta + 2 \sin L + \frac{1}{2}\xi \sin 2L - \frac{1}{2}\eta \cos 2L, \quad (61)$$

$$H(L) = D \sin L_0 - E (\sin L + \xi \sin(L - L_0) - \eta \cos(L - L_0)), \quad (62)$$

$$I(L) = -D \cos L_0 + E (\cos L - \xi \cos(L - L_0) - \eta \sin(L - L_0)), \quad (63)$$

$$u^{-2} = 1 - P^2 - Q^2. \quad (64)$$

In equations above $a, \xi, \eta, P, Q, L_0, p_a, p_\xi, p_\eta, p_P, p_Q, p_L$ are constants of integration.

The "primer" vector along a coast-arc in a noncentral gravity field

The generalized canonical formulation presented in the preceding section permits to study perturbative effects of additional forces - drag, oblateness of the central body, ... etc - by means of the canonical perturbation methods of Celestial Mechanics, in particular the ones based on Lie series or transforms ^{2,3}.

Consider the problem of determining the evolution of the "primer" vector along a coast-arc in a noncentral gravity field generated by an ellipsoid.

In this case the Hamiltonian function describing the evolution of the "primer" vector is given by

$$H = \mathbf{p_r} \cdot \mathbf{v} - \frac{\mu}{r^3} \mathbf{p_v} \cdot \mathbf{r} + \mathbf{p_v} \cdot \left(\frac{\partial V_2}{\partial \mathbf{r}} \right)^T, \quad (65)$$

being V_2 the disturbing force function

$$V_2 = -\mu a_e^2 \frac{J_2}{r^3} P_2(\sin \varphi), \quad (66)$$

where a_e is the mean equatorial radius, J_2 is the coefficient for the second zonal harmonic of the potential,

φ is the latitude and P_2 is the Legendre polynomial of second order. The Hamiltonian H can be written as

$$H = H_0 + H_{J_2}, \quad (67)$$

with

$$H_0 = \mathbf{p_r} \cdot \mathbf{v} - \frac{\mu}{r^3} \mathbf{p_v} \cdot \mathbf{r}, \quad (68)$$

$$H_{J_2} = \mathbf{p_v} \cdot \left(\frac{\partial V_2}{\partial \mathbf{r}} \right)^T. \quad (69)$$

Here H_0 is the undisturbed Hamiltonian (describes the motion in Newtonian central field) and H_{J_2} is the disturbing function concerning the asphericity (oblateness) of the central body.

The general solution of the dynamical system governed by the undisturbed Hamiltonian function is given by Eqns (2)-(7) and defines a Mathieu transformation between the Cartesian elements and the orbital ones,

$$(\mathbf{p_r}, \mathbf{p_v}; \mathbf{r}, \mathbf{v})^{\text{MATHIEU}} (p_a, \dots, p_M; a, \dots, M).$$

For simplicity, only nonequatorial quasi-circular orbits will be considered. Consequently a set of nonsingular orbital elements must be used. Consider the following one

a - semi-major axis

$$h = e \cos \omega$$

$$k = e \sin \omega$$

I - inclination of the orbital plane

Ω - longitude of the ascending node

$$l = M + \omega, \quad (70)$$

whose adjoint variables are

$$p_a = p_a$$

$$p_h = p_e \cos \omega - \left(\frac{p_\omega - p_M}{e} \right) \sin \omega$$

$$p_k = p_e \sin \omega + \left(\frac{p_\omega - p_M}{e} \right) \cos \omega$$

$$p_I = p_I$$

$$p_\Omega = p_\Omega$$

$$p_l = p_M. \quad (71)$$

Two canonical transformations are defined by Eqns (2)-(7) and (70)-(71). The Hamiltonian function \mathcal{H} resulting from these transformations is given by

$$\mathcal{H} = np_l + n\varepsilon \left\{ -2a \sin^2 I \sin 2l p_a + \left[-\sin l + \frac{1}{4} \sin^2 I (5 \sin l - 7 \sin 3l) \right] p_h \right\}$$

$$\begin{aligned}
& + \left[\cos l + \frac{1}{4} \sin^2 l (-7 \cos l + 7 \cos 3l) \right] p_k \\
& - \frac{1}{2} \sin 2l \sin 2l p_l + (\cos 2l - 1) \cos l p_\Omega \\
& \left[4 \sin^2 l (\cos 2l - 1) + (3 - \cos 2l) \right] p_l \}, \quad (72)
\end{aligned}$$

where $\varepsilon = \frac{3}{2} J_2 \left(\frac{a_e}{a} \right)^2$.

A first order analytical solution of the dynamical system governed by the Hamiltonian function \mathcal{H} is obtained by applying Hori's method². So, the evolution of the "primer" vector along a coast-arc in a noncentral gravity field for nonequatorial quasi-circular orbits is given by

$$\begin{aligned}
p\mathbf{v} &= \frac{1}{na} \{ \{-2p_l + p_h \sin l - p_k \cos l\} r \\
& + \{2ap_a + 3n\tau p_l + 2p_h \cos l + 2p_k \sin l\} s \\
& + \left\{ p_l \cos l + \left(\frac{p_\Omega}{\sin l} - \cot l p_l \right) \sin l \right\} w \}. \quad (73)
\end{aligned}$$

The orbital elements and the adjoint variables are obtained from the transformation equations of Hori's method. At first order solution

$$\begin{aligned}
x &= x^* + \frac{\partial S}{\partial p_x^*} \\
p_x &= p_x^* - \frac{\partial S}{\partial x^*}, \quad (74)
\end{aligned}$$

where x denotes the orbital elements, p_x is the adjoint variable, and the star '*' denotes the mean orbital elements whose equations of motion are governed by the Hamiltonian function \mathcal{H}^* ,

$$\begin{aligned}
\mathcal{H}^* &= n^* p_l^* + \frac{3}{2} n^* J_2 \left(\frac{a_e}{a^*} \right)^2 \{ -\cos l^* p_\Omega^* \\
& - (1 - 4 \cos^2 l^*) p_l^* \}, \quad (75)
\end{aligned}$$

and S is the generating function

$$\begin{aligned}
S &= \frac{3}{2} J_2 \left(\frac{a_e}{a^*} \right)^2 \left\{ \left[\frac{1}{2} \sin^2 l^* \cos 2l^* \right] 2a^* p_a^* \right. \\
& + \left[\cos l^* + \frac{1}{2} \sin^2 l^* \left(-\frac{5}{2} \cos l^* + \frac{7}{6} \cos 3l^* \right) \right] p_k^* \\
& + \left[\sin l^* + \frac{1}{2} \sin^2 l^* \left(-\frac{7}{2} \sin l^* + \frac{7}{6} \sin 3l^* \right) \right] p_k^* \\
& + \left[\frac{1}{4} \sin 2l^* \cos 2l^* \right] p_l^* + \left[\frac{1}{2} \cos l^* \sin 2l^* \right] p_\Omega^* \\
& \left. \left[\frac{1}{4} (3 - 5 \cos^2 l^*) \sin 2l^* \right] p_l^* \right\}. \quad (76)
\end{aligned}$$

Conclusion

The coast-arc problem was solved using a Hamiltonian formalism based on some properties of "generalized canonical system". The evolution of the "primer" vector along a coast-arc was derived for circular, elliptical, parabolic and hyperbolic motions in Newtonian central field and for nonequatorial quasi-circular motion in a noncentral gravity field.

References

- Da Silva Fernandes, S.: Generalized canonical systems. I - General properties. em *Acta Astronautica* (accepted for publication).
- Hori, G.: Theory of general perturbations with unspecified canonical variables. *Publ. Astron. Soc. Japan* 18, p.287-295, 1966.
- Deprit, A.: Canonical transformations depending on a small parameter. *Celest. Mech.* 1, p.12-30, 1969.
- Marec, J.-P.: *Optimal space trajectories*. Elsevier, New York, 1979.
- Da Silva Fernandes, S.: Generalized canonical systems. II - Derivation of Lagrange's and Gauss' equations. *Acta Astronautica* (accepted for publication).
- Da Silva Fernandes, S.: Generalized canonical systems. III - Space dynamics applications: solution of the coast-arc problem. *Acta Astronautica* (accepted for publication).
- Giacaglia, G.E.O.: The equations of motion of an artificial satellite in nonsingular variables. *Celest. Mech.* 15, p.191-215, 1977.
- Roth, E.A.: The Gaussian form of the variational of parameter equations formulated in equinoctial elements - applications: air drag and radiation pressure. *Acta Astronautica* 12, p.719-730, 1985.

Appendix

Some properties of "generalized canonical systems" are briefly presented in this appendix, for more details see reference¹.

Consider the autonomous "generalized canonical system",

$$\begin{aligned}
\frac{d\mathbf{x}}{dt} &= \mathbf{F}(\mathbf{x}) \\
\frac{d\lambda}{dt} &= - \left[\frac{\partial \mathbf{F}(\mathbf{x})}{\partial \mathbf{x}} \right]^T \lambda, \quad (A.1)
\end{aligned}$$

governed by the Hamiltonian function H ,

$$H = \lambda \cdot \mathbf{F}(\mathbf{x}), \quad (A.2)$$

where $\mathbf{x} = [x_1 \dots x_n]^T$ is a $n \times 1$ vector of coordinates (state variables), $\lambda = [\lambda_1 \dots \lambda_n]^T$ is a $n \times 1$ vector of momenta (adjoint variables), $\mathbf{F} = [F_1 \dots F_n]^T$ is a $n \times 1$

vector of functions of the coordinates. Dot denotes the scalar vector product and T denotes the transposition. The Hamiltonian function H is separable into two parts,

$$H = H_0 + R, \quad (A.3)$$

where

$$H_0 = \lambda \cdot \mathbf{f}(\mathbf{x}), \quad (A.4)$$

governs an integrable dynamical system, and

$$R = \lambda \cdot \mathbf{g}(\mathbf{x}), \quad (A.5)$$

is the remaining part.

The general solution of the dynamical system governed by H_0 is, in the case of periodic solution, given by

$$\begin{aligned} \mathbf{x} &= \Psi(c_1, \dots, c_{n-1}, \theta) \\ \lambda &= (\Delta_\Psi^{-1})^T \mathbf{b}, \end{aligned} \quad (A.6)$$

where Δ_Ψ is the Jacobian matrix defined by

$$\Delta_\Psi = \left[\frac{\partial \mathbf{x}}{\partial \mathbf{c}} \right], \quad (A.7)$$

with $\mathbf{c} = [c_1 \dots c_{n-1} \theta]^T$, c_1, \dots, c_{n-1} are arbitrary constants of integration, θ is the fast phase depending on the frequency $\omega(c_1)$ and \mathbf{b} is a $n \times 1$ vector involving n arbitrary constants of integration and the fast phase θ . If another set of arbitrary constants of integration and phase is used for describing this general solution then there exists the following relation connecting two sets of arbitrary parameters,

$$\begin{aligned} [C_1 \dots C_{n-1} \Theta]^T &= C(c_1, \dots, c_{n-1}, \theta) \\ \mathbf{B} &= (\Delta_C^{-1})^T \mathbf{b}, \end{aligned} \quad (A.8)$$

where C_1, \dots, C_{n-1} , Θ and \mathbf{B} are the new arbitrary parameters of integration.

Therefore, the following results can be stated:

- i- A time independent Mathieu transformation is defined by Eq.(A.6) between the variables of the system and the arbitrary parameters of integration.
- ii- A time independent Mathieu transformation is defined by Eq.(A.8) between two different sets of arbitrary parameters of integration;
- iii- The Hamiltonian function H is invariant with respect to these transformations.

Similar results can be obtained for systems involving time-independent constraints on the coordinates.

SPACE DYNAMICS II

ORBITAL ANALYTICAL MODEL
FOR GEOSYNCHRONOUS SATELLITE

1. Campan, G. and Brousse, P. (CNES-France):
"ORANGE - Orbital Analytical Model for Geosynchronous Satellite" 561
2. Andrade, E.P. and Andrade, J.R.C. (EMBRATEL-Brazil):
"Mission Designs for Satellites Injected into Storage Orbit" 573
3. Fitz-Coy, N. and Chatterjee, A. (University of Florida-USA):
"On Stability of Satellite Capture" 577
4. Giacaglia, G.E.O. (University of São Paulo-Brazil):
"Long-Period Perturbations in the Inclination of Sun-Synchronous Satellites" 583
5. Nan, Y.; Chen, S. and Lu, X. (Northwestern Polytechnical University-China):
"The Determination of Navigation Information for Space Vehicle by GPS (or INS)/Equations of Motions" 590

ORANGE ORBITAL ANALYTICAL MODEL FOR GEOSYNCHRONOUS SATELLITE

Genevieve CAMPAN
Pascal BROUSSE
CNES, Toulouse, France

Abstract

ORANGE semi-analytical model is an approximate representation of the centered orbital parameters evolution of a geosynchronous orbit built with the symbolic computation tool MAPLE. The centered orbital parameters correspond to geostationary orbit adapted parameters from which short term variations are removed and daily average is computed to remove small amplitude variations.

The method we have applied consists in expanding the perturbation functions in adapted orbit parameters and incorporating these developments into the Lagrange equations. All the computations are done with the symbolic computation tool MAPLE what considerably decreases the risk of error and then, also allows to develop the equation to a higher order. The targeted accuracy is after 30 days of extrapolation, 10 meters on the semi-major axis, 10^{-5} on the eccentricity, 10^{-3} degrees on the inclination and 10^{-3} degrees for the mean longitude. This accuracy is got in a validity domain such as the semi-major axis is closer than 500 km from the geosynchronous one, the eccentricity is lower than 0.01 and the inclination 5 deg, what represents a wide window around a geostationary position.

Key words: Geosynchronous, Analytical Model, Symbolic Computation.

1. Presentation

ORANGE semi-analytical model is an approximate representation of the evolution of the orbit parameters of a geosynchronous satellite.

1.1. Parameters involved

Instead of the conventional keplerian parameters, not really adequate to figure almost circular and equatorial orbits the following parameters are used:

- semi-major axis a

- eccentricity vector
$$\begin{aligned} e_x &= e \cos \omega + \Omega \\ e_y &= e \sin \omega + \Omega \end{aligned}$$

where e is the eccentricity
 ω is the argument of perigee
 Ω is the right ascension of the ascending node

- inclination vector
$$\begin{aligned} i_x &= \sin i \cos \Omega \\ i_y &= \sin i \sin \Omega \end{aligned}$$

where i is the inclination

- mean longitude
$$lm = \omega + \Omega + M - \theta$$

where M is the mean anomaly and θ is the sidereal time.

Nota : lm has not to be confused with the right ascension of the satellite $\alpha = \omega + \Omega + M$. In one revolution, α varies from 0 to 360 deg and lm varies around the station longitude ls .

Moreover, these parameters are centered, that is to say short term variations are removed and a daily average is calculated to remove small amplitude variations. The use of the centered parameters allows to simplify the algorithms since the instantaneous effect of the short period terms, having not to be considered in the design of the corrections, is already removed from the parameters.

1.2. Force model

We took the three main following sources for geostationary orbit perturbations:

- unhomogeneity and not sphericity of the Earth. The used Earth potential model is the GEM10 model, the maximal degree of zonal and tesseral terms is 4;
- the lunar and solar attraction;
- the solar radiation pressure. This force is considered as deriving from a pseudo-potential since we neglected the shadow passages.

1.3. Evolution equations

The used equations are derived from Lagrange equations through adapted parameters.

The original equation are:

$$\begin{aligned} \frac{da}{dt} &= \frac{2}{na} \frac{\partial R}{\partial M} & \text{[eq 1]} \\ \frac{de}{dt} &= \frac{1-e^2}{na^2 e} \frac{\partial R}{\partial M} - \frac{(1-e^2)^{1/2}}{na^2 e} \frac{\partial R}{\partial \omega} \\ \frac{di}{dt} &= -\frac{1}{na^2 (1-e^2)^{1/2} \sin i} \frac{\partial R}{\partial \Omega} + \frac{\cos i}{na^2 (1-e^2)^{1/2} \sin i} \frac{\partial R}{\partial \omega} \\ \frac{d\Omega}{dt} &= \frac{\cos i}{na^2 (1-e^2)^{1/2} \sin i} \frac{\partial R}{\partial i} \\ \frac{d\omega}{dt} &= \frac{(1-e^2)^{1/2}}{na^2 e} \frac{\partial R}{\partial e} - \frac{\cos i}{na^2 (1-e^2)^{1/2} \sin i} \frac{\partial R}{\partial i} \\ \frac{dM}{dt} &= n - \frac{2}{na} \frac{\partial R}{\partial a} - \frac{1-e^2}{na^2 e} \frac{\partial R}{\partial e} \end{aligned}$$

After some derivative computations we obtained with adapted parameters:

$$\begin{aligned} \frac{da}{dt} &= \frac{2}{na} \frac{\partial R}{\partial M} & \text{[eq 2]} \\ \frac{dex}{dt} &= \frac{-\sqrt{1-e^2}}{na^2} \frac{\partial R}{\partial ey} - \frac{ey(1-tg^2 i / 2)}{2na^2 \sqrt{1-e^2}} \left[hx \frac{\partial R}{\partial hx} + hy \frac{\partial R}{\partial hy} \right] \\ &\quad - \frac{ex \sqrt{1-e^2}}{na^2 [1+\sqrt{1-e^2}]} \frac{\partial R}{\partial lm} \\ \frac{dey}{dt} &= \frac{\sqrt{1-e^2}}{na^2} \frac{\partial R}{\partial ex} + \frac{ex(1-tg^2 i / 2)}{2na^2 \sqrt{1-e^2}} \left[hx \frac{\partial R}{\partial hx} + hy \frac{\partial R}{\partial hy} \right] \\ &\quad - \frac{ey \sqrt{1-e^2}}{na^2 [1+\sqrt{1-e^2}]} \frac{\partial R}{\partial lm} \\ \frac{dhx}{dt} &= \frac{-\cos i}{na^2 \sqrt{1-e^2}} \frac{\partial R}{\partial hy} + \frac{hx(1-tg^2 i / 2)}{2na^2 \sqrt{1-e^2}} \left[ey \frac{\partial R}{\partial ex} - ex \frac{\partial R}{\partial ey} \right] \\ &\quad - \frac{hx(1-tg^2 i / 2)}{2na^2 \sqrt{1-e^2}} \frac{\partial R}{\partial lm} \end{aligned}$$

$$\frac{dhy}{dt} = \frac{\cos i}{na^2 \sqrt{1-e^2}} \frac{\partial R}{\partial hx} + \frac{hy(1-tg^2 i / 2)}{2na^2 \sqrt{1-e^2}} \left[ey \frac{\partial R}{\partial ex} - ex \frac{\partial R}{\partial ey} \right]$$

$$- \frac{hy(1-tg^2 i / 2)}{2na^2 \sqrt{1-e^2}} \frac{\partial R}{\partial lm}$$

$$\begin{aligned} \frac{dlm}{dt} &= n - \omega_T - \frac{2}{na} \frac{\partial R}{\partial a} + \frac{\sqrt{1-e^2}}{na^2 [1+\sqrt{1-e^2}]} \left[ex \frac{\partial R}{\partial ex} + ey \frac{\partial R}{\partial ey} \right] \\ &\quad + \frac{1-tg^2 i / 2}{2na^2 \sqrt{1-e^2}} \left[hx \frac{\partial R}{\partial hx} + hy \frac{\partial R}{\partial hy} \right] \end{aligned}$$

$\sin i$ can be replaced by $\sqrt{hx^2 + hy^2}$.
 e can be replaced by $\sqrt{ex + ey}$.

We searched to develop evolution equations at order 2 in inclination and 1 in eccentricity (i evolving more quickly than e , it generally is bigger, so an order is added to inclination).

The terms present in the evolution equation are i , i^2 and e .

So as these equations are computed from partial derivative from perturbation potentials with regard to orbital parameters, to establish the expressions of perturbation potential the following terms are consequently kept: i , i^2 , i^3 , e , e^2 , ie , $i^2 e$.

Taking into account this latter point, a simplified form of the equations [eq.2] can be used. As previously said ORANGE model is at order 2 in i and 1 in e so the evolution equation used are the following:

$$\begin{aligned} \frac{da}{dt} &= \frac{2}{na} \frac{\partial R}{\partial M} & \text{[eq 3]} \\ \frac{dex}{dt} &= \frac{-1}{na^2} \frac{\partial R}{\partial ey} - \frac{ex}{2na^2} \frac{\partial R}{\partial M} \\ \frac{dey}{dt} &= \frac{1}{na^2} \frac{\partial R}{\partial ex} - \frac{ey}{2na^2} \frac{\partial R}{\partial M} \\ \frac{dhx}{dt} &= \frac{-\left(1 - \frac{1}{2} \sin^2 i\right)}{na^2} \frac{\partial R}{\partial hy} - \frac{hx}{2na^2} \frac{\partial R}{\partial M} \\ \frac{dhy}{dt} &= \frac{1 - \frac{1}{2} \sin^2 i}{na^2} \frac{\partial R}{\partial hx} - \frac{hy}{2na^2} \frac{\partial R}{\partial M} \end{aligned}$$

$$\frac{d\mathbf{m}}{dt} = \mathbf{n} - \omega_T - \frac{2}{na} \frac{\partial R}{\partial a} + \frac{1}{2na^2} \left[ex \frac{\partial R}{\partial ex} + ey \frac{\partial R}{\partial ey} \right] + \frac{1}{2na^2} \left[hx \frac{\partial R}{\partial hx} + hy \frac{\partial R}{\partial hy} \right]$$

which is more complete than the ones taken in MASQ (order 1 in e and i (ref. 1)).

1.4. MAPLE generalities about ORANGE utilizations

The MAPLE tool is easy to use and very useful for the development of complex equations: it ensures reliable conversions of any equation: if an error slips into the computations, it is due to an error of the user, either in entering the equation or in typing the command. This is appreciable enough when, as in this study, expressions that can be several pages long before simplification are manipulated.

In addition to classical arithmetical operators, a great number of mathematical, algebraical, graphical... functions are in MAPLE library.

In this study, the evolution equations are developed to order 2 in inclination and to order 1 in eccentricity. But one of the ORANGE aim study is to prepare the work to a higher order. When possible, the computations are written so as to they are valid to any orders ni in inclination and ne in eccentricity. For that, functions having ni and ne as parameters were developed and put in library under $-m$ form.

The computations for which it was not possible to automate and write as function of ni and ne were stored in executable files $.ms$.

Considering the length of computation time (for instance the Earth potential development, once the intermediate variables was computed, takes 1 or 2 hours on an ELC sparc station) and the SWAP memory place used for some sessions (for instance 10 Mega for the Moon-Sun potential computation), we did not create a main program allowing to execute the complete ORANGE developments from A to Z. We preferred developments done variable after variable, and stored in different files (executable or functions); the results of each development being stored in files. For each step of the development we begin to read in these files the results of preceding steps. Hence the user has to better know the way the computations take place but it is more interesting than a huge computation able to saturate the SWAP memory of a machine.

2. Expression of the perturbational forces

The total perturbation force is computed at the sum of the three main contributions:

$$R = R_{\text{earth}} + (R_{\text{moon}} + R_{\text{sun}}) + R_{\text{pressure}}$$

All "potentials" are developed at the same order.

2.1. Expression of the Earth potential

We can define the perturbational function as follows:

$$R_{\text{earth}} = \sum_{k=2}^{\infty} \sum_{m=0}^k R_{k,m} (r, \lambda, \varphi)$$

where:

$$R_{k,m} (r, \lambda, \varphi) = \frac{\mu}{r} \left(\frac{R_e}{r} \right)^k P_{k,m} (\sin \varphi) (C_{k,m} \cos m\lambda + S_{k,m} \sin m\lambda)$$

where:

R_e = equatorial radius of the Earth

φ = satellite latitude

λ = satellite longitude

$P_k, P_{k,m}$ = Legendre polynoms and associated function

$C_{k,m}, S_{k,m}$ = harmonic coefficient degree k order m

μ = Earth attraction constant

r = range between Earth center and satellite

To obtain this potential as a function of adapted parameters (to compute partial derivatives in the Lagrange equations second members) we have to explicit r , $\sin \varphi$, λ and Legendre polynoms.

2.2. Expression of lunar and solar attraction

The expression of this perturbational function is given by:

$$R_p = n_p^2 \beta_p a^2 \sum_{k=2}^{\infty} \left(\frac{r}{a} \right)^k \left(\frac{a}{ap} \right)^{k-2} \left(\frac{ap}{rp} \right)^{k+1} P_k (\cos S)$$

where:

P indicates either the Moon or the Sun

r = range between Earth center and satellite

$\cos S$ = cosinus of (Earth-satellite, Earth-perturbator body) angle

$$\beta_p = \frac{m_p}{m_p + m_t}$$

where:

m_t = earth mass

m_p = p mass

a_p = semi-major axis of P orbit

r_p = range between Earth center and P center

n_p = mean motion of P

To obtain this potential as a function of adapted parameters we have to explicit r and $\cos S$.

Nota: The position of Moon and Sun in an inertial reference frame is assumed known at any time T . A call to a CNES library gives corresponding values thanks to a subroutine applying Newton theory for the Sun and Brown theory for the Moon.

2.3. Expression of the solar radiation pressure

As the periods of passing through shadow are neglected we can say that this perturbational force derives from a potential whose expression is given by:

$$R_{\text{pressure}} = -\sigma r \cos S$$

where: $\sigma = C_p \frac{A}{m} P_0$

- with C_p = reflectivity coefficient
- A = effective area
- m = satellite mass
- P_0 = solar pressure per surface unit
- r = range between Earth center and the satellite
- $\cos S$ = cosinus of (Earth-satellite, Earth-Sun) angle

To obtain this pseudo-potential as a function of adapted parameters we have to explicit r and $\cos S$.

2.4. MAPLE developments

As explained just before we have to explicit r , $\sin \phi$, λ , $\cos S$ and P_k , P_{km} .

This needs the development of intermediate variables and functions like the true anomaly v (occurring in many expressions) or unit vector the Earth \rightarrow satellite direction, etc.

All these variables are developed at order 3 in i and 2 in e since the Lagrange equation second members have to be at order 2 in e and 1 in e , hence before partial derivatives any variable is developed at one more order.

To develop, we write for instance:

$$v = M + 2e \sin M + \frac{5}{4} e^2 \sin 2M + O(e^3)$$

$$\cos i = 1 - \frac{1}{2} \sin^2 i + O(i^4)$$

$$v = (v - M) + M$$

$$M = \alpha - (\omega + \Omega)$$

$$r = \frac{a(1-e^2)}{1+e \cos v} = a - ae \cos v - ae^2 + ae^2 \cos^2 v + O(e^3)$$

...

You can see that a major part of the variable changes to do consists in manipulation of sums of trigonometrical terms. However it is not obvious to automatically do that with a symbolic computation tool.

Indeed there are a lot of forms for writing a sum of trigonometrical terms. MAPLE has an internal logical that allows to choose a form among every possible ones but this form is not necessarily the one needed for the variable change. MAPLE has two functions that mainly allow to manipulate trigonometrical forms:

- Expand (x) transforming cosinus (or sinus, tangent,...) of an angle sum into products of simple cosinus. If $x = \cos(a + b)$ is entered, the result of expand (x) is $\cos a \cos b - \sin a \sin b$.
- Combine (x, trig) transforming the products of cosinus (or sinus, tangent,...) into cosinus of an angle sum. "Trig" is an option of the general function "combine". If $x = \cos^2 a$ is entered the result of combine (x) is $\frac{1}{2} \cos 2x + \frac{1}{2}$.

When one of these both functions is applied to an expression, all the terms of the expression undergo the same fate. Nevertheless when a variable exchange is done, the most often time we need to do "expand" on some terms and "combine" on other terms. The expression has to be separated in several expressions to be separately processed or substitutions have to be done in order to prevent MAPLE to consider some terms as trigonometric terms (for instance $\cos(a)$ can be replaced by the simple variable $\cos a$). This is why it is difficult to automate this kind of variable change.

To lighten the manipulations, three main utility functions were written:

a) "Simplif function":

In each development, we were going to simplify the got expressions at either order 3 in i and 2 in e , or 2 in i and 1 in e .

We created the "simplif (ni, ne, expr)" function which simplifies the expression expr at order ni in inclination an ne in eccentricity. This function calls some sub-functions like "Ordre3i2e (expr)" which simplifies at order 3 in i and 2 in e or "Ordre2i1e (expr)" which simplifies at order 2 in i and 1 in e . It is obvious that to carry out simplifications at other orders, other sub-functions OrdreXiYe will have to be added.

These functions use the MAPLE function simplify (expr, eqn). It allows to simplify an expression according to the equation list given in eqn.

Nota 1 : "Simplify" function is used rather the MAPLE "subs (eqn, expr)" function because this latter do substitutions of simple variables in expression expr. It can be substitute 0 to i^n but not to $e^n \times i^m$.

Nota 2 : We have preferred to use several time the "simplify" function with short equation list rather only one time with a big equation list. Indeed, in using a big equation list, MAPLE tool uses a much more important memory place and the computation take more time. It is better to split the equations.

The function "Ordre211e" writes the following terms are nul: ex^2 , ey^2 , $ex.ey$, hx^3 , hy^3 , $ex.hx$, $ex.hy$, $ey.hy$, $hx.hy^2$ and $hx^2.hy$ as well as any higher power.

Likewise the function "ordre3i2e" writes the following terms are nul: ex^3 , ey^3 , hx^4 , hy^4 , $ex^2.ey$, $ex.ey^2$, $ex^2.hx$, $ex^2.hy$, $ey^2.hx$, $ey^2.hy$, $ex.hx^3$, $ex.hy^3$, $ey.hx^3$, $ey.hy^3$, $ex.hx.hy^2$, $ex.hx^2.hy$, $ey.hx^2.hy$, $ex.ey.hx$, $ex.ey.hy$, $hx^2.hy^2$, $hx.hy^3$ and $hx^3.hy$, as well as any higher power.

```
> ordre211e := proc(expr)
  simplification in a polynomial in ex, ey, hx, hy in terms at order higher than 2
  in h and than l in e
> local eqn1,eqn2,eqn3,eqn4,expr1;
> eqn1 := { ex^2=0,ey^2=0,ex*ey=0};
> eqn2 := {hx^3=0,hy^3=0};
> eqn3 := {ex*hx=0,ex*hy=0,ey*hx=0,ey*hy=0};
> eqn4 := {hx^2*hy=0,hx*hy^2=0};
> expr1 := simplify( expr,eqn1 );
> expr1 := simplify( expr1,eqn2 );
> expr1 := simplify( expr1,eqn3 );
> simplify( expr1,eqn4 );
> end;

> ordre3i2e := proc(expr)
  simplification in a polynomial in ex, ey, hx, hy in terms at order higher than 3
  in h and than 2 in e
> eqn1 := {ex^3=0,ey^3=0};
> eqn2 := {hx^4=0,hy^4=0};
> eqn3 := {ex^2*ey=0,ex*ey^2=0};
> eqn4 := {ex^2*hx=0,ex^2*hy=0,ey^2*hx=0,ey^2*hy=0};
> eqn5 := {ex*hx^3=0,ex*hy^3=0,ey*hx^3=0,ey*hy^3=0};
> eqn6 := {ex*hx*hy^2=0,ex*hx^2*hy=0,ey*hx*hy^2=0,ey*hx^2*hy=0};
> eqn7 := {ex*ey*hx=0,ex*ey*hy=0};
> eqn8 := {hx^2*hy^2=0,hx*hy^3=0,hy*hx^3=0};
>
> expr1 := simplify( expr,eqn1);
> expr1 := simplify( expr1,eqn2);
> expr1 := simplify( expr1,eqn3);
> expr1 := simplify( expr1,eqn4);
> expr1 := simplify( expr1,eqn5);
> expr1 := simplify( expr1,eqn6);
> expr1 := simplify( expr1,eqn7);
>
> simplify( expr1,eqn8);
>
> end;

> simplif := proc(ni,ne,expr)
  simplification of a polynomial in ex, ey, hx, hy at order ni in h and ne in e
> if (ni=3 and ne=2) then
  ordre3i2e(expr)
> elif(ni=2 and ne=1) then
  ordre211e(expr)
> else ERROR('la fonction de simplification',ni,ne, 'n existe pas encore')
fi;
> end;
```

b) "Long period" function:

The evolution is only studied for centered orbital parameter, the expressions have to be simplified to remove short period terms. That is to say to average the terms $\cos \alpha$, $\sin \alpha$, $\cos 2\alpha$, $\sin 2\alpha$... where α is the right ascension of the satellite.

The "long period (expr)" function was written stating the terms $\cos i\alpha$ or $\sin i\alpha$ for i going from 1 to 10 are nul in the expression expr.

```
>
  Definition of a function removing short period terms
> longperiod := proc(expr)
> local l,expr1;
> expr1:=expr;
> for l from 1 by 1 to 10 do
>   expr1 := subs(cos(l*alpha)=0,sin(l*alpha)=0,expr1);
> od;
> expr1;
> end;
```

c) "Legendre" function:

In the developments of the perturbarator potentials, Legendre polynoms and associated functions are needed. In a MAPLE package Legendre polynoms can be found they are the "orthopoly [P] (k, x)" functions which give the Legendre Polynom $P_k(x)$.

On the other hand the associated functions do not exist in the MAPLE library. The function "Legendre (K, m, x)" was created, giving the expression of the associated function to the Legendre Polynome $P_k(x)$.

$$P_{km}(x) = (1-x^2)^{m/2} \frac{d^m P_k(x)}{dx^m}$$

If m is within 1 and k and gives the Legendre polynome $P_k(x)$ if m is nul.

```
> legendre:=proc(l,m,x)
  Definition of Legendre associated function
> if (m>1) then ERROR('la fonction de legendre',l,m,'n existe pas') fi;
> if m=0 then
>   orthopoly[P](l,x);
> else
>   (1-x^2)^(m/2)*diff(orthopoly[P](l,x),x$m);
> fi;
  expression of Plm Legendre associated function
> end;
```

The part corresponding to computation of intermediate variables or to preparation of generic function was an important point of the study. An example of writing of an intermediate variable is given just hereafter: it is r the range between Earth center and the satellite. In bold, the MAPLE command is written in italic the result of MAPLE is given.

> r0 := a*(1-e^2)/(1+ecosv);

$$r0 := \frac{a(1-e^2)}{1+ecosv}$$

readin of cos(v-M) and sin(v-M)

> read 'cosAsinA';

$$A := 2e \sin(M) + \frac{5}{4} e^2 \sin(2M)$$

$$\cos A := 1 - 2 \cos(\alpha)^2 e y^2 - 2 \sin(\alpha)^2 e x^2 + 4 \sin(\alpha) \cos(\alpha) e y e x$$

$$\sin A := -2 \cos(\alpha) e y - \frac{5}{4} e y^2 \sin(2\alpha) + \frac{5}{4} e x^2 \sin(2\alpha) + 2 \sin(\alpha) e x - \frac{5}{2} e y e x \cos(2\alpha)$$

Development in serie of 1/(1+ecosv) when ecosv is near 0 at order 6
(default value)

> r1 := series(r0,ecosv=0);

$$r1 := a(1-e^2) + a(-1+e^2)ecosv - a(-1+e^2)ecosv^2 + a(-1+e^2)ecosv^3 - a(-1+e^2)ecosv^4 + a(-1+e^2)ecosv^5 + O(ecosv^6)$$

> r1 := convert(r1,polynomial);

$$r1 := a(1-e^2) + a(-1+e^2)ecosv - a(-1+e^2)ecosv^2 + a(-1+e^2)ecosv^3 - a(-1+e^2)ecosv^4 + a(-1+e^2)ecosv^5$$

ecosv is replaced by its value: e*cos(v)

> r2 := subs(ecosv=e*cos(v),r1);

$$r2 := a(1-e^2) + a(-1+e^2)e \cos(v) - a(-1+e^2)e^2 \cos(v)^2 + a(-1+e^2)e^3 \cos(v)^3 - a(-1+e^2)e^4 \cos(v)^4 + a(-1+e^2)e^5 \cos(v)^5$$

> r2 := expand(r2);

$$r2 := a - a e^2 - a e \cos(v) + a e^3 \cos(v) + a e^2 \cos(v)^2 - a e^4 \cos(v)^2 - a e^3 \cos(v)^3 + a e^5 \cos(v)^3 + a e^4 \cos(v)^4 - a e^6 \cos(v)^4 - a e^5 \cos(v)^5 + a e^2 \cos(v)^5$$

Simplification at order 2 in e

> r3 := simplify(r2,{e^3=0});

$$r3 := a - a e \cos(v) + a(\cos(v)^2 - 1)e^2$$

v is replaced by its value: alpha - A1 - pompgom, A1=v-M, pompgom = omega+Omega

> subs(v=alpha+A1-pompgom,r3);

$$a - a e \cos(\alpha + A1 - pompgom) + a(\cos(\alpha + A1 - pompgom)^2 - 1)e^2$$

> r4 := expand("");

$$\begin{aligned} r4 := & a - a e \cos(\alpha) \cos(A1) \cos(pompgom) - a e \cos(\alpha) \sin(A1) \sin(pompgom) \\ & + a e \sin(\alpha) \sin(A1) \cos(pompgom) - a e \sin(\alpha) \cos(A1) \sin(pompgom) \\ & + a e^2 \cos(\alpha)^2 \cos(A1)^2 \cos(pompgom)^2 \\ & + 2 a e^2 \cos(\alpha)^2 \cos(A1) \cos(pompgom) \sin(A1) \sin(pompgom) \\ & - 2 a e^2 \cos(\alpha) \cos(A1) \cos(pompgom)^2 \sin(\alpha) \sin(A1) \\ & + 2 a e^2 \cos(\alpha) \cos(A1)^2 \cos(pompgom) \sin(\alpha) \sin(pompgom) \\ & + a e^2 \cos(\alpha)^2 \sin(A1)^2 \sin(pompgom)^2 \\ & - 2 a e^2 \cos(\alpha) \sin(A1)^2 \sin(pompgom) \sin(\alpha) \cos(pompgom) \\ & + 2 a e^2 \cos(\alpha) \sin(A1) \sin(pompgom)^2 \sin(\alpha) \cos(A1) \\ & + a e^2 \sin(\alpha)^2 \sin(A1)^2 \cos(pompgom)^2 \\ & - 2 a e^2 \sin(\alpha)^2 \sin(A1) \cos(pompgom) \cos(A1) \sin(pompgom) \\ & + a e^2 \sin(\alpha)^2 \cos(A1)^2 \sin(pompgom)^2 - a e^2 \end{aligned}$$

Introduction of ex and ey

> rgen := simplify(r4,(e*cos(pompgom)=ex,e*sin(pompgom)=ey));

$$\begin{aligned} rgen := & -a (\cos(\alpha) \cos(A1) - \sin(\alpha) \sin(A1)) ex \\ & + a (\cos(\alpha)^2 \cos(A1)^2 - 2 \cos(\alpha) \cos(A1) \sin(\alpha) \sin(A1) + \sin(\alpha)^2 \sin(A1)^2) ex^2 - 2 \\ & a (\cos(\alpha)^2 \cos(A1) \sin(A1) + \cos(\alpha) \cos(A1)^2 \sin(\alpha) - \sin(\alpha)^2 \sin(A1) \cos(A1)) \\ & - \cos(\alpha) \sin(A1)^2 \sin(\alpha)) ey ex + a - a e^2 - a (\cos(\alpha) \sin(A1) + \sin(\alpha) \cos(A1)) ey \\ & + a (\cos(\alpha)^2 \sin(A1)^2 - \sin(\alpha)^2 \cos(A1)^2 + 2 \cos(\alpha) \cos(A1) \sin(\alpha) \sin(A1)) ey^2 \end{aligned}$$

>

General form of r, whatever the development of v in f(M) is. We have

A1=v-M.

It is sufficient to replace A1 by its value before going on the development.

In this file A1=2*e*sin(M)+5/4*e2*sin(2M)

2.

cos(v-M) and sin(v-M) are replaced by their value read at the beginning of the program

> r5 := subs(cos(A1)=cosA,sin(A1)=sinA,rgen);

$$\begin{aligned} r5 := & -a (\cos(\alpha) \%2 - \sin(\alpha) \%1) ex \\ & + a (\cos(\alpha)^2 \%2^2 - 2 \cos(\alpha) \%2 \sin(\alpha) \%1 + \sin(\alpha)^2 \%1^2) ex^2 - 2 \\ & a (\cos(\alpha)^2 \%2 \%1 + \cos(\alpha) \%2^2 \sin(\alpha) - \sin(\alpha)^2 \%1 \%2 - \cos(\alpha) \%1^2 \sin(\alpha)) ey ex \\ & - a - a e^2 - a (\cos(\alpha) \%1 + \sin(\alpha) \%2) ey \\ & - a (\cos(\alpha)^2 \%1^2 - \sin(\alpha)^2 \%2^2 + 2 \cos(\alpha) \%2 \sin(\alpha) \%1) ey^2 \\ \%1 := & -2 \cos(\alpha) ey - \frac{5}{4} ey^2 \sin(2\alpha) + \frac{5}{4} ex^2 \sin(2\alpha) + 2 \sin(\alpha) ex - \frac{5}{2} ey ex \cos(2\alpha) \end{aligned}$$

$$\%2 := 1 - 2 \cos(\alpha)^2 ey^2 - 2 \sin(\alpha)^2 ex^2 + 4 \sin(\alpha) \cos(\alpha) ey ex$$

Simplification at order 2 in e

> r5 := simplify(r5,(ex^3=0,ey^3=0,ex^2*ey=0,ex*ey^2=0));

$$\begin{aligned} r5 := & -a ex \cos(\alpha) + a (\cos(\alpha)^2 + 2 \sin(\alpha)^2) ex^2 - 2 a ex \sin(\alpha) \cos(\alpha) ey - a (-1 + e^2) \\ & - a ey \sin(\alpha) + a (\sin(\alpha)^2 + 2 \cos(\alpha)^2) ey^2 \end{aligned}$$

> r5 := expand(r5);

$$\begin{aligned} r5 := & -a ex \cos(\alpha) + a ex^2 \cos(\alpha)^2 + 2 a ex^2 \sin(\alpha)^2 - 2 a ex \sin(\alpha) \cos(\alpha) ey + a - a e^2 \\ & - a ey \sin(\alpha) + a ey^2 \sin(\alpha)^2 + 2 a ey^2 \cos(\alpha)^2 \end{aligned}$$

> r5 := simplify(r5,(e^2=ex^2+ey^2));

$$\begin{aligned} r5 := & -a ex \cos(\alpha) + a (\cos(\alpha)^2 + 2 \sin(\alpha)^2 - 1) ex^2 - 2 a ex \sin(\alpha) \cos(\alpha) ey + a \\ & - a ey \sin(\alpha) + a (\sin(\alpha)^2 + 2 \cos(\alpha)^2 - 1) ey^2 \end{aligned}$$

> r := simplify(r5);

$$\begin{aligned} r := & -a ex \cos(\alpha) + a ex^2 - a ex^2 \cos(\alpha)^2 - 2 a ex \sin(\alpha) \cos(\alpha) ey + a - a ey \sin(\alpha) \\ & + a ey^2 \cos(\alpha)^2 \end{aligned}$$

Save of the result in the file named "developr"

> save r,'developr';

>

When the simple variables and their power are computed, they are stored in files and will be used by the main functions like terrestre (nl, ni, ne) or lunisolaire or pressionsolaire.

These main functions correspond to centered potentials after utilization of function "Long period". Indeed it is not necessary to keep the short period since after derivation they will be eliminated (only centered evolution is searched). The example of solar radiation pressure potential is given in terms of MAPLE commands. Intermediate store file can be noticed.

```
> pressionsolaire := proc(nl,ne)
>
>   Development of solar radiation pressure pseudo potential at order ni in i
and ne in e
>
>   reading of intermediate variables
> read 'developvar';
>
>   potential expression
> prsol := -sigma*(rx*tx+ry*ty+rz*tz);
>   simplification at order ni in i and ne in e
> prsol := simplif(nl,ne,prsol);
> prsol := combine(prsol,trig);
>   removing of short period terms
> prsol := longperiod(prsol);
>
> save prsol,'potpressol';
> end;
```

3. Lagrange equation's

The perturbational potential is spelt:

$$R = R_{\text{earth}} + R_{\text{moon}} + R_{\text{sun}} + R_{\text{pressure}}$$

$$\text{So: } \frac{\partial R}{\partial P} = \frac{\partial R_{\text{earth}}}{\partial P} + \frac{\partial R_{\text{moon}}}{\partial P} + \frac{\partial R_{\text{sun}}}{\partial P} + \frac{\partial R_{\text{pressure}}}{\partial P}$$

for any adapted parameters.

Lagrange equations are consequently established for each perturbation. The sum is later done at the time of the integration.

To establish these equations a Lagrange function was written. From a potential pot it returns the expression list:

$$\frac{da}{dt}, \frac{dex}{dt}, \frac{dey}{dt}, \frac{dhx}{dt}, \frac{dhy}{dt}, \frac{dlm}{dt}$$

This function Lagrange (pot, ni, ne) computes, from a general expression (not simplified) of Lagrange equation in orbital parameters, the contribution of a potential to the evolution of the orbital parameters at the order ni in i and ne in e. As soon as the potential expression is written at order (ni + 1) in i and (ne + 1) in e, the parameters evolution can be computed for any ni and ne.

When the instruction list := [Lagrange (pot, 2, 1)] is typed, the list of the 6 orbital parameters evolution due to potential pot at order 2 in i and 1 in e is got.

The corresponding list of MAPLE commands is given hereafter:

```
> Lagranges := proc(pot,ni,ne)
>
>   Computation of Lagrange equations 2nd members in adapted parameters
for the potential named "pot".
>   These equations are simplified at order ni in i and ne in e.
> local dp1,dp2,dp3,dp4,dp5,dp6,d1,d2,d3,d4,d5,d6,na2,dna2;
>
> na2 := n*a^2;
> dna2 := 2*n*a^2;
> calcexpr(nl,ne,'expr1','expr2','expr3','expr4');
>   Simplification of some variable expressions in 2nd members
>
>   Derivative computation
> dp1 := diff(pot,a);
> dp2 := diff(pot,ex);
> dp3 := diff(pot,ey);
> dp4 := diff(pot,hx);
> dp5 := diff(pot,hy);
> dp6 := diff(pot,lm);
>
> d1 := (2/(n*a)) * dp6;
> d1 := simplif(nl,ne,d1);
>
> d2 := -(expr1/na2) * dp3
>   - simplif(nl,ne,ey*expr2*hx/dna2) * dp4
>   - simplif(nl,ne,ey*expr2*hy/dna2) * dp5
>   - simplif(nl,ne,ex*expr3/na2) * dp6;
> d2 := simplif(nl,ne,d2);
>
> d3 := (expr1/na2) * dp2
>   + simplif(nl,ne,ex*expr2*hx/dna2) * dp4
>   + simplif(nl,ne,ex*expr2*hy/dna2) * dp5
>   - simplif(nl,ne,ey*expr3/na2) * dp6;
> d3 := simplif(nl,ne,d3);
>
> d4 := -(expr4/na2) * dp5
>   + simplif(nl,ne,hx*ey*expr2/dna2) * dp2
>   - simplif(nl,ne,hx*ex*expr2/dna2) * dp3
>   - simplif(nl,ne,hx*ex*expr2/dna2) * dp6;
> d4 := simplif(nl,ne,d4);
>
> d5 := (expr4/na2) * dp4
>   + simplif(nl,ne,hy*ey*expr2/dna2) * dp2
>   - simplif(nl,ne,hy*ex*expr2/dna2) * dp3
>   - simplif(nl,ne,hy*ex*expr2/dna2) * dp6;
> d5 := simplif(nl,ne,d5);
>
> d6 := -(2/(n*a)) * dp1
>   + simplif(nl,ne,ex*expr3/na2) * dp2
>   + simplif(nl,ne,ey*expr3/na2) * dp3
>   + simplif(nl,ne,hx*expr2/dna2) * dp4
>   + simplif(nl,ne,hy*expr2/dna2) * dp5;
> d6 := simplif(nl,ne,d6);
>
> d1,d2,d3,d4,d5,d6;
> end;
```

Then for each potential, we have built a function that reads the potential previously stored in a file, loads the "Lagranges" function and run it, carries out some sorts and gatherings to give a more readable form to results and stores the results in files. These functions always have ni and ne as parameters.

4. Fortran language source code generation

Through section 1 to 4, for each perturbation force, we have got the evolution expression due to this force of orbital parameters. Now the objective is to use these computations in a language compatible with our other space dynamics software, for example FORTRAN language.

Without leaving MAPLE, a generation of Fortran source code is possible while using the MAPLE function Macrofor.m.

The utilization of such a function is very easy. What the Fortran subroutine has to contain, has to be written line by line in Macrofor language.

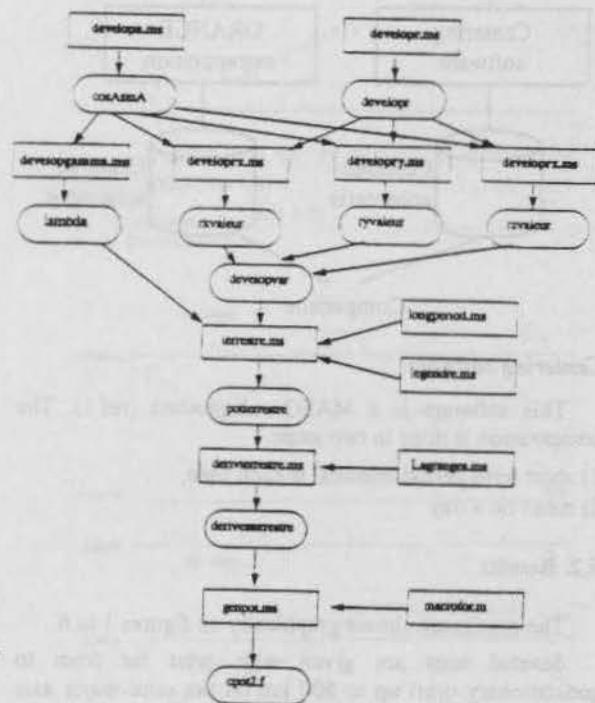
The example for the Earth potential is given just hereafter:

```
> genpot := proc()
>
>   reading of derivate formulas in save file
> read 'derivate terrestre';
>   Preparation of Maple formulas to Fortran language writing
> for i from 1 to 6 do
>   der.i := subs('Rt/a')=Rt/a, n=xna, hz=six, hy=siy, der.i);
>   for i1 from 1 to 4 do
>     for i2 from 1 to 4 do
>       in Modele, cim and sim coefficients are equal to Rt^i1*cim et Rt^i2*sim
>       der.i := subs(C(i1,i2)=cim(i1,i2)/Rt^i1, S(i1,i2)=sim(i1,i2)/Rt^i1, der.i);
>     od;
>     der.i := subs(J(i1)=xj(i1)/Rt^i1, der.i);
>     der.i := subs(cos(i1*lm)=co(i1), sin(i1*lm)=si(i1), der.i);
>   od;
>   der.i := simplify(der.i);
>   evalf writes integers under real form, allowing to write the fractions of
>   Maple formulas (2/3, 4/5, ...) under understandable form in Fortran
>   language (2./3., 4./5., ...);
>   der.i := evalf(der.i);
> od;
>
> init_genfor();
> precision := double;
> #optimized := true;
>
>   Instructions for writing the subroutine
> potpot := [ subroutinem , cpot , [p,dp] , [
> [commentf, 'Version ORANGE Juin 1993 .N Marcille',
> [commentf, 'Contribution du potentiel terrestre aux equations',
> [commentf, 'differentielles d evolution des parametres centre. ],
> [commentf, 'p(6) tableau des parametres centres (km,rad) ',
> [commentf, 'dp(6) derivees des parametres centres (km,rad) '],
> [commentf, 'Ce programme initialise le vecteur dp',
> [declaref, 'implicit double precision', [(a-n,o-z)']],
> [declaref, 'dimension', [p(6),dp(6)']],
> [declaref, 'dimension', [co(4),si(4)']],
> [commentf, 'coefficients du potentiel terrestre calcules dans Modele'],
> ],
> [commentf, 'poten', [xj(4),cim(4,4),sim(4,4)']],
> [parameterf, [pi:=evalf(Pi,14),rad:=evalf(pi/180)']],
> [parameterf, [xmu:=398600.47,omt:=360.985612*rad]],
> ],
> [equalf, a, p(1)],
> [equalf, ex, p(2)],
> [equalf, oy, p(3)],
> ],
> [equalf, six, p(4)],
> [equalf, siy, p(5)],
> ],
> [equalf, xna, sqrt(xmu/a)/a^86400],
> ],
> [dom, 1, 1, 4, [
> [equalf, co(i), cos(dfloat(i)*p(6))],
> [equalf, si(i), sin(dfloat(i)*p(6))]]
> ],
> ],
> [commentf, 'Effet sur le demi-grand axe' ],
> [equalf, dp(1), der1 ],
```

```
> [commentf, 'Effet sur l'excentricite' ],
> [equalf, dp(2), der2 ],
> [equalf, dp(3), der3 ],
> [commentf, 'Effet sur l'inclinaison' ],
> [equalf, dp(4), der4 ],
> [equalf, dp(5), der5 ],
> [commentf, 'Effet sur la longitude moyenne' ],
> [equalf, dp(6), xna - omt + der6 ]
> ];
```

```
Writing of the Fortran subroutine in the file named cpot2.f
> writeto('cpot2.f');
> genfor(potpot);
> writeto(terminal);
>
> end;
```

To summarize, the development of the pertinent subroutine is the fruit of several MAPLE actions whom the example for the Earth potential is given in the following schema.



Earth potential

Inside the boxes (square angles) there are the MAPLE software or functions.

Inside the other boxes (round angles) there are the storage file of intermediate results.

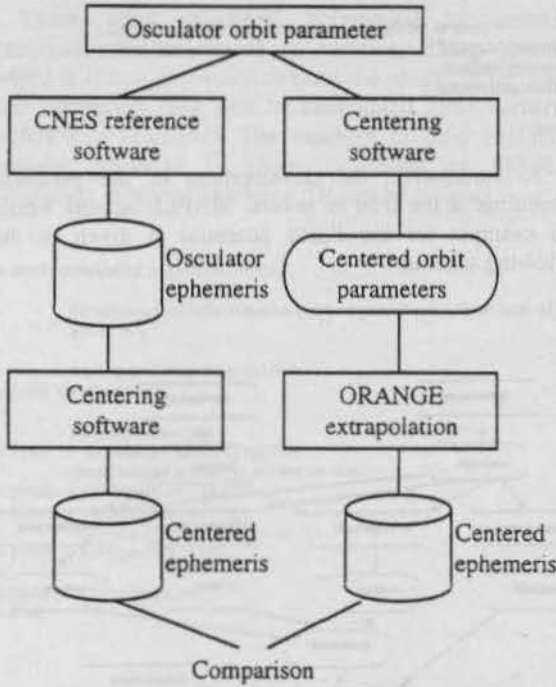
5. Results

5.1. Method

To test the ORANGE library, we add an integrator to it, in order to have a complete extrapolation software.

And using a CNES reference software doing osculator parameter extrapolation with a very good accuracy, comparisons have been done on around one month.

As explained before, ORANGE is for centered parameters, hence the reference orbit bulletins were regularly centered in order to have comparable data.



Centering software

This software is a MASQ sub-product (ref.1). The computation is done in two steps:

- 1) short term period removal at each time,
- 2) mean on a day.

5.2. Results

The results are shown graphically on figures 1 to 6.

Several tests are given with orbit far from to geostationary orbit up to 500 km on the semi-major axis and 3 deg on the inclination.

For all the tests, the following deviations are obtained after 30 extrapolation days:

- on $a < 5$ m for 10 m specified
- $e < 4.10^{-6}$ for 10^{-5} specified
- $i < 5.10^{-4}$ deg for 10^{-3} deg specified
- $l < 5.10^{-4}$ deg for 10^{-3} deg specified

These results are good and definitively sufficient for station keeping.

However some supplementary developments might improve some terms for which some residual periodical terms are remained. It is mainly the case of inclination which could be improved by a higher order development of moon-solar potential.

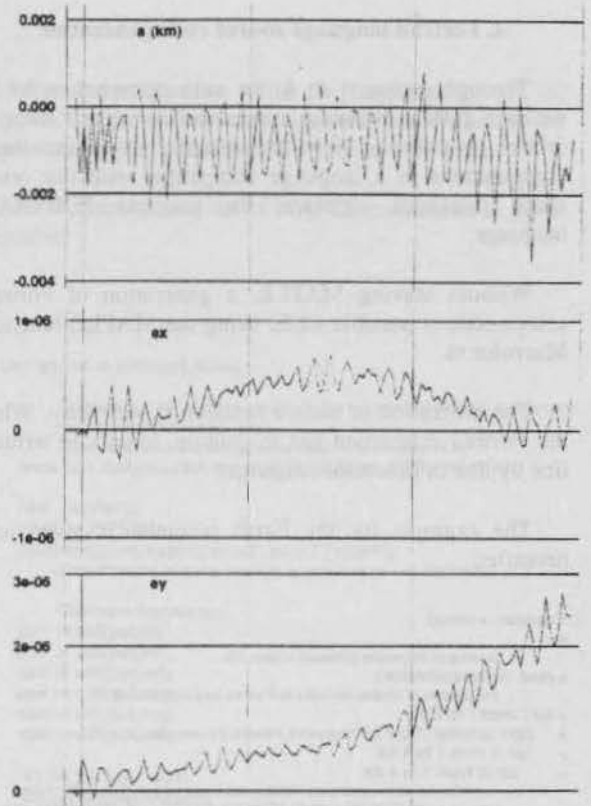


Figure 1 : a, ex, ey deviation versus time
- 30 days extrapolation
- geostationary orbit

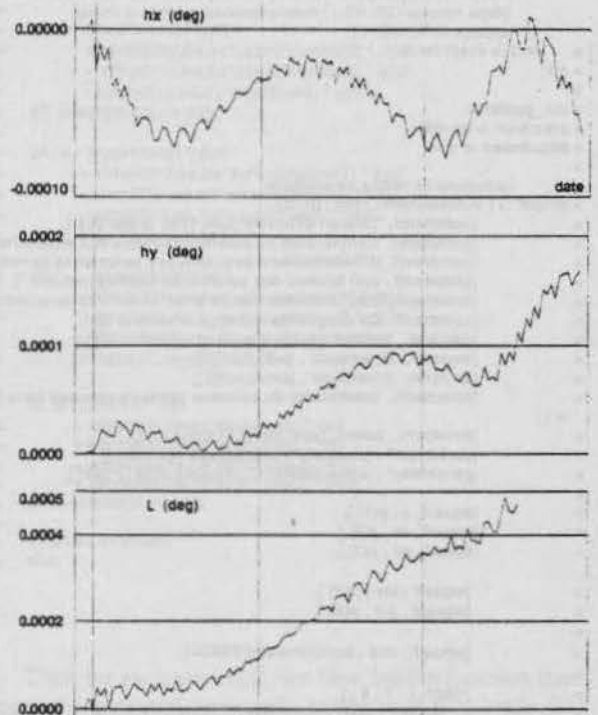


Figure 2 : hx, hy, l deviation versus time
30 days of extrapolation
geostationary orbit

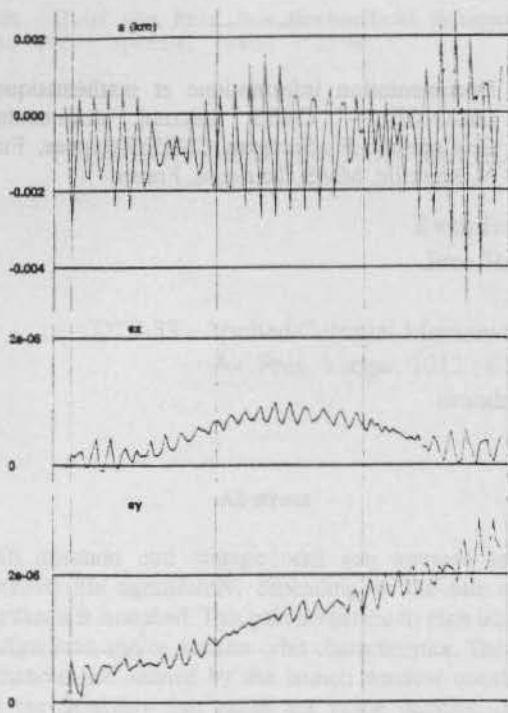


Figure 3 : a, ex, ey deviation versus time

30 extrapolation days
geosynchronous satellite
3° of inclination

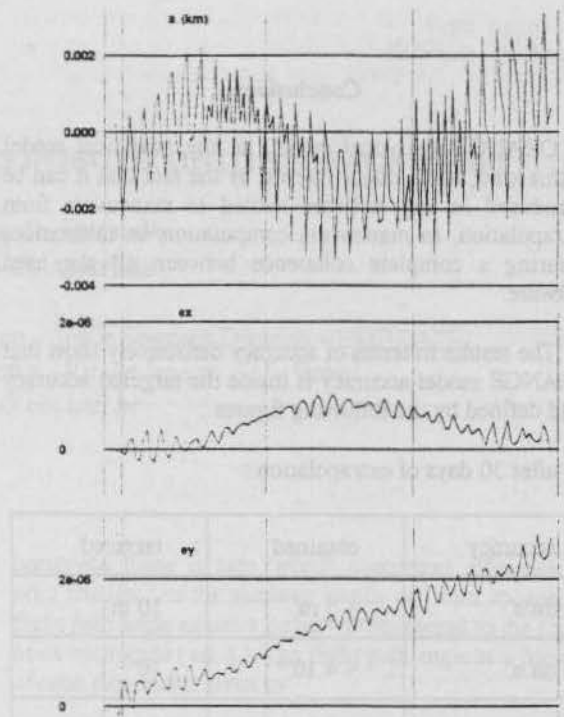


Figure 5 : a, ex, ey deviations versus time

30 extrapolation days
 $a - a_{\text{synchronous}} = -500 \text{ km}$
3° of inclination

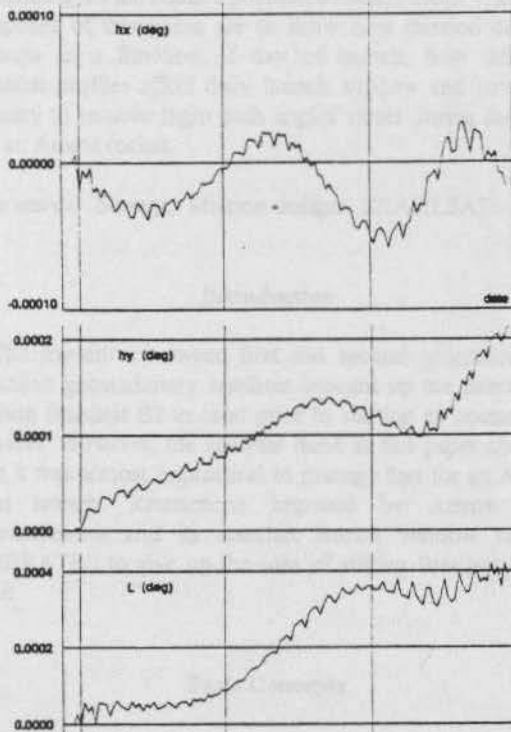


Figure 4 : hx, hy, l deviation versus time

30 extrapolation days
geosynchronous satellite
3° of inclination

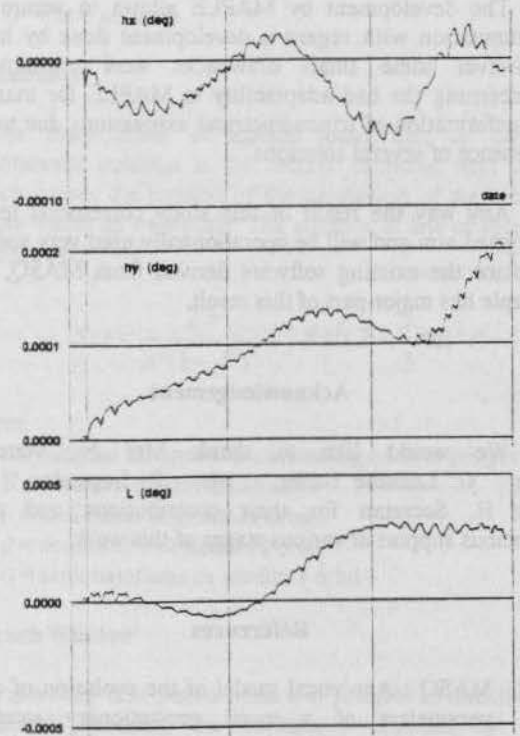


Figure 6 : hx, hy, l deviations versus time

30 extrapolation days
 $a - a_{\text{asynchronous}} = -500 \text{ km}$
3° of inclination

Conclusions

ORANGE analytical model, as any analytical model of this kind, has a major interest by the fact that it can be introduced in any software related to maneuvers from extrapolation, to maneuvers computation or calibration, ensuring a complete coherence between all the used software.

The results in terms of accuracy definitively show that ORANGE model accuracy is inside the targeted accuracy field defined by the following figures :

after 30 days of extrapolation :

accuracy	obtained	targeted
on a	< 5 m	10 m
on e	< $4 \cdot 10^{-6}$	10^{-5}
on i	< 0.0005 deg	0.001 deg
on lm	< 0.0005 deg	0.001 deg

The development by MAPLE allows to secure the computation with regard a development done by hand. However some small drawbacks were encountered concerning the bad adaptability to MAPLE for massive transformation of trigonometrical expressions due to the presence of several solutions.

Any way the result of this study correspond to the targeted aim and will be operationnally used very soon to replace the existing software derived from MASQ, and Maple has major part of this result.

Acknowledgement

We would like to thank Mrs N. Marcille, Mr G. Lassalle Balier, Mr P. Legendre and Mr H. Secretan for their contributions and their precious support at various stages of this work.

Références

- [1] MASQ : Analytical model of the evolution of orbit parameters of a quasi geostationary satellite. P. Legendre - CNES - Toulouse - France IAF - Budapest - Oct. 83
- [2] Evolution de l'orbite d'un satellite geostationnaire D. COT - Thésis presented in Université Paul Sabatier Toulouse, France 31/10/84

- [3] Documentation informatique et mathématique de ORANGE - CNES internal documentation G. Campan, H. Secretan CNES Toulouse, France N. Marcille, MMS, Toulouse, France

MISSION DESIGNS FOR SATELLITES INJECTED INTO STORAGE ORBIT

Evandro Paiva de Andrade
Jose Roberto C. Andrade

DTS-33 - Applied Celestial Mechanics Section - Space Segment Division - EMBRATEL
Av. Pres. Vargas, 1012 / 610 - Centro - Rio de Janeiro - RJ - Brasil
evandro@dts-3.ebt.anrj.br

Abstract

An injection into storage orbit can increase satellite maneuver life significantly, depending on the date of the year that it is launched. This gain is specific to each launcher configuration and/or transfer orbit characteristics. The main restrictions are defined by the launch window constraints and the flexibility that either the single launcher or the perigee stage can give. In order to avoid large flight path angle during injection, there are two scenarios to be considered when the launcher cannot place transfer orbit apogee properly: earth's oblateness can either make it converge or diverge to the desired orbit transfer point, depending on the relative position between them. The main purposes of this paper are to show how mission designs change as a function of day of launch, how different mission profiles affect daily launch window and how fuel penalty to remove flight path angles varies during the year for an Ariane rocket.

Key words: Storage, Mission designs, BRASILSATs.

Introduction

The transition between first and second generations of Brazilian geostationary satellites brought up the interest of storing Brasilsat B2 in orbit prior to starting its operational services. However, the analysis done in this paper showed that it was almost unpractical to manage that for an Ariane dual launch. Restrictions imposed by Ariane orbit characteristics and its standart launch window caused EMBRATEL to give up the idea of storing Brasilsat B2 in orbit.

Basic Concepts

Flight Path Angle (γ)

Apogee and perigee are the only two points in an elliptical orbit where the angle γ between velocity vector and local

horizontal plane is zero, which maximizes efficiency for orbit transfer. As the satellites stands off from apogee, the flight path angle causes a penalty proportional to the square of its magnitude (eq. 5). The flight path angle as a function of orbit elements is given by:

$$\tan \gamma = \frac{e \sin \nu}{1 + e \sin \nu} \quad (1)$$

where:

e = eccentricity of the orbit
 ν = true anomaly.

Oblateness

The main effect in transfer orbit due to earth's gravitational potential is the second harmonic term J_2 , which causes the rotation of the orientation of the orbital ellipse within its own plane. The advance of line of apsides is given by:

$$\Delta \omega = \frac{2\pi}{a^2(1-e^2)^2} J_2 R_e^3 \left(2 - \frac{5}{2} \sin^2 i\right) \quad (2)$$

where:

ω = angular distance from ascending node to perigee
 R_e = earth's equatorial radius
 i = inclination of satellite's orbit
 e = eccentricity of satellite's orbit
 a = semimajor axis of satellite's orbit.

Launch Window

It is a daily time period when it is possible to launch the spacecraft attending the constraints imposed by the launcher and by the health, communications and control conditions of the satellite. The main restrictions are:

power for solar panel to charge batteries
temperature

- . eclipse duration restrictions
- . sun sensor visibility
- . earth sensor interference

Ariane Orbit Characteristic

For the standart midnight Ariane launch, the right ascension of the ascending node of transfer orbit is always around sun right ascension.

Inclination Vector Definition and Control

The inclination vector is defined pointing towards the ascending node of the orbit and is given by:

$$\vec{j} = [K_1, H_2] = j \exp(j\Omega) \quad (3)$$

Considering that the satellite is usually injected into transfer orbit at the descending node, apogee motor firing occur at the ascending node with the satellite pointing downwards. In such cases, the change in inclination caused by the firing is given by:

$$\Delta i = \frac{\Delta V_N}{V_s} \exp(-j\alpha_{s/c}) \quad (4)$$

where:

- ΔV_N = normal correction delta velocity
- V_s = synchronous velocity
- $\alpha_{s/c}$ = sun right ascension.

Reaching Storage Orbit From Ariane Transfer Orbit

Considering that the effect of luni-solar perturbation on the inclination vector of a geostationary satellite has a well determined inertial direction, one can anticipate it and position the orbit in space such that over the required period of storage, nature itself brings the satellite to a geostationary condition.

If this is the case and considering also that the ascending node of transfer orbit, and so the direction of its inclination vector, depends on the day of launch, the relative position between transfer orbit apogee and the crossing point of the orbits to accomplish optimum transfer will also vary accordingly. Roughly the injection point occurs after transfer orbit apogee from December to June and before apogee for the rest of the year. This angular distance at the moment of the firing is going to cause a flight path angle and, as a consequence, a penalty given by^[1]:

$$\frac{\partial V_B}{\partial \gamma_s^2} = \frac{V_s}{V_B} \frac{\partial V_s}{\partial \gamma_s^2} + \frac{V_T}{V_B} \frac{\partial V_T}{\partial \gamma_s^2} +$$

$$\frac{\cos i}{V_B} \left[\left(\frac{V_s V_T}{2} \right) - \left(1 - \frac{r_s^2}{2} \right) \left(V_s \frac{\partial V_T}{\partial \gamma_s^2} + V_T \frac{\partial V_s}{\partial \gamma_s^2} \right) \right] \quad (5)$$

where:

$$\frac{\partial V_s}{\partial \gamma_s^2} = \frac{\mu(1-e)}{2V_s r_s e} \quad (6)$$

and

$$\frac{\partial V_T}{\partial \gamma_s^2} = \frac{\mu(1-e)}{2V_T r_s e} \quad (7)$$

$$\frac{\partial V_B}{\partial a} = \frac{V_s V_T}{V_B} \sin i \quad (8)$$

where:

- V_s = arrival velocity
- V_T = target velocity
- i = transfer orbit inclination
- $V_B = \Delta V$ required at AMF to achieve the target orbit
- r_s = radius at AMF

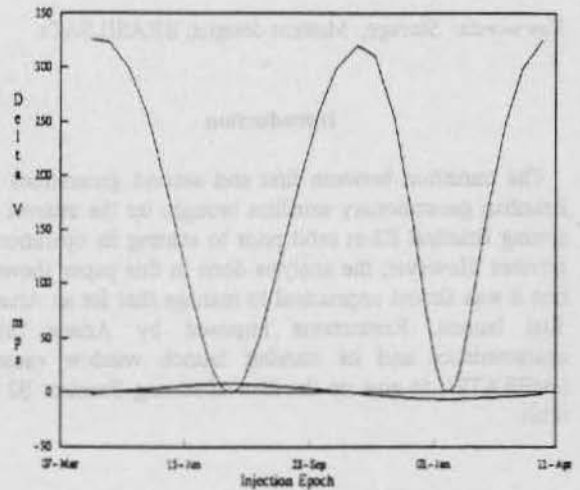


Figure 1: Storage Orbit Injection 1.5 deg - Brasilsat B2

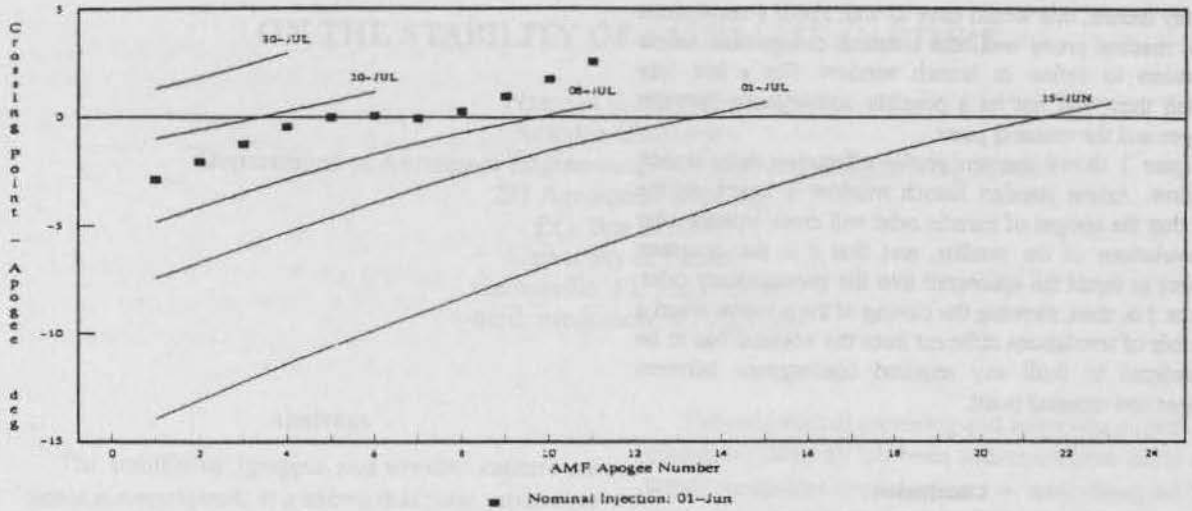


Figure 2: Mission Designs Change x Day of Launch

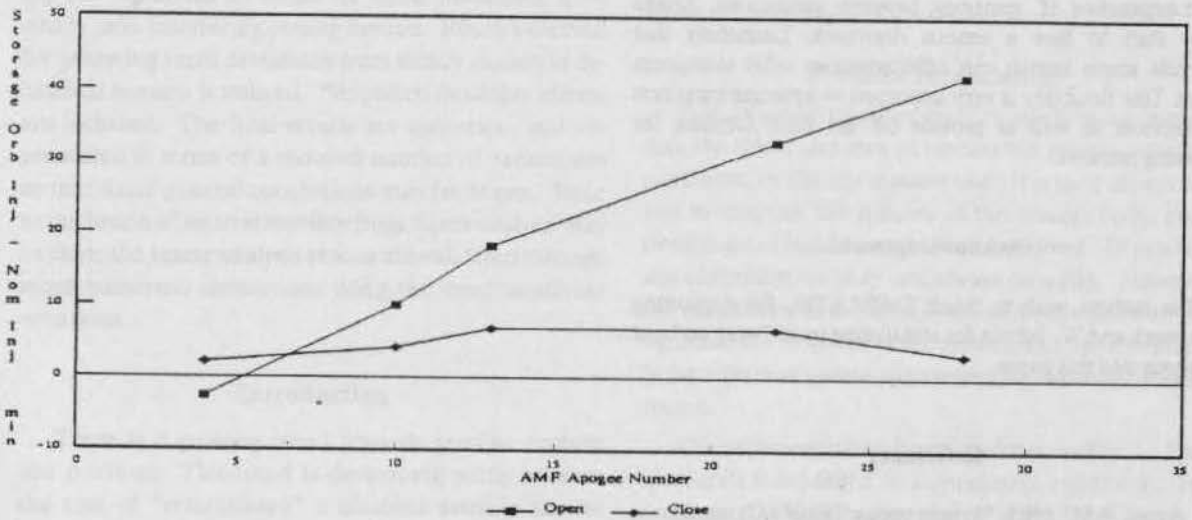


Figure 3: Mission Profiles x Launch Window Closing

γ_a = vertical flight path angle at AMF

Figure 1 shows graphically the ΔV penalty due to the flight path angle as a function of day of launch. The penalty from the variation of the right ascension of the ascending node standpoint, given by equation (9), and of a lower order of magnitude, is also shown^[2].

$$\Delta \Delta V_B = \frac{V_d V_T \pi}{V_{Bo} 180} \left[\frac{1}{2} \left(\frac{\pi}{180} \right) i_{tar} \cos i + \right. \\ \left. - \sin i \cos(\Delta \Omega) \right] \quad (9)$$

where:

V_{Bo} = required velocity for a stationary target orbit

$\Delta \Omega$ = $RAAN_{transfer\ orbit} - RAAN_{target\ orbit}$

i_{tar} = storage orbit inclination target

Figure 2 shows how mission design changes as a function of day of launch from 15 of June until 30 of July for a 1.5 degree storage orbit. For a 15 of June launch, one has to wait 22 revolutions in transfer orbit in order to make apogee converge to the crossing point. That may cause an undesirable impact on the standard launch window. For a 15

of July launch, one would have to wait about 6 revolutions what matches pretty well the nominal design that Ariane considers to define its launch window. For a late July launch there will not be a possible convergence between apogee and the crossing point.

Figure 3 shows mission profile effects on daily launch window. Ariane standard launch window is based on the fact that the apogee of transfer orbit will cross equator after 6 revolutions of the satellite, and that it is the optimum apogee to inject the spacecraft into the geostationary orbit. Figure 3 is, then, showing the closing of the window when a number of revolutions different from the nominal has to be considered to fulfil any required convergence between apogee and crossing point.

Conclusion

Although Ariane presents one of the most successful rocket of the market for the latest years, now, when most owners of geostationary satellites are going through their first experience of transition between generations, Ariane may start to face a serious drawback. Launchers that provide single launch can offer whatever orbit customers want. This flexibility is very important to optimize transition of services as well as provide off the shelf satellites for growing markets.

Acknowledgement

The authors wish to thank EMBRATEL for supporting this work and W. Schulz for stimulating us to "wrap up" our analysis into this paper.

References

- 1] Anzel, B.M.; 1983, "Synchronous Satellite Dynamics and Operations", Ref. F1532SCG NO8410068 - Hughes, El Segundo, CA.
- 2] Anzel, B.M.; 1989, "Hughes Proposal of Geostationary Satellites to EMBRATEL" - Hugues, El Segundo, CA.

ON THE STABILITY OF SATELLITE CAPTURE

Norman G. Fitz-Coy[†]
Anindya Chatterjee*

Department of Aerospace Engineering, Mechanics & Engineering Science
231 Aerospace Building
P.O. Box 116250
University of Florida
Gainesville, FL 32611-6250
e-mail: nfc@snow.aero.ufl.edu

Abstract

The stability of "grapple and wrestle" capture scenarios is investigated. It is shown that these capture scenarios may become unstable. The dynamic system is analyzed assuming there are no control forces and torques. The system is examined for stability by linearizing the equations in terms of small deviations from steady, non-interfering coning motion. Routh's method for analyzing small deviations from steady motion in dynamical systems is utilized. Simplified flexibility effects are included. The final results are numerical, and are presented in terms of a reduced number of parameters so that some general conclusions may be drawn. Since a conclusion of neutral stability from linear analysis may be false, the linear analysis results are validated through some numerical simulations using the exact nonlinear equations.

Introduction

There is a growing trend towards satellite capture and retrieval. This trend is developing partly because the cost of "refurbishing" a disabled satellite can be much cheaper than the cost of replacing the satellite. Further motivation comes from the "cost" of human lives in the event of a manned space vehicle being disabled for some reason. Satellite capture/retrieval could also be utilized in addressing the mounting problem of space debris.

In recent years, some satellites have been retrieved as well as repaired in orbit. Examples are the Long Duration Exposure Facility (LDEF), the Intelsat 6 communication satellite, the Eureka satellite, and more recently, the Hubble Space Telescope. In all missions, the rescue vehicle was the space shuttle. For the purpose of capturing disabled spacecraft, the space shuttle has limitations: (i) it is incapable of reaching high orbits, (ii) its manipulator arm may not withstand the dynamic loading that will occur during a retrieval operation, and (iii) the possibility of injury to the shuttle's crew makes its use too dangerous for routine capture operations.

The dynamics of capturing and retrieving a (possibly manned) spacecraft has been addressed from many different viewpoints over the years — most being ad hoc numerical simulations. In this paper, we address the stability of capture when one vehicle (rescue) is significantly larger than the other vehicle (disabled). The rescue approach most commonly used in these scenarios is referred to as "grapple and wrestle".¹

Problem Formulation

It is assumed that one body is much more massive than the other, and thus its motion will remain relatively unaffected by the less massive one. It is then only necessary to examine the stability of the smaller body, and a smaller set of equations needs to be solved. In practice, this simplification may not always be valid. However, the simplification is useful because it provides some insight into the behavior of the system, and helps to identify the effects of system parameters on the stability of the system.

The representative system is shown in Fig. 1. Each spacecraft is modelled as a symmetric, rigid body. It is assumed that both bodies can be brought to a state of steady coning motion in which the attachment point of

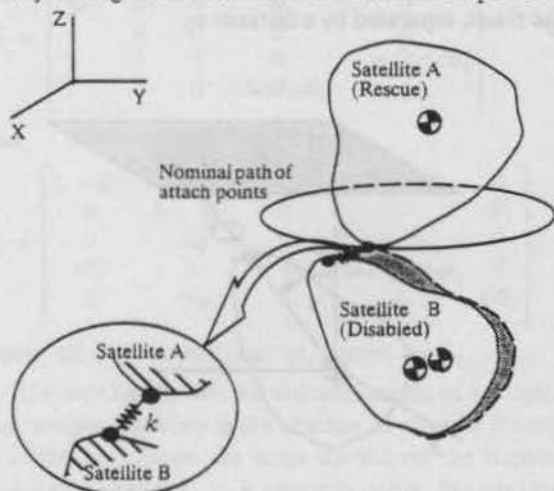


Fig. 1. Representative System

each body describes identical circles in space. The two bodies are then connected by a ball-and-socket joint, which is assumed frictionless — via a frictionless joint, forces are not exerted on either body and therefore the coning motion should continue undisturbed. The basic premise of this paper is that if the system is unstable, then slight perturbations can lead to large deviations from this reference state of steady coning motion. In a spacecraft retrieval situation, this will lead to greater demands on the attitude control system of the rescue vehicle.

To investigate the effects of perturbations on the stability of the system, a coordinate system which rotates at a constant angular rate is utilized (Fig. 2). The advantage of using this coordinate system is that the palpable (non-ignorable) coordinates are constant during steady coning motion (i.e., they are in an equilibrium state). Therefore, upon elimination of the cyclic (ignorable) coordinates, small disturbance theory can be utilized to obtain a linear gyroscopic system in terms of the palpable coordinates. This type of analysis is referred to as Routh's procedure in the literature.^{2,3} Stability about the nominal equilibrium states can then be analyzed by appropriate methods.

Note: There is a disadvantage to using the coordinate system shown in Fig. 2. For small coning angles (i.e., conditions close to pure spin), the equations are not as valid since the precession and spin angles become indistinguishable (gimbal lock). These cases require special formulation and are not addressed in this paper.⁴

A linear spring is used to model flexibility in the system. The spring deformation, δ , is the instantaneous distance between the attachment points, assuming both bodies were perfectly rigid (see Fig. 1). The reference positions of the centers of mass of the two bodies lie on the z-axis, separated by a distance z_0 .

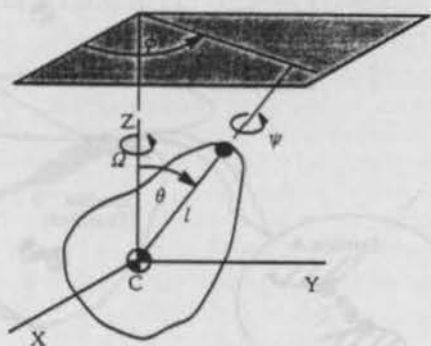


Fig. 2. Coordinate System

The Lagrangian

With the assumption of one body being significantly more massive than the other, we need consider only the motion of the less massive body. In that case, the translational kinetic energy is given by

$$T_v = \frac{m}{2} \{ (\dot{x} - \Omega y)^2 + (\dot{y} + \Omega x)^2 + \dot{z}^2 \}, \quad (1)$$

where m is the mass of the body, (x, y, z) describes the displacement of the center of mass (c.m.) of the body from its nominal position and are measured in the rotating frame, and $\underline{\Omega} = \Omega \mathbf{k}$ is the angular velocity of the rotating frame. The rotational kinetic energy is

$$T_{rot} = \frac{I}{2} (\dot{\theta}^2 + (\dot{\phi} + \Omega)^2 \sin^2 \theta + \mu(\dot{\psi} + (\dot{\phi} + \Omega) \cos \theta)^2), \quad (2)$$

where the principal moments of inertia of the body are I , I and μI from the assumption of symmetry; $\dot{\psi}$, $\dot{\theta}$, and $\dot{\phi}$ are the spin, nutation, and precession rates, respectively, of the body with respect to the rotating frame.

The potential energy is

$$V = \frac{k}{2} \delta^2 = \frac{k}{2} \{ (x + l \sin \theta \cos \phi - l \sin \theta_0 \cos \phi_0)^2 + (y + l \sin \theta \sin \phi - l \sin \theta_0 \sin \phi_0)^2 + (z + l \cos \theta - l \cos \theta_0)^2 \}, \quad (3)$$

where l is the distance between c.m. and attach point (see Fig. 2), k is the stiffness of the spring modelling system flexibility, and θ_0 and ϕ_0 are the reference nutation and precession angles of the system, (by appropriate choice, $\phi_0 = 0$).

The Lagrangian then becomes

$$\begin{aligned} \mathcal{L} = T_{rot} + T_v - V \\ = \frac{I}{2} \{ \dot{\theta}^2 + (\dot{\phi} + \Omega)^2 \sin^2 \theta + \mu(\dot{\psi} + (\dot{\phi} + \Omega) \cos \theta)^2 \} \\ + \frac{m}{2} \{ (\dot{x} - \Omega y)^2 + (\dot{y} + \Omega x)^2 + \dot{z}^2 \} \\ - \frac{k}{2} \{ (x + l \sin \theta \cos \phi - l \sin \theta_0)^2 \\ + (y + l \sin \theta \sin \phi)^2 \\ + (z + l \cos \theta - l \cos \theta_0)^2 \}. \end{aligned} \quad (4)$$

Through nondimensionalization, it is possible to reduce the number of parameters which affect the stability of the system.⁵ Since the dimensionality of the Lagrangian is ML^2T^{-2} , the quantity $ml^2\omega^2$ can be used to nondimensionalize the Lagrangian; m is the reference mass of the body, l is the reference length, and ω is the reference frequency ($\omega^2 = \frac{k}{m}$). Defining a nondimensionalized time, τ , as $\tau = \omega t$, derivatives with respect to time ($\frac{d}{dt}$) can be replaced with a nondimensional time derivative ($\omega \frac{d}{d\tau}$).

Nondimensionalization of the Lagrangian results in

$$\begin{aligned} \mathcal{L} = & \frac{A}{2} (\dot{\theta}^2 + (\dot{\phi} + \dot{\Omega})^2 \sin^2 \theta) \\ & + \frac{A\mu}{2} (\dot{y} + (\dot{\phi} + \dot{\Omega}) \cos \theta)^2 \\ & + \frac{1}{2} \{ (\dot{x} - \dot{\Omega}y)^2 + (\dot{y} + \dot{\Omega}x)^2 + \dot{z}^2 \} \\ & - \frac{1}{2} \{ (x + \sin \theta \cos \phi - \sin \theta_0)^2 \\ & \quad + (y + \sin \theta \sin \phi)^2 \\ & \quad + (z + \cos \theta - \cos \theta_0)^2 \}, \end{aligned} \quad (5)$$

where

$$\bar{x} = \frac{x}{l}, \bar{y} = \frac{y}{l}, \bar{z} = \frac{z}{l}, \bar{\omega} = \omega \frac{d(\bar{\cdot})}{d\bar{t}}, A = \frac{I}{ml^2}.$$

For Convenience, the over bar is now dropped with the understanding that for the rest of this paper, we refer only to the nondimensionalized variables. Also, dots over a variable indicate differentiation with respect to the nondimensionalized time τ .

Routh's Method for Stability

Since $\mathcal{L} = \mathcal{L}(x, y, z, \dot{\phi}, \dot{\theta}, \psi, x, y, z, \phi, \theta)$, then ψ is a cyclic coordinate (ignorable); the palpable (non-ignorable) coordinates are x, y, z, ϕ and θ . For the cyclic coordinate ψ , an integral of motion exists (momentum conjugate):^{2,3}

$$P_\psi = \frac{\partial \mathcal{L}}{\partial \dot{\psi}} = A\mu(\dot{\psi} + (\dot{\phi} + \dot{\Omega}) \cos \theta). \quad (6)$$

Since P_ψ is constant, it can be evaluated at any point during the motion; evaluation of P_ψ during steady motion, yields

$$P_\psi = A\mu\Omega \cos \theta_0.$$

The Routhian function, is defined as^{2,3}

$$\mathcal{R} = \mathcal{L} - \psi P_\psi. \quad (7)$$

For this problem,

$$\begin{aligned} \mathcal{R} = & \frac{A}{2} (\dot{\theta}^2 + (\dot{\phi} + \dot{\Omega})^2 \sin^2 \theta) \\ & - \frac{P_\psi^2}{2A\mu} + P_\psi(\dot{\phi} + \dot{\Omega}) \cos \theta \\ & + \frac{1}{2} \{ (\dot{x} - \dot{\Omega}y)^2 + (\dot{y} + \dot{\Omega}x)^2 + \dot{z}^2 \} \\ & - \frac{1}{2} \{ (x + \sin \theta \cos \phi - \sin \theta_0)^2 \\ & \quad + (y + \sin \theta \sin \phi)^2 \\ & \quad + (z + \cos \theta - \cos \theta_0)^2 \}. \end{aligned} \quad (8)$$

(Note: $\mathcal{R} = \mathcal{R}(x, y, z, \phi, \theta, x, y, z, \phi, \theta, P_\psi)$. For the palpable coordinates, \mathcal{R} behaves like a Lagrangian function while, for the cyclic coordinates, \mathcal{R} behaves like a Hamiltonian function.)

Via small deformation theory, the i^{th} palpable coordinate can be expressed as $q_i = q_{i0} + \delta q_i$, where the zero subscript implies steady motion conditions and the prefix δ implies perturbed motion conditions; thus,

$q_i = \delta q_i$. The Routhian function can be expanded in a Taylor series about the steady motion conditions as

$$\begin{aligned} \mathcal{R} = & \mathcal{R}_0 + \sum_{i=1}^k \left(\frac{\partial \mathcal{R}}{\partial q_i} \right)_0 \delta q_i + \sum_{i=1}^k \left(\frac{\partial^2 \mathcal{R}}{\partial q_i^2} \right)_0 \delta q_i^2 \\ & + \frac{1}{2} \sum_{i=1}^k \sum_{j=1}^k \left(\frac{\partial^2 \mathcal{R}}{\partial q_i \partial q_j} \right)_0 \delta q_i \delta q_j \\ & + \frac{1}{6} \sum_{i=1}^k \sum_{j=1}^k \sum_{l=1}^k \left(\frac{\partial^3 \mathcal{R}}{\partial q_i \partial q_j \partial q_l} \right)_0 \delta q_i \delta q_j \delta q_l \\ & + \frac{1}{24} \sum_{i=1}^k \sum_{j=1}^k \sum_{l=1}^k \sum_{m=1}^k \left(\frac{\partial^4 \mathcal{R}}{\partial q_i \partial q_j \partial q_l \partial q_m} \right)_0 \delta q_i \delta q_j \delta q_l \delta q_m + (h.o.t.) \end{aligned} \quad (9)$$

Application of Lagrange's equation to the expanded Routhian function eliminates the constant term and the linear terms; the linear terms identically satisfy the steady motion equations. The first non-trivial contribution to the perturbed state equations of motion are from the quadratic terms. Neglecting the higher order terms, a linear, constant coefficient ordinary differential equation of the form

$$M\delta\ddot{q} + G\delta\dot{q} + K\delta q = 0 \quad (10)$$

is obtained, where

$$\begin{aligned} M_{ij} = & \left(\frac{\partial^2 \mathcal{R}}{\partial q_i \partial q_j} \right)_0, \quad G_{ij} = \left(\frac{\partial^2 \mathcal{R}}{\partial q_i \partial \dot{q}_j} \right)_0 - \left(\frac{\partial^2 \mathcal{R}}{\partial \dot{q}_i \partial q_j} \right)_0 \\ & \text{and } K_{ij} = - \left(\frac{\partial^2 \mathcal{R}}{\partial q_i \partial q_j} \right)_0. \end{aligned}$$

For $q = [x, y, z, \theta - \theta_0, \phi]^T$, and \mathcal{R}_0 given in Eq. (8)

$$\begin{aligned} M = & \begin{bmatrix} 1 & 0 & 0 & 0 & 0 \\ 0 & 1 & 0 & 0 & 0 \\ 0 & 0 & 1 & 0 & 0 \\ 0 & 0 & 0 & A & 0 \\ 0 & 0 & 0 & 0 & A s^2 \theta_0 \end{bmatrix}, \\ G = & \begin{bmatrix} 0 & -2\Omega & 0 & 0 & 0 \\ 2\Omega & 0 & 0 & 0 & 0 \\ 0 & 0 & 0 & 0 & 0 \\ 0 & 0 & 0 & 0 & -A\Omega s \theta_0 c \theta_0 \\ 0 & 0 & 0 & A\Omega s \theta_0 c \theta_0 & 0 \end{bmatrix}, \end{aligned}$$

and

$$K = \begin{bmatrix} 1 - \Omega^2 & 0 & 0 & c \theta_0 & 0 \\ 0 & 1 - \Omega^2 & 0 & 0 & s \theta_0 \\ 0 & 0 & 1 & -s \theta_0 & 0 \\ c \theta_0 & 0 & -s \theta_0 & 1 + A\Omega^2 s \theta_0 & 0 \\ 0 & s \theta_0 & 0 & 0 & s^2 \theta_0 \end{bmatrix},$$

where $s\theta_0$ implies $\sin \theta_0$ and $c\theta_0$ implies $\cos \theta_0$.

It is well known that the attitude motion of a weightless, torque free body in the absence of external forcing is stable; also, under the same conditions, the translational motion of the c.m. is neutrally stable. For the case above, as $k \rightarrow 0$, the system approaches the weightless,

torque-free case; therefore, we should expect the system above to exhibit similar stability characteristics. Note, as $k \rightarrow 0, \Rightarrow \omega \rightarrow 0 \Rightarrow \Omega \rightarrow \infty$ (NB, Ω is nondimensionalized; i.e., Ω/ω). Therefore, all terms of less than leading order in Ω may be discarded from the system matrices. Thus, all terms in K not containing Ω^2 are discarded; M and G are unchanged. With these simplification, the system matrices decouple into translational (x, y, z) and rotational ($\theta - \theta_0, \phi$) blocks. It has been shown that a linear conservative gyroscopic system is unstable if $(4K + G^T M^{-1}G)$ is negative definite.⁶ The translational blocks yield $(4K + G^T M^{-1}G) = 0$, while the rotational blocks yield a positive definite matrix. Since the zero matrix is negative semi-definite, the translational coordinates are neutrally (un)stable and the rotational coordinates are stable, as expected.

A general investigation of the stability of the linearized system expressed in Eq. (10) requires the solution of the associated eigenvalue problem for a large range of values of the system parameters. After nondimensionalization, only three parameters are required — A, Ω and θ_0 .

Stability of Linear Gyroscopic Systems

The matrices M and K are symmetric, while G is skew symmetric. Such systems are referred to as gyroscopic systems.⁶ The eigenvalues of the system can be found by solving the equation,

$$\det(\lambda^2 M + \lambda G + K) = 0$$

Note that because of the properties of M, K and G ,

$$\begin{aligned} \det(\lambda^2 M + \lambda G + K) &= \det(\lambda^2 M + \lambda G + K)^T \\ &= \det(\lambda^2 M - \lambda G + K). \end{aligned}$$

Therefore, the coefficients of odd powers of λ in the characteristic equation must be zero. Thus, if λ is an eigenvalue of the system, then so is $-\lambda$. This property has the following consequences: (i) if $\lambda = a \pm i\beta, a, \beta \neq 0$ are eigenvalues of the system, then $\lambda = -a \pm i\beta$ are automatically eigenvalues; (ii) if zero is an eigenvalue of the system, then it has a multiplicity of at least two; (iii) if any eigenvalue of the system has a non-zero real part, then the system *must* be unstable. Thus complex eigenvalues occur in sets of four. Purely imaginary and purely real eigenvalues occur in pairs.

Numerical Results

Validation of Linear Analysis

The object of this analysis is to identify regions where instability results from exponential growth as opposed to approximately linear drift. Results from a linear stability analysis are then useful if information is available

about what the linear range is. However, as indicated above, the linearized system has at most, *neutral* stability. Since a conclusion of neutral stability from linear analysis is usually a weak one by itself (the nonlinear system may be unstable by the usual stability definitions), validation of the results obtained through linear analysis is presented through numerical simulations using the "exact" nonlinear equations.

The numerical simulation results for a representative system are obtained and presented in the following format. First, the normalized nutation angle, θ_0 , is fixed at some value. Then for different values of the normalized precession rate, Ω , the equations of motion are solved numerically for a suitable time period. For each value of Ω , the initial values used for the system are the *same* small perturbation of steady state conditions. The common perturbation imparted at the start of each simulation was randomly generated. The normalized distance of the c.m. from its nominal position is taken to be a measure of the system's deviation from its steady motion. A surface plot with Ω and normalized time, τ , along two axes and the deviation of the center of mass along the third axis then shows those values of Ω for which the system shows exponential growth at the chosen value of θ_0 .

Figures 3 and 4 show the results obtained for the case when $A=1$. Although the linear analysis shows that the stability of the system is μ -independent, for the numerical simulation μ was chosen to be 1.5. For Fig. 3, θ_0 was chosen to be 0.5 while for Fig. 4, θ_0 was chosen to be 1.1. Finally, to verify μ -independence, provided ψ is consistent with Ω and θ_0 , a final simulation result is given in Fig. 5, for $\theta_0 = 1.1$ as in Fig. 4 but with $\mu=0.7$. Although the numerical results are not identical, the regions of exponential growth are seen to be the same, verifying the μ -independence. In these plots, approximately linear drift from equilibrium is observed in regions where the

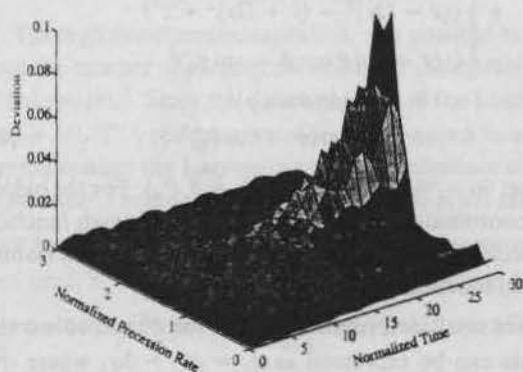


Fig. 3. Time simulation; $A=1, \mu=1.5, \theta_0=0.5$

linearized system has purely imaginary eigenvalues (cf., Figs 6-8).

Effect of Varying Parameters

Figures 3 - 5 can now be compared to the results from linear analysis. If the largest of the real parts of the eigenvalues of the linearized system is taken as a measure of instability, then the time response need not be plotted any more. Instead, that axis can now be used to plot the nominal coning angle, θ_0 . Thus, each surface plot gives a picture of the stability of the system for a range of values of Ω and θ_0 at a fixed value of A . A number of such surface plots for different values of A can then be expected to provide a reasonably complete picture of the system's behavior.

Figures 6, 7, and 8 show surface plots of the largest of the real parts of the eigenvalues of the linearized system. The precession rate Ω is varied from 0 to 3, while the coning angle θ_0 is varied from 0.01 to 1.57 (from close to 0 to just under $\pi/2$). A comparison of the eigen-

value (positive real part) surface plot for the case $A=1$ (i.e., Fig. 7), with the numerical results given in Figs. 3 - 5, shows perfect agreement between the two approaches. It is seen that significant qualitative changes

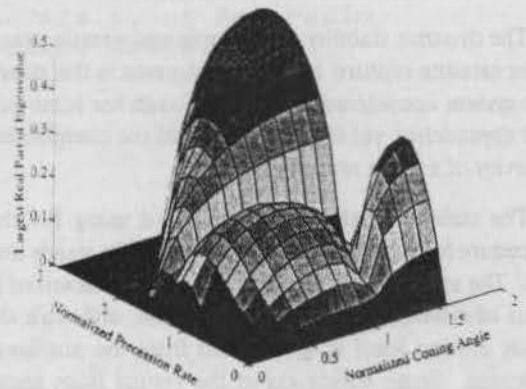


Fig. 6. Unstable regime for $A=0.3$

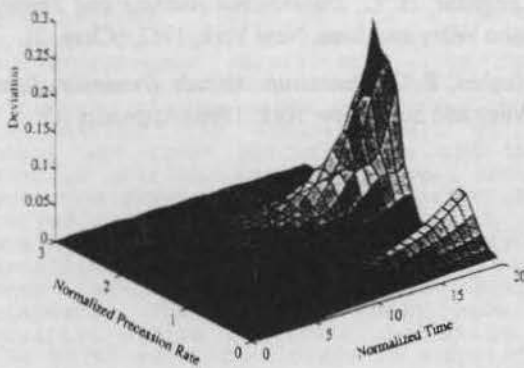


Fig. 4. Time simulation; $A=1, \mu=1.5, \theta_0=1.1$

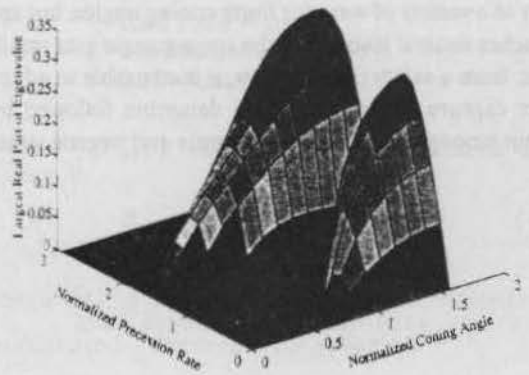


Fig. 7. Unstable regime for $A=1.0$

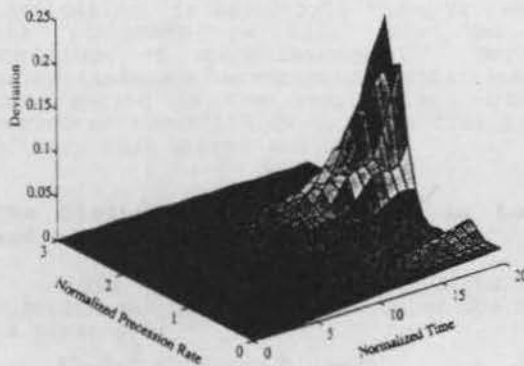


Fig. 5. Time simulation; $A=1, \mu=0.7, \theta_0=1.1$

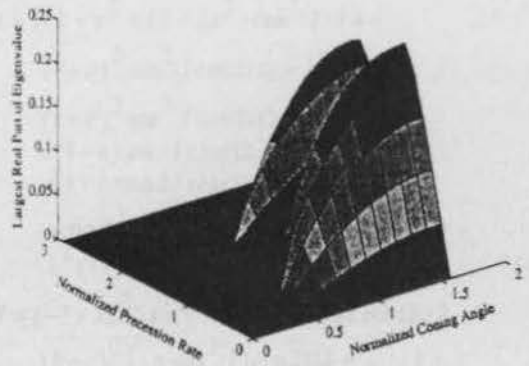


Fig. 8. Unstable regime for $A=5.0$

occur in the behavior of the system as the three nondimensional parameters A , Ω , and θ_0 are varied.

Summary & Conclusions

The dynamic stability of a grapple and wrestle strategy for satellite capture has been addressed in this paper. The system considered is simple enough for semi-analytic approaches, yet it exhibits most of the complicated behavior of a more realistic system.

The stability analysis was conducted using Routh's procedure for studying small deviations from steady motion. The stability results are for equations linearized in terms of deviations from steady motion, although the steady motion itself is determined from the nonlinear equations. Some validation of the results from linear analysis is presented through numerical solution of the nonlinear equations of motion for a few configurations.

The principal conclusion from the analysis is that the grapple and wrestle approach can lead to dynamic instability in a variety of ways for finite coning angles, but approaches neutral stability as the coning angle gets small. Thus, from a safety point of view, it is advisable to adopt other capture strategies (e.g., a detumble followed by despin strategy) rather than a grapple and wrestle strategy.

For future work, the problem of identifying patterns of stable behavior for different values of system parameters needs to be examined in detail. Another area for future investigation is the effects of slight asymmetry in the body.

References

1. Fitz-Coy, N. G., and Chatterjee, A., "Spacecraft Detumbling Through Energy Dissipation," *NASA CP-3186 (Proceedings of Flight Mechanics/Estimation Theory Symposium)*, 1992, pp. 23-37.
2. Goldstein, H., *Classical Mechanics, 2nd Ed.*, Addison Wesley, Reading, MA, 1980.
3. Pars, L. A., *A Treatise on Analytical Dynamics*, Heinemann Educational Books Ltd., London, 1965.
4. Fitz-Coy, N. G., and Chatterjee, A., "Stability of Rendezvous and Capture; The Pure Spin Case," In preparation for submission to the *Journal of the Astronautical Sciences*.
5. Langhaar, H. L., *Dimensional Analysis and Theory*, John Wiley and Sons, New York, 1952, (Chap. 2).
6. Hughes, P. C., *Spacecraft Attitude Dynamics*, John Wiley and Sons, New York, 1986 (Appendix A).

LONG-PERIOD PERTURBATIONS IN THE INCLINATION OF SUN-SYNCHRONOUS SATELLITES

Giorgio E.O. Giacaglia
 Polytechnical School - University of Sao Paulo
 05508-900, Sao Paulo, Brazil

Abstract

Performance of sun-synchronous satellites depends critically on lunar and solar perturbations in inclination, since a large change in this elements alters radically the motion of the ascending node and, therefore, the synchronism with the motion of the sun. A good knowledge of the perturbations affecting the inclination is, therefore of paramount importance for the purpose of mission planning. Of course, for very high satellites, the lunar and solar influences are so large that they could cause an enormous oscillations in the eccentricity, causing the satellite either to escape from the earth, to collide with the earth or the moon, or to be ejected from the gravitational field of the earth-moon system. This is not the case for usual sun-synchronous satellites, since their initial eccentricity is very small, so the attention of this paper is focused on the inclination. The dominant part of the solar and lunar perturbations and their average over the satellite's mean anomaly are considered, so that only major long-period and secular perturbations are evaluated. In fact, for sun-synchronous satellites, these perturbations are the ones which mostly interest mission planners. The sun and moon move in elliptic orbits and their inclination to the earth equatorial plane is supposed to be constant. The earth gravitational field includes zonal harmonics through J_2 and several possible resonances with tesseral and zonal harmonics are discussed. Due to luni-solar perturbations, corresponding to the arguments $j\omega' + k\Omega' + l(\Omega - \lambda')$, the very long period perturbation of the inclination, is about 5×10^{-2} deg/yr, while the six-month periodic term, has an amplitude of approximately 10^{-3} deg/yr. Major tesseral harmonics perturbations of long period in the inclination, with a period of about 550 days, arise from terms of very high degree and order.

The Disturbing Function due to Lunar and Solar Attractions

The main part of the disturbing function due to either the sun or the moon is given by ¹⁻⁵

$$R = \beta n^2 r^2 (a'/r')^3 P_2(\cos S) \quad (1)$$

where for the sun $\beta=1$ and for the moon $\beta=0.012$. In Eq. (1), one has the following definitions:

$$\begin{aligned} \cos S &= A \cos u + B \sin u \\ u &= \omega + f \\ A &= \cos \delta' \cos(\Omega - \alpha') \\ B &= -\cos \delta' \cos I \sin(\Omega - \alpha') + \sin \delta' \sin I \end{aligned} \quad (2)$$

Taking the equatorial plane as reference and the vernal equinox as the origin for the right ascension, considering ϵ to be either the obliquity of the ecliptic or the inclination of the lunar orbit to the earth equator, one has the usual relations:

$$\begin{aligned} \cos \delta' \cos \alpha' &= \cos \lambda' \\ \cos \delta' \sin \alpha' &= \sin \lambda' \cos \epsilon \\ \sin \delta' &= \sin \lambda' \sin \epsilon \end{aligned} \quad (3)$$

Secular and long-periodic terms are given by

$$R_S = \frac{1}{2\pi} \int_0^{2\pi} R dM \quad (4)$$

where M is the satellite's mean anomaly. The major terms of this averaged disturbing function are given by ²⁻⁵

$$\begin{aligned} R_S &= \beta n^2 a^2 (a'/r')^3 ((3A-2)(2+3e^2)/8 + \\ &+ 15e^2 (B \cos 2\omega + 2C \sin 2\omega)/8) \end{aligned} \quad (5)$$

where:

$$\begin{aligned} A &= ((2+s^2 + (2-3s^2)\cos^2 I)/4 + \\ &+ (1-c)^2 \sin^2 I \cos 2(\Omega + \lambda')/8 + \\ &+ (1+c)^2 \sin^2 I \cos 2(\Omega - \lambda')/8 + \\ &+ s(1-c) \sin 2I \cos(\Omega + 2\lambda')/4 - \\ &+ s(1+c) \sin 2I \cos(\Omega - 2\lambda')/4 + \\ &+ sc \sin 2I \cos \Omega / 2 + s^2 \sin^2 I \cos 2\Omega / 4 - \\ &+ s^2 (1-2\sin^2 I) \cos 2\lambda' / 4 \end{aligned} \quad (6)$$

$$\begin{aligned} B &= (-1+3c^2) \sin^2 I / 4 - sc \sin 2I \cos \Omega / 2 + \\ &+ (1-c)^2 (1+\cos^2 I) \cos 2(\Omega + \lambda')/8 + \\ &+ (1+c)^2 (1+\cos^2 I) \cos 2(\Omega - \lambda')/8 + \end{aligned}$$

$$s^2(1+\cos^2 I)\cos 2\Omega/4+3s^2\sin^2 I\cos 2\lambda'/2+s(1+c)\sin 2I\cos(\Omega-2\lambda')/4-s(1-c)\sin 2I\cos(\Omega+2\lambda')/4 \quad (7)$$

$$C = sc\sin I\sin \Omega/2 - s^2\cos I\sin 2\Omega/4 - ((1-c)^2\sin 2(\Omega+\lambda')+(1+c)^2\sin 2(\Omega-\lambda'))\cos I/8 + ((1-c)\sin(\Omega+2\lambda')-(1+c)\sin(\Omega-2\lambda'))s\sin I/4 \quad (8)$$

where $s = \sin \epsilon$, $c = \cos \epsilon$, $\eta = (1-e^2)^{1/2}$

From Lagrange's Planetary Equation given by

$$na^2\eta\sin I\frac{dI}{dt} = (\cos I\frac{\partial}{\partial \omega} - \frac{\partial}{\partial \Omega})R_s \quad (9)$$

it is found that

$$\frac{n\eta\sin I}{n^2}\frac{dI}{dt} = 15e^2\cos I(-2B\sin 2\omega+4C)/8 - 3\frac{\partial}{\partial \Omega}((2+3e^2)A/8+5e^2B\cos 2\omega/8+5e^2C\sin 2\omega/4) - 9e'\eta\cos(\lambda'-\varpi')\frac{\partial A}{4\partial \Omega} \quad (10)$$

where a/a' , e^2e' and higher powers of these quantities have been neglected. One notes that, for the sun, a/a' is about 0.0048 and for the moon is about 0.0187. Also, e' for the sun is 0.017 and for the moon 0.055, while a typical value of e for an earth observing sun-synchronous satellite is 0.002.

The complete expression for third-body perturbation of the satellite's inclination is given by Eq. (11) below:

$$\frac{16n}{3n^2\beta}\frac{dI}{dt} = D + \frac{2e^2(-10E\cos I+20F\cos I-eG-5H-10J)}{\eta\sin I} \quad (11)$$

where D , E , F , G , H and J are given below. β is equal to 1 for the sun and equal to approximately 0.012 ($m'/(m+m')$) for the moon. The values of the constants appearing in the equations are given in Table I. It should be noted that, for $e=0$, the motion of the node induced by the larger zonal harmonics is given by

$$d\Omega/dt = -1.5(a_e/a)^2nJ_2C_i(1+0.75(a_e/a)^2 \times J_2(3-5S_i^2/3)-0.625(a_e/a)^2(J_4/J_2) \times (7C_i^2-3))-0.75(n_i^2\beta_s+n_m^2\beta_m)C_i \times (1+1.5e^2)(1-1.5S_i^2)/n\eta\eta^3$$

where C_i and S_i stand for $\cos I$ and $\sin I$.

The above mentioned coefficients are:

$$D = (1-c)^2\sin(2\Omega+2\lambda')\sin I + (1+c)^2\sin(2\Omega-2\lambda')\sin I + 2s^2\sin I\sin 2\Omega - 2s(1+c)\cos I\sin(\Omega-2\lambda') + 2s(1-c)\cos I\sin(\Omega+2\lambda') + 4sc\cos I\sin \Omega + 1.5e'(1-c)^2\sin I\sin(2\Omega+3\lambda'-\varpi') - 1.5e'(1-c)^2\sin I\sin(2\Omega+\lambda'+\varpi') + 1.5e'(1+c)^2\sin I\sin(2\Omega-\lambda'-\varpi') - 1.5e'(1+c)^2\sin I\sin(2\Omega-3\lambda'+\varpi') + 3e's^2\sin I\sin(2\Omega-\lambda'+\varpi') + 3e's^2\sin I\sin(2\Omega+\lambda'+\varpi') - 3e's(1+c)\cos I\sin(\Omega-3\lambda'+\varpi') - 3e's(1+c)\cos I\sin(\Omega-\lambda'+\varpi') + 3e's(1-c)\cos I\sin(\Omega+\lambda'+\varpi') + 3e's(1-c)\cos I\sin(\Omega+3\lambda'+\varpi') + 6e'sc\cos I\sin(\Omega-\lambda'+\varpi') + 6e'sc\cos I\sin(\Omega+\lambda'+\varpi')$$

$$E = (1/4)(-1+3e^2)\sin^2 I\sin 2\omega + (1/16)(1-c)^2(1+\cos^2 I)(\sin(2\varpi+2\lambda') - \sin(2\Omega-2\omega+2\lambda')) + (1/16)(1+c)^2 \times (1+\cos^2 I)(\sin(2\varpi-2\lambda') - \sin(2\Omega-2\omega-2\lambda')) + (1/8)s^2(1+\cos^2 I)(\sin 2\varpi - \sin(2\Omega-2\omega) + (3/4)s^2\sin^2 I(\sin(2\omega+2\lambda') + \sin(2\omega-2\lambda')) + 0.25s(1+c)\sin I\cos I \times (\sin(\Omega+2\omega-2\lambda') - \sin(\Omega-2\omega-2\lambda')) + 0.25s(1-c)\sin I\cos I \times (\sin(\Omega-2\omega+2\lambda') - \sin(\Omega+2\omega+2\lambda')) - 0.5sc\sin I\cos I(\sin(\Omega+2\omega) - \sin(\Omega-2\omega))$$

$$F = -(1/8)s^2\cos I(\sin 2\varpi - \sin(2\Omega-2\omega)) + 0.25sc\sin I(\sin(\Omega+2\omega) + \sin(\Omega-2\omega)) - (1/16)(1-c)^2\cos I(\sin(2\varpi+2\lambda') + \sin(2\Omega-2\omega+2\lambda')) - (1/16)(1+c)^2\cos I \times (\sin(2\varpi-2\lambda') + \sin(2\Omega-2\omega-2\lambda')) + (1/8)s(1-c)\sin I(\sin(\Omega+2\omega+2\lambda') + \sin(\Omega-2\omega+2\lambda')) - (1/8)s(1+c)\sin I \times (\sin(\Omega+2\omega-2\lambda') + \sin(\Omega-2\omega-2\lambda'))$$

$$G = -0.25\sin^2 I((1-c)^2\sin(2\Omega+2\lambda') + (1+c)^2\sin(2\Omega-2\lambda') + 2s^2\sin 2\Omega) + 0.25s\sin 2I((1+c)\sin(\Omega-2\lambda') - (1-c)\sin(\Omega+2\lambda') - 2c\sin \Omega)$$

$$H = -(1/8)(1 + \cos^2 I)((1-c)^2 (\sin 2(\varpi + \lambda') + \sin 2(\Omega - \omega + \lambda') + 2 \sin 2\varpi + 2 \sin 2(\Omega - \omega)) + (1+c)^2 (\sin 2(\varpi - \lambda') + \sin 2(\Omega - \omega - \lambda')) - (1/8)s \sin 2I((1+c)(\sin(\Omega + 2\omega - 2\lambda') + \sin(\Omega - 2\omega - 2\lambda')) - (1-c)(\sin(\Omega + 2\omega + 2\lambda') + \sin(\Omega - 2\omega + 2\lambda'))) + (1/4)sc \sin 2I(\sin \varpi + \sin(\Omega - \omega))$$

$$J = 0.25s^2 \cos I(\sin(2\Omega - 2\omega) - \sin 2\varpi) + 0.25sc \sin I(\sin(\Omega + 2\omega) - \sin(\Omega - 2\omega)) - (1/8)(1-c)^2 \cos I(\sin(2\varpi + 2\lambda') - \sin(2\Omega - 2\omega + 2\lambda')) - (1/8)(1+c)^2 \times \cos I(\sin(2\varpi - 2\lambda') - \sin(2\Omega - 2\omega - 2\lambda')) + (1/8)s(1-c) \sin I(\sin(\Omega + 2\omega + 2\lambda') - \sin(\Omega - 2\omega + 2\lambda')) - (1/8)s(1+c) \sin I \times (\sin(\Omega + 2\omega - 2\lambda') - \sin(\Omega - 2\omega - 2\lambda'))$$

For a sunsynchronous satellite one has the approximate relation $d\Omega/dt = n'$.

TABLE I - Constant Parameters for the Moon and Sun

	SUN	MOON
n'	$360^\circ / \text{yr}$	$360^\circ / 27.321 \text{ days}$
e'	0.017	0.055
ϵ	23.45°	5.15°
β	1	0.01234
a'	$150 \times 10^6 \text{ km}$	$385 \times 10^3 \text{ km}$
$d\omega'/dt$	-	0.008573 n'
$d\Omega'/dt$	-	-0.003999 n'
$\beta n'^2/n$	6.93×10^{-2}	$1.549 \times 10^{-1} \text{ (deg/yr)}$

The orbital expansion induced by the oblateness of the earth is given by ²

$$a = \left(\frac{\mu}{n^2}\right)^{1/3} (1 + 0.25J_2(a_e/a)^2(1 - 3\cos^2 I - 0.25J_2(a_e/a)^2(11 - 126(\cos^2 I + \cos^4 I))) \quad (19)$$

while the solar and lunar perturbations do not introduce any measurable amplification or contraction ⁵. For a ground repeating track period of 19 days (270 days repeating orbit), and for $e=0$, one finds the following values:

$$a = 7201.36 \text{ km}, I = 98.725 \text{ deg.}$$

The fundamental adopted values are ³⁻⁴⁻⁶:

$$\mu = 398\,600.9 \text{ km}^2 \text{ s}^{-2}$$

$$\begin{aligned} a_e &= 6\,378.135 \text{ km} \\ J_2 &= 1\,082.64 \times 10^{-6} \\ J_3 &= -2.55 \times 10^{-6} \\ J_4 &= -1.65 \times 10^{-6} \\ J_5 &= -0.21 \times 10^{-6} \end{aligned} \quad (20)$$

Very long period perturbations

The total amplitude of very long period terms in dI/dt is given by the coefficients of terms with argument

$$j\varpi' + k\Omega' + l(\Omega - \lambda')$$

since, even for the moon, ϖ' and Ω' are very long periodic arguments as compared with the period of the satellite. For such terms, the collected coefficients are given in Table 2 below.

TABLE 2 - Numerical Values of Perturbing Terms in dI/dt

ARGUMENT	COEFFICIENT	VALUE (deg/yr)
$2\Omega - 2\lambda'$	$\frac{3(n_s^2(1+c_s)^2 + \beta_m n_m^2(1+c_m)^2) \sin I}{16n}$	4.724×10^{-2}
$\Omega - \lambda' - \varpi'$	$\frac{9(n_s^2 e'_s s_s (1+c_s) + \beta_m n_m^2 e'_m s_m (1+c_m)) \cos I}{16n}$	0.773×10^{-4}
$\Omega - \lambda' + \varpi'$	$\frac{9(n_s^2 e'_s s_s c_s + \beta_m n_m^2 e'_m s_m c_m) \cos I}{16n}$	0.333×10^{-5}
$2\Omega - 2\lambda'$	$\frac{9e^2(n_s^2(1+c_s)^2 + \beta_m n_m^2(1+c_m)^2) \sin I}{32n(1-e^2)^{1/2}}$	2.834×10^{-5}

Terms pertaining to the sun and moon have been added, despite a possible phase shift, since one is interested in the maximum amplitude in the perturbations. Adding these terms, one finds for the maximum amplitude of the very long terms in dI/dt the value $4.735 \times 10^{-2} \text{ deg/yr}$.

Six-month perturbations in dI/dt

In Table 3 the larger six-month period terms have been collected.

They show a maximum total amplitude of about $2.532 \times 10^{-4} \text{ deg/yr}$. The eccentricity e of the satellites in all calculations has been taken equal to 0.002.

TABLE 3 - Six months perturbations in dl/dt

ARGUMENT	COEFFICIENT	VALUE (deg/yr)
2Ω	$\frac{3(n_s^2 s_s + \beta_m n_m^2 s_m) \sin I}{8n}$	1.753×10^{-4}
2Ω	$\frac{9e^2 \sin I (n_s^2 s_s^2 + \beta_m n_m^2 s_m^2)}{16n(1-e^2)^{1/2}}$	0.517×10^{-6}
$\Omega + \lambda' + \omega'$	$\frac{9(n_s^2 e'_s s_s (1-c_s) + \beta_m n_m^2 e'_m s_m (1-c_m)) \cos I}{16n}$	0.333×10^{-5}
$\Omega + \lambda' - \omega'$	$\frac{9(n_s^2 e'_s s_s c_s + \beta_m n_m^2 e'_m s_m c_m) \cos I}{8n}$	0.740×10^{-4}

Perturbations due to Tesseral and Zonal Harmonics

The inclination is affected by all zonal harmonics. The largest terms are given by Eq. (21):

$$\delta I = \frac{e \cos I}{1-e^2} (P \cos 2\omega + Q \sin \omega + R \sin 3\omega) \quad (21)$$

where

$$P = -\frac{ea_e^2 \sin I (2J_2 (1-15 \cos^2 I) + 5 \frac{J_4}{J_2} (1-7 \cos^2 I))}{16(1-e^2)(1-5 \cos^2 I)a^2} \quad (22)$$

$$Q = \frac{5}{32} \left(\frac{ae}{a} \right)^3 \frac{J_5}{J_2} \frac{3e^2 + 4}{(1-e^2)^2} (1-4 \cos^2 I - \frac{24 \cos^4 I}{1-5 \cos^2 I}) + 2 \frac{ae}{a} \frac{J_3}{J_2} \quad (23)$$

$$R = -\frac{315e^2}{192(1-e^2)^2} \left(\frac{ae}{a} \right)^3 \frac{J_5}{J_2} \times (1-5 \cos^2 I - \frac{16 \cos^4 I}{1-5 \cos^2 I}) \quad (24)$$

It is important to verify whether any important resonance with the earth potential field is present. From a linear perturbation theory¹, a harmonic of degree l and order m generates terms with arguments

$$(l-2p+q)M + (l-2p)\omega + m(\Omega - \theta)$$

where $p=0,1,2,\dots,l$ and $m \in R$. After integration, the corresponding denominator is

$$D = (l-2p+q)dM/dt + (l-2p)d\omega/dt + md(\Omega - \theta)/dt$$

For the sun-synchronous satellite, one has

$$n_\Omega = d\Omega/dt = n' = 1.14077106 \times 10^{-5} \text{ deg/sec}$$

$$n_\theta = d\theta/dt = 4.166666 \times 10^{-3} \text{ deg/sec}$$

$$n = dM/dt = 5.9210526 \times 10^{-2} \text{ deg/sec}$$

Since the corresponding term² is factored by $e^{|q|}$, the relevant terms correspond to $q=0$. One may also assume, for the purpose of this calculation, that $n+n\omega \approx n$. The repeating ground track is every 19 days and every 270 orbital periods. Then the nodal period is $(19/270)(2\pi/(n_\theta - n_\Omega))$, while the anomalistic period is 19/270 days. Resonance for $e=0$ occurs when $\alpha n = \beta(n_\theta - n_\Omega)$ for α, β relative primes. In the present case, one has

$$\frac{\beta}{\alpha} = \frac{n}{n_\theta - n'} \approx 14.249539 \approx 14.25 = \frac{57}{4}$$

so that $\alpha=4, \beta=57$. The resonant terms correspond to

$$|l-2p| = \gamma \alpha = 4\gamma, \quad m = \gamma \beta = 57\gamma, \quad \text{for } \gamma=1, 2, 3, \dots$$

In decreasing order of importance, the resonant harmonics are, therefore:

- a) $l = \beta + 1 = 58, m = \beta = 57, p = (\beta - \alpha + 1)/2 = 27$
 - b) $l = \beta + 3 = 60, m = \beta = 57, p = (\beta - \alpha + 3)/2 = 28$
 - c) $l = 62, m = 57, p = 29$
- etc.

To a lesser degree of resonance, one could assume

$$\beta/\alpha \approx 56/4 = 14/1$$

so that some large terms could arise from the following harmonics:

- a') $l = 15, m = 14, p = 7.$
 - b') $l = 17, m = 14, p = 8.$
 - c') $l = 19, m = 14, p = 9,$
- etc.

For the dominant term (a) one has

$$D = 4n - 57(n_\theta - n') = 7.648 \times 10^{-6} \text{ deg/sec}$$

and the corresponding period is

$$P = \frac{360}{D} \text{ sec} = \frac{0.1}{24D} \text{ days} = 545 \text{ days}$$

All other terms (b), (c), ..., have the same period but decreasing amplitudes. For the weaker resonance condition, the dominant term (a') corresponds to

$D = n - 14(n_0 - n') = 1.0369028 \times 10^{-3}$ deg/sec and $P = 4$ days, a very short period. Shallower resonances correspond to the approximation

$$\beta/\alpha = 14.3 = 43/3 \quad (m=3, l=43, 45, 47, \text{etc}),$$

$$\beta/\alpha = 14.2 = 71/5 \quad (m=5, l=71, \text{etc})$$

and so on, but they correspond to very short periods. Thus, the deepest resonance comes from terms of order $m=57$ and degrees $l=58, 60, 62, \dots$ with the corresponding values $p=27, 28, 29, \dots$

The contribution of the (58,57) harmonic corresponds to an amplitude given by

$$\frac{dI}{dt} = nJ_{58,57} (a_e/a)^{58} F_{58,57,28}(I) \frac{57-4 \cos I}{\sin I} \quad (25)$$

where $J_{58,57} = (C_{58,57}^2 + S_{58,57}^2)^{1/2}$. A computation performed at The University of Texas by Prof. Schutz⁸ gives to $F_{58,57,27}$ the normalized value of 0.25157 for an inclination of $98^\circ.725$. The order of magnitude of $J_{58,57}$ is about 10^{-9} so that the all thing amount to $dI/dt = 5 \times 10^{-9}$ deg/rev approximately

For any values of l, m, p the equation for the perturbation in inclination is

$$\frac{dI}{dt} = nJ_{lm} (a_e/a)^l F_{lmp}(I) \frac{\alpha \cos I - \beta}{\sin I} \sin \Psi_{\alpha\beta} \quad (26)$$

where $\Psi_{\alpha\beta} = \alpha(M + \omega) + \beta(\Omega - \theta) + \gamma_{lm}$, and

γ_{lm} is a phase constant.

Terms factored by the eccentricity with general argument

$$\Psi_{lmpq} = (l-2p)\omega + (l-2p+q)M + m(\Omega - \theta)$$

correspond to $q = \pm 1$, and considering only long period perturbations $l-2p+q = 0$. In the case under consideration one may assume

$$\begin{aligned} d\omega/dt &= -\frac{3nJ_2 a_e^2}{4a^2(1-e^2)} (1-5\cos^2 I) \cong \\ &\cong -1.671 \times 10^{-5} \text{ deg/sec} \end{aligned}$$

so that the associated period is about 250 days. Also

$$d(\Omega - \theta)/dt \cong -4.15526 \times 10^{-3} \text{ deg/day}$$

with an associated period of 1.0027 days.

Therefore only zonal perturbations ($m=0$) will give the largest contribution over a long period of time. Taking $m=0$ and $l-2p = \pm 1$ the corresponding denominator is given by $(l-2p)d\omega/dt = \pm d\omega/dt$, with corresponding period given by

$$2\pi/\omega \cong 250 \text{ days.}$$

Long period terms with period of about 250 days may therefore arise from odd zonal harmonics. For the inclination, one has the amplitude¹

$$\Delta I_{10pq} = -\frac{\mu J_1 a_e^l F_{10p}(I) G_{1pq}(e)(l-2p) \cos I}{na^{l+3} (1-e^2)^{1/2} \sin I}$$

and for $l-2p = \pm 1$, $e \cong 0.002$, one finds

$$\Delta I_{10pq} = 9.0816371 \times 10^{-3} (0.88568)^l J_{1q} F_{10p}(I) G_{1pq}(e) \text{ deg/sec}$$

As an example consider $l=3$, $p=1, 2$, $q=+1$ and -1 . Table 4 gives the corresponding F and G functions up to e^3 . The F functions are in closed forms.

TABLE 4 - F and G Functions

l	p	q	F	G
3	1	1	$\frac{15}{16} \sin^3 I - \frac{3}{4} \sin I$	$3e + \frac{11}{4} e^3 + \dots$
3	1	-1	"	$e(1-e^2)^{-5/2}$
3	2	1	$-\frac{15}{16} \sin^3 I + \frac{3}{4} \sin I$	"
3	2	-1	"	$3e + \frac{11}{4} e^3$

Assuming the value $J_3 \cong -2.5 \times 10^{-6}$ and using the relation

$$\Delta I = 360 \Delta i / 2\pi q \omega \text{ deg}$$

where

$$\Delta I_{30pq} = -1.5773 \times 10^{-8} q F_{30p} G_{3pq}$$

one finds the values presented in Table 5.

TABLE 5 - 250 days period perturbations in Inclination

l	p	q	$10^4 \Delta I_{10pq}$ (deg/yr)	$10^5 \Delta I_{10pq}$ (deg/250 days)
3	1	1	+4.9	+5.3
3	1	-1	-1.6	-1.7
3	2	1	-1.6	-1.7
3	2	-1	+4.9	+5.3

Thus, for J_3 the amplitude in I with a period of about 250 days is about

$$\Delta I \cong 7.2 \times 10^{-5} \text{ deg while } \Delta \dot{I} \cong 6.6 \times 10^{-4} \text{ deg/yr}$$

Conclusions

Due to luni-solar perturbations, the very long periodic change in inclination is given by

$$dI/dt = \frac{3\sin I (n_s^2 (1 + \cos \epsilon)^2 + \beta (1 + \cos I_m)^2)}{16n} \cong 4.735 \times 10^{-2} \text{ deg/yr}$$

$$(\beta \cong 0.0123; \epsilon \cong 23^\circ 27'; I_m \cong 5^\circ)$$

There is a six-month periodic term with amplitude given by

$$\begin{aligned} \frac{dI}{dt} = & \frac{6n_s^2 \sin \epsilon (\sin \epsilon + 3e_s (1 - \cos \epsilon) \cos I)}{16n} + \\ & \frac{18n_s^2 \sin \epsilon (e_s \cos \epsilon \cos I + e^2 \sin \epsilon \sin I)}{16n} + \\ & \frac{9\beta n_m^2 e_m \sin I_m (2 \cos I_m + (1 - \cos I_m) \cos I)}{16n} + \\ & \frac{9\beta n_m^2 e^2 \sin^2 I_m \sin I}{16n} \cong 2.532 \times 10^{-4} \text{ deg/yr} \end{aligned}$$

Long period perturbations due to tesseral harmonics have a period of about 550 days and an amplitude given by

$$\begin{aligned} dI/dt = & nJ_{58,57} \left(\frac{a_e}{a}\right)^{58} F_{58,57,27}(I) \frac{57-4 \cos I}{\sin I} \\ \cong & 5 \times 10^{-9} \text{ deg/rev} \end{aligned}$$

Long period terms for the inclination, with period of about 250 days due to zonal harmonics have an amplitude given by

$$\frac{dI}{d\omega} = \frac{e}{1-e^2} \cos I (-2P \sin 2\omega + Q \cos \omega + 3R \cos 3\omega)$$

where P, Q, R are given by Eqs. (22), (23) and (24), and ²⁻⁷

$$\begin{aligned} d\omega/dt \cong & -\frac{3nJ_2 a_e^2}{4a^2 (1-e^2)} (1 - 5 \cos^2 I) \cong \\ & -1.671 \times 10^{-5} \text{ deg/sec} \end{aligned}$$

Since to a first approximation² one has:

$$\frac{d\Omega}{dt} = -\frac{3}{2} n (a_e/a)^2 J_2 \cos I$$

the deviation from sun-synchronism is given by the relation:

$$\frac{d}{dt} \Omega = \frac{3}{2} n (a_e/a)^2 J_2 \sin I \frac{dI}{dt}$$

which can be evaluated using the above derived equations for dI/dt . Considering the values³

$$a = 7201360 \text{ km}$$

$$a_e = 6378.135 \text{ km}$$

$$I = 98^\circ 725$$

$$n = 5.9210526 \times 10^{-2} \text{ deg/sec } (P = 1\text{h } 4\text{min})$$

$$J_2 = 1082.63 \times 10^{-6}$$

one finds for the coefficient of dI/dt in $d\Omega/dt$ the value $7.36916 \times 10^{-5} \text{ deg/sec}$ or 0.448 deg/rev or $2.3255 \times 10^3 \text{ deg/yr}$.

References

- 1 Kaula, W.M., Theory of Satellite Geodesy, Blaisdell Publ. Co. Waltham-Toronto-London, 1966, 124 p.
- 2 Brouwer, D. and Clemence, G. M., Methods of Celestial Mechanics, Academic Press, New York, London, 1961, 598 p.
- 3 Melbourne, W. G. et alii, Constants and Related Informations for Astrodynamics Calculations, 1968. NASA TR 32-1306, Pasadena, California, 1968. 57 p.
- 4 Lundquist, C.A. and Veis, G. (Edit.) Geodetic Parameters for a 1966 Smithsonian Institution Standard Earth, vol. I, SAO Special Report N. 200, 1966. 231 p.
- 5 Giacaglia, G.E.O., Third Body Perturbations on Satellites. Artificial Satellite Theory Workshop, U.S. Naval Observatory, Washington, D.C. Nov. 8-9, 1993.
- 6 Lerch, F.J. et alii, Geopotential Models of the Earth: GEM-T3 and GEM-T3S, NASA TM 104555, 1992. 108 p.
- 7 Alfried, T. Review of Status of Analytical Satellite Theories, Artificial Satellite Theory Workshop, U.S. Naval

Observatory, Washington, D.C., Nov. 8-9, 1993.

⁸Schutz, B. (Private communication), Dec. 1993

Acknowledgments

The author acknowledges the financial support given by Dr. Pavel Rosenfeld of INPE and by the Escola Politécnica of the University of São Paulo for the participation in this International Symposium.

THE DETERMINATION OF NAVIGATION INFORMATION FOR SPACE VEHICLE BY GPS(OR INS)/ EQUATIONS OF MOTION

Nan Ying

Chen Shilu Lu Xuefu

College of Astronautics, Northwestern Polytechnical University
Xi'an, 710072, People's Republic of China

Abstract

Based on the normal trajectory of aeroassisted orbital transfer, the paper gives a new navigation scheme for the space vehicle: Navigation hardware / Equation of Motion (EM) . GPS / EM, INS / EM are studied for the vehicle to determine the navigation information (such as position velocity, attitude, and so on) during aeroassisted orbital transfer. Supersonic aerodynamic calculation formulas are introduced to deduce the equations of the filter and observation for the hybrid navigation systems. The numerical results show that the navigation precision of GPS (or INS) / EM are more higher than the one of single EM, GPS(or INS). The GPS(or INS) / EM has more redundancy than the single GPS(or INS).

Key Words: Space vehicle, Orbit and attitude determination, Equations of motion, GPS, INS, Numerical method

Introduction

It is an important problem for the navigation system of the space vehicle to increase the information redundancy. In generally, there are three kinds of methods to obtain the information redundancy. The hardware redundancy is restrictedly used in space vehicle because of a lot of hardware equipments and expensive cost.

In theory, analytical (and mix) redundancy can make up the defect of hardware redundancy. However, analytical (and mix) redundancy are

based on the system mathematic models. The navigation precisions become decreased because of the errors of the mathematic models. To make up the shortcoming of the analytical redundancy, this paper gives a navigation hardware / EM to estimate the errors in the system mathematic models. Because the estimated errors are introduced to the equations of motion, the navigation precision of analytical redundancy become increased.

The Equations of Motion and the Approximate Solution of Disturbance Equation during Aeroassisted Orbit Transfer

In theory, Equations of motion can accurately estimate the 6-radom navigation. However, the EM always neglect a lot of stochastic disturbances existing in the realistic flight environment. So, the trajectories integrated from the ideal EM deviate from the real trajectories. These disturbances include: error of drag coefficient ΔC_D , and of lift coefficient ΔC_L , errors of aerodynamic pressure center ΔX_T , ΔY_T , ΔZ_T , errors of kinds of aerodynamic moment derivatives $\Delta m_x^{\delta x}$, $\Delta m_x^{\omega x}$, $\Delta m_y^{\omega x}$, $\Delta m_y^{\omega y}$, $\Delta m_z^{\delta z}$, $\Delta m_z^{\omega z}$, $\Delta m_z^{\omega x}$, errors of the inertia ΔI_x , ΔI_y , ΔI_z , error of Earth gravitation acceleration Δg , and of the atmospheric density $\Delta \rho$, horizontal wind W . The first fifteen disturbances are supposed to be the functions of Mach number, the appearance parameters of the

vehicle, the position, velocity and attitude of the vehicle. Wind W is supposed to be the Gauss white noise of zero mean. $\Delta\rho$ and Δg are the functions of flight height of the vehicle. There are the other errors in estimating the navigation information by EM, such as: the integration errors.

The Equations of Motion of Space Vehicle

The equations of mass center motion are:

$$\left\{ \begin{aligned} \frac{dV}{dt} &= -\frac{\rho V^2 C_D}{2m} - g \sin \gamma \\ &+ \omega_x^2 r \cos \varphi (\cos \varphi \sin \gamma - \sin \psi \sin \varphi \cos \gamma) = f_1 \\ V \frac{d\gamma}{dt} &= \frac{SC_L \rho V^2 \cos \alpha}{2m} - g \cos \gamma + \frac{V^2}{r} \cos \gamma \\ &+ 2\omega_x V \cos \psi \cos \varphi + \omega_x^2 r \cos \varphi (\cos \gamma \cos \varphi \\ &+ \sin \gamma \sin \psi \sin \varphi) = f_2 \\ V \frac{d\psi}{dt} &= \frac{SC_L \rho V^2 \sin \alpha}{2m} - \frac{V^2}{r} \cos \gamma \sin \varphi \cos \psi \\ &+ 2\omega_x V (t g \gamma \sin \psi \cos \varphi - \sin \varphi) \\ &- \frac{\omega_x^2 r}{\cos \gamma} \cos \psi \sin \varphi \cos \varphi = f_3 \\ \frac{dr}{dt} &= V \sin \gamma = f_4 \\ \frac{d\theta}{dt} &= \frac{V \cos \gamma \cos \psi}{r \cos \varphi} = f_5 \\ \frac{d\varphi}{dt} &= \frac{V \cos \gamma \sin \psi}{r} = f_6 \end{aligned} \right. \quad (1)$$

The equations of attitude motion are:

$$\left\{ \begin{aligned} I_x \frac{d\omega_x}{dt} &= (I_y - I_z) \omega_y \omega_z - I_{yz} (\omega_y^2 - \omega_z^2) \\ &- I_{xy} (\omega_x + \omega_x \omega_y) - I_{xz} (\omega_x - \omega_y \omega_z) \\ &+ 0.5 \rho V^2 S l (m_z^2 \delta_z + m_x^2 \omega_x + C_x \Delta Z_T \\ &+ C_z \Delta Y_T) = f_7 \\ I_y \frac{d\omega_y}{dt} &= (I_x - I_z) \omega_x \omega_z - I_{xz} (\omega_x^2 - \omega_z^2) \\ &- I_{xy} (\omega_x + \omega_y \omega_z) - I_{yz} (\omega_x - \omega_y \omega_z) \\ &+ 0.5 \rho V^2 S l (m_y^2 \omega_y + m_z^2 \omega_z + C_x \Delta Z_T \\ &+ C_z \Delta X_T) = f_8 \\ I_z \frac{d\omega_z}{dt} &= (I_x - I_y) \omega_x \omega_y - I_{xy} (\omega_x^2 - \omega_y^2) \\ &- I_{xz} (\omega_x + \omega_x \omega_y) - I_{yz} (\omega_x - \omega_y \omega_z) \end{aligned} \right. \quad (2)$$

$$\left\{ \begin{aligned} &+ 0.5 \rho V^2 S l (m_z^2 \delta_z + m_z^2 \omega_z + m_z^2 \alpha \\ &+ C_z \Delta Y_T + C_y \Delta X_T) = f_9 \\ \dot{\Theta} &= \omega_y \sin \Gamma + \omega_x \cos \Gamma = f_{10} \\ \dot{\Phi} &= (\omega_x \cos \Gamma - \omega_y \sin \Gamma) / \cos \Theta = f_{11} \\ \dot{\Gamma} &= \omega_x - t g \Theta (\omega_y \cos \Gamma - \omega_x \sin \Gamma) = f_{12} \end{aligned} \right.$$

Angle of attack α , side-slip angle β and bank angle σ obey the following equations:

$$\left\{ \begin{aligned} \sin \gamma &= \sin \Phi \cos \alpha \cos \beta - \cos \Gamma \cos \Theta \sin \alpha \cos \beta \\ &- \sin \Gamma \cos \Theta \sin \beta \\ \cos \sigma &= (\sin \Theta \sin \alpha + \cos \Gamma \cos \Theta \cos \alpha) / \cos \alpha \\ \sin(\psi - \Phi) &= \sin \Gamma \sin \alpha \cos \beta - \cos \Gamma \sin \beta / \cos \gamma \\ \rho &= \rho_0 \exp(-h/B_T), \quad g = g(r_0/r)^2, \\ r &= r_0 + h \end{aligned} \right. \quad (3)$$

in above equations (1)~(3), V —the velocity of the vehicle, γ —flight path angle, ψ —heading, r —radial distance from center of the planet, ω_x —the angular velocity of the Earth, θ —longitude, φ —latitude, m —mass of the vehicle, ω_x , ω_y and ω_z —the angular velocity of the vehicle round the vehicle body-axis x_1 , y_1 and z_1 , respectively, I_x , I_y and I_z —the inertia of the vehicle round the body-axis x_1 , y_1 and z_1 , respectively, I_{xy} , I_{xz} and I_{yz} —the inertia product, Θ , Φ and Γ —the Euler angles of the vehicle, ρ_0 , g_0 , r_0 are respectively the atmospheric density, gravitation acceleration and the radius of the Earth at the sea level. The flight velocity during the aeroassisted orbital transfer in the atmosphere is more large than 7km/s. It is a course of high supersonic, large angle-of-attack, and sharp variation of the atmospheric density, so the aerodynamic characteristic is very complex. Aerodynamic lift and drag coefficients and moment derivatives can be approximately by the following equations.

Lift coefficient and drag coefficient are:

$$C_N = (1 + \frac{1}{\sqrt{M^2 - 1}}) (0.0292\alpha - 0.207) \quad (5)$$

$$C_D = (1 + \frac{1}{\sqrt{M^2 - 1}}) (6.21 \times 10^{-4} \alpha^2 - 6.16 \times 10^{-3} \alpha + 0.0785) \quad (6)$$

where, M is the Mach number, $M = V/a$, a is

velocity of sound.

The pitching damping moment derivative, static steady moment derivative and operation moment are respectively represented by

$$m_z^{\omega_z} = (1 + \frac{1}{\sqrt{M^2 - 1}}) (0.00193 \omega_z + 0.043) \quad (7)$$

$$m_z^{\alpha} = -0.0016(\alpha - 10^\circ) (1 + \frac{1}{\sqrt{M^2 - 1}}) \quad (8)$$

$$m_z^{\delta_z} = C_{LW}^* n K_q (K_{\infty})_w \frac{S_w}{S} (\bar{X}_G - \bar{X}_T) \quad (9)$$

where, $C_{LW}^* = 2.4\alpha$, n —operation efficiency of steering plane, K_q , $(K_{\infty})_w$ —interference factor, S_w —area of a wing, \bar{X}_G , \bar{X}_T —the position of the mass center, the position of the aerodynamic pressure center (nondimension).

Longitudinal damping moment derivative and operation moment, are respectively:

$$m_x^{\omega_x} = \frac{13C_L^*}{Vl} \exp(-\sqrt{M^2 - 1}) \frac{S}{S_{sh}} (l/l_{sh})^2 \quad (10)$$

$$m_x^{\delta_x} = -\frac{\lambda_f}{4} \cos \chi_f - \bar{l}_f^2 (L + N \bar{l}_f) \xi_s \quad (11)$$

where, subscript 'sh' represents vehicle body, λ_f —the ratio of span and chord of aileron, χ_f —sweep angle, \bar{l}_f —relative aileron length, ξ_s —experience correct coefficient, and

$$L = \frac{0.02}{\lambda_f \sqrt{M^2 - 1}}, \quad N = \frac{0.01}{\lambda_f \sqrt{M^2 - 1}}$$

equation (10) is obtained by the ratio of wingroot and wingtip $\eta = 3$.

Intersect moment derivative is:

$$m_y^{\omega_y} = 256 \left(\frac{1}{\eta}\right)^3 \left[\beta \lambda \left(1 + \frac{1}{\eta}\right) - \frac{1}{\eta}\right] / 3\pi \beta^2 \lambda^3 \left(1 + \frac{1}{\eta}\right)^4 \frac{S_l}{S_w b} \quad (12)$$

where, $\beta = \sqrt{M^2 - 1}$, λ —the ratio of the span and chord of wing.

Crossrange damping moment derivative $m_y^{\omega_y}$

is

$$m_y^{\omega_y} = k m_x^{\omega_x} \quad (13)$$

where, $k \approx \text{constant}$.

Disturbance Equation and Its Solution

The 6-radom disturbance equation of the space vehicle can be written as:

$$\Delta \dot{X}_1 = A \Delta X_1 + B \Delta U \quad (14)$$

where,

$$\Delta X_1 = \{\Delta V, \Delta \gamma, \Delta \psi, \Delta r, \Delta \theta, \Delta \phi, \Delta \omega_x, \Delta \omega_y, \Delta \omega_z, \Delta \Theta, \Delta \Phi, \Delta \Gamma\} \\ = \{\Delta x_1, \Delta x_2, \dots, \Delta x_{12}\}$$

$$\Delta U = \{\Delta C_N, \Delta C_X, \Delta X_T, \Delta Y_T, \Delta Z_T,$$

$$\Delta m_x^{\delta_z}, \Delta m_x^{\omega_z}, \Delta m_y^{\delta_z}, \Delta m_y^{\omega_z},$$

$$\Delta m_z^{\delta_z}, \Delta m_z^{\omega_z}, \Delta m_z^{\delta_x}, \Delta I_x, \Delta I_y, \Delta I_z,$$

$$\Delta g, \Delta \rho, W\} = \{\Delta u_1, \Delta u_2, \dots, \Delta u_{18}\}$$

The elements of A and B can be calculated by

$$a_{ij} = \frac{\partial f_i}{\partial x_j} \quad i = 1, 2, \dots, 12, \\ j = 1, 2, \dots, 18 \quad (15)$$

$$b_{ij} = \frac{\partial f_i}{\partial u_j} \quad i = 1, 2, \dots, 12, \\ j = 1, 2, \dots, 18 \quad (16)$$

Being calculated by the predetermined normal trajectory and "fixed" hypothesis, a_{ij} and b_{ij} approximately equal to constant in a certain time. So, equation (14) becomes a constant coefficient linear differential equation. The solution of equation (14) is

$$\Delta X_1(t) = L^{-1} [(SI - A)^{-1}] \Delta X_1(t_0) \\ + L^{-1} [(SI - A)^{-1} B \Delta U] \quad (17)$$

where, L^{-1} —Laplace inverse transformation, I —unit matrix. As ΔU slowly varies with time, equation can be rewritten as

$$\Delta U = \{L^{-1} [(SI - A)^{-1} B]\}^{-1} \{\Delta X_1(t) \\ - L^{-1} [(SI - A)^{-1}] \Delta X_1(t_0)\} \quad (18)$$

As the initial errors $X(t_0)$ are eliminated by GN&C of the vehicle during the flight, that is, $\Delta X_1(t)$ is not affected by $\Delta X_1(t_0)$, equation (18) is rewritten as

$$\Delta U = \{L^{-1} [(SI - A)^{-1} B]\}^{-1} \Delta X_1(t) \quad (19)$$

$$\Delta X_1 = \{AL^{-1} [(SI - A)^{-1} B] + B\} \Delta U \quad (19a)$$

The Filter Equation of GPS(or INS)/ Equations of Motion

The Filter Equation of Equations of Motion

Suppose the disturbances obey the following equation:

$$\Delta \dot{U} = T_1 \Delta U + \xi_U \quad (20)$$

where, T_1 is the matrix of 18×18 . ξ_U is supposed as white noise of zero mean.

$$\xi_U = \{ \xi_{CN}, \xi_{CX}, \xi_{XT}, \xi_{YT}, \xi_{ZT}, \xi_{mXDZ}, \xi_{mXWZ}, \xi_{mYDZ}, \xi_{mYWY}, \xi_{mZDZ}, \xi_{mZx}, \xi_{mZWZ}, \xi_{I_x}, \xi_{I_y}, \xi_{I_z}, \xi_{\epsilon}, \xi_{\rho}, \xi_{W} \}$$

and

$$E[\xi_U(i)\xi_U^T(j)] = Q(i)\delta_{ij} \quad (21)$$

Getting the function of ΔU and $\frac{d\Delta U}{dt}$ from equations (5)~(13), the elements of matrix T_1 are obtained. That is,

$$\Delta \dot{U} = P \Delta X_1 + Q \Delta X_1 \quad (22)$$

where, P and Q are the matrix of 18×12 . Considering equation (14) and (19),

$$\Delta \dot{U} = [(P + QA)\{AL^{-1}[(SI - A)^{-1}B]\} + QB]\Delta U = T_1 \Delta U \quad (23)$$

and the elements of matrix P and Q are

$$Q_{ij} = \frac{\partial g_i}{\partial x_j} \quad i = 1, 2, 6, 7, 8, 11, 12, \quad j = 1, 4, 9 \quad (24)$$

$$P_{ij} = \frac{d}{dt} Q_{ij} \quad i = 1, 2, 6, 7, 8, 9, 11, 12, \quad j = 1, 4, 9 \quad (25)$$

$$P_{ij} = Q_{ij} = 0 \quad i = 3, 4, 5, 10, 13, 14, \dots, 18, \quad j = 2, 3, 5, 6, 7, 8, 9, 11, 12 \quad (26)$$

$$P_{ij} = \frac{d}{dt} Q_{ij} \quad i = 3, 4, 5, 10, 13, 14, \dots, 18, \quad j = 2, 3, 5, 6, 7, 8, 9, 11, 12 \quad (27)$$

The Filter Equation of GPS

The Filter Equation of GPS can be written as:

$$\Delta \dot{X}_2 = T_2 \Delta X_2 + \xi_{\Delta X_2} \quad (28)$$

where, $\Delta X_2 = [\delta b, \delta n]^T$, δb —clock bias error, δn —clock drift error, $\xi_{\Delta X_2}$ is the vector of

Gauss white noise of zero mean.

$$E[\xi_{\Delta X_2}(i)\xi_{\Delta X_2}^T(j)] = Q_{\Delta X_2}(i)\delta_{ij}$$

and

$$T_2 = \begin{bmatrix} 0 & 1 \\ 0 & -1/\tau_{Gb} \end{bmatrix} \quad (29)$$

where, τ_{Gb} is the time constant.

The Filter Equation of INS

The filter equation of INS can be written as:

$$\Delta \dot{X}_3 = T_3 \Delta X_3 + b + \xi_{\Delta X_3} \quad (30)$$

where, $\Delta X_3 = [\delta V, \delta \gamma, \delta \psi, \delta h, \delta \theta, \delta \phi, \delta \Theta, \delta \Phi, \delta \Gamma, \epsilon_E, \epsilon_N, \epsilon_U, \nabla_E, \nabla_N, \nabla_U]^T$, $\epsilon_E, \epsilon_N, \epsilon_U$ the drift errors of the platform, $\nabla_E, \nabla_N, \nabla_U$ the zero drift of the accelerometer, $\xi_{\Delta X_3}$ is the vector of white noise of zero mean.

$$b = C_3[\nabla_E, \nabla_N, \nabla_U, 0, 0, 0,$$

$$\epsilon_E, \epsilon_N, \epsilon_U, 0(1 \times 6)]^T \quad (31)$$

$$T_3 = C_3 \begin{bmatrix} T_{31} & & \\ & T_{32} & \\ & & T_{33} \end{bmatrix} \quad (33)$$

$$T_{32} = -diag(1/\tau_E, 1/\tau_N, 1/\tau_U) \quad (35)$$

$$T_{33} = -diag(\tau_{VE}, \tau_{VN}, \tau_{VU}) \quad (36)$$

where, $\tau_E, \tau_N, \tau_U, \tau_{VE}, \tau_{VN}, \tau_{VU}$ are the time constants.

The Filter Equation of The Hybrid Systems

The filter equation of EM/GPS is

$$\begin{bmatrix} \Delta \dot{U} \\ \Delta \dot{X}_2 \end{bmatrix} = \begin{bmatrix} T_1 & \\ & T_2 \end{bmatrix} \begin{bmatrix} \Delta U \\ \Delta X_2 \end{bmatrix} + \begin{bmatrix} \xi_{\Delta U} \\ \xi_{\Delta X_2} \end{bmatrix} \quad (37)$$

The filter equation of EM/INS is

$$\begin{bmatrix} \Delta \dot{U} \\ \Delta \dot{X}_3 \end{bmatrix} = \begin{bmatrix} T_1 & \\ & T_3 \end{bmatrix} \begin{bmatrix} \Delta U \\ \Delta X_3 \end{bmatrix} + \begin{bmatrix} \xi_{\Delta U} \\ \xi_{\Delta X_3} \end{bmatrix} \quad (38)$$

The Equations of the Observation

The Observation Equations of EM/GPS

The observation values of EM/GPS are the difference between the pseudorange of GPS and the range (calculated by EM) between the selected GPS satellite and the vehicle, that is, $Z_1 = (Y_{\rho_1},$

$Y_{\rho 2}, Y_{\rho 3}, Y_{\rho 4}$) and the difference between the pseudorange rate of GPS and the range rate (calculated by EM) between the selected GPS satellite and the vehicle, that is, $Z_2 = (Y_1, Y_2, Y_3, Y_4)$. So, the observation equations of EM/GPS can be deduced as

$$\begin{bmatrix} Z_1 \\ Z_2 \end{bmatrix} = \begin{bmatrix} H_1 \\ H_2 \end{bmatrix} \begin{bmatrix} \Delta U \\ \Delta X_2 \end{bmatrix} + V_1 \quad (39)$$

where, V_1 is measurement noise vector with the zero mean, and

$$H_1 = \{D_B D'_A L^{-1}[(SI - A)^{-1} B] \quad 0(3 \times 2)\}$$

$$D_B = [D_{B1} \quad D_{B2} \quad D_{B3} \quad D_{B4}]^T$$

$$D_{Bi} = \left[\frac{X_{si} - X_r}{\rho_{ri}}, \frac{Y_{si} - Y_r}{\rho_{ri}}, \frac{Z_{si} - Z_r}{\rho_{ri}} \right]$$

$$(i = 1, 2, 3, 4)$$

$$D_A = \begin{bmatrix} r \cos \varphi & 0 & \sin \varphi \\ -r \sin \varphi \cos \theta & -r \cos \varphi \sin \theta & \cos \varphi \cos \theta \\ -r \sin \varphi \sin \theta & r \cos \varphi \cos \theta & \cos \varphi \sin \theta \end{bmatrix}$$

$$D'_A = [0(3 \times 3) \quad D_A \quad 0(3 \times 6)]$$

in the above equations, X_{si}, Y_{si}, Z_{si} the position of the selected GPS satellite in the coordinate system of the center of Earth—the equator (E), X_r, Y_r, Z_r the real position of the vehicle in the E coordinate system, ρ_{ri} real range between the vehicle and i th satellite.

$$H_2 = [D_C D_F \quad 0(3 \times 2)]$$

$$D_C = [D_{C1} \quad D_{C2} \quad D_{C3} \quad D_{C4}]^T$$

$$D_{Ci} = \frac{1}{\rho_{ri}} \begin{bmatrix} Z_r - Z_{si} + \dot{\rho}_{ri}(Z_{si} - Z_r) / \rho_{ri} \\ \dot{X}_r - \dot{X}_{si} + \dot{\rho}_{ri}(X_{si} - X_r) / \rho_{ri} \\ \dot{Y}_r - \dot{Y}_{si} + \dot{\rho}_{ri}(Y_{si} - Y_r) / \rho_{ri} \end{bmatrix}$$

$$(i = 1, 2, 3, 4)$$

$$D_F = D_C D_A L^{-1}[(SI - A)^{-1} B] + D_B D_A$$

$$[0(3 \times 3) \quad I \quad 0(3 \times 6)] \cdot L^{-1}[(SI - A)^{-1} B]$$

$$+ D_B D_A [0(3 \times 3) \quad I \quad 0(3 \times 6)]$$

$$\cdot \{AL^{-1}[(SI - A)^{-1} B] + B\}$$

where, the elements of D_A are

$$D_{A11} = \theta \cos^2 \varphi \cos \theta - \dot{\varphi} \sin \theta$$

$$D_{A12} = \dot{r} \sin \varphi \sin \theta - r \dot{\theta} \cos^2 \varphi \sin \theta - r \dot{\varphi} \cos \theta$$

$$D_{A13} = -\dot{r} \cos \varphi \cos \theta - 2r \dot{\theta} \cos \varphi \sin \varphi \cos \theta$$

$$D_{A21} = \theta \cos^2 \varphi \sin \theta + \dot{\varphi} \cos \theta$$

$$D_{A22} = -\dot{r} \sin \varphi \cos \theta + r \dot{\theta} \cos^2 \varphi \cos \theta - r \dot{\varphi} \sin \theta$$

$$D_{A23} = -\dot{r} \cos \varphi \sin \theta - r \dot{\theta} \sin 2\varphi \sin \theta$$

$$D_{A31} = \theta \cos \varphi \sin \varphi$$

$$D_{A32} = 0$$

$$D_{A33} = -\dot{r} \sin \varphi - r \dot{\theta} \sin \varphi \cos \varphi$$

$$D_E = \begin{bmatrix} -\sin \varphi \cos \theta & r \cos^2 \varphi \cos \theta & -r \sin \theta \\ -\sin \varphi \sin \theta & r \cos^2 \varphi \sin \theta & r \cos \theta \\ \cos \varphi & r \cos \varphi \sin \varphi & 0 \end{bmatrix}$$

The Observation Equation of EM/INS.

The observation values of EM/INS are the differences of position, velocity and attitude between the calculated values and the observation values of INS.

$$Z_3 = [\delta V_m, \delta \gamma_m, \delta \psi_m, \delta r_m, \delta \theta_m, \delta \varphi_m, \delta \Theta, \delta \Phi_m, \delta \Gamma_m]^T$$

The observation equation is:

$$Z_3 = H_3 \begin{bmatrix} \Delta U \\ \Delta X_3 \end{bmatrix} + V_3 \quad (40)$$

where, V_3 is measurement noise vector with the zero mean, and,

$$H_3 = [H'_3, I_-, 0(9 \times 6)]$$

$$H'_3 = H''_3 \{L^{-1}[(SI - A)^{-1} B]\}$$

$$H''_3 = \begin{bmatrix} I(6 \times 6) & 0(6 \times 6) \\ 0(3 \times 9) & I(3 \times 3) \end{bmatrix}$$

$$I_- = \text{diag}(-1, -1, \dots, -1)_{(9 \times 9)}$$

Numerical Results

In this paper, a residual decoupled kalman filter is used to obtain the numerical results. The Kalman filter uses the decoupled estimation algorithm of state and deviation. The calculation time of the algorithm is no more than 1/3~1/2 of the general Kalman filters. On the other hand,

the algorithm maintains high accuracy under the condition of high order vector and matrix. The filter is not given in this paper, and can be seen also in reference [5].

The nominal trajectory used in numerical emulation is given by [3]. The time for the vehicle to fly along the trajectory in atmosphere is 700~1500 seconds, where during the middle one-third time the GPS receiver can't work because of the 'dark obstruction area'. During the first one-third trajectory, the GDOP(geometric dilution of precision) is minimum, that is, the navigation precision of GPS is the highest. The characters of GPS errors can be seen also [7]~[9]. The characters of INS errors are: Gyro g-sensitive bias is 1.0deg/h/g, the accelerometer bias is 0.01m/s², the accelerometer scale factor is less 0.1%.

The performance index appraising the navigation precision is

$$\Delta x_i = \sqrt{\int_{t_0}^{t_f} \Delta x_i^2(t) dt} / t_f \quad (41)$$

EM can't accurately estimate the navigation information; A single GPS receiver can't provide navigation information during the atmospheric flight because of 'the dark obstruction area'. INS can provide better navigation information because of the short flight time during the asroassisted orbital transfer; Finally, GPS/EM, INS/EM can provide the higher precision navigation information than single INS or GPS does. This is because GPS(or INS)/EM can estimate the errors during the initial flight time (< 100 seconds). The estimated errors are introduced into the EM which considers all disturbances to calculate the navigation parameters. So the navigation information precision keeps at the precision of GPS (or INS) at the around initial reentry point, so GPS(or INS)/EM can get the best navigation information precision.

CONCLUSION

Based on the nominal trajectory of

Table 1 The Accuracy of EM, GPS, INS, EM/GPS, EM/INS

Equipment Errors	EM ^①	GPS	INS	GPS/EM ^①	INS/EM ^①
$\Delta V(m/s)$	20.17	∞	10.50	9.50	6.43
$\Delta \gamma(deg)$	1.42	∞	0.38	0.20	0.17
$\Delta \psi(deg)$	0.51	∞	0.40	0.20	0.17
$\Delta r(m)$	6337.5	∞	786.8	35.61	28.86
$\Delta X(m)$	3942.0	∞	317.5	35.61	27.54
$\Delta Z(m)$	1543.1	∞	213.4	35.61	28.70
$\Delta \Theta(deg)$	2.32	∞	0.25	0.20	0.17
$\Delta \Phi(deg)$	0.91	∞	0.27	0.20	0.16
$\Delta \Gamma(deg)$	0.57	∞	0.26	0.20	0.17

① $\Delta g = -5\%g$, $\Delta C_N = 5\%C_N$ in the equations of motion.

So table 1 is obtained for the navigation precision of space vehicle during the atmospheric flight. In table 1, the navigation precision of EM is very low because EM didn't consider affect of the disturbances (such as Δg , ΔC_N). It is clear that

aeroassisted orbital transfer, the paper gives a new navigation scheme for the space vehicle: Navigation hardware/ Equations of Motion, GPS/EM, INS/EM are studied for the vehicle to determine the navigation informa-

tion during aeroassisted orbital transfer. Supersonic aerodynamic calculation formulas are introduced to deduce the equations of the filter and observation for the hybrid navigation system. Equations of disturbance (14), filter equations (20), (28), (30), (37) and (38), observation equations (39) and (40) (including the matrix A , B , T_1 , T_2 , T_3 , H_1 , H_2 , H_3) are deduced. Numerical results are obtained. The navigation precisions of GPS(or INS)/EM are higher than the one of single EM, GPS (or INS).

References

1. Mease, K. D., Optimization of Aeroassisted Orbital Transfer: Current Status. *The Journal of the Astronautical Sciences*, Vol.36, January ~ June, 1988.
2. Nan Ying, et al. *The Trajectory and Control of Space Vehicle: Current Status*. The Conference paper in Chinese National 10th Conference of Flight Dynamics and Flight Experiment, Oct. 1993, Chengde, China.
3. Nan Ying, Chen Shilu, Optimal Aeroassisted Guidance using Loh's Term Approximations, *Journal of Chinese Space Science*, 1994.(In Chinese)
4. Zhan Xuetang, et al. *Celestial Mechanics and Astronomy Dynamics*, Beijing Teachers Univesity Publishing House, 1989, 10.(In Chinese)
5. Gu Qitai, Implementation of Integrated INS / GPS Navigation System & Its Applications, *Navigation*, No.2, 1992.(In Chinese)
6. Nan Ying, Chen Shilu, The Determination of Navigation information for the Space Vehicle by GPS / Equations of Motion, *Navigation*, No.1, 1994.(In Chinese)
7. Jance, H.L., *Space Shuttle Navigation Analysis*, NASA-CR-15113, 1977.
8. Dennis, A., *A Kalman Filter Design for the Space Shuttle Orbiter Inertial Measuring Ulnite during Deorbit/ Reentry Using Global Positioning System Satellite Information*, AD / A-055465, 1977.
9. Matchett G A et al. *Space Shuttle Navigation Analysis, Final Report, Volume 1: GPS Aided Navigation*, NASA-CR-160765, 30, May, 1980.
10. Nan Ying, Lu Xuefu, A New Fault-tolerant Navigation Scheme of Space Shuttle, *NPU paper*, YH9218, Oct. 1992.

AUTHOR INDEX

A

- Alby, F. - OD I.1
Alonso, R. - A&OC II.3
Ambrósio, A.M. - GSH&S II.3
Andrade, E.P. - C&C I.3, SD II.2
Andrade, J.R.C. - SD II.2
Anigstein, P.A. - A&OC II.3
Aubron, R. - GSH&S III.4

B

- Baetz, O. - C&C I.2
Baize, L. - GSH&S II.2, GSH&S II.5
Becceneri, J.C. - GSH&S I.2, GSH&S I.4
Beltan, T. - GSH&S I.3
Bianco, G. - OD I.1
Bollner, M. - A&OC II.1
Booty, K. - OP I.5
Brenot, J.M. - OP I.1
Brittinger, P. - OP II.5
Broucke, R. - SD I.4
Brousse, P. - OP II.4, OD I.3, SD II.1
Brum, A.G.V. - AD.3
Boutonnet, G. - GS II.5

C

- Campan, G. - GS I.2, OP II.4, OD I.3, SD II.1
Carrara, V. - A&OC II.2
Carrou, J.P. - GS I.2
Chatterjee, A. - SD II.3
Chen, S. - SD II.5

D

- Darrigan, C. - A&OC I.1
Darroy, J.M. - OP I.1
Dias Jr., O.P. - IP
Donat, M. - OP II.6
Drexler, M. - GSH&S I.1
Dulot, J.L. - A&OC I.1
Durand, J.C. - GS II.1
Dyachenko, A.I. - A&OC III.5

E

- Eismont, N. - AD.4

F

- Feng, X. - A&OC III.4
Fernandes, S.S. - SD I.5, SD I.6
Ferrari, C.A. - GSH&S III.2
Feucht, U. - A&OC II.1
Fitz-Coy, N.G. - SD II.3
Foliard, J. - GS I.2
Forcioli, D. - A&OC I.1
Fourcade, J. - GS I.2, OD I.1
Fournier, D. - GS II.5
Francken, P. - C&C I.4
Frank, H. - A&OC II.1, GSH&S I.5
Fronton, J.F. - GSH&S I.3

G

- Garlick, D. - GS II.2
Garton, D. - GSH&S I.5
Gaullier, F. - GS II.3, OP I.1, OP I.4
Giacaglia, G.E.O. - SD II.4
Gill, E. - OD I.1
Girolamo, S. di - C&C I.1
Goertz, C. - GSH&S III.1
Goettlich, P. - GSH&S II.4
Grahn, S. - GS II.6
Graziani, F. - C&C II.2
Gremillon, P. - GS II.3
Guedes, U.T.V. - AD.1, A&OC II.2

H

- Haire, A.G. - OP I.5
Hardsten, G. - OP I.2
Hashimoto, M. - GSH&S III.7
Head, N. - GSH&S I.6, GSH&S III.5
Hechler, M. - OP II.3
Heyler, G.A. - C&C II.1
Holmqvist, B. - GS II.6
Huc, C. - GSH&S III.4
Hucke, S. - GSH&S II.4

I

- Itami, S.N. - GSH&S I.2

J

- Jalbaud, M. - GSH&S I.3
Jansen, N. - GSH&S III.6
Jarnmark, J. - OP I.2
Jáuregui, M. - A&OC II.3
Jones, M. - GSH&S I.6, GSH&S III.5

K

- Kaufeler, J.F. - GSH&S III.8
Kaufeler, P. - GSH&S III.8
Kehr, J. - GS II.4
Keyte, K. - GSH&S III.5, GS I.1
Kirschner, M. - OD I.1
Klas, J. - AD.4
Konemba, M. - SD I.1
Kono, J. - A&OC II.4
Kruse, W. - GS I.3
Kuga, H.K. - AD.1, GSH&S II.3, OD I.2

L

- Leconat, F. - OP I.1
Leibold, A.F. - A&OC I.3
Liberio, C. de - A&OC III.2
Lima Jr., P.H.C.N. de - SD I.5
Limouzin, G. - OP I.4
Lin, H. - A&OC III.4
Lopes, R.V.F. - AD.1
Lu, X. - SD II.5
Luceri, V. - OD I.1
Lundin, S. - GS II.6
Luongo, M. - C&C I.1

M

- Maisonobe, L. - OD I.3
Mara, S. - OP I.5
Martins Neto, A.F. - A&OC III.1
Mauceri, G. - A&OC III.2
Mesnard, R. - OD I.1
Micheau, P. - A&OC I.1
Montenbruck, O. - OD I.1
Moraes, R.V. de - SD I.1, SD I.3
Mukai, T. - GSH&S III.7

N

- Nan, Y. - SD II.5
Nagarajan, N. - A&OC II.4
Nakatani, I. - GSH&S III.7
Nazirov, R. - A&OC I.5, OD I.6
Nishigori, N. - GSH&S III.7

O

- Obara, T. - GSH&S III.7
Oberto, J.M. - GSH&S III.3
Oku, Y. - GSH&S II.4
Ono, S. - OD II.2
Orlando, V. - AD.1, OP II.1
Orsal, E. - GS II.5
Ovchinnikov, M.Y. - A&OC III.5

P

- Pacholczyk, P. - OP II.2
Pacola, L.C. - GSH&S III.2
Pallaschke, S. - OD I.4
Palmerini, G.B. - C&C II.2
Parkes, A. - GSH&S III.8
Pasquier, H. - GSH&S II.2, GSH&S II.5
Pena, R.S.S. - A&OC II.3
Pessah, P. - OP I.1
Pham, P. - OP I.1
Pieplu, J.L. - GSH&S III.4, GS II.5
Pilgram, M. - GSH&S III.1, GS I.3
Pinheiro, M.P. - OD I.5
Pivovarov, M. - A&OC III.6
Prado, A.F.B.A. - SD I.4
Pujo, O. - GSH&S I.6

R

- Rao, K.R. - AD.1, OD I.2
Rayan, H.R. - A&OC II.4
Reich, R. - GSH&S III.4
Ribeiro, E.A. - GSH&S I.2
Ricci, M.C. - AD.3
Rodrigues, D.L.F. - SD I.2
Rozenfeld, P. - OP II.1
Rupp, T. - A&OC II.1

S

- Saint Vicent, A. de - OP I.1
Salter, W. - GS II.4
Santana, C.E. - A&OC II.4
Schneider, E.M. - OP II.1
Schneller, M. - OD I.1
Schoemaekers, J. - OD I.1
Schulz, W. - C&C I.3
Sessin, W. - SD I.5
Shimonek, J. - AD.4
Shuster, M.D. - AD.2
Sitruk, F. - OP I.3
Soddu, C. - C&C I.1
Soppa, U. - C&C I.2
Souza, L.C.G. de - A&OC III.3
Souza, M.L.O. e - SD I.2
Spindler, K. - OD II.1
Suard, N. - GS II.1
Symonds, M. - GSH&S.5

T

- Teofillatto, P. - C&C II.2
Thomas, G.R. - A&OC I.2
Timokhova, T.A. - A&OC I.5, OD I.6
Triska, P. - A&OC III.6
Twynam, D. - GSH&S II.1

U

- Uesugi, K. - GSH&S III.7

V

- Voita, J. - A&OC III.6

W

- Wauthier, P. - C&C I.4
Wilde, D. - C&C I.2
Williams, P. - GSH&S II.1

Y

- Yamaguti, W. - GSH&S I.2
Yasielski, R. - A&OC II.3
Yu, S. - C&C II.3

Z

- Zanardi, M.C. - SD I.3

SCOPE AND POLICY

• The purpose of the journal of the Brazilian Society of Mechanical Sciences is to publish papers of permanent interest dealing with research, development and design related to science and technology in Mechanical Engineering, encompassing interfaces with Civil, Electrical, Chemical, Naval, Nuclear, Agricultural, Materials, Petroleum, Aerospace, Food, System Engineering, etc., as well as with Physics and Applied Mathematics.

• The Journal publishes Full-Length Papers, Review Papers and Letters to the Editor. Authors must agree not to publish elsewhere a paper submitted to and accepted by the journal. Exception can be made for papers previously published in proceedings or conferences. In this case it should be cited as a footnote on the title page. Copies of the conference referees reviews should be also included. Review articles should constitute a critical appraisal of published information.

• The decision of acceptance for publication lies with the Editors and is based on the recommendations of at least two ad hoc reviewers, and of the Editorial Board, if necessary.

• Manuscripts and all the correspondence should be sent to the Editor or, alternatively, to the appropriate Associate Editor.

• Four(4) copies of the manuscript are required. The author should submit the original figures, which will be returned if the paper is not accepted after the review process.

• Manuscripts should be submitted in English or Portuguese. Spanish will also be considered.

• A manuscript submitted for publication should be accompanied by a cover letter containing the full name(s) of author(s), mailing addresses, the author for contact, including phone and fax number, and, if the authors so wish, the names of up to five persons who could act as referees.

• Manuscripts should begin with the title, including the English title, the abstract and up to five key words. If the paper's language is not English, an extended summary of about 500 words should be included. The manuscript should not contain the author(s) name(s).

• In research papers, sufficient information should be provided in the text or by referring to papers in generally available Journals to permit the work to be repeated.

• Manuscripts should be typed double-spaced, on one side of the page, using A-4 sized paper, with 2 cm margins. The pages should be numbered and not to exceed 24 pages, including tables and figures. The lead author of a RBCM paper which exceeds the standard length of pages will be assessed an excess page charge.

• All symbols should be defined in the text. A separate nomenclature section should list, in alphabetical order, the symbols used in the text and their definitions. The Greek symbols follow the English symbols, and are followed by the subscripts and superscripts. Each dimensional symbol must have SI (Metric) units mentioned at the end. In addition, English units may be included parenthetically. Dimensionless groups and coefficients must be so indicated as dimensionless after their definition.

• Uncertainties should be specified for experimental and numerical results.

• Figures and Tables should be referred in consecutive arabic numerals. They should have a caption and be placed as close as possible to the text first reference.

• Line drawings should be prepared on tracing paper or vellum, using India Ink; line work must be even and black. Laser print output is acceptable. The drawings with technical data/results should have a boundary on all four sides with scale indicators (tick marks) on all four sides. The legend for the data symbols should be put in the figure as well as labels for each curve wherever possible.

• Illustrations should not be larger than 12 x 17 cm. Lettering should be large enough to be clearly legible (1.5-2.0 mm).

• Photographs must be glossy prints.

• References should be cited in the text by giving the last name of the author(s) and the year of publication of the reference: either "Recent work (Smith and Jones, 1985)..." or "Recently Smith and Jones (1985). With four or more names, use the form "Smith et al. (1985)" in the text. When two or more references would have the same text identification, distinguish them by appending "a", "b", etc., to the year of publication.

• Acceptable references include: journal articles, dissertations, published conference proceedings, numbered paper preprints from conferences, books, submitted articles if the journal is identified, and private communications.

• References should be listed in alphabetical order, according to the last name of the first author, at the end of paper. Some sample references follow:

Bordalo, S.N., Ferziger, J.H. and Kline, S.J., 1989, "The Development of Zonal Models for Turbulence", Proceedings, 10th ABCM - Mechanical Engineering Conference, Vol. I, Rio de Janeiro, Brazil, pp. 41-44.

Clark, J.A., 1986, Private Communication, University of Michigan, Ann Arbor, MI.

Coimbra, A.L., 1978, "Lessons of Continuum Mechanics", Editora Edgard Blucher Ltda, São Paulo, Brazil.

Kandikar, S.G. and Shah, R.K., 1989, "Asymptotic Effectiveness - NTU Formulas for Multiphase Plate Heat Exchangers", ASME Journal of Heat Transfer, Vol. 111, pp. 314-321.

McCormack, R.W., 1988, "On the Development of Efficient Algorithms for Three Dimensional Fluid Flow", Journal of the Brazilian Society of Mechanical Sciences, Vol. 10, pp. 323-346.

Silva, L.H.M., 1988, "New Integral Formulation for Problems in Mechanics", (In Portuguese), Ph.D. Thesis, Federal University of Santa Catarina, Florianópolis, SC, Brazil.

Sparrow, E.M., 1980a, "Forced-Convection Heat Transfer in a Duct Having Spanwise-Periodic Rectangular Protuberances", Numerical Heat Transfer, Vol. 3, pp. 149-167.

Sparrow, E.M., 1980b, "Fluid-to-Fluid Conjugate Heat Transfer for a Vertical Pipe-Internal Forced Convection and External Natural Convection", ASME Journal of Heat Transfer, Vol. 102, pp. 402-407.

SUBMISSION

FORMAT

ILLUSTRATIONS AND
TABLES

REFERENCES

Vol. XVI - Special Issue - 1994

<i>Invited Paper</i>	001
<i>Attitude Determination (AD)</i>	009
<i>Attitude and Orbit Control I (A&OC-I)</i>	039
<i>Attitude and Orbit Control II (A&OC-II)</i>	075
<i>Attitude and Orbit Control III (A&OC-III)</i>	101
<i>Constellation and Co-location I (C&C-I)</i>	141
<i>Constellation and Co-location II (C&C-II)</i>	171
<i>Ground System Hardware and Software I (GSH&S-I)</i>	197
<i>Ground System Hardware and Software II (GSH&S-II)</i>	235
<i>Ground System Hardware and Software III (GSH&S-III)</i>	265
<i>Ground Systems I (GS-I)</i>	317
<i>Ground Systems II (GS-II)</i>	339
<i>Operations I (OP-I)</i>	383
<i>Operations II (OP-II)</i>	419
<i>Orbit Determination I (OD-I)</i>	459
<i>Orbit Determination II (OD-II)</i>	503
<i>Space Dynamics I (SD-I)</i>	521
<i>Space Dynamics II (SD-II)</i>	559
<i>Author Index</i>	599
